British Journal of Pharmacology

June 1994

Volume 112 Number 2 pages 347–716

Br. J. Pharmacol. (1994), **112**, 347–348

SPECIAL REPORT

Dexamethasone-induced translocation of lipocortin (annexin) 1 to the cell membrane of U-937 cells

Egle Solito, *Sandra Nuti & [1]Luca Parente

Departments of Pharmacology and *Immunology, Immunobiology Research Institute Siena, Via Fiorentina, 1-53100 Siena, Italy

Lipocortin (annexin) 1 is a putative mediator of the inflammatory effects of glucocorticoids. By flow cytometric analysis (FACS) we have studied the effect of dexamethasone on the cellular localization of lipocortin 1. U-937 cells were incubated with or without 10 nM phorbol 12-myristate 13-acetate (PMA) to induce cell differentiation. Then 1 μM dexamethasone was added and incubation carried out for increasing times (1–24 h). Dexamethasone caused a time-dependent biphasic translocation of lipocortin 1 from the intracellular compartment to the cell membrane with maximal membrane expression at 4 and 24 h. In differentiated U-937 cells the steroid-induced membrane accumulation of lipocortin 1 was significantly higher than that of undifferentiated cells. The accumulation of the protein in the cell membrane may precede its release which is stimulated by dexamethasone in differentiated U-937 cells. Since extracellular lipocortin 1 has anti-inflammatory properties the modulation of the translocation/secretion process of the protein by glucocorticoids may be part of their mechanism of action.

Keywords: Lipocortin 1; dexamethasone; flow cytometry; membrane translocation

Introduction Lipocortin (annexin) 1 is a member of a family of proteins endowed with calcium and phospholipid binding properties which has been proposed as a putative mediator of the anti-inflammatory action of glucocorticoids. This hypothesis is based on experimental evidence showing that steroid drugs are able to induce the synthesis and/or release of the protein (Goulding *et al.*, 1990) and that extracellular lipocortin 1 shares many of the anti-inflammatory effects of glucocorticoids (Becherucci *et al.*, 1993). The extracellular release of lipocortin 1 has been questioned by experimental evidence showing that it is an intracellular protein lacking in hydrophobic signal peptide (Frey *et al.*, 1991). On the other hand Christmas *et al.* (1991) have observed that lipocortin 1 is secreted by the human prostate gland through a novel secretory mechanism of high sorting efficiency.

We have previously shown that dexamethasone induces the expression of the mRNA of lipocortin 1 and the secretion of the protein in differentiated, but not undifferentiated U-937 cells (Solito *et al.*, 1991). These cells have been used in the present paper to investigate by flow cytometric analysis (FACS) the effect of dexamethasone on the cellular localization of lipocortin 1.

Methods *Intracellular and cell membrane immunofluorescence of U-937 cells* U-937 cells plated at 5×10^5 ml^{-1} were incubated for 24 h either with or without 10 nM PMA. Then, in the appropriate experiments, 1 μM dexamethasone was added and cells further incubated for increasing times (1–24 h). To assess intracellular expression, cells were fixed and permeabilized according to Dent *et al.* (1989). Immunofluorescence was performed as described in the Beckton Dickinson Monoclonal Handbook. Briefly, cells resuspended in phosphate-buffered saline (PBS) containing 1% BSA were incubated with human IgG (1 mg ml^{-1}) for 20 min at 4°C to prevent non-specific binding. After washing, the cells were incubated either with the anti-CD14 antibody (1:10 dilution) or with the anti-lipocortin 1 antibody (1:100 dilution) for 20 min at 4°C. After washing the FITC anti-rabbit Ig antibody (5 μg ml^{-1}) was added and cells further incubated for 20 min at 4°C. Before FACS cell viability was assessed by the propidium iodide method, as described by Shapiro (1988). Only viable cells have been used for the analysis.

Flow cytometric analysis (FACS) The quantitative FACS was performed on a FACSTAR flow cytometer (Beckton Dickinson) equipped with an Argon ion laser beam operating at 488 nm using 200 mW of power to excite the FITC and the propidium iodide. Log fluorescence histograms (256-channel) were obtained from approx. 10000 viable cells for each sample. With the Consort 30 Data Analysis System from Beckton Dickinson, mean channel number fluorescence was used to assess differences in fluorescence intensity.

Materials Human monocytic U-937 cells were obtained from the American Type Culture Collection and cultured as previously described (Solito *et al.*, 1991). Dexamethasone-21-phosphate, phorbol 12-myristate 13-acetate (PMA), propidium iodide, were purchased from the Sigma Chemical Company. Fluorescein isothiocyanate (FITC)-labelled antibodies anti-human and anti-rabbit Ig were from Boehringer Mannheim Biochemica, Germany. FITC-labelled antibody against CD14 was from Beckton-Dickinson, Mountain View, CA, U.S.A. Human IgG were from Cappel, West Chester, PA, U.S.A. Anti-human lipocortin 1 rabbit polyclonal antibody (no. 842) was kindly supplied by Dr J.L. Browning, Biogen, Cambridge, MA, U.S.A. This antibody recognized a human recombinant lipocortin 1 endowed with anti-inflammatory activity (Becherucci *et al.*, 1993).

Results U-937 cells incubated for 24 h with 10 nM PMA showed a dramatic increase in the membrane positivity (59.1 ± 14.6% of positive cells) to CD14, a specific macrophage antigen, compared to control cells (0.3 ± 0.1%, $n = 6$, $P < 0.01$). This result demonstrates that 24 h treatment with 10 nM PMA induced immature monocytic U-937 cells to differentiate into macrophage-like cells confirming previous observations (Hoff *et al.*, 1992).

Table 1 shows the results of intracellular and cell membrane expression of lipocortin 1. U-937 cells incubated for 24 h with 10 nM PMA (i.e. differentiated cells) showed an approximately 30 fold increase of intracellular lipocortin 1 expression (60.3 ± 0.4 mean fluorescence) as compared with control (i.e undifferentiated) cells (2.4 ± 0.1). On the other hand, the extent of lipocortin 1 expression on the membrane was very similar in both differentiated (36.4 ± 2.4) and undifferentiated cells (38.0 ± 3.1). Treatment with dexamethasone of differentiated cells caused a decrease of the intracellular expression of the protein (6.9 ± 0.1 at 2 h) and a

[1] Author for correspondence.

Table 1 Intracellular and cell membrane expression of lipocortin 1 in U-937 cells

Dexamethasone incubation-times (h)	*Intracellular*		*Cell membrane*	
	Control cells	*PMA-treated cells*	*Control cells*	*PMA-treated cells*
	(mean fluorescence)			
0	2.4 ± 0.1	60.3 ± 0.4**	38.0 ± 3.1	36.4 ± 2.4
1	2.3 ± 0.1	8.4 ± 0.2**	19.2 ± 2.0	45.8 ± 1.6**
2	5.8 ± 0.3	6.9 ± 0.1	53.9 ± 2.4	233.2 ± 12.4**
4	25.1 ± 0.5	25.6 ± 0.5	184.0 ± 4.2	290.6 ± 6.5**
8	5.0 ± 0.1	13.1 ± 0.1**	3.7 ± 0.1	2.6 ± 0.1
16	16.9 ± 0.4	21.8 ± 0.6*	41.6 ± 0.9	80.6 ± 1.3**
24	15.1 ± 0.3	10.3 ± 0.3*	47.6 ± 1.1	193.7 ± 8.2**

U-937 cells were incubated with or without 10 nM phorbol 12-myristate 13-acetate (PMA) for 24 h. Then 1 μM dexamethasone was added and incubation carried out for different times. At the end of incubations, intracellular and cell membrane expression of lipocortin 1 was determined by FACS as described in Methods. Data are means ± s.e.mean of the channel number fluorescence measured in the scans of 6 different cell preparations ($n = 6$). The mean non-specific fluorescence measured with the FITC-labelled anti-human Ig antibody (intracellular: 11.5 ± 0.8, $n = 6$; cell membrane: 5.9 ± 0.2, $n = 20$) has been subtracted from the table values. *$P < 0.005$, **$P < 0.001$ vs corresponding control cell values (Student's two-tailed t test).

concurrent dramatic increase of membrane protein accumulation (233.2 ± 12.4 at 2 h) which peaked at 4 h (290.6 ± 6.5). At 8 h, membrane expression fell to negligible amounts and again increased at 16 and especially at 24 h (193.7 ± 8.2). In control cells the glucocorticoid also induced a biphasic membrane translocation of the protein which again peaked at 4 h (184.0 ± 4.2) and 24 h (47.6 ± 1.1). These values were, however, significantly lower than those of PMA-treated cells. In separate experiments after 24 h PMA incubation, cells were further incubated for increasing times (1–24 h) in absence of dexamethasone. In these cells both intracellular and cell membrane positivity of lipocortin 1 did not significantly change with time as compared with the values observed after 24 h PMA (not shown).

Discussion These results demonstrate that dexamethasone induces a biphasic translocation of lipocortin 1 from the intracellular compartment to the cell membrane of U-937 cells. The steroid effect is probably specific inasmuch as glucocorticoids do not interfere with the differentiation process induced by PMA in these cells (Hoff *et al.*, 1992). We have previously observed the release of lipocortin 1 from differentiated U-937 cells stimulated with dexamethasone (Solito *et al.*, 1991). Since the steroid-induced membrane accumulation is significantly higher in differentiated U-937 cells, the translocation of large amounts of lipocortin 1 to the membrane may precede the release of the protein in the extracellular milieu. Extracellular lipocortin 1 has anti-inflammatory properties (Becherucci *et al.*, 1993); it is then conceivable that the modulation of the translocation/secretion of the protein by glucocorticoids represents part of their mechanisms of action.

The time-course of steroid-induced membrane accumulation of lipocortin 1 in differentiated U-937 cells shows that the expression peaks at 4 h, decreases to very low amounts at 8 h and increases again at 16 and 24 h. This pattern is somewhat specular to what occurs intracellularly where the initial high level of the protein decreases at 1–2 h and increases again at later times. The biphasic accumulation of lipocortin 1 on cell membrane induced by dexamethasone may appear surprising; however, a very similar time-course has been reported previously for the release of 'macrocortin' (an earlier name for lipocortin 1) induced by hydrocortisone in rat macrophages (Blackwell *et al.*, 1981; Carnuccio *et al.*, 1981). These authors have shown that macrocortin is stored preformed in macrophages and that hydrocortisone induces a biphasic release of the protein. On the basis of the previous and the present experimental evidence we propose that glucocorticoids initially stimulate the translocation to the membrane and release of the preformed lipocortin 1 with subsequent depletion of intracellular stores. This process is then followed by a new wave of synthesis which allows for new protein to be translocated and released. Further work is necessary to ascertain whether the resynthesis phase is a steroid-stimulated event or whether there is an internal feedback mechanism which initiates protein synthesis when intracellular concentrations fall below a certain level.

An account of this work was presented at the Vth Joint Meeting between the Societa' Italiana di Farmacologia and the British Pharmacological Society, Rome, 14th–16th September, 1993.

References

BECHERUCCI, C., PERRETTI, M., SOLITO, E., GALEOTTI, C.L. & PARENTE, L. (1993). Conceivable difference in the anti-inflammatory mechanisms of lipocortins 1 and 5. *Med. Inflamm.*, **2**, 109–113.

BLACKWELL, G.J., CARNUCCIO, R., DI ROSA, M., FLOWER, R.J. & PARENTE, L. (1981). Storage and steroid-induced release from rat macrophages of a phospholipase inhibitor. *Br. J. Pharmacol.*, **72**, 136–137P.

CARNUCCIO, R., DI ROSA, M., FLOWER, R.J. & PINTO, A. (1981). The inhibition by hydrocortisone of prostaglandin biosynthesis in rat peritoneal leucocytes is correlated with intracellular macrocortin levels. *Br. J. Pharmacol.*, **74**, 322–324.

CHRISTMAS, P., CALLAWAY, J., FALLON, J., JONES, J. & HAIGLER, H.T. (1991). Selective secretion of annexin 1, a protein without a signal sequence, by the human prostate gland. *J. Biol. Chem.*, **266**, 2499–2507.

DENT, G.A., LEGLISE, M.C., PRYZWANSKY, K.B. & ROSS, D.W. (1989). Simultaneous paired analysis by flow cytometry of surface markers, cytoplasmic antigens, or oncogene expression with DNA content. *Cytometry*, **10**, 192–198.

FREY, B.M, FREY, F.J., LINGAPPA, V.R. & TRACHSEL, H. (1991). Expression of human recombinant lipocortin I in a wheat-germ cell-free system and *Xenopus* oocytes. Lipocortin is not secreted. *Biochem. J.*, **275**, 219–225.

GOULDING, N.J., GODOLPHIN, J.L., SHARLAND, P.R., PEERS, S.H., SAMPSON, M., MADDISON, P.J. & FLOWER, R.J. (1990). Anti-inflammatory lipocortin 1 production by peripheral blood leucocytes in response to hydrocortisone. *Lancet*, **335**, 1416–1418.

HOFF, T., SPENCKER, T., EMMENDOERFFER, A. & GOPPELT-STRUEBE, M. (1992). Effect of glucocorticoids on the TPA-induced monocytic differentiation. *J. Leukoc. Biol.*, **52**, 173–182.

SHAPIRO, H.M. (1988). *Practical Flow Cytometry*. 2nd ed. New York: Alan R. Liss.

SOLITO, E., RAUGEI, G., MELLI, M. & PARENTE, L. (1991). Dexamethasone induces the expression of the mRNA of lipocortin 1 and 2 and the release of lipocortin 1 and 5 in differentiated, but not undifferentiated U-937 cells. *FEBS Lett.*, **291**, 238–244.

(Received February 4, 1994
Accepted February 17, 1994)

Br. J. Pharmacol. (1994), **112**, 349–351

SPECIAL REPORT

Biological actions of purines on rat megakaryocytes: potentiation by adenine of the purinoceptor-operated cytoplasmic Ca^{2+} oscillation

[1]Chikako Uneyama, *Hisayuki Uneyama, Michihito Takahashi & *Norio Akaike

Division of Pathology, National Institute of Health Sciences, Setagaya-ku, Tokyo 158, and *Department of Bio-Plasticity, Faculty of Medicine, Kyushu University, Fukuoka, 812 Japan

We have found that adenine enhanced the purinoceptor-operated cytoplasmic Ca^{2+} oscillation in rat megakaryocytes at submillimolar concentrations. Guanine and other nucleic acid bases had no effect on this system. Adenine enhanced the reaction intensity but had no effect on the threshold concentration of ATP to evoke the oscillation.

Keywords: Adenine; purinoceptor; cytoplasmic Ca^{2+} oscillation; rat megakaryocyte; Ca^{2+}-activated K^+ current

Introduction We have previously reported that rat megakaryocytes responded to extracellularly applied ATP and ADP by showing periodic activation of a Ca^{2+}-dependent K^+ current (I_{KCa}) reflecting oscillatory changes in cytoplasmic Ca^{2+} concentration ($[Ca^{2+}]_i$) induced by novel subtype of purinoceptor (Uneyama *et al.*, 1993a). As the feature of I_{KCa} oscillation in megakaryocytes is an advantage in investigating the physiological properties of single cells, we can obtain many interesting data with this experimental system (Uneyama *et al.*, 1993b,c; Akaike *et al.*, 1993; Uneyama *et al.*, 1994). Thus we studied the effect of purines and pyrimidines, and found that adenine had an enhancing effect on the purinoceptor-induced I_{KCa} oscillation. This is the first account of the modulatory effect of adenine on receptor function.

Methods The isolation technique for megakaryocytes was described previously (Uneyama *et al.*, 1993a). Megakaryocytes were used for electrical experiments within 8 h after isolation. Electrical measurements were performed with the modified perforated patch recording of Horn & Marty (1988) as previously described (Uneyama *et al.*, 1993a,b). The resistance between the recording electrode filled with internal solution and the reference electrode in external solution was 4–6 MΩ. The liquid junctional potential between the pipette solution and the standard external solution was approximately −3 mV. The data were not compensated for this potential. All experiments were performed at room temperature (20–22°C). The ionic composition of standard external solution was (in mM): NaCl 150, KCl 5, $MgCl_2$ 1, $CaCl_2$ 2, *N*-2-hydroxyethylpiperazine-*N'*-2-ethanesulphonic acid (HEPES) 10 and glucose 10. The pH was adjusted to 7.4 with tris [hydroxymethyl]aminomethane (Tris)-OH. The composition of the patch-pipette solution was (in mM): KCl 150 and HEPES 10. The pH was adjusted to 7.2 with Tris-OH.

H-8 (N-[2-methylamino)ethyl]-5-isoquinoline sulphonamide dihydrochloride) was obtained from Seikagaku Kogyo (Tokyo, Japan) and all other drugs were obtained from Sigma (St. Louis, U.S.A.). All drugs were dissolved in the standard external solution just before use. Drugs were applied by a rapid application method termed the 'Y-tube' method, as described by Murase *et al.* (1990). With the use of this technique, the drugs could be applied rapidly to megakaryocytes within 20 ms.

Results At first, we examined the Ca^{2+} mobilizing effects of purines (adenine and guanine) and pyrimidines (cytosine and uracil) on rat megakaryocytes. None of these drugs induced any detectable outward current at concentrations up to 1 mM (data not shown). However, in the presence of ATP (1 μM) or ADP (0.01 μM), adenine markedly enhanced I_{KCa} spikes induced by the purinoceptor stimuli. A typical current trace is shown in Figure 1a. Adenine (1 mM) evoked I_{KCa} spikes only in the presence of ATP in a good reproducible manner, but another purine, guanine, had no effect. Pyrimidines also had no enhancing effect on the I_{KCa} at concentrations up to 1 mM (data not shown). The action of adenine occurred 14 ± 3 s ($n = 7$) after the drug application and diminished 31 ± 11 s ($n = 7$) after the drug wash out.

As previously reported (Uneyama *et al.*, 1993a), the EC_{50} value for ATP was about 3 μM, and the concentration (1 μM) of ATP used in Figure 1a was the threshold one to evoke I_{KCa}. The synergistic action of adenine and sub-threshold (0.3 μM) and over-maximal (100 μM) concentrations of ATP was, therefore, examined (Figure 1b). Adenine (1 mM) had no effect in the presence of these sub-threshold or supramaximal concentrations of ATP. Thus, the enhancing effect by adenine was dependent on the ATP concentration, but the receptor sensitivity for ATP was not so dramatically changed as in the case of Ca^{2+} and Mg^{2+} (Uneyama *et al.*, 1993a).

The concentration-dependency of the enhancing action of adenine was investigated. The cells were pretreated with adenine for 1 min before 3 μM ATP application. Adenine increased the frequency of I_{KCa} spikes in a concentration-dependent manner, but did not enhance the current amplitude (Figure 2a). In Figures 2b and c, the quantitative results are shown. Adenine exerted its enhancing action on the current frequency from 1 μM, and the ED_{50} value was about 80 μM, but it failed to increase current amplitude at concentrations up to 1 mM.

Then, we examined whether the enhancing action of adenine was apparent when another agonist was used instead of ATP. We used thrombin as the Ca^{2+} mobilizer, because thrombin also evoked repetitive I_{KCa} spikes in rat megakaryocytes. However, in contrast to purinoceptor stimulation, adenine (1 mM) failed to enhance 5 u ml^{-1} thrombin-induced I_{KCa} oscillation (data not shown). Thrombin-1 5 u ml^{-1} was a submaximal concentration to evoke I_{KCa} oscillation in rat megakaryocytes. In addition, co-administration of adenine (300 μM) and ATP (1 μM) showed the synergistic action in the presence of H-8 (10 μM), an inhibitor of adenosine 3':5'-cyclic monophosphate (cyclic AMP)-dependent protein kinase, or forskolin (1 μM), an activator of adenylate cyclase (data not shown). Moreover, even in the absence of Mg^{2+} and Ca^{2+} in the external solution, adenine enhanced the ATP-induced responses (data not shown).

[1] Author for correspondence.

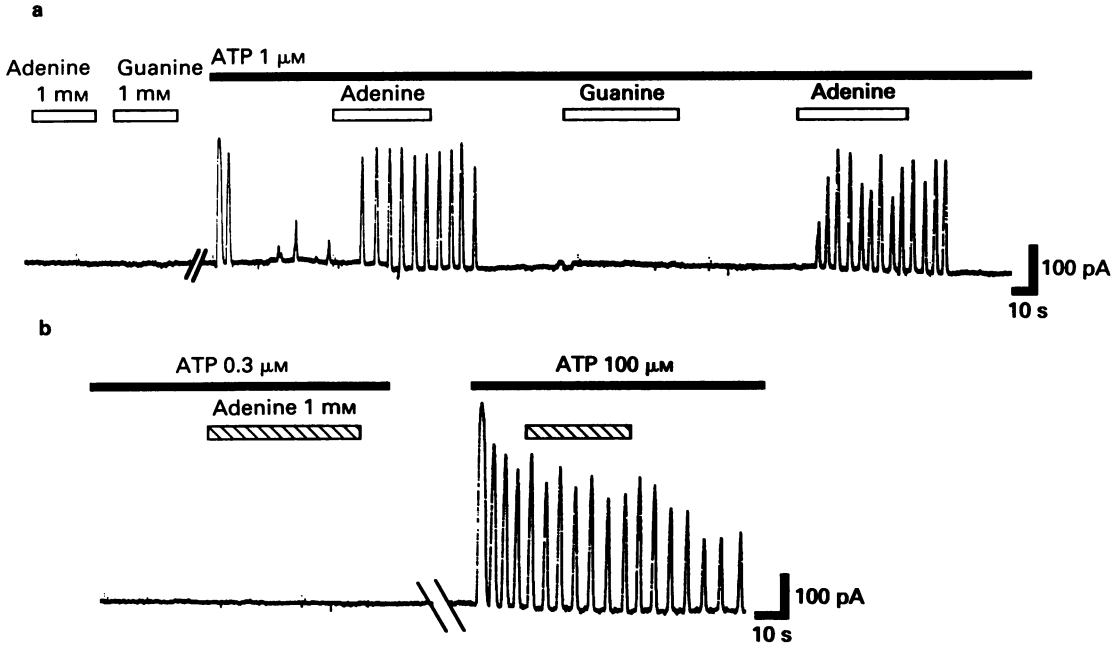

Figure 1 (a) Response to adenine and guanine in the presence and absence of ATP. Note the adenine (1 mM) evoked I_{KCa} spikes only in the presence of 1 μM ATP. (b) Effect of adenine on the responses induced by low (0.3 μM) and high (100 μM) concentrations of ATP. The megakaryocyte was voltage-clamped at a V_H of − 40 mV. Drugs were continuously applied for the period shown by the bars above each response. Each current trace was obtained from two different cells.

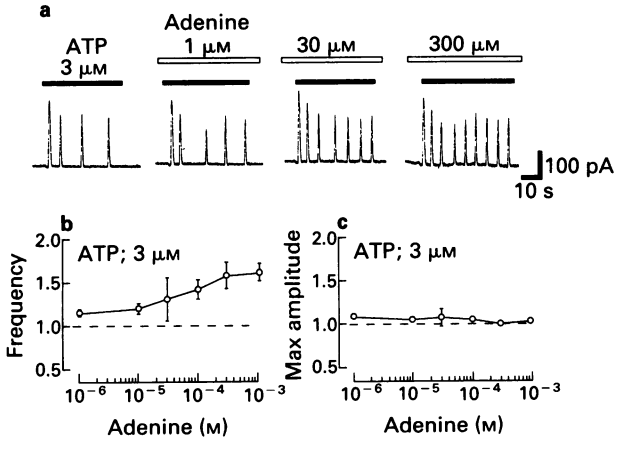

Figure 2 Concentration-dependent enhancement by adenine of the ATP-induced I_{KCa} oscillation. (a) Typical current traces obtained from the same cell. V_H was − 40 mV. Adenine at each concentration was applied 1 min prior to the application of ATP. The current traces were obtained from a single cell, and a typical one of 5 cells examined. (b) Quantitative results obtained from (a). The value of frequency and maximum current amplitude (I_{max}) were normalized to the value obtained with 3 μM ATP alone. Each value represents the mean ± s.e.mean of five to six cells.

Discussion Here we demonstrate that adenine enhanced the purinoceptor-induced I_{KCa} oscillation in a concentration-dependent manner. The other nucleic acid bases examined had no effect. The modulatory action was independent of cyclic AMP and the presence of divalent cations. In previous work, the purinoceptor-operated I_{KCa} was potentiated by reduction of the extracellular divalent cations and inhibited by elevation of intracellular cyclic AMP concentrations (Uneyama *et al.*, 1993a,b; Akaike *et al.*, 1993). Therefore, the modulatory effect of cyclic AMP and the binding of divalent cation to ATP and ADP is not involved in the action of adenine. The thrombin-operated I_{KCa} was, moreover, unaffected by adenine, although that might also be induced by an intracellular signal transduction pathway similar, in part, to the purinoceptor-mediated one. These results suggested that adenine might have a specific receptor site on megakaryocytes. It may be an adenine receptor or a part of a purinoceptor. Though the word 'purinoceptor' is the usual term, the true agonists are not purines, but purine nucleosides or nucleotides (Burnstock & Kennedy, 1985). Thus the discovery of the pharmalogical activity of adenine may provide new insight in this area.

Adenine itself is a major intermediate compound of biologically active substances such as ATP and cyclic AMP or nucleic acids consisting of DNA and RNA. When cells are injured or die, these might be released from the intracellular to extracellular spaces and the free base, adenine, might be generated. Furthermore, though adenine has been used as a component of blood preservatives (McShine *et al.*, 1990), adenine has not been regarded as an agonist with any pharmacological function. The findings indicated here will contribute not only to the understanding of the physiology of megakaryocytes but also to the mechanism of blood coagulation.

References

AKAIKE, N., UNEYAMA, H., KAWA, K. & YAMASHITA, Y. (1993). Existence of rolipram-sensitive phosphodiesterase in rat megakaryocyte. *Br. J. Pharmacol.*, **109**, 1020–1023.

BURNSTOCK G. & KENNEDY, C. (1985). Is there a basis for distinguishing two types of P_2-purinergic receptor? *Gen. Pharmacol.*, **16**, 433–440.

HORN, R. & MARTY, A. (1988). Muscarinic activation of ionic currents measured by a new whole-cell recording method. *J. Gen. Physiol.*, **92**, 145–159.

McSHINE, R.L., SIBINGA, S. & BROZOVIC, B. (1990). Differences between the effects of EDTA and citrate anticoagulants on platelet count and mean platelet volume. *Clin. Lab. Haematol.*, **12,** 277–285.

MURASE, K., RYU, T.D. & RANDIC, M. (1990). Excitatory and inhibitory amino acids- and peptide-induced responses in acutely isolated rat spinal dorsal horn neurons. *Neurosci. Lett.*, **103,** 56–63.

UNEYAMA, C., UNEYAMA, H. & AKAIKE, N. (1993a). Cytoplasmic calcium oscillation of rat megakaryocyte evoked by novel type of purinoceptor. *J. Physiol.*, **470,** 731–749.

UNEYAMA, H., UNEYAMA, C. & AKAIKE, N. (1993b). Intracellular mechanisms of cytoplasmic Ca^{2+} oscillation in rat megakaryocyte. *J. Biol. Chem.*, **268,** 168–174.

UNEYAMA, H., UNEYAMA, C., EBIHARA, S. & AKAIKE, N. (1994). Suramin and reactive blue 2 are antagonists for newly identified purinoceptor on rat megakaryocyte. *Br. J. Pharmacol.*, **111,** 245–249.

UNEYAMA, C., UNEYAMA, H., TAKAHASHI, M. & AKAIKE, N. (1993c). Cytoplasmic pH regulates ATP-induced Ca^{2+} dependent K^+ current oscillation in rat megakaryocyte. *Biochem. J.*, **295,** 317–320.

(Received February 2, 1994
Accepted February 18, 1994)

Br. J. Pharmacol. (1994), **112**, 352–354

SPECIAL REPORT

The nonpeptide neurotensin antagonist, SR 48692, used as a tool to reveal putative neurotensin receptor subtypes

I. Dubuc, J. Costentin, *J.P. Terranova, *M.C. Barnouin, *P. Soubrié, *G. Le Fur, †W. Rostène & [1,]‡P. Kitabgi

Unité de Neuropsychopharmacologie Expérimentale, UA 1170 CNRS, Faculté de Médecine-Pharmacie de Rouen, 76800 St-Etienne du Rouvray, France; *Sanofi Recherche, Département de Neuropsychiatrie, 371 rue du Prof. J. Blayac, 34184 Montpellier Cedex 04, France; †INSERM U339, Hôpital St. Antoine, 184 rue du Fbg St. Antoine, 75571 Paris Cédex 12, France and ‡Institut de Pharmacologie Moléculaire et Cellulaire du CNRS, Université de Nice-Sophia Antipolis, Sophia Antipolis, 660 Route des Lucioles, 06560 Valbonne, France

The nonpeptide neurotensin (NT) antagonist, SR 48692, was recently shown to inhibit NT binding to the cloned rat and human NT receptor and to antagonize NT effects in a variety of *in vitro* and *in vivo* assays. Here, we show that, in contrast to its antagonistic action on NT-induced hypomotility in the rat, SR 48692 failed to antagonize NT-induced hypothermia and analgesia in the mouse and rat. We suggest that these effects might be mediated through a subtype of SR 48692-insensitive NT receptor.

Keywords: Nonpeptide neurotensin antagonist; SR 48692; neurotensin receptor subtypes; hypothermia; analgesia

Introduction Expression cloning studies have identified one type of neurotensin (NT) receptor expressed in the central nervous system and peripheral tissues of mammals (Tanaka *et al.*, 1990; Vita *et al.*, 1993). Based on structure-activity studies with peptide and pseudopeptide agonist analogues of NT, it has been suggested recently that NT exerts its hypothermic and analgesic effects in the rat and the mouse through a central receptor subtype distinct from the cloned NT receptor (Al Rhodan *et al.*, 1991; Labbé-Jullié *et al.*, 1994). Distinction of receptor subtypes on pharmacological grounds can be established with selective antagonists. We recently described the biochemical and pharmacological properties of SR 48692, a potent nonpeptide antagonist of the cloned NT receptor (Gully *et al.*, 1993; Vita *et al.*, 1993). In the present study, we show that SR 48692 antagonizes the hypolocomotor effect induced by i.c.v. injection of NT in the rat. In contrast, the compound fails to inhibit the hypothermic and analgesic responses to i.c.v. injected NT in the mouse and in the rat.

Methods *Studies in mice* Tests were performed on male Swiss albino mice (CD1-Charles River, St-Aubin les Elbeuf, France). NT was dissolved in saline and SR 48692 in dimethyl sulphoxide (DMSO) and diluted in distilled water (final DMSO concentration, 5%). Corresponding vehicles were administered to controls. I.c.v. injections were performed according to Haley & McCormick (1957). SR 48692 was administered either i.p. 30 min before or i.c.v. simultaneously with the i.c.v. injection of NT (100 ng). Hypothermia and analgesia were evaluated 30 min after NT injection. Colonic temperature was measured with a thermistor probe (Ellab RM6, Copenhagen). Analgesic activity was evaluated by the tail flick test of D'Amour & Smith (1941) adapted for mice. Statistical analysis was conducted using two-way ANOVA.

Studies in rats Male OFA rats (130–160 g) from Iffa Credo (l'Arbresle, France) were used for NT-induced hypothermia, analgesia and hypomotility. I.c.v. injections (2 µl) of NT dissolved in sterile saline were made free-hand in the right lateral ventricle of conscious, non-restrained rats. SR 48692 suspended in 0.01% of Tween 80 in distilled water was administered orally (p.o.) at 5 ml kg^{-1}. Corresponding vehicles were administered to controls.

For hypothermia studies, the rectal temperature of all animals was measured with a thermocouple probe (Bailey Instrument) and animal groups with matched mean rectal temperature were constituted. Sixty minutes later, various doses of NT were injected i.c.v. The rectal temperature was measured twice just before and 30 min after NT injection. A dose of 400 ng NT was chosen for studies with SR 48692 which was administered p.o. at the indicated doses 60 min before NT injection.

For NT-induced antinociception against phenyl-*p*-benzoquinone-induced writhings (PBQ test), the animals were fasted 12 h before the test and isolated throughout the experiment. PBQ (20 mg kg^{-1}, 12.5 ml kg^{-1}) was given i.p. immediately after i.c.v. injections of increasing doses of NT. A dose of 100 ng NT was selected for antagonism studies with SR 48692 which was given p.o. at the indicated doses, 60 min before NT injection. Abdominal writhings were recorded visually between 5 and 30 min post PBQ.

For hypomotility experiments, animals were injected i.c.v. with vehicle or various doses of NT. A dose of 100 ng NT was selected for antagonism studies with SR 48692 which was given p.o. at the indicated doses 60 min before NT injection. Immediately after NT injection, the rats were placed in the test cages, motility being automatically recorded (digital image analysis system, Videotrack 512, View Point) during a 30 min period.

Statistical analysis was performed using ANOVA for motility studies and the Kruskall Wallis test for the other studies.

Drugs SR 48692, {2-[1-(7-chloro-4-quinolinyl)-5-(2,6-dimethoxyphenyl) pyrazol-3-yl) carbonylamino] tricyclo (3.3.1.1.^{3,7}) decan-2-carboxylic acid}, was synthesized at Sanofi Recherche (Montpellier, France). NT was from Neosystem (Strasbourg, France) or Sigma (St Louis, MO, U.S.A.). Phenyl-*p*-benzoquinone (PBQ) from Sigma was solubilized with 5% ethanol in distilled water.

Results *Studies in mice* SR 48692 (0.1–2.5 mg kg^{-1}, i.p.) did not significantly affect the hypothermic and analgesic responses to i.c.v. injections of 100 ng NT (Table 1). Note also that SR 48692 alone has no intrinsic activity on body temperature and tail flick latency (Table 1). When mice were injected i.c.v. with a mixture of NT (100 ng) and SR 48692 (1 µg), their body temperature (32.7 ± 0.5°C) and tail flick latency (7.5 ± 0.5 s) as measured 30 min later were similar to

[1] Author for correspondence.

Table 1 Effect of SR 48692 on the hypothermic and analgesic resposes to neurotensin (NT) in mice

Treatment	*Colonic temperature* (°C)	*Tail flick latency* (s)
Vehicle	37.0 ± 0.2	4.8 ± 0.4
NT 100 ng	33.0 ± 0.1*	7.8 ± 0.5*
SR 48692 0.1 mg kg^{-1}	37.0 ± 0.1	4.8 ± 0.6
SR 48692 0.3 mg kg^{-1}	36.7 ± 0.4	5.6 ± 0.5
SR 48692 2.5 mg kg^{-1}	37.2 ± 0.1	5.6 ± 0.6
SR 48692 0.1 mg kg^{-1} + NT 100 ng	33.5 ± 0.5*	7.8 ± 0.6*
SR 48692 0.3 mg kg^{-1} + NT 100 ng	33.2 ± 0.3*	7.2 ± 0.4*
SR 48692 2.5 mg kg^{-1} + NT 100 ng	32.7 ± 0.2*	8.6 ± 0.4*

SR 48692 was administered i.p. 30 min before i.c.v. injection of NT. Colonic temperature and tail flick latency were measured 30 min after NT injection. Values represent the mean ± s.e.mean from 6–15 mice per group. Two-way ANOVA indicates a lack of interaction between SR 48692 and NT, and a lack of intrinsic activity of SR 48692 in both tests.
*$P<0.001$ as compared to vehicle-injected animals.

those measured in animals injected with NT alone (32.9 ± 0.3°C; 7.7 ± 0.4 s) (means ± s.e.mean from 6 mice per group). It was also noted that SR 48692 (1 μg, i.c.v.) displayed no intrinsic effect on either parameter.

Studies in rats As shown in Figure 1a left, NT (400 ng, i.c.v.) induced a significant hypothermia in rats. SR 48692 (0.5, 1, 2, 4 mg kg^{-1}) did not significantly modify the hypothermia induced by 400 ng NT (Figure 1a, right). In the dose-range studied, SR 48692 by itself did not affect body temperature.

NT (100 ng, i.c.v.) significantly reduced the number of writhings induced by PBQ in rats (Figure 1b, left). SR 48692 at 0.5, 1, 2 and 4 mg kg^{-1} did not significantly affect the analgesia induced by 100 ng NT (Figure 1b, right).

I.c.v. administration of NT induced a dose-dependent and significant reduction of spontaneous locomotor activity in the rat (Figure 1c, left). SR 48692 (2 mg kg^{-1}) significantly ($P<0.05$) antagonized the hypomotility induced by 100 ng NT (Figure 1c, right).

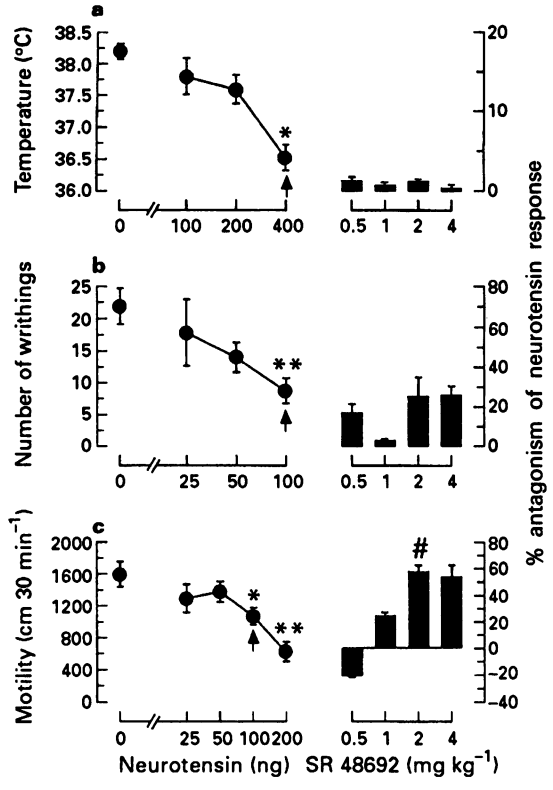

Figure 1 Effect of SR 48692 on neurotensin (NT)-induced hypothermia (a), analgesia (b) and hypomotility (c) in rats. Left panels present the NT dose-response relationships, right panels present the effects of SR 48692 against NT i.c.v. injected at the dose indicated by arrows in the corresponding left panels. In all studies, SR 48692 was administered p.o. 60 min prior to NT injection. Rectal temperature was measured 30 min after NT or vehicle injection. Antinociception (writhing test) was evaluated between 5 and 30 min post phenyl-*p*-benzoquinone (PBQ) which was given i.p. immediately after NT or vehicle injection. Motility was monitored during a 30 min period immediately following NT or vehicle injection. Values represent the mean ± s.e.mean from 10–30 rats per group. *$P<0.05$; **$P<0.01$ as compared to controls. #$P<0.05$ as compared to NT alone.

Discussion Previous studies have shown that SR 48692 inhibited the binding of NT to and antagonized NT responses mediated through the cloned rat and human NT receptors (Gully *et al.*, 1993; Vita *et al.*, 1993). The present data show that SR 48692 fails to antagonize the hypothermic and analgesic responses elicited by NT in the mouse and the rat. A lack of central bioavailability of i.p. or p.o. administered SR 48692 can be ruled out since both routes of administration of the antagonist led to a marked inhibition of the turning behaviour induced by intrastriatal injection of NT in the mouse (Gully *et al.*, 1993). Furthermore, SR 48692 given p.o. to rats significantly antagonizes the hypokinetic effect elicited by NT as reported here. Finally, we show that direct injection of SR 48692 in the central nervous sytem also fails to antagonize the hypothermic and analgesic effects of NT in the mouse. We therefore propose as a possible explanation for the present findings that NT-induced hypothermia and analgesia may be initiated through a receptor pharmacologically distinct from the cloned NT receptor. This conclusion is in full agreement with that recently proposed on the basis of structure-activity studies with NT agonists (Al-Rhodan *et al.*, 1991; Labbé-Jullié *et al.*, 1994). Further studies will be necessary to characterize the structure, biochemical properties and tissue distribution of the SR 48692-insensitive NT receptor.

References

AL-RHODAN, N.R.F., RICHELSON, E., GILBERT, J.A., MCCORMICK, D.J., KANBA, K.S., PFENNING, M.A., LARSON, E.W. & YAKSH, T.L. (1991). Structure-antinociceptive activity of neurotensin and some novel analogues in the periaqueductal gray region of the brainstem. *Brain Res.*, **557**, 227–235.

D'AMOUR, F.E. & SMITH, D.L. (1941). A method for determining loss of pain sensation. *J. Pharmacol. Exp. Ther.*, **72**, 74–77.

GULLY, D., CANTON, M., BOIGEGRAIN, R., JEANJEAN, F., MOLIMARD, J.C., PONCELET, M., GUEUDET, C., HEAULME, M., LEYRIS, R., BROUARD, A., PELAPRAT, D., LABBE-JULLIE, C., MAZELLA, J., SOUBRIE, P., MAFFRAND, J.P., ROSTENE, W., KITABGI, P. & LE FUR, G. (1993). Biochemical and pharmacological profile of a potent and selective nonpeptide antagonist of the neurotensin receptor. *Proc. Natl. Acad. Sci. U.S.A.*, **90**, 65–69.

HALEY, T.J. & MCCORMICK, W.G. (1957). Pharmacological effects produced by intracerebral injection of drugs in the conscious mouse. *Br. J. Pharmacol. Chemother.*, **12**, 12–15.

LABBE-JULLIE, C., DUBUC, I., BROUARD, A., DOULUT, S., BOURDEL, E., PELEPRAT, D., MAZELLA, J., MARTINEZ, J., ROSTENE, W., COSTENTIN, J. & KITABGI, P. (1994). In vivo and in vitro structure-activity studies with peptide and pseudopeptide neurotensin analogs suggest the existence of distinct central neurotensin receptor subtype. *J. Pharmacol. Exp. Ther.*, **268**, 328–336.

TANAKA, K., MASU, M. & NAKANISHI, S. (1990). Structure and functional expression of the cloned rat neurotensin receptor. *Neuron*, **4**, 847–854.

VITA, N., LAURENT, P., LEPORT, S., CHALON, P., DUMONT, X., KAGHAD, M., GULLY, D., LE FUR, G., FERRARA, P. & CAPUT, D. (1993). Cloning and expression of a complementary DNA encoding a high affinity human neurotensin receptor. *FEBS Lett.*, **317**, 139–142.

(Received February 17, 1994
Accepted March 7, 1994)

Br. J. Pharmacol. (1994), 112, 355-356

SPECIAL REPORT

Inhibition by spermine of the induction of nitric oxide synthase in J774.2 macrophages: requirement of a serum factor

Csaba Szabó, Garry J. Southan, Elizabeth Wood, [1]Christoph Thiemermann & John R. Vane

The William Harvey Research Institute, St. Bartholomew's Hospital Medical College, Charterhouse Square, London EC1M 6BQ

Polyamines are endogenous regulators of various cell functions. Nitric oxide (NO) is a cytostatic and cytotoxic free radical which is produced by the inducible NO synthase (iNOS) in immuno-stimulated macrophages. We tested whether spermine modulates the induction of iNOS in J774.2 macrophages. Stimulation of macrophages by bacterial lipopolysaccharide (LPS) or γ-interferon increased the accumulation of nitrite in the culture medium. Spermine (10^{-6}–10^{-4} M) inhibited nitrite production without causing cytotoxicity. This inhibition of NO formation by spermine was significantly reduced when it was given 6 h after LPS. Spermine did not inhibit nitrite accumulation when foetal calf serum was omitted from the tissue culture medium. Thus, spermine is an inhibitor of the induction of iNOS, and its inhibitory activity requires the presence of a serum factor.

Keywords: Nitric oxide; lipopolysaccharide; spermine; polyamines

Introduction Endotoxin (bacterial lipopolysaccharide, LPS), interleukin-1, tumour-necrosis factor and γ-interferon (IFN) either alone or in combination induce nitric oxide (NO) synthase (iNOS) in macrophages resulting in the formation of large quantities of NO, which serves as a cytotoxic molecule with a key role in the antimicrobial activity of immune-stimulated macrophages (Green & Nacy, 1993).

The polyamines, spermine, spermidine and putrescine are endogenous regulators of proliferation, differentiation, functional activation and macromolecular biosynthesis in all mammalian cells (Selmeci *et al.*, 1985; Morgan, 1987). High concentrations of polyamines occur in foetal and neoplastic tissues and in seminal fluid. These tissues represent antigenic challenges that often do not elicit appropriate immune response of the host organism (see: Selmeci *et al.*, 1985; Normann, 1985; Morgan, 1987; Bulmer, 1992 for reviews). Here we show that spermine inhibits the induction of iNOS in activated macrophages.

Methods The mouse macrophage cell line J774.2 was cultured in Dulbecco's modified Eagle's medium (DMEM) with 4×10^{-3} M L-glutamine and 10% foetal calf serum (FCS) (Szabó *et al.*, 1993). Cells were cultured in 96-well plates until confluence. To induce iNOS, fresh DMEM containing *E. coli* LPS (1 μg ml^{-1}) or γ-interferon (IFN, 50 u ml^{-1}) was added to the medium. Nitrite was measured after 24 h by the Griess reaction (Szabó *et al.*, 1993). Where appropriate, spermine (10^{-6}–10^{-4} M), dexamethasone (10^{-6} M) or N^G-monomethyl-L-arginine (L-NMMA, 3×10^{-3} M) were added to the medium either together with LPS or 6 h after LPS. The effect of spermine (10^{-6}–10^{-4} M) was also tested in DMEM without FCS. Mitochondrial respiration was assessed by the mitochondrial-dependent reduction of MTT [3-(4,5-dimethylthiazol-2-yl)-2,5-diphenyltetrazolium bromide] to formazan (Szabó *et al.*, 1993). DMEM, L-glutamine, LPS (*E. coli*, serotype No. 0127:B8), dexamethasone phosphate, MTT and spermine hydrochloride were from Sigma (Poole, Dorset). N^G-monomethyl-L-arginine monoacetate (L-NMMA) was from Calbiochem (Nottingham). FCS was from AAP (West Midlands). Murine γ-interferon was from Genzyme (West Malling, Kent). Values are expressed as mean ± s.e.mean of n observations, where n represents the number of wells studies (9 wells from 3 independent experiments). Student's unpaired t test was used to compare means between groups. A P value <0.05 was considered significant.

Results LPS or IFN increased nitrite concentrations in the culture medium at 24 h (Figure 1). Co-administration of spermine with LPS dose-dependently reduced the accumulation of nitrite (Figure 1a). Nitrite production is due to induction of iNOS, for both L-NMMA (a NOS inhibitor, 3×10^{-6} M) and dexamethasone (an inhibitor of iNOS induction, 10^{-6} M) inhibited nitrite accumulation (Figure 1). The induction of iNOS in the cells was associated with an inhibition of mitochondrial respiration, which was prevented by spermine or L-NMMA (Figure 1b).

The effects of spermine or dexamethasone were reduced when added to the medium 6 h after LPS (Figure 1a). This reduction was not due to accumulation of nitrite before addition of spermine or dexamethasone at 6 h, as there was no significant nitrite accumulation at this stage (nitrite concentration was 1.8 ± 0.5 μM 6 h after LPS vs. 1.4 ± 0.3 μM in control, $n = 12$).

Spermine did not inhibit nitrite accumulation when FCS was omitted from the medium (Figure 1a). Without FCS, the induction of nitrite production was attenuated by LPS, while it was slightly enhanced by IFN (Figure 1a).

Discussion We show that spermine inhibits the accumulation of nitrite in the medium of immune-stimulated J774.2 macrophages. This effect of spermine is less when added to the medium 6 h after stimulation, suggesting that spermine inhibits the induction, rather than activity of iNOS. Similarly, other inhibitors of iNOS induction, such as dexamethasone (Figure 1a), interleukin-10 (Cunha *et al.*, 1992) or dihydropyridine calcium channel modulators (Szabó *et al.*, 1993) also show less potency in inhibiting the formation of nitrite when given several hours after the stimulus of induction.

Cytotoxicity and/or a non-specific depression of cellular respiration does not account for the inhibition of nitrite accumulation seen with spermine, for spermine up to 10^{-4} M did not reduce viability. On the contrary, spermine partially reverses the LPS-induced inhibition of cellular respiration. This is likely to be due to inhibition of NO production by spermine, for NO mediates the inhibition of mitochondrial respiration in immune-stimulated macrophages (Green & Nacy, 1993).

The inhibitory effect of spermine on nitrite accumulation was only seen in the presence of FCS. This indicates that serum modulates the activity of spermine, possibly by providing an endogenous inhibitor of iNOS induction which synergizes with spermine or by activating spermine, e.g. through its metabolism.

[1] Author for correspondence.

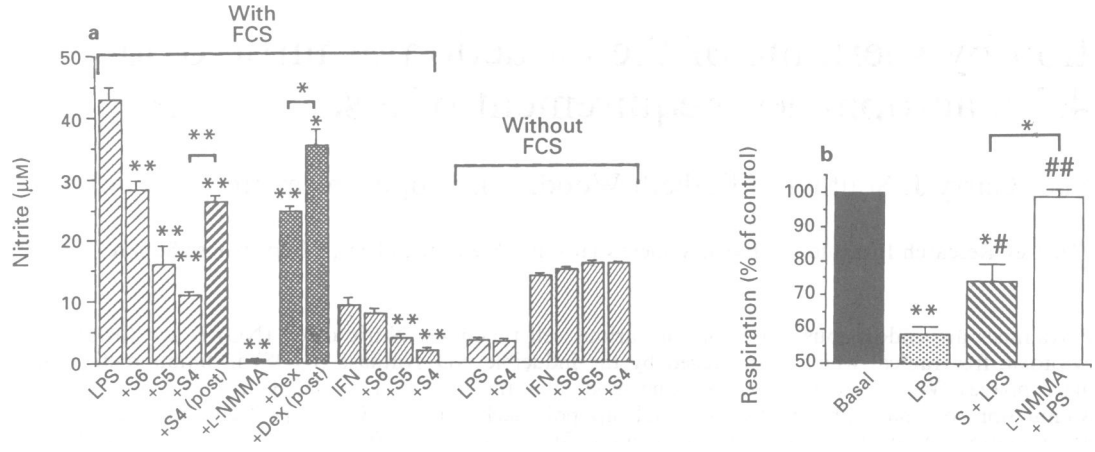

Figure 1 Nitrite concentration in the supernatant of J774.2 macrophages 24 h after stimulation by bacterial lipopolysaccharide (LPS) or γ-interferon (IFN). Experiments were performed in DMEM either with 10% foetal calf serum (FCS) or without FCS. Basal nitrite (~2.5 μM) has been subtracted from the values. Depicted are the effects of spermine (10^{-6}, 10^{-5} and 10^{-4} M; S6, S5 and S4 respectively), N^G-monomethyl-L-arginine (L-NMMA, 3×10^{-3} M) or dexamethasone (Dex, 1 μM) on nitrite accumulation. The effect of 100 μM spermine or Dex on nitrite accumulation was also studied when these agents were given 6 h after LPS (post). Data are expressed as means ± s.e.mean of $n = 9$ wells from 3 experimental days. $^*P < 0.05$ and $^{**}P < 0.01$ represent significant differences in the presence of various inhibitors, when compared to control, or between groups as indicated. (b) Spermine (S) or L-NMMA inhibit the depression of cellular respiration by LPS in J774.2 macrophages. Depicted are the effects of spermine (10^{-4} M) and L-NMMA (3×10^{-3} M) on mitochondrial respiration in J774.2 macrophages stimulated by LPS for 24 h. Data are expressed as means ± s.e.mean of $n = 9$ wells from 3 experimental days. $^*P < 0.05$ and $^{**}P < 0.01$ represent significant differences when compared to basal values or between groups are compared as indicated; $^{\#}P < 0.05$ and $^{\#\#}P < 0.001$ represent significant restoration of the mitochondrial respiration in the presence of spermine or L-NMMA (together with LPS) when compared to LPS alone.

Interestingly, the induction of iNOS by LPS was markedly reduced in the absence of FCS. A likely explanation for this finding is that some serum factor is required for the induction of iNOS by LPS. A candidate is LPS-binding protein (LBP) which binds to LPS to form an LBD-LPS complex which then binds to the CD14 receptor on the cell membrane (Raetz *et al.*, 1991). Induction of NOS by IFN, however, was enhanced in the absence of FCS. This may be related to a possible non-specific binding of IFN to plasma proteins present in FCS.

Immunosuppression is frequently seen in tissues or biological fluids containing high levels of polyamines. We speculate that prevention of iNOS induction by polyamines may contribute to the well-documented host immunosuppression seen in pregnancy (see Bulmer, 1992) or in tumour-bearing organisms (see Normann, 1985). Polyamines are produced by various bacteria (see Morgan *et al.*, 1987), and so bacteria-derived polyamines may attenuate the host immune responses associated with the systemic inflammatory response syndrome.

This work was supported by a grant from Glaxo Group Research Ltd. C.S. is supported by Lloyd's of London Tercenernary Foundation. C.T. is supported by a grant from the commission of the European Communities (Biomed I, BMHI, CT 92/1893).

References

BULMER, J. (1992). Immune aspects of pathology of the placental bed contributing to pregnancy pathology. *Balliere's Clin. Obstet. Gynecol.*, **6**, 461–488.

CUNHA, F.Q., MONCADA, S. & LIEW, F.Y. (1992). IL-10 inhibits the induction of nitric oxide synthase by IFNγ in murine macrophages. *Biochem. Biophys. Res. Commun.*, **182**, 1155–1159.

GREEN, S.J. & NACY, C.A. (1993). Antimicrobial and immunopathologic effects of cytokine-induced nitric oxide synthesis. *Current. Op. Infect. Dis.*, **6**, 384–396.

MORGAN, D.M. (1987). Polyamines. *Essays Biochem.*, **23**, 82–115.

NORMANN, S.J. (1985). Macrophage infiltration and tumor progression. *Cancer Metastas. Rev.*, **4**, 277–291.

RAETZ, C.R.H., ULEVITCH, R.J., WRIGHT, S.D., SIBLEY, C.H., DING, A. & NATHAN, C.F. (1991). Gram-negative endotoxin: an extraordinary lipid with profound effects on eukaryotic signal transduction. *FASEB J.*, **5**, 2652–2660.

SELMECI, L., BROSNAN, M.E. & SEILER, N. (1985). *Recent Progress in Polyamine Research*. Budapest: Akademiai Kiado.

SZABÓ, C., THIEMERMANN, C. & VANE, J.R. (1993). Dihydropyridine modulators of calcium channels inhibit the induction of nitric oxide synthase by endotoxin in cultured J774.2 cells. *Biochem. Biophys. Res. Commun.*, **196**, 825–830.

(Received March 2, 1994
Accepted March 14, 1994)

Br. J. Pharmacol. (1994), **112**, 357–359

SPECIAL REPORT

Evidence from desensitization studies for distinct receptors for ATP and UTP on the rat superior cervical ganglion

Gerald P. Connolly

Department of Physiology, University College London, Gower Street, London WC1E 6BT

Prolonged contact of the rat superior cervical ganglia (SCG) with the purine α,β-methylene-ATP (α,β-Me-ATP) selectively depressed responses to ATP and α,β-Me-ATP but not responses to uridine 5'-triphosphate (UTP), potassium or adenosine. Prolonged contact with the pyrimidine UTP selectively depressed responses to UTP but not responses evoked by α,β-Me-ATP, potassium or adenosine. These results are consistent with the presence of P_2-purinoceptors and pyrimidinoceptors on the rat SCG and the hypothesis that pyrimidinoceptors exist within the nervous system.

Keywords: rat superior cervical ganglion; uridine-5'-triphosphate (UTP); α,β-methylene-ATP (α,β-Me-ATP); pyrimidinoceptor; P_2-purinoceptor

Introduction Based on the results of studies of the relative order of potency of purine and pyrimidine 5'-nucleotides on non-neuronal tissues it has been suggested that some tissues contain distinct receptors that recognize either purines, e.g. adenosine 5'-triphosphate (ATP) or pyrimidines e.g. uridine 5'-triphosphate (UTP), i.e. P_2-purinoceptors and pyrimidinoceptors respectively (Seifert & Schultz, 1989; O'Connor *et al.*, 1991). In addition to agonist studies the effect of selective desensitization by α,β-methylene-ATP (α,β-Me-ATP), a slowly degradable analogue of ATP has been employed to establish if P_2-purinoceptors are involved in the actions of ATP (Burnstock & Kennedy, 1985; Von Kugelgen *et al.*, 1987; Saiag *et al.*, 1990). Comparable studies to support the existence and presence of pyrimidinoceptors have been reported using UTP which desensitizes responses of blood vessels evoked by UTP (Von Kugelgen *et al.*, 1987; Saiag *et al.*, 1990) and rat perfused liver (Haussinger *et al.*, 1987). In contrast other tissues have been shown to exhibit cross desensitization between ATP and UTP suggesting these responses are mediated via a common nucleotide receptor that recognizes ATP and UTP (Pfeilschifter, 1990).

The effects of pyrimidines and their 5'-nucleotides on the nervous system have received little attention from pharmacologists. Some evidence for the presence of distinct P_2-purinoceptors and pyrimidinoceptors on sympathetic neurones has been obtained by use of P_2-purinoceptor antagonists, suramin (Connolly *et al.*, 1993), pyridoxalphosphate-6-azophenyl-2',5'-disulphonic acid (Connolly & Harrison, 1994) and reactive blue 2 (unpublished observations) which selectively antagonized α,β-Me-ATP but not UTP-evoked depolarizations of the rat superior cervical ganglion (SCG). In order to assess whether purine and pyrimidine 5'-nucleotides activate distinct receptors on the rat SCG the effects of desensitization by UTP or α,β-Me-ATP on responses evoked by these nucleotides was determined.

Methods Ganglia were prepared for recording of d.c. potentials via the internal carotid nerve and the body of the ganglion as described before (Connolly *et al.*, 1993). SCG removed from male Sprague-Dawley rats (230–330 g) killed with a lethal dose of urethane were desheathed and placed in a recording bath and superfused (approx. 2 ml min^{-1}) with a solution at pH 7.4 and 25 ± 1°C, containing (mM) NaCl 125, $NaHCO_3$ 25, KCl 1, KH_2PO_4 1, $MgSO_4$ 1, glucose 10, $CaCl_2$ 0.1 and pre-oxygenated (5% CO_2/95% O_2).

Purines and UTP or potassium were applied for 2 or 1 min respectively. To produce desensitization the flow of superfusate was stopped (approx. 30 min), ganglia were kept oxygenated and after adjusting the volume of the bath (Ca. 0.5 ml) 50 μl of superfusate was replaced with concentrated α,β-Me-ATP or UTP and left in contact for 25 min before restarting superfusion. Responses evoked by ATP (100 μM) were recorded in the presence of an A_1-purinoceptor antagonist, 8-cyclopentyl-1,3-dipropylxanthine (DPCPX) at 1 μM, added to the superfusate throughout an experiment. All drugs except for DPCPX (Research Biochemicals Inc.) were bought from Sigma Chemical Co. (U.K.) and dissolved as 10 or 100 mM stock solutions in superfusate. Salts were of Analar grade. Differences between responses (mean ± s.e.mean) from eight ganglia unless stated otherwise were considered significant (paired *t* test) if $P<0.05$ and n = number of ganglia.

Results The effect of a single or repeated application of α,β-Me-ATP, UTP, potassium and adenosine on the d.c. potential of single ganglia are shown in Figure 1. Prolonged contact with 1 mM α,β-Me-ATP evoked a sustained depolarization (378 ± 73 μV) and a significant depression of subsequent depolarization to α,β-Me-ATP but not depolarizations evoked by UTP (Figure 1a,b) or potassium (5 mM) (responses 163 and 65 min before (144 ± 9 μV, 141 ± 17 μV respectively) and 12 and 109 min after (143 ± 17 μV, 119 ± 22 μV respectively)), or hyperpolarization by adenosine (100 μM) (responses 120 min before (94 ± 18 μV) and 67 min after (102 ± 23 μV)) (Figure 1a).

Prolonged contact with 1 mM α,β-Me-ATP in the presence of DPCPX (1 μM) evoked a sustained depolarization (765 ± 188 μV) and a significant depression ($P<0.05$) of all subsequent depolarizations to ATP (cf. responses 132 and 74 min before (238 ± 16 μV, 207 ± 36 μV respectively) and 15, 60 and 129 min after (119 ± 52, 119 ± 14, and 134 ± 23 μV respectively)) but not depolarizations evoked by 100 μM UTP (responses 162 and 101 min before (276 ± 20 μV, 282 ± 50 μV respectively) and 36 min after (209 ± 41 μV)) or 5 mM potassium (186 min before (194 ± 11 μV) and 151 min after (255 ± 54 μV)).

Prolonged contact with UTP at 1 or 10 mM evoked a sustained depolarization (185 ± 46 μV, $n=4$; 891 ± 55 μV, $n=8$) and a concentration-dependent depression of depolarization evoked by UTP (Figure 1d,e). Depolarizations evoked by α,β-Me-ATP (Figure 1d) or 5 mM potassium were not significantly altered by prolonged contact with 1 mM UTP (responses to potassium 112 and 18 min before (180 ± 28 μV, 206 ± 42 μV respectively) and 46 min after 1 mM UTP (183 ± 31 μV) ($n=4$)). Depolarizations evoked by α,β-Me-ATP (Figures 1c,e) or 5 mM potassium (responses 154 and 69 min before (165 ± 25 μV, 131 ± 10 μV respectively) and 10 mM 17 and 120 min after 10 mM UTP (156 ± 30 μV and 118 ± 192 μV respectively)) or hyperpolarizations evoked by

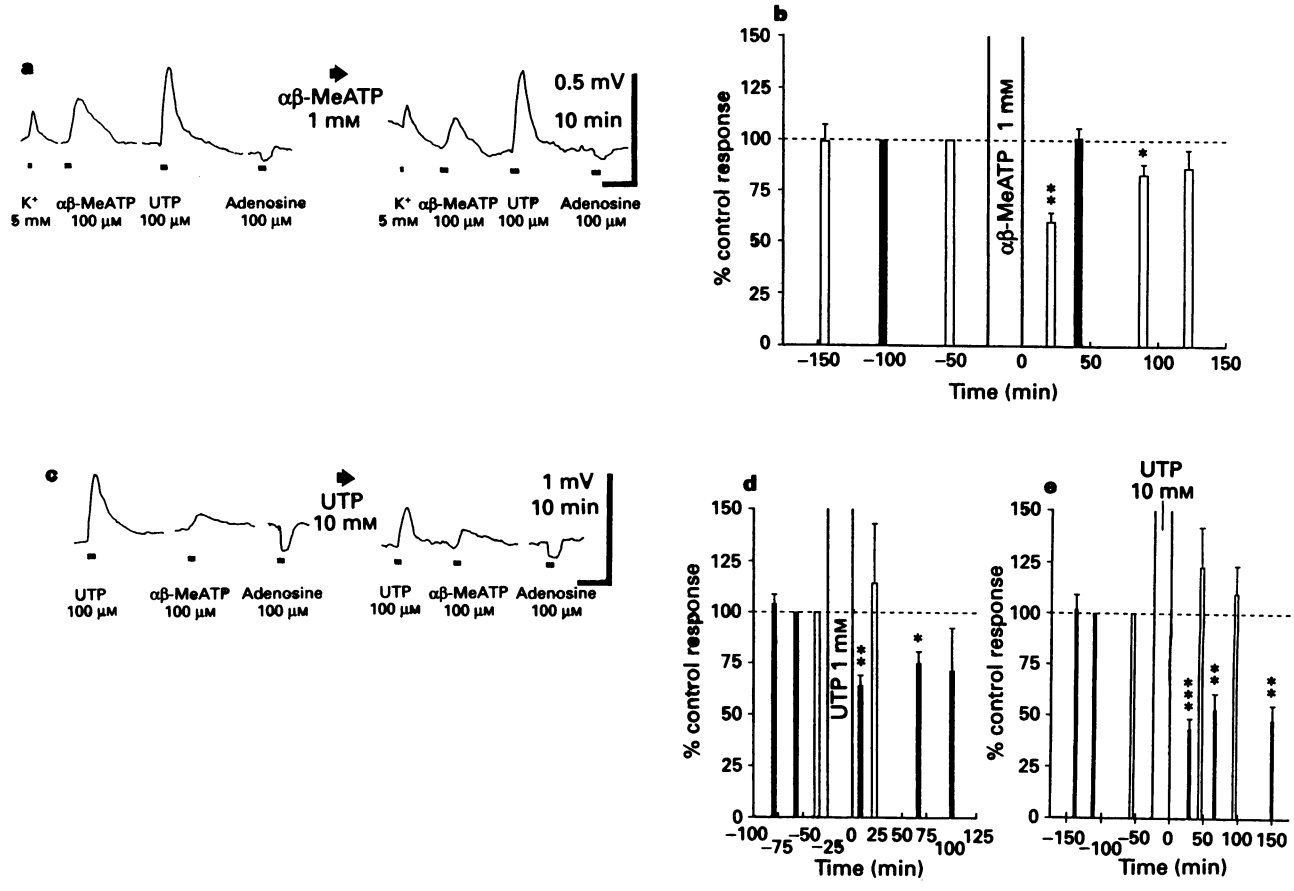

Figure 1 Effect of prolonged contact with α,β-methylene-ATP (α,β-Me-ATP) or uridine 5'-triphosphate (UTP) on the response of the rat superior ganglion to α,β-Me-ATP, UTP, potassium or adenosine. (a) Response of a single ganglion evoked by potassium (K^+), α,β-Me-ATP, UTP and adenosine before (left hand) and after (right hand) 1 mM α,β-Me-ATP. (b) Summary of the effect of 1 mM α,β-Me-ATP on depolarizations evoked by 100 μM α,β-Me-ATP (open columns) or 100 μM UTP (solid columns). Responses are expressed as a percentage of the control response evoked by α,β-Me-ATP 53 min (177 ± 16 μV) or UTP (355 ± 29 μV) 102 min before 1 mM α,β-Me-ATP. (c) Response of a single ganglion evoked by UTP, α,β-Me-ATP and adenosine before (left hand) and after (right hand) 10 mM UTP. (d) and (e) Summary of the effect of 1 or 10 mM UTP on depolarizations evoked by 100 μM α,β-Me-ATP (open columns) or 100 μM UTP (solid columns). Responses before application of 1 or 10 mM UTP ($n = 4$ or 8 respectively) are expressed as a percentage of the control response evoked by α,β-Me-ATP (150 ± 21 μV, 118 ± 15 μV respectively) or UTP (208 ± 6 μV, 390 ± 66 μV respectively). In (b), (d) and (e) statistical differences between responses before (control) and after application of α,β-Me-ATP or UTP are indicated by $*P<0.05$; $**P<0.01$ and $***P<0.001$.

100 μM adenosine (responses 86 min before (183 ± 20 μV) and 138 min (149 ± 17 μV) after 10 mM UTP, see Figure 1c) were not significantly altered by prolonged contact with 10 mM UTP.

Discussion Selective desensitization by α,β-Me-ATP provides a means of identifying P_{2X}-purinoceptors (Burnstock & Kennedy, 1985) and prolonged contact with α,β-Me-ATP selectively antagonized both ATP and α,β-Me-ATP-evoked depolarizations of the rat SCG but not depolarizations evoked by UTP, potassium and adenosine, indicating that depolarization by ATP and α,β-Me-ATP but not by the other agonists tested was mediated by P_{2X}-purinoceptors. These results also indicate that UTP-evoked depolarizations were due to activation of distinct receptors, i.e. pyrimidinoceptors. This hypothesis is supported by the observation that prolonged application of UTP produced a concentration-dependent depression of subsequent responses to UTP but not responses mediated by α,β-Me-ATP, potassium or adenosine. Both the present observations and the inability of selective P_2-purinoceptor antagonists to antagonize depolarizations of the rat SCG by UTP (Connolly *et al.*, 1993; Connolly & Harrison, 1994) strongly indicate that these rat SCG neurones possess pyrimidinoceptors and support the idea that pyrimidinoceptors exist within the nervous system.

I thank Dr P.J. Harrison (UCL) for his encouragement during this study.

References

BURNSTOCK, G. & KENNEDY, C. (1985). Is there a basis for distinguishing two types of P_2-purinoceptors? *Gen. Pharmacol.*, **16**, 433–440.

CONNOLLY, G.P., HARRISON, P.J. & STONE, T.W. (1994). αβ-MethyleneATP but not UTP evoked depolarisations of the rat superior cervical ganglion are antagonised by a P_{2X}-purinoceptor antagonist. *Br. Pharmacol.*, **112**, 408P.

CONNOLLY, G.P., HARRISON, P.J. & STONE, T.W. (1993). Action of purine and pyrimidine nucleotides on the rat superior cervical ganglion. *Br. J. Pharmacol.*, **110**, 1297–1304.

HAUSSINGER, D., STEHLE, T. & GEROK, W. (1987). Actions of extracellular UTP and ATP in perfused rat liver. *Eur. J. Pharmacol.*, **167**, 65–71.

O'CONNOR, S.E., DAINTY, I.A. & LEFF, P. (1991). Further subclassifications of ATP receptors based on agonist studies. *Trends Pharmacol. Sci.*, **12**, 137–141.

PFEILSCHIFTER, J. (1990). Comparison of extracellular ATP and UTP signalling in rat renal mesangial cells. *Biochem. J.*, **272**, 469–472.

SAIAG, B., MILON, D., ALLAIN, H., RAULT, B. & VAN DEN DRIESSCHE, J. (1990). Constriction of smooth muscle of rat tail and femoral arteries and dog saphenous vein is induced by uridine triphosphate via 'Pyrimidinoceptors', and by adenosine triphosphate via P2x purinoceptors. *Blood Vessels*, **27**, 352–364.

SEIFERT, R. & SCHULTZ, G. (1989). Involvement of pyrimidinoceptors in the regulation of cell functions by uridine and by uracil nucleotides. *Trends Pharmacol. Sci.*, **10**, 365–369.

VON KUGELGEN, I., HAUSSINGER, D. & STARK, K. (1987). Evidence for a vasoconstriction-mediating receptor for UTP, distinct from the P_2-purinoceptor, in rabbit ear artery. *Naunyn-Schmied. Arch. Pharmacol.*, **336**, 556–560.

(Received March 15, 1994
Accepted March 24, 1994)

Br. J. Pharmacol. (1994), **112**, 360–368

Interdependence of contractile responses of rat small mesenteric arteries on nitric oxide and cyclo-oxygenase and lipoxygenase products of arachidonic acid

X.C. Wu, E. Johns, *J. Michael & [1]*N.T. Richards

Department of Physiology, University of Birmingham, Edgbaston, Birmingham B15 2TT and *Department of Nephrology, Queen Elizabeth Hospital, Edgbaston, Birmingham B15 2TH

1 We have examined the effects of nitric oxide inhibition, indomethacin and the dual lipoxygenase/cyclo-oxygenase inhibitor, 3-amino-1-[*m*-(trifluoromethyl)-phenyl]-2-pyrazoline (BW755C), on the responses of small mesenteric arteries of Wistar rats, with and without endothelium, to noradrenaline, potassium chloride, endothelin-1, acetylcholine and sodium nitroprusside.

2 Noradrenaline, potassium chloride and endothelin-1 caused concentration-dependent contraction of small mesenteric arteries. Indomethacin (14 μM) attenuated the contractile response to both noradrenaline and potassium chloride. The inhibitory action of indomethacin persisted in vessels treated with CHAPS.

3 Acetylcholine produced concentration-dependent relaxation in these vessels. Indomethacin (14 μM) had no significant effect on the acetylcholine concentration-response relationship.

4 N^G-nitro-L-arginine methyl ester (L-NAME, 100 μM) potentiated the contractile response to both noradrenaline and potassium chloride and inhibited acetylcholine-induced relaxation. Indomethacin attenuated the effects of L-NAME.

5 BW755C inhibited the contractile response to noradrenaline and potassium chloride but not to endothelin-1. The inhibitory effects of BW755C persisted in the presence of indomethacin and in vessels treated with CHAPS.

6 BW755C enhanced endothelium-dependent relaxation, as assessed by the response to acetylcholine. In the presence of indomethacin, BW755C produced a shift to the right of the concentration-response curve to acetylcholine.

7 Inhibition of nitric oxide synthase with L-NAME, reversed the inhibitory effect of BW755C on noradrenaline- and potassium-induced contraction. L-NAME and BW755C in combination resulted in a shift to the right of the concentration-response curve to acetylcholine.

8 Sodium nitroprusside produced concentration-dependent relaxation of the vessels. Endothelium removal reduced the maximum relaxation to nitroprusside. BW755C did not alter the response to sodium nitroprusside in vessels with or without endothelium.

9 These data support the existence of two vasoconstrictor products of arachidonic acid released during contraction of small mesenteric arteries with noradrenaline and potassium chloride: a cyclo-oxygenase product and a lipoxygenase product both of which appear to be largely endothelium-independent.

Keywords: Mesenteric arteries; cyclo-oxygenase; lipoxygenase; nitric oxide; BW755C

Introduction

Endothelium-derived relaxing factors play a central role in the control of vascular smooth muscle tone and therefore vascular resistance (Baylis *et al.*, 1990; Moncada *et al.*, 1991). Endothelium-dependent contracting factors have also been described in a number of different vascular beds including the aorta (Lüscher & Vanhoutte, 1986; Diederich *et al.*, 1990; Dohi *et al.*, 1990; Kato *et al.*, 1990) and renal arcuate arteries of spontaneously hypertensive rats (SHR) (Fu-Xiang *et al.*, 1992). Similar factors have also been described in Wistar-Kyoto (WKY) rats, (Diederich *et al.*, 1989; Koga *et al.*, 1989; Kato *et al.*, 1990) although not consistently. Koga *et al.* (1989) have shown that in the WKY aorta, endothelium-dependent vasoconstrictor prostanoids develop with age. Noradrenaline is known to release both endothelium-dependent relaxing and contracting factors from rat arteries (Nigro *et al.*, 1990). The contracting factors described are cyclo-oxygenase-dependent (Diederich *et al.*, 1990; Lüscher *et al.*, 1990) but the compounds responsible vary, depending upon the species and vascular bed studied. In the aorta of both WKY and SHR the contracting factor appears to be either prostaglandin H_2 (Kato *et al.*, 1990; Fu-Xiang *et al.*, 1992) or thromboxane A_2 (Lin & Nasjletti, 1991); however, in mesenteric resistance vessels from SHR, Jameson *et al.* (1993) have proposed that cyclo-oxygenase-generated superoxide anions are responsible.

Kanner *et al.* (1992) have demonstrated that nitric oxide inhibits lipid oxidation by both lipoxygenase and cyclo-oxygenase, raising the possibility of an inter-relationship between the endothelium-derived nitric oxide vasodilator system and endothelium-derived vasoconstrictor prostanoids.

Arachidonic acid may be metabolised by at least three different enzyme systems, namely, cyclo-oxygenase, lipoxygenases (5-, 12- and 15-) and a cytochrome P450-dependent mono-oxygenase. Products of the cytochrome P450-dependent mono-oxygenase may be further transformed by cyclo-oxygenase (Carroll *et al.*, 1992). A physiological role has yet to be defined for many of the resulting compounds although interest has focused on a possible role for lipoxygenase and cytochrome P450 dependent mono-oxygenase products in the control of vascular tone, the development of hypertension (McGiff *et al.*, 1991) and in compensatory renal hypertrophy (Takahashi *et al.*, 1993).

Lipoxygenase activity (5-, 12-, 15-) has been demonstrated

[1] Author for correspondence.

within the endothelium and vascular smooth muscle from a variety of vascular beds in all species studied (Larrue *et al.*, 1983; Farber *et al.*, 1985; Revtyak *et al.*, 1988; Shannon *et al.*, 1991). The main vasoactive products of the 5-lipoxygenase enzyme are leukotriene C_4 and leukotriene D_4. A number of workers have shown that these two leukotrienes constrict mesenteric arteries from rats and dogs (Feigen, 1983; Chapnick, 1984; Eimerl *et al.*, 1986) although this is not a universal finding (Stanton & Coupar, 1986).

Hydroxyeicosatetraenoic (HETE) acids, (products of the lipoxygenase system) are also potent vasoactive compounds with a variety of actions. 12-HETE, a product of the 12-lipoxygenase pathway, is a directly acting vasoconstrictor (Ma *et al.*, 1991), and contributes to the effector mechanisms of angiotensin II-induced vasoconstriction and modulates the intracellular calcium response to arginine vasopressin, angiotensin II and endothelin (Saito *et al.*, 1992). 15-HETE is the major lipoxygenase product of cultured endothelial cells (Larrue *et al.*, 1983) and of the atherosclerotic vessel wall (Henriksson *et al.*, 1985). It is also a directly acting vasoconstrictor in a number of vascular beds of the dog and under certain circumstances may act as an endothelium-independent vasodilator (Van Diest *et al.*, 1990).

Metabolism of arachidonic acid via the lipoxygenase rather than cyclo-oxygenase pathway may lead to the production of reactive oxygen species (Hänsch, 1990) which may accelerate the destruction of nitric oxide and thus in the presence of nitric oxide, will act as a vasoconstrictor. This raises the possibility of a further link between the lipoxygenase and nitric oxide pathways.

Lipoxygenase products of arachidonic acid metabolism are potent vasoactive compounds with a variety of actions in different vascular beds. There are very few data on their effects in resistance sized arteries despite their postulated roles in the development of hypertension. In this study we have used the nitric oxide synthase inhibitor, N^G-nitro-L-arginine-methyl ester (L-NAME), indomethacin and the combined lipoxygenase/cyclo-oxygenase blocker, 3-amino-1-[*m*-(trifluoromethyl)phenyl]-2-pyrazoline (BW755C) (Higgs *et al.*, 1979) to examine the relative roles of cyclo-oxygenase and lipoxygenase products of arachidonic acid and their relationship to nitric oxide in the contractile properties of rat small mesenteric arteries.

Methods

Preparation of blood vessels

Small mesenteric arteries (mean internal diameter of 165 ± 8 μm, $n = 102$) were isolated from male Wistar rats (age 3–4 months, weight range 250–400 g, killed by CO_2 asphyxia or pentobarbitone injection). The proximal jejunum was removed into iced buffer and third branch mesenteric arteries were identified and dissected free of surrounding connective tissue. The vessels were mounted on 40 μm tungsten wires in a small vessel myograph (Cambustion, Cambridge, UK) capable of measuring isometric tension. The arteries were bathed in a physiological salt solution (PSS) containing (mM): NaCl 119, KCl 4.7, $CaCl_2$ 2.5, $MgSO_4$ 1.17, $NaHCO_3$ 25, KH_2PO_4 1.18, EDTA 0.026, glucose 5.5, pH 7.4, at 37°C, bubbled with 5% CO_2 in O_2. Maximal potassium activation was achieved by KPSS (PSS with equimolar substitution of KCl for NaCl resulting in final K^+ concentration 125 mM).

After equilibration for 1 h in PSS the passive tension/internal circumference characteristics were determined (Mulvany & Halpern, 1977). The vessels were then set to an internal circumference equivalent to 90% of that they would have had when relaxed *in situ* under a transmural pressure of 100 mmHg. The maximum active tension is developed at approximately this circumference (Mulvany & Halpern, 1977). The arteries were then maximally contracted for 2 min every 10 min on five occasions, the first two contractions being with KPSS and 5 μM noradrenaline followed by noradrenaline 5 μM, KPSS alone and finally noradrenaline 5 μM with KPSS. Any vessel that failed to develop a maximum tension equivalent to a pressure of 100 mmHg was excluded. In a series of vessels, the endothelium was removed, before mounting, by perfusion with 0.3% 3-[(3-cholamidopropyl)-dimethylammonio]-1-propanesulfonate (CHAPS) for 3 min. The absence of functioning endothelium was confirmed by the loss of relaxation to acetylcholine.

Experiment protocol

Cumulative concentration-response curves were constructed to acetylcholine 0.01–100 μM for vessels with endothelium, pre-contracted with 5 μM noradrenaline. The vessels were then washed for 10 min in PSS and cumulative concentration-response curves were constructed to noradrenaline 0.01–10 μM. The vessels were washed again for 10 min in PSS, and cumulative concentration-response curves were constructed to potassium chloride 12–125 mM. Following this, the vessels were further washed for 10 min in PSS and then incubated in a number of different agents: indomethacin 14 μM; L-NAME 100 μM; indomethacin 14 μM and L-NAME 100 μM; BW755C 50 μM or 180 μM; BW755C 50 μM and indomethacin 14 μM; BW755C 50 μM and L-NAME 100 μM. Concentration-response curves were then repeated to acetylcholine, noradrenaline and potassium chloride in the presence of the above combinations of BW755C, indomethacin and L-NAME. The above protocol was repeated in a series of vessels pretreated with CHAPS. Time controls were obtained for the response to noradrenaline, potassium chloride and acetylcholine, by repetition of the above protocol in the absence of any other agent.

In further sets of vessels, concentration-response curves were constructed to endothelin-1 0.1 nM–1 μM alone or in the presence of BW755C 50 μM and sodium nitroprusside 0.1 nM–10 μM, in vessels precontracted with 5 μM noradrenaline, with or without pretreatment with CHAPS, prior to and following incubation with BW755C 50 μM.

Drugs

The following were used: acetylcholine, indomethacin, L-NAME, CHAPS, endothelin-1, (Sigma, Poole, Dorset), sodium nitroprusside (Central Laboratories, Dublin, Ireland), noradrenaline (Winthrop Laboratories, Guildford, Surrey), BW755C (Welcome Laboratories, Beckenham, Kent). All other reagents were obtained from BDH (Poole, Dorset). All reagents were of Analar grade and solutions were prepared fresh daily.

Statistically analysis

A Hill plot was constructed for each concentration-response relationship. The – log concentration of the drug required to produce 50% of the maximum response (pEC_{50} M) was calculated with a computerised curve fitting software package (Graphpad Inplot version 3.14). Where curve fitting was not appropriate the maximum responses were compared. In the figures, concentrations are given as negative logarithms in molar units. Tension was expressed as mN mm^{-1} artery length. Relaxation to acetylcholine and sodium nitroprusside was expressed as a percentage of the initial pre-contraction to noradrenaline. All values are given as mean ± s.e.mean. Differences between means were assessed with Student's *t* test for paired or unpaired data as appropriate. $P < 0.05$ was taken as statistically significant.

Results

Noradrenaline, potassium chloride and endothelin-1 produced concentration-dependent contraction and acetylcholine

and sodium nitroprusside concentration-dependent relaxation of the vessels. Repetition of the concentration-response curves, as timed controls, did not significantly alter the response to either noradrenaline (pEC_{50} 5.89 ± 0.02 and 5.90 ± 0.01; maximum response 2.57 ± 0.29 mN mm^{-1} and 2.61 ± 0.32 mN mm^{-1}) or potassium chloride (pEC_{50} 1.26 ± 0.02 and 1.23 ± 0.02; maximum response 2.08 ± 0.39 mN mm^{-1} and 1.83 ± 0.35). However repetition of the acetylcholine concentration-response curve led to a shift to the right of the curve (pEC_{50} 6.95 ± 0.02 and 6.52 ± 0.03, $P<0.01$), but no reduction in the maximum relaxation seen (96.5 ± 1.2% and 93.3 ± 2.4%).

Indomethacin

Indomethacin attenuated the maximum contractile response to noradrenaline (3.17 ± 0.22 mN mm^{-1} versus 2.37 ± 0.21 mN mm^{-1} with indomethacin, $P<0.05$) and caused a shift to the right of the concentration-response curve (pEC_{50} 5.88 ± 0.08 versus 5.61 ± 0.09 with indomethacin, $P<0.05$) (Figure 1). Indomethacin reduced the maximum contractile response of the arteries to potassium chloride (3.27 ± 0.26 mN mm^{-1} versus 2.58 ± 0.30 mN mm^{-1} with indomethacin, $P<0.001$) without a shift of the concentration-response curve (Figure 1). Indomethacin did not affect the acetylcholine response of mesenteric arteries (Figure 1).

L-NAME

Inhibition of nitric oxide synthase with L-NAME produced a shift to the left of the concentration-response curves to noradrenaline (pEC_{50} 5.75 ± 0.08 versus 6.24 ± 0.06 with L-NAME, $P<0.001$) and to potassium chloride (pEC_{50} 1.10 ± 0.01 versus 1.43 ± 0.03 with L-NAME, $P<0.01$) and an increase in the maximum contractile response to potassium chloride (3.99 ± 0.57 mN mm^{-1} versus 5.56 ± 0.69 mN mm^{-1} with L-NAME, $P<0.05$) (Figure 2). Acetylcholine induced relaxation was virtually abolished by L-NAME (maximum

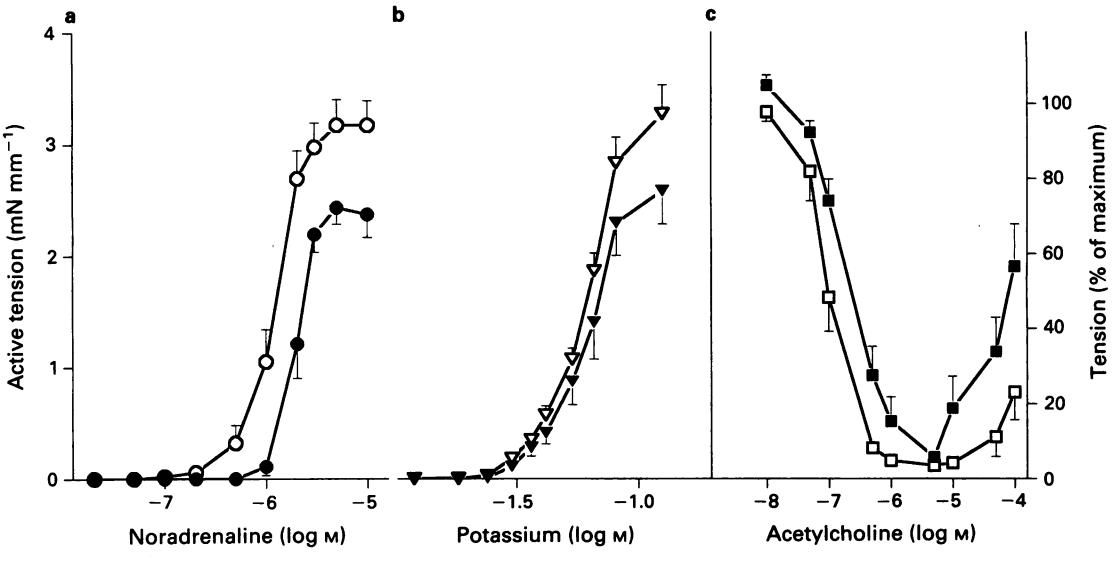

Figure 1 The effect of indomethacin, 14 μM on the concentration-response relationship of small mesenteric arteries to noradrenaline (a), potassium chloride (b) and acetylcholine (c). Indomethacin indicated by (●) in (a); (▼) in (b) and (■) in (c); open symbols indicate control values. In (a) and (b) $n = 8$ and diameter = 167 ± 9 μm; in (c) $n = 9$ and diameter = 185 ± 9 μm.

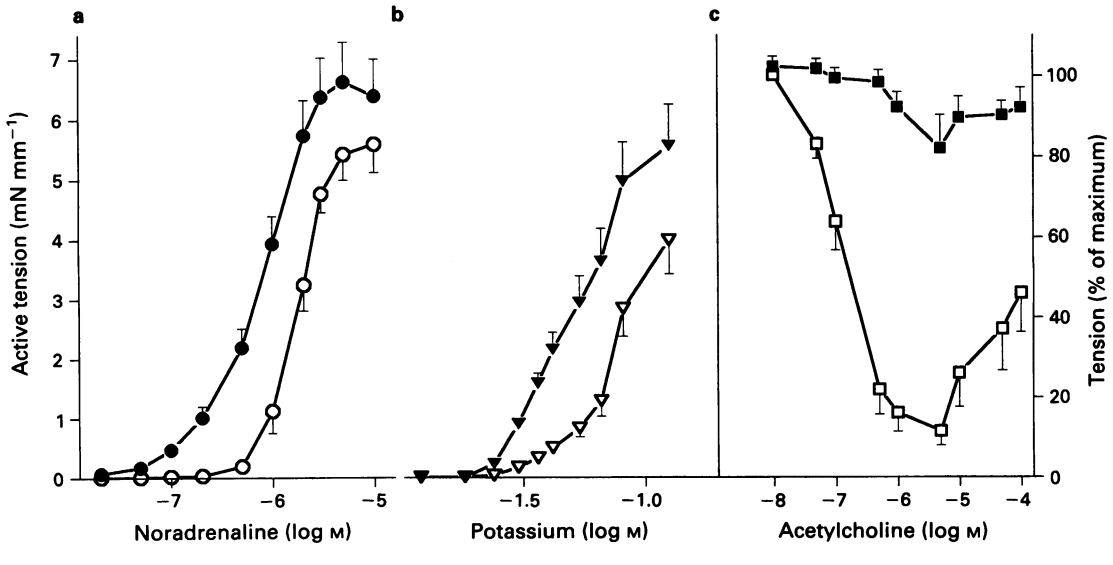

Figure 2 The effect of N^G-nitro-L-arginine methyl ester (L-NAME, 100 μM), on the concentration-response relationship of small mesenteric arteries to noradrenaline (a), potassium chloride (b) and acetylcholine (c). L-NAME indicated by (●) in (a), (▼) in (b) and (■) in (c); open symbols show control values. In (a) and (b), $n = 8$ and diameter = 168 ± 9 μm; in (c) $n = 10$ and diameter = 160 ± 10 μm.

relaxation 98.5 ± 3.6 versus 17.9 ± 8.2% with L-NAME, $P<0.001$) (Figure 2).

Indomethacin and L-NAME

Indomethacin attenuated the shift to the left of the concentration-response curve and increase in the maximum response to both noradrenaline, $P<0.02$, and potassium, $P<0.01$, seen with L-NAME alone (Figure 3). Whilst L-NAME alone virtually abolished acetylcholine-induced relaxation (Figure 2), in the presence of the combination of indomethacin and L-NAME, although there was a reduction in the maximum relaxation seen (91.3% versus 58.2 ± 13.3% with indomethacin and L-NAME, $P<0.05$), there was no shift to the right of the concentration-response curve and the maximum relaxation obtained was greater than that seen with L-NAME alone, $P<0.01$, (Figure 3).

BW755C

BW755C decreased the maximum constrictor response of the mesenteric arteries to potassium in a concentration-dependent manner (3.33 ± 0.22 mN mm^{-1} versus 2.24 ± 0.18 mN mm^{-1} with BW755C 50 μM, $P<0.001$; 3.22 ± 0.48 mN mm^{-1} versus 1.72 ± 0.38 mN mm^{-1} with BW755C 180 μM, $P<0.001$). Reductions in the maximum constrictor response to noradrenaline did not reach statistical significance (Figure 4). There was a shift to the right of the concentration-response curves to noradrenaline (pEC_{50} 6.06 ± 0.06 versus 5.78 ± 0.06 with BW755C 50 μM, $P<0.01$; 5.93 ± 0.01 versus 5.68 ± 0.01 with BW755C 180 μM, $P<0.001$) and to potassium chloride (pEC_{50} 1.22 ± 0.01 versus 1.18 ± 0.01 with BW755C 50 μM, $P<0.01$; 1.20 ± 0.01 versus 1.19 ± 0.01 with BW755C 180 μM). BW755C did not alter either the pEC_{50} (6.82 ± 0.07 versus 6.82 ± 0.06 with BW755C 50 μM) or max-

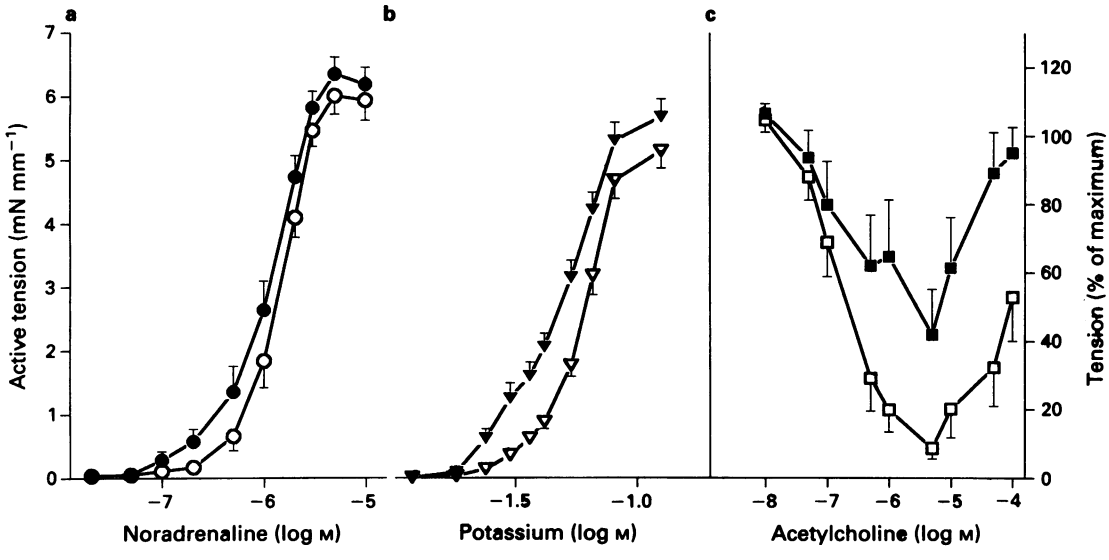

Figure 3 The effect of N^G-nitro-L-arginine methyl ester (L-NAME, 100 μM), on the concentration-response relationship of small mesenteric arteries to noradrenaline (a), potassium chloride (b) and acetylcholine (c) in the presence of indomethacin (14 μM). Indomethacin plus L-NAME indicated by (●) in (a), (▼) in (b) and (■) in (c); open symbols show control values. In (a) and (b) $n = 8$, diameter = 182 ± 9 μm; in (c) $n = 8$ and diameter = 173 ± 12 μm.

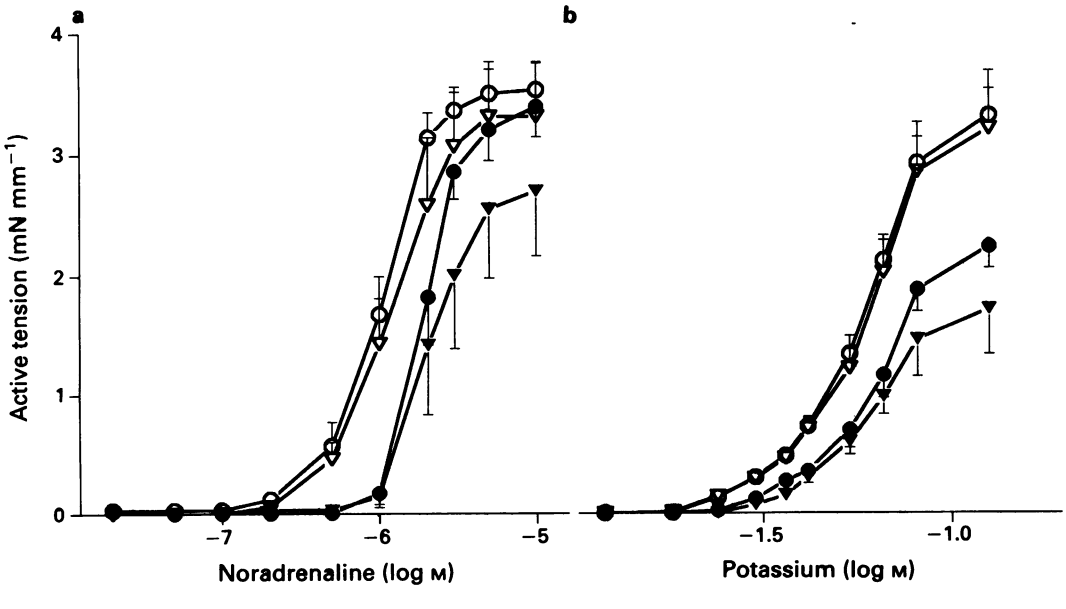

Figure 4 The effect of BW755C on the concentration-response relationship of rat small mesenteric arteries to noradrenaline (a) and potassium chloride (b). (○) Control; (●) BW755C 50 μM; diameter = 162 ± 8 μm, $n = 7$. (▽) Control; (▼) BW755C 180 μM; diameter = 164 ± 8 μm, $n = 6$.

imum response (95.6 ± 1.3% versus 96.4 ± 0.6% with BW-755C 50 μM) to acetylcholine relative to its paired control (Figure 5). However, repetition of the acetylcholine concentration-response curve led to a shift to the right of the curve (pEC_{50} 6.95 ± 0.02 curve 1 versus 6.52 ± 0.03 curve, $P<0.05$) (Figure 5). When the acetylcholine response, in the presence of BW755C, was compared to its time control it was apparent that BW755C caused a significant shift to the left of the concentration-response curve to acetylcholine, $P<0.01$ (Figure 5). BW755C did not alter either the pEC_{50} (8.12 ± 0.39 versus 8.09 ± 0.21 with BW755C 50 μM) or the maximum response (3.05 ± 0.64 mN mm^{-1} versus 3.42 ± 0.26 mN mm^{-1} with BW755C 50 μM) to endothelin-1.

BW755C and indomethacin

In the presence of indomethacin, BW755C still depressed the maximum response to potassium (4.04 ± 0.78 mN mm^{-1} versus 3.20 ± 0.58 mN mm^{-1} with BW755C and indomethacin, $P<0.01$). The pEC_{50} for potassium remained unchanged. There was a small, although statistically significant, shift to the right of the concentration-response curve to noradrenaline (pEC_{50} 5.69 ± 0.03 versus 5.61 ± 0.02 with BW755C and indomethacin, $P<0.05$). The fall in the maximum response to noradrenaline was not statistically significant (4.07 ± 0.67 mN mm^{-1} versus 3.71 ± 0.67 mN mm^{-1} with BW755C and indomethacin). In the presence of indomethacin, BW755C induced a shift to the right of the concentration-response curve to acetylcholine of the order of that seen in the appropriate timed control (pEC_{50} 7.14 ± 0.01 versus 6.60 ± 0.09 with BW755C and indomethacin, $P<0.01$) the maximum relaxation remained unchanged (97.8 ± 0.5% versus 96.1 ± 1.0% with BW755C and indomethacin) (Figure 5).

BW755C and L-NAME

Inhibition of nitric oxide synthase with L-NAME in the presence of BW755C abolished the shift to the right of the concentration-response curves to noradrenaline and potas-

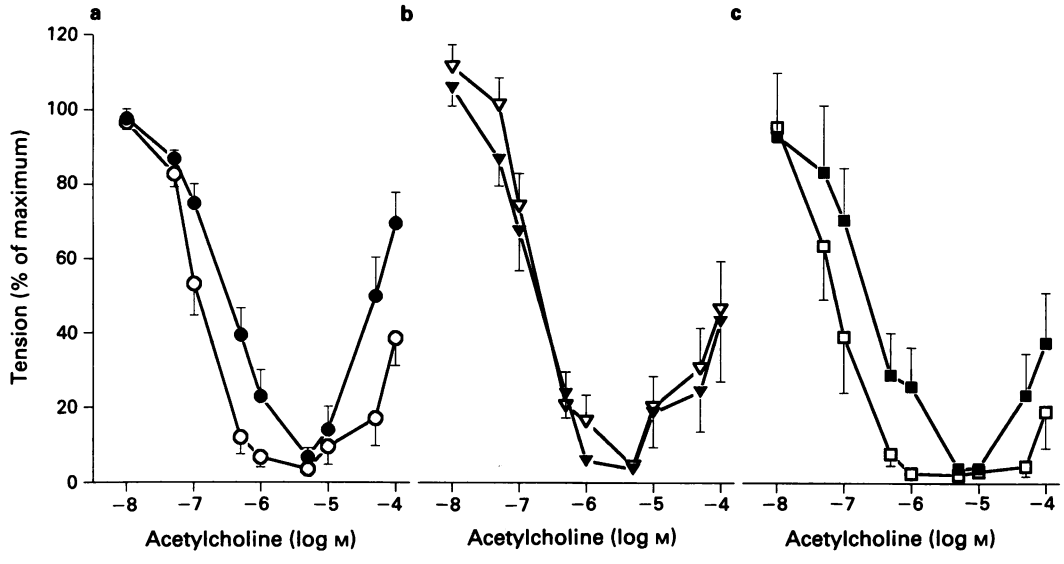

Figure 5 Acetylcholine concentration-response relationships of rat small mesenteric arteries (a) following repetition, (b) with BW755C and (c) with indomethacin 14 μM and BW755C. The vessels were pre-constricted with noradrenaline. In (a) (○) control 1; (●) control 2, $n = 9$, diameter = 162 ± 9 μm; in (b) (▽) control; (▼) BW755C 50 μM, $n = 9$, diameter = 187 ± 12 μm; in (c) (□) indomethacin; (■) indomethacin plus BW755C, $n = 8$, diameter = 166 ± 4 μm.

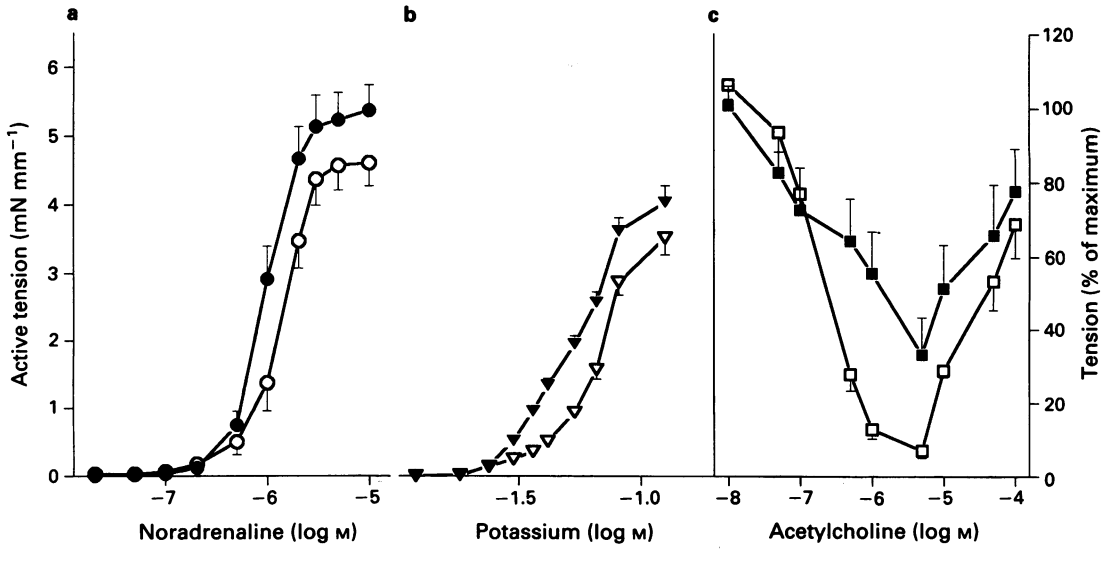

Figure 6 The effect BW755C on the concentration-response relationship of rat small mesenteric arteries to noradrenaline (a), potassium chloride (b) and acetylcholine (c) in the presence of N^G-nitro-L-arginine methyl ester (L-NAME, 100 μM). In (a) (○) control, (●) L-NAME plus BW755C 50 μM, $n = 8$, diameter = 144 ± 5 μm; (b) (▽) control, (▼) L-NAME plus BW755C 50 μM, $n = 8$, diameter = 144 ± 5 μm; in (c) (□) control; (■) L-NAME + BW755C 50 μM, $n = 10$, diameter = 159 ± 10 μm.

sium seen with BW755C alone (Figure 4), and resulted in an increase in the maximum response to noradrenaline (4.61 ± 0.34 versus 5.37 ± 0.37 with BW755C and L-NAME, $P<0.01$) and shift to the left of the concentration-response curve to potassium (pEC_{50} 1.17 ± 0.01 versus 1.27 ± 0.02 with BW755C and L-NAME, $P<0.01$) (Figure 6). For both noradrenaline and potassium there was a shift to the left of the concentration-response curves and increase in the maximum response with the combination of L-NAME and BW755C relative to BW755C alone, $P<0.02$ and $P<0.001$, respectively. The combination of L-NAME and BW755C produced a shift to the right of the concentration-response curve to acetylcholine (pEC_{50} 6.72 ± 0.03 versus 6.44 ± 0.10 with BW755C and L-NAME, $P<0.01$) and reduced the maximum relaxation seen (93.1 ± 1.9% versus 66.8 ± 10.1% with BW755C and L-NAME, $P<0.05$) (Figure 6).

CHAPS

Endothelial removal with CHAPS largely abolished acetylcholine-induced relaxation (maximum relaxation 96.5 ± 1.2% versus 4.3 ± 3.1% following CHAPS, $P<0.001$) and resulted in a shift to the left of the concentration-response curves and increase in the maximum contractile response to both noradrenaline (pEC_{50} 5.89 ± 0.02 versus 5.96 ± 0.08 following CHAPS, $P<0.05$; maximum response 2.57 ± 0.29 mN mm^{-1} versus 4.41 ± 0.48 mN mm^{-1} following CHAPS, $P<0.01$) and potassium chloride (pEC_{50} 1.26 ± 0.02 versus 1.21 ± 0.01 following CHAPS, $P<0.05$; maximum response 2.08 ± 0.39 mN mm^{-1} versus 3.88 ± 0.47 mN mm^{-1} following CHAPS, $P<0.02$).

CHAPS and indomethacin

In arteries pretreated with CHAPS, indomethacin caused a shift to the right of the concentration-response curve to noradrenaline (pEC_{50} 5.96 ± 0.08 versus 5.75 ± 0.06 with indomethacin, $P<0.05$) and potassium (pEC_{50} 1.21 ± 0.01 versus 1.07 ± 0.05 with indomethacin, $P<0.01$) and reduced the maximum contractile response to potassium (3.88 ± 0.47 mN mm^{-1} versus 3.51 ± 0.45 mN mm^{-1}, $P<0.01$) but not noradrenaline (4.41 ± 0.48 mN mm^{-1} versus 4.22 ± 0.41 mN mm^{-1} with indomethacin) (Figure 7). Maximum relaxation to acetylcholine increased in the presence of indomethacin (4.3 ± 3.1% versus 10.7 ± 2.6% with indomethacin, $P<0.05$).

CHAPS and BW755C

In arteries pretreated with CHAPS, BW755C still caused a shift to the right of the concentration-response curves to noradrenaline (pEC_{50} 6.42 ± 0.08 versus 5.75 ± 0.02 with BW755C, $P<0.001$) and potassium chloride (pEC_{50} 1.34 ± 0.02 versus 1.24 ± 0.03 with BW755C, $P<0.01$) and reduced the maximum contractile response to potassium (2.70 ± 0.39 mN mm^{-1} versus 1.70 ± 0.25 mN mm^{-1} with BW755C, $P<0.01$) (Figure 8). Acetylcholine-induced relaxation was virtually abolished in vessels pretreated with CHAPS, as would be expected. However the addition of BW755C increased the maximum relaxation seen (20.6 ± 3.2% versus 30.2 ± 3.6% with BW755C, $P<0.05$) (Figure 8).

CHAPS and BW755C with indomethacin

In the presence of indomethacin, BW755C produced a small though significant shift to the right of the concentration-response curve to noradrenaline (pEC_{50} 5.87 ± 0.08 versus 5.72 ± 0.03 with BW755C and indomethacin, $P<0.05$) and reduced the maximum response to potassium (4.57 ± 0.52 mN mm^{-1} versus 3.39 ± 0.44 mN mm^{-1} with BW755C and indomethacin, $P<0.001$) (Figure 9). The increased relaxation to acetylcholine seen with BW755C alone, in these vessels, was not seen with the combination of BW755C and indomethacin (19.5 ± 5.6% versus 18.8 ± 3.2% with BW755C and indomethacin) (Figure 9).

Sodium nitroprusside

BW755C did not affect either the maximum response or the pEC_{50} to sodium nitroprusside in vessels with (pEC_{50} 7.58 ± 0.86 versus 6.75 ± 1.24 with BW755C; maximum relaxation 81.9 ± 4.4% versus 93.6 ± 3.5% with BW755C) or without endothelium (pEC_{50} 7.09 ± 0.18 versus 7.21 ± 0.16 with BW755C; maximum relaxation 63.3 ± 1.4% versus 69.8 ± 2.5% with BW755C). However, the maximum relaxation to nitroprusside was reduced in vessels pretreated with CHAPS (81.9 ± 4.4% versus 63.3 ± 1.6% following CHAPS, $P<0.01$).

Discussion

In this study we have demonstrated the presence of vasoactive cyclo-oxygenase and non-cyclo-oxygenase derivatives of

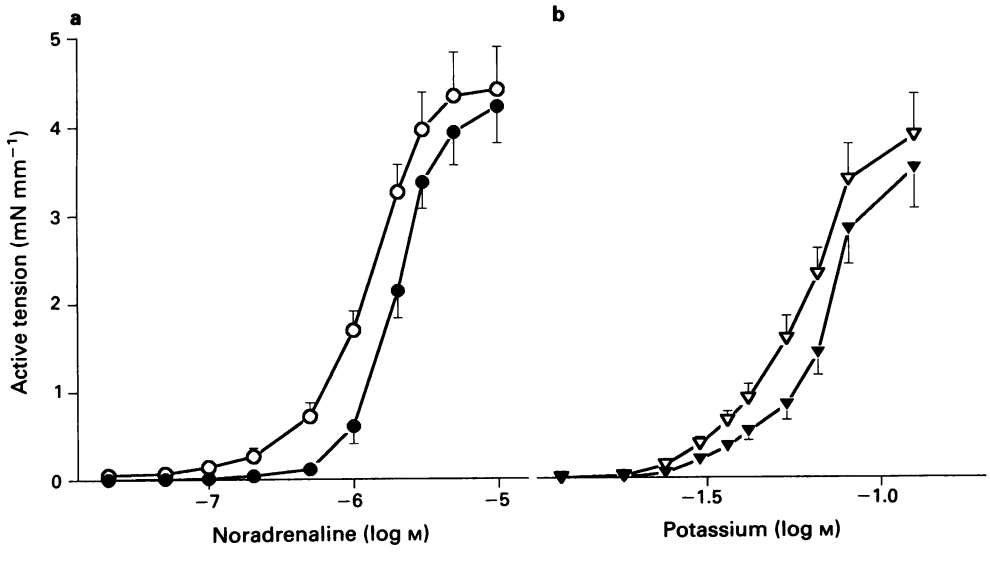

Figure 7 The effect of indomethacin (14 μM), on the concentration-response relationship of small mesenteric arteries, pretreated with CHAPS, to noradrenaline (a) and potassium chloride (b). In (a) indomethacin (●); in (b) indomethacin (▼); control values are shown by open symbols and $n = 7$, diameter = 143 ± 6 μm in both (a) and (b).

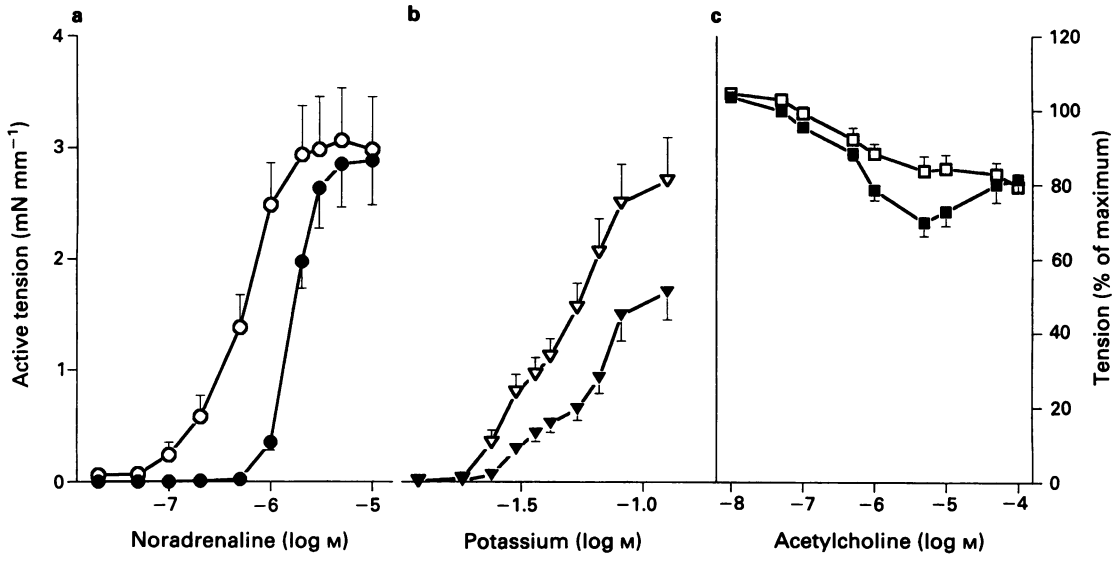

Figure 8 The effect of BW755C on the concentration-response relationship of rat small mesenteric arteries, pretreated with CHAPS, to noradrenaline (a), potassium chloride (b) and acetylcholine (c). BW755C 50 μM shown by (●) in (a); (▼) in (b) and (■) in (c); open symbols show control values. In (a) and (b), $n = 7$ and diameter = 168 ± 9 μm; in (c) $n = 9$ and diameter = 187 ± 12 μm.

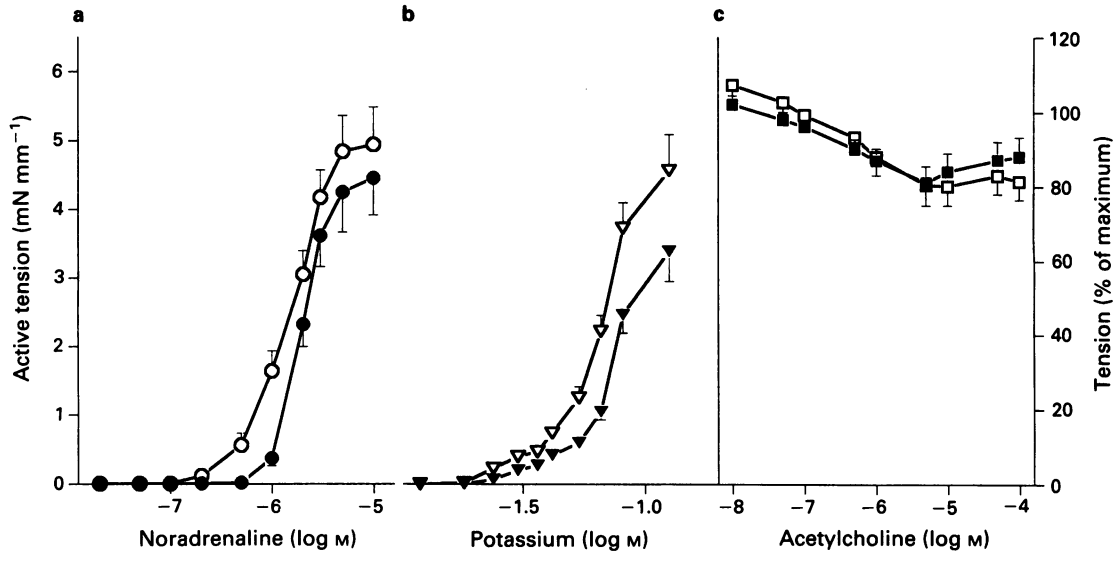

Figure 9 The effect of BW755C on the concentration-response relationship of rat small mesenteric arteries, pretreated with CHAPS, in the presence of indomethacin, to noradrenaline (a), potassium chloride (b) and acetylcholine (c). In (a) indomethacin shown by (○); indomethacin plus BW755C (50 μM) shown by (●). In (b) indomethacin (▽); indomethacin plus BW755C (50 μM) (▼). In (c) indomethacin (□); indomethacin plus BW755C (50 μM) (■). In (a) and (b), $n = 8$ and diameter = 168 ± 9 μm; in (c) $n = 8$ and diameter = 166 ± 4 μm.

arachidonic acid in small mesenteric arteries of the rat. These data also support the possibility of an interrelationship between arachidonic acid products and nitric oxide.

Indomethacin attenuated the contractile responses of small mesenteric arteries to noradrenaline and potassium chloride. Endothelium-dependent relaxation, as assessed by the response to acetylcholine, was not affected. These data support the presence of a cyclo-oxygenase-derived vasoconstrictor released by both noradrenaline and potassium chloride in these vessels. Similar vasoconstrictors have been previously described in renal arcuate, but not in small mesenteric arteries in WKY rats (Kato *et al.*, 1990). The inhibitory effect of indomethacin persisted in the absence of a functioning endothelium suggesting that the vasoconstrictor cyclo-oxygenase product responsible, originates within the vascular smooth muscle rather than the endothelium. However, despite pretreatment of the vessels with CHAPS, acetylcholine-induced relaxation was not completely abolished; thus, it is not possible totally to exclude the endothelium as the source of the vasoconstrictor.

Inhibition of nitric oxide synthase, with L-NAME, potentiated the contractile response to noradrenaline and potassium and inhibited endothelium-dependent relaxation of mesenteric arteries. The change in noradrenaline and potassium sensitivity probably result from a combination of a decrease in both basal and agonist-stimulated nitric oxide release. A number of vasoconstrictors, including noradrenaline, have been shown to stimulate nitric oxide release (Peach *et al.*, 1985). Repeated exposure of the mesenteric vessels to acetylcholine led to a loss of sensitivity. This is in keeping with the findings of Furchgott *et al.* (1990) and suggests that there are two stores of nitric oxide. The first is limited and readily

available, released immediately on exposure to an endothelium-dependent agonist such as acetylcholine but becomes exhausted. The exposure to the agonist then initiates synthesis of nitric oxide from L-arginine.

Kanner *et al.* (1992) suggested that nitric oxide may inhibit arachidonic acid metabolism via both cyclo-oxygenase and lipoxygenase pathways modulating the arachidonic acid cascade and the generation of reactive oxygen species. In these arteries the action of the combination of indomethacin and L-NAME, on noradrenaline and potassium chloride-induced contraction, could be explained by the sum of their individual actions, i.e. the negative effects of indomethacin and positive effects of L-NAME. L-NAME alone virtually completely inhibited acetylcholine-induced relaxation; however, in the presence of indomethacin and L-NAME, appreciable relaxation occurred. This may be explained by the combination of inhibition of the cyclo-oxygenase-derived vasoconstrictor, released by both noradrenaline and acetylcholine and incomplete inhibition of nitric oxide synthase by L-NAME. Alternatively, it is known that acetylcholine can release another endothelium-derived relaxing factor (Raij *et al.*, 1988). This substance, endothelium-derived hyperpolarizing factor, relaxes vascular smooth muscle through hyperpolarization as a result of opening of potassium channels (Van de Voorde *et al.*, 1992). Rees *et al.* (1990) demonstrated that L-NAME (100 μM) completely inhibited acetylcholine-induced relaxation in rat aorta; however, indomethacin was not used. Bennett *et al.* (1992) examined the effect of L-NAME and N^G-nitro-L-arginine (L-NOARG) on small rat mesenteric arteries. They demonstrated that the potency of the two inhibitors was time-dependent and that cyclo-oxygenase inhibition with indomethacin, potentiated acetylcholine-induced relaxation in the presence of both L-NAME and L-NOARG.

BW755C predominantly inhibits 5- and 12-lipoxygenase in addition to cyclo-oxygenase, having little activity against 15-lipoxygenase (Higgs *et al.*, 1979; Salmon *et al.*, 1983). BW-755C, attenuated the contractile responses of the small mesenteric arteries to noradrenaline and potassium chloride and enhanced acetylcholine-induced relaxation (endothelium-dependent). The effect of BW755C on the response to noradrenaline and potassium was additional to that of the cyclo-oxygenase inhibitor, indomethacin. Whilst BW755C alone enhanced acetylcholine-induced relaxation, in the presence of indomethacin this effect was lost. The effect of BW755C on constrictor responses was independent of the presence of an intact endothelium, whereas BW755C still potentiated the residual response to acetylcholine after endothelial removal. In vessels pre-treated with CHAPS, BW755C had an additional effect to that of indomethacin. Thus these data support the presence of two vasoconstrictors, one a lipoxygenase derivative, which contributes to tension development induced by noradrenaline and potassium chloride and the other a cyclo-oxygenase derivative, produced in response to acetylcholine.

A cyclo-oxygenase-derived vasoconstrictor has been described by ourselves (Richards *et al.*, 1990) and others (Lüscher *et al.*, 1990) and is probably prostaglandin H_2 (Kato *et al.*, 1990). The ability of BW755C to modify the contractile responses of rat isolated small mesenteric arteries has not been previously studied, although Stanton & Coupar (1986) using an isolated perfused mesentery preparation of the rat demonstrated that BW755C and meclofenamate depressed vasoconstrictor responses to noradrenaline. They found the combined actions of meclofenamate and BW755C could be partially reversed by addition of prostaglandin E_2, but not by leukotriene C_4 or leukotriene D_4 (products of 5-lipoxygenase) neither of which had any effect on vascular tone in this preparation. Conversely Eimerl *et al.* (1986) and Chapnick (1984) have demonstrated that leukotriene C_4 and leukotriene D_4 are potent vasoconstrictors in the mesenteric vascular bed. These intermediates cannot therefore be discounted from mediating the responses seen in this study. The majority of published work on products of the lipoxygenase pathway has been carried out in conduit arteries or whole vascular beds and the results obtained depend on the species and vascular bed studied (Van Diest *et al.*, 1991). Thomas & Ramwell (1986) and Van Diest *et al.* (1991) have demonstrated that 15-HETE is capable of invoking endothelium-independent relaxation and producing vasoconstriction in canine and rat isolated arteries depending upon the conditions studied.

Whilst it is possible that BW755C is inhibiting the production of a 5- or 12-lipoxygenase-derived vasoconstrictor, another possibility is that inhibition of cyclo-oxygenase and 5- and 12-lipoxygenase leads to increased metabolism of arachidonic acid by either 15-lipoxygenase or cytochrome P450-dependent mono-oxygenase and the interactions seen are related to a vasoactive product of one of these pathways. Enhanced production of a 15-lipoxygenase-derived vasodilator could also explain the enhanced acetylcholine-induced relaxation seen with BW755C, although this may also be the result of inhibition of a vasoconstrictor. If this were so the loss of this action in the presence of indomethacin cannot be readily explained.

Inhibition of nitric oxide synthase with L-NAME reversed the effect of BW755C on noradrenaline- and potassium-induced contraction. This raises the possibility that BW755C may lead to the generation of nitric oxide or inhibit its destruction. A number of workers have suggested that BW-755C inhibits oxygen free radical production from arachidonic acid (Semb & Vaage, 1991; Hänsch, 1990) although Moncada *et al.* (1986), suggested that BW755C promotes superoxide anion production. If BW755C inhibits lipoxygenase-dependent free radical production it would potentiate the action of nitric oxide and thus inhibit contraction and potentiate acetylcholine-induced relaxation and its effect would be attenuated by the absence of nitric oxide. However the action of BW755C was largely independent of the endothelium, arguing against the direct involvement of endothelium-derived nitric oxide. Rees *et al.* (1990) demonstrated that L-NAME (100 μM) completely inhibited acetylcholine-induced relaxation in rat aorta. In our study in the presence of BW755C, L-NAME inhibited acetylcholine-induced relaxation, although the effect was much less than would have been expected, implying that BW755C promotes relaxation by an independent mechanism.

In conclusion we have demonstrated the presence of endothelium-independent cyclo-oxygenase and lipoxygenase-derived vasoconstrictors in small mesenteric arteries of WKY rats. BW755C attenuates noradrenaline and potassium chloride-induced contraction and potentiates endothelium-dependent relaxation of small mesenteric arteries. The effects on contraction were additional to those seen with indomethacin alone, were endothelium-independent and may be inhibited by blockade of nitric oxide synthase. The exact mechanism of action of BW755C in this system has not been elucidated and further work is required to define the roles of the individual lipoxygenase enzymes in the production of vasoactive substances including reactive oxygen species.

We thank Dr L. Poston for her help and advice in preparation of the manuscript. BW755C was a kind gift from Wellcome Research Laboratories, Beckenham, Kent. This work was supported by a grant from the West Midlands Regional Health Authority.

References

BAYLIS, C., HARTON, P. & ENGELS, K. (1990). Endothelial-derived relaxing factor controls renal hemodynamics in the normal rat kidney. *J. Am. Soc. Nephrol.*, **1**, 875–881.

BENNETT, M.A., WATT, P.A.C. & THURSTON, H. (1992). Endothelium-dependent modulation of resistance vessel contraction: studies with N^G-nitro-L-arginine methyl ester and N^G-nitro-L-arginine. *Br. J. Pharmacol.*, **107**, 616–621.

CARROLL, M.A., GARCIA, M.P., FALCK, J.R. & McGIFF, J.C. (1992). Cyclooxygenase dependency of the renovascular actions of cytochrome P450-derived arachidonate metabolites. *J. Pharmacol. Exp. Ther.*, **260**, 104–109.

CHAPNICK, B.M. (1984). Divergent influences of leukotrienes C4, D4 and E4 on mesenteric and renal blood flow. *Am. J. Physiol.*, **246**, H518–H524.

DIEDERICH, D., SKOPEC, J., DIEDERICH, A. & JEMESON, M. (1989). Acetylcholine releases relaxing and contracting factors from renal arcuate arteries of rats. *Kidney Int.*, **37**, 550.

DIEDERICH, D., YANG, Z., BÜHLER, B.R. & LÜSCHER, T.F. (1990). Impaired endothelium-dependent relaxations in hypertensive resistance arteries involve cyclooxygenase pathway. *Am. J. Physiol.*, **258**, H445–H451.

DOHI, Y., THIEL, M.A., BÜHLER, F.R. & LÜSCHER, T.F. (1990). Activation of endothelial L-arginine pathway in resistance arteries. Effect of age and hypertension. *Hypertension*, **15**, 170–179.

EIMERL, J., SIRÉN, A.L. & FEUERSTEIN, G. (1986). Systemic and regional hemodynamic effects of leukotrienes D4 and E4 in the conscious rat. *Am. J. Physiol.*, **251**, H700–H709.

FARBER, H.W., CENTER, D.M. & RIWADSM, S. (1985). Bovine and human endothelial cell production of neutrophil chemoattractant activity in response to components of the angiotensin system. *Circ. Res.*, **57**, 898–902.

FEIGEN, L.P. (1983). Differential effects of leukotrienes C4, D4 and E4 in the canine renal and mesenteric vascular beds. *J. Pharmacol. Exp. Ther.*, **225**, 682–687.

FURCHGOTT, R.F., DESINGARO, J. & FREAY, A.D. (1990). Endothelium-derived relaxing factor: some old and new findings. In *Nitric Oxide from L-arginine: a Bioregulatory System.* ed. Moncada, S. & Higgs, E.A. pp. 5–17. Amsterdam: Elsevier Science.

FU-XIANG, D., SKOPEC, J., DIEDERICH, A. & DIEDERICH, D. (1992). Prostaglandin H2 and thromboxane A2 are contractile factors in intrarenal arteries of spontaneously hypertensive rats. *Hypertension*, **19**, 796–798.

HANSCH, J.G.M. (1990). Oxygen radical generation in human platelets: Dependence on 12-lipoxygenase activity and the glutathione cycle. *Int. Arch. Allergy. Appl. Immunol.*, **93**, 73–79.

HENRIKSSON, P., HAMBERG, M. & DICZFALUSY, U. (1985). Formation of 15-HETE as the major hydroxyeicosatetraenoic acid in the atherosclerotic vessel wall. *Biochem. Biophys. Acta.*, **834**, 272–274.

HIGGS, G.H., FLOWER, R.J. & VANE, J.R. (1979). A new approach to anti-inflammatory drugs. *Biochem. Pharmacol.*, **28**, 1959–1961.

JAMESON, M., FU-XIANG, D., LÜSCHER, T., SKOPEC, J., DIEDERICH, A. & DIEDERICH, D. (1993). Endothelium-derived contracting factors in resistance arteries of young spontaneously hypertensive rats before development of overt hypertension. *Hypertension*, **21**, 280–288.

KANNER, J., HAREL, S. & GRANIT, R. (1992). Nitric oxide, and inhibitor of lipid oxidation by lipoxygenase, cyclooxygenase and haemoglobin. *Lipids*, **27**, 46–49.

KATO, T., IWAMA, Y., OKUMURA, K., HASHIMOTO, H., ITO, T. & SATAKE, T. (1990). Prostaglandin H_2 may be the contracting factor released by acetylcholine in the aorta of the rat. *Hypertension*, **5**, 475–481.

KOGA, T., TAKATA, Y., KOBAYASHI, K., TAKISHITA, S., YAMASHITA, Y. & FUJISHIMA, M. (1989). Age and hypertension promote endothelium-dependent contractions to acetylcholine in the aorta of the rat. *Hypertension*, **14**, 542–548.

LARRUE, J., RIGAUD, M., RAZAKA, G., DARET, D., DEMOND-HENRI, J. & BRICAUD, H. (1983). Formation of monohydroxyeicosatetraenoic acids from arachidonic acid by cultured rabbit aortic smooth muscle cells. *Biochem. Biophys. Res. Commun.*, **112**, 242–249.

LIN, L. & NASJLETTI, A. (1991). Role of endothelium-derived prostanoid in angiotensin-induced vasoconstriction. *Hypertension*, **18**, 158–164.

LÜSCHER, T.F. & VANHOUTTE, P.M. (1986). Endothelium-dependent contractions to acetylcholine in the aorta of spontaneously hypertensive rats. *Hypertension*, **8**, 344–348.

LÜSCHER, T., AARHUS, L.L. & VANHOUTTE, P.M. (1990). Indomethacin improves the impaired endothelium-dependent relaxations in small mesenteric arteries of the spontaneously hypertensive rats. *Am. J. Hypertens.*, **3**, 55–58.

MA, Y.-H., HARDER, D.R., CLARK, J.E. & ROMAN, R.J. (1991). Effects of 12-HETE on isolated dog renal arcuate arteries. *Am. J. Physiol.*, **261**, H451–H456.

McGIFF, J.C., CARROLL, M.A. & ESCALANTE, B. (1991). Arachidonate metabolites and kinins in blood pressure regulation. *Hypertension*, **18** (suppl III), III-150–III-157.

MONCADA, S., PALMER, R.M.J. & GRYGLEWSKI, R.J. (1986). Mechanism of action of some inhibitors of endothelium-derived relaxing factor. *Proc. Natl. Acad. Sci.*, **83**, 9164–9168.

MONCADA, S., PALMER, R.M.J. & HIGGS, E.A. (1991). Nitric oxide: physiology, Pathophysiology and Pharmacology. *Pharmacol. Rev.*, **43**, 109–142.

MULVANY, M.J. & HALPERN, W. (1977). Contractile properties of small arterial resistance vessels in spontaneously hypertensive and normotensive rats. *Circ. Res.*, **41**, 19–26.

NIGRO, D., FORTES, Z.B., SCIVOTETTO, R. & CARVALHO, M.H.C. (1990). Simultaneous release of endothelium derived relaxing and contracting factors induced by noradrenaline in normotensive rats. *Gen. Pharmac.*, **21(4)**, 443–446.

PEACH, M.J., LOEB, A.L., SINGER, H.A. & SAYE, J. (1985). Endothelium-derived relaxing factor. *Hypertension*, suppl I, **7**, I-94–I-100.

RAIJ, L., LÜSCHER, T.F. & VANHOUTTE, P.M. (1988). High potassium diet augments endothelium-dependent relaxations in the Dahl rat. *Hypertension*, **12**, 562–567.

REES, D.D., PALMER, R.M.J., SCHULZ, R., HODSON, H.F. & MONCADA, S. (1990). Characterisation of three inhibitors of endothelial nitric oxide synthase *in vitro* and *in vivo*. *Br. J. Pharmacol.*, **101**, 746–752.

REVTYAK, G.E., HUGHES, M.J., JOHNSON, A.R. & CAMPBELL, W.B. (1988). Histamine stimulation of prostaglandin and HETE synthesis in human endothelial cells. *Am. J. Physiol.*, **255**, C214–C225.

RICHARDS, N.T., POSTON, L. & HILTON, P.J. (1990). Evidence for the release of an indomethacin sensitive vasoconstrictor from renal arcuate arteries. *Nephrol. Dial. Transplant.*, **5**, 641.

SAITO, F., HORI, M.T., IDEGUCHI, Y., BERGER, M., GOLUB, M., STERN, N. & TUCK, M.L. (1992). 12-Lipoxygenase products modulate calcium signals in vascular smooth muscle cells. *Hypertension*, **20**, 138–143.

SALMON, J.A., SIMMONS, P.M. & MONCADA, S. (1983). The effects of BW755C and other anti-inflammatory drugs on eicosanoid concentration and leucocyte accumulation in experimentally-induced acute inflammation. *J. Pharm. Pharmacol.*, **35**, 808–813.

SEMB, A.G. & VAAGE, J. (1991). Oxygen free radical-injury in isolated rat hearts: effects of ibuprofen and BW 755C. *Scand. J. Clin. Lab. Invest.*, **51**, 377–384.

SHANNON, V.R., CROUCH, E.C., TAKAHASHI, Y., UEDA, N., YAMAMOTO, S. & HOLTZMAN, M.J. (1991). Related expression of arachidonate 12- and 15-lipoxygenases in animal and human lung tissue. *Am. J. Physiol.*, **261**, L399–L405.

STANTON, B.J. & COUPAR, I.M. (1986). The effect of BW755C and nordihydroguaiaretic acid in the rat isolated perfused mesenteric vasculature. *Prost. Leu. Med.*, **25**, 199–207.

TAKAHASHI, K., HARRIS, R.C., CAPDEVILA, J.H., KARARA, A., MAKITA, K., JACOBSON, H.R., MUNGER, K.A. & BADR, K.F. (1993). Induction of renal arachidonate cytochrome P-450 epoxygenase after uninephrectomy: Counterregulation of hyperfiltration. *J. Am. Soc. Nephrol.*, **8**, 1496–1500.

THOMAS, G. & RAMWELL, P. (1986). Induction of vascular relaxation by hydroperoxides. *Biochem. Biophys. Res. Commun.*, **139**, 102–108.

VAN DE VOORDE, J., VANHEEL, B. & LEUSEN, I. (1992). Endothelium-dependent relaxation and hyperpolarisation in aorta from control and renal hypertensive rats. *Circ. Res.*, **70**, 1–8.

VAN DIEST, M.J., VERBEUREN, T.J. & HERMAN, A.G. (1991). 15-lipoxygenase metabolites of arachidonic acid evoke contractions and relaxations in isolated canine arteries: Role of thromboxane receptors, endothelial cells and cyclooxygenase. *J. Pharm. Exp. Ther.*, **256**, 194–203.

(Received October 6, 1993
Revised December 20, 1993
Accepted January 17, 1994)

Br. J. Pharmacol. (1994), **112**, 369–376

Relative roles of nitric oxide and cyclo-oxygenase and lipoxygenase products of arachidonic acid in the contractile responses of rat renal arcuate arteries

X.C. Wu, [1,*]N.T. Richards, *J. Michael & E. Johns

Department of Physiology, University of Birmingham, Edgbaston, Birmingham B15 2TT and *Department of Nephrology, Queen Elizabeth Hospital, Edgbaston, Birmingham B15 2TH

1 We have examined the effects of inhibition of nitric oxide synthase, cyclo-oxygenase and lipoxygenase on the responses of renal arcuate arteries of Wistar rats, with and without endothelium, to noradrenaline, potassium chloride, endothelin-1, acetylcholine and sodium nitroprusside.

2 Noradrenaline, potassium chloride and endothelin-1 caused concentration-dependent contraction of the vessels. Indomethacin (14 μM) attenuated the contractile response to noradrenaline and to potassium chloride. The inhibitory effect of indomethacin persisted following endothelial removal.

3 Acetylcholine produced concentration-dependent relaxation of the vessels which was potentiated by indomethacin (14 μM).

4 N^G-nitro-L-arginine methyl ester (L-NAME, 100 μM) did not affect the contractile response to either noradrenaline or potassium chloride but abolished relaxation to acetylcholine. In addition, L-NAME abolished the affects of indomethacin on acetylcholine-induced relaxation and noradrenaline- and potassium chloride-induced contraction.

5 BWC755C attenuated noradrenaline and potassium chloride-induced contraction. This effect persisted in the presence of indomethacin.

6 In vessels pretreated with CHAPS, BW755C inhibited both noradrenaline and potassium chloride-induced contraction. In these vessels BW755C had no additional inhibitory effect to indomethacin on noradrenaline- and potassium-induced contraction.

7 Inhibition of nitric oxide synthase with L-NAME (100 μM) attenuated the effect of BW755C on noradrenaline- and potassium-induced contraction.

8 BW755C alone did not affect endothelium-dependent relaxation as assessed by the response to acetylcholine. However, in the presence of indomethacin, BW755C inhibited acetylcholine-induced relaxation.

9 BW755C did not affect endothelium-independent relaxation as assessed by the response to sodium nitroprusside in vessels with or without endothelium.

10 These data support the existence of two vasoconstrictor products of arachidonic acid released during contraction of renal arcuate arteries with noradrenaline and potassium chloride. A cyclo-oxygenase product which appears to be endothelium-independent and the other an endothelium-dependent lipoxygenase product.

Keywords: Renal arcuate arteries; cyclo-oxygenase; lipoxygenase; nitric oxide; Wistar rats

Introduction

Endothelium-derived relaxing factors play a central role in the control of vascular smooth muscle tone and therefore vascular resistance (Baylis *et al.*, 1990; Moncada *et al.*, 1991). Nitric oxide is known to be tonically released and has major influences on regional haemodynamics in particular within the kidney, although the exact site of action remains contentious (Tolins *et al.*, 1990; Radermacher *et al.*, 1990). Endothelium-dependent contracting factors have also been described in a number of different vascular beds including the aorta (Lüscher & Vanhoutte, 1986; Diederich *et al.*, 1990; Dohi *et al.*, 1990; Kato *et al.*, 1990) and renal arcuate arteries of spontaneously hypertensive rats (SHR) (Fu-Xiang *et al.*, 1992). Similar factors have also been described in Wistar-Kyoto (WKY) rats, (Diederich *et al.*, 1989; Koga *et al.*, 1989; Kato *et al.*, 1990) although not consistently. Koga *et al.* (1989) have shown that in WKY aorta, endothelium-dependent vasoconstrictor prostanoids develop with age. Noradrenaline is known to release both endothelium-dependent relaxing and contracting factors from rat arteries (Nigro *et al.*, 1990). The contracting factors described are cyclo-oxygenase-dependent (Diederich *et al.*, 1990; Lüscher *et al.*, 1990) but the compounds responsible vary depending upon the species and vascular bed studied. In the aorta and intrarenal arteries of both WKY and SHR the contracting factor appears to be either prostaglandin H_2 (Kato *et al.*, 1990; Fu-Xiang *et al.*, 1992) or thromboxane A_2 (Lin & Nasjletti, 1991).

Arachidonic acid may be metabolized into its vasoactive products by lipoxygenases (5-, 12- and 15-) a cytochrome P450-dependent mono-oxygenase and by cyclo-oxygenase. Lipoxygenase activity (5-, 12-, 15-) has been demonstrated in human, bovine and rabbit vascular endothelium and vascular smooth muscle, by functional studies, by the ability to convert arachidonic acid to monohydroxyeicosatetraenoic acids and by immunochemical techniques (Larrue *et al.*, 1983; Farber *et al.*, 1985; Revtyak *et al.*, 1988; Shannon *et al.*, 1991). Interest has focused on the role of lipoxygenase and cytochrome P450-dependent mono-oxygenase products of arachidonic acid in the control of vascular tone and the development of hypertension. However, the role of lipoxygenase products in the control of vascular tone is controversial.

The main vasoactive products of the 5-lipoxygenase en-

[1] Author for correspondence.

zyme are leukotriene C_4 and leukotriene D_4 which are potent vasoconstrictors of intrarenal arteries of rats (Badr *et al.*, 1987). 12-Hydroxyeicosatetraenoic acid (HETE), a product of the 12-lipoxygenase pathway, likewise appears to have vasoconstrictor properties and has been found to contribute to the effector mechanisms of angiotensin II-induced vasoconstriction (Saito *et al.*, 1992). 12-HETE also modulates the intracellular calcium response to arginine vasopressin, angiotensin II and endothelin. Other actions of 12-HETE include inhibition of prostacyclin-induced renin secretion by rat renal cortical slices (Antonipillai, 1990), and direct vasoconstrictor actions in dog renal arcuate arteries (Ma *et al.*, 1991). A product of the 15-lipoxygenase pathway, 15-HETE, is a directly acting vasoconstrictor in a number of vascular beds of the dog (Van Diest *et al.*, 1990). In addition, 15-HETE may act as an endothelium-independent vasodilator in vessels pre-contracted with prostaglandin $F_{2\alpha}$ (Van Diest *et al.*, 1990). This may have physiological relevance as Larrue *et al.* (1983) suggest that 15-HETE is the major lipoxygenase product of cultured endothelial cells and 15-HETE is also the major HETE of atherosclerotic vessel wall (Henriksson *et al.*, 1985).

There are at least two possible mechanisms by which the nitric oxide pathway may interact with the lipoxygenase pathway. Firstly lipoxygenase-dependent metabolism of arachidonic acid can lead to superoxide anion production (Hänsch, 1990), which may accelerate the breakdown of nitric oxide. Secondly there is evidence that nitric oxide may inhibit lipid oxidation by both lipoxygenase and cyclo-oxygenase (Kanner *et al.*, 1992).

It is clear that the lipoxygenase products of arachidonic acid are potent vasoactive compounds. There are few data on their effects on renal arcuate arteries. In this study we have used indomethacin, the combined lipoxygenase/cyclo-oxygenase blocker, 3-amino-1-[*m*-(trifluoromethyl)phenyl]-2-pyrazoline (BW755C, Higgs *et al.*, 1979) and the nitric oxide synthase blocker, N^G-nitro-L-arginine-methyl ester (L-NAME), to examine the relative roles of cyclo-oxygenase and lipoxygenase products of arachidonic acid and their relationship to nitric oxide in the contractile properties of rat renal arcuate arteries.

Methods

Preparation of blood vessels

Renal arcuate arteries (mean internal diameter of 168 ± 10 μm, $n = 114$) were isolated from male Wistar rats (age 3–4 months, weight range 250–400 g). The rats were either killed by CO_2 asphyxia or pentabarbitone injection. Pentabarbitone was used, in a series of animals, to allow cannulation of the main renal artery and perfusion of the kidney with 0.1% 3-[(3-cholamidopropyl)-dimethylammonio]-1-propanesulphonate (CHAPS) for 4 min, prior to nephrectomy, to effect endothelium removal. The method of killing does not affect the vascular responses obtained. The kidneys were removed into iced physiological salt solution (PSS) containing (mM): NaCl 119, KCl 4.7, $CaCl_2$ 2.5, $MgSO_4$ 1.17, $NaHCO_3$ 25, KH_2PO_4 1.18, EDTA 0.026 and glucose 5.5, pH 7.4; the arcuate arteries were identified and dissected free of surrounding connective tissue. The vessels were mounted on 40 μm tungsten wires in a small vessel myograph (Cambustion, Cambridge), capable of measuring isometric tension. The arteries were bathed in PSS at 37°C, bubbled with 5% CO_2 in O_2. Maximal potassium activation was achieved by KPSS (PSS with equimolar substitution of KCl for NaCl resulting in final K concentration of 125 mM).

After an equilibration period of 1 h in PSS, the passive tension/internal circumference characteristics were determined (Mulvany & Halpern, 1977). The vessels were then set to an internal circumference equivalent to 90% of that they would have had when relaxed *in situ* under a transmural pressure of 100 mmHg. The maximum active tension is developed at approximately this circumference (Mulvany & Halpern, 1977). The arteries were then maximally contracted for 2 min every 10 min on four occasions. The first two contractions being with KPSS and 5 μM noradrenaline followed by 5 μM noradrenaline and finally KPSS. Any vessel which failed to develop a maximum tension equivalent to a pressure of 100 mmHg was discarded.

Experiment protocol

Cumulative concentration-response curves were constructed sequentially, to acetylcholine, 0.01–100 μM, (arteries precontracted with 5 μM noradrenaline), noradrenaline 0.01–10 μM and potassium chloride 12–125 mM. Each concentration of agonist was left in contact with the vessels for 2 min, the tension being recorded at the end of the period. Following each concentration-response curve the vessels were washed with PSS and rested in PSS for 10 min. Following the three concentration-response curves the vessels were washed again and allowed to rest for a further 10 min. Groups of vessels (6–8 vessels in each group) were then incubated in a number of different agents (one agent or pair of agents per group): indomethacin 14 μM; L-NAME 100 μM; indomethacin 14 μM and L-NAME 100 μM; BW755C 50 μM or 180 μM; BW755C 50 μM and indomethacin 14 μM; BW755C 50 μM and L-NAME 100 μM. Concentration-response curves were then repeated to acetylcholine, noradrenaline and potassium chloride in the presence of the appropriate agent or combination of agents. The above protocol was repeated in groups of vessels pretreated with CHAPS.

The experimental protocol involves repeating concentration-response curves to acetylcholine, noradrenaline and potassium chloride on two occasions. In order to exclude changes in sensitivity of the vessels with repeated exposure, timed controls were performed. Concentration-response curves were obtained to acetylcholine, noradrenaline and potassium chloride as above; the vessels were washed in PSS and allowed to rest for 10 min. The concentration-response curves were then repeated.

In two groups of vessels concentration-response curves were constructed to endothelin-1 0.1 nM–1 μM, alone and to endothelin-1 in the presence of BW755C 50 μM. Due to the irreversible nature of endothelin-1-induced contraction it was not possible to perform sequential concentration-response curves to endothelin-1 alone and then with BW755C. Concentration-response curves were also constructed to sodium nitroprusside 0.1 nM–10 μM, in vessels precontracted with 5 μM noradrenaline, with or without pretreatment with CHAPS, alone and in the presence of BW755C 50 μM.

Drugs

Acetylcholine, indomethacin, L-NAME, CHAPS, endothelin-1 (Sigma, Poole, Dorset), sodium nitroprusside (Central Laboratories, Dublin, Ireland), noradrenaline (Winthrop Laboratories, Guildford, Surrey) and BW755C (Wellcome Laboratories, Beckenham, Kent) were used. All other reagents were obtained from BDH (Poole, Dorset). All reagents were of Analar grade and solutions were prepared fresh daily.

Statistical analysis

A Hill plot was constructed for each concentration-response relationship. The – log concentration of the drug required to produce 50% of the maximum response (pEC_{50} M) was calculated with a computerised curve fitting software package (Graphpad Inplot version 3.14). Where curve fitting was not appropriate, the maximum responses were compared. In the figures, concentrations are given as negative logarithms in molar units. Tension was expressed as mN mm^{-1} artery length. Relaxation to acetylcholine and sodium nitroprusside

was expressed as a percentage of the initial precontraction to noradrenaline. All values are given as mean ± s.e.mean. Differences between means were assessed by Student's t test for paired or unpaired data as appropriate. $P<0.05$ was taken as statistically significant.

Results

Noradrenaline, potassium chloride and endothelin-1 produced concentration-dependent contraction and acetylcholine and sodium nitroprusside concentration-dependent relaxation of the vessels. Repetition of the concentration-response curves, as timed controls did not significantly affect either the pEC_{50} or maximum response obtained to noradrenaline (pEC_{50} 6.22 ± 0.02 curve 1, versus 6.22 ± 0.02 curve 2; maximum response 2.03 ± 0.34 mN mm^{-1} curve 1, versus 2.02 ± 0.37 mN mm^{-1} curve 2), potassium chloride (pEC_{50} 1.35 ± 0.02 curve 1, versus 1.40 ± 0.02 curve 2); maximum response 1.09 ± 0.18 mN mm^{-1} curve 1, versus 0.98 ± 0.18 mN mm^{-1} curve 2) and acetylcholine (pEC_{50} 5.95 ± 0.30 curve 1 versus 6.26 ± 0.11 curve 2; maximum response 23.8 ± 4.7% curve 1 versus 23.1 ± 2.4% curve 2).

Indomethacin

Indomethacin attenuated the contractile response to noradrenaline (pEC_{50} 6.28 ± 0.04 versus 6.13 ± 0.06 with indomethacin, $P<0.05$; maximum response 1.84 ± 0.27 mN mm^{-1} versus 1.48 ± 0.21 mN mm^{-1} with indomethacin, $P<0.01$) and potassium (maximum response 0.77 ± 0.20 mN mm^{-1} versus 0.55 ± 0.11 mN mm^{-1} with indomethacin, $P<0.01$) (Figure 1). Indomethacin potentiated acetylcholine-induced relaxation (pEC_{50} 5.96 ± 0.06 versus 6.80 ± 0.13 with indomethacin, $P<0.001$; maximum response 17.2 ± 1.7% versus 36.5 ± 3.3% with indomethacin, $P<0.001$) (Figure 1).

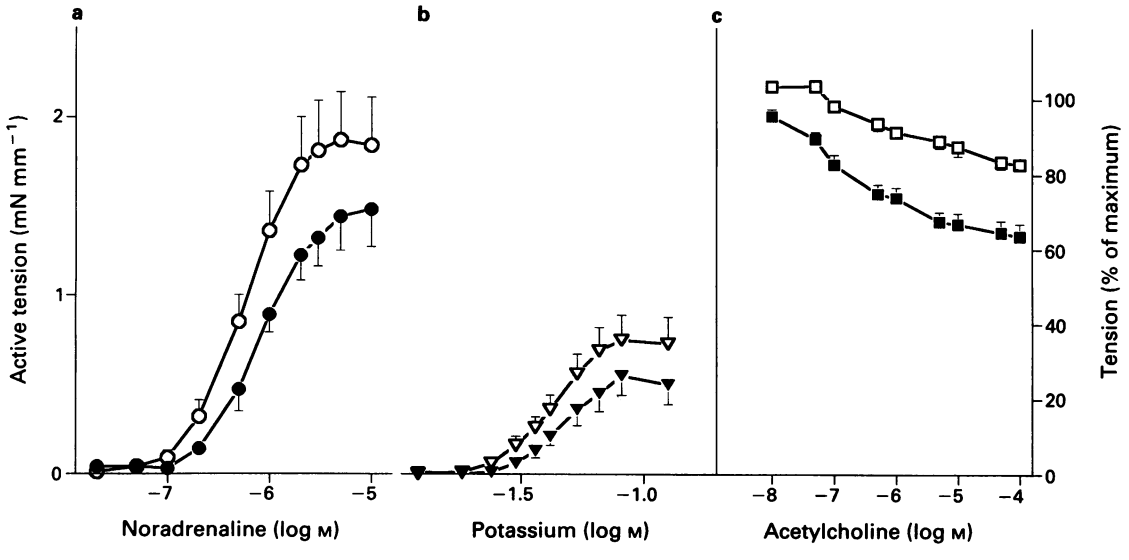

Figure 1 The effect of indomethacin, 14 μM, on the concentration-response relationship of renal arcuate arteries to (a) noradrenaline, (b) potassium chloride and (c) acetylcholine. In (a) and (b): (○, ▽) control; (●, ▼) indomethacin; $n = 8$; diameter = 180 ± 7 μm. In (c): (□) control, (■) indomethacin; $n = 8$; diameter = 160 ± 7 μm.

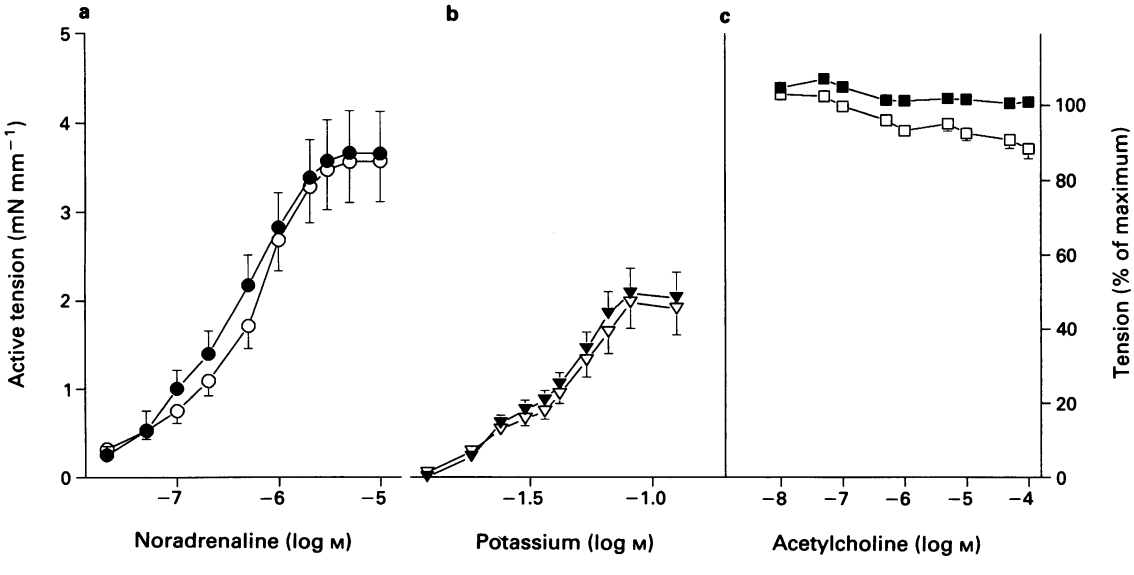

Figure 2 The effect of indomethacin and N^G-nitro-L-arginine methyl ester (L-NAME) on the concentration-response relationship of rat renal arcuate arteries to (a) noradrenaline, (b) potassium chloride and (c) acetylcholine. In (a) and (b): (○, ▽) control; (●, ▼) indomethacin plus L-NAME; $n = 8$; diameter = 184 ± 10 μm. In (c); (□) control; (■) indomethacin plus L-NAME; $n = 8$; diameter = 156 ± 11 μm.

L-NAME

L-NAME had no significant effect on the concentration-response curves to either noradrenaline (pEC_{50} 6.38 ± 0.05 versus 6.47 ± 0.05 with L-NAME; maximum response 2.03 ± 0.28 mN mm^{-1} versus 2.20 ± 0.34 mN mm^{-1} with L-NAME) or to potassium chloride (pEC_{50} 1.43 ± 0.04 versus 1.43 ± 0.03 with L-NAME). Acetylcholine-induced relaxation was virtually abolished by L-NAME (maximum relaxation 19.1 ± 2.2% versus − 3.2 ± 1.2% with L-NAME, $P<0.001$. Negative relaxation implies contraction).

Indomethacin and L-NAME

In these vessels, the inhibitory effect of indomethacin on the contractile response to noradrenaline and potassium was abolished by the presence of L-NAME (noradrenaline pEC_{50} 6.22 ± 0.04 versus 6.41 ± 0.05 with indomethacin and L-NAME, $P<0.05$; maximum response 3.57 ± 0.46 mN mm^{-1} versus 3.65 ± 0.47 mN mm^{-1} with indomethacin and L-NAME, NS; potassium pEC_{50} 1.40 ± 0.06 versus 1.44 ± 0.05 with indomethacin and L-NAME, NS; maximum response 1.98 ± 0.03 mN mm^{-1} versus 2.08 ± 0.28 mN mm^{-1} with indomethacin and L-NAME, NS) (Figure 2). The enhanced acetylcholine-induced relaxation seen in the presence of indomethacin, was abolished by L-NAME (maximum relaxation 11.5 ± 2.7% versus − 0.5 ± 1.7% with indomethacin and L-NAME, $P<0.05$) (Figure 2).

BW755C

BW755C attenuated the contractile response of the vessels, in a concentration-dependent manner, to noradrenaline (pEC_{50} 6.47 ± 0.03 versus 6.02 ± 0.01 with BW755C 50 μM, $P<0.001$, 6.48 ± 0.03 versus 5.56 ± 0.04 with BW755C 180 μM, $P<0.01$; maximum response 1.94 ± 0.53 mN mm^{-1} versus 1.27 ± 0.15 mN mm^{-1} with BW755C 50 μM, NS, 2.32 ± 0.59 mN mm^{-1} versus 0.72 ± 0.22 mN mm^{-1} with BW755C 180 μM, $P<0.05$) and potassium (pEC_{50} 1.45 ± 0.04 versus 1.40 ± 0.03 with BW755C 50 μM, NS, 1.40 ± 0.07 versus 1.13 ± 0.22 with BW755C 180 μM, NS; maximum response 0.77 ± 0.20 mN mm^{-1} versus 0.20 ± 0.08 mN mm^{-1} with BW755C 50 μM, $P<0.05$, 0.92 ± 0.31 mN mm^{-1} versus 0.10 ± 0.06 mN mm^{-1} with BW755C 180 μM, $P<0.05$) (Figure 3). BW755C did not alter the response to either acetylcholine (pEC_{50} 5.49 ± 0.12 versus 5.67 ± 0.35 with BW755C, NS; maximum response 11.5 ± 2.3% versus 12.1 ± 5.1% with BW755C, NS) or endothelin-1 (pEC_{50} 7.13 ± 0.13 versus 7.44 ± 0.18 with BW755C, NS; maximum response 2.24 ± 0.71 mN mm^{-1} versus 1.83 ± 0.16 mN mm^{-1} with BW755C, NS).

BW755C and indomethacin

In the presence of indomethacin, BW755C still attenuated the contractile response to potassium (maximum response 1.02 ± 0.22 mN mm^{-1} versus 0.38 ± 0.10 mN mm^{-1} with BW755C and indomethacin, $P<0.01$) and caused a shift to the right of the concentration-response curve to noradrenaline (pEC_{50} 6.05 ± 0.04 versus 5.88 ± 0.03 with BW755C and indomethacin, $P<0.01$) although the magnitude of the effect was small compared to that seen with BW755C alone (Figure 4). The combination of BW755C and indomethacin caused a shift to the right of the acetylcholine concentration-response curve (pEC_{50} 6.58 ± 0.09 versus 5.97 ± 0.15 with BW755C and indomethacin, $P<0.001$) and reduced the maximum relaxation seen (23.2 ± 1.15% versus 9.4 ± 2.24% with BW755C and indomethacin, $P<0.05$). This effect was directly opposite to that seen with indomethacin alone (Figure 1).

BW755C and L-NAME

Inhibition of nitric oxide synthase with L-NAME significantly reduced the shift to the right of the concentration-response curves to noradrenaline and abolished that for potassium, seen in the presence of BW755C alone, (noradrenaline pEC_{50} 6.12 ± 0.04 versus 5.93 ± 0.02 with L-NAME and BW755C, $P<0.01$; potassium pEC_{50} 1.33 ± 0.01 versus 1.34 ± 0.07 with L-NAME and BW755C, NS) (Figure 5). The maximum response to both noradrenaline and potassium in the presence of BW755C and L-NAME (2.00 ± 0.24 mN mm^{-1} and 0.55 ± 0.14 mN mm^{-1} respectively) were significantly greater than that seen with BW755C alone (1.27 ± 0.15 mN mm^{-1} and 0.20 ± 0.08 mN mm^{-1} respectively), $P<0.02$ and $P<0.05$ respectively. The combination of BW755C and L-NAME virtually abolished acetylcholine-induced relaxation (maximum relaxation 1.30 ± 2.10%). This effect was not significantly different from that seen with L-NAME alone.

CHAPS

Endothelial removal with CHAPS increased the maximum contractile response to both noradrenaline (2.03 ± 0.34 mN

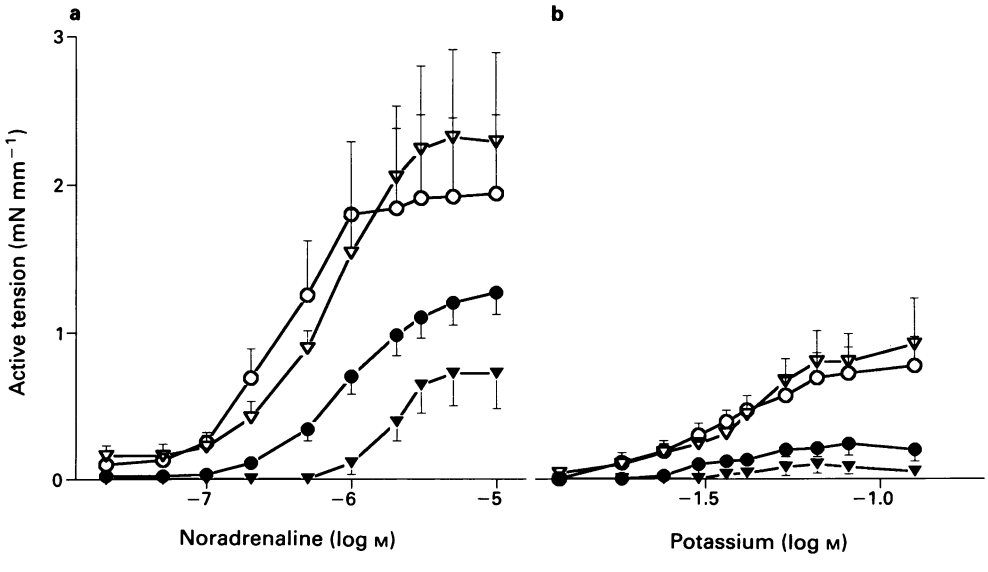

Figure 3 The effect of BW755C on the concentration-response relationship of rat renal arcuate arteries to (a) noradrenaline and (b) potassium chloride. In (a) and (b): (○) control; (●) BW755C 50 μM; $n = 7$, mean diameter = 183 ± 10 μm; (▽) control; (▼) BW755C 180 μM; $n = 5$; mean diameter = 175 ± 15 μm.

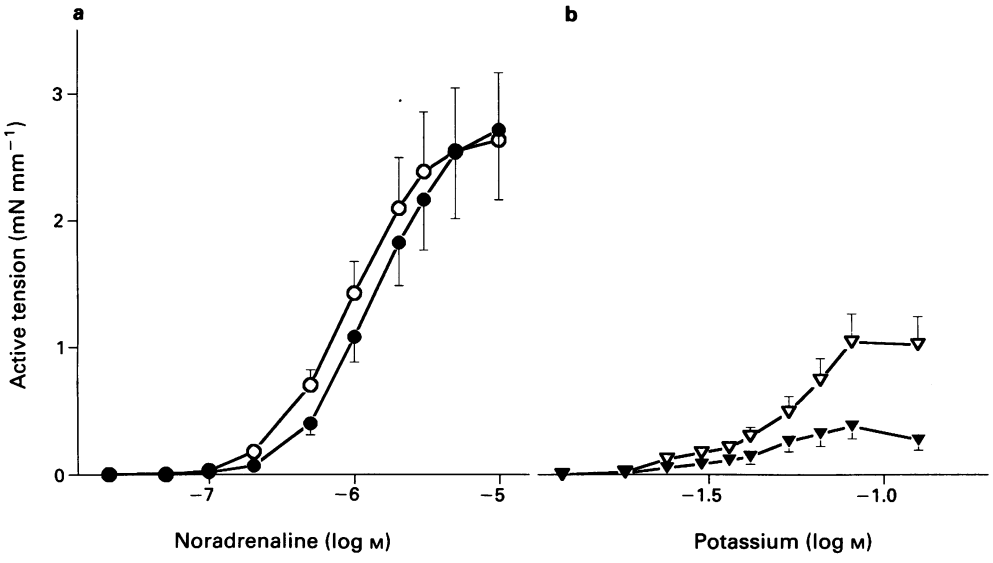

Figure 4 The effect of BW755C on the concentration-response relationship of rat renal arcuate arteries to (a) noradrenaline and (b) potassium chloride in the presence of indomethacin (1.4 μM). In (a): (○) indomethacin; (●) indomethacin plus BW755C 50 μM. In (b): (▽) indomethacin; (▼) indomethacin plus BW755C 50 μM. In (a) and (b): $n = 6$; diameter = 197 ± 8 μm.

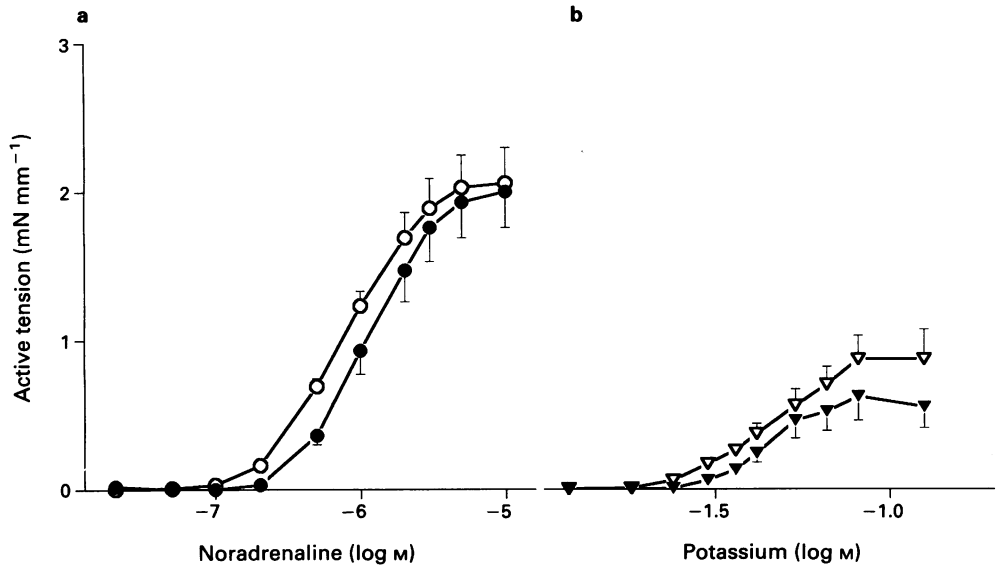

Figure 5 The effect of BW755C on the concentration-response relationship of rat renal arcuate arteries to (a) noradrenaline and (b) potassium chloride in the presence of N^G-nitro-L-arginine methyl ester (L-NAME 100 μM). In (a): (○) control; (●) L-NAME plus BW755C 50 μM. In (b): (▽) control; (▼) L-NAME plus BW755C 50 μM. In (a) and (b): $n = 8$; diameter = 138 ± 6 μm.

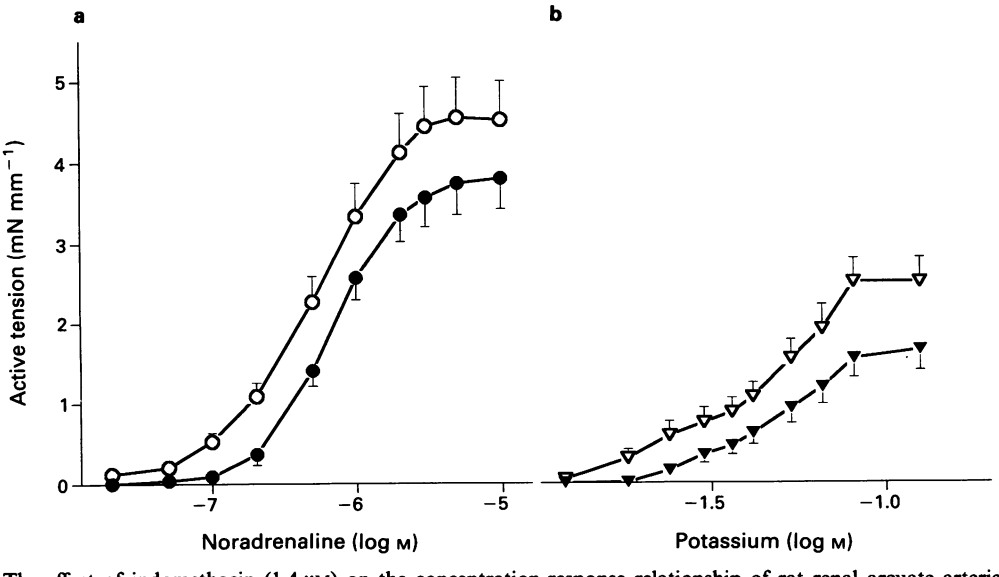

Figure 6 The effect of indomethacin (1.4 μM) on the concentration-response relationship of rat renal arcuate arteries, pretreated with CHAPS, to (a) noradrenaline and (b) potassium chloride. In (a): (○) control; (●) indomethacin. In (b): (▽) control; (▼) indomethacin. In (a) and (b): $n = 7$; diameter = 162 ± 13 μm.

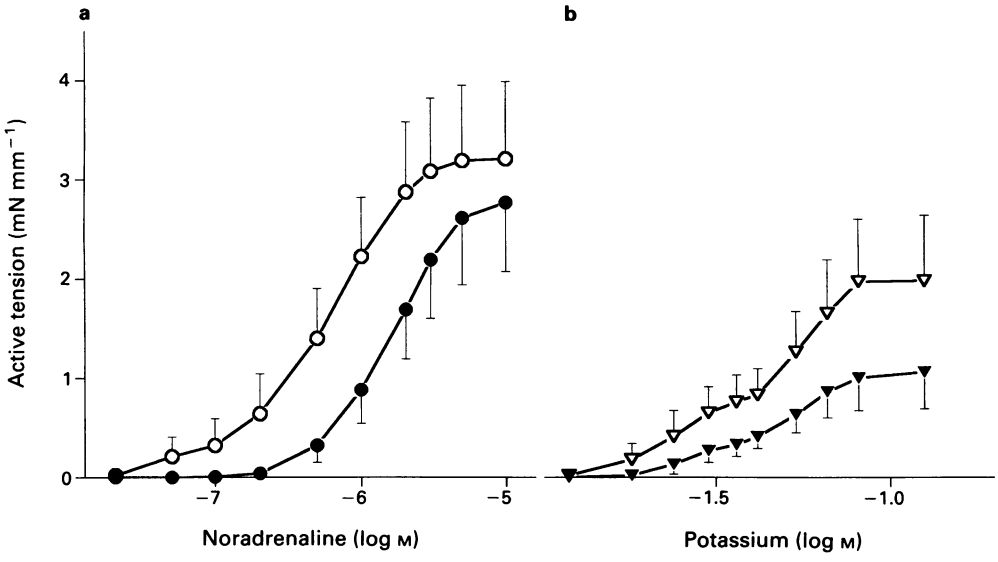

Figure 7 The effect of BW755C (50 μM) on the concentration-response relationship of rat renal arcuate arteries, pretreated with CHAPS, to (a) noradrenaline and (b) potassium chloride. In (a): (○) control; (●) BW755C. In (b): (▽) control; (▼) BW755C. In (a) and (b), $n = 6$; diameter = 180 ± 18 μm.

mm^{-1} versus 4.52 ± 0.48 mN mm^{-1} following CHAPS, $P <$ 0.001) and potassium chloride (1.09 ± 0.18 versus 2.50 ± 0.31 following CHAPS, $P < 0.006$) without causing a shift of the concentration-response curve. Acetylcholine-induced relaxation was largely abolished (maximum relaxation 23.8 ± 4.7% versus 5.10 ± 1.4% following CHAPS, $P < 0.003$).

CHAPS and indomethacin

In renal arcuate arteries pretreated with CHAPS, indomethacin reduced the maximum contractile response to noradrenaline, (4.52 ± 0.48 mN mm^{-1} versus 3.80 ± 0.38 mN mm^{-1} with indomethacin, $P < 0.01$) and potassium (2.50 ± 0.31 mN mm^{-1} versus 1.65 ± 0.26 mN mm^{-1} with indomethacin, $P <$ 0.001). There was a tendency for a shift to the right of the concentration-response curves to both noradrenaline and potassium but this did not reach statistical significance (Figure 6).

CHAPS and BW755C

Following endothelial removal, BW755C still produced a shift to the right of the concentration-response curve to noradrenaline (pEC_{50} 6.20 ± 0.02 versus 5.78 ± 0.01 with BW755C, $P < 0.01$) and depressed the maximum response to both noradrenaline (3.21 ± 0.78 mN mm^{-1} versus 2.77 ± 0.70 mN mm^{-1} with BW755C, $P < 0.05$) and potassium (1.98 ± 0.66 mN mm^{-1} versus 1.06 ± 0.37 mN mm^{-1} with BW755C, $P < 0.05$) (Figure 7).

CHAPS and BW755C with indomethacin

In the presence of indomethacin, in vessels pretreated with CHAPS, there was no additional effect of BW755C on either the maximum response or pEC_{50} for noradrenaline (pEC_{50} 5.90 ± 0.06 versus 5.81 ± 0.04 with indomethacin and BW-755C; maximum response 4.88 ± 0.62 versus 4.78 ± 0.61 with indomethacin and BW755C). In the presence of indomethacin, BW755C still reduced the maximum contractile response to potassium (2.75 ± 0.40 versus 1.63 ± 0.30 with indomethacin and BW755C, $P < 0.001$).

Sodium nitroprusside

Neither endothelial removal nor BW755C affected either the maximum response or the pEC_{50} to sodium nitroprusside (pEC_{50} 4.30 ± 0.09 versus 4.41 ± 0.28 with BW755C; 3.90 ± 0.18 versus 4.17 ± 0.32 with BW755C following CHAPS; maximum response 99.8 ± 0.10% versus 98.4 ± 0.80 with BW755C; 95.6 ± 0.30% versus 98.3 ± 0.40% with BW755C following CHAPS).

Discussion

In these vessels indomethacin enhanced endothelium-dependent relaxation, as assessed by the response to acetylcholine and attenuated the contractile responses to noradrenaline and potassium chloride. These data confirm previous findings of a cyclo-oxygenase-dependent vasoconstrictor in renal arcuate arteries (Kato *et al.*, 1990). The inhibitory effect of indomethacin persisted in the absence of a functioning endothelium suggesting that the vasoconstrictor responsible originates within the vascular smooth muscle rather than the endothelium.

Inhibition of nitric oxide synthesis with L-NAME had no effect on the contractile response to either noradrenaline or potassium, but inhibited acetylcholine-induced relaxation. This suggests that there is little stimulated nitric oxide release during contraction of these vessels with noradrenaline or potassium chloride. This may also explain the relatively poor relaxation to acetylcholine and resistance to sodium nitroprusside, but does not explain the potentiation of contraction seen following endothelial removal. These findings are compatible with those of Imig & Roman (1992) who examined the effect of nitric oxide inhibition on the pressure-diameter relationship of renal arterioles. Nitric oxide inhibition had no effect on the diameter of either arcuate or interlobular vessels whilst reducing the diameter of afferent arterioles at all perfusion pressures studied.

Kanner *et al.* (1992) have suggested that nitric oxide may inhibit arachidonic acid metabolism via both cyclo-oxygenase and lipoxygenase pathways modulating the arachidonic acid cascade and the generation of reactive oxygen species. In these arteries, indomethacin potentiated acetylcholine-induced relaxation; this relaxation was inhibited by L-NAME. Indomethacin alone attenuated the contractile response to both noradrenaline and potassium and this affect again was inhibited by L-NAME. Thus these data suggest that nitric oxide is released in these vessels by acetylcholine and on contraction with noradrenaline and potassium chloride. However the effects of nitric oxide are only apparent follow-

ing removal of the cyclo-oxygenase-derived vasoconstrictor.

Inhibition of the lipoxygenase/cyclo-oxygenase pathway with BW755C reduced the contractile responses of rat renal arcuate arteries to noradrenaline and potassium chloride. Acetylcholine-induced relaxation (endothelium-dependent) was not affected by BW755C. The effect of BW755C on the contractile response was unlikely to have been the result of cyclo-oxygenase inhibition alone as the shift to the right of the noradrenaline concentration-response curve seen with BW755C alone was greater than that seen with indomethacin alone and in the presence of indomethacin, BW755C still caused a shift to the right of the noradrenaline concentration-response curve and reduced the maximum response to potassium chloride. Endothelial removal with CHAPS attenuated the effect of BW755C and in these vessels BW755C had little additional effect in the presence of indomethacin. Thus these data support the presence of two vasoconstrictors, one an endothelium-dependent lipoxygenase derivative and the other an endothelium-independent cyclo-oxygenase derivative. The cyclo-oxygenase derived vasoconstrictor has been previously described by ourselves (Richards *et al.*, 1990) and others (Lüscher *et al.*, 1990) and is probably prostaglandin H_2 (Kato *et al.*, 1990). BW755C predominately inhibits 5- and 12-lipoxygenase in addition to cyclo-oxygenase having little activity against 15-lipoxygenase (Higgs *et al.*, 1979; Salmon *et al.*, 1983). There has been very little investigation of the effects of lipoxygenase products in the renal vasculature but Badr *et al.* (1987) demonstrated that leukotriene D_4 constricted intra-renal and efferent arterioles in the rat and Ma *et al.* (1991) have shown that 12-HETE is a directly acting vasoconstrictor in dog renal arcuate arteries. Thus it is entirely feasible that these intermediates are active in mediating the responses seen in this study.

Whilst it is possible that BW755C is inhibiting the production of a 5- or 12-lipoxygenase-derived vasoconstrictor, another possibility is that inhibition of cyclo-oxygenase and 5- and 12-lipoxygenase leads to increased metabolism of arachidonic acid by either 15-lipoxygenase or cytochrome P450-dependent mono-oxygenase and the effects seen are related to a vasoactive product of one of these pathways such as 15-HETE or 5,6-, 8,9- and 11,12-EET which have all been shown to have vasodilator properties (Van Diest *et al.*, 1990; Carroll *et al.*, 1992).

The vasoconstrictor response to endothelin-1 was not affected by BW755C. This finding is contrary to the data of Fretschner *et al.* (1991) who examined the effect of endothelin-1 in the split hydronephrotic kidney model. They demonstrated that the response to endothelin-1 was attenuated by a competitive leukotriene antagonist. The differences between our findings are not readily explained but may relate to differences in the model or inhibitors used.

L-NAME, greatly attenuated the inhibitory effect of BW755C suggesting that BW755C may either induce nitric oxide release or inhibit its breakdown. Moncada *et al.* (1986), using a rabbit aortic strip bioassay system, suggested that BW755C inhibited endothelium-dependent relaxation through cyclo-oxygenase-mediated production of superoxide anions. However, Semb & Vaage (1991) demonstrated that BW755C prevented oxygen free radical-induced injury in rat isolated heart and Hänsch (1990) showed that oxygen free radical generation from arachidonic acid was dependent on lipoxygenase rather than cyclo-oxygenase activity. Both these findings contradict those of Moncada *et al.* (1986) suggesting that BW755C decreases rather than increases free radical production. Reactive oxygen species accelerate nitric oxide breakdown, thus agents which either prevent free radical production or are free radical scavengers will potentiate the action of nitric oxide. If BW755C inhibits lipoxygenase-dependent free radical production it would potentiate the action of nitric oxide and thus inhibit contraction. If this were the case then the effect of BW755C should be inhibited by a nitric oxide synthase blocker, which is consistent with our findings. However, BW755C had no effect on endothelium-dependent relaxation which was unexpected as BW755C should enhance endothelium-dependent relaxation if it reduces free radical synthesis. The opposite was seen as BW755C reduced the response to acetylcholine in the presence of indomethacin and the action of BW755C was only partially endothelium-dependent which also argues against an action through nitric oxide.

In conclusion we have demonstrated that BW755C inhibits contraction of renal arcuate arteries induced by both noradrenaline and potassium chloride in the rat. This effect is additional to that seen with indomethacin, is partially endothelium-dependent and may be inhibited by blockade of nitric oxide synthase. The exact mechanism of action of BW755C in the renal vasculature has not been elucidated but it would appear that lipoxygenase derivatives could be involved in the control of renal vascular tone. Further work is required to define the roles of the individual lipoxygenase enzymes in the production of vasoactive substances, including reactive oxygen species.

We acknowledge the help and advice of Dr L. Poston in the preparation of this manuscript. BW755C was a kind gift from Wellcome Research Laboratories, Beckenham, Kent. This work was supported by a grant from the West Midlands Regional Health Authority.

References

ANTONIPILLAI, I. (1990). 12-Lipoxygenase products are potent inhibitors of prostacyclin-induced renin release. *Proc. Soc. Exp. Biol. Med.*, **194**, 224–230.

BADR, K.F., BRENNER, B.M. & ICHIKAWA (1987). Effects of leukotriene D4 on glomerular dynamics in the rat. *Am. J. Physiol.*, **253**, F239–F243.

BAYLIS, C., HARTON, P. & ENGELS, K. (1990). Endothelial-derived relaxing factor controls renal hemodynamics in the normal rat kidney. *J. Am. Soc. Nephrol.*, **1**, 875–881.

CARROLL, M.A., GARCIA, M.P., FALCK, J.R. & MCGIFF, J.C. (1992). Cyclooxygenase dependency of the renovascular actions of cytochrome P450-derived arachidonate metabolites. *J. Pharmacol. Exp. Ther.*, **260**, 104–109.

DIEDERICH, D., SKOPEC, J., DIEDERICH, A. & JAMESON, M. (1989). Acetylcholine releases relaxing and contracting factors from renal arcuate arteries of rats. *Kidney Int.*, **37**, 550.

DIEDERICH, D., YANG, Z., BÜHLER, B.R. & LÜSCHER, T.F. (1990). Impaired endothelium-dependent relaxations in hypertensive resistance arteries involve cyclooxygenase pathway. *Am. J. Physiol.*, **258**, H445–H451.

DOHI, Y., THIEL, M.A., BÜHLER, F.R. & LÜSCHER, T.F. (1990). Activation of endothelial L-arginine pathway in resistance arteries. Effect of age and hypertension. *Hypertension*, **15**, 170–179.

FARBER, H.W., CENTER, D.M. & RIWADSM, S. (1985). Bovine and human endothelial cell production of neutrophil chemoattractant activity in response to components of the angiotensin system. *Circ. Res.*, **57**, 898–902.

FRETSCHNER, M., ENDLICH, K., GULBINS, E., LANG, R.E., SCHLOTTMANN, K. & STEINHAUSEN, M. (1991). Effects of endothelin on the renal microcirculation of the split hydronephrotic rat kidney. *Renal. Physiol. Biochem.*, **414**, 112–127.

FU-XIANG, D., SKOPEC, J., DIEDERICH, A. & DIEDERICH, D. (1992). Prostaglandin H2 and thromboxane A2 are contractile factors in intrarenal arteries of spontaneously hypertensive rats. *Hypertension*, **19**, 796–798.

HANSCH, J.G.M. (1900). Oxygen radical generation in human platelets: dependence on 12-lipoxygenase activity and the glutathione cycle. *Int. Arch. Allergy Appl. Immunol.*, **93**, 73–79.

HENRIKSSON, P., HAMBERG, M. & DICZFALUSY, U. (1985). Formation of 15-HETE as the major hydroxyeicosatetraenoic acid in the atherosclerotic vessel wall. *Biochem. Biophys. Acta*, **834**, 272–274.

HIGGS, G.H., FLOWER, R.J. & VANE, J.R. (1979). A new approach to anti-inflammatory drugs. *Biochem. Pharmacol.*, **28**, 1959–1961.

IMIG, J.D. & ROMAM, R.J. (1992). Nitric oxide modulates vascular tone in preglomerular arterioles. *Hypertension*, **19**, 770–774.

KANNER, J., HAREL, S. & GRANT, R. (1992). Nitric oxide, and inhibitor of lipid oxidation by lipoxygenase, cyclooxygenase and haemoglobin. *Lipids*, **27**, 46–49.

KATO, T., IWAMA, Y., OKUMURA, K., HASHIMOTO, H,. ITO, T. & SATAKE, T. (1990). Prostaglandin H_2 may be the contracting factor released by acetylcholine in the aorta of the rat. *Hypertension*, **5**, 475–481.

KOGA, T., TAKATA, Y., KOBAYASHI, K., TAKISHITA, S., YAMASHITA, Y. & FUJISHIMA, M. (1989). Age and hypertension promote endothelium-dependent contractions to acetylcholine in the aorta of the rat. *Hypertension*, **14**, 542–548.

LARRUE, J., RIGAUD, M., RAZAKA, G., DARET, D., DEMOND-HENRI, J. & BRICAUD, H. (1983). Formation of monohydroxy-eicosatetraenoic acids from arachidonic acid by cultured rabbit aortic smooth muscle cells. *Biochem. Biophys. Res. Commun.*, **112**, 242–249.

LIN, L. & NASJLETTI, A. (1991). Role of endothelium-derived prostanoid in angiotensin-induced vasoconstriction. *Hypertension*, **18**, 158–164.

LÜSCHER, T.F. & VANHOUTTE, P.M. (1986). Endothelium-dependent contractions to acetylcholine in the aorta of spontaneously hypertensive rats. *Hypertension*, **8**, 344–348.

LÜSCHER, T., AARHUS, L.L. & VANHOUTTE, P.M. (1990). Indomethacin improves the impaired endothelium-dependent relaxations in small mesenteric arteries of the spontaneously hypertensive rat. *Am. J. Hypertens.*, **3**, 55–58.

MA, Y.-H., HARDER, D.R., CLARK, J.E. & ROMAN, R.J. (1991). Effects of 12-HETE on isolated dog renal arcuate arteries. *Am. J. Physiol.*, **261**, H451–H456.

MONCADA, S., PALMER, R.M.J. & GRYGLEWSKI, R.J. (1986). Mechanism of action of some inhibitors of endothelium-derived relaxing factor. *Proc. Natl. Acad. Sci. U.S.A.*, **83**, 9164–9168.

MULVANY, M.J. & HALPERN, W. (1977). Contractile properties of small arterial resistance vessels in spontaneously hypertensive and normotensive rats. *Circ. Res.*, **41**, 19–26.

NIGRO, D., FORTES, Z.B., SCIVOTETTO, R. & CARVALHO, M.H.C. (1990). Simultaneous release of endothelium derived relaxing and contracting factors induced by noradrenaline in normotensive rats. *Gen. Pharmacol.*, **21**, 443–446.

RADERMACHER, J., FÖRSTERMANN, U. & FRÖLICH, J.C. (1990). Endothelium-derived relaxing factor influences renal vascular resistance. *Am. J. Physiol.*, **259**, F9–F17.

REVTYAK, G.E., HUGHES, M.J., JOHNSON, A.R. & CAMPBELL, W.B. (1988). Histamine stimulation of prostaglandin and HETE synthesis in human endothelial cells. *Am. J. Physiol.*, **255**, C214–C225.

RICHARDS, N.T., POSTON, L. & HILTON, P.J. (1990). Evidence for the release of an indomethacin sensitive vasoconstrictor from renal arcuate arteries. *Nephrol. Dial. Transplant.*, **5**, 641.

SAITO, F., HORI, M.T., IDEGUCHI, Y., BERGER, M., GOLUB, M., STERN, N. & TUCK, M.L. (1992). 12-Lipoxygenase products modulate calcium signals in vascular smooth muscle cells. *Hypertension*, **20**, 138–143.

SALMON, J.A., SIMMONS, P.M. & MONCADA, S. (1983). The effects of BW755C and other anti-inflammatory drugs on eicosanoid concentration and leucocyte accumulation in experimentally-induced acute inflammation. *J. Pharm. Pharmacol.*, **35**, 808–813.

SEMB, A.G. & VAAGE, J. (1991). Oxygen free radical-injury in isolated rat hearts: effects of ibuprofen and BW755C. *Scand. J. Clin. Lab. Invest.*, **51**, 377–384.

SHANNON, V.R., CROUCH, E.C., TAKAHASHI, Y., UEDA, N., YAMAMOTO, S. & HOLTZMAN, M.J. (1991). Related expression of arachidonate 12- and 15-lipoxygenase in animal and human lung tissue. *Am. J. Physiol.*, **261**, L399–L405.

TOLINS, J.P., PALMER, R.M.J., MONCADA, S. & RAIJ, L. (1990). Role of endothelium-derived relaxing factor in regulation of renal haemodynamic responses. *Am. J. Physiol.*, **258**, H655–H662.

VAN DIEST, M.J., VERBEUREN, T.J. & HERMAN, A.G. (1991). 15-lipoxygenase metabolites of arachidonic acid evoke contractions and relaxations in isolated canine arteries: role of thromboxane receptors, endothelial cells and cyclooxygenase. *J. Pharmacol. Exp. Ther.*, **256**, 194–203.

(Received October 6, 1993
Revised January 10, 1994
Accepted January 24, 1994)

Br. J. Pharmacol. (1994), **112**, 377–385

Molecular cloning and expression of human EP_3 receptors: evidence of three variants with differing carboxyl termini

[1]J.W. Regan, T.J. Bailey, *J.E. Donello, K.L. Pierce, D.J. Pepperl, D. Zhang, *K.M. Kedzie, *C.E. Fairbairn, *A.M. Bogardus, *D.F. Woodward & *D.W. Gil

Departments of Pharmacology & Toxicology, and Physiology and the Program in Neuroscience, University of Arizona, Tucson, AZ 85721 and *Allergan, Inc., Biological Sciences, Irvine, CA 92713, U.S.A.

1 The polymerase chain reaction (PCR) was used in combination with plaque hybridization analysis to clone four variants of the EP_3 prostaglandin receptor from a human small intestine cDNA library.

2 Three of these variants, i.e. the EP_{3A}, EP_{3E} and EP_{3D}, share the same primary amino acid sequence except for their carboxyl termini, which diverge from one another at the same point, approximately 10 amino acids away from the end of the seventh membrane spanning domain of the receptor. The fourth variant (EP_{3A1}) has a nucleotide coding sequence identical to EP_{3A} but has a completely different 3' untranslated sequence.

3 The carboxyl termini of the three isoforms differ most obviously in length with the EP_{3A} being the longest (41 amino acids) and the EP_{3E} being the shortest (16 amino acids). They also differ in content with the EP_{3A} containing 9 serine and threonines in its carboxyl terminus and the EP_{3E} none.

4 Transient expression in eukaryotic cells showed that the human EP_3 receptor variants had similar but not identical radioligand binding properties and differed in their functional coupling to second messenger pathways. Up to 3 pmol mg^{-1} protein of [^{3}H]-prostaglandin E_2 binding could be obtained with more than 95% specific binding. Using a reporter gene assay, as a measure of intracellular cyclic AMP levels, the EP_{3A} coupled more efficiently to the inhibition of adenylyl cyclase than did the EP_{3E}.

5 PCR was used to confirm the presence of mRNAs encoding the four human EP_3 receptor variants in tissues of the human small intestine, heart and pancreas. These findings indicate that the EP_3 receptor variants identified here are likely to be expressed in tissues. The differences in the carboxyl termini at the protein level, and in the 3' untranslated regions at the mRNA level, could be profound in terms of the regulation and functional coupling of these receptor isoforms.

Keywords: Prostaglandin; small intestine; cDNA; G-protein coupled; adenylyl cyclase; cyclic AMP inhibition; CAT assays

Introduction

The prostaglandins are locally acting hormones derived from the metabolism of arachidonic acid by prostaglandin endoperoxide synthase (cyclo-oxygenase). They are very widely distributed in animal tissues where they act on cell surface receptors to produce a diverse range of physiological effects. The prostaglandin receptors elicit cellular responses by activating guanine nucleotide regulatory proteins (G-proteins). Like other members of the superfamily of G-protein coupled receptors their molecular structure is dominated by seven hydrophobic regions that appear to represent membrane-spanning α-helices.

The prostanoid receptor family is comprised of several members according to the current classification (Coleman *et al.*, 1982). Separate receptors for prostaglandin D_2 (PGD_2), PGE_2, $PGF_{2\alpha}$, PGI_2 and thromboxane A_2 were originally proposed based largely on agonist studies: these receptors were respectively defined as DP, EP, FP, IP and TP. This classification received further support by the development of TP (Coleman *et al.*, 1982) and DP receptor (Giles *et al.*, 1989) antagonists. A further subdivision of EP receptors into 3 subtypes (EP_1, EP_2 and EP_3) was proposed based on functional studies and by the development of an EP receptor antagonist (Coleman *et al.*, 1982; 1987). Similar heterogeneity of the other prostanoid receptors appears likely. Thus, subdivisions within the TP (Masuda *et al.*, 1991; Furci *et al.*, 1992) and DP receptors (Woodward *et al.*, 1993) have been suggested.

The advent of a more detailed classification of the prostaglandin receptors came with the cloning of a human TP receptor (Hirata *et al.*, 1991). Its deduced amino acid sequence confirmed that the TP receptors are in the superfamily of G-protein coupled receptors and provided the basis for the subsequent cloning of the mouse EP_2 (Honda *et al.*, 1993) and EP_3 receptors (Sugimoto *et al.*, 1992). The subsequent cloning of two isoforms of the mouse EP_3 receptor revealed heterogeneity that was not anticipated by previous functional studies (Sugimoto *et al.*, 1993). With respect to their deduced amino acid sequences, the two isoforms, $EP_{3\alpha}$ and $EP_{3\beta}$, differ only in the sequence of their carboxyl-terminal domains, this difference affecting approximately 30 amino acids changes both the interaction of these receptor isoforms with G-proteins and their patterns of agonist-promoted desensitization (Negishi *et al.*, 1993).

An important benefit of having a cloned receptor is the ability to study its pharmacology in the absence of potentially interfering receptors by the use of heterologous expression. Such types of studies have revealed significant species differences in the pharmacology of cloned rodent G-protein coupled receptors as compared with their human homologues. It has been found that a change in just one amino acid is sufficient to cause differences. For example, the rat 5-HT_{1B} and human 5-HT_{1D} receptors are actually biochemical homologues but a ^{355}T→N mutation in transmembrane (TM) 7 of the human 5-HT_{1D} changes its pharmacology to the extent that these receptors came to be defined as different subtypes (Oksenberg *et al.*, 1992). Similarly, a ^{201}S→C mutation in TM5 of the mouse α_{2A} adrenoceptor dramatically

[1] Author for correspondence.

increases its affinity for the antagonist yohimbine relative to the human α_{2A} (Link *et al.*, 1992). This is significant because [^{3}H]-yohimbine is one of the main radioligands for the characterization of α_2-adrenoceptors. To improve our understanding of the pharmacology of the human EP_3 receptors we sought to clone and express these receptors. Using the polymerase chain reaction (PCR) and homology-based screening we found four human variants of this receptor. Three of the variants represent changes at the protein level and one at the mRNA level. One of the variants corresponds to the mouse $EP_{3\alpha}$ but the other three do not correspond to any of the previously described mouse EP_3 receptors.

Methods

Reverse transcription/PCR

A sense primer was designed from nucleotides (nt's) 301–326 of the published mouse EP_3 receptor sequence (Sugimoto *et al.*, 1992) and corresponds to the proposed first extracellular loop of the receptor. Its sequence is:

5'GA(T/C)CC GTCG(T/G) GICGI CTITG (C/T)(C/A)(C/G)ITT3'

An antisense primer was designed from nucleotides 775–797 of the published mouse EP_3 receptor sequence (Sugimoto *et al.*, 1992) and corresponds to the proposed sixth transmembrane domain of the receptor. Its sequence is:

5'AC(A/G)CA CATIA T(A/T/G/C)CCC AT(A/T/G/C)A(A/G) (T/C)TG3'

The sense and antisense primers were used in a combined reverse transcription/PCR reaction with total RNA from human small intestine (Clontech). The reverse transcription reaction (final volume, 140 µl) contained 14 µl 10 × PCR buffer (Perkin Elmer), 3.5 µl RNasin (Boehringer Mannheim, 40 u ul^{-1}), 35 µl dNTP's (5 mM), 7 µl random primers (1 mg ml^{-1}), 14 µl RNA (1 µg µl^{-1}) and 7 µl AMV reverse transcriptase (Boehringer Mannheim, 25 u µl^{-1}). The reaction was incubated at room temperature (~24°C) for 10 min, 42°C for 1 h, 95°C for 5 min and was placed on ice. The PCR reaction (final volume, 50 µl) contained 20 µl from the reverse transcription reaction, 3 µl 10 × PCR buffer, 5 µl dimethylsulphoxide (DMSO), 5 µl sense primer (20 µM), 5 µl antisense primer (20 µM) and 1 µl *Taq* polymerase (Perkin Elmer, 2.5 u µl^{-1}). The following programme was used for the PCR: 94°C, 3 min; 50°C, 2 min; 72°C, 3 min; followed by 59 cycles of 94°C, 1 min; 50°C, 2 min; 72°C, 3 min; and a final cycle of 72°C, 15 min; 4°C, 12 h.

Agarose gel electrophoresis of a sample (15 µl) of the PCR reaction showed a single product of ~500 base pairs (bp). The product was purified (Geneclean, Bio101 Inc.) and was cloned into pBluescript-II KS(+) (Stratagene) using a G/C tailing reaction according to the manufacturer's instructions (Boehringer Mannheim). Briefly, terminal transferase was used to add a poly-dC extension on the purified PCR product and a poly-dG extension on PstI digested pBluescript. The samples were annealed and were used to transform *E. coli* DH10B cells by electroporation. A positive clone (B_1) was obtained and the nucleotide sequence of the PCR product/insert was determined using ΔTaq-PCR sequencing according to the manufacturer's instructions (United States Biochemicals). The sequence of clone B_1 shared ~80% identity with the mouse EP_3 receptor and was consistent with its being a human homologue.

Isolation of a genomic clone

A human genomic library in λFixII (Stratagene) was screened by plaque hybridization analysis (Sambrook *et al.*, 1989) using a ^{32}P-labelled probe derived from clone B_1. Nitrocellulose filters were used to take impressions of 440,000 recombinants (~20,000 recombinants/filter) which were denatured, neutralized and baked for 2 h at 80°C. The filters were prehybridized for 2 h at 37°C in 50% formamide/1 M NaCl/1% SDS/100 µg ml^{-1} herring sperm DNA and then hybridized with the probe overnight at 37°C in the same solution. The probe was labelled by nick-translation (Gibco/BRL) and was used at a concentration of ~5 × 10^6 d.p.m. ml^{-1}. The filters were washed for 1 h at 37°C in 2 × SSC/0.1% SDS and then for 1 h at 53°C in 0.1 × SSC/0.1% SDS. Autoradiographs were obtained and a positive clone was identified (EP_3λ12) and was isolated following 2 additional rounds of plaque hybridization analysis.

DNA was prepared from plate lysates of EP_3λ12 using LambdaSorb (Promega). The DNA was digested with EcoRI and an insert of ~13 kilobasepairs (kb) was obtained. Further restriction enzyme analysis and Southern blotting (Sambrook *et al.*, 1989) revealed a 2.4 kb BamHI fragment that hybridized with the ^{32}P-labelled PCR product. This 2.4 kb BamHI fragment was subcloned into pBluescript and its nucleotide sequence was determined using Sequenase (United States Biochemicals). An open reading frame was present that had ~80% identity with the mouse EP_3 receptor sequence. The amino terminus of this open reading frame started in approximately the same region as that of the mouse EP_3 amino terminus but the carboxyl terminus of the human sequence ended at a point equivalent to TM6 of the mouse EP_3 receptor. Examination of the nucelotide sequence in this region of the human genomic clone was consistent with an intron/exon boundary.

Isolation of cDNA clones

A human small intestine cDNA library in λgt10 (Clontech) was screened with the nick-translated PCR product using the same conditions as described above for the genomic library. From ~860,000 recombinants, 2 clones were obtained ($EP_3$27 and $EP_3$32). Another ~460,000 recombinants were screened under the same conditions except that the filters were washed for 1 h at 50°C in 1 × SSC/0.1% SDS. Four clones were obtained ($EP_3$1, $EP_3$4, $EP_3$19 and $EP_3$21). All were subcloned into the EcoRI site of pBluescript and were found to contain nucleotide sequence identical to the genomic clone. Although none contained complete open reading frames, between the six clones three distinct alternative splicing variants were present and complete open reading frames could be constructed for all of them (see below). A third screen of ~500,000 recombinants yielded a clone ($EP_3$11.2) that represented a fourth alternative splicing variant and which contained a complete open reading frame. The latter was obtained using a ^{32}P-labelled RNA probe corresponding to nt's 506–952 (Figure 1) of the genomic clone. Filters were prehybridized at 60°C in 6 × SSC/20 mM NaH_2PO_4 (pH 7.6)/1 × Denhardts/1 mM DTT/100 µg ml^{-1} poly-A (United States Biochemical) and were hybridized overnight in the same solution containing 2 × 10^6 d.p.m. ml^{-1} of the probe. Filters were washed under increasingly stringent conditions with the final wash at 60°C for 20 min in 0.1 × SSC/0.1% SDS. $EP_3$11.2 was plaque purified and subcloned into the EcoRI site of pBluescript.

Full length plasmids encoding human EP_3 receptors

A sense PCR primer containing adjacent BstXI and SspI restriction sites was made to nucleotide sequence upstream of the apparent translation start site (nt 57 in Figure 1). The sequence of this primer, shown below, contained sequence identical to that in the cDNA and genomic clones (nt's 1–22 in Figure 1) as well as additional 5' sequence (the additional sequence is shown below in the smaller font, the BstXI site is bold and the SspI site is underlined).

5'GATCCACCGCGGTGGAATATTGCCCCCTCCCGCTGCGGCTCT3'

This primer was used with an antisense primer (corresponding to nt's 657–679 in Figure 1) in a PCR reaction with the 2.4 kb BamHI genomic clone as a template. A product of ~700 bp was obtained that was purified with Geneclean (Bio101) and digested with BstXI, cleaving it at the 5′ end and at a position corresponding to nt's 499–510 in Figure 1. The larger, ~500 bp, fragment was isolated from a low-melting-point agarose gel and was used in a solid phase ligation (Sambrook *et al.*, 1989) with the 4.2 kb fragment isolated from the digestion of the pBluescript $EP_3$27 cDNA clone with BstXI. [$EP_3$27 starts at a position corresponding to nt 497 in Figure 1 and thus contains the downstream BstXI site as well as BstXI site immediately upstream in the multiple cloning site of pBluescript.] *E. coli* XL1-Blue cells were transformed and a clone was obtained (KS/EP_{3A}, Figure 1) containing 1170 bases of the complete open reading frame, 56 bases of 5′-untranslated sequence and 504 bases of 3′-untranslated sequence. KS/EP_{3A} was digested with SspI and the coding fragment was ligated to EcoRV digested pBluescript to yield KS/EPS in which the orientation of the coding sequence was such that the translation start site (nt's 57–59) was downstream of the T3 promotor.

A full length construct of EP_{3E} (KS/EP_{3E}) was obtained by digesting the pBluescript clone of $EP_3$19 with Bgl2 and HindIII and ligating the resulting small fragment with the large fragment obtained from the digestion of KS/EP_{3A} with the same enzymes. The pBluescript clone of $EP_3$11.2 was digested with BamHI and the resulting small fragment was ligated to the large fragment obtained from the digestion of KS/EPS with BamHI to yield KS/EP_{3D}.

Functional expression

The KS/EP_{3A} clone was digested with SspI which cleaved it 2 bases upstream of nt 1 and again at nt 1421. The digest was electrophoresed on a 1% agarose gel and the 1.4 kb fragment was cut out and purified with Geneclean (Bio101). The eukaryotic expression vector, pBC12BI (Cullen, 1987), was digested with HindIII and BamHI, was blunt-ended with Klenow, and was electrophoresed on a 1% low-melting-point agarose gel. The 3.9 kb fragment was isolated and was used in a solid phase ligation with the 1.4 kb SspI fragment from KS/EP_{3A}. Cells were transformed and a clone was obtained (pBC/EP_{3A}).

The KS/EP_{3E} clone was used to prepare pBC/EP_{3E} by digesting pBC12BI with HindIII and BamHI, blunting, and ligating the large fragment to the blunt-ended 1.2 kb fragment obtained from digestion of KS/EP_{3E} with SspI and HinfI. pBC/EP_{3D} was made by digesting KS/EP_{3D} with HindIII and SspI and ligating the coding fragment to the large fragment obtained from pBC12BI which had been cleaved with BamHI, blunt-ended, and then cleaved with HindIII.

Functional expression was determined as previously described (Pepperl & Regan, 1993) in a transient assay using JEG-3 cells and an adenosine 3′:5′-cyclic monophosphate (cyclic AMP)-responsive chloramphenicol acetyl transferase reporter gene (CRE-CAT). Briefly, JEG-3 cells were cotransfected with DNA encoding pBC/EP_3 receptor variants and the reporter gene using calcium phosphate precipitation. The cells were maintained in DMEM/5% FBS for 36–40 h and were then rinsed twice with DMEM and drugs were added. They were incubated for 4 h at 37°C and were harvested. CAT assays were done using 50 µl cytosol, 200 nCi [^{3}H]-chloramphenicol and 300 µM butyryl CoA. The butyrylated chloramphenicol was extracted into xylenes and the radiolabelled product was measured by liquid scintillation counting.

Radioligand binding

COS-7 cells were transfected as previously described (Regan *et al.*, 1988) with the pBC/EP_3 receptor constructs. Three days later the cells were harvested and membranes were prepared by homogenization and differential centrifugation. Membranes were resuspended in 50 mM Tris-HCl/10 mM $MgCl_2$/1 mM EDTA/pH 7.4 at a concentration of ~1 mg ml^{-1} and were frozen at −80°C. The membranes were thawed, diluted with ice-cold 50 mM Tris HCl/pH 7.4 (TB), and were dispersed with sonication. Binding was determined in triplicate in a final volume of 200 µl for 30 min at 25°C. Non-specific binding was defined with 10 µM PGE_2. Reactions were started by the addition of membranes and were terminated by the addition of 4 ml of ice-cold TB followed by rapid filtration through Whatman GF/B filters and 3 additional 4 ml washes with a cell harvester (Brandel). The filters were dried, placed in 5 ml of scintillation fluid (Ready Protein, Beckman), and counted (Beckman LS-380). Competition studies were done with a final concentration of 5 nM [^{3}H]-PGE_2. Data were analyzed by computer using the EBDA/Ligand programme (McPherson, 1985).

Northern blot analysis

Preparation of human polyA$^+$-RNA, electrophoresis and transfer to a nylon membrane was done by the manufacturer (Clontech, Multiple Tissue Northern, catalogue No. 7760-1). Accordingly, polyA$^+$-RNA was prepared by oligo(dT) cellulose chromatography and electrophoresis was on 1.2% agarose/formaldehyde gels. Probes were radiolabelled with ^{32}P-dCTP by nick translation (Gibco/BRL) and were purified by size exclusion chromatography (Chromaspin-10, Clontech). Prehybridization was in 10 ml of 44% formamide/8.8 × Denhardt's/88 µg ml^{-1} herring sperm DNA/4.4 × SSPE/1.8% SDS for 3 h at 42°C. Hybridization was for ~16 h at 42°C in 8 ml of the prehybridization buffer containing ~1.5×10^6 c.p.m. ml^{-1} of probe. Blots were rinsed 6 × 5 min at 24°C in 2 × SSC/0.5% SDS and then 2 × 20 min at 50°C in 0.1 × SSC/0.1% SDS. Exposures were made at −80°C using Kodak AR film.

PCR analysis of variant expression

Sense and antisense primers corresponding to TM5 and the 3′-untranslated regions, respectively, of the human EP_3 receptor variants were used in RT/PCR reactions to confirm the expression of the variants in total RNA from human tissues. The sense primer represents nt's 774–791 (Figure 1) which is common to all of the variants. The antisense primers are as follows: EP_{3A}, nt's 1257–1274; EP_{3A1}, nt's 1356–1373; EP_{3E}, nt's 1164–1181; EP_{3D}, nt's 1166–1183 (Figure 2). The reverse transcription reaction (final volume, 60 µl) contained 6 µl 10 × PCR buffer (Boehringer Mannheim), 2 µl RNasin, 6 µl dNTP's (10 mM), 6 µl random primers (6-mers, 0.04 A_{260}, μl^{-1}) or 6 µl p(dT)$_{15}$ (0.02 A_{260} μl^{-1}), 2 µl denatured (65°C for 10 min) RNA (1 µg ul^{-1}), 12 µl $MgCl_2$ (25 mM), 0.6 µl acetylated BSA (10 mg ml^{-1}) and 7 µl AMV reverse transcriptase. The reaction was incubated at room temperature (~24°C) for 10 min, 42°C for 45 min, 95°C for 5 min and was placed on ice. The PCR reaction (final volume, 50 µl) contained 4 µl from the reverse transcription reaction, 5 µl 10 × PCR buffer, 0.6 µl sense primer (25 µM), 0.6 µl antisense primer (25 µM), 3µl $MgCl_2$, 2 µl dNTP's (1.25 mM), 1 µl tetra-methyl-ammonium chloride (2.5 mM) and 0.3 µl *Taq* polymerase (Perkin Elmer, 5 u μl^{-1}). An initial denaturation step at 94°C for 2 min was followed by 35 cycles of 94°C, 15 s; 60°C, 15 s; 72°C, 36 s and a final step at 72°C for 6 min. Products were analyzed by agarose gel (1.5%) electrophoresis followed by staining with ethidium bromide.

Results

Using the polymerase chain reaction (PCR) and primers designed from the first extracellular loop and sixth transmembrane (TM) domain of the mouse EP_3 prostaglandin receptor (Sugimoto *et al.*, 1992), a product of ~500 base

pairs was obtained from human small intestine RNA. Analysis of the product's nucleotide and deduced amino acid sequence indicated that it was the human homologue of the mouse EP_3 receptor. The PCR product was labelled with ^{32}P and was used to screen a human genomic library by plaque hybridization analysis. A clone was isolated and was found to contain nucleotide sequence identical to the PCR product, however, downstream of nt 953 (Figure 1) the sequence of the genomic clone diverged radically from the mouse EP_3 receptor sequence. This divergence, which in the deduced amino acid sequence corresponds to TM6, marks the beginning of an intron. Subsequent Southern blot analysis of the genomic clone with a probe encoding TM7 from the human EP_{3A} receptor cDNA was negative, indicating that the downstream exon(s) were not present in this clone.

The ^{32}P-labelled PCR product was then used to screen a human small intestine cDNA library. A total of 7 clones were isolated and sequenced. One of these clones appeared to correspond to the mouse $EP_{3\alpha}$ (Sugimoto *et al.*, 1993) but it lacked some of the 5′ coding region. Between it and the genomic clone, a full length clone encoding the human EP_{3A} was constructed. Later, two of the other cDNA clones were found to have complete 5′ coding sequences which confirmed the sequence of the recombinant receptor. The complete nucleotide and deduced amino acid sequence of the human EP_{3A} clone is shown in Figure 1. The overall amino acid identity of this clone with the mouse $EP_{3\alpha}$ sequence is 79% and identity in the transmembrane domains is 91%. Like the mouse sequence, the human EP_{3A} has a short third intracellular loop (~26 amino acids), two consensus sites for N-linked glycosylation in the amino terminus and an aspartate residue in TM7 that is conserved in other prostanoid receptors but is an asparagine in other G-protein coupled receptors.

Among the other cDNA clones was one (EP_{3A1}) that had a coding sequence identical to the EP_{3A} but which had a completely different 3′ untranslated sequence beginning in the

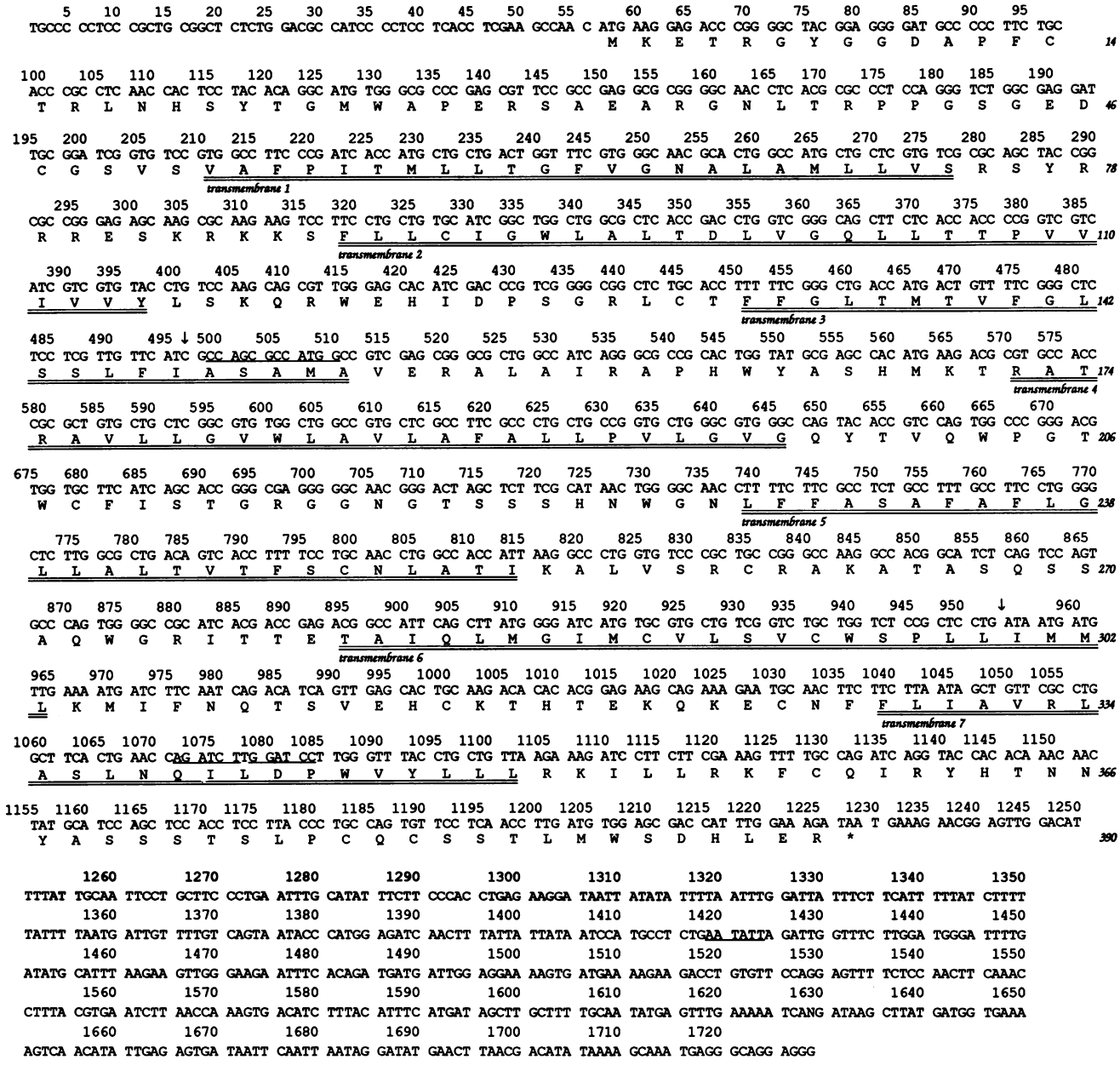

Figure 1 Nucleotide (nt) and deduced amino acid sequence of the human EP_{3A} receptor. The coding sequence is from nt's 57 to 1226 and the 390 amino acid sequence is indicated using the single letter code. Putative transmembrane regions are indicated by the double underline. The beginning of cDNA clone $EP_{3}27$ is indicated by the arrow (↓) at nt 497. The beginning of an intron in the genomic sequence is indicated by the arrow (↓) after nt 953. The single underlines are restriction enzymes sites that were used in making recombinants: they are as follows, BstXI, nt's 499–510; Bgl2, nt's 1072–1077; BamHI, nt's 1079–1084; and SspI nt's 1419–1424.

stop codon at nt 1227. The nucleotide and deduced amino acid sequence of this and 2 other variants are shown in Figure 2. The other 2 variants, EP_{3E} and EP_{3D}, share the same nucleotide sequence as the EP_{3A} up to nt 1133 but then they diverge from each other and from the EP_{3A}. With respect to their amino acid sequences, this gives rise to 3 possible carboxyl terminal variants of the human EP_3 receptor. Assuming that ^{350}R marks the beginning, the carboxyl terminus of the EP_{3A} would consist of 41 amino acids, while the EP_{3E} and EP_{3D} would consist of 16 and 39 amino acids, respectively. There is no amino acid identity between the variants in these regions nor is there any nucleotide sequence

EP_{3A1}

```
       1130          1140          1150          1160          1170
AAG TTT TGC CAG ATC AGG TAC CAC ACA AAC AAC TAT GCA TCC AGC TCC ACC TCC TTA
 K   F   C   Q   I   R   Y   H   T   N   N   Y   A   S   S   S   T   S   L

           1190          1200          1210          1220          1230
CCC TGC CAG TGT TCC TCA ACC TTG ATG TGG AGC GAC CAT TTG GAA AGA TGA G AAAAA
 P   C   Q   C   S   S   T   L   M   W   S   D   H   L   E   R   *

 1240          1250          1260          1270          1280          1290          1300
GAAGA CTCAG AGAGC AATTC TGGAG GCCGG CAAGT TCAGG ATCAG GGTGC CAGCA GATTC GGTGT
       1310          1320          1330          1340          1350          1360
CTGAC TGGAG TGCAG TGGAG TGATT TCCGC TCACT GCAAC CTTCA CCTCC TCCAC TCACT GCAAT
 1370          1380          1390          1400          1410          1420          1430
CTTCG CCTCC TGGGT TCAAG TGATT CTCCT GCCTC AGCCT CCCAA GTAGC TGGAA TTGCA CGATG
       1440          1450          1460          1470          1480          1490
CGCCA CAAGC CTGGC TAATT TTTGC ATTTT TAGTA GAGAT GAGTT TCACC ATGTT TGCCA GGCTG
 1500          1510          1520          1530          1540          1550          1560
GTCTT GAACA CCTGA CCTCA AGTAA CCCAC CCACC TTGGC CTCCC AAAGA GCTGG GATTA CAGGC
       1570          1580          1590          1600          1610          1620
ATGAG CCAAC GTGCC TGGCC ATGTT CTGAT CGTTT AATGA TAGCA ACATT TAGTA TTATA GAGCA
1630          1640          1650
TGAAA ATGTC AAAGC CGCCC GGAAT TC
```

EP_{3E}

```
       1130          1140          1150          1160          1170
AAG TTT TGC CAG GAG GAA TTT TGG GGA AAT TAA A ACCTG CCTTT CTGCC AGGAT
 K   F   C   Q   E   E   F   W   G   N   *

 1180          1190          1200          1210          1220          1230          1240
CACAT CACTG GAAGC TCCAT GACTC TCTTT TTGTA AAAGA AAAAA AAATC ACAGA AACAC CCACC
       1250          1260          1270          1280          1290          1300
TCCCA AACTA TTCTC TTTTA CTTCT TCCCC CAAGC CCACC CCCAA ATATA ACTGT TATCC AGAAG
 1310          1320          1330          1340          1350          1360          1370
CTGTT ATGTC CTGTT TCCAT ACATG TTTTT GTACT TTTAC TATAT CTACA TACAT CAATT AAACT
       1380          1390          1400          1410          1420
TATGT CCTAT TGTTT TGTGA ATTTA TATTT GCGTA TACAT TATCG TATGT CCGGA ATTC
```

EP_{3D}

```
       1130          1140          1150          1160          1170
AAG TTT TGC CAG GTA GCA AAT GCT GTC TCC AGC TGC TCT AAT GAT GGA CAG AAA GGG
 K   F   C   Q   V   A   N   A   V   S   S   C   S   N   D   G   Q   K   G

           1190          1200          1210          1220          1230
CAG CCT ATC TCA TTA TCT AAT GAA ATA ATA CAG ACA GAA GCA TGA AA GAAAA CACTT
 Q   P   I   S   L   S   N   E   I   I   Q   T   E   A   *

 1240          1250          1260          1270          1280          1290          1300
AACTT GCATG TGCAC AGCTT TTGGT AACAA ATATC GCTAA ACCTT ACTGT GAATT AGGCA TCTCT
       1310          1320          1330          1340          1350          1360
GGCAT GCCAC TGTTA TGCAT TGAAT GTGGA ATTTT GGTAT AAAGC TAAAT GGTCT TAGAA GCATA
 1370          1380          1390          1400          1410          1420          1430
GAAAA TCCCC TATGT GCCAA AAGTA GTGAA CACAA CAAAG GAAAA TATAT TAATA ACAGT CTAGT
       1440          1450          1460          1470          1480          1490
GTTTT GTTGA GTCTG CCATT GTAGC TGAAT ATGTG ATTAA TTATG TGATG AAAAC ATTTT TTATA
 1500          1510          1520          1530          1540
AATGA TCTTG GTCTA TTGGG GAGCG GGGAT AGTTA ATATT CCACC GG
```

Figure 2 Nucleotide and deduced amino acid sequences of the human EP_3 receptor variants in their carboxyl termini and 3'-untranslated regions. From top to bottom: the EP_{3A1}, the EP_{3E} and the EP_{3D}. Sequences start with nt 1122 (aa. No 356) with upstream sequences the same as in Figure 1 for the EP_{3A}. Amino acid sequences that overlap with the EP_{3A} are in bold type face. The single underlines from nt's 1196–1200 in the EP_{3E} and nt's 1530–1535 in the EP_{3D} are HinfI and SspI sites, respectively, that were used in making recombinants.

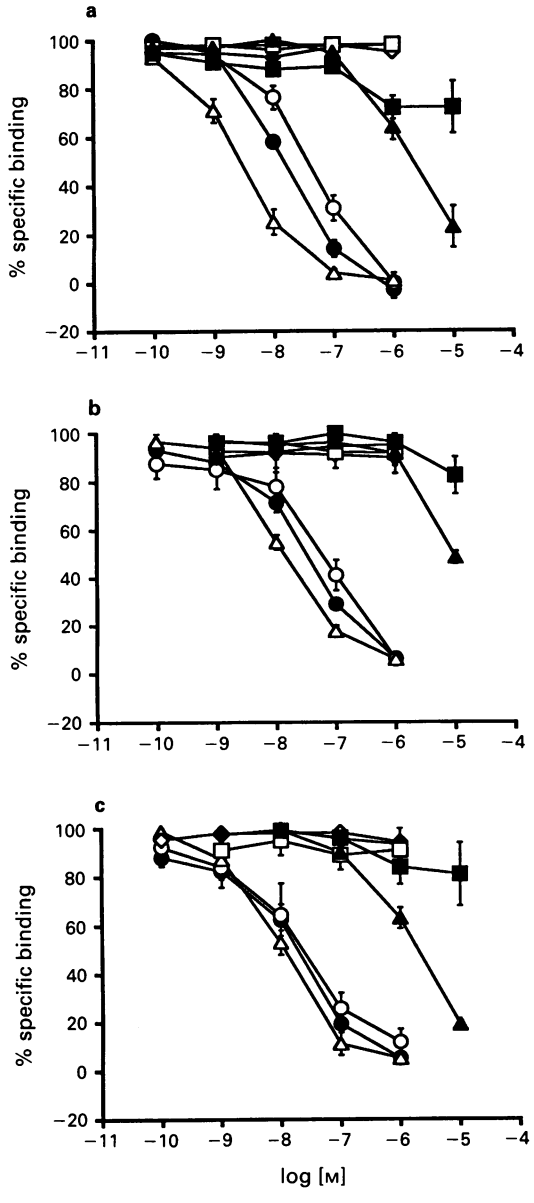

Figure 3 Inhibition of specific [^{3}H]-PGE_2 binding to membranes prepared from COS-7 cells that have been transfected with plasmid DNA encoding the three human EP_3 receptor variants. Competitors include natural prostaglandins and compounds that are selective for the various prostaglandin receptor subtypes and are as follows: PGE_2 (●), PGE_1 (○), MB28767 (△), AH13205 (◇), AH6809 (◆), U46619 (□), $PGF_{2\alpha}$ (▲), PGD_2 (■). (a) EP_{3A}; (b) EP_{3D}; (c) EP_{3E}. Binding was done as described in Methods with a final concentration of 5 nM [^{3}H]-PGE_2. Data represent the means ± s.e.mean from three separate experiments, each performed in triplicate.

Table 1 Competition for the binding of [^{3}H]-prostaglandin E_2 ([^{3}H]-PGE_2) to membranes prepared from COS-7 cells transfected with plasmid DNA encoding alternative splicing variants of the human EP_3 prostaglandin receptor[1]

	Receptor variants (IC_{50} in nM)		
Competitor	*EP_{3A}*	*EP_{3D}*	*EP_{3E}*
MB28767	3	14	12
PGE_2	15	32	20
PGE_1	39	60	25
$PGF_{2\alpha}$	2300	9300	1200

[1]IC_{50}'s were calculated from the data shown in Figure 3 and represent the pooled data from 3 separate experiments. K_ds for the equilibrium saturation binding of [^{3}H]-PGE_2 were: 1, 8 and 6 nM for the EP_{3A}, EP_{3D}, and EP_{3E}, respectively.

identity. This is in contrast to the mouse EP_3 receptor variants which differ from one another because of a deletion and frame-shift (Sugimoto *et al.*, 1993).

The EP_3 receptor variants were cloned into a mammalian expression vector and were expressed transiently in COS-7 cells. Membranes were prepared and radioligand binding was determined using [^{3}H]-PGE_2. Figure 3 shows the results of competition studies using compounds predicted to have varying degrees of affinity for the EP_3 receptor. PGE_2, PGE_1, and MB28767 (EP_3 selective) all potently inhibited [^{3}H]-PGE_2 binding; the rank order of potency for all the variants being MB28767 > PGE_2 > PGE_1. There were, however, differences between the variants in the IC_{50}s for some of the competitors (Table 1). For example, a 13 fold difference separated the IC_{50}s of MB28767 and PGE_1 at the EP_{3A}, whereas, only a 2 fold difference separated them at the EP_{3E}. Most of this difference could be accounted for by a higher affinity of MB28767 for the EP_{3A}. $PGF_{2\alpha}$ also seemed to discriminate between the variants to some extent, showing higher affinity for the EP_{3A} and EP_{3E} as compared with the EP_{3D}. The other compounds competed very poorly or not at all. These included the selective thromboxane receptor agonist, U46619, the EP_1 selective antagonist, AH6809, the EP_2 selective agonist AH13205, and PGD_2.

The EP_3 receptor variants were also co-transfected into JEG-3 cells with a cyclic AMP responsive-chloramphenicol acetyltransferase reporter plasmid (CRE-CAT). This plasmid responds to changes in intracellular cyclic AMP and has been developed into a transient functional assay for receptors that interact with adenylyl cyclase (Pepperl & Regan, 1993). Figure 4 shows the inhibition of forskolin-stimulated CAT activity by sulprostone for the EP_{3A}, EP_{3D} and EP_{3E} receptor variants. The curves are biphasic with an inhibition of CAT activity occurring at low concentrations of sulprostone and a reversal at higher concentrations. A similar type of dose-response pattern has also been observed for α_2-adrenoceptor subtypes (Pepperl & Regan, 1993) and for muscarinic receptors (Jones *et al.*, 1991) using both this assay and/or direct measurements of cyclic AMP. Figure 4 also shows that the EP_{3A} inhibited forskolin-stimulated CAT activity to a greater extent than either the EP_{3D} or EP_{3E}. With respect to the potency of sulprostone, large differences were not observed between the variants, although, there was a tendency for sulprostone to have a lower EC_{50} at the EP_{3A}.

The full coding sequence of the human EP_{3A} was radiolabelled with ^{32}P by nick-translation and was used as a probe in Northern blot analyses to examine the distribution of EP_3 receptor message in several human tissues. Figure 5 shows that mRNA from human kidney hybridized strongly with the probe. The most abundant message size was ~2.4 kb but other bands at 5.1 and 7 kb were also observed. Longer exposures revealed a small amount of the 2.4 kb message in mRNA from the pancreas and heart.

The polymerase chain reaction (PCR) was used with primer combinations that were specific for each of the cDNA variants of the EP_3 receptor to determine if human tissues contained mRNA that corresponded to these variants. Figure 6 shows that using human small intestine RNA and reverse transcription followed by PCR, products were obtained that represented each of the cloned EP_3 receptor variants. Similar results were obtained with RNA from the human heart and pancreas except that only a single band was observed with primers that were specific for the EP_{3E}.

Discussion

A human small intestine cDNA library was screened with a PCR product encoding a portion of a human EP_3 receptor and 4 unique cDNA variants of this receptor were identified. One of these variants, the human EP_{3A} appears to be the homologue of the mouse $EP_{3\alpha}$ (Sugimoto *et al.*, 1993). A second variant (EP_{3A1}) contains the same coding sequence as

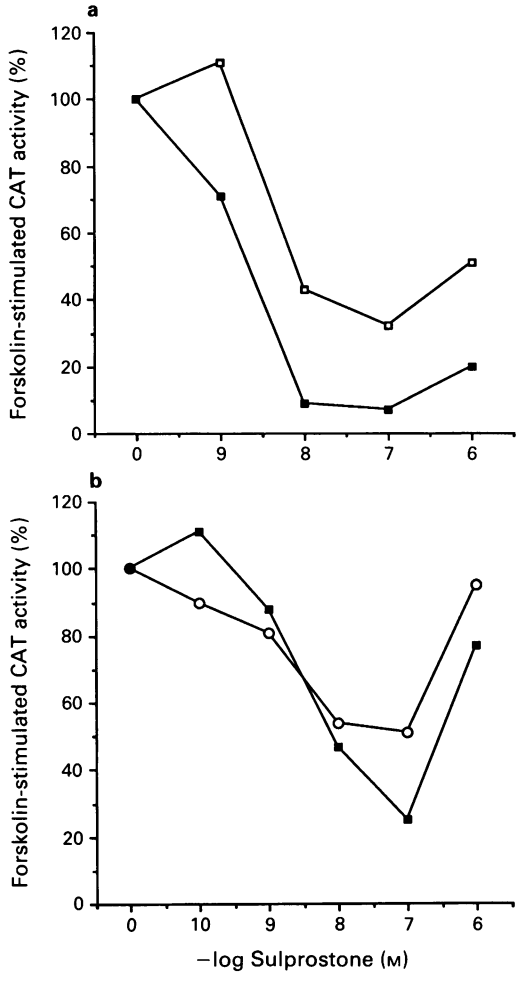

Figure 4 Effects of sulprostone on forskolin-stimulated CRE-CAT reporter gene activity after transient transfection of JEG-3 cells with DNA encoding either: (a) the EP_{3A} (■) and EP_{3D} (□); or (b) the EP_{3A} (■) and EP_{3E} (○). Each curve is expressed as a percentage of the forskolin-stimulated activity in the absence of sulprostone. Transfections and CAT assays were done as described in Methods. Forskolin was used at a final concentration of 1 μM. For (a) data are representative of 2 experiments and for (b) data are representative of 4 experiments.

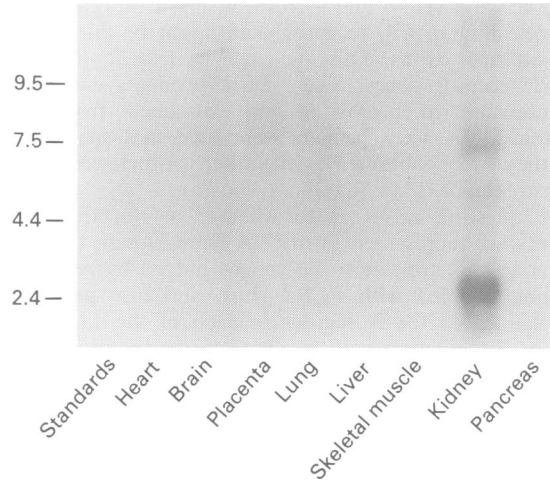

Figure 5 Northern Blot of human mRNA's hybridized with the full coding sequence (nt's − 2 to 1421) of the human EP_{3A} radiolabelled with ^{32}P by nick-translation. Hybridization, wash and exposure conditions are described in Methods. Lane 1, heart; lane 2, brain; lane 3, placenta; lane 4, lung; lane 5, liver; lane 6, skeletal muscle; lane 7, kidney; lane 8, pancreas. The position of the size standards are indicated. The blot was stripped and probed with a β-actin probe that indicated that similar amounts of RNA were loaded in each lane.

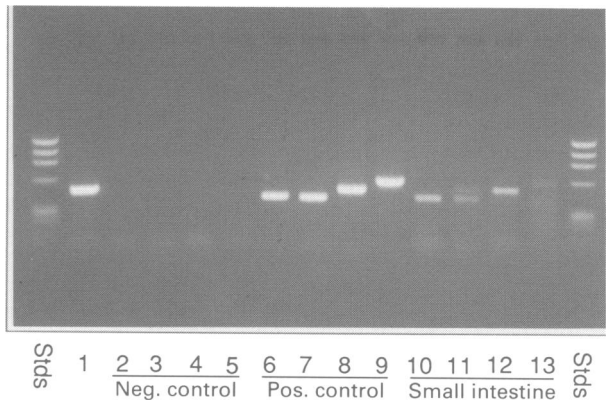

Figure 6 Photograph of ethidium-stained agarose gel of the products of a reverse transcription/PCR reaction with primers specific for each of the human EP_3 receptor cDNA variants. Lane 1 is a positive control for the PCR reaction; lanes 2–5 are negative controls (no templates); lanes 6–9 are positive controls using plasmid DNA encoding each of the human EP_3 receptor variants; lanes 10–13 are the results of the RT/PCR reaction using RNA from human small intestine. In each set of reactions (ie. negative control, positive control, small intestine), primers specific for the following variants were used EP_{3D}, EP_{3E}, EP_{3A} and EP_{3A1}. The expected product sizes (bp) were as follows: EP_{3D}, 409; EP_{3E}, 407; EP_{3A}, 500; and EP_{3A1}, 599. Standards (stds) are HaeIII cleaved ΦX174.

the EP_{3A} but has a completely divergent 3′ untranslated region beginning with the stop codon. The last two variants, the human EP_{3E} and EP_{3D}, encode receptors with the same amino acid sequence as the EP_{3A} except for their predicted carboxyl terminal domains. These carboxyl terminal sequence differences appear to affect some of the ligand binding properties of these variants and their functional coupling to a cyclic AMP responsive reporter gene. In addition, since the 3′-untranslated region can affect mRNA stability, the existence of EP_3 receptor variants with alternative 3′-untranslated sequences may also be important for regulating the expression of these receptors.

It is interesting that nucleotide sequences of the human EP_{3E} and EP_{3D} diverge from each other and from the EP_{3A} at exactly the same point (nt 1133, Figure 1); which is also where the mouse $EP_{3\beta}$ diverges from the $EP_{3\alpha}$ (Sugimoto *et al.*, 1993). In the case of cDNAs encoding the mouse EP_3 receptors, the origin of this divergence involves a deletion of 89 nucleotides which results in a frame shift that changes the sequence of the next 26 amino acids before a new termination codon is reached. For our human variants such a mechanism is not in evidence because the nucleotide sequences in the divergent regions do not share identity. In either case mRNA splicing involving exons encoding alternative carboxyl termini appears to be operational. The use of alternative splicing, as a mechanism of creating receptor heterogeneity, does not appear to be common among the G-protein coupled receptors but it has been described for rhodopsin and for the dopamine receptors. Thus, two variants of the D_2-dopamine receptor are known in which the use of alternative splicing creates 'long' and 'short' forms of the receptor which differ in the lengths of their third intracellular loops (Giros *et al.*, 1989; Monsma *et al.*, 1989; Dal Toso *et al.*, 1989). In addition, splice variants of the D_3-dopamine receptor have been described (Giros *et al.*, 1991).

Besides the cDNAs encoding carboxyl terminal variants of the EP_3 receptor we found evidence of an intron in the human EP_3 receptor gene in a region corresponding to TM6. We did not, however, find any cDNA clones that were variants at this position. Considering that separate exons

may encode TM1–6 and 7, respectively, it appears that the complete human EP_3 receptor gene might be fairly complex with multiple exons. This may also be true for other prostanoid receptor genes. Thus, PCR products encoding the thromboxane receptor were not obtained from human genomic DNA when primers were used that spanned TM6 but they were obtained with other primer combinations downstream of TM6 (data not shown).

The question arises as to whether or not these cDNA variants are represented in mRNA from human tissues. The answer to this appears to be yes, as judged by reverse transcription coupled with PCR. Thus, antisense primers that were unique to the 3′ regions of each of the variants were used in combination with a sense primer common to all of the variants. Four PCR products, corresponding to each of the variants, were obtained using RNA from human small intestine, as well as with RNA from human heart and pancreas. With RNA from human small intestine, however, the primers specific for the EP_{3E} consistently yielded two products: one of expected size and another that was 50–100 nt longer. By analogy to the mouse $EP_{3\beta}$, which contains an 89 bp deletion relative to the mouse $EP_{3\alpha}$, it is possible that the human EP_{3E} receptor represents a deletion of yet another human EP_3 receptor variant. The finding that the larger of the two products was obtained only with RNA from small intestine and not with RNA from heart or pancreas, suggests that EP_3 receptor variants may be uniquely expressed in tissues. Additional studies, however, will be needed to define the tissue specific expression of EP_3 receptor variants.

Further evidence that the EP_3 receptor cDNA clones encoded functional receptors was obtained by radioligand binding studies of the cloned receptors expressed in mammalian cells lacking endogenous EP_3 receptors. Thus, expression of the human EP_3 receptor variants in COS-7 cells followed by radioligand binding with [^{3}H]-PGE_2 have established an EP_3 pharmacology. PGE_2 was found to bind with high affinity as did the EP_3-selective agonist, MB28767. The EP_2-selective agonist, AH13205, and the EP_1 selective antagonist, AH6809, did not inhibit [^{3}H]-PGE_2 binding which further confirms these receptors as EP_3. The inhibitory potency of $PGF_{2\alpha}$ in the human variants was similar to that reported for the cloned murine EP_3 receptors (Sugimoto *et al.*, 1993) and to native EP_3 receptors in the renal, gastrointestinal and reproductive tissues from various nonprimate species (Sonnenberg *et al.*, 1990; Watanabe *et al.*, 1991; Woodward *et al.*, 1994). In contrast, PGD_2 exhibited minimal activity at the human EP_3 variants, whereas, it is more active at some nonprimate EP_3 receptors. Other differences in potency also exist between the cloned murine and human EP_3 receptors. For example, MB28767 is ~10 fold more potent than PGE_1 at the human EP_{3A} as compared with the murine $EP_{3\alpha}$. In this regard, the murine $EP_{3\alpha}$ is more similar pharmacologically to the human EP_{3E}.

The radioligand binding of [^{3}H]-PGE_2 to membranes prepared from cells transfected with these EP_3 receptors offers some distinct advantages over the use of naturally occurring animal tissues. For example, at a concentration of 5 nM [^{3}H]-PGE_2, 35 μg of membrane protein from COS-7 cells transiently transfected with the EP_{3A} yielded ~37,100 d.p.m. of specific [^{3}H]-PGE_2 binding activity (3.2 pmol mg^{-1} protein) with only 2% nonspecific binding. Using membranes prepared from the rat uterus, 20 μg of membrane protein yielded ~2,100 d.p.m. of specific binding (309 fmol mg^{-1} protein) with 33% nonspecific binding (Woodward *et al.*, 1994). The recognition of EP_3 receptor heterogeneity combined with the ability to study these variants in isolation increases the likelihood that the biochemical differences between these variants will be exploited pharmacologically.

The apparent differences in agonist binding between EP_3 receptor variants could reflect differences in the efficiency of coupling, or pattern of coupling, to G-proteins and second messenger pathways. Native EP_3 receptors, previously characterized in cells and tissues, inhibit adenylyl cyclase as part of their second messenger pathway (Sonnenburg *et al.*, 1990; Matthews & Jones, 1993). The mouse EP_3 receptors that have been stably expressed in cultured CHO cells (Sugimoto *et al.*, 1993) differ markedly in their inhibition of forskolin-stimulated cyclic AMP formation. Thus, PGE_2 is ~3 orders of magnitude more potent at the $EP_{3\alpha}$ than it is at the $EP_{3\beta}$. The isoforms also differ with respect to desensitization with the $EP_{3\alpha}$ being relatively sensitive and the $EP_{3\beta}$ resistant (Negishi *et al.*, 1993). The human EP_3 receptor variants also seem to show differences with respect to their patterns of coupling with adenylyl cyclase. In transiently transfected human JEG-3 cells there was a biphasic effect on forskolin-stimulated cyclic AMP-responsive CAT reporter gene activity: first inhibition, and then reversal. It also appeared that sulprostone could produce a greater degree of inhibition at the EP_{3A} as compared with either the EP_{3D} or EP_{3E}.

Phosphorylation of G-protein coupled receptors on serines and/or threonines present in the carboxyl terminal or third intracellular loop is known to be critical in the process of receptor desensitization (Lefkowitz, 1993). In addition, tyrosines present in the carboxyl terminus of the β-adrenoceptor may have a role in the more specific process of down-regulation, although, it is unknown if this also involves phosphorylation (Valiquette *et al.*, 1990). It is notable, therefore, that the composition of the carboxyl termini of the human EP_3 receptor variants differ markedly in these regards. Thus, the carboxyl terminus of the EP_{3A} contains 7 serines, 3 threonines and 2 tyrosines; the EP_{3E} contains none of these amino acids and the EP_{3D} contains 5 serines, 1 threonine and 1 tyrosine. If desensitization of EP_3 receptors specifically involves phosphorylation of the carboxyl terminus, then the human EP_{3A} and EP_{3D} would be expected to be more affected than the EP_{3E}.

Very recently the cloning of four EP_3 receptor variants (EP_{3A}, EP_{3B}, EP_{3C}, EP_{3D}) from the bovine adrenal medulla was reported (Namba *et al.*, 1993). Interestingly, all of these bovine isoforms were variants starting with the same amino acid in the carboxyl terminus as in the human variants; however, only one is an actual homologue of the human clones. Thus, the bovine EP_{3D}, is a homologue of the human EP_{3D}. The human EP_{3A}, which is a homologue of the mouse $EP_{3\alpha}$, is not a homologue of the bovine EP_{3A}. In addition, none of the bovine variants are homologues of the mouse $EP_{3\beta}$. In total, therefore, up to seven EP_3 receptor variants may exist in any given species.

The identification and characterization of these EP_3 receptor variants demonstrates a greater degree of complexity with respect to alternative RNA splicing than previously thought for the G-protein coupled receptors. It also raises intriguing questions concerning the regulation and expression of these isoforms and their physiological roles in mediating the actions of endogenous prostaglandins. The potential for tissue specific expression of each of the human EP_3 receptor variants exists, as well as the possibility that the regulation of receptor number rests not only at the level of the protein but at the level of the mRNA. The differential expression of these EP_3 receptor variants could affect a target tissue's sensitivity to drugs both in terms of responsiveness and the ability to desensitize. Such differences could potentially be exploited for therapeutic benefit.

Note added in proof

We have recently cloned a cDNA from a human skin fibroblast library (Clontech) that represents an additional carboxyl terminal variant of the EP_3 prostaglandin receptor. This variant, the EP_{3F}, is related to the human EP_{3E} and probably explains the doublet that was observed in the PCR reaction (Figure 6, lane 11; also see paragraph 4 of Discussion). As compared with the EP_{3E} (Figure 2), the EP_{3F} contains an additional 27 bases between nt's 1133 and 1134. The nucleotide and deduced amino acid sequence of this insert is shown as follows.

5'ATG AGA AAA AGA AGA CTC AGA GAG CAA3'
M R K R R L R E Q

The radioligand binding and functional coupling of this variant have not been presently characterized.

This work has been supported by Allergan Inc. with additional support provided to J.W.R. by the National Institutes of Health (EY09355), the Arizona Affiliate of the American Heart Association and the Arizona Disease Control Research Commission.

References

COLEMAN, R.A., HUMPHREY, P.P.A. & KENNEDY, I. (1982). Prostanoid receptors in smooth muscle: further evidence for a proposed classification. *Trends. Autonom. Pharmacol.*, **3**, 35–49.

COLEMAN, R.A., HUMPHREY, P.P.A., KENNEDY, I., SHELDRICKS, R.L.G. & TOLOWINKSA, I.Y. (1987). Further evidence for the existence of three subtypes of PGE_2-sensitive (EP-) receptors. *Br. J. Pharmacol.*, **91**, 407P.

CULLEN, B.R. (1987). Use of eukaryotic expression technology in the functional analysis of cloned genes. *Methods Enzymol.*, **152**, 684–704.

DAL TOSO, R., SOMMER, B., EWERT, M., HERB, A., PRITCHETT, D.B., BACH, A., SHIVERS, B.D. & SEEBURG, P.H. (1989). The dopamine D_2 receptor: two molecular forms generated by alternative splicing. *EMBO J.*, **8**, 4025–4034.

FURCI, L., FITZGERALD, D.J. & FITZGERALD, G.A. (1991). Heterogeneity of prostaglandin H2/thromboxane A2 receptors: distinct subtypes mediate vascular smooth muscle contraction and platelet aggregation. *J. Pharmacol. Exp. Ther.*, **258**, 74–81.

GILES, H., LEFF, P., BOLOFO, M.L., KELLY, M.G. & ROBERTSON, A.D. (1989). The classification of prostaglandin DP-receptors in platelets and vasculature using BWA868C, a novel, selective and potent competitive antagonist. *Br. J. Pharmacol.*, **96**, 291–300.

GIROS, B., SOKOLOFF, P., MARTRES, M.-P., RIOU, J.-F., EMORINE, L.J. & SCHWARTZ, J.-C. (1989). Alternative splicing directs the expression of two D_2 dopamine receptor isoforms. *Nature*, **342**, 923–926.

GIROS, B., MARTRES, M.-P., PILON, C., SOKOLOFF, P. & SCHWARTZ, J.-C. (1991). Shorter variants of the D_3 dopamine receptor produced through various patterns of alternative splicing. *Biochem. Biophys. Res. Commun.*, **176**, 1584–1592.

HIRATA, M., HAYASHI, Y., USHIKUBI, F., YOKOTA, Y., KAGEYAMA, R., NAKANISHI, S. & NARUMIYA, S. (1991). Cloning and expression of cDNA for a human thromboxane A_2 receptor. *Nature*, **349**, 617–620.

HONDA, A., SUGIMOTO, Y., NAMBA, T., WATABE, A., IRIE, A., NEGISHI, M., NARUMIYA, S. & ICHIKAWA, A. (1993). Cloning and Expression of a cDNA for mouse prostaglandin E receptor EP_2 subtype. *J. Biol. Chem.*, **268**, 7759–7762.

JONES, S.V.P., HEILMAN, C.J. & BRANN, M.R. (1991). Functional responses of cloned muscarinic receptors expressed in CHO-K1 cells. *Mol. Pharmacol.*, **40**, 242–247.

LEFKOWITZ, R.J. (1993). G protein-coupled receptor kinases. *Cell*, **74**, 409–412.

LINK, R., DAUNT, D., BARSH, G., CHRUSCINSKI, A. & KOBILKA, B. (1992). Cloning of two mouse genes encoding α_2-adrenergic subtypes and identification of a single amino acid in the mouse α_2-C10 homolog responsible for an interspecies variation in antagonist binding. *Mol. Pharmacol.*, **42**, 16–27.

MASUDA, A., MAIS, D.E., OATIS, J.E & HALUSHKA, P.V. (1991). Platelet and vascular thromboxane A_2/prostaglandin H_2 receptors: evidence for different subclasses in the rat. *Biochem. Pharmacol.*, **42**, 537–544.

MATTHEWS, J.S. & JONES, R.L. (1993). Potentiation of aggregation and inhibition of adenylate cyclase in human platelets by prostaglandin E analogues. *Br. J. Pharmacol.*, **108**, 363–369.

MCPHERSON, G.A. (1985). Analysis of radioligand binding experiments: a collection of computer programs for the IBM PC. *J. Pharmacol. Methods*, **14**, 213–228.

MONSMA, F.J., MCVITTIE, L.D., GERFEN, C.R., MAHAN, L.C. & SIBLEY, D.R. (1989). Multiple D_2 dopamine receptors produced by alternative RNA splicing. *Nature*, **342**, 926–929.

NAMBA, T., SUGIMOTO, Y., NEGISHI, M., IRIE, A., USHIKUBI, F., KAKIZUKA, A., ITO, S., ICHIKAWA, A. & NARUMIYA, S. (1993). Alternative splicing of C-terminal tail of prostaglandin E receptor subtype EP3 determines G-protein specificity. *Nature*, **365**, 166–170.

NEGISHI, M., SUGIMOTO, Y., IRIE, A., NARUMIYA, S. & ICHIKAWA, A. (1993). Two isoforms of prostaglandin E receptor EP_3 subtype: Different COOH-terminal domains determine sensitivity to agonist-induced desensitization. *J. Biol. Chem.*, **268**, 9517–9521.

OKSENBERG, D., MARSTERS, S.A., O'DOWD, B.F., JIN, H., HAVLIK, S., PEROUTKA, S.J. & ASHKENAZI, A. (1992). A single amino-acid difference confers major pharmacological variation between human and rodent 5-HT_{1B} receptors. *Nature*, **360**, 161–163.

PEPPERL, D.J. & REGAN, J.W. (1993). Selective coupling of α_2-adrenergic receptor subtypes to cAMP-dependent reporter gene expression in transiently transfected JEG-3 cells. *Mol. Pharmacol.*, **44**, 802–809.

REGAN, J.W., KOBILKA, T.S., YANG-FENG, T.L., CARON, M.G., LEFKOWITZ, R.J. & KOBILKA, B.K. (1988). Cloning and expression of a human cDNA for an α_2-adrenergic receptor subtype. *Proc. Natl. Acad. Sci. U.S.A.*, **85**, 6301–6305.

SAMBROOK, J., FRITSCH, E.F. & MANIATIS, T. (1989). In *Molecular Cloning: a Laboratory Manual*, Cold Spring Harbor, NY: Cold Spring Harbor Laboratory Press.

SONNENBURG, W.K., ZHU, J. & SMITH, W.L. (1990). A prostaglandin E receptor coupled to a pertussis toxin-sensitive guanine nucleotide regulatory protein in rabbit cortical collecting tubule cells. *J. Biol. Chem.*, **265**, 8479–8483.

SUGIMOTO, Y., NEGISHI, M., HAYASHI, Y., NAMBA, T., HONDA, A., WATABE, A., HIRATA, M., NARUMIYA, S. & ICHIKAWA, A. (1993). Two isoforms of the EP_3 receptor with different carboxyl-terminal domains: identical ligand binding properties and different coupling properties with G_i proteins. *J. Biol. Chem.*, **268**, 2712–2718.

SUGIMOTO, Y., NAMBA, T., HONDA, A., HAYASHI, Y., NEGISHI, M., ICHIKAWA, A. & NARUMIYA, S. (1992). Cloning and expression of a cDNA for mouse prostaglandin E Receptor EP_3 Subtype. *J. Biol. Chem.*, **267**, 6463–6466.

TAKEUCHI, K., ABE, T., TAKAHASHI, N. & ABE, K. (1993). Molecular cloning and intrarenal localization of rat prostaglandin E_2 receptor EP_3 subtype. *Biochem. Biophys. Res. Comm.*, **194**, 885–891.

VALIQUETTE, M., BONIN, H., HNATOWICH, M., CARON, M.G., LEFKOWITZ, R.J. & BOUVIER, M. (1990). Involvement of tyrosine residues located in the carboxyl tail of the human β_2-adrenergic receptor in agonist-induced down-regulation of the receptor. *Proc. Natl. Acad. Sci. U.S.A.*, **87**, 5089–5093.

WATANABE, T., SHIMIZU, T., NAKAO, A., TANIGUCHI, S., ARATA, T., TERAMOTO, T., SEYAMA, Y., UI, M. & KUROKAWA, K. (1991). Characterization of partially purified prostaglandin E_2 receptors form canine renal medulla: evidence for physical association of the receptor protein with the inhibitory guanine nucleotide-binding protein. *Biochem. Biophys. Acta*, **1074**, 398–405.

WOODWARD, D.F., FAIRBURN, C.E. & LAWRENCE, R.A. (1994). Identification of the FP-receptor as a discrete entity by radioligand binding in biosystems that exhibit different functional rank orders of potency to prostanoids. In *Eicanosoids and Other Bioactive Lipids in Cancer, Inflammation, and Radiation Injury*, (In press).

WOODWARD, D.F., SPADA, C.S., HAWLEY, S.B., WILLIAMS, L.S., PROTZMAN, D.C. & NIEVES, A.L. (1993). Further studies on ocular responses to DP receptor stimulation. *Eur. J. Pharmacol.*, **230**, 327–333.

(Received November 15, 1993
Revised January 27, 1994
Accepted February 3, 1994)

Br. J. Pharmacol. (1994), **112**, 386–389

The effect of the ET_A receptor antagonist, FR 139317, on [^{125}I]-ET-1 binding to the atherosclerotic human coronary artery

[1]Michael R. Dashwood, *Sean P. Allen, *Thin N. Luu & John R. Muddle

Departments of Physiology and Neurological Science, Royal Free Hospital School of Medicine, Rowland Hill Street, London NW3 2PF and *NHLI, Harefield Hospital, Uxbridge, Middlesex

1 The distribution of [^{125}I]-endothelin (ET-1) binding sites on atherosclerotic human epicardial coronary arteries has been studied by *in vitro* receptor autoradiography.

2 [^{125}I]-ET-1 binding was to the tunica media and regions of neovascularization.

3 Competition studies were carried out in the presence of ET-1 and the ET_A receptor antagonist, FR 139317. The IC_{50} values for ET-1 at the tunica media and regions of neovascularization were similar (mean ± s.e.mean of $n = 4$ patients, 2.5 ± 0.9 nM and 2.9 ± 0.9 nM, respectively) whereas IC_{50} values for FR 139317 at regions of neovascularization (607 ± 34 nM) were significantly higher than those of the tunica media (12.6 ± 2.4 nM) ($P < 0.0001$).

4 These results indicate that ET_A receptors are present on the tunica media of the diseased human coronary artery whereas a different ET receptor subtype exists at regions of neovascularization.

Keywords: Endothelin; FR 139317; ET_A binding site; tunica media; neovascularization; human coronary artery; atherosclerosis

Introduction

Endothelin (ET) is a vasoconstrictor peptide that also possesses mitogenic activity on cultured vascular smooth muscle cells (see Yanagisawa & Masaki, 1989). [^{125}I]-ET-1 binding to the tunica media, vasa vasorum and regions of neovascularization of normal and diseased human coronary arteries has been described (Dashwood *et al.*, 1991; 1993). Neovascularization associated with regions of atherosclerotic plaque has been demonstrated in the human coronary artery (Barger *et al.*, 1984) and intimal hyperplasia is induced following manipulation of the adventitial vasa vasorum (Barker *et al.*, 1993). Two ET receptor subtypes have been cloned from cDNA libraries, ET_A (where the affinity of ET-1 > ET-2 ➤ ET-3) and ET_B (which shows equipotent affinity for all three ET receptor isoforms and for sarafotoxins, Sakurai *et al.*, 1992). Here we have studied the effect of the ET_A receptor antagonist, FR 139317 ((**R**)2-[(**R**)-2-[(S)-2-[[1-(hexahydro-1H-azepinyl)]-carbonyl]amino-4-methyl-pentanoyl]amino-3-[3-(1-methyl-1H-indolyl)]propionyl]amino-3-(2-pyridyl) proprionic acid] (Sogabe *et al.*, 1992) on [^{125}I]-ET-1 binding to atherosclerotic human coronary arteries from patients undergoing cardiac transplantation.

Methods

[^{125}I]-ET-1 binding to coronary arteries from 7 patients undergoing cardiac transplantation for ischaemic heart disease was studied by *in vitro* autoradiography. Tissue was obtained at surgery, frozen immediately in liquid nitrogen and stored at −70°C until 10 μm serial sections were cut at −20°C and thaw-mounted onto gelatinized microscope slides. High- and low-resolution autoradiography was performed as previously described (Moody *et al.*, 1990). For saturation analysis, slide-mounted sections were incubated in buffer containing 1 to 1000 pM [^{125}I]-ET-1 alone (specific activity 1800 to 2000 Ci mmol^{-1}, Amersham International, Amersham, Bucks) and in the presence of 500 nM ET-1 (Bachem Fine Chemicals) to determine the degree of non-specific binding. Competition studies were carried out by incubating consecutive sections in the presence of 10^{-10} M to 1.5×10^{-5} M unlabelled ET-1 or the ET_A receptor antagonist, FR 139317 (Fujisawa Pharmaceutical Co. Ltd., Osaka, Japan). After incubation, low-resolution autoradiography was carried out by apposing tissue to Hyperfilm ^{3}H (Amersham, Bucks) for 6 to 16 days. Densitometric analysis was performed on an IBAS imaging system (Kontron, Watford) and the degree of binding to the tunica media and regions of neovascularization determined from curves generated by ^{125}I microscales (Amersham, Bucks). High-resolution autoradiographs were produced by dipping post-fixed tissue in nuclear emulsion (LM-1, Amersham, Bucks) and exposing for up to 11 days. Underlying tissue was stained with haematoxylin and eosin for histological examination and standard immunocytochemical techniques used on selected sections to identify endothelial cells. Binding to the tunica media and microvessels (vasa vasorum and regions of neovascularization) was confirmed on high-resolution autoradiographs. IC_{50} values were calculated using non-linear regression analysis of competitive binding curves (GraphPad InPlot, GraphPad Software, San Diego, U.S.A.) from densitometric measurements of ^{3}H Hyperfilm images. Analysis of high-resolution autoradiographs was also carried out, where grain-counting was performed on emulsion-coated sections that had been incubated in [^{125}I]-ET-1 in the presence of increasing concentrations of ET-1 and FR 139317, at 200 times magnification, on an Olympus Vanox microscope.

Results

[^{125}I]-ET-1 bound to all vessels examined, binding being to smooth muscle cells of the tunica media as well as to perivascular structures, identified as regions of neovascularization (Figure 1). Abundant perivascular binding was associated with regions of atherosclerotic plaque of diseased vessels (Figure 2). The characteristics of [^{125}I]-ET-1 binding to vascular tissue ($K_D \sim 150$ pM) were essentially as previously described by others (see Yanagisawa & Masaki, 1989). There was a concentration-dependent reduction in [^{125}I]-ET-1 binding to sections incubated in the presence of unlabelled ET-1 and FR 139317 (Figure 3). Densitometric analysis of film images indicated that binding to the tunica media and perivascular sites was inhibited by low concentrations of ET-1 (mean ± s.e.mean IC_{50} values, for $n = 4$ patients, 2.5 ± 0.9 nM and 2.9 ± 0.9 nM respectively). Interestingly reduction of [^{125}I]-ET-1 binding to the tunica media by FR 139317 was also achieved at low concentrations (mean

[1] Author for correspondence.

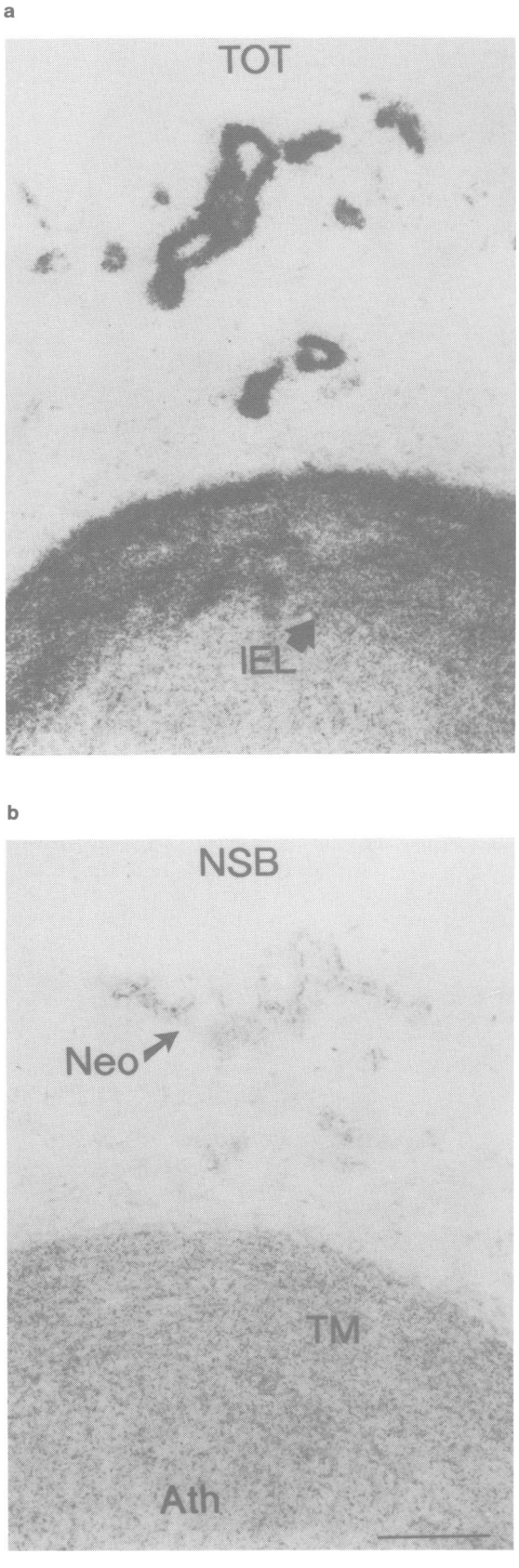

Figure 1 High-resolution autoradiographs of [^{125}I]-endothelin-1 ([^{125}I]-ET-1) binding to atherosclerotic human coronary artery. Autoradiographs from competition study generated on nuclear emulsion. (a) Section incubated in 150 pM [^{125}I]-ET-1 (TOT). (b) Binding to section incubated in the presence of 100 nM unlabelled ET-1 (reduced to non-specific level, NSB). Underlying haematoxylin and eosin stained tissue. TM = tunica media; Ath = atherosclerotic plaque; IEL = internal elastic lamina; Neo = regions of neovascularization; scale bar = 100 μm.

IC_{50}, $n = 4$ patients, 12.6 ± 2.4 nM) whereas the IC_{50} at perivascular sites was significantly higher (mean IC_{50}, $n = 4$ patients 607 ± 34 nM: $P < 0.0001$, Table 1). Perivascular binding was confirmed to be to microvessels, or regions of neovascularization, on high-resolution autoradiographs and sections used for immunocytochemistry. Grain counts of high-resolution autoradiographs from one patient ($n = 56$ sections) showed similar effects of FR 139317 on [^{125}I]-ET-1 binding to the tunica media and regions of neovascularization (see Table 1).

Discussion

The constrictor effects of ET-1 and the distribution of [^{125}I]-ET-1 binding sites on segments of human coronary artery have been described previously (Dashwood *et al.*, 1991; 1993). ET-1-induced vasoconstriction is suggested to be via smooth muscle ET_A receptors (Sakurai *et al.*, 1992) and the ET_A receptor antagonist, FR 139317, has been shown to inhibit ET-induced contractions of the guinea-pig pulmonary artery (Cardell *et al.*, 1993). A recent *in vitro* study has demonstrated that distal portions of human coronary arteries are more sensitive to the constrictor effects of ET-1 than proximal portions and that this vasoconstriction is mediated via different ET receptors (Godfraind, 1993).

Raised plasma ET-1 levels have been reported in patients with symptomatic atherosclerosis and atherosclerotic vessels display ET-1-like immunoreactivity that is localized to endothelial and smooth muscle cells (Lerman *et al.*, 1991; Dashwood *et al.*, 1993). Neovascularization in the walls of human coronary arteries has been reported using a cinematographic technique (Barger *et al.*, 1984), the extent of which is correlated with the severity of disease (Kamat *et al.*, 1987). Our autoradiographic data indicate that these regions exhibit dense [^{125}I]-ET-1 binding (Dashwood *et al.*, 1991; 1993).

ET_A and ET_B receptors have been cloned (Sakurai *et al.*, 1992) and a number of subtype-selective compounds have recently been synthesized. In the present study we have shown that [^{125}I]-ET-1 binding to the atherosclerotic human coronary artery is inhibited by the ET_A selective antagonist, FR 139317, in a concentration-dependent manner and have demonstrated regional variations in the affinity of FR 139317 in diseased vessels. The IC_{50} for this compound at the tunica media is similar to that reported for porcine and human aortic microsomes (Sogabe *et al.*, 1992) whereas, at regions of neovascularization, FR 139317 displayed a significantly lower inhibitory potency, approaching the low-affinity for [^{125}I]-ET-1 binding sites in porcine brain (Sogabe *et al.*, 1992).

It has been suggested that a 'microvessel' ET receptor exists at regions of neovascularization of the atherosclerotic coronary artery and that this receptor differs in some way

Table 1 Inhibition of [^{125}I]-endothelin-1 ([^{125}I]-ET-1) binding to atherosclerotic human coronary artery: effect of un- labelled ET-1 and FR 139317

		Tunica media IC_{50} (nM)		*Neovascularization* IC_{50} (nM)
A	ET-1	2.5 ± 0.9	NS	2.9 ± 0.9
	FR139317	12.6 ± 2.4	$P < 0.0001$	607 ± 34
B	ET-1	0.52 ± 0.2	NS	0.58 ± 0.2
	FR139317	6.5 ± 0.2	$P < 0.0006$	619 ± 173

IC_{50} (nM) values derived from non-linear regression analysis of competition experiments. The values represent mean ± s.e.mean, unpaired *t* test; NS, not significant.

A Values derived from densitometric analysis of autoradiographs generated on film ($n = 200$ sections from 4 patients).

B Values derived from grain-counts of high-resolution images from one patient ($n = 56$ sections).

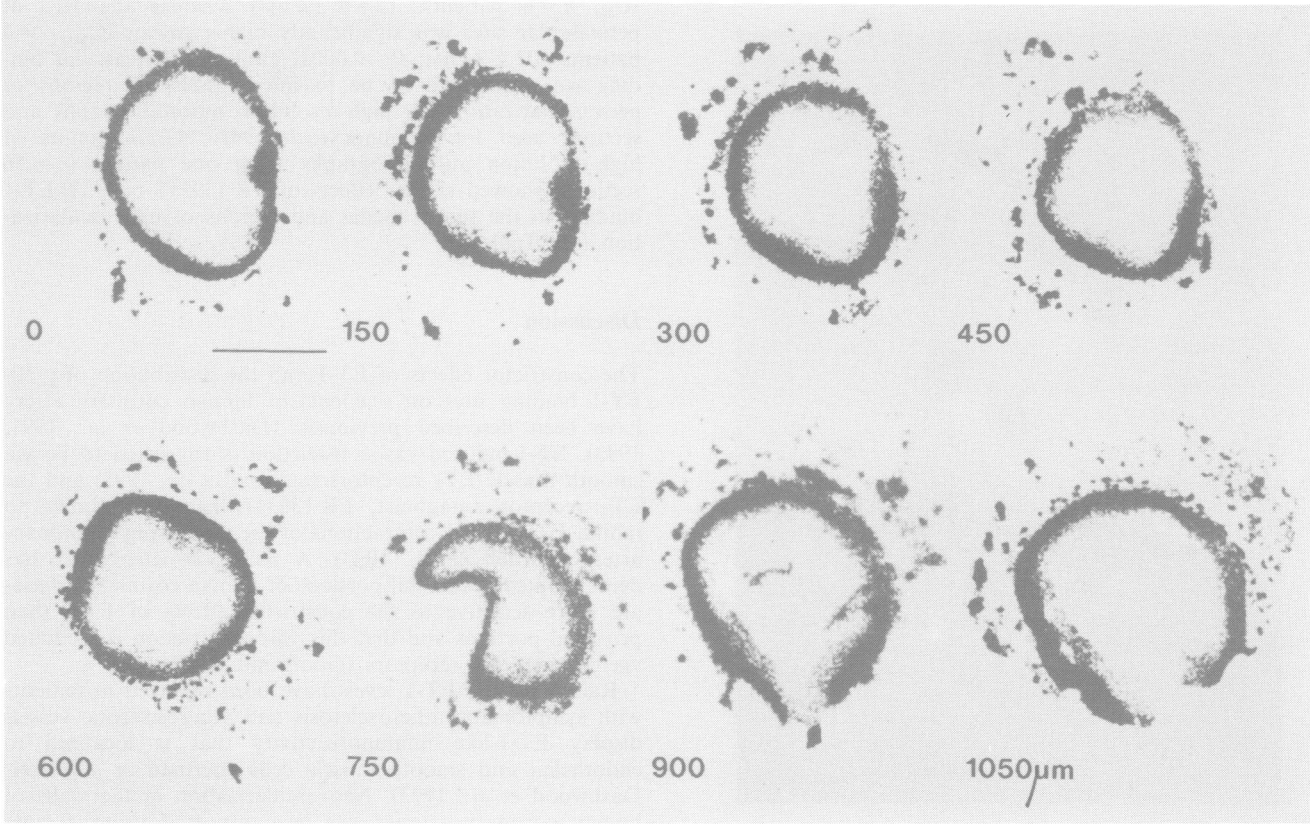

Figure 2 [^{125}I]-endothelin-1 ([^{125}I]-ET-1) binding to perivascular regions of atherosclerotic human coronary artery. Autoradiographs of binding to transverse sections (at 150 μm intervals) through the atheromatous region of a human coronary artery. Tissue incubated in 150 pM [^{125}I]-ET-1; scale bar = 1 mm.

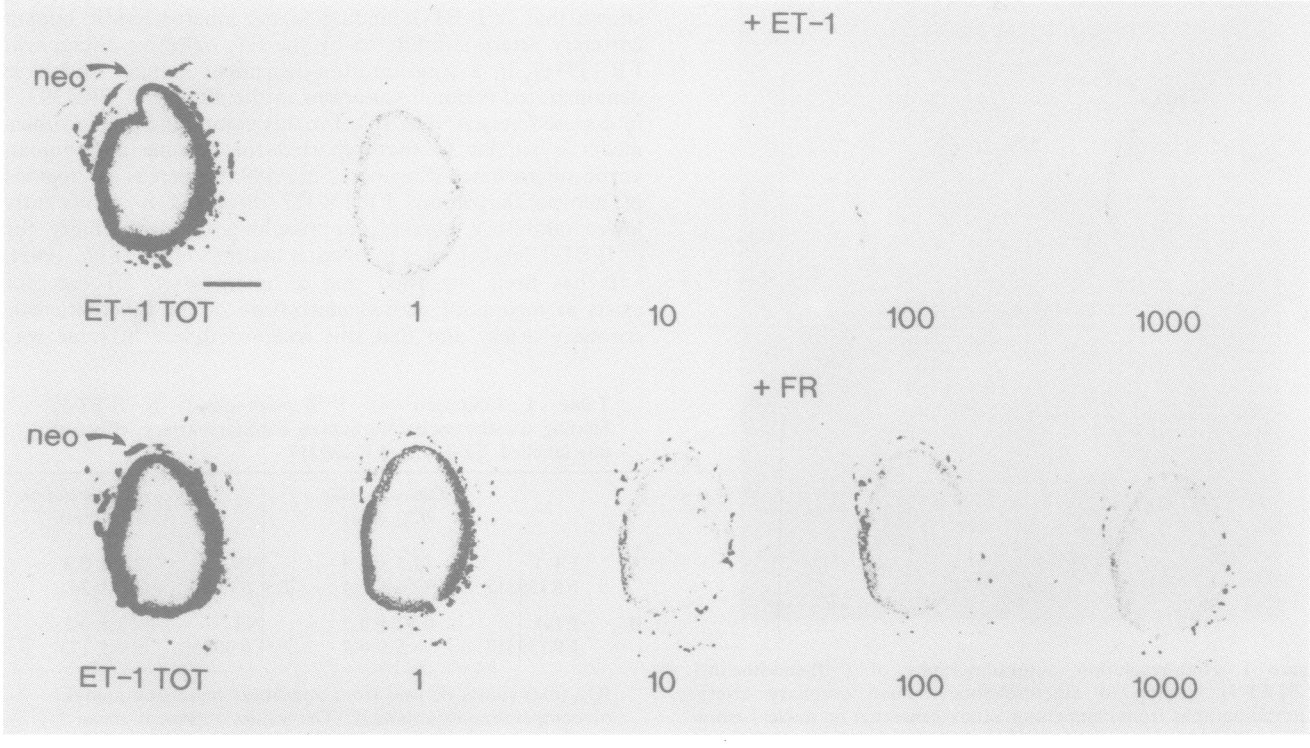

Figure 3 Effects of endothelin-1 (ET-1) and FR139317 (FR) on [^{125}I]-ET-1 binding to atherosclerotic human coronary artery. Above: autoradiographs from consecutive sections incubated in 150 pM [^{125}I]-ET-1 alone (total binding) and in the presence of increasing concentrations of unlabelled ET-1 (1 to 1000 nM). Below: autoradiographs from sections incubated in [^{125}I]-ET-1 in the presence of 1 to 1000 nM FR 139317. Arrows indicate binding to regions of neovascularization; scale bar = 1 mm.

from the binding site at the tunica media (Dashwood *et al.*, 1991). Our results with FR 139317 support this hypothesis and provide evidence that this receptor is not of the ET_A subtype. FR 139317 has a low affinity for ET_B binding sites (Sogabe *et al.*, 1992) and it is possible that this receptor may predominate on microvessels. Alternatively binding may be to non-isopeptide-selective ET receptors (Haynes *et al.*, 1993).

The role of ET at vasa vasorum and regions of neovascularization is so far unclear. ET_B-mediated constriction of resistance vessels has recently been described (Rigel & Lappe, 1993) and it is possible that ET-induced constriction of the vasa vasorum may lead to local ischaemia of the blood vessel wall and subsequent intimal hyperplasia. Whether proliferation of the vasa vasorum precedes or follows plaque formation in diseased vessels is not known. It has been suggested that this vascular proliferation represents an example of the normal tissue response to injury and that neovascularization at regions of plaque in diseased coronary arteries may play a 'fundamental role in the pathogenesis of the atherosclerotic process and its sequelae' (Barger *et al.*, 1984). It is possible that the microvessel binding sites identified in this study are associated with ET-induced vessel growth at regions of coronary artery demonstrating extensive atherosclerotic change.

We thank the British Heart Foundation and Stanley Thomas Johnson Foundation for support and are grateful to the Fujisawa Pharmaceutical Co Ltd, Osaka, Japan for generously supplying FR 139317.

References

BARGER, A.C., BEEUWKES, R. III, LAINEY, L.L. & SILVERMAN, K.J. (1984). Hypothesis: vaso vasorum and neovascularisation of human coronary arteries: a possible role in the pathophysiology of atherosclerosis. *N. Engl. J. Med.*, **310**, 175–177.

BARKER, S.G.E., TALBERT, A., COTTAM, S., BASKERVILLE, P.A. & MARTIN, J.F. (1993). Arterial intimal hyperplasia follows occlusion of the adventitial vasa vasorum in the pig: the potential role of hypoxia in atherogenesis. *Arteriosclerosis*, **13**, 70–77.

CARDELL, L.O., UDDMAN, R. & EDVINSSON, L. (1993). A novel ET_A receptor antagonist, FR 139317, inhibits endothelium-induced contractions of guinea-pig pulmonary arteries, but not trachea. *Br. J. Pharmacol.*, **108**, 448–452.

DASHWOOD, M.R., BARKER, S.G.E., MUDDLE, J.R., YACOUB, M.H. & MARTIN, J.F. (1993). [^{125}I]endothelin-1 binding to vas vasorum and regions of neovascularization in human and porcine blood vessels: a possible role for endothelin in intimal hyperplasia and atherosclerosis. *J. Cardiovasc. Pharmacol.*, **22** (Suppl. 8), S343–347.

DASHWOOD, M.R., SYKES, R.M., MUDDLE, J.R., COLLINS, M.J., PREHAR, S., THEODOROPOULOS, S. & YACOUB, M.H. (1991). Autoradiographic localization of [^{125}I]endothelin binding sites in human blood vessels and coronary tissue: functional correlates. *J. Cardiovasc. Pharmacol.*, **17** (Suppl. 7), S458–462.

GODFRAIND, T. (1993). Evidence for heterogeneity of endothelin receptor distribution in human coronary artery. *Br. J. Pharmacol.*, **110**, 1201–1205.

HAYNES, W.G., DAVENPORT, A.P. & WEBB, D.J. (1993). Endothelin: progress in pharmacology and physiology. *Trends Pharmacol. Sci.*, **14**, 225–228.

KAMAT, B.R., GALLI, S.J., BARGER, A.G., LAINEY, L.L. & SILVERMAN, K.J. (1987). Neovascularization and coronary atherosclerotic plaque: cinematographic localization and quantitative histologic analysis. *Human Pathol.*, **18**, 1036–1042.

LERMAN, A., EDWARDS, B.S., HALLETT, J.W., HEUBLIN, D.M., SANDBERG, S.M. & BURNETT, M.D. (1991). Circulating and tissue endothelin immunoreactivity in advanced atherosclerosis. *N. Engl. J. Med.*, **325**, 997–1001.

MOODY, C.J., DASHWOOD, M.R., SYKES, R.M., CHESTER, M., JONES, S.M., YACOUB, M.H. & HARDING, S.E. (1990). Functional and autoradiographic evidence for endothelin 1 receptors on human and rat myocytes comparison with single smooth muscle cells. *Circ. Res.*, **67**, 764–769.

RIGEL, D.F. & LAPPE, R.W. (1993). Differential responsiveness of conduit and resistance coronary arteries to endothelin A and B receptor stimulation in anesthetized dogs. *J. Cardiovasc. Pharmacol.*, **22** (Suppl. 8), S243–247.

SAKURAI, T., YANAGISAWA, M. & MASAKI, T. (1992). Molecular characterization of endothelin receptors. *Trends Pharmacol. Sci.*, **13**, 103–108.

SOGABE, T., NIREI, H., SHOUBO, M., NOMOTO, A., HENMI, K., NOTSU, Y. & ONO, T. (1992). A novel endothelin receptor antagonist: studies with FR 139317. *Jpn. J. Pharmacol.*, **58** Suppl., 105P.

YANAGISAWA, M. & MASAKI, T. (1989). Molecular biology and biochemistry of the endothelins. *Trends Pharmacol. Sci.*, **10**, 374–379.

(Received January 20, 1994
Accepted February 7, 1994)

Br. J. Pharmacol. (1994), **112**, 390–395

Lithium-induced decrease in spontaneous Ca^{2+} oscillations in single GH_3 rat pituitary cells

[1]Mark A. Varney, Antony Galione & Steve P. Watson

University Department of Pharmacology, Mansfield Road, Oxford OX1 3QT

1 Measurement of $[Ca^{2+}]_i$ in single rat pituitary GH_3 cells by dynamic single cell imaging techniques demonstrated that under basal conditions there is a large variation in the temporal pattern of $[Ca^{2+}]_i$ signalling between individual cells ranging from high frequency asynchronous oscillations to quiescence.

2 We have reported previously that treatment of GH_3 cells with 1 mM Li^+ (a concentration used therapeutically in the treatment of manic depression) for 7 days reduces basal and thyrotrophin-releasing hormone (TRH)-stimulated levels of mass inositol 1,4,5-trisphosphate [Ins(1,4,5)P_3]. In the present study, we show that this is associated with a reduction in the number of cells exhibiting basal Ca^{2+} oscillations over a sampling period of 60 s, whereas the maximum amplitude of oscillations is unaffected.

3 The pattern of $[Ca^{2+}]_i$ responses to the agonist TRH varied considerably between individual cells, making quantitation of the responses difficult; however, data obtained from measurements made on a population of cells showed that increases in peak $[Ca^{2+}]_i$ induced by high concentrations of TRH were reduced in cells treated with 1 mM Li^+ for 7 days relative to control cells.

4 The sensitivity of the phosphoinositide pathway to $[Ca^{2+}]_i$ was investigated by loading GH_3 cells with BAPTA/AM at a concentration sufficient to lower 'basal' $[Ca^{2+}]_i$ in a population of cells and to inhibit agonist-stimulated increases in $[Ca^{2+}]_i$. Under these conditions, basal and TRH-stimulated mass Ins(1,4,5)P_3 levels were unaffected.

5 These results demonstrate that a 7-day Li^+ treatment leads to an alteration in Ca^{2+} signalling, in particular by reducing the number of cells exhibiting high frequency Ca^{2+} oscillations under basal conditions. The significance of these results to the clinical effectiveness of Li^+ in the treatment of manic depression is discussed.

Keywords: Rat pituitary; GH_3 cells; lithium; Ca^{2+} oscillations; inositol 1,4,5-trisphosphate; TRH; BAPTA

Introduction

Lithium ions are used therapeutically at a serum level of approximately 1 mM in the treatment of manic depression to alleviate both the manic and depressive phases of this disorder (reviewed in Wood & Goodwin, 1987). The mechanism by which Li^+ produces its therapeutic effects is not known although there is evidence for inhibition of the adenylyl cyclase (Newman & Belmaker, 1987) and phosphoinositide pathways (Berridge *et al.*, 1982; 1989) and it has been proposed that these effects are mediated at the level of G-proteins (Avissar *et al.*, 1988). However, this does not provide an explanation for the selectivity of action of Li^+ to manic depressive disease and a more widely accepted hypothesis is the ability of Li^+ to inhibit metabolism of certain inositol phosphates. At therapeutic concentrations, Li^+ uncompetitively inhibits inositol monophosphatase (Hallcher & Sherman, 1980), a key enzyme in the metabolism of inositol monophosphates. Inhibition of this enzyme by Li^+ leads to a large accumulation of inositol monophosphates in rat brain, and a corresponding reduction in inositol levels (Allison & Stewart, 1971; Allison *et al.*, 1976). In tissues which have access to limited supplies of inositol, such as brain because of the relatively poor ability of inositol to cross the blood brain barrier, reduced inositol levels may lead to reduced synthesis of phosphoinositides, and ultimately impair receptor-stimulated phosphoinositide activity by reducing production of the Ca^{2+}-mobilizing second messenger Ins(1,4,5)P_3 and 1,2-diacylglycerol which activates protein kinase C (Berridge *et al.* 1982; 1989). In support of this, the majority of studies have reported a reduction in agonist-stimulated generation of inositol phosphates and mass Ins(1,4,5)P_3 in brain slices following chronic treatment with Li^+ (reviewed by Nahorski *et al.*, 1991), although an enhanced accumulation of Ins(1,4,5)P_3 has been described in a few cases (Whitworth *et al.*, 1990; Lee *et al.*, 1992; Dixon *et al.*, 1992).

In order to investigate the interaction of Li^+ with the phosphoinositide cycle in further detail, we have previously set up a model using rat pituitary GH_3 cells. These cells were chosen because, like neurones, they are electrically excitable neurosecretory cells giving robust Ca^{2+} and phosphoinositide responses. Using these cells we have previously shown that chronic treatment with 1 mM Li^+ reduces both basal and agonist-stimulated levels of mass Ins(1,4,5)P_3 and that this is correlated with a reduction in Ca^{2+} signalling and prolactin secretion (Varney *et al.*, 1992). The magnitude of the inhibitory effects observed, however, were relatively small (~20% inhibition), although we suggested that heterogeneity may exist between cells in their susceptibility to Li^+. In this study we have addressed this by examining the effect of Li^+ treatment on Ca^{2+} signalling in individual GH_3 cells using dynamic Ca^{2+} imaging techniques.

Methods

Li^+ treatment of rat pituitary cells

Rat pituitary GH_3 cells were grown in Hams F10 medium supplemented with 16% foetal calf serum. For experiments however, cells were seeded into either flasks or 16-well plates and grown in inositol-free Hams F10 medium (Gibco BRL) supplemented with 5% foetal calf serum either in the absence or presence of 1 mM LiCl as described previously (Varney *et al.*, 1992). All experiments were performed after a period of 7 days of treatment with Li^+. Measurements of mass Ins(1,4,5)P_3 was generally performed in multiwell plates,

[1] Author for correspondence at present address: Institute de Recherche Servier, Centre de Recherches de Croissy, 125, Chemin de Ronde, 78290 Croissy sur Seine, France.

although essentially identical results were obtained with cellular suspensions following removal of cells from flasks by incubation with trypsin.

Where appropriate, cells were loaded with BAPTA either by incubation with 100 μM BAPTA/AM alone or with 100 μM BAPTA/AM and 1 μM fura-2/AM (for Ca^{2+} measurements). After 45 min incubation cells were washed, resuspended in fresh buffer, and mass Ins(1,4,5)P_3 and population $[Ca^{2+}]_i$ levels measured as described previously (Varney *et al.*, 1992).

Measurement of cytosolic free Ca^{2+} in single GH_3 cells

Cytosolic Ca^{2+} levels ($[Ca^{2+}]_i$) were measured in GH_3 cells using the Ca^{2+}-sensitive dye fura-2. Measurements of $[Ca^{2+}]_i$ were carried out in cells grown on borosilicate glass coverslips. After 4 to 5 days in culture, cells were loaded with 3 μM fura-2/AM in 3 ml of Hanks buffer in the presence of 0.1% Pluronic for 45 min at room temperature. Coverslips were washed twice in Hanks buffer, left for a further 10 min, and transferred to a Teflon coverslip holder (Digitimer Ltd.; Welwyn Garden City, Herts). All $[Ca^{2+}]_i$ measurements were performed at 22°C. The coverslip dish was placed on the stage of a Zeiss Axiovert 35 inverted microscope equipped for fluorescence microscopy. A 75 W xenon arc lamp combined with interference filters of 350 and 380 nm, present in a filter wheel changer (Ludl Electronic Products Ltd., Hawthorne, New York) was used for excitation of the loaded fura-2. Excitation light was deflected by a dichroic mirror (Zeiss FT 395 nm) into the microscope objective (× 40 Achrostigmat oil immersion lens; n.a. 1.30) and onto the sample. Excited light was collected from the sample through the dichroic mirror and a 510 nm interference filter and directed into an intensified CCD camera (Extended ISIS-M; Photonic Science, U.K.). Care was taken to attenuate the excitation light as much as possible to avoid bleaching of the dye and photodamage to cells. Pairs of images were captured every 2–3 s with an image grabbing board (PixelPipeline; Perceptics Corp., Knoxville, TN, U.S.A.) fitted to an Apple Macintosh Quadra 900 and controlled by the software IonVision (Improvision, Coventry). Four frames were normally averaged at each excitation wavelength, and the 350/380 nm ratio calculated for each pair of images after subtraction of the backgrounds. The mean $[Ca^{2+}]_i$ levels were calculated from each ratio image using the software IonVision. Calibration of the signals as a function of $[Ca^{2+}]_i$ was performed with standard Ca^{2+} solutions (Williams & Fay, 1990), and a viscosity correction factor determined and applied as described by Poenie (1990).

Agonists were added directly to the coverslip chamber at the appropriate time with a Gilson pipette. A relatively large volume of agonist was added to the chamber so as to ensure rapid mixing (i.e. 0.5 ml agonist added to 2.5 ml bath volume).

Statistical analysis

Results are shown as mean ± s.e.mean of at least three separate experiments. Statistical analysis were performed by the Wilcoxon Rank sum test, or Student's *t* test following a non-significant Wilk-Shapiro Normality test. Statistical significance was taken as $P < 0.05$.

Materials

[^{3}H]-Ins(1,4,5)P_3 (specific activity 17-54 Ci mmol^{-1}) was obtained from New England Nuclear or Amersham International. Fura-2/AM and BAPTA/AM were obtained from Molecular Probes. Thyrotrophin-releasing hormone (TRH) and Ins(1,4,5)P_3 were purchased from Sigma. Tissue culture

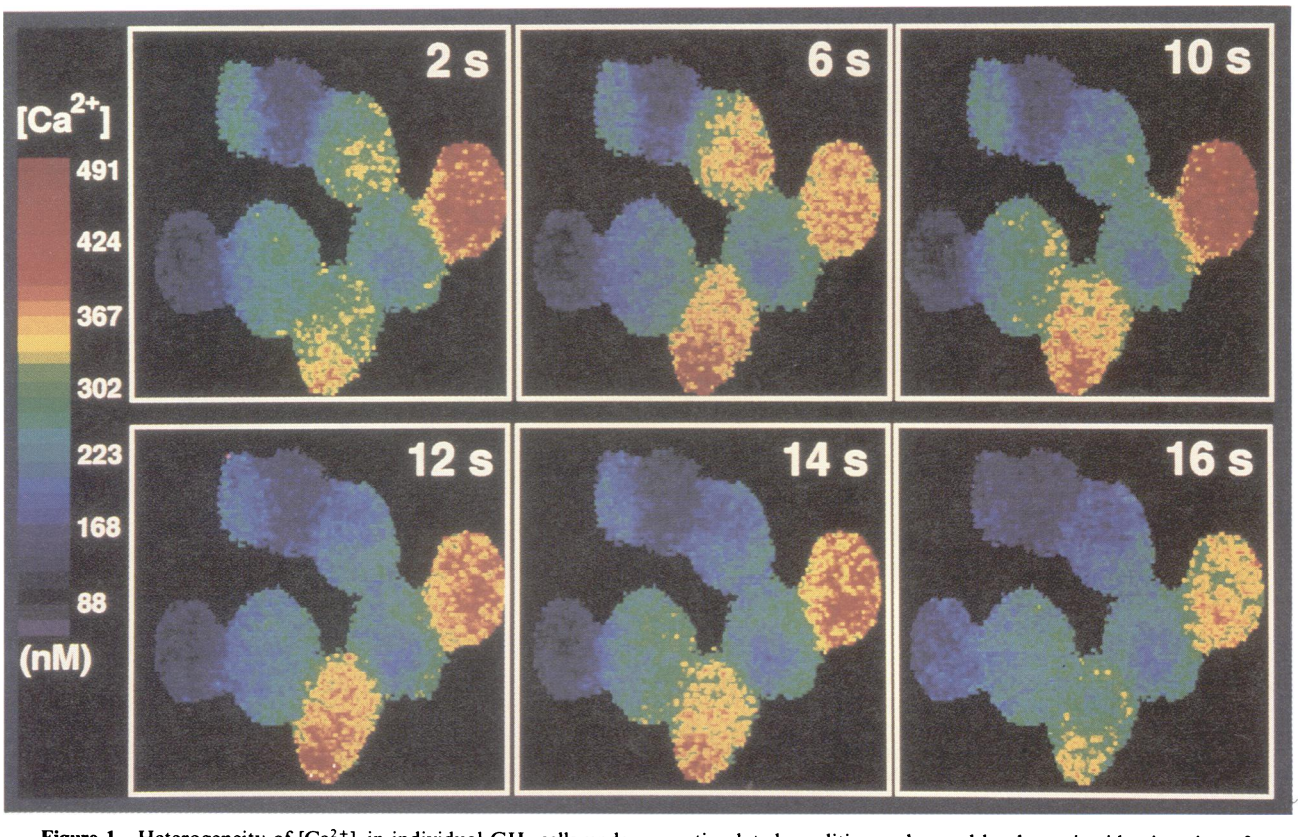

Figure 1 Heterogeneity of $[Ca^{2+}]_i$ in individual GH_3 cells under non-stimulated conditions, observed by dynamic video-imaging of fura-2 at various time points (indicated on each time frame). The images are the ratios of those observed at 350 nm and 380 nm, following background subtraction, and calibrated against Ca^{2+} standards, as described in the Methods section. Images are displayed in pseudocolour, with red representing high Ca^{2+}, and blue low Ca^{2+}.

reagents such as medium (including custom-made inositol-free Hams F10) were obtained from GIBCO, and plastic tissue culture equipment from Griffiths & Neilson. All other standard laboratory reagents were of Analytical grade.

Results

Single cell $[Ca^{2+}]_i$ measurements

Measurement of Ca^{2+} revealed a wide variation in basal levels of $[Ca^{2+}]_i$ between individual cells as exemplified in Figure 1; some cells appeared quiescent since $[Ca^{2+}]_i$ levels did not change significantly over the recording period, whilst others exhibited frequent, irregular spontaneous oscillations in $[Ca^{2+}]_i$. Two extreme examples of this behaviour are shown in Figure 2a. In order to examine the action of Li^+ on individual cells, the mean $[Ca^{2+}]_i$ throughout a 60 s recording period was measured in 370 cells treated with 1 mM Li^+ for 7 days and compared to the same number of control cells. The frequency distribution histogram of mean $[Ca^{2+}]_i$ levels over a 60 s recording period revealed a clear shift to the left in the Li^+-treated group (Figure 2b). When results in individual cells were pooled, cells treated with Li^+ had a significantly ($P<0.05$) lower mean $[Ca^{2+}]_i$ of 160 ± 7 nM as compared to 195 ± 9 nM in control cells (Figure 3a) a result which is similar to values previously obtained in whole cell populations (Varney *et al.*, 1992). This reduction in intracellular Ca^{2+} did not appear to be due to a change in cell viability as

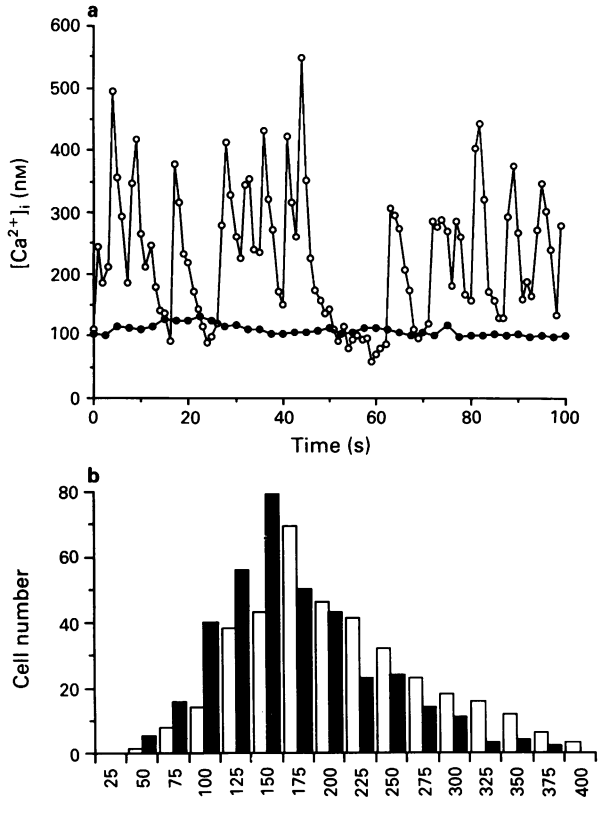

Figure 2 (a) A time-course of $[Ca^{2+}]_i$ levels in 2 individual cells, one of which displays $[Ca^{2+}]_i$ oscillations (○), whilst the other is quiescent (●). A pair of images were acquired every 2 s, and $[Ca^{2+}]_i$ levels calculated by image analysis of the time-sequence of images. (b) A frequency distribution histogram of mean $[Ca^{2+}]_i$ levels in GH_3 cells under non-stimulated conditions, recorded over a 60 s period, with images acquired every 2 s. Mean $[Ca^{2+}]_i$ levels were assigned into groups which differed by 25 nM (i.e. 0–25, 26–50, etc) for a total of 370 control cells (open columns) and 370 chronic Li^+-treated cells (solid columns) Numbers on the abscissa scale refer to the upper limit of the range.

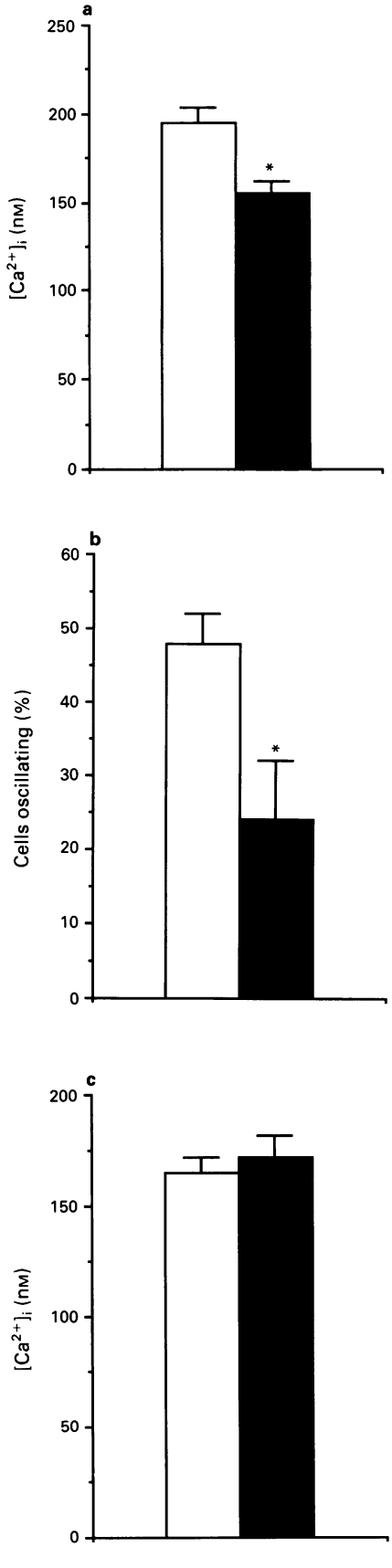

Figure 3 Summary of $[Ca^{2+}]_i$ measurement in control GH_3 cells (open columns) and chronic Li^+-treated cells (solid columns). (a) Mean basal $[Ca^{2+}]_i$, (b) numbers of cells showing $[Ca^{2+}]_i$ oscillations, and (c) the mean maximum amplitude of these $[Ca^{2+}]_i$ oscillations. Data are summarised from 370 control and Li^+-treated cells, obtained from 21 experiments; values are mean with s.e.mean. *represents a significantly different value from the control value ($P<0.05$).

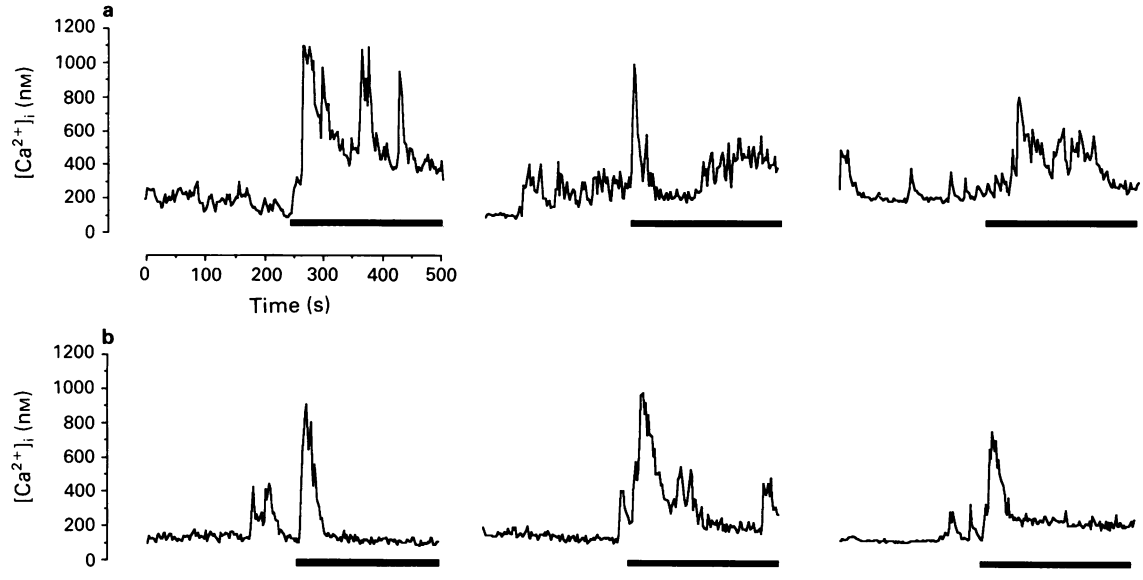

Figure 4 $[Ca^{2+}]_i$ measurements in GH_3 cells. (a) Example traces of basal $[Ca^{2+}]_i$ levels, and 1 μM TRH-stimulated levels (indicated by the solid bar), in both control (a) and chronic Li^+-treated cells (b). Note the variability of $[Ca^{2+}]_i$ levels between cells under basal conditions, and in response to TRH. Calibration bars indicating $[Ca^{2+}]_i$ and time are shown, and apply to all traces.

both groups of cells exhibited a similar ability to exclude trypan blue (not shown).

A more detailed analysis of basal $[Ca^{2+}]_i$ levels was performed through the study of Ca^{2+} oscillations in individual GH_3 cells. Since the Ca^{2+} oscillations were not easily defined into individual oscillations or patterns (see Figure 2a), their frequency could not be reliably calculated, and instead, cells were defined as either oscillating or quiescent. A change in $[Ca^{2+}]_i$ of greater than 100 nM over a 60 s recording period was taken to define a cell as oscillating. The maximum amplitude (maximum minus minimum $[Ca^{2+}]_i$ level) was also measured from cells which were defined as oscillating. This analysis revealed that under non-stimulated conditions 48 ± 4% of control cells showed oscillations in Ca^{2+} and that following Li^+ treatment this number was significantly reduced to 24 ± 8% ($P<0.05$; Figure 3b). The maximal amplitude of oscillations, however, was unaffected in cells which displayed Ca^{2+} oscillations in the two treatment regimes (Figure 3c). This decrease in frequency of basal Ca^{2+} oscillations can also be seen by comparison of the representative Ca^{2+} traces in single GH_3 cells before agonist stimulation (Figure 4).

TRH-stimulated $[Ca^{2+}]_i$ responses varied considerably between individual GH_3 cells. Although, the majority of cells responded to TRH with a rapid peak increase in $[Ca^{2+}]_i$, this was followed by more variable behaviour with some cells showing an increase and some a decrease in frequency of oscillations, while in others, a maintained increase in $[Ca^{2+}]_i$ was observed (see Figure 4 for example traces). This heterogeneity in $[Ca^{2+}]_i$ responses to TRH prevented a detailed quantitative analysis of traces from single cell experiments. However, measuring the mean of TRH-stimulated $[Ca^{2+}]_i$ responses from many individual cells revealed that a high concentration of TRH (1 μM) induces a larger peak Ca^{2+} response in control cells (658 ± 59 nM), as compared to Li^+-treated cells (492 ± 49 nM, $n = 5$, 15–20 observations per experiment: $P<0.05$). This small (~25%) inhibitory effect of Li^+ against high concentrations of TRH is similar to that described previously in a population of cells (Varney *et al.*, 1992).

Effect of $[Ca^{2+}]_i$ levels on mass Ins(1,4,5)P_3

When cells were loaded with 100 μM BAPTA/AM for 30 min, there was a reduction in basal $[Ca^{2+}]_i$ in cell suspensions from

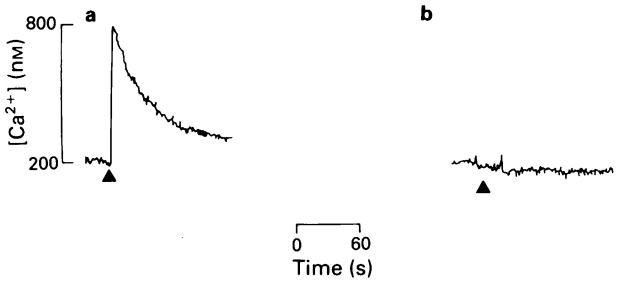

Figure 5 Effect of TRH (100 nM) on $[Ca^{2+}]_i$ responses in control (a) and BAPTA-loaded cells (b) obtained from recordings made from a whole coverslip. Traces are representative of two further experiments. The addition of the agonist is shown by the arrow head, and the relevant $[Ca^{2+}]_i$ calibration bar is shown alongside the traces.

209 ± 17 to 57 ± 7 nM ($n = 3$, 12 observations) and little or no detectable increase in $[Ca^{2+}]_i$ was observed in BAPTA-loaded cells on challenge with TRH (100 nM) or K^+ (70 mM) (see Figure 5 for example traces). In contrast, mass Ins(1,4,5)P_3 levels were similar in control (12.4 ± 1.4 pmol mg^{-1} protein) and BAPTA-treated cells (11.3 ± 1.2 pmol mg^{-1} protein), and in control (36.6 ± 3.2 pmol mg^{-1} protein) and BAPTA-loaded cells (43.7 ± 3.5 pmol mg^{-1} protein) challenged with 100 nM TRH for 10 s.

Discussion

$[Ca^{2+}]_i$ measurements

In a previous study we demonstrated that chronic treatment of GH_3 cells with a therapeutic concentration of Li^+ reduced basal and agonist-stimulated intracellular Ca^{2+} levels in a suspension of GH_3 cells (Varney *et al.*, 1992). In this study we have extended these observations to single cells using dynamic video imaging techniques. The results demonstrate a marked heterogeneity in $[Ca^{2+}]_i$ signalling between single GH_3 cells. A sub-population of cells exhibit spontaneous, irregular $[Ca^{2+}]_i$ oscillations under basal conditions which are asynchronous with respect to neighbouring cells. Although

the limited sampling period used in this study (60 s) may underestimate the actual percentage of cells displaying $[Ca^{2+}]_i$ oscillations, our result that approximately 50% of the GH_3 cell population display oscillations within this period is in agreement with results obtained for GH_4C_1 cells where considerably longer sampling times were used (Wagner *et al.*, 1993). The number of cells exhibiting $[Ca^{2+}]_i$ oscillations in the recording period was reduced in cells treated with Li^+, although the amplitude of the oscillations in the remaining cells was not changed. The present results, therefore, demonstrate that the previously reported decrease in 'basal' Ca^{2+} observed in a suspension of GH_3 cells following Li^+ treatment (Varney *et al.*, 1992) is mediated by either a reduction in the frequency of spontaneous $[Ca^{2+}]_i$ oscillations or an increase in the sub-population of cells exhibiting quiescent behaviour.

We have shown previously that chronic Li^+ treatment of GH_3 cells results in a decrease in basal and TRH-stimulated levels of mass Ins(1,4,5)P_3. Since the role of Ins(1,4,5)P_3 is to release Ca^{2+} from intracellular stores, the altered Ca^{2+} signalling in GH_3 cells following Li^+ treatment might be explained by a Li^+-induced decrease in phosphoinositide turnover. An alternative explanation that the Li^+-induced decrease in Ca^{2+} signalling results in a decreased phosphoinositide pathway activity seems unlikely as BAPTA-loaded cells did not exhibit reduced basal or TRH-stimulated levels of Ins(1,4,5)P_3 despite a marked reduction in intracellular Ca^{2+}. Consistent with this, increasing $[Ca^{2+}]_i$ levels using high K^+ or addition of a Ca^{2+} ionophore did not alter basal or TRH-stimulated formation of [^{3}H]-inositol phosphates (M.A.V., unpublished observations). These data argue against a role for Ca^{2+} in the regulation of phospholipase C in GH_3 cells.

The reduction in $[Ca^{2+}]_i$ oscillations under non-stimulated conditions may underlie the decrease in 'basal' prolactin secretion reported previously following Li^+-treatment (Varney *et al.*, 1992) as $[Ca^{2+}]_i$ oscillations are believed to control basal secretion in GH_3 cells (Schlegel *et al.*, 1987). The previously reported reduction in basal level of Ins(1,4,5)P_3 following Li^+-treatment (Varney *et al.*, 1992) may be responsible for the reduced $[Ca^{2+}]_i$ oscillations. In GH_3 cells, Ca^{2+} oscillations are completely dependent on the presence of extracellular Ca^{2+} since they are blocked by addition of dihydropyridine calcium channel blockers e.g. nifedipine, or by the lowering of extracellular Ca^{2+} (Schlegel *et al.*, 1987; Wagner *et al.*, 1993). Ca^{2+} oscillations are thus driven by entry of Ca^{2+} through voltage-dependent Ca^{2+} channels. Recent models of Ca^{2+} oscillations suggest that Ca^{2+} enhances its own release through a process of Ca^{2+}-induced Ca^{2+} release (CICR) through ryanodine and Ins(1,4,5)P_3 receptors (reviewed by Berridge, 1993). Ins(1,4,5)P_3-sensitive stores become more sensitive to Ins(1,4,5)P_3 as they fill up with Ca^{2+}, and once the Ca^{2+} reaches a critical amount the basal levels of Ins(1,4,5)P_3 may be sufficient to release Ca^{2+} through a process of CICR (Missiaen *et al.*, 1991). Thus in GH_3 cells, the voltage-dependent entry of Ca^{2+} through spontaneous action potentials may serve to prime the Ins(1,4,5)P_3-sensitive stores such that basal levels of Ins(1,4,5)P_3 are sufficient to cause Ca^{2+} release, resulting in the initiation of an oscillation. However, in Li^+-treated cells, lower basal levels of Ins(1,4,5)P_3 effectively reduce the sensitivity of the stores, resulting in a longer period between Ca^{2+} discharge and therefore a reduction in the frequency of $[Ca^{2+}]_i$ oscillations.

In conclusion, these results show that treatment of GH_3 cells with low concentrations of Li^+ reduces the likelihood of spontaneous $[Ca^{2+}]_i$ oscillations in single rat pituitary GH_3 cells. An inhibitory action of an acute treatment with Li^+ on oscillatory changes in a Ca^{2+}-activated Cl^- current in blowfly salivary gland has also been described (Galione & Berridge, 1988). It can be speculated that the reduced levels of Ins(1,4,5)P_3 observed in rat cerebral cortex following chronic treatment with Li^+ may also lead to a decrease in Ca^{2+} signalling (Varney *et al.*, 1992). The observation that $[Ca^{2+}]_i$ oscillations occur in neurones (Murphy & Miller, 1989; Friel & Tsien, 1992) and glia (Cornell-Bell *et al.*, 1990), and that CICR may play an important role within neurones (Marrion & Adams; 1992), suggest that changes in Ca^{2+} mobilization will induce a change in neuronal activity. Changes in basal Ca^{2+} levels can also influence responses to agonists. For example, in acinar cells the pattern of agonist-induced Ca^{2+} oscillations is dependent on basal Ca^{2+} levels (Toescu *et al.*, 1993), while hippocampal neurones with higher resting levels of $[Ca^{2+}]_i$ show increased responses to NMDA and K^+ depolarization (Nakajima *et al.*, 1993). An altered Ca^{2+} signalling may therefore be an important modulatory mechanism in Li^+-sensitive cells.

This work was supported by Bristol-Myers Squibb Incorporation. S.P.W. is a Royal Society University Research Fellow. A.G. is a Beit Fellow.

References

ALLISON, J.H. & STEWART, M.A. (1971). Reduced brain inositol in lithium-treated rats. *Nature*, **233**, 267–268.

ALLISON, J.H., BLISNER, M.E., HOLLAND, W.H., HIPPS, P.P. & SHERMAN, W.R. (1976). Increased brain *myo*-inositol 1-phosphate in lithium-treated rats. *Biochem. Biophys. Res. Commun.*, **71**, 664–670.

AVISSAR, S., SCHREIBER, G., DANSON, A. & BELMAKER, R.H. (1988). Lithium inhibits adrenergic and cholinergic increases in GTP binding in rat cortex. *Nature*, **331**, 440–442.

BERRIDGE, M.J. (1993). Inositol trisphosphate and calcium signalling. *Nature*, **361**, 315–325.

BERRIDGE, M.J., DOWNES, C.P. & HANLEY, M.R. (1982). Lithium amplifies agonist-dependent phosphatidylinositol responses in brain and salivary glands. *Biochem. J.*, **206**, 587–595.

BERRIDGE, M.J., DOWNES, C.P. & HANLEY, M.R. (1989). Neural and developmental actions of lithium: a unifying hypothesis. *Cell*, **59**, 411–419.

CORNELL-BELL, A.H., FINKBEINER, S.M., COOPER, M.S. & SMITH, S.J. (1990). Glutamate induces calcium waves in cultured astrocytes: long-range glial signalling. *Science*, **247**, 470–473.

DIXON, J.F., LEE, C.H., LOS, G.V. & HOKIN, L.E. (1992). Lithium enhances accumulation of [^{3}H]inositol radioactivity and mass of second messenger inositol 1,4,5-trisphosphate in monkey cerebral cortex slices. *J. Neurochem.*, **59**, 2332–2335.

FRIEL, D.D. & TSIEN, R.W. (1992). Phase-dependent contributions from Ca^{2+} entry and Ca^{2+} release to caffeine-induced $[Ca^{2+}]_i$ oscillations in bullfrog sympathetic neurones. *Neuron*, **8**, 1109–1125.

GALIONE, A.G. & BERRIDGE, M.J. (1988). Pharmacological modulation of oscillations in the blowfly salivary gland. *Biochem. Soc. Trans.*, **16**, 987–989.

HALLCHER, L.M. & SHERMAN, W.R. (1980). The effects of lithium ion and other agents on the activity of myo-inositol-1-phosphatase from bovine brain. *J. Biol. Chem.*, **255**, 10896–10901.

LEE, C.H., DIXON, J.F., REICHMAN, M., MOUMMI, C., LOS, G. & HOKIN, L.E. (1992). Li^+ increase accumulation of inositol 1,4,5-trisphosphate and inositol 1,3,4,5-tetrakisphosphate in cholinergically stimulated brain slices in guinea-pig, mouse and rat. *Biochem. J.*, **282**, 377–385.

MARRION, N.V. & ADAMS, P.R. (1992). Release of intracellular Ca^{2+} and modulation of membrane currents by caffeine in Bull-frog sympathetic neurones. *J. Physiol.*, **445**, 515–535.

MISSIAEN, L., TAYLOR, C.W. & BERRIDGE, M.J. (1991). Spontaneous calcium release from inositol trisphosphate-sensitive stores. *Nature*, **352**, 241–244.

MURPHY, S.N. & MILLER, R.J. (1989). Two distinct quisqualate receptors regulate Ca^{2+} homeostasis in hippocampal neurones *in vitro*. *Mol. Pharmacol.*, **35,** 671–680.

NAHORSKI, S.R., RAGAN, C.I. & CHALLISS, R.A.J. (1991). Lithium and the phosphoinositide cycle: an example of uncompetitive inhibition and its pharmacological consequences. *Trends Pharmacol. Sci.*, **12,** 297–303.

NAKAJIMA, K., HARADA, K., EBINA, Y., YOSHIMURA, T., ITO, H., BAN, T. & SHINGAI, R. (1993). Relationship between resting cytosolic Ca^{2+} and responses induced by *N*-methyl-D-aspartate in hippocampal neurones. *Brain Res.*, **603,** 321–323.

NEWMAN, M.E. & BELMAKER, R.H. (1987). Effects of lithium *in vitro* and *in vivo* on components of the adenylate cyclase from rat brain. *Neuropharmacol.*, **26,** 211–217.

POENIE, M. (1990). Alteration of intracellular Fura-2 fluorescence by viscosity: A simple correction. *Cell Calcium*, **11,** 85–92.

SCHLEGEL, W., WINIGER, B.P., MOLLARD, P., VACHER, P., WUARIN, F., ZAHND, G.R., WOLLHEIM, C. & DUFY, B. (1987). Oscillations of cytosolic Ca^{2+} in pituitary cells due to action potentials. *Nature*, **329,** 719–721.

TOESCU, E.C., LAWRIE, A.M., GALLACHER, D.V. & PETERSON, O.H. (1993). The pattern of agonist-evoked cytosolic Ca^{2+} oscillations depends on the resting intracellular Ca^{2+} concentration. *J. Biol. Chem.*, **268,** 18654–18658.

VARNEY, M.A., GODFREY, P.P., DRUMMOND, A.H. & WATSON, S.P. (1992). Chronic lithium treatment inhibits basal and agonist-stimulated responses in rat cerebral cortex and GH_3 cells. *Mol. Pharmacol.*, **42,** 671–678.

WAGNER, K.A., YACONO, P.W., GOLAN, D.E. & TASHJIAN, H. (1993). Mechanism of spontaneous intracellular calcium fluctuations in single GH_4C_1 rat pituitary cells. *Biochem. J.*, **292,** 175–182.

WHITWORTH, P., HEAL, D.J. & KENDALL, D.A. (1990). The effects of acute and chronic lithium treatment on pilocarpine-stimulated phosphoinositide hydrolysis in mouse brain *in vivo*. *Br. J. Pharmacol.*, **101,** 39–44.

WILLIAMS, D.A. & FAY, F.S. (1990). Intracellular calibration of the fluorescent calcium indicator Fura-2. *Cell Calcium*, **11,** 75–84.

WOOD, A.J. & GOODWIN, G.M. (1987). A review of the biochemical and neuropharmacological actions of lithium. *Psychol. Med.*, **17,** 579–600.

(Received January 5, 1994
Accepted February 2, 1994)

Br. J. Pharmacol (1994), **112**, 396–402

Induction of nitric oxide synthase in cultured vascular smooth muscle cells: the role of cyclic AMP

K. Hirokawa, K. O'Shaughnessy, K. Moore, P. Ramrakha & [1]M.R. Wilkins

Department of Clinical Pharmacology, Royal Postgraduate Medical School, Du Cane Rd, London W12 0NN

1 Interleukin-1β (IL-1β) is a potent stimulant of inducible nitric oxide synthase (iNOS) mRNA and nitric oxide (NO) production in vascular smooth muscle (VSM) cells in culture. These studies investigate the role of adenosine 3':5'-cyclic monophosphate (cyclic AMP) in this process.

2 Dibutyryl cyclic AMP (db cyclic AMP, 0.1–1 mM), forskolin (1–10 μM) and the phosphodiesterase inhibitor, Ro 20-1724 (1–10 μM), all of which increase intracellular cyclic AMP, had no effect on NO production when added alone but markedly enhanced NO production by IL-1β-stimulated VSM cells in a dose-dependent manner. Consistent with a cyclic AMP-mediated action, isoprenaline (1–10 μM) increased NO production from IL-1β-stimulated cells. Dibutyryl cyclic GMP (db cyclic GMP) had no effect at concentrations up to 1 mM.

3 Pursuing these observations, iNOS protein levels were examined by Western blot analysis and iNOS mRNA levels were measured by reverse transcription and amplification of the resultant cDNA using the polymerase chain reaction. In addition to enhancing NO production, db cyclic AMP increased iNOS protein and mRNA above that produced by IL-1β alone.

4 These data demonstrate a major effect of cyclic AMP on cytokine-induced NOS activity in VSM cells, mediated at least in part by regulating synthesis of iNOS, and has implications for the pathogenesis and management of septic shock.

Keywords: Nitric oxide; nitric oxide synthase; cyclic AMP; mRNA; polymerase chain reaction; vascular smooth muscle

Introduction

Nitric oxide (NO) is a potent vasodilator produced locally in the vessel wall from L-arginine by the action of nitric oxide synthase (NOS) (Moncada *et al.*, 1991). Two major subtypes of NOS have been described. One subtype is calcium-dependent, expressed constitutively in endothelium and produces picomol amounts of NO. A second form of NOS is calcium-insensitive and can be induced in endothelium and vascular smooth muscle cells by endotoxin and some cytokines to generate nanomol quantities of NO.

It is now clear that induction of NOS synthesis and markedly increased NO production play a primary role in the pathogenesis of septic shock. This condition is characterized by pronounced hypotension which is resistant to treatment with vasoconstrictor agents. In contrast, inhibition of NO production with the L-arginine analogue, L-monomethyl-arginine, has been shown to increase blood pressure in this condition (Petros *et al.*, 1991) and has indicated a novel therapeutic strategy. Reservations have been expressed, however, about the value of global inhibition of NO synthesis (Nava *et al.*, 1991) as NO released from other cells, such as macrophages, may be important in combating infection. Specific inhibition of iNOS activity in vascular tissues requires a better understanding of the factors governing the expression and function of this enzyme. Some progress has been made in elucidating factors regulating iNOS activity in endothelial, macrophage and neuronal cell lines (Nakane *et al.*, 1991; Brune & Lapetina, 1991; Gaillard *et al.*, 1991; 1992; Bredt *et al.*, 1992; Severn *et al.*, 1992; Marotta *et al.*, 1992; Hortelano *et al.*, 1992; 1993; Feinstein *et al.*, 1993). One factor that appears to play a role in regulating NO production is adenosine 3':5'-cyclic monophosphate (cyclic AMP) but the effect of increasing cyclic AMP levels appears to differ in different tissues such that it is not possible to extrapolate from these studies to VSM cells. The purpose of this study was to examine the effect of increasing cyclic AMP on cytokine-stimulated iNOS activity in vascular smooth muscle (VSM) cells.

[1] Author for correspondence.

Methods

Isolation and primary culture of rat aortic smooth muscle cells

VSM cells were harvested from enzymatically dissociated rat thoracic aorta according to the method of Beasley *et al.* (1991) with some minor modifications. The thoracic aorta was excised under sterile conditions from male Wistar rats (300–350 g) and placed in ice cold Dulbecco's Phosphate Buffered Saline (PBS, Ca^{2+} and Mg^{2+}-free) with penicillin-streptomycin 200 u ml^{-1} and amphotericin B 25 μg ml^{-1}. The aorta was washed and transferred into a petri dish containing Hanks Balanced Salt Solution (HBSS). Fat, connective tissue, and adventitia were removed by blunt dissection. The cleaned aortae were opened and the endothelium carefully scraped off. Fine pieces of aorta were transferred into a 15 ml plastic centrifuge tube and incubated for 90 min at 37°C in HBSS containing $CaCl_2$ (0.2 mM), HEPES (15 mM), collagenase (type II-S, 1 mg ml^{-1}), elastase (type III, 0.125 mg ml^{-1}), and bovine serum albumin (2 mg ml^{-1}). The digested tissue was triturated 10 times through an 18-gauge needle, sieved through nylon mesh, and the resulting cell suspension centrifuged at 200 *g* for 5 min. The cells were resuspended in Dulbecco's modified Eagle's medium (DMEM) containing 20% foetal calf serum, L-glutamine (2 mM), penicillin-streptomycin (50 μl ml^{-1}) and amphotericin B (2.5 μg ml^{-1}) and seeded into 25 cm^2 flasks. After reaching confluence, cells were passaged by harvesting with trypsin-EDTA, seeded at a ratio of 1:5 into 96-well plates, and grown in DMEM supplemented with 10% foetal calf serum, L-glutamine (2 mM), penicillin-streptomycin (50 u ml^{-1}) and amphotericin B (2.5 μg ml^{-1}). The cells were characterized as smooth muscle cells by morphology and immunostaining with antibodies to smooth muscle α-actin.

Experimental protocol and measurement of NO production

All studies were carried out on VSM cells obtained between the 4th and 10th passage. Cells were stimulated by incuba-

tion with interleukin-1β (IL-1β) at different concentrations for varying periods of time up to 48 h. In preliminary experiments we observed that IL-1β-stimulated nitrite production was reduced in the presence of foetal calf serum (Figure 1a). Foetal calf serum also stimulates mitosis. In order to maximise the nitrite signal and to study quiescent cells, all subsequent experiments were conducted in the absence of foetal calf serum. Thus, 24 h prior to study, the medium was changed to DMEM without phenol red containing 0.1% bovine serum albumin (low endotoxin) in place of foetal calf serum; each well contained 100 μl of culture medium.

NOS activity was assessed by measurement of nitrite production (Griess reaction) over a timed period according to the method of Zembowicz & Vane (1992) with some modifications. Supernatants (100 μl) were mixed with 100 μl of Griess reagent (1% sulphanilamide in 5% H_3PO_4 and 0.1% naphthylethylenediamine dihydrochloride in a ratio of 1:1). Following a 10 min incubation at room temperature, the absorbance was read at 540 nm in a Titertek Multiscan Plus MKII 96 well plate spectrophotometer. Standard curves were determined by use of known concentrations of sodium nitrite. Nitrite levels reflect NOS activity in this system since no other potential source of this ion exists.

This assay was used to examine the effect of a variety of agents on NOS activity. The agents used were selected on the basis of their known actions on protein kinases. Unless indicated, all experiments were carried out using IL-1β 10 ng ml^{-1} and were repeated on at least 4 occasions. Appropriate controls were included in each 96-well plate to overcome variation produced by differences in cell density. All wells in each experiment were judged microscopically to be of similar confluence.

Western blotting

VSM cells were cultured in 75 cm^2 culture flasks with serum-free DMEM without phenol red containing antibiotics, L-glutamine (2 mM) and 0.1% bovine serum albumin (fatty acid-free and low endotoxin) for 24 h and then stimulated with IL-1β (10 ng ml^{-1}) in the presence or absence of db cyclic AMP for periods of time up to 48 h. Culture supernatant was then removed, divided into aliquots and stored for the measurement of nitrite. The cells were washed with PBS (5 ml) 3 times and released by treatment with trypsin-EDTA (2 ml). The cells were then pelleted by centrifugation (500 *g*, 5 min), resuspended in PBS and recentrifuged. The final cell pellet was resuspended in 300 μl lysis buffer (Tris HCl, 50 mM, pH 7.4) containing pepstatin A (5 μg ml^{-1}), chymostatin (1 μg ml^{-1}), aprotinin (5 μg ml^{-1}), leupeptin (1 μg ml^{-1}), dithiothreitol (1 mM) and phenylmethylsulphonyl fluoride (100 μM) and then lysed by quick freeze and thaw 3 times. The lysate was centrifuged at 16,000 *g* for 10 min and the resultant clear supernatant stored at −70°C until further analysis.

Aliquots of cells lysate were used for protein assay (BCA protein assay reagent, Pierce, Illinois, U.S.A.) and Western blot analysis. VSM cell lysate containing 25 to 400 μg of protein was reduced and separated on 7.5% SDS–PAGE using prestained molecular weight markers (Sigma). Proteins were electroblotted in 20% methanol, Tris (25 mM), glycine (192 mM) pH 8.3 on nitrocellulose membranes (ECL-Hyperbond, Amersham International plc, Amersham, UK). The membranes were blocked with 4% low fat milk in PBS for 2 h, washed 3 times in PBS containing 0.05% BSA, 0.05% Tween-20, then incubated with rabbit anti-rat iNOS antibody (diluted 1:5,000 in PBS, 0.1% BSA, Riveros-Moreno *et al.*, 1993) for 2 h, washed and finally incubated with a 1:20,000 dilution of goat anti-rabbit IgG conjugated to horseradish peroxidase (ICN Flow, Oxford, UK) for 2 h. After successive washes as before, the immunocomplexes were developed using an enhanced horseradish peroxidase/luminol chemiluminescence reaction (ECL Western blotting detection reagents, Amersham International plc, Amersham, UK) and detected with X-ray film.

Extraction of total RNA from VSM cells and analysis of iNOS mRNA by reverse transcription-polymerase chain reaction (RT-PCR)

Total RNA was extracted from VSM cells according to the method of Chomczynski & Sacchi (1987). VSM cells cultured in 96-well plates were homogenized in 1.5 ml Eppendorf tubes using 0.5 ml of a solution containing guanidium isothiocyanate (4 M), sodium citrate (25 mM, pH 7.0), 0.5% N-lauroyl-sarcosinate and 2-mercaptoethanol (0.1 M). In order, homogenates were mixed thoroughly with 50 μl sodium acetate (2 M, pH 4.0), 0.5 ml water-saturated phenol and finally 0.2 ml chloroform/isoamyl alcohol (49:1 v/v). Homogenates were left on ice for 15 min and then centrifuged at 16,000 *g* for 15 min at 4°C. The upper aqueous layer was transferred to a new tube and RNA was precipitated twice with isopropanol. The RNA pellet was finally washed with 70% ice-cold ethanol, dried, and dissolved in 20 μl of nuclease-free water.

Quantitative RT-PCR was performed using a method which has previously been extensively validated (Nunez *et al.*, 1992). Two μl aliquots of total RNA were mixed with 25 pmol of a 15 mer random sequence primer before incubation for 2 h at 37°C with 10 u Moloney murine leukaemia virus reverse transcriptase (Pharmacia). The cDNA samples were then diluted with nuclease-free water to a volume of 100 μl and stored at −20°C. Both iNOS and the 'housekeeper' gene glyceraldehyde-3-phosphate dehydrogenase (GAPDH) were measured in each sample. The primers used were as follows: iNOS, sense 5'-CCTACCAAGGTGACCTGAAAG and antisense 5'-TAATGAATTCAATGGCTTGA (Nunokawa *et al.*, 1993), GAPDH sense 5'-GGTGTGAAACACGAGAAATATGAC and antisense 5'-TTGCAGGCTGGGTCCTCATTGTCA (Fort *et al.*, 1985). PCR was performed using 2.5 μl of the diluted cDNA sample in a total reaction volume of 25 μl with 1 μM iNOS or GAPDH primers, 1 unit of Taq DNA polymerase (Promega Corporation, Madison, U.S.A.) and 0.5 μCi of [α-^{32}P]-dCTP (> 5000 Ci $mmol^{-1}$; Amersham International plc) (Brown *et al.*, 1993). Preliminary experiments were performed to ensure that the PCR was terminated during the exponential phase of amplification (data not shown). The amplification conditions were: 26 cycles for GAPDH, 36 cycles for iNOS; each cycle comprised 93°C for 30 s, 60°C for 30 s, 73°C for 1 min. An aliquot (15 μl) of each PCR reaction was then separated by electrophoresis through a 6% polyacrylamide gel. The gels were exposed to Kodak-X-Omat XAR5 autoradiography film to locate the specific product bands (of the expected size) on the gel. These were excised and the amount of ^{32}P incorporated quantified by liquid scintillation counting. The specificity of the iNOS band was verified by DNA sequencing using the deoxy chain termination method (Sanger *et al.*, 1977). The relative amounts of template cDNA at the start of the PCR was assessed by measuring the quantity of PCR product during the exponential phase of amplification. For each cDNA sample, the counts (in c.p.m.) incorporated into iNOS DNA were divided by the amount in the GAPDH band to correct for variation in the extraction of RNA and the efficiency of reverse transcription.

Materials

Interleukin-1β (IL-1β) was obtained from British Biotechnology (Oxford, UK), L-NMMA (N^G-monomethyl-L-arginine) and RO-20-1724 ([4-(3-butoxy-4-methoxybenzyl)-2-imidazolidinone]) from Calbiochem (Nottingham, UK). Dibutyryl cyclic AMP (db cyclic AMP) was a kind gift from Dr Une, Daiichi Pharmaceutical Co Ltd (Tokyo, Japan). Anti-rat iNOS antiserum was provided by Drs Riveros-Moreno and Moncada, Wellcome Reserach Laboratories (Beckenham,

Kent). All culture media, antibiotics, antifungal agents, trypsin and EDTA were obtained from ICN Flow (Oxford, UK). Plastics for culture were purchased from Falcon (Oxford, UK). Fetal calf serum was from Imperial laboratories (West Portway, UK). Unless stated otherwise, all reagents for RT-PCR and all other reagents were obtained from Sigma Ltd (Poole, UK).

Statistics

Where appropriate, data were analysed by ANOVA (Complete Statistical System, StatSoft software) and statistical significance assessed by Student's unpaired 2-tailed t test. Differences were considered statistically significant when the P-value was less than 0.05.

Results

Production of nitrite by VSM cells stimulated with IL-1β

Mean nitrite concentration in media from unstimulated cells, cultured in 96 well plates for 24 h and used in the studies described here, was $2.9 \pm 0.22\,\mu M$ ($n = 28$ plates). Exposure of cultured VSM cells to IL-1β increased nitrite concentration in the supernatant in both a dose- and time-dependent manner (Figure 1a and b). Mean nitrite concentration in media from VSM cells cultured for 24 h with IL-1β (10 ng ml^{-1}) was $24.2 \pm 2.6\,\mu M$ ($n = 28$ plates). The variation between plates was largely due to differences in the density of plated cells; therefore for all experiments described, each 96 well plate contained controls appropriate to the treatment examined.

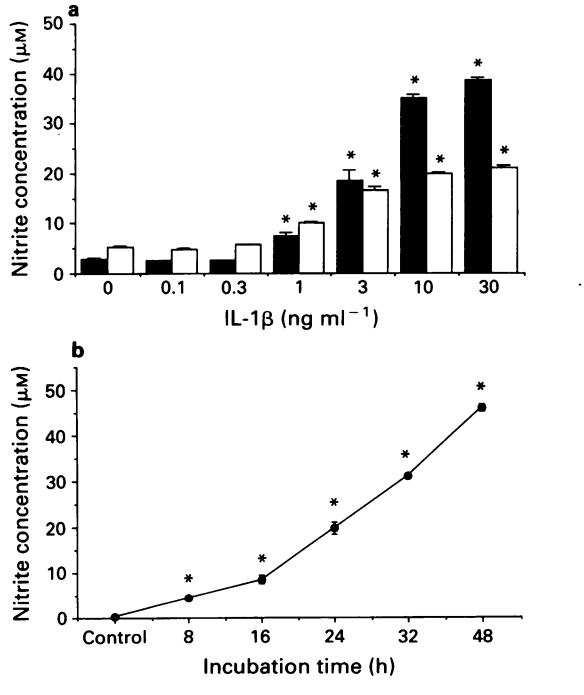

Figure 1 (a) Incubation of vascular smooth muscle (VSM) cells with interleukin-1β (IL-1β) for 24 h results in a dose-dependent increase in nitrite concentration in the culture medium. This response was greater in the presence of 0.1% BSA (solid columns) than with 10% foetal calf serum (open columns). Data are mean ± s.e.mean of 4 wells. *$P<0.01$, IL-1β-treated cells relative to cells not exposed to this cytokine. (b) Increase in nitrite concentration in culture medium with time during incubation of VSM cells with IL-1β (10 ng ml^{-1}). Control represents cells cultured for 24 h without IL-1β. Data are mean ± s.e.mean of 4 wells at each time point. *$P<0.01$, IL-1β-treated cells relative to control cells.

Accumulation of nitrite following incubation of cells with IL-1β (10 ng ml^{-1}) was inhibited by cycloheximide at all concentrations and by L-NMMA in a dose-dependent manner (Figure 2). Consistent with other reports (Szabo *et al.*, 1993), dexamethasone also had a significant inhibitory effect at 10 μM (results not shown).

Effect of agents that increase cyclic AMP levels

Once the cellular response to IL-1β was characterized, we studied the effect of a variety of agents that act to increase intracellular cyclic AMP levels. Specifically, we examined the effect of direct addition of cyclic AMP using the stable analogue, db cyclic AMP; stimulating adenylyl cyclase (e.g. with forskolin, isoprenaline); and inhibiting cyclic AMP phosphodiesterase (e.g. with Ro 20-1724). These observations were compared with the effect of increasing intracellular cyclic GMP levels by the addition of db cyclic GMP.

db cyclic AMP increased nitrite levels in a dose-dependent manner (0.01 – 1 mM) when co-incubated with IL-1β (10 ng ml^{-1}) for 24 h, in contrast to db cyclic GMP which had no effect (Figure 3). The mean increase in nitrite levels with

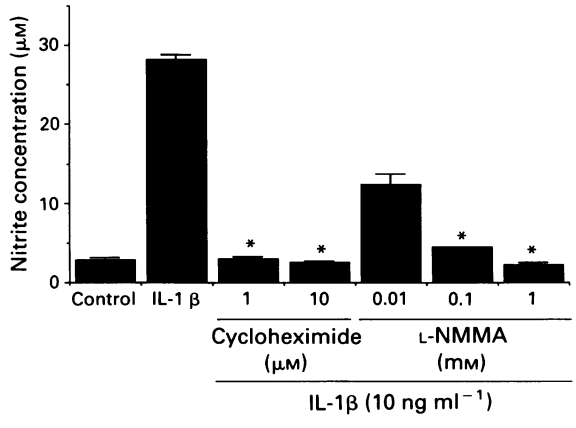

Figure 2 Effect of cycloheximide and the L-arginine analogue, N^G-monomethyl-L-arginine (L-NMMA), on nitrite concentration in culture medium during incubation of VSM cells with interleukin-1β (IL-1β, 10 ng ml^{-1}) for 24 h. Data are mean ± s.e.mean of 4 wells. *$P<0.01$ compared to IL-1β alone.

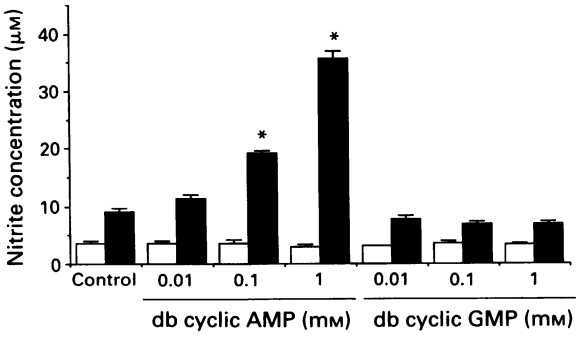

Figure 3 Effects of db cyclic AMP (0.01 – 1 mM) and db cyclic GMP (0.01 – 1 mM) on nitrite concentration in culture medium from VSM cells incubated in the presence (solid columns) and absence (open columns) of interleukin-1β (IL-1β, 10 ng ml^{-1}) for 24 h. The cyclic nucleotides were present throughout the 24 h incubation period. Increasing cyclic AMP levels with db cyclic AMP increased nitrite concentration in the presence of IL-1β above that produced by the cytokine alone (control, solid). In contrast, db cyclic GMP did not affect the response to IL-1β. Neither db cyclic AMP nor db cyclic GMP had any measurable effect on nitrite production in the absence of IL-1β. Data are mean ± s.e.mean of 4 wells. *$P<0.01$ compared to control cells incubated with IL-1β alone.

IL-1β (10 ng ml^{-1}) plus db cyclic AMP (1 mM) over that produced by IL-1β (10 ng ml^{-1}) alone was 393 ± 71% ($n = 8$ plates). Further experiments showed that potentiation of IL-1β induced elevation of nitrite levels could be produced by short, early exposure of the cells to db cyclic AMP i.e. for the first 4 h of a 28 h incubation with IL-1β (Figure 4a). To examine the effects of cyclic AMP on the activity of the induced enzyme, VSM cells were incubated with IL-1β for 20 h, then washed and incubated with media containing db cyclic AMP (1 mM) for 8 h; the final nitrite concentration in the media was not significantly different from that in media from cells similarly treated but incubated in the absence of db cyclic AMP (Figure 4b). These data support a role for cyclic AMP in the regulation of iNOS induction rather than the activity of the enzyme itself.

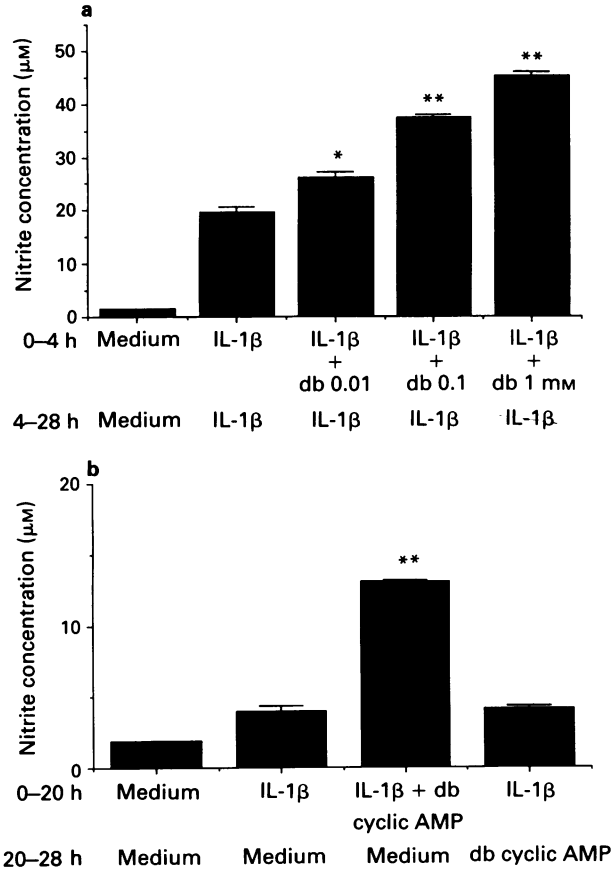

Figure 4 (a) VSM cells were incubated with interleukin-1β (IL-1β, 10 ng ml^{-1}) in the presence and absence of db cyclic AMP (0.01–1 mM) for 4 h; cells were then washed and incubated with IL-1β (10 ng ml^{-1}) alone for a further 24 h. Control cells were incubated without cytokine or cyclic nucleotide for 4 + 24 h. Nitrite concentration therefore represents nitrite accumulation in culture media during the last 24 h incubation period. Co-incubation with db cyclic AMP resulted in a dose-dependent increase in nitrite concentration in the medium above that produced by the cytokine alone. Data are mean ± s.e.mean of 4 wells and are representative of 4 experiments. *$P < 0.01$, **$P < 0.001$ compared to control cells incubated with IL-1β alone. (b) VSM cells were incubated with IL-1β (10 ng ml^{-1}) in the presence or absence of AMP (1 mM) for 20 h; cells were then washed and cultured for a further 8 h without IL-1β. One group of wells previously exposed to IL-1β only for 0–20 h received db cyclic AMP (1 mM) during last 8 h incubation (20–28 h). Control cells were incubated without cytokine or cyclic nucleotide for 20 + 8 h. Nitrite concentration reflects nitrite accumulation in the media during the last 8 h incubation period. The presence of db cyclic AMP during the first 20 h incubation period but not the subsequent 8 h period enhanced nitrite levels above that produced by the effect of the cytokine alone. Data are mean ± s.e.mean of 4 wells and are representative of 4 experiments. *$P < 0.01$, **$P < 0.001$ compared to control cells incubated with IL-1β alone.

Forskolin (0.1–10 μM) and Ro 20-1724 (1–10 μM) had no detectable effect on nitrite levels in the absence of IL-1β but enhanced the production of nitrite in response to IL-1β in a dose-dependent manner (Figure 5a). The mean increase in nitrite concentration with IL-1β (10 ng ml^{-1}) and forskolin (10 μM) above that produced by the cytokine alone was 259 ± 48% ($n = 5$ plates). An inactive derivative of forskolin, 1,9-dideoxyforskolin (0.1–10 μM), had no effect on IL-1β-stimulated nitrite production. The Ro 20-1724 potentiated the effect of forskolin on IL-1β stimulated nitrite production (Figure 5a), in keeping with cyclic AMP as the common mediator of this effect.

To pursue these observations further, the effect of receptor-mediated changes in intracellular cyclic nucleotide levels on nitrite levels was examined. The β-adrenoceptor agonist, isoprenaline which elevates cyclic AMP, enhanced nitrite production by IL-1β-stimulated VSM cells dose-dependently (Figure 5b) but had no detectable effect in the absence of the cytokine. The mean increase in nitrite levels with IL-1β (10 ng ml^{-1}) and isoprenaline (10 μM) above that produced by the cytokine alone was 142 ± 15% ($n = 4$ plates). Ro 20-1724 increased further the effect of isoprenaline on IL-1β-stimulated nitrite production (Figure 5b). The α-adrenoceptor agonist, phenylephrine, had no effect on nitrite levels with or without IL-1β (data not shown).

Measurement of iNOS protein levels by Western blotting

Incubation of VSM cells with IL-1β (10 ng ml^{-1}) produced a single band (~130 kDa) on immunoblotting with anti-iNOS antibody, consistent with iNOS protein. This band was not detected in control cells (cultured in the absence of cytokine) and increased in a time-dependent manner during culture with IL-1β from 0–48 h (Figure 6a). Co-incubation of IL-1β (10 ng ml^{-1}) and db cyclic AMP (1 mM) increased the density of staining with anti-iNOS antibody at any given protein concentration compared to IL-1β alone, while db cyclic AMP alone produced no detectable band (Figure 6b). These data

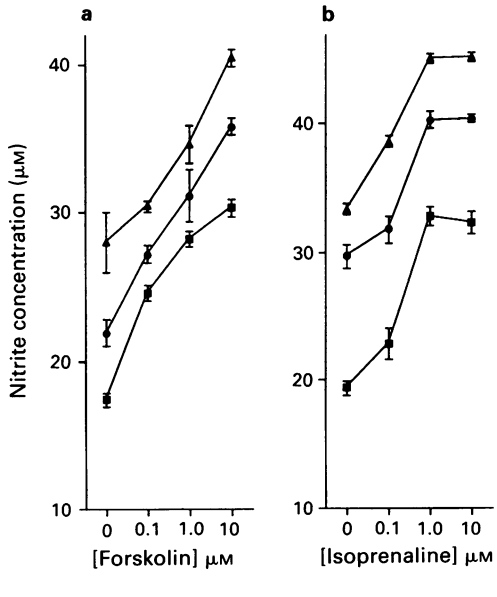

Figure 5 Effect of 2 doses of Ro 20-1724 (●, 1 μM and ▼, 10 μM), a cyclic AMP phosphodiesterase inhibitor, on nitrite levels in media from VSM cells incubated with interleukin-1β (IL-1β, 10 ng ml^{-1}) for 24 h together with increasing doses of (a) forskolin (0.1–10 μM) or (b) isoprenaline (0.1–10 μM): (■) represents cells incubated without Ro 20-1724. Forskolin, isoprenaline and Ro 20-1724 alone caused dose-dependent enhancement of IL-1β-induced nitrite production. Both doses of Ro 20-1724 increased significantly the effect of forskolin or isoprenaline on IL-1β-induced nitrite production ($P < 0.05$, ANOVA). Data are mean ± s.e.mean of 4 wells and are representative of 4 experiments.

are consistent with cyclic AMP enhancing IL-1β-induced iNOS protein synthesis.

Measurement of iNOS mRNA in VSM cells

In unstimulated VSM cells, iNOS mRNA was not detectable after 36 cycles of PCR. However, after incubation with IL-1β (10 ng ml^{-1}), iNOS mRNA levels were readily detectable at 3 h and continued to increase up to 48 h (data not shown). Consistent with the effect of cyclic AMP on IL-1β-stimulated nitrite production, incubation of VSM cells for 4 h with IL-1β and db cyclic AMP (1 mM) markedly enhanced mRNA levels above that produced by IL-1β alone (Figure 7). IL-1β did not affect the prevalence of GADPH mRNA.

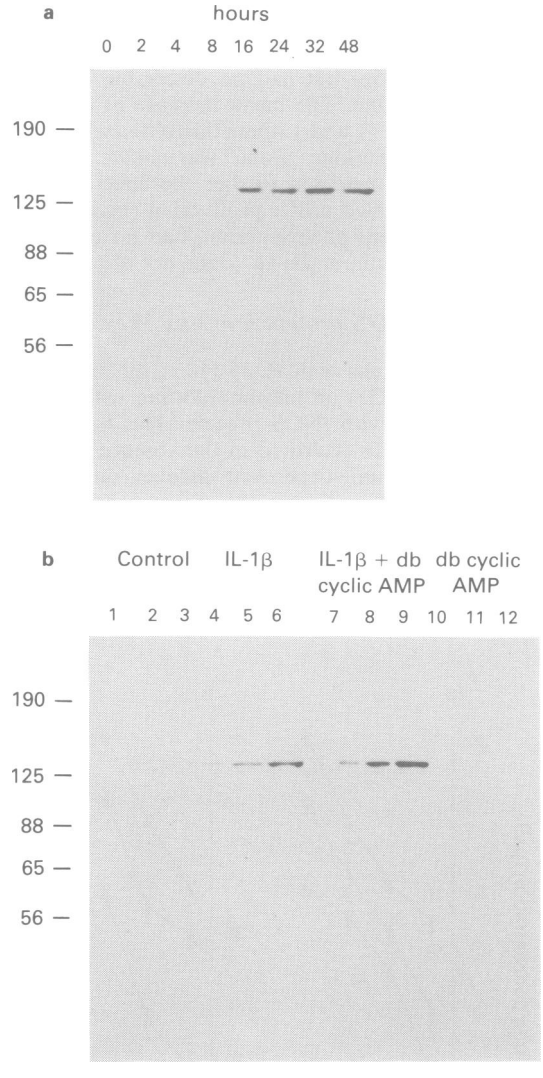

Figure 6 Western blot analysis of iNOS in VSM cells. Supernatant fraction of cell lysate was separated by SDS–PAGE, transferred to nitrocellulose and blotted with anti-iNOS antibody. A single band was seen at ~130 kDa, of appropriate molecular weight for iNOS protein. (a) Time-dependent increase in iNOS protein in VSM cells incubated with interleukin-1β (IL-1β, 10 ng ml^{-1}) for 0, 2, 4, 8, 16, 24, 32 and 48 h (lanes 1–8 respectively, 100 μg protein per lane). (b) Enhancement of IL-1β-induced increase in iNOS protein levels by db cyclic AMP. VSM cells were incubated with media alone (lane 1, 2), IL-1β (10 ng ml^{-1}, lanes 3–6), IL-1β plus db cyclic AMP (1 mM, lanes 7–9), or db cyclic AMP alone (1 mM, lanes 10–12) for 24 h. Different amounts of protein were subjected to SDS–PAGE (25 μg, lanes 3, 7; 50 μg, lanes 4, 8; 100 μg, lane 1, 5, 9, 10; 200 μg, lanes 2, 6, 11; 400 μg, lane 12) to enable semi-quantitation of iNOS protein. iNOS was readily detected in the 25 μg of protein of cells incubated with IL-1β plus db cyclic AMP (lane 7) but required 100 μg of protein from cell incubated with IL-1β alone (lane 5), consistent with db cyclic AMP enhancing iNOS protein synthesis. Data are representative of 3 experiments.

Discussion

Several groups have reported that IL-1β is a powerful stimulant of NO production in VSM cells in culture (Busse & Mulsch, 1990; Beasley *et al.*, 1991; Nakayama *et al.*, 1992; Scott-Burden *et al.*, 1992). This effect is thought to be mediated largely by increased synthesis of NOS. In support of this we have shown that exposure to IL-1β is accompanied by increased iNOS protein and mRNA levels and that the effect of this cytokine on NO production is inhibited by cycloheximide.

More importantly, however, these studies demonstrate a clear effect of cyclic AMP in IL-1β-stimulated NO production in VSM cells. Increasing intracellular cyclic AMP concentration directly by the addition of db cyclic AMP produced a marked shift to the left of the dose-response curve for IL-1β. Similarly, indirect elevation of cyclic AMP levels with forskolin, a phosphodiesterase inhibitor and isoprenaline augmented significantly the production of NO at a given concentration of IL-1β. Insight into some of the mechanisms underlying this effect is provided by the measurements of iNOS protein and mRNA levels. The effects of db cyclic AMP on IL-1β-stimulated NO production were accompanied by a further increase in iNOS protein levels and

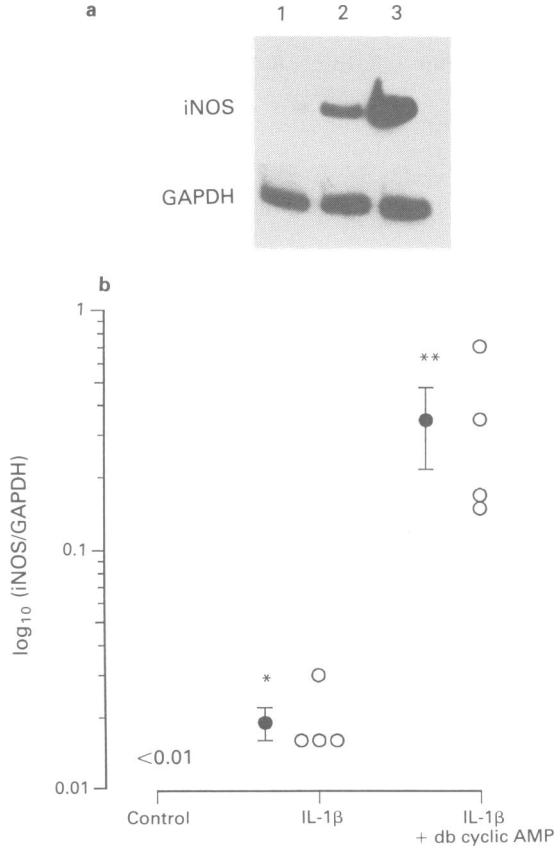

Figure 7 Measurement of mRNA levels for iNOS and GAPDH by RT-PCR in VSM cells cultured for 4 h without interleukin-1β (IL-1β) (1) control, with IL-1β 10 ng ml^{-1} (2) and with IL-1β 10 ng ml^{-1} plus db cyclic AMP 1 mM (3). (a) Inducible NOS mRNA was not detected at 36 cycles of PCR in control cells. IL-1β increased iNOS mRNA levels and this was increased further in the presence of db cyclic AMP. GAPDH measured at 26 cycles did not increase with IL-1β with or without db cyclic AMP. (b) $\log_{10}$ ratio of iNOS to GAPDH mRNA levels. Data (●) are mean ± s.e.mean for 4 experiments. *$P<0.01$ compared to control; **$P<$ compared to IL-1β.

mRNA transcripts for iNOS, above that produced by IL-1β alone. This would suggest that cyclic AMP acts at least in part by influencing iNOS synthesis by altering the steady-state level of iNOS mRNA (but whether this is by increasing transcription or reducing degradation rate is unknown). Since submission of this paper Koide *et al.* (1993) have shown that cyclic AMP-elevating agents such as forskolin and prostaglandin E_1 enhance NO production by interferon-γ, IL-1β and tumour necrosis factor in VSM cells at the level of iNOS mRNA expression, findings in agreement with our own results.

Cyclic AMP can regulate the expression of a number of genes through a conserved cyclic AMP-response element, CRE (Yamamoto *et al.*, 1988). The CRE is a palindromic octanucleotide (TGACGTCA) which binds a number of structurally related proteins constituting the ATF/CREB family. These proteins usually bind as homodimers and can exert both positive and negative effects on transcription (Yamamoto *et al.*, 1988; Karpinski *et al.*, 1992). Evidence for the existence of CRE domains in association with the iNOS gene is currently lacking (there is no CRE sequence present in the 5'-flanking region of mouse iNOS, Xie *et al.*, 1993). The absence of an effect of db cyclic AMP alone on nitrite production suggests, however, that if CRE-dependent transcription is operating in our system then this must be conditional on the activation of the numerous cytokine-response elements which have been identified in the iNOS promoter region (Xie *et al.*, 1993). The interactions are complex and appear to vary between different cell types. Thus, isoprenaline, 8-bromo cyclic AMP, db cyclic AMP and PGE_2 have been reported to potentiate cytokine-stimulated NO production in endothelial cells and Kupffer cells (Gaillard *et al.*, 1992; Durieu-Trautmann *et al.*, 1993), whereas db cyclic AMP inhibits this effect in macrophage and astroglial cells (Marotta *et al.*, 1992; Feinstein *et al.*, 1993). Although species differences may contribute to these apparent discrepancies, it is also possible that there are differences between tissues in the regulation of inducible NOS synthase activity which it may be possible to exploit therapeutically.

Our data show that cyclic AMP enhances IL-1β-stimulated elevation of iNOS protein and mRNA levels but this does not exclude the possibility that cyclic AMP-mediated phosphorylation of iNOS protein itself may also be involved in regulating its activity. Both the constitutive and inducible forms of NOS exhibit sites for cyclic AMP-dependent phosphorylation (Dinermann *et al.*, 1993). Against this, addition of db cyclic AMP to VSM cells in which synthesis of iNOS had already been induced (by incubation with IL-1β for 20 h) did not increase NO levels above that produced by IL-1β alone, suggesting little effect of cyclic AMP on the activity of the enzyme. It is noteworthy that phosphorylation of purified constitutive NOS from brain or the recombinant enzyme in transfected cells by protein kinase A does not alter its activity (Brune & Lapetina, 1991; Bredt *et al.*, 1992). Phosphorylation by other protein kinases may regulate iNOS activity although the effect of phosphorylation by protein kinase C remains unclear; one study has reported activation of protein kinase C decreases (Bredt *et al.*, 1992) and another that it increases (Nakane *et al.*, 1991) iNOS activity. Recent studies have shown that phosphorylation of constitutive NOS affects the site of action of this enzyme, as phosphorylation influences translocation of the enzyme from membrane to cytosol (Michel *et al.*, 1993).

In summary, induction of NOS activity in VSM cells by IL-1β is enhanced by cyclic AMP. Moreover, the effect of cyclic AMP is mediated, at least in part, by an increase in iNOS protein levels and mRNA prevalence. These data have implications for the pathogenesis and treatment of septic shock. Specifically, endogenous factors such as adrenaline that elevate cyclic AMP and are increased in septic shock may facilitate the production of NO and hypotension. Similarly, therapeutic agents, for example dobutamine, that act by increasing cyclic AMP may be best avoided in the management of septic shock.

The authors thank Dr D.J. Nunez for his helpful comments on the manuscript. This work was supported in part by a grant from Daiichi Pharmaceutical Co Ltd.

References

BEASLEY, D., SCHWARTZ, J.H. & BRENNER, B.M. (1991). Interleukin 1 induces prolonged L-arginine-dependent cyclic guanosine monophosphate and nitrite production in rat vascular smooth muscle cells. *J. Clin. Invest.*, **87**, 602–608.

BREDT, D.S., FERRIS, C.D. & SNYDER, S.H. (1992). Nitric oxide synthase regulatory sites. Phosphorylation by cyclic AMP-dependent protein kinase, protein kinase C, and calcium/calmodulin protein kinase; identification of flavin and calmodulin binding sites. *J. Biol. Chem.*, **267**, 10976–10981.

BROWN, L.A., NUNEZ, D.J. & WILKINS, M.R. (1993). Differential regulation of natriuretic peptide receptor messenger RNAs during the development of cardiac hypertrophy in the rat. *J. Clin. Invest.*, **92**, 2702–2712.

BRUNE, B. & LAPETINA, E.G. (1991). Phosphorylation of nitric oxide synthase by protein kinase A. *Biochem. Biophys. Res. Commun.*, **181**, 921–926.

BUSSE, R. & MULSCH, A. (1990). Induction of nitric oxide synthase by cytokines in vascular smooth muscle cells. *FEBS Lett.*, **275**, 87–90.

CHOMCZYNSKI, P. & SAACHI, N. (1987). Single step method of RNA isolation by acid guanidium isothiocyanate-phenol-chloroform extraction. *Anal. Biochem.*, **162**, 156–159.

DINERMAN, J.L., LOWENSTEIN, C.J. & SNYDER, S.H. (1993). Molecular mechanisms of nitric oxide regulation: potential relevance to cardiovascular disease. *Circ. Res.*, **73**, 217–222.

DURIEU-TRAUTMANN, O., FEDERICI, C., CREMON, C., FOIGNANT-CHAVEROT, N., ROUX, F., CLAIRE, M., STROSBERG, A.D. & COURAUD, P.O. (1993). Nitric oxide and endothelin secretion by brain microvessel endothelial cells: regulation by cyclic nucleotides. *J. Cell. Physiol.*, **155**, 104–111.

FEINSTEIN, D.L., GALEA, E. & REI, D.J. (1993). Norepinephrine suppress inducible nitric oxide synthase activity in rat astroglial cultures. *J. Neurochem.*, **60**, 1945–1948.

FORT, P.L., MARTY, L., PIECHACZYK, M., SABROUTY, S.E., DANI, C., JEANTEUR, P. & BLANCHARD, J.M. (1985). Various rat tissues express only one major form of mRNA species from the glyceraldehyde-3-phosphate dehydrogenase multigenic family. *Nucleic Acids Res.*, **13**, 1431–1442.

GAILLARD, T., MULSCH, A., BUSSE, R., KLEIN, H. & DECKER, K. (1991). Regulation of nitric oxide production by stimulated rat kupffer cells. *Pathobiol.*, **59**, 280–283.

GAILLARD, T., MULSCH, A., KLEIN, H. & DECKER, K. (1992). Regulation by prostaglandin E_2 of cytokine-elicited nitric oxide synthesis in rat liver macrophages. *Biol. Chem. Hoppe-Seyler.*, **373**, 897–902.

HORTELANO, S., GENARO, A.M. & BOSCA, L. (1992). Phorbol esters induce nitric oxide synthase activity in rat hepatocytes. Antagonism with the induction elicited by lipopolysaccharide. *J. Biol. Chem.*, **267**, 24937–24940.

HORTELANO, S., GENARO, A.M. & BOSCA, L. (1993). Phorbol esters induce nitric oxide synthase and increase arginine influx in cultured peritoneal macrophages. *FEBS Lett.*, **320**, 135–139.

KARPINSKI, B.A., MORLE, G.D., HUGGENVIK, J., UHLER, M. & LEIDEN, J.M. (1992). Molecular cloning of human CREB-2: an ATF/CREB transcription factor that can negatively regulate transcription from the cAMP response element. *Proc. Natl. Acad. Sci. U.S.A.*, **89**, 4820–4824.

KOIDE, M., KAWAHARA, Y., NAKAYAMA, I., TSUDA, T. & YOKOYAMA, M. (1993). Cyclic AMP-elevating agents induce an inducible type of nitric oxide synthase in cultured vascular smooth muscle cells; synergism with the induction elicited by inflammatory cytokines. *J. Biol. Chem.*, **268**, 24959–24966.

MAROTTA, P., SAUTEBIN, L. & DI ROSA, M. (1992). Modulation of the induction of nitric oxide synthase by eicosanoids in murine macrophage cell line J774. *Br. J. Pharmacol.*, **107**, 640–641.

MICHEL, T., LI, G.K. & BUSCONI, L. (1993). Phosphorylation and subcellular translocation of endothelial nitric oxide synthase. *Proc. Natl. Acad. Sci. U.S.A.*, **90,** 6252–6256.

MONCADA, S., PALMER, R.M.J. & HIGGS, E.A. (1991). Nitric oxide: physiology, pathophysiology and pharmacology. *Pharmacol. Rev.*, **43,** 109–142.

NAKANE, M., MITCHELL, J., FRORSTERMANN, U. & MURAD, F. (1991). Phosphorylation by calcium calmodulin-dependent protein kinase II and protein kinase C modulates the activity of nitric oxide synthase. *Biochem. Biophys. Res. Commun.*, **180,** 1396–1402.

NAKAYAMA, D.K., GELLER, D.A., LOWENSTEIN, C.J., DAVIES, P., PITT, B.R., SIMMOMS, R.L. & BILLIAR, T.R. (1992). Cytokines and lipopolysaccharide induce nitrice oxide synthase in cultured rat pulmonary artery smooth muscle cells. *Am. J. Respir. Cell. Mol. Biol.*, **7,** 471–476.

NAVA, E., PALMER, R.M.J. & MONCADA, S. (1991). Inhibition of nitric oxide synthesis in septic shock: how much is beneficial? *Lancet*, **338,** 1555–1557.

NUNEZ, D.J.R, DICKSON, M.C. & BROWN, M.J. (1992). Natriuretic peptide receptor mRNAs in the rat and human heart. *J. Clin. Invest.*, **90,** 1966–1971.

NUNOKAWA, Y., ISHIDA, N. & TANAKA, S. (1993). Cloning of inducible nitric oxide synthase in rat vascular smooth muscle. *Biochem. Biophys. Res. Commun.*, **191,** 89–94.

PETROS, A., BENNETT, D. & VALLANCE, P. (1991). Effect of nitric oxide synthase inhibitors on hypotension in septic shock. *Lancet*, **338,** 1557–1558.

RIVEROS-MORENO, V., BEDDELL, C. & MONCADA, S. (1993). Nitric oxide synthase: Structural studies using anti-peptide antibodies. *Eur. J. Biochem.*, **215,** 801–808.

SANGER, F., NICKLEN, S. & COULSEN, A.R. (1977). DNA sequencing with chain terminating inhibitors. *Proc. Natl. Acad. Sci. U.S.A.*, **74,** 5463–5467.

SCOTT-BURDEN, T., SCHINI, V.B., ELIZONDO, E., JUNQUERO, D.C. & VANHOUTTE, P.M. (1992). Platelet-derived growth factor suppresses and fibroblast growth factor enhances cytokine-induced production of nitric oxide by cultured smooth muscle cells. Effects on cell proliferation. *Circ. Res.*, **71,** 1088–1100.

SEVERN, A., WAKELAM, M.J.O. & LIEW, F.Y. (1992). The role of protein kinase C in the induction of nitric oxide synthesis by murine macrophages. *Biochem. Biophys. Res. Commun.*, **188,** 997–1002.

SZABO, C., MITCHELL, J.A., GROSS, S.S., THIEMERMANN, C. & VANE, J.R. (1993). Nifedipine inhibits the induction of nitric oxide synthase by bacterial lipopolysaccharide. *J. Pharmacol. Exp. Ther.*, **265,** 674–680.

XIE, Q., WHISNANT, R. & NATHAN, C. (1993). Promoter of the mouse gene encoding calcium-independent nitric oxide synthase confers inducibility of interferon γ and bacterial lipopolysaccharide. *J. Exp. Med.*, **177,** 1779–1784.

YAMAMOTO, K.K., GONZALEZ, G.A., BIGGS, W.H. & MONTMINY, M.R. (1988). Phosphorylation-induced binding and transcriptional efficacy of nuclear CREB. *Nature*, **334,** 494–498.

ZEMBOWICZ, A. & VANE, J.R. (1992). Induction of nitric oxide synthase activity by toxic shock syndrome toxin 1 in a macrophage-monocyte cell line. *Proc. Natl. Acad. Sci. U.S.A.*, **89,** 2051–2055.

(Received November 1, 1993
Revised January 31, 1994
Accepted February 15, 1994)

Br. J. Pharmacol. (1994), **112**, 403–410

Noradrenergic-nitrergic interactions in the rat anococcygeus muscle: evidence for postjunctional modulation by nitric oxide

[1]Lübomir Kasakov, Abebech Belai, [2]Mila Vlaskovska & [3]Geoffrey Burnstock

Department of Anatomy and Developmental Biology, University College London, Gower Street, London WC1E 6BT

1 The distribution of NADPH-diaphorase positive and catecholamine-containing nerve structures, and functional noradrenergic-nitrergic interactions, were studied in the rat anococcygeus muscle.

2 The morphological findings demonstrated NADPH-diaphorase positive neurones mostly as aggregates in intramural ganglia, nerve tracts and few single nerve fibres forming plexus-like structures.

3 The nitric oxide synthase inhibitor N^G-nitro-L-arginine (L-NOARG) inhibited concentration-dependently the nitrergic relaxation, an effect reversed by L-arginine. The drug had dual effects on noradrenergic contractile responses: at lower concentrations (0.1–10 μM) it decreased the amplitude of contractions and this was not affected by L-arginine; higher concentrations (50–500 μM) potentiated the contractions, an effect that was prevented by L-arginine.

4 The electron acceptor, nitro blue tetrazolium (NBT) produced a rapid inhibition of the noradrenergic contractile responses (EC_{50} 0.178 ± 0.041 μM). The drug decreased the tone of the preparations. However, it potentiated concentration-dependently the nitrergic relaxations.

5 NBT (1 μM) had no significant effect on the relaxations induced by exogenously applied nitric oxide (NO)-donor sodium nitroprusside (SNP, 0.01–50 μM). However, the effect of NBT (0.1–10 μM) on the electrically induced relaxation was significantly decreased by L-NOARG (10 and 50 μM). The inhibition was of a non-competitive type.

6 Neither L-NOARG (100 μM) nor NBT (1 μM) had any effect on the spontaneous or electrically-induced release of ^{3}H-radioactivity from the tissues preincubated in [^{3}H]-noradrenaline.

7 It is concluded that L-arginine-NO pathway can modulate noradrenergic transmission in the rat anococcygeus muscle at postjunctional, but not prejunctional site(s).

Keywords: Anococcygeus muscle (rat); NADPH-diaphorase; N^G-nitro-L-arginine; nitro blue tetrazolium; [^{3}H]-noradrenaline release.

Introduction

Following the identification of the endothelium-derived relaxing factor (EDRF; Furchgott & Zawadzki, 1980) as the free radical of nitric oxide ($NO^{\cdot}$; Palmer *et al.*, 1987; Ignarro *et al.*, 1987) the so-called L-arginine-NO pathway has been suggested to represent a widespread mechanism for the regulation of cell function and communication (Moncada *et al.*, 1989; 1991; Moncada, 1992). The action of NO is mediated by the stimulation of a soluble guanylyl cyclase (Arnold *et al.*, 1977) leading to the elevation of guanosine 3′:5′-cyclic monophosphate (cyclic GMP) levels within the target cells (Snyder & Bredt, 1991). It is well documented that elevation of cyclic GMP can increase the release of acetylcholine (ACh) from PC12 cells and noradrenaline (NA) from the adrenal chromaffin cells, or decrease release of ACh in the hippocampus, cerebral cortex, and skeletal neuromuscular junction, and that of NA from adrenergic nerves and PC12 cells (for review see: Garthwaite, 1991). Recently, NO has been implicated as an inhibitor transmitter-like substance in the non-adrenergic, non-cholinergic (NANC) neurotransmission in various preparations (Bult *et al.*, 1990; Rand, 1992; Sanders & Ward, 1992). However, the interaction of NO with other types of neurotransmission needs further study. Controversial results have been reported that NO inhibits the release of NA from the adrenergic nerves in canine blood vessels (Cohen & Weisbrod, 1988; Greenberg *et al.*, 1989; 1990), that NO increases the release of NA in rat mesenteric vasculature (Yamamoto *et al.*, 1992), or that NO has no effect on either NA release from the noradrenergic nerve terminals in the vasculature (Cederquist *et al.*, 1991; Toda & Okamura, 1992), or ACh release from the cholinergic nerves in guinea-pig ileum (Gustafsson *et al.*, 1990b).

The rat anococcygeus muscle is a suitable non-vascular autonomically-innervated tissue to study the noradrenergic-nitrergic interactions. The electrical stimulation of intramural nerves evokes a fast high-amplitude contractile response which is largely mediated by NA (Gillespie, 1980); after guanethidine the application of identical stimulation evokes a rapid relaxation of the precontracted anococcygeus muscle (for review see Gillespie, 1980) which is mediated mainly by NO-related mechanisms (Hobbs & Gibson, 1990; Martin & Gillespie, 1990). The nerve terminals supplying the anococcygeus muscle comprise a dense network in which 60–70% of the fibres are noradrenergic and up to 40% are considered NANC terminals, with only about 5% of all nerve terminals having cholinergic characteristics (Burnstock *et al.*, 1978). More data are required about the presence and pattern of distribution of NO-containing nerve fibres and neurones in the rat anococcygeus muscle.

In preliminary experiments we found that the inhibition or potentiation of the relaxant responses produced by N^G-nitro-L-arginine (L-NOARG) or nitro blue tetrazolium (NBT) respectively, which are chemical agents that may alter the activity of nitric oxide synthesis (EC 1.14.23; NOS) (Palmer *et al.*, 1988; Gibson *et al.*, 1990; Hobbs & Gibson, 1990; Hope *et al.*, 1990), corresponded to marked reciprocal effects on the contractile responses (Kasakov *et al.*, 1991). The aim of the present investigation was to characterize further the effects of L-NOARG and NBT on the neurogenic responses of the rat anococcygeus muscle and to investigate the effect of L-NOARG amd NBT on the basal, as well as stimulus-

Present address: [1] Department of Comparative Physiology, Institute of Physiology, Bulgarian Academy of Sciences, Sofia 1113, Bulgaria.
[2] Department of Pharmacology, Higher Medical School, Sofia 1431, Bulgaria.
[3] Author for correspondence.

evoked, release of tritium (^3H) from the noradrenergic terminals in the muscle preincubated with [^3H]-NA. In addition we have examined the distribution and localization of NADPH-diaphorase containing neuronal structures in the rat anococcygeus muscle.

Methods

General

Male Sprague-Dawley rats (200–250 g) were killed by an overdose of CO_2 and exsanguination and the anococcygeus muscles were excised. The isolated preparations were placed horizontally between pairs of platinum ring (4 mm diameter) electrodes (10 mm apart) in 1 ml plastic (high density polythene) double-jacketed organ baths (37°C). Tissues were perfused at a constant flow of 1.2 ml min^{-1} (0.6 ml min^{-1} in ^3H release experiments) by means of a peristaltic pump (Watson-Marlow) with a medium of the following composition (mM): NaCl 136.9, KCl 2.7, $CaCl_2$ 1.8, $MgCl_2$ 0.6, $NaHCO_3$ 11.9, KH_2PO_4 0.5, glucose 11.5, containing (mg l^{-1}) albumin 25, ascorbic acid 100, atropine 0.7, bacitracin 30, EDTA 10, and gassed with 5% CO_2 in O_2 (pH 7.4–7.6). The preparations were stretched to a 5 mN initial tension and allowed to equilibrate for 90 min. One end of the preparation was tied to a Grass FT 03C force-displacement transducer connected to a Gould 2200S recorder for registration of the isometric changes of the tension. The preparations were stimulated electrically for 10 s (60 s in ^3H release experiments) with trains of rectangular pulses of 0.6 ms duration, 20 Hz and 60 V delivered by Grass SD9 stimulators triggered by a D100 Digitimer (Digitimer Ltd, Herts) every 130 s (twice at 45 min intervals in ^3H release experiments). Drugs were added to the medium reservoir (continuous treatment) or infused for short periods of time into the perfusate at a flow rate of 0.3 ml min^{-1} close to the preparation via a side-way canula by means of a peristaltic pump (intermittent treatment).

Fluorescence histochemistry

The anococcygeus muscles were dissected and stretched on a Slygard silicone rubber plate, and fat and connective tissues were cleared carefully. The stretched tissues were immersed in a 2% glyoxylic acid solution in 0.1 M phosphate buffer, pH 7.4, for 1.5 h at room temperature. After incubation the tissue samples were transferred onto clean glass slides, dried until translucent and placed in an oven at 80°C for 4 min. The tissues were then mounted with liquid paraffin and catecholamine containing nerve fibres were viewed under a Zeiss photomicroscope fitted for epifluorescence with ultraviolet filters.

NADPH-diaphorase staining

Stretched and cleaned tissues were fixed in 4% paraformaldehyde in phosphate buffered saline (PBS) for 2 h at 4°C. The tissues were then washed 10 times (each for 10 min) with 80% alcohol, dehydrated, rehydrated and washed 3 times (each for 5 min) with PBS containing 0.1% Triton X-100. For NADPH-diaphorase staining the tissues were incubated in 0.1 M Tris. HCl (pH 7.4) containing 1.2 mM β-NADPH, 2.4 mM NBT and 15.2 mM L-malic acid at 37°C for 1.5–2 h. After incubation the tissues were transferred onto clear glass slides, mounted with citifluor (glycerol:PBS) and the neurones and nerve fibres stained for NADPH-diaphorase were viewed with a light microscope.

Radiolabelled release experiments

The changes in NA-levels were monitored by the levels of ^3H-radioactivity in the perfusate and in the tissue. After isolation (as described above) the tissues were incubated for 60 min in continuously gassed medium containing 0.1 μM tritium labelled (−)-noradrenaline ([^3H]-NA, Amersham; Sp. Act. 1850 GBq $mmol^{-1}$; two preparations in 2 ml medium) at 37°C. After rinsing 5 times with 3 ml medium each preparation was placed in an organ bath between stimulating electrodes as described above. The bath chambers were perfused (0.6 ml min^{-1}) with a cocaine-containing (10 μM) medium.

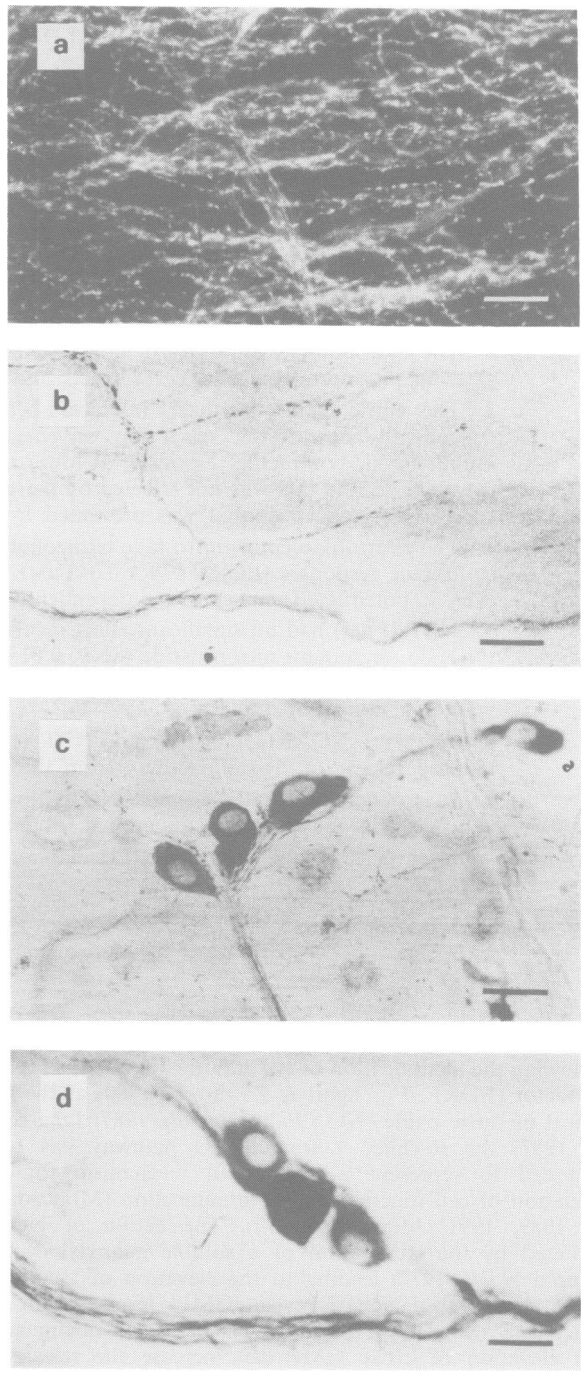

Figure 1 Microphotographs showing: (a) The distribution of catecholamine-containing nerve fibres on whole-mount preparation of the rat anococcygeus muscle. (b) NADPH-diaphorase containing single fibres forming plexus-like structures. (c) NADPH-diaphorase stained neurones in groups forming ganglion structures. Sometimes single neurones were seen lying between the ganglia structures. (d) Prominent nerve tracts which could be followed across the preparations and connecting ganglion structures. Calibration bars = 30 μm.

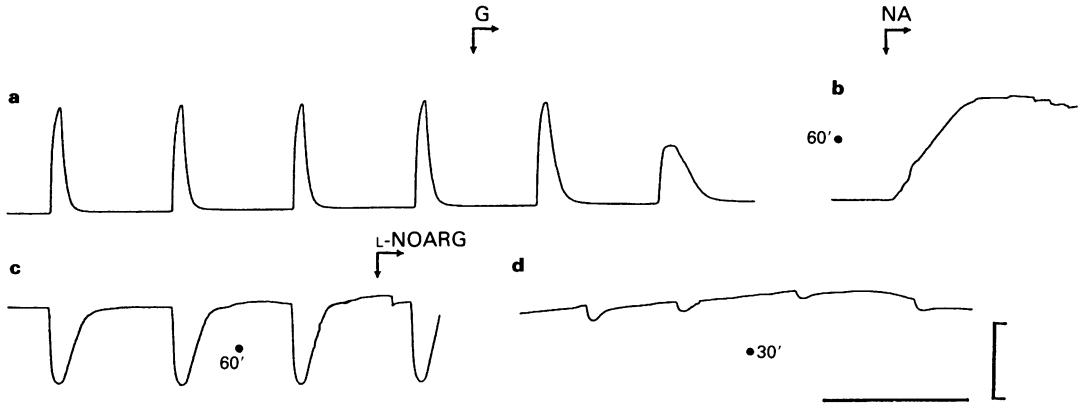

Figure 2 The neurogenic responses of the rat anococcygeus muscle induced by electrical field stimulation (60 V, 20 Hz, 0.6 ms, 10 s duration at 130 s interval). The mechanograms are original recordings of the consecutive responses of one preparation and are representative of all experiments of this series. (a) The electrically induced contractions in the presence of atropine (1 μM) an inhibition of the contractile response by guanethidine (G; 50 μM). (b) Complete block of the contractile response to electrical stimulation applied at 60th min of the guanethidine treatment and the effect of exogenously applied noradrenaline (NA; 1 μM). (c) The electrically induced relaxations (guanethidine 50 μM and atropine 1 μM present) of the precontracted (NA 1 μM) muscle and the application of N^G-nitro-L-arginine (L-NOARG, 100 μM). (d) The inhibition of relaxation after 30 min L-NOARG treatment. The time elapsed after each treatment is indicated by the dot. Arrows show the beginning and onward flow of the medium containing the respective drug(s). Note that atropine (1 μM) is present from (a) to (d). The bars represent 10 mN (vertical) and 2 min (horizontal).

After 90 min pre-collection period the perfusate was collected for 63 min divided into 21 consecutive intervals of 3 min each (collections 7, 8, 10, 11, 12, 19, 20 were discarded). Drugs were applied with the perfusion medium at the end of collection 9 (27th min) and were present throughout the next 12 collections. Samples (1 ml) from each collection were added to 2 ml Ready-gel (Beckman) scintillation cocktail and ^{3}H-radioactivity was counted in a Beckman 5300 liquid scintillation system. The perfusion was stopped immediately after the last collection, the preparations were weighed and dissolved in 0.2 ml Soluene 100 (Packard) tissue solubilizer, and the total tissue ^{3}H-radioactivity was counted as described above. The basal outflow, as well as stimulus-evoked overflow, of tritium was calculated as a percentage fractional rate (FR%) as described previously (Kasakov *et al.*, 1988). The FR values of the discarded collections were estimated by a linear approximation from d.p.m. (disintegrations per minute) values in the collections prior to and after the discarded period. The changes in the stimulus-evoked release or spontaneous efflux of ^{3}H were quantified as S_2/S_1 ratio (the integral increase of ^{3}H release over the basal level in collections 16, 17 and 18 versus the identical increase of ^{3}H release in collections 4, 5 and 6) or as B_{15}/B_3 ratio (the level of ^{3}H in collection 15 versus the level of ^{3}H in collection 3). The basal levels of ^{3}H release during S_1 and S_2 were estimated by a linear approximation from the values in collections 3 and 9 or collections 15 and 21.

Drugs used

The drugs used were: albumin (bovine, fraction V), L-ascorbic acid, atropine sulphate, bacitracin, cocaine hydrochloride, ethylenediamine tetraacetic acid disodium salt (EDTA), N^G-nitro-L-arginine (L-NOARG), nitro blue tetrazolium (NBT), noradrenaline hydrochloride, β-NADPH, sodium nitroprusside (all from Sigma) and guanethidine monosulphate (Ismelin, CIBA). All drugs were first prepared in distilled water as stock solutions.

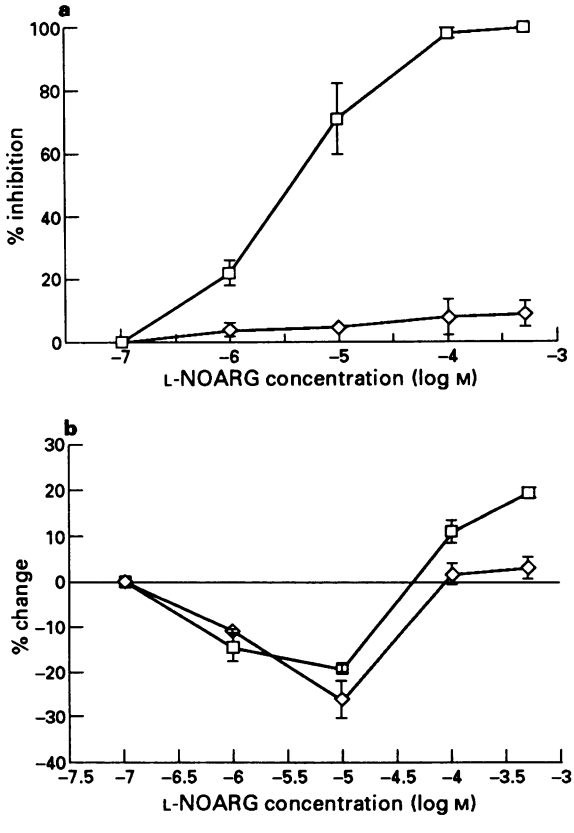

Figure 3 The effect of N^G-nitro-L-arginine (L-NOARG) on the neurogenic relaxation (a) and contraction (b) of the rat anococcygeus muscle induced by electrical field stimulation (see legend for Figure 2). The effect of L-NOARG in the absence (□) and presence (◇) of L-arginine is shown. Each point represents the mean ± s.e.mean of 4 to 7 experiments.

Statistical analysis

Quantitative data are expressed as mean ± s.e.mean and the differences between two means were evaluated by Student's two-tailed *t* test for paired or unpaired observations as appropriate. A probability of less than 0.05 was considered statistically significant. *n* denotes the number of preparations.

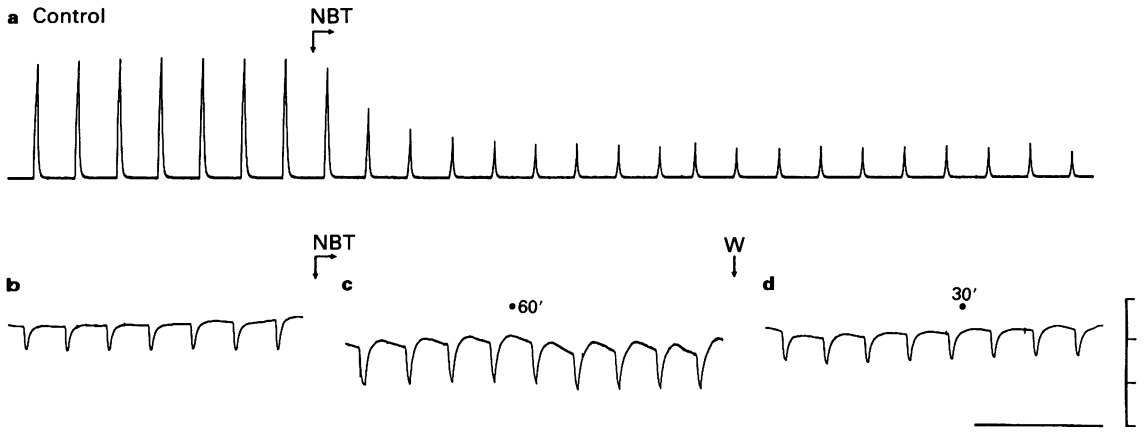

Figure 4 The effect of nitro blue tetrazolium (NBT) on the electrically induced responses of the rat anococcygeus muscle induced by electrical field stimulation (see legend to Figure 2). The mechanographs are original recordings from two experiments and are representative of all experiments of this series. (a) Neurogenic contractions and the inhibitory effect of NBT (1 μM) in the absence of guanethidine. (b) Neurogenic relaxations of the precontracted muscle (by noradrenaline, NA, 1 μM) in the presence of guanethidine (50 μM) and atropine (1 μM). (c) Neurogenic relaxations in the presence of NBT (1 μM). (d) Restoration of the initial tone and neurogenic relaxations after the wash out of NBT (W). Note that atropine (1 μM) is present from (a) to (b). The bars represent 30 mN (vertical) and 5 min (horizontal). The time elapsed after NBT and W is indicated by the dot.

Results

NADPH-diaphorase and catecholamine staining

The NADPH-diaphorase reaction used for the histochemical studies is based on the NADPH-dependent reduction of NBT (an electron accepting substrate for NADPH-diaphorase and one of the constituent chemicals of the staining solution) to produce a visible formazan product (Hope *et al.*, 1990). There were single nerve fibres, nerve tracts and neuronal cell bodies that stained for NADPH-diaphorase (Figure 1b,c,d). The neurones were found mostly in aggregates as intramural ganglia with some single neurones lying between the ganglion structures (Figure 1c,d). There were few single nerve fibres forming plexus-like structures (Figure 1b). However, several thin and thick nerve tracts could be followed across the preparations connecting ganglionic structures (Figure 1c,d).

The fluorescence histochemistry revealed a dense innervation of the rat anococcygeus muscle by catecholamine-containing nerve fibres (Figure 1a).

Effect of L-NOARG and NBT on the contractile and relaxant responses

In atropine-containing medium the preparations responded to electrical stimulation with fast high-amplitude contractions which increased in amplitude as stimulation continued and rapidly relaxed to the prestimulation level at its cessation (Figure 2a). After application of guanethidine (50 μM) the contractile responses rapidly attenuated and in 46–60 min were almost completely inhibited (Figure 2b). The application of NA (1 μM) in the presence of guanethidine (1 μM) and atropine (1 μM) induced a sustained increase of the tone that reached similar or higher amplitude than the neurogenic contractions and remained unchanged until NA was present (Figure 2b). Applied at that level, the electrical stimulation with identical parameters evoked fast high-amplitude relaxations which reached the maximum before the stimulation terminated followed by a slow restoration of the prestimulation tone (Figure 2c). The relaxations were inhibited by L-NOARG (100 μM). This effect was combined in many preparations with a slight increase of the tone (Figure 2d).

The effect of L-NOARG on the mechanical responses of the rat anococcygeus muscle was studied in a concentration range of 0.1 to 500 μM. It was found that L-NOARG inhibited concentration-dependently the relaxant responses

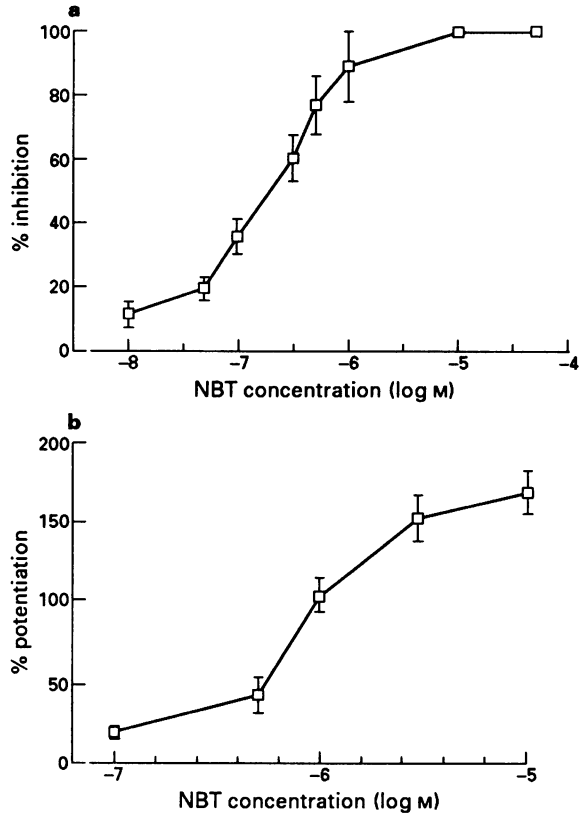

Figure 5 The effect of nitro blue tetrazolium (NBT) on neurogenic contraction (a) and relaxation (b) of the rat anococcygeus muscle induced by electrical field stimulation (see legend to Figure 2). Each point represents the mean ± s.e.mean of 7 to 9 experiments.

(Figure 3a). This inhibitor effect was antagonized by L-arginine (500 μM) (Figure 3a). When L-NOARG was applied in concentrations higher than 10 μM it caused in 50% of all preparations an additional rise in tension which varied from 15 to 30% of the tone generated in the presence of NA. As is shown in Figure 3b, lower concentrations of L-NOARG (0.1–50 μM) attenuated concentration-dependently the con-

tractile responses. On the contrary higher concentrations (100–500 μM) L-NOARG induced a potentiation of the contractile responses. L-Arginine (500 μM) antagonized the L-NOARG-induced potentiation of the contractile responses but did not affect L-NOARG-induced decrease of the neurogenic contractions. NBT was applied in a concentration range of 0.01–50 μM. It was found that NBT produced a rapid inhibition of the contractile response (Figure 4a). The results of these experiments are summarized in Figure 5a. EC_{50} estimated for the inhibition of contractile response was 0.178 ± 0.041 μM. The response to exogenously applied NA (1 μM) was inhibited by NBT (0.5 μM) by 30–35% (not shown). In another series of experiments the effect of NBT on the neurogenic relaxation was investigated. It was found that NBT produced a rapid decline of the tone. Despite the lower tone of the preparation, relaxations evoked by electrical field stimulation were greatly potentiated in the presence of NBT (Figure 4c). The effect was concentration-dependent and eliminated soon after the wash out of the substance (Figure 4d). The results of these experiments are summarized in Figure 5b. The Effect of NBT on the relaxations induced by the exogenously applied NO-donor sodium nitroprusside (SNP) was investigated. It was found that NBT (1 μM) did not change significantly the relaxation induced by SNP. The results of these experiments are shown in Figure 6. However

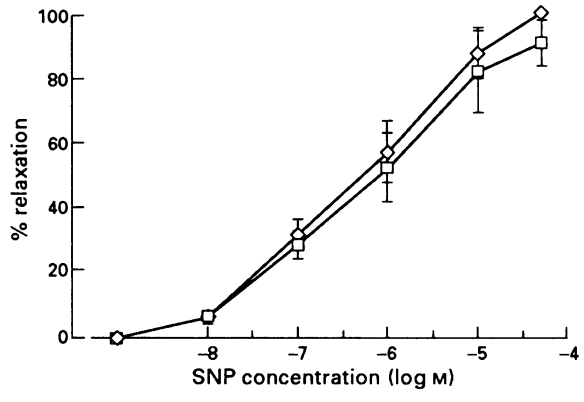

Figure 6 Sodium nitroprusside (SNP)-induced relaxation of rat anococcygeus muscle in the absence (□) and presence (◇) of nitro blue tetrazolium (NBT, 1 μM). SNP was applied intermittently for 4 min at 20 min intervals. The initial concentrations were appropriately adjusted to give the final concentrations required. With this experimental protocol no tachyphylaxis towards SNP was observed. Each point represents the mean ± s.e.mean of 7 experiments.

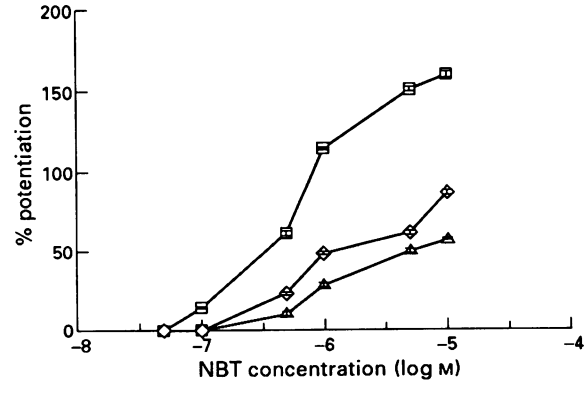

Figure 7 The effect of nitroblue tetrazolium (NBT) on the neurogenic relaxation of the rat anococcygeus muscle induced by electrical field stimulation (see legend to Figure 2) in the absence (□) and presence of N^G-nitro-L-arginine at concentrations of 10 μM (◇) and 50 μM (△). Each point represents the mean ± s.e.mean of 6 or 7 experiments.

the potentiating effect of NBT on the electrically evoked relaxation was significantly antagonized in a non-competitive manner by L-NOARG (Figure 7).

Effect of L-NOARG and NBT on ^3H release

The data presented above showed that L-NOARG and NBT may strongly inhibit and potentiate respectively the nitrergic relaxant responses in the rat anococcygeus muscle. At the same time L-NOARG and NBT were powerful modulators of the noradrenergic contractile responses. These effects might result from a pre-junctional or a postjunctional nitrergic modulation of the noradrenergic transmission in the anococcygeus muscle. Therefore the next step was to investigate the effect of L-NOARG and NBT on the spontaneous as well as the electrically induced release of ^3H in the anococcygeus muscle. The electrical stimulation of non-treated preparations induced a rapid substantial increase in the level of ^3H in the perfusate which corresponded to the twitch contractile response of the muscle. A second stimulation produced similar contractile response and ^3H release (Figure 8). L-NOARG applied at a concentration of 100 μM, which produced a nearly complete block of the relaxations, potentiated the contractile response but did not change the spontaneous or the electrically induced release of ^3H. NBT at a concentration of 1 μM, which strongly inhibited the contractile response, also did not change the release of ^3H. It was found that some 15% of the total ^3H activity which accumulated in the tissue during the incubation period was released in the superfusate under this experimental protocol. The total release was changed neither by L-NOARG nor NBT. The results of these experiments are summarized in Table 1.

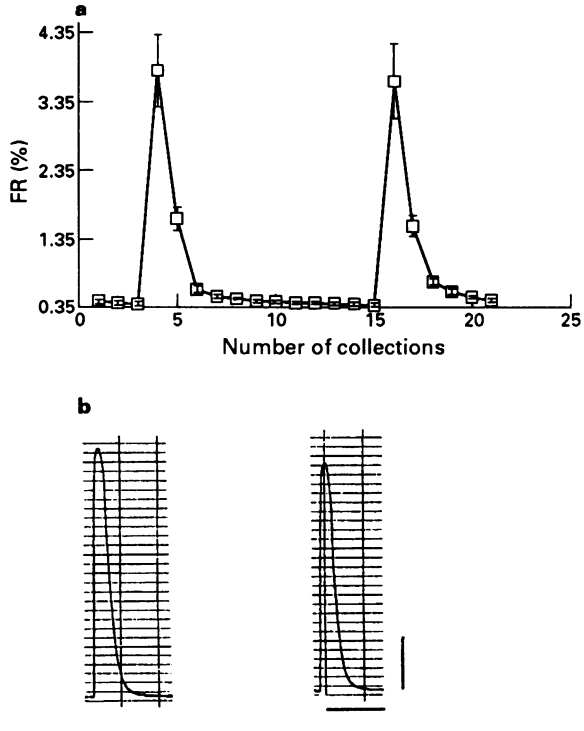

Figure 8 'No drugs' contractile response of the rat anococcygeus muscle induced by electrical field stimulation (b; 60 V, 20 Hz, 0.6 ms, 60 s duration twice at 45 min interval). The corresponding fractional rate (FR %) of ^3H release measured in the perfusate is shown in (a). The mechanogram is an original recording from one experiment and is representative of all experiments of this series. The bars represent 10 mN (vertical) and 5 min (horizontal). Note the different time scales; the mechanical activity is recorded at a paper advance of 3 mm min^{-1}. Each point in the ^3H fractional rate graph represents the values of ^3H-radioactivity in the superfusate of 21 consecutive 3 min collections of 4–8 experiments.

Table 1 The effect of N^G-nitro-L-arginine (L-NOARG) and nitro blue tetrazolium (NBT) on the contractile response and corresponding ^3H release in the rat anococcygeus muscle

	B_{15}/B_3	S_2/S_1	A_2/A_1	*Total release 0–63 min (%)*
Control	0.95 ± 0.05 ($n = 6$)	0.98 ± 0.03 ($n = 5$)	0.91 ± 0.02 ($n = 6$)	18.79 ± 1.22 ($n = 6$)
L-NOARG (100 μM)	0.09 ± 0.03 ($n = 8$)	0.93 ± 0.04 ($n = 8$)	1.22 ± 0.08** ($n = 8$)	15.46 ± 1.29 ($n = 8$)
NBT (1 μM)	0.91 ± 0.08 ($n = 4$)	1.01 ± 0.07 ($n = 4$)	0.67 ± 0.02** ($n = 4$)	15.2 ± 0.66 ($n = 4$)

The effect of L-NOARG and NBT on spontaneous (B_{15}/B_3, the ratio of ^3H-radioactivity in collections 15 and 3), electrically induced (S_2/S_1, the ratio of the integral increase of ^3H release over the basal level in collections 16, 17 and 18 and the identical increase of ^3H release in collections 4, 5 and 6) at 60 V, 20 Hz, 0.6 ms, 60 s duration twice at 45 min interval, percentage total release of ^3H and amplitude of the contractile responses (A_2/A_1, the ratio of the amplitude of contractile responses (mm) induced by S_2 and S_1), in the rat anococcygeus muscle. n denotes number of preparations. $^{**}P < 0.01$.

Discussion

The morphological findings in the present study have demonstrated the presence of neurones and nerve fibres that contain NADPH-diaphorase in the rat anococcygeus, similar to that reported by Dail *et al.* (1993). Hope *et al.* (1991) have revealed that neuronal NADPH-diaphorase is an NO-synthase (NOS) and the co-localization of NOS and NADPH-diaphorase has been shown by others, establishing that NADPH-diaphorase staining accounts for the presence of NOS in neuronal structures (Bredt *et al.*, 1991; Belai *et al.*, 1992; Bredt & Snyder, 1992). The brain tissue has been shown to contain a cystolic (soluble) isoform of NOS while vascular endothelium contains a particulate isoform (Bredt & Snyder, 1990; Schmidt *et al.*, 1991; Mitchell *et al.*, 1991a). Unlike brain and endothelium, the rat anococcygeus muscle is reported to contain both particulate and soluble NOS activity (Mitchell *et al.*, 1991b). The authors have demonstrated that NOS is localized specifically in the NANC neuronal components rather than smooth muscle cells, as the activity of NOS in the rat anococcygeus is dependent on the presence of calcium, unlike the inducible NOS which has calcium/calmodulin independent activity (Mitchell *et al.*, 1991b). These findings suggest that NO (or a related molecule) is one of the NANC neurotransmitters in the rat anococcygeus muscle. The presence of dense catecholamine-containing nerve fibres supports the previous findings that the majority of the fibres supplying the muscle are noradrenergic (Burnstock *et al.*, 1978).

The present investigation has demonstrated that modulation of the NO-dependent relaxation of rat anococcygeus muscle corresponded to reciprocal modulatory effects on the neurogenic contractile responses of the muscle.

We utilized this finding to study the level at which the interaction between two neurotransmitter mechanisms may occur. The inhibition of the relaxation corresponded to an increase in the amplitude of the contractions evoked by electrical nerve stimulation or exogenously applied NA. However, the corresponding release of ^3H from the nerve terminals supplying the tissue remained unchanged. Furthermore, the potentiation of NO-related relaxation corresponded to a marked inhibition of the contractile response. Again there were no changes in the release of ^3H from the nerve terminals. These findings strongly suggest that NO-modulation of noradrenergic responses occurs at postjunctional but not prejunctional site(s). Similar findings have been reported recently for the rat tail artery (Bucher *et al.*, 1992), in which neurogenic vasoconstriction is modulated by NO and this modulation is not due to a prejunctional action of NO. In a recent investigation Brave *et al.* (1993) found that L-NOARG did not change the electrically-induced release of ^3H in the rat anococcygeus preloaded with [^3H]-NA. The authors concluded that endogenous nitrate NANC transmitter did not influence release of NA from the sympathetic nerves in the rat anococcygeus muscle. The negative postjunctional modulation of the contractile response of the rat anococcygeus muscle by NO is an example of the physiological antagonism between the excitatory (NA) and inhibitory (NO) transmitter mechanisms which may contribute to the balance of the excitatory and inhibitory inputs in the autonomically innervated tissues.

The data presented here show that inhibition of NOS by high concentrations of L-NOARG (0.1–0.5 μM) potentiates the neurogenic contraction. Similar potentiation of the contractile responses by NOS-inhibitors has also been described by other authors (Gustafsson *et al.*, 1990a; Belvisi *et al.*, 1991). This effect is most likely due to elimination of the relaxant effect of NO. This seems to be a specific effect since: (1) at the same concentrations, L-NOARG completely inhibited the neurogenic relaxations of the rat anococcygeus muscle that are mediated by NO-related mechanism(s) (Martin & Gillespie, 1990); (2) potentiation was reversed by L-arginine. This also implies that generation of NO may contribute to the continuous low, or negligible, tone of this smooth muscle. This is further supported by the observation that in a great number of preparations L-NOARG inhibited the relaxation and induced a further rise of the tone of the precontracted tissue. The existence of a physiologically significant continuous generation of NO has also been suggested in the gastrointestinal tract (Wiklund *et al.*, 1993). It may serve as an ubiquitous mechanism for a physiological adjustment of the tone of the smooth muscles. In the present study it has been additionally found that L-NOARG at lower concentrations (0.1–50 μM) attenuated the neurogenic contractions and that L-arginine did not reverse this effect. Similar results have been reported for dog mesenteric artery (Toda & Okamura, 1990). Recently it has been found that N^G-monomethyl-L-arginine but not L-NOARG (20 μM) was a partial agonist for NOS (Archer & Hampl, 1992). In the present investigation L-NOARG produced its maximal inhibitory effect on the contractile responses at concentrations of 1–50 μM. It is most likely to be a non-specific effect of which the mechanism has yet to be unravelled.

NBT is an electron acceptor in the NADPH-diaphorase reaction and a constituent of the recipes for the NADPH-diaphorase visualization (Hope *et al.*, 1990). We reported here that NBT dose-dependently potentiated the NO-mediated relaxation of the rat anococcygeus muscle. It is unlikely to be primarily due to an inhibition of the excitatory transmitter mechanisms since atropine and guanethidine were present throughout the experiment. NBT might potentiate the neurogenic relaxation in the rat anococcygeus muscle by a stimulation of NO synthesis/release. As NO is not stored in the nerve terminals, NOS is more likely to be the primary target for the action of NBT. This suggestion is supported by two findings: (1) NBT had no effect on the relaxation

induced by the NO-donor molecule SNP and (2) NBT-induced potentiation of the electrically induced relaxation of rat anococcygeus muscle was significantly decreased by the specific NOS inhibitor L-NOARG. This is however a non-competitive antagonist effect. Recently, Davisson *et al.* (1993) reported that NBT produced substantial hypotension and vasodilatation in rats. The authors suggested that these effects of NBT involve an augmentation of NO synthesis/release. It has been shown that NBT at a concentration of 50 μM completely inhibited NOS with a K_i, with respect to L-arginine, of 11 μM (Hope *et al.*, 1991). In the present investigation, NBT potentiated the relaxation at much lower concentrations (0.01–1 μM). The present study does not verify the exact mechanism of this activation but it seems plausible to suggest that at these lower concentrations NBT acts as a substrate activator of NOS, whereas at higher concentrations it is a competitive inhibitor of NOS. The finding that NBT is able, at lower concentrations, to potentiate the NO-dependent relaxation in the rat anococcygeus muscle could be a useful tool in future investigations.

This work was supported by the Wellcome Trust (Grant to L.K.) and the Bulgarian Ministry of Education, Science & Culture (Project L1/91). We thank Dr D. Christie for her editorial assistance.

References

ARCHER, S.L. & HAMPL, V. (1992). N^G-monomethyl-L-arginine causes nitric oxide synthesis in isolated arterial rings: trouble in paradise. *Biochem. Biophys. Res. Commun.*, **188**, 590–596.

ARNOLD, W.P., MITTAL, C.K., KATSUKI, S. & MURAD, F. (1977). Nitric oxide activates guanylate cyclase and increases guanosine 3′,5′-cyclic monophosphate levels in various tissue preparations. *Proc. Natl. Acad. Sci. U.S.A.*, **74**, 3203–3207.

BELAI, A., SCHMIDT, H.H.H.W., HOYLE, C.H.V., HASSALL, C.J.S., SAFFREY, M.J., MOSS, J., FÖRSTERMANN, U., MURAD, F. & BURNSTOCK, G. (1992). Colocalization of nitric oxide synthase and NADPH-diaphorase in the myenteric plexus of the rat gut. *Neurosci. Lett.*, **143**, 60–64.

BELVISI, M.G., STRETTON, D. & BARNES, P.J. (1991). Nitric oxide as an endogenous modulator of cholinergic neurotransmission in guinea-pig airways. *Eur. J. Pharmacol.*, **198**, 219–221.

BRAVE, S.R., BHAT, S., HOBBS, A.J., TUCKER, J.F. & GIBSON, A. (1993). The influence of L-N^G-Nitro-arginine in sympathetic nerve induced contraction and noradrenaline release in the rat isolated anococcygeus muscle. *J. Auton. Pharmacol.*, **13**, 219–225.

BREDT, D.S., GLATT, C.E., HWANG, P.M., FOTUHI, M., DAWSON, T.M. & SNYDER, S.H. (1991). Nitric oxide synthase protein and mRNA are discreetly localised in neuronal populations of the mammalian CNS together with NADPH diaphorase. *Neuron.*, **7**, 615–624.

BREDT, D.S. & SNYDER, S. (1990). Isolation of nitric oxide synthase, a calmodulin-requiring enzyme. *Proc. Natl. Acad. Sci. U.S.A.*, **87**, 682–685.

BREDT, D.S. & SNYDER, S.H. (1992). Nitric oxide, a novel neuronal messenger. *Neuron*, **8**, 3–11.

BUCHER, B., OUEDRAOGO, S., TSCHÖPL, M., PAYA, D. & STOCLET, J.C. (1992). Role of the L-arginine-NO pathway and cyclic GMP in electrical field-induced noradrenaline release and vasoconstriction in the rat tail artery. *Br. J. Pharmacol.*, **107**, 976–982.

BULT, H., BOECKXSTAENS, G.E., PELCKMANS, P.A., JORDAENS, F.H., VAN MAERCKE, Y.M. & HERMAN, A.G. (1990). Nitric oxide as an inhibitory non-adrenergic non-cholinergic neurotransmitter. *Nature*, **345**, 346–347.

BURNSTOCK, G., COCKS, T. & CROWE, R. (1978). Evidence for purinergic innervation of the anococcygeus muscle. *Br. J. Pharmacol.*, **64**, 13–20.

CEDERQUIST, B., WIKLUND, N.P., PERSSON, M.G. & GUSTAFSSON, L.E. (1991). Modulation of neuroeffector transmission in the guinea-pig pulmonary artery by endogenous nitric oxide. *Neurosci. Lett.*, **127**, 67–69.

COHEN, R.A. & WEISBROD, R.M. (1988). Endothelium inhibits norepinephrine release from adrenergic nerves of rabbit carotid artery. *Am. J. Physiol.*, **254**, H871–H877.

DAIL, W.G., GALLOWAY, B. & BORDEGARAY, J. (1993). NADPH diaphorase innervation of the rat anococcygeus and retractor penis muscles. *Neurosci. Lett.*, **160**, 17–20.

DAVISSON, R.L., WALTON, T.M., JOHNSON, A.K. & LEWIS, S.J. (1993). Cardiovascular effects produced by systemic injections of nitro blue tetrazolium in the rat. *Eur. J. Pharmacol.*, **241**, 135–137.

FURCHGOTT, R.F. & ZAWADZKI, J.V. (1980). The obligatory role of endothelial cells in the relaxation of arterial smooth muscle by acetylcholine. *Nature*, **288**, 373–376.

GARTHWAITE, J. (1991). Glutamate, nitric oxide and cell-cell signalling in the nervous system. *Trends Neurol. Sci.*, **14**, 60–67.

GIBSON, A., MIRZAZADEH, S., HOBBS, A.J. & MOORE, P.K. (1990). L-N^G-monomethyl arginine and L-N^G-nitro arginine inhibit non-adrenergic, non-cholinergic relaxation of the mouse ancoccygeus muscle. *Br. J. Pharmacol.*, **99**, 601–606.

GILLESPIE, J.S. (1980). The physiology and pharmacology of the anococcygeus muscle. *Trends Pharmacol. Sci.*, **16**, 453–457.

GREENBERG, S., DIECKE, F.P., PEEVY, K. & TANAKA, T.P. (1989). The endothelium modulates adrenergic neurotransmission to canine pulmonary arteries and veins. *Eur. J. Pharmacol.*, **162**, 67–70.

GREENBERG, S., DIECKE, F.P.J., PEEVY, K. & TANAKA, T.P. (1990). Release of norepinephrine from adrenergic nerve endings of blood vessels is modulated by endothelium-derived relaxing factor. *Am. J. Hypertens.*, **3**, 211–218.

GUSTAFSSON, L.E., WIKLUND, P.N., WIKLUND, C.U., CEDERQUIST, B., PERSSON, M.G. & MONCADA, S. (1990b). Modulation of autonomic neuroeffector transmission by nitric oxide-like activity in guinea-pig smooth muscle. In *Nitric Oxide from L-Arginine: A Biomodulatory System.* ed. Moncada, S. & Higgs, E.A. pp. 177–181. Amsterdam: Elsevier.

GUSTAFSSON, L.E., WIKLUND, C.U., WIKLUND, P.N., PERSSON, M.G. & MONCADA, S. (1990a). Modulation of autonomic neuroeffector transmission by nitric oxide in guinea-pig ileum. *Biochem. Biophys. Res. Commun.*, **173**, 106–110.

HOBBS, A.J. & GIBSON, A. (1990). L-N^G-nitro-arginine and its methyl ester are potent inhibitors of non adrenergic, non-cholinergic transmission in the rat anococcygeus. *Br. J. Pharmacol.*, **100**, 749–752.

HOPE, B.T., MICHAELS, G.J., KNIGGE, K.M. & VINCENT, S.R. (1990). NADPH-diaphorase synthesizes a second messenger: Yes or No. *Abstracts Soc. Neurosci.*, **16**, 228.7.

HOPE, B.T., MICHAELS, G.J., KNIGGE, K.M. & VINCENT, S.R. (1991). Neuronal NADPH-diaphorase is a nitric oxide synthase. *Proc. Natl. Acad. Sci. U.S.A.*, **88**, 2811–2814.

IGNARRO, L.J., BUGA, G.M., WOOD, K.S., BYRNS, R.E. & CHAUDHURY, G. (1987). Endothelium-derived relaxing factor produced and released from artery and vein is nitric oxide. *Proc. Natl. Acad. Sci. U.S.A.*, **84**, 9265–9269.

KASAKOV, L., ELLIS, J., KIRKPATRICK, K., MILNER, P. & BURNSTOCK, G. (1988). Direct evidence for concomitant release of noradrenaline, adenosine 5′-triphosphate and neuropeptide Y from sympathetic nerves supplying guinea-pig vas deferens. *J. Auton. Nerv. Syst.*, **22**, 75–82.

KASAKOV, L., BELAI, A., VLASKOVSKA, M. & BURNSTOCK, G. (1991). Potentiation of nitric oxide-mediated neurogenic relaxation of the rat anococcygeus muscle by nitro blue tetrazolium. *Proc. 5th Natl. Congress Bulg. Physiol. Soc.*, **7**.

MARTIN, W. & GILLESPIE, J.S. (1990). L-arginine-derived nitric oxide: the basis of inhibitory transmission in the anococcygeus and retractor penis muscle. In *Novel Peripheral Neurotransmitters.* ed. Bell, C. pp. 65–79. Oxford: Pergamon Press.

MITCHELL, J.A., FÖRSTERMANN, U., WARNER, T.D., POLLOCK, J.S., SCHMIDT, H.H.H.W., HELLER, M. & MURAD, F. (1991a). Endothelial cells have a particulate enzyme system responsible for EDRF formation: measurement by vascular relaxation. *Biochem. Biophys. Res. Commun.*, **176**, 1417–1423.

MITCHELL, J.A., SHANG, H., FÖRSTERMANN, U. & MURAD, F. (1991b). Characterization of nitric oxide synthase in non-adrenergic non-cholinergic nerve containing tissue from the rat anococcygeus muscle. *Br. J. Pharmacol.*, **104**, 289–291.

MONCADA, S. (1992). The L-arginine: nitric oxide pathway. *Acta Physiol. Scand.*, **145**, 201–227.

MONCADA, S., PALMER, R.M.J. & HIGGS, E.A. (1989). Biosynthesis of nitric oxide from L-arginine. A pathway for the regulation of cell function and communication. *Biochem. Pharmacol.*, **38**, 1709–1715.

MONCADA, S., PALMER, R.M.J. & HIGGS, E.A. (1991). Nitric oxide: physiology, pathophysiology and pharmacology. *Pharmacol. Rev.*, **43**, 109–142.

PALMER, R.M.J., FERRIGE, A.S. & MONCADA, S. (1987). Nitric oxide release accounts for the biological activity of endothelium-derived relaxing factor. *Nature*, **327**, 524–526.

PALMER, R.M.J., REES, D.D., ASHTON, D.S. & MONCADA, S. (1988). L-Arginine is the physiological precursor for the formation of nitric oxide in endothelium-dependent relaxation. *Biochem. Biophys. Res. Commun.*, **153**, 1251–1256.

RAND, M.J. (1992). Nitrergic transmission: nitric oxide as a mediator of non-adrenergic, non-cholinergic neuro-effector transmission. *Clin. Exp. Pharmacol. Physiol.*, **19**, 147–169.

SANDERS, K.M. & WARD, S.M. (1992). Nitric oxide as a mediator of nonadrenergic noncholinergic neurotransmission. *Am. J. Physiol.*, **262**, G379–G392.

SCHMIDT, H.H.H.W., POLLOCK, J.S., NAKANE, M., GORSKY, L.D., FÖRSTERMANN, U. & MURAD, F. (1991). Purification of a soluble isoform of guanyl cyclase-activating synthase. *Proc. Natl. Acad. Sci. U.S.A.*, **88**, 365–369.

SNYDER, S.H. & BREDT, D.S. (1991). Nitric oxide as a neuronal messenger. *Trends Pharmacol. Sci.*, **12**, 125–128.

TODA, H. & OKAMURA, T. (1990). Modification by L-N^G-monomethyl arginine (L-NMMA) on the response to nerve stimulation in isolated dog mesenteric and cerebral arteries. *Jpn. J. Pharmacol.*, **52**, 170–173.

TODA, H. & OKAMURA, T. (1992). Mechanism of neurally induced monkey mesenteric artery relaxation and contraction. *Hypertension*, **19**, 161–166.

WIKLUND, N.P., LEONE, A.M., GUSTAFSSON, L.E. & MONCADA, S. (1993). Release of nitric oxide evoked by nerve stimulation in guinea-pig intestine. *Neuroscience*, **53**, 607–611.

YAMAMOTO, R., WADA, A., ASADA, Y., NIINA, H. & SUMIYOSHI, A. (1992). N^G-nitro-L-arginine, an inhibitor of nitric oxide synthesis, decreases noradrenaline outflow in rat isolated perfused mesenteric vasculature. *Naunyn-Schmied. Arch. Pharmacol.*, **319**, 29–33.

(Received October 20, 1993
Revised January 25, 1994
Accepted February 1, 1994)

Br. J. Pharmacol. (1994), **112**, 411–416

Mechanisms of sympathetic enhancement and inhibition of parasympathetically induced salivary secretion in anaesthetized dogs

Mary A. Lung

Department of Physiology, Faculty of Medicine, University of Hong Kong, Sassoon Road, Hong Kong

1 The effects of superimposed and continuous sympathetic nerve stimulation on submandibular parasympathetic salivation were investigated in anaesthetized dogs.

2 Superimposed sympathetic nerve stimulation (1–2 min) initially enhanced and later inhibited salivary secretion induced by parasympathetic nerve stimulation (2–8 Hz) in glands with uncontrolled blood supply or constant-flow vascular perfusion. Propranolol (0.05 mg kg^{-1}, i.a.) did not affect the diphasic sympathetic action whereas phentolamine (0.1 mg kg^{-1}, i.a.) abolished it. Prazosin (0.025 mg kg^{-1}, i.a.) greatly lessened the initial enhancement while yohimbine (0.025 mg kg^{-1}, i.a.) alleviated the late inhibition.

3 Salivary secretion, induced by parasympathetic nerve stimulation (4 Hz) or acetylcholine infusion (10 $\mu g\ kg^{-1}\ min^{-1}$, i.a.), was abolished by atropine (0.05 mg kg^{-1}, i.a.), increased by phenylephrine infusion (0.25 $\mu g\ kg^{-1}\ min^{-1}$, i.a.) and depressed by clonidine infusion (0.75 $\mu g\ kg^{-1}\ min^{-1}$, i.a.). Hexamethionium (12.5 mg kg^{-1}, i.a.) abolished the nerve-induced secretion but had no effect on the acetylcholine-induced secretion.

4 Continuous background sympathetic nerve stimulation decreased parasympathetic nerve-induced salivary secretion in glands with uncontrolled blood supply or constant-flow vascular perfusion.

5 These results show that parasympathetic salivation can be modified by the sympathetic system at the postsynaptic level; enhancement is via α_1-adrenoceptors whereas inhibition is via α_2-adrenoceptors.

Keywords: Parasympathetic salivation; sympathetic enhancement of salivary flow; sympathetic inhibition of salivary flow; postsynaptic α_1-adrenoceptors; postsynaptic α_2-adrenoceptors

Introduction

In experimental animals, parasympathetically induced salivary secretion from the submandibular gland is usually diminished by superimposed sympathetic nerve stimulation (Langley, 1878; Emmelin, 1955). This effect has long been thought to be the result of a reduced blood flow brought about by sympathetic vasoconstriction (Garrett, 1987). However, Lung (1990a) has recently demonstrated, in canine submandibular gland having either uncontrolled blood supply or constant flow vascular perfusion, that superimposed sympathetic nerve stimulation (1–2 min) initially enhances but later diminishes the parasympathetically induced secretion, indicating that the sympathetic action on parasympathetic salivation, apart from being independent of the concurrent blood flow response, is diphasic. The present study was therefore undertaken to investigate the mechanisms underlying the diphasic sympathetic influence on the parasympathetic salivary secretion. Some of the results have been presented in abstracts (Lung, 1990b; 1991; 1992).

Methods

Mongrel dogs (18–22 kg body weight) of either sex were anaesthetized by intravenously administered sodium pentobarbitone (30 mg kg^{-1}); supplementary doses (10 mg kg^{-1}) were given when necessary. Body temperature (rectal) was maintained at 37°C by placing an electric heating pad underneath the animal. Ventilation was monitored via a tracheal cannula and systemic arterial pressure from a cannulated femoral artery. Heparin (1000 u h^{-1}) was given via a cannulated femoral vein.

Measurement of submandibular arterial blood flow and pressure

Submandibular arterial blood flow and pressure were measured as previously described (Lung, 1990a). For determining the arterial flow, an ultrasonic flow sensor (2S, Transonic System) was placed around the facial artery just proximal to the origin of the glandular branch, the major arterial supply to the dog submandibular gland. A catheter was inserted retrogradely into the facial artery with its tip advanced to the origin of the glandular branch for measuring the submandibular arterial pressure or for intra-arterial injection of drugs.

Vascular perfusion of submandibular gland

Vascular perfusion of the gland was performed as previously described (Lung, 1990a). The glandular branch was perfused at a constant flow rate with blood from a femoral artery. The perfusion rate was adjusted to give a perfusion pressure close to the systemic arterial pressure. Changes in vascular resistance were reflected by changes in the mean arterial perfusion pressure.

Measurement of salivary secretion

Salivary secretion was measured as previously described (Lung, 1990a). The submandibular duct was retrogradely cannulated and the catheter was connected to a bottle in which the secreted saliva displaced a saline solution. Drops of saline (0.025 ml in volume) displaced from the bottle were measured; salivary flow was calculated from the time interval between falling drops.

Electrical stimulation of autonomic nerves

Electrical stimulation of the autonomic nerves to the submandibular gland was carried out as previously described (Lung, 1990a). The tied peripheral ends of both nerves were stimulated by bipolar platinum electrodes with varying frequency at fixed supramaximal voltage (5 V for parasympathetic nerve and 20 V for sympathetic nerve) and pulse duration (1 ms).

Drugs

Drugs were dissolved in saline solution and all were infused intra-arterially at the rate of 0.1 ml min^{-1} into the submandibular gland, either via the facial arterial catheter in preparations with uncontrolled blood supply or via the perfusion circuit in preparations with constant flow vascular perfusion. They included: acetylcholine chloride (Sigma), noradrenaline hydrochloride (Sigma), phenylephrine hydrochloride (Sigma), clonidine hydrochloride (Sigma), propranolol hydrochloride (Sigma), phentolamine hydrochloride (Regitine, Ciba), prazosin hydrochloride (Pfizer), yohimbine hydrochloride (Sigma), atropine sulphate (Merck) and hexamethonium bromide (Sigma). Doses are expressed as weights of the salts.

Experimental protocol

Salivary secretion was induced by either parasympathetic nerve stimulation or intra-arterial acetylcholine infusion; salivary flow reached a maximum within 10 s and then declined to a steady level within 30 s as previously reported for parasympathetic stimulation (Lung & Wang, 1990). The steady state parasympathetic salivary secretion was found to remain unchanged throughout a stimulation period of 5–6 min. Sympathetic nerve stimulation or arterial application of a sympathomimetic drug was superimposed for a period of 1–2 min after the parasympathetic nerve stimulation had attained a steady salivary response. In some experiments, parasympathetic salivary secretion was studied against a background of continuous sympathetic nerve stimulation. Ganglionic, cholinergic as well as adrenergic (β-adrenoceptor, α-adrenoceptor or its sub-types) blockades were induced 5 min before the stimulation of parasympathetic salivary secretion. The adequacy of parasympathetic ganglionic blockade was tested by the abolition of the secretory response to preganglionic nerve stimulation. The individual receptor blockade was tested by the abolition of the response of corresponding receptor agonist.

Data recording and analysis

All pressure and flow variables were recorded on magnetic tape (Store 14, Racal) and an oscillographic chart-recorder (2800S, Gould) and mean values were calculated. Data were given as means ± s.e.means. Student's *t* tests were used to determine the level of significance of difference between the means.

Results

Parasympathetic nerve stimulation induced a frequency-dependent steady state salivary flow (2–8 Hz) in dog submandibular glands having uncontrolled blood supply or constant flow vascular perfusion. The response was abolished by hexamethonium (12.5 mg kg^{-1}, i.a., $P<0.05$, $n=4$) or atropine (0.05 mg kg^{-1}, i.a., $P<0.05$, $n=4$). Superimposed sympathetic nerve stimulation (20 Hz for 1 min) initially enhanced (at 5–10 s) but later inhibited (at 50–60 s) parasympathetically induced salivary secretion, whether or not the gland received uncontrolled blood supply or constant-flow vascular perfusion (Figure 1); the inhibitory response persisted with slow recovery after the end of sympathetic stimulation (Figure 4).

Against a background of continuous sympathetic nerve stimulation (20 Hz), salivary secretion induced by parasympathetic nerve stimulation at various frequencies (2–8 Hz) was significantly reduced, whether or not the gland received uncontrolled blood flow or constant-flow vascular perfusion (Figure 2).

The effects of various adrenoceptor blockers on the diphasic sympathetic action on parasympathetic nerve-induced salivary secretion were studied in glands with constant-flow vascular perfusion (Figure 3). Propranolol had

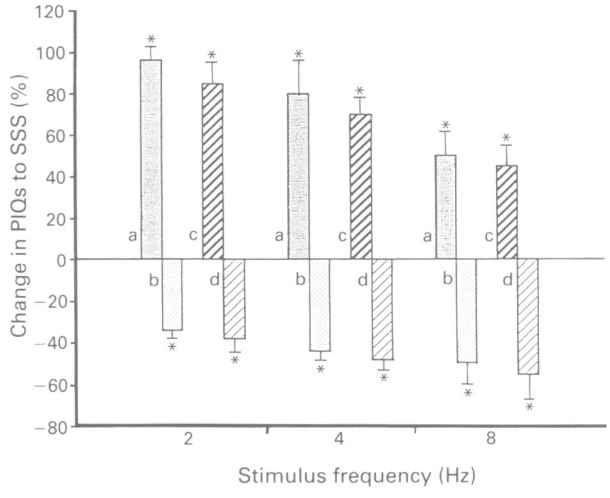

Figure 1 Effects of superimposition of sympathetic nerve stimulation (SSS; 20 Hz of 1 min duration) on parasympathetic nerve-induced salivary secretion (PIQs) in dog submandibular glands with uncontrolled blood supply (a and b) or constant-flow vascular perfusion at a normal blood flow rate (c and d). Change in PIQs to SSS at 5–10 s (a and c); change in PIQs to SSS at 50–60 s (b and d). Number of animals in each group is 15. $*P<0.05$ when compared to the corresponding control (the steady state parasympathetic salivary flow just prior to sympathetic nerve stimulation).

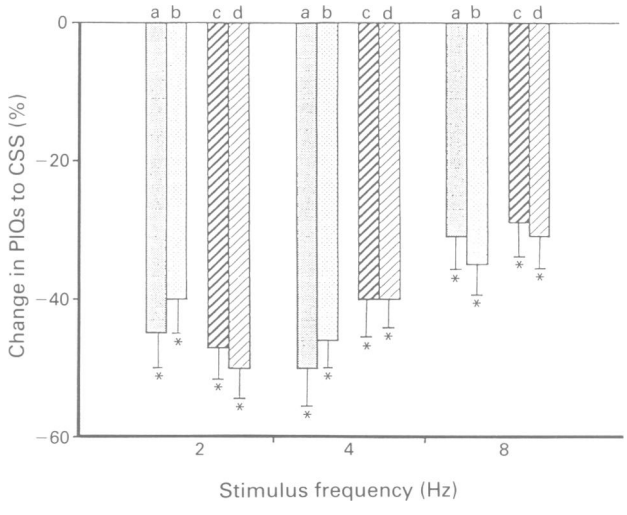

Figure 2 Effects of continuous background sympathetic nerve stimulation (CSS; 20 Hz) on the parasympathetic nerve induced salivary secretion (PIQs; of 1 min duration) in dog submandibular glands with uncontrolled blood supply (a and b) or constant-flow vascular perfusion at a normal blood flow rate (c and d). Change in PIQs to CSS at 5–10 s (a and c); change in PIQs to CSS at 50–60 s (b and d). Number of animals in each group is 6. $*P<0.05$ when compared to corresponding normal response (the parasympathetic salivary response without background sympathetic nerve stimulation).

no effect on the sympathetic action whereas phentolamine abolished the diphasic response. Prazosin greatly lessened the initial response but yohimbine alleviated the late response (Figure 4).

Salivation was also induced by intra-arterial infusion of acetylcholine (10 μg kg^{-1} min^{-1}). As with parasympathetic nerve stimulation, salivary flow showed an initial peak followed by a slight decline to a steady state flow (Figure 6). The salivary flow to acetylcholine was found to be unaffected by hexamethonium (12.5 mg kg^{-1}, i.a., P = NS, n = 4) but abolished by atropine (0.05 mg kg^{-1}, i.a., $P<0.05$, n = 4).

The effects of various adrenoceptor agonists on salivary secretion induced by parasympathetic nerve stimulations or by intra-arterial acetylcholine infusion were studied in glands with constant-flow vascular perfusion (Figure 5). Phenylephrine potentiated parasympathetic salivation with a maximum occurring at 10 s after the onset of the response (Figure 6); but subsequent additional superimposed sympathetic nerve stimulation could only elicit the late inhibitory action (Figure 7). Clonidine decreased parasympathetic salivation with the steady response reached at 60 s after the onset of the response (Figure 6) with the succeeding additional superimposed sympathetic nerve stimulation capable of causing an initial enhancement and a late inhibition on secretion (Figure 7).

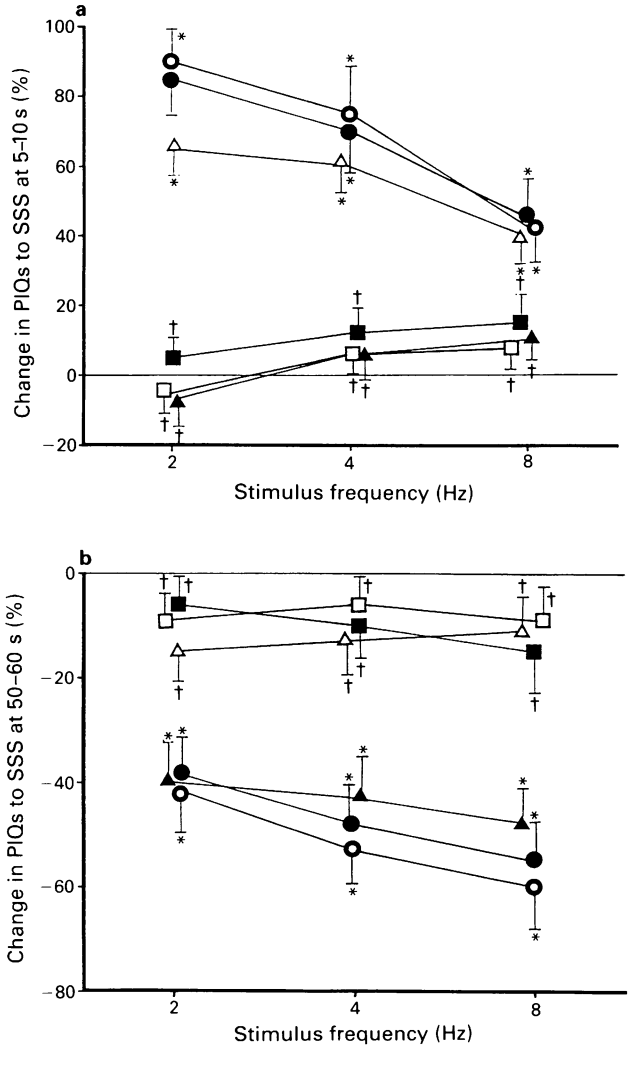

Figure 3 Effects of adrenoceptor blocking agents on the effects of superimposed sympathetic nerve stimulation (SSS; 20 Hz of 1 min) on the parasympathetic nerve-induced salivary secretion (PIQs) in dog submandibular glands with constant-flow vascular perfusion at a normal blood flow rate. (a) Changes in PIQs to SSS at 5–10 s; (b) change in PIQs to SSS at 50–60 s. Normal (●, n = 15); after propranolol (0.05 mg kg^{-1} min^{-1}, ○, n = 8); after phentolamine (0.1 mg kg^{-1} min^{-1}, ■, n = 6); after prazosin (0.025 mg kg^{-1} min^{-1}, ▲, n = 8); after yohimbine (0.025 mg kg^{-1} min^{-1}, △, n = 8); after prazosin and yohimbine (0.025 mg kg^{-1} min^{-1} each, □, n = 8). *$P<0.05$ when compared to the corresponding control (the steady state parasympathetic salivary flow just prior to sympathetic nerve stimulation). †$P<0.05$ when compared to the normal response.

Discussion

This study demonstrated, for the first time, that maximal sympathetic nerve stimulation could exert a diphasic action, an initial enhancement followed by an inhibition, over a wide range of salivary flow caused by parasympathetic nerve stimulation (2–8 Hz) (Figure 1). The events occurred whether the submandibular gland received uncontrolled blood supply or constant-flow vascular perfusion at resting blood flow rate. We have previously shown that as long as blood flow to the gland is maintained at a normal flow rate, secretory response to parasympathetic nerve stimulation (0.5–32 Hz) is not significantly affected (Lung, 1990a). Therefore, the sympathetic diphasic action on parasympathetic salivary secretion is not related to concurrent vascular changes. Interestingly, continuous background sympathetic nerve stimulation was found to exert a single action on parasym-

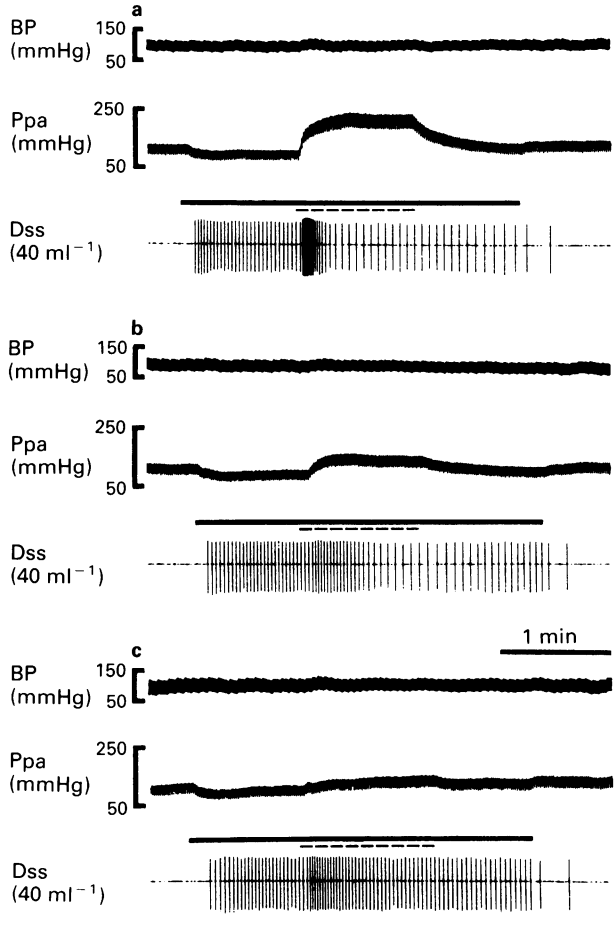

Figure 4 Experimental record illustrating the effects of adrenoceptor blockers on the effects of superimposed sympathetic nerve stimulation (20 Hz) on parasympathetic nerve induced salivary secretion (2 Hz) in a submandibular gland with vascular perfusion. (a) Normal response; (b) after prazosin (0.025 mg kg^{-1} min^{-1}); (c) after prazosin (0.025 mg kg^{-1} min^{-1}) and yohimbine (0.025 mg kg^{-1} min^{-1}). Systemic arterial pressure (BP); arterial perfusion pressure (Ppa); salivary flow measured by a drop-counter (Dss); duration of parasympathetic nerve stimulation (———); duration of superimposed sympathetic nerve stimulation (– – – –).

pathetic salivation, decreasing salivary flow (Figure 2). Hence, it seems that the initial enhancement in parasympathetic salivary flow in response to superimposed sympathetic intervention is a relatively transient event whereas the late inhibition is the steady-state response and the two sympathetic effects may be operating via different mechanisms.

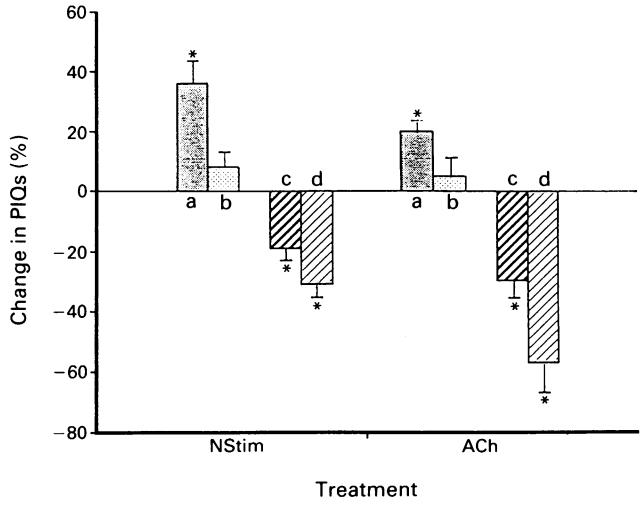

Figure 5 Effects of adrenoceptor agonists on parasympathetic salivation (PIQs) induced by nerve stimulation (NStim; 4 Hz) or acetylcholine infusion (ACh, 10 $\mu g\,kg^{-1}\,min^{-1}$) in glands with constant-flow vascular perfusion at a normal blood flow rate. After phenylephrine (0.25 $\mu g\,kg^{-1}\,min^{-1}$, a and b); after clonidine (0.75 $\mu g\,kg^{-1}\,min^{-1}$, c and d). Change in PIQs at 5–10 s (a and c); change in PIQs at 50–60 s (b and d). Number of animals in each group is 5. $^*P<0.05$ when compared to the corresponding control (the steady state parasympathetic salivary flow just prior to adrenoceptor agonist infusion).

The inhibitory effect of superimposed sympathetic stimulation on parasympathetic salivation was observed to persist with slow recovery after the end of sympathetic stimulation (Figure 4). Since the sympathetic nerve was maximally stimulated in the present study, a very high concentration of sympathetic neurotransmitter(s) would be expected to occur in the vicinity of the responding receptors. Unlike acetylcholine which is rapidly hydrolysed after its release from parasympathetic nerves, enzymatic metabolism is not the primary mechanism for termination of action of the primary neurotransmitter, noradrenaline, released from sympathetic nerves and several processes including simple diffusion away from the receptor sites and reuptake into the nerve terminals or effective cells are involved (Katzung, 1992). The persistence of the inhibitory response after the end of maximal sympathetic nerve stimulation may be related to the slow clearance of the sympathetic neurotransmitter from the receptor site.

The inhibitory effect of superimposed sympathetic stimulation on parasympathetic salivation was greater at higher salivary flows (at 4–8 Hz parasympathetic nerve stimulation) whereas the inhibition in response to continuous background sympathetic nerve stimulation was much stronger at low salivary flow (at 2 Hz parasympathetic nerve stimulation). (Figures 1 and 2). The difference in the degree of inhibition in the two types of sympathetic interventions at various salivary flow states may be related to the presence of initial enhancement in the superimposed type and its absence in the continuous one; the stronger initial enhancing effect on low salivary flow state may have a bigger counterbalancing effect on the late inhibitory action than in the higher salivary flow situation.

The diphasic sympathetic effects on parasympathetic salivation were greatly lessened by phentolamine but unaffected by propranolol, suggesting that the sympathetic nerve exerts its action via the α-adrenergic mechanism. Prazosin, an α_1-adrenoceptor blocker, was found to abolish the initial enhancing effect but not affect the late inhibitory response. Yohimbine, an α_2-adrenoceptor blocker, had no

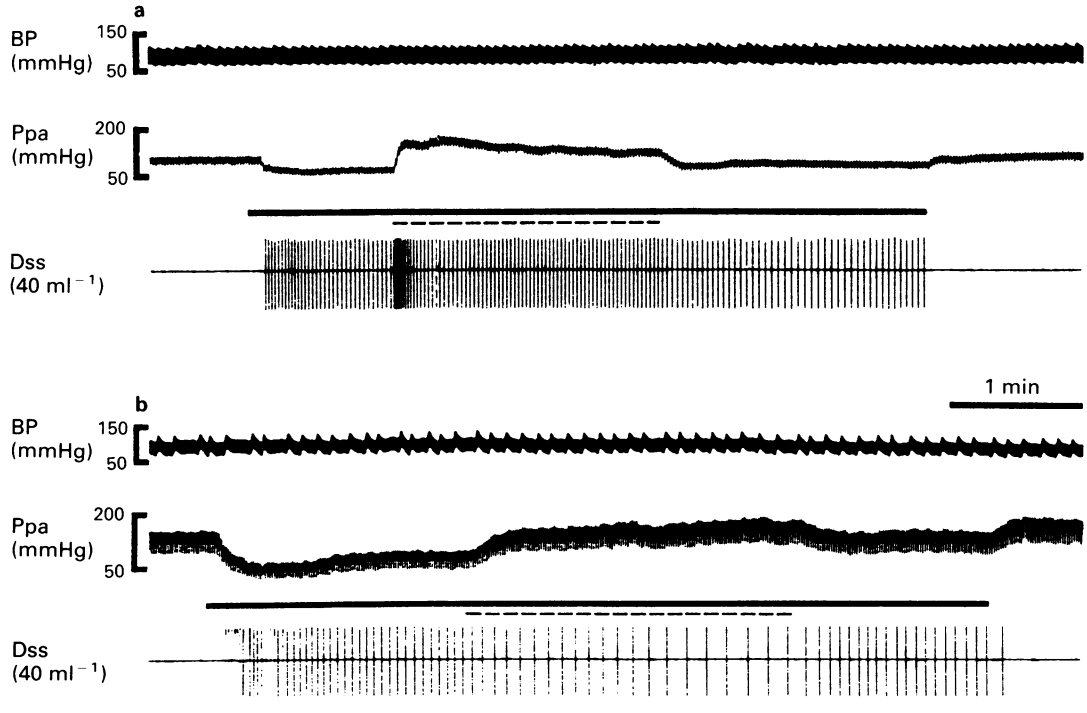

Figure 6 Experimental record illustrating the effects of adrenoceptor agonists on parasympathetic salivary secretion induced by acetylcholine. Acetylcholine infusion (10 $\mu g\,kg^{-1}\,min^{-1}$, ———); phenylephrine (0.25 $\mu g\,kg^{-1}\,min^{-1}$, – – –) in (a) and clonidine (0.75 $\mu g\,kg^{-1}\,min^{-1}$, – – –) in (b). Abbreviations as in Figure 4.

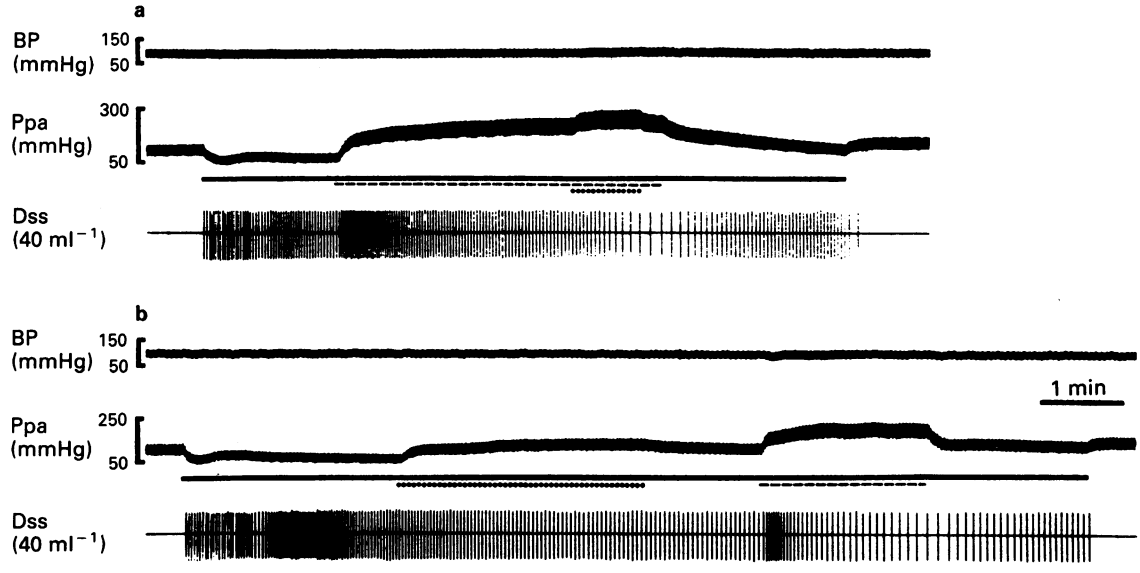

Figure 7 Experimental record illustrating the effects of superimposed sympathetic nerve stimulation and adrenoceptor agonists on parasympathetic nerve-induced salivary secretion. Parasympathetic nerve stimulation, (4 Hz, ———); sympathetic nerve stimulation (20 Hz, · · · ·); phenylephrine (0.25 $\mu g\,kg^{-1}\,min^{-1}$, – – – –) in (a) and clonidine (0.75 $\mu g\,kg^{-1}\,min^{-1}$, – – – –) in (b).

effect on the initial response but abolished the late inhibitory action. Simultaneous administration of both α-adrenoceptor sub-type blockers resulted in a significant reduction of the diphasic sympathetic response (Figure 3). Hence, the sympathetic enhancing action on parasympathetic salivation is related to the α_1-adrenoceptor mechanism while the sympathetic inhibitory action is through the α_2-adrenoceptor mechanism.

Parasympathetic salivation, induced whether by nerve stimulation or by intra-arterial administration of acetylcholine, was found to be abolished by atropine, enhanced by phenylephrine and depressed by clonidine (Figure 5); however, hexamethonium abolished the nerve-induced response without affecting the acetylcholine-induced salivary flow. The findings, apart from providing further support for the suggestion that the enhancing effect is via an α_1-adrenergic mechanism and the inhibitory effect via the α_2-adrenergic mechanism, indicate that the interactions between the parasympathetic and sympathetic nerve stimulations on salivary secretion may have occurred at the postsynaptic level.

Since the initial augmentation in salivary secretion by sympathetic superimposition appears to be a transient event, the response may be due to a heightened excitability of the secretory cells caused by preceding parasympathetic nerve stimulation (Langley, 1889) or the contraction of the myoepithelial cells which help in the squeezing of saliva from the ductal system (Emmelin *et al.*, 1969). Sympathetic contraction of myoepithelial cells has been found to be exclusively an α-adrenergic activity; this is in agreement with our finding that the sympathetic enhancing effect is via an α_1-adrenergic activity. It has also been shown that the myoepithelial cells are affected by both divisions of the autonomic nervous system in the same direction (Garrett, 1987). A continuous background maximal sympathetic nerve stimulation would have maximally contracted the myoepithelial cells and this would result in the elimination of their enhancing effect on salivary secretion in the subsequent parasympathetic nerve stimulation, favouring the manifestation of the steady state sympathetic inhibitory action. This may explain why a continuous background sympathetic nerve stimulation causes only a single depreciating action on the parasympathetic nerve induced salivary secretion. However, further experiments are required for verification.

Some workers have reported a presynaptic α_2-adrenoceptor inhibition of cholinergic transmission in the dog submandibular gland, based on the finding that intravenous yohimbine induces spontaneous salivary secretion with the response abolished after the section of the chorda tympani nerve (Montastruc *et al.*, 1989). Postsynaptic α_2-adrenoceptor receptors have been localized in the submandibular gland of some animal species (Bylund & Martinez, 1981). Results of this study have clearly demonstrated the functional occurrence of sympathetic and parasympathetic interactions on salivary secretion at postsynaptic level, suggesting the presence of inhibitory postsynaptic α_2-adrenoceptors in the dog submandibular gland. It is reasonable to assume that the tonic sympathetic discharge to the gland as well as the circulatory catecholamines, especially under stress conditions, would have inhibited salivary secretion via the postsynaptic α_2-adrenoceptors. Initiation of secretory action of the acinar cells under normal circumstances may depend not only on parasympathetic activation but also on the removal of the postsynaptic α_2-adrenoceptor inhibition. In the studies of Montastruc and his co-workers, yohimbine infusion could have removed the α_2-adrenoceptor postsynaptic inhibition resulting in predominant parasympathetic activation and spontaneous salivary secretion; absence of yohimbine-induced spontaneous salivary secretion after the section of the chorda tympani nerve can occur if the secretory activity of the acinar cells requires direct activation by the parasympathetic nerve. However, further experiments with the use of antagonists or agonists with selectivity for either presynaptic or postsynaptic α_2-adrenoceptors are required to rule out the possibility of a presynaptic α_2-adrenoceptor-mediated inhibition. Hence parasympathetic salivary secretion in the dog can be inhibited by the sympathetic system, not only at presynaptic level as suggested by other workers (Monstastruc, 1989) but also at the postsynaptic level as shown in this study.

This work was supported by the University of Hong Kong Research Fund (337/034/0011, 337/034/0016, 337/034/0018 & 377/030/7840). The author is grateful to Dr James C.C. Wang for helpful comments, to Mr K.K. Tsang for technical assistance, and to the Laboratory Animal unit of the University of Hong Kong for the supply of experimental animals.

References

BYLUND, D.B. & MARTINEZ, J.R. (1981). Postsynaptic localization of alpha 2 adrenergic receptors in rat submandibular gland. *J. Neurosci.*, **1**, 1003–1007.

EMMELIN, N. (1955). On the innervation of the submaxillary gland cells in cats. *Acta Physiol. Scand.*, **34**, 22–28.

EMMELIN, N., GARRETT, J.R. & OHLIN, P. (1969). Motor nerves of salivary epithelial cells in dogs. *J. Physiol.*, **200**, 539–546.

GARRETT, J.R. (1987). The proper role of nerves in salivary secretion: a review. *J. Dent. Res.*, **66**, 387–397.

KATZUNG, B.G. (1992). Introduction to autonomic pharmacology. In *Basic and Clinical Pharmacology*. Fifth edition. ed. Katzung, B.G. pp. 69–81. New York, U.S.A.: Appleton & Lange.

LANGLEY, J.N. (1878). On the physiology of the salivary secretion. I. The influence of the chorda tympani and sympathetic nerves upon the secretion of the submaxillary gland of the cat. *J. Physiol.*, **1**, 96–103.

LANGLEY, J.N. (1889). On the physiology of the salivary secretion. V. The effects of stimulating the cerebral secretory nerves upon the amount of saliva obtained by stimulating the sympathetic nerve. *J. Physiol.*, **10**, 291–328.

LUNG, M.A. (1990a). Variations in blood flow on mandibular glandular secretion to autonomic nervous stimulations in anaesthetized dogs. *J. Physiol.*, **431**, 479–493.

LUNG, M.A. (1990b). Effects of sympathetic nerve stimulation on parasympathetically induced salivary secretion in anaesthetized dogs. *J. Physiol.*, **432**, 17P.

LUNG, M.A. (1991). Mechanisms involved in sympathetic enhancement and inhibition of parasympathetically induced salivary secretion in dogs. *Proc. 6th SE Asia/West. Pac. Reg. Meeting Pharmacol.*, **151**, P129.

LUNG, M.A. (1992). Action of sympathetic drugs on parasympathetic salivary secretion in dogs. *Br. J. Pharmacol.*, **107**, 148P.

LUNG, M.A. & WANG, J.C.C. (1990). Direct measurement of arterial inflow, venous outflow and saliva secretion of mandibular gland in anaesthetized dogs: effects of parasympathetic stimulation. *J. Physiol.*, **422**, 80P.

MONTASTRUC, P., BERLAN, M. & MONTASTRUC, J.L. (1989). Effects of yohimbine on submaxillary salivation in dogs. *Br. J. Pharmacol.*, **98**, 101–104.

(Received September 20, 1993
Revised January 24, 1994
Accepted February 3, 1994)

Br. J. Pharmacol. (1994), **112**, 417–422

The renal handling of dopamine originating from L-DOPA and γ-glutamyl-L-DOPA

[1]M. Pestana & [2]P. Soares-da-Silva

Department of Pharmacology and Therapeutics, Faculty of Medicine, 4200, Porto, Portugal

1 The formation and outflow of dopamine and its deaminated metabolite 3,4-dihydroxyphenylacetic acid (DOPAC) was studied in cortical fragments of the rat kidney loaded with L-β-3,4-dihydroxyphenylalanine (L-DOPA) or γ-glutamyl-L-DOPA (GluDOPA). Dopamine and DOPAC in the tissues and in the effluent were assayed by means of h.p.l.c. with electrochemical detection.

2 In rats given 30 mg kg^{-1} L-DOPA, tissue and outflow levels of both dopamine and DOPAC were 3 fold those observed with a lower dose of L-DOPA (10 mg kg^{-1}). In rats given GluDOPA (16.7 mg kg^{-1}) levels of dopamine in renal tissues and in perifusate samples were found to be higher than those obtained with an equimolar dose of L-DOPA (10 mg kg^{-1}); however, no significant difference was observed for DOPAC. The outflow of both dopamine and DOPAC in kidney slices of rats injected with L-DOPA (10 and 30 mg kg^{-1}) or GluDOPA (16.7 mg kg^{-1}) was found to decline monophasically with similar slopes of decline. The rate constants of loss (k, min^{-1}) of DOPAC (10 mg kg^{-1} L-DOPA, $k = 0.0070$; 30 mg kg^{-1} L-DOPA, $k = 0.0087$; 16.7 mg kg^{-1} GluDOPA, $k = 0.0080$) were 2 to 3 fold those of dopamine (10 mg kg^{-1} L-DOPA, $k = 0.0027$; 30 mg kg^{-1} L-DOPA, $k = 0.0034$; 16.7 mg kg^{-1} GluDOPA, $k = 0.0030$). With both precursors the DOPAC/dopamine ratio in perifusate samples were 2.0 fold those in the tissues.

3 Tissue and outflow levels of dopamine after incubation of renal tissues with L-DOPA, 50 and 100 μM were found to be lower than those observed with GluDOPA (50 and 100 μM). DOPAC/dopamine ratios in tissues and perifusate samples of experiments performed with L-DOPA were significantly higher ($P < 0.01$) than those observed with GluDOPA. The outflow of both dopamine and DOPAC in renal slices incubated with L-DOPA (50 and 100 μM) were found to decline with time, but presented a biphasic shape. DOPAC/dopamine ratios in perifusate samples were 3 fold that in the tissues with both precursors.

4 In conclusion, the present results show that both L-DOPA and GluDOPA give origin to substantial amounts of dopamine and the newly-formed amine undergoes considerable deamination to DOPAC. However, dopamine originating from GluDOPA was less deaminated than that resulting from L-DOPA; it appears that this different behaviour may concern aspects related to the formation of the amine and also those related to its deamination and disposition, namely the processes involved in the access of newly-formed dopamine to MAO.

Keywords: L-DOPA; GluDOPA; dopamine; DOPAC; rat kidney

Introduction

Epithelial cells of renal proximal convoluted tubules are endowed with a high aromatic L-amino acid decarboxylase (AAAD) activity (Hayashi *et al.*, 1990) and a considerable amount of the renal dopamine is believed to derive largely from the decarboxylation of circulating or filtered 3,4-dihydroxyphenylalanine (DOPA) in these cellular elements. In the last few years, increasing evidence has suggested that renal dopamine, through the activation of specific receptors, may be of importance in the regulation of tubular sodium reabsortion as a result of the inhibition of both Na^+-K^+ ATPase and Na^+-H^+ antiport activities (Bertorello *et al.*, 1988; Felder *et al.*, 1990). Since dopamine can be formed in the cells or in the proximity of the cells which are endowed with dopamine receptors, it has been hypothesized that dopamine in the kidney may act as a paracrine and/or autocrine substance (Siragy *et al.*, 1989). The fate and outflow of newly-formed dopamine in tubular epithelial cells is a matter of considerable importance since, in order to be active at its receptor sites, the amine is expected to be able to leave this cellular compartment. On the other hand, renal tissues are endowed with one of the highest monoamine oxidase (MAO) activities in the body (Youdim *et al.*, 1988) and deamination of newly-formed dopamine into 3,4-dihydroxyphenylacetic acid (DOPAC) represents a major pathway for the inactivation of the amine (Fernandes & Soares-da-Silva, 1990; Fernandes *et al.*, 1991).

The physiological role of renal dopamine has recently gained further relevance with the observations that in some hypertensive patients, namely those with sodium sensitive hypertension, an inherited or acquired defect in the renal handling of dopamine may be of some pathophysiological importance (Gill *et al.*, 1988; Lee *et al.*, 1990; Williams *et al.*, 1990). Neither dopamine nor its precursor L-DOPA appear, however, particularly suitable for the correction of the hypothetical deficit of renal dopaminergic mechanisms in hypertension, mainly because of their extrarenal actions (Lee, 1988). γ-Glutamyl-L-DOPA (GluDOPA), on the other hand, is a synthetic dipeptide which also gives origin to dopamine (Wilk *et al.*, 1978; Worth *et al.*, 1985; Boateng *et al.*, 1990; Soares-da-Silva *et al.*, 1992b). GluDOPA itself is devoid of pharmacological actions but it is converted, preferentially in the kidney, to L-DOPA and subsequently to dopamine by the sequential actions of the brush border enzyme γ-glutamyl transpeptidase (γ-GT) and the intracellular AAAD (Lee, 1988). GluDOPA has been demonstrated to increase effective renal plasma flow, glomerular filtration rate and sodium and water excretion and to decrease plasma renin activity; these effects are antagonized by either carbidopa or (+)-sulpiride (Jeffrey *et al.*, 1988; MacDonald *et al.*, 1988). Infusion of

[1] On leave from Dept. of Nephrology, Faculty of Medicine, 4200 Porto, Portugal.
[2] Author for correspondence.

GluDOPA (25 μg kg^{-1} min^{-1}) in healthy volunteers over 10 h has been demonstrated to result in an increased output of urinary L-DOPA, dopamine and DOPAC (MacDonald *et al.*, 1989). Apparently, some of the L-DOPA originating from GluDOPA escapes decarboxylation into dopamine and the deamination of the newly-formed amine to DOPAC also appears to be a quantitatively important process. These two events may tend to limit the intrarenal availability of dopamine originating from GluDOPA.

The aim of the present work was to compare the renal handling of dopamine originating from either L-DOPA or GluDOPA and additionally to determine the kinetic parameters of the outflow of newly-formed dopamine and of its deaminated metabolite DOPAC. A preliminary account of some of these findings has been presented (Pestana & Soares-da-Silva, 1992).

Methods

Male Wistar rats (Biotério do Instituto Gulbenkian de Ciência, Oeiras, Portugal) 45–60 days old and weighing 200–250 g were used. Animals were kept three per cage under controlled environmental conditions (12 h light/dark cycle and room temperature 24°C). Food and tap water were allowed *ad libitum* and the experiments were all carried out during daylight hours. In some experiments, rats were given L-3,4-dihydroxyphenylalanine (L-DOPA; 10 and 30 mg kg^{-1}, i.p.) or γ-L-glutamyl-L-DOPA (GluDOPA; 16.7 mg kg^{-1}, i.p., an equimolar dose for 10 mg kg^{-1} L-DOPA) and killed by decapitation under ether anaesthesia 15 min after the dopamine precursor had been given; control rats were given the vehicle. The kidneys were removed, rinsed free from blood with saline (0.9% NaCl), placed on an ice-cold glass plate and the kidney poles removed; thereafter, slices approximately 2.0 mm thick were obtained and four cortical fragments weighing about 60 mg were prepared with a scalpel and placed in glass perifusion chambers; the process of preparing the renal fragments and placing them in the perfusion chambers took no more than 15 min.

In another series of experiments, rats were killed by decapitation under ether anaesthesia and four cortical fragments were prepared as described above. The preparations were preincubated for 30 min with 2 ml of warm (37°C) and gassed (95% O_2 and 5% CO_2) Krebs solution. Thereafter, the cortical slices were incubated for 15 min in 2 ml Krebs solution with added L-DOPA (50 μM and 100 μM), GluDOPA (50 μM and 100 μM) or in the absence of either substrate. After the incubation, the renal tissues were transferred to individual glass perifusion chambers.

In both series of experiments the preparations were perifused with warm (37°C) and gassed (95% O_2 and 5% CO_2) Krebs solution at a rate of 350 μl min^{-1} and allowed a 30 min stabilization period. Thereafter, five consecutive 10 min perifusate samples were collected into glass test tubes kept on ice and containing 500 μl of 2 M perchloric acid. The composition of the Krebs solution was as follows (in mM): NaCl 118, KCl 4.7, $CaCl_2$ 2.4, $MgSO_4$ 1.4, $NaHCO_3$ 25, KH_2PO_4 1.2, EDTA 0.4 and glucose 11, tropolone (50 μM) was added to the Krebs solution in order to inhibit the enzyme catechol-*O*-methyltransferase (COMT). At the end of the perifusion period, renal fragments were collected, blotted with filter paper and placed in 2 ml of 0.2 M perchloric acid.

Several attempts were made in order to reproduce in *in vitro* experiments the conditions obtained under *in vitro ex vivo* experiments. In some experiments the washing period was prolonged up to 50 min, whereas in others, two additional perifusate samples (10 min each) were collected. In order to have a reasonable wash of the preparations and to obtain detectable amounts of dopamine and DOPAC in the effluent, the optimal timing is the 30 min washing period and to collect the perifusate samples for up to 50 min. As shown below (in the results section), in the *in vitro* series of experiments the outflow of both dopamine and DOPAC failed to exhibit a monophasic decline, as evidenced by their upward concave shape; for this reason no kinetic analysis of the outflow of both dopamine and DOPAC was performed. In both series of experiments (*in vitro ex vivo* and *in vitro* experiments), the acidified perifusates and tissue fragments maintained in perchloric acid were kept at 4°C for the next 24 h till quantification of catecholamines. The assay of dopamine and DOPAC in renal tissues and samples of the perifusate was performed by means of high performance liquid chromatography (h.p.l.c.) with electrochemical detection, as previously described (Soares-da-Silva & Fernandes, 1992). The lower limit for detection of dopamine and DOPAC was, respectively, 8 and 14 pmol g^{-1}.

Statistics

The levels (in nmol g^{-1} 10 min^{-1}) of dopamine and DOPAC in the perifusate were logarithmically transformed, plotted against the time of perifusion and the slope of decline calculated by linear regression analysis. The rate constants of efflux of dopamine or DOPAC were calculated by dividing the levels of the amine or amine metabolite (nmol g^{-1} min^{-1}) in the last efflux sample by the tissue content (nmol g^{-1}) at the end of the experiment (k = rate of efflux/tissue content). Results are means ± s.e.mean of values for the indicated number of experiments. Values for the rate constant of loss (k) are geometric means with 95% confidence intervals. Statistical significance was determined by the Tuckey-Kramer method (Sokal & Rohlf, 1981). A P value less than 0.05 was assumed to denote a significant difference.

Results

As shown in Table 1, administration of L-DOPA resulted in an increased accumulation of newly-formed dopamine and of its deaminated metabolite DOPAC in cortical tissues of the rat kidney; the tissue levels of dopamine (DOPAC was not detectable) of rats given the vehicle were substantially lower than those observed in rats treated with the lowest dose of L-DOPA used. The tissue levels of both dopamine and DOPAC after 30 mg kg^{-1} L-DOPA had been given were found to be 3 fold those observed after the administration of a lower dose of L-DOPA (10 mg kg^{-1}). DOPAC/dopamine tissue ratios were found to be similar with both 10 and 30 mg kg^{-1} L-DOPA. Administration of GluDOPA (16.7 mg kg^{-1}) also resulted in a substantial accumulation of dopamine and DOPAC in renal tissues; however, the tissue accumulation of dopamine was nearly twice that found with an equimolar dose of L-DOPA (10 mg kg^{-1}). By contrast, the tissue accumulation of DOPAC in the group of animals injected with GluDOPA was 30% less than that in the group treated with an equimolar dose of L-DOPA. This resulted in the DOPAC/dopamine tissue ratio in the group injected with GluDOPA being lower ($P<0.01$) than that in the group of rats given L-DOPA (10 mg kg^{-1}).

The outflow of both dopamine and DOPAC in renal tissues of animals injected with L-DOPA (10 and 30 mg kg^{-1}) or GluDOPA (16.7 mg kg^{-1}) was found to decline progressively with time and reflected the dopamine and DOPAC tissue contents (Figure 1). Under these conditions, similar values for the slope (min^{-1}) of decline of both dopamine (10 mg kg^{-1} L-DOPA, slope = 0.0206; 30 mg kg^{-1} L-DOPA, slope = 0.0193; 16.7 mg kg^{-1} GluDOPA, slope = 0.0172) and DOPAC (10 mg kg^{-1} L-DOPA, slope = 0.0171; 30 mg kg^{-1} L-DOPA, slope = 0.0189; 16.7 mg kg^{-1} GluDOPA, slope = 0.0153) were found to occur; this was observed in experiments performed with both L-DOPA and GluDOPA. The rate constant of loss (k) of DOPAC was found to be 2.5 fold lower than that obtained for dopamine (Table 2). However, no significant differences were observed in k values in experiments performed with either L-DOPA or GluDOPA.

Table 1 Tissue levels of dopamine and DOPAC (in nmol g^{-1}) and DOPAC/dopamine ratios at the end of perifusions performed in slices of renal cortex of rats given L-DOPA (10 and 30 mg kg^{-1}), GluDOPA (16.7 mg kg^{-1}) and control animals (injected with the vehicle)

	Dopamine (nmol g^{-1})	*DOPAC* (nmol g^{-1})	*DOPAC/Dopamine*
Control	0.032 ± 0.003	< 0.014	
L-DOPA 10 mg kg^{-1}	13.6 ± 2.7	4.0 ± 1.2	0.35 ± 0.05
L-DOPA 30 mg kg^{-1}	40.9 ± 5.4*	15.4 ± 1.2*	0.40 ± 0.08
GluDOPA 16.7 mg kg^{-1}	22.4 ± 3.4*	2.7 ± 0.8	0.14 ± 0.01*

Results shown are means ± s.e.mean of 8 to 12 experiments per group.
Significantly different (*$P < 0.01$) from corresponding values for L-DOPA 10 mg kg^{-1}.

For both L-DOPA and GluDOPA, DOPAC/dopamine ratios in the perifusate were 2 fold those observed in the tissues and remained constant with time (Figure 2). However, the DOPAC/dopamine ratio in the perifusate of experiments performed with tissues from rats injected with 10 and 30 mg kg^{-1} L-DOPA, respectively 0.79 ± 0.09 and 0.73 ± 0.10, was twice that observed in the group of animals treated with GluDOPA (0.34 ± 0.02) (Figure 2).

It might be hypothesized that the comparatively higher formation of dopamine after the administration of GluDOPA than after L-DOPA could be related to its preferential metabolism in renal tissues. However, the fact that the increased accumulation of the amine is accompanied by a significant reduction in its deamination to DOPAC suggests that the dopamine formed from GluDOPA is handled differently from that originating from L-DOPA. To evaluate this possibility, a series of experiments was performed under *in vitro* conditions, i.e., the renal tissues were incubated with either L-DOPA or GluDOPA before being perifused; the preferential decarboxylation of L-DOPA in other tissues was eliminated in this way. The accumulation of dopamine and DOPAC in renal tissues previously loaded with L-DOPA (50 and 100 μM) and GluDOPA (50 and 100 μM) was found to be dependent on the concentration of the amine precursor used (Table 3); the tissue levels of dopamine (DOPAC was not detectable) in renal fragments incubated in the absence of either substrate was 100 fold lower than those observed in tissues incubated with the lowest concentration of L-DOPA. The tissue accumulation of dopamine after incubation with L-DOPA was lower than that observed with equimolar concentrations of GluDOPA; this was particularly evident at the higher concentrations of L-DOPA and GluDOPA. In contrast, the levels of DOPAC at 50 and 100 μM L-DOPA did not differ significantly from those obtained in the presence of GluDOPA (50 and 100 μM). This resulted in the DOPAC/dopamine ratio in renal tissues loaded with L-DOPA 50 and 100 μM being significantly higher ($P < 0.01$) than that observed in cortical slices previously incubated with equimolar concentrations of GluDOPA (Table 3).

The outflow of dopamine and DOPAC in renal tissues loaded with L-DOPA (50 and 100 μM) or GluDOPA (50 and 100 μM), was found to decrease progressively with time, but did not exhibit a monophasic decline, as evidenced by their upward concave shape (Figure 3). In some experiments, the collection of the perifusate was extended up to 70 min, but the levels of dopamine in the perifusate were too low (especially with 50 μM L-DOPA) to perform a kinetic analysis. The levels of dopamine in the overflow of renal tissues incubated with GluDOPA (50 and 100 μM) were higher than those observed with L-DOPA (Figure 3). This was particularly evident ($P < 0.01$) at the higher concentrations of the two precursors; dopamine levels in the effluent were 4 fold higher with GluDOPA (100 μM) than with L-DOPA (100 μM). By contrast, the levels of DOPAC in the overflow were similar (GluDOPAC 50 μM) or increased 2 fold over (GluDOPA 100 μM) those observed with L-DOPA.

DOPAC/dopamine ratios in the perifusate were found to be higher ($P < 0.01$) than those in the tissues and to increase

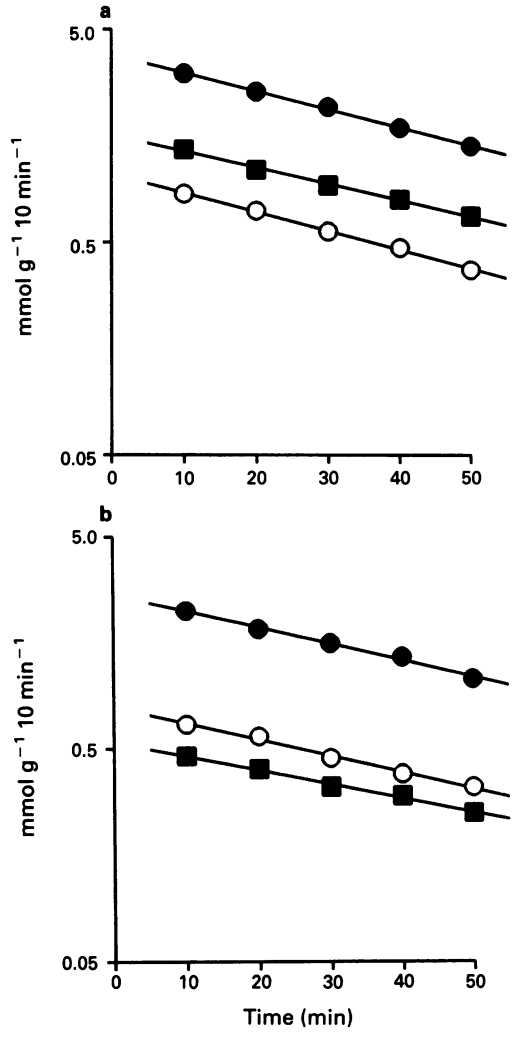

Figure 1 Outflow (in nmol g^{-1} 10 min^{-1}) of (a) dopamine and (b) DOPAC in perifusate samples of renal cortical slices obtained from rats injected with L-DOPA (10 and 30 mg kg^{-1}) and GluDOPA (16.7 mg kg^{-1}). Each point represents the mean of 8 to 12 experiments per group; s.e. mean values were less than 10% of respective mean values. Linear coefficient values were in rats given 10 mg kg^{-1} L-DOPA; dopamine, $r = 0.9991$, $n = 40$; DOPAC, $r = 0.9968$, $n = 40$; in rats given 30 mg kg^{-1} L-DOPA; dopamine, $r = 0.9988$, $n = 60$; DOPAC, $r = 0.9964$, $n = 60$; and in rats given 16.7 mg kg^{-1} GluDOPA; dopamine, $r = 0.9975$; $n = 40$; DOPAC, $r = 0.9970$, $n = 40$. L-DOPA (10 mg kg^{-1}, ○); L-DOPA (30 mg kg^{-1}, ●) and GluDOPA (16.7 mg kg^{-1}, ■).

progresssively throughout the perifusion period (Figure 4); this was found to be particularly evident with L-DOPA. In addition, the DOPAC/dopamine ratio in the perifusate of experiments performed in tissues loaded with L-DOPA (50 and 100 μM) was significantly higher ($P < 0.01$) than that

Table 2 Rate constant of loss (k) of dopamine and DOPAC in renal cortical slices of rats given L-DOPA 10 and 30 mg kg^{-1} or GluDOPA 16.7 mg kg^{-1}

	Dopamine k (min^{-1})	*DOPAC* k (min^{-1})
L-DOPA 10 mg kg^{-1}	0.0027 (0.0034, 0.0022)	0.0070 (0.0085, 0.0061)*
L-DOPA 30 mg kg^{-1}	0.0034 (0.0042, 0.0027)	0.0087 (0.0099, 0.0075)*
GluDOPA 16.7 mg kg^{-1}	0.0030 (0.0040, 0.0023)	0.0080 (0.0112, 0.0057)*

Results shown are means ± s.e.mean of 8 to 12 experiments per group.
Significantly different from corresponding values for dopamine (*$P<0.05$).

Table 3 Tissue levels of dopamine and DOPAC (in nmol g^{-1}) and DOPAC/dopamine ratios at the end of perifusions of slices of rat renal cortex previously loaded with L-DOPA (50 and 100 μM) and controls (tissues incubated in the absence of either substrate)

	Dopamine (nmol g^{-1})	*DOPAC* (nmol g^{-1})	*DOPAC/Dopamine*
Control	0.024 ± 0.006	<0.014	
L-DOPA 50 μM	2.4 ± 0.3	0.7 ± 0.2	0.31 ± 0.07
L-DOPA 100 μM	3.4 ± 0.4	0.1 ± 0.2	0.31 ± 0.02
GluDOPA 50 μM	3.2 ± 0.6	0.5 ± 0.1	0.15 ± 0.02*
GluDOPA 100 μM	8.4 ± 0.9*†	1.6 ± 0.3†	0.19 ± 0.01*

Results shown are means ± s.e.mean of 4 to 8 experiments per group.
Significantly different from corresponding values for L-DOPA (*$P<0.01$) and 50 GluDOPA (†$P<0.05$).

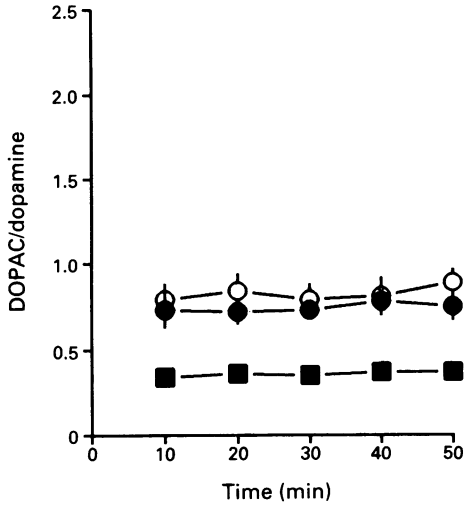

Figure 2 Proportion of DOPAC to dopamine in 10 min perifusate samples collected from renal cortical fragments obtained from rats injected with 10 mg kg^{-1} L-DOPA (○) and 30 mg kg^{-1} L-DOPA (●) and 16.7 mg kg^{-1} GluDOPA (■). Each point represents the mean with s.e.mean of 4 to 5 experiments per group. Significantly different from corresponding values for GluDOPA (*$P<0.01$) using the Tuckey-Kramer method.

observed in the effluent of renal slices incubated with GluDOPA (50 and 100 μM) (Figure 4).

Discussion

The results presented here show that, in the kidney, both L-DOPA and GluDOPA give origin to substantial amounts of dopamine and the newly-formed amine undergoes considerable deamination to DOPAC. The analysis of the outflow of dopamine and DOPAC in the *in vitro ex vivo* experiments reveals the presence of a monocompartmental system with MAO activity which is in a steady state of efflux. Under these conditions, a significantly higher rate constant of loss of DOPAC in comparison with that for dopamine indicates that the amine metabolite leaves the cellular com-

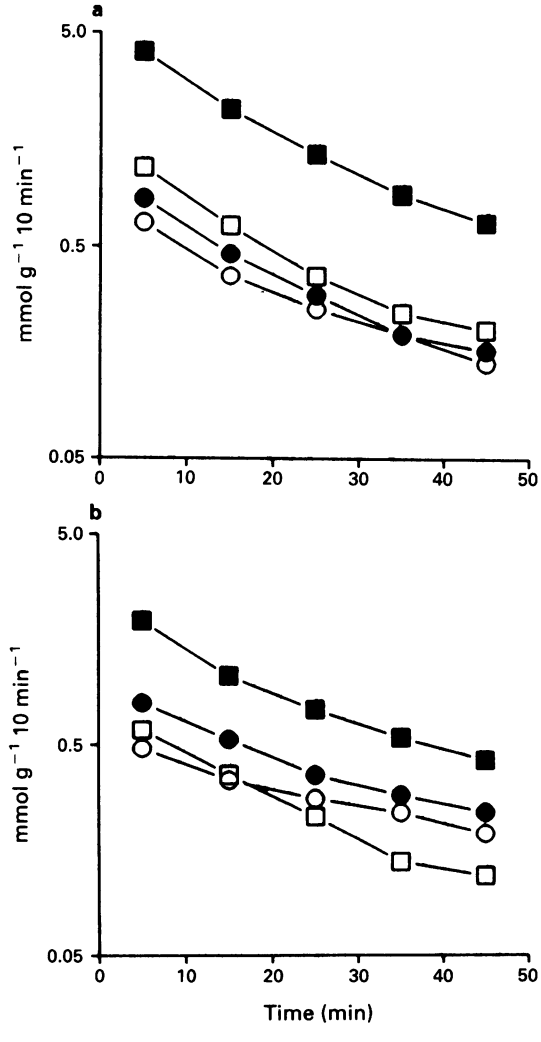

Figure 3 Outflow (in nmol g^{-1} 10 min^{-1}) of (a) dopamine and (b) DOPAC in perifusate samples of renal cortical slices previously incubated with 50 μM L-DOPA (○), 100 μM L-DOPA (●), 50 μM GluDOPA (□) and 100 μM GluDOPA (■). Each point represents the mean of 4 to 8 experiments per group; s.e.mean values were less than 10% of respective mean values.

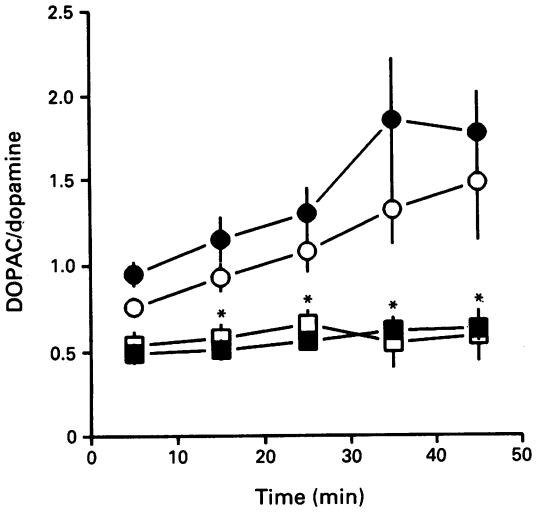

Figure 4 Proportion of DOPAC to dopamine in 10 min perifusate samples collected from renal cortical slices previously incubated with 50 μM L-DOPA (○), 100 μM L-DOPA (●), 50 μM GluDOPA (□) and 100 μM GluDOPA (■). Each point represents the mean with s.e.mean of 4 to 5 experiments per group. Significantly different from corresponding values for GluDOPA (*$P<0.01$) using the Tuckey-Kramer method.

partment more easily than does the parent amine. The data presented here also provide evidence favouring the view that dopamine formed from GluDOPA does not behave similarly to dopamine originating from L-DOPA; this different behaviour concerns the aspects related to the formation of the amine and also those related to its deamination and disposition, namely the processes involved in the access of newly-formed dopamine to MAO.

Several lines of evidence support the view that most of the renal dopamine has its origin in tubular epithelial cells as a result of decarboxylation of circulating or filtered L-DOPA by AAAD; the conversion of L-DOPA to dopamine in renal sympathetic nerves has, on other hand, been demonstrated to be of minor importance (Baines, 1982; Soares-da-Silva *et al.*, 1992a). The results presented here show that both L-DOPA and GluDOPA, either after systemic administration of the compounds or following incubation of renal tissues, give origin to substantial amounts of dopamine. The levels of dopamine were, however, significantly higher both in the tissues and in the effluent of cortical slices of animals given GluDOPA than in animals given an equimolar dose of L-DOPA. This is in agreement with the results of previous studies (Wilk *et al.*, 1978) and appears to be consistent with the preferential metabolism of GluDOPA in renal tissues, which is dependent on the fact that the kidney has by far the greatest activity of γ-GT in the body (Albert *et al.*, 1961). However, the finding that the levels of dopamine were also significantly higher both in the tissues and in the effluent of cortical slices incubated with GluDOPA suggests that tubular epithelial cells may have handled differently the dopamine originating from GluDOPA and L-DOPA. This suggestion is supported by the findings that the levels of DOPAC were comparatively lower, both in tissues and perifusate samples of experiments performed with GluDOPA both *in vitro ex vivo* conditions and in *in vitro* conditions; this would favour the view that the dopamine formed from GluDOPA is less available for deamination than the amine formed from L-DOPA.

Following systemic administration, circulating L-DOPA has access to tubular epithelial cells after being taken up at the basolateral cell border, whereas filtered L-DOPA may enter the cell through the apical border (Chan, 1976; Baines & Chan, 1980; Barthelmebs *et al.*, 1990); in both cases, L-DOPA undergoes rapid decarboxylation by cytosolic AAAD. Considering the predominant localization of γ-GT in the brush border membrane of proximal tubular cells (Wilk *et al.*, 1978), GluDOPA must have access to this cell border (Barthelmebs *et al.*, 1990), before giving origin to L-DOPA and subsequently to dopamine. This sequence of events would favour the possibility that the dopamine formed from GluDOPA may behave similarly to that dopamine formed from L-DOPA entering the tubular cell mainly through the luminal border; the observation that the DOPAC/dopamine ratios in perifusate samples of experiments in which rats were given L-DOPA were similar to those observed when kidney slices were incubated with GluDOPA agrees with this suggestion. On the other hand, DOPAC/dopamine ratios in perifusate samples of kidney slices loaded *in vitro* with L-DOPA, a situation in which most of L-DOPA appears to enter the cell through the basolateral border, were found to present a pattern which indicates an increased degree of deamination of newly-formed dopamine. MAO activity is exclusively located in the mitochondria and in epithelial cells of proximal tubules; these organelles have a predominant localization in the basal pole of the cell. Thus, it might be hypothesized that the dopamine formed from GluDOPA would be less available to be deaminated. Differences in the extent of deamination of dopamine are, therefore, one possible explanation for the increased dopamine levels observed in both the tissues and the perifusate samples of cortical slices previously loaded with GluDOPA.

In spite of differences in the extent of deamination of dopamine, the results presented here show that the dopamine originating from either L-DOPA or GluDOPA undergoes considerable deamination before reaching the perifusion fluid. Apparently, the *in vitro ex vivo* model represents a monocompartmental system which has MAO activity, which is in a steady state of efflux and in which the efflux of the metabolite is characterized by a rate constant (k_{DOPAC}) that is 2 to 3 times higher than the k-value for the efflux of the parent amine (k_{DA}). In spite of this pronounced difference, the efflux curves for parent amine and metabolite were parallel (Figure 1a and b); this parallelism is due to the deamination of dopamine to DOPAC which continues throughout the perifusion period. The increased ability of DOPAC to leave the cellular compartment endowed with MAO activity, as evidenced by the higher k values, is dictated by its higher lipophilicity (Trendelenburg *et al.*, 1979). Therefore, the rate of efflux of DOPAC must be proportional to the rate of deamination of dopamine. The finding that the proportion of DOPAC to dopamine in the perifusate is 2 fold that found to occur in the tissues, further reinforces the conclusion that a considerable amount of renal dopamine which is in the process of leaving the tubular epithelial cell is a constant source for DOPAC. An alternative explanation for these findings concerns the possibility that the dopamine produced in tubular epithelial cells, after being released into the extracellular medium, would be submitted to an uptake process into cellular compartment rich in MAO. Evidence has been gained favouring the view that the cellular compartment in which renal dopamine undergoes deamination is rather unlikely to be the neuronal one. Firstly, most of renal MAO appears to be located extraneuronally (Caramona & Soares-da-Silva, 1990; Soares-da-Silva *et al.*, 1992a). Secondly, it has been shown that the levels of noradrenaline in kidney slices did not change when up to 2500 μM L-DOPA was added to the incubation medium, thus suggesting that the dopamine formed in renal tissues loaded with L-DOPA has no access to nerve terminals (Fernandes *et al.*, 1991). If the released dopamine is in fact subject to an uptake process into the tubular cells, it might be suggested that this is most likely to occur at the basolateral cell border of tubular cells, namely when using kidney slices. Two different sets of arguments support this suggestion: (1) under *in vitro* experimental conditions the lumen of renal tubules may be collapsed and, therefore, the tubular uptake in those conditions

would occur mainly via the basolateral membrane (Wedeen & Weiner, 1973); (2) dopamine is not taken up into tubular cells through the luminal cell border (Chan, 1976).

In conclusion, the results presented here show that the renal handling of the dopamine with origin in GluDOPA is similar to that with origin in L-DOPA with the exception that the amine formed from GluDOPA is less available to be deaminated. Apart from its preferential metabolism in renal tissues, it is suggested that another advantage of GluDOPA over L-DOPA is that concerning a lower rate in the deamination of the dopamine originating from GluDOPA in comparison with that from L-DOPA.

References

ALBERT, Z., ORLOWSKI, M. & SZEWCZUK, A. (1961). Histochemical demonstration of γ-glutamyl-transpeptidase. *Nature*, **191**, 767–768.

BAINES, A.D. (1982). Effects of salt intake and renal denervation on catecholamine catabolism and excretion. *Kidney Int.*, **21**, 316–322.

BAINES, A.D. & CHAN, W. (1980). Production of urine free dopamine from dopa: a micropuncture study. *Life Sci.*, **26**, 253–259.

BARTHELMEBS, M., CAILLETTE, A., EHRHARDT, J.-D., VELLY, J. & IMBS, J.L. (1990). Metabolism and vascular effects of γ-glutamyl-L-dopa on the isolated rat kidney. *Kidney Int.*, **37**, 1414–1422.

BERTORELLO, A., HÖKFELT, T., GOLDSTEIN, M. & APERIA, A. (1988). Proximal tubule Na^+-K^+-ATPase activity is inhibited during high-salt diet: evidence for DA-mediated effect. *Am. J. Physiol.*, **254**, F795–F801.

BOATENG, Y.A., BARBER, H.E., MACDONALD, T.M., PETRIE, J.C., LEE, M.R. & WHITING, P.H. (1990). The pharmacokinetics of γ-glutamyl-L-DOPA in normal and anephric rats and rats with glycerol-induced acute renal failure. *Br. J. Pharmacol.*, **101**, 301–306.

CARAMONA, M.M. & SOARES-DA-SILVA, P. (1990). Evidence for an extraneuronal location of monoamine oxidase in renal tissues. *Naunyn-Schmied. Arch. Pharmacol.*, **341**, 411–413.

CHAN, Y.L. (1976). Cellular mechanisms of renal tubular transport of L-DOPA and its derivatives in the rat: microperfusion studies. *J. Pharmacol. Exp. Ther.*, **199**, 17–24.

FELDER, C.C., CAMPBELL, T., ALBRECHT, F. & JOSE, P.A. (1990). Dopamine inhibits Na^+-H^+ exchanger activity in renal BBMV by stimulation of adenylate cyclase. *Am. J. Physiol.*, **259**, F297–F303.

FERNANDES, M.H., PESTANA, M. & SOARES-DA-SILVA, P. (1991). Deamination of newly-formed dopamine in rat renal tissues. *Br. J. Pharmacol.*, **102**, 778–782.

FERNANDES, M.H. & SOARES-DA-SILVA, P. (1990). Effects of MAO-A and MAO-B selective inhibitors Ro 41-1049 and Ro19-6327 on the deamination of newly-formed dopamine in the rat kidney. *J. Pharmacol. Exp. Ther.*, **255**, 1309–1313.

GILL, J.R. Jr., GULLNER, H.G., LAKE, R., LAKATUA, D. & LAN, G. (1988). Plasma and urinary catecholamines in salt-sensitive idiopathic hypertension. *Hypertension*, **11**, 312–319.

HAYASHI, M., YAMAJI, Y., KITAJIMA, W. & SARUTA, T. (1990). Aromatic L-amino acid decarboxylase activity along the rat nephron. *Am. J. Physiol.*, **258**, F28–F33.

JEFFREY, R.F., MACDONALD, T.M., MARWICK, K. & LEE, M.R. (1988). The effects of carbidopa and indomethacin on the renal responses to γ-glutamyl-L-dopa in normal man. *Br. J. Clin. Pharmacol.*, **25**, 195–201.

LEE, M.R. (1988). Dopamine prodrugs. In *Peripheral Actions of Dopamine*, ed. Bell, C. & McGrath, B. pp. 207–218. London: Macmillan Press.

LEE, M.R., CRITCHLEY, J.A.J.H., GORDON, C.J., MAKARANANDA, K., SRIWATANAKUL, K., BALALI-MOOD, M. & BOYE, G.L. (1990). Ethnic difference in the renal sodium dopamine relationship. A possible explanation for regional variations in the prevalence of hypertension? *Am. J. Hypertens.*, **3**, 100s–103s.

MACDONALD, T.M., JEFFREY, R.F., FREESTONE, S. & LEE, M.R. (1988). (+)-Sulpiride antagonises the renal effects of γ-glutamyl-L-dopa in man. *Br. J. Clin. Pharmacol.*, **25**, 203–212.

MACDONALD, T.M., JEFFREY, R.F. & LEE, M.R. (1989). The renal and haemodynamic effects of a 10 h infusion of γ-glutamyl-L-dopa in normal man. *Br. J. Clin. Pharmacol.*, **27**, 811–822.

PESTANA, M. & SOARES-DA-SILVA, P. (1992). Renal outflow of dopamine: a comparative study with L-DOPA and γ-glutamyl-L-DOPA. *Br. J. Pharmacol.*, **106**, 82P.

SIRAGY, H.M., FELDER, R.A., HOWELL, N.L., CHEVALIER, R.L., PEACH, M.J. & CAREY, R.M. (1989). Evidence that intrarenal dopamine acts as a paracrine substance at the renal tubule. *Am. J. Physiol.*, **257**, F469–F477.

SOARES-DA-SILVA, P. (1993). Kinetic study of the tubular dopamine outward transporter in the rat and dog kidney. *Br. J. Pharmacol.*, **109**, 577–580.

SOARES-DA-SILVA, P. & FERNANDES, M.H. (1992). Sodium-dependence and ouabain-sensitivity of the synthesis of dopamine in renal tissues of the rat. *Br. J. Pharmacol.*, **105**, 811–816.

SOARES-DA-SILVA, P., FERNANDES, M.H., ALBINO-TEIXEIRA, A., AZEVEDO, I. & PESTANA, M. (1992a). Brief transient ischemia induces long-term depletion of norepinephrine without affecting the aromatic amino acid decarboxylase and monoamine oxidase activities in the rat kidney. *J. Pharmacol. Exp. Ther.*, **260**, 902–908.

SOARES-DA-SILVA, P., FERNANDES, M.H. & PESTANA, M. (1992b). L-DOPA and γ-glutamyl-L-DOPA as precursors for dopamine in human renal tissues. *Br. J. Clin. Pharmacol.*, **33**, 539P.

SOKAL, R.R. & ROHLF, F.J. (1981). *Biometry. The Principles and Practice of Statistics in Biological Research*. New York: Freeman and Company.

TRENDELENBURG, U., BÖNISCH, H., GRAEFE, K.-H. & HENSELING, M. (1979). The rate constant for the efflux of metabolites of catecholamines and phenylethylamines. *Pharmacol. Rev.*, **31**, 179–203.

WEDEEN, R.P. & WEINER, B. (1973). The distribution of p-aminohippuric acid in rat kidney slices. I. Tubular localization. *Kidney Int.*, **3**, 205–213.

WILK, S., MIZOGUCHI, H. & ORLOWSKI, M. (1978). γ-glutamyl-DOPA: A kidney specific dopamine precursor. *J. Pharmacol. Exp. Ther.*, **206**, 227–232.

WILLIAMS, G.H., GORDON, M.S., STUENKEL, C.A., CONLIN, P.R. & HOLLBERG, N.K. (1990). Dopamine and nonmodulating hypertension. *Am. J. Hypertens.*, **3**, 112s–115s.

WORTH, D.P., HARVEY, J.N., BROWN, J. & LEE, M.R. (1985). γ-L-glutamyl-L-dopa is a dopamine prodrug, relatively specific for the kidney in normal subjects. *Clin. Sci.*, **69**, 207–214.

YOUDIM, M.B.H., FINBERG, J.P.M. & TIPTON, K.F. (1988). Monoamine oxidase. In *Catecholamines*, Vol. 1. ed. Trendelenburg, U. & Weiner, N. pp. 119–192. Berlin: Springer-Verlag.

(Received March 15, 1993
Revised January 28, 1994
Accepted February 4, 1994)

Br. J. Pharmacol. (1994), **112**, 423–428

Comparison of the ability of nicardipine, theophylline and zaprinast to restore cardiovascular haemodynamics following inhibition of nitric oxide synthesis

[1]N.A. Herity, *J.D. Allen, **B. Silke & A.A.J. Adgey

Regional Medical Cardiology Centre, Royal Victoria Hospital, Belfast BT12 6BA and Departments of *Physiology and **Therapeutics and Clinical Pharmacology, Queen's University, Belfast BT9 7BL

1 The use of pharmacological inhibitors of nitric oxide (NO) synthesis to treat patients with septic shock is limited by the observation that they cause a fall in cardiac output in some subjects. The aim of this work was to investigate this fall and to test whether it was reversible by subsequent administration of nicardipine, theophylline or the cyclic GMP-selective phosphodiesterase inhibitor, zaprinast (M&B 22948).

2 In pentobarbitone-anaesthetized pigs, haemodynamic indices were measured before and after intravenous administration of N^G-nitro-L-arginine methyl ester (L-NAME) in a dose-response protocol (0.2–20 mg kg^{-1}; $n = 6$) and as a single bolus of 10 mg kg^{-1} either alone or followed by increasing doses of nicardipine, theophylline or zaprinast ($n = 8$ in each group).

3 L-NAME caused a dose-dependent rise in systemic vascular resistance and mean systemic arterial pressure and a dose-dependent fall in cardiac output. A single bolus of L-NAME (10 mg kg^{-1}) produced these effects within 15 min.

4 Subsequent administration of nicardipine (0.05–0.2 mg kg^{-1}) caused complete reversal of systemic vasoconstriction and hypertension and in doing so completely restored cardiac output. Theophylline (7.5–10 mg kg^{-1}) partially reversed the rise in systemic vascular resistance and partially restored cardiac output but the effect was small compared to that of nicardipine. Zaprinast (1–5 mg kg^{-1}) had no significant effect on any of these variables.

5 These results suggest that reduced cardiac output following inhibition of NO synthesis is an effect of increased afterload on the heart and is reversible by nicardipine and to a lesser extent by theophylline. These findings may have potential value for those using NO synthase inhibitors to treat patients with septic shock.

Keywords: Nitric oxide; nicardipine; theophylline; zaprinast; N^G-nitro-L-arginine methyl ester; cardiovascular haemodynamics

Introduction

Endothelium-derived relaxing factor (EDRF) is a physiological vasodilator thought to be the nitric oxide radical (NO; for review see Moncada *et al.*, 1991) or a closely related molecule, perhaps the nitroxyl radical (Fukuto *et al.*, 1992) or both. NO is synthesized from its precursor L-arginine in a reaction catalysed by NO synthase of either the constitutive or inducible form. It activates guanylate cyclase accelerating formation of guanosine 3':5'-cyclic monophosphate (cyclic GMP) in vascular smooth muscle cells thus causing relaxation and vasodilatation (Moncada *et al.*, 1991). Although the details of this mechanism remain uncertain the evidence suggests that a cyclic GMP-dependent protein kinase activates a calcium transport protein causing a reduction in intracellular free calcium concentration and thus relaxation (Lincoln, 1989).

NO synthesis is competitively inhibited by L-arginine analogues such as N^G-monomethyl-L-arginine and N^G-nitro-L-arginine methyl ester (L-NMMA and L-NAME; Rees *et al.*, 1990). Administration of such agents to experimental animals causes widespread vasoconstriction, increased peripheral vascular resistance and arterial hypertension (Moncada *et al.*, 1991) and a fall in cardiac output in rats (Gardiner *et al.*, 1990; Amrani *et al.*, 1992), rabbits (Persson *et al.*, 1990), dogs (Kilbourn *et al.*, 1990) and sheep (Tresham *et al.*, 1991). In the present study we have documented the effects of intravenous administration of L-NAME to pentobarbitone-anaesthetized pigs in a dose-response protocol (0.2–20 mg kg^{-1}) and as a single large bolus (10 mg kg^{-1}). A fall in cardiac output has also been observed in human subjects receiving NO synthase inhibitors (Petros *et al.*, 1991) or the guanylate cyclase inhibitor, methylene blue (Schneider *et al.*, 1992) as treatment for septic shock resulting in limitation of their use to treat this condition. The reason for the fall in cardiac output is unknown although increased afterload (Gardiner *et al.*, 1990; Persson *et al.*, 1990), reduced preload (Persson *et al.*, 1990) direct myocardial action (Gardiner *et al.*, 1990; Persson *et al.*, 1990; Schulz *et al.*, 1992), coronary vasoconstriction (Gardiner *et al.*, 1990; Persson *et al.*, 1990; Amrani *et al.*, 1992; Schulz *et al.*, 1992) and activation of baroreceptor reflexes (Kilbourn *et al.*, 1990) have all been suggested. Inhibition of endocardial (Schulz *et al.*, 1991) or myocardial (Schulz *et al.*, 1992) NO synthesis are further potential mechanisms. We have investigated the observed reduction in cardiac output by testing the hypothesis that it could be restored by subsequent administration of vasodilator agents. The agents used, nicardipine (a highly vasoselective calcium channel blocker), theophylline (a non-selective phosphodiesterase inhibitor) and zaprinast (M&B 22948; a cyclic GMP-selective phosphodiesterase inhibitor) were chosen because increased cyclic GMP levels and a fall in intracellular free calcium concentration are central to NO-mediated vasodilatation and thus we felt that each had the potential to mimic restoration of NO to the vascular smooth muscle cell.

Methods

Adult pigs of either sex (32–52 kg) were sedated with azaperone (Stresnil 160 mg, i.m.) and anaesthetized with pen-

[1] Author for correspondence.

tobarbitone (Sagatal, May and Baker, 30 mg kg^{-1} i.v. initially and supplemented as required) via an ear vein. They were intubated and ventilated with room air by a Palmer Ideal pump at a rate and tidal volume adjusted according to end-tidal carbon dioxide concentration ($ETCO_2$). A warming blanket maintained body temperature above 36.5°C as measured by a rectal thermistor (Harvard). A cannula was inserted into a forelimb vein for drug administration.

Haemodynamic measurements

The right common carotid artery was cannulated and connected via a transducer (Druck PDCR 75) to a 4-channel electronic recorder (Gould 2400S) to register arterial blood pressure. A continuous surface electrocardiogram (lead III) was recorded with electronic measurement of heart rate (Neurolog). A transcutaneous pulse oximeter (Ohmeda 4700 Oxicap) measured tissue oxygen saturation (SaO_2) and $ETCO_2$.

For measurement of cardiac output, a triple lumen balloon-tipped thermodilution catheter (Edwards Laboratories or Baxter) of either 7.0 or 7.5 French gauge was passed through the right external jugular vein to the main pulmonary artery under fluoroscopic control. The proximal lumen was used for delivery of the injectate and for measurement of right atrial pressure. One litre of injectate (5% dextrose in water cooled to 0–0.5°C) was stored in a flask over ice. A thermistor probe inside the flask measured injectate temperature. A short length of plastic tubing connected the solution via a three way tap to the injectate syringe (Braun). For each measurement 10 ml of injectate was drawn into the syringe and infused by a gas-powered injector gun (USCI No. 372000) through the proximal port of the catheter. The resultant change in blood temperature was measured by a thermistor 4 cm from the catheter tip, the cardiac output was calculated by an on line cardiac output computer (American Edwards Laboratories 9520A) and the thermodilution curve recorded (American Edwards Laboratories 9812). This procedure was repeated eight times for each data point and the first two readings disregarded to correct for catheter warming between measurements. Cardiac output was calculated as the mean of the remaining six readings.

Systemic vascular resistance (SVR) was calculated from the formula:

$$SVR = \frac{(MAP - MRAP) \times 8}{CO} \text{ kPa l}^{-1}\text{s}$$

where MAP represents mean arterial pressure, MRAP represents mean right atrial pressure, CO represents cardiac output, 8 (= 60/7.5) converts mmHg l^{-1} min to kPa l^{-1}s.

Experimental protocols

(a) Dose-response effects of L-*NAME* ($n = 6$) Following the initial preparation, two pretreatment sets of haemodynamic measurements were made 15 min apart to ensure stability. L-NAME was then administered intravenously initially as a bolus of 0.2 mg kg^{-1}. The cumulative dose was increased every 20 min to 0.5 mg kg^{-1}, 1 mg kg^{-1}, 2 mg kg^{-1}, 5 mg kg^{-1}, 10 mg kg^{-1}; 20 mg kg^{-1} in three of the six pigs. Haemodynamic measurements were recorded 15 min after each dose. The results obtained were compared with those in a control group of six pigs who followed the same protocol but received equal volumes of isotonic saline rather than L-NAME.

(b) Effects of a single bolus of L-*NAME alone* ($n = 8$) Following the initial two pretreatment sets of measurements, L-NAME (10 mg kg^{-1}, i.v.) was administered as a single bolus. Haemodynamic measurements were recorded 15, 30, 45 and 60 min later and the results compared with the second pretreatment value.

(c) Effects of a single bolus of L-*NAME followed by nicardipine* ($n = 8$) Following the initial two pretreatment sets of measurements, L-NAME (10 mg kg^{-1}, i.v.) was administered as a single bolus. Haemodynamic measurements were recorded 15 min later. Nicardipine was then administered intravenously initially at a dose of 0.05 mg kg^{-1}. The cumulative dose was increased at 15 min intervals to 0.1 mg kg^{-1} and then to 0.2 mg kg^{-1}. Haemodynamic measurements were repeated 10 min after each dose. The results obtained were compared with those in the group of eight pigs who received only the bolus of L-NAME and no further drug (group (b) above).

(d) Effects of a single bolus of L-*NAME followed by theophylline* ($n = 8$) Following the initial two pretreatment sets of measurements, L-NAME (10 mg kg^{-1}, i.v.) was administered as a single bolus. Haemodynamic measurements were recorded 15 min later. Theophylline was then administered intravenously initially at a dose of 7.5 mg kg^{-1}. The cumulative dose was increased after 15 min to 10 mg kg^{-1}. Haemodynamic measurements were repeated 10 min after each dose. The results obtained were compared with those in the group of eight pigs receiving only the bolus of L-NAME (group (b) above).

(e) Effects of a single bolus of L-*NAME followed by zaprinast* ($n = 8$) Following the initial two pretreatment sets of measurements L-NAME (10 mg kg^{-1}, i.v.) was administered as a single bolus. Haemodynamic measurements were recorded 15 min later. Zaprinast was then administered intravenously initially at a dose of 1 mg kg^{-1}. The cumulative dose was increased at 15 min intervals to 3 mg kg^{-1} and then to 5 mg kg^{-1}. Haemodynamic measurements were repeated 10 min after each dose. The results obtained were compared with those in the group of eight pigs receiving only the bolus of L-NAME (group (b) above).

Drugs used

L-NAME (Sigma) was administered as a solution of 10 mg ml^{-1} dissolved in normal saline. Nicardipine (a gift from Syntex Research) was administered as the manufacturer's solution of 2.5 mg ml^{-1}. Theophylline (Sigma) was administered as a solution of 2 mg ml^{-1} in normal saline. Zaprinast (M&B 22948; a gift from Rhône-Poulenc Rorer) was administered as a solution of 10 mg ml^{-1} in 5% triethanolamine in normal saline.

Statistical analysis

Results are expressed as mean ± standard error of the mean (s.e.mean). The Mann-Whitney U test (SPSS) analysed the change produced in a given haemodynamic variable caused by administration of each active drug by comparison with that produced by its corresponding control (viz: effects of L-NAME compared with those of normal saline; effects of L-NAME followed by nicardipine, theophylline and zaprinast compared with those of L-NAME followed by no further drug). The null hypothesis stated that there was no difference between drug groups and was rejected if $P < 0.05$. The Wilcoxon matched-pairs signed-ranks test (SPSS) compared post-treatment values with the second pretreatment value within each group. The null hypothesis stated that there was no difference within a drug group and was rejected if $P < 0.05$.

Results

(a) Dose-response effects of L-*NAME* (Figure 1)

Administration of L-NAME caused a dose-dependent rise in systemic vascular resistance significantly different to saline at

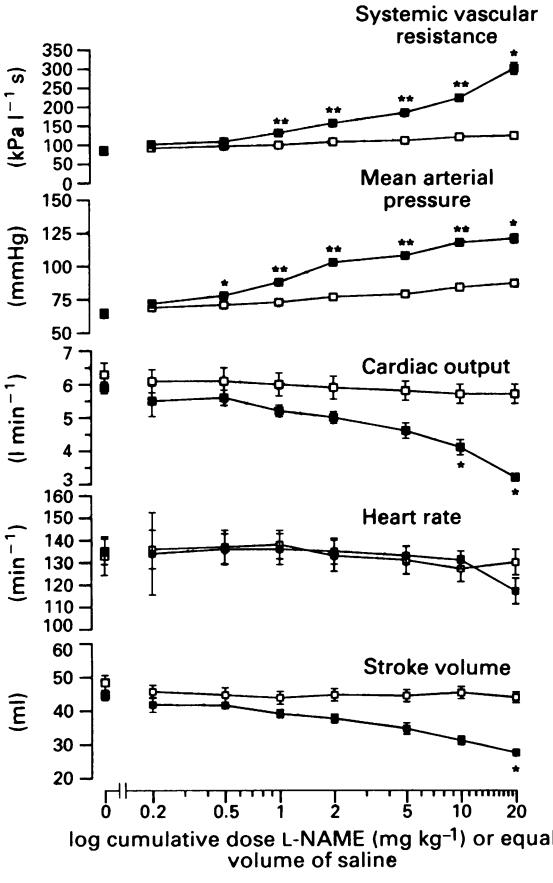

Figure 1 Log dose-response effects of N^G-nitro-L-arginine methyl ester (L-NAME) (■) or saline (□) on systemic vascular resistance, mean arterial pressure, cardiac output, heart rate and stroke volume. Mean ± s.e.mean; six pigs in each group. $*P<0.05$ versus saline. $**P<0.01$ versus saline.

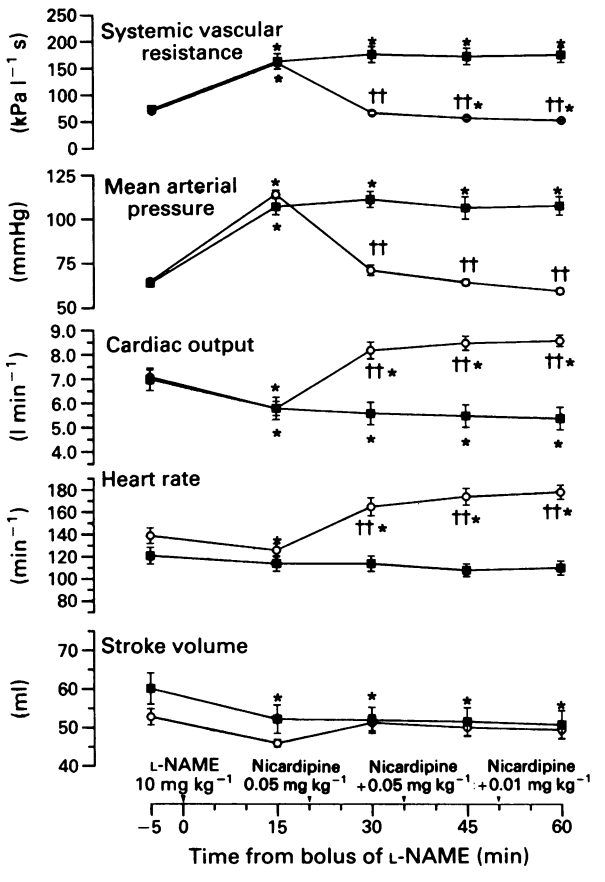

Figure 2 Effects of a single bolus of N^G-nitro-L-arginine methyl ester (L-NAME) (10 mg kg^{-1}) alone (■) and followed by increasing doses (marked) of nicardipine (○) on systemic vascular resistance, mean arterial pressure, cardiac output, heart rate and stroke volume. Mean ± s.e.mean; eight pigs in each group. $*P<0.05$ versus the pretreatment value. $\dagger\dagger P<0.01$ versus the effect produced by no further drug after the bolus of L-NAME.

doses $\geqslant$ 1 mg kg^{-1}. The accompanying rise in mean arterial pressure was significantly different to saline at doses $\geqslant$ 0.5 mg kg^{-1}. This was associated with a dose-dependent fall in cardiac output significantly different from saline at doses of 10 and 20 mg kg^{-1}. The changes in heart rate following L-NAME were not significantly different from those following saline but there was a dose-dependent fall in stroke volume significantly different from the effects of saline at 20 mg kg^{-1}.

(b) Effects of a single bolus of L-NAME alone (Figures 2–4)

Administration of L-NAME (10 mg kg^{-1}) as a single bolus caused increases in systemic vascular resistance and mean arterial pressure and a reduction in cardiac output all of which variables were significantly different from the pretreatment value after 15 min and remained so for at least 60 min. There was no significant change in heart rate from the pretreatment value but stroke volume was significantly reduced.

(c) Effects of a single bolus of L-NAME followed by nicardipine (Figure 2)

Administration of L-NAME caused increases in systemic vascular resistance and mean arterial pressure and a reduction in cardiac output all of which variables were significantly different from the pretreatment value after 15 min. There was no significant change in stroke volume from the pretreatment value but heart rate was significantly reduced.

Subsequent administration of nicardipine caused substantial reductions in systemic vascular resistance (0.05 mg kg^{-1}: 159.1 to 65.5 kPa l^{-1} s) and mean arterial pressure (0.05 mg kg^{-1}: 114 to 71 mmHg) such that, following the lowest dose of nicardipine (0.05 mg kg^{-1}), neither variable was significantly different from the pretreatment value. Higher cumulative doses of nicardipine were associated with further reductions in systemic vascular resistance and at 0.1 and 0.2 mg kg^{-1} these values were significantly lower than the pretreatment value. Cardiac output was completely and supramaximally restored (0.05 mg kg^{-1}: 5.8 to 8.2 l min^{-1}) such that, from the lowest dose used, values were significantly higher than the pretreatment value. The major component of this increase in cardiac output was due to a rise in heart rate (0.05 mg kg^{-1}: 126 to 165 min^{-1}).

(d) Effects of a single bolus of L-NAME followed by theophylline (Figure 3).

Administration of L-NAME caused increases in systemic vascular resistance and mean arterial pressure and a reduction in cardiac output all of which variables were significantly different from the pretreatment value after 15 min. Both heart rate and stroke volume were significantly reduced.

Subsequent administration of theophylline produced a statistically significant fall in systemic vascular resistance (10 mg kg^{-1}: 236.9 to 199.4 kPa l^{-1} s) and mean arterial pressure (7.5 mg kg^{-1}: 121 to 117 mmHg) but these effects were small compared to those of nicardipine and each variable

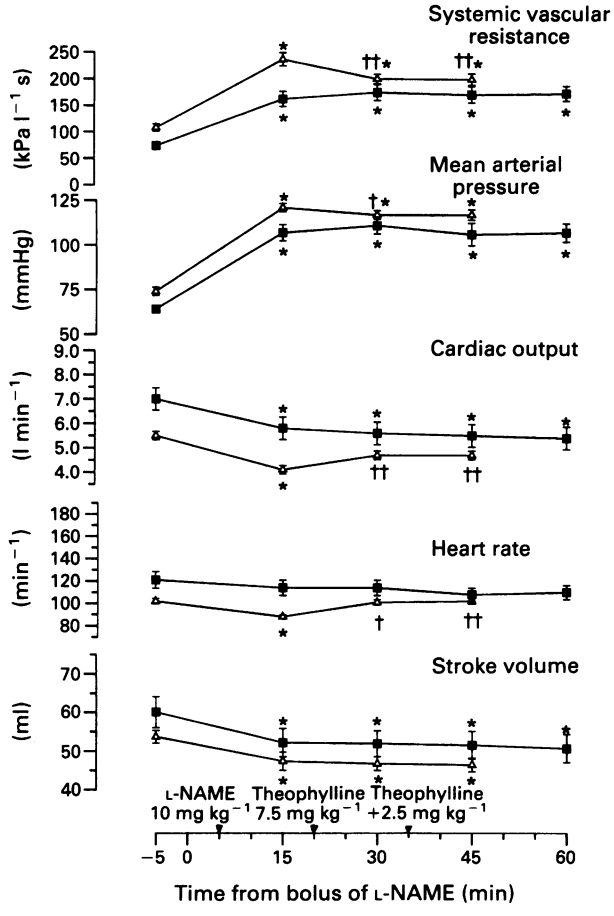

Figure 3 Effects of a single bolus of N^G-nitro-L-arginine methyl ester (L-NAME) (10 mg kg^{-1}) alone (■) and followed by increasing doses (marked) of theophylline (Δ) on systemic vascular resistance, mean arterial pressure, cardiac output, heart rate and stroke volume. Mean ± s.e.mean; eight pigs in each group. *$P<0.05$ versus the pretreatment value. †$P<0.05$ versus the effect produced by no further drug after the bolus of L-NAME. ††$P<0.01$ versus the effect produced by no further drug after the bolus of L-NAME.

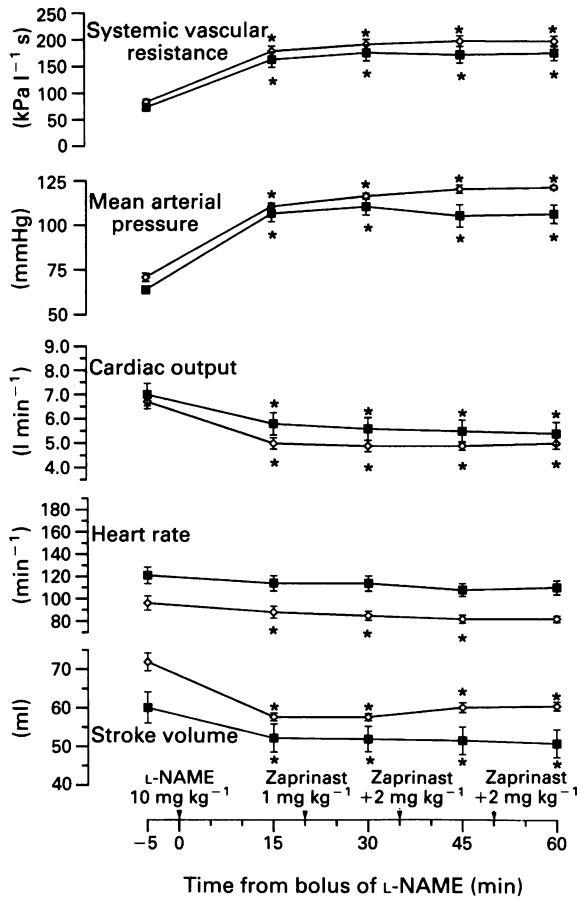

Figure 4 Effects of a single bolus of N^G-nitro-L-arginine methyl ester (L-NAME) (10 mg kg^{-1}) alone (■) and followed by increasing doses (marked) of zaprinast (◇) on systemic vascular resistance, mean arterial pressure, cardiac output, heart rate and stroke volume. Mean ± s.e.mean; eight pigs in each group. *$P<0.05$ versus the pretreatment value.

remained significantly higher than the pretreatment value. Cardiac output was partially restored (10 mg kg^{-1}: 4.1 to 4.7 l min^{-1}) and, from the first dose, was no longer significantly different from the pretreatment value. As with nicardipine this increase in cardiac output was due to a rise in heart rate, stroke volume remaining unchanged.

(e) Effects of a single bolus of L-NAME followed by zaprinast (Figure 4)

Administration of L-NAME caused increases in systemic vascular resistance and mean arterial pressure and a reduction in cardiac output all of which variables were significantly different from the pretreatment value after 15 min. Both heart rate and stroke volume were significantly reduced. Subsequent administration of zaprinast (1 to 5 mg kg^{-1}) had no significant tendency to reverse any of these effects. In four separate experiments we found that the effects of administration of L-NAME followed by 5% triethanolamine in saline, the solution used to dissolve zaprinast were not significantly different from those of L-NAME followed by no further drug.

Discussion

In these experiments in pentobarbitone-anaesthetized pigs, inhibition of NO synthesis with L-NAME caused a dose-dependent rise in systemic vascular resistance and mean arterial pressure with a dose-dependent fall in cardiac output caused by reduced stroke volume, or bradycardia, or both. These effects were reproduced 15 min after a single bolus of L-NAME (10 mg kg^{-1}) and were maintained for at least 60 min when no further drug was administered. Subsequent administration of the highly vasoselective calcium channel blocker nicardipine completely reversed systemic vasoconstriction and hypertension at low doses and in doing so completely restored cardiac output. Administration of theophylline had similar effects to nicardipine but was much less potent. Administration of zaprinast had no significant effect on any of these variables.

Nitric oxide is synthesized in the endocardium (Schulz *et al.*, 1991) and in the myocardium (Schulz *et al.*, 1992; Brady *et al.*, 1992; de Belder *et al.*, 1993) of human and animal hearts where it elevates myocardial cyclic GMP levels (Fort & Lewis, 1991; Schulz *et al.*, 1992) and depresses myocardial contractility (Fort & Lewis, 1991). This mechanism may contribute to myocardial dysfunction in endotoxic shock (Brady *et al.*, 1992) and in dilated cardiomyopathy (de Belder *et al.*, 1993). Thus we would expect that inhibition of endocardial or myocardial NO synthesis by L-NAME would increase myocardial contractility if it is to have any direct effect. In fact, previous work has shown that administration of NO synthase inhibitors to isolated cardiac myocytes from healthy animals neither augments nor reduces their contractility (Amrani *et al.*, 1992; Brady *et al.*, 1992). In our experiments cardiac output decreased following inhibition of NO synthesis and was completely restored by nicardipine

which is a vasodilator with little or no direct inotropic action (Rousseau *et al.*, 1985). We conclude that reduction of cardiac output by L-NAME is unlikely to be due to inhibition of endocardial or myocardial NO synthesis.

Increased systemic vascular resistance and systemic arterial pressure follow inhibition of NO synthesis in the rat (Gardiner *et al.*, 1990), rabbit (Persson *et al.*, 1991), dog (Kilbourn *et al.*, 1990; Chu *et al.*, 1990; Richard *et al.*, 1991), sheep (Tresham *et al.*, 1991) and guinea-pig (Aisaka *et al.*, 1989) associated with a dose-dependent bradycardia thought to be caused by activation of the baroreceptor reflex (Kilbourn *et al.*, 1990; Chu *et al.*, 1990). This has been proposed as the mechanism by which cardiac output falls in these circumstances (Kilbourn *et al.*, 1990). However, inhibition of the baroreflexes by pretreatment with atropine and atenolol does not prevent the fall in cardiac output in rats (Widdop *et al.*, 1992). In our experiments inhibition of NO synthesis caused increased systemic vascular resistance and mean arterial pressure with a variable heart rate response. When a large intravenous bolus of L-NAME (10 mg kg^{-1}) was administered it was accompanied by reduced cardiac output and reduced stroke volume or bradycardia or both, suggesting activation of baroreceptor reflexes. However, a progressive, dose-dependent fall in cardiac output observed in the dose-response experiments was not accompanied by progressive bradycardia and bradycardia appeared for the first time at the highest dose used (20 mg kg^{-1}). Baroreceptor reflexes have been demonstrated in pigs but their sensitivity is lower than that observed in other less sedentary species (Booth *et al.*, 1966). Barbiturate anaesthesia is known to depress baroreceptor reflexes (Bristow *et al.*, 1969) and this may have contributed to their variable sensitivity in our experiments. We conclude that the baroreceptor-mediated response to hypertension does not adequately account for the observed fall in cardiac output that follows L-NAME.

Inhibition of NO synthesis causes proximal coronary vasoconstriction demonstrated by increased coronary perfusion pressure (Amezcua *et al.*, 1989) or increased coronary resistance (Richard *et al.*, 1991), or by reduced coronary diameter (Chu *et al.*, 1990). However, workers who have measured myocardial perfusion as regional myocardial blood flow (Richard *et al.*, 1991) or as phasic blood flow (Chu *et al.*, 1990) in the presence of such proximal vasoconstriction have found it to be minimally affected if at all, suggesting that this pattern of coronary vasoconstriction does not produce true myocardial ischaemia. Further evidence for this conclusion comes from concomitant measurement of left ventricular dP/dt which is also unchanged (Chu *et al.*, 1990) except where coronary flow is severely reduced (Amrani *et al.*, 1992). Thus although proximal coronary vasoconstriction is a well-described effect of inhibition of NO synthesis, this is not necessarily associated with myocardial ischaemia or with negative inotropism and consequently we conclude that restoration of cardiac output by nicardipine after L-NAME is unlikely to be mediated by its coronary vasodilator properties.

Calcium channel blockers act by inhibiting calcium influx across the slow channel of cardiac and vascular smooth muscle cell membranes (Thorens & Hauesler, 1979) resulting in decreased intracellular calcium concentration and relaxation. Nicardipine is a highly vasoselective example. Intravenous or intracoronary administration of nicardipine causes systemic and coronary vasodilatation (Rousseau *et al.*, 1985). A slight increase in left ventricular peak dP/dt follows intravenous administration. This effect is not statistically significant when heart rate changes are controlled by pacing and intracoronary administration of nicardipine is not associated with a positive inotropic effect suggesting that nicardipine has little or no direct inotropic effect on the myocardium. These properties of nicardipine allowed us to study the effects of acute peripheral and coronary vasodilatation on cardiac output following inhibition of NO synthesis without directly affecting left ventricular contractility.

In our experiments, cardiac output reduced by L-NAME was completely restored by nicardipine. Given that this is unlikely to be mediated by coronary vasodilatation or by direct positive inotropism, we suggest that peripheral vasodilatation with consequent reduction of afterload on the ventricle allowed cardiac output to increase. The fact that the increase in cardiac output was primarily due to tachycardia with only a small rise in stroke volume is consistent with an inability of ventricular preload to rise sufficiently to match the fall in afterload produced by nicardipine. A similar phenomenon was observed in rats when a nitric oxide donor, S-nitroso-*N*-acetyl penicillamine (SNAP), was administered following N^G, N^G,dimethyl-L-arginine (ADMA; Gardiner *et al.*, 1993). In our experiments, measurement of pulmonary capillary wedge pressure (9.3 mmHg before nicardipine and 9.6 mmHg after the highest dose) and mean right atrial pressure (6.2 mmHg before nicardipine and 5.5 mmHg after the highest dose) supports the hypothesis, although the value of these indices as true markers of preload may be less reliable following major alterations in peripheral vascular tone.

Theophylline is a non-selective phosphodiesterase inhibitor, although the importance of this property at therapeutic doses remains controversial. At these levels its cardiovascular effects may be mediated by its ability to block myocardial and vascular adenosine receptors (Rall, 1990). Haemodynamic effects previously described include tachycardia, vasodilatation and positive inotropism but wide variation occurs between individuals (Ogilvie *et al.*, 1977). In our experiments theophylline slightly reversed systemic vasoconstriction but its effects were small compared to those of nicardipine. Cardiac output was partly restored by a combination of tachycardia and afterload reduction.

Zaprinast selectively inhibits cyclic GMP hydrolysis and the resulting increase in cyclic GMP levels is associated with vascular smooth muscle relaxation (Martin *et al.*, 1986). Administration of zaprinast to dogs causes systemic vasodilatation, hypotension and increased cardiac output at doses comparable to those used in pigs in our experiments (Weishaar *et al.*, 1990). However, we observed no significant tendency of zaprinast to reverse the changes in systemic vascular resistance brought about by L-NAME. Heart rate was unaffected and cardiac output was not restored. This may be explained by species variability or by total depletion of cyclic GMP in vascular smooth muscle cells as a result of administration of L-NAME which could not then be adequately restored by administration of zaprinast. Compared to vasoselective calcium channel blockade with nicardipine, inhibition of cyclic GMP breakdown using phosphodiesterase inhibitors was a less effective method of reversing the effects of L-NAME on the cardiovascular system and in particular, of restoring cardiac output.

The clinical relevance of these present findings concerns the excessive production of NO during septic shock (Gray *et al.*, 1991) when circulating bacterial lipopolysaccharide induces NO synthase (Smith *et al.*, 1991). This pathway may mediate pathological vasodilatation and hypotension which is characteristically unresponsive to sympathomimetic agents (Parratt, 1973). Inhibitors of NO synthase restore arterial pressure and vascular resistance (Kilbourn *et al.*, 1990) in animal models of septic shock, but worsen the prognosis if excessive doses are given (Nava *et al.*, 1991). NO synthase inhibitors (Petros *et al.*, 1991) and the guanylate cyclase inhibitor, methylene blue (Schneider *et al.*, 1992) have been administered to patients with septic shock but depression of cardiac index has been observed (Petros *et al.*, 1991; Schneider *et al.*, 1992), prompting other authors to advise caution (Hotchkiss *et al.*, 1992).

The conclusions from the present study are that the fall in cardiac output is mainly an effect of altered loading conditions on the heart, and that in healthy pigs, it is reversible by the subsequent administration of highly selective vasodilator agents. The hypothesis generated is that the same effect occurs in animal models of sepsis where myocardial depres-

sion and disrupted vascular reactivity may confound the problem. This hypothesis remains to be tested before drawing conclusions about clinical management.

N.A.H. was a Royal Victoria Hospital research fellow. We are grateful to the staff of the Medical Research Unit, Queen's University for their technical assistance. We are grateful to Syntex Research for the gift of nicardipine solution and to Rhône-Poulenc Rorer for the gift of zaprinast.

References

AISAKA, K., GROSS, S.S., GRIFFITH, O.W. & LEVI, R. (1989). N^G-methylarginine, an inhibitor of endothelium-derived nitric oxide synthesis, is a potent pressor agent in the guinea pig: does nitric oxide regulate blood pressure in vivo? *Biochem. Biophys. Res. Commun.*, **160**, 881–886.

AMEZCUA, J.L., PALMER, R.M.J., DE SOUZA, B.M. & MONCADA, S. (1989). Nitric oxide synthesized from L-arginine regulates vascular tone in the coronary circulation of the rabbit. *Br. J. Pharmacol.*, **97**, 1119–1124.

AMRANI, M., O'SHEA, J., ALLEN, N.J., HARDING, S.E., JAYAKUMAR, J., PEPPER, J.R., MONCADA, S. & YACOUB, M.H. (1992). Role of basal release of nitric oxide on coronary flow and mechanical performance of the isolated rat heart. *J. Physiol.*, **456**, 681–687.

BOOTH, N.H., BREDECK, H.E. & HERIN, R.A. (1966). Baroceptor and chemoceptor reflex mechanisms in swine. In *Swine in Biomedical Research*. ed. Bustad, G. pp. 331–346. London: Detweiler.

BRADY, A.J.B., POOLE-WILSON, P.A., HARDING, S.E. & WARREN, J.B. (1992). Nitric oxide production within cardiac myocytes reduces their contractility in endotoxemia. *Am. J. Physiol.*, **263**, H1963–H1966.

BRISTOW, J.D., PRYS-ROBERTS, C., FISHER, A., PICKERING, T.G. & SLEIGHT, P. (1969). Effects of anesthesia on baroreflex control of heart rate in man. *Anesthesiology*, **31**, 422–428.

CHU, A., CHAMBERS, D.E., LIN, C.-C., KUEHL, W.D. & COBB, F.R. (1990). Nitric oxide modulates epicardial coronary basal vasomotor tone in awake dogs. *Am. J. Physiol.*, **258**, H1250–H1254.

DE BELDER, A.J., RADOMSKI, M.W., WHY, H.J.F., RICHARDSON, P.J., BUCKNALL, C.A., SALAS, E., MARTIN, J.F. & MONCADA, S. (1993). Nitric oxide synthase activities in human myocardium. *Lancet*, **341**, 84–85.

FORT, S. & LEWIS, M.J. (1991). Regulation of myocardial contractile performance by sodium nitroprusside in the isolated perfused heart of the ferret. *Br. J. Pharmacol.*, **102**, 351P.

FUKUTO, J.M., CHIANG, K., HSZIEH, R., WONG, P. & CHAUDHURI, G. (1992). The pharmacological activity of nitroxyl: a potent vasodilator with activity similar to nitric oxide and/or endothelium-derived relaxing factor. *J. Pharmacol. Exp. Ther.*, **263**, 546–551.

GARDINER, S.M., COMPTON, A.M., KEMP, P.A. & BENNETT, T. (1990). Regional and cardiac haemodynamic effects of N^G-nitro-L-arginine methyl ester in conscious, Long Evans rats. *Br. J. Pharmacol.*, **101**, 625–631.

GARDINER, S.M., KEMP, P.A., BENNETT, T., PALMER, R.M.J. & MONCADA, S. (1993). Regional and cardiac haemodynamic effects of N^G,N^G,dimethyl-L-arginine methyl ester and their reversibility by vasodilators in conscious rats. *Br. J. Pharmacol.*, **110**, 1457–1464.

GRAY, G.A., SCHOTT, C., JULOU-SCHAEFFER, G., FLEMING, I., PARRATT, J.R. & STOCLET, J.-C. (1991). The effect of inhibitors of the L-arginine/nitric oxide pathway on endotoxin-induced loss of vascular responsiveness in anaesthetized rats. *Br. J. Pharmacol.*, **103**, 1218–1224.

HOTCHKISS, R.S., KARL, I.E., PARKER, J.L. & ADAMS, H.R. (1992). Inhibition of NO synthesis in septic shock [letter]. *Lancet*, **339**, 434–435.

KILBOURN, R.G., JUBRAN, A., GROSS, S.S., GRIFFITH, O.W., LEVI, R., ADAMS, J. & LODATO, R.F. (1990). Reversal of endotoxin-mediated shock by N^G-methyl-L-arginine, an inhibitor of nitric oxide synthesis. *Biochem. Biophys. Res. Commun.*, **172**, 1132–1138.

LINCOLN, T.M. (1989). Cyclic GMP and mechanisms of vasodilation. *Pharmac. Ther.*, **41**, 479–502.

MARTIN, W., FURCHGOTT, R.F., VILLANI, G.M. & JOTHIANANDAN, D. (1986). Phosphodiesterase inhibitors induce endothelium-dependent relaxation of rat and rabbit aorta by potentiating the effects of spontaneously released endothelium-derived relaxing factor. *J. Pharmacol. Exp. Ther.*, **237**, 539–547.

MONCADA, S., PALMER, R.M.J. & HIGGS, E.A. (1991). Nitric oxide: physiology, pathophysiology, and pharmacology. *Pharmacol. Rev.*, **43**, 109–142.

NAVA, E., PALMER, R.M.J. & MONCADA, S. (1991). Inhibition of nitric oxide synthesis in septic shock: how much is beneficial? *Lancet*, **338**, 1555–1557.

OGILVIE, R.I., FERNANDEZ, P.G. & WINSBERG, F. (1977). Cardiovascular response to increasing theophylline concentrations. *Eur. J. Clin. Pharmacol.*, **12**, 409–414.

PARRATT, J.R. (1973). Myocardial and circulatory effects of E. coli endotoxin; modification of responses to catecholamines. *Br. J. Pharmacol.*, **47**, 12–25.

PERSSON, M.G., GUSTAFSSON, L.E., WIKLUND, N.P., MONCADA, S. & HEDQVIST, P. (1990). Endogenous nitric oxide as a probable modulator of pulmonary circulation and hypoxic pressor response in vivo. *Acta Physiol. Scand.*, **140**, 449–457.

PERSSON, M.G., WIKLUND, N.P. & GUSTAFSSON, L.E. (1991). Nitric oxide requirement for vasomotor nerve-induced vasodilatation and modulation of resting blood flow in muscle microcirculation. *Acta Physiol. Scand.*, **141**, 49–56.

PETROS, A., BENNETT, D. & VALLANCE, P. (1991). Effect of nitric oxide synthase inhibitors on hypotension in patients with septic shock. *Lancet*, **338**, 1557–1558.

RALL, T.W. (1990). Drugs used in the treatment of asthma. In *The Pharmacological Basis of Therapeutics*. ed. Goodman Gilman, A., Rall, T.W., Nies, A.S. & Taylor, P. pp. 618–637. New York: Pergamon Press.

REES, D.D., PALMER, R.M.J., SCHULZ, R., HODSON, H.F. & MONCADA, S. (1990). Characterisation of three inhibitors of endothelial nitric oxide synthase *in vitro* and *in vivo*. *Br. J. Pharmacol.*, **101**, 746–752.

RICHARD, V., BERDEAUX, A., LA ROCHELLE, C.D. & GIUDICELLI, J.-F. (1991). Regional coronary haemodynamic effects of two inhibitors of nitric oxide synthesis in anaesthetized, open-chest dogs. *Br. J. Pharmacol.*, **104**, 59–64.

ROUSSEAU, M.F., VINCENT, M.F., CHERON, P., VAN DEN BERGHE, G., CHARLIER, A.A. & POULEUR, H. (1985). Effects of nicardipine on coronary blood flow, left ventricular inotropic state and myocardial metabolism in patients with angina pectoris. *Br. J. Clin. Pharmacol.*, **20** (Suppl. 1), 147S–157S.

SCHNEIDER, F., LUTUN, Ph., HASSELMANN, M., STOCLET, J.C. & TEMPE, J.D. (1992). Methylene blue increases systemic vascular resistance in human septic shock. *Int. Care Med.*, **18**, 309–311.

SCHULZ, R., SMITH, J.A., LEWIS, M.J. & MONCADA, S. (1991). Nitric oxide synthase in cultured endocardial cells of the pig. *Br. J. Pharmacol.*, **104**, 21–24.

SCHULZ, R., NAVA, E. & MONCADA, S. (1992). Induction and potential biological relevance of a Ca^{2+}-independent nitric oxide synthase in the myocardium. *Br. J. Pharmacol.*, **105**, 575–580.

SMITH, R.E.A., PALMER, R.M.J. & MONCADA, S. (1991). Coronary vasodilatation induced by endotoxin in the rabbit isolated perfused heart is nitric oxide-dependent and inhibited by dexamethasone. *Br. J. Pharmacol.*, **104**, 5–6.

THORENS, S. & HAEUSLER, G. (1979). Effects of some vasodilators on calcium translocation in intact and fractionated vascular smooth muscle. *Eur. J. Pharmacol.*, **54**, 79–91.

TRESHAM, J.J., DUSTING, G.J., COGHLAN, J.P. & WHITWORTH, J.A. (1991). Haemodynamic and hormonal effects of N-nitro-L-arginine, an inhibitor of nitric oxide biosynthesis, in sheep. *Clin. Exp. Pharmacol. Physiol.*, **18**, 327–330.

WEISHAAR, R.E., KOBYLARZ-SINGER, D.C., KEISER, J., HALEEN, S.J., MAJOR, T.C,. RAPUNDALO, S., PETERSON, J.T. & PANEK, R. (1990). Subclasses of cyclic GMP-specific phosphodiesterase and their role in regulating the effects of atrial natriuretic factor. *Hypertension*, **15**, 528–540.

WIDDOP, R.E., GARDINER, S.M., KEMP, P.A. & BENNETT, T. (1992). The influence of atropine and atenolol on the cardiac haemodynamic effects of N^G-nitro-L-arginine methyl ester in conscious, Long Evans rats. *Br. J. Pharmacol.*, **105**, 653–656.

(Received November 3, 1993
Revised February 2, 1994
Accepted February 4, 1994)

Br. J. Pharmacol. (1994), **112**, 429–434

Benzodiazepine/cholecystokinin interactions at functional CCK receptors in rat brain

[1]P.R. Boden & G.N. Woodruff

Parke-Davis Neuroscience Research Centre, Addenbrookes Hospital Site, Hills Road, Cambridge, CB2 2QB

1 The effects of benzodiazepines on cholecystokinin (CCK) responses produced following activation of CCK_B receptors by pentagastrin in the ventromedial hypothalamus (VMH) or CCK_A receptors by CCK-8S in the dorsal raphe of the rat brain *in vitro* have been investigated.

2 The benzodiazepine agonist, flurazepam, at high concentrations, blocked pentagastrin-induced excitations in the rat VMH yielding an equilibrium constant (K_e) value of 12.5 μM.

3 In the rat dorsal raphe, where activation of CCK_A receptors leads to neuronal depolarization, flurazepam also produced a weak block of the CCK response.

4 Flurazepam blocked CCK responses but not carbachol-induced excitations of VMH neurones. The inhibition of CCK responses by flurazepam was not blocked by the benzodiazepine antagonist, flumazenil.

5 These data suggest that flurazepam is a weak antagonist at central CCK_B receptors.

6 At central CCK_A receptors, flurazepam blocked CCK-8S responses but the inhibition was not competitive, with a reduction in the peak CCK-8S obtainable in the presence of flurazepam. These results suggest that flurazepam acts at a site other than the CCK_A receptor itself to block CCK responses in the dorsal raphe.

Keywords: Cholecystokinin; CCK_B; CCK_A; ventromedial hypothalamus; dorsal raphe; benzodiazepines

Introduction

Benzodiazepines have been shown to inhibit both central and peripheral cholecystokinin (CCK) responses. In the periphery, the benzodiazepines diazepam and chlordiazepoxide were both competitive inhibitors of CCK-induced contractions of guinea-pig gall bladder (Kubota *et al.*, 1985b) where the CCK response is traditionally associated with CCK_A receptor activation. In mice, flurazepam and the benzodiazepine antagonist, flumazenil, have also both been shown to block the antinociceptive actions of intracisternal CCK (Kubota *et al.*, 1985a). Iontophoretic application of the water-soluble benzodiazepine, flurazepam, produced a selective block of CCK-induced increases in firing rate of CA1 and CA3 hippocampal neurones *in vivo* (Bradwejn & De Montigny, 1984), an effect that was reversed by application of flumazenil. They proposed that this selective block of CCK responses by benzodiazepines acting via neuronal benzodiazepine receptors could account for the anxiolytic effects of these drugs, which is made more interesting by recent evidence that CCK_B antagonists are also potent anxiolytics (Hughes *et al.*, 1990; Singh *et al.*, 1991). Benzodiazepine inverse agonists have been shown to induce panic (Dorrow *et al.*, 1983; Baldwin & File, 1988; Little, 1991). The proposal that CCK-4 might induce panic by acting as an inverse agonist at the benzodiazepine receptor has been eliminated by data from healthy human subjects showing that flumazenil had no effect on the behavioural and cardiovascular responses induced by CCK-4, thus proving that benzodiazepine receptors are not involved in CCK-4-induced panicogenesis (Harro *et al.*, 1993). Whether benzodiazepine agonist prevention of CCK-4-induced panicogenesis in man, as shown in the study of De Montigny (1989), is via benzodiazepine receptor activation would require such experiments to be performed in the presence of a benzodiazepine antagonist. There is evidence that chronic benzodiazepine treatment can alter both the functional responses to CCK application and the density of CCK binding sites in the rodent brain. Long-term treatment of rats with flurazepam (15 mg daily, i.p.) reduced the neuronal responsiveness to CCK of rat CA3 hippocampal neurones (Bouthillier & De Montigny, 1988). In behavioural studies, cessation of chronic diazepam administration produced an increase in [^{3}H]-CCK-8S binding sites in rat cortex and hippocampus (Harro *et al.*, 1990) and recent *in situ* hybridisation studies showed that CCK mRNA levels in non-pyramidal cells (where CCK and GABA co-exist) increased following a single injection of diazepam (2 mg kg^{-1}) or withdrawal from chronic diazepam treatment (Rattray *et al.*, 1993).

We have addressed the possible interactions between benzodiazepine moieties and CCK using *in vitro* electrophysiological studies with selective CCK agonists and antagonists. Two benzodiazepines, the agonist flurazepam and the antagonist flumazenil, were chosen since these agents had been shown previously to be effective in modulating CCK excitation *in vivo* (Bradwejn & De Montigny, 1984) and we made use of two models for central CCK receptor activation, the rat ventromedial hypothalamus or VMH (Boden & Hill, 1988a) and the rat dorsal raphe (Boden *et al.*, 1991), both of which have been fully characterized pharmacologically.

Methods

Brain slice preparation and recording

Studies of benzodiazepine/CCK_B receptor interactions were performed using extracellular recordings from rat VMH neurones contained in coronal slices of rat midbrain. To ensure that only CCK_B responses were evoked in the VMH and to eliminate any influence from CCK_A receptors, we used pentagastrin, which is a selective CCK_B agonist, and Cl-988 as the CCK_B antagonist. Benzodiazepine/CCK_A interactions were studied by intracellular recording from a sub-population of 5-hydroxytryptamine (5-HT)-sensitive, CCK-responsive, neurones. The presence of only CCK_A receptors in the dorsal raphe (Boden *et al.*, 1991) meant that CCK-8S was used in these studies. Slices of hypothalamus or dorsal raphe were prepared from the brains of male Wistar rats (100–200 g) as

[1] Author for correspondence.

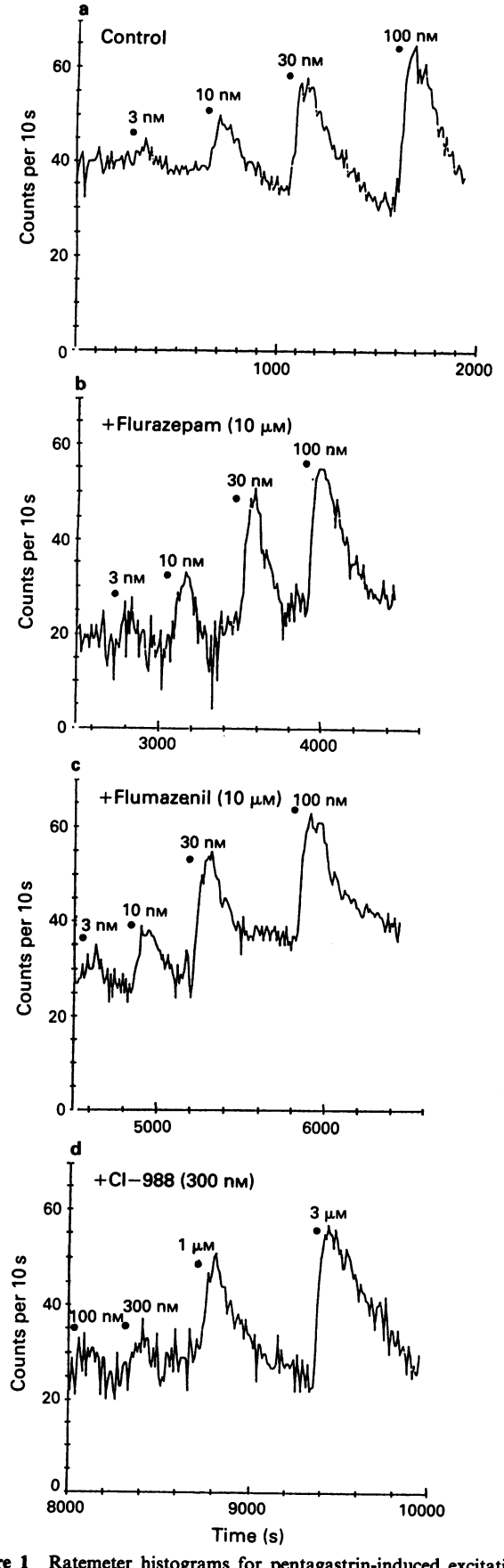

Figure 1 Ratemeter histograms for pentagastrin-induced excitation of a VMH neurone in the absence and presence of benzodiazepines and CI-988. The traces show control dose-responses to increasing concentrations of pentagastrin (3–100 nM) applied for 1 min. In the presence of flurazepam (10 μM, 20 min) (b) or flumazenil (10 μM, 20 min) (c) the pentagastrin responses were still present. When CI-988 (300 nM, 20 min) was included in the perfusing ACSF the response to pentagastrin (100 nM) was abolished but the block could be overcome by increasing the concentration of pentagastrin (d).

described previously (Boden & Hill, 1988a; Boden *et al.*, 1991) and incubated in pre-gassed (95%O_2:5%CO_2) artificial cerebrospinal (ACSF) fluid of the following composition (mM); NaCl 124, KCl 5, $CaCl_2$ 2.4, NaH_2PO_4 1.2, $MgCl_2$ 1.2, glucose 11 and $NaHCO_3$ 25 at room temperature (21–23°C). One hour prior to recording, one slice was transferred to a Perspex chamber where it was perfused with ACSF at 37°C flowing at 4 ml min^{-1}. Drugs were applied directly in the perfusing medium following dilution in ACSF to the required concentration from dimethyl sulphoxide (DMSO) stock solutions. CI-988(4-{[2-[[3-(1H-indol-3-yl)-2-methyl-1-oxo-2-[[(tricylo-[3.3.1.1.^{3,7}]-dec-2-yloxy)-carbonyl]-amino]-propyl]-amino]-1-phenylethyl]-amino}-4-oxo-[**R**-(**R***,**R***)]-butanoate-*N*-methyl-D-glucamine) was synthesized in the Medicinal Chemistry Laboratories of Parke-Davis, Cambridge, U.K. Flurazepam and flumazenil were from Roche.

Data analysis

Data collection and analysis was performed according to previously described methodology (Boden & Hill, 1988a; Hughes *et al.*, 1990; Pinnock *et al.*, 1992). Final ratemeter histograms and dose-response curves were obtained by importing the files into a graphics and statistics software package (RS1, version 12.10E BBN software products, Cambridge, Massachusetts, U.S.A.). Best-fit curves were obtained by fitting a simple hyperbolic function ($f\{x\} = (B.x)/(x + A)$). The equilibrium constant (K_e) was then calculated from the equation, Dose-ratio $- 1 = [\text{antagonist}]/K_e$.

Results

Results were obtained from a total of 26 VMH neurones (16 slice preparations) and 14 dorsal raphe neurones (14 preparations).

Effects of benzodiazepines on CCK_B responses

Dose-response curves to pentagastrin obtained from VMH neurones were not changed in the presence of flurazepam or flumazenil at concentrations up to and including 10 μM

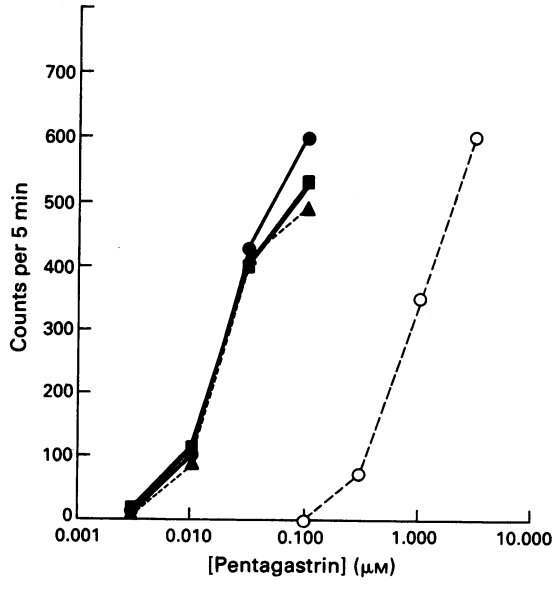

Figure 2 Dose-response curves plotted from the data obtained in the experiment shown in Figure 1. Note that the dose-response curves for pentagastrin under control (●) conditions and in the presence of flurazepam, 10 μM (■) or flumazenil, 10 μM (▲) are superimposed. The dose-response curve for pentagastrin in the presence of CI-988 (300 nM) (○) was shifted to the right with a K_e of 8.2 nM.

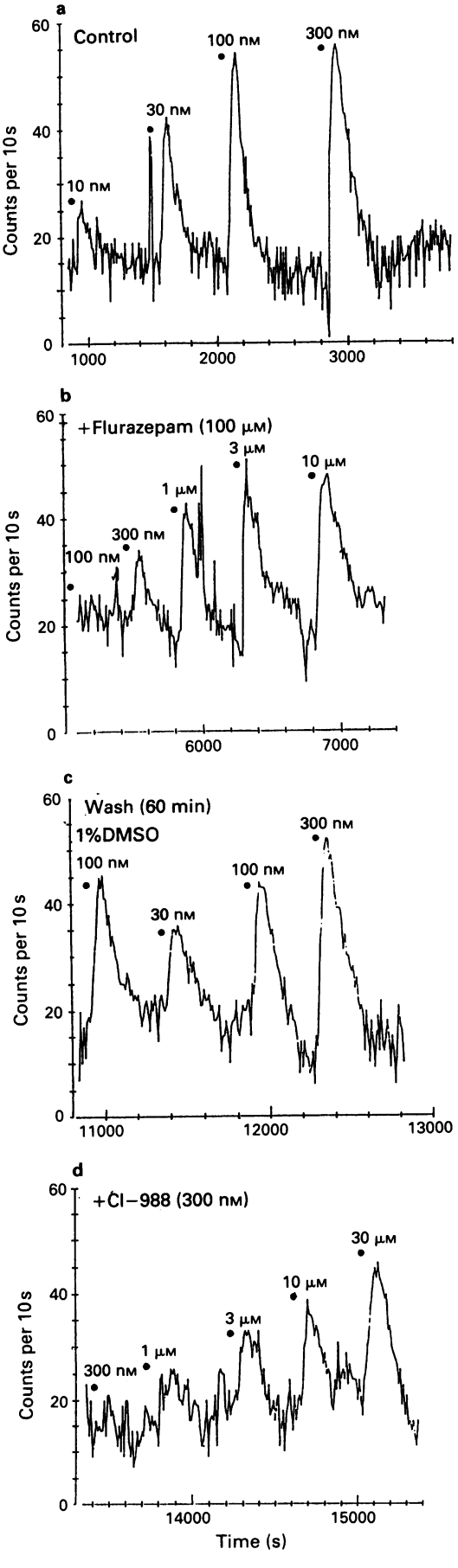

Figure 3 Data obtained for pentagastrin-induced excitation of a VMH neurone in the absence (a) and presence of flurazepam (100 μM) (b). This concentration of flurazepam blocked the pentagastrin response (K_e = 5.4 μM). After removal of flurazepam, pentagastrin was applied (100 nM, 1 min) every 10 min for approximately 1 h. Recovery of the pentagastrin response was evident (c). After recovery (c) solvent controls were performed (100 nM pentagastrin in 1% dimethylsulphoxide (DMSO)) to ensure that 1% DMSO did not affect the pentagastrin response. Finally the slice was treated with CI-988 (300 nM, 20 min). The resulting block of the pentagastrin response is shown in (d). The K_e for CI-988 in this instance was 2.0 nM.

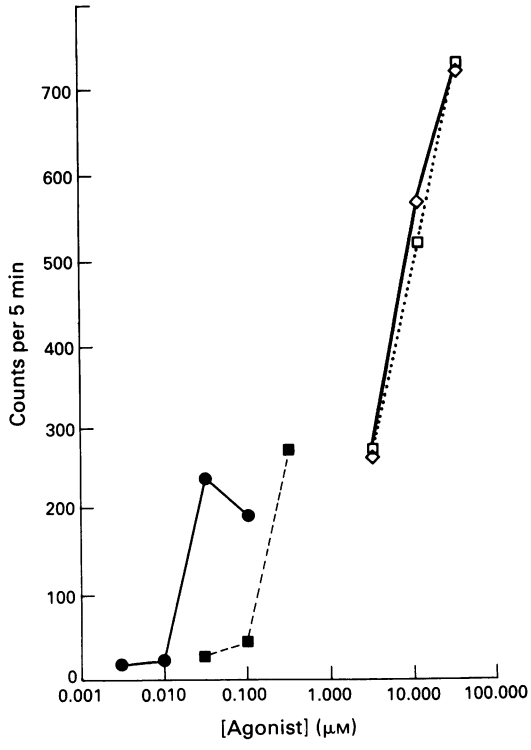

Figure 4 Flurazepam (100 μM) affects only pentagastrin-induced excitations of VMH neurones. In this experiment the action of flurazepam was tested on both carbachol-induced and pentagastrin-induced responses. No equivalent block of the carbachol response was evident, with little reduction in the carbachol excitation seen at a carbachol concentration of 10 μM in the presence of flurazepam (100 μM), a dose of the benzodiazepine which produced a tenfold shift in the pentagastrin dose-response curve. Control (pentagastrin) (●); control (carbachol) (□); carbachol + flurazepam 100 μM (◇); pentagastrin + flurazepam 100 μM (■).

(n = 6). Figure 1 shows ratemeter histograms from one experiment in normal conditions and in the presence of flurazepam or flumazenil (10 μM). Neither drug altered the pentagastrin dose-response curve, plotted in Figure 2, but subsequent addition of the selective CCK_B antagonist CI-988 (300 nM) produced the expected rightward shift in the pentagastrin dose-response curve.

Dose-response curves to pentagastrin were shifted to the right in a competitive fashion by flurazepam (100 μM). This weak blocking effect of the benzodiazepine (Figure 3b) could be overcome by washing the preparation in drug-free solution. Recovery times for the reversal of the block by flurazepam varied between 40 and 90 min. One example of the reversal is shown by the ratemeter recording in Figure 3c which shows data obtained 60 min after removal of the benzodiazepine from the perfusing ACSF. CI-988 was then applied, and produced a profound block of the pentagastrin response (Figure 3d). The selectivity of the benzodiazepine for CCK was confirmed by using either pentagastrin or the muscarinic agonist carbamylcholine (carbachol) to excite the VMH neurone in the same experiment. Under these condi-

tions only the dose-response curve to pentagastrin was affected (Figure 4). The equilibrium constant (K_e) value for flurazepam from these experiments was 12.5 μM (range 5.4–21.4 μM, $n = 5$).

Whilst the results indicated that flurazepam was a weak antagonist at the rat central CCK_B receptor we wanted to eliminate any possibility that the benzodiazepine effects were the result of interaction of flurazepam with a benzodiazepine receptor. Experiments were performed to see whether the flurazepam block of CCK responses in the rat VMH could be prevented by prior administration of the benzodiazepine antagonist, flumazenil.

Addition of flumazenil (100 μM) had no effect on the pentagastrin dose-response curve. Flurazepam (100 μM) still produced a weak block of the pentagastrin excitation in the continued presence of flumazenil (Figure 5). These data confirmed flurazepam to be acting as a CCK_B antagonist and not via neuronal benzodiazepine receptors in the rat VMH.

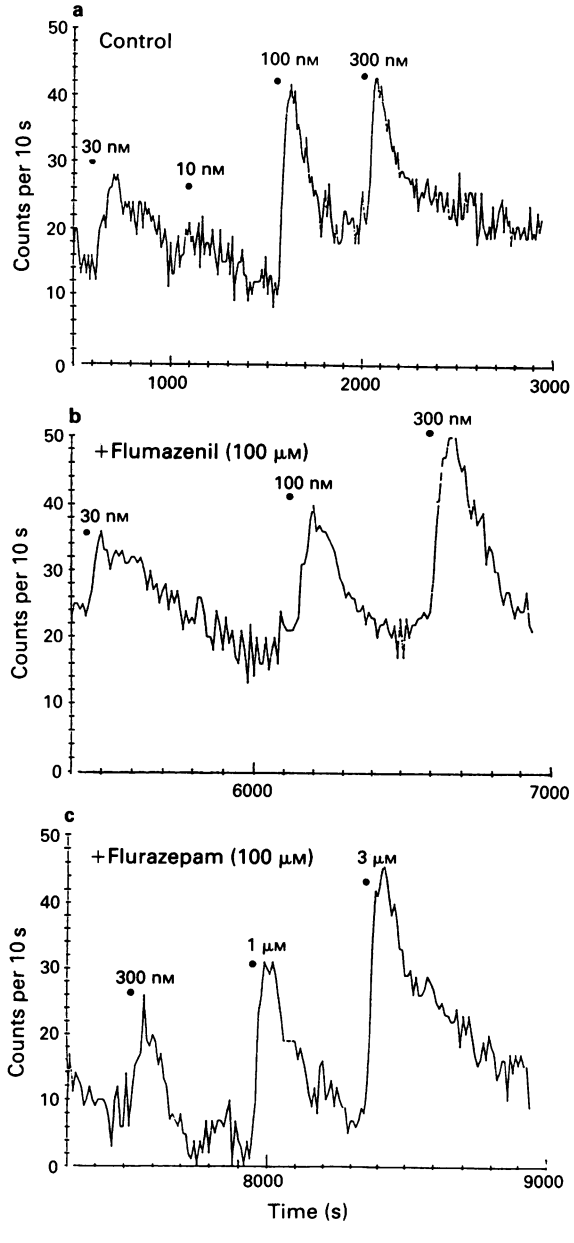

Figure 5 The effect of flurazepam on pentagastrin responses in the rat VMH are not blocked by prior treatment with flumazenil (100 μM, 20 min): (a) shows control dose-response data; (b) shows that flumazenil had no effect alone on the pentagastrin response and failed to influence the subsequent block of the pentagastrin response by flurazepam (100 μM, 20 min) (c). The K_e value for the block by flurazepam in this experiment was 21.4 μM.

Flurazepam also inhibits CCK_A responses in the rat dorsal raphe

We have also investigated whether flurazepam can block CCK_A-mediated excitations of rat dorsal raphe neurones. In this series of experiments application of the sulphated octapeptide of CCK, CCK-8S, produced a concentration-dependent depolarization concomitant with an increase in action potential firing rate in 14 out of 42 5-HT neurones tested (using a total of 14 dorsal raphe slice preparations). In the majority of these (11 out of 14) flurazepam (500 nM–10 μM) reduced the CCK response. However, the block by flurazepam was not readily surmountable with concentration-response curves suggesting a non-competitive interaction for flurazepam and CCK at CCK_A receptors. Increasing the concentration of flurazepam did increase the block produced by the benzodiazepine agonist, as seen in Figure 6. The flurazepam block of CCK-8S responses in the dorsal raphe was not altered by the presence of 100 μM flumazenil ($n = 4$). In the remaining three experiments we found that application of flurazepam at the highest concentration alone to a CCK-8S-sensitive raphe neurone produced an excitation analogous to that seen using the peptide. Subsequent responses obtained to CCK-8S application showed an enhancement of the CCK response at low concentrations and a block at high concentrations, with a pronounced reduction in the time course of the response to CCK-8S following flurazepam application. The low incidence of this type of effect produced a full investigation into the nature of the interaction between flurazepam and CCK.

Discussion

We have used two pharmacologically well defined *in vitro* models of functional CCK receptor activation in the rat brain to study the interactions between benzodiazepines and CCK. Our results provide the first evidence for a block, albeit weak, of functional CCK_B responses by a benzodiazepine agonist in the hypothalamus which is competitive in nature and thus indicative of an effect of flurazepam at the CCK_B receptor. The inability of the benzodiazepine antagonist, flumazenil, to reverse the block induced by flurazepam, combined with the high concentration of flurazepam required to produce a shift in the dose-response curves for CCK ligands are in contrast to the results reported by Bradwejn & De Montigny (1984), who showed that low doses of flurazepam acting at neuronal benzodiazepine receptors could attenuate CCK responses in the hippocampus. The data presented here suggest that flurazepam, a benzodiazepine agonist, is a weak competitive antagonist at rat central CCK_B receptors.

We were unable to find any effect of either flurazepam or flumazenil at concentrations up to and including 10 μM. With higher concentrations (100 μM) of flurazepam a competitive block of the pentagastrin response was found yielding a K_e of approximately 12 μM. The flurazepam effect was selective for pentagastrin and reversible on washing in drug-free saline, after which time the preparation could be treated with CI-988 to produce the predicted block of pentagastrin. However, no change in the ability of flurazepam to attenuate pentagastrin-induced excitations was seen when the preparation was pretreated with the benzodiazepine antagonist, flumazenil (100 μM). From this series of experiments we conclude that the only interaction between flurazepam and CCK_B receptors occurs at high concentrations when the benzodiazepine interacts competitively with CCK_B agonists at the CCK_B receptor. The low probability that such high concentrations of benzodiazepines would occur at CCK_B receptors to block the CCK_B response when anxiolytic doses of ben-

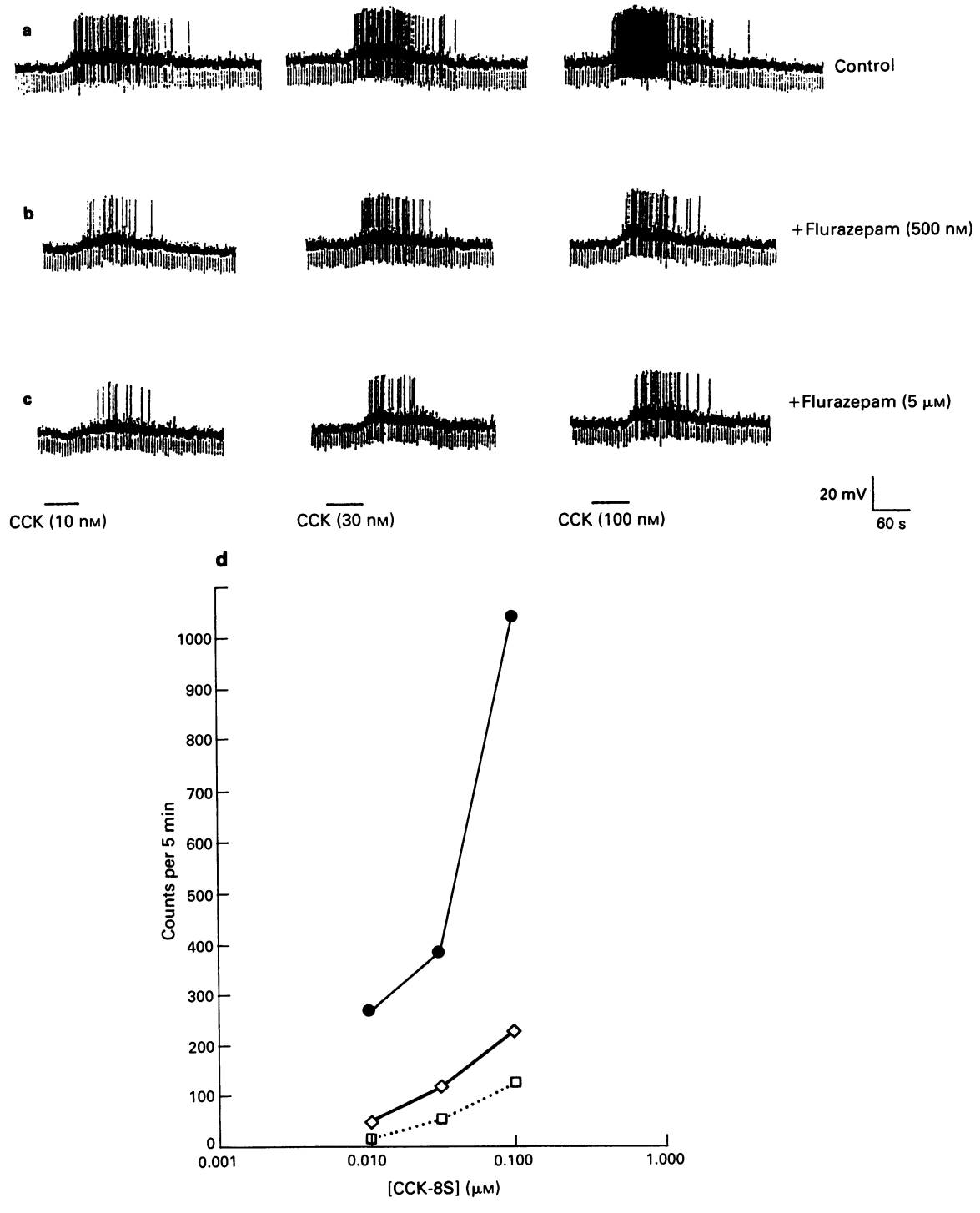

Figure 6 Flurazepam blocks CCK-8S-induced excitation of rat dorsal raphe neurones. The figure shows pen recorder traces of an intracellular recording from a single dorsal raphe neurone. Resting potential of the neurone was − 54 mV. CCK was applied at known concentrations for 1 min, as indicated by the horizontal bars. The top three traces (a) are control (drug-free) responses. In (b) are shown pen recordings taken during flurazepam (500 nM) treatment, showing attenuation of the CCK responses. This is more evident in (c) where the slice was bathed in flurazepam at a final concentration of 5 μM. The concentration-response curves for the experiment (d) are shown to illustrate the lack of evidence for a competitive interaction between flurazepam and CCK-8S; control (●); flurazepam 500 nM (◇); flurazepam 5 μM (□).

zodiazepines are given precludes us from suggesting a common pathway between CCK_B antagonist and benzodiazepine agonist-induced anxiolysis.

We also obtained evidence that flurazepam inhibits excitations mediated by CCK acting via central CCK_A receptors. CCK_A responses recorded from rat dorsal raphe neurones were attenuated by flurazepam at micromolar concentrations. The lack of effect of the benzodiazepines receptor antagonist on the block produced by flurazepam again suggests that the benzodiazepine agonist is a weak antagonist at the central CCK_A receptor. However, we found this action of the benzodiazepine to be much more difficult to surmount with increasing CCK concentrations. From our limited concentration-response data we are not able to define the nature of the interaction other than it appears not to be competitive. These results would imply that the interaction between the benzodiazepine agonist and CCK at the central CCK_A receptor may be occurring at a site distinct from the CCK_A

receptor. As such this effect of the benzodiazepine agonist differs from that seen at the CCK_B receptor. The flurazepam block of pentagastrin in the VMH and CCK-8S in the raphe are similar in their requirement for high benzodiazepine agonist concentrations and lack of effect of the benzodiazepine antagonist flumazenil, either alone or in blocking the flurazepam inhibition.

What can also be concluded from these data is that a discrepancy exists between the *in vitro* results described herein and the *in vivo* electrophysiological experiments of Bradwejn & De Montigny (1984). We were unable to reverse any of the actions of flurazepam at either of the CCK receptors with the same benzodiazepine antagonist used to block successfully the inhibition of CCK responses in hippocampus by these authors. One possible explanation would be the existence of regional differences with regard to the functional association between CCK and benzodiazepines. Neuronal benzodiazepine binding sites are present in the rat VMH but may not modulate CCK action in this nucleus whilst interacting more intimately with the hippocampal CCK receptor. The data would be more analogous if *in vitro* studies using CCK responses in the rat hippocampus were used. However, two problems would need to be overcome before *in vitro* studies using hippocampal slices could be undertaken. The first is the profound CCK receptor desensitization which is seen in hippocampal slice preparations (Dodd & Kelly, 1981; Boden & Hill, 1988b). Secondly, *in vitro* studies on the CCK response in hippocampus suggests a CCK_B receptor on CA1 hippocampal neurones (Dodd & Kelly, 1981; Boden & Hill, 1988b), which is in stark contrast to the lack of efficacy of the non-sulphated octapeptide of CCK reported by Bradwejn & De Montigny which implies that CCK_A receptors are involved in pyramidal neurone excitation by the peptide *in vivo*. We did test flurazepam against CCK_A sites in the rat brain in an endeavour to find a similar phenomena to that reported by Bradwejn & De Montigny but were without success, finding no evidence for an involvement of a neuronal benzodiazepine receptor in the block of CCK responses in the rat dorsal raphe by flurazepam. Although further studies would be required to identify the exact nature of the benzodiazepine/central CCK_A receptor interaction the effect produced by flurazepam at the central CCK_A receptor does not mirror the competitive interaction reported at the peripheral CCK_A receptor (Kubota *et al.*, 1985b).

In conclusion, we have investigated the effects of a benzodiazepine agonist and antagonist on CCK_A and CCK_B responses recorded from rat brain slices *in vitro*. Our data suggest that the effects seen with flurazepam occur as a consequence of a direct interaction between the benzodiazepine agonist and the CCK_B receptor. In the dorsal raphe, we could find no evidence to support a competitive interaction between flurazepam and the CCK_A receptor, but the benzodiazepine agonist was still able to inhibit CCK_A-mediated responses. In both cases flumazenil was unable to prevent flurazepam from inhibiting the CCK response, suggesting that the benzodiazepine effects on CCK in these experiments do not involve a neuronal benzodiazepine receptor.

References

BALDWIN, H.A. & FILE, S.E. (1988). Reversal of increased anxiety during benzodiazepine withdrawal: evidence for an anxiogenic endogenous ligand for benzodiazepine receptor. *Brain Res. Bull.*, **20**, 603–606.

BODEN, P.R. & HILL, R.G. (1988a). Effect of cholecystokinin and related peptides on neuronal activity in the ventromedial nucleus of the rat hypothalamus. *Br. J. Pharmacol.*, **94**, 246–252.

BODEN, P.R. & HILL, R.G. (1988b) Effects of cholecystokinin and pentagastrin on rat hippocampal neurones maintained *in vitro*. *Neuropeptides*, **12**, 95–103.

BODEN, P.R., PINNOCK, R.D. & WOODRUFF, G.N. (1991). Pharmacology of a cholecystokinin receptor on 5-hydroxytryptamine neurones in the dorsal raphe of the rat brain. *Br. J. Pharmacol.*, **102**, 635–638.

BOUTHILLIER, A. & DE MONTIGNY, C.D. (1988). Long-term benzodiazepine treatment reduces neuronal responsiveness to cholecystokinin: an electrophysiological study in the rat. *Eur. J. Pharmacol.*, **151**, 135– 138.

BRADWEJN, J. & DE MONTIGNY, C.D. (1984). Benzodiazepines antagonize cholecystokinin-induced activation of rat hippocampal neurones. *Nature*, **312**, 363–364.

DE MONTIGNY, C. (1989). Cholecystokinin tetrapeptide induces panick-like attacks in healthy volunteers. *Arch. Gen. Psychiatry*, **46**, 511–517.

DODD, J. & KELLY, J.S. (1981). The actions of cholecystokinin and related peptides on pyramidal neurones of the mammalian hippocampus. *Brain Res.*, **205**, 337–350.

DOROW, R., HOROWSKI, R., PASCHELKE, G., AMIN, M. & BRAESTRUP, C. (1983). Severe anxiety induced by FG7142, a β-carboline ligand for the benzodiazepine receptor. *Lancet*, **ii**, 98–99.

HARRO, J., LANG, A. & VASAR, E. (1990). Long-term diazepam treatment produces changes in cholecystokinin receptor binding in rat brain. *Eur. J. Pharmacol.*, **180**, 77–83.

HARRO, J., VASAR, E. & BRADWEJN, J. (1993). CCK in animal and human research on anxiety. *Trends Pharmacol. Sci.*, **14**, 244–249.

HUGHES, J., BODEN, P., COSTALL, B., DOMENEY, A., KELLY, E., HORWELL, D.C., HUNTER, J.C., PINNOCK, R.D. & WOODRUFF, G.N. (1990). Development of a class of cholecystokinin type B receptor antagonists having potent anxiolytic activity. *Proc. Natl. Acad. Sci. U.S.A.*, **87**, 6728–6732.

KUBOTA, K., SUGAYA, K., MATSUDA, M., MATSUOKA, Y. & TERAWAKI, Y. (1985a). Reversal of antinociceptive effect of cholecystokinin by benzodiazepines and a benzodiazepine antagonist flumazenil. *Jpn. J. Pharmacol.*, **37**, 101–105.

KUBOTA, K., SUGAYA, K., SUNAGANE, N., MATSUDA, I. & URUNO, T. (1985b). Cholecystokinin antagonism by benzodiazepines in the contractile response of the isolated guinea-pig gall bladder. *Eur. J. Pharmacol.*, **110**, 225–232.

LITTLE, H.J. (1991). The benzodiazepines: anxiolytic and withdrawal effects. *Neuropeptides*, **19**, 11–14.

PINNOCK, R.D., BODEN, P.R., RICHARDSON, R.S. & WOODRUFF, G.N. (1992). CCK receptors in rat brain *in vitro*: sensitivity to CCK_A and CCK_B receptor agonists and antagonists. *Mol. Neuropharmacol.*, **4**, 211–219.

RATTRAY, M., ANDREWS, N., WU, P.-Y., SINGHVI, S. & FILE, S.E. (1993). Diazepam treatment modulates mRNA for GAD and CCK in several rat brain regions. *Br. J. Pharmacol.*, **108**, 292P.

SINGH, L., FIELD, M.J., HUGHES, J., MENZIES, R., OLES, R.J., VASS, C.A. & WOODRUFF, G.N. (1991). The behavioural properties of CI-988, a selective cholecystokinin$_B$ receptor antagonist. *Br. J. Pharmacol.*, **104**, 239–245.

(Received October 22, 1993
Revised January 20, 1994
Accepted February 7, 1994)

Br. J. Pharmacol. (1994), **112**, 435–442

AT_1 receptor characteristics of angiotensin analogue binding in human synovium

[1]*†David A. Walsh, *#Takahiro Suzuki, *Gregory A. Knock, †David R. Blake, *Julia M. Polak & *John Wharton

*Department of Histochemistry, Royal Postgraduate Medical School, Hammersmith Hospital, Du Cane, Road, London; †Inflammation Group, Arthritis and Rheumatism Council Building, The London Hospital Medical College, Whitechapel, London and #Government Industrial Research Institute, Nagoya, Japan

1 Angiotensin II (AII) reduces blood flow, modulates vascular remodelling and is a growth factor. Human inflammatory arthritides are characterized by synovial hypoperfusion, hypoxia and proliferation. We aimed to localize and characterize receptors for AII in human synovium.

2 We used quantitative *in vitro* receptor autoradiography with [^{125}I]-(Sar^1, Ile^8)AII and [^{125}I]-AII on human synovium from patients with chondromalacia patellae, osteoarthritis and rheumatoid arthritis.

3 [^{125}I]-(Sar^1, Ile^8)AII and [^{125}I]-AII bound to similar sites on synovial blood vessels, lining cells and stroma. Binding to microvessels (<100 μm diameter) was more dense than to arteriolar media, and vascular binding was more dense than that to lining cells and stroma.

4 Microvessels and arterioles which displayed angiotensin converting enzyme-like immunoreactivity also displayed specific binding of [^{125}I]-(Sar^1, Ile^8)AII.

5 Specific binding of [^{125}I]-(Sar^1, Ile^8)AII to each structure was completely inhibited by 10 μM dithiothreitol and was inhibited by unlabelled ligands with the rank order of potency (Sar^1, Ile^8)AII > AII > losartan = SKF108566 ≫ PD123319 indicating an AT_1 subclass of angiotensin receptor.

6 GTPγS (1 μM) abolished specific binding of [^{125}I]-AII and abolished the high affinity component of the binding inhibition curve for AII against [^{125}I]-(Sar^1, Ile^8)AII, indicating G protein coupling.

7 The distribution of [^{125}I]-(Sar^1, Ile^8)AII binding sites was similar in all disease groups and no significant differences in binding densities, affinities or specificities were observed between disease groups.

8 Locally generated AII may act on synovial AT_1 receptors to modulate synovial perfusion and growth. Specific AT_1 receptor antagonists should help elucidate the role of angiotensins in human arthritis.

Keywords: Angiotensin-II; receptors; synovium; rheumatoid arthritis; osteoarthritis; chondromalacia patellae; angiotensin converting enzyme; autoradiography

Introduction

Angiotensin II (AII) is an octopeptide produced by enzymatic cleavage of angiotensin I by angiotensin converting enzyme (ACE, EC 3.4.15.1). In peripheral tissues AII is a potent vasoconstrictor and has also been implicated in vascular intimal hyperplasia and stenosis following endothelial damage (Laport & Escher, 1992; Azuma *et al.*, 1992). In addition, AII stimulates angiogenesis in some animal models (Fernandez *et al.*, 1985; Le Noble *et al.*, 1991), induces expression of growth factors by vascular smooth muscle (Naftilan *et al.*, 1989) and may itself regulate proliferation of some cell types (Araki *et al.*, 1990).

Human inflammatory arthritides such as rheumatoid arthritis are characterized by chronic synovial hypoxia, indicative of synovial hypoperfusion (Levick, 1990; Stevens *et al.*, 1991), and by synovial proliferation. We have previously demonstrated the localization of ACE in normal and inflamed human joints (Walsh *et al.*, 1993) and it is likely that AII is generated in human synovium. Locally generated AII may therefore contribute to the pathogenesis of human inflammatory arthritis.

AII acts via specific cell surface receptors, of which two subtypes have been defined pharmacologically. The human AT_1 subtype has been cloned (Furuta *et al.*, 1992; Takayanagi *et al.*, 1992; Bergsma *et al.*, 1992), and, recently, a distinct gene has been identified, encoding the rat AT_2 receptor (Kambayashi *et al.*, 1993; Mukoyama *et al.*, 1993). Both are members of the seven-transmembrane-domain superfamily of receptors. AT_1 receptors can be distinguished from the AT_2 subtype by their sensitivity to specific AT_1 antagonists such as losartan (DuP753, Ex 89) (Whitebread *et al.*, 1989) and SKF 108566 (Weinstock *et al.*, 1991), sensitivity to reducing agents such as dithiothreitol (DTT) (Whitebread *et al.*, 1989) and to guanine nucleotides (Bottari *et al.*, 1991). By contrast, AT_2 receptors are sensitive to specific AT_2 receptor antagonists such as PD123319 (Dudley *et al.*, 1990; 1991), are not inhibited by DTT and agonist binding is not sensitive to guanine nucleotides.

We have used quantitative *in vitro* receptor autoradiography to localize and characterize receptors for angiotensin in human synovium in order to assess potential sites of action of locally generated AII and to assess whether specific angiotensin receptor antagonists can interact with angiotensin receptors in human synovium.

Methods

Human tissues

Human knee synovium was collected at surgery from patients undergoing total knee replacement for osteoarthritis ($n = 6$, mean age 70, range 59 to 78, 2 male) or rheumatoid arthritis ($n = 8$, mean age 62, range 39 to 70, 4 male). Samples were also obtained at surgery for carbon fibre resurfacing of articular cartilage in patients with chondromalacia patellae

[1] Author for correspondence at: Department of Histochemistry, Royal Postgraduate Medical School, Hammersmith Hospital, Du Cane Road, London W12 0NN.

($n = 7$, mean age 44, range 22 to 60, 5 male). Tissue samples were immediately embedded in Tissue-Tek (Miles Inc., Elkhart, Indiana, U.S.A.) and frozen to cork mounts in melting isopentane without prior fixation. Specimens were stored at −40°C until use: 10 μm thick sections were cut in a cryostat and thaw mounted onto Vectabond (Vector Laboratories, Peterborough, U.K.) treated slides, air dried and used immediately, or stored at −20°C with silica gel for up to 5 days until use.

Ligand binding

Sections of human synovium were preincubated for 10 min in 10 mM phosphate buffered saline, pH 7.4, containing 5 mM $MgCl_2$, 5 mM ethylenediamine tetraacetic acid (EDTA) and 0.004% bacitracin (buffer A). Excess buffer was removed and sections were incubated for 90 min with ligand in buffer B (buffer A plus 1% bovine serum albumin). Ligand comprised 0.25 nM [^{125}I]-(Sar^1, Ile^8)AII or 0.25 nM [^{125}I]-AII alone (total binding), or together with an excess (1 μM) of unlabelled (Sar^1, Ile^8)AII or AII respectively (non-specific binding). In experiments using [^{125}I]-AII as ligand and those investigating the effect of guanosine 5'-O-(3-thiotriphosphate) (GTPγS) on inhibition of [^{125}I]-(Sar^1, Ile^8)AII binding by AII, EDTA was omitted from both buffer A and B. Following incubations, sections were washed twice for 5 min at 4°C in buffer A and rinsed in distilled water before being rapidly dried under a stream of cold air. Except where stated, incubations were performed at 22°C.

Quantification

Labelled sections were apposed to radiosensitive film (Hyperfilm-^{3}H, Amersham, U.K.) and exposed at 4°C for 4 days ([^{125}I]-(Sar^1, Ile^8)AII) or 17 days ([^{125}I]-AII). Films were developed in Kodak D19 for 3 min at 15°C. Autoradiographic images were analysed by an IBAS 386 image processing system. Synovial structures were identified, where necessary, by comparison of films with tissue sections counterstained with haematoxylin and eosin. Tissue structures (blood vessels, lining cells and regions of subintimal stroma displaying specific binding) were each delineated interactively. Binding was quantified on the 20 blood vessels in each section with the most dense specific binding. Binding density was derived from grey values by comparison with ^{125}Iodine standards (Amersham, Bucks) co-exposed with each film, and corrected for the activity date of the ligand.

Microautoradiography

Tissue sections freshly labelled with [^{125}I]-(Sar^1, Ile^8)AII were air dried then fixed in dry paraformaldehyde vapour for 30 min at 90°C with silica gel dessicant. Sections were then dipped in radiosensitive emulsion (Ilford K5) at 42°C and rapidly dried under a stream of cold air. Following exposure for 3 weeks at 4°C, emulsion-dipped slides were developed as for film autoradiograms, then counterstained with haematoxylin and eosin, dehydrated and mounted in dibutylpthalate polystyrene xylene (DPX, Raymond Lamb, London). Preliminary experiments revealed that 'wet' fixation techniques in Bouin's fixative for 60 min did not prevent dissociation of specific binding during dipping. 'Dry' fixation in paraformaldehyde vapour for 30 min was found to be optimal for preventing dissociation of ligand, while avoiding the near total loss of haematoxylin and eosin reactivity which resulted from longer fixation.

Characterization of binding sites

Specific binding was defined as total minus non-specific binding. Characterization of specific binding was performed on samples of synovium from patients with osteoarthritis. The association rate of 0.25 nM [^{125}I]-(Sar^1, Ile^8)AII to specific binding sites was assessed with incubation times from 5 to 300 min. Dissociation was measured as the decline in specific binding following incubation with 0.25 nM [^{125}I]-(Sar^1, Ile^8)AII for 90 min, then transfer of sections to an excess (400 ml) of buffer A without added ligand for 5 to 120 min.

Saturability of binding and K_d and B_{max} values were measured by 'hot' saturation studies with 25 to 700 pM [^{125}I]-(Sar^1, Ile^8)AII.

Specificity of binding was measured by binding inhibition studies with 0.25 nM [^{125}I]-(Sar^1, Ile^8)AII together with unlabelled ligands at concentrations between 100 pM and 10 μM. Inhibiting ligands included the agonist AII, the dual AT_1/AT_2 antagonist (Sar^1, Ile^8)AII, the selective AT_1 antagonists, losartan and SKF 108566 and the selective AT_2 antagonist, PD123319. Sensitivity of specific binding to dithiothreitol (DTT) was assessed by incubation with 0.25 nM [^{125}I]-(Sar^1, Ile^8)AII together with 10 mM DTT. For comparison of receptor subtypes in synovia from patients with rheumatoid arthritis with those from patients with osteoarthritis, sections were incubated with 0.25 nM [^{125}I]-(Sar^1, Ile^8)AII alone (total binding), together with 1 μM unlabelled (Sar^1, Ile^8)AII (nonspecific binding), with 10 μM PD123319 (AT_1 receptors remain unblocked) or with 10 μM losartan (AT_2 receptors remain unblocked). Guanine nucleotide sensitivity of AII binding was assessed by coincubating sections with 0.25 nM [^{125}I]-AII and 1 μM guanosine 5'-O-(3-thiotriphosphate (GTPγS) and by measuring the inhibition of binding of 0.25 nM [^{125}I]-(Sar^1, Ile^8)AII by unlabelled AII in the presence and absence of 1 μM GTPγS.

Statistical analysis

Kinetic and equilibrium constants were derived from specific binding values by iterative non-linear regression assuming single site models using GraphPAD Inplot4 (San Diego). Equilibrium binding densities (B_{eq}) were obtained with 0.25 nM [^{125}I]-(Sar^1, Ile^8)AII incubated for 90 min at 22°C. Values for binding inhibition constants (K_i) and Hill coefficients (n_H) were derived by fitting sigmoid curves. Data from inhibition of [^{125}I]-(Sar^1, Ile^8)AII binding by AII in the presence and absence of GTPγS were fitted to one and two site models and the goodness of fit compared by F tests using GraphPAD Inplot4. Descriptive data are expressed as means (95% confidence interval) and between group comparisons were made by one way or repeated measured ANOVA and Student's t test with Bonferroni correction on geometric data.

Immunohistochemistry

To investigate further the cellular localization of specific [^{125}I]-(Sar^1, Ile^8)AII binding, consecutive sections to those used for emulsion-dipped preparations were immunostained using primary antibodies to platelet-endothelial cell adhesion molecule PECAM, CD31 (clone JC/70A, Parums *et al.*, 1990), smooth muscle α-actin (clone IA4, Skalli *et al.*, 1986), to the macrophage marker CD14 (clone UCHM 1, Hogg *et al.*, 1984), to the fibroblast marker prolyl-4-hydroxylase (clone 5B5, Höyhtyä *et al.*, 1984), and to the T cell antigen, CD2 (clone OKT11, Verbi *et al.*, 1982). Correspondence of binding site localization with angiotensin converting enzyme was assessed with the affinity purified polyclonal antibody, RH179 (Walsh *et al.*, 1993). Cryosat sections (10 μm thick) were stained by the avidin-biotin complex (ABC) method of Hsu *et al.* (1981). In brief, sections were fixed in acetone for 5 min at 4°C, incubated with primary antibody for 2 h at room temperature, then with biotinylated horse antimouse IgG or biotinylated goat antirabbit IgG for 1 h, avidin-biotin complex for 30 min and finally developed in diaminobenzidine, dehydrated and mounted in DPX.

Materials

[^{125}I]-(Sar^1, Ile^8)AII and [^{125}I]-AII (specific activities 2200 Ci mmol^{-1}) were obtained from DuPont-New England

Nuclear Research Products (UK) Ltd., Stevenage, Herts. ^{125}Iodine standards, and Hyperfilm-^{3}H were obtained from Amersham International plc, Amersham, Bucks. Losartan (DuP 753, 2-n-butyl-4-chloro-5-(hydroxymethyl)-1-[2'(1H-tetrazol-5-yl)biphenyl-4-yl)-methyl]imidazole) was kindly provided by DuPont Merck, Wilmington, De, U.S.A. SKF 108566 ((E-α-2-[2-butyl-1-[(caboxyphenyl)methyl)1H-imidazol-5-yl)methylene]-2-thiophenepropanoic acid) was from Smith-Kline Beecham, King of Prussia, PA, U.S.A. and PD123319 (1(4-amino-3-methylphenyl)methyl-5-diphenylacetyl-4,5,6,7-tetrahydro-1H-imidazo[4,5-c]pyridine -6-carboxylic acid-2HCl) from Parke-Davis, Ann Arbor, MI, U.S.A. Other unlabelled peptides, guanine nucleotides, DTT, bacitracin and enzyme free bovine serum albumin were obtained from Sigma Chemical Co., Poole, Dorset. Primary antibodies were obtained from DAKO Ltd., High Wycombe, Bucks (JC/70A, 5B5), Ortho Diagnostics Systems Ltd., High Wycombe, Bucks (OKT11), and Sigma Chemical Co., Poole, Dorset (IA4, UCHM 1). Antibody RH179 to human angiotensin converting enzyme was a kind gift of Dr A.J. Kenny, Medical Research Council Membrane Peptidase Group, Leeds. Biotinylated horse anti-mouse IgG and biotinylated goat anti-rabbit affinity purified IgG and avidin-biotin complex were from Vector Laboratories, Peterborough.

Results

Localization

[^{125}I]-(Sar^{1}, Ile^{8})AII bound specifically and with high affinity to microvessels, lining cells and stromal cells in all cases

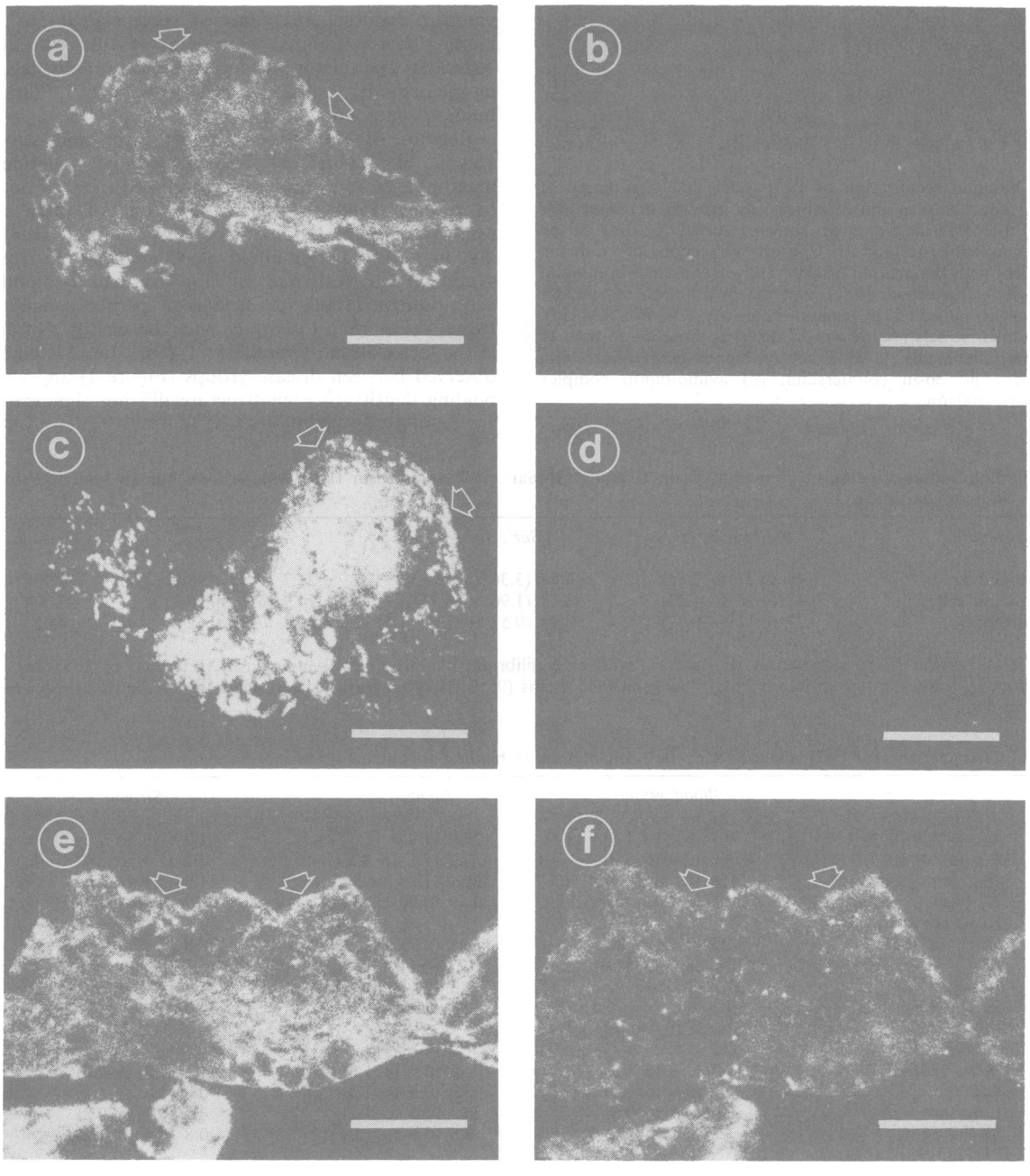

Figure 1 (a) Total binding of [^{125}I]-(Sar^{1}, Ile^{8})angiotensin II ([^{125}I]-(Sar^{1}, Ile^{8})AII) to synovium from a patient with chondromalacia patellae demonstrating punctate binding to blood vessels and more diffuse binding to synovial stroma and to the lining cell layer (arrows). (b) Nonspecific binding of [^{125}I]-(Sar^{1}, Ile^{8})AII in the presence of 1 μM unlabelled (Sar^{1}, Ile^{8})AII to a section consecutive to that shown in (a). (c,e) Total binding of [^{125}I]-(Sar^{1}, Ile^{8})AII to synovium from patients with rheumatoid arthritis showing a similar distribution to that in (a). (d) Nonspecific binding to a section consecutive to that shown in (c). (f) Total binding of ^{125}I-labelled angiotensin II to a consecutive section to that shown in (e) showing an identical distribution but lower density. Reversal prints of film autoradiograms. Arrows: synovial surface. Bars: 2 mm.

(Figures 1 and 2). Specific binding of [^{125}I]-AII had an identical distribution to that of [^{125}I]-(Sar^1, Ile^8)AII, as demonstrated in consecutive sections, although specific [^{125}I]-AII binding to each structure was only 15 to 22% as dense as the corresponding binding of [^{125}I]-(Sar^1, Ile^8)AII (Figure 1, Table 1). In synovium from all disease groups the densest binding of [^{125}I]-(Sar^1, Ile^8)AII was observed to synovial microvessels, with lining cells displaying less dense specific binding and binding to stromal cells being even less dense (Table 2).

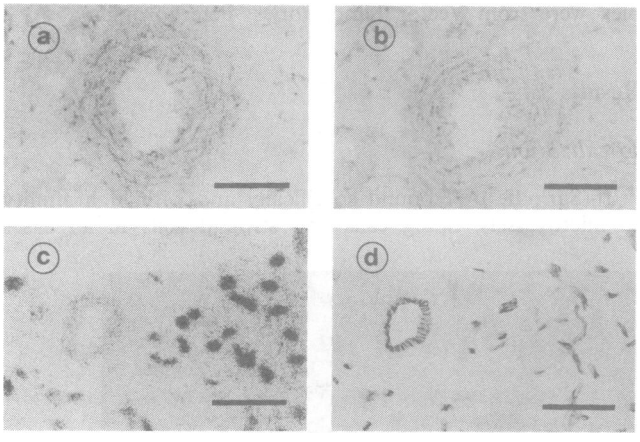

Figure 2 Vascular localization of [^{125}I]-(Sar^1, Ile^8) angiotensin II binding. (a) Total binding and (b) nonspecific binding in consecutive sections of osteoarthritic synovium showing specific binding to the media of an arteriole. (c) and (d) Consecutive sections of synovium from a patient with rheumatoid arthritis showing vascular binding of [^{125}I]-(Sar^1, Ile^8) angiotensin II (c), and the distribution of vascular endothelium as indicated by immunoreactivity for PECAM (d). Binding to microvessels (< 100 μm diameter) is more dense than to adjacent arteriolar media. (a–c) Emulsion-dipped preparations with haematoxylin and eosin counterstain; (d) avidin-biotin complex method. Bars: 100 μm.

In emulsion-dipped preparations, vascular binding of [^{125}I]-(Sar^1, Ile^8)AII was seen to comprise binding to arteriolar media (external diameter > 100 μm) (Figure 2a,b) and to microvessels (external diameter < 100 μm) identified by immunoreactivity in consecutive sections for the endothelial marker PECAM (platelet-endothelial cell adhesion molecule, Figure 2b,c) and the vascular smooth muscle marker α-smooth muscle actin. Binding to microvessels appeared more dense than that to arteriolar media (Figure 2c,d). Even the smallest microvessels identified by PECAM-immunoreactive endothelia also displayed α-smooth muscle actin immunoreactivity, and it was not possible to resolve whether microvascular endothelium possessed specific [^{125}I]-(Sar^1, Ile^8)AII binding sites in addition to those on vascular smooth muscle. Arterioles and microvessels with intense endothelial ACE-like immunoreactivity also displayed specific [^{125}I]-(Sar^1, Ile^8)AII binding (data not shown).

Regions of the synovial lining layer and stroma with specific [^{125}I]-(Sar^1, Ile^8)AII binding contained both macrophage- and fibroblast-derived cells. It was not possible to resolve whether both or only one of these cell types displayed specific binding. Specific [^{125}I]-(Sar^1, Ile^8)AII binding in follicular lymphoid accumulations in rheumatoid synovium was restricted to PECAM- and α-smooth muscle actin-positive blood vessels and to perifollicular connective tissue, rather than to lymphocytes themselves. No differences in the localization of specific [^{125}I]-(Sar^1, Ile^8)AII binding were observed between disease groups (Figure 1) and equilibrium binding density to each structure did not significantly differ

Table 1 Equilibrium binding of [^{125}I]-angiotensin II and [^{125}I]-(Sar^1, Ile^8) angiotensin II to structures in human synovium from 5 patients with osteoarthritis

Structure	*Angiotensin II*	*(Sar^1, Ile^8)AII*	*Ratio* (%)	P *value*
Blood vessel	1.48 (0.77 to 2.86)	6.83 (3.30 to 14.13)	21.7 (9.8 to 48.2)	0.006
Lining cell	0.47 (0.18 to 1.23)	3.18 (1.96 to 6.23)	14.9 (6.3 to 35.3)	0.004
Stroma	0.21 (0.12 to 0.37)	0.98 (0.57 to 1.68)	21.8 (7.6 to 62.3)	0.02

(Sar^1, Ile^8)AII = (Sar^1, Ile^8) angiotensin II. Ratio = ratio of equilibrium binding of [^{125}I]-angiotensin II to that of [^{125}I]-(Sar^1, Ile^8) angiotensin II. Values are given in amol mm^{-2} as geometric means (95% CI). Comparisons were made by Student's paired *t* test on geometric data.

Table 2 Characteristics of [^{125}I]-labelled (Sar^1, Ile^8) angiotensin II binding to human osteoarthritic synovium

	Blood vessels	*Lining cells*	*Stroma*
k_{obs} ($s^{-1} \times 10^{-4}$)	0.7 (0.2 to 1.8)	2.0 (1.2 to 3.3)	1.2 (0.6 to 2.5)
k_{-1} ($s^{-1} \times 10^{-4}$)	1.6 (0.9 to 3.0)	2.0 (1.1 to 3.6)	2.2 (1.3 to 3.7)
B_{max} (amol mm^{-2})	[a]154 (69 to 344)	[b]26.9 (12.7 to 57.2)	11.8 (5.1 to 27.1)
K_d (nM)	0.55 (0.34 to 0.89)	0.40 (0.20 to 0.81)	0.32 (0.20 to 0.51)
K_i *values* (nM)			
(Sar^1, Ile^8)AII	[c]1.55 (0.69 to 2.95)	[c]1.38 (0.93 to 2.00)	[c]3.39 (2.19 to 5.25)
AII	[d]12.6 (6.6 to 24.6)	[d]8.32 (4.17 to 16.2)	[d]15.1 (7.41 to 31.6)
Losartan	[e]37.2 (15.9 to 87.1)	[e]102.3 (33.1 to 316.2)	[e]75.9 (32.4 to 177.8)
SKF 108566	49.0 (29.5 to 79.4)	60.3 (25.1 to 144.5)	81.3 (38.0 to 177.8)
PD123319	> 10,000	> 10,000	> 10,000
n_H *values*			
(Sar^1, Ile^8)AII	1.0 (0.8 to 1.3)	1.2 (0.9 to 1.6)	1.6 (1.2 to 2.0)
AII	1.0 (0.6 to 1.5)	0.9 (0.5 to 1.2)	0.8 (0.5 to 1.2)
Losartan	0.6 (0.4 to 0.8)	0.9 (0.5 to 1.2)	0.6 (0.3 to 0.8)
SKF 108566	1.2 (0.9 to 1.4)	0.8 (0.6 to 1.0)	0.8 (0.4 to 1.2)
PD123319	–	–	–

[a]Maximal binding capacity (B_{max}) significantly greater to blood vessels than lining cells and than stroma (each $P < 0.001$) and [b]significantly greater to lining cells than to stroma ($P < 0.01$, paired *t* tests). No significant differences observed between structures for other parameters. For each structure, [c](Sar^1, Ile^8)AII was significantly more potent than AII (each $P < 0.05$); [d]AII was significantly more potent than losartan in lining cells ($P < 0.05$), and more potent than SKF 108566 in all structures (each $P < 0.05$). [e]No significant differences were observed in K_i values between losartan and SKF 108566.
Values are expressed as geometric or arithmetic (n_H) means (95% confidence interval) and *P* values are corrected for multiple comparisons.

between synovium from patients with chondromalacia patellae, rheumatoid arthritis or osteoarthritis (data not shown).

Characterization

Specific binding of [^{125}I]-(Sar^1, Ile^8)AII to each synovial structure was time-dependent and reversible (Table 2). Binding was saturable, with maximum binding densities greatest for synovial blood vessels and least for synovial stroma (Table 2, Figure 3). Binding to each structure was of high affinity, and no significant differences were found between structures in association and dissociation rates, nor in K_d values (Table 2).

Specific binding of [^{125}I]-(Sar^1, Ile^8)AII was inhibited by related compounds with a rank order of potencies (Sar^1, Ile^8)AII > AII > losartan = SKF 108566 ➤ PD 123319 (Table 2, Figure 4). No significant differences in K_i values were observed between structures. In synovium from patients with osteoarthritis and those with rheumatoid arthritis, specific [^{125}I]-(Sar^1, Ile^8)AII binding to each structure was completely inhibited by the AT_1 antagonist, losartan (10 μM), but was not significantly inhibited by the specific AT_2 antagonist, PD123319 (10 μM) (Table 3). Specific binding to each structure was completely inhibited by 10 mM DTT (Table 4).

Binding of the agonist [^{125}I]-AII to each structure was inhibited by the non-hydrolysable GTP analogue, GTPγS (1 μM), to levels not significantly different from nonspecific binding (data not shown). GTPγS (1 μM) did not inhibit specific binding of the antagonist [^{125}I]-(Sar^1, Ile^8)AII. For each structure, inhibition of [^{125}I]-(Sar^1, Ile^8)AII binding by the agonist AII in the absence of EDTA and GTPγS was better described by a 2 site model than by a single site model (Table 5) with 15 to 26% of the sites being of high affinity (IC_{50} values <0.4 nM) and the remaining 74 to 85% of lower affinity (IC_{50} values ≥ 7.0 nM). In the presence of 1 μM GTPγS, inhibition curves were described by a one site model corresponding to the lower affinity state (Table 5) indicating abolition of the high affinity state by GTPγS.

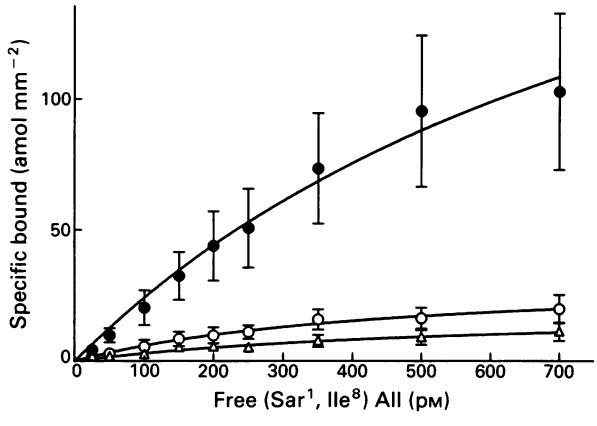

Figure 3 Specific equilibrium binding of increasing concentrations of [^{125}I]-(Sar^1, Ile^8) angiotensin II to synovium from patients with osteoarthritis. Maximal binding was greater to blood vessels (●) than to lining cells (○) ($P<0.001$), and greater to lining cells than to stroma (△) ($P<0.01$). Data are means (± s.e.mean) of 6 cases.

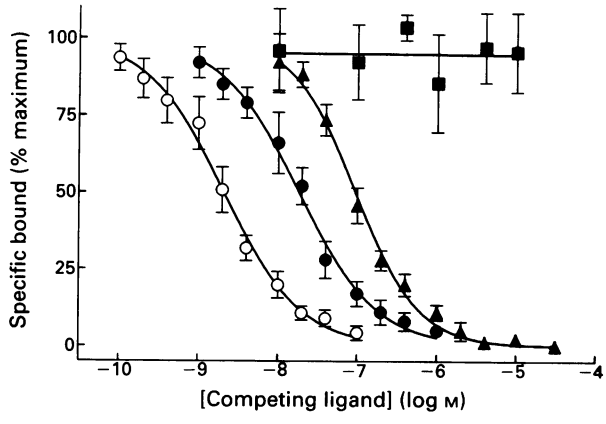

Figure 4 Inhibition of specific binding of [^{125}I]-(Sar^1, Ile^8) angiotensin II to blood vessels in synovium from patients with osteoarthritis by unlabelled (Sar^1, Ile^8) angiotensin II (○), angiotensin II (●), the AT_1 specific antagonist, SKF 108566 (▲) and the AT_2 specific antagonist, PD123319 (■). Data are means (± s.e.mean) of 6 cases.

Table 3 Effect of specific AT_1 antagonist, losartan, and AT_2 antagonist, PD123319, on binding of [^{125}I]-(Sar^1, Ile^8) angiotensin II to human synovium

		Total	*Nonspecific*	*Losartan*	*PD123319*
Blood vessels	OA	7.9 (6.0 to 10)	2.4 (2.2 to 2.6)	[a]2.9 (2.4 to 3.5)	[b]7.1 (5.1 to 9.9)
	RA	14 (5.6 to 36)	2.6 (2.3 to 3.1)	[a]2.8 (2.3 to 3.3)	[b]12 (5.1 to 29)
Lining cells	OA	3.6 (2.8 to 4.8)	1.6 (1.4 to 1.8)	[a]1.7 (1.5 to 1.8)	[b]3.8 (2.9 to 4.4)
	RA	5.7 (3.2 to 10)	1.7 (1.6 to 1.9)	[a]1.8 (1.7 to 2.0)	[b]5.5 (3.5 to 8.7)
Stroma	OA	2.4 (1.8 to 3.2)	1.5 (1.4 to 1.6)	[a]1.5 (1.4 to 1.6)	[b]2.2 (1.8 to 2.6)
	RA	3.0 (2.3 to 4.0)	1.6 (1.5 to 1.7)	[a]1.5 (1.5 to 1.6)	[b]2.9 (2.1 to 4.1)

[a]Losartan (10 μM) significantly inhibits binding to each structure in synovium from patients with osteoarthritis (OA) or rheumatoid arthritis (RA) (each $P<0.01$), reducing binding to values not significantly different from nonspecific binding observed in the presence of 1 μM unlabelled (Sar^1, Ile^8)angiotensin II (each $P>0.05$). [b]PD123319 did not significantly inhibit binding to any structure in either OA or RA synovium (each $P>0.05$). Values are given in amol mm^{-2} as geometric means (95% CI).

Table 4 Inhibition by dithiothreitol (DTT) of [^{125}I]-(Sar^1, Ile^8) angiotensin II binding to structures in synovium from patients with osteoarthritis

	Blood vessels	*Lining cells*	*Stroma*
Total	10.2 (6.6 to 15.7)	5.1 (3.3 to 7.9)	2.6 (2.1 to 3.3)
Nonspecific	3.2 (2.6 to 3.9)	2.1 (1.8 to 2.3)	1.7 (1.5 to 1.9)
+10 mM DTT	[a]3.2 (2.9 to 3.5)	[a]2.0 (1.8 to 2.3)	[a]1.6 (1.5 to 1.7)

[a]Binding of [^{125}I]-(Sar^1, Ile^8)AII in the presence of DTT is significantly lower than in the absence of DTT (each $P<0.02$), and not significantly different from nonspecific binding observed in the presence of 1 μM unlabelled (Sar^1, Ile^8)AII. Values are given in amol mm^{-2} as geometric means (95% CI) and P values derived from paired t tests are corrected for multiple comparisons.

Table 5 Effect of 1 μM guanosine 5'-O-(3-thiotriphosphate) (GTPγS) on inhibition of [^{125}I]-(Sar^1, Ile^8) angiotensin II binding to osteoarthritic human synovium by unlabelled angiotensin II

		IC_{50} (nM)			1 vs 2 site model		
Structure		*Site 1*	*Site 2*	*% Site 1*	*F*	*d.f.*	P
Blood vessels	−GTPγS	7.0 (5.2 to 9.4)	0.06 (0.01 to 0.63)	83 (76 to 91)	13.9	5	0.009
	+GTPγS	11.5 (7.9 to 16.5)	–	–	5.7	5	0.052
Lining cells	−GTPγS	9.1 (6.3 to 13.3)	0.37 (0.06 to 3.5)	85 (70 to 99)	8.9	5	0.022
	+GTPγS	16 (12 to 21)	–	–	1.5	5	0.309
Stroma	−GTPγS	8.6 (5.0 to 15.0)	0.06 (0.01 to 0.72)	74 (62 to 85)	11.6	5	0.013
	+GTPγS	20 (12 to 35)	–	–	1.2	5	0.373

Best fitting curves representing mean data from synovia from 6 cases of osteoarthritis were generated according to a 2 site model when this gave a significantly better fit than a single site model, and otherwise according to a single site model. Estimates (95% CI) of IC_{50} values and percentage of sites in the lower affinity state (site 1) are given for the best fitting curves. In the absence of GTPγS (−GTPγS) the data for each structure best fit to 2 site models. In the presence of 1 μM GTPγS, single site models describe the data, with estimated IC_{50} values corresponding to the lower affinity site observed in the absence of GTPγS.

Discussion

We have demonstrated specific binding sites for [^{125}I]-(Sar^1, Ile^8)AII and [^{125}I]-AII in human synovium. The identical distributions of binding and the inhibitory effect of GTPγS on agonist binding with either ligand, and inhibition of [^{125}I]-(Sar^1, Ile^8)AII binding by unlabelled AII suggest that both ligands label the same population of angiotensin receptors. The rank order of potencies for inhibition of specific binding, (Sar^1, Ile^8)AII > AII > losartan = SKF 108566 ≫ PD 123319, inhibition of binding by DTT and of agonist binding by GTPγS are characteristic of the AT_1 subclass of angiotensin receptor (Whitebread *et al.*, 1989; Dudley *et al.*, 1990; 1991; Weinstock *et al.*, 1991; Bottari *et al.*, 1991). Binding studies performed in the presence of losartan or PD123319 provided no evidence for the presence of AT_2 receptors in synovium from any disease group. Our data indicate that distinct synovial structures bear different densities of AT_1 receptors rather than different receptor subtypes.

Specific binding of [^{125}I]-(Sar^1, Ile^8)AII and ACE-like immunoreactivity were observed in media and endothelium of synovial arterioles, respectively, suggesting that these vessels may be subject to the actions of locally generated AII. AT_1-like binding sites have previously been demonstrated in media of large and medium sized arteries in man (Urata *et al.*, 1989) and on cultured vascular smooth muscle cells (Whitebread *et al.*, 1989) and are believed to mediate vasoconstriction (Chiu *et al.*, 1990) and smooth muscle hypertrophy (Millet *et al.*, 1992), both of which may reduce tissue perfusion. Synovial hypoperfusion has been implicated in the pathogenesis of human arthritis (Levick, 1990), and the potential of AT_1 antagonists to enhance tissue perfusion (Azuma *et al.*, 1992) deserves further study.

The most dense binding of [^{125}I]-(Sar^1, Ile^8)AII in human synovium was observed to synovial microvessels (< 100 μm diameter). These microvessels also displayed endothelial ACE-like immunoreactivity. It was not possible to determine whether [^{125}I]-(Sar^1, Ile^8)AII bound to microvascular endothelium in addition to binding to smooth muscle cells, but specific binding of [^{125}I]-AII has been previously demonstrated to each of these cell types in culture (Whitebread *et al.*, 1989; Patel *et al.*, 1989). Binding of angiotensins has previously been demonstrated to microvessels in brain (Speth & Harik, 1985), retina (Ferrari-Dileo *et al.*, 1991) and kidney (Sechi *et al.*, 1992). In addition to effects on vascular tone and smooth muscle growth, microvascular angiotensin receptors may regulate endothelial permeability (Morel *et al.*, 1990) and neovascularisation (Fernandez *et al.*, 1985; Le Noble *et al.*, 1991).

We have also demonstrated specific binding sites for [^{125}I]-(Sar^1, Ile^8)AII and [^{125}I]-AII to lining cells and stroma in human synovium, corresponding to the distribution of macrophages and fibroblasts. Both macrophages (Thomas & Hoffman, 1994) and fibroblasts (Millan *et al.*, 1989) have previously been shown to express angiotensin receptors in culture. *In vitro*, angiotensin inhibits macrophage migration (Weinstock & Blum, 1983) and may increase phagocytosis (Weinstock & Kassab, 1984), although the relevance of these observations to macrophage function *in vivo* remains uncertain.

Angiotensin receptor subtypes have been extensively studied in foetal rat skin fibroblasts. These cells express both AT_1 and AT_2 receptors (Tsutsumi *et al.*, 1991; Johnson & Aguilera, 1991), AT_2 receptors predominating on foetal skin fibroblasts. In the rat, however, there is a dramatic decrease in angiotensin receptors on skin fibroblasts following birth (Millan *et al.*, 1989), and in the adult rat, dermal angiotensin receptors are predominantly of the AT_1 subtype (Kimura *et al.*, 1992). Specific binding of [^{125}I]-(Sar^1, Ile^8)AII to adult human synovial stroma and lining cells was exclusively to AT_1-like sites, and was observed both in inflamed and uninflamed tissues. It appears, therefore, that chronic synovial inflammation is not associated with a switching from AT_1- to AT_2-like receptors. Angiotensins have been implicated in tissue growth (Millan *et al.*, 1989) and their possible role in synovial hypertrophy in inflammatory arthritis deserves further investigation.

Studies to date on the role of angiotensins in chronic synovial inflammation have been limited by the lack of specificity of the interventions studied. Open, uncontrolled studies of ACE inhibition in inflammatory arthritis have been inconclusive, providing some evidence that ACE inhibitor, captopril may be of therapeutic benefit (Martin *et al.*, 1984), although such beneficial effects need not necessarily be attributable to the inhibition of ACE (Bird *et al.*, 1990). Furthermore, AI is not the only substrate for ACE, which also inactivates proinflammatory peptides such as bradykinin and substance P (Kenny *et al.*, 1987), both of which may be involved in arthritis (Caspritz *et al.*, 1986; Walsh *et al.*, 1992; Miao *et al.*, 1992). Inhibition of ACE may therefore have multiple actions which may mask any beneficial effect of reducing AII generation. We have demonstrated that two specific AT_1 antagonists, losartan and SKF 108566, potently and completely inhibit binding of [^{125}I]-(Sar^1, Ile^8)AII to microvessels, lining cells and stroma in inflamed human synovium. Specific antagonists such as these will be valuable in elucidating the role of angiotensins in chronic arthritis, and may provide novel approaches to therapy.

Supported by the Arthritis and Rheumatism Council. We are grateful to Dr R.D. Smith, DuPont Merck, Wilmington, DE, U.S.A. for supplying us with losartan, to Dr J.B. Reese, SmithKline Beecham, King of Prussia, PA, U.S.A. for SKF 198566 and to Dr J.A. Keiser, Parke-Davis, Ann Arbor, MI, U.S.A. for PD123319. D.A.W. is an Arthritis and Rheumatism Council Clinical Research Fellow, and D.R.B. is an Arthritis and Rheumatism Council Professor of Rheumatology.

References

ARAKI, S.-I., KAWAHARA, Y., KRIYA, K.-I., SUNAKO, M., TSUDA, T., FUKUZAKI, H. & YOSHIMI, T. (1990). Stimulation of platelet-derived growth factor-induced DNA synthesis by angiotensin II in rabbit vascular smooth muscle cells. *Biochem. Biophys. Res. Commun.*, **168**, 350–357.

AZUMA, H., NIIMI, Y. & HAMASAKI, H. (1992). Prevention of intimal thickening after endothelial removal by a nonpeptide angiotensin II receptor antagonist, losartan. *Br. J. Pharmacol.*, **106**, 665–671.

BERGSMA, D.J., ELLIS, C., KUMAR, C., NUTHULAGANTI, P., KERSTEN, H., ELSHOURBAGY, N., GRIFFIN, E., STADEL, J.M. & ALYAR, N. (1992). Cloning and characterisation of a human angiotensin II type 1 receptor. *Biochem. Biophys. Res. Commun.*, **183**, 989–995.

BIRD, H.A., LE GALLEZ, P., DIXON, J.S., CATALANO, M.A., TRAFICANTE, A., LIAUW, L.A., SUSSMAN, H., ROTMAN, H. & WRIGHT, V. (1990). A clinical and biochemical assessment of a nonthiol ACE inhibitor (pentopril; CGS-13945) in active rheumatoid arthritis. *J. Rheumatol.*, **17**, 603–608.

BOTTARI, S.P., TAYLOR, V., KING, N.I., BOGDAL, Y., WHITEBREAD, S. & DE GASPARO, M. (1991). Angiotensin II AT_2 receptors do not interact with guanine nucleotide binding proteins. *Eur. J. Pharmacol.*, **207**, 157–163.

CASPRITZ, G., ALPERMANN, H.G. & SCHLEYERBACH, R. (1986). Influence of the new angiotensin converting enzyme inhibitor ramipril on several models of acute inflammation and the adjuvant arthritis in the rat. *Arzneimittelforschung*, **36**, 1605–1608.

CHIU, A.T., MCCALL, D.E., PRICE, W.A., WONG, P.C., CARINI, D.J., DUNCIA, J.V., WEXLER, R.R., YOO, S.E., JOHNSON, A.L. & TIMMERMANS, P.B.M.W.M. (1990). Nonpeptide angiotensin II receptor antagonists. VII. Cellular and biochemical pharmacology of DuP 753, an orally active antihypertensive agent. *J. Pharmacol. Exp. Ther.*, **252**, 711–718.

DUDLEY, D.T., HUBBELL, S.E. & SUMMERFLET, R.M. (1991). Characterization of angiotensin (AT_2) binding sites in R3&3 cells. *Mol. Pharmacol.*, **40**, 360–367.

DUDLEY, D.T., PANEL, R.L., MAJOR, T.C., LU, G.H., BRUNS, R.F., KLINKEFUS, B.A., HODGES, J.C. & WEISHAAR, R.E. (1990). Subclasses of angiotensin II binding sites and their functional significance. *Mol. Pharmacol.*, **38**, 370–377.

FERNANDEZ, L.A., TWICKLER, J. & MEAD, A. (1985). Neovascularization produced by angiotensin II. *J. Lab. Clin. Med.*, **105**, 141–145.

FERRARI-DILEO, G., DAVIS, E.B. & ANDERSON, D.R. (1991). Angiotensin II binding receptors in retinal and optic nerve head blood vessels. *Invest. Ophthalmol. Vis. Sci.*, **32**, 21–26.

FURUTA, H., GUO, D.-F. & INAGAMI, T. (1992). Molecular cloning and sequencing of the gene encoding human angiotensin II type 1 receptor. *Biochem. Biophys. Res. Commun.*, **183**, 8–13.

HOGG, N., MACDONALD, S., SLUSARENKO, M. & BEVERLY, P.C.L. (1984). Monoclonal antibodies specific for human monocytes, granulocytes and endothelium. *Immunology*, **53**, 753–767.

HÖYHTYÄ, M., MYLLYLÄ, R., SIUVA, J., KIVIRIKKO, K.I. & TRYGGVASON, K. (1984). Monoclonal antibodies to human prolyl 4-hydroxylase. *Eur. J. Biochem.*, **141**, 477–482.

HSU, S-M., RAINE, L. & FANGER, H. (1981). Use of avidin-biotin-peroxidase complex (ABC) method in immunoperoxidase techniques: a comparison between ABC and unlabelled antibody (PAP) procedures. *J. Histochem. Cytochem.*, **29**, 577–580.

JOHNSON, M.C. & AGUILERA, G. (1991). Angiotensin-II receptor subtypes and coupling to signaling systems in cultured fetal fibroblasts. *Endocrinology*, **129**, 1266–1274.

KAMBAYASHI, Y., BARDHAN, S., TAKAHASHI, K., TSUZUKI, S., INUI, H., HAMAKUBO, T. & INAGAMI, T. (1993). Molecular cloning of a novel angiotensin II receptor isoform involved in phosphotyrosine phosphatase inhibition. *J. Biol. Chem.*, **268**, 24543–24546.

KENNY, A.J., STEPHENSON, S.L. & TURNER, A.J. (1987). Cell surface peptidases. In *Mammalian Ectoenzymes*. ed. Kenny, A.J. & Turner, A.J. pp. 169–210. Amsterdam, New York, Oxford: Elsevier.

KIMURA, B., SUMNERS, C. & PHILLIPS, M.I. (1992). Changes in skin angiotensin II receptors in rats during wound healing. *Biochem. Biophys. Res. Commun.*, **187**, 1083–1090.

LAPORT, S. & ESCHER, E. (1992). Neointima formation after vascular injury is angiotensin II mediated. *Biochem. Biophys. Res. Commun.*, **187**, 1510–1516.

LE NOBLE, F.A., HEKKING, J.W., VAN STRAATEN, H.W., SLAAF, D.W. & STRUYKER-BOUDIER, H.A. (1991). Angiotensin II stimulates angiogenesis in the chorio-allantoic membrane of the chick embryo. *Eur. J. Pharmacol.*, **195**, 305–306.

LEVICK, J.R. (1990). Hypoxia and acidosis in chronic inflammatory arthritis: relation to vascular supply and dynamic effusion pressure. *J. Rheumatol.*, **17**, 579–582.

MARTIN, M.F.R., SURRALL, K.E., MCKENNA, F., DIXON, J.S., BIRD, H.A. & WRIGHT, V. (1984). Captopril: a new treatment for rheumatoid arthritis? *Lancet*, **i**, 1325–1328.

MIAO, F.J.-P., HELMS, C., BENOWITZ, N.L., BASBAUM, A.I., HELLER, P.H. & LEVINE, J.D. (1992). Chronically administered nicotine attenuates bradykinin-induced plasma extravasation and aggravates arthritis-induced joint injury in the rat. *Neuroscience*, **51**, 649–655.

MILLAN, M.A., CARVALLO, P., IZUMI, S.-I., ZEMEL, S., CATT, K.J. & AGUILERA, G. (1989). Novel sites of expression of functional angiotensin II receptors in the late gestation fetus. *Science*, **244**, 1340–1342.

MILLET, D., DESGRANGES, C., CAMPAN, M., GADEAU, A.-P. & COSTEROUSSE, O. (1992). Effects of angiotensins on cellular hypertrophy and c-*fos* expression in cultured arterial smooth muscle cells. *Eur. J. Biochem.*, **206**, 367–372.

MOREL, N.M., PETRUZZO, P.P., HECHTMAN, H.B. & SHEPRO, D. (1990). Inflammatory agonists that increase microvascular permeability in vivo stimulate cultured pulmonary microvessel endothelial cell contraction. *Inflammation*, **14**, 571–583.

MUKOYAMA, M., NAKAJIMA, M., HORIUCHI, M., SASAMURA, H., PRATT, R.E. & DZAU, V.J. (1993). Expression of cloning type 2 angiotensin II receptor reveals a unique class of seven-transmembrane receptors. *J. Biol. Chem.*, **268**, 24539–24542.

NAFTILAN, A.J., PRATT, R.E. & DZAU, V.J. (1989). Induction of platelet-derived growth factor A-chain and c-*myc* gene expressions by angiotensin II in cultured rat vascular smooth muscle cells. *J. Clin. Invest.*, **83**, 1419–1424.

PARUMS, D.V., CORDELL, J.L., MICKLEM, K., HERYET, A.R., GATTER, K.C. & MASON, D.Y. (1990). JC70: a new monoclonal antibody that detects vascular endothelium associated antigen on routinely processed tissue sections. *J. Clin. Pathol.*, **43**, 752–757.

PATEL, J.M., YARID, F.R., BLOCK, E.R. & RAIZADA, M.K. (1989). Angiotensin receptors in pulmonary arterial and aortic endothelial cells. *Am. J. Physiol.*, **256**, C987–C993.

SECHI, L.S., GRADY, E.F., GRIFFEN, C.A., KALINYAK, J.E. & SHAMBELAN, M. (1992). Distribution of angiotensin II receptor subtypes in rat and human kidney. *Am. J. Physiol.*, **262**, F236–F240.

SKALLI, O., ROPRAZ, P., TRZECIAK, A., BEZONANA, G., GILLESSEN, D. & GABBIANI, G. (1986). A monoclonal antibody against α-smooth muscle actin: a new probe for smooth muscle differentiation. *J. Cell. Biol.*, **103**, 2787–2796.

SPETH, R.C. & HARIK, S.I. (1985). Angiotensin II receptor binding sites in brain microvessels. *Proc. Natl. Acad. Sci. U.S.A.*, **82**, 5340–6343.

STEVENS, C.R., BLAKE, D.R., MERRY, P., REVELL, P.A. & LEVICK, J.R. (1991). A comparative study by morphometry of the microvasculature in normal and rheumatoid synovium. *Arthritis Rheum.*, **34**, 1508–1513.

TAKAYANAGI, R., OHNAKA, K., SAKAI, Y., NAKAO, R., YANASE, T., HAJI, M., INAGAMI, T., FURUTA, H., GOU, D.-F., NAKAMUTA, M. & NAWATA, H. (1992). Molecular cloning, sequence analysis and expression of a cDNA encoding human type-1 angiotensin II receptor. *Biochem. Biophys. Res. Commun.*, **183**, 910–916.

THOMAS, D.W. & HOFFMAN, M.D. (1984). Identification of macrophage receptors for angiotensin: a potential role in antigen uptake for T lymphocyte responses? *J. Immunol.*, **132**, 2807–2812.

TSUTSUMI, K., STRÖMBERG, C., VISWANATHAN, M. & SAAVEDRA, J.M. (1991). Angiotensin-II receptor subtypes in fetal tissues of the rat: autoradiography, guanine nucleotide sensitivity, and association with phosphoinositide hydrolysis. *Endocrinology*, **129**, 1075–1082.

URATA, H., HEALY, B., STEWART, R.W., BUMPUS, F.M. & HUSAIN, A. (1989). Angiotensin II receptors in normal and failing human hearts. *J. Clin. Endocrinol. Metab.*, **69**, 54–66.

VERBI, W., GREAVES, M.F., SCHNEIDER, C., KOUBEK, K., JANOSSY, G., STEIN, H., KUNG, P. & GOLDSTEIN, G. (1982). Monoclonal antibodies OKT11 and OKT11A have pan-T reactivity and block sheep erythrocyte 'receptors'. *Eur. J. Immunol.*, **12**, 81–86.

WALSH, D.A., MAPP, P.I., WHARTON, J., POLAK, J.M. & BLAKE, D.R. (1993). Neuropeptide degrading enzymes in normal and inflamed human synovium. *Am. J. Pathol.*, **142**, 1610–1621.

WALSH, D.A., MAPP, P.I., WHARTON, J., RUTHERFORD, R.A.D., KIDD, B.L., REVELL, P.A., BLAKE, D.R. & POLAK, J.M. (1992). Localisation and characterisation of substance P binding to human synovial tissue in rheumatoid arthritis. *Ann. Rheum. Dis.*, **51**, 313–317.

WEINSTOCK, J.V. & BLUM, A.M. (1983). Isolated liver granulomas of murine *Schistosoma mansoni* contain components of the angiotensin system. *J. Immunol.*, **131**, 2529–2532.

WEINSTOCK, J.V. & KASSAB, J.T. (1984). Angiotensin II stimulation of granuloma macrophage phagocytosis and actin polymerization in murine schistosomiasis mansonii. *Cell. Immunol.*, **89**, 46–54.

WEINSTOCK, J., KEEMAN, R.M., SAMANEN, J., HEMPEL, J., FINKELSTEIN, J.A., FRANZ, R.G., GAITANOPOULOS, D.E., GIRARD, G.R., GLEASON, J.G., HILL, D.T., MORGAN, T.M., PEISOFF, C.E., AIYAR, N., BROOKS, T.M., FREDRICKSON, T.A., OHLSTEIN, E.H., RUFFOLO, R.R., STACK, E.J., SULPIZIO, A.C., WEIDLEY, E.F. & EDWARDS, R.M. (1991). 1-(Carboxybenzyl)imidazole-5-arcyclic acids: potent and selective angiotensin II receptor antagonists. *J. Med. Chem.*, **34**, 1514–1517.

WHITEBREAD, S., MELE, M., KAMBER, B. & DE GASPARO, M. (1989). Preliminary biochemical characterization of two angiotensin II receptor subtypes. *Biochem. Biophys. Res. Commun.*, **163**, 264–291.

(Received October 14, 1993
Revised January 21, 1994
Accepted February 8, 1994)

Br. J. Pharmacol. (1994), **112**, 443–448

Enhancement of noradrenergic constriction of large coronary arteries by inhibition of nitric oxide synthesis in anaesthetized dogs

[1]Owen L. Woodman & Patchareewan Pannangpetch

Department of Pharmacology, University of Melbourne, Parkville, Victoria, 3052, Australia

1 Coronary vascular responses to bilateral carotid occlusion (BCO) and the intravenous infusion of tyramine (Tyr, 20 $\mu g\,kg^{-1}\,min^{-1}$) and noradrenaline (NA, 0.5 $\mu g\,kg^{-1}\,min^{-1}$) were examined after bilateral vagotomy and antagonism of β-adrenoceptors. BCO, Tyr and NA decreased large coronary artery diameter and increased mean coronary resistance and systemic arterial pressure without affecting heart rate.

2 Inhibition of nitric oxide (NO) synthase with N^G-nitro-L-arginine (L-NNA, 5 and 15 $mg\,kg^{-1}$) significantly increased mean arterial pressure and decreased heart rate and large coronary artery diameter. Mean coronary resistance was unaffected by either dose of L-NNA. L-NNA significantly reduced depressor and coronary vasodilator responses to the endothelium-dependent vasodilator acetylcholine (ACh, 10 $\mu g\,kg^{-1}$, i.v.). Systemic and coronary vasodilator responses to sodium nitroprusside (SNP, 5 $\mu g\,kg^{-1}$) were unaffected by L-NNA with the exception that the dilatation of the large coronary artery was significantly enhanced by the higher dose.

3 L-NNA significantly enhanced constriction of the large coronary arteries caused by BCO, Tyr and NA but did not affect the increases in mean coronary resistance or systemic arterial pressure.

4 Inhibition of NO synthesis enhances adrenergic constriction of large coronary arteries caused by both neuronally released and exogenous noradrenaline. In contrast, L-NNA did not affect adrenergic constriction of coronary or systemic resistance vessels. Endothelium-derived NO may play an important role in the modulation of noradrenergic vasoconstriction in coronary conductance arteries.

Keywords: Bilateral carotid occlusion; large coronary arteries; N^G-nitro-L-arginine; noradrenaline; tyramine; vasoconstriction

Introduction

There is considerable evidence that the endothelium can modulate vasoconstriction produced by a variety of stimuli. In isolated blood vessels, removal of the endothelium enhances contraction to exogenous noradrenaline (Cocks & Angus, 1983; Miller & Vanhoutte, 1985; Martin *et al.*, 1986; McGrath *et al.*, 1990) and to electrical field stimulation (Tesfamariam *et al.*, 1987; Hynes *et al.*, 1988; Gonzalez *et al.*, 1990; Urabe *et al.*, 1991). The ability of the endothelium to inhibit vasoconstriction appears to be related to the release of the potent vasodilator, nitric oxide (NO). The endothelium synthesizes NO, or a closely related molecule (Palmer *et al.*, 1987), from the terminal guanidino nitrogen atom(s) of L-arginine (Palmer *et al.*, 1988). Analogues of L-arginine such as N^G-nitro-L-arginine (L-NNA) and N -monomethyl-L-arginine (L-NMMA) impair NO synthesis by inhibition of the catalysing enzyme NO synthase (Rees *et al.*, 1989). We (Du *et al.*, 1992; Pannangpetch & Woodman, 1992) and others (Tresize *et al.*, 1992; Vo *et al.*, 1992) have shown that inhibition of NO synthesis enhances adrenergic constriction in both isolated arteries and in intact vascular beds. These studies have led to suggestions that in various cardiovascular disease states, such as atherosclerosis and myocardial ischaemia, endothelial damage could contribute to enhanced vasoconstriction and in the coronary circulation perhaps lead to vasospasm.

The aim of this study was to examine the influence that inhibition of NO synthesis has on coronary vasoconstrictor responses to exogenous and neuronally released NA. Two different methods were used to stimulate the neuronal release of NA. Firstly, bilateral carotid occlusion was applied to stimulate the baroreceptor reflex to low carotid sinus pressure and secondly, tyramine (Tyr), an indirectly acting sympathomimetic, was infused to displace NA from intraneuronal stores. Responses to these stimuli were compared to the effects of the intravenous infusion of noradrenaline. All experiments were performed in anaesthetized dogs after bilateral vagotomy and antagonism of β-adrenoceptors to prevent any changes in cardiac contractility which would have confounded the effects on coronary vascular tone. Large coronary artery diameter and coronary blood flow were measured in order to allow comparison of effects in conduit and resistance arteries.

Methods

Mongrel and greyhound dogs of either sex weighing 13–31 kg were anaesthetized with thiopentone (25–30 $mg\,kg^{-1}$, i.v.) followed by α-chloralose (70 $mg\,kg^{-1}$, i.v., supplemented as necessary). The dogs were ventilated with room air plus additional oxygen as necessary to maintain arterial blood P_{O_2}, P_{CO_2} and pH within the normal range (P_{O_2}: 90–110 mmHg; P_{CO_2} 30–35 mmHg; pH: 7.25–7.35). Pressure in the thoracic aorta was measured by passing a catheter from the right femoral artery and connecting the catheter to a pressure transducer (Spectromed). The ECG was recorded from standard limb leads and was used to trigger a cardiotachometer to provide a continuous measurement of heart rate.

A thoracotomy was performed at the left fifth intercostal space and the pericardium was opened. A pair of 7 MHz piezoelectric transducers were sutured to opposing surfaces of the left circumflex artery. The external diameter of the artery was measured with an ultrasonic transit-time dimension gauge (Triton). Blood flow through the artery was measured with a cuff type electromagnetic flow probe (Skalar) placed on the artery. Care was taken during the placement of the transducers to limit dissection and damage to any visible

[1] Author for correspondence.

nerves. Arterial pressure, coronary blood flow, coronary artery diameter and heart rate were recorded on a Grass (Model 7D) polygraph. Mean coronary resistance was calculated as the quotient of mean arterial pressure and mean coronary blood flow.

Experimental protocol

All experiments were performed after bilateral cervical vagotomy and antagonism of β-adrenoceptors with propranolol (1 mg kg^{-1}, i.v. plus 0.5 mg kg^{-1} h^{-1}) to prevent any reflex or β-adrenoceptor-mediated changes in heart rate. Responses to three stimuli, applied in random order, were compared: clamping of both common carotid arteries for 2 min to induce the baroreceptor reflex to low carotid sinus pressure and infusion of NA (0.5 μg kg^{-1} min^{-1}) or Tyr (20 μg kg^{-1} min^{-1}) intravenously for 5 min. We have previously found that these three stimuli produced similar pressor responses in anaesthetized dogs (Woodman, 1987) and that observation was confirmed in this study. Responses to these stimuli were also examined after inhibition of NO synthesis with two doses of N^G-nitro-L-arginine (L-NNA, 5 and 15 mg kg^{-1}, i.v.). L-NNA was infused intravenously over 15 to 20 min and a further 15 min was allowed after completing the infusion to allow arterial pressure, coronary artery diameter and coronary blood flow to stabilize before examination of further responses. Selective inhibition of NO synthesis was confirmed by examining responses to bolus injections of the endothelium-dependent vasodilator, ACh (10 μg kg^{-1}, i.v.) and the endothelium-independent dilator, sodium nitroprusside (SNP, 5 μg kg^{-1}, i.v.) at the end of each experiment. In some experiments the effect of ACh was also tested 15 min after L-NNA infusion, and before the constrictor stimuli, and the responses compared to those observed at the end of the experiment to ensure that L-NNA had a stable effect over the duration of these experiments. To test whether

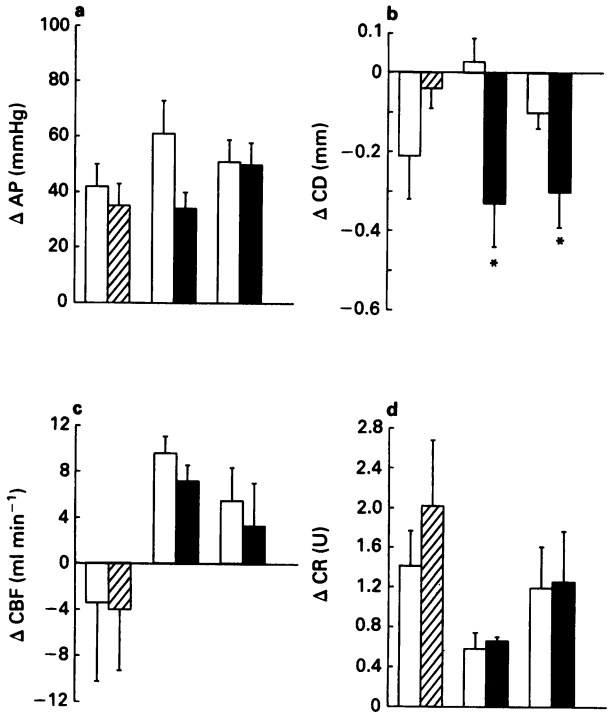

Figure 2 Effect of the 5 min intravenous infusion of tyramine (20 mg kg^{-1} min^{-1}) on (a) mean arterial pressure (ΔAP), (b) large coronary artery diameter (ΔCD), (c) mean coronary blood flow (ΔCBF) and (d) mean coronary resistance (ΔCR) before (open columns) and after infusion of saline (widely hatched columns, $n = 8$), N^G-nitro-L-arginine 5 mg kg^{-1} (closely hatched columns, $n = 6$) or 15 mg kg^{-1} (solid columns, $n = 11$). The values shown are the mean with s.e.mean. $^*P < 0.05$, Wilcoxon's matched pairs test.

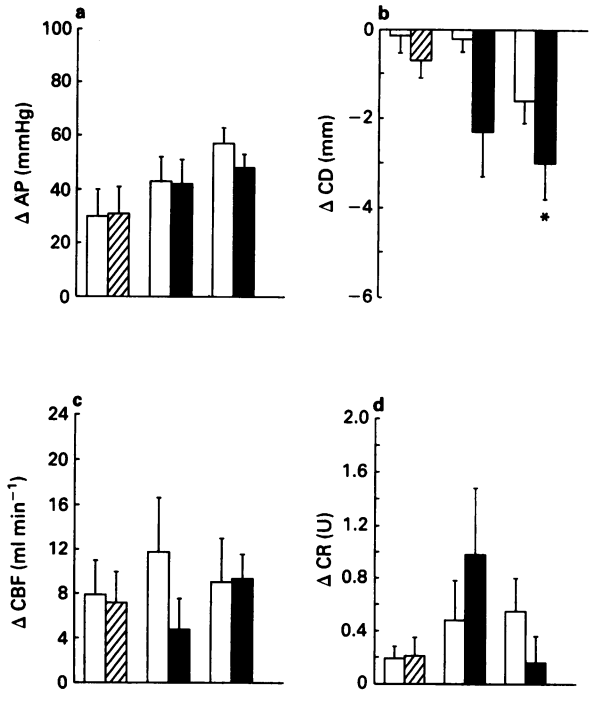

Figure 1 Effect of bilateral carotid occlusion for 2 min on (a) mean arterial pressure (ΔAP), (b) large coronary artery diameter (ΔCD), (c) mean coronary blood flow (ΔCBF) and mean coronary resistance (ΔCR) before (open columns) and after infusion of saline (widely hatched columns, $n = 7$), N^G-nitro-L-arginine 5 mg kg^{-1} (closely hatched columns, $n = 8$) or 15 mg kg^{-1} (solid columns, $n = 13$). The values shown are the mean with s.e.mean. $^*P < 0.05$, Wilcoxon's matched pairs test.

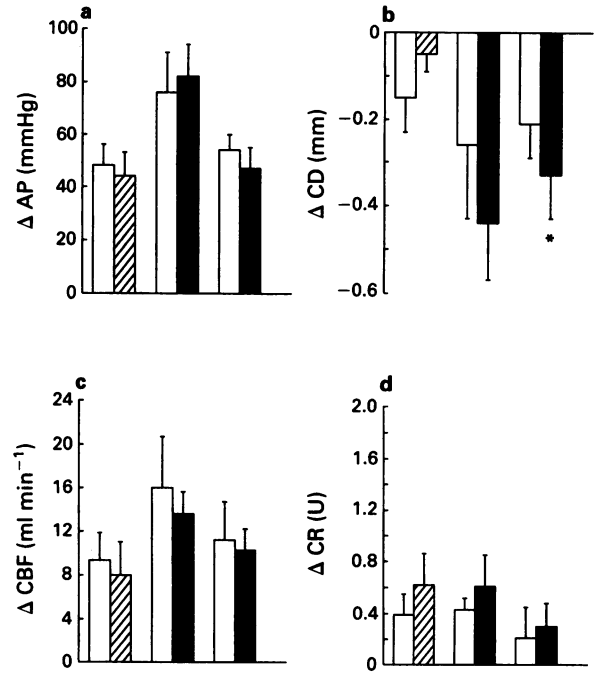

Figure 3 Effect of the 5 min intravenous infusion of noradrenaline (0.5 μg kg^{-1} min^{-1}) on (a) mean arterial pressure (ΔAP), (b) large coronary artery diameter (ΔCD), (c) mean coronary blood flow (ΔCBF) and (d) mean coronary resistance (ΔCR) before (open columns) and after infusion of saline (widely hatched columns, $n = 8$), N^G-nitro-L-arginine 5 mg kg^{-1} (closely hatched columns, $n = 6$) or 15 mg kg^{-1} (solid columns, $n = 11$). The values shown are the mean with s.e.mean. $^*P < 0.05$, Wilcoxon's matched pairs test.

there was any change in vascular reactivity over time in a separate group of dogs responses to BCO, Tyr and NA were tested before and after the infusion of saline.

Drugs

Drugs used were: acetylcholine perchlorate (BDH); (−)-noradrenaline bitartrate (Sigma); N^G-nitro-L-arginine (Sigma); (±)-propranolol hydrochloride (Sigma); sodium nitroprusside (Sigma); tyramine hydrochloride (Sigma). All drugs were dissolved in saline with the exception of L-NNA and propranolol which were dissolved in distilled water. Further dilutions of all drugs were made in saline.

Statistics

As it was found that there was some variability in the coronary vascular responses to BCO and Tyr between dogs, the experiments were designed so that each dog acted as its own control. Results are expressed as the mean ± s.e.mean of n experiments and only one experiment was performed in each dog. Baseline values of the haemodynamic variables and responses to vasodilator and vasoconstrictor stimuli were compared by Wilcoxon's matched pairs test.

Results

All of the data were collected after bilateral vagotomy and antagonism of β-adrenoceptors with propranolol.

Response to BCO, tyramine and noradrenaline

Control responses to BCO for 2 min and the intravenous infusion of Tyr (20 μg kg^{-1} min^{-1}) or NA (0.5 μg kg^{-1} min^{-1}) for 5 min are shown in Figures 1–3. Each of these stimuli increased mean arterial pressure and mean coronary resistance and decreased large coronary artery diameter without affecting heart rate (data not shown).

Effect of the intravenous infusion of N^G-nitro-L-arginine on baseline parameters

L-NNA (5 or 15 mg kg^{-1}) was infused intravenously over 15–20 min. The preparation was then allowed to stabilize for 15 min and the effects of L-NNA on the baseline haemodynamic values were measured (Tables 1 and 2). Both doses of L-NNA significantly increased mean arterial pressure and decreased large coronary artery diameter and heart rate. L-NNA had no significant effect on coronary blood flow. In

Table 1 The effect of intravenous administration of N^G-nitro-L-arginine (5 mg kg^{-1}) on baseline haemodynamic variables in each experiment

	Baseline haemodynamic variables									
	Mean arterial pressure (mmHg)		*Mean coronary blood flow* (ml min^{-1})		*Mean coronary resistance* (mmHg min ml^{-1})		*Mean coronary artery diameter* (mm)		*Heart rate* (beats min^{-1})	
Experiment number	*Control*	*L-NNA*	*Control*	*L-NNA*	*Control*	*L-NNA*	*Control*	*L-NNA*	*Control*	*L-NNA*
2391	100	110	54	50	1.85	2.2	3.93	3.89	118	114
2491	93	103	20	22	4.65	4.68	3.2	3.16	118	118
2591	108	140	20	28	5.4	5.0	–	–	144	140
192	105	100	–	–	–	–	2.88	2.79	148	140
292	93	105	48	52	1.94	2.02	6.43	6.36	126	120
392	120	125	42	40	2.86	3.13	3.32	3.2	120	116
293	115	115	44	44	2.61	2.61	3.78	3.7	132	130
593	115	128	30	32	3.83	4.0	4.92	4.86	126	128
993	125	125	48	40	2.6	3.13	3.5	3.52	112	108
Mean	108	117*	38	38	3.2	3.3	4.0	3.94*	127	124*
s.e.mean	4	4	5	4	0.4	0.4	0.41	0.41	4	4

*$P < 0.05$, Wilcoxon's matched pairs test.

Table 2 The effect of intravenous administration of N^G-nitro-L-arginine (15 mg kg^{-1}) on baseline haemodynamic variables in each experiment

	Baseline haemodynamic variables									
	Mean arterial pressure (mmHg)		*Mean coronary blood flow* (ml min^{-1})		*Mean coronary resistance* (mmHg min ml^{-1})		*Mean coronary artery diameter* (mm)		*Heart rate* (beats min^{-1})	
Experiment number	*Control*	*L-NNA*	*Control*	*L-NNA*	*Control*	*L-NNA*	*Control*	*L-NNA*	*Control*	*L-NNA*
1091	120	135	15	16	8.0	8.44	–	–	128	124
1191	103	120	34	48	3.03	2.5	3.6	3.52	160	152
1291	110	133	48	52	2.3	2.56	3.34	3.23	124	116
1391	93	105	28	32	3.32	3.28	2.48	2.37	136	128
1491	113	120	18	18	6.28	6.67	3.03	2.84	124	112
1591	95	113	62	64	1.53	1.77	4.24	4.2	140	132
1691	135	150	24	20	5.62	7.5	2.72	2.6	128	120
2091	93	115	32	40	2.91	2.88	3.53	3.46	110	106
2191	140	147	80	66	1.75	2.23	3.7	3.28	156	152
2291	125	145	80	82	1.56	1.77	4.39	4.3	128	128
293	115	130	44	36	2.61	3.61	3.8	3.52	132	124
593	115	160	26	44	5.96	3.64	4.92	4.61	126	126
993	125	125	48	36	2.6	3.47	3.5	3.46	112	104
2693	165	180	72	72	2.29	2.5	4.15	4.08	144	144
Mean	118	134*	44	45	3.5	3.8	3.7	3.5*	132	126*
s.e.mean	5	5	6	5	0.5	0.6	0.2	0.2	4	4

*$P < 0.05$, Wilcoxon's matched pairs test.

most experiments mean coronary resistance increased; however, in 2 dogs (2591, Table 1; 593, Table 2) coronary resistance decreased. In each of these experiments the pressor response was larger than that seen in any other members of the group and may have initiated reflex changes in coronary resistance not seen in the other experiments.

Effect of N^G-nitro-L-arginine on haemodynamic responses to BCO, tyramine and noradrenaline

Responses to BCO, tyramine and NA were examined before and after inhibition of NO synthesis with the 2 doses of L-NNA, 5 and 15 mg kg^{-1}, i.v. Increases in mean arterial pressure and mean coronary resistance caused by any of these stimuli were unaffected by either dose of L-NNA (Figures 1–3). In contrast, the Tyr-induced constriction of the large coronary artery was significantly enhanced by the lower dose of L-NNA and the large artery constrictor responses to each of the stimuli were enhanced by the higher dose of L-NNA (Figures 1–3). Responses to BCO, Tyr and NA were unaffected by treatment with saline (Figures 1–3).

Effect of N^G-nitro-L-arginine on haemodynamic responses to acetylcholine and sodium nitroprusside

Responses to bolus injections of the endothelium-dependent dilator, ACh (10 μg kg^{-1}, i.v.) and the endothelium-independent dilator, SNP (5 μg kg^{-1}, i.v.) were examined before and after inhibition of NO synthesis with the 2 doses of L-NNA, 5 and 15 mg kg^{-1}, i.v. When measured at the end of the experiment, ACh-induced systemic and coronary dilatation were significantly attenuated by both doses of L-NNA (Figure 4). To test whether L-NNA caused a stable level of inhibition, responses to ACh were also tested 15 min after L-NNA infusion in some dogs (L-NNA 5 mg kg^{-1}, $n = 5$; L-NNA 15 mg kg^{-1}, $n = 9$) and again at the end of the experiment. In those experiments there were no significant differences in the responses to the first and second administration of ACh after NO synthesis inhibition (data not shown). In contrast, L-NNA did not affect responses to SNP with the exception that there was a significant enhancement of the large artery dilatation in the presence of the higher dose of L-NNA (Figure 5).

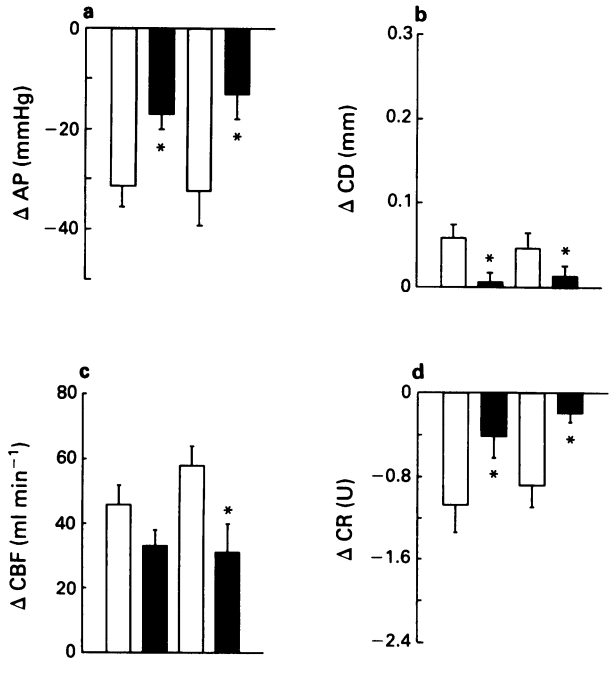

Figure 4 Effect of the bolus intravenous injection of acetylcholine 10 μg kg^{-1} (ACh) before (open columns) and after infusion of N^G-nitro-L-arginine 5 mg kg^{-1} (stippled columns, $n = 9$) or 15 mg kg^{-1} (solid columns, $n = 14$). The values shown are the mean with s.e.mean. *$P < 0.05$, Wilcoxon's matched pairs test.

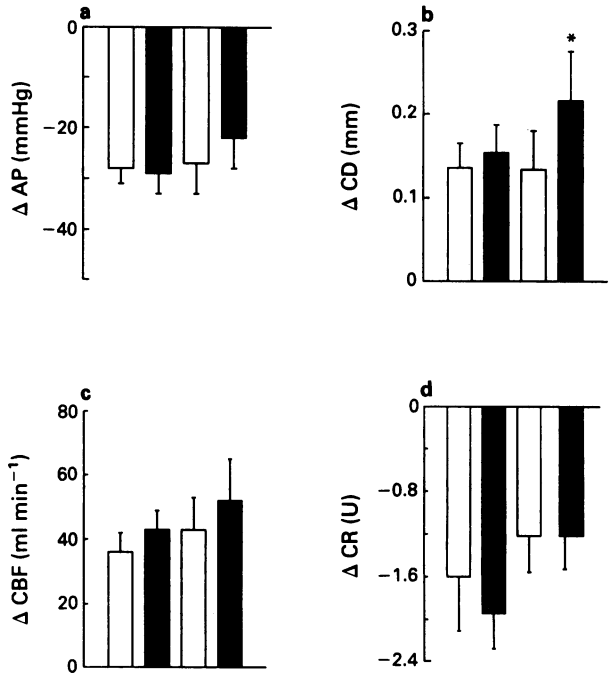

Figure 5 Effect of the bolus intravenous injection of sodium nitroprusside (SNP) before (open columns) and after infusion of N^G-nitro-L-arginine 5 mg kg^{-1} (stippled columns, $n = 9$) or 15 mg kg^{-1} (solid columns, $n = 14$). The values shown are the mean with s.e.mean. *$P < 0.05$, Wilcoxon's matched pairs test.

Discussion

This study demonstrated that in the anaesthetized dog, inhibition of NO synthesis with L-NNA enhanced adrenergic constriction of the large coronary arteries without affecting responses in the coronary resistance vessels or in the systemic circulation. L-NNA caused similar enhancement of responses to NA released from sympathetic nerves due to stimulation of the baroreceptor reflex by bilateral carotid occlusion or due to administration of the indirectly acting sympathomimetic tyramine. Large artery constrictor responses to the infusion of exogenous NA were also enhanced by L-NNA.

It is well established that removal of the endothelium enhances noradrenaline-induced contraction in isolated conductance arteries, including coronary arteries, from dogs and other species (Cocks & Angus, 1983; Miller & Vanhoutte, 1985; Berkenboom *et al.*, 1991). The inhibitory effect of the endothelium appears to be mediated by nitric oxide as inhibitors of NO synthesis also enhance noradrenaline-induced contraction of dog isolated coronary arteries (Berkenboom *et al.*, 1991).

The increased vasoconstriction in response to BCO in the presence of L-NNA could involve a prejunctional action of NO as well as an effect on vascular smooth muscle reactivity. Tesfamariam *et al.* (1987) found that in rabbit isolated carotid arteries the stimulation-induced release of NA was reduced by the presence of the endothelium. In contrast other reports suggested that endothelium-derived NO does not influence NA release (Bucher *et al.*, 1992; Vo *et al.*, 1992). In the present study, neuronal release of NA was stimulated by two means, activation of the baroreceptor reflex to cause a release that would be subject to prejunctional modulation and infusion of Tyr that displaces NA from sympathetic nerves which is therefore not subject to prejunctional control.

Tyr-induced constriction was enhanced by L-NNA in a similar manner to constriction to BCO suggesting that if there is any influence of NO over NA release it is only a minor contributor to the enhanced responses.

It is not known whether the endothelium-mediated inhibition of adrenergic constriction is due to a basal or a stimulated release of NO. Observations that inhibition of NO synthesis increases coronary vascular tone (Benyo *et al.*, 1991; Humphries *et al.*, 1991; Woodman & Dusting, 1991; Sonntag *et al.*, 1992) indicate that there is a significant basal release of NO that could non-selectively oppose constrictor stimuli. In the present study, L-NNA significantly constricted the large coronary artery without significantly affecting coronary blood flow or coronary resistance, a finding consistent with our previous study with L-NNA (Woodman & Dusting, 1990) and the observations of Chu *et al.* (1990) who examined the effect of L-NMMA in conscious dogs. In contrast Richard *et al.* (1991) reported that L-NNA and L-NMMA caused significant increases in coronary resistance in anaesthetized dogs. However, it is interesting that in the same study myocardial tissue perfusion, measured with radioactive microspheres, was unaffected by the inhibitors of NO synthesis. Given that the inhibition of NO synthesis also causes systemic vasoconstriction and hypertension which will initiate metabolic and reflex modulation of coronary vascular tone, it is difficult to assess the level to which the basal release of NO modulates coronary vascular tone. In the present study L-NNA increased coronary resistance in the majority of experiments; however, in 2 experiments where the pressor response to L-NNA was large, coronary resistance surprisingly decreased. Consequently in the whole group there was no statistically significant change in coronary resistance in response to L-NNA. In addition NA has been reported to stimulate the release of EDRF (NO) through the stimulation of α_2-adrenoceptors on endothelial cells (Angus *et al.*, 1986). It is not possible to distinguish between the potential role of basal and stimulated release of NO in the modulation of noradrenergic coronary vasoconstriction in these experiments.

A surprising finding of this study was that although L-NNA enhanced constriction of the large coronary arteries in response to neuronally-released or exogenous NA, there was no enhancement of the constriction of coronary resistance vessels nor of the systemic pressor response. NO is an important regulator of resistance vessel tone and inhibitors of NO synthesis have been reported to enhance adrenergic constriction of resistance vessels. We have found that in the rat autoperfused mesentery, L-NNA enhances responses to both NA and stimulation of sympathetic nerves (Pannangpetch & Woodman, 1992). We have also observed that in conscious rabbits in the presence of autonomic blockade, L-NNA enhances hindquarters constriction caused by the infusion of NA and Tyr (Du *et al.*, 1992) although there is no enhancement of the systemic pressor response. Together with the present study this suggests that the extent to which NO influences adrenergic constriction of resistance vessels may vary in different vascular beds. The absence of an effect of L-NNA was not due to an inability to inhibit NO synthesis in resistance arteries as the ACh-induced increase in coronary blood flow and reduction in arterial pressure were both significantly attenuated.

In conclusion, impaired synthesis of NO enhanced sympathetic nervous constriction of the large coronary artery but not of the resistance vessels. In atherosclerotic arteries or after ischaemia and reperfusion, where NO-mediated dilatation is impaired (Sobey & Woodman, 1993), sympathetic vasoconstriction may be enhanced, resulting in impaired blood flow to the heart.

References

ANGUS, J.A., COCKS, T.M. & SATOH, K. (1986). α2-Adrenoceptors and endothelium-dependent relaxation in canine large arteries. *Br. J. Pharmacol.*, **88**, 767–777.

BENYO, Z., KISS, G., SZABO, C., CSAKI, C. & KOVACH, A.G.B. (1991). Importance of basal nitric oxide synthesis in regulation of myocardial blood flow. *Cardiovasc. Res.*, **25**, 700–703.

BERKENBOOM, G., UNGER, P., FANG, Z.Y. & FONTAINE, J. (1991). Endothelium-derived relaxing factor and protection against contraction to norepinephrine in isolated canine and human coronary arteries. *J. Cardiovasc. Pharmacol.*, **17** (Suppl. 3), S127–S132.

BUCHER, B., QUEDRAOGO, S., TSCHOPL, M., PAYA, D. & STOCLET, J.-C. (1992). Role of the L-arginine-NO pathway and of cyclic GMP in electrical field-induced noradrenaline release and vasoconstriction in the rat tail artery. *Br. J. Pharmacol.*, **107**, 976–982.

CHU, A., CHAMBERS, D.E., LIN, C.C., KUEHL, W.D. & COBB, F.R. (1990). Nitric oxide modulates epicardial coronary vasomotor tone in awake dogs. *Am. J. Physiol.*, **258**, H1250–H1254.

COCKS, T.M. & ANGUS, J.A. (1983). Endothelium-dependent relaxation of coronary arteries by noradrenaline and serotonin. *Nature*, **305**, 627–630.

DU, Z.Y., DUSTING, G.J. & WOODMAN, O.L. (1992). Inhibition of nitric oxide synthase specifically enhances adrenergic vasoconstriction in rabbits. *Clin. Exp. Pharmacol. Physiol.*, **19**, 523–530.

GONZALEZ, C., MARTIN, C., HAMEL, E., GALEA, E., GOMEZ, B., LLUCH, S. & ESTRADA, C. (1990). Endothelial cells inhibit the vascular response to adrenergic stimulation by a receptor-mediated mechanism. *Can. J. Physiol. Pharmacol.*, **68**, 104–109.

HUMPRHIES, R.G., CARR, R.D., NICOL, A.K., TOMLINSON, W. & O'CONNOR, S.E. (1991). Coronary vasoconstriction in the conscious rabbit following intravenous infusion of L-N^G-nitro-arginine. *Br. J. Pharmacol.*, **102**, 565–566.

HYNES, M.R., DANG, H. & DUCKLES, S.P. (1988). Contractile responses to adrenergic nerve stimulation are enhanced with removal of endothelium in rat caudal artery. *Life Sci.*, **42**, 357–365.

MARTIN, W., FURCHGOTT, R.F., VILLANI, G.M. & JOTHIANANDAN, D. (1986). Depression of contractile responses in rat aorta by spontaneously released endothelium-derived relaxing factor. *J. Pharmacol. Exp. Ther.*, **237**, 529–538.

MCGRATH, J.C., MONAGHAN, S., TEMPLETON, A.G.B. & WILSON, V.G. (1990). Effects of basal and acetylcholine-induced release of endothelium-derived relaxing factors on contraction to α-adrenoceptor agonists in a rabbit artery and corresponding veins. *Br. J. Pharmacol.*, **99**, 77–86.

MILLER, V.M. & VANHOUTTE, P.M. (1985). Endothelial α2-adrenoceptors in canine pulmonary and systemic blood vessels. *Eur. J. Pharmacol.*, **118**, 123–129.

PALMER, R.M., ASHTON, D.S. & MONCADA, S. (1988). Vascular endothelial cells synthesize nitric oxide from L-arginine. *Nature*, **333**, 664–666.

PALMER, R.M., FERRIGE, A.G. & MONCADA, S. (1987). Nitric oxide release accounts for the biological activity of endothelium-derived relaxing factor. *Nature*, **327**, 524–526.

PANNANGPETCH, P. & WOODMAN, O.L. (1992). Nitric oxide synthase inhibition enhances sympathetic constriction of the rat autoperfused mesentery. *Pharmacol. Commun.*, **2**, 241–252.

REES, D.D., PALMER, R.M.J., HODSON, H.F. & MONCADA, S. (1989). A specific inhibitor of nitric oxide formation from L-arginine attenuates endothelium-dependent relaxation. *Br. J. Pharmacol.*, **96**, 418–424.

RICHARD, V., BERDEAUX, A., DRIEU LA ROCHELLE, C. & GIUDICELLI, J.-F. (1991). Regional coronary haemodynamic effects of two inhibitors of nitric oxide synthesis in anaesthetized, open-chest dogs. *Br. J. Pharmacol.*, **104**, 59–64.

SOBEY, C.G. & WOODMAN, O.L. (1993). Myocardial ischaemia: what happens to the coronary arteries? *Trends Pharmacol. Sci.*, **14**, 448–453.

SONNTAG, M., DEUSSEN, A. & SCHRADER, J. (1992). Role of nitric oxide in local blood flow control in the anaesthetized dog. *Pflugers Arch. Eur. J. Physiol.*, **420**, 194–199.

TESFAMARIAM, B., WEISBROD, R.M. & COHEN, R.A. (1987). Endothelium inhibits responses of rabbit carotid artery to adrenergic nerve stimulation. *Am. J. Physiol.*, **253**, H792–H798.

TRESIZE, D.J., DREW, G.M. & WESTON, A.H. (1992). Analysis of the depressant effect of the endothelium on contractions of rabbit isolated basilar artery to 5-hydroxytryptamine. *Br. J. Pharmacol.*, **106**, 587–592.

URABE, M., KAWASAKI, H. & TAKASAKI, K. (1991). Effect of endothelium removal on the vasoconstrictor response to neurally released 5-hydroxytryptamine and noradrenaline in the rat isolated mesenteric and femoral arteries. *Br. J. Pharmacol.*, **102**, 85–90.

VO, P.A., REID, J.J. & RAND, M.J. (1992). Attenuation of vasoconstriction by endogenous nitric oxide in rat caudal artery. *Br. J. Pharmacol.*, **107**, 1121–1128.

WOODMAN, O.L. (1987). The role of α1- and α2-adrenoceptors in the coronary vasoconstrictor responses to neuronally released and exogenous noradrenaline in the dog. *Naunyn-Schmied. Arch. Pharmacol.*, **336**, 161–168.

WOODMAN, O.L. & DUSTING, G.J. (1991). N^G-nitro L-arginine causes coronary vasoconstriction and inhibits endothelium-dependent vasodilatation in anaesthetized greyhounds. *Br. J. Pharmacol.*, **103**, 1407–1410.

(Received November 8, 1993
Revised January 31, 1994
Accepted February 8, 1994)

Br. J. Pharmacol. (1994), **112**, 449–452

Increase of extracellular brain calcium involved in interleukin-1β-induced pyresis in the rabbit: antagonism by dexamethasone

[1]M. Palmi, M. Frosini, [2]C. Becherucci, G.P. Sgaragli & [2]L. Parente

Istituto di Scienze Farmacologiche, Università di Siena, Via Piccolomini 170, 53100 Siena, Italy

1 This study investigates the role of extracellular brain calcium in the hyperthermia induced by interleukin-1β (IL-1β).

2 Intracerebroventricular (i.c.v.) injection of IL-1β (12.5 ng kg^{-1}) in rabbits caused a prompt and sustained rise in cerebrospinal fluid (CSF) Ca^{2+} concentration ($[Ca^{2+}]$) followed by enhanced prostaglandin E_2 (PGE_2) release and hyperthermia.

3 A linear and significant correlation was observed between the increase in $[Ca^{2+}]$ induced by IL-1β and the rise in body temperature.

4 Ventriculo-cisternal perfusion with artificial CSF containing the calcium chelator EGTA (1.3 mM) blocked the IL-1-induced PGE_2 release and countered the febrile response.

5 I.c.v. administration of dexamethasone (Dex) (2.4 and 24 μg kg^{-1}) 100 min prior to IL-1β, dose-dependently antagonized the cytokine-induced Ca^{2+} increase, the PGE_2 release and the febrile response.

6 These results suggest that changes in extracellular brain calcium are involved in the regulation of body temperature. In this light, the antipyretic action of Dex may be related to its effect on Ca^{2+} uptake.

Keywords: Interleukin-1β; dexamethasone; CSF-calcium; prostaglandin E_2; fever

Introduction

It has been proposed that the set point of body temperature in mammals is regulated by extracellular changes of Ca^{2+} concentrations within the hypothalamus (Myers & Veale, 1970). It is also well established that interleukin-1 (IL-1) is a key host mediator of the febrile response to infectious agents and bacterial pyrogens (for review see Rothwell, 1991). The pyrogenic effect of IL-1 appears to lie in the cytokine's ability to induce the synthesis/release of prostaglandin E_2 (PGE_2) (Dinarello & Bernheim, 1981; Davidson *et al.*, 1990). We recently showed that intracerebroventricular (i.c.v.) injection of human recombinant IL-1β in rabbits caused fever accompanied by a significant increase of Ca^{2+} concentration ($[Ca^{2+}]$) in the cerebrospinal fluid (CSF), whereas i.c.v. injection of PGE_2 induced fever with no corresponding increase in CSF Ca^{2+}. The administration of acetylsalicylic acid counteracted the increases in both body temperature and CSF $[Ca^{2+}]$ elicited by IL-1 (Palmi *et al.*, 1992). The role of calcium in thermoregulation is also to be seen from dose-correlation studies where i.c.v. calcium antagonists, such as verapamil, nifedipine and cinnarizine induced hyperthermia, whereas the calcium agonist, Bay-K-8644 caused hypothermia and antagonized fever induced by endotoxin (Palmi & Sgaragli, 1989). In this study we tested the hypothesis that increases in CSF $[Ca^{2+}]$ induced by IL-1 triggers PGE_2 synthesis causing fever. We also investigated whether the well-known antipyretic activity of dexamethasone (Milton *et al.*, 1989) could be related to its antagonism of the CSF Ca^{2+} increase.

Methods

Animal surgery

Adult male New Zealand rabbits weighing 2.0 to 2.5 kg under sodium pentobarbitone (Nembutal) anaesthesia (i.v., 30 mg kg^{-1}) were chronically implanted with cannulae in one lateral ventricle and the *cisterna magna* by means of a stereotaxic apparatus (Stoelting Instrument, Chicago, IL, U.S.A.) and CSF samples were collected from the *cisterna magna* in conscious rabbits restrained in stainless steel cages following a procedure detailed elsewhere (Palmi *et al.*, 1992).

Ventriculo-cisternal perfusion

Artificial pyrogen-free CSF was perfused through the ventricle for 25 min at a constant rate of 5 μl min^{-1} with concurrent withdrawal of CSF from the *cisterna magna*. At this juncture sampling of CSF was continued from the *cisterna magna* only. This procedure was run alternatively with Ca^{2+} and EGTA both at a concentration of 1.3 mM. Perfusion pressure was monitored throughout the experimental series. In a few cases where the pressure increased above 30 cmH_2O and could not be reduced by proper adjustment of the cannulae, the perfusion was terminated and the experiment excluded.

Sample collection and measurement of $[Ca^{2+}]$, $[PGE_2]$ and RT

Reference values for CSF $[Ca^{2+}]$, PGE_2 and rectal temperature (RT) were collected in the first 100 min (4 fractions) of each experimental series.

Calcium concentrations were determined colorimetrically at 573 nm by the method of Stern & Lewis (1957) using ortho-cresolphthalein (OCPC) as Ca^{2+} complexing agent and 8-hydroxyquinoline-5-sulphonic acid to eliminate Mg^{2+} interference (see Palmi *et al.*, 1992). PGE_2 levels in CSF were determined by radioimmunoassay (RIA) with minimal (3.7%) PGE_1 cross reactivity (NEN-Du Pont, Dreieich, Germany).

Rectal temperature (RT) was measured every 5 min by a thermocouple thermometer (Columbus, Ohio, U.S.A.) connected to a Personal Computer with an iso-thermex programme (Columbus, Ohio, U.S.A.).

To isolate any experimental artefact arising from animal

[1] Author for correspondence.
[2] Present address: Dipartimento di Farmacologia, Istituto di Ricerca Immunobiologica Siena (IRIS), 53100 Siena, Italy.

restraint, manipulation or glucocorticoid vehicling, a control group of 6 animals was injected with 10 µl of 1:1 (v/v) ethanol:H_2O and liquor withdrawn for a total of 250 min. Pre and post vehicle values for $[Ca^{2+}]$, PGE_2 and RT showed no statistically significant differences (data not shown).

Chemicals

The following drugs were used: dexamethasone (Dex) acetate, dissolved directly prior to use in a 1:1 (v/v) mixture of ethanol:H_2O, and ethylene glycol-*bis*(β-aminoethylether) *N,N,N'N'*-tetraacetic acid (EGTA) were purchased from Sigma Chemical Co. (St. Louis, MO, U.S.A.). Calcium test reagent, hrIL-1β (specific activity 1.0×10^{-9} u mg^{-1} protein), and 'pyrogen-free' water were obtained as previously reported (Palmi *et al.*, 1992).

Statistical analysis

Values are expressed as means ± s.e.mean. Data were compared statistically by one way analysis of variance. Group data of $[Ca^{2+}]$, $[PGE_2]$ and RT were compared across all treatment conditions: hrIL-1β alone, hrIL-1β in the presence of 2.4 µg kg^{-1} Dex and hrIL-1β in the presence of 24 µg kg^{-1} Dex. Pre (control) and post-treatment data comparisons were only performed for the hrIL-1β treatment. Linear regression analysis was used to plot the single values of $[Ca^{2+}]$ against RT. A $P<0.05$ was considered significant.

Results

Figure 1c shows that i.c.v. IL-1β (12.5 ng kg^{-1}) prompted an immediate and significant rise ($P<0.05$; $n=6$) in CSF $[Ca^{2+}]$ which was sustained throughout the experiment. Individual percentage increases of CSF $[Ca^{2+}]$ ranged between 4.1 and 20.6 with an average peak of 8.2 ± 1.4 over controls (1.41 ± 0.02 mM) 25 min after IL-1β administration. Treatment with two different doses of dexamethasone (Dex) (2.4 and 24 µg kg^{-1}), 100 min prior to IL-1β, dose-dependently and significantly ($P<0.01$) antagonized the increase in $[Ca^{2+}]$. With the lower dose, CSF $[Ca^{2+}]$ fell transiently by an average 4.5 ± 1.0% compared to controls (1.48 ± 0.04 mM), with basal values regained within 6 h. Response to the higher dose was more sustained and lasted the entire experimental period with no return to basal conditions. Four hours post-administration of the high dose of Dex, the CSF $[Ca^{2+}]$ averaged 10 ± 2.4% less than controls (1.45 ± 0.03 mM).

After 50 min lag phase following IL-1β administration, concentrations of PGE_2 ($[PGE_2]$) in CSF steadily rose to an average of 703 ± 278% over controls (0.829 ± 0.085 ng ml^{-1}) at 100 min after IL-1β administration (Figure 1b). When time-courses for $[Ca^{2+}]$ and $[PGE_2]$ increases were compared, it was found that $[PGE_2]$ increased with a 25 min delay compared to that of CSF $[Ca^{2+}]$. Both doses of Dex significantly ($P<0.01$) antagonized the increase of PGE_2 induced by IL-1β. At the lower Dex dose, PGE_2 elevation was 223.9 ± 68.9% over controls (0.754 ± 0.097 ng ml^{-1}) whereas at the higher Dex dose it was 153.8 ± 51.7% of controls (0.907 ± 0.200 ng ml^{-1}). Dex counteracted RT increases in a dose-dependent way (IL-1-induced RT increase: 1.58 ± 0.2°C; RT increase with low Dex was 0.87 ± 0.12°C ($P<0.01$), while RT with high Dex declined to 0.63 ± 0.22°C below basal values (Figure 1a)). In all three conditions (low, high and no Dex) basal parameters remained unaltered over the 100 min interval preceding IL-1 administration and did not differ significantly one from another, demonstrating that Dex action is dependent on the presence of pyresis. Convergent results were obtained when the Ca^{2+} chelator, EGTA (1.3 mM) was added to the artificial CSF perfusion. The addition of the Ca^{2+} chelator EGTA significantly ($P<0.01$) lowered $[PGE_2]$ and RT to 302.8 ± 63.1% of controls (0.882 ± 0.109) and 0.76 ± 0.10°C respectively (Figure 2).

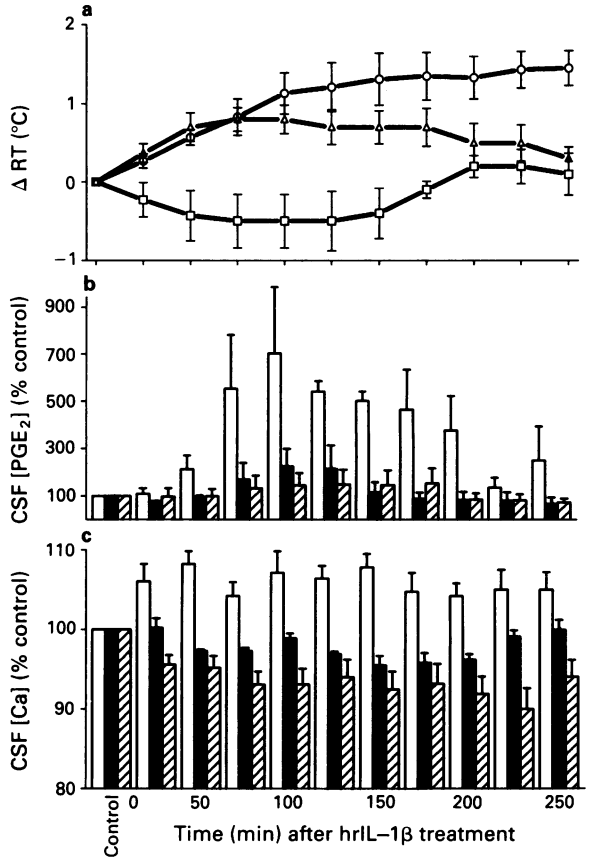

Figure 1 Effects of pretreatment with dexamethasone (Dex) on (a) rectal temperature (RT), (b) prostaglandin E_2 concentration ($[PGE_2]$) and (c) calcium concentration ($[Ca^{2+}]$) in rabbit cerebrospinal fluid (CSF) after intracerebroventricular (i.c.v.) injection of interleukin 1β (IL-1β). (○) and open columns indicate IL-1β; (△) and solid columns indicate IL-1β + Dex at 2.4 µg kg^{-1}; (□) and hatched columns indicate IL-1β + Dex at 24 µg kg^{-1}. Dex was administered i.c.v. 100 min before IL-1β injection (zero min). Columns (mean of triplicate determinations of CSF fractions from 6 animals) with s.e.mean show percentage deviations in $[Ca^{2+}]$ and $[PGE_2]$ over controls. Controls (100%) represent the average concentration from 4 fractions collected over a period −100–0 min. Group data of RT, $[Ca^{2+}]$ and $[PGE_2]$ were compared statistically by ANOVA across all treatment conditions: IL-1β alone, with Dex at 2.4 (IL-1β + $Dex_{2.4}$) and with Dex at 24 (IL-1β + Dex_{24}) µg kg^{-1}. Control vs IL-1β: $[Ca^{2+}]$, $[PGE_2]$, $P<0.05$; RT, $P<0.01$. IL-1β vs ($Dex_{2.4}$ + IL-1β) or (Dex_{24} + IL-1β): $[Ca^{2+}]$, $[PGE_2]$, RT, $P<0.01$. ($Dex_{2.4}$ + IL-1β) vs (Dex_{24} + IL-1β): $[Ca^{2+}]$, RT, $P<0.01$; $[PGE_2]$, NS.

Basal parameters were unaffected by 25 min of perfusion at maximum initial EGTA concentration, whereas after pyretic induction, EGTA promptly and sustainedly halved RT and PGE_2 values, despite its progressive dilution by CSF, exhibiting the chelator's specificity of action. The slight remaining increase in temperature after perfusion with EGTA is probably due to the chelator's progressive dilution over the long time span of the experimental session.

To seek a possible direct relationship between CSF calcium and RT, individual changes of CSF calcium in several animals treated with IL-1β (12.5 ng kg^{-1}) were plotted against the corresponding maximal RT variations which occurred 150 to 250 min after IL-1 treatment. Calcium concentration in febrile animals was calculated by averaging calcium values of 5 CSF fractions collected over the same time span and subtracting these from the corresponding pretreatment levels. The animals exhibited a wide range of ΔRT, from 0.6 to 2°C, with corresponding calcium variations between 0.01 and 0.39 mM. These two parameters, as shown in Figure 3, were linearly and positively correlated in a highly

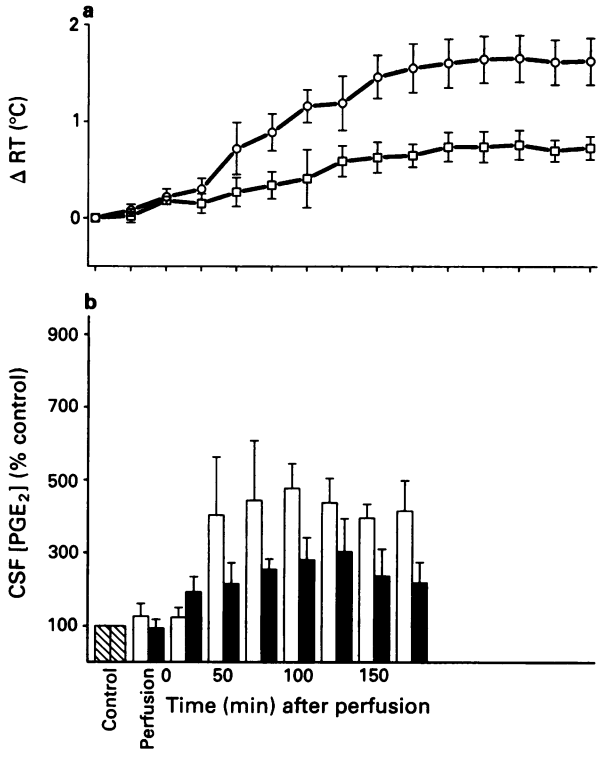

Figure 2 Effect of EGTA on changes of (a) rectal temperature (RT) and (b) prostaglandin E_2 concentration ([PGE_2]) in rabbit cerebrospinal fluid (CSF) induced by i.c.v. injection of interleukin 1β (IL-1β). Artificial CSF containing EGTA was perfused (5 μl min^{-1}) ventriculo-cisternally during a −25–0 min interval, preceding IL-1β (12.5 ng kg^{-1}) injection (zero min). (○) and open columns indicate perfusion without EGTA; (□) and solid columns indicate perfusion with EGTA (1.3 mM); hatched columns indicate preperfused control. Columns (mean of triplicate determinations of CSF fractions from 5 animals) with s.e.mean show percentage deviations in [PGE_2] over controls (cf. Figure 1). Statistical analysis was performed by ANOVA and compared post-perfusion data obtained in absence (−EGTA) and in presence (+EGTA) of EGTA: −EGTA vs +EGTA:[PGE_2] and RT, $P<0.01$.

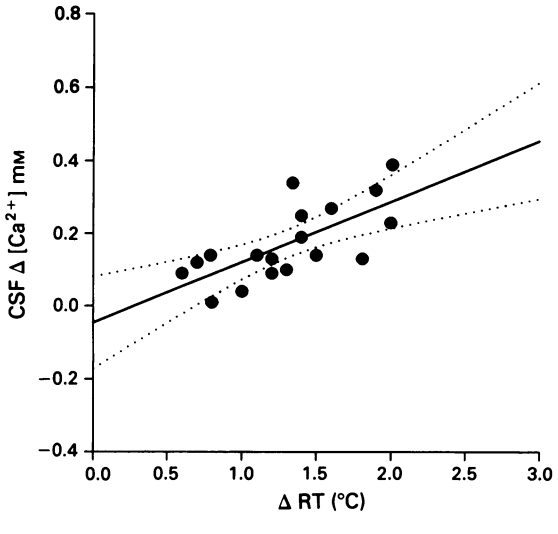

Figure 3 Correlation between variations in rectal temperature (ΔRT) and calcium concentration (Δ[Ca^{2+}]) in cerebrospinal fluid (CSF) of rabbits ($n = 18$) submitted to intracerebral (i.c.v.) injection of hrIL-1β (12.5 ng kg^{-1}). Individual CSF [Ca^{2+}] values represent the mean of triplicate determinations from 5 CSF fractions collected at 25 min intervals in a 150–250 min period post hrIL-1β administration. ΔRT values represent the average of 25 measurements at 5 min intervals during the period of CSF collection. Regression and correlation analysis showed $P<0.01$ and $r = 0.695$. Dotted lines represent 95% confidence intervals.

statistically significant way. Figure 3 shows that mean CSF calcium increase in concentration per unit temperature in febrile animals was in the order of 0.12 mM which represents a 8.5% increase over mean calcium concentration in controls (1.41 ± 0.02 mM see above).

Discussion

The present study suggests that compounds of known pyretic and antipyretic activity may exert their effect via regulation of extracellular brain calcium. The findings show that IL-1 caused an increase of CSF [Ca^{2+}] accompanied by elevation of RT and [PGE_2]. These effects were promptly reversed by the well known antipyretic, dexamethasone, in a dose-dependent manner, supporting the growing evidence for the involvement of extracellular brain calcium in body temperature regulation. Preliminary quantitative high performance liquid chromatography (h.p.l.c.) anlaysis indicates that concentrations of other cations, such as Na^+, K^+, and Mg^{2+} do not increase following IL-1β (Frosini *et al.*, unpublished data), pointing to a specificity of action of the cytokine on Ca^{2+}. The hypothesis that changes in CSF [Ca^{2+}] trigger the synthesis of PGE_2, the probable final effector of the hyperthermic response, and not *viceversa*, is also supported by prior research (Palmi *et al.*, 1992) showing that i.c.v. PGE_2 leaves CSF [Ca^{2+}] unmodified.

Support for this sequence of events is provided by the perfusion series with EGTA (Figure 2) where the extracellular calcium chelator antagonized PGE_2 and consequently the febrile response induced by IL-1, substantiating *in vivo*, a previous finding concerning cultured fibroblasts (Wienhold *et al.*, 1991).

Direct evidence that calcium elevation is critical in IL-1β hyperthermia is also provided by Figure 3 which shows that increased calcium levels are linearly correlated to degree of temperature gain. The value obtained, showing an 8.5% (0.12 mM) increase of [Ca^{2+}] per unit temperature change substantially agrees with previous data concerning spontaneous post-surgical fever in rabbits. In these animals the average calcium increase per unit RT change was 0.15 mM corresponding to 10% variation in [Ca^{2+}] (Palmi *et al.*, 1992). The modest changes observed may be ascribed both to the distance separating the possible site of IL-1 action (brain extracellular space) from the site of calcium monitoring (*cisterna magna*) and/or to an overall diluting effect of the cerebrospinal fluid.

It is in fact known that the rate limiting step in prostanoid synthesis is the availability of the arachidonate precursor released from cellular phospholipids upon activation of phospholipase A_2 (PLA_2) (Flower & Blackwell, 1976). The activity of extracellular PLA_2 enzymes is dependent on calcium and their role in inflammation and eicosanoid generation, recently reviewed by Glaser *et al.* (1993) warrants the legitimate speculation that increased CSF calcium concentration may activate extracellular PLA_2 leading to enhanced PGE_2 synthesis. It has been shown that IL-1 and glucocorticoids have opposite effects on PLA_2 enzymes. While IL-1 stimulates mRNA synthesis (Lyons-Giordano *et al.*, 1989), release (Pfeilschifter *et al.*, 1989) and action (Burch *et al.*, 1988) of PLA_2, glucocorticoids block mRNA synthesis and post-transcriptional expression of PLA_2 (Nakano *et al.*, 1990) and inhibit enzymatic activity by inducing the synthesis of lipocortins which possess anti-inflammatory and antipyretic activity (Solito & Parente, 1989; Solito *et al.*, 1991; Davidson *et al.*, 1991). Reverse modulation of extracellular calcium levels by IL-1 and glucocorticoids may represent an additional regulatory mechanism of extracellular PLA_2 enzymes.

The means by which IL-1 and dexamethasone affect extracellular calcium requires further elucidation; however, opposite disruptive effects on the voltage-gated calcium channels may be postulated. IL-1 in fact depresses inward calcium currents in guinea-pig hippocampal neurones (Plata-Salaman

& Ffrench-Mullen, 1992) whereas dexamethasone increases calcium uptake in rat aortic smooth muscle cells (Hayashi *et al.*, 1991). In conclusion this study shows that thermal states can be manipulated as a function of CSF [Ca^{2+}], highlighting again the cation's central role in thermoregulation.

This work was supported by contributions of MURST (40 + 60%) Rome, Italy and BIOMED 1 (European Community). The authors thank Dr R. Raikes for helpful advice and critical reading of this manuscript.

References

BURCH, R.M., CONNOR, J.R. & AXELROD, J. (1988). Interleukin-1 amplifies receptor-mediated activation of phospholipase A_2 in 3T3 fibroblasts. *Proc. Natl. Acad. Sci. U.S.A.*, **85**, 6305–6309.

DAVIDSON, J., FLOWER, R.J., MILTON, A.S., PEERS, S.H. & ROTONDO, D. (1991). Antipyretic action of human recombinant lipocortin-1. *Br. J. Pharmacol.*, **102**, 7–9.

DAVIDSON, J., MILTON, A.S. & ROTONDO, D. (1990). A study of the pyrogenic action of interleukin-1α and interleukin-1β: interaction with a steroidal and a non steroidal antiinflammatory agent. *Br. J. Pharmacol.*, **100**, 542–546.

DINARELLO, C.A. & BERNHEIM, H.A. (1982). Ability of human leukocyte pyrogen to stimulate brain prostaglandin synthesis in vitro. *J. Neurochem.*, **37**, 702–708.

FLOWER, R.G. & BLACKWELL, G.J. (1976). The importance of phospholipase A_2 in prostaglandin biosynthesis. *Biochem. Pharmacol.*, **25**, 285–291.

GLASER, K.B., MOBILIO, D., CHANG, J.Y. & SENKO, N. (1993). Phospholipase A_2 enzymes: regulation and inhibition. *Trends Pharmacol. Sci.*, **14**, 92–98.

HAYASHI, T., NAKAI, T. & MIYABO, S. (1991). Glucorticoids increase Ca^{2+} uptake and [^{3}H]dihydropyridine binding in A7r5 vascular smooth muscle cells. *Am. J. Physiol.*, **261**, C106–C114.

LYONS-GIORDANO, B., DAVIS, G.L., GALBRAITH, W., PRATTA, M.A. & ARNER, E.C. (1989). Interleukin-1β stimulates phospholipase A_2 mRNA in rabbit articular chondrocytes. *Biochem. Biophys. Res. Commun.*, **164**, 488–495.

MILTON, A.S., ABUL, H.T., DAVIDSON, J. & ROTONDO, D. (1989). Antipyretic action of dexamethasone. In *Thermoregulation: Research and Clinical Applications*. ed. Lomax, P. & Schonbaum, E. pp. 74–77. Basel: Karger.

MYERS, R.D. & VEALE, W.L. (1970). Body temperature: possible ionic mechanism in the hypothalamus controlling the set-point. *Science*, **170**, 95–97.

NAKANO, T., OHARA, O., TERAOKA, H. & ARITA, H. (1990). Glucocorticoids suppress group II phospholipase A_2 production by blocking mRNA synthesis and post-transcriptional expression. *J. Biol. Chem.*, **265**, 12745–12748.

PALMI, M., FROSINI, M. & SGARAGLI, G.P. (1992). Calcium changes in rabbit CSF during endotoxin, IL-1β and PGE_2 fever. *Pharmacol. Biochem. Behav.*, **43**, 1253–1262.

PALMI, M. & SGARAGLI, G.P. (1989). Hyperthermia induced in the rabbit by organic calcium antagonists. *Pharmacol. Biochem. Behav.*, **34**, 325–330.

PFEILSCHIFTER, J., PIGNAT, W., VOSBECK, K. & MARKI, F. (1989). Interleukin-1 and tumor necrosis factor sinergistically stimulate prostaglandin synthesis and phospholipase A_2 release from rat mesangial cells. *Biochem. Biophys. Acta*, **159**, 385–394.

PLATA-SALAMAN, C.R. & FFRENCH-MULLEN, J.M.H. (1992). Interleukin-1β depresses calcium currents in CA1 hyppocampal neurons in phathophysiological concentrations. *Brain Res. Bull.*, **29**, 221–223.

ROTHWELL, N.J. (1991). Functions and mechanisms of interleukin-1 in the brain. *Trends Pharmacol. Sci.*, **12**, 430–435.

SOLITO, E. & PARENTE, L. (1989). Modulation of phospholipase A_2 activity in human fibroblasts. *Br. J. Pharmacol.*, **96**, 656–660.

SOLITO, E., RAUGEI, G., MELLI, M. & PARENTE, L. (1991). Dexamethasone induces the expression of the mRNA of lipocortin 1 and 2 and the release of lipocortin 1 and 5 in differentiated but not undifferentiated U-937 cells. *FEBS Lett.*, **291**, 238–244.

STERN, J. & LEWIS, W.H.P. (1957). The colorimetric estimation of calcium in serum with o-cresolphtalein complexone. *Clin. Chim. Acta*, **2**, 576–580.

WIENHOLD, L. SPECKING, A.S. & DEKER, K. (1991). Signal transduction in endotoxin-stimulated synthesis of TNF-α and prostaglandin E_2 by rat kupffer cells. Role of extracellular calcium ions and protein kinase C. *Biol. Chem. Hoppe-Seyler*, **372**, 829–834.

(Received October 6, 1993
Revised January 25, 1994
Accepted February 8, 1994)

Br. J. Pharmacol. (1994), **112**, 453–460

Mediation by bradykinin of rat paw oedema induced by collagenase from *Clostridium histolyticum*

F.J. Legat, T. Griesbacher & [1]F. Lembeck

Department of Experimental and Clinical Pharmacology, University of Graz, Universitätsplatz 4/1, A-8010 Graz, Austria

1 Collagenases are thought to play a major role in the pathology of gas gangrene caused by *Clostridium histolyticum*, because they can destroy the connective tissue barriers. We investigated possible mediators involved in the oedema formation and plasma protein extravasation which follow the injection of a collagenase (EC 3.4.24.3) from *Clostridium histolyticum* into one hind paw of anaesthetized rats.

2 The magnitude of the oedema following a subplantar injection was dependent on the dose of collagenase (30, 100 and 300 μg) injected. It reached its maximum within 30 min and remained unchanged for at least 5 h. Plasma protein extravasation into the paw was most pronounced within 20 min of the injection. Heat-inactivated collagenase was ineffective.

3 The B_2 bradykinin (BK) antagonist icatibant (D-Arg-[Hyp^3-Thi^5-D-Tic^7-Oic^8] bradykinin, formerly named Hoe-140) reduced oedema formation in a dose-dependent manner with a maximal reduction of around 65% at a dose of 100 nmol kg^{-1} (s.c.). A significant effect could already be observed at a dose of 10 nmol kg^{-1}. The duration of the effect of icatibant (100 nmol kg^{-1}) was found to be at least 3 h. These results demonstrate the high potency and long duration of action of icatibant. Pretreatment of rats with the bradykinin B_1 antagonist, des-Arg^9-[Leu^8]-BK did not affect collagenase-induced paw oedema. Thus, the observed collagenase-induced effects are mainly mediated by BK through activation of B_2 receptors.

4 Pretreatment of adult rats with capsaicin (125 mg kg^{-1}, s.c.) three weeks before the collagenase injection caused a significant attenuation of the paw oedema and of plasma extravasation but was significantly less effective than icatibant (100 nmol kg^{-1}, s.c.). The non-peptide substance P antagonist, CP-96,345 (10 μmol kg^{-1}, i.v.) significantly reduced collagenase-induced oedema formation to a degree comparable with that seen after capsaicin pretreatment. The inhibition by the substance P antagonist was significantly smaller than that seen after icatibant. The inhibitory effect of icatibant in capsaicin-pretreated rats, or of icatibant together with CP-96,345 in untreated rats, was not greater than that of icatibant alone in rats treated with the vehicle for either capsaicin or CP-96,345. CP-96,344 (10 μmol kg^{-1}, i.v.), the inactive enantiomer of CP-96,345, did not affect collagenase-induced paw oedema. In capsaicin-pretreated rats, CP-96,345 (10 μmol kg^{-1}, i.v.) did not reduce collagenase-induced paw oedema.

The subplantar injection of bradykinin (30 nmol) induced a paw oedema comparable with that induced by collagenase (100 μg). CP-96,345 (10 μmol kg^{-1}, i.v.), but not CP-96,344 (10 μmol kg^{-1}, i.v.), significantly reduced the bradykinin-induced paw oedema. These findings indicate that collagenase leads to the release of bradykinin; bradykinin then stimulates afferent C-fibre terminals and causes the release of substance P and probably also neurokinin A, which augment the oedema-inducing effect of bradykinin.

5 Indomethacin or mepyramine plus cimetidine failed to inhibit collagenase-induced paw oedema. Thus, prostaglandins and histamine do not seem to be involved in collagenase-induced paw oedema.

6 After subplantar injection of collagenase, the sensitivity scores in a modified formalin-test rapidly increased during the first 10 min. This increase was abolished by pretreatment with icatibant (100 nmol kg^{-1}, s.c.) indicating that the stimulation of nociceptive afferent neurones following injection of collagenase is due to the action of released kinins.

7 In conclusion, bradykinin appears to be the main mediator of inflammation induced by a collagenase from *Clostridium histolyticum*. As well as having direct relevance to a known pathological condition, collagenase-induced paw oedema could prove to be a useful model in inflammation research and in the investigation of bradykinin antagonists. The present results might provide an experimental basis for clinical investigations of the effects of icatibant in infectious diseases where the release of collagenases from bacteria causes rapid spreading of inflammation.

Keywords: Collagenase; *Clostridium histolyticum*; bradykinin; icatibant; CP-96,345; capsaicin; paw oedema; plasma protein extravasation

Introduction

Clostridium histolyticum is one of the bacteria that are found in clostridial myonecrosis, i.e. gas gangrene. This life-threatening disease is caused by toxins produced by clostridial bacteria. Such bacteria are present throughout the environment. Although the majority of cases occur after injuries such as open fractures, wounds, or burns, clostridial myonecrosis has also been reported in cases of 'clean' surgery (Parker, 1969). The management of patients with gas gangrene is difficult and requires intensive and aggressive medical intervention including extensive resection of necrotic tissue or even amputation to save the patient's life. The earliest signs of gas gangrene are disproportionate pain and pronounced oedema at the site of the wound. These symptoms spread as the Clostridia invade neighbouring tissue.

Collagenases, which are components of the β-toxin produced by *C. histolyticum*, are thought to play a major role in

[1] Author for correspondence.

the pathology of gas gangrene because they destroy the connective tissue barriers and thereby facilitate the invasion of the tissue by bacteria (Hatheway, 1990). It has been reported that anti-inflammatory drugs such as aspirin and dexamethasone inhibited to some degree collagenase-induced inflammation (Vargaftig *et al.*, 1976). The aim of the present study was to elucidate further which mediators are involved in the oedema and plasma protein extravasation following a subplantar injection in rats of collagenase (EC 3.4.24.3) from *C. histolyticum*.

Some of these results have been presented to the British Pharmacological Society (Legat *et al.*, 1993).

Methods

Female Sprague Dawley rats (200–280 g) were anaesthetized with pentobarbitone sodium (50 mg kg^{-1}, i.p.). Collagenase (EC 3.4.24.3) from *C. histolyticum*, 100 μg dissolved in 100 μl of a 154 mM NaCl solution (saline), was given, as a subplantar injection (s.p.), into one hind paw. In experiments in which the time course of development of paw oedema after the injection of different doses of collagenase was studied, 30 or 300 μg doses of the enzyme were also used. In all experiments, the contralateral hind paw served as control and was injected with 100 μl saline.

The magnitude of the oedema was assesssed by measuring the paw volume with a plethysmometer (Ugo Basile, Italy) before, and at given time intervals during, the first hour after the collagenase injection; in some experiments it was also measured 300 min after the injection.

For the quantitative evaluation of plasma protein extravasation, the extravasation of Evans blue dye into the paws was measured (Gamse *et al.*, 1980). Evans blue (20 mg kg^{-1}) was injected i.v. 5 min before the subplantar injection of collagenase. At the end of the experiment, the rats were exsanguinated, each hind paw was cut off at the ankle joint and immersed in 5 ml formamide for 24 h at 50°C. The concentration of Evans blue in the formamide was determined photometrically at 620 nm.

The time course of plasma protein extravasation after the subplantar injection of collagenase into one hind paw and of saline into the contralateral hind paw was studied by measuring the Evans blue extravasation in the paws during 4 consecutive 10 min periods following the collagenase injection. A separate group of rats was used for each of the 4 consecutive 10 min periods. In the first group of rats, Evans blue was injected at the same time as the collagenase; in the second, third and fourth groups of rats Evans blue was injected 10, 20 and 30 min after the collagenase, respectively. In each group of rats, the hind paws were detached 10 min after the Evans blue injection and Evans blue extravasation determined as described above.

Oedema formation and plasma extravasation in the hind paw was also measured after the subplantar injection of heat-inactivated collagenase (exposure to 60°C for 30 min).

In another set of experiments, oedema formation was measured after a subplantar injection of bradykinin (30 nmol in 100 μl saline).

Bradykinin (BK) antagonists

Icatibant In order to study the effectiveness of this bradykinin B_2 antagonist, rats were given a s.c. injection of 1, 3, 10, 30, 100, 300 or 1000 nmol kg^{-1} icatibant, 60 min before a subplantar injection of 100 μg collagenase and the paw volume was measured during the 60 min period following the collagenase injection. The duration of action of icatibant was measured by injecting rats with 100 nmol kg^{-1} icatibant 10, 30, 60, 180, 360 or 540 min before the subplantar injection of collagenase (100 μg).

Des-Arg^9-[Leu^8]-bradykinin Rats received i.v. injections of this bradykinin B_1 antagonist (200 nmol kg^{-1}) 10 min before the subplantar injection of 100 μg collagenase.

The ensuing paw oedema was measured after both bradykinin antagonists.

Capsaicin pretreatment

Adult rats were treated with capsaicin three weeks before the collagenase experiments according to a regimen similar to that used by Esplugues *et al.* (1989). Capsaicin, 25 mg kg^{-1}, was injected into rats, under ether anaesthesia, twice on day one and in the morning of day two; in the afternoon of day two the dose used was 50 mg kg^{-1}. Before the morning injections of capsaicin, the rats were given a mixture of terbutaline (0.2 mg kg^{-1}), aminophylline (20 mg kg^{-1}) and atropine (0.1 mg kg^{-1}) i.p. to prevent bronchoconstriction by capsaicin. An equal number of rats was treated similarly, but received vehicle instead of capsaicin. One group of capsaicin-pretreated rats and one group of vehicle-pretreated rats received icatibant (100 nmol kg^{-1}, s.c.), 60 min before the collagenase injection. The corresponding control groups received a s.c. injection of 1 ml kg^{-1} saline. Paw volume was measured during the 60 min following the subplantar injection of collagenase (100 μg) and plasma extravasation was determined at the end of the experiment.

The non-peptide substance P antagonist, CP-96,345

Rats were pretreated either with CP-96,345 (10 μmol kg^{-1}, i.v.) 10 min prior to the injection of collagenase, or with icatibant (100 nmol kg^{-1}, s.c.) 60 min before collagenase. In another group of rats both pretreatments were combined. Control rats received the vehicles by the corresponding routes. Paw volume was measured during the 60 min period following the collagenase injection and plasma protein extravasation was determined at the end of the experiment.

In order to verify that the effects of CP-96,345 were specific, control experiments were carried out in rats which were injected i.v. 10 min before collagenase with the inactive enantiomer, CP-96,344 (10 μmol kg^{-1}).

Pretreatment of rats with capsaicin combined with CP-96,345

Rats were pretreated with capsaicin as described above. Three weeks later they were injected with CP-96,345 (10 μmol kg^{-1}, i.v.) or saline 10 min before the subplantar injection of collagenase. The magnitude of the oedema was determined as above.

Bradykinin-induced paw oedema: pretreatment with CP-96,345 or CP-96,344

Paw oedema was induced by a subplantar injection of bradykinin (30 nmol in 100 μl saline). Rats were pretreated with CP-96,345 (10 μmol kg^{-1}, i.v.), CP-96,344 (10 μmol kg^{-1}, i.v.) or saline (i.v.) 10 min before the subplantar injection of bradykinin.

Blockade of histamine receptors or inhibition of prostaglandin formation

Mepyramine (35 μmol kg^{-1}) and cimetidine (40 μmol kg^{-1}) were injected i.p. 60 min before collagenase (100 μg); indomethacin (30 μmol kg^{-1}) was injected i.p. 60 min before collagenase (100 μg). The corresponding control rats received the appropriate vehicles. Paw volume was measured either during the 60 min period (mepyramine plus cimetidine) or the 300 min period (indomethacin) following the collagenase injection.

Activity scores

The behavioural reactions of rats after subplantar injection of collagenase (100 μg in 100 μl saline) were rated in a modified formalin-test (Cohen *et al.*, 1984) by sensitivity scores (0 = walking or sitting normally; 1 = walking or sitting favouring the paw not injected with collagenase; 2 = lifting the injected paw off the ground; 3 = licking the injected paw). The integrated sensitivity scores for consecutive 5 min periods after the injection of collagenase were calculated for each rat; the total observation period after the subplantar injection was 60 min. The integrated sensitivity score was calculated by summing the score values of each second during a 5 min period and dividing the resulting sum by 300.

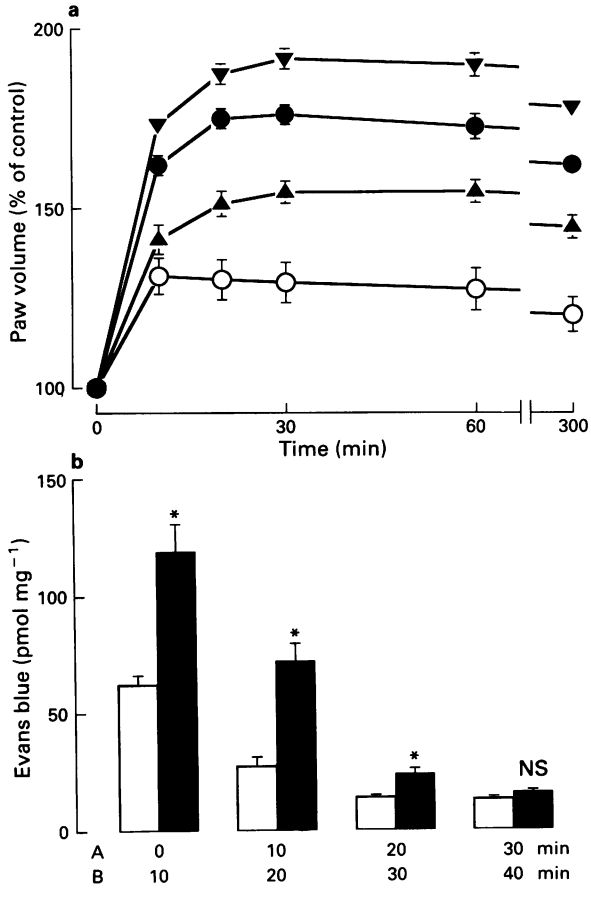

Figure 1 Collagenase-induced paw oedema. (a) Time course and dose-response relationship of collagenase-induced paw oedema. Collagenase (30 ▲, 100 ●, 300 μg ▼) or saline (○) was administered as a subplantar injection (100 μl) into rat hind paws at time 0 min. Paw volume was monitored during the following 300 min. Volume of paw oedema is expressed as a percentage of the paw volume before the subplantar injection of collagenase or saline. Data are means ± s.e.mean; ($n = 6$). (b) Collagenase-induced extravasation of plasma proteins as indicated by the Evans blue content of the paws in 4 consecutive 10 min periods following the subplantar injection of collagenase (100 μg in 100 μl saline) at time 0. The contralateral hind paws were injected with 100 μl saline. The plasma protein extravasation during each of the 4 consecutive 10 min periods after collagenase injection was evaluated by using a separate group of rats for each 10 min period. 'Time A' gives the time after the injection of collagenase at which the rats in the different groups were injected with Evans blue (20 mg kg^{-1}, i.v.). 'Time B' gives the time after the injection of collagenase at which the hind paws of rats in the different groups were detached for the determination of their Evans blue content. Data are means ± s.e.mean of the Evans blue extravasation, given as pmol mg^{-1} wet weight, in the paws injected with collagenase (solid columns) and the contralateral paws injected with saline (open columns). Significance of difference from saline control: *$P < 0.05$, NS = not significant ($P < 0.10$). $n = 6$.

Sixty min before the subplantar injection of collagenase, rats were treated either with icatibant (100 nmol kg^{-1}, s.c.) or with saline.

Materials

Collagenase (EC 3.4.24.3) from *Clostridium histolyticum* (Type II, Sigma), Evans blue, aminophylline and des-Arg^9-[Leu^8]-bradykinin (Sigma, St. Louis, MO, U.S.A.); icatibant (D-Arg-[Hyp^3-Thi^5-D-Tic^7-Oic^8-bradykinin] formerly named Hoe-140, mol. wt. = 1863) (Hoechst AG, Frankfurt/Main, Germany); CP-96,345 {(2S,3S)-*cis*-2-(diphenylmethyl)-*N*-((2-methoxyphenyl)-methyl)-1-azabicyclo[2.2.2]octan-3-amine dihydrochloride; mol. wt. = 499.02} CP-96,344 {[2R,3R)-*cis*-2-(diphenylmethyl)-*N*-((2-methoxyphenyl)-methyl)-1-azabicyclo-[2.2.2]octan-3-amine dihydrochloride; mol. wt. = 499.02} (Pfizer Inc., Groton, Conn., U.S.A.); mepyramine and cimetidine (Smith Kline Beecham, U.K.); indomethacin and atropine sulphate (Merck Sharp & Dohme, U.S.A.); pentobarbitone sodium (Sanofi Santé, France); capsaicin (Fluka, Buchs, Switzerland); terbutaline sulphate (Astra, Wedel/Holstein, Germany); ethanol and Tween 80 (Merck, Darmstadt, Germany); bradykinin (mol. wt. = 1306.45) (Bachem, Bubendorf, Switzerland).

Capsaicin was dissolved in a mixture of 10% (v/v) ethanol and 10% (v/v) Tween 80 in saline.

Statistical analysis

The paw volumes measured after the subplantar injections of collagenase, bradykinin or of saline were expressed as a % of the value determined immediately prior to the injection. From the values obtained at regular intervals during the course of the experiment the area under the curve was calculated. The data obtained for paw volume and for Evans blue extravasation were tested for deviation from normality by the Shapiro-Wilk test (Conover, 1980). In order to test for a possible heteroskedasticity, the Levene test (Sachs, 1984) was used. Multiple comparisons between the treatment groups were then made using the least significance difference test (Sachs, 1984). The mean sensitivity scores for each consecutive 5 min period obtained after the subplantar injection of collagenase were compared with the values for saline-injected control rats using the Mann-Whitney U test. In the experiments in which the time course of plasma protein extravasation after subplantar injection of collagenase was studied, the extravasation in paws injected with collagenase was compared with that in the contralateral paws injected with saline using the Wilcoxon matched pairs signed rank test. Multiple nonparametric comparisons with a control were used to compare the net amount of plasma protein which leaked out of paw vessels in the 2nd, 3rd and 4th 10 min period with that in the 1st 10 min period after the collagenase injection.

Results

Time course of development of paw oedema after injection of three different doses of collagenase

Subplantar injection of collagenase (30, 100 and 300 μg in 100 μl saline) into rat hind paws induced a dose-dependent increase in paw volume (Figure 1a). The paw oedema reached its maximum within 30 min; it was only slightly smaller after 300 min. The collagenase-injected paws were significantly larger ($P < 0.001$) than the control paws injected with 100 μl saline. Subplantar injection of heat-inactivated collagenase (100 μg) did not induce paw oedema or plasma protein extravasation. Paw volume was increased to 119 ± 3% after 30 min and 120 ± 3% after 60 min in paws injected with saline, and to 120 ± 3% after 30 min and 121 ± 4% after 60 min in paws injected with heat-inactivated col-

lagenase ($n = 6$). Extravasation of Evans blue was 59 ± 11 pmol mg^{-1} wet weight in paws injected with saline and 68 ± 11 pmol mg^{-1} wet weight in paws injected with heat-inactivated collagenase ($n = 6$).

Time course of plasma protein extravasation after collagenase injection

The amount of plasma protein which leaked out of the paw vessels after the injection of collagenase (100 μg, s.p.) was largest during the first 10 min and, thereafter, declined with time. In the contralateral hind paws injected with saline, the extravasation of plasma proteins was also largest during the 1st 10 min and then declined. In the 1st, 2nd and 3rd 10 min period, the extravasation of plasma proteins in paws injected with collagenase was significantly ($P<0.05$) larger than in the contralateral paws injected with saline; in the 4th 10 min period the difference was not significant ($P<0.10$) (Figure 1b).

The net amount of plasma protein extravasated, i.e. the difference between the values for collagenase-injected and for saline-injected paws, was similar in the 1st and 2nd 10 min periods but was significantly smaller in the 3rd and 4th observation periods ($P<0.05$, $P<0.001$, respectively).

Effects of bradykinin antagonists on collagenase-induced oedema

Icatibant: dose-response relationship Icatibant, 10–1000 nmol kg^{-1}, given s.c. 60 min before a subplantar injection of collagenase (100 μg), significantly ($P<0.01$) reduced the resulting paw oedema. The inhibition caused by doses of 30–1000 nmol kg^{-1} icatibant was not significantly different from that caused by 10 nmol kg^{-1} (Figure 2a).

Icatibant: duration of action Icatibant (100 nmol kg^{-1}, s.c.) given up to 3 h before the subplantar injection of collagenase significantly ($P<0.01$) reduced collagenase-induced paw oedema (Figure 2b). Icatibant did not reduce the oedema when administered 6 or 9 h before collagenase.

Icatibant: effect on plasma protein extravasation Icatibant (100 nmol kg^{-1}, s.c.) given 60 min before a subplantar injection of collagenase (100 μg) caused a reduction in plasma extravasation that was similar to the reduction in the paw oedema (Figure 3b and Figure 4b).

Des-Arg^9-[Leu^8]-bradykinin Pretreatment of rats with the bradykinin B_1 antagonist des-Arg^9-[Leu^8]-BK (200 nmol kg^{-1}, i.v.) 10 min before a subplantar injection of collagenase did not affect collagenase-induced paw oedema (Table 1).

Effects of capsaicin on collagenase-induced paw oedema

Pretreatment of adult rats with capsaicin (125 mg kg^{-1}, s.c. three weeks before collagenase) significantly ($P<0.05$) reduced the collagenase-induced paw oedema (Figure 3a). However, the reduction brought about by capsaicin was significantly ($P<0.05$) smaller than that caused by icatibant (100 nmol kg^{-1}, s.c.). The inhibitory effect of icatibant in capsaicin-pretreated rats was not different from that in control rats.

The extravasation of Evans blue induced by collagenase was significantly reduced by capsaicin pretreatment ($P<0.001$), but to a significantly ($P<0.05$) lesser degree than by icatibant. The inhibitory effects of icatibant and capsaicin were not additive (Figure 3b).

Effect of the substance P antagonist, CP-96,345, on collagenase-induced oedema

CP-96,345 (10 μmol kg^{-1}, i.v.) significantly ($P<0.05$) reduced the collagenase-induced paw oedema (Table 1) to a degree

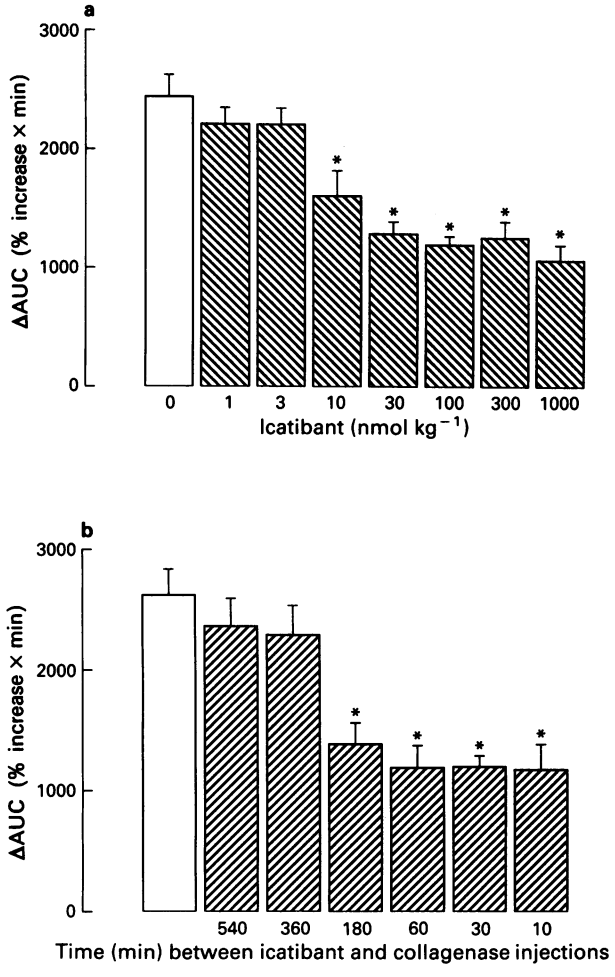

Figure 2 Effect of icatibant on collagenase-induced paw oedema. The area under the volume-time curve (AUC) of paw volume increase above the pre-injection volume was calculated for paws injected with collagenase and for the contralateral paws injected with saline. The difference between the two AUC values gives the net increase in paw volume induced by collagenase. (a) Effect of increasing doses of icatibant on collagenase-induced paw oedema. Icatibant (1, 3, 10, 30, 100, 300, or 1000 nmol kg^{-1} in 1 ml kg^{-1} saline, s.c.) was injected 60 min before collagenase (hatched columns). Control rats received the corresponding volume of saline s.c. (open column). Paw volume was measured repeatedly for 60 min after the injection of collagenase (100 μg) into one hind paw and saline (100 μl) into the contralateral paw. Data are means ± s.e.mean of the net increase of paw volume (ΔAUC) after injection of collagenase. Significance of difference from saline control: $^*P<0.01$; $n = 6$. (b) Effect of increasing the pretreatment interval on the inhibitory effect of icatibant. Icatibant (100 nmol kg^{-1}, s.c.) was injected 10, 30, 60, 180, 360 or 540 min before the subplantar injection of collagenase (100 μg) or saline (100 μl) into the rat hind paws. Data are means ± s.e.mean of the ΔAUCs (net increase of paw volume) after injection of collagenase. Significance of difference from saline control: $^*P<0.01$; $n = 6$.

similar to that caused by capsaicin pretreatment, but was significantly ($P<0.05$) less effective than icatibant (100 nmol kg^{-1}, s.c.). The effects of icatibant and CP-96,345 were not additive (Figure 4a). In capsaicin-pretreated rats CP-96,345 (10 μmol kg^{-1}, i.v.) did not further reduce collagenase-induced paw oedema (data not shown).

In contrast to icatibant, CP-96,345 (10 μmol kg^{-1}) did not significantly reduce collagenase-induced plasma extravasation, nor did it augment the effect of icatibant on plasma extravasation (Figure 4b).

CP-96,344, the inactive enantiomer of CP-96,345, did not affect collagenase-induced paw oedema (Table 1).

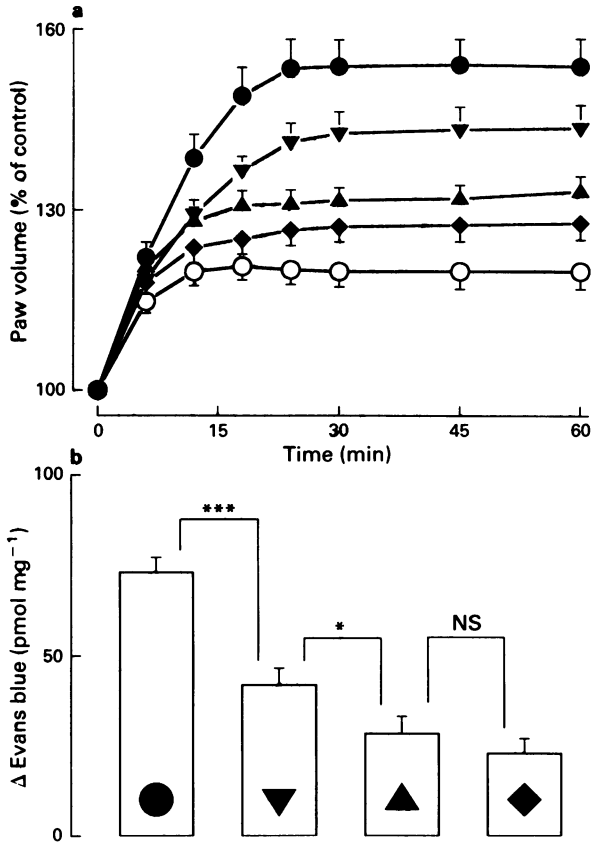

Figure 3 Effect of capsaicin on collagenase-induced paw oedema and plasma extravasation. Paw oedema was induced by subplantar injection of collagenase (●, 100 μg). The contralateral hind paws were injected with 100 μl saline (○). Rats were pretreated either with capsaicin (▼, 125 mg kg^{-1}, s.c., 3 weeks prior to the collagenase injection), or with icatibant (▲, 100 nmol kg^{-1}, s.c., 60 min before collagenase injection) or with capsaicin together with icatibant (◆). (a) Effect of capsaicin and/or icatibant on collagenase-induced paw oedema. Paw volume was measured for 60 min after subplantar injection of collagenase or saline. The values given are means ± s.e.mean ($n = 6$) of paw volumes expressed as a percentage of the pre-injection paw volume. For reasons of clarity only the paw volume-time curve of saline-injected paws of non pretreated control rats is given. This was not different from the curve obtained with pretreated rats ($n = 6$). (b) Effect of capsaicin and/or icatibant on collagenase-induced extravasation of plasma proteins. Evans blue (20 mg kg^{-1}) was injected i.v. 5 min before the subplantar injection of collagenase or saline. Immediately after the last measurement of paw volume, i.e. 60 min after collagenase injection, rats were exsanguinated, the hind paws cut off and the Evans blue content determined. Column heights are means ± s.e.mean of the difference (Δ) between Evans blue extravasation in paws injected with collagenase and Evans blue extravasated in the contralateral paws injected with saline. The amount of Evans blue extravasated in paws injected with saline was about 50 pmol mg^{-1} wet weight in each group of rats. Significance of differences between groups: $^{*}P < 0.05$, $^{***}P < 0.001$; NS, not significant. $n = 6$.

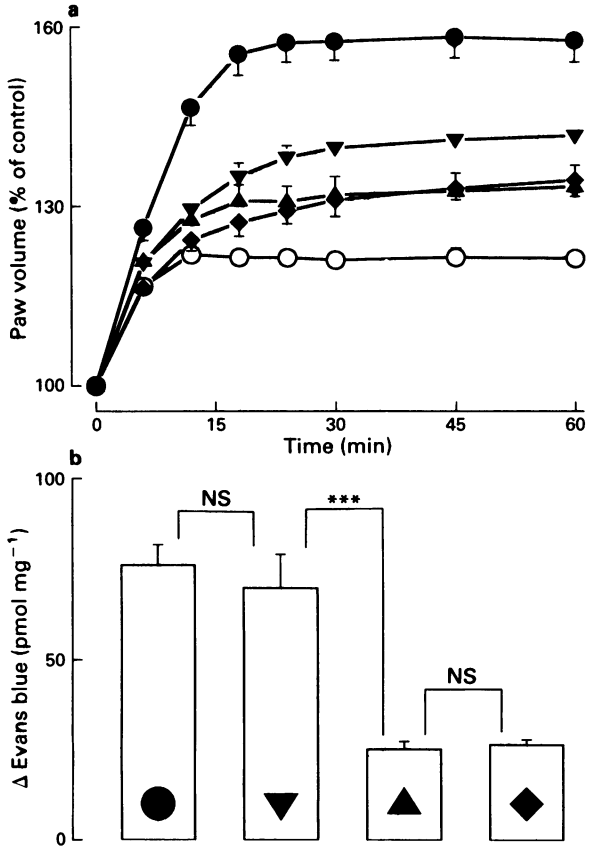

Figure 4 Effect of pretreatment with CP-96,345 on collagenase-induced paw oedema and plasma extravasation. Paw oedema was induced by subplantar injection of collagenase (●, 100 μg), the contralateral hindpaws were injected with 100 μl saline (○). Rats were pretreated with CP-96,345 (▼, 10 μmol kg^{-1}, i.v., 10 min before collagenase), or with icatibant (▲, 100 nmol kg^{-1}, s.c., 60 min before collagenase) or with both CP-96,345 and icatibant (◆). (a) Effect of the substance P antagonist, CP-96,345 and/or icatibant on collagenase-induced paw oedema. Paw volume was measured during the 60 min period after subplantar injection of collagenase or saline. The values given are means ± s.e.mean ($n = 6$–11) of paw volumes expressed as a percentage of the pre-injection paw volume. For reasons of clarity only the paw volume-time curve of saline-injected paws of control rats is given; it is similar to the curve obtained for the saline injected paws of drug-pretreated rats. (b) Effect of substance P antagonist, CP-96,345 and/or icatibant on collagenase-induced extravasation of plasma proteins. Evans blue (20 mg kg^{-1}) was injected i.v. 5 min before the subplantar injection of collagenase or saline. Sixty min after the collagenase injection the rats were exsanguinated, the hind paws cut off and the Evans blue content determined. Column heights represent means ± s.e.mean of the difference (Δ) between Evans blue extravasation in paws injected with collagenase and Evans blue extravasation in the contralateral paws injected with saline. The amount of Evans blue extravasated in paws injected with saline was about 50 pmol mg^{-1} wet weight in each group of rats. Significance of difference between treatments: $^{***}P < 0.001$; NS, not significant. $n = 6$–11.

Effect of CP-96,345 or CP-96,344 on bradykinin-induced paw oedema

Subplantar injection of BK (30 nmol) caused a paw oedema comparable with that caused by collagenase (100 μg, s.p.), i.e. about 160% of the pre-injection paw volume.

Pretreatment of rats with the substance P antagonist, CP-96,345 (10 μmol kg^{-1}, i.v.) significantly reduced both paw oedema induced by bradykinin (30 nmol) (Figure 5) and collagenase-induced paw oedema to a similar extent, i.e. to about 140% of the pre-injection paw volume.

The inactive enantiomer CP-96,344 had no effect on bradykinin-induced oedema formation (Figure 5).

Effects of drugs that block histamine receptors or inhibit prostaglandin formation

The pretreatment of rats with mepyramine (35 μmol kg^{-1}, i.p.) combined with cimetidine (40 μmol kg^{-1}, i.p.) did not reduce collagenase-induced paw oedema (Table 1). Indomethacin (30 μmol kg^{-1}, i.p.) also had no effect on collagenase-induced paw oedema (Table 1).

Behaviour after subplantar injection of collagenase

Immediately after subplantar injection of collagenase into the hind paws of saline-pretreated rats, there was a rapid in-

Table 1 Effect of drugs, which block histamine or substance P receptors or prostaglandin formation, on collagenase-induced oedema in the hind paw of the rat

Drug	Pretreatment Dose (μmol kg^{-1})	Route	% increase in paw volume Time after collagenase 30 min	60 min	300 min
			%	%	%
des-Arg^9[Leu^8]-BK	0.2	i.v.	178 ± 6	178 ± 4	–
Saline			175 ± 3	178 ± 3	–
Mepyramine	35	i.p.			
+ cimetidine	40	i.p.	177 ± 4	172 ± 3	–
Saline			179 ± 5	175 ± 4	–
Indomethacin	30	i.p.	182 ± 2	182 ± 1	176 ± 2
Saline			181 ± 3	181 ± 3	177 ± 3
CP-96,345	10	i.v.	140 ± 1*	142 ± 1*	–
Saline			157 ± 3	158 ± 4	–
CP-96,344	10	i.v.	171 ± 3	174 ± 3	–
Saline			170 ± 2	168 ± 3	–

The dose of collagenase given by subplantar injection was 100 μg (dissolved in 100 μl saline). Results are expressed as a percentage of paw volume before collagenase injection. Data are means ± s.e.mean. $n = 6-9$. Significance of difference from saline control: *$P < 0.05$.

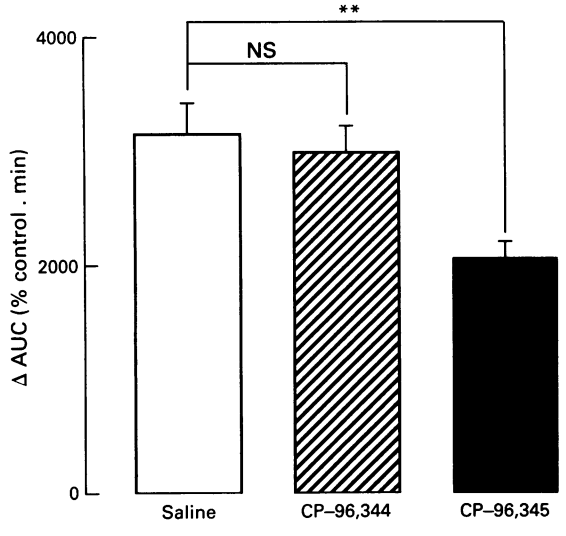

Figure 5 Effect of pretreatment with CP-96,345 or CP-96,344 on bradykinin-induced paw oedema. The area under the paw volume-time curve (AUC) above the level of pre-injection volume was calculated for paws injected with bradykinin (BK, 30 nmol in 100 μl saline) and for the contralateral paws injected with 100 μl saline. The difference between the two AUC values gives the net increase in paw volume induced by BK. Rats were pretreated either with CP-96,345 (10 μmol kg^{-1}, i.v., 10 min before BK; solid column) or with CP-96,344 (10 μmol kg^{-1}, i.v., 10 min before BK; hatched column). Control rats received the corresponding volume of saline i.v. (open column). Paw volume was measured repeatedly for 60 min after the injection of BK into one hind paw and after the injection of saline into the contralateral hind paw. Data are means ± s.e.mean of the net increase of paw volume (ΔAUC) after the injection of BK. Significance of difference from saline control: **$P < 0.01$; NS, not significant. $n = 10$.

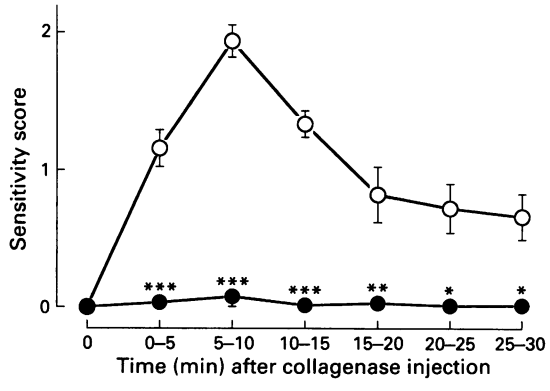

Figure 6 Sensitivity scores after subplantar injection of collagenase. Behavioural reactions of rats which received a subplantar injection of collagenase (100 μg) were rated with sensitivity scores from 0 to a maximum of 3. Sixty min before the collagenase injection, rats were pretreated s.c. either with icatibant (●, 100 nmol kg^{-1}) or with a similar volume of saline (○). The total observation period following the injection of collagenase was 60 min. For reasons of clarity only the first 30 min after the collagenase injection are given in the graph; thereafter, until the end of the observation period, the difference in the sensitivity scores for rats pretreated with icatibant and for control rats remained unchanged (*$P < 0.02$). Values are means ± s.e.mean of the integrated sensitivity scores in consecutive 5 min periods after the injection of collagenase. The integrated sensitivity score in a 5 min period was calculated by summing the sensitivity scores for each second during the 5 min period and dividing the sum by 300. Significance of difference between control and icatibant-pretreated rats: *$P < 0.02$; **$P < 0.01$; ***$P < 0.002$. $n = 6-9$.

crease in the sensitivity scores (Figure 6). A peak in the integrated sensitivity score was reached in the second 5 min period after the injection of collagenase. Thereafter, the score declined rapidly. Pretreatment of rats with icatibant (100 nmol kg^{-1}, s.c.) 60 min before collagenase almost completely ($P < 0.002$) prevented the effect of collagenase.

Discussion

The β-toxin of *Clostridium histolyticum* is comprised of a mixture of at least seven collagenases, which differ from mammalian collagenases in their mode of action (Hatheway, 1990). Clostridial collagenases act on all known types of collagen and can cleave native triple helical collagen into small fragments, mostly tripeptides, whereas mammalian collagenases are specific for certain types of collagen and often cleave only one protein bond in a polypeptide chain of triple helical collagen, resulting in two polypeptide fragments (Han *et al.*, 1992). Thus, clostridial collagenases are very effective in destroying the connective tissue barrier. Breakdown of connective tissue facilitates bacterial invasion into tissues and provides conditions necessary for bacterial proliferation and growth.

The subplantar injection of collagenase from *C. his-*

tolyticum into rat hind paws induced a dose-dependent paw oedema. Injection of heat-inactivated collagenase did not cause oedema, as has previously been shown by Vargaftig *et al.* (1976), and also did not cause extravasation of plasma proteins. Paw oedema development and plasma protein extravasation were most pronounced during the first 20 min after subplantar injection of collagenase and in most experiments the paw oedema reached its maximum within 30 min. The time course of sensitivity scores showed a peak in the 2nd 5 min period after the challenge with collagenase. The rapid onset of the effects of clostridial collagenase implies that the collagenase itself and/or the immediate release of fast acting inflammatory mediators, rather than breakdown of the tissues, leads to an increase in vascular permeability and to stimulation of sensory nerves. This contrasts with the report by Vargaftig *et al.* (1976) who suggested that the early phase of paw oedema development after injection of clostridial collagenase into rat hind paws is only of minor importance for the inflammatory action of this enzyme.

Pretreatment of rats with a potent bradykinin B_2 receptor antagonist, icatibant [formerly named compound I (Lembeck *et al.*, 1991) or Hoe-140 (Hock *et al.*, 1991; Wirth *et al.*, 1991)], caused a pronounced reduction of the collagenase-induced paw oedema and of plasma protein extravasation. In addition, icatibant abolished the increase in sensitivity scores in a behaviour test after subplantar injection of collagenase in unanaesthetized rats.

Icatibant has been shown to be inactive against a great variety of mediators including angiotensin II, noradrenaline, histamine, acetylcholine, 5-hydroxytryptamine, substance P and neurokinin A (Lembeck *et al.*, 1991; Wirth *et al.*, 1991; Damas & Remacle-Volon, 1992; Rhaleb *et al.*, 1992). Since icatibant does not inhibit the action of des-Arg^9-BK at the B_1 receptor (Hock *et al.*, 1991; Rhaleb *et al.*, 1992), the present results point towards an involvement of B_2, but not B_1 receptors in collagenase-induced paw oedema.

Pretreatment of adult rats with capsaicin in a dose sufficient to impair the function of sensory afferent nerve fibres (Gamse *et al.*, 1980; 1981) significantly decreased the collagenase-induced paw oedema and the plasma protein extravasation. A significant reduction of the paw oedema, similar to that caused by capsaicin, was also induced by CP-96,345, a non-peptide antagonist of substance P which is specific for NK_1-receptors (McLean *et al.*, 1991; Snider *et al.*, 1991). The reduction of the collagenase-induced paw oedema brought about by icatibant was, however, significantly greater than that caused by capsaicin or by CP-96,345. The effect of pretreatment with icatibant together with capsaicin or icatibant together with CP-96,345 did not exceed that of icatibant alone. These results suggest that the collagenase-induced paw oedema is caused firstly by a direct action of BK and secondly by the action of neuropeptides released from sensory afferent neurones by BK. The ability of BK to release neuropeptides from peripheral terminals of capsaicin-sensitive primary afferents has recently been reviewed by Geppetti (1993). In addition, our findings indicate that, in collagenase-induced paw oedema, the effects of neuropeptides released from sensory afferent neurones are mainly mediated by activation of NK_1-receptors. Thus, tachykinins, especially substance P and probably also neurokinin A, seem to be the most important of the neuropeptides involved in the inflammatory effect of collagenase. The assumption that bradykinin releases tachykinins which then act on NK_1-receptors is further supported by our findings that CP-96,345 not only significantly reduced the collagenase-induced paw oedema but also caused a similar reduction of rat paw oedema induced by an equipotent dose of BK. Nonspecific effects of CP-96,345, reported to appear when it is used in high doses (Constantine *et al.*, 1991; Donnerer *et al.*, 1992; Griesbacher *et al.*, 1992; Lembeck *et al.*, 1992a), can be ruled out since the inactive enantiomer, CP-96,344, did not affect the oedema induced by collagenase or BK. In addition, CP-96,345 did not affect collagenase-induced paw oedema in rats which had been pretreated with capsaicin. This indicates that CP-96,345 blocks tachykinins released from capsaicin-sensitive afferent neurones.

Whereas CP-96,345 significantly reduced collagenase-induced formation of paw oedema, no significant reduction of collagenase-induced plasma protein extravasation by CP-96,345 was observed. At present there is no satisfactory explanation for this discrepancy. It may indicate differences in the mechanisms which lead to the increases in the vascular permeabilities for protein-free fluid and for plasma proteins.

It has been reported previously (Lembeck *et al.*, 1992b) that infusion of BK into the femoral artery of rat isolated hind legs does not cause histamine release. In the present study, a role for histamine in the formation of the paw oedema induced by clostridial collagenase was excluded since it was not affected by pretreatment with mepyramine and cimetidine. These findings are in accordance with observations of Vargaftig *et al.* (1976). However, we could not confirm a reduction of the collagenase-induced paw oedema by indomethacin. Our findings thus suggest that prostaglandins are not involved in collagenase-induced paw oedema.

The part of the paw oedema which is prevented by icatibant but is not affected by CP-96,345 or capsaicin is probably mediated by a direct action of BK on endothelial cells and/or other parts of the blood vessel walls. This action could involve vasodilatation of pre-capillary arterioles, constriction of post-capillary venules, and increase of microvascular leakage as a result of endothelial cell contraction and widening of intracellular junctions (Johnson, 1979).

The BK-induced increase in vascular permeability after injection of collagenase is mediated through activation of bradykinin B_2 receptors, since the bradykinin B_1 antagonist des-Arg^9-[Leu^8]-BK had no effect on the formation of the oedema. This also applies to the action of BK on sensory afferent neurones leading to the peripheral release of tachykinins.

From the time course of the formation of the collagenase-induced paw oedema, it can be seen that the inhibitory effects of icatibant, capsaicin and CP-96,345 are present during the first minutes of the oedema formation. This indicates that BK and tachykinins are released very shortly after the subplantar injection of collagenase and that later than 30 min after the injection of collagenase no further mediator with a noticable impact on oedema formation is released.

Icatibant was found to be a potent agent for counteracting the collagenase-induced paw oedema and plasma protein extravasation. However, icatibant was not able to prevent these effects completely. In addition to the oedema, haemorrhages were observed in the paws injected with collagenase, but not in the paws injected with saline. This has already been described by Vargaftig *et al.* (1976). Just *et al.* (1970) reported that the ability of collagenase to cause haemorrhage is due to a direct collagenolytic action on the basement membranes of small vessels, thereby destroying the integrity of the vessel walls. They also showed that BK, by itself, is not able to induce haemorrhage. Thus, destruction of vessel walls leading to bleeding might account for that part of collagenase-induced paw oedema which could not be blocked by treatment with icatibant. However, the involvement of other, as yet undetected, inflammatory mediators cannot be excluded.

In conclusion, collagenase from *Clostridium histolyticum* causes severe paw oedema and plasma protein extravasation. Bradykinin, acting on bradykinin B_2 receptors, appears to be the main mediator of this inflammatory response. Part of the effect of BK is due to the release of substance P, and possibly also neurokinin A, from the peripheral terminals of sensory afferent neurones. Histamine and prostaglandins are apparently not involved in the inflammatory action of collagenase.

Icatibant could provide a new direction for supportive therapy in the prevention of tissue destruction and bacterial invasion in infectious diseases where the release of col-

lagenase from bacteria causes rapid spread of tissue inflammation.

The authors thank Mrs E. Painsipp for expert technical assistance. The work was supported by grants from the Austrian Academy of Sciences and from the Franz-Lanyar-Stiftung.

References

COHEN, S.R., ABBOTT, F.V. & MELZACK, R. (1984). Unilateral analgesia produced by intraventricular morphine. *Brain Res.*, **303**, 277–287.

CONOVER, W.J. (1980). *Practical Nonparametric Statistics*. 2nd edition. New York: Wiley.

CONSTANTINE, I.W., LEBEL, W.S. & WOODY, H.A. (1991). Inhibition of tachykinin-induced hypotension in dogs by CP-96,345, a selective blocker of NK_1 receptors. *Naunyn-Schmied. Arch. Pharmacol.*, **344**, 471–477.

DAMAS, J. & REMACLE-VOLON, G. (1992). Influence of a long-acting bradykinin antagonist, Hoe 140, on some acute inflammatory reactions in the rat. *Eur. J. Pharmacol.*, **211**, 81–86.

DONNERER, J., STARK, U., TRITTHART, H.A. & LEMBECK, F. (1992). CP-96,345, a non-peptide antagonist of substance P: III. Cardiovascular effects in mammals unrelated to actions on substance P receptors. *Naunyn-Schmied. Arch. Pharmacol.*, **346**, 328–332.

ESPLUGUES, J.V., WHITTLE, B.J.R. & MONCADA, S. (1989). Local opioid-sensitive afferent sensory neurones in the modulation of gastric damage induced by Paf. *Br. J. Pharmacol.*, **97**, 579–585.

GAMSE, R., HOLZER, P. & LEMBECK, F. (1980). Decrease of substance P in primary afferent neurones and impairment of neurogenic plasma extravasation by capsaicin. *Br. J. Pharmacol.*, **68**, 207–213.

GAMSE, R., LEEMAN, S.E., HOLZER, P. & LEMBECK, F. (1981). Differential effects of capsaicin on the content of somatostatin, substance P, and neurotensin in the nervous system of the rat. *Naunyn-Schmied. Arch. Pharmacol.*, **317**, 140–148.

GEPPETTI, P. (1993). Sensory neuropeptide release by bradykinin: mechanisms and pathophysiological implications. *Regulat. Pept.*, **47**, 1–23.

GRIESBACHER, T., DONNERER, J., LEGAT, F.J. & LEMBECK, F. (1992). CP-96,345, a non-peptide antagonist of substance P: II. Actions on substance P-induced hypotension and bronchoconstriction, and on depressor reflexes in mammals. *Naunyn-Schmied. Arch. Pharmacol.*, **346**, 323–327.

HAN, S., BLUMENFELD, O.O. & SEIFTER, S. (1992). Specific identification of collagens and their fragments by clostridial collagenase and anti-collagenase antibody. *Anal. Biochem.*, **201**, 336–342.

HATHEWAY, C.L. (1990). Toxigenic clostridia. *Clin. Microbiol. Rev.*, **3**, 66–98.

HOCK, F.J., WIRTH, K., ALBUS, U., LINZ, W., GERHARDS, H.J., WIEMER, G., HENKE, S., BREIPOHL, G., KÖNIG, W., KNOLLE, J. & SCHÖLKENS, B.A. (1991). Hoe 140 a new potent and long acting bradykinin-antagonist: *in vitro* studies. *Br. J. Pharmacol.*, **102**, 769–773.

JOHNSON, A.R. (1979). Effects of kinins on organ systems. In *Bradykinin, Kallidin and Kallikrein. (Handb. Exp. Pharmacol.*, Vol. 25, Suppl.). ed. Erdös, E.G. pp. 357–399. Berlin, Heidelberg, New York: Springer.

JUST, D., URBANITZ, D. & HABERMANN, E. (1970). Pharmakologische Charakterisierung der vaskulären Schrankenfunktion gegenüber Erythrocyten und Albumin. *Naunyn-Schmied. Arch. Pharmakol.*, **267**, 399–420.

LEGAT, F.J., GRIESBACHER, T. & LEMBECK, F. (1993). Bradykinin is the main mediator of collagenase-induced oedema in the rat paw. *Br. J. Pharmacol.*, **108**, 57P.

LEMBECK, F., DONNERER, J., TSUCHIYA, M. & NAGAHISA, A. (1992a). The non-peptide tachykinin antagonist, CP-96,345, is a potent inhibitor of neurogenic inflammation. *Br. J. Pharmacol.*, **105**, 527–530.

LEMBECK, F., GRIESBACHER, T., ECKHARDT, M., HENKE, S., BREIPOHL, G. & KNOLLE, J. (1991). New, long-acting, potent bradykinin antagonists. *Br. J. Pharmacol.*, **102**, 297–304.

LEMBECK, F., GRIESBACHER, T. & LEGAT, F.J. (1992b). Lack of significant unspecific effects of Hoe 140 and other novel bradykinin antagonists *in vitro* and *in vivo*. *Agents Actions* Suppl., **38/II**, 414–422.

MCLEAN, S., GANONG, A.H., SEEGER, T.F., BRYCE, D.K, PRATT, K.G., REYNOLDS, L.S., SIOK, C.J., LOWE III, J.A. & HEYM, J. (1991). Activity and distribution of binding sites in brain of a nonpeptide substance P (NK_1) receptor antagonist. *Science*, **251**, 437–439.

PARKER, M.T. (1969). Postoperative clostridial infections in Britain. *Br. Med. J.*, **3**, 671–676.

RHALEB, N.-E., ROUISSI, N., JUKIC, D., REGOLI, D., HENKE, S., BREIPOHL, G. & KNOLLE, J. (1992). Pharmacological characterization of a new highly potent B_2 receptor antagonist (HOE 140: D-Arg-[Hyp^3,Thi^5,D-Tic^7,Oic^8] bradykinin). *Eur. J. Pharmacol.*, **210**, 115–120.

SACHS, L. (1984). *Angewandte Statistik*. 6th edition. Berlin, Heidelberg, New York, Tokyo: Springer.

SNIDER, R.M., CONSTANTINE, J.W., LOWE III, J.A., LONGO, K.P., LEBEL, W.S., WOODY, H.A., DROZDA, S.E., DESAI, M.C., VINICK, F.J., SPRENGER, R.W. & HESS, H.-J. (1991). A potent nonpeptide antagonist of the substance P (NK_1) receptor. *Science*, **251**, 435–437.

VARGAFTIG, B.B., LEFORT, J. & GIROUX, E.L. (1976). Haemorrhagic and inflammatory properties of collagenase from C. histolyticum. *Agents Actions*, **6**, 627–635.

WIRTH, K., HOCK, F.J., ALBUS, U., LINZ, W., ALPERMANN, H.G., ANAGNOSTOPOULOS, H.,, HENKE, S., BREIPOHL, G., KÖNIG, W., KNOLLE, J. & SCHÖLKENS, B.A. (1991). Hoe 140 a new potent and long acting bradykinin-antagonist: *in vivo* studies. *Br. J. Pharmacol.*, **102**, 774–777.

(Received July 23, 1993
Revised January 31, 1994
Accepted February 9, 1994)

Br. J. Pharmacol. (1994), **112**, 461–464

Effects of a novel nonpeptide bradykinin B_2 receptor antagonist on intestinal and airway smooth muscle: further evidence for the tracheal B_3 receptor

[1]Stephen G. Farmer & Mark A. DeSiato

Pulmonary Pharmacology, ZENECA Pharmaceuticals Group, 1800 Concord Pike, Wilmington, DE 19897-2300, U.S.A.

1 We examined the effects of phosphonium, [[4-[[2-[[*bis*(cyclohexylamino)methylene] amino]-3-(2-naphthalenyl) 1-oxopropyl]amino]-phenyl]-tributyl, chloride, monohydrochloride (WIN 64338), a novel, nonpeptide bradykinin B_2 receptor antagonist, on bradykinin-induced contractions of guinea-pig isolated ileum, and guinea-pig and ferret trachea.

2 WIN 64338 potently and competitively antagonized ileal contractions, in response to bradykinin, exhibiting a pA_2 value of 7.97 ± 0.10. The compound was without effect on contractions elicited by methacholine, a muscarinic receptor antagonist. Thus, WIN 64338 is a competitive and selective antagonist of ileal B_2 receptors.

3 In contrast, WIN 64338 was completely without effect on bradykinin-induced contractions of guinea-pig or ferret trachea. Thus, even at a concentration of 1 μM, which was sufficient to cause a 100 fold decrease in ileal sensitivity to bradykinin, WIN 64338 failed to shift the bradykinin log concentration-response curves in trachea isolated from either species.

4 These data confirm that WIN 64338 represents the first reported nonpeptide antagonist of guinea-pig ileal B_2 receptors. They also provide additional evidence for heterogeneity of bradykinin receptors within the same species (guinea-pig) and, furthermore, indicate that the tracheal bradykinin receptor (B_3?) is different from that in ileal tissue (B_2).

Keywords: Bradykinin; bradykinin receptors; B_2 receptor; B_3 receptor; nonpeptide; antagonist; WIN 64338; ileum; trachea; smooth muscle

Introduction

Bradykinin receptors are typically subdivided into B_1 and B_2 subtypes, based on the rank orders of potencies of agonists and antagonists (reviewed in Farmer & Burch, 1992; Hall, 1992). For example, B_2 receptors are preferentially activated by bradykinin, [Tyr(Me)[8]]-bradykinin and kallidin, and are antagonized by analogues of [D-Phe[7]]-bradykinin (Burch *et al.*, 1990). Conversely, desArg[9]-bradykinin is a specific B_1 receptor agonist and desArg[9]-[Leu[8]]-bradykinin, a B_1 receptor antagonist (Farmer & Burch, 1992; Hall, 1992).

A few years ago, it was reported that bradykinin-induced contraction of guinea-pig trachea was very weakly inhibited by B_1 or B_2 receptor antagonists (Farmer *et al.*, 1989b). Furthermore, we found that these antagonists did not displace [^{3}H]-bradykinin binding from guinea-pig and sheep tracheal membranes, and did not inhibit bradykinin-induced $^{45}Ca^{2+}$ efflux from tracheal smooth muscle (Farmer *et al.*, 1991b). This led to the proposal that guinea-pig tracheal smooth muscle cells may express a novel B_3 receptor (Farmer *et al.*, 1989b; 1991b). Interestingly, Field and colleagues (1992) noted that several analogues of [D-Phe[7]]-bradykinin did inhibit [^{3}H]-bradykinin binding in guinea-pig trachea. The reason for these contrasting binding results is unknown.

More recently, Pyne & Pyne (1993) reported that bradykinin-stimulated phospholipase C activity in guinea-pig trachea was inhibited by D-Arg-[Hyp[3],D-Phe[7]]-bradykinin (NPC 567), a B_2 receptor antagonist, whereas activation of phospholipase D was unaffected. These investigators proposed that guinea-pig tracheal smooth muscle cells, maintained in tissue culture, express both B_2 and B_3 receptors. We also reported that bradykinin-induced prostaglandin biosynthesis in the same cell type was inhibited by NPC 567 (Farmer *et al.*, 1991b).

Until recently, B_2 receptor antagonists, including those utilized in the studies discussed above, were peptides that exhibited weak affinity (pK_b values of 6–7) for B_2 receptors and, often, displayed agonist-like activity in isolated smooth muscle preparations (Burch *et al.*, 1990). The discovery of a series represented by D-Arg-[Hyp[3],Thi[5],D-Tic[7],Oic[8]]-bradykinin (Hoe 140) (Hock *et al.*, 1991; Lembeck *et al.*, 1991) and D-Arg-[Hyp[3], D-HypS(transphenyl)[7],Oic[8]]-bradykinin (NPC 17761) (Kyle *et al.*, 1991; Burch & Kyle, 1992) yielded B_2 receptor antagonists with affinities two to three orders of magnitude greater than earlier agents. Several of these novel peptides, including Hoe 140 (Field *et al.*, 1992; Trifilieff *et al.*, 1992), NPC 17761 (Trifilieff *et al.*, 1993) and D-Arg-[Hyp[3], Thi[5],D-Tic[7],Tic[8]]-bradykinin (NPC 16731) (Farmer *et al.*, 1991a), potently antagonize bradykinin-induced responses of guinea-pig trachea. Thus, these novel agents may be antagonists of both B_2 and the putative B_3 receptors (Farmer *et al.*, 1991a; Perkins *et al.*, 1991; Pyne & Pyne, 1993).

WIN 64338 (phosphonium, [[4-[[2-[[*bis*(cyclohexylamino) methylene]amino]- 3- (2-naphthalenyl) 1-oxopropyl]amino]-phenyl]-methyl]-tributyl, chloride, monohydrochloride) is a recently discovered, nonpeptide, competitive antagonist of B_2 receptors in human lung fibroblasts and guinea-pig ileum (Sawutz *et al.*, 1993; Salvino *et al.*, 1993). In the present study, we examined the effects of WIN 64338 on the sensitivity of guinea-pig isolated ileum and trachea to bradykinin. Since ferret trachea contracts in response to bradykinin, we also investigated the effect of WIN 64338 in this tissue.

Methods

Tissue preparation

Male Dunkin-Hartley guinea-pigs (250–350 g) (Hazelton, PA, U.S.A) were killed by stunning and exsanguination.

[1] Author for correspondence.

Transverse strips of epithelium-denuded trachea, and strips of terminal ileal longitudinal smooth muscle were prepared essentially as described previously (Farmer *et al.*, 1986; 1989a). Male ferrets (1.5–2.5 kg; Marshall Farms, PA), were killed with sodium pentobarbitone, (80 mg kg^{-1}, i.p.). The chest was opened along its midline, and the trachea was removed, cleared of surrounding fat and connective tissue, cut longitudinally along its ventral surface and divided into transverse strips containing 2–3 cartilaginous rings. The epithelium was not removed from ferret trachea as this procedure has been reported not to alter sensitivity to bradykinin (Dusser *et al.*, 1988).

Each tissue was suspended, under a resting tension of 1.5 g (guinea-pig trachea and ileum) or 3 g (ferret trachea), in a 4 ml water-jacketed tissue bath containing modified Krebs-Henseleit solution (mM: NaCl 118, KCl 4.7, $CaCl_2$ 2.5, KH_2PO_4 1.2, $MgSO_4$ 1.2, $NaHCO_3$ 25.0, glucose 10.0) maintained at 37°C, and gassed with 5% CO_2 in O_2. Experiments with ileum and ferret trachea were conducted in buffer containing indomethacin (3 μM), tetrodotoxin (1 μM) and (+)-chlorpheniramine (1 μM). Indomethacin, which inhibits bradykinin-induced contraction of guinea-pig trachea (Farmer *et al.*, 1989b), was omitted from experiments with this tissue. Tissues were equilibrated for at least 60 min and the buffer replaced every 15 min. After this period, each preparation was exposed to methacholine (MCh, 10 μM) to ascertain tissue viability and obtain a reference contraction. After washout and relaxation to baseline tension, experiments were started.

Experimental protocols

For guinea-pig tissues, log concentration-response curves to bradykinin (10^{-10}–10^{-3} M) were obtained following its addition in a noncumulative fashion. After each agonist response was obtained, tissues were washed at least three times with fresh buffer until initial resting tension was recovered. Log concentration-response curves to bradykinin in ferret trachea were constructed after cumulative addition of the peptide to the bath. To obviate possibly confounding effects of tachyphylaxis (Farmer *et al.*, 1989a), only one curve was obtained in each ileal or tracheal preparation. Where appropriate, WIN 64338 was added to the bath 20 min prior to exposure to agonists. Although only one antagonist concentration was tested in a single tissue, several concentrations of WIN 64338 could be examined in tissues from the same animal. In order to test the selectivity of WIN 64338, its effect on ileal sensitivity to MCh was tested. At the end of each experiment, MCh (10 mM) was added to the bath, and all tissue responses expressed as a percentage of this maximum contraction.

Agonist pD_2 values were obtained from regression analyses of logit-transformed log concentration-response curves (InPlot, GraphPad Software, San Diego, CA). EC_{50} ratios for bradykinin in the absence and presence of WIN 64338 were calculated, and pA_2 values for the antagonist were obtained from Schild plots. All data are expressed as mean ± s.e.mean, and data between different experimental groups were compared by analysis of variance (InStat, GraphPad Software, San Diego, CA, U.S.A.).

Drugs

Bradykinin was purchased from Bachem California (Torrance, CA, U.S.A.), and acetyl-β-methylcholine chloride (methacholine, MCh), indomethacin, (+)-chlorpheniramine maleate, and tetrodotoxin were obtained from Sigma (St. Louis, MO, U.S.A.). WIN 64338, which was a kind gift from Dr David G. Sawutz, Sterling-Winthrop Pharmaceuticals (Collegeville, PA, U.S.A.), was prepared as a 30 mM stock solution in dimethyl sulphoxide (DMSO). Indomethacin was prepared as a 30 mM stock solution in 100 mM Na_2CO_3 and stored at −20°C until required. All other drugs were dissolved extemporaneously in 0.9% w/v NaCl solution (saline), and all drug dilutions were made in saline.

Results

Guinea-pig ileum

Bradykinin elicited concentration-dependent contractions in this tissue, demonstrating a pD_2 value of 8.51 ± 0.13 (n = 13). WIN 64338 caused concentration-dependent right shifts in bradykinin concentration-response curves with no significant depression in maximum response (Figure 1a). The antagonist had no spasmogenic effects at any concentration tested. WIN 64338 was a competitive B_2 receptor antagonist in guinea-pig ileum, yielding a straight line Schild plot whose slope was 1.09 ± 0.19, and not significantly different from unity (Figure 1b). The pA_2 value for WIN 64338, determined from the intercepts of regression lines of individual Schild plots through the abscissa scale, was 7.97 ± 0.10 (n = 4–7) (Figure 1b). Even at a concentration of 1 μM, WIN 64388 was without effect on ileal sensitivity to MCh (Figure 2).

Guinea-pig and ferret trachea

At a concentration of 1 μM, which was sufficient to decrease ileal sensitivity to bradykinin by more than two log units, WIN 64338 was without effect on guinea-pig tracheal sensitivity to the kinin (Figure 3a). Similarly, WIN 64338 did

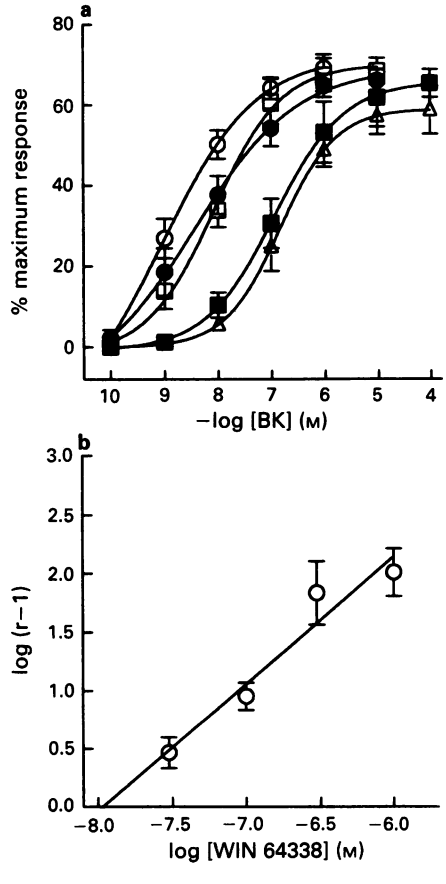

Figure 1 (a) Log concentration-response curves for bradykinin (BK) in guinea-pig isolated ileum in the absence (○) and presence of the B_2 receptor antagonist, WIN 64338: (●) 30 nM; (□) 100 nM; (■) 300 nM; (△) 1 μM. (b) Schild plot for antagonism of bradykinin-induced ileal contractions by WIN 64338. Slope was 1.09 ± 0.19, and the intercept of the abscissa was 7.97. Data are expressed as the mean ± s.e.mean of 4–13 observations in tissues from different animals.

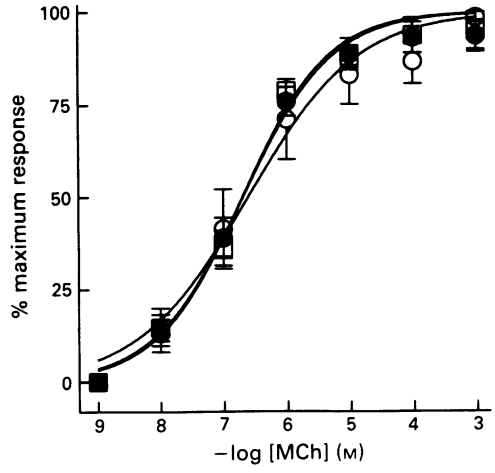

Figure 2 Log concentration-response curves for methacholine (MCh) in guinea-pig isolated ileum in the absence (○) and presence of the B_2 receptor antagonist, WIN 64338 100 nM (●); 1 μM (□). Data are expressed as the mean ± s.e.mean of four observations in tissues from different animals.

not significantly alter the sensitivity of ferret isolated trachea to bradykinin (Figure 3b).

Discussion

We examined the effects of WIN 64338, the first described nonpeptide antagonist of bradykinin B_2 receptor (Sawutz *et al.*, 1993; Salvino *et al.*, 1993), in guinea-pig ileum and guinea-pig and ferret trachea. This drug was reported recently to inhibit competitively bradykinin-induced contraction of guinea-pig ileum (Sawutz *et al.*, 1993). In the present study, we have confirmed that WIN 64338 is a competitive antagonist of bradykinin-induced contraction of guinea-pig ileum with a potency (pA_2 7.97) essentially identical to that reported by Sawutz and colleagues (1993) (pA_2 8.20). It has also been shown that WIN 64338 is selective for bradykinin receptors in that it had considerably lower activity at muscarinic receptors (Sawutz *et al.*, 1993; Salvino *et al.*, 1993). Furthermore, the drug appeared specific for B_2 receptors in that it was inactive as a B_1 receptor antagonist in rabbit aorta (Sawutz *et al.*, 1993). We also found that WIN 64338 was devoid of antagonist effects against methacholine-induced contractions of ileum.

In initial studies with WIN 64338, there appeared to be some species or, perhaps, tissue differences in its bradykinin receptor antagonist potencies (Sawutz *et al.*, 1993). For example, the antagonist was approximately ten times more potent against bradykinin-induced guinea-pig ileal contraction than against $^{45}Ca^{2+}$ efflux in foetal human lung fibroblasts (IMR 90 cells) (Sawutz *et al.*, 1993). In binding experiments in IMR 90 cells, WIN 64338 had a pK_i value of 6.19, and this is significantly less potent than its pK_i in guinea-pig ileum binding (8.10 ± 0.23, $n = 4$, unpublished data). Indeed, in preliminary experiments, we also found that WIN 64338 was around tenfold less potent in displacing [^{3}H]-bradykinin binding from human B_2 receptors expressed in murine erythroleukemia cells (pK_i 7.01 ± 0.15, $n = 4$, unpublished data) than in guinea-pig ileum. These data suggest that the guinea-pig ileal B_2 receptor has a higher affinity for WIN 64338 than human B_2 receptors. This may be indicative of species differences in B_2 receptors.

Alternatively, the different affinities for this novel antagonist may result from heterogeneity of bradykinin receptors in different tissues. In the present study, WIN 64338 displayed typical competitive antagonist activity in guinea-pig ileum.

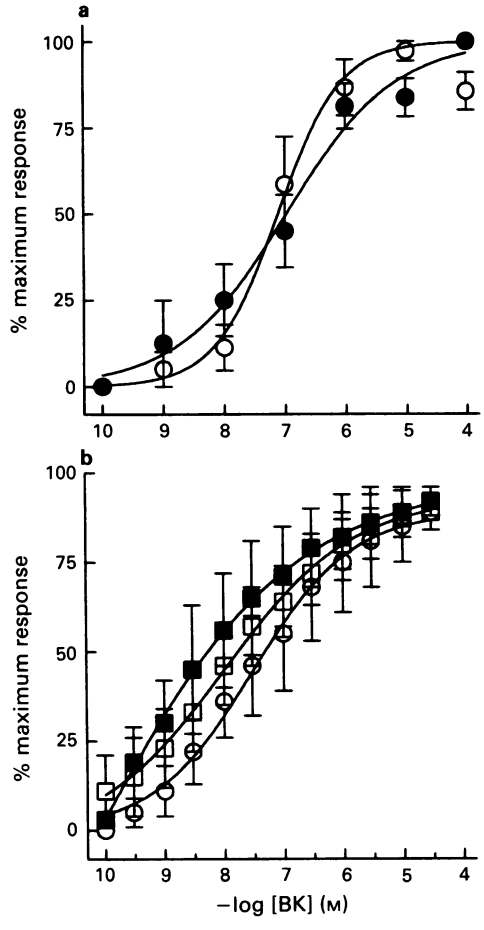

Figure 3 (a) Log concentration-response curves for bradykinin in guinea-pig isolated trachea in the absence (○) and presence of the B_2 receptor antagonist, WIN 64338 (●) 1 μM. (b) Log concentration-response curves for bradykinin in ferret isolated trachea in the absence (○) and presence of WIN 64338: (□) 1 μM; (■) 10 μM. Data are expressed as the mean ± s.e.mean of four observations in tissues from different animals.

The drug potently inhibited bradykinin-induced contractions, yielding a Schild slope of unity. Moreover, there was no decrease in the maximum contractile response to bradykinin, no partial agonist effects were evident even at high concentrations, and WIN 64338 had no effect on contractions in response to a muscarinic receptor agonist. Yet, even at a concentration (1 μM) that shifted the bradykinin log concentration-response curve 100 fold to the right in ileum, WIN 64338 was inactive as an antagonist of bradykinin-induced contractions in guinea-pig or ferret trachea.

Previous studies noted that several [D-Phe^7]-substituted analogues of bradykinin, which are B_2 receptor antagonists (Burch *et al.*, 1990), did not displace [^{3}H]-bradykinin binding in guinea-pig and sheep tracheal smooth muscle membranes (Farmer *et al.*, 1989b), and were very weak or inactive as inhibitors of bradykinin-induced tracheal contraction (Farmer *et al.*, 1989b; Perkins *et al.*, 1991). In addition, in guinea-pig tracheal smooth muscle cells, bradykinin-stimulated efflux of $^{45}Ca^{2+}$ (Farmer *et al.*, 1991b) and phospholipase D activity (Pyne & Pyne, 1993) are not affected by NPC 567, a peptide B_2 receptor antagonist. These data led to the proposal that tracheal smooth muscle may express B_3 receptors (reviewed by Farmer & Burch, 1991, 1992).

Newer, more potent bradykinin receptor antagonists such as NPC 16731 (Farmer *et al.*, 1991a), Hoe 140 (Field *et al.*, 1992; Trifilieff *et al.*, 1992), and NPC 17761 (Trifilieff *et al.*, 1993) potently antagonize bradykinin-induced responses of

guinea-pig trachea. Thus, these peptides may represent antagonists of B_2 and B_3 receptors. Conversely, it has been suggested that effects of bradykinin in guinea-pig trachea are not mediated by receptors at all, and this possibility was cited as the reason for the lack of effect of NPC 567 and other similar antagonists (Regoli & Nantel, 1990; Rhaleb *et al.*, 1992). This proposal is fallacious since, as noted above, Hoe 140, NPC 17761 and NPC 16731 do inhibit bradykinin-induced tracheal contraction. Because of the observation that Hoe 140 is much less potent as an antagonist of guinea-pig tracheal (and intestinal) responses to bradykinin than in tissues from other species (Rhaleb *et al.*, 1992; Field *et al.*, 1992), it has also been proposed that guinea-pig B_2 receptors are 'different' from B_2 receptors in other species (Regoli *et al.*, 1992; Rhaleb *et al.*, 1992). It has even been suggested that '. . . the proposed B_3 receptor might perhaps be regarded as a B_2 receptor from a guinea-pig' (Field *et al.*, 1992).

The present study may refute these arguments. WIN 64338 has been demonstrated to be a potent antagonist of B_2 receptors in human and guinea-pig tissues, albeit with approximately 10 fold differences in potency (Sawutz *et al.*, 1993; Salvino *et al.*, 1993; present study). Nevertheless, this agent was completely devoid of antagonist activity in tracheal preparations isolated from guinea-pigs or ferrets. These results indicate strongly that the bradykinin receptor subtypes expressed in tracheal smooth muscle from these two species differ from those expressed in guinea-pig ileum or human lung fibroblasts (B_2). Thus, like trachea from guinea-pigs, that from ferrets also appears to express a novel bradykinin receptor. In the absence of a drug that specifically inhibits bradykinin-induced tracheal contraction, however, the existence of the B_3 receptor remains to be proven.

References

BURCH, R.M., FARMER, S.G. & STERANKA, L.R. (1990). Bradykinin receptor antagonists. *Med. Res. Rev.*, **10**, 237–269.

BURCH, R.M. & KYLE, D.J. (1992). Recent developments in the understanding of bradykinin receptors. *Life Sci.*, **50**, 829–838.

DUSSER, D.J., NADEL, J.A., SEKIZAWA, K., GRAF, P.D. & BORSON, D.B. (1988). Neutral endopeptidase and angiotensin converting enzyme inhibitors potentiate kinin-induced contraction of ferret trachea. *J. Pharmacol. Exp. Ther.*, **244**, 531–536.

FARMER, S.G. & BURCH, R.M. (1991). Airway bradykinin receptors. *Ann N.Y. Acad. Sci.*, **629**, 237–249.

FARMER, S.G. & BURCH, R.M. (1992). Biochemical and molecular pharmacology of kinin receptors. *Annu. Rev. Pharmacol. Toxicol.*, **32**, 511–536.

FARMER, S.G., BURCH, R.M., DEHAAS, C.J., TOGO, J. & STERANKA, L.R. (1989a). [Arg^1-DPhe^7]-sustained analogues of bradykinin inhibit vasopressin- and bradykinin-induced contractions of uterine smooth muscle. *J. Pharmacol. Exp. Ther.*, **248**, 677–681.

FARMER, S.G., BURCH, R.M., KYLE, D.J., MARTIN, J.A., MEEKER, S.N. & TOGO, J. (1991a). D-Arg[Hyp^3-Thi^5-D-Tic^7-Tic^8]-bradykinin, a potent antagonist of smooth muscle BK_2 receptors and BK_3 receptors. *Br. J. Pharmacol.*, **102**, 785–787.

FARMER, S.G., BURCH, R.M., MEEKER, S.N. & WILKINS, D.E. (1989b). Evidence for a pulmonary bradykinin B_3 receptor *Mol. Pharmacol.*, **36**, 1–8.

FARMER, S.G., DESIATO, M.A. & BROOM, T. (1992). Effects of kinin receptor agonists and antagonists in ferret isolated tracheal smooth muscle. Evidence that bradykinin-induced contractions are mediated by B_2 receptors. *Br. J. Pharmacol.*, **107**, 32P.

FARMER, S.G., ENSOR, J.E. & BURCH, R.M. (1991b). Evidence that cultured airway smooth muscle cells contain bradykinin B_2 and B_3 receptors. *Am. J. Respir. Cell Mol. Biol.*, **4**, 273–277.

FARMER, S.G., FEDAN, J.S., HAY, D.W.P. & RAEBURN, D. (1986). The effects of epithelium removal on the sensitivity of guinea-pig isolated trachealis to bronchodilator drugs. *Br. J. Pharmacol.*, **89**, 407–414.

FIELD, J.L., HALL, J.M. & MORTON, I.K.M. (1992). Putative novel bradykinin B_3 receptors in the smooth muscle of the guinea-pig taenia caeci and trachea. *Agents Actions*, **38**, Suppl. I, 540–545.

HALL, J.M. (1992). Bradykinin receptors: pharmacological properties and biological roles. *Pharmacol. Ther.*, **56**, 131–190.

HOCK, F.J., WIRTH, K., ALBUS, U., LINZ, W., GERHARDS, H.J., WIEMER, G., ST. HENKE, G., BREIPOHL, G., KÖNIG, W., KNOLLE, J. & SCHÖLKENS, B.A. (1991). Hoe 140 a new potent and long acting bradykinin-antagonist: *in vitro* studies. *Br. J. Pharmacol.*, **102**, 769–773.

KYLE, D.J., MARTIN, J.A., FARMER, S.G. & BURCH, R.M. (1991). Design and conformation analysis of several highly potent bradykinin receptor antagonists. *J. Med. Chem.*, **34**, 1230–1233.

LEMBECK, F., GRIESBACHER, T., ECKHARDT, M., HENKE, S., BREIPOHL, G. & KNOLLE, J. (1991). New, long-acting, potent bradykinin antagonists. *Br. J. Pharmacol.*, **102**, 297–304.

PERKINS, M.N, BURGESS, G.M, CAMPBELL, E.A., HALLETT, A., MURPHY, R.J., NAEEM, S., PATEL, I.A., RUEFF, A. & DRAY, A. (1991). HOE140: a novel bradykinin analogue that is a potent antagonist at both B_2 and B_3 receptors *in vitro*. *Br. J. Pharmacol.*, **102**, 171P.

PYNE, S. & PYNE, N.J. (1992). Differential effects of B_2 receptor antagonists upon bradykinin-stimulated phospholipase C and D in guinea-pig cultured tracheal smooth muscle. *Br. J. Pharmacol.*, **110**, 477–481.

REGOLI, D., JUKIC, D., TOUSIGNANT, C. & RHALEB, N.-E. (1992). Kinin receptor classification. *Agents Actions*, **38**, 475–486.

REGOLI, D. & NANTEL, F. (1990). Receptor-independent action of bradykinin. Direct activation of G proteins. *Trends Pharmacol. Sci.*, **11**, 400–401.

RHALEB, N.-E., ROUISSI, N., JUKIC, D., REGOLI, D., HENKE, S., BREIPOHL, G. & KNOLLE, J. (1992). Pharmacological characterization of a new highly potent B_2 receptor antagonist (Hoe 140: D-Arg-[Hyp^3,Thi^5,D-Tic^7,Oic^8]bradykinin). *Eur. J. Pharmacol.*, **210**, 115–120.

SALVINO, J.M., SEOANE, P.R., DOUTY, B.D., AWAD, M.M.A., DOLLE, R.E., HOUCK, W.T., FAUNCE, D.M. & SAWUTZ, D.G. (1993). Design of potent non-peptide competitive antagonists of the human bradykinin B_2 receptor. *J. Med. Chem.*, **36**, 2583–2584.

SAWUTZ, D.G., SALVINO, J.M., DOLLE, R.E., CASIANO, F., WARD, S.J., HOUCK, W.T., FAUNCE, D.M, DOUTY, B., AWAD, M. & SOEANE, P. (1993). Discovery and *in vitro* biological activity of the nonpeptide bradykinin receptor antagonist WIN 64338. *Pharmacologist*, **35**, 142.

TRIFILIEFF, A., DA SILVA, A., LANDRY, Y. & GIES, J.-P. (1992). Effect of Hoe 140, a new B_2 noncompetitive antagonist, on guinea pig tracheal bradykinin receptors. *J. Pharmacol. Exp. Ther.*, **263**, 1377–1382.

TRIFILIEFF, A., AMRANI, Y., LANDRY, Y. & GIES, J.-P. (1993). Comparative action of new highly potent bradykinin receptor antagonists in the guinea-pig trachea. *Eur. J. Pharmacol.*, **239**, 227–229.

(Received December 6, 1993
Revised February 3, 1994
Accepted February 10, 1994)

Br. J. Pharmacol. (1994), **112**, 465–470

Triflocin, a novel inhibitor for the Na-HCO_3 symport in the proximal tubule

Fouzia Belachgar, Philippe Hulin, Takis Anagnostopoulos & [1]Gabrielle Planelles

INSERM U. 323, CHU Necker Enfants-Malades, 156 rue de Vaugirard-75730-Paris Cedex 15, France

1 Triflocin, applied at millimolar concentration hyperpolarizes the basolateral membrane of *Necturus* proximal convoluted tubular cells, *in vivo*.

2 Barium, 2.5×10^{-3} M, ouabain, 10^{-3} M, or amiloride 10^{-4} M, fail to prevent this hyperpolarization.

3 Triflocin has no effect on the intracellular chloride activity.

4 In physiological acid base conditions, Triflocin increases intracellular pH.

5 Upon an acute isohydric hypercapnia, Triflocin depolarizes the basolateral membrane potential.

6 It is concluded that, Triflocin inhibits the basolateral electrogenic Na-$(HCO_3)_{n>1}$ cotransport in proximal tubules.

Keywords: Triflocin; Na-$(HCO_3)_{n>1}$ cotransport; proximal tubule; intracellular pH

Introduction

About 60% of the sodium filtered by the kidney is reabsorbed by the proximal convoluted tubule (PCT), mainly across the cell pathway. The basolateral step for this sodium transport is accomplished mainly by the Na,K/ATPase and the basolateral Na-$(HCO_3)_{n>1}$ symport. However, some studies suggest a third mechanism for Na^+ reabsorption, namely a distinct sodium pump: indeed, several *in vitro* studies on PCT cells (Del Castillo *et al.*, 1982; El Mernissi *et al.*, 1991) report that a sodium-stimulated, ouabain-insensitive ATPase is inhibited by Triflocin (4[3trifluoromethylanilino-] nicotinic acid); such a sodium-stimulated ouabain-insensitive ATPase activity is also reported in other tissues (Marin *et al.*, 1990; Orsenigo *et al.*, 1991).

In vivo, a natriuretic effect of Triflocin has been reported in both the PCT and the thick ascending limb (TAL) of Henle's loop (Gussin *et al.*, 1986). In the latter segment, this natriuresis is due to inhibition of the Na-K-2Cl cotransport (Wangemann *et al.*, 1986), whereas in the PCT the mechanism is not yet clearly established.

In the present work, we studied the effects of Triflocin on *Necturus* PCT *in vivo* using an electrophysiological approach. Our results provide no direct evidence for the inhibition of a Na-pump but indicate rather that Triflocin inhibits the Na-$(HCO_3)_{n>1}$ cotransport. This inhibitory effect may account for the drug-induced reduction of solute and water reabsorption in the proximal tubule.

Methods

Preparation of the animal

All experiments were carried out on the PCT of *Necturus maculosus in vivo*. Before the experiment, anaesthesia was achieved by immersion of the animal in a tricaine methanesulphonate solution (700 $\mu g\,ml^{-1}$) and was maintained throughout the experiment by immersion of the branchia in the same solution diluted by 1/5th. Dissection of the animal, exposure of the peritoneal cavity, and superfusion of the kidney throughout the experiment have been described elsewhere (Planelles *et al.*, 1984).

Peritubular perfusions

A double-barrelled micropipette was inserted into a peritubular capillary vessel (portal) with a micromanipulator (Leitz). The two barrels of the pipette were connected to polyethylene catheters filled with two solutions differing by only a single parameter, thus allowing alternative delivery of the two solutions using a gravimetric system. In some experiments, an additional double-barrelled micropipette was inserted into the same vessel in order to study a greater number of perfusates.

In experiments with equilibrated CO_2 solutions, the polyethylene tubes were enclosed in a gas-tight tube in which the appropriate P_{CO_2} was maintained throughout the experiment. This arrangement avoids CO_2 leaks, as described elsewhere (Planelles & Anagnostopoulos, 1991).

The composition of the solutions is indicated in Table 1.

Electrophysiological determinations

Transmembrane potential, V_m, was measured with a single intracellular microelectrode. Microelectrodes were pulled from capillary tubes (o.d. 2 mm, i.d. 1.6 mm, Clark) using a vertical puller (PE2, Narishige) and were then filled with KCl, 1 M. The microelectrodes were connected via a Ag/AgCl junction to the input of an electrometer (WPI FD 223), and the output was connected to a chart recorder (Sefram, Servofram). A KCl 1 M, Ag/AgCl macroelectrode, introduced into the animal's peritoneal cavity, closed the electrical circuit.

In some experimental series, we simultaneously measured both V_m and a given intracellular ionic activity, e.g. chloride, Cl_i, or pH, pH_i, using double-barrelled microelectrodes. The manufacture of such electrodes in our laboratory has been described in detail elsewhere (Anagnostopoulos & Planelles, 1987). Briefly, two borosilicate capillary tubes (o.d. 1.2 mm, i.d. 0.7 mm) were joined at two points with beeswax, were twisted 360° under a microflame and were finally pulled into two symmetrical double-barrelled microelectrodes. One of the barrels was exposed to dimethyltrimethylsililamine (Fluka) in order to render the inner surface hydrophobic. The microelectrodes were then baked for 2 h (120°C). Finally, a droplet of ion exchanger (approximately 0.5 μl of the Fluka proton cocktail or 477913 Corning chloride exchanger) was introduced and was allowed to slip down to the extreme tip. The next day, the selective barrel was filled either with NaCl, 0.1 M, (for the Cl-electrodes) or with a solution containing NaCl 0.067, KH_2PO_4 0.04, NaOH 0.023 M (for the pH electrodes), whereas the conventional barrel was filled with KCl, 1 M. The slope per decade, S, of these microelectrodes was 45–50 mV for the Cl-selective electrodes, and 55–60 mV for the pH electrodes. Cl_i was calculated as $Cl_i = Cl_{ref}$

[1] Author for correspondence.

Table 1 Composition of control solutions

	NaCl (mM)	*Na gluconate* (mM)	*KCl* (mM)	*$CaCl_2$* (mM)	*$MgCl_2$* (mM)	*TES* (mM)	*$NaHCO_3$* (mM)	*CO_2* (kPa)	*pH*
Ringer	100	0	3	1.8	1	5	0	0	7.6
Low Cl solution	0	82	3	5.4	1	5	0	0	7.6
Physiological acid base status	10.8	81	3	5.4	1	0	8.2	1	7.6
Isohydric hypercapnia	18	0	3	1.8	1	0	82	10	7.6

In some experiments, Ringer was supplemented with 2.5 mM $BaCl_2$ (at pH 7.6 or 6.9), 1 mM ouabain or 0.1 mM amiloride. In low chloride solutions, $CaCl_2$ was increased due to calcium chelation by gluconate. The physiological acid base and isohydric hypercapnia solutions were designed to have equal constant chloride concentrations.

Table 2 Transmembrane potential differences, V_m (mV), in the presence of blood and under various control conditions

	V_m				ΔV_m	
Blood	*Ringer*	*Ringer Ba pH 7.6*	*Ringer Ba pH 6.9*	*Ringer Ba Ouabain*	*Ringer Amil*	*Triflocin*	n
− 69.1 ± 2.2	− 60.9 ± 2.2					− 6.4 ± 0.9 ***	14
− 51.8 ± 3.4		− 35.6 ± 2.6				− 6.4 ± 1.2 ***	5
− 54.2 ± 2.2			− 26.7 ± 2.1			− 5.0 ± 1.1 **	4
− 58.4 ± 2.6		− 33.4 ± 1.9		− 20.8 ± 2.6		− 5.6 ± 1.3 **	5
− 64.0 ± 3.9					− 57.8 ± 4.1	− 5.8 ± 0.4 ***	6

ΔV_m Triflocin column indicates the V_m changes (mV) upon Triflocin (1 mM) addition.
n = number of tubules. Significance of the results were assessed by paired t test. $^{**}P<0.01$, $^{***}P<0.001$.
Ba = barium, 2.5 mM; Amil = amiloride 0.1 mM; oubain 1 mM.

$\times 10^{(V_{Cl}-V_m)/S}$, where Cl_{ref} is the chloride activity in the superfusion solution (activity coefficient $\gamma = 0.75$) and V_{Cl} is the measured electrochemical potential difference for Cl^-. In the same manner, pH_i was calculated as $pH_i = pH_{ref}-(V_H-V_m)/S$, where pH_{ref} is the pH in the superfusion solution and V_H is the measured electrochemical potential difference for H^+.

Chemicals

Triflocin was a generous gift of Drs B. Clark and P. Poitou (Lederle).

Statistics

The data are expressed as mean ± s.e.mean; n = number of single tubules. Unless stated in the text, statistical significance was assessed by Student's paired t test (two tailed).

Results

Effects of Triflocin on membrane potential

In a first series of experiments, we looked for changes in basolateral membrane potential in the presence of Triflocin. To this end, we delivered into a superficial peritubular vessel a physiological solution (Ringer) and then switched the perfusate to an identical solution supplemented with Triflocin, 1 mM. The results show (Table 2) that the drug leads to hyperpolarization of V_m. This hyperpolarization effect of Triflocin was observed in every single cell, but the amplitude of the response varied over a wide range (from − 3 to − 12 mV, with a mean of − 6.4 ± 0.9 mV, n = 14). We therefore looked to find out whether the amplitude of the ΔV_m response was dependent upon the site along the PCT. After recording their ΔV_m values, four single tubules were injected with coloured mineral oil from their respective glomeruli up to the puncture site. We observed that the two largest hyperpolarizations (− 9 and − 12 mV) occurred in the early PCT, whereas the two smallest hyperpolarizations (− 3 and − 4 mV) were located further downstream.

Effects of Triflocin on membrane potential in presence of several inhibitors

That the introduction of Triflocin results in hyperpolarization is consistent with its postulated effect on a rheogenic transport mechanism across the basolateral membrane. To test whether this effect involves a basolateral K^+ conductance, G_K, we introduced barium (2.5 mM) (a known inhibitor of the basolateral G_K in PCT (Planelles *et al.*, 1981)) into the perfusate. A tracing of V_m from one of these experiments (Figure 1) shows that Triflocin still hyperpolarizes the membrane even in the presence of an acid extracellular pH, a condition used to inhibit fully G_K (Oberleithner *et al.*, 1988). The data (Table 2) indicate that the membrane hyperpolarization induced by Triflocin is not due to the activation of a barium- or low pH-sensitive G_K.

In the presence of a solution containing barium (2.5 mM) supplemented with ouabain (1 mM), the hyperpolarizing effect of Triflocin on V_m is still present (Figure 2 and Table 2). This suggests that the effect of Triflocin on membrane potential is not due to stimulation of the basolateral ouabain-sensitive Na,K/ATPase.

Application of amiloride (10^{-4} M) in the basolateral capillaries also does not affect the hyperpolarization associated with Triflocin (Figure 3, Table 2), indicating that it is not the consequence of the inhibition of an amiloride-sensitive sodium conductance, G_{Na}.

Effect of Triflocin upon chloride conductance

The hyperpolarization induced by Triflocin could be associated with inhibition of a chloride conductance, G_{Cl}. To test this hypothesis, we looked initially at Triflocin effects during a low-Cl basolateral perfusate. In this condition, Triflocin

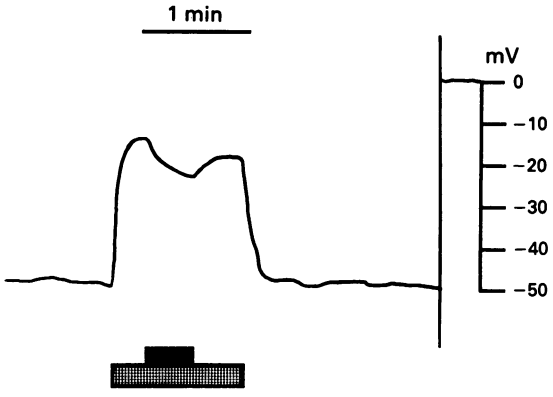

Figure 1 Effect of Triflocin, 10^{-3} M, on basolateral membrane potential (mV) in the presence of barium, 2.5×10^{-3} M at pH 6.9. Original tracing, obtained with a conventional intracellular microelectrode, is shown. Timing of perfusion with experimental solutions is indicated by horizontal bars (shaded for barium, pH 6.9; solid black for Triflocin) below the graph. Before and after these experimental solutions, perfusion was with blood from normal circulation.

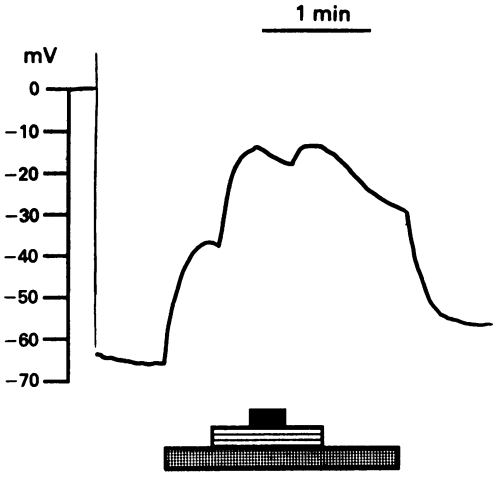

Figure 2 Effect of Triflocin, 10^{-4} M, on basolateral membrane potential (mV) in the presence of ouabain, 10^{-3} M, and barium, 2.5×10^{-3} M. Original tracing, obtained with a conventional intracellular microelectrode, is shown. Timing of perfusion with experimental solutions is indicated by horizontal bars (shaded for barium, stripes for ouabain, and solid black for Triflocin) below the graph. Before and after these experimental solutions, perfusion was with blood from normal circulation.

resulted in a hyperpolarization (-6.7 ± 0.9 mV, $n = 7$) comparable, by using an unpaired t test, to that obtained in the separate Ringer series (-6.4 ± 0.9 mV, Table 2). This result argues against, but does not totally rule out, an inhibitory effect of the drug upon a G_{Cl} (see Discussion). We thus did another experimental series (two double peritubular micropipettes) to compare, by a paired t test, the size of Triflocin-induced hyperpolarization in the presence of a physiological concentration of peritubular Cl (Ringer) to that in the presence of a low chloride solution. In this experimental series ($n = 7$), Triflocin hyperpolarized V_m by -8.6 ± 0.8 mV in the Ringer solution, whereas in the low-Cl solution, the observed hyperpolarization was -7.2 ± 0.9 mV: the difference between these values is only borderline significant, $P = 0.046$.

To delineate better the effects of Triflocin upon G_{Cl}, we decided to measure the intracellular Cl^- activity directly in the absence and in the presence of the drug. Indeed, if

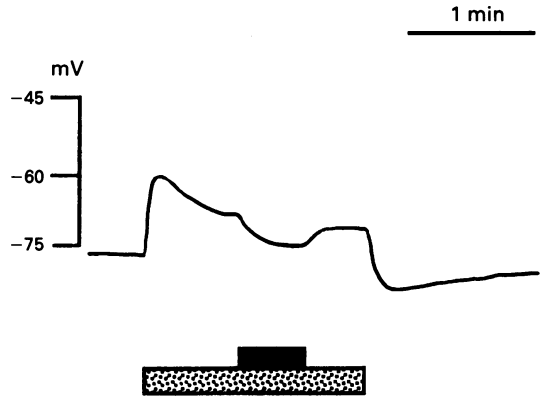

Figure 3 Effect of Triflocin, 10^{-3} M, on basolateral membrane potential (mV) in the presence of amiloride, 10^{-4} M. Original tracing, obtained with a conventional intracellular microelectrode, is shown. Timing of perfusion with experimental solutions is indicated by horizontal bars (stippled for amiloride; solid black for Triflocin) below the graph.

Triflocin does inhibit a basolateral G_{Cl}, thereby reducing that anion's efflux, one would expect at least a transient increase of Cl_i upon introduction of Triflocin. The following results were obtained: in the presence of the blood stream in the capillaries, V_m was -66.7 ± 4.4 mV and Cl_i was 12.55 ± 1.09 mM; then the basolateral perfusion of the Ringer solution yields a V_m of -60.0 ± 5.0 mV, without significant alteration of Cl_i (12.64 ± 1.12 mM); addition of Triflocin results in hyperpolarization of -5.9 ± 0.7 mV ($P < 0.001$) without significant changes in Cl_i ($Cl_i = 13.15 \pm 1.42$ mM).

Taken together, these data indicate that the predominant effect of Triflocin is not related to the inhibition of a basolateral Cl conductance.

Inhibition of the Na-$(HCO_3)_{n>1}$ cotransport by Triflocin

In the last experimental series, we looked for an inhibitory effect of Triflocin on the basolateral Na-$(HCO_3)_{n>1}$ cotransport, which physiologically promotes extrusion of $nHCO_3^-$ ions together with 1 Na^+ ion. Thus, a drug-induced membrane hyperpolarization could reflect the inhibition of this rheogenic carrier. The changes of V_m under Triflocin were assessed under physiological acid-base conditions for the salamander (defined by a PCO_2 of 1 kPa, HCO_3 8.2 mM and pH 7.6, cf. Table 1) and during acute iso-hydric hypercapnia (PCO_2 10 kPa, HCO_3 82 mM, pH 7.6, cf. Table 1). We have already demonstrated that the basolateral Na-$(HCO_3)_{n>1}$ cotransport reverses its net flux (thus promoting the influx of sodium plus HCO_3 equivalents) during acute iso-hydric hypercapnia (Planelles *et al.*, 1993). Under physiological acid-base conditions, Triflocin significantly hyperpolarizes V_m by -7.6 ± 0.3 mV ($n = 10$, $P < 0.001$) (Figure 4), whereas during acute iso-hydric hypercapnia, Triflocin significantly depolarizes V_m by 4.7 ± 0.3 mV ($n = 7$, $P < 0.001$) (Figure 5). These data are consistent with the inhibition of a Na-$(HCO_3)_{n>1}$ cotransport that functions respectively in the outward (PCO_2 1 kPa) or the inward direction (PCO_2 10 kPa).

To obtain further information as to whether Triflocin is an inhibitor of the Na-$(HCO_3)_{n>1}$ cotransport, we simultaneously measured V_m and pH_i under physiological acid-base conditions (PCO_2 1 kPa, HCO_3 8.2 mM, pH 7.6) in the absence and in the presence of the drug. As shown in Figure 6, intracellular pH increases significantly upon introduction of Triflocin (mean alkalinization $+0.05 \pm 0.01$ pH U, $n = 10$, $P < 0.001$). This pH_i increase associated with the membrane hyperpolarization (-4.6 ± 0.5 mV in this series) in the presence of the drug is consistent with the inhibition of Triflocin of the physiologically outward-directed Na-$(HCO_3)_{n>1}$ symport.

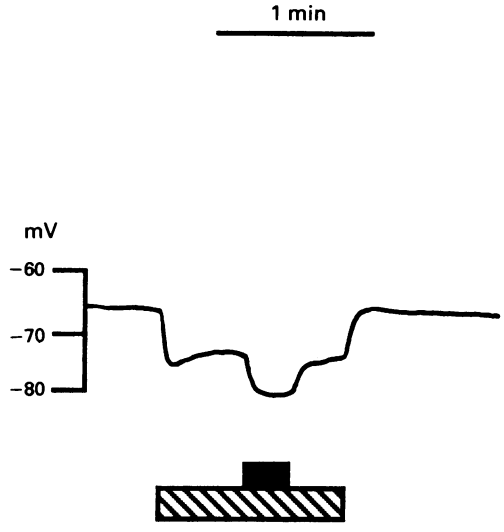

Figure 4 Effect of Triflocin, 10^{-3} M, on basolateral membrane potential (mV) in the presence of a physiological acid-base condition, CO_2 1% (see Table 1 for complete description of the perfusion solution). Original tracing, obtained with a conventional intracellular microelectrode, is shown. Timing of perfusion with experimental solutions is indicated by horizontal bars (hatched for CO_2 1%; solid black for Triflocin).

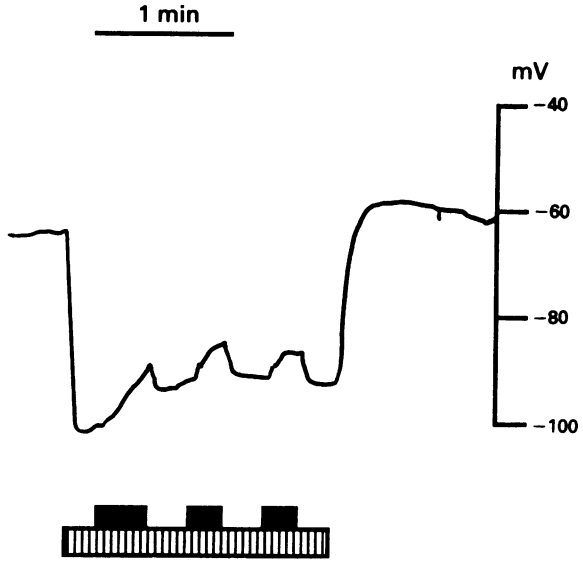

Figure 5 Effect of Triflocin, 10^{-3} M, on basolateral membrane potential (mV), under conditions of acute peritubular isohydric hypercapnia, CO_2 10% (see Table 1 for complete description of the perfusion solution). Original tracing, obtained with a conventional intracellular microelectrode, is shown. Timing of perfusion with experimental solutions is indicated by horizontal bars (vertical stripes for CO_2 10%; solid black for Triflocin).

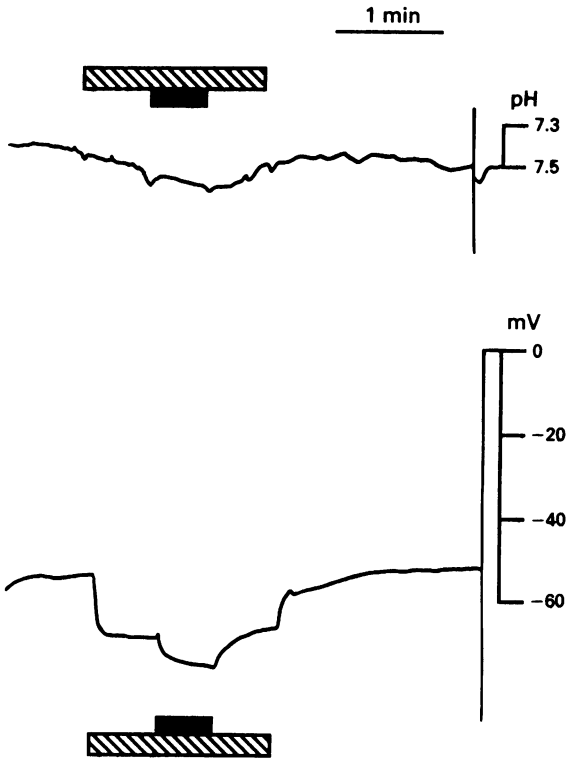

Figure 6 Effect of Triflocin, 1 mM, on basolateral membrane potential (mV, lower trace) and intracellular pH (upper trace), under physiological acid base conditions (CO_2 1%). Note that pH trace precedes the voltage trace, due to placement of pens on the chart recorder. Original tracing, obtained with an intracellular double-barreled pH microelectrode, is shown. Timing of perfusion with experimental solutions is indicated by horizontal bars (hatched for CO_2 1%; solid black for Triflocin).

Discussion

The natriuretic effect of Triflocin is mainly restricted to the PCT and to the TAL (Gussin *et al.*, 1969). In the TAL, luminal application of Triflocin inhibits the Na-K-2Cl cotransport with an IC_{50} of 3×10^{-5} M (Wangemann *et al.*, 1986), whereas basolateral Triflocin exposure fails to produce significant effects, especially upon the large basolateral chloride conductance of this segment (Wangemann *et al.*, 1986). By contrast, the mechanism of the Triflocin effect on the proximal tubule has not been clearly established. Several biochemical studies report that the drug inhibits a sodium-stimulated, ouabain-insensitive ATPase (Del Castillo *et al.*, 1982; El Mernissi *et al.*, 1991). These data suggest that a distinct Na-ATPase could contribute to proximal Na^+ reabsorption (Marin *et al.*, 1990), whereas the conventional view of basolateral sodium absorption is restricted to two transporters, the Na,K/ATPase and the Na-$(HCO_3)_{n>1}$ cotransport. In the present study, our goal was to define the mechanism of Triflocin on the PCT *in vivo*.

An important experimental observation presented here opposes the hypothesis of a putative sodium-only pump, namely, Triflocin exerts a swift hyperpolarization of V_m. In a previous study (Planelles & Anagnostopoulos, 1982), we established that ouabain fails to evoke an immediate change in V_m in the PCT, due to the small current flow across the low membrane resistance. That Triflocin results in a quasi-immediate hyperpolarization would suggest that the putative Na-ATPase (assuming it to be located on the basolateral membrane and to be perfectly functional) carries a current higher than the Na,K/ATPase. In addition, membrane hyperpolarization is incompatible with the simplest model for a 'sodium pump', i.e. the translocation of a single Na^+ ion out of the cell, the inhibition of which should result in membrane depolarization. The occurrence of a hyperpolarization, if in fact related to the inhibition of a Na-pump contributing to sodium absorption, could account for the arrest of influx of n ($n > 1$) positive charges exchanged for a single Na^+ ion, or for the cessation of the efflux of n ($n > 1$) negative charges cotransported with one Na^+ out of the cell. Theoretically, NaCl reabsorption by a Na^+, nCl^-/ATPase could be conceivable, but this contingency is not supported by biochemical studies (El Mernissi *et al.*, 1991), which showed that

Triflocin-inhibited sodium-dependent ATPase activity is chloride-independent.

We considered several alternative hypotheses: first, if Triflocin effectively inhibited a pump mediating Na^+ efflux (Marin *et al.*, 1990), an increase of intracellular sodium activity under Triflocin is conceivable, thereby triggering activation of the Na,K/ATPase (Harris, 1965; Karlish & Stein, 1985), thus yielding membrane hyperpolarization. With this in mind, we studied the effects of the drug in the presence of ouabain. These experiments were carried out in the presence of barium to increase the membrane resistance, thereby revealing the inhibitory effect of the cardiac glucoside by a depolarization of the basolateral membrane (Planelles & Anagnostopoulos, 1982). In the presence of barium and ouabain, a persistent hyperpolarization under Triflocin is obtained, ruling out the above hypothesis.

At this stage, we wondered whether the Triflocin-associated hyper-polarization might rather be accounted for by an effect on an already identified basolateral membrane rheogenic mechanism. We inquired whether the rise of V_m reflected an increase of G_K, which should draw V_m closer to the equilibrium potential for K^+. However, our observation of the persistence of the Triflocin effect on V_m in the presence of barium and an acidic extracellular pH rules out activating-effects of Triflocin on G_K. Inhibition of a sodium conductance by the drug would also trigger a membrane hyperpolarization. Thus, we wondered whether Triflocin-associated hyperpolarization persisted in the presence of amiloride at 10^{-4} M, i.e. a concentration largely sufficient to inhibit epithelial sodium channels (Frelin *et al.*, 1987). The persistence of the membrane effect of Triflocin under amiloride rules out inhibition of a sodium conductance.

Since Triflocin is a nitro-trifluoromethyl derivative of diphenylamine-2-carboxylate (DPC), which is an inhibitor of G_{Cl} (Di Stefano *et al.*, 1985), we wondered whether our results could be accounted for by a blockade of G_{Cl} by Triflocin, even though this compound was shown to be ineffective towards the basolateral G_{Cl} of the thick ascending limb of Henle (Wangemann *et al.*, 1986). We therefore first compared the membrane hyperpolarization induced by Triflocin in the presence of plain Ringer solution to its effects in a low chloride solution. We found no evidence for an effect of G_{Cl}. To confirm the lack of significance (as emphasized in the Results section, the magnitude of the Triflocin-induced hyperpolarization is variable, thereby possibly introducing a bias in the unpaired statistical analysis), another experimental series was conducted, in order to carry out a paired *t* test statistical analysis: a sequence of four peritubular solutions (Ringer and low chloride solutions, supplemented or not with the drug) was delivered via a single capillary, and V_m was recorded in a single cell during the whole series. In this configuration, a borderline statistical significance ($P = 0.046$) was obtained when comparing the Triflocin-induced V_m changes. This weak significance prompted us to use yet another approach, by looking at the effect of the drug on the intracellular chloride activity to ascertain definitively whether Triflocin inhibits a chloride conductance. Since the electrochemical potential for chloride *in vivo* favours basolateral efflux (Edelman *et al.*, 1981), inhibition of a G_{Cl} should lead, at least transiently, to elevation of Cl_i. We failed to observe any systematic Cl_i change in the presence of Triflocin, suggesting that the effects of Triflocin on V_m do not relate to inhibition of a putative G_{Cl}. It should be noted that an increase of Cl_i (if it were observed) in the presence of Triflocin would be difficult to interpret: indeed, our tests *in vitro* reveal that the addition of Triflocin to a physiological solution interferes with the microelectrode determination of the chloride activity in bulk solution (apparent overestimation); thus an apparent increase of Cl_i could be ascribed either to entry of the drug into the cell or to a real Cl_i augmentation.

Last, we looked for Triflocin-associated inhibition of the Na-$(HCO_3)_{n>1}$ cotransport. This SITS-inhibited cotransporter was initially described in the basolateral membrane of the amphibian PCT (Boron & Boulpaep, 1983), then in mammalian PCT (Yoshitomi *et al.*, 1985; Alpern, 1985). Membrane hyperpolarization induced by SITS reflects inhibition of the outward-directed Na-$(HCO_3)_{n>1}$ cotransport (Lopes *et al.*, 1987; Planelles *et al.*, 1993), while membrane depolarization induced by SITS reflects inhibition of the inward-directed Na-$(HCO_3)_{n>1}$ (Hughes *et al.*, 1989; Planelles *et al.*, 1993). In the present study, we were able to reverse the Triflocin effect on V_m from hyperpolarization (under physiological acid-base conditions) to depolarization (under imposed iso-hydric hypercapnia). This reversal can be understood in the light of our recent studies (Planelles *et al.*, 1993) demonstrating reversal of the net flux of sodium and bicarbonate via the transporter under conditions of isohydric hypercapnia. A second experimental argument strengthens the hypothesis of Triflocin-associated inhibition of Na-$(HCO_3)_{n>1}$, namely, under physiological conditions and while the cotransport carries net efflux of bicarbonate, the addition of Triflocin leads to cytoplasmic alkalinization. Finally, the diminution of the drug-induced ΔV_m responses observed here along the PCT may be accounted for by the fact that the activity of the Na-$(HCO_3)_{n>1}$ cotransport varies along the superficial loops of single PCTs, with a higher activity in the early PCT (Kondo & Frömter, 1987).

We show in this paper that Triflocin applied at millimolar concentrations inhibits the Na-$(HCO_3)_{n>1}$ cotransport. Due to the variability of the ΔV_m responses, we did not establish dose-response curves with this inhibitor. To date, no specific inhibitor for the Na-$(HCO_3)_{n>1}$ symport has been reported: millimolar concentrations of stilbene-derivatives, SITS or DIDS (Soleimani & Aronson, 1989a), and of Harmalin (Soleimani & Aronson, 1989b) inhibit Na-$(HCO_3)_{n>1}$ cotransport. Since Triflocin, while less potent than bumetamide, has inhibitory effects on the Na-K-2Cl cotransport (Wangemann *et al.*, 1986), it cannot be considered as a specific inhibitor for the Na-$(HCO_3)_{n>1}$ cotransport. Niflumic acid, an isomer of Triflocin, in addition to its inhibitory effect on cationic (Gögelein *et al.*, 1990) and Cl channels (Gögelein, 1988) inhibits the band 3 of erythrocytes (Cousin & Motais, 1982a,b). To our knowledge, the effect of Triflocin on band 3 has not been tested, while stilbene derivates like SITS and DIDS are known to inhibit this Cl/HCO_3 exchanger; thus, it would be interesting to check the effects of the Triflocin on band 3, and, as a corollary, to test the effects of alternative inhibitors of the Cl/HCO_3 exchanger on the Na-$(HCO_3)_{n>1}$ cotransport. Inhibition of the Na-$(HCO_3)_{n>1}$ cotransport and Cl/HCO_3 exchanger by the same molecules could reflect a common sequence to both transporters. This hypothetical scenario may be a useful approach in order to tackle the molecular structure of the Na-$(HCO_3)_{n>1}$ cotransport. At present, our data nevertheless suggest that the natriuretic effect of Triflocin is related to inhibition of net absorption of sodium and base-equivalents in the proximal tubule.

The Na-$(HCO_3)_{n>1}$ cotransport, initially described in the kidney (Boron & Boulpaep, 1983), is present in numerous epithelial and non-epithelial tissues (Boron & Boulpaep, 1989). This transporter may play a major role in the regulation of the aqueous humour in the eye (Jentsch *et al.*, 1984) and in the control of extracellular pH in the nervous system (Deitmer, 1991). Consequently, novel inhibitors could lead to the development in the near future of a pharmacopoeia that could be applied to some physiopathological states.

The authors wish to thank Mireille Blonde for her technical assistance and Michèle Poitou for her expert secretarial work.

References

ALPERN, R.J. (1985). Mechanism of basolateral membrane $H^+/OH^-/HCO_3^-$ transport in the rat proximal convoluted tubule. *J. Gen. Physiol.*, **86**, 613–636.

ANAGNOSTOPOULOS, T. & PLANELLES, G. (1987). Cell and luminal activities of chloride, potassium, sodium and protons in the late distal tubule of Necturus kidney. *J. Physiol.*, **393**, 73–89.

BORON, W.F. & BOULPAEP, E.L. (1983). Intracellular pH regulation in the renal proximal tubule of the salamander. Basolateral HCO_3 transport. *J. Gen. Physiol.*, **81**, 53–94.

BORON, W.F. & BOULPAEP, E.L. (1989). The electrogenic Na/HCO_3 cotransporter. *Kidney Intern.*, **36**, 392–402.

COUSIN, J.L. & MOTAIS, R. (1982a). Inhibition of anion transport in the red blood cell by anionic amphiphilic compounds I. Determination of the flufenamate-binding site by proteolytic dissection of the band 3 protein. *Biochem. Biophys. Acta*, **687**, 147–155.

COUSIN, J.L. & MOTAIS, R. (1982b). Properties of anion transport in the red blood cell by anionic amphiphilic compounds II. Chemical properties of the flufenamate-binding site on the band 3 protein. *Biochem. Biophys. Acta*, **687**, 156–164.

DEITMER, J.W. (1991). Electrogenic sodium-dependent bicarbonate secretion by glial cells of the leech central nervous system. *J. Gen. Physiol.*, **98**, 637–655.

DEL CASTILLO, J.R., MARIN, R., PROVERBIO, T. & PROVERBIO, F. (1982). Partial characterization of the ouabain-insensitive, Na^+ stimulated ATPase activity of kidney basal-lateral plasma membrane. *Biochem. Biophys. Acta*, **692**, 61–68.

DI STEFANO, A., WITTNER, M., SCHLATTER, E., LANG, H.J., ENGLERT, H. & GREGER, R. (1985). Diphenylamine-2-carboxylate, a blocker of the Cl^--conductive pathway in Cl^- transporting epithelia. *Pflügers Arch.*, **405** (Suppl. 1), S95–S100.

EDELMAN, A., BOUTHIER, M. & ANAGNOSTOPOULOS, T. (1981). Chloride distribution in the proximal convoluted tubule of Necturus kidney. *J. Memb. Biol.*, **62**, 7–17.

EL MERNISSI, G., BARLET-BAS, C., KHADOURI, C., MARSY, S., CHEVAL, L. & DOUCET, A. (1991). Characterization and localisation of ouabain-insensitive Na-dependent ATPase activities along the rat nephron. *Biochem. Biophys. Acta*, **1064**, 205–211.

FRELIN, C., VIGNE, P., BARBRY, P. & LAZDUNSKI, M. (1987). Molecular properties of amiloride action and of its Na^+ transporting targets. *Kidney Intern.*, **32**, 785–793.

GÖGELEIN, H. (1988). Chloride channels in epithelia. *Biochem. Biophys. Acta*, **947**, 521–547.

GÖGELEIN, H., DAHLEM, D., ENGLERT, H.C. & LANG, H.J. (1990). Flufenamic acid, mefenamic acid and niflumic acid inhibit single non selective channels in the rat exocrin pancreas. *FEBS Lett*, **268**, 79–82.

GUSSIN, R.Z., CUMMINGS, J.R., STROKEY, E.H. & RONSBERG, M.A. (1969). CL 65, 562(4-(ααα-trifluoro-m-toluidino)nicotinic acid), a novel 'high ceiling' diuretic. *J. Pharmacol. Exp. Ther.*, **167**, 194–206.

HARRIS, E.J. (1965). The dependence of efflux of sodium from frog muscle on internal Na+ and external potassium. *J. Physiol.*, **177**, 355–376.

HUGHES, B.A., ADORANTE, J.S., MILLER, S.S. & LIN, H. (1989). Apical electrogenic $Na-HCO_3$ cotransport. A mechanism for HCO_3 absorption across the retinal pigment epithelium. *J. Gen. Physiol.*, **94**, 125–150.

JENTSCH, T.J., KELLER, S.K., KOCH, M. & WIEDERHOLT, T. (1984). Evidence for coupled transport of bicarbonate and sodium in cultured bovine corneal endothelial cells. *J. Memb. Biol.*, **81**, 189–204.

KARLISH, S.J.D. & STEIN, W.D. (1985). Cation activation of the pig kidney sodium pump, transmembrane allosteric effects of sodium. *J. Physiol.*, **359**, 119–149.

KONDO, Y. & FRÖMTER, E. (1987). Axial heterogeneity of sodium-bicarbonate cotransport in proximal straight tubule of rabbit kidney. *Pflügers Arch.*, **410**, 481–486.

LOPES, A.G., SIEBENS, A.W., GIEBISCH, G. & BORON, W.F. (1987). Electrogenic Na/HCO_3 cotransport across basolateral membrane of isolated perfused Necturus proximal tubule. *Am. J. Physiol.*, **253**, F340–F350.

MARIN, R., GOMEZ, D.C., RODRIGUEZ, G.A., PROVERBIO, T. & PROVERBIO, F. (1990). Ouabaïn-insensitive, Na-ATPase activity in pure suspensions of rat kidney proximal tubules. *FEBS Lett.*, **269**, 77–78.

OBERLEITHNER, H., KERSTING, U. & HUNTER, M. (1988). Cytoplasmic pH determines K^+ conductance in fused epithelial cells. *Proc. Natl. Acad. Sci. U.S.A.*, **85**, 8345–8349.

ORSENIGO, M.N., TOSCO, M,. ESPOSITO, G. & FAELLI, A. (1991). The ouabain-insensitive sodium pump. *Comp. Biochem. Physiol.*, **99A**, 279–283.

PLANELLES, G. & ANAGNOSTOPOULOS, T. (1982). Effects of ouabain on the electrical responses of proximal tubular cells. *J. Pharmacol. Exp. Ther.*, **223**, 841–847.

PLANELLES, G. & ANAGNOSTOPOULOS, T. (1991). Basolateral electrogenic Na/HCO_3 symport in the amphibian distal tubule. *Pflügers Arch.*, **417**, 582–590.

PLANELLES, G., KURKDJIAN, A. & ANAGNOSTOPOULOS, T. (1984). Cell and luminal pH in the proximal tubule of Necturus kidney. *Am. J. Physiol.*, **247**, F932–F938.

PLANELLES, G., TEULON, J. & ANAGNOSTOPOULOS, T. (1981). The effects of barium on the electrical properties of the basolateral membrane in proximal tubule. *Naunyn-Schmied. Arch. Pharmacol.*, **318**, 135–141.

PLANELLES, G., THOMAS, S.R. & ANAGNOSTOPOULOS, T. (1993). Change of apparent stoichiometry of proximal tubule Na^+-HCO_3^- cotransport upon experimental reversal of its orientation. *Proc. Natl. Acad. Sci. U.S.A.*, **90**, 7406–7410.

SOLEIMANI, M. & ARONSON, P.S. (1989a). Ionic mechanism of Na^+-HCO_3^- cotransport in rabbit renal basolateral membrane vesicles. *J. Biol. Chem.*, **264**, 18302–18308.

SOLEIMANI, M. & ARONSON, P.S. (1989b). Effects of acetazolamide on Na^+-HCO_3^- cotransport in basolateral membrane vesicles isolated from rabbit renal cortex. *J. Clin. Invest.*, **83**, 945–951.

WANGEMANN, P., WITTNER, M., DI STEFANO, A., ENGLERT, H.C., LANG, H.J., SCHLATTER, E. & GREGER, R. (1986). Cl^--channel blockers in the thick ascending limb of the loops of Henle. Structure activity relationship. *Pflügers Arch.*, **407** (Suppl. 2), S128–S141.

YOSHITOMI, K., BUCKHARDT, B.Ch. & FRÖMTER, E. (1985). Rheogenic sodium-bicarbonate cotransport in the peritubular cell membrane of rat. *Pflügers Arch.*, **405**, 360–366.

(Received December 3, 1993
Revised February 10, 1994
Accepted February 11, 1994)

Br. J. Pharmacol. (1994), **112**, 471–476

Vasoconstrictor responses after neo-intima formation and endothelial removal in the rabbit carotid artery

[1]Guido R.Y. De Meyer, Hidde Bult, *Levent Üstünes, †Mark Kockx, François H. Jordaens, Ludo L. Zonnekeyn & Arnold G. Herman

Division of Pharmacology, University of Antwerp (UIA), Antwerp, Belgium; *Department of Pharmacology, Faculty of Pharmacy, Ege University, Izmir, Turkey and †Department of Pathology, General Hospital Middelheim, Antwerp, Belgium

1 The present study examined the responses of the rabbit carotid artery to five vasoconstrictors after neo-intima formation induced by perivascular collar treatment and evaluated the role of constitutive and inducible nitric oxide (NO) synthase and endothelial cells (ECs).

2 Ring segments of the rabbit carotid artery were mounted in organ chambers for isometric tension recording. Neo-intima-bearing vessels developed less force (E_{max}) in response to KCl, the thromboxane-mimetic U-46619 and 5-hydroxytryptamine (5-HT), but not to angiotensin I and II.

3 The collar-treatment increased the sensitivity to 5-HT, and decreased the sensitivity to angiotensin II. The sensitivity to U-46619 and angiotensin I remained unchanged.

4 Mechanical removal of ECs and inhibition of NO biosynthesis by N^G-monomethyl-L-arginine (L-NMMA) and N^G-nitro-L-arginine (L-NOARG) increased the sensitivity to 5-HT in sham and collar-treated segments to the same extent. The effects of collar-treatment and endothelial removal or treatment with inhibitors of NO biosynthesis were additive. Inhibition of NO biosynthesis failed to augment sensitivity to 5-HT after endothelial denudation. L-NOARG increased the force development to KCl in sham and collar-treated segments to the same extent. However, L-NMMA and L-NOARG failed to augment the contractile responses of neo-intima-bearing vessels to 5-HT and KCl after endothelial removal.

5 The responses to angiotensin I were not altered, either by the neo-intima or by endothelial removal. In arteries with a neo-intima the sensitivity to angiotensin II was decreased. Removal of the endothelium or incubation with L-NOARG counteracted this rightward shift and increased E_{max}.

6 Our results demonstrate that contractions to 5-HT, angiotensin II and KCl are modulated by NO in both sham and neo-intima-bearing vessels. Inhibition of NO biosynthesis and collar treatment resulted in additive effects on the EC_{50} values, suggesting that the 5-HT and angiotension (AT) receptors on the smooth muscle cells are also modified by the formation of a neo-intima. Furthermore, the reduced contractile responses of segments with a neo-intima are not due to NO formed by an inducible NO synthase in those vessels.

Keywords: Nitric oxide; inducible nitric oxide synthase (iNOS); endothelium; neo-intima; 5-HT; angiotensin; U-46619; potassium chloride; silicone collar

Introduction

Patients with atherosclerosis are prone to the development of vasospasm (Maseri *et al.*, 1978). In animals, cholesterol feeding produces augmented responses to vasoconstrictor stimuli (Heistad *et al.*, 1984; Verbeuren *et al.*, 1986). However, very little is known about the vascular responsiveness in early atherosclerosis. Recently, a new model of early atherosclerosis has been developed (Booth *et al.*, 1989). By positioning a non-occlusive, soft silicone collar around the rabbit carotid artery, a neo-intima develops within seven days via smooth muscle cell infiltration into the subendothelium (Kockx *et al.*, 1992). A neo-intima can be considered as a site of predilection for atherosclerosis (Wilens, 1951; Stary *et al.*, 1992). Previously, it has been demonstrated that the nitric oxide synthase: guanosine 3':5'-cyclic monophosphate (cyclic GMP) system remains intact in neo-intima-bearing vessels, but that muscarinic endothelium-dependent relaxation becomes selectively impaired (De Meyer *et al.*, 1991; 1992; Arthur & Dusting, 1992).

Furthermore, during the formation of a neo-intima the sensitivity to 5-HT but not to noradrenaline, is increased even without a cholesterol-rich diet (De Meyer *et al.*, 1990). Thus, the presence of a neo-intima can selectively alter contractile responses. On the other hand, several lines of evidence suggest that endothelial cells can modulate the responses to vasoconstricting agents (for review, see Vanhoutte *et al.*, 1986). In view of this, we studied the contribution of the endothelial cells to the altered 5-HT-responses in vessels with a neo-intima. In addition, another platelet-derived constrictor, thromboxane A_2 (via its stable analogue, U-46619) and angiotensin I and II were investigated. A depolarizing potassium chloride solution was used to evaluate non-receptor mediated force development by the various tissues. Furthermore, the hypothesis that reduced contractile responses of segments with a neo-intima might be due to NO formed by an inducible NO synthase in those vessels was also tested.

Methods

Induction of a neo-intima and preparation of segments

Male New Zealand white rabbits (2.5–3.0 kg) were anaesthetized with sodium pentobarbitone (30 mg kg^{-1}, i.v.) and both carotid arteries were exposed surgically. A non-occlusive silicone collar of 2.2 cm length was placed around the left carotid artery as described by Booth *et al.* (1989). The right carotid artery was sham-operated, i.e., it was separated from the surrounding connective tissue and the

[1] Author for correspondence.

vagus nerve and received a similar stretch to the contralateral collared artery. The rabbits were fed a standard laboratory chow. Seven days later they were given heparin (150 u kg^{-1}, i.v.) as an anticoagulant and anaesthetized with sodium pentobarbitone (30 mg kg^{-1}, i.v.). The sham and collar-treated carotid artery were dissected and immediately placed in a gassed (95% O_2:5% CO_2) physiological salt solution. The vessels were carefully cleaned of loose connective tissue. Subsequently, two rings (3 mm long) were cut from the right (sham-treated) and left (central collar-treated region) carotid artery. One segment was manipulated very carefully in order to preserve the endothelium; the second segment was denuded of endothelial cells by rubbing the tip of a pair of forceps against the intimal or neo-intimal surface. In another series of experiments a collar was positioned around both the left and right carotid artery for 14 days. In this case the segment proximal to the collar was used as sham.

The rings were mounted in organ chambers filled with 25 ml physiological salt solution, maintained at 37°C and continuously gassed with 95% O_2:5% CO_2. Tension was measured isometrically with a Statham UC_2 force transducer. After an equilibration period of 15 min, the segments were gradually stretched and placed at the optimal point of their length tension relationship (7.2 g ± 0.2 g for 26 control segments and 6.9 g ± 0.2 g for 26 collar-treated segments) using 50 mM KCl. The rings were then allowed to equilibrate for 45 min at their optimal length. The bath medium was changed every 15 min during equilibration.

Experimental protocol

Cumulative (0.5 log unit) concentration-response curves were made to 5-HT (10^{-10} to 10^{-5} M), U-46619 (10^{-8} to 10^{-6} M), angiotensin I (10^{-8} to 10^{-5} M) and angiotensin II (10^{-11} to 10^{-6} M). Concentration-response curves to the various agonists were randomized. Maximum contractile force to a single concentration of 120 mM KCl (Tesfamariam *et al.*, 1989) was also determined at the end of each experiment. Between agonists the bath medium was exchanged three times and tissues were allowed to equilibrate for 30 min. The efficacy of the endothelial removal was evaluated in each segment with acetylcholine (Furchgott & Zawadzki, 1980). In a second experiment we examined the effects of N^G-nitro-L-arginine (L-NOARG, 2×10^{-5} M, Moore *et al.*, 1990) on the contractions induced by 5-HT and angiotensin II in endothelium-intact sham-treated and collar-treated arteries. In a third experiment the effect of N^G-monomethyl-L-arginine (L-NMMA, 10^{-4} M) on 5-HT-induced contractions in rubbed and unrubbed sham-treated and collar-treated arteries was investigated after 14 days of collar treatment. L-NOARG and L-NMMA were added to the organ chambers 40 min prior to experimentation. To inhibit prostaglandin biosynthesis, indomethacin (3×10^{-6} M) was present in the physiological salt solution in the second and third series of experiments.

Materials

Acetylcholine chloride, angiotensin I (acetate salt, human) and angiotensin II (acetate salt, human) were obtained from Sigma, St. Louis, MO, U.S.A. 5-Hydroxytryptamine creatinine sulphate monohydrate and L-NOARG (N^G-nitroamidino-L-2,5-diaminopentanoic acid) from Janssen Chimica, Beerse, Belgium. U-46619 (9,11-dideoxy-11α,9α-epoxymethano-prostaglandin $F_{2\alpha}$) and L-NMMA were gifts from Dr S. Moncada, Wellcome Research Laboratories, Beckenham, Kent, UK. Indomethacin sodium was obtained from Merck, Sharp and Dohme, München, Germany. All drugs were made up in distilled water each day before experimentation. Sodium pentobarbitone was obtained from Psyphac, Brussels, Belgium and heparin Leo from Therabel Pharma, Brussels, Belgium. Silicone (Silastic 732, Dow Corning) was kindly provided by CCMP, Antwerp, Belgium. The physiological salt solution contained (mM): NaCl 118, KCl 4.7, $CaCl_2$ 2.5, KH_2PO_4 1.2, $MgSO_4$ 1.2, $NaHCO_3$ 25, CaEDTA 0.025 and glucose 11.1. Potassium 50 mM and 120 mM were prepared by equimolar replacement of sodium in the salt solution.

Data analysis

The concentration-response curves were analysed as increase in tension (g) from resting and the maximum response (E_{max}) was determined. The negative logarithm of the concentration of agonist that produced a contraction halfway between the minimal and maximal contraction obtained with that agonist ($-\log EC_{50}$) was calculated for each segment, using linear regression analysis (Tallarida & Murray, 1981). The data were analysed by analysis of variance (ANOVA) (Sokal & Rohlf, 1981) with collar (two levels, present or not) as within rabbit factor and endothelial cells (two levels, with or without), L-NOARG (two levels, with or without) or L-NMMA (two levels, with or without) as within artery factor. Only when the interaction between two factors in ANOVA was statistically significant was the ANOVA test supplemented by an additional statistical analysis (Student's *t* test). The SPSS/PC^+ package (SPSS, Chicago, IL, U.S.A.) was applied for these purposes. A probability of error less than 0.05 was selected as the criterion for statistical significance. All data are given as the mean ± s.e.mean. The number of carotid arteries reported (*n*) equals the number of rabbits used.

Results

Maximum contractile force to KCl (120 mM)

The arteries which had been surrounded by the collar developed significantly less tension (E_{max}) in response to KCl than did the sham-treated vessels. Mechanical removal of the endothelial cells did not influence E_{max} (Table 1).

Influence of collar and ECs on responses to 5-HT

As indicated by the decrease of the EC_{50} values, removal of the endothelial cells from sham-treated arteries marginally enhanced the sensitivity to 5-HT (1.7 fold, Table 2). This effect was also observed after collar-treatment (1.9 fold). However, collar-treatment by itself also induced an increased sensitivity to 5-HT as compared to the sham vessels (4.7 fold and 5.2 fold in arteries with ECs and without ECs respectively). The tendency to a diminished maximum contractile force development in response to 5-HT in collared arteries was statistically not significant either in vessels with ECs or in vessels without ECs (Table 1).

Influence of collar and ECs on responses to U-46619

The sensitivity to U-46619 remained unchanged after collar-treatment or endothelial removal (Table 2). However, the maximum contractile force developed by this agent was slightly (i.e. 1.5 g or 20%) decreased in the segments surrounded by the collar (Table 1).

Influence of collar and ECs on responses to angiotensin I and II

The reactivity (EC_{50} and E_{max} values) in response to angiotensin I was not altered, either by the collar-treatment, or by the removal of the endothelial cells (Tables 1 and 2).

The carotid arteries were about 30 times more sensitive to angiotensin II than to angiotensin I. Analysis of the EC_{50} values showed that the effects of neo-intima and endothelial removal were not additive. Indeed, removal of the endothelial cells increased the potency of angiotensin II but this was only seen in segments with collar-induced neo-intima formation and not in sham-treated segments (Table 2). The sensitivity

Table 1 Maximum contractile force (E_{max}) to 5-hydroxytryptamine (5-HT), U-46619, angiotensin I, angiotensin II and KCl in rings from rabbit carotid arteries without (sham) and with a silicone collar in position for 7 days and influence of the removal of the endothelial cells

E_{max} (g)	*5-HT* ($n = 9$)	*U-46619* ($n = 8$)	*Angiotensin I* ($n = 5$)	*Angiotensin II* ($n = 8$)	*KCl* 120 mM ($n = 9$)
Sham (contralateral)					
+ ECs	6.7 ± 0.5	7.0 ± 0.8	3.9 ± 0.9	2.9 ± 0.4	8.2 ± 0.8
− ECs	6.8 ± 0.5	6.9 ± 0.8	3.5 ± 0.5	2.7 ± 0.5	7.8 ± 0.7
Collar					
+ ECs	6.2 ± 0.6	5.6 ± 0.8	4.0 ± 0.8	2.8 ± 0.4	4.7 ± 0.6
− ECs	5.5 ± 0.7	5.4 ± 0.7	4.3 ± 0.4	4.1 ± 0.6	4.3 ± 0.7
Significance of factors in ANOVA:					
Collar	NS	$P = 0.025$	NS	$P = 0.036$	$P < 0.001$
ECs	NS	NS	NS	NS	NS
Collar by ECs	NS	NS	NS	NS	NS

Values are shown as means ± s.e.mean. n represents the number of animals.
NS: not significant. ECs: endothelial cells.

Table 2 EC_{50} values of 5-hydroxytryptamine (5-HT), U-46619, angiotensin I and angiotensin II in rings from rabbit carotid arteries without (sham) and with a silicone collar in position for 7 days and influence of the removal of the endothelial cells

EC_{50} (− log M)	*5-HT* ($n = 9$)	*U-46619* ($n = 8$)	*Angiotensin I* ($n = 5$)	*Angiotensin II* ($n = 8$)
Sham (contralateral)				
+ ECs	7.10 ± 0.06	7.10 ± 0.08	7.00 ± 0.09	8.44 ± 0.08
− ECs	7.34 ± 0.08	6.91 ± 0.11	6.83 ± 0.06	8.43 ± 0.07
Collar				
+ ECs	7.77 ± 0.12	7.14 ± 0.13	6.62 ± 0.27	8.06 ± 0.12*
− ECs	8.06 ± 0.05	7.19 ± 0.07	6.74 ± 0.07	8.56 ± 0.17
Significance of factors in ANOVA:				
Collar	$P < 0.001$	NS	NS	NS
ECs	$P = 0.002$	NS	NS	$P = 0.012$
Collar by ECs	NS	NS	NS	$P < 0.001$

Values are shown as means ± s.e.mean. n represents the number of animals.
NS: not significant. ECs: endothelial cells. *Significantly different from corresponding sham (Student's two-tailed paired t test).

Table 3 Maximum contractile force (E_{max}) to 5-hydroxytryptamine (5-HT) and angiotensin II in rings from rabbit carotid arteries without (sham) and with a silicone collar in position for 7 days and influence of N^G-nitro-L-arginine (L-NOARG, 2×10^{-5} M)

E_{max} (g)	*5-HT* ($n = 6$)	*Angiotensin II* ($n = 7$)
Sham (contralateral)		
− L-NOARG	8.5 ± 1.2	3.0 ± 1.0
+ L-NOARG	9.5 ± 0.7	4.0 ± 1.1
Collar		
− L-NOARG	3.8 ± 0.6	1.5 ± 0.7
+ L-NOARG	3.9 ± 0.8	3.1 ± 0.8
Significance of factors in ANOVA:		
Collar	$P = 0.013$	NS
L-NOARG	NS	$P = 0.014$
Collar by L-NOARG	NS	NS

Values are shown as means ± s.e.mean. n represents the number of animals. NS: not significant.

Table 4 EC_{50} values of 5-hydroxytryptamine (5-HT) and angiotensin II in rings from rabbit carotid arteries without (sham) and with a silicone collar in position for 7 days and influence of N^G-nitro-L-arginine (L-NOARG, 2×10^{-5} M)

EC_{50} (− log M)	*5-HT* ($n = 6$)	*Angiotensin II* ($n = 7$)
Sham (contralateral)		
− L-NOARG	6.85 ± 0.07	9.01 ± 0.19
+ L-NOARG	7.06 ± 0.10	9.28 ± 0.18
Collar		
− L-NOARG	7.06 ± 0.04	8.40 ± 0.18
+ L-NOARG	7.44 ± 0.08	8.81 ± 0.19
Significance of factors in ANOVA:		
Collar	$P = 0.001$	$P = 0.012$
L-NOARG	$P = 0.026$	$P = 0.007$
Collar by L-NOARG	NS	NS

Values are shown as means ± s.e.mean. n represents the number of animals. NS: not significant.

to angiotensin II decreased in the endothelium intact collar-surrounded segments ($P < 0.05$, Student's t test). Mechanical removal of the endothelial cells of these rings restored the EC_{50} to the sham values (Table 2).

Influence of L-NOARG on the contractions induced by 5-HT, angiotensin II and KCl

In contrast to the first series of experiments, the diminished E_{max} of 5-HT in collar-treated arteries was statistically significant (Table 3). L-NOARG (2×10^{-5} M) decreased the EC_{50} of 5-HT, both in sham and collar-treated segments. The effects of the collar and L-NOARG were additive, as indicated by the absence of interaction (Table 4). The concentration-response curve for angiotensin II shifted to the right in collar-treated segments, confirming the first series of experiments. L-NOARG induced a leftward shift of the angiotensin II curve and enhanced its E_{max} both in control and collar-treated vessels (Table 3). L-NOARG increased the force development to KCl in sham and collar-treated seg-

ments to the same extent. However, L-NOARG failed to augment contractile responses to KCl after endothelial denudation (Table 5).

Influence of L-NMMA on responses to 5-HT in sham and collar-treated arteries with or without ECs

The maximum contractile force developed (E_{max}) in response to 5-HT was significantly increased after L-NMMA treatment both in sham- and collar-treated segments with ECs (Table 6). This increase in E_{max} occurred to the same extent in sham and collar-treated rings. E_{max} was also augmented in the rubbed sham and collar-treated segments after L-NMMA incubation. However, in the rubbed collar-treated segments this was to a smaller extent (Table 6).

The increased sensitivity of the collared segments to 5-HT persisted after L-NMMA incubation (Table 7). L-NMMA incubation increased the sensitivity to 5-HT both in sham and in collar-treated segments to the same extent (1.6 fold). On the other hand, the sensitivity to 5-HT in endothelium denuded sham- and endothelium denuded collar-treated segments was not significantly influenced by L-NMMA.

Table 5 Maximum contractile force (E_{max}) to KCl in rings from rabbit carotid arteries without (sham) or with a silicone collar in position for 14 days and influence of the endothelial cells and N^G-nitro-L-arginine (L-NOARG, 2×10^{-5} M)

E_{max} (g)	*KCl + ECs* ($n = 13$)	*KCl − ECs* ($n = 13$)
Sham (proximal)		
− L-NOARG	6.5 ± 0.6	7.3 ± 0.4
+ L-NOARG	8.3 ± 0.4	7.7 ± 0.5
Collar		
− L-NOARG	4.5 ± 0.6	5.6 ± 0.7
+ L-NOARG	6.1 ± 0.6	6.0 ± 0.6

Significance of factors in ANOVA:

Collar: $P = 0.001$; ECs: NS; L-NOARG: $P = 0.039$; Collar by ECs: NS; Collar by L-NOARG: NS; ECs by L-NOARG: $P = 0.005$; Collar by ECs, by L-NOARG: NS

Values are shown as means ± s.e.mean. n represents the number of animals. NS: not significant. ECs: endothelial cells.

Table 6 Maximum contractile force (E_{max}) to 5-hydroxytryptamine (5-HT) in rings from rabbit carotid arteries without (sham) or with a silicone collar in position for 14 days and influence of the endothelial cells and N^G-monomethyl-L-arginine (L-NMMA, 10^{-4} M)

E_{max} (g)	*5-HT + ECs* ($n = 13$)	*5-HT − ECs* ($n = 13$)
Sham (proximal)		
− L-NMMA	6.9 ± 0.5	7.0 ± 0.6
+ L-NMMA	8.0 ± 0.3	8.3 ± 0.5
Collar		
− L-NMMA	5.6 ± 0.6	6.9 ± 0.7
+ L-NMMA	6.6 ± 0.4	7.3 ± 0.7

Significance of factors in ANOVA:

Collar: NS; ECs: NS; L-NMMA: $P = 0.025$; Collar by ECs: NS; Collar by L-NMMA: NS; L-NMMA by ECs: NS; Collar by ECs, by L-NMMA: NS

Values are shown as means ± s.e.mean. n represents the number of animals. NS: not significant. ECs: endothelial cells.

Table 7 EC_{50} values of 5-hydroxytryptamine (5-HT) in rings from rabbit carotid arteries without (sham) or with a silicone collar in position for 14 days and influence of the endothelial cells and N^G-monomethyl-L-arginine (L-NMMA, 10^{-4} M)

EC_{50} (− log M)	*5-HT + ECs* ($n = 13$)	*5-HT − ECs* ($n = 13$)
Sham (proximal)		
− L-NMMA	6.78 ± 0.06	6.89 ± 0.06
+ L-NMMA	6.98 ± 0.06	6.95 ± 0.06
Collar		
− L-NMMA	6.92 ± 0.06	7.09 ± 0.07
+ L-NMMA	7.11 ± 0.11	7.05 ± 0.07

Significance of factors in ANOVA:

Collar: $P = 0.009$; L-NMMA: $P = 0.004$; ECs: NS; Collar by ECs: NS; Collar by L-NMMA: NS; ECs by L-NMMA: $P = 0.016$; Collar by ECs, by L-NMMA: NS

Values are shown as means ± s.e.mean. n represents the number of animals. NS: not significant. ECs: endothelial cells.

Discussion

5-HT and KCl

The present studies confirmed that the collar-induced neo-intima formation is associated with an increased sensitivity to 5-HT (De Meyer *et al.*, 1990). They also indicated that the EC_{50} for 5-HT decreased after mechanical removal of the endothelial cells. Moreover, both effects were additive, as indicated by the absence of interaction (Table 2). L-NOARG and L-NMMA, which block NO biosynthesis (Moore *et al.*, 1990), shifted the 5-HT curve of normal and collared segments with ECs to the left, indicating that NO modulates 5-HT-induced contractions. However, since L-NOARG and L-NMMA decreased the EC_{50} of 5-HT in normal and collar-treated segments to a similar extent, and since the effects of neo-intima formation and L-NOARG or L-NMMA were additive, the increased sensitivity to 5-HT in collar-treated rings cannot be explained by an impaired release of NO. Furthermore, there was an interaction between the presence of ECs and the efficacy of L-NOARG in sham and collared rings. The EC_{50} shift due to L-NOARG was not significant after endothelial removal from normal or collared segments. Therefore, the endothelial cells appear to be the source of NO which modulates the 5-HT responses both in normal and in collared segments. Since indomethacin, a cyclo-oxygenase inhibitor was used throughout the organ chamber experiments with L-NOARG and L-NMMA, it is unlikely that the increased sensitivity to 5-HT after collar treatment is due to an impaired release of prostacyclin or other vasodilator prostaglandins. Hence, these results suggest that the 5-HT receptors on the smooth muscle cells (SMCs) are modified by the collar treatment. Alternatively, the uptake of 5-HT by the endothelium could be compromised, facilitating the access of the amine to the vascular SMCs. This assumption implies a selective alteration of the 5-HT-carrier, since the response to noradrenaline, another amine metabolized by the ECs, was unaltered (De Meyer *et al.*, 1990).

In accordance with the previous experiments, the force development to KCl was always reduced, whereas the reduction of the E_{max} of 5-HT was decreased in the second series of experiments. This discrepancy may be explained by the biological variability in the extent of neo-intima formation. Indeed, previous experiments have shown that the E_{max} of 5-HT decreases significantly as the neo-intima becomes thicker. The cells in the neo-intima are mainly smooth muscle cells, orientated in a longitudinal direction, thus perpen-

dicular to their original position in the media (De Meyer *et al.*, 1991; Kockx *et al.*, 1992). This could further explain the decreased maximum contractile force developed by KCl, U-46619, and 5-HT (in the second experiment). A change of the smooth muscle phenotype from a contractile to a synthetic stage may be another explanation. This phenomenon is observed in smooth muscle cells either adjacent to or within atheromatous plaques (Mosse *et al.*, 1985; Kocher & Gabbiani, 1986). Also during the development of neo-intimal thickening induced by injury with an inflated balloon catheter an altered phenotype is expressed (Manderson *et al.*, 1989a). Under the latter circumstances the maximum contractile force developed by KCl was also decreased (Manderson *et al.*, 1989b).

Joly *et al.* (1992) have shown that balloon denudation leads to expression of an inducible NO synthase. This inducible NO synthase (NOS2) produces NO continuously, in contrast to the calcium-dependent constitutive enzyme (NOS1) in ECs (Moncada *et al.*, 1991). A continuous NO supply could possibly explain the hyporeactivity of the SMCs. Since inflammatory components may be involved in the formation of a neo-intima, we tested the hypothesis that the reduced contractile responses of segments with a neo-intima was due to NO formed by NOS2 in those vessels.

Since after 14 days of collar treatment, L-NMMA as well as L-NOARG increased the force development to 5-HT and KCl in sham- and collar-treated segments to the same extent, the possibility of a continuous release of NO in collar-treated rings seems to be unlikely. This was further confirmed by the observation that L-NMMA and L-NOARG did not augment contractile responses of the neo-intima bearing vessels to 5-HT and KCl after endothelial denudation. Therefore, these results fail to support the assumption that the diminished force development in collared segments was due to the expression of an inducible NOS2 in either media or neo-intima.

Angiotensin

The presence of an intact endothelium may (Oshiro *et al.*, 1985; Bullock *et al.*, 1986; Gruetter *et al.*, 1988) or may not (Saye *et al.*, 1984; D'Orleans-Juste *et al.*, 1985; Gruetter *et al.*, 1988) inhibit vasoconstrictor responses to angiotensin II, depending upon the species and (or) vascular bed from which the vessels are isolated. In the present study endothelial denudation of the control arteries did not alter the reactivity (EC_{50}, E_{max}) to angiotensin II. However, in the arteries with a neo-intima and with an intact endothelium, the sensitivity to this potent vasoconstrictor was decreased. Removal of the endothelial cells of the neo-intima-bearing vessels increased the maximum contractile force and restored the EC_{50} to its value in the sham-treated arteries. This was also indicated by the significant interaction between collar-treatment and endothelial denudation.

Several explanations are conceivable for the decreased sensitivity to angiotensin II. First, an altered sensitivity of the angiotensin II receptors on the smooth muscle cells of neo-intima-bearing vessels. Second, the endothelial cells may produce more vasodilator substances after neo-intima formation. Evidence exists that angiotensin II can stimulate the release of dilator prostaglandins (Desjardins-Giasson *et al.*, 1982) and that angiotensin II-induced endothelium-dependent relaxations of canine renal arteries may be mediated by release of cyclo-oxygenase products from the endothelium (Toda, 1984). Another possible mediator of the decreased sensitivity to angiotensin II is endothelium-derived NO. Third, the endothelial cells of neo-intima-bearing vessels may have an enhanced capacity for degrading angiotensin II.

To elucidate some of these possibilities we performed a second series of experiments and investigated the effects of L-NOARG on the contractions elicited by angiotensin II. L-NOARG evoked a sensitization and slightly enhanced the contractions to angiotensin II. Hence, in the rabbit carotid artery, angiotensin II-induced contractions are modulated by NO. These effects seemed to be more pronounced in neo-intima-bearing vessels. However, the effects of the collar and L-NOARG treatment were additive, suggesting that AT receptors on the SMCs are modified as well by the formation of a neo-intima. The responsiveness to angiotensin I had not been changed by endothelial denudation. Although there was a tendency to a decreased sensitivity to angiotensin I after denudation of ECs, (a finding that would be compatible with angiotensin II formation by angiotensin converting enzyme) this was not statistically significant. The latter is in agreement with Saye *et al.* (1984), who demonstrated that conversion of angiotensin I to angiotensin II in endothelial-disrupted rabbit aortic rings was the same as in intact rings, 5 min after the addition of angiotensin I. As angiotensin I is converted to angiotensin II at the luminal side of the endothelium and then immediately diluted into the organ chamber before it can react with the underlying smooth muscle cells, it was not very likely that significant effects of the endothelial denudation would become apparent in the present experimental set-up. Indeed, neither removal of the endothelial cells, nor the development of a neo-intima affected the responses to angiotensin I.

In conclusion, our results indicate that the presence of a neo-intima diminishes the reactivity to KCl and slightly to U-46619, but not to angiotensin I. NO modulates the contractions to 5-HT and angiotensin II both in sham and neo-intima-bearing vessels. However, the 5-HT and AT receptors on the SMCs seem to be modified as well by the formation of a neo-intima. Furthermore, the reduced contractile responses of segments with a neo-intima are not due to NO formed by an inducible NO synthase in those vessels.

The authors wish to thank Mrs Liliane Van den Eynde and Mrs Lydie Van Laerhoven for typing the manuscript. G.R.Y.DeM. is Senior Research Assistant of the National Fund for Scientific Research, Belgium. This study was supported by the BEKALES Foundation and by a grant of the FGWO (No. 3.9036.91) and by the Belgian Programme on Interuniversity Poles of Attraction.

References

ARTHUR, J.F. & DUSTING, G.J. (1992). Selective endothelial dysfunction in early atheroma-like lesions in the rabbit. *Coron. Artery Dis.*, **3**, 623–629.

BOOTH, R.F.G., MARTIN, J.F., HONEY, A.C., HASSALL, D.G., BEESLEY, J.E. & MONCADA, S. (1989). Rapid development of atherosclerotic lesions in the rabbit carotid artery induced by perivascular manipulation. *Atherosclerosis*, **76**, 257–268.

BULLOCK, G.R., TAYLOR, S.G. & WESTON, A.H. (1986). Influence of the vascular endothelium on agonist-induced contractions and relaxations in rat aorta. *Br. J. Pharmacol.*, **89**, 819–830.

DE MEYER, G.R.Y., BULT, H. & HERMAN, A.G. (1992). Selective muscarinic alterations of nitric oxide-mediated relaxations by neo-intima. *J. Cardiovasc. Pharmacol.*, **20** (suppl 12), S205–S207.

DE MEYER, G.R.Y., BULT, H., MARTIN, J.F., VAN HOYDONCK, A.-E. & HERMAN, A.G. (1990). The effect of a developing neo-intima on serotonergic and adrenergic contractions. *Eur. J. Pharmacol.*, **187**, 519–524.

DE MEYER, G.R.Y., BULT, H., VAN HOYDONCK, A.-E., JORDAENS, F.H., BUYSSENS, N. & HERMAN, A.G. (1991). Neo-intima formation impairs endothelial muscarinic receptors while enhancing prostacyclin mediated responses in the rabbit carotid artery. *Circ. Res.*, **68**, 1669–1680.

DESJARDINS-GIASSON, S., GUTKOWSKA, J., GARCIA, R. & GENEST, J. (1982). Effect of angiotensin II and norepinephrine on release of prostaglandins E_2 and I_2 by the perfused rat mesenteric artery. *Prostaglandins*, **24**, 105–114.

D'ORLEANS-JUSTE, P., DION, S., MIZRAHI, J. & REGOLI, D. (1985). Effects of peptides and non-peptides on isolated arterial smooth muscles: role of endothelium. *Eur. J. Pharmacol.*, **114**, 9–21.

FURCHGOTT, R.F. & ZAWADZKI, J.V. (1980). The obligatory role of endothelial cells in the relaxation of arterial smooth muscle by acetylcholine. *Nature*, **288**, 373–376.

GRUETTER, C.A., RYAN, E.T., LEMKE, S.M., BAILLY, D.A., FOX, M.K. & SCHOEPP, D.D. (1988). Endothelium-dependent modulation of angiotensin II-induced contraction in blood vessels. *Eur. J. Pharmacol.*, **146**, 85–95.

HEISTAD, D.D., ARMSTRONG, M.L., MARCUS, M.L., PIEGORS, D.J. & MARK, A.L. (1984). Augmented responses to vasoconstrictor stimuli in hypercholesterolemic and atherosclerotic monkeys. *Circ. Res.*, **54**, 711–718.

JOLY, G.A., SCHINI, V.B. & VANHOUTTE, P.M. (1992). Balloon injury and interleukin-1β induce nitric oxide synthase activity in rat carotid arteries. *Circ. Res.*, **71**, 331–338.

KOCHER, O. & GABBIANI, G. (1986). Cytoskeletal features of normal and atheromatous human arterial smooth muscle cells. *Hum. Pathol.*, **17**, 875–880.

KOCKX, M.M., DE MEYER, G.R.Y., JACOB, W.A., BULT, H. & HERMAN, A.G. (1992). Triphasic sequence of neo-intimal formation in the cuffed carotid artery of the rabbit. *Arterioscler. Thromb.*, **12**, 1447–1457.

MANDERSON, J.A., MOSSE, P.R.L., SAFSTROM, J.A., YOUNG, S.B. & CAMPBELL, G.R. (1989a). Balloon catheter injury to rabbit carotid artery. I. Changes in smooth muscle phenotype. *Arteriosclerosis*, **9**, 289–298.

MANDERSON, J.A., COCKS, T.M. & CAMPBELL, G.R. (1989b). Balloon catheter injury to rabbit carotid artery. II. Selective increase in reactivity to some vasoconstrictor drugs. *Arteriosclerosis*, **9**, 299–307.

MASERI, A., L'ABBATE, A., BAROLD, G., CHIERCHIA, S., MARZILLI, M., BALLESTRA, A.M., SEVERIJ, S., PARODI, O., BIAGINI, A., DISTANTE, A. & PESULA, A. (1978). Coronary vasospasm as a possible cause of myocardial infarction, a conclusion derived from the study of preinfarction angina. *N. Engl. J. Med.*, **299**, 1271–1277.

MOORE, P.K., AL-SWAYEH, O.A., CHONG, N.W.S., EVANS, R.A. & GIBSON, A. (1990). L-N^G-nitro arginine (L-NOARG), a novel, L-arginine-reversible inhibitor of endothelium-dependent vasodilatation *in vitro*. *Br. J. Pharmacol.*, **99**, 408–412.

MONCADA, S., PALMER, R.M.J. & HIGGS, E.A. (1991). Nitric oxide: physiology, pathophysiology, and pharmacology. *Pharmacol. Rev.*, **43**, 109–142.

MOSSE, P.R., CAMPBELL, G.R., WANG, Z.L. & CAMPBELL, J.H. (1985). Smooth muscle phenotypic expression in human carotid arteries. I. Comparison of cells from diffuse initimal thickenings adjacent to atheromatous plaques with those of the media. *Lab. Invest.*, **53**, 556–562.

OSHIRO, M.E., PAIVA, A.C. & PAIVA, T.B. (1985). Endothelium-dependent inhibition of the use of extracellular calcium for the arterial response to vasoconstrictor agents. *Gen. Pharmacol.*, **16**, 567–572.

SAYE, J.A., SINGER, H.A. & PEACH, M.J. (1984). Role of endothelium in conversion of angiotensin I to angiotensin II in rabbit aorta. *Hypertension*, **6**, 216–221.

SOKAL, R.R. & ROHLF, F.J. (1981). *Biometry: The Principles and Practice of Statistics in Biological Research*. 2nd edition. pp. 179–453. New York: W.H. Freeman and Company.

STARY, H.C., BLANKENHORN, D.H., CHANDLER, A.B., GLAGOV, S., INSULL, W. Jr., RICHARDSON, M., ROSENFELD, M.E., SCHAFFER, S.A., SCHWARTZ, C.J., WAGNER, W.D. & WISSLER, R.W. (1992). AHA Medical/Scientific Statement: a definition of the intima of human arteries and of its atherosclerosis prone regions: a report from the committee on vascular lesions of the council on arteriosclerosis. American Heart Association. *Arterioscler. Thromb.*, **92**, 120–134.

TALLARIDA & MURRAY (1981). *Manual of Pharmacologic Calculations*. pp. 1–150. Berlin, Heidelberg, New York: Springer-Verlag.

TESFAMARIAM, B., WEISBROD, R.M. & COHEN, R.A. (1989). Augmented adrenergic contractions of carotid arteries from cholesterol-fed rabbits due to endothelial cell dysfunction. *J. Cardiovasc. Pharmacol.*, **13**, 820–835.

TODA, N. (1984). Endothelium-dependent relaxation induced by angiotensin II and histamine in isolated arteries of the dog. *Br. J. Pharmacol.*, **81**, 301–307.

VANHOUTTE, P.M., RUBANYI, G.M., MILLER, V.M. & HOUSTON, D.S. (1986). Modulation of vascular smooth muscle contractions by the endothelium. *Annu. Rev. Physiol.*, **48**, 307–320.

VERBEUREN, T.J., JORDAENS, F.H., ZONNEKEYN, L.L., VAN HOVE, C.E., COENE, M.-C. & HERMAN, A.G. (1986). Effect of hypercholesterolemia on vascular reactivity in the rabbit. I. Endothelium-dependent and endothelium-independent contractions and relaxations in isolated arteries of control and hypercholesterolemic rabbits. *Circ. Res.*, **58**, 552–564.

WILENS, S.L. (1951). The nature of diffuse intimal thickening of arteries. *Am. J. Pathol.*, **27**, 825–839.

(Received September 27, 1993
Revised January 31, 1994
Accepted February 11, 1994)

Br. J. Pharmacol. (1994), 112, 477-486

Effects of an ET_1-receptor antagonist, FR139317, on regional haemodynamic responses to endothelin-1 and [$Ala^{11,15}$]Ac-endothelin-1 (6-21) in conscious rats

[1]S.M. Gardiner, P.A. Kemp, J.E. March, T. Bennett, *A.P. Davenport & †L. Edvinsson

Department of Physiology & Pharmacology, University of Nottingham Medical School, Queen's Medical Centre, Nottingham NG7 2UH; *Department of Clinical Pharmacology, University of Cambridge and †Department of Experimental Research, University of Lund, Sweden

1 In conscious, Long Evans rats, chronically instrumented for the measurement of regional haemodynamics, we compared responses to the putative, selective ET_B-receptor agonist, [$Ala^{1,3,11,15}$]endothelin-1 (ET-1), obtained from two sources (Microchemical Laboratory, Cambridge (MLC) and Neosystem Laboratory, France (NLF)). [$Ala^{1,3,11,15}$]ET-1 (0.15, 0.3, 1 and 10 nmol kg^{-1}) from MLC caused dose-dependent pressor effects, accompanied by reductions in renal and, particularly, mesenteric flows and vascular conductances; there was an initial hyperaemic vasodilatation in the hindquarters which was not dose-dependent, and only with the highest dose was there a subsequent vasoconstriction. There was no significant initial depressor response to [$Ala^{1,3,11,15}$]ET-1 from MLC at any dose. However, the peptide from NLF exerted dose-dependent depressor and hindquarters vasodilator actions, and subsequent pressor effects. The difference between the two peptide preparations remains unexplained, but it appears that the [$Ala^{1,3,11,15}$]ET-1 from MLC may activate ET_B-receptors mediating vasoconstriction, more effectively than those mediating vasodilatation.

2 We also assessed responses to the putative ET_B-receptor agonist, [$Ala^{11,15}$]Ac-ET-1 (6-21) (BQ-3020), and determined the effects of the selective ET_A-receptor antagonist, FR139317, on responses to ET-1 and BQ-3020 at doses matched for their initial depressor and subsequent pressor effects (ET-1, 0.5 nmol kg^{-1}, BQ-3020, 10 nmol kg^{-1}), and also at doses that did not affect mean arterial blood pressure, but which were matched for their renal vasoconstrictor effects (ET-1, 7.5 pmol kg^{-1}; BQ-3020, 0.15 nmol kg^{-1}).

3 BQ-3020 (0.15, 0.3 and 1 nmol kg^{-1}) had dose-dependent pressor effects accompanied by reductions in renal and, particularly, mesenteric flows and vascular conductances. BQ-3020 at a dose of 10 nmol kg^{-1} elicited an initial depressor response which coincided with an attenuated mesenteric vasoconstrictor effect, accompanying a marked hindquarters vasodilatation. Hence, it appears that BQ-3020 may activate both vasoconstrictor and vasodilator ET_B-receptors.

4 FR139317 (0.5 μmol kg^{-1}) caused attenuation of the pressor, and renal, mesenteric and hindquarters vasoconstrictor effects of ET-1 (0.5 nmol kg^{-1}) and of BQ-3020 (10 nmol kg^{-1}), but the reductions of the pressor and renal vasoconstrictor effects of ET-1 were greater than those of BQ-3020. However, in the presence of FR139317, significant pressor and renal, mesenteric and hindquarters vasoconstrictor responses to ET-1 and BQ-3020 still occurred, and the initial depressor and hindquarters vasodilator responses to both peptides were unchanged.

5 ET-1 at a dose of 7.5 pmol kg^{-1} and BQ-3020 at a dose of 0.15 nmol kg^{-1} had similar renal vasoconstrictor effects. However, the response to ET-1 was almost abolished by FR139317 whereas that to BQ-3020 was unaffected. Moreover, under these conditions, the mesenteric vasoconstrictor and hindquarters vasodilator responses to ET-1 and to BQ-3020 were not changed by FR139317.

6 Collectively, these results are consistent with the haemodynamic effects of ET-1 and BQ-3020 involving ET_A-receptors or ET_B-receptors, or ET_A- and ET_B-receptors, depending on the dose of agonist and the regional haemodynamic effect considered.

Keywords: ET_A-receptors; ET_B-receptors; FR139317; regional haemodynamics in Long Evans rats

Introduction

It has been suggested that endothelin (ET) receptors can be classified into three prototypes, namely, ET_A-receptors that exist on vascular smooth muscle and are responsible for vasoconstriction, ET_B-receptors that exist on endothelial cells and are responsible for vasodilatation, and ET_C-receptors that exist on neurones (Masaki *et al.*, 1992). However, already there is evidence that ET_B-receptors may mediate vasoconstriction (e.g. Hiley *et al.*, 1989; Randall, 1991; Bigaud & Pelton, 1992; Clozel *et al.*, 1992; Gardiner *et al.*, 1992b; Moreland *et al.*, 1992; Cristol *et al.*, 1992; Douglas *et al.*, 1992; McMurdo *et al.*, 1993).

Recently, it was reported that the renal and coeliac vasoconstrictor effects of ET-1 in anaesthetized rats were resistant to antagonism by the ET_A-receptor antagonist, BQ-123 (Bigaud & Pelton, 1992; Cristol *et al.*, 1993; Pollock & Opgenorth, 1993). This observation is consistent with these effects of ET-1 being mediated by ET_B-receptors. However, the picture is confused by the finding that the renal and coeliac, but not the mesenteric, vasoconstrictor effects of the ET_B-receptor agonist, [$Ala^{1,3,11,15}$]ET-1 (Hiley *et al.*, 1990; Saeki *et al.*, 1991), were blocked by BQ-123 (Bigaud & Pelton, 1992). In addition, Bigaud & Pelton (1992) found that the mesenteric vasoconstrictor effect of ET-1 was significantly inhibited by BQ-123, whereas Douglas *et al.* (1992) found it was not. In order to determine if these anomalous findings pertain only to the use of [$Ala^{1,3,11,15}$]ET-1 and BQ-123 in anaesthetized rats we have assessed, in conscious rats, regional haemodynamic responses to [$Ala^{1,3,11,15}$]

[1] Author for correspondence.

ET-1 and to [Ala^{11,15}]Ac-ET-1 (6-21) (BQ-3020) (Ihara *et al.*, 1992; Molenaar *et al.*, 1992), which is also a selective ET_B-receptor agonist. In addition, we analysed the effect of the ET_A-receptor antagonist, FR139317 (i.e., ((**R**) 2-[(**R**)-2-[(**S**)-2[[1-(hexahydro-1H-azepinyl)]-carbonyl] amino-4-methyl-pentanoyl] amino-3-[3-(1-methyl-1H-indolyl)]propionyl]amino-3-(2-pyridyl) propionic acid) (Sun *et al.*, 1992; Sogabe *et al.*, 1993; Cardell *et al.*, 1993) on regional haemodynamic responses to doses of ET-1 and BQ-3020, matched for their initial depressor and subsequent pressor effects, or for their renal vasoconstrictor effects. Parts of this work have been presented to the British Pharmacological Society (Gardiner *et al.*, 1992b; 1993; Bennett *et al.*, 1993).

Methods

Male, Long Evans rats (350–450 g) were studied. Animals were anaesthetized (sodium methohexitone, Brietal, Lilly, 40–60 mg kg^{-1}, i.p., supplemented as required) and had pulsed Doppler flow probes (Haywood *et al.*, 1981) fitted around the left renal and superior mesenteric arteries, and the distal abdominal aorta (to monitor flow to the hindquarters) (Gardiner *et al.*, 1991; 1992a). At least 7 days later, rats were anaesthetized (sodium methohexitone, 40 mg kg^{-1}, i.p.) and a catheter was inserted into the distal abdominal aorta (via the ventral caudal artery) and three catheters were inserted into the right jugular vein. Catheters ran subcutaneously to emerge at the back of the neck at the same point as the probe wires; the latter were soldered into a microconnector (Microtech Inc, Boothwyn, U.S.A.) that was clamped into a harness fitted to the rat. A flexible spring was connected to the harness, and the catheters were threaded through this for protection. The spring was supported by a counterbalanced lever that allowed the animals free movement in their individual home cages in which they were left for at least 24 h with free access to food and water before experiments were begun. The experiments performed were as follows:-

Protocol 1: regional haemodynamic responses to [Ala^{1,3,11,15}]ET-1

Increasing i.v. bolus doses of [Ala^{1,3,11,15}]ET-1 (0.15, 0.3, 1 and 10 nmol kg^{-1}) were administered to seven Long Evans rats. The doses were separated by intervals of at least 1 h to allow all variables to return to baseline before the next dose was administered. The peptide used in these experiments was synthesized in the microchemical laboratory in Cambridge (MLC) and the results showed no significant depressor responses at any dose (see Results) whereas Bigaud & Pelton (1992) reported marked depressor responses to [Ala^{1,3,11,15}]ET-1. Since the experiments of Bigaud & Pelton (1992) were carried out in pentobarbitone-anaesthetized Sprague-Dawley rats, we also investigated the effect of the [Ala^{1,3,11,15}]ET-1 obtained from MLC under identical conditions; it had no depressor effect.

The [Ala^{1,3,11,15}]ET-1 used by Bigaud & Pelton (1992) was obtained from Neosystem Laboratory, France (NLF). Therefore, in a second group of rats ($n = 6$) we assessed haemodynamic responses to this peptide at doses of 0.15, 0.3, 1 and 10 nmol kg^{-1}. While we were able to confirm this peptide had dose-dependent initial depressor effects (see Results) these were very transient (duration about 30 s) in contrast to the effects reported by Bigaud & Pelton (1992) which lasted for at least 3 min. In order to determine if the depressor effect of the [Ala^{1,3,11,15}]ET-1 from NLF was more prolonged in the experimental model studied by Bigaud & Pelton (1992) we also investigated its effects in pentobarbitone-anaesthetized Sprague-Dawley rats ($n = 2$).

Protocol 2: regional haemodynamic responses to BQ-3020

Increasing bolus doses of BQ-3020 (0.1, 0.3, 1 and 10 nmol kg^{-1}) were administered to another eight Long Evans rats, using the same dosing schedule as above.

Protocol 3: regional haemodynamic responses to ET-1 or BQ-3020 before and after FR139317

From the above experiments, we determined that the initial depressor and subsequent pressor effects of ET-1 at a dose of 0.5 nmol kg^{-1}, and BQ-3020 at a dose of 10 nmol kg^{-1}, were similar. Therefore, we then assessed (in the same animals, but on different days) regional haemodynamic responses to ET-1 or BQ-3020 at these doses before and 5 min after FR139317 at a dose of 0.5 μmol kg^{-1}. This dose was chosen because higher doses of FR139317 had pressor effects, and did not cause any greater inhibition of responses to ET-1 or BQ-3020 than did the dose of 0.5 μmol kg^{-1}.

Six of the animals that underwent this protocol came from the group of eight studied in protocol 2 (on another experimental day). An additional two animals were investigated to make $n = 8$ for the assessment of the effects of FR139317 on responses to ET-1 or BQ-3020. Four extra animals, together with some of those in this protocol (i.e. protocol 3) were also investigated on another day to determine the reproducibility of responses to ET-1 ($n = 8$) or BQ-3020 ($n = 7$) before and after saline administration (0.1 ml), to control for the effect of FR139317 vehicle.

From our initial findings (see Results) it appeared that some of the effects of the 10 nmol kg^{-1} dose of BQ-3020 were inhibited by FR139317. This raised the possibility that this relatively high dose of BQ-3020 was acting on ET_A-receptors. Therefore, in a separate group of eight rats we assessed responses to low doses of ET-1 (7.5 pmol kg^{-1}) and BQ-3020 (0.15 nmol kg^{-1}), before and after saline, and before and after FR139317 (0.5 μmol kg^{-1}) administration. The doses of ET-1 and BQ-3020 were matched for their renal vasoconstrictor effects.

Drugs and peptides

ET-1 was obtained from the Peptide Institute (Osaka, Japan) through their UK agents (Scientific Marketing Associates); FR139317 was a gift from Dr Jo Mori (Fujisawa Pharmaceutical Co., Osaka, Japan). [Ala^{1,3,11,15}]ET-1 and BQ-3020, obtained from MLC, were preparaed by solid phase t-Boc chemistry, purified by gel filtration, and the sequence confirmed by microsequence analysis; peptide concentration was determined by u.v. spectrophotometry. Peptide purity was confirmed by analytical high performance liquid chromatography using a Vydac C18 column. The gradient was 30% acetonitrile in water containing 0.1% trifluoroacetic acid at time 0 to 38% acetonitrile in water (0.1% trifluoroacetic acid) after 45 min. For each MLC peptide, a single peak was found using spectrophotometric detection at 206 nm.

All substances were dissolved in sterile isotonic saline (154 nmol l^{-1} NaCl) containing 1% bovine serum albumin (Sigma). Bolus injections were given in a volume of 100 μl and flushed in with 150 μl of isotonic saline.

Data analysis

Throughout an experimental protocol, continuous recordings were made of instantaneous heart rate, phasic and mean arterial blood pressures, and phasic and mean Doppler shift signals. Percentage changes in mean Doppler shift signals were taken as an index of flow changes, and the corresponding % changes in vascular conductances were calculated by dividing the mean Doppler shift signal by the mean arterial blood pressure (Gardiner *et al.*, 1991; 1992a).

Responses to [Ala^{1,3,11,15}]ET-1, BQ-3020, or ET-1 were

assessed from the values measured at 0.25, 0.5, 0.75, 1, 2, 3, 4 and 5 min; these responses were analysed by Friedman's test applied to the changes relative to the pretreatment baseline. Comparisons of the responses to [$Ala^{1,3,11,15}$]ET-1 or BQ-3020 under different conditions were made by the Mann-Whitney U test applied to integrated responses (i.e. areas under or over curves; AUC and AOC 0–5 min, respectively). The effects of FR139317 on responses to ET-1 or BQ-3020 were assessed by comparing integrated responses in the absence and presence of FR139317 by Wilcoxon's test. A value of $P<0.05$ was taken as significant.

Results

Regional haemodynamic responses to [$Ala^{1,3,11,15}$]ET-1

The injection of [$Ala^{1,3,11,15}$]ET-1 obtained from MLC caused dose-dependent pressor effects and bradycardia. There was an initial, variable tachycardia (Figures 1 and 2), but there was not a consistent, initial hypotensive response to [$Ala^{1,3,11,15}$]ET-1 at doses of 0.15, 0.3 or 1 nmol kg^{-1} (Figure 1). Even at a dose of 10 nmol kg^{-1}, the peptide did not have an early depressor effect in all animals, and in those animals in which such a response occurred it was slight, and so brief (Figure 2) that it had gone by the first post-injection measurement (i.e. 0.25 min; Figure 1). [$Ala^{1,3,11,15}$]ET-1 from MLC in doses as high as 30 nmol kg^{-1}, in pentobarbitone-anaesthetised Sprague-Dawley rats (i.e., the model studied by Bigaud & Pelton (1992)), caused no initial depressor response (data not shown).

The pressor effects of [$Ala^{1,3,11,15}$]ET-1 obtained from MLC were accompanied by dose-dependent reductions in renal and mesenteric flows and vascular conductances; the changes in the mesenteric vascular bed were greatest (Figures 1 and 2). In the hindquarters vascular bed there was an initial hyperaemia and vasodilatation, although the latter was not dose-dependent (Figures 1 and 2). Only with the highest dose of [$Ala^{1,3,11,15}$]ET-1 was there a subsequent hindquarters vasoconstriction (Figure 1).

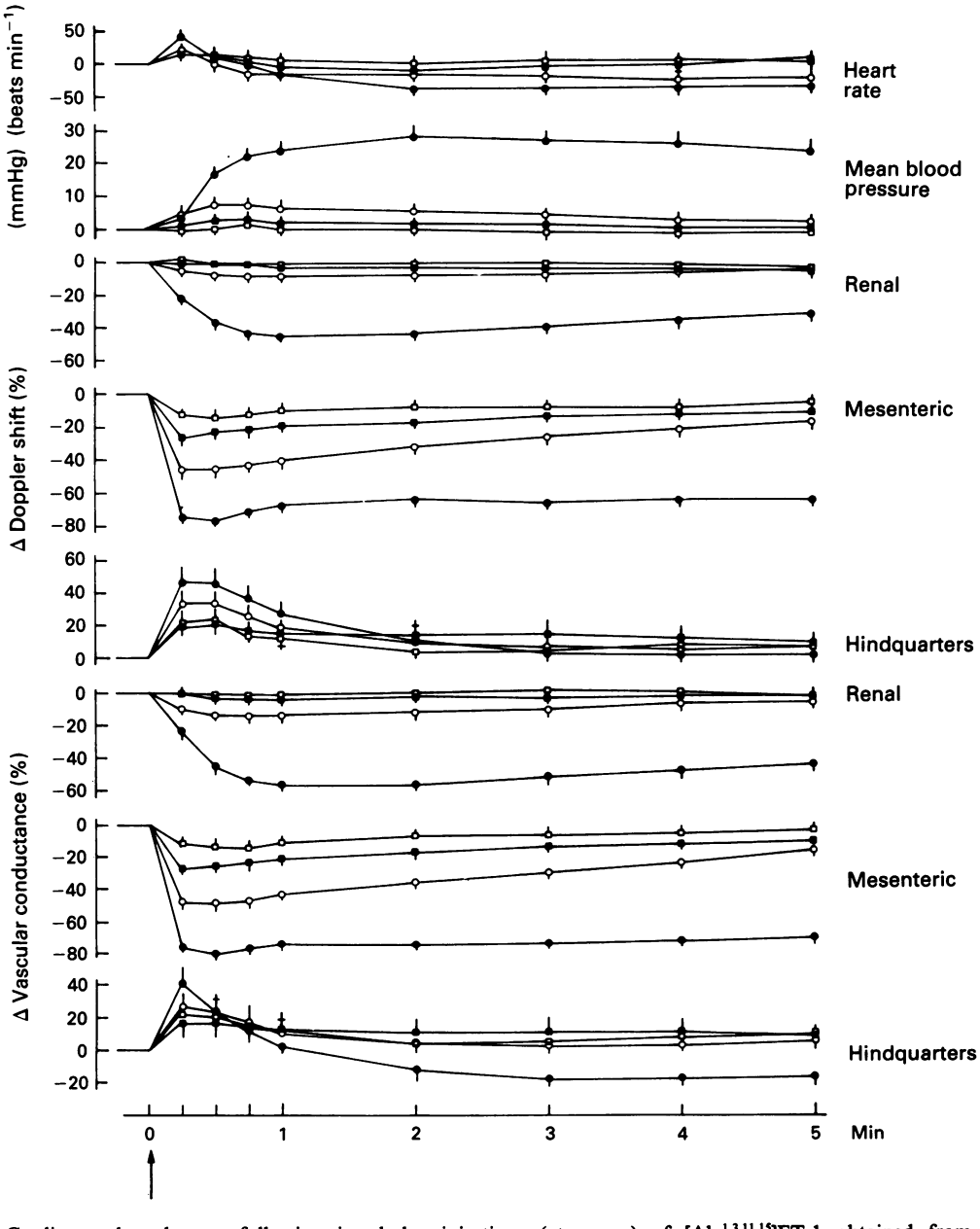

Figure 1 Cardiovascular changes following i.v. bolus injections (at arrow) of [$Ala^{1,3,11,15}$]ET-1 obtained from MLC (□, 0.15 nmol kg^{-1}; ■, 0.3 nmol kg^{-1}; ○, 1 nmol kg^{-1}; ●, 10 nmol kg^{-1}) in the same conscious Long Evans rats ($n = 7$). Values are mean with s.e.mean.

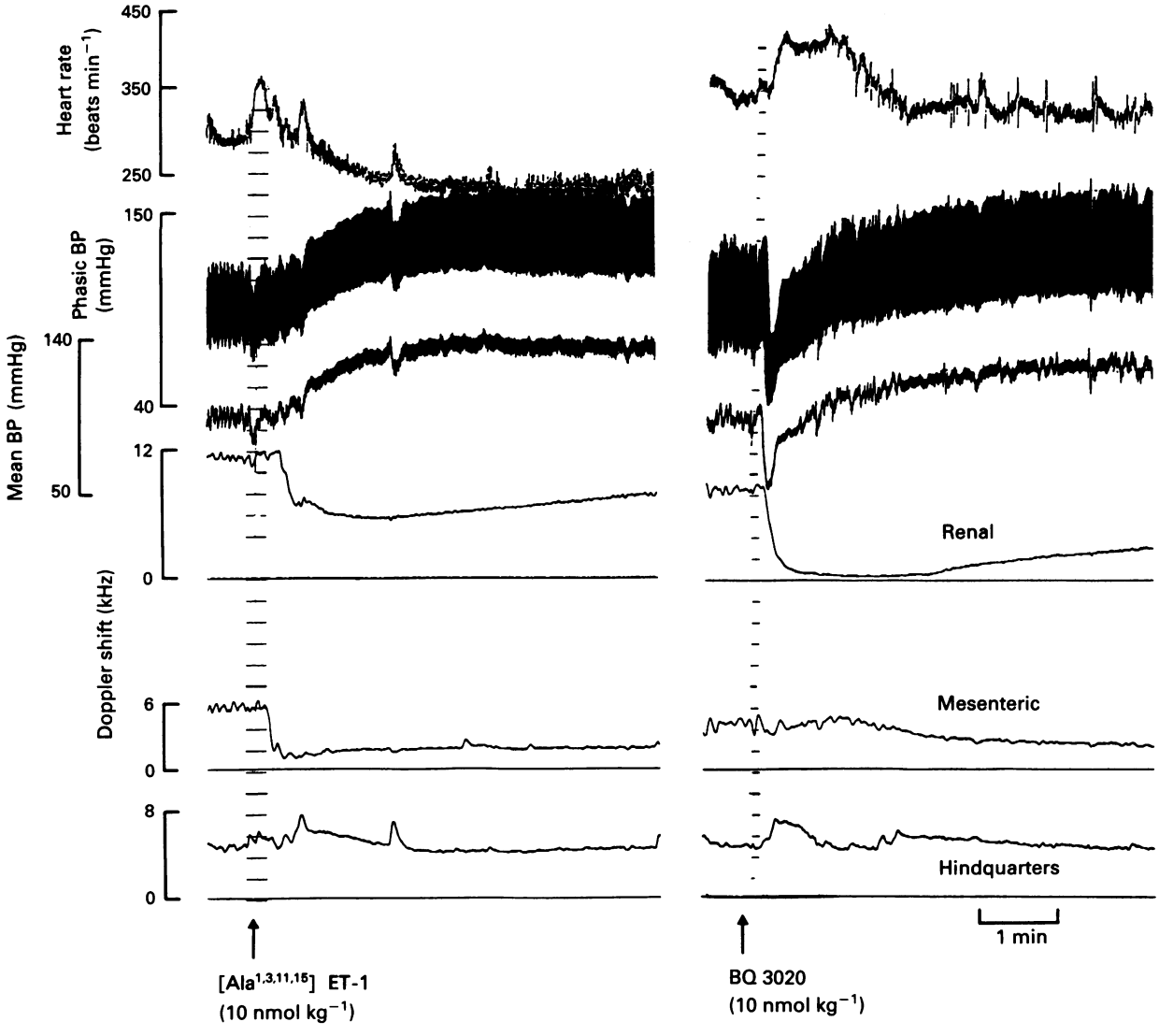

Figure 2 Cardiovascular changes following i.v. injection of [Ala^{1,3,11,15}]ET-1 or [Ala^{11,15}]Ac-ET-1 (6–21) (i.e., BQ-3020) (both from MLC) (10 nmol kg^{-1}) in conscious Long Evans rats.

[Ala^{1,3,11,15}]ET-1 obtained from NLF exerted initial, dose-dependent depressor effects accompanied by hindquarters hyperaemic vasodilatation, and reductions in renal and mesenteric flows and conductances (Figure 3). Thereafter, there was a variable pressor effect and hindquarters vasoconstriction (Figure 3). Although this pattern of effect was more similar to that observed by Bigaud & Pelton (1992) than that seen with [Ala^{1,3,11,15}]ET-1 obtained from MLC (see above), the depressor effect of the peptide from NLF was very transient (i.e., lasting about 30 s) in contrast to the findings of Bigaud & Pelton (1992) (i.e., a depressor effect lasting at least 3 min). The depressor effect of [Ala^{1,3,11,15}]ET-1 from NLF was no more prolonged in pentobarbitone-anaesthetized Sprague-Dawley rats (data not shown).

Regional haemodynamic responses to BQ-3020

BQ-3020 at doses of 0.15, 0.3 and 1 nmol kg^{-1} caused increasing pressor effects with no initial hypotensive response (Figure 4). However, at a dose of 10 nmol kg^{-1}, BQ-3020 had a substantial early depressor effect (Figures 2 and 4) which opposed its subsequent pressor action (Figures 2 and 4). The heart rate changes following BQ-3020, were not dose-dependent (Figures 2 and 4).

The pressor effects of BQ-3020 were accompanied by dose-dependent reductions in renal flow and vascular conductance (Figure 4). There were also dose-dependent reductions in mesenteric flow and vascular conductance with BQ-3020 at doses of 0.15, 0.3 and 1 nmol kg^{-1}, and over this dose-range the effects in the mesenteric vascular bed were greater than those in the kidney (Figure 4). However, with the 10 nmol kg^{-1} dose of BQ-3020, the reduction in mesenteric flow and vascular conductance was delayed (Figures 2 and 3), such that the integrated response was not different from that seen with BQ-3020 at a dose of 1 nmol kg^{-1}. Moreover, the mesenteric vascular response to the highest dose of BQ-3020 was less than that seen in the renal vascular bed (Figures 2 and 4).

In the hindquarters vascular bed, there was an initial, hyperaemic vasodilator response to BQ-3020; the effect on hindquarters vascular conductance was greatest with the highest dose of BQ-3020 (Figure 4). There was a subsequent hindquarters vasoconstriction, although the flow changes were variable (Figure 4).

Regional haemodynamic responses to ET-1 and BQ-3020 in the absence and presence of FR139317

ET-1 (0.5 nmol kg^{-1}) caused an initial hypotension and tachycardia followed by a pressor effect and bradycardia

(Figure 5, Table 1). There were reductions in renal and mesenteric flows and vascular conductances and an initial increase, and subsequent decrease, in hindquarters flow and vascular conductance (Figure 5, Table 1).

In the presence of FR139317 (0.5 μmol kg^{-1}) the pressor, and renal, mesenteric and hindquarters vasoconstrictor effects of ET-1 were significantly reduced (Figure 5, Table 1). However, the initial depressor and hindquarters vasodilator effects

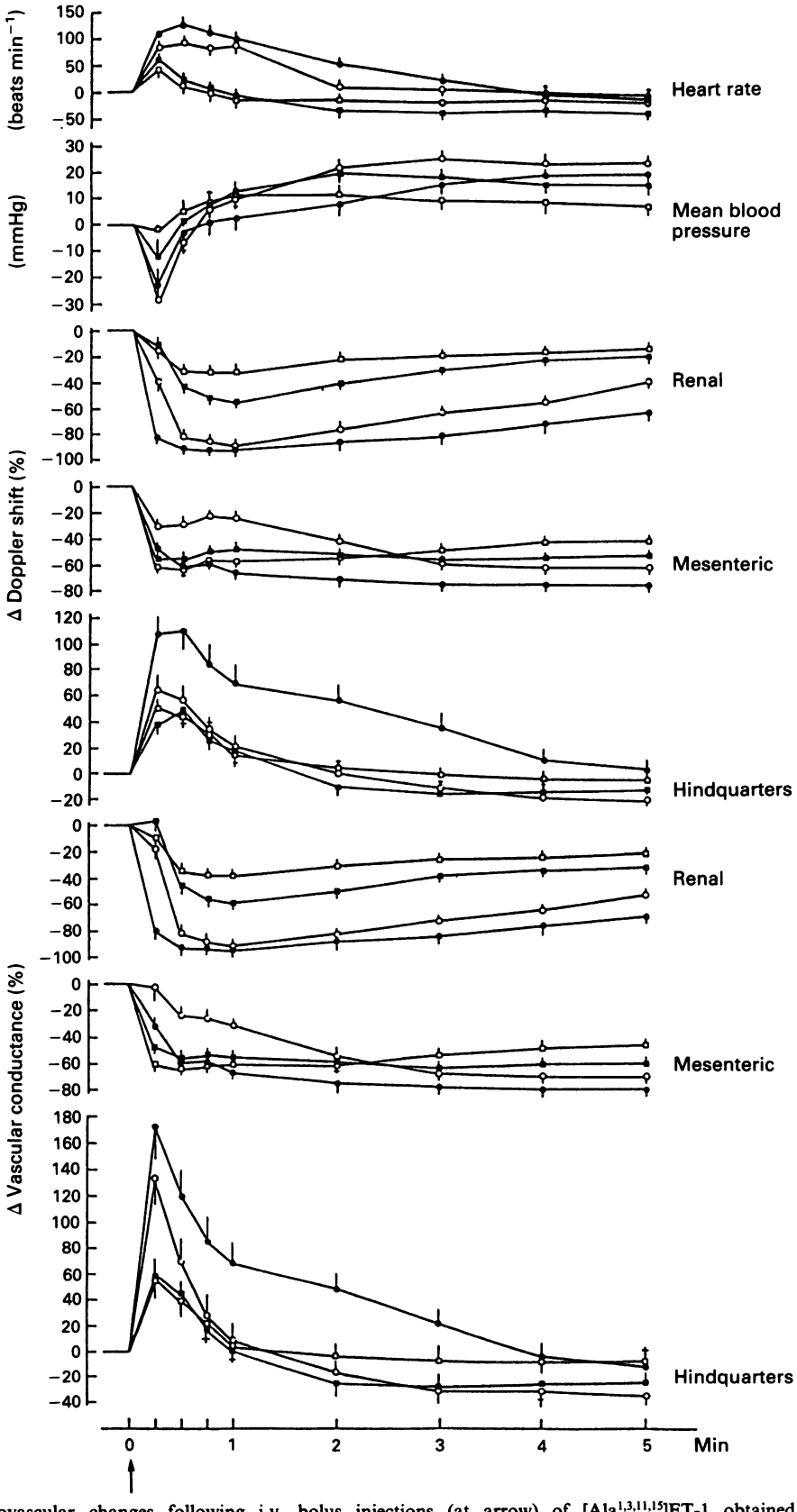

Figure 3 Cardiovascular changes following i.v. bolus injections (at arrow) of [$Ala^{1,3,11,15}$]ET-1 obtained from NLF (□, 0.15 nmol kg^{-1}; ■, 0.3 nmol kg^{-1}; ○, 1 nmol kg^{-1}; ●, 10 nmol kg^{-1}) in the same conscious Long Evans rats ($n = 7$). Values are mean with s.e.mean.

of ET-1 were not affected significantly by FR139317 although the duration of the former tended to be increased (Figure 5, Table 1).

FR139317 also attenuated the pressor and renal, mesenteric and hindquarters vasoconstrictor effects of BQ-3020 (10 nmol kg^{-1}) while leaving its depressor and hindquarters vasodilator action intact (Figure 6, Table 1). The inhibitory effects of FR139317 on the pressor and renal vasoconstrictor actions of BQ-3020 were significantly less than on those of ET-1, whereas the inhibition of the mesenteric vasoconstriction and of the hindquarters vasoconstriction were not significantly different from ET-1 and BQ-3020 (Table 1). In

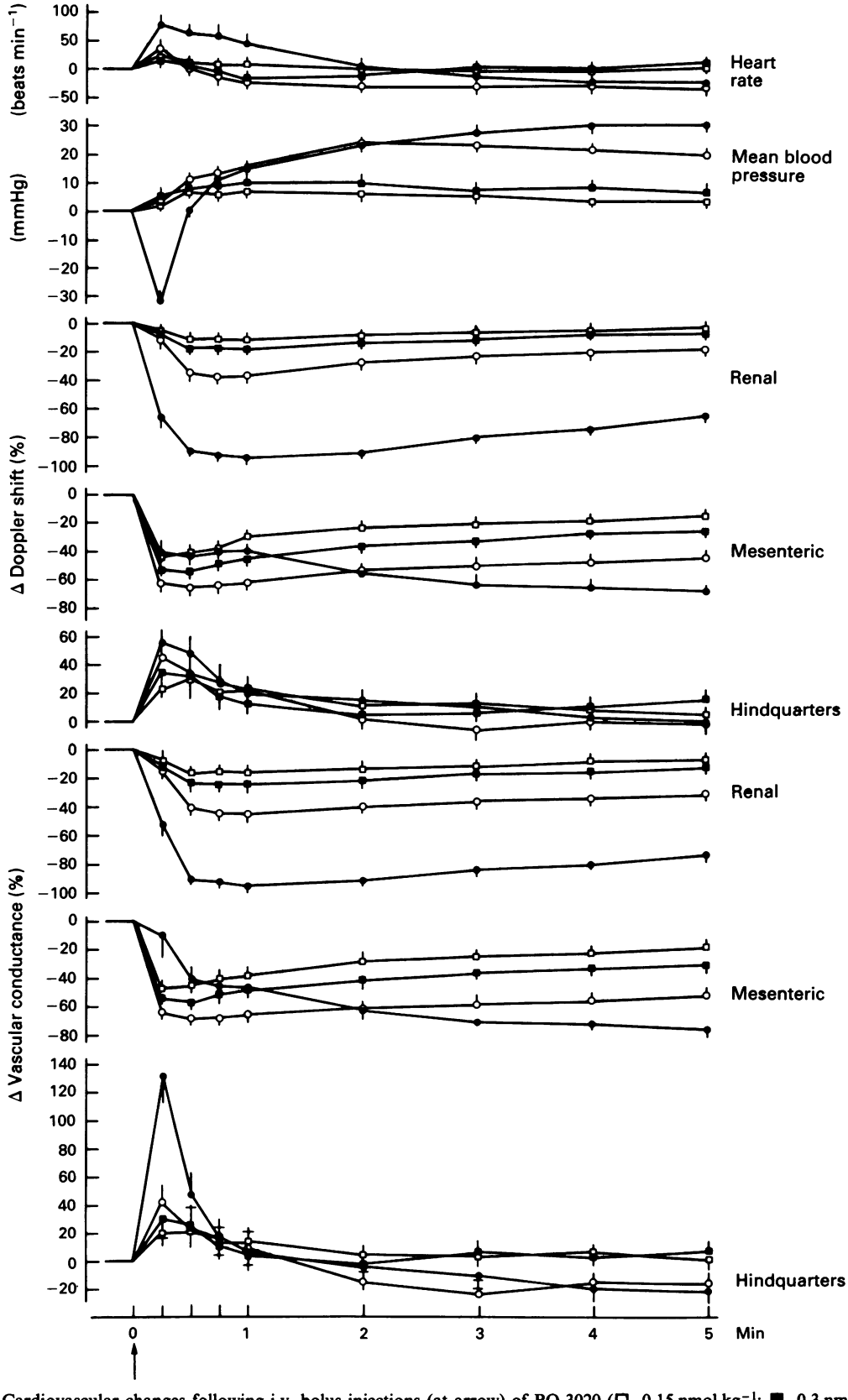

Figure 4 Cardiovascular changes following i.v. bolus injections (at arrow) of BQ-3020 (□, 0.15 nmol kg^{-1}; ■, 0.3 nmol kg^{-1}; ○, 1 nmol kg^{-1}; ●, 10 nmol kg^{-1}) in the same conscious Long Evans rats ($n = 8$). Values are mean with s.e.mean.

the presence of FR139317, both ET-1 and BQ-3020 still elicited significant haemodynamic effects (Figures 5 and 6, Table 1).

With repeated administration of ET-1 or BQ-3020 in the presence of saline, rather than FR139317, there were no significant changes in haemodynamic responses (data not shown).

As explained in Methods, we carried out an additional experiment to determine if FR139317 (0.5 μmol kg^{-1}) affected the haemodynamic responses to low doses of ET-1 or BQ-3020. ET-1 at a dose of 7.5 pmol kg^{-1} had no significant effect on mean arterial blood pressure, but it caused significant reductions in renal and mesenteric flows (AOC, -43 ± 9 and -50 ± 4% min, respectively) and vascular conductances (AOC, -44 ± 10 and -50 ± 5% min, respectively), and significant increases in hindquarters flow (AUC, 61 ± 10% min) and vascular conductance (65 ± 22% min). In the presence of FR139317, the ET-1-induced reductions in renal flow (AOC, -10 ± 4% min) and vascular conductance (AOC -9 ± 3% min) were significantly attenuated, but the reductions in mesenteric flow (AOC, -60 ± 5% min) and vascular conductance (AOC, -54 ± 7% min), and the increases in hindquarters flow (AUC, 47 ± 17% min) and vascular conductance (AUC, 55 ± 18% min) were not different from those seen in the absence of FR139317.

In this experiment, BQ-3020 at a dose of 0.15 nmol kg^{-1} had similar haemodynamic effects to those in the previous experiment (renal flow, AOC -43 ± 7; mesenteric flow,

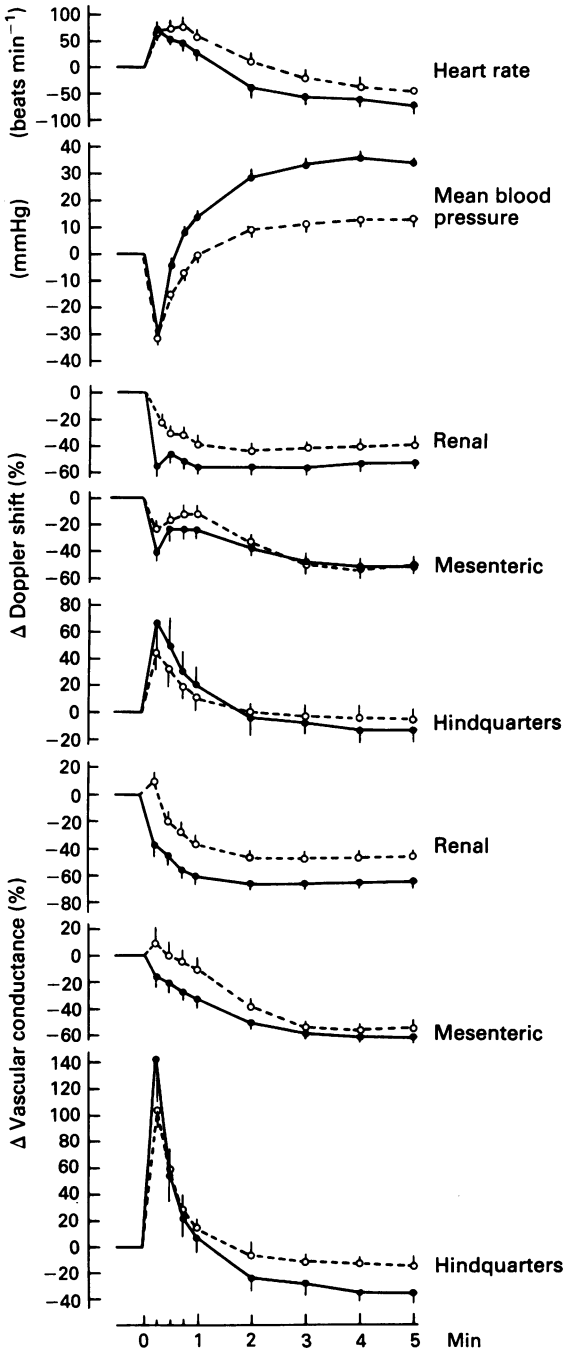

Figure 5 Cardiovascular changes in response to endothelin-1 (0.5 nmol kg^{-1}) in the absence (●) or presence (○) of FR139317 (0.5 μmol kg^{-1}) in the same conscious, Long Evans rats ($n = 8$). The statistics for the differences in the integrated responses are shown in Table 1. Values are mean with s.e.mean.

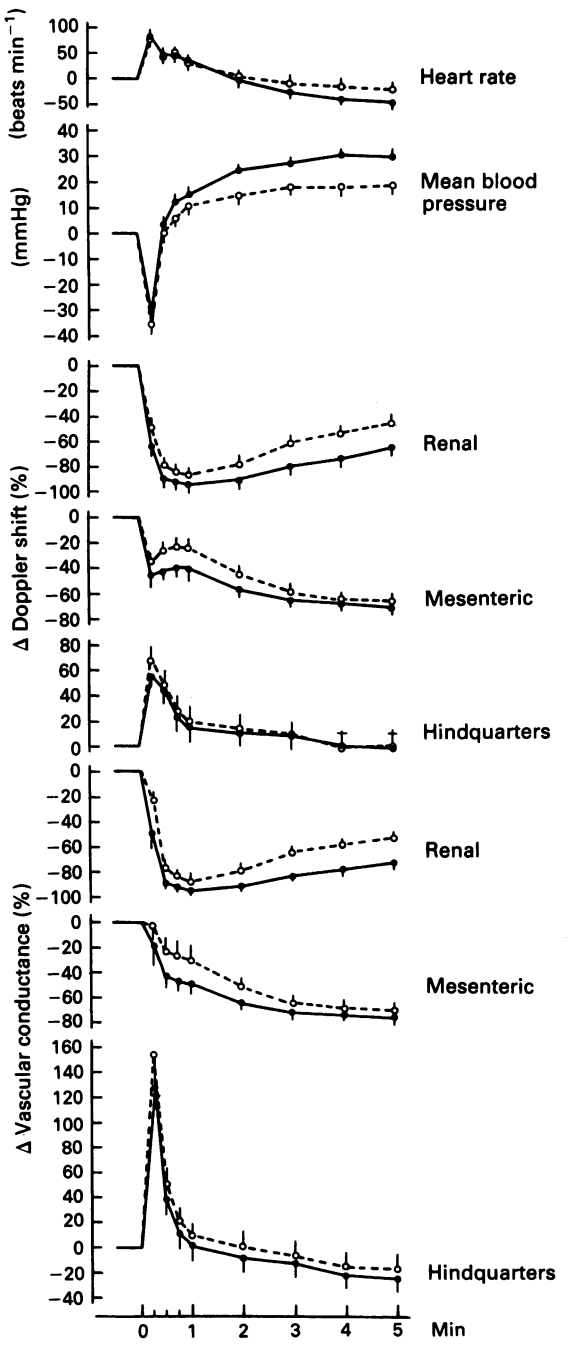

Figure 6 Cardiovascular changes in response to BQ-3020 (10 nmol kg^{-1}) in the absence (●) or presence (○) of FR139317 (0.5 μmol kg^{-1}) in the same conscious, Long Evans rats ($n = 8$). The statistics for the differences in the integrated responses are shown in Table 1. Values are mean with s.e.mean.

Table 1 Integrated cardiovascular responses (areas under or over curves; AUC, $AOC_{0-5\,min}$) following bolus injection of endothelin-1 (ET-1, 0.5 nmol kg^{-1}) or BQ-3020 (10 nmol kg^{-1}) in the absence and presence of FR139317 (0.5 μmol kg^{-1}) in the same conscious Long Evans rats

	ET-1	*ET-1 + FR139317*	*BQ-3020*	BQ3020 + *FR139317*
Heart rate (AUC; beats)	72 ± 17	107 ± 13	90 ± 15	101 ± 29
Heart rate (AOC; beats)	− 213 ± 52	− 101 ± 21	− 108 ± 33	− 66 ± 33
Mean blood pressure (AOC; mmHg min)	− 14 ± 1	− 18 ± 2	− 13 ± 1	− 15 ± 2
Mean blood pressure (AUC; mmHg min)	126 ± 7	40 ± 5*	113 ± 10	72 ± 9*
Renal flow (AOC; % min)	− 269 ± 16	− 190 ± 9*	− 405 ± 13	− 323 ± 7*
Mesenteric flow (AOC; % min)	− 202 ± 16	− 187 ± 13*	− 289 ± 23	− 244 ± 25*
Hindquarters flow (AUC; % min)	83 ± 39	54 ± 19	100 ± 49	97 ± 31
Hindquarters flow (AOC; % min)	− 65 ± 20	− 28 ± 11*	− 38 ± 16	− 28 ± 14
Renal conductance (AOC; % min)	− 305 ± 17	− 198 ± 9*	− 417 ± 12	− 355 ± 9*
Mesenteric conductance (AOC; % min)	− 245 ± 15	− 195 ± 12*	− 314 ± 22	− 259 ± 25*
Hindquarters conductance (AUC; % min)	76 ± 29	67 ± 16	81 ± 37	91 ± 27
Hindquarters conductance (AOC; % min)	− 120 ± 26	− 48 ± 14*	− 92 ± 23	− 57 ± 21*

$n = 8$
*$P < 0.05$ versus corresponding response in the absence of FR139317 (Wilcoxon's test).

AOC − 153 ± 20; hindquarters flow, AUC 56 ± 8; renal vascular conductance, AOC − 54 ± 8; mesenteric vascular conductance, AOC − 161 ± 21; hindquarters vascular conductance, AUC 49 ± 5% min). In the presence of FR139317, the responses to BQ-3020 were not changed significantly (renal flow, AOC − 41 ± 8; mesenteric flow, AOC − 146 ± 13; hindquarters flow, AUC 56 ± 13; renal vascular conductance, AOC − 53 ± 10; mesenteric vascular conductance, AOC − 157 ± 14; hindquarters vascular conductance, AUC 49 ± 12% min).

Discussion

Our objectives were: (1) to determine if the regional haemodynamic effects of [$Ala^{1,3,11,15}$]ET-1 in conscious rats were as described for anaesthetized rats; (2) to ascertain if BQ-3020 had effects similar to [$Ala^{1,3,11,15}$]ET-1; and (3) to delineate effects of FR139317 on responses to ET-1 and BQ-3020 in order to assess the possible involvement of ET_A- and ET_B-receptors, and to compare the results with those obtained by others using the ET_A-receptor antagonist, BQ-123, in anaesthetized rats.

Regional haemodynamic responses to [$Ala^{1,3,11,15}$]ET-1 and BQ-3020

Bigaud & Pelton (1992) recently described the regional haemodynamic effects of [$Ala^{1,3,11,15}$]ET-1 in pentobarbitone-anaesthetized Sprague-Dawley rats, acutely instrumented with pulsed Doppler flow probes. They found that [$Ala^{1,3,11,15}$]ET-1 obtained from NLF caused dose-dependent, early depressor, and subsequent pressor, effects accompanied by renal and mesenteric vasoconstriction; there was an early hindquarters vasodilatation, but no subsequent vasoconstriction, and no change in heart rate at any stage. Our results with [$Ala^{1,3,11,15}$]ET-1 obtained from NLF showed a similar pattern of change in regional haemodynamics. However, under all experimental conditions we found the depressor effect of the peptide was very transient (about 30 s) in contrast to the long duration (at least 3 min) of the effect described by Bigaud & Pelton (1992); we cannot explain this difference. The [$Ala^{1,3,11,15}$]ET-1 obtained from MLC was confirmed in structure and purity, i.e., no shorter analogues or contaminants were detectable. Thus, the finding that this peptide caused only modest hindquarters vasodilatation and was completely devoid of an initial depressor effect in doses up to 30 nmol kg^{-1} indicates it activated ET_B-receptors mediating vasoconstriction more effectively than ET_B-receptors mediating vasodilatation. This is consistent with the recent report from Gray & Clozel (1994) showing that the mixed, non-peptide endothelin antagonist, bosentan, distinguished between those ET_B-receptors on vascular smooth muscle and those on endothelial cells. However, the reason for the difference between the effects of [$Ala^{1,3,11,15}$]ET-1 from MLC and NLF is unknown.

Neither [$Ala^{1,3,11,15}$]ET-1 obtained from MLC or NLF, nor BQ-3020, showed any signs of preferential activation of vasodilator responses, except in the hindquarters vascular bed. The 3 nmol kg^{-1} dose of [$Ala^{1,3,11,15}$]ET-1 (from NLF) and the 10 nmol kg^{-1} dose of BQ-3020 caused less marked initial mesenteric vasoconstriction than was seen with lower doses, possibly due to recruitment of an opposing vasodilator mechanism (see below). However, such a phenomenon was not apparent with [$Ala^{1,3,11,15}$]ET-1 obtained from MLC. Nonetheless, collectively, the results are consistent with ET_B-receptors being responsible for renal, and mesenteric vasoconstrictor, and hindquarters vasodilator, responses to [$Ala^{1,3,11,15}$]ET-1 and BQ-3020, but these observations, particularly with higher doses of the peptides, do not exclude the involvement of ET_A-receptors, or other receptor sub-types.

Effects of FR139317 on responses to ET-1 and BQ-3020

Since, in our experiments, [$Ala^{1,3,11,15}$]ET-1 from MLC or NLF did not elicit a pattern of haemodynamic responses entirely like that of ET-1, we compared the effects of the ET_A-receptor antagonist, FR139317, on responses to ET-1

and BQ-3020, both at doses matched for their initial depressor and subsequent pressor effects, and at doses matched for their renal vasoconstrictor effects.

FR139317 (0.5 μmol kg^{-1}) abolished the renal vasoconstrictor effect of ET-1 (7.5 pmol kg^{-1}), but did not change its mesenteric vasoconstrictor or hindquarters vasodilator action. Moreover, the renal and mesenteric vasoconstrictor, and hindquarters vasodilator, effects of BQ-3020 (0.15 nmol kg^{-1}) were all uninfluenced by FR139317. These results are consistent with the renal vasoconstriction caused by low doses of ET-1 being mediated through ET_A-receptors, while ET_B-receptors (or other receptor subtypes) appear to be responsible for the mesenteric vasoconstrictor and hindquarters vasodilator action of ET-1, and for all the effects of BQ-3020 at a low dose.

Recent studies, in anaesthetized rats, have reported that the renal vasoconstrictor effects of ET-1 are not influenced by the ET_A-receptor antagonist, BQ-123 (Bigaud & Pelton, 1992; Cristol *et al.*, 1993; Pollock & Opgenorth, 1993). However, Bigaud & Pelton (1992) used a higher dose of ET-1 than we did, and hence these effects may have been harder to antagonize; this proposition is consistent with the finding that BQ-123 had some inhibitory effect on the renal vasoconstrictor response to ET-1 at a dose of 0.1 nmol kg^{-1} (Cristol *et al.*, 1993). Since Pollock & Opgenorth (1993) used infusions of ET-1, it is feasible that steady-state responses to the peptide are more dependent on ET_B-receptors. It is also possible that FR139317 is more effective than BQ-123 in blocking ET_A receptors, possibly because the physicochemical properties of a modified linear tripeptide (FR139317) may confer greater stability and/or bioavailability compared to BQ-123.

However, it could also be argued that FR139317 is less selective for ET_A-receptors than is BQ-123; but the lack of effect of FR139317 against the responses to BQ-3020 (0.15 nmol kg^{-1}) argues against this, at least as far as ET_B-receptors are concerned. By the same token, the failure of FR139317 to influence the mesenteric vasoconstrictor or hindquarters vasodilator effects of low doses of ET-1 or BQ-3020 is consistent with these actions being mediated by ET_B-receptors. It is notable that the hindquarters vasodilator effect of BQ-3020 was not different from that of ET-1 whereas its mesenteric vasoconstrictor effect was much more marked. This, together with the lack of dose-dependency of the hindquarters vasodilator effect of BQ-3020 indicates that mechanisms other than, or in addition to, activation of ET_B-receptors may be involved in the responses in the two vascular beds.

A different pattern of effects of FR139317 was seen when responses to higher doses of ET-1 (0.5 nmol kg^{-1}) and BQ-3020 (10 nmol kg^{-1}) were studied. FR139317 (0.5 μmol kg^{-1}) caused 66% inhibition of the pressor effects of ET-1 (0.5 nmol kg^{-1}) and 36% inhibition of the pressor effects of BQ-3020 (10 nmol kg^{-1}). Considering the results above, indicating that FR139317 (0.5 μmol kg^{-1}) does not inhibit ET_B-receptor-mediated events, it is likely that the inhibitory actions of FR139317 on the pressor effect of BQ-3020 was due to the high dose of the latter acting on ET_A-receptors, although we cannot exclude the possibility that both FR 139317 and BQ-3020 interact with non-ET_A- and non-ET_B-receptors.

The fact that FR139317 had a significantly greater inhibitory effect on the pressor action of ET-1 than on that of BQ-3020 is consistent with a predominance of ET_A-receptors in the former response, but, even with ET-1, a significant pressor response still occurred in the presence of FR139317. These results are consistent with a variable component of the pressor response to ET-1 and BQ-3020 being due to ET_B-receptors, depending on the agonist, and are consistent with the findings of Bigaud & Pelton (1992) and Cristol *et al.* (1993). As mentioned in Methods, a 10 fold higher dose of FR139317 had no greater inhibitory effect on responses to ET-1 or BQ-3020, so our results were probably not due to incomplete antagonism of ET_A-receptors.

FR139317 also caused greater inhibition of the renal vasoconstrictor effect of ET-1 (35%) than of BQ-3020 (19%), indicating differential involvement of ET_A- and ET_B-receptors. Our results, showing total loss of the renal vasoconstrictor effects of a low dose of ET-1, and a significant inhibition of the renal vasoconstrictor effect of a high dose of ET-1, are consistent with a predominance of ET_B-receptors in this latter event, compared to an exclusive involvement of ET_A-receptors in the former. The slight inhibitory effect of FR139317 on the renal vasoconstrictor response to BQ-3020 is consistent with the latter agonist influencing ET_A- as well as ET_B-receptors at high doses.

The small inhibition of the mesenteric vasoconstrictor effects of high doses of ET-1 and BQ-3020 by FR139317 indicates a slight involvement of ET_A-receptors. Since at low doses, these agonists caused mesenteric vasoconstriction that was unaffected by FR139317, then both results are consistent with a preponderance of ET_B-receptors in this action (see also Bigaud & Pelton, 1992). It is notable that at low doses, ET-1 appeared to act selectively on ET_A-receptors in the kidney and on ET_B-receptors in the mesenteric vascular bed, possibly because of differences in receptor populations.

Inhibition of the late hindquarters vasoconstrictor effects of ET-1 and BQ-3020 by FR139317 was not significantly different; assuming the effect of FR139317 on the response to BQ-3020 was due to the latter acting on ET_A-receptors, it appears about half the hindquarters vasoconstrictor effect of ET-1 and BQ-3020 was due to stimulation of ET_B-receptors. In contrast, the whole of the hindquarters vasodilator (and depressor) effect of ET-1 and BQ-3020 was uninfluenced by FR139317, consistent with this being entirely dependent on ET_B-receptors. But, as mentioned above, the hindquarters vasodilator response was not clearly dose-dependent, although, at the highest dose of BQ-3020, there was a marked increase in the rise in calculated hindquarters vascular conductance that it caused. However, this was due to the occurrence of an initial depressor effect coinciding with a relative attenuation of the mesenteric vasoconstriction. Thus, at higher doses it may be that BQ-3020 (and ET-1) activate additional (possibly non ET_A-, non ET_B-receptor-mediated) vasodilator mechanisms.

In summary, one explanation of our results is that, at a low dose (7.5 pmol kg^{-1}), ET-1 activates renal ET_A-receptors (vasoconstriction), mesenteric ET_B-receptors (vasoconstriction) and hindquarters ET_B-receptors (vasodilatation). At a higher dose (0.5 nmol kg^{-1}), ET-1 has a pressor effect (dependent on ET_A- $>$ ET_B-receptors), and vasoconstrictor effects in the renal (ET_B- $>$ ET_A-receptors), mesenteric (ET_B- $>>$ ET_A-receptors) and hindquarters (ET_A- $\geq$ ET_A-receptors) vascular beds, together with an initial depressor and hindquarters vasodilator effect (ET_B-receptors only).

BQ-3020 at a low dose (0.5 nmol kg^{-1}) causes renal and mesenteric vasoconstriction (ET_B-receptors), and hindquarters vasodilatation (ET_B-receptors). At a dose of 10 nmol kg^{-1}, BQ-3020 has a pressor effect (ET_B $>$ ET_A-receptors) and causes vasoconstriction in renal (ET_B- $>>$ ET_A-receptors), mesenteric (ET_B- $>>$ ET_A-receptors) and hindquarters (ET_B- $\geq$ ET_A-receptors) vascular beds preceded by an early depressor and hindquarters vasodilator effect (ET_B-receptors). However, it is feasible that some, or all, the effects here attributed to ET_B-receptors involve, to varying extents, subtypes of ET_B-receptors and/or ET-receptors that are not of the ET_A- or ET_B-receptor subtype.

References

BENNETT, T., GARDINER, S.M., KEMP, P.A., DAVENPORT, A.P. & EDVINSSON, L. (1993). Influence of an ET_A-receptor antagonist on regional haemodynamic responses to endothelin-1 (ET-1) and [$Ala^{11,15}$]Ac-ET-1(6-21) in conscious rats. *Br. J. Pharmacol.*, **109**, 57p.

BIGAUD, M. & PELTON, J.T. (1992). Discrimination between ET_A- and ET_B-receptor-mediated effects of endothelin-1 and [$Ala^{1,3,11,15}$] endothelin-1 by BQ-123 in the anaesthetized rat. *Br. J. Pharmacol.*, **107**, 912–918.

CARDELL, L.O., UDDMAN, R. & EDVINSSON, L. (1993). A novel ET_A-receptor antagonist, FR139317, inhibits endothelin-induced contractions of guinea-pig pulmonary arteries, but not trachea. *Br. J. Pharmacol.*, **108**, 448–452.

CLOZEL, M., GRAY, G.A., BREU, V., LÖFFLER, B.-M. & OSTERWALDER, R. (1992). The endothelin ET_B-receptor mediates both vasodilatation and vasoconstriction *in vivo*. *Biochem. Biophys. Res. Commun.*, **186**, 867–873.

CRISTOL, J.-P., WARNER, T.D., THIEMERMANN, C. & VANE, J.R. (1993). Mediation via different receptors of the vasoconstrictor effects of endothelins and sarafotoxins in the systemic circulation and renal vasculature of the anaesthetized rat. *Br. J. Pharmacol.*, **108**, 776–779.

DOUGLAS, S.A., ELLIOT, J.D. & OHLSTEIN, E.H. (1992). Regional vasodilataton to endothelin-1 is mediated by a non ET_A receptor subtype in the anaesthetized rat: effect of BQ-123 on systemic haemodynamic responses. *Eur. J. Pharmacol.*, **221**, 315–324.

GARDINER, S.M., COMPTON, A.M., KEMP, P.A. & BENNETT, T. (1991). The effects of phosphoramidon on the regional haemodynamic responses to human proendothelin [1-38] in conscious rats. *Br. J. Pharmacol.*, **103**, 2009–2015.

GARDINER, S.M., KEMP, P.A. & BENNETT, T. (1992a). Inhibition by phosphoramidon of the regional haemodynamic effects of proendothelin-1 and -3 in conscious rats. *Br. J. Pharmacol.*, **107**, 584–590.

GARDINER, S.M., KEMP, P.A., BENNETT, T. & DAVENPORT, A.P. (1992b). Regional haemodynamic response to [$Ala^{1,3,11,15}$]endothelin-1 in conscious rats. *Br. J. Pharmacol.*, **107**, Suppl. 415P.

GARDINER, S.M., KEMP, P.A., BENNETT, T. & DAVENPORT, A.P. (1993). Regional haemodynamic responses to the ET_B-receptor-selective agonist, BQ3020, in conscious rats. *Br. J. Pharmacol.*, **109**, Suppl. 131P.

GRAY, G.A. & CLOZEL, M. (1994). Three endothelin receptor subtypes suggested by the differential potency of bosentan, a novel endothelin receptor antagonist, in isolated tissues. *Br. J. Pharmacol.*, Suppl. (in press).

HAYWOOD, J.R., SHAFFER, R.A., FASTENOW, C., FINK, G.D. & BRODY, M.J. (1981). Regional blood flow measurement with pulsed Doppler flow meter in conscious rat. *Am. J. Physiol.*, **241**, H273–H278.

HILEY, C.R., DOUGLAS, S.A. & RANDALL, M.D. (1989). Pressor effects of endothelin-1 and some analogs in the perfused superior mesenteric arterial bed of the rat. *J. Cardiovasc. Pharmacol.*, **13**, (suppl. 5), S197–S199.

HILEY, C.R., JONES, C.R., PELTON, J.T. & MILLER, R.C. (1990). Binding of [^{125}I]-endothelin-1 to rat cerebellar homogenates and its interactions with some analogues. *Br. J. Pharmacol.*, **101**, 319–324.

IHARA, M., SAEKI, T., FUKURODA, T., KIMURA, S., OZAKI, S., PATEL, A.C. & YANO, M. (1992). A novel radioligand [^{125}I]BQ-3020 selective for endothelin (ET_B) receptors. *Life Sci.*, **51**, 47–52.

MASAKI, T., YANAGISAWA, M. & GOTO, K. (1992). Physiology and pharmacology of endothelins. *Med. Res. Rev.*, **12**, 391–421.

MOLENAAR, P., KUC, R.E. & DAVENPORT, A.P. (1992). Characterisation of two new ET_B selective radioligands [^{125}I]-BQ-3020 and [^{125}I]-[$Ala^{1,3,11,15}$]ET-1 in human heart. *Br. J. Pharmacol.*, **107**, 637–639.

MCMURDO, L., CORDER, R., THIEMERMANN, C. & VANE, J.R. (1993). Incomplete inhibition of the pressor effects of endothelin-1 and related peptides in the anaesthetized rat with BQ-123 provides evidence for more than one vasoconstrictor receptor. *Br. J. Pharmacol.*, **108**, 557–561.

MORELAND, S., MCMULLEN, D.M., DELANEY, C.L., LEE, V.G. & HUNT, J.T. (1992). Venous smooth muscle contains vasoconstrictor ET_B-like receptors. *Biochem. Biophys. Res. Commun.*, **184**, 100–106.

POLLOCK, D.M & OPGENORTH, T.J. (1993). Evidence for endothelin-induced renal vasoconstriction independent of ET_A-receptor activation. *Am. J. Physiol.*, **264**, R222–R226.

RANDALL, M.D. (1991). Vascular activities of the endothelins. *Pharmacol. Ther.*, **50**, 73–93.

SAEKI, T., IHARA, M., FUKURODA, T., YAMAGIWA, M. & YANO, M. (1991). [$Ala^{1,3,11,15}$]endothelin-1 analogs with ET_B agonistic activity. *Biochem. Biophys. Res. Commun.*, **179**, 286–292.

SOGABE, K., NIREI, H., SHOUBO, M., NOMOTO, A., AO, S., NOTSU, Y. & ONO, T. (1993). Pharmacological profile of FR139317, a novel, potent endothelin ET_A receptor antagonist. *J. Pharmacol. Exp. Ther.*, **264**, No. 3.

SUN, X., HEDNER, T., FONG, Q. & EDVINSSON, L. (1992). Inhibition of endothelin (ET-1) induced pressor responses by the endothelin (ET_A) receptor antagonist FR139317 in the pithed rat. *Blood Press.*, **1**, 108–112.

(Received April 23, 1993
Revised January 21, 1994
Accepted February 14, 1994)

Br. J. Pharmacol. (1994), **112**, 487–492

Discrimination between citrulline and arginine transport in activated murine macrophages: inefficient synthesis of NO from recycling of citrulline to arginine

Anwar R. Baydoun, [1]Richard G. Bogle, Jeremy D. Pearson & [2]Giovanni E. Mann

Vascular Biology Research Centre, Biomedical Sciences Division, King's College, Campden Hill Road, London W8 7AH

1 The kinetics, specificity, pH- and Na^+-dependency of L-citrulline transport were examined in unstimulated and lipopolysaccharide (LPS)-activated murine macrophage J774 cells. The dependency of nitric oxide production on extracellular arginine or citrulline was investigated in cells activated with LPS (1 $\mu g\ ml^{-1}$) for 24 h.

2 In unstimulated J774 cells, transport of citrulline was saturable ($K_t = 0.16$ mM and $V_{max} = 32$ pmol μg^{-1} protein min^{-1}), pH-insensitive and partially Na^+-dependent. In contrast to arginine, transport of citrulline was unchanged in LPS-activated (1 $\mu g\ ml^{-1}$, 24 h) cells.

3 Kinetic inhibition experiments revealed that arginine was a relatively poor inhibitor of citrulline transport, whilst citrulline was a more potent inhibitor ($K_i = 3.4$ mM) of arginine transport but only in the presence of extracellular Na^+. Neutral amino acids inhibited citrulline transport ($K_i = 0.2–0.3$ mM), but were poor inhibitors of arginine transport.

4 Activated J774 cells did not release nitrite in the absence of exogenous arginine. Addition of citrulline (0.01–10 mM), in the absence of exogenous arginine, could only partially restore the ability of cells to synthesize nitrite, which was abolished by 100 μM N^G-nitro-L-arginine methyl ester or N^G-iminoethyl-L-ornithine.

5 Intracellular metabolism of L-[^{14}C]-citrulline to L-[^{14}C]-arginine was detected in unstimulated J774 cells and was increased further in cells activated with LPS and interferon-γ.

6 We conclude that J774 macrophage cells transport citrulline via a saturable but nonselective neutral carrier which is insensitive to induction by LPS. In contrast, transport of arginine via the cationic amino acid system y^+ is induced in J774 cells activated with LPS.

7 Our findings also confirm that citrulline can be recycled to arginine in activated J774 macrophage cells. Although this pathway provides a mechanism for enhanced arginine generation required for NO production under conditions of limited arginine availability, it cannot sustain maximal rates of NO synthesis.

Keywords: Murine macrophage cell line J774; macrophages; nitric oxide; nitrite; citrulline transport; arginine transport; citrulline metabolism; bacterial lipopolysaccharide

Introduction

Synthesis and release of nitric oxide (NO) by activated macrophages is an important cytotoxic/cytostatic mechanism in non-specific immunity (see review by Moncada *et al.*, 1991). In macrophages, NO and citrulline are generated from arginine by a Ca^{2+}/calmodulin-insensitive NO synthase, which is induced following exposure of these cells to lipopolysaccharide (LPS) and/or cytokines such as interferon-γ (Hibbs *et al.*, 1988; Marletta *et al.*, 1988; Bogle *et al.*, 1992a). Production of NO by activated macrophages is critically dependent on extracellular arginine (Drapier & Hibbs, 1988; Granger *et al.*, 1990; Keller *et al.*, 1990; Takema *et al.*, 1991; Bogle *et al.*, 1992a; Assreuy & Moncada, 1992).

Recent studies in macrophages have demonstrated that arginine (Bogle *et al.*, 1992a; Sato *et al.*, 1992) and lysine (Sato *et al.*, 1991) are transported by a high-affinity carrier, resembling the cationic amino acid system y^+ identified in a variety of other cell types (White, 1985). We have reported that induction of arginine transport activity in LPS-stimulated J774 macrophage cells involves *de novo* protein synthesis, suggesting that enhanced uptake of arginine is important for sustained NO biosynthesis (Baydoun *et al.*, 1993). In view of the fact that peritoneal macrophages can recycle citrulline to arginine (Wu & Brosnan, 1992), we were interested in establishing whether this pathway could sustain NO production in LPS-activated J774 cells. We have therefore investigated the ability of J774 cells to convert citrulline to arginine, and examined whether this generates sufficient arginine for sustained NO production under conditions of limited arginine availability. In addition, we have fully characterized citrulline transport in unstimulated and LPS-activated J774 cells with the aim of determining whether separate pathways mediate the entry of citrulline and arginine. A preliminary account of this work has been presented in abstract form (Bogle *et al.*, 1992b).

Methods

Cell culture

The murine monocyte/macrophage cell line J774 was obtained from the European Collection of Animal Cell Cultures (ECACC, Wiltshire). J774 cells were maintained in continuous culture in T75 tissue culture flasks in Dulbecco's modified Eagles medium (DMEM) containing 0.4 mM L-arginine and no L-citrulline but supplemented with 4 mM glutamine, penicillin (100 units ml^{-1}), streptomycin (100 $\mu g\ ml^{-1}$) and 10% foetal calf serum (providing a further

[1] Present address: Department of Pharmacology and Clinical Pharmacology, St. George's Hospital Medical School, Cranmer Terrace, London SW17 0RE.
[2] Author for correspondence.

0.08 mM L-arginine and 0.01 mM L-citrulline). Cells were harvested by gentle scraping and passaged every 3–6 days by dilution of a suspension of the cells 1:10 in fresh medium.

Measurement of amino acid transport

J774 cells were plated at a density of 10^5 cells per well in 96-well microtiter plates and allowed to adhere for 2 h. Medium was then replaced either with fresh DMEM or with DMEM containing LPS (1 μg ml^{-1}) and/or other compounds for specific time periods. After each incubation, cells were rinsed twice with a modified HEPES-buffered Krebs solution maintained at 37°C (Bogle *et al.*, 1992a). Amino acid uptake was initiated by adding HEPES-buffered Krebs (50 μl per well; 37°C) containing either 0.1 mM L-[^{14}C]-citrulline (1 μCi ml^{-1}) or 0.1 mM L-[^{3}H]-arginine (1 μCi ml^{-1}) to the monolayers. Incubations were terminated by placing the plates on melting ice and rinsing cells three times with 200 μl ice-cold Dulbecco's phosphate-buffered saline (mM: NaCl 138, KCl 2.6, Na_2HPO_4 1.8, KH_2PO_4 1.5, pH 7.4) containing either 10 mM unlabelled citrulline or arginine to remove extracellular radiolabelled amino acids. In some experiments an extracellular reference tracer, either D-[^{3}H]-mannitol or D-[^{14}C]-mannitol, was included in the incubation medium. In all experiments $<0.01\%$ of D-mannitol applied was recovered in cell lysates. Cell protein was determined using the BioRad reagent and radioactivity (d.p.m.) in formic acid digests of the cells was determined by liquid scintillation counting. Uptake was then calculated and expressed in units of pmol μg^{-1} protein min^{-1}.

Metabolism of L-citrulline to L-arginine

Metabolism of L-[^{14}C]-citrulline was assessed by thin-layer chromatography (t.l.c.). J774 cells were seeded into 35 mm dishes (3×10^6 cells) and allowed to adhere for 2 h. Thereafter, the medium was removed and replaced with DMEM containing 1 μCi ml^{-1} L-[^{14}C]-citrulline alone or supplemented with LPS (1 μg ml^{-1}) and IFN-γ (100 units ml^{-1}). Following a 24 h incubation period, the medium was collected and centrifuged at 10,000 *g* for 5 min. Cells were washed with ice-cold phosphate buffered saline and lysed with 100% methanol. Medium and methanol cell lysate samples were stored at −70°C for chromatographic analysis.

Methanol extracts were evaporated to dryness under a stream of nitrogen and resuspended in 20 μl methanol of which 10 μl was spotted onto silica-coated t.l.c. plates (Whatman, 150A). For analysis of culture medium, 20 μl of deproteinized sample was spotted onto t.l.c. plates. The plates were developed in a solvent system of chloroform: methanol:ammonium hydroxide:water (5:45:20:10 v/v) over a distance of 18 cm (Iynengar *et al.*, 1987). After drying, plates were scanned with a Berthold t.l.c. linear analyzer (Berthold, Germany). The R_F-values for ^{14}C-labelled L-arginine and L-citrulline (0.32 and 0.87) were identical to those of authentic amino acid standards.

Measurement of nitrite formation

Production of NO in intact J774 cells was assessed as described previously (Bogle *et al.*, 1992a) by measuring the accumulation of nitrite in the medium using the Griess reaction with sodium nitrite as standard (Green *et al.*, 1982).

Materials

The HEPES-buffered Krebs solution was of the following composition (mM): NaCl 131, KCl 5.5, $MgCl_2$ 1, $CaCl_2$ 2.5, $NaHCO_3$ 25, NaH_2PO_4 1, D-glucose 5.5, HEPES 20, pH 7.4, 37°C. In some experiments the standard Krebs solution was titrated with 0.1N HCl or 0.1N NaOH to achieve pH values ranging pH 5 to pH 8. In sodium-free experiments, the buffer was modified by replacing NaCl, $NaHCO_3$ and NaH_2PO_4 with choline chloride, choline bicarbonate and KH_2PO_4, respectively.

All reagents for cell culture except foetal calf serum (Sigma) were from Gibco (Paisley, U.K.). Arginine-free DMEM was prepared in the laboratory and was supplemented with 10% dialysed foetal calf serum. Serum was dialysed twice for 48 h at 4°C using a membrane with a 10,000 M_r cut off and confirmed to be free of amino acids by high performance liquid chromatography (h.p.l.c.) (Baydoun *et al.*, 1993). LPS extracted from *Escherichia coli* (serotype 055:B5) was obtained from Difco, Michigan, U.S.A. Recombinant murine IFN-γ was from Holland Biotechnologies. Other chemicals were from Sigma or BDH and of the highest grade obtainable. Radioactive tracers, L-[2,3-^{3}H]-arginine (53 Ci mmol^{-1}) and L-[carbamoyl-^{14}C]-citrulline (54.3 mCi mmol^{-1}) were obtained from New England Nuclear, Dreieich, Germany. Purity of L-[^{14}C]-citrulline was >99% as assessed by t.l.c.

Statistics

All values are means ± s.e. of at least three separate experiments with six replicates per experiment. Statistical analyses were performed by Student's *t* test with $P<0.05$ considered statistically significant.

Results

Characteristics of citrulline transport

Time course experiments revealed that transport of 0.1 mM L-[^{14}C]-citrulline was linear for up to 1 min but lower in LPS-activated cells over prolonged periods (inset Figure 1). In unstimulated J774 cells transport of citrulline was temperature-dependent and unaffected by changes in extracellular pH, ranging from 5–8 (data not shown). In contrast to arginine, citrulline transport was partially dependent on extracellular Na^+ and was unaltered by LPS (Table 1).

Transport of citrulline was saturable and a single Michaelis-Menten entry site analysis revealed an apparent K_t of 0.16 ± 0.02 mM and V_{max} of 32 ± 1 pmol μg^{-1} protein min^{-1} in control J774 cells (Figure 1). Activation of cells with LPS (1 μg ml^{-1}) for 24 h had no significant effect on the kinetics of citrulline transport (K_t = 0.11 ± 0.02 mM and V_{max} = 31 ±

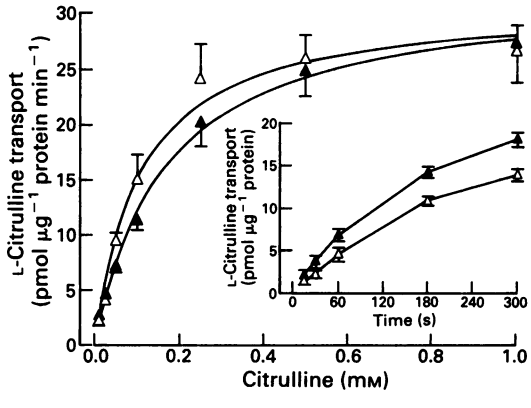

Figure 1 Kinetics and time course of citrulline uptake in unstimulated and LPS-activated J774 cells. Initial uptake rate kinetics were measured for citrulline (0.025–1 mM) in unstimulated (▲) and LPS-activated (△, 1 μg ml^{-1} for 24 h) cells. Rectangular hyperbolae were fitted to the mean influx data weighted for the reciprocal of the standard error at each mean. Values are the mean ± s.e. of 6 replicate measurements in 3 separate experiments. The inset shows the time course of L-[^{14}C]-citrulline transport (0.1 mM) measured in unstimulated cells (▲) or cells pretreated with LPS (△, 1 μg ml^{-1} for 24 h) over 15–300 s incubation periods. Values are the mean ± s.e. of 6 replicate measurements in 3 different experiments.

Table 1 Sodium-dependency of L-citrulline and L-arginine transport in J774 cells

	Unstimulated J774 cells (pmol μg^{-1} protein min^{-1})		+ *LPS* (1 $\mu g\,ml^{-1}$) (pmol μg^{-1} protein min^{-1})	
	+ Na^+	− Na^+	+ Na^+	− Na^+
L-Citrulline	11.7 ± 0.6	6.8 ± 0.3*	11.6 ± 0.9	7.8 ± 0.4*
L-Arginine	4.0 ± 0.1	3.8 ± 0.1	6.5 ± 0.2	6.0 ± 0.2

Transport of L-[^{14}C]-citrulline (0.1 mM) or L-[^{3}H]-arginine (0.1 mM) was measured over 30 s and 5 min, respectively, during incubation of J774 cells in a Krebs solution containing 143 or 0 mM Na^+. Cells were activated with LPS for 24 h in DMEM before assessing the Na^+-dependency of amino acid transport during incubation with Krebs. Values are the mean ± s.e. of 12–18 replicate measurements in 3 separate experiments.
*$P < 0.05$, unpaired t test versus values in the presence of Na^+.

1 pmol μg^{-1} protein min^{-1}). The insensitivity of citrulline transport to LPS contrasts markedly with our earlier findings that the V_{max} for arginine transport was increased in LPS-activated J774 cells (Bogle *et al.*, 1992a).

Selectivity of citrulline transport

In kinetic inhibition experiments, both citrulline and arginine caused a marked self-inhibition of transport (Figure 2a and b). Arginine (0.5–5 mM) was a poor inhibitor of citrulline transport (Figure 2a), whereas citrulline signicantly inhibited (K_i = 3.4 ± 0.5 mM) arginine uptake (Figure 2b). Although arginine transport in J774 cells is Na^+-independent (Table 1), the inhibition of arginine uptake by citrulline was abolished in the absence of extracellular Na^+ (Figure 2b).

The substrate specificities of citrulline and arginine transporters were examined further by screening the inhibitory effects of a series of 1 mM unlabelled amino acids. As shown in Figure 3, the cationic substrates for system y^+, arginine and lysine, and the system A analogue, 2-methylaminoisobutyric acid (MeAIB), were weak inhibitors of citrulline (0.1 mM) transport in unstimulated and LPS-activated cells. In contrast, transport was inhibited markedly by naturally occurring and synthetic neutral amino acids, and the pattern of inhibition was similar in both unstimulated and activated cells (Figure 3). Thus, in J774 macrophage cells transport of citrulline seems to be mediated by a neutral carrier with broad substrate specificity, resembling the neutral amino acid system identified by Sato *et al.* (1987) in murine peritoneal macrophages.

In contrast, transport of arginine (0.1 mM) was inhibited significantly by cationic amino acids, β-2-amino-bicyclo-(2,2,1)-heptane-2-carboxylic acid (BCH) and citrulline, but not by MeAIB, phenylalanine, 6-diazo-5-oxo-L-norleucine (DON) or glutamine (data not shown). No significant change in the pattern of inhibition occurred when cells were activated with LPS.

Metabolism of citrulline to arginine in cultured J774 cells

Metabolism of L-[^{14}C]-citrulline by cultured J774 cells was investigated by thin-layer chromatography. Incubation of unstimulated J774 cells with L-[^{14}C]-citrulline for 24 h resulted in the production of L-[^{14}C]-arginine which was detected in both cell extracts and the culture medium (Table 2). Activation of cells with LPS (1 $\mu g\,ml^{-1}$) and interferon-γ (IFN-γ, 100 units ml^{-1}) for 24 h resulted in a significantly greater intracellular conversion of L-[^{14}C]-citrulline into L-[^{14}C]-arginine.

Effects of citrulline on nitrite production from arginine-deprived J774 cells

In a previous study we reported that nitrite release from activated J774 cells was not detectable when L-arginine was omitted from the culture medium (Bogle *et al.*, 1992a). Since citrulline has been reported to recycle to arginine intracellularly in both endothelial cells (Hecker *et al.*, 1990) and peritoneal macrophages (Wu & Brosnan, 1992), we designed experiments to investigate whether citrulline could restore nitrite production in cultured J774 cells activated in the absence of exogenous arginine. When activated cells were incubated in an arginine-free medium containing citrulline (0.01–10 mM), nitrite production was detectable, reaching a maximum of 2.1 ± 0.1 nmol μg^{-1} protein 24 h^{-1} in the presence of 10 mM citrulline (Figure 4). Maximal rates of nitrite production (8.1 ± 0.22 nmol μg^{-1} protein 24 h^{-1}) were achieved at extracellular arginine concentrations of less than 0.3 mM. Thus, citrulline supply can only sustain ~20% of

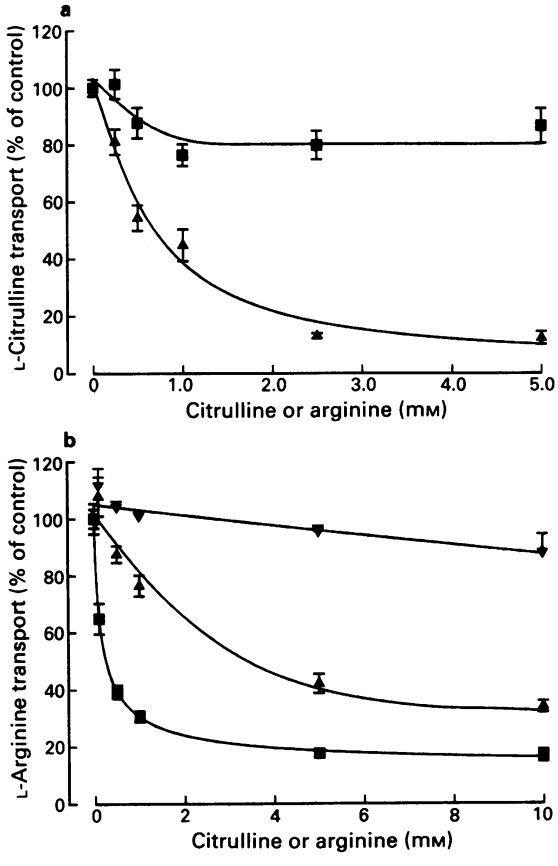

Figure 2 Discrimination of citrulline and arginine transport. (a) Inhibition of 0.1 mM L-[^{14}C]-citrulline transport was measured in the presence of Na^+ and increasing concentrations (0–5 mM) of unlabelled L-citrulline (▲) or L-arginine (■). Values are the mean ± s.e. of 6 replicate measurements in 3 separate experiments. (b) Inhibition of 0.1 mM L-[^{3}H]-arginine influx by increasing concentrations (0–10 mM) of unlabelled L-arginine (■) or L-citrulline (▲) in cells incubated in the presence of Na^+. Inhibition of arginine transport by citrulline was abolished in the absence of extracellular Na^+ (▼). Values are the mean ± s.e. of 10 replicate measurements in 3 experiments.

Table 2 Metabolism of L-[^{14}C]-citrulline to L-[^{14}C]-arginine in cultured J774 cells

	% L-[^{14}C]-arginine	% L-[^{14}C]-citrulline
Unstimulated J774 cells		
Culture medium	30 ± 3	70 ± 3
Cell extracts	17 ± 1	71 ± 2
J774 cells + LPS/IFN-γ		
Culture medium	24 ± 1	76 ± 1
Cell extracts	40 ± 4*	42 ± 8*

J774 cells were cultured in 35 mm dishes (3×10^6 cells) in the absence or presence of LPS (1 μg ml^{-1}) and IFN-γ (100 units ml^{-1}). L-[^{14}C]-citrulline (1 μCi ml^{-1}) was added at time zero and 24 h later cells and media were analysed for ^{14}C-labelled metabolites of citrulline by t.l.c. Results are shown as the % radioactivity associated with each detected peak and denote the mean ± s.e. of 3 experiments.

*$P < 0.05$, values significantly different from control cells, Student's unpaired t test.

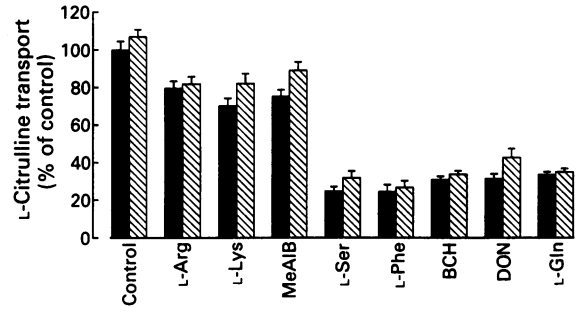

Figure 3 Specificity of citrulline transport in unstimulated and LPS-activated J774 cells. Transport of 0.1 mM L-[^{14}C]-citrulline was measured in the absence (control) or presence of a given inhibitor amino acid (1 mM). Cross-inhibition studies were performed in unstimulated (solid columns) and lipopolysaccharide-activated (1 μg ml^{-1}, 24 h, hatched columns) cells in the presence of Na^+. Data are expressed as a percentage of the transport rate measured in unstimulated cells in the absence of an inhibitor. Abbreviations denote standard amino acid nomenclature: arginine (Arg), lysine (Lys, system y^+); 2-methylaminoisobutyric acid (MeAIB, system A); serine (Ser, system ASC/asc); phenylalanine (Phe), β-2-amino-bicyclo-(2,2,1)-heptane-2-carboxylic acid (BCH, system L); 6-diazo-5-oxo-L-norleucine (DON), glutamine (Gln, system N). Values denote the mean ± s.e. of 6 replicate measurements in 3 experiments.

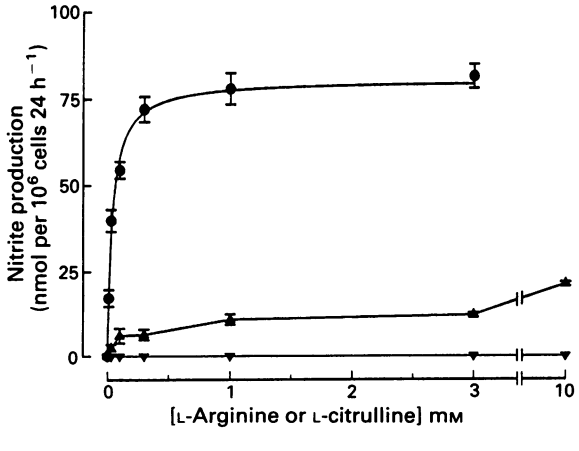

Figure 4 Dependency of nitrite production on extracellular citrulline or arginine in activated J774 cells. Cells were preincubated for 24 h with lipopolysaccharide (1 μg ml^{-1}) and interferon-γ (100 units ml^{-1}) in an arginine-free medium supplemented with either L-citrulline (0.01–10 mM), in the absence (▲) or presence of N^G-imidoethyl-L-ornithine (L-NIO, ▼, 0.1 mM). Accumulation of nitrite in the medium was then assayed using the Griess reaction. The dependency of nitrite production on extracellular L-arginine (●, 0–3 mM) is shown for comparison and was replotted from Figure 2 in Bogle *et al.* (1992a). Values are the mean ± s.e. of 6 replicate measurements in 3 experiments.

the maximal nitrite production generated from physiological concentrations of extracellular arginine.

In arginine-deprived J774 cells nitrite production, generated from citrulline, was abolished during co-incubation of cells with either N^G-nitro-L-arginine methyl ester (L-NAME; 0.1 mM; data not shown) or N^G-imidoethyl-L-ornithine (L-NIO; 0.1 mM; Figure 4), both potent inhibitors of inducible NO synthase (Rees *et al.*, 1990; McCall *et al.*, 1991).

Discussion

The present study confirms that uptake of citrulline and arginine by J774 cells is mediated by different amino acid transporters: a neutral amino acid carrier with broad substrate specificity and the cationic amino acid system y^+. Although metabolism of citrulline to arginine occurs in J774 macrophages and is enhanced following activation of cells with LPS, citrulline can only sustain limited NO synthesis in the absence of exogenous arginine. The rate of NO production approximates only ~20% of the maximal rate achieved with arginine, despite comparable or greater transport rates for citrulline.

Little information is available on the mechanism(s) mediating cellular uptake of citrulline. Studies *in vivo* suggest that citrulline is synthesized and released from the intestine as an end product of glutamine nitrogen metabolism (Windmueller & Spaeth, 1981). In the circulation, citrulline is rapidly cleared by the kidney and subsequently metabolised and released as arginine (Dhanakoti *et al.*, 1990). Thus, uptake and metabolism of citrulline may contribute to the maintenance of plasma arginine levels which appear to be important for sustained NO production *in vivo* (Aisaka *et al.*, 1989).

In our studies, uptake of citrulline by J774 cells occurred against a 5 fold concentration gradient (Baydoun *et al.*, 1993), was saturable, partially Na^+-dependent and reduced at low temperature. Moreover, the kinetics of citrulline transport were not altered in LPS-activated J774 cells. This contrasts with our previous report that arginine transport via system y^+ was induced in activated J774 cells (Bogle *et al.*, 1992a). Recent studies have also identified another cationic amino acid transporter (mouse cationic amino acid transporter, MCAT-2), of low affinity (K_m >2 mM), in mouse hepatocytes and the murine macrophage cell line RAW264.7 (Closs *et al.*, 1993a,b). Although the MCAT-2 transporter reveals a similar sequence and structure to MCAT-1 (high affinity cationic y^+ transporter, Kim *et al.*, 1991), only 5–10% of MCAT-2 transport would be occupied by substrate at physiological plasma concentrations. As the specificity of the arginine transporter is similar in unstimulated and activated J774 cells (Bogle *et al.*, 1992a,b; Baydoun *et al.*, 1993) and murine peritoneal macrophages (Sato *et al.*, 1992), it is likely that in these cell types the activity of system y^+ is upregulated by LPS.

Very few studies have investigated the relationship between

citrulline and arginine transport. Inhibition of arginine transport by citrulline has been observed in the chicken small intestine (Herzberg *et al.*, 1971). In the present experiments inhibition of arginine uptake by citrulline was observed but was abolished when Na^+ was removed from the incubation medium. This phenomenon of Na^+-dependent inhibition of Na^+-independent cationic amino acid transport has been observed previously in both reticulocytes and Ehrlich cells (Christensen & Antonioli, 1969). At physiological pH, citrulline carries no net charge and can therefore be classified as a neutral amino acid. It is likely that Na^+ serves as a substitute for the positively charged side chain of arginine, thus allowing a fraction of citrulline to enter J774 cells via system y^+. The inhibition of arginine transport by neutral amino acids in the presence of sodium is indeed a feature of system y^+ (Munck, 1980; White, 1985; Lawless *et al.*, 1987; Sweiry *et al.*, 1991).

Although activation of J774 cells did not markedly alter the kinetics of citrulline transport, net accumulation of ^{14}C from [^{14}C]-citrulline over a 60 min incubation period was reduced by $\sim$50% in LPS-treated cells (data not shown). Since in these cells the V_{max} for citrulline transport was not altered, this difference may reflect increased metabolism and subsequent efflux of either citrulline itself or a radiolabelled metabolite. In this respect we have previously shown by reverse-phased h.p.l.c. that citrulline accumulates in the culture medium of activated cells (Baydoun *et al.*, 1993). Our present results indicate that J774 cells can synthesize L-[^{14}C]-arginine from L-[^{14}-C]-citrulline, which is increased further following activation of J774 cells with LPS and IFN-γ. These findings suggest that the enzymatic pathway, arginosuccinate synthase/lyase (Hoffman *et al.*, 1978), responsible for citrulline metabolism is induced by treatment of J774 cells with these agents. Wu & Brosnan (1992) have reported a 3 fold increase in the metabolism of citrulline to arginine in LPS-treated rat peritoneal macrophages. Moreover, recent studies in rat smooth muscle cells and the RAW 264.7 macrophage cell line demonstrate that LPS and cytokines induce arginosuccinate synthase gene expression which appears to be essential for sustaining NO production in cells expressing inducible NO synthase (Morris *et al.*, 1993).

At sites of macrophage activation *in vivo*, rapid depletion of extracellular arginine occurs due to the metabolism of arginine by both arginase and NO synthase (Currie *et al.*, 1978; Albina *et al.*, 1989; Granger *et al.*, 1990). Under these conditions the availability of arginine may become rate-limiting for NO production. Thus, metabolism of citrulline to arginine could be an important mechanism not only for the maintenance of intracellular arginine levels but also for the production of NO. Our results, however, demonstrate that this process is at best very inefficient, emphasising the importance of an adequate supply of extracellular arginine to sustain NO synthesis in activated macrophages.

G.E.M. and A.R.B. thank the British Heart Foundation (1180150, 1890453) for financial support. R.G.B. was the recipient of a SERC/CASE PhD award in collaboration with Wellcome Research Laboratories. We gratefully acknowledge the valuable comments of Dr Salvador Moncada FRS on this manuscript.

References

AISAKA, K., GROSS, S.S., GRIFFITH, O.W. & LEVI, R. (1989). L-arginine availability determines the duration of acetylcholine-induced systemic vasodilatation in vivo. *Biochem. Biophys. Res. Commun.*, **163**, 710–717.

ALBINA, J.E., MILLS, C.D., HENRY, W.L. & CALDWELL, M.D. (1989). Regulation of macrophage physiology by L-arginine: role of the oxidative deiminase pathway. *J. Immunol.*, **143**, 3641–3646.

ASSREUY, J. & MONCADA, S. (1992). A perfusion system for the long term study of macrophage activation. *Br. J. Pharmacol.*, **107**, 317–321.

BAYDOUN, A.R., BOGLE, R.G., PEARSON, J.D. & MANN, G.E. (1993). Selective inhibition by dexamethasone of induction of NO synthase, but not of induction of L-arginine transport, in activated murine macrophage J774 cells. *Br. J. Pharmacol.*, **110**, 1401–1406.

BOGLE, R.G., BAYDOUN, A.R., PEARSON, J.D., MONCADA, S. & MANN, G.E. (1992a). L-arginine transport is increased in macrophages generating nitric oxide. *Biochem. J.*, **284**, 15–18.

BOGLE, R.G., BAYDOUN, A.R., PEARSON, J.D. & MANN, G.E. (1992b). Citrulline can restore the ability of activated macrophages to generate nitric oxide in the absence of extracellular arginine. *Br. J. Pharmacol.*, **107**, 286P.

CHRISTENSEN, H.N. & ANTONIOLI, J.A. (1969). Cationic amino acid transport in the rabbit reticulocyte. Na^+-dependent inhibition of Na^+-independent transport. *J. Biol. Chem.*, **244**, 1497–1504.

CLOSS, E.I., ALBRITTON, L.M., KIM, J.W. & CUNNINGHAM, J.M. (1993a). Identification of a low affinity, high capacity transporter of cationic amino acids in mouse liver. *J. Biol. Chem.*, **268**, 7538–7544.

CLOSS, E.I., LYONS, C.R., MITCHELL, M. & CUNNINGHAM, J.M. (1993b). Expression of cationic amino acid transporters in NO-producing macrophages. *Endothelium*, **1**, S16.

CURRIE, G.A. (1978). Activated macrophages kill tumour cells by releasing arginase. *Nature*, **273**, 758–759.

DHANAKOTI, S.N., BROSNAN, J.T., HERZBERG, G.R. & BROSNAN, M.E. (1990). Renal arginine synthesis: studies in vitro and in vivo. *Am. J. Physiol.*, **259**, E437–E442.

DRAPIER, J.-C. & HIBBS, J.B. Jr. (1988). Differentiation of murine macrophages to express nonspecific cytotoxicity for tumor cells in L-arginine dependent inhibition of mitochondrial iron-sulphur enzymes in the macrophage effector cells. *J. Immunol.*, **140**, 2829–2838.

GREEN, L.C., WAGNER, D.A., GLOGOWSKI, J., SKIPPER, P.L., WISHNOK, J.S. & TANNENBAUM, S.R. (1982). Analysis of nitrate, nitrite and [^{15}N]nitrite in biological fluids. *Anal. Biochem.*, **126**, 131–138.

GRANGER, D.L., HIBBS, J.B. Jr., PERFECT, J.R. & DURACK, D.T. (1990). Metabolic fate of L-arginine in relation to microbiostatic capability of murine macrophages. *J. Clin. Invest.*, **85**, 264–273.

HECKER, M., SESSA, W.C., HARRIS, H.J., ANGGARD, E.E. & VANE, J.R. (1990). The metabolism of L-arginine and its significance for the biosynthesis of endothelium-derived relaxing factor: cultured endothelial cells recycle L-citrulline to L-arginine. *Proc. Natl. Acad. Sci. U.S.A.*, **87**, 8612–8616.

HERZBERG, G.R., SHEERIN, H. & LERNER, J. (1971). Cationic amino acid transport in chicken small intestine. *Comp. Biochem. Physiol.*, **40A**, 229–247.

HIBBS, J.B. Jr, TAINTOR, R.R., VAVRIN, Z. & RACHLIN, E.M. (1988). Nitric oxide: a cytotoxic activated macrophage effector molecule. *Biochem. Biophys. Res. Commun.*, **157**, 87–94.

HOFFMAN, F., KREUSCH, J., MAIER, K.-P., MUNDER, P.G. & DECKER, K. (1978). The urea cycle in different types of macrophages. *Biochem. Soc. Trans.*, **6**, 990–992.

IYNENGAR, R., STUEHR, D.J. & MARLETTA, M.A. (1987). Macrophage synthesis of nitrite, nitrate and N-nitrosoamines: precursors and the role of the respiratory burst. *Proc. Natl. Acad. Sci. U.S.A.*, **84**, 6369–6373.

KELLER, R., GEIGES, M. & KEIST, R. (1990). L-arginine dependent reactive nitrogen intermediates as mediators of tumour cell killing by activated macrophages. *Cancer Res.*, **50**, 1421–1425.

KIM, J.W., CLOSS, E.I., ALBRITTON, L.M. & CUNNINGHAM, J.M. (1991). Transport of cationic amino acids by the mouse ecotropic retrovirus receptor. *Nature*, **352**, 725–728.

LAWLESS, K., MAENZ, D. & CHEESEMAN, C. (1987). Is leucine an allosteric modulator of the lysine transporter in the intestinal basolateral membrane? *Am. J. Physiol.*, **253**, G637–G642.

MARLETTA, M.A., YOON, P.S., IYENGAR, R., LEAF, C.D. & WISHNOK, J.S. (1988). Macrophage oxidation of L-arginine to nitrite and nitrate: nitric oxide is an intermediate. *Biochemistry*, **27**, 8706–8711.

MCCALL, T.B., FEELISCH, M., PALMER, R.M.J. & MONCADA, S. (1991). Identification of N-iminoethyl-L-ornithine as an irreversible inhibitor of nitric oxide in phagocytic cells. *Br. J. Pharmacol.*, **102**, 235–238.

MONCADA, S., PALMER, R.M.J. & HIGGS, E.A. (1991). Nitric oxide: physiology, pathophysiology and pharmacology. *Pharmacol. Rev.*, **43**, 109–142.

MORRIS, S.M., NAKAYAMA, D.K., NUSSLER, A.K., LIU, Z., DAVIES, P., PITT, B.R., SIMMONS, R.L. & BILLIAR, T.R. (1993). Co-induction of NO synthase and arginnosuccinate synthetase (AS) gene expression. Implications for regulation of NO synthesis. *Endothelium*, **1**, S9.

MUNCK, B.G. (1980). Lysine transport across the small intestine. Stimulating and inhibitory effects of neutral amino acids. *J. Memb. Biol.*, **53**, 45–53.

PALMER, R.M.J., ASHTON, D.S. & MONCADA, S. (1988). Vascular endothelial cells synthesize nitric oxide from L-arginine. *Nature*, **333**, 664–666.

REES, D.D., SCHULZ, R., HODSON, H.F., PALMER, R.M.J. & MONCADA, S. (1990). Characterization of three inhibitors of endothelial cell nitric oxide synthase *in vitro* and *in vivo*. *Br. J. Pharmacol.*, **101**, 746–752.

SATO, H., FUJIWARA, M. & BANNAI, S. (1992). Effect of lipopolysaccharide on transport and metabolism of arginine in mouse peritoneal macrophages. *J. Leuk. Biol.*, **52**, 161–164.

SATO, H., ISHII, T., SUGITA, Y. & BANNAI, S. (1991). Induction of cationic amino acid transport activity in mouse peritoneal macrophages by lipopolysaccharide. *Biochim. Biophys. Acta*, **1069**, 46–52.

SATO, H., WATANABE, H., ISHII, T. & BANNAI, S. (1987). Neutral amino acid transport in mouse peritoneal macrophages. *J. Biol. Chem.*, **262**, 13015–13019.

SWEIRY, J.H., MUÑOZ, M & MANN, G.E. (1991). Cis-inhibition and trans-stimulation of cationic amino acid transport in the perfused rat pancreas. *Am. J. Physiol.*, **261**, C506–C514.

TAKEMA, M., INABA, K., UNO, K., KAKIHARA, K.-I., TAWARA, K. & MURAMATSU, S. (1991). Effect of L-arginine on the retention of macrophage tumoricidal activity. *J. Immunol.*, **146**, 1928–1933.

WHITE, M.F. (1985). The transport of cationic amino acids across the plasma membrane of mammalian cells. *Biochem. Biophys. Acta*, **822**, 355–374.

WINDMUELLER, H.G. & SPAETH, A.E. (1981). Source and fate of circulating citrulline. *Am. J. Physiol.*, **241**, E473–E480.

WU. G. & BROSNAN, M.T. (1992). Macrophages can convert citrulline into arginine. *Biochem. J.*, **281**, 45–48.

(Received November 9, 1993
Revised February 1, 1994
Accepted February 14, 1994)

Br. J. Pharmacol. (1994), **112**, 493–498

Effect of salmeterol on human nasal epithelial cell ciliary beating: inhibition of the ciliotoxin, pyocyanin

K. Kanthakumar, D.R. Cundell, *M. Johnson, P.J. Wills, †G.W. Taylor, P.J. Cole & [1]R. Wilson

Host Defence Unit, Department of Thoracic Medicine, Royal Brompton National Heart and Lung Institute, Emmanuel Kaye Building, Manresa Road, London SW3 6LR; *Department of Cardiovascular and Respiratory Pharmacology, Glaxo Group Research Limited, Ware, Herts SG12 0DP and †Department of Clinical Pharmacology, Royal Postgraduate Medical School, Hammersmith Hospital, Du Cane Road, London W12 0HS

1 Patients with airway infection by *Pseudomonas aeruginosa* have impaired mucociliary clearance. Pyocyanin is a phenazine pigment produced by *P. aeruginosa* which is present in the sputum of colonized patients, slows human ciliary beat frequency (CBF) *in vitro* and slows mucociliary transport *in vivo* in the guinea-pig.

2 We have investigated the effect of salmeterol, a long-acting β_2-adrenoceptor agonist, on pyocyanin-induced slowing of human CBF *in vitro*. Salmeterol (2×10^{-7} M) was found to reduce pyocycanin ($20\ \mu g\ ml^{-1}$)-induced slowing of CBF by 53% and the fall in intracellular adenosine 3':5'-cyclic monophosphate (cyclic AMP) by 26% and ATP by 29%.

3 Another β_2-adrenoceptor agonist, isoprenaline (2×10^{-7} M), also inhibited pyocyanin-induced slowing of CBF by 39%.

4 The effects of salmeterol (30 min preincubation) persisted after washing the cells.

5 Propranolol (10^{-7} M) and the β_2-specific antagonist, ICI 118551 (10^{-6} M) blocked the protective effects of salmeterol completely, but atenolol (10^{-6} M) was less effective. These results suggested that the effects of salmeterol on pyocyanin-induced effects were mediated primarily via the stimulation of β_2-adrenoceptors.

6 Pyocyanin-induced ciliary slowing is associated with a substantial fall in intracellular cyclic AMP and ATP. Salmeterol reversed the effects of pyocyanin on cyclic AMP and ATP.

7 Mucociliary clearance is an important defence mechanism of the airways against bacterial infection. Salmeterol may benefit patients colonized by *P. aeruginosa*, not only by its bronchodilator action, but also by protecting epithelial cells from pyocyanin-induced slowing of CBF.

Keywords: Salmeterol; cilia; ciliotoxin; pyocyanin; *Pseudomonas aeruginosa*; β agonist; cyclic AMP; ATP

Introduction

Many patients with chronic airways infection by bacteria such as *Pseudomonas aeruginosa* have airflow obstruction and impaired mucociliary clearance (Hoiby, 1982; Fick, 1989; Cole & Wilson, 1989). Pyocyanin is a phenazine pigment produced by *P. aeruginosa* which is present in the sputum of colonized patients at high concentrations up to $27\ \mu g\ ml^{-1}$ (Wilson *et al.*, 1988). Pyocyanin slows human ciliary beat frequency (CBF) *in vitro*, and later disrupts the integrity of the epithelial surface (Wilson *et al.*, 1987); it also slows tracheal mucociliary transport in guinea-pigs *in vivo* (Munro *et al.*, 1989). *P. aeruginosa* also produces 1-hydroxyphenazine (Wilson *et al.*, 1987) and rhamnolipid (Read *et al.*, 1992) which both slow human ciliary beating, and collectively these products are likely to play a part in bacterial colonisation of the lower respiratory tract. We have recently shown that pyocyanin-induced slowing of human ciliary beat *in vitro* is associated with a fall in intracellular adenosine 3':5'-cyclic monophosphate (cyclic AMP) and adenosine 5'-triphosphate (ATP). Ciliary beat slowing could be prevented by treating the epithelial cells with agents known to increase cyclic AMP levels (Kanthakumar *et al.*, 1993).

Studies investigating the effects of inhaled β_2-adrenoceptor agonists on mucociliary clearance in humans *in vivo* have indicated that this may be an important aspect of their therapeutic efficacy, especially in infective lung disease (Pavia, 1984; Devalia *et al.*, 1992). The mechanism is unclear but it has been suggested that it involves increase of ciliary activity and intracellular cyclic AMP levels by stimulation of β_2-adrenoceptors on the epithelial surface (Devalia *et al.*, 1992; Lansley *et al.*, 1992). Studies by Verdugo and colleagues (1980) and Di Benedetto and colleagues (1991) have suggested that cyclic AMP is a regulator of ciliary activity in airway epithelium, possibly by affecting the availability or use of ATP by the ciliary axoneme (Lansley *et al.*, 1992). Salmeterol is a potent β_2 agonist with a prolonged action and causes a greater increase in intracellular cyclic AMP than salbutamol (Devalia *et al.*, 1992). We have investigated the effect of salmeterol on pyocyanin-induced changes in ciliary beating, and intracellular cyclic AMP and ATP levels, in human nasal epithelial cells, and have compared salmeterol with isoprenaline.

Methods

Human nasal epithelium

Strips of normal human nasal ciliated epithelium were obtained with a cytology brush (Rutland & Cole, 1980) from the inferior turbinate of healthy volunteers who had been free of respiratory infection for at least 4 weeks and dispersed by agitation in cell culture medium 199 with Earle's salts and HEPES (N-hydroxyethylpiperazine-N'-2-ethanesulphonic acid) (Flow Laboratories, Canada). The sample of epithelium was divided, and sealed microscope coverslip-slide preparations were constructed for assessment by light microscopy. CBF was measured photometrically from ten identified sites on at

[1] Author for correspondence.

least six strips of epithelium at 37°C as previously described (Wilson et al., 1987; 1988; Kanthakumar et al., 1993). Ciliary dyskinesia (loss of the normal coordinated pattern of ciliary beating), ciliostasis (absence of ciliary beating), and disruption of the integrity of the epithelial surface (irregularity and break-up of the previously smooth intact surface) were recorded when present. Although every effort was made to make recordings of CBF at the same point of a strip at each experimental time-point, this was not always possible because epithelial strips sometimes move or change shape during an experiment because of ciliary beating. For this reason a recording of zero CBF was made only when ciliary beating had ceased on the whole epithelial strip. A sample of epithelium from a volunteer was used for only one experiment. Each experiment was repeated on six separate occasions with nasal epithelial samples obtained from six separate volunteers.

Effect of salmeterol on pyocyanin-induced ciliary slowing

Pyocyanin ($20\ \mu g\ ml^{-1}$) was used in all experiments. This concentration has been observed in the sputum of infected patients (Wilson et al., 1988), and in previous experiments in our laboratory (Kanthakumar et al., 1993) caused CBF to fall to about half of control by 4 h, disruption of epithelium integrity at 3 h, and marked falls in both intracellular cyclic AMP and ATP. For each experiment the sample of nasal epithelial strips in medium 199 was divided into four equal aliquots. Four sealed microscope coverslip-slide preparations were then constructed containing medium 199 alone, pyocyanin ($20\ \mu g\ ml^{-1}$), salmeterol ($1-4 \times 10^{-7}$ M) or salmeterol and pyocyanin. Epithelium for preparations containing salmeterol was preincubated with salmeterol for 15 min. The preparations were allowed to stabilize for a further 15 min after slide construction, and then CBF was measured at hourly intervals for 4 h. The experiment was repeated with isoprenaline (2×10^{-7} M).

One aliquot of nasal epithelial strips was pre-incubated with salmeterol (2×10^{-7} M) for 5 min, 15 min or 30 min. The aliquots were washed twice in medium 199. Each aliquot was centrifuged (800 g, 5 min) to pellet the epithelium, the supernatant was carefully removed with a pipette, and the epithelium resuspended in fresh medium 199. This procedure was repeated a second time. Four microscope-slide preparations were then constructed containing medium 199 alone, pyocyanin (epithelium not exposed to salmeterol), pyocyanin (epithelium incubated with salmeterol for 5, 15 or 30 min), and pyocyanin and salmeterol (present throughout the experiment, as in the concentration-response experiments described above).

Effect of salmeterol on pyocyanin-induced ciliary slowing in the presence of β-adrenoceptor antagonists

For each series of experiments, samples of nasal epithelium were incubated with salmeterol (2×10^{-7} M, 30 min at 37°C), washed twice and then exposed to pyocyanin ($20\ \mu g\ ml^{-1}$) and either propranolol (10^{-7} M), ICI 118551 (10^{-6} M) or atenolol (10^{-6} M). Five microscope-slide preparations were constructed for each experiment containing medium 199 alone, β-adrenoceptor antagonist, pyocyanin, pyocyanin (epithelium incubated with salmeterol), and pyocyanin and β-antagonist (epithelium incubated with salmeterol). Atenolol is a selective β_1-antagonist ($pA_2\ \beta_1 = 7.1$, $pA_2\ \beta_2 = 5.6$; O'Donnell & Wanstall, 1979) and ICI 118551 a selective β_2 antagonist ($pA_2\ \beta_2 = 8.8$, $pA_2\ \beta_1 = 6.7$; O'Donnell & Wanstall, 1981). Therefore at the concentrations of atenolol and ICI 118551 used, selective blockade of β_1 and β_2 adrenoceptors respectively was achieved.

ATP and cyclic AMP measurement

Levels of ATP in nasal epithelium were measured spectrophotometrically (Sigma, UK). Cyclic AMP levels were measured by enzyme immunoassay (Amersham, UK) (Kanthakumar et al., 1993). Nasal epithelial samples ($n = 6$) were treated with pyocyanin ($20\ \mu g\ ml^{-1}$) for 2 h in the presence or absence of salmeterol (2×10^{-7} M). This incubation time was chosen since the effects of pyocyanin are completely reversible at this point (Kanthakumar et al., 1993). Cellular protein levels were assessed by the method of Lowry et al. (1951), and levels of adenosine nucleotides were expressed as mg^{-1} of cellular protein.

Materials

Pyocyanin was prepared by photolysis of phenazine methosulphate (Knight et al., 1979) (Aldrich Chemicals, U.S.A.) and purified and characterized by its h.p.l.c.-u.v. profile as previously described (Wilson et al., 1988). Pyocyanin was tested at a final concentration of $20\ \mu g\ ml^{-1}$ ($\sim 10^{-4}$ M) in all experiments. Salmeterol hydroxynaphthoate (Glaxo, UK) was initially dissolved in glacial acetic acid and then diluted in phosphate buffered saline (PBS, pH 7.0); isoprenaline sulphate (Sigma, UK) was dissolved in distilled water. The β_2-specific antagonist, erythro-DL-1(7-methylindan-4-yloxy)-3-iso propylamino-butan-2-ol (ICI 118551, ICI, UK; Lemoine et al., 1988) was dissolved in PBS (pH 7.0). The β_1-specific antagonist, atenolol (Sigma, UK) and the non-specific β-antagonist, propranolol hydrochloride (Sigma, UK) were dissolved in distilled water.

Statistical analysis

Statistical analysis was carried out with the Wilcoxon signed ranks paired test. Data were expressed as mean ± standard error of the mean (s.e.mean). The mean percentage inhibition of pyocyanin-induced effects (protection) afforded by salmeterol and isoprenaline was calculated after 4 h as 100 × [mean ($n = 6$) CBF of pyocyanin with β-agonist − mean ($n = 6$) CBF of pyocyanin without β agonist]/[mean ($n = 6$) CBF of control − mean ($n = 6$) CBF of pyocyanin without β-agonist].

Results

Effect of salmeterol on pyocyanin-induced ciliary slowing

Salmeterol (1, 2 and 4×10^{-7} M) had no effect on baseline CBF compared to control CBF in medium 199 alone. Pyocyanin caused progressive slowing of CBF over 4 h (58% compared with control cells). Epithelial disruption was observed at 3 h and ciliary dyskinesia at 4 h. All three concentrations of salmeterol reduced pyocyanin-induced ciliary slowing with mean percentage protection at 4 h of 37%, 53% and 60% for 1, 2 and 4×10^{-7} M, respectively (Figure 1). Ciliary dyskinesia was not observed in any of the experiments incorporating salmeterol. Salmeterol (2 and 4×10^{-7} M) delayed the appearance of epithelial disruption from 3 h to 4 h. A salmeterol concentration of 2×10^{-7} M was chosen for use in all further experiments.

In a separate series of experiments, the effect of washing the tissue after exposure to salmeterol, before incubation with pyocyanin was studied. Incubation of epithelial cells with salmeterol (2×10^{-7} M) for 5 or 15 min, before washing, had no significant effect on pyocyanin-induced ciliary slowing, ciliary dyskinesia or epithelial damage. However, incubation with salmeterol for 30 min before washing produced a similar effect to that produced with salmeterol present throughout the experiment (Figure 2).

Effect of salmeterol on pyocyanin-induced ciliary slowing in the presence of β-adrenoceptor antagonists

Propranolol (10^{-7} M; Figure 3a) and ICI 118551 (10^{-6} M, Figure 3b) completely abolished the protective effect afforded

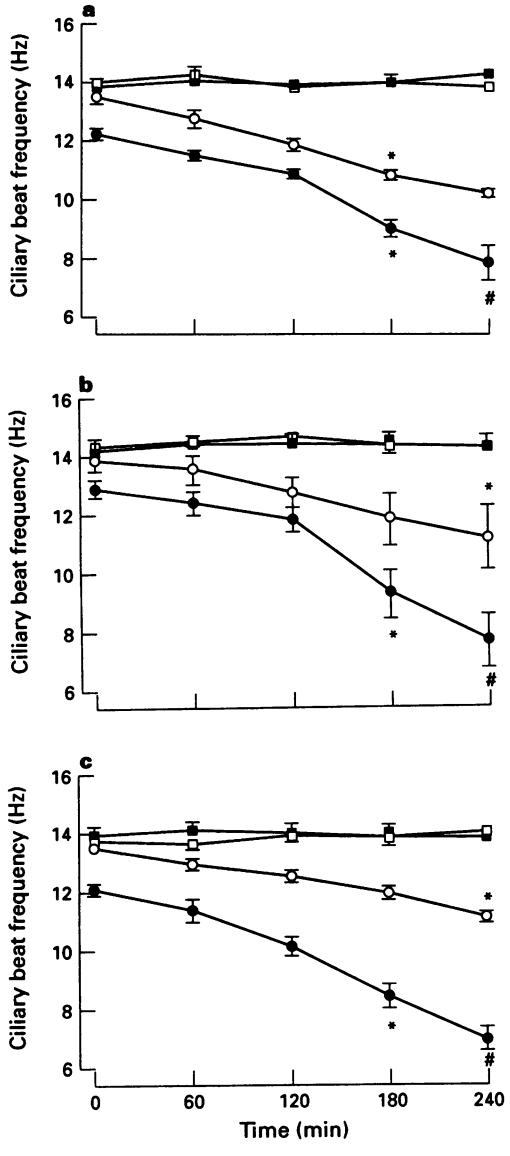

Figure 1 The effect of salmeterol on pyocyanin-induced ciliary beat slowing. Salmeterol was present throughout the experiment. Salmeterol alone (□) had no effect on baseline ciliary beat frequency (CBF) compared to control CBF in medium 199 alone (■) at any of the concentrations tested: (a) 1×10^{-7} M, (b) 2×10^{-7} M or (c) 4×10^{-7} M. Salmeterol (○) at all three concentrations significantly ($P<0.05$) reduced ciliary slowing and ciliary dyskinesia (#) produced by pyocyanin (●). The two higher concentrations were also able to delay the appearance of epithelial disruption (*) by 1 h.

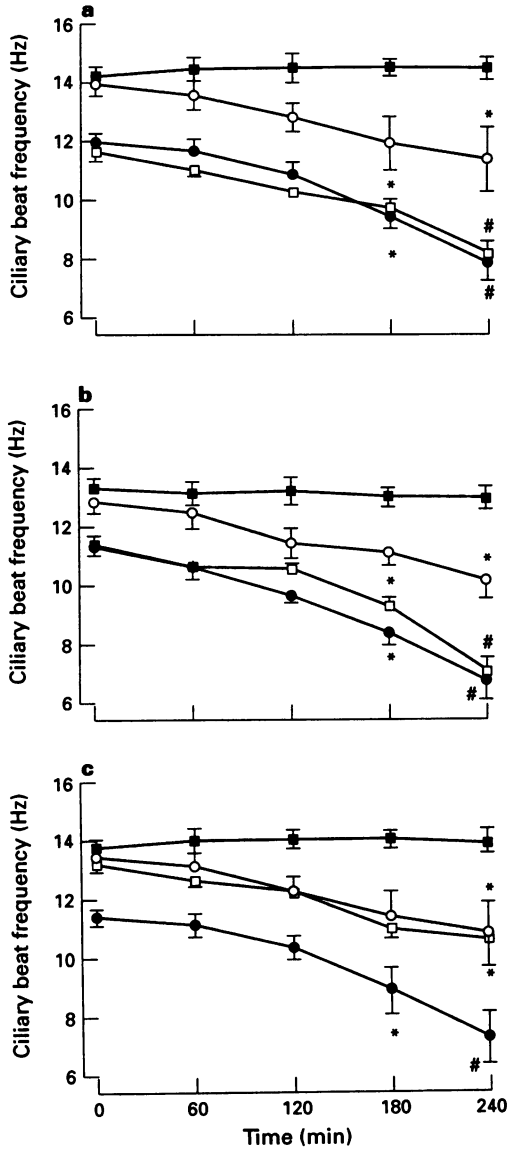

Figure 2 The effect of preincubation time on the protection afforded by salmeterol on pyocyanin-induced ciliary beat slowing. Incubation of cells with salmeterol (2×10^{-7} M) (□) for (a) 5 min and (b) 15 min followed by washing did not influence pyocyanin-induced ciliary beat slowing (●), but (c) incubation for 30 min gave equivalent results to salmeterol present throughout the experiment (○) (e.g. Figure 1b). Control medium 199 alone (■), # = ciliary dyskinesia, * = epithelial disruption.

by salmeterol (2×10^{-7} M) on pyocyanin-induced ciliary slowing, ciliary dyskinesia and epithelial disruption. Atenolol (10^{-6} M) partially inhibited the protective effect of salmeterol (2×10^{-7} M) on pyocyanin-induced ciliary slowing (Figure 3c), but had no effect on the protection afforded by salmeterol against pyocyanin-induced ciliary dyskinesia and epithelial disruption.

Effect of isoprenaline on pyocyanin-induced ciliary slowing

Isoprenaline (2×10^{-7} M) alone had no effect on baseline CBF, but significantly protected (39% inhibition) against pyocyanin-induced slowing of CBF; this effect compared with 53% inhibition by salmeterol at the same concentration. Isoprenaline also prevented ciliary dyskinesia, and delayed the appearance of epithelial disruption by 1 h.

Effect of salmeterol on pyocyanin-induced fall in intracellular cyclic AMP and ATP

Incubation of epithelial cells with pyocyanin for 2 h produced a 93% fall in intracellular cyclic AMP and 88% fall in ATP levels compared with controls (Figure 4). Incubation of cells with salmeterol (2×10^{-7} M) had no effect on basal levels of either nucleotide but did significantly protect against pyocyanin-induced falls in both cyclic AMP (26% protection), and ATP (29% protection).

Discussion

Pyocyanin is a phenazine pigment produced by *P. aeruginosa* that has a number of important effects during infections of the respiratory tract. Pyocyanin slows ciliary beating and

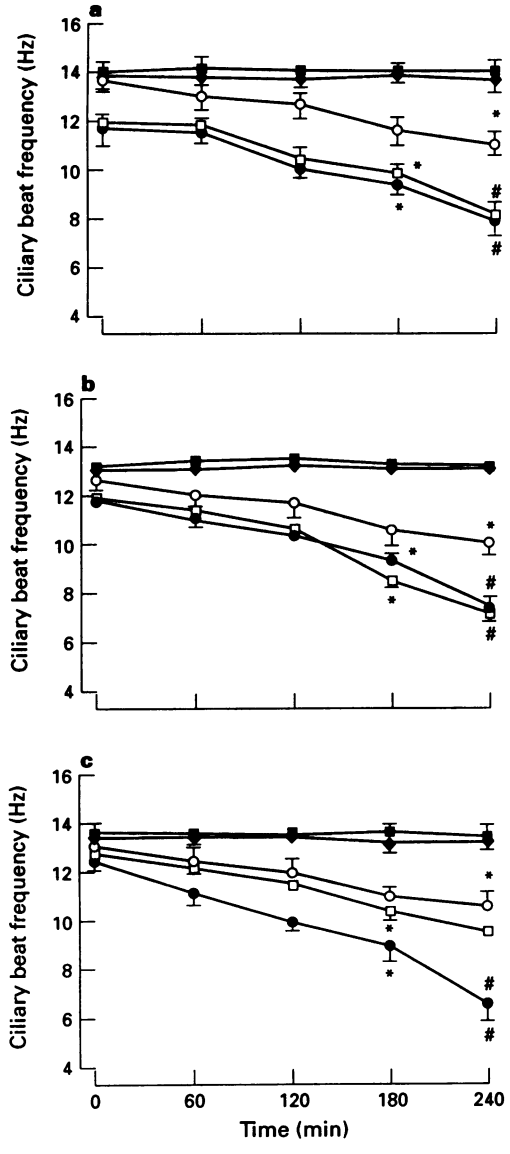

Figure 3 The effect of propranolol, ICI 118551 and atenolol on the protection afforded by salmeterol on pyocyanin-induced ciliary beat slowing. (a) Propranolol (10^{-7} M), (b) ICI 118551 (10^{-6} M) and (c) atenolol (10^{-6} M) alone (◆) had no effect on baseline ciliary beat frequency (CBF) compared to control CBF in medium 199 alone (■). All three β-antagonists (□) did significantly ($P<0.05$) reduce the protective effect of salmeterol (○) on pyocyanin-induced ciliary slowing (●). # = ciliary dyskinesia, * = epithelial disruption.

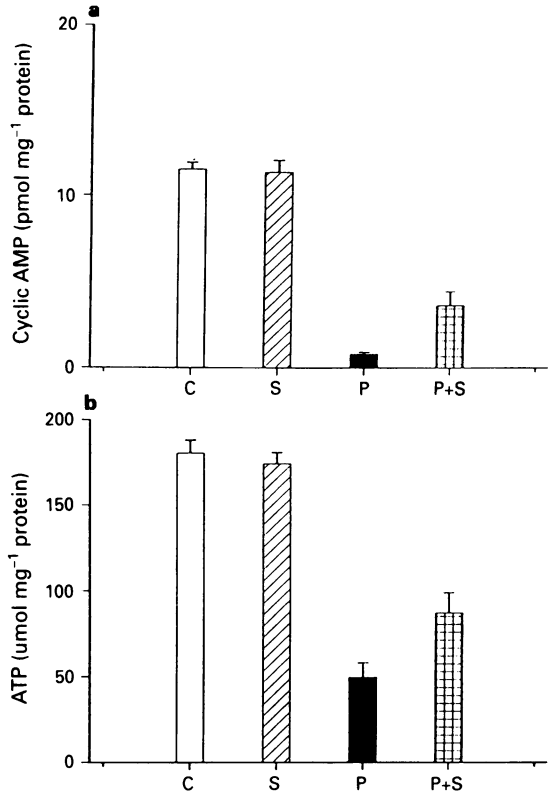

Figure 4 The effect of salmeterol on pyocyanin-induced reduction in intracellular cyclic AMP and ATP. Pyocyanin (P) produced a 93% reduction in cyclic AMP (a) and an 88% reduction in ATP (b) compared to controls (c) in medium 199 alone. Treatment of the cells with salmeterol (S) 2×10^{-7} M had no effect on basal levels of adenosine nucleotides but did significantly ($P<0.05$) protect (P + S) by 26% and 29% respectively against the reduction produced by pyocyanin in intracellular cyclic AMP and ATP.

reduces mucociliary clearance (Wilson *et al.*, 1987; Munro *et al.*, 1989; Kanthakumar *et al.*, 1993). Pyocyanin also enhances the oxidative metabolism of neutrophils (Ras *et al.*, 1990), inhibits epithelial cell growth (Cruickshank *et al.*, 1953) and affects lymphocytes function (Nutman *et al.*, 1987). Pyocyanin is found in the sputum of colonized patients at concentrations as high as 27 μg ml^{-1} (Wilson *et al.*, 1988) which is sufficient to cause all these *in vitro* effects.

Pyocyanin (20 μg ml^{-1}) caused CBF to slow by >50% during 4 h, and this was associated with epithelial disruption after 3 h and ciliary dyskinesia after 4 h. Salmeterol reduced the effects of pyocyanin on epithelial cells. The concentrations of salmeterol that were studied were chosen because 2×10^{-7} M salbutamol just provides maximum stimulation of β_2-adrenoceptors in a range of tissues (Coleman & Nials, 1989; Ball *et al.*, 1991). In the presence of salmeterol there was less ciliary slowing, no ciliary dyskinesia and the onset of epithelial disruption was delayed. The interaction of salmeterol with the epithelium was such that the drug could be removed by washing after 30 min without affecting its action. This suggests that the drug persists in the tissue after this time, and may result from its lipid solubility (Bradshaw *et al.*, 1987; Nials *et al.*, 1993). These data are consistent with the studies of Johnson (1990) on guinea-pig smooth muscle and Devalia *et al.* (1992) on human cultured bronchial epithelial cells. Previous studies using animal tracheal tissue have shown CBF to increase with β-agonists at similar concentrations to those used in the present study (Verdugo *et al.*, 1980; Wong *et al.*, 1988). In our studies, 2×10^{-7} M salmeterol had no effect on baseline CBF, nor intracellular cyclic AMP and ATP levels. This difference is likely to be related to the species studied, or possibly the site from which the epithelial cells were obtained. The effects of β-agonists on human CBF may be concentration-dependent because high concentrations of salmeterol (10^{-6} M) have been shown to stimulate an approximate 10% increase in CBF of human cultured bronchial epithelial cells. This was associated with an approximate 10 fold increase in intracellular cyclic AMP levels (Devalia *et al.*, 1992).

The non-specific β-receptor antagonist, propranolol and the β_2-selective receptor antagonist, ICI 118551 (Nials *et al.*, 1993) both completely abolished the action of salmeterol on pyocyanin-induced ciliary slowing, ciliary dyskinesia and epithelial disruption. Our findings on the effect of propranolol are in agreement with those of Ball *et al.* (1991) who suggested from their studies of guinea-pig trachea that a simple competitive interaction existed between the two com-

pounds. The selective β_1-receptor antagonist, atenolol had only a small effect on the action of salmeterol on pyocyanin-induced ciliary slowing, and had no effect on either ciliary dyskinesia or epithelial disruption. The effects of atenolol could be ascribed to its weak β_2-antagonist activity (Nials *et al.*, 1993). Isoprenaline, which has short-acting β_2-adrenoceptor agonist activity, was also able to inhibit pyocyanin-induced ciliary slowing, ciliary dyskinesia and epithelial disruption, although, as in other studies (Nials *et al.*, 1993), it was less potent than salmeterol.

We have previously shown that ciliary beat slowing by pyocyanin is associated with a fall in intracellular cyclic AMP and ATP, and is prevented by the cyclic AMP analogue, dibutyryl cyclic AMP, the phosphodiesterase inhibitor isobutyl methylxanthine, and the adenylate cyclase stimulant, forskolin (Kanthakumar *et al.*, 1993). Salmeterol protected against the pyocyanin-induced fall in intracellular adenosine nucleotides, and this was associated with a reduction in pyocyanin-induced ciliary slowing, which suggests that these events could be mediated via a common mechanism. As ATP is an essential energy source for beating cilia (Satir, 1989; Satir & Sleigh, 1990), it is possible that the effects of pyocyanin on CBF and coordination of ciliary beat are directly mediated through the fall in intracellular ATP levels. Lansley and colleagues (1992) have proposed that the concentration of intracellular cyclic AMP may affect the availability or utilisation of ATP by ciliary axonemes. β_2-Adrenoceptor agonists have been shown to increase cyclic AMP levels in both animal and human respiratory epithelial cells (Lansley *et al.*, 1992; Devalia *et al.*, 1992) and this is likely, therefore, to explain the effect of salmeterol on pyocyanin-induced ciliary beat slowing. In our previous studies pyocyanin-induced ciliary slowing after 2 h was completely reversed after washing, and the associated fall in adenosine nucleotides at 2 h occurred at a time when the epithelial cells were not damaged as assessed by lactate dehydrogenase release and trypan blue exclusion. These observations suggest that cell damage is not the primary cause of slowed CBF, and reduced levels of cyclic AMP and ATP (Kanthakumar *et al.*, 1993). Agents which raise intracellular cyclic AMP, including salmeterol in the present study, also prevent pyocyanin-induced disruption of the integrity of the epithelial surface.

Salmeterol may benefit patients colonised by *P. aeruginosa*, not only by its bronchodilator action, but by protecting epithelial cells from pyocyanin-induced slowing and disorganisation of CBF, disruption of epithelial integrity, and the consequent reduction of mucociliary transport (Wilson, 1988; Yeates *et al.*, 1976).

This work was supported by Glaxo Group Research Ltd. We are grateful to Miss Jane Burditt for secretarial assistance.

References

BALL, D.I., BRITTAIN, R.T., COLEMAN, R.A., DENYER, L.H., JACK, D., JOHNSON, M., LUNTS, L.H.C., NIALS, A.T., SHELDRICK, K.E. & SKIDMORE, I.F. (1991). Salmeterol, a novel long-acting β_2-adrenoceptor agonist: characterization of pharmacological activity *in vitro* and *in vivo*. *Br. J. Pharmacol.*, **104**, 665–671.

BRADSHAW, J., BRITTAIN, R.T., COLEMAN, R.A., JACK, D., KENNEDY, I., LUNTS, L.H.C. & SKIDMORE, I.F. (1987). The design of salmeterol, a long-acting β_2-adrenoceptor agonist. *Br. J. Pharmacol.*, **92**, 520P.

COLE, P.J. & WILSON, R. (1989). Host-microbial interrelationships in respiratory infection. *Chest* (Suppl.) **95**, 217S–221S.

COLEMAN, R.A. & NIALS, A.T. (1989). Novel and versatile superfusion system. Its use in the evaluation of some spasmogenic and spasmolytic agents using guinea-pig isolated tracheal smooth muscle. *J. Pharmacol. Methods*, **21**, 71–86.

CRUICKSHANK, C.N.D. & LOWBURY, E.J.L. (1953). The effect of pyocyanin on human skin cells and leukocytes. *Br. J. Exp. Pathol.*, **34**, 583.

DEVALIA, J.L., SAPSFORD, R.J., RUSZNAK, C., TOUMBIS, M.J. & DAVIES, R.J. (1992). The effects of salmeterol and salbutamol on ciliary beat frequency of cultured human bronchial epithelial cells, in vitro. *Pulmonary Pharmacol.*, **5**, 257–263.

DI BENEDETTO, G., MARARA-SHEDIAC, F.S. & MEHTA, S. (1991). Effect of cyclic AMP on ciliary activity of human respiratory epithelium. *Eur. Respir. J.*, **4**, 789–795.

FICK, R.B. (1989). Pathogenesis of the Pseudomonas lung lesion in cystic fibrosis. *Chest*, **96**, 158–164.

HOIBY, N. (1982). Microbiology of lung infections in cystic fibrosis. *Acta Paediatr. Scand.*, **301** (Suppl.), 33–54.

JOHNSON, M. (1990). The pharmacology of salmeterol. *Lung*, (Suppl.), 115–119.

KANTHAKUMAR, K., TAYLOR, G., TSANG, K.W.T., CUNDELL, D.R., RUTMAN, A., SMITH, S., JEFFERY, P.K., COLE, P.J. & WILSON, R. (1993). Mechanisms of action of *Pseudomonas aeruginosa* pyocyanin on human ciliary beat in vitro. *Infect. Immun.*, **61**, 2848–2853.

KNIGHT, M., HARTMAN, P.E., HARTMAN, Z. & YOUNG, V.M. (1979). A new method of preparation of pyocyanin and demonstration of an unusual bacterial sensitivity. *Anal. Biochem.*, **95**, 19–23.

LANSLEY, A.B., SANDERSON, M.J. & DIRKSEN, E.R. (1992). Control of the beat cycle of respiratory tract cilia by Ca^{++} and cAMP. *Am. J. Physiol.*, **263**, L232–L242.

LEMOINE, H., SCHONELL, H. & KAUMANN, A.J. (1988). Contribution of β_1- and β_2-adrenoceptors of human atrium and ventricle to the effects of noradrenaline and adrenaline as assessed with atenolol. *Br. J. Pharmacol.*, **95**, 55–56.

LOWRY, O.H., ROSEBROUGH, N.J., FARR, A.L. & RANDALL, R.J. (1951). Protein measurement with the Folin phenol reagent. *J. Biol. Chem.*, **193**, 265–275.

MUNRO, N.C., BARKER, A., RUTMAN, A., TAYLOR, G,. WATSON, D., McDONALD-GIBSON, W.J., TOWART, R., TAYLOR, W.A., WILSON, R. & COLE, P.J. (1989). Effect of pyocyanin and 1-hydroxyphenazine on *in vivo* tracheal mucus velocity. *J. Appl. Physiol.*, **67**, 316–323.

NIALS, A.T., SUMNER, M.J., JOHNSON, M. & COLEMAN, R.A. (1993). Investigations into factors determining the duration of action of the β_2-adrenoceptor agonist, salmeterol. *Br. J. Pharmacol.*, **108**, 507–515.

NUTMAN, J., BERGER, M., CHASE, P.A., DEARBORN, D.G., MILLER, K.M., WALLER, R.L. & SORENSEN, R.U. (1987). Studies on the mechanism of T cell inhibition by the *Pseudomonas aeruginosa* pigment pyocyanine. *J. Immunol.*, **138**, 3481–3487.

O'DONNELL, S.R. & WANSTALL, J.C. (1979). The importance of choice of agonist in studies designed to predict $\beta 2$:$\beta 1$ adrenoceptor selectivity of antagonists from pA2 values on guinea-pig trachea and atria. *Arch. Pharmacol.*, **308**, 183–190.

O'DONNELL, S.R. & WANSTALL, J.C. (1981). Pharmacological approaches to the characterisation of beta-adrenoceptor populations in tissue. *J. Auton. Pharmacol.*, **1**, 305–312.

PAVIA, D. (1984). Lung mucociliary clearance. In *Aerosols and the Lung*. ed. Clarke, S.W. & Pavia, D. pp. 122–155. London: Butterworths.

RAS, G.J., ANDERSON, R., TAYLOR, G.W., SAVAGE, J.E., VAN NIEKERK, E., WILSON, R. & COLE, P.J. (1990). Pro-inflammatory interactions of pyocyanin and 1-hydroxyphenazine with human neutrophils, *in vitro*. *J. Infect. Dis.*, **162**, 178–185.

READ, R.C., ROBERTS, P., MUNRO, N., RUTMAN, A., HASTIE, A., SHRYOCK, T., HALL, R., McDONALD-GIBSON, W., LUND, V., TAYLOR, G., COLE, P.J. & WILSON, R. (1992). The effect of *Pseudomonas aeruginosa* rhamnolipid on guinea pig tracheal mucociliary transport *in vivo* and human ciliary beating *in vitro*. *J. Appl. Physiol.*, **72**, 2271–2277.

RUTLAND, J. & COLE, P.J. (1980). Non-invasive sampling of nasal cilia for measurement of beat frequency and study of ultrastructure. *Lancet*, **ii**, 564–565.

SATIR, P. (1989). The role of axonemal components in ciliary motility. *Comp. Biochem. Physiol.*, **94A**, 351–357.

SATIR, P. & SLEIGH, M.A. (1990). The physiology of cilia and mucociliary interactions. *Annu. Rev. Physiol.*, **52**, 137–155.

VERDUGO, P., JOHNSON, N.T. & TAM, P.Y. (1980). β-Adrenergic stimulation of respiratory ciliary activity. *J. Appl. Physiol.*, **48**, 868–871.

WILSON, R. (1988). Secondary ciliary dysfunction. *Clin. Sci.*, **75**, 113–120.

WILSON, R., PITT, T., TAYLOR, G., WATSON, D., McDERMOT, J., SYKES, D., ROBERTS, D. & COLE, P.J. (1987). Pyocyanin and 1-hydroxyphenazine produced by *Pseudomonas aeruginosa* inhibit human ciliary beating *in vitro*. *J. Clin. Invest.*, **79**, 221–229.

WILSON, R., SYKES, D.A., WATSON, D., RUTMAN, A., TAYLOR, G.W. & COLE, P.J. (1988). Measurement of *Pseudomonas aeruginosa* phenazine pigments in sputum and assessment of their contribution to sputum sol toxicity for respiratory epithelium. *Infect. Immun.*, **56**, 2515–2517.

WONG, L.B., MILLER, I.F. & YEATES, D.B. (1988). Regulation of ciliary beat frequency to autonomic mechanisms: in vitro. *J. Appl. Physiol.*, **65**, 1895–1901.

YEATES, D.B., STURGESS, J.M., KAHN, S.R., LEVISON, H. & ASPIN, N. (1976). Mucociliary transport in trachea of patients with cystic fibrosis. *Arch. Dis. Childhood*, **51**, 28–33.

(Received October 18, 1993
Revised January 10, 1994
Accepted February 16, 1994).

Br. J. Pharmacol (1994), **112**, 499–504

Rapid desensitization of adrenaline- and neuropeptide Y-stimulated Ca^{2+} mobilization in HEL-cells

Martin C. Michel, with the technical assistance of Annette Kötting

Dept. Medicine, University of Essen, Essen, Germany

1 Desensitization of G_s-coupled receptors, the β_2-adrenoceptor for example, involves rapid and slower components but little is known regarding the existence of rapid desensitization of G_i-coupled receptors and its possible mechanisms. In HEL-cells stimulation of α_{2A}-adrenoceptors by adrenaline or Y_1-like neuropeptide Y receptors by neuropeptide Y, transiently mobilizes Ca^{2+} from intracellular stores via a G_i-protein. We have used this model to study the existence and possible mechanisms of rapid desensitization of a G_i-mediated cellular response.

2 Following stimulation by adrenaline or neuropeptide Y Ca^{2+} levels returned towards baseline a few minutes after agonist addition and were refractory to a second agonist exposure demonstrating rapid desensitization. Cross-desensitization experiments with neuropeptide Y, adrenaline and moxonidine demonstrated the presence of homologous (both receptors) and heterologous desensitization (neuropeptide Y receptors only), and that the α_{2A}-adrenoceptor desensitization was not specific for phenylethylamine (adrenaline) or imidazoline agonists (moxonidine).

3 The protein kinase C activator, phorbol ester, rapidly desensitized the hormonal Ca^{2+} responses and inhibitors of protein kinase C enhanced the hormonal responses inconsistently. The tyrosine kinase inhibitor, herbimycin, enhanced Ca^{2+} mobilization by adrenaline and neuropeptide Y, whereas the protein phosphatase inhibitor, okdadaic acid, did not affect Ca^{2+} mobilization or its desensitization.

4 In the absence of extracellular Ca^{2+} the endoplasmic reticulum Ca^{2+}-ATPase inhibitor, thapsigargin, reduced hormone-stimulated Ca^{2+} elevations, demonstrating that mobilization occurs from a thapsigargin-sensitive pool in the endoplasmic reticulum. The inositol phosphate-independent Ca^{2+} release modulator, ryanodine, significantly enhanced adrenaline- and neuropeptide Y-stimulated Ca^{2+} elevations. Blockade of the endoplasmic reticulum Ca^{2+}-ATPase by thapsigargin in the presence of extracellular Ca^{2+} enhanced hormone-stimulated Ca^{2+} increases, demonstrating the importance of this enzyme for the termination of the Ca^{2+} signal.

5 It is concluded that adrenaline and neuropeptide Y-stimulated Ca^{2+} mobilization in HEL-cells occurs from a thapsigargin- and ryanodine-sensitive store in the endoplasmic reticulum and desensitizes rapidly; this appears to involve multiple mechanisms including protein kinases, possibly acting on receptors, and Ca^{2+} release and sequestration mechanisms.

Keywords: α_2-Adrenoceptor; neuropeptide Y receptor; Ca^{2+} mobilization; desensitization

Introduction

Desensitization is a general physiological mechanism by which cells adapt to a changing environment. Desensitization in response to agonist exposure has been best studied for a G_s-coupled receptor, the β_2-adrenoceptor (Lefkowitz *et al.*, 1990; Lorenz *et al.*, 1991). It involves rapid and slower components which are at least partly mediated by the action of multiple protein kinases. Much less is known regarding the desensitization of G_i-coupled receptors. Most previous studies on the regulation of G_i-coupled receptor function have focused on slow desensitization, i.e. that occuring within hours or days (Green *et al.*, 1990; Wojcikiewicz & Nahorski, 1991; Shreve *et al.*, 1991). Whether rapid desensitization exists for G_i-coupled receptors and how it may occur is largely unknown. This may be due in part, to the fact that the classical signalling pathway of G_i-coupled receptors, inhibition of adenylate cyclase, is difficult to study at early time points.

We have recently demonstrated that G_i-coupled receptors such as the α_{2A}-adrenoceptor and the Y_1-like neuropeptide Y (NPY) receptor in HEL-cells can, in addition to inhibition of adenylate cyclase, also couple to mobilization of Ca^{2+} from intracellular stores (Motulsky & Michel, 1988; Michel *et al.*, 1989). Similar Ca^{2+} elevations have been shown in SK-N-MC neuroblastoma cells (Aakerlund *et al.*, 1990; Feth *et al.*, 1991), cultured neurones (Ewald *et al.*, 1988; Perney & Miller, 1989), pituitary cells (Shangold & Miller, 1990; Crowley *et al.*, 1990) and smooth muscle cells (Mihara *et al.*, 1989; Erdbrügger *et al.*, 1993). These Ca^{2+} elevations occur in less than 1 min, are mediated by a G_i-protein, and do not involve a Na^+/H^+-antiporter or cyclo-oxygenase or lipoxygenase products of arachidonic acid (Motulsky & Michel, 1988; Michel *et al.*, 1989). Our previous data suggest that inositol phosphates are not involved (Motulsky & Michel, 1988; Michel *et al.*, 1989) but this is controversial (Daniels *et al.*, 1989). The α_{2A}-adrenoceptor and NPY-receptor-stimulated Ca^{2+} mobilization in HEL-cells and other cell types is only transient and usually lasts less than 3 min. Therefore, this may be a suitable model to investigate the existence of rapid desensitization of G_i-coupled receptor function and its possible mechanisms.

Methods

Cell culture

HEL-cells were originally obtained from Dr Papayannopoulou (Dept. Medicine, University of Washington, Seattle, WA, U.S.A.) and maintained in the chemically defined CG medium (Camon, Wiesbaden, Germany) in an atmosphere of

[1] Author for correspondence: Nephrol. Lab. IG1, Klinikum, Hufelandstr. 55, D-45122 Essen, Germany.

95% air/5% CO_2 at 37°C at a density of 4–6 × 10^5 cells ml^{-1} by daily dilution with fresh medium. In some experiments phorbol-myristate-acetate, herbimycin or dimethylsulphoxide were added to the culture medium in the indicated concentrations for the indicated times.

Ca^{2+} measurements

The free intracellular Ca^{2+} concentration was determined with the fluorescent inhibitor dye, fura-2, in a Hitachi F2000 spectrofluorometer as previously described (Feth *et al.*, 1992). Briefly, experiments were performed in buffer of the following composition (mM): HEPES 20, NaCl 120, KH_2PO_4 5, Mg acetate 1, $CaCl_2$ 1 and glucose 1 mg ml^{-1} at pH 7.4 using approximately 6–8 × 10^5 cells ml^{-1}. After 1 h of loading with the dye the cells were washed twice, resuspended in fresh buffer and used for fluorescence measurements within the next hour. Excitation was alternating at 340 and 380 nm with emission being read at 510 nm. Unless otherwise indicated, fluorescence data were converted into Ca^{2+} concentrations with software supplied by the manufacturer.

In some experiments a single-wavelength method with excitation at 340 nm only was used as previously described (Motulsky & Michel, 1988). In this case fluorescence data were converted into Ca^{2+} concentrations with the formula

$$[Ca^{2+}] = K \times (F - F_{min})/(F_{max} - F)$$

In this formula, K is the affinity of fura-2 for Ca^{2+} ions, 224 nM, F is the fluorescence of the intracellular fura-2, F_{max} is its fluorescence when saturated with Ca^{2+}, and F_{min} is its fluorescence in the absence of Ca^{2+}.

Unless otherwise indicated compounds were added to the cell suspension 30–60 s before the receptor agonists. In the thapsigargin experiments receptor agonists were added when the thapsigargin effects on intracellular Ca^{2+} had reach a plateau, i.e. after 3–5 min. In some experiments, extracellular Ca^{2+} was chelated by addition of 5 mM EGTA 30–60 s before the other agents. Dimethylsulphoxide and herbimycin were added to the culture medium 4 days and 1 day respectively before the experiment. All drugs were added to the assay from stock solutions which were concentrated 100 fold in order to minimize dilution of the cell suspension. Whenever solvent concentrations reached (dimethylsulphoxide and methanol) or exceeded (other solvents) 0.1% in the final assay, samples were compared to vehicle-treated controls. All experiments were performed at room temperature to minimize dye leakage from the cells.

Chemicals

Fura-2 AM (obtained from Molecular Probes, Eugene, OR, U.S.A.) was dissolved at 1 mM in dimethylsulphoxide and used at 1 μM to load the cells. Adrenaline (obtained from Sigma, Munich, Germany) and NPY (obtained from Saxon Biochemicals, Hannover, Germany) were dissolved (at 10 and 1 mM, respectively) and further diluted in 10 mM HCl. Adrenaline was dissolved fresh daily whereas NPY solutions were stored at 4°C for up to three months; no decline in NPY activity could be observed during this period as assessed by its EC_{50} to mobilize Ca^{2+} in HEL-cells. Thapsigargin (obtained from Calbiochem, La Jolla, CA, U.S.A.) was dissolved to 10 mM with dimethylsulphoxide, diluted to 1 mM with ethanol and then further diluted in 10 mM HCl. Herbimycin (from Gibco, Eggenstein, Germany) was dissolved at 1.75 mM in dimethylsulphoxide and diluted with cell culture medium. Ryanodine (obtained from Research Biochemicals Inc., Natick, MA, U.S.A.) was dissolved at 10 mM with methanol and diluted with buffer. The phorbol ester, phorbol-12-myristate-13-acetate (obtained from Calbiochem), was dissolved at 1 mM in dimethylsulphoxide and further diluted in water. H8 (N-[2-(methylamino)-ethyl]-5-isoquinolinesulphonamide dihydrochloride; obtained from Research Biochemicals Inc.) was dissolved at 10 mM in dilute HCl. Staurosporine (obtained from Sigma) and calphostin C (obtained from Calbiochem) were dissolved at 10 mM in dimethylsulphoxide and further diluted in water.

Data elevation

Data are given as mean ± s.e.mean of n experiments. The statistical significance of differences between control and treated cells determined in paired two-tailed t tests using the InStat programme (GraphPAD Software, San Diego, CA, U.S.A.).

Results

Nearly maximally effective concentrations of adrenaline and NPY (1 μM and 100 nM, respectively) increased intracellular free Ca^{2+} in HEL-cells with NPY responses being approximately 2.5 times those of adrenaline (192 ± 8 nM vs 73 ± 10 nM peak Ca^{2+} increase; $n = 11$; Figure 1). The agonist-stimulated Ca^{2+} increases were only transient; they peaked within 20–40 s and thereafter declined, reaching values close to baseline within 2–3 min (Figure 1). A second addition of a receptor agonist 3 min after the first exposure elicited responses of only 26 ± 7% (adrenaline) or 3 ± 1% (NPY) of the first ($n = 11$; Figure 1, Table 1). This desensitized state towards adrenaline and NPY was maintained for at least 30 min following washout of the agonists.

Since adrenaline and NPY appear to use similar mechanisms to increase Ca^{2+} in HEL-cells (Motulsky & Michel, 1988; Michel *et al.*, 1989), we determined whether desensitization of the response to one hormone also desensitizes the response to the other: 30 s after the second dose of adrenaline a dose of NPY was administered and in other cuvettes 30 s after the second dose of NPY a dose of adrenaline was given. Following two additions of adrenaline the subsequent response to NPY was not significantly altered (Figure 1, Table 1); following two additions of NPY the subsequent response to adrenaline, however, was considerably reduced (Figure 1, Table 1). Thus, adrenaline and NPY preferentially desensitize the responsiveness of their own receptors but the more efficacious Ca^{2+} mobilizer, NPY, can also partially (≈80%) desensitize the adrenaline response.

The phenylethylamine agonist, adrenaline (1 μM), and the

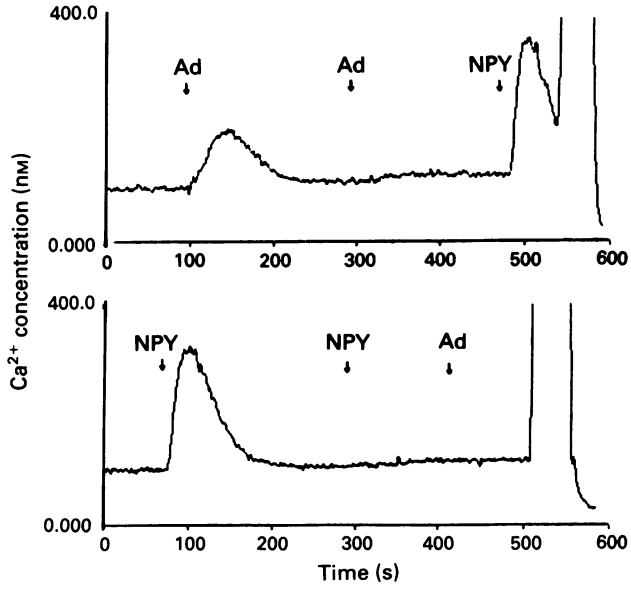

Figure 1 Representative traces showing Ca^{2+} mobilization by adrenaline (Ad, 1 μM) and neuropeptide Y (NPY, 100 nM) in HEL cells. Also shown is the cross desensitization of the agonists.

imidazoline agonist, moxonidine (100 μM), yielded quantitatively similar homologous desensitization of the α_{2A}-adrenoceptor-mediated response (Table 1). In cross-desensitization experiments adrenaline and moxonidine desensitized responses to each other to the same extent as their own responses (Table 1).

A 4-day treatment with 1.25% dimethylsulphoxide in the culture medium did not significantly alter basal intracellular Ca^{2+} levels (72 ± 4 nM in control vs. 64 ± 2 nM in treated cells, $n = 11$, $P > 0.05$) but attenuated adrenaline- and NPY-stimulated peak Ca^{2+} increases by 30% ($n = 5$, $P = 0.0226$) and 54% ($n = 6$, $P < 0.0001$; Table 2), respectively; the time course of the Ca^{2+} elevations, however, was not appreciably altered.

Addition of the protein kinase C activator, phorbol-12-myristate-13-acetate, 30 s before adrenaline or NPY, concentration-dependently inhibited Ca^{2+} mobilization; threshold inhibition occured at 10 nM phorbol ester, and 100 nM inhibited the effects of adrenaline and NPY by 75 ± 3% and 60 ± 5%, respectively (Figure 2, Table 2).

Among the three protein kinase C inhibitors tested (100 μM H8, 1 μM staurosporine, 1 μM calphostin C) only staurosporine significantly enhanced the Ca^{2+} response to adrenaline and only staurosporine and calphostin C enhanced the response to NPY (Table 2); the duration of the Ca^{2+} increases was not consistently prolonged by any protein kinase C inhibitor and lower staurosporine concentrations did not significantly alter peak receptor agonist-stimulated Ca^{2+} increases.

Cells were also treated with 100 nM phorbol-12-myristate-13-acetate overnight in order to down-regulate the cellular protein kinase C. Phorbol ester treatment desensitized stimulated Ca^{2+} elevations (13 ± 4 vs. 61 ± 7 nM for adrenaline and 14 ± 4 vs. 124 ± 17 nM for NPY in treated and control cells, respectively; $n = 3$ each, $P < 0.05$ vs. vehicle-treated cells).

In HEL-cells treated for 24 h with 1 μM of the irreversible tyrosine kinase inhibitor, herbimycin (June *et al.*, 1990), both adrenaline and NPY caused greater peak Ca^{2+} increases than in vehicle-treated cells (Table 2).

Okadaic acid (1 μM), a protein phosphatase inhibitor (Mattingly & Garrison, 1992), by itself induced a minor elevation of intracellular Ca^{2+} (15 ± 1 nM, $n = 8$) but this was not different from that induced by vehicle (1% ethanol, 14 ± 1 nM, $n = 8$). The Ca^{2+} elevations in response to adrenaline and NPY, however, were not affected by addition of okadaic acid 1 min before the hormones (Table 2).

Addition of 30 mM KCl did not affect the basal intracellular Ca^{2+} concentration but reduced adrenaline- and NPY-stimulated Ca^{2+} increases by 68 ± 3% and 30 ± 4%, respec-

Table 1 Cross-desensitization of Ca^{2+} mobilization by neuropeptide Y (NPY), adrenaline and moxonidine in HEL cells

First agonist	*Second agonist*	*% desensitization*
NPY	NPY	97 ± 1
NPY	adrenaline	82 ± 4
Adrenaline	NPY	2 ± 6
Adrenaline	adrenaline	74 ± 7
Adrenaline	moxonidine	81 ± 9
Moxonidine	adrenaline	82 ± 3
Moxonidine	moxonidine	78 ± 5

The ability of a first agonist (1 μM adrenaline, 100 μM moxonidine or 100 nM NPY) to desensitize responses to a second agonist was tested. When intracellular Ca^{2+} had returned to baseline (usually within 3–5 min) after addition of an agonist, a second agonist was added. Desensitization of the response to the second agonist was determined as % reduction in its response when compared to its response in control cells. Data are mean ± s.e.mean of 7–11 experiments. A representative tracing of such experiments is shown in Figure 1.

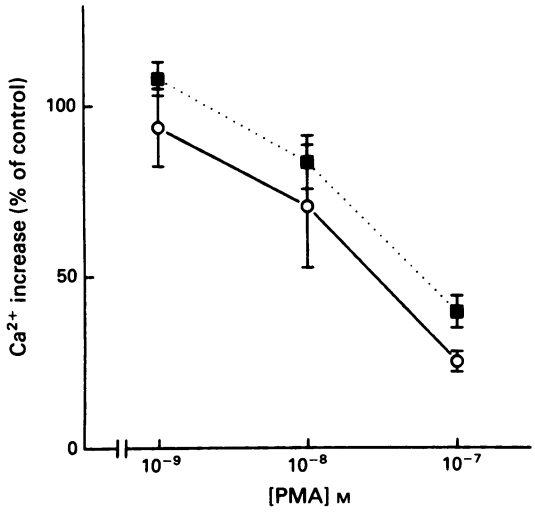

Figure 2 Effect of phorbol-12-myristate-13-acetate (PMA) added 30 s before adrenaline (1 μM, ○) or neuropeptide Y (NPY, 100 nM, ■) on the agonist-stimulated peak Ca^{2+} increases, expressed as % of those obtained in matched cuvettes in the absence of PMA. Control Ca^{2+} increases were 40 ± 6 and 156 ± 9 nM for adrenaline and NPY, respectively. Data are the mean ± s.e.mean of 4–5 experiments.

Table 2 Effects of various compounds on adrenaline- and neuropeptide Y (NPY)-stimulated Ca^{2+} mobilization in HEL-cells

	Adrenaline (1 μM) response in % of control		*NPY* (100 nM) response in % of control	
KCl (30 mM)	32 ± 3*	(3)	70 ± 4*	(4)
NaCl (30 mM)	32 ± 3*	(3)	67 ± 5*	(5)
Thapsigargin (50 nM)	155 ± 18*	(7)	288 ± 68*	(10)
Ryanodine (10 μM)	142 ± 10*	(12)	120 ± 6*	(11)
DMSO treatment (1.25%, 4 days)	70 ± 4*	(5)	46 ± 4*	(6)
Phorbol ester (100 nM)	24 ± 3*	(5)	40 ± 5*	(4)
H8 (100 μM)	106 ± 22	(5)	84 ± 10	(6)
Staurosporine (1 μM)	142 ± 15*	(6)	122 ± 8*	(6)
Calphostin C (1 μM)	110 ± 9	(5)	124 ± 7*	(6)
Herbimycin (1 μM, 24 h)	188 ± 35*	(7)	138 ± 5*	(8)
Okadaic acid (1 μM)	104 ± 13	(4)	99 ± 3	(4)

All compounds were added 30–60 s before adrenaline or NPY except for dimethylsulphoxide (DMSO) and herbimycin which were added to the culture medium 4 days and 1 day beforehand, respectively, and washed out prior to the Ca^{2+} measurements. Phorbol-12-myristate-13-acetate was the phorbol ester. Data are mean ± s.e.mean of the number of experiments indicated in parentheses. Data are expressed as % of the Ca^{2+} increase observed in paired vehicle-controlled cells. *$P < 0.05$.

Table 3 Ca^{2+} elevations caused by thapsigargin, adrenaline, neuropeptide Y (NPY) and their combinations in the presence and absence of extracellular Ca^{2+}

	$[Ca^{2+}]$ 1 mM	$[Ca^{2+}]$ 0 mM (5 mM EGTA added)
Thapsigargin (50 nM)	564 ± 46	425 ± 32
Adrenaline (1 μM)	56 ± 10	119 ± 17
Adrenaline following thapsigargin	140 ± 25*	25 ± 33*
NPY (100 nM)	145 ± 25	353 ± 79
NPY following thapsigargin	323 ± 55*	154 ± 43*

Ca^{2+} increases were determined by a single-wave-length method in standard buffer containing 1 mM Ca^{2+} or following chelation of extracellular Ca^{2+} by addition of 5 mM EGTA 30 s before the addition of thapsigargin adrenaline or NPY. Data are mean ± s.e.mean of 7 experiments (15–17 for effects of thapsigargin alone), and Ca^{2+} increases are expressed in nM. *$P<0.05$ vs results obtained in the absence of thapsigargin.

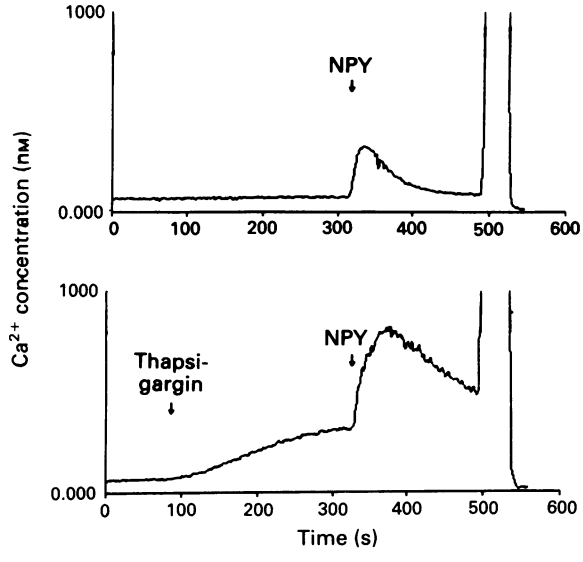

Figure 3 Representative effects of 50 nM thapsigargin on neuropeptide Y (NPY)-stimulated Ca^{2+} mobilization in HEL cells. NPY-stimulated Ca^{2+} elevations were 186 ± 11 nM in the absence, and 287 ± 26 nM in the presence, of thapsigargin ($n = 7$; $P<0.05$).

tively. Similar data were obtained with addition of 30 mM NaCl (Table 2).

In standard buffer containing 1 mM Ca^{2+} and using the double-wavelength method, 50 nM thapsigargin increased intracellular Ca^{2+} from 77 ± 2 to 405 ± 39 nM (mean increase 328 ± 38 nM, $n = 19$). Despite the already elevated cytoplasmic Ca^{2+} concentration, adrenaline and NPY further increased intracellular Ca^{2+} and these increases significantly exceeded those in the absence of thapsigargin (Figure 3, Table 2). Similar data were obtained in the presence of extracellular Ca^{2+} by the single-wavelength method (Table 3). In Ca^{2+}-free buffer, 50 nM thapsigargin elicited slightly smaller Ca^{2+} elevations than were seen in Ca^{2+}-containing buffer (Table 3) as determined by the single-wavelength method. The subsequent Ca^{2+} responses to adrenaline and NPY in Ca^{2+}-free buffer were significantly reduced in the presence of thapsigargin (Table 3).

Ryanodine, an inositol phosphate-independent modulator of Ca^{2+} release, did not alter the basal intracellular Ca^{2+} concentration. Ryanodine enhanced adrenaline-stimulated peak Ca^{2+} increases from 65 ± 6 to 89 ± 8 nM ($n = 12$, $P = 0.0008$, Table 2) and NPY-stimulated Ca^{2+} increases from 215 ± 18 to 253 ± 17 nM ($n = 11$, $P<0.0060$, Table 2).

Discussion

The mechanisms involved in the desensitization of G_s-coupled receptors, for example the β_2-adrenoceptor, have been extensively characterized (Lefkowitz *et al.*, 1990; Lorenz *et al.*, 1991). It is now clear that β_2-adrenoceptor desensitization involves rapid (uncoupling and sequestration for example) and slower components (down-regulation for example) which are mediated at least partly by protein kinases such as adenosine 3':5'-cyclic monophosphate (cyclic AMP)-dependent protein kinase or β-adrenoceptor kinase, which specifically recognizes the agonist-occupied form of the receptor. In contrast, little is known of the regulation of G_i-coupled receptors. Previous studies have demonstrated that prolonged agonist exposure may down-regulate some G_i-coupled receptors such as A_1 adenosine (Green *et al.*, 1990) and muscarinic receptors (Wojcikiewicz & Nahorski, 1991) or α_2-adrenoceptors (Shreve *et al.*, 1991). Whether rapid desensitization of G_i-coupled receptor function also exists is unclear, and for NPY receptor function neither rapid nor slow desensitization has been studied.

Since an inhibitory response, inhibition of adenylate cyclase, is difficult to study at early time points, we have used a stimulatory response, elevation of intracellular Ca^{2+}, to investigate the existence and possible underlying mechanisms of rapid desensitization of G_i-coupled receptors. In HEL-cells, adrenaline and NPY increase intracellular Ca^{2+} via α_{2A}-adrenoceptors and Y_1-like receptors, respectively, and both responses are G_i-coupled (Motulsky & Michel, 1988; Michel *et al.*, 1989). Adrenaline- and NPY-stimulated Ca^{2+} elevations are only transient and return towards baseline within a few minutes. Our data show that the rapid decline of intracellular Ca^{2+} concentration in the continued presence of agonist is caused by desensitization rather than by removal or inactivation of the agonist since the HEL-cells remained unresponsive to a second dose of agonist. Thus, rapid desensitization exists for α_2-adrenergic and NPY receptor-mediated Ca^{2+} elevations in HEL-cells.

Desensitization of receptor responsiveness can occur at multiple levels including receptors, G-proteins and effector enzymes. Our cross-desensitization experiments with adrenaline and NPY demonstrate that adrenaline induced only homologous desensitization whereas NPY also caused considerable heterologous desensitization of the adrenaline response. This may be related to the fact that NPY is a considerably more effective agonist which may in turn be related to the fact that HEL-cells have only approximately 6,000 α_2-adrenoceptors (McKernan *et al.*, 1987) but more than 40,000 NPY receptors per cell (Feth *et al.*, 1992). Homologous desensitization of the α_2-adrenoceptor response is not specific for phenylethylamine or imidazoline agonists since adrenaline and moxonidine desensitized each others responses to the same extent as their own. Thus, the previously reported imidazoline-specific mechanisms of α_2-adrenoceptor desensitization in vascular smooth muscle

(Ruffolo *et al.*, 1977) are not involved in the desensitization mechanism in HEL-cells.

Differentiation with dimethylsulphoxide activates protein kinase C in murine erythroleukaemia cells (Chakraverthy *et al.*, 1992) and accelerates the desensitization rate of G_s-coupled prostaglandin E receptors in human erythroleukaemia cells (HEL-cells; Ashby *et al.*, 1991). This differentiation also lowered peak adrenaline- or NPY-stimulated Ca^{2+} elevations, which is compatible with the idea of enhanced desensitization rates for these G_i-mediated responses. HEL-cells contain the β- and δ-forms of protein kinase C, and activation of the enzymes can desensitize Ca^{2+} mobilization by other receptors in these cells (Grabarek *et al.*, 1992; Brass, 1992). Our data show that phorbol ester rapidly desensitizes adrenaline- and NPY-stimulated Ca^{2+} elevations. Desensitization of NPY-stimulated Ca^{2+} elevations by phorbol ester has also been demonstrated by other investigators, who additionally found that it can be prevented by specific protein kinase C inhibitors (Daniels *et al.*, 1992) indicating that it is mediated by protein kinase C. The structural basis for this desensitzation may be the presence of protein kinase C phosphorylation sites in the cytoplasmic domains of α_{2A}-adrenoceptors (Kobilka *et al.*, 1987) and Y_1-like NPY receptors (Krause *et al.*, 1992). It is also possible that phorbol ester exposure stimulates Ca^{2+} uptake into the endoplasmic reticulum, since it has recently been shown that phorbol ester enhances and that the protein kinase C inhibitor, calphostin C, reduces the V_{max} of this Ca^{2+} removal mechanism in human platelets (Tao *et al.*, 1992).

The desensitization of adrenaline- and NPY-stimulated Ca^{2+} elevations by phorbol ester, however, does not necessarily imply that protein kinase C activation is important in the rapid desensitization of agonist-stimulated Ca^{2+} mobilization. The protein kinase C inhibitors staurosporine, H8 and calphostin C yielded contradictory results and none of them completely prevented desensitization. The protein kinase C inhibitor, H7, also failed to prevent desensitization of NPY-stimulated Ca^{2+} mobilization in HEL-cells, although it effectively prevents the desensitization caused by phorbol ester (Daniels *et al.*, 1992). Together these data indicate that activation of protein kinase C is unlikely to play a major role in the rapid desensitization of adrenaline- or NPY-stimulated Ca^{2+} mobilization.

The human Y_1-like NPY receptor contains a consensus site for tyrosine phosphorylation in its cytoplasmic domain (Larhammar *et al.*, 1992). Our data demonstrate that the specific tyrosine kinase inhibitor, herbimycin, enhanced adrenaline- and NPY-stimulated Ca^{2+} mobilization, and thus are consistent with the idea that a tyrosine kinase may participate in the rapid desensitization of Ca^{2+} mobilization. However, these data are not easy to interpret on a molecular level since a 24 h incubation with herbimycin was necessary to achieve this effect, and because the substrate of tyrosine kinase activity may also be G-protein α-subunits which can undergo tyrosine phosphorylation (Hausdorff *et al.*, 1992). The overall role of phosphorylation events in the rapid desensitization of adrenaline- or NPY-stimulated Ca^{2+} mobilization remains unclear since the protein phosphatase inhibitor, okadaic acid, had no detectable effects, although similar okadaic acid treatment enhances desensitization of thrombin-stimulated Ca^{2+} elevations in HEL-cells (Brass, 1992).

The simultaneous presence of homologous and heterologous desensitization suggests that alterations downstream of the receptors may also be involved. Candidates for this would be the Ca^{2+} release and sequestration mechanisms. In some cells depolarization impairs the responses to Ca^{2+} elevating agonists (Randriamampita *et al.*, 1991). In HEL-cells, depolarization by addition of a high potassium concentration impaired Ca^{2+} responses to adrenaline and NPY, but addition of an equal concentration of sodium had the same effect. Thus, osmolarity rather than depolarization or membrane potential appears to be involved in this attenuation.

Intracellular Ca^{2+} stores can be depleted when the inhibitor of the endoplasmic reticulum Ca^{2+}-ATPase, thapsigargin, is applied to cells in Ca^{2+}-free buffer (Thastrup *et al.*, 1990) and treatment with this agent attenuated adrenaline- and NPY-stimulated Ca^{2+} mobilization. Qualitatively similar data for NPY-stimulated Ca^{2+} increases in HEL- and SK-N-MC-cells have been described (Aakerlund *et al.*, 1990; Daniels *et al.*, 1992). In the endoplasmic reticulum thapsigargin acts on both inositol phosphate-sensitive and -insensitive compartments (Thastrup *et al.*, 1990; Lytton *et al.*, 1991) and adrenaline and NPY mediate Ca^{2+} mobilization independently of inositol phosphates (Motulsky & Michel, 1988; Michel *et al.*, 1989). A modulator of inositol phosphate-insensitive Ca^{2+} release, ryanodine (Sorrentino & Vople, 1993), enhanced adrenaline- and NPY-stimulated Ca^{2+} mobilization. Together these data suggest that depletion of intracellular Ca^{2+} pools may desensitize adrenaline- and NPY-stimulated Ca^{2+} mobilization. However, we consider it unlikely that this plays a role in the rapid desensitization following agonst addition because it is seen in Ca^{2+}-free and in Ca^{2+}-containing buffer, whereas depletion of the store apparently occurs only in Ca^{2+}-free buffer.

Our results demonstrate that adrenaline- and NPY-stimulated Ca^{2+} elevations rapidly desensitize in HEL-cells. This involves homologous and heterologous components. Ca^{2+} increases by both agonists are enhanced by the endoplasmic reticulum Ca^{2+}-ATPase inhibitor, thapsigargin, in the presence of extracellular Ca^{2+}, by the inositol phosphate-independent Ca^{2+} release modulator, ryanodine, and by the tyrosine kinase inhibitor, herbimycin. They can be attenuated by increased osmolarity, Ca^{2+} store depletion, and a protein kinase C activating phorbol ester. Whether protein kinase C activation plays an important role in the rapid desensitization following agonist exposure remains unclear since protein kinase C inhibitors had inconsistent effects.

This work was supported by the Deutsche Forschungsgemeinschaft.

References

AAKERLUND, L., GETHER, U., FUHLENDORFF, J., SCHWARTZ, T.W. & THASTRUP, O. (1990). Y_1 receptors for neuropeptide Y are coupled to mobilization of intracellular calcium and inhibition of adenylate cyclase. *FEBS Lett.*, **260**, 73–78.

ASHBY, B., ALMONOR, G.O., WERNICK, E. & SELAK, M.A. (1991). Prostaglandin-concentration-dependent desensitization of adenylate cyclase in human erythroleukemia (HEL) cells is abolished by pertussis toxin and enhanced by induction by dimethyl sulphoxide. *Biochem. J.*, **280**, 801–804.

BRASS, L.F. (1992). Homologous desensitization of HEL cell thrombin receptors. Distinguishable roles for proteolysis and phosphorylation. *J. Biol. Chem.*, **267**, 6044–6050.

CHAKRAVERTHY, B.R., TREMBLAY, R., MACDONALD, P., KRSMANOVIC, V., WHITFIELD, J.F. & DURKIN, J.P. (1992). The activation of inactive membrane-associated protein kinase C is associated with DMSO-induced erythroleukemia cell differentiation. *Biochem. Biophys. Acta.*, **1136**, 83–90.

CROWLEY, W.R., SHAH, G.V., CARROLL, B.L., KENNEDY, D., DOCKTER, M.E. & KALRA, S.P. (1990). Neuropeptide-Y enhances luteinizing hormone (LH)-releasing hormone-induced LH release and elevations in cytosolic Ca^{2+} in rat anterior pituitary cells: evidence for involvement of extracellular Ca^{2+} influx through voltage-sensitive channels. *Endocrinol.*, **127**, 1487–1494.

DANIELS, A.J., LAZAROWSKI, E.R, MATTHEWS, J.E. & LAPETINA, E.G. (1989). Neuropeptide Y mobilizes intracellular Ca^{2+} and increases inositol phosphate production in human erythroleukemia cells. *Biochem. Biophys. Res. Commun.*, **165**, 1138–1144.

DANIELS, A.J., MATTHEWS, J.E., VIVEROS, O.H. & LAZAROWSKI, E.R. (1992). Characterization of the neuropeptide Y-induced intracellular calcium release in human erythroleukemia cells. *Mol. Pharmacol.*, **41**, 767–771.

ERDBRÜGGER, W., VISCHER, P., BAUCH, H.-J. & MICHEL, M.C. (1993). Norepinephrine and neuropeptide Y increase intracellular Ca^{2+} in cultured porcine aortic smooth muscle cells. *J. Cardiovasc. Pharmacol.*, **22**, 97–102.

EWALD, D.A., STERNWEIS, P.C. & MILLER, R.J. (1988). Guanine nucleotide-binding protein G_o-induced coupling of neuropeptide Y receptors to Ca^{2+} channels in sensory neurons. *Proc. Natl. Acad. Sci. U.S.A.*, **85**, 3633–3637.

FETH, F., RASCHER, W. & MICHEL, M.C. (1991). G-Protein coupling and signalling of Y_1-like neuropeptide Y receptors in SK-N-MC cells. *Naunyn-Schmied. Arch. Pharmacol.*, **344**, 1–7.

FETH, F., RASCHER, W. & MICHEL, M.C. (1992). Neuropeptide Y (NPY) receptors in HEL cells: comparison of binding and functional parameters for full and partial agonists and a non-peptide antagonist. *Br. J. Pharmacol.*, **105**, 71–76.

GRABAREK, J., RAYCHOWDHURY, M., RAVID, K., KENT, K.C., NEWMAN, P.J. & WARE, J.A. (1992). Identification and functional characterization of protein kinase C isozymes in platelets and HEL cells. *J. Biol. Chem.*, **267**, 10011–10017.

GREEN, A., JOHNSON, J.L. & MILLIGAN, G. (1990). Down-regulation of G_i sub-types by prolonged incubation of adipocytes with an A_1 adenosine receptor agonist. *J. Biol. Chem.*, **265**, 5206–5210.

HAUSDORFF, W.P., PITCHER, J.A., LUTTRELL, D.K., LINDER, M.E., KUROSE, H., PARSONS, S.J., CARON, M.G. & LEFKOWITZ, R.J. (1992). Tyrosine phosphorylation of G protein α subunits by $pp60^{c\text{-}src}$. *Proc. Natl. Acad. Sci. U.S.A.*, **89**, 5720–5724.

JUNE, C.H., FLETCHER, M.C., LEDBETTER, J.A., SCHIEVEN, G.L., SIEGEL, J.N., PHILLIPS, A.F. & SAMELSON, L.E. (1990). Inhibition of tyrosine phosphorylation prevents T-cell receptor-mediated signal transduction. *Proc. Natl. Acad. Sci. U.S.A.*, **87**, 7722–7726.

KOBILKA, B.K., MATSUI, H., KOBILKA, T.S., YANG-FENG, T.L., FRANCKE, U., CARON, M.G., LEFKOWITZ, R.J. & REGAN, J.W. (1987). Cloning, sequencing, and expression of the gene coding for the human platelet α_2-adrenergic receptor. *Science*, **238**, 650–656.

KRAUSE, J., EVA, C., SEEBURG, P.H. & SPRENGEL, R. (1992). Neuropeptide Y_1 subtype pharmacology of a recombinantly expressed neuropeptide receptor. *Mol. Pharmacol.*, **41**, 817-821.

LARHAMMAR, D., BLOMQVIST, A.G., YEE, F., JAZIN, E., YOO, H. & WAHLESTEDT, C. (1992). Cloning and functional expression of a human neuropeptide Y/peptide YY receptor of the Y1 type. *J. Biol. Chem.*, **267**, 10935–10938.

LEFKOWITZ, R.J., HAUSDORFF, W.P. & CARON, M.G. (1990). Role of phosphorylation in desensitization of the β-adrenoceptor. *Trends Pharmacol. Sci.*, **11**, 190–194.

LORENZ, W., INGLESE, J., PALCZEWSKI, K., ONORATO, J.J., CARON, M.G. & LEFKOWITZ, R.J. (1991). The receptor kinase family: primary structure of rhodopsin kinase reveals similarities to the β-adrenergic receptor kinase. *Proc. Natl. Acad. Sci. U.S.A.*, **88**, 8715–8719.

LYTTON, J., WESTLIN, M. & HANLEY, M.R. (1991). Thapsigargin inhibits the sarcoplasmic or endoplasmic reticulum Ca-ATPase family of calcium pumps. *J. Biol. Chem.*, **266**, 17067–17071.

MATTINGLY, R.R. & GARRISON, J.C. (1992). Okadaic acid inhibits angiotension II stimulation of $Ins(1,4,5)P_3$ and calcium signalling in rat hepatocytes. *FEBS Lett.*, **296**, 225–230.

MCKERNAN, R.M., HOWARD, M.J., MOTULSKY, H.J. & INSEL, P.A. (1987). Compartmentation of α_2-adrenergic receptors in human erythroleukemia (HEL) cells. *Mol. Pharmacol.*, **32**, 258–265.

MICHEL, M.C., BRASS, L.F., WILLIAMS, A., BOKOCH, G.M., LAMORTE, V.J. & MOTULSKY, H.J. (1989). α_2-Adrenergic receptor stimulation mobilizes intracellular Ca^{2+} in human erythroleukemia cells. *J. Biol. Chem.*, **264**, 4986–4991.

MIHARA, S.-I., SHIGERI, Y. & FUJIMOTO, M. (1989). Neuropeptide Y-induced intracellular Ca^{2+} increases in vascular smooth muscle. *FEBS Lett.*, **259**, 79–82.

MOTULSKY, H.J. & MICHEL, M.C. (1988). Neuropeptide Y mobilizes Ca^{++} and inhibits adenylate cyclase in human erythroleukemia cells. *Am. J. Physiol.*, **255**, E880–E885.

PERNEY, T.M. & MILLER, R.J. (1989). Two different G-proteins mediate neuropeptide Y and bradykinin-stimulated phospholipid breakdown in cultured rat sensory neurons. *J. Biol. Chem.*, **264**, 7317–7327.

RANDRIAMAMPITA, C., BISMUTH, G., DEBRE, P. & TRAUTMANN, A. (1991). Nitrendipine-induced inhibition of calcium influx in a human T-cell clone: role of cell depolarization. *Cell Calcium*, **12**, 313–323.

RUFFOLO, R.R. Jr., TUROWSKI, B.S. & PATIL, P.N. (1977). Lack of cross-desensitization between structurally dissimilar α-adrenoceptor agonists. *J. Pharm. Pharmacol.*, **29**, 378–380.

SHANGOLD, G.A. & MILLER, R.J. (1990). Direct neuropeptide Y-induced modulation of gonadotrope intracellular calcium transients and gonadotropin secretion. *Endocrinol.*, **126**, 2336–2342.

SHREVE, P.E., TOEWS, M.L. & BYLUND, D.B. (1991). α_{2A}- and α_{2C}-adrenoceptor subtypes are differentially down-regulated by norepinephrine. *Eur. J. Pharmacol.*, **207**, 275–276.

SORRENTINO, V. & VOPLE, P. (1993). Ryanodine receptors: how many, where and why? *Trends Pharmacol. Sci.*, **14**, 98–103.

TAO, J., JOHANSSON, J.S. & HAYNES, D.H. (1992). Protein kinase C stimulates dense tubular Ca^{2+} uptake in the intact human platelet by increasing the V_m of the Ca^{2+}-ATPase pump: stimulation by phorbol ester, inhibition by calphostin C. *Biochem. Biophys. Acta*, **1107**, 213–222.

THASTRUP, O., CULLEN, P.J., DROBAK, B.K., HANLEY, M.R. & DAWSON, A.P. (1990). Thapsigargin, a tumor promoter, discharges intracellular Ca^{2+} stores by specific inhibition of the endoplasmic reticulum Ca^{2+}-ATPase. *Proc. Natl. Acad. Sci. U.S.A.*, **87**, 2466–2470.

WOJCIKIEWICZ, R.J.H. & NAHORSKI, S.R. (1991). Chronic muscarinic stimulation of SH-SY5Y neuroblastoma cells suppresses inositol 1,4,5-trisphosphate action. Parallel inhibition of inositol 1,4,5-trisphosphate induced Ca^{2+} mobilization and inositol 1,4,5-trisphosphate binding. *J. Biol. Chem.*, **266**, 22234–22241.

(Received June 21, 1993
Revised December 6, 1993
Accepted February 16, 1994)

Br. J. Pharmacol. (1994), **112**, 505–514

Binding and functional properties of hexocyclium and sila-hexocyclium derivatives to muscarinic receptor subtypes

[1]M. Waelbroeck, J. Camus, M. Tastenoy, *[2]R. Feifel, *E. Mutschler, †R. Tacke, †C. Strohmann, †K. Rafeiner, ‡J.F. Rodrigues de Miranda & *G. Lambrecht

Department of Biochemistry and Nutrition, Medical School, Université Libre de Bruxelles, Building G/E, CP 611, Route de Lennik 808, B-1070 Brussels, Belgium; *Department of Pharmacology, Biocentre Niederursel, University of Frankfurt, Marie-Curie-Strasse 9, Geb.N 260, D-60439 Frankfurt/M, Germany; †Institute of Inorganic Chemistry, University of Karlsruhe, Engesserstraße, Geb. 30.45, D-76128 Karlsruhe, Germany and ‡Department of Pharmacology, University of Nijmegen, P.O. Box 9101, NL-6500 HB Nijmegen, The Netherlands

1 We have compared the binding properties of several hexocyclium and sila-hexocyclium derivatives to muscarinic M_1 receptors (in rat brain, human neuroblastoma (NB-OK 1) cells and calf superior cervical ganglia), rat heart M_2 receptors, rat pancreas M_3 receptors and M_4 receptors in rat striatum, with their functional antimuscarinic properties in rabbit vas deferens (M_1/M_4-like), guinea-pig atria (M_2), and guinea-pig ileum (M_3) muscarinic receptors.

2 Sila-substitution (C/Si exchange) of hexocyclium (→ sila-hexocyclium) and demethyl-hexocyclium (→ demethyl-sila-hexocyclium) did not significantly affect their affinities for muscarinic receptors. By contrast, sila-substitution of *o*-methoxy-hexocyclium increased its affinity 2 to 3 fold for all the muscarinic receptor subtypes studied.

3 The *p*-fluoro- and *p*-chloro-derivatives of sila-hexocyclium had lower affinities than the parent compound at the four receptor subtypes, in binding and pharmacological studies.

4 In binding studies, *o*-methoxy-sila-hexocyclium ($M_1 = M_4 \geqslant M_3 \geqslant M_2$) had a much lower affinity than sila-hexocyclium for the four receptor subtypes, and discriminated the receptor subtypes more poorly than sila-hexocyclium ($M_1 = M_3 > M_4 > M_2$). This is in marked contrast with the very clear selectivity of *o*-methoxy-sila-hexocyclium for the prejunctional M_1/M_4-like heteroreceptors in rabbit vas deferens.

5 The tertiary amines demethyl-hexocyclium, demethyl-sila-hexocyclium and demethyl-*o*-methoxy-sila-hexocyclium had 10 to 30 fold lower affinities than the corresponding quaternary ammonium derivatives.

Keywords: Hexocyclium/sila-hexocyclium derivatives; *o*-methoxy-sila-hexocyclium; muscarinic receptor subtypes; structure/affinity relationships; binding/functional correlations; muscarinic receptor antagonists

Introduction

Following the discovery that pirenzepine is able to discriminate several muscarinic receptor binding sites (Hammer *et al.*, 1980), the subclassification and characterization of various muscarinic receptor subtypes has aroused increasing interest. Molecular biology studies suggest that at least five genes encoding muscarinic receptor subtypes (m1–m5) are expressed in mammalian tissues (see Hulme *et al.*, 1990; Levine & Birdsall, 1993). Functional and binding experiments revealed the existence of four different native subtypes, termed M_1–M_4. Comparison of the radioligand binding properties and functional coupling of the native M_1–M_4 receptors with those of the expressed m1–m4 proteins showed a good correlation (Hulme *et al.*, 1990; Lazareno *et al.*, 1990; Waelbroeck *et al.*, 1990; Dörje *et al.*, 1991; Levine & Birdsall, 1993).

Although several drugs have been reported to discriminate the M_1 from M_2, M_3 and M_4 receptors in binding and/or functional studies, most of these drugs possess tertiary amino groups. Their binding properties, like those of pirenzepine, might therefore be strongly pH-dependent (Barlow & Chan, 1982), a factor which may complicate the identification of receptor subtypes. It was interesting, therefore, that a quaternary ammonium compound, *o*-methoxy-sila-hexocyclium, was found to have very clear M_1 selectivity in functional studies (Lambrecht *et al.*, 1988; Boddeke *et al.*, 1989; Polidori *et al.*, 1990).

The goal of the present study was to evaluate the structural requirements for binding of the carbon/silicon analogues hexocyclium and sila-hexocyclium and related compounds (Figure 1) to M_1, cardiac M_2, glandular/smooth muscle M_3 and brain M_4 sites. To achieve this goal, we analysed the binding properties of the compounds to [^{3}H]-pirenzepine-labelled M_1 sites in rat brain cortex, [^{3}H]-telenzepine-labelled M_1 sites in calf superior cervical ganglia (Feifel *et al.*, 1991) or [^{3}H]-N-methyl-scopolamine ([^{3}H]-NMS)-labelled NB-OK 1 (M_1) sites (Waelbroeck *et al.*, 1987b; 1988), [^{3}H]-NMS-labelled rat cardiac M_2 sites (Waelbroeck *et al.*, 1987a), [^{3}H]-NMS-labelled rat pancreas M_3 sites (Waelbroeck *et al.*, 1987a) and [^{3}H]-NMS-labelled M_4 sites in rat striatum, sites with a slow dissociation rate for NMS (Waelbroeck *et al.*, 1987b; 1990).

We compared the binding affinity profiles at these four receptor subtypes with the pharmacological properties of the compounds at prejunctional muscarinic heteroreceptors in rabbit vas deferens (Eltze, 1988; Eltze *et al.*, 1988; Grimm *et al.*, 1994; Lambrecht *et al.*, 1993), M_2 receptors in guinea-pig atria, and M_3 receptors in guinea-pig ileum (see review by Caulfield, 1993).

The affinities of a number of antagonists for the prejunctional muscarinic receptors mediating inhibition of neurogenic contractions of rabbit vas deferens clearly indicate that these receptors are not the M_2, M_3 or m5 subtype (Eltze, 1988; Eltze *et al.*, 1988; 1993; Lambrecht *et al.*, 1989; Dörje *et al.*, 1991; Grimm *et al.*, 1994). The most prominent features of these prejunctional inhibitory receptors are: (i) a high affinity for the M_1-selective antagonist pirenzepine (pA_2 values = 8.08–8.52; Lambrecht *et al.*, 1989; Choo & Mitchelson, 1990; Micheletti *et al.*, 1990a; Dörje *et al.*, 1990; Eltze *et al.*, 1993; Sagrada *et al.*, 1993); (ii) a high affinity for the M_2/M_4-selective antagonist himbacine (pA_2

[1] Author for correspondence.
[2] Present address: Preclinical Research, Sandoz Pharma AG, CH-4002 Basle, Switzerland

values = 8.5–8.17; Dörje et al., 1990; Eltze et al., 1993; Sagrada et al., 1993); and (iii) a low affinity for methoctramine (pA_2 value = 6.85; Lambrecht et al., 1989). It is also worth noting that there is immunoreactivity to specific anti-m1 receptor antibodies, but not to anti-m4 antibodies, in rabbit vas deferens (Dörje et al., 1991). Thus, we are left with arguments for and against the presence of inhibitory muscarinic M_1 and M_4 heteroreceptors in rabbit vas deferens. Perhaps the data may be reconciled by multiple, M_1 and M_4, prejunctional muscarinic receptors.

Further experiments are needed to clarify this issue. To reflect this lack of final definition of the prejunctional rabbit vas deferens receptor subtype, in this paper we will use the term M_1/M_4-like for these receptors.

Preliminary accounts of this study have been communicated to the German Society for Pharmacology and Toxicology, Hamburg, September 1988 (Mutschler et al., 1988) and to the IUPHAR, Amsterdam, July 1990 (Feifel et al., 1990).

Methods

Radioligand binding experiments: general considerations

Protein concentrations were determined according to Lowry et al. (1951), using bovine serum albumin as standard. Male Wistar albino rats were killed by decapitation and the brain, heart or pancreas immediately removed. Calf superior cervical ganglia were obtained from a regional slaughterhouse and brought into the laboratory within 70 min. NB-OK 1 cells were cultured as previously described (Waelbroeck et al., 1988), in RPMI 1640 medium enriched with 10% foetal calf serum, 100 units ml^{-1} penicillin and 100 $\mu g\,ml^{-1}$ streptomycin. All the following operations were performed at 4°C.

Preparation of the homogenates or crude membranes used for binding studies

M_1 receptors For [^{3}H]-NMS binding experiments, the NB-OK 1 cells were rinsed, harvested and centrifuged in 20 mM sodium phosphate buffer (pH 7.4) containing 150 mM NaCl and 1 mM EDTA, resuspended and homogenized in 20 mM Tris/HCl buffer (pH 7.5) enriched with 5 mM $MgCl_2$ and stored in liquid nitrogen.

The rat brain cortex was homogenized in 15 ml of 20 mM Tris/HCl buffer (pH 7.5) enriched with 250 mM sucrose, in a glass-teflon homogenizer (7 up and down strokes). The resulting homogenate was stored in liquid nitrogen until use, and diluted 5 fold with the same buffer immediately before the experiment.

After separation of surrounding tissue, the calf superior cervical ganglia were minced with scissors and homogenized in ice-cold buffer solution (30 g tissue wet weight/100 ml of 50 mM Tris/HCl buffer (pH 7.4) enriched with 120 mM NaCl and 5 mM $MgCl_2$), with an Ultra-Turrax (maximal speed, for 2 × 30 s). The homogenate was centrifuged at 160 *g* for 10 min, and the pellet was ground a second time and processed as before. The supernatants were combined and centrifuged for 1 h at 100,000 *g*. The pellets (corresponding to 20% of the original wet weight of the original tissue) were stored at − 20°C until use. For binding studies, the pellets were resuspended in ice-cold buffer with a Potter-Elvejhem homogenizer.

M_2 receptors The rat heart was rinsed in isotonic NaCl, then homogenized in 2.5 ml of 20 mM Tris/HCl buffer (pH 7.5), enriched with 250 mM sucrose, with an Ultra-Turrax (maximal speed, for 5 s) followed by addition of 12.5 ml of the same buffer, 7 up and down strokes with a glass-teflon homogenizer and filtration on 2 layers of medical gauze.

M_3 receptors The rat pancreas was minced with scissors and homogenized with a glass-teflon homogenizer (7 up and down strokes) in 8 ml of 300 mM sucrose enriched with 0.2 $mg\,ml^{-1}$ bacitracin and 500 kallikrein inhibitor units (KIU) ml^{-1} of trasylol. The resulting homogenate was immediately filtered over two layers of medical gauze and diluted 11 fold with the incubation buffer (66 mM sodium phosphate buffer, pH 7.4, enriched with 2.6 mM $MgCl_2$ and with 13 $mg\,ml^{-1}$ bovine serum albumin, 0.24 $mg\,ml^{-1}$ bacitracin and 600 KIU ml^{-1} of trasylol).

M_4 receptors Rat striatum homogenates were prepared in 2 ml of 20 mM Tris/HCl buffer (pH 7.5), enriched with 250 mM sucrose, and stored in liquid nitrogen until use. The homogenates were diluted 20 fold with the homogenization buffer, immediately before the incubation with [^{3}H]-NMS.

Binding studies

Most binding studies were performed at 25°C, at equilibrium, in a 50 mM sodium phosphate buffer (pH 7.4) enriched with 2 mM $MgCl_2$ and 1% bovine serum albumin (and, for incubations with pancreas, 0.2 $mg\,ml^{-1}$ bacitracin and 500 KIU ml^{-1} trasylol), [^{3}H]-NMS or [^{3}H]-pirenzepine and the indicated unlabelled drugs concentrations, in a total volume of 1.2 ml. In contrast, [^{3}H]-telenzepine binding studies were performed at 37°C, in a 50 mM Tris/HCl buffer enriched with 120 mM NaCl, 5 mM $MgCl_2$, [^{3}H]-telenzepine, and the indicated unlabelled drugs concentrations, in a total volume of 350 µl.

To measure [^{3}H]-pirenzepine binding to brain cortex homogenates, we used 80 µl of the homogenate, corresponding to a protein concentration of 200 µg per assay. A 2 h incubation allowed equilibrium binding. The [^{3}H]-pirenzepine concentration was 5 nM. To measure [^{3}H]-telenzepine binding to calf superior cervical ganglia, we used 250 µl of the homogenate (corresponding to 1.25 mg crude membrane wet weight). The [^{3}H]-telenzepine concentration was 0.8 nM. A 2 h incubation allowed equilibrium binding. To measure [^{3}H]-NMS binding to NB-OK 1 homogenates, we used 80 µl of homogenate, corresponding to about 200 µg protein per assay. The incubation period was 2 h to achieve equilibrium binding in the presence of 0.25 nM [^{3}H]-NMS. For incubations with rat heart homogenates, we used 80 µl of the homogenate, corresponding to 400 to 500 µg protein per assay. The 2 h incubation period was sufficient to allow equilibrium binding. The [^{3}H]-NMS concentration used was 1.0 nM. To analyse [^{3}H]-NMS binding to pancreas homogenates, we used 80 µl of homogenate, corresponding to 800 µg pancreas protein per assay. A 4 h incubation period was necessary to allow full equilibration of [^{3}H]-NMS binding at 25°C. The tracer concentration used was 0.25 nM. In rat striatum homogenates, [^{3}H]-NMS labels M_1, very few M_2 and M_3, and a majority of M_4 sites. It dissociates faster from the M_1 and M_2 sites. (Waelbroeck et al., 1987b; 1990). We preincubated 80 µl of the homogenate (equivalent to about 30 µg protein) in a total volume of 1.2 ml, in the presence of [^{3}H]-NMS and unlabelled drugs. A 2 h preincubation period allowed equilibrium binding. We then added 1 µM atropine and allowed tracer dissociation for 35 min before filtration. This procedure allowed us to investigate tracer binding to the striatum M_4 sites. The tracer concentration used in these experiments was 0.25 nM.

The incubations were stopped by addition of 2 ml ice-cold filtration buffer (50 mM sodium phosphate buffer, pH 7.4). Bound and free tracer were immediately separated by filtration on glass fibre GFC filters presoaked overnight in 0.05% polyethyleneimine. The samples were rinsed three times with filtration buffer. The filters were then dried, and the bound radioactivity counted by liquid scintillation. Non specific [^{3}H]-telenzepine, [^{3}H]-NMS or [^{3}H]-pirenzepine binding was defined as tracer bound in the presence of 10 µM atropine.

For more experimental details, see Waelbroeck *et al.* (1987a,b; 1988; 1990) and Feifel *et al.* (1991).

Analysis of binding data

All competition curves were repeated three times in duplicate. IC_{50} values were determined by a computer-aided procedure described by Richardson & Humrich (1984), assuming the existence of only one receptor subtype. K_i values were determined from IC_{50} values by the Cheng & Prusoff (1973) equation, using the radioligand K_D values obtained in the same tissue. The pK_i values shown in Table 1 correspond to $-\log K_i$ values.

The standard deviations of pK_i values were equal to or below 0.1 log unit.

Pharmacological experiments

Rabbit vas deferens Male New Zealand white rabbits (2.5–3.0 kg) were killed by i.v. injection of 120 mg kg^{-1} pentobarbitone sodium. The vasa deferentia were excised, dissected free of connective tissue and divided into four segments of approximately 1.5 cm length. The preparations were set up in 7 ml organ baths containing modified Krebs buffer which consisted of (mM): NaCl 118, KCl 4.7, $CaCl_2$ 2.5, $MgSO_4$ 0.6, KH_2PO_4 1.2, $NaHCO_3$ 25.0 and (+)-glucose 11.1; 1 μM yohimbine was included to block α_2-adrenoceptors. The bathing fluid was maintained at pH 7.4, 31°C, and aerated with 95% O_2/5% CO_2. A basal tension of 750 mg was applied. After a 30 min equilibration period, isometric twitch contractions were elicited by electrical field stimulation (0.05 Hz, 0.5 ms, 30 V) with platinum electrodes. These effects were concentration-dependently inhibited by the M_1 receptor agonists 4-(3-chlorophenylcarbamoyloxy)-2-butynyltrimethylammonium chloride (McN-A-343) and 4-(4-chlorophenylcarbamoyloxy)-2-butynyltrimethylammonium iodide (4-Cl-McN-A-343) (Eltze, 1988; Eltze *et al.*, 1988; Boddeke, 1991; Lambrecht *et al.*, 1993). The neurogenic contractions were measured by a force-displacement transducer connected to a Hellige amplifier and a Rikadenki polygraph.

Guinea-pig atria and ileum Adult guinea-pigs of either sex were killed by cervical dislocation and the organs required were removed. Left atria and strips of ileal longitudinal smooth muscle of 1.5 cm length (Paton & Zar, 1968) were set up in 6 ml organ baths, under 500 mg tension, in oxygenated (95% O_2/5% CO_2) Tyrode solution, composed of (mM): NaCl 137, KCl 2.7, $CaCl_2$ 1.8, $MgCl_2$ 1.05, $NaHCO_3$ 11.9, NaH_2PO_4 0.42 and (+)-glucose 5.6. All experiments were conducted at 32°C (pH 7.4). The agonist used was arecaidine propargyl ester (Mutschler & Lambrecht, 1984; Barlow & Weston-Smith, 1985; Lambrecht *et al.*, 1993).

Left atria were electrically paced by means of platinum electrodes (2 Hz, 3 ms duration, supramaximal voltage). Atrial responses to the agonist were measured as changes in isometric tension, and these effects were expressed as the percentage inhibition of the force of contraction. Responses of ileal longitudinal smooth muscle strips to arecaidine propargyl ester were measured as isotonic contractions. The effects in atria and ileum were recorded as with the rabbit vas deferens.

Antagonist affinities

After 1 h equilibration, concentration-response curves were obtained by cumulative addition of the agonists (Van Rossum, 1963). When these responses were constant, concentration-response curves were repeated in the presence of at least 3 concentrations (in most cases, log interval = 0.48) of antagonists, allowing 15–45 min equilibration time. Each concentration of antagonist was tested 3 to 5 times and the ratios of agonist molar EC_{50} values obtained in the presence and absence of antagonists were calculated. The slopes of the Arunlakshana-Schild plots (Arunlakshana & Schild, 1959) were determined by linear regression using the method of least squares. pA_2 values were estimated by fitting to the data the best straight line with a slope of unity (Arunlakshana & Schild, 1959; Tallarida *et al.*, 1979).

To assess whether *o*-methoxy-sila-hexocyclium (**3b**) had actions at a site in addition to that occupied by the M_1-selective agonist, McN-A-343, in rabbit vas deferens, combination antagonist studies were performed on the basis of dose-ratio analysis (Paton & Rang, 1965). The concentration-response curves to McN-A-343 in these experiments were obtained under control conditions and then in the presence of compound **3b** (50 μM) or pirenzepine (50 μM) alone or with the two antagonists combined. The contact time for pirenzepine and **3b** was always 30 min. The experimental data for individual antagonist applications were used to calculate dose-ratios (DR) expected for the combination for two models: expected single-site = $DR_1 + DR_2 - 1$ and expected independent sites = $DR_1 \times DR_2$. These dose-ratios were compared with the experimentally observed combined mean dose-ratio.

Data analysis

All data are presented as means ± s.e.mean of the indicated number (n) of experiments. Linear regression analyses were

Table 1 pK_i values obtained in binding studies on NB-OK 1 cells, rat brain cortex and calf superior cervical ganglia (CSCG; M_1 sites), rat heart (M_2 sites), rat pancreas (M_3 sites) and to the slowly-dissociating (M_4) sites in rat striatum[a]

Antagonist	*NB-OK 1*	*M_1 Cortex*	*CSCG*	*M_2 Heart*	*M_3 Pancreas*	*M_4 Striatum*
1a Hexocyclium[b]	8.8	8.9[c]		7.7	8.4	8.8
1b Sila-hexocyclium[b]	8.9	8.8[c]	8.9	7.6	8.4	8.8
2a Demethyl-hexocyclium[b]	8.0	8.0		6.7	7.4	8.0
2b Demethyl-sila-hexocyclium[b]	7.9	7.9		6.6	7.4	8.0
3a *o*-Methoxy-hexocyclium	6.8	6.8		5.9	6.2	6.8
3b *o*-Methoxy-sila-hexocyclium	7.1	7.1	6.9	6.3	6.6	7.0
4 Demethyl-*o*-methoxy-sila-hexocyclium	6.5	6.4	6.7	5.3	5.6	6.2
5 *p*-Fluoro-sila-hexocyclium	7.9	7.9	7.8	6.9	7.3	7.9
6 *p*-Chloro-sila-hexocyclium	7.4	7.5	7.4	6.4	7.0	7.1

[a]The standard deviations of the pK_i values were typically ± 0.1 log unit, always below 0.15 log unit. The Hill coefficients varied between 0.95 and 1.05 (standard deviation ± 0.1) except for the [^{3}H]-pirenzepine/**1a**/**1b** competition curves in brain cortex (Hill coefficients of 0.85 were obtained for these compounds).

[b]The pK_i values of these compounds in NB-OK 1 cells, pancreas and heart homogenates have been published previously (Waelbroeck *et al.*, 1989).

[c]The competition curves were biphasic (see text). The pK_i values indicated correspond to the major 'subclass' of binding sites (85 to 90% of tracer binding).

carried out by the method of least squares (Tallarida *et al.*, 1979). Differences between mean values were tested for statistical significance by Student's t test; $P<0.05$ was accepted as being significant.

Compounds

[^{3}H]-N-methylscopolamine methyl chloride ([^{3}H]-NMS, 80 to 85 Ci mmol^{-1}) was obtained from Amersham International (Bucks, England). [^{3}H]-pirenzepine (80 to 85 Ci mmol^{-1}) was from New England Nuclear, Boston, MA, U.S.A. Racemic [^{3}H]-telenzepine (85 Ci mmol^{-1}) was a generous gift from Byk Gulden Lomberg, Konstanz, Germany, 4-(3-chlorophenylcarbamoyloxy)-2-butynyltrimethylammonium chloride (McN-A-343), atropine sulphate, bovine serum albumin (Fraction V) and polyethyleneimine were from Sigma Chemical Co. (St Louis, MO, U.S.A.), and glass fibre filters GFC from Whatmann (Maidstone, England). All other reagents were of the highest grade available. Pirenzepine dihydrochloride was a generous gift from Thomae (Biberach, Germany). 4-(4-Chlorophenylcarbamoyloxy)-2-butynyltrimethylammonium iodide (4-Cl-McN-A-343; Nelson *et al.*, 1976), arecaidine propargyl ester (Mutschler & Hultzsch, 1973), hexocyclium (**1a**; as methyl sulphate; Zaugg *et al.*, 1958), sila-hexocyclium (**1b** as methyl sulphate; Tacke *et al.*, 1989a), demethyl-hexocyclium (**2a**; Zaugg *et al.*, 1958), demethyl-sila-hexocyclium (**2b**; as dihydrochloride), *o*-methoxy-hexocyclium (**3a**; as methyl sulphate; Strohmann, 1990), *o*-methoxy-sila-hexocyclium (**3b**; as methyl sulphate; Tacke *et al.*, 1989b) and demethyl-*o*-methoxy-sila-hexocyclium (**4**; as dihydrochloride; Tacke *et al.*, 1989b) were synthesized in our laboratories according to the literature. *p*-Fluoro-sila-hexocyclium (**5**; as methyl sulphate; m.p. 108°C) and *p*-chloro-sila-hexocyclium (**6**; as methyl sulphate; m.p. 149–150°C) were prepared by analogy to the parent compound sila-hexocyclium (**1b**; Tacke *et al.*, 1989b). Compounds **5** and **6** were characterized by ^{1}H-NMR, ^{13}C-NMR and EI-MS measurements as well as by elemental analyses.

Compounds **1a/1b–3a/3b** and **4–6** (see Figure 1) possess a centre of chirality, the carbinol and silanol, respectively, carbon and silicon atom, and therefore exist in two enantiomers. In this study, all compounds were used as racemates.

Results

Radioligand binding studies

All compounds inhibited tracer binding to muscarinic receptors. Most competition curves did not deviate significantly from results expected for competitive inhibition of tracer binding to a single receptor (see for example Figures 2 and 3). The only exceptions to this rule were the [^{3}H]-pirenzepine/hexocyclium (**1a**) and [^{3}H]-pirenzepine/sila-hexocyclium (**1b**) competition curves in rat cortex (Figure 2): these two quaternary compounds inhibited [^{3}H]-pirenzepine binding to 85 or 90% of the receptors with a high affinity, and to 10 or 15% of the receptor with a very low affinity (Figure 2). However, the affinities of compounds **1a/1b–3a/3b** and **4–6** for the majority of M_1 receptors in rat cortex were very similar to that for M_1 receptors in NB-OK 1 cells and calf superior cervical ganglia (Table 1, Figures 2 and 3). The structure-affinity relationships of the hexocyclium and sila-hexocyclium derivatives at each receptor subtype are summarized in Table 1 and Figure 4.

The hexocyclium and sila-hexocyclium derivatives studied in this work, like the parent compounds hexocyclium and sila-hexocyclium, had a clear preference for M_1, M_3 and M_4 over M_2 receptors (Table 1). The same affinity profile ($M_1 \approx M_3 \approx M_4 > M_2$) has been reported for hexocyclium as well as for sila-hexocyclium at cloned muscarinic m_1–m_4 receptors expressed in CHO-K1 cells (Buckley *et al.*, 1989).

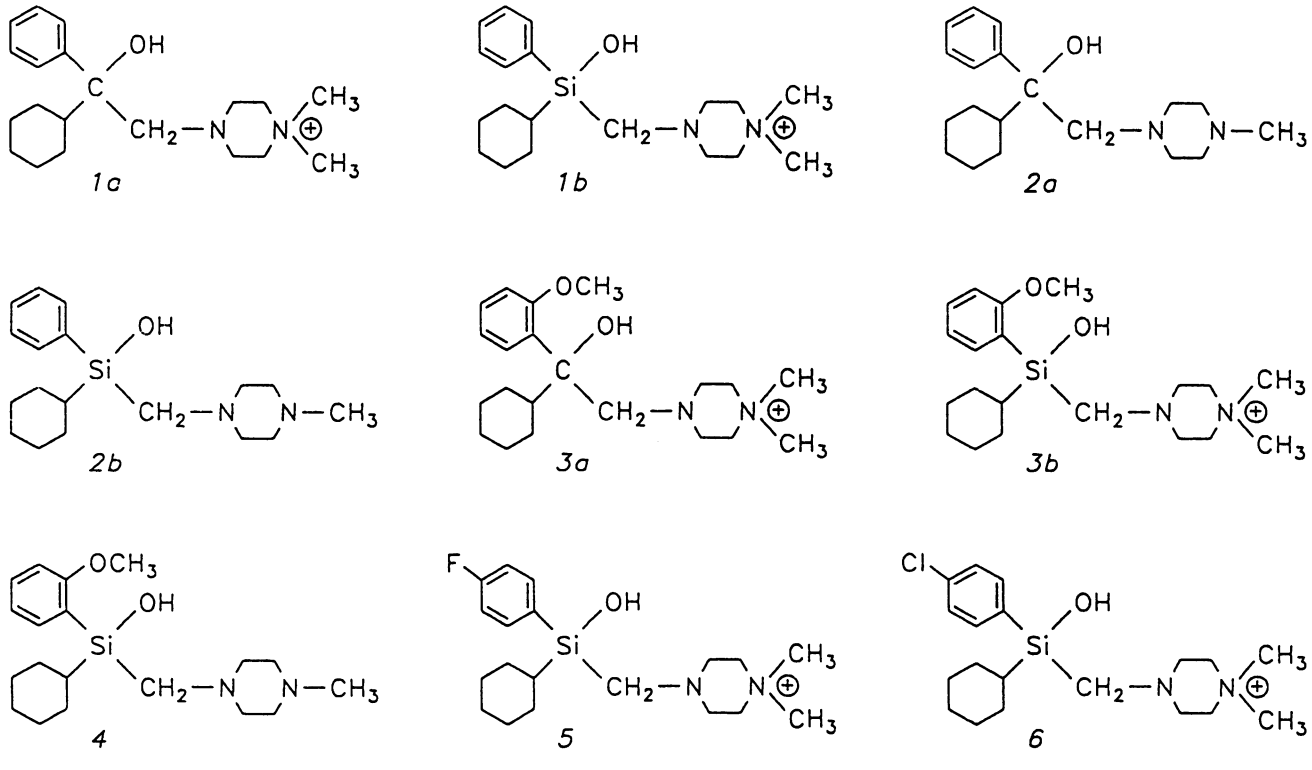

Figure 1 Structural formulas of the compounds studied: hexocyclium (**1a**) and sila-hexocyclium (**1b**), demethyl-hexocyclium (**2a**) and demethyl-sila-hexocyclium (**2b**), *o*-methoxy-hexocyclium (**3a**) and *o*-methoxy-sila-hexocyclium (**3b**), demethyl-*o*-methoxy-sila-hexocyclium (**4**), *p*-fluoro-sila-hexocyclium (**5**) and *p*-chloro-sila-hexocyclium (**6**). All compounds possess a centre of chirality and therefore exist in two enantiomers. In this study, they were used as racemates.

Pharmacological studies

All compounds antagonized the inhibition of neurogenic contractions of rabbit vas deferens by McN-A-343 or 4-Cl-McN-A-343 as well as the negative inotropic effects in electrically stimulated guinea-pig left atria and the contractions of the guinea-pig ileum to arecaidine propargyl ester. This is shown for *o*-methoxy-sila-hexocyclium (**3b**) in Figure 5. With the exception of demethyl-*o*-methoxy-sila-hexocyclium (**4**) in atria (Table 2), there was a concentration-dependent parallel shift to the right of agonist dose-response curves without either the basal tension or the maximal responses being affected. The Schild plots were linear throughout the antagonist concentration-range studied, and slopes were not significantly different from unity ($P > 0.05$), except for *o*-methoxy-sila-hexocyclium (**3b**) at M_2 receptors (Figure 5 and Table 2). The pA_2 value of **3b** in guinea-pig atria (6.41) might therefore be regarded as a purely experimental quantity. However, the binding affinity of **3b** to M_2 receptors in rat heart ($pK_i = 6.3$; Table 1) was very similar to that obtained in functional studies in guinea-pig atria. In the radioligand binding studies (Figure 3), competition curves with **3b** in rat heart homogenates did not deviate significantly from results expected for competitive inhibition of [^{3}H]-NMS binding at a single binding site. Thus, compounds **1a**/**1b**–**3a**/**3b** and **4**–**6** were apparently simple competitive antagonists in the preparations studied. The pA_2 values are shown in Table 2.

Hexocyclium (**1a**), sila-hexocyclium (**1b**) and the derivatives studied in this work had a greater affinity for the M_1/M_4-like heteroreceptors in rabbit vas deferens as compared to guinea-pig (M_2) receptors (Table 2). Most of the compounds also had a higher affinity for guinea-pig ileum M_3 receptors (Table 2). *o*-Methoxy-sila-hexocyclium (**3b**) had a different selectivity pattern: it had a 30 fold and 100 fold higher affinity for M_1/M_4-like receptors in rabbit vas deferens over M_3 receptors in guinea-pig ileum and M_2 receptors in guinea-pig atria, respectively (Table 2).

To investigate whether *o*-methoxy-sila-hexocyclium (**3b**) was interacting solely at the muscarinic receptor in rabbit vas deferens occupied by the agonist McN-A-343, combination concentration-ratio experiments were undertaken with pirenzepine using the method of Paton & Rang (1965).

The concentration-ratios, determined in separate tissues

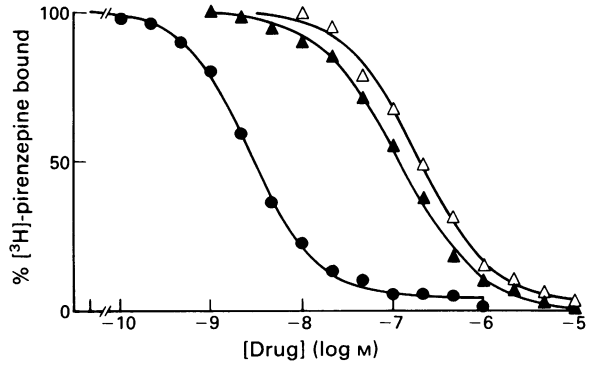

Figure 2 [^{3}H]-pirenzepine competition curves in rat cortex were obtained as explained in Methods, using **1a** or **1b** (●) (the experimental data were within 2% of the means; we therefore used a single symbol for the two compounds), **3a** (△) and **3b** (▲).

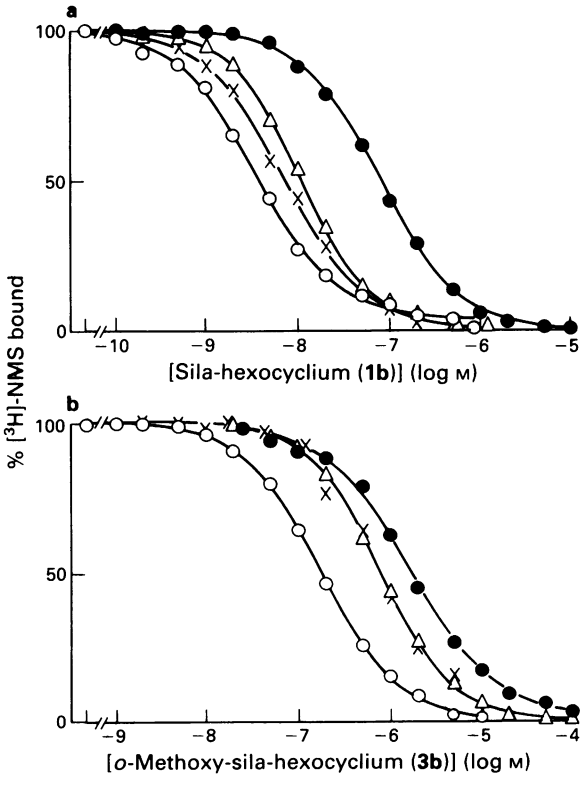

Figure 3 Competition curves obtained at four muscarinic receptor subtypes: (a) [^{3}H]-NMS/sila-hexocyclium (**1b**) competition curves were obtained as explained in Methods, using NB-OK 1 cells (○), heart (●), pancreas (△) or striatum M_4 (x) sites. (b) [^{3}H]-NMS/*o*-methoxy-sila-hexocyclium (**3b**) competition curves were obtained as explained in Methods, using NB-OK 1 cells (○), heart (●), pancreas (△), or striatum M_4 (x) sites.

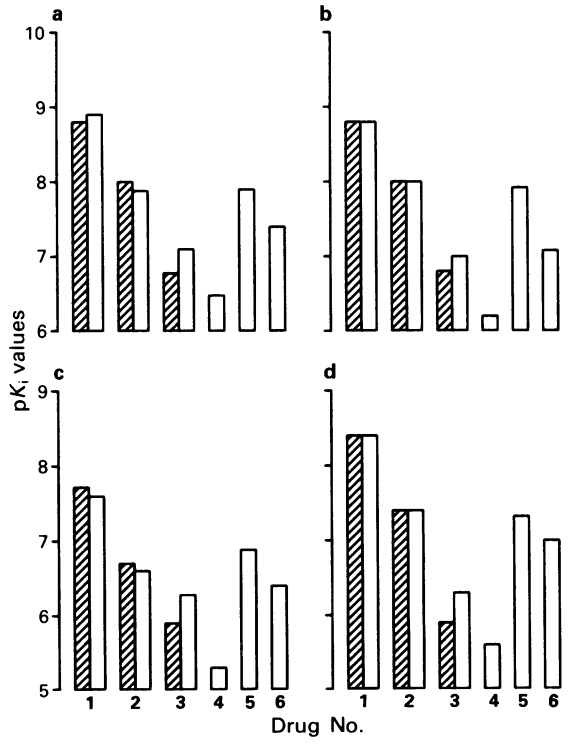

Figure 4 Structure-activity relationships for binding of compounds structurally related to hexocyclium (hatched columns) or to sila-hexocyclium (open columns). The receptors investigated were: NB-OK-1 receptors (M_1) (a); rat heart (M_2) (c); rat pancreas (M_3) (d); and M_4 in rat striatum (b). The compounds were: hexocyclium and sila-hexocyclim (**1**, open and hatched bars), demethyl-hexocyclium and demethyl-sila-hexocyclium (**2**, open and hatched bars), *o*-methoxy-hexocyclium and *o*-methoxy-sila hexocyclium (**3**, open and hatched bars), demethyl-*o*-methoxy-sila-hexocyclium (**4**), *p*-fluoro-sila-hexocyclium (**5**) and *p*-chloro-sila-hexocyclium (**6**). Their pK_i values at the four muscarinic receptor subtypes were measured as explained in Methods.

Table 2 Affinity profiles of hexocyclium, sila-hexocyclium and related muscarinic antagonists at muscarinic M_1/M_4-like receptors in rabbit vas deferens, M_2 receptors in guinea-pig atria, and M_3 receptors in guinea-pig ileum

Antagonist	*M_1/M_4-like Rabbit vas deferens*	*M_2 Guinea-pig atria*	*M_3 Guinea-pig ileum*
1a Hexocyclium	8.89 ± 0.03	7.75 ± 0.03[a]	8.49 ± 0.04[a]
	(1.03 ± 0.07)	(0.97 ± 0.06)	(1.05 ± 0.07)
1b Sila-hexocyclium	9.01 ± 0.07	7.57 ± 0.04[a]	8.78 ± 0.05[a]
	(1.04 ± 0.09)	(0.94 ± 0.07)	(1.04 ± 0.09)
2a Demethyl-hexocyclium	7.69 ± 0.06	6.51 ± 0.08[a]	7.63 ± 0.03[a]
	(0.94 ± 0.11)	(1.05 ± 0.09)	(1.08 ± 0.06)
2b Demethyl-sila-hexocyclium	7.73 ± 0.12	6.65 ± 0.04[a]	7.87 ± 0.04[a]
	(1.11 ± 0.09)	(1.02 ± 0.11)	(0.94 ± 0.08)
3a *o*-Methoxy-hexocyclium	7.23 ± 0.04	6.18 ± 0.05	6.77 ± 0.02
	(0.95 ± 0.12)	(0.89 ± 0.10)	(1.07 ± 0.04)
3b *o*-Methoxy-sila-hexocyclium	8.39 ± 0.05	6.41 ± 0.01[b]	6.96 ± 0.03[b]
	(1.01 ± 0.09)	(1.25 ± 0.06)[c]	(0.93 ± 0.06)
4 Demethyl-*o*-methoxy-sila-hexocyclium	6.44 ± 0.06	5.51 ± 0.03[d]	6.36 ± 0.04
	(1.11 ± 0.14)	–	(0.93 ± 0.06)
5 *p*-Fluoro-sila-hexocyclium	8.32 ± 0.07	7.40 ± 0.04	8.25 ± 0.06
	(1.04 ± 0.14)	(0.92 ± 0.07)	(0.99 ± 0.10)
6 *p*-Chloro-sila-hexocyclium	7.79 ± 0.04	6.93 ± 0.02	7.67 ± 0.04
	(0.98 ± 0.07)	(1.00 ± 0.03)	(1.07 ± 0.06)

pA_2 values and slopes of Schild plots (in parentheses) are presented as means ± s.e.mean ($n = 3-5$).
[a]Data taken from Waelbroeck *et al.* (1989).
[b]Data taken from Lambrecht *et al.* (1988).
[c]Significantly different from unity ($P<0.05$). [d]Only one concentration (10 μM: $n = 5$) was investigated due to the negative inotropic effects of the compound itself at higher concentrations. The pA_2 values were therefore determined from the individual dose-ratios according to Tallarida *et al.* (1979).

($n = 5$) for pirenzepine (50 nM; $DR_1 = 11.8 \pm 1.5$, $pA_2 = 8.32 \pm 0.05$) and compound **3b** (50 nM; $DR_2 = 7.4 \pm 0.6$, $pA_2 = 8.10 \pm 0.01$) were first ascertained. Again, in separate tissues ($n = 5$), the effect of compound **3b** was determined in the presence of pirenzepine ($DR = 18.3 \pm 2.4$). This combined mean dose-ratio obtained experimentally was very close to that calculated for the two antagonists acting by competing with the agonist for the receptor site ($DR_1 + DR_2 - 1 = 19.2$). The results were not consistent ($P<0.05$, unpaired t test) with a multiplication of dose-ratios ($DR_1 \times DR_2 = 87.0$) which would be expected if the two antagonists interacted at independent sites.

Discussion

The native muscarinic receptors are currently divided, in binding and functional studies, into four subtypes (M_1-M_4), the M_1 receptors being recognized by their higher affinity for pirenzepine (see, Hulme *et al.*, 1990; Waelbroeck *et al.*, 1990; Lazareno *et al.*, 1990; Dörje *et al.*, 1991; Doods *et al.*, 1993; Lazareno & Birdsall, 1993; Levine & Birdsall, 1993).

As pointed out some years ago by Barlow & Chan (1982), the fact that pirenzepine is a tertiary amine may lead to problems in determining its antimuscarinic potency. Indeed, titration of the amino group of pirenzepine by variation of the pH of the bath fluid affects markedly its affinity for muscarinic receptors in smooth muscle (Barlow & Chan, 1982). *o*-Methoxy-sila-hexocyclium (**3b**) is the first M_1-selective quaternary muscarinic antagonist in functional studies (Lambrecht *et al.*, 1988; Boddeke *et al.*, 1989; Polidori *et al.*, 1990). It has a large functional $M_1 > M_3$ selectivity, and an even greater $M_1 > M_2$ selectivity than pirenzepine. With this in mind, we decided to measure its affinity for four muscarinic receptor subtypes, and to investigate the structure-activity relationships of various tertiary and quaternary hexocyclium and sila-hexocyclium derivatives (Figure 1) at different muscarinic receptor subtypes. These studies were also performed as a part of our systematic investigations on carbon/silicon bioisosterism (Tacke & Zilch, 1986; Tacke & Linoh, 1989; Waelbroeck *et al.*, 1989).

General considerations

In functional experiments, hexocyclium, sila-hexocyclium and their derivatives behaved as competitive muscarinic antagonists (Figure 5 and Table 2).

In binding studies, most of the competition curves were also compatible with competitive antagonism at a single site (Figures 2 and 3). Hexocyclium and sila-hexocyclium, however, recognized a small fraction (10–15%) of the [^{3}H]-pirenzepine-labelled receptors with a very low affinity (Figure 2). We observed the same type of competition curves with other quaternary antagonists having a high affinity (results not shown), using either [^{3}H]-quinuclidinyl benzylate or [^{3}H]-pirenzepine as tracer, i.e. two tertiary amines. As demonstrated by Ellis (1988), this population of receptors with very low affinity for quaternary antagonists is not correlated with the M_1, M_2, M_3 or M_4 receptor category. We are not aware of the existence of muscarinic receptors having (in functional studies) a comparable affinity profile. We therefore believe that this reflects the existence of binding sites accessible only through a hydrophobic barrier (for instance facing inside closed vesicles) (see Ellis, 1988).

Structure-activity relationships

Sila-substitution of hexocyclium (**1a→1b**) and demethyl-hexocyclium (**2a→2b**) increased only slightly their affinities for the different muscarinic receptor subtypes (Waelbroeck *et al.*, 1989). The effect of sila-substitution on *o*-methoxy-hexocyclium (**3a→3b**) was somewhat greater (Figure 3a and Table 1). In binding studies, we observed a 2 to 3 fold greater affinity for **3b** than for **3a**, at all the muscarinic receptor subtypes (Table 1). In pharmacological studies, **3b** had a 15 fold higher affinity than **3a** for the M_1/M_4-like receptors in rabbit vas deferens (Table 2).

Demethylation of hexocyclium (**1a→2a**), sila-hexocyclium (**1b→2b**) and *o*-methoxy-sila-hexocyclium (**3b→4**) decreased affinities for all muscarinic receptor subtypes by at least 5 fold (Waelbroeck *et al.*, 1989, and this work). This very large effect cannot be explained solely by the stabilization of the positive charge on the quaternary ammonium group, and

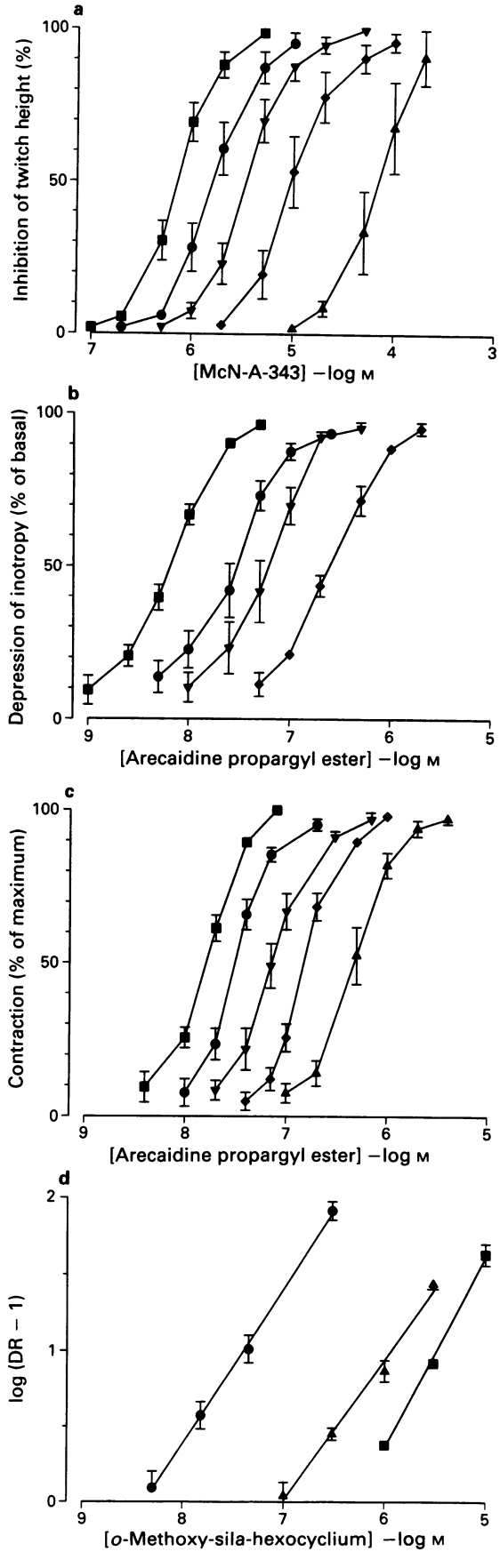

Figure 5 Antagonism of responses to McN-A-343 in rabbit vas deferens and to arecaidine propargyl ester in guinea-pig paced left atria and ileum by different concentrations of *o*-methoxy-sila-hexocyclium (**3b**). Data are means ± s.e.mean. Error bars falling within the area covered by a symbol are not shown. (a) Concentration-response curves for McN-A-343-induced inhibition of neurogenic twitch contractions in rabbit vas deferens in the absence (■; $n = 12$) and presence ($n = 4$) of 5 (●), 15 (▼), 45 (◆) and 300 (▲) nM **3b**. (b) Concentration-response curves for arecaidine propargyl ester-induced negative inotropy in guinea-pig atria in the absence (■; $n = 6$) and presence ($n = 3$) of 1 (●), 3 (▼) and 10 (◆) μM **3b**. (c) Concentration-response curves for arecaidine propargyl ester-induced contractions in guinea-pig isolated ileum longitudinal smooth muscle in the absence (■; $n = 6$) and presence ($n = 3$) of 0.1 (●), 0.3 (▼), 1 (◆) and 3 (▲) μM **3b**. (d) Schild regression from experiments in rabbit vas deferens (●), guinea-pig atria (■) and guinea-pig ileum smooth muscle (▲).

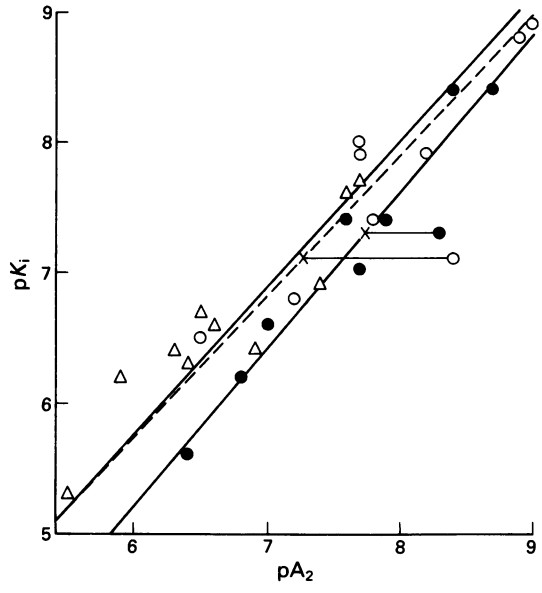

Figure 6 Comparison of the pK_i and pA_2 values of hexocyclium, sila-hexocyclium and related compounds. The pK_i values obtained in NB-OK-1 cells were compared to pA_2 values in rabbit vas deferens (○), the pK_i values obtained in rat heart with the pA_2 values in guinea-pig atria (△) and the pK_i values obtained in rat pancreas, with the pA_2 values in guinea-pig ileum (●). The lines were obtained by linear regression of the data, excluding *o*-methoxy-sila-hexocyclium (**3b**) on the M_1–M_1/M_4-like receptors, and *p*-fluoro-sila-hexocyclium (**5**) on the M_3 receptors.

therefore suggests that this ammonium group fits in a hydrophobic pocket.

Substitutions of the phenyl ring in the *para*-position (*p*-fluoro- and *p*-chloro-derivatives, **5** and **6**) and in the *ortho*-position (*o*-methoxy derivatives, **3a**, **3b** and **4**) decreased the affinities of the respective parent drugs **1a**, **1b** and **2b** at the four muscarinic receptor subtypes (Figure 4). The affinity loss due to replacement of a hydrogen by a (small) fluorine atom varied between 5 and 10 fold, depending on the receptor subtype studied. This suggested that the introduction of a fluorine atom not only induced steric repulsions between the phenyl group and the muscarinic binding site, but probably also modified the electronic properties of the whole phenyl ring (polarization), with unfavourable effects on the interaction with the muscarinic receptors.

In binding studies, the affinity loss due to introducing an *o*-methoxy group was very impressive (20 to 160 fold lower affinity). Binding to all subtypes was similarly affected by the modification (compare **1a**→**3a**, **1b**→**3b**, **2b**→**4**). In contrast, *o*-methoxy-sila-hexocyclium (**3b**) had a high potency in pharmacological experiments at M_1 receptors (pA_2 value of 8.31 in rat superior cervical ganglia, Lambrecht *et al.*, 1988; Boddeke *et al.*, 1989) and at M_1/M_4-like receptors in rabbit vas deferens (pA_2 value = 8.39; this study).

Comparison of the binding and pharmacological properties

The affinities of the compounds studied in this work for the M_2 receptors in rat heart (binding) and guinea-pig atria (functional studies) were very similar, both individually and in rank order (Figure 6). The affinities of the compounds for the M_3 receptors in rat pancreas (binding) were consistently 2–3 fold less than in guinea-pig ileum (functional studies). This might explain part of the difference between the pK_i and pA_2 values of *p*-fluoro-sila-hexocyclium, which was 10 fold less potent in binding than in pharmacological studies on M_3 receptors. The binding affinities of most of the compounds for M_1 receptors in rat cortex, human neuroblastoma (NB-OK 1) cells and calf superior cervical ganglia were very close to their potencies obtained in pharmacological assays at M_1/M_4-like heteroreceptors in rabbit vas deferens (Tables 1 and 2 and Figure 6). However, *o*-methoxy-sila-hexocyclium (**3b**) had a significantly lower affinity in binding compared to pharmacological assays (see also Lambrecht *et al.*, 1988; Boddeke *et al.*, 1989; Polidori *et al.*, 1990; Lazareno & Birdsall, 1993). This is particularly frustrating, since *o*-methoxy-sila-hexocyclium had a remarkable selectivity, in pharmacological studies, for the rabbit vas deferens and rat superior cervical ganglia receptors. It is noteworthy that the pA_2 values obtained for hexocyclium (**1a**; 8.89), sila-hexocyclium (**1b**; 9.01), demethyl-sila-hexocyclium (**2b**; 7.73) and *o*-methoxy-sila-hexocyclium (**3b**; 8.39) in rabbit vas deferens (this study) were very similar to those at M_1 receptors in rat superior cervical ganglia (Eltze *et al.*, 1988; Lambrecht *et al.*, 1988: **1a** = 8.8; **1b** = 9.6; **2b** = 7.6; **3b** = 8.3). In addition, the functional affinity of sila-hexocyclium (**1b**; $pA_2 = 8.78$) for muscarinic M_3 receptors in guinea-pig ileum (this study) was very close to reported M_3 affinity data obtained in other tissues (rat parietal cells: K_i–[^{3}H]-NMS binding = 3.2 nM; K_i–inositol phosphate production = 1.5 nM; K_i–[^{14}C]-aminopyrine accumulation = 2.7 nM; Pfeiffer *et al.*, 1990b. Human HT-29 colon carcinoma cells: K_i–[^{3}H]-NMS binding = 3.1 nM; Kopp *et al.*, 1989. Human gastric mucosa: K_i–[^{3}H]-NMS binding = 5.6 nM; Pfeiffer *et al.*, 1990a).

We checked whether there could be an additional action of *o*-methoxy-sila-hexocyclium (other than on muscarinic receptors) in rabbit vas deferens by measuring the dose-ratio for McN-A-343 in the presence either of pirenzepine, of **3b**, or of a combination of the two antagonists. The results confirmed that there is no additional action of compound **3b** which cannot be accounted for by a competitive mechanism of action. We then decided to compare its binding properties to several different M_1 binding sites of different origins (different animal species and different rat brain regions), in the hope of finding an assay system with M_1 receptors having a high affinity for **3b**. However, the binding properties of pirenzepine and of compounds **2a**, **2b**, **3a**, **3b**, **5** and **6** were identical in the three 'M_1' systems used for these studies (NB-OK 1 cells, rat brain cortex and calf superior cervical ganglia; Table 1). *o*-Methoxy-sila-hexocyclium (**3b**)/[^{3}H]-pirenzepine competition curves in three different rat brain regions (cortex, hippocampus and striatum) were also superimposable, and compatible with the existence of a single binding site with low affinity for **3b** (unpublished results).

In the hope of identifying binding sites with a high affinity for **3b**, we attempted to measure binding of racemic [^{3}H]-*o*-methoxy-sila-hexocyclium (70 Ci mmol^{-1}, lot 2423-148; developed in collaboration with Dr S. Hurt, New England Nuclear, Boston, MA, U.S.A.) to calf superior cervical ganglia. The experiments were carried out in the same way as for [^{3}H]-telenzepine binding, and revealed almost 95% non-specific binding. It was therefore impossible to estimate this tracer's ([^{3}H]-**3b**) affinity (unpublished results). It is possible that the data obtained in pharmacological studies reflect the properties of a very small receptor population, undetectable in binding studies. Further experiments are needed to clarify this issue. Here, it is noteworthy that the hexocyclium derivative N-iminomethyl-*N'*-[(2-hydroxy-2-phenyl-2-cyclohexyl)-ethyl]piperazine (DAC 5945) has also been shown to display a high degree (204 fold M_3 over M_2) of functional *in vitro* selectivity (pA_2, M_3/guinea-pig ileum = 8.56, pA_2, M_2/guinea-pig atria = 6.25, pA_2, M_1–M_4-like/rabbit vas deferens = 7.97; Micheletti *et al.*, 1990b; Lambrecht *et al.*, unpublished results), but the binding affinities of DAC 5945 (pK_i values) to muscarinic M_1 (8.3/8.3), M_2 (7.5/7.4), M_3 (8.4/7.9) and M_4 receptors (8.4/8.6) differed only 16 fold (M_4 over M_2; Doods *et al.*, 1993; Waelbroeck *et al.*, unpublished results).

In conclusion, the present study shows that sila-substitution of *o*-methoxy-hexocyclium (**3a**→**3b**) had a greater effect on the binding properties than observed for the carbon/silicon pairs **1a**/**1b** and **2a**/**2b**: this might reflect differences in the relative importance of the bonds formed between the hydroxyl and phenyl groups and muscarinic receptors. Furthermore, the presence of a quaternary ammonium group is important for binding of antagonists of the hexocyclium/sila-hexocyclium type to muscarinic receptors. Substitution of the phenyl group in the *o*- and *p*-positions of hexocyclium and sila-hexocyclium decreased affinity. Although *o*-methoxy-sila-hexocyclium was found to be remarkably M_1 (M_1/M_4-like)- selective in pharmacological studies, we were unable to confirm this property in binding studies.

The authors thank the Fund for Medical Scientific Research of Belgium (Grant 3.4525.91), the Deutsche Forschungsgemeinschaft (G.L., R.T.) and the Fonds der Chemischen Industrie (G.L., E.M., R.T.) for financial support.

References

ARUNLAKSHANA, O. & SCHILD, H.O. (1959). Some quantitative uses of drug antagonists. *Br. J. Pharmacol. Chemother.*, **14**, 48–58.

BARLOW, R.B. & CHAN, M. (1982). The effects of pH on the affinity of pirenzepine for muscarinic receptors in the guinea-pig ileum and rat fundus strip. *Br. J. Pharmacol.*, **77**, 559–563.

BARLOW, R.B. & WESTON-SMITH, P. (1985). The relative potencies of some agonists at M_2 muscarinic receptors in guinea-pig ileum, atria and bronchi. *Br. J. Pharmacol.*, **85**, 437–440.

BODDEKE, H.W.G.M. (1991). Different effects of muscarinic agonists in rat superior cervical ganglion and hippocampal slices. *Eur. J. Pharmacol.*, **201**, 191–197.

BODDEKE, H.W.G.M., MEIGEL, I.M. & ENZ, A. (1989). Pharmacological characterization of M_1 subtypes in rat superior cervical ganglion and the CA1 and dendate gyrus region of the hippocampus. *Fundam. Clin. Pharmacol.*, **3**, 427.

BUCKLEY, N.J., BONNER, T.I., BUCKLEY, C.M. & BRANN, M.R. (1989). Antagonist binding properties of five cloned muscarinic receptors expressed in CHO-K1 cells. *Mol. Pharmacol.*, **35**, 469–476.

CAULFIELD, M.P. (1993). Muscarinic receptors – characterization, coupling and function. *Pharmacol. Ther.*, **58**, 319–379.

CHENG, Y. & PRUSOFF, W.H. (1973). Relationship between the inhibition constant (K_i) and the concentration of inhibitor (I_{50}) which causes a 50 percent inhibition of an enzymatic reaction. *Biochem. Pharmacol.*, **22**, 3099–3108.

CHOO, L.K. & MITCHELSON, F. (1990). Selective inhibition of responses to carbachol and McN-A-343 in the rabbit vas deferens. *Clin. Exp. Pharmacol. Physiol.*, **17**, 601–611.

DOODS, H.N., WILLIM, K., BODDEKE, H.W.G.M. & ENZEROTH, M. (1993). Characterization of muscarinic receptors in guinea-pig uterus. *Eur. J. Pharmacol.*, **250**, 223–230.

DÖRJE, F., FRIEBE, T., TACKE, R., MUTSCHLER, E. & LAMBRECHT, G. (1990). Novel pharmacological profile of muscarinic receptors mediating contraction of the guinea-pig uterus. *Naunyn-Schmied. Arch. Pharmacol.*, **342**, 284–289.

DÖRJE, F., WESS, J., LAMBRECHT, G., TACKE, R., MUTSCHLER, E. & BRANN, M.R. (1991). Antagonist binding profiles of five cloned human muscarinic receptor subtypes. *J. Pharmacol. Exp. Ther.*, **256**, 727–733.

ELLIS, J. (1988). Method for comparing selectivities of unlabeled subpopulation-selective ligands: application to muscarinic receptors. *J. Rec. Res.*, **8**, 885–900.

ELTZE, M. (1988). Muscarinic M_1- and M_2-receptors mediating opposite effects on neuromuscular transmission in rabbit vas deferens. *Eur. J. Pharmacol.*, **151**, 205–221.

ELTZE, M., GMELIN, G., WESS, J., STROHMANN, C., TACKE, R., MUTSCHLER, E. & LAMBRECHT, G. (1988). Presynaptic muscarinic receptors mediating inhibition of neurogenic contractions in rabbit vas deferens are of the ganglionic M_1-type. *Eur. J. Pharmacol.*, **158**, 233–242.

ELTZE, M., ULLRICH, B., MUTSCHLER, E., MOSER, U., BUNGARDT, E., FRIEBE, T., GUBITZ, C., TACKE, R. & LAMBRECHT, G. (1993). Characterization of muscarinic receptors mediating vasodilation in rat perfused kidney. *Eur. J. Pharmacol.*, **238**, 343–355.

FEIFEL, R., RODRIGUES DE MIRANDA, J.F., STROHMANN, C., TACKE, R., AASEN, A.J., MUTSCHLER, E. & LAMBRECHT, G. (1991). Selective labelling of muscarinic M_1 receptors in calf superior cervical ganglia by [^{3}H](±)-telenzepine. *Eur. J. Pharmacol.*, **195**, 115–123.

FEIFEL, R., RODRIGUES DE MIRANDA, J.F., WAELBROECK, M., CHRISTOPHE, J., RAFEINER, K., TACKE, R., WAGNER-RÖDER, M., MUTSCHLER, E. & LAMBRECHT, G. (1990). Binding and functional properties of sila-hexocyclium derivatives to muscarinic receptor subtypes. *Eur. J. Pharmacol.*, **183**, 1726.

GRIMM, U., FUDER, H., MOSER, U., BÄUMERT, H.G., MUTSCHLER, E. & LAMBRECHT, G. (1994). Characterization of the prejunctional muscarinic receptors mediating inhibition of evoked release of endogenous noradrenaline in rabbit isolated vas deferens. *Naunyn-Schmied. Arch. Pharmacol.*, **349**, 1–10.

HAMMER, R., BERRIE, C.P., BIRDSALL, N.J.M., BURGEN, A.S.V. & HULME, E.C. (1980). Pirenzepine distinguishes between different subclasses of muscarinic receptors. *Nature*, **283**, 90–92.

HULME, E.C., BIRDSALL, N.J.M. & BUCKLEY, N.J. (1990). Muscarinic receptor subtypes. *Annu. Rev. Pharmacol. Toxicol.*, **30**, 633–673.

KOPP, R., LAMBRECHT, G., MUTSCHLER, E., MOSER, U., TACKE, R. & PFEIFFER, A. (1989). Human HT-29 colon carcinoma cells contain muscarinic M_3 receptors coupled to phosphoinositide metabolism. *Eur. J. Pharmacol.*, **172**, 397–405.

LAMBRECHT, G., FEIFEL, R., WAGNER-RÖDER, M., STROHMANN, C., ZILCH, H., TACKE, R., WAELBROECK, M., CHRISTOPHE, J., BODDEKE, H. & MUTSCHLER, E. (1989). Affinity profiles of hexahydro-sila-difenidol analogues at muscarinic receptor subtypes. *Eur. J. Pharmacol.*, **168**, 71–80.

LAMBRECHT, G., GMELIN, G., RAFEINER, K., STROHMANN, C., TACKE, R. & MUTSCHLER, E. (1988). o-Methoxy-sila-hexocyclium: a new quaternary M_1-selective muscarinic antagonist. *Eur. J. Pharmacol.*, **151**, 155–156.

LAMBRECHT, G., MOSER, U., GRIMM, U., PFAFF, O., HERMANNI, U., HILDEBRANDT, C., WAELBROECK, M., CHRISTOPHE, J. & MUTSCHLER, E. (1993). New functionally selective muscarinic agonists. *Life Sci.*, **52**, 481–488.

LAZARENO, S. & BIRDSALL, N.J.M. (1993). Pharmacological characterization of acetylcholine-stimulated [^{35}S]-GTPγS binding mediated by human muscarinic m1–m4 receptors: antagonist studies. *Br. J. Pharmacol.*, **109**, 1120–1127.

LAZARENO, S., BUCKLEY, N.J. & ROBERTS, F.F. (1990). Characterization of muscarinic M_4 binding sites in rabbit lung, chicken heart, and NG 108-15 cells. *Mol. Pharmacol.*, **38**, 805–815.

LEVINE, R.R. & BIRDSALL, N.J.M. (eds.) (1993). Subtypes of muscarinic receptors V. *Life Sci.*, **52**, 405–597.

LOWRY, O.H., ROSEBROUGH, N.J., FARR, A.L. & RANDALL, R.J. (1951). Protein measurement with the Folin phenol reagent. *J. Biol. Chem.*, **193**, 265–275.

MICHELETTI, R., GIUDICI, L., TURCONI, M. & DONETTI, A. (1990a). 4-DAMP analogues reveal heterogeneity of M_1 muscarinic receptors. *Br. J. Pharmacol.*, **100**, 395–397.

MICHELETTI, R., SCHIAVONE, A., CEREDA, E. & DONETTI, A. (1990b). Hexocyclium derivatives with a high selectivity for smooth muscle muscarinic receptors. *Br. J. Pharmacol.*, **100**, 150–152.

MUTSCHLER, E. & HULTZSCH, K. (1973). Über Struktur-Wirkungs-Beziehungen von ungesättigten Estern des Arecaidins und Dihydroarecaidins. *Arzneim.-Forsch.*, **23**, 732–737.

MUTSCHLER, E. & LAMBRECHT, G. (1984). Selective muscarinic agonists and antagonists in functional tests. *Trends Pharmacol. Sci.*, Suppl., **5**, 39–44.

MUTSCHLER, E., MOSER, U., FEIFEL, R., RAFEINER, K., STROHMANN, C., TACKE, R. & LAMBRECHT, G. (1988). o-Methoxy-sila-hexocyclium: a novel quaternary M_1-selective muscarinic antagonist. *Naunyn-Schmied. Arch. Pharmacol.*, **338** (Suppl.), R61.

NELSON, W.L., FREEMAN, D.S. & VINCENZI, F.F. (1976). Stereochemical analogs of a muscarinic, ganglionic stimulant. 2. Cis and trans olefinic, epoxide, and cyclopropane analogs related to 4-[N-(3-chlorophenyl)carbamoyloxy]-2-butynyl trimethylammonium chloride (McN-A-343). *J. Med. Chem.*, **19**, 153–158.

PATON, W.D.M. & RANG, H.P. (1965). The uptake of atropine and related drugs by intestinal smooth muscle of the guinea-pig in relation to acetylcholine receptors. *Proc. R. Soc. B.*, **163**, 1–44.

PATON, W.D.M. & ZAR, M.A. (1968). The origin of acetylcholine release from guinea-pig intestine and longitudinal muscle strips. *J. Physiol.*, **194**, 13–33.

PFEIFFER, A., HANACK, C., KOPP, R., TACKE, R., MOSER, U., MUTSCHLER, E., LAMBRECHT, G. & HERAWI, M. (1990a). Human gastric mucosa expresses glandular M3 subtype of muscarinic receptors. *Dig. Dis. Sci.*, **35**, 1468–1472.

PFEIFFER, A., ROCHLITZ, H., NOELKE, B., TACKE, R., MOSER, U., MUTSCHLER, E. & LAMBRECHT, G. (1990b). Muscarinic receptors mediating acid secretion in isolated rat gastric parietal cells are of M3 type. *Gastroenterology*, **98**, 218–222.

POLIDORI, C., MASSI, M., LAMBRECHT, G., MUTSCHLER, E., TACKE, R. & MELCHIORRE, C. (1990). Selective antagonists provide evidence that M_1 muscarinic receptors may mediate carbachol-induced drinking in the rat. *Eur. J. Pharmacol.*, **179**, 159–165.

RICHARDSON, A. & HUMRICH, A. (1984). A microcomputer program for the analysis of radioligand binding curves and other dose-response data. *Trends Pharmacol. Sci.*, **5**, 47–49.

SAGRADA, A., DURANTI, P., GIUDICI, L. & SCHIAVONE, A. (1993). Himbacine discriminates between two M_1 receptor-mediated responses. *Life Sci.*, **52**, 574.

STROHMANN, C. (1990). E in Beitrag zur C/Si-Bioisosteine. Ph.D. Thesis, *Technical University of Braunschweig, Germany.*

TACKE, R. & LINOH, H. (1989). Bioorganosilicon chemistry. In *The Chemistry of Organic Silicon Compounds*, Part 2. ed. Patai, S. & Rappoport, Z. pp. 1143–1206. Chichester: John Wiley & Sons Ltd.

TACKE, R., LINOH, H., RAFEINER, K., LAMBRECHT, G. & MUTSCHLER, E. (1989a). Synthese und Eigenschaften des selektiven Antimuscarinikums Sila-Hexocyclium-methylsulfat. *J. Organomet. Chem.*, **359**, 159–168.

TACKE, R., RAFEINER, K., STROHMANN, C., MUTSCHLER, E. & LAMBRECHT, G. (1989b). Synthesis of the selective anti-muscarinic agent 4-{[cyclohexylhydroxy(2-methoxyphenyl)silyl] methyl}-1,1-dimethylpiperazinium methyl sulfate (o-methoxy-sila-hexocyclium methyl sulfate). *Appl. Organomet. Chem.*, **3**, 129–132.

TACKE, R. & ZILCH, M. (1986). Sila-substitution – a useful strategy for drug design? *Endeavour, New Series*, **10**, 191–197.

TALLARIDA, R.J., COWAN, A. & ADLER, M.W. (1979). pA_2 and receptor differentiation: a statistical analysis of competitive antagonism. *Life Sci.*, **25**, 637–654.

VAN ROSSUM, J.M. (1963). Cumulative dose-response curves. II. Technique for the making of dose-response curves in isolated organs and the evaluation of drug parameters. *Arch. Int. Pharmacodyn.*, **143**, 299–330.

WAELBROECK, M., CAMUS, J., TASTENOY, M. & CHRISTOPHE, J. (1988). 80% of muscarinic receptors expressed by the NB-OK 1 human neuroblastoma cell line show high affinity for pirenzepine and are comparable to rat hippocampus M_1 receptors. *FEBS Lett.*, **226**, 287–290.

WAELBROECK, M., CAMUS, J., WINAND, J. & CHRISTOPHE, J. (1987a). Different antagonist binding properties of rat pancreatic and cardiac muscarinic receptors. *Life Sci.*, **41**, 2235–2240.

WAELBROECK, M., GILLARD, M., ROBBERECHT, P. & CHRISTOPHE, J. (1987b). Muscarinic receptor hereogeneity in rat central nervous system. I. Binding of four selective antagonists to three muscarinic receptor subclasses: a comparison with M_2 cardiac muscarinic receptors of the C type. *Mol. Pharmacol.*, **32**, 91–99.

WAELBROECK, M., TASTENOY, M., CAMUS, J. & CHRISTOPHE, J. (1990). Binding of selective antagonists to four muscarinic receptors (M_1 to M_4) in rat forebrain. *Mol. Pharmacol.*, **38**, 267–273.

WAELBROECK, M., TASTENOY, M., CAMUS, J., CHRISTOPHE, J., STROHMANN, C., LINOH, H., ZILCH, H., TACKE, R., MUTSCHLER, E. & LAMBRECHT, G. (1989). Binding and functional properties of antimuscarinics of the hexocyclium/sila-hexocyclium and hexahydro-diphenidol/hexahydro-sila-diphenidol type to muscarinic receptor subtypes. *Br. J. Pharmacol.*, **98**, 197–205.

ZAUGG, H.E., MICHAELS, R.J., GLENN, H.J., SWETT, L.R., FREIFELDER, M., STONE, G.R. & WESTON, A.W. (1958). Tertiary carbinols of the piperazine series. I. *J. Am. Chem. Soc.*, **80**, 2763–2768.

(Received November 11, 1993
Revised February 21, 1994
Accepted February 22, 1994)

Br. J. Pharmacol. (1994), **112**, 515–518

Recovery after dietary vitamin E supplementation of impaired endothelial function in vitamin E-deficient rats

[1]Annalisa Rubino & Geoffrey Burnstock

Department of Anatomy and Developmental Biology, University College London, Gower Street, London WC1E 6BT

1 Thoracic aortae, isolated from rats supplemented with dietary vitamin E after vitamin E deficiency, were analysed for changes in vascular reactivity.

2 Following 4 or 12 months of dietary vitamin E deficiency, endothelium-dependent vasodilator responses to acetylcholine were significantly impaired. However, when animals were fed after the first 4 months of vitamin E deprivation with a vitamin E-supplemented diet for 8 months, endothelium-mediated responses were completely restored.

3 In contrast, the endothelium-independent vasodilator or vasoconstrictor responses to sodium nitroprusside and noradrenaline, respectively were not altered either by vitamin E deficiency or supplementation.

4 These data indicate that vitamin E supplementation reversed the impairment of endothelial cell function which occurs during vitamin E deficiency.

Keywords: Vitamin E deficiency; rat aorta; endothelium-dependent vasodilatation; vitamin E supplementation

Introduction

Vitamin E is widely recognised as a naturally occurring antioxidant in biological systems, having an apparent specificity as lipid antioxidant. It is thought to act by trapping lipid peroxy radical (LOO·) and lipid (L·) radical species, thus breaking the lipid peroxidation chain (Burton *et al.*, 1982; 1983). Vitamin E has been shown to protect animal tissues against oxidative damage, such as lipid peroxidation, both *in vitro* and *in vivo* (Tappel, 1980; Leibovitz *et al.*, 1990) and it is now accepted that vitamin E has physiological and pharmacological roles in certain disorders. Neural tissues appear to be particularly susceptible to a deficiency of vitamin E probably because neuronal cells have a special vulnerability to oxidative injury and subsequently a special need for antioxidant to protect their lipid membranes (Harding, 1987; Muller & Goss-Sampson, 1989; 1990). The complete neurological syndrome due to vitamin E deficiency involves central and peripheral nervous system, retina and skeletal muscles (Muller & Goss-Sampson, 1990). However, it has been reported that treatment with vitamin E at a sufficiently early stage of the syndrome prevents its development and can halt or reverse its progression (Muller, 1986). Also the vascular system is constantly subject to oxidative stress and the endothelium is one of the first targets of oxygen-derived free radical-mediated reactions. Several investigations have shown that vitamin E prevents oxidative injury of endothelial cells (Hennig *et al.*, 1990; Kaneko *et al.*, 1991). In addition to its role as antioxidant, vitamin E may modulate a variety of endothelial cell functions, such as prostacyclin synthesis and cell growth and/or repair (Hennig *et al.*, 1988; Huang *et al.*, 1988). In an earlier study we have shown the impairment of endothelium-mediated vascular events during dietary vitamin E deprivation (Rubino *et al.*, 1993).

In the present study we have examined the possibility of preventing and/or reversing the vascular effects of vitamin E deficiency. To this end, endothelium-mediated vasodilator responses to acetylcholine (ACh) were evaluated in aortae isolated from rats fed with a diet supplemented with vitamin E after dietary vitamin E deprivation. The effects of sodium nitroprusside (SNP) and noradrenaline (NA) which also act on smooth muscle cells were examined in vitamin E-supplemented rats, although their actions were not impaired in the vitamin E-depleted rats.

[1] Author for correspondence.

Methods

Animal treatment

The animal model of vitamin E deficiency was set up according to Goss-Sampson *et al.* (1990). Post-weaning (21–23 days old) male Wistar rats (Charles Rivers Ltd., U.K.) were kept on a vitamin E-deficient diet (Machlin/Draper-HLR No. 814, supplied by Dyets, Pennsylvania, U.S.A.) which consisted of tocopherol-stripped corn oil (10%), glucose (65%), salt mix (4%), vitamin-free casein (20%) and full vitamin supplementation (excluding vitamin E). The diet was sterilized by irradiation (1.5 Mrads). Control animals were fed the same diet with the addition of α-tocopherol acetate (40 mg kg^{-1} diet, approx. 1360 iu g^{-1}). The two groups of animals were kept on their respective diets for 12 months, being allowed free access to food and water. After 4 months treatment with vitamin E-deficient diet, a group of animals was fed with a diet repleted with vitamin E for the following 8 months; another group of animals was killed at this stage of the study. Previous investigations had indicated that after 16 weeks of treatment the content of α-tocopherol was undetectable in serum and concentrations in liver and adipose tissue were $<2\%$ of control values (see Goss-Sampson *et al.*, 1988). Body weights of vitamin E-deficient animals were significantly different from controls, indicating an impairment of growth during vitamin E deficiency. Body weights were 704.2 ± 28.5 ($n = 15$) and 585.2 ± 29.9 ($n = 7$; $P < 0.01$) g in control and 12 months-treated animals, respectively. The body weight of rats fed with repleted diet was not significantly different from the age-matched controls, being 687.4 ± 17.2 ($n = 7$) g. Impairment of growth was already observed after 4 months treatment, body weights being 412.8 ± 14.2 ($n = 6$) and 500 ± 21.3 g ($n = 6$; $P < 0.05$) in 4 months vitamin E-deficient and control rats, respectively. Animals were heparinised (1000 units i.p.) 15 min before they were killed by an overdose of sodium pentobarbitone (Sagatal, RMB Animals Health, Dagenham, Essex) and exsanguination.

Tissue preparation

The experimental model used was as described elsewhere (Rubino *et al.*, 1992). Briefly, the descending thoracic aorta was removed and cleaned of all loosely adherent connective tissue; 4–5 mm wide rings were prepared and mounted between two hooks in 10 ml organ baths containing a Krebs

solution of the following composition (mM): NaCl 133, KCl 4.7, NaH_2PO_4 1.35, $NaHCO_3$ 16.3, $MgSO_4$ 0.61, $CaCl_2$ 2.52 and glucose 7.8, gassed with 95% O_2; 5% CO_2 and maintained at 37°C. Preparations were allowed to equilibrate for 60 min, under a resting tension of 1.5 g. After 30 min, the tension on the rings was readjusted to 1.5 g and the experiments were begun after a further 30 min equilibration period. Isometric responses were recorded by use of a Grass FT03C transducer and displayed on a Grass ink-writing polygraph (model 79). Cumulative concentrations of NA were added to the bath to detect contractile responses. In order to evaluate vasodilatation, rings were preconstricted to their EC_{75} value with NA to obtain a stable plateau and challenged with increasing concentrations of the vasodilator tested. The next concentration of the agonist was added to the bath when the previous response had reached a plateau. Cumulative concentration-response curves were obtained in each preparation at intervals of 20 min.

Calculations and statistics

Vascular responses were evaluated as changes in tension (mg) and vasodilatation was calculated as a percentage of the NA sustained tone. EC_{50} values were estimated from the concentration of drug which produced 50% of its maximal response in each concentration-response curve. In the text and figures all results are expressed as means ± s.e.mean. *n* refers to the number of animals from which vessels were used. Statistical analysis was performed by Student's *t* test for unpaired data for comparison between two groups of data; analysis of variance followed by Tuckey's test was used when a comparison among three groups was made. Results were considered significantly different when $P<0.05$.

Results

Vascular responses to acetylcholine (ACh)

The cumulative application of ACh (0.01–10 μM) to raised tone preparations induced concentration-dependent vasodilator responses which were significantly impaired in 12 months-treated animals, compared to the age-matched controls. The maximal effect achieved (ACh 3 μM) was 75.8 ± 3.8 ($n = 10$) and 57.5 ± 2.9 ($n = 7$) % vasodilatation of the NA sustained tone in control and vitamin E-depleted rings, respectively (EC_{50} values were 60.0 ± 2.7 versus 77.3 ± 1.6 nM). However, when the vasodilator responses to ACh were evaluated in rings isolated from vitamin E-repleted animals, the concentration-effect curve for ACh was superimposible on that obtained in control experiments, showing a maximal relaxation of 79.5 ± 8.3 ($n = 7$; $EC_{50} = 68.0 \pm 3.6$ nM) % (Figure 1a). Vasodilator responses to ACh were significantly impaired after 4 months vitamin E-deprivation. The effect of 10 μM ACh was a vasodilatation of 82.8 ± 4.7 ($n = 4$; $EC_{50} = 320.0 \pm 21.0$ nM) % in control experiments and of 45.7 ± 10.7 ($n = 4$; $EC_{50} = 291.7 \pm 34.6$ nM) % in vitamin E- deficient rings (Figure 1b).

Vascular responses to sodium nitroprusside (SNP)

When the endothelium-independent vasodilator responses to SNP (1–300 nM) were evaluated, no significant difference was detected between vitamin E-deficient and age-matched control animals. Control rings from 12 months old rats responded to the maximal concentration of SNP with a relaxation of 94.0 ± 3.5 ($n = 10$), 100.0 ± 0 ($n = 6$), and 100.0 ± 0 ($n = 6$) % in control, vitamin E-depleted and vitamin E-repleted preparations, respectively (Figure 2a). Similarly, SNP induced concentration-dependent vasodilatation up to 90.4 ± 3.5 ($n = 6$) and up to 99.0 ± 0.9 ($n = 6$) % relaxation of the NA sustained tone in control and 4 months-depleted preparations, respectively (Figure 2b).

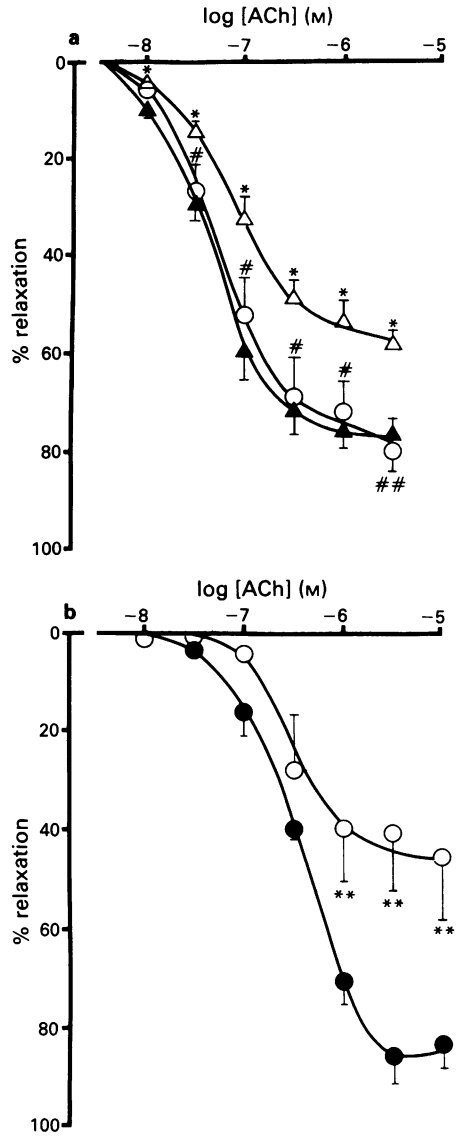

Figure 1 Vasodilator responses to increasing concentrations of acetylcholine (ACh) in aortic rings isolated from 12 (a) and 4 months (b)-treated and age-matched control rats. (a) (▲) Control; (△) vitamin E-depleted; (○) vitamin E-repleted preparations. Statistically significant differences were determined among control, vitamin E-depleted and vitamin E-repleted preparations. $^{*}P<0.05$ vs control; $^{\#}P<0.05$ and $^{\#\#}P<0.02$ vs depleted. (b) (●) Control; (○) vitamin E-depleted preparations. Statistically significant differences were found between control and treated animals: $^{**}P<0.02$ vs control.

Vascular responses to noradrenaline (NA)

Increasing concentrations of NA (1–300 nM) induced contractile responses that were similar in control and vitamin E-deficient preparations. When the effect of NA was evaluated on 12 months-depleted preparations, the concentration-effect curve obtained was slightly shifted to the right, in respect to that obtained on the age-matched controls. However, the contractile responses to the highest concentration of NA used were 865.2 ± 58.0 ($n = 11$) and 779.9 ± 128.7 ($n = 6$) mg tension in control and treated preparations, respectively (Figure 3a). Furthermore, the EC_{50} values for NA responses in control and depleted rings were not significantly different (49.2 ± 21 versus 70.5 ± 12.6 nM). Aortic rings isolated from repleted vitamin E rats showed a maximal contractile response to NA of 872.2 ± 68.8 ($n = 7$) mg and an EC_{50} value (67.9 ± 8.6 nM) superimposable on that of control preparations (Figure 3a). The maximal effect

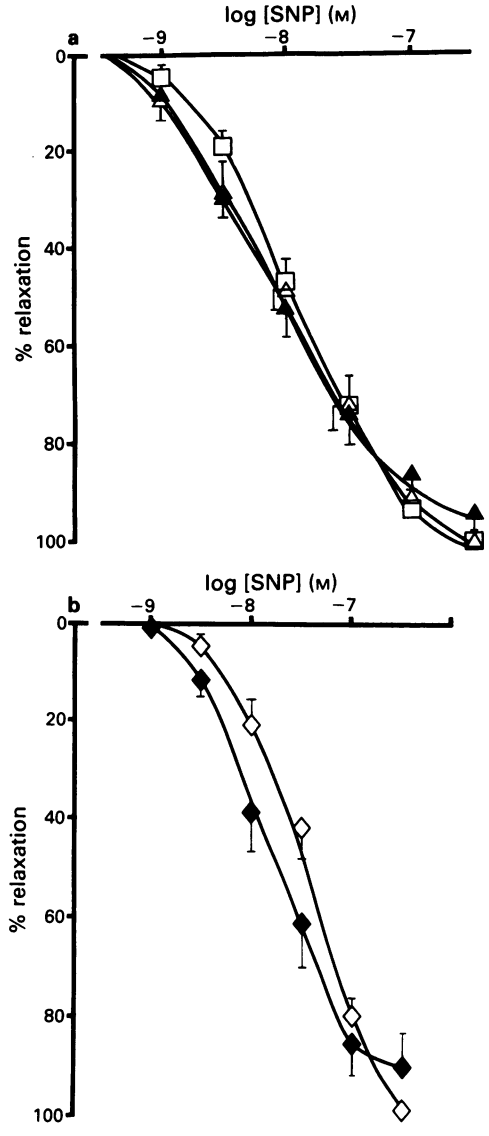

Figure 2 Vasodilator responses to increasing concentrations of sodium nitroprusside (SNP) in 12 (a) and 4 months (b)-treated and age-matched control vessel groups. (a) (▲) Control; (△) vitamin E-depleted; (□) vitamin E-repleted preparations. No statistically significant difference was determined among control, vitamin E-depleted and vitamin E-repleted preparations at any of the concentrations of SNP tested. (b) (◆) Control; (◇) vitamin E-depleted preparations. No statistically significant difference was found between control and treated animals.

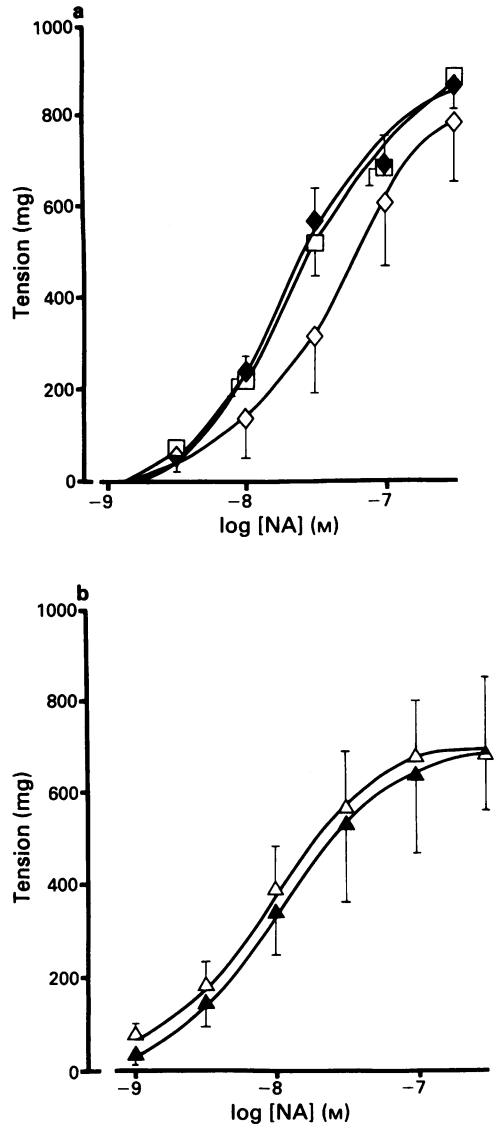

Figure 3 Contractile responses to increasing concentrations of noradrenaline (NA) in 12 (a) and 4 months (b)-treated and age-matched control vessel groups. (a) (◆) Control; (◇) vitamin E-depleted; (□) vitamin E-repleted preparations. No statistically significant difference was determined among control, vitamin E-depleted and vitamin E-repleted animals at any of the concentrations of NA tested. (b) (▲) Control; (△) vitamin E-depleted preparations. No statistically significant difference was found between control and treated animals.

of NA was a contraction of 687.6 ± 198.6 ($n = 6$) and 680.0 ± 122.8 ($n = 6$) mg in rings isolated from control and 4 months-treated rats, respectively (Figure 3b).

Discussion

This study provides the original observation that the impairment of endothelial function which occurs during vitamin E deficiency can be reversed by dietary vitamin E supplementation. Previous investigations showed that following dietary vitamin E deprivation, the endothelial function of the thoracic aorta was drastically affected (Rubino *et al.*, 1993). In keeping with those observations, the present study shows that after 12 months of dietary vitamin E deficiency, endothelium-mediated vasodilatation to ACh was reduced, while direct vasodilatation to SNP was unaffected by vitamin E deficiency. However, when the dietary supplementation of vitamin E was restored, following 4 months of vitamin E deprivation, endothelium-mediated responses to ACh were completely restored. Consistent with findings indicating a drastic reduction of vitamin E tissue contents following 16 weeks of vitamin E deprivation (Goss-Sampson *et al.*, 1988), our data indicate that 4 months of vitamin E deprivation significantly impaired vasodilator responses to ACh. Therefore, the fact that animals fed with a vitamin E-repleted diet showed endothelial function similar to controls indicated that vitamin E supplementation reversed the endothelial malfunction caused by 4 months of vitamin E deprivation.

A reduced rate of growth in the vitamin E-deficient rats has been previously reported (Goss-Sampson *et al.*, 1988). The endothelial malfunction observed during this study could be explained by general malnutrition. However, the groups of animals used received the same basal diet. Further, as far as we are aware, there have been no reports on the effect of malnutrition on endothelial function. Therefore, the impair-

ment of endothelium-mediated relaxation appears to be a specific consequence of vitamin E deficiency. The pharmacological evidence obtained in this study does not indicate whether the recovery of the endothelial function following vitamin E supplementation is due to the reversal of an endothelial defect or to the replacement of endothelial cells which were lost during vitamin E deficiency. Ultrastructural investigations revealed that following 12 months of vitamin E deficiency, normal tissue organisation was disrupted, the endothelial layer being partially detached from underlying tissue (Rubino *et al.*, unpublished observations). Further, Hennig and coworkers (1988) showed that vitamin E stimulates cell proliferation of cultured endothelial cells. Based on these observations it might be speculated that dietary vitamin E supplementation allowed the normal growth and turnover of endothelial cells which was affected during vitamin E deficiency.

Vascular endothelium disruption and increased lipid peroxidation are the major pathogenic factors of cardiovascular diseases such as atherosclerosis and hypertension. Many well documented reports state a positive effect of vitamin E on these factors (see Introduction). Studies on endothelial cells in culture indicated that acute oxidative injury could be prevented by pretreatment, but not by post-treatment, with vitamin E (Block, 1991). Other authors showed that in cultured aortic endothelial cells, vitamin E did not affect basal prostacyclin (PGI_2) production, but it restored the production of PGI_2, prostaglandin E_2 (PGE_2) and thromboxane A_2 (TXA_2) which was reduced by high concentrations of glucose (Kunisaki *et al.*, 1992). It was suggested that vitamin E may restore depressed prostacyclin production by the vascular wall in hyperglycaemic conditions such as those seen in patients with diabetes mellitus (Kunisaki *et al.*, 1992). Further, a study by scanning electron microscopy in aortae of rats which spontaneously developed cataract and neutrophilia, demonstrated that oral administration of vitamin E reduced the extent of endothelial injury observed at 8 and 16 weeks after birth (Masuda *et al.*, 1989). These authors observed that in vitamin E-treated animals, the luminal surfaces of the aortae became similar to that seen in rats at 4 and 6 weeks after birth, before developing morphological changes and detaching of endothelium (Masuda *et al.*, 1989). The observation that endothelial impairment caused by vitamin E deficiency can be successfully reversed by vitamin E supplementation is consistent with investigations on the neurological syndrome related to vitamin E deficiency, showing that an appropriate supplementation of vitamin E can halt and sometimes revert neurological features of vitamin E deprivation (Muller, 1986).

In summary, the present study shows that vitamin E supplementation reversed the impairment of endothelial function in rat aorta. Since endothelial damage is one of the recognised malfunctions associated with cardiovascular disease, these findings suggest a crucial role for dietary vitamin E in the maintenance of vascular function. Further, the reversal of vascular damage via dietary vitamin E supplementation, might indicate vitamin E as an eligible candidate for protection from vascular injury occurring during some cardiovascular diseases.

The authors are grateful to Dr Mark Goss-Sampson and Dr Peter Milla for their comments and suggestions and for providing the tissue used in this study. This work was supported by The British Heart Foundation.

References

BLOCK, E.R. (1991). Hydrogen peroxide alters the physical state and function of the plasma membrane of pulmonary artery endothelial cells. *J. Cell. Physiol.*, **146**, 362–369.

BURTON, G.W., JOYCE, A. & INGOLD, K.U. (1982). First proof that vitamin E is a major lipid soluble, chain-breaking antioxidant in human blood plasma. *Lancet*, **ii**, 327.

BURTON, G.W., JOYCE, A. & INGOLD, K.U. (1983). Is vitamin E the only lipid soluble, chain breaking antioxidant in human blood plasma and erythrocyte membranes? *Arch. Biochem. Biophys.*, **221**, 281–286.

GOSS-SAMPSON, M.A., MAC EVILLY, C.J. & MULLER, D.P.R. (1988). Longitudinal studies of the neurobiology of vitamin E and other antioxidant systems, and neurological function in the vitamin E deficient rat. *J. Neurol. Sci.*, **87**, 25–35.

GOSS-SAMPSON, M.A., KRISS, A. & MULLER, D.P.R. (1990). A longitudinal study of somatosensory, brainstem auditory and peripheral sensory-motor conduction during vitamin E deficiency in the rat. *J. Neurol. Sci.*, **100**, 79–84.

HARDING, A.E. (1987). Vitamin E and the nervous system. *Crit. Rev. Neurobiol.*, **3**, 89–103.

HENNIG, B., BOISSONEAULT, G.A., FISCUS, L.J. & MARRA, M.E. (1988). Effect of vitamin E on oxysterol- and fatty-acid hydroperoxide-induced changes of repair and permeability properties of cultured endothelial cell monolayers. *Int. J. Vitam. Nutr. Res.*, **58**, 41–47.

HENNIG, B., BOISSONEAULT, G.A., CHOW, C.K. & WANG, Y. (1990). Effect of vitamin E on linoleic acid-mediated induction of peroxisomal enzymes in cultured porcine endothelial cells. *J. Nutr.*, **120**, 331–337.

HUANG, N., LINEBERG, B. & STEINER, M. (1988). Alpha-tocopherol, a potent modulator of endothelial cell function. *Thromb. Res.*, **50**, 547–557.

KANEKO, T., NAKANO, S. & MATSUO, M. (1991). Protective effect of vitamin E on linoleic acid hydroperoxide-induced injury to human endothelial cells. *Lipids*, **26**, 345–348.

KUNISAKI, M., UMEDA, F., INOGUCHI, T. & NAWATA, H. (1992). Vitamin E restores reduced prostacyclin synthesis in aortic endothelial cells cultured with high concentration of glucose. *Metabolism*, **41**, 613–621.

LEIBOVITZ, B., HU, M.-L. & TAPPEL, A. (1990). Dietary supplements of vitamin E, β-carotene, coenzyme Q^{10} and selenium protect tissues against lipid peroxidation in rat tissue slices. *J. Nutr.*, **120**, 97–104.

MASUDA, M., IHARA, N., KURIKI, H., KOMIYAMA, Y., NISHIKADO, H., EGAWA, H. & MURATA, K. (1989). Spontaneous injuries in the aortic endothelium of the inherited cataract rats and their prevention by tocopherol. A study by scanning electron microscopy. *Atherosclerosis*, **75**, 23–30.

MULLER, D.P.R. (1986). Vitamin E – Its role in neurological function. *Postgrad. Med. J.*, **62**, 107–109.

MULLER, D.P.R. & GOSS-SAMPSON, M.A. (1989). The role of vitamin E in neural tissue. *Ann. N.Y. Acad. Sci.*, **570**, 146–155.

MULLER, D.P.R. & GOSS-SAMPSON, M.A. (1990). Neurochemical, neurophysiological, and neuropathological studies in vitamin E deficiency. *Crit. Rev. Neurobiol.*, **5**, 239–263.

RUBINO, A., GOSS-SAMPSON, M.A., HOYLE, C.H.V. & BURNSTOCK, G. (1993). Impaired endothelial-mediated vasodilatation in aorta of rats with vitamin E deficiency. *Br. J. Pharmacol.*, **108**, 6P.

RUBINO, A., THOMANN, H., HENLIN, J., SCHILLING, W. & CRISCIONE, L. (1992). Endothelium-dependent relaxant effect of neurokinins on rabbit aorta is mediated by the NK_1 receptor. *Eur. J. Pharmacol.*, **212**, 237–240.

TAPPEL, A.L. (1980). Vitamin E and selenium protection from in vivo lipid peroxidation. *N.Y. Acad. Sci.*, **355**, 18–31.

(Received December 2, 1993
Revised February 17, 1994
Accepted March 1, 1994)

Br. J. Pharmacol. (1994), **112**, 519–524

Mediation by M_3-muscarinic receptors of both endothelium-dependent contraction and relaxation to acetylcholine in the aorta of the spontaneously hypertensive rat

[1]Chantal M. Boulanger, Keith J. Morrison & Paul M. Vanhoutte

Center for Experimental Therapeutics, Baylor College of Medicine, Houston, Texas 77030, U.S.A.

1 Experiments were designed to characterize the subtype(s) of endothelial muscarinic receptor that mediate(s) endothelium-dependent relaxation and contraction in the aorta of spontaneously hypertensive rats (SHR).

2 Rings of SHR aorta with endothelium were suspended in organ baths for the measurement of isometric force. Ecothiopate (an inhibitor of acetylcholinesterase) was present throughout the experiments. Endothelium-dependent contraction to acetylcholine was studied in quiescent aortic rings in the presence of N^G-nitro-L-arginine (to prevent the formation of nitric oxide). Endothelium-dependent relaxation to acetylcholine was obtained during contraction to phenylephrine and in the presence of indomethacin (to inhibit cyclo-oxygenase activity). Responses to acetylcholine were assessed against the non-preferential muscarinic receptor antagonist, atropine, and the preferential antagonists pirenzepine (M_1), methoctramine (M_2) and 4-diphenylacetoxy-*N*-methylpiperidine methobromide (4-DAMP; M_3).

3 The potency of acetylcholine in inducing endothelium-dependent contraction was 6.54 ± 0.07 (EC_{50}). Atropine, pirenzepine, methoctramine and 4-DAMP displayed competitive antagonism towards the endothelium-dependent contraction to acetylcholine. The pA_2 values for these muscarinic receptor antagonists were estimated from Arunlakshana-Schild plots to be ($-\log M$) 9.48 ± 0.07, 6.74 ± 0.22, 6.30 ± 0.20 and 9.39 ± 0.22 respectively. The potency of acetylcholine in inducing endothelium-dependent relaxation was 7.82 ± 0.09 (IC_{50}). Atropine, pirenzepine and 4-DAMP displayed competitive antagonism towards the endothelium-dependent relaxation to acetylcholine but methoctramine had no effect. The pA_2 values for atropine and 4-DAMP for the relaxation to acetylcholine were estimated from Arunlakshana-Schild plots to be ($-\log M$) 9.15 ± 0.23 and 9.63 ± 0.28, respectively. These results suggest that the muscarinic M_3 receptor subtype mediates both endothelium-dependent relaxation and contraction to acetylcholine in SHR aorta.

Keywords: Endothelium-derived relaxing factor; endothelium-derived contracting factor; muscarinic receptors; spontaneously hypertensive rats (SHR)

Introduction

Endothelial cells contribute to the local regulation of vasomotor tone by releasing dilator and constrictor substances. The relaxing substances which are generated by the endothelium include endothelium-derived relaxing (EDRF; identified as nitric oxide or a related nitrogen-containing compound) and hyperpolarizing (EDHF) factors (e.g. Furchgott & Zawadzki, 1980; Furchgott & Vanhoutte, 1989; Lüscher & Vanhoutte, 1990; Moncada *et al.*, 1991). Candidates for endothelium-derived contracting substances include endoperoxides, thromboxane A_2, superoxide anions and possibly endothelins (e.g. Furchgott & Vanhoutte, 1989; Yanagisawa & Masaki, 1989; Lüscher & Vanhoutte, 1990; Bassenge & Heusch, 1990). In the aorta of the normotensive rat, acetylcholine causes an endothelium-dependent relaxation, which is mediated via both the activation of a constitutive, calmodulin-dependent nitric oxide synthase enzyme and the subsequent production of nitric oxide (Lüscher & Vanhoutte, 1986; Schini & Vanhoutte, 1992), and the release of EDHF (Chen *et al.*, 1988). In the aorta of the adult spontaneously hypertensive rat (SHR), low concentrations of acetylcholine (10^{-9} to 3×10^{-7} M) induce an endothelium-dependent relaxation which is comparable to that observed in the aorta from normotensive control rats (Lüscher & Vanhoutte, 1986). However, relaxation to higher concentrations of acetylcholine (3×10^{-7} to 3×10^{-5} M) is attenuated in the hypertensive strain, due to the concomitant release of an endothelium-derived contracting factor (EDCF). Endothelium-dependent contractions to acetylcholine are not observed in the aorta of normotensive rats (Lüscher & Vanhoutte, 1986). In the SHR, they are abolished in the presence of inhibitors of cyclo-oxygenase; the EDCF involved may be an endoperoxide (Lüscher & Vanhoutte, 1986; Auch-Schwelk *et al.*, 1990; Ito *et al.*, 1991). Thus, acetylcholine elicits both endothelium-dependent contraction and relaxation in the aorta of SHRs (Lüscher & Vanhoutte, 1986).

In blood vessels, the release of EDRF evoked by acetylcholine is mediated via the activation of different muscarinic receptors. The M_1 subtype mediates endothelium-dependent relaxations in the canine femoral artery (Rubanyi *et al.*, 1987), the bovine pial artery (Garcia-Villalon *et al.*, 1991), the rabbit saphenous artery (Komori & Suzuki, 1987) and the rabbit pulmonary artery (Orphanos & Catravas, 1989). Activation of the M_2 subtype causes the release of EDRF in the bovine coronary artery (Duckles, 1988), the rabbit ear artery (Hynes *et al.*, 1986), the porcine cerebral artery (Van Charldorp & Van Zwieten, 1989) and the canine femoral artery (Rubanyi *et al.*, 1987). The M_3 muscarinic receptors mediate endothelium-dependent relaxation in pial arterioles of mice (Shimizu *et al.*, 1983), the rabbit ear artery (Duckles & Garcia-Villalon, 1990), the rat pulmonary artery (McCormack *et al.*, 1988), the bovine coronary artery (Brunner *et al.*, 1991), the rabbit aorta (Jaiswal *et al.*, 1991), the rabbit pial artery (Garcia-Villalon *et al.*, 1991) and the cat cerebral artery (Dauphin & Hamel, 1990; Alonso *et al.*, 1991). In addition, activation of different muscarinic receptor subtypes in the same preparation can cause the release of different endothelial vasoactive factors; indeed, in the rabbit

[1] Author for correspondence.

saphenous artery, the release of EDRF and that of endothelium-derived hyperpolarizing factor are mediated by activation of M_2 and M_1 subtypes, respectively (Komori & Suzuki, 1987).

In the SHR aorta, the endothelium-dependent contraction to acetylcholine is blocked by the non-preferential muscarinic antagonist, atropine, but not by the nicotinic receptor antagonist, hexamethonium (Lüscher & Vanhoutte, 1986). Furthermore, the release of EDCF occurs in response to higher concentrations of acetylcholine than are required to elicit the release of EDRF; this suggests that different subtypes of muscarinic receptors may mediate the two responses.

The present series of experiments used preferential muscarinic receptor antagonists to characterize the muscarinic receptor subtype(s) that mediate(s) the endothelium-dependent contraction and relaxation in response to acetylcholine in the aorta from SHR.

Methods

Organ bath experiments

Experiments were performed on thoracic aortae from male SHR (8–10 months old; weight 350–412 g; Harlan Sprague Dawley, Indianapolis, IN, U.S.A). All procedures using animals were in accordance with the guidelines of the Animal Protocol Review Committee of Baylor College of Medicine. Systolic arterial blood pressure was measured by the tail cuff method, and averaged 213 ± 6 mmHg ($n = 41$). The rats were anaesthetized with pentobarbitone sodium (50 mg kg^{-1}, intraperitoneally). The thoracic aorta was dissected free, excised, and placed in cold modified Krebs-Ringer bicarbonate solution of the following composition (mM): NaCl 118.3, KCl 4.7, $MgSO_4$ 1.2, KH_2PO_4 1.2, $CaCl_2$ 2.5, $NaHCO_3$ 25.0, calcium disodium edetate (EDTA) 0.026, and glucose 11.1 (control solution). The blood vessels were cleaned of adherent connective tissue and cut into rings (4–5 mm long). In some preparations, the endothelium was removed by gently rubbing the intimal surface with a small forceps. In the remaining rings, care was taken not to touch the inner surface of the blood vessel. The presence or absence of functional endothelial cells was confirmed by the presence or absence of relaxation in response to thrombin (1 u ml^{-1}), respectively (Lüscher & Vanhoutte, 1986).

The rings were suspended horizontally between two stainless steel wires in organ baths, which contained 25 ml of control solution (37°C) aerated with 95% O_2 5% CO_2. The preparations were connected to force transducers (Statham Universal UC2 or Grass FT 03C, Quincy, MA, U.S.A.) for recording of changes in isometric tension. Prior to experimentation, the preparations were stretched progressively and exposed to phenylephrine (3×10^{-7} M) at each level of force until the optimal point of the length-active force relationship was reached. After the procedure the rings were allowed to equilibrate for 40 min. All rings were then exposed to phenylephrine (3×10^{-5} M) to determine maximal responsiveness. Experiments were performed on parallel rings with endothelium, in the presence of ecothiopate (3×10^{-6} M) to prevent degradation of acetylcholine by acetylcholinesterases. Ecothiopate did not affect the endothelium-dependent responses to acetylcholine in this preparation (data not shown). Responses to acetylcholine were assessed against the non-preferential muscarinic receptor antagonist, atropine, and the preferential antagonists, pirenzepine (M_1), methoctramine (M_2) and 4-diphenylacetoxy-*N*-methylpiperidine methobromide (4-DAMP; M_3). Unless otherwise stated, the incubation period with the different antagonists was 40 min.

When endothelium-dependent contraction to acetylcholine was investigated, aortic rings with endothelium were incubated with N^G-nitro-L-arginine (10^{-4} M, 20 min) to prevent the formation of nitric oxide (Schini & Vanhoutte, 1992) and to optimize the endothelium-dependent contractile response (Ito *et al.*, 1991; Auch-Schwelk *et al.*, 1992). The response to acetylcholine was investigated under control conditions and in the presence of increasing concentrations of the muscarinic antagonists. Only one concentration of antagonist was studied per tissue.

Endothelium-dependent relaxation to acetylcholine was studied in aortic rings, with endothelium, in the presence of indomethacin (10^{-5} M; 40 min; to prevent the formation of vasoactive prostanoids). Responses to acetylcholine were measured in tissues which were contracted with phenylephrine (3×10^{-8} M to 3×10^{-7} M; to match the level of contraction between preparations) under control conditions and in the presence of increasing concentrations of the muscarinic antagonists. Only one concentration of antagonist was studied per tissue.

Drugs

The following drugs were used: acetylcholine HCl, atropine sulphate, indomethacin, phenylephrine, thrombin (Sigma Chemical, St. Louis, MO, U.S.A.), N^G-nitro-L-arginine (Aldrich Chemical Company, Milwaukee, WI, U.S.A.); ecothiopate iodide (as phospholine iodide, 1.8% ophthalmic solution, St Lukes Hospital Pharmacy, Houston, TX, U.S.A.); pirenzepine, methoctramine and 4-diphenylacetoxy-*N*-methylpiperidine methiodide (4-DAMP) (Research Biochemical Inc., Natick, MA, U.S.A.). Drug concentrations are expressed as final molar concentrations in the bath solution. Drugs were prepared in distilled water, except indomethacin which was dissolved in distilled water containing $NaCO_3$ (3×10^{-5} M) and sonicated before use. A stock solution of ecothiopate was prepared in sterile diluent (composition: chlorobutanol, 0.55%; mannitol, 1.2%; boric acid, 0.06% and sodium phosphate, 0.026%). Subsequent dilutions were made in control solution.

Statistical analysis

Experiments with each muscarinic antagonist were performed on rings from the same animals studied in parallel.

In the experiments in which concentration-contraction curves to acetylcholine were determined in quiescent preparations (endothelium-dependent contraction), the results of each experiment are expressed as percentage of the maximal response to acetylcholine (10^{-5} M) observed in control preparations. EC_{50} represents the negative logarithm of the concentration of acetylcholine that elicits fifty percent (50%) of its maximal response (measured at 10^{-5} M).

In the experiments in which endothelium-dependent relaxation to acetylcholine was studied, aortic rings were contracted with equi-effective concentrations of phenylephrine (3×10^{-8} to 3×10^{-7} M) [mean contractile response 1.6 ± 0.1 g; $n = 24$]. For each preparation, the relaxation is expressed as percentage inhibition of the contraction to phenylephrine. IC_{50} represents the negative logarithm of the concentration of acetylcholine that induces fifty percent (50%) inhibition of the contraction to phenylephrine (3×10^{-8} to 3×10^{-7} M).

pA_2 values (estimates of the equilibrium dissociation constants) for the muscarinic receptor antagonists were determined from graphs of log concentration-ratios minus 1 (CR – 1) versus log concentration of antagonist (Arunlakshana & Schild, 1959). CR is defined as the concentration of agonist required to induce 50% maximal response in the presence of antagonist divided by the agonist concentration that elicits the same degree of response in the absence of antagonist. The pA_2 values were calculated if the slope of the plot was not significantly different from unity.

Results are given as means ± s.e.mean. Statistical evaluation was done by Student's *t* test for paired or unpaired observations. When more than two means were compared, two-way analysis of variance (ANOVA) was used. Means

were considered significantly different when P was less than 0.05.

Results

Contraction

Acetylcholine induced concentration- and endothelium-dependent contraction of rings of aorta from SHR treated with N^G-nitro-L-arginine (10^{-4} M; 20 min) (Figure 1). The EC_{50} value for acetycholine for contraction under control conditions was 6.54 ± 0.07 ($n = 12$). The contraction evoked by acetylcholine was $60.6 \pm 4.1\%$ of that induced by phenylephrine (3×10^{-5} M; 4.0 ± 0.4 g, $n = 7$), whereas in rings denuded of endothelium, the maximal contraction to acetylcholine (10^{-4} M) was $12.0 \pm 1\%$ of that to phenylephrine (3×10^{-5} M) ($n = 7$; $P < 0.05$).

Atropine (3×10^{-9} M–3×10^{-7} M) caused a parallel rightward displacement of the concentration-response curve to acetylcholine. The response to acetylcholine (10^{-4} M) was reduced in preparations incubated in the presence of atropine (3×10^{-8} and 3×10^{-7} M) (Figure 1). Pirenzepine (10^{-6} M–10^{-5} M) (Figure 1), methoctramine (10^{-6} M–10^{-5} M) (Figure 2) and 4-DAMP (10^{-9} M–10^{-7} M) (Figure 2) caused parallel dextral shifts in the concentration-contraction curve (at the linear portion of the curve) to acetylcholine, with no change in the maximal response.

The pA_2 values for atropine, pirenzepine, methoctramine and 4-DAMP for contraction to acetylcholine were (– log M) 9.48 ± 0.07, 6.74 ± 0.22, 6.30 ± 0.20 and 9.39 ± 0.22, respectively (Table 1). The effect of 4-DAMP on endothelium-

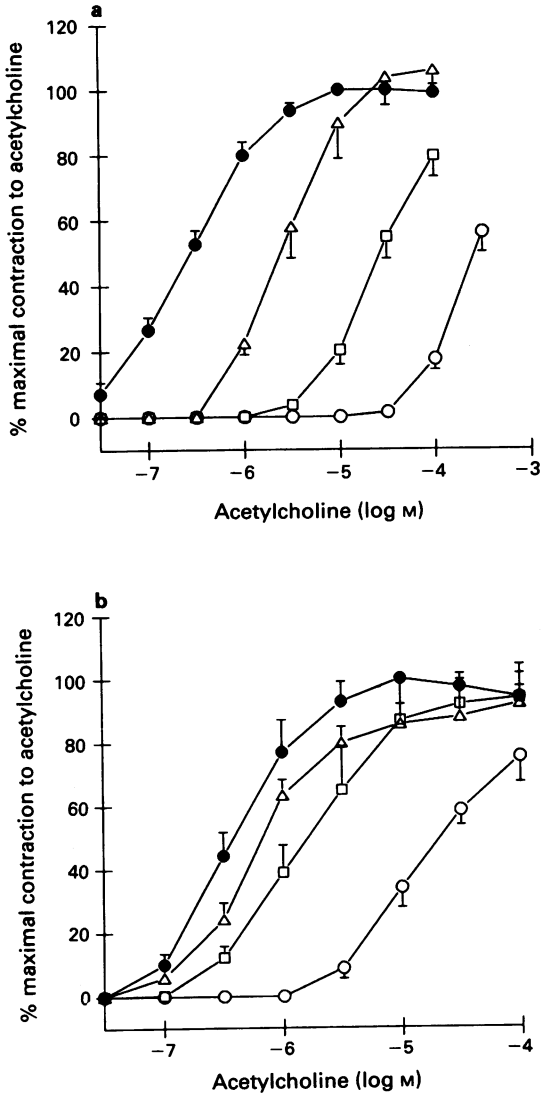

Figure 1 Effect of the non-preferential muscarinic antagonist atropine (a) and the preferential M_1 muscarinic antagonist pirenzepine (b) on the endothelium-dependent contraction evoked by acetylcholine in the SHR rat aorta in the presence of N^G-nitro-L-arginine (10^{-4} M). The experiments were performed on parallel rings with endothelium under control conditions (●) and in the presence of either atropine (a: 3×10^{-9} M (Δ), 3×10^{-8} M (□), 3×10^{-7} M (○)) or pirenzepine (b: 10^{-6} M (Δ), 3×10^{-6} M (□), 10^{-5} M (○)). The data are given as mean ± s.e.mean and are expressed as percentage of the maximal contraction to acetylcholine (10^{-5} M) obtained under control conditions (experiments with atropine: 2.0 ± 0.3 g, $n = 6$; experiments with pirenzepine: 2.0 ± 0.3 g, $n = 6$).

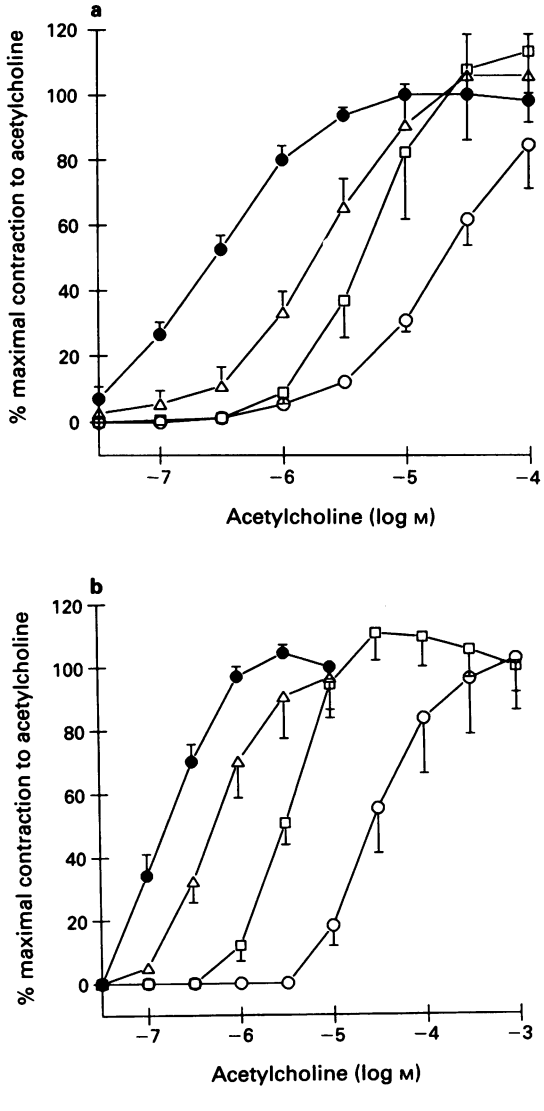

Figure 2 Effect of the preferential M_2 muscarinic antagonist methoctramine (a) and the preferential M_3 muscarinic antagonist 4-DAMP (b) on the endothelium-dependent contraction evoked by acetylcholine in the SHR rat aorta in the presence of N^G-nitro-L-arginine (10^{-4} M). The experiments were performed on parallel rings with endothelium, under control conditions (●) and in the presence of either methoctramine (a: 3×10^{-7} M (Δ), 3×10^{-6} M (□), 3×10^{-5} M (○)) or 4-DAMP (b: 10^{-9} M (Δ), 10^{-8} M (□), 10^{-7} M (○)). The data are given as mean ± s.e.mean and are expressed as percentage of the maximal contraction to acetylcholine (10^{-5} M) obtained under control conditions (experiments with methoctramine: 2.8 ± 0.4 g, $n = 7$; experiments with 4-DAMP: 2.6 ± 0.3, $n = 6$).

dependent contraction to acetylcholine was evaluated after 60 min incubation with the antagonist. Indeed, in a previous set of experiments performed at 40 min incubation, the slope of the Arunlakshana-Schild plot was significantly greater than unity, suggesting non-equilibrium conditions.

Relaxation

Acetylcholine induced an endothelium-dependent relaxation of rings of aorta from SHR treated with indomethacin (10^{-5} M; 45 min) (Figure 3). The IC_{50} value for acetylcholine for relaxation under control conditions was 7.82 ± 0.09 ($n = 12$).

Atropine (3×10^{-9} M–3×10^{-7} M) (Figure 3), pirenzepine (10^{-6}M–10^{-5} M) (Figure 3) and 4-DAMP (10^{-9}–10^{-8} M) (Figure 4) caused parallel dextral shifts in the concentration-relaxation curve (at the linear portion of the curve) to acetylcholine, with no change in the maximal response. Methoctramine (10^{-6} M–10^{-5} M) (Figure 4) did not significantly affect the relaxation to acetylcholine. The IC_{50} values for acetylcholine under control conditions and in the presence of methoctramine (10^{-6} M, 3×10^{-6} M and 10^{-5} M) were 7.79 ± 0.13, 7.41 ± 0.13, 7.48 ± 0.12 and 7.28 ± 0.15, respectively.

The pA_2 values for the muscarinic antagonists for relaxation to acetylcholine are shown in Table 1. A pA_2 value for pirenzepine was not calculated because the slope of the Arunlakshana-Schild plot was significantly greater than unity (Table 1).

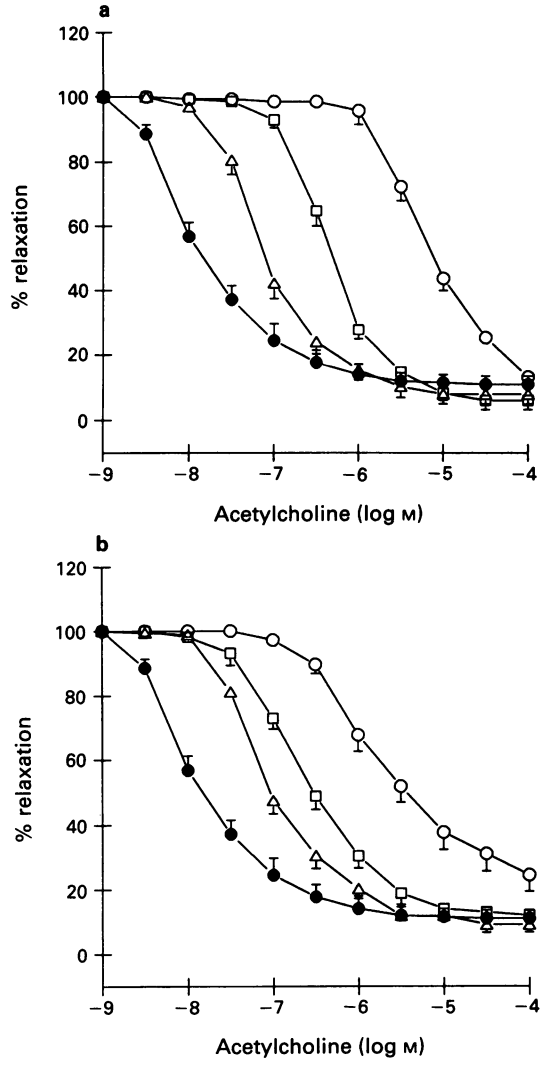

Figure 3 Effect of the non-preferential muscarinic antagonist atropine (a) and the preferential M_1 muscarinic antagonist pirenzepine (b) on the endothelium-dependent relaxation evoked by acetylcholine in the SHR rat aorta in the presence of indomethacin (10^{-5} M). The experiments were performed on parallel rings with endothelium under control conditions (●) and in the presence of either atropine (a: 3×10^{-9} M (Δ), 3×10^{-8} M (□), 3×10^{-7} M (○)) or pirenzepine (b: 10^{-6} M (Δ), 3×10^{-6} M (□), 10^{-5} M (○)). The data are given as mean ± s.e.mean and are expressed as percentage inhibition of the contraction to phenylephrine (3×10^{-8} M to 3×10^{-7} M). In the experiments with atropine (a), the contraction to phenylephrine averaged 1.6 ± 0.1 g (control), 1.4 ± 0.1 g (atropine 3×10^{-9} M), 1.5 ± 0.1 g (atropine 3×10^{-8} M) and 1.7 ± 0.2 g (atropine 3×10^{-7} M) ($n = 6$). In the set of experiments involving pirenzepine (b), the contraction evoked by phenylephrine averaged 1.6 ± 0.1 g (control), 1.8 ± 0.1 g (pirenzepine 10^{-6} M), 1.4 ± 0.1 g (pirenzepine 3×10^{-6} M) and 1.9 ± 0.3 g (pirenzepine 10^{-5} M) ($n = 6$).

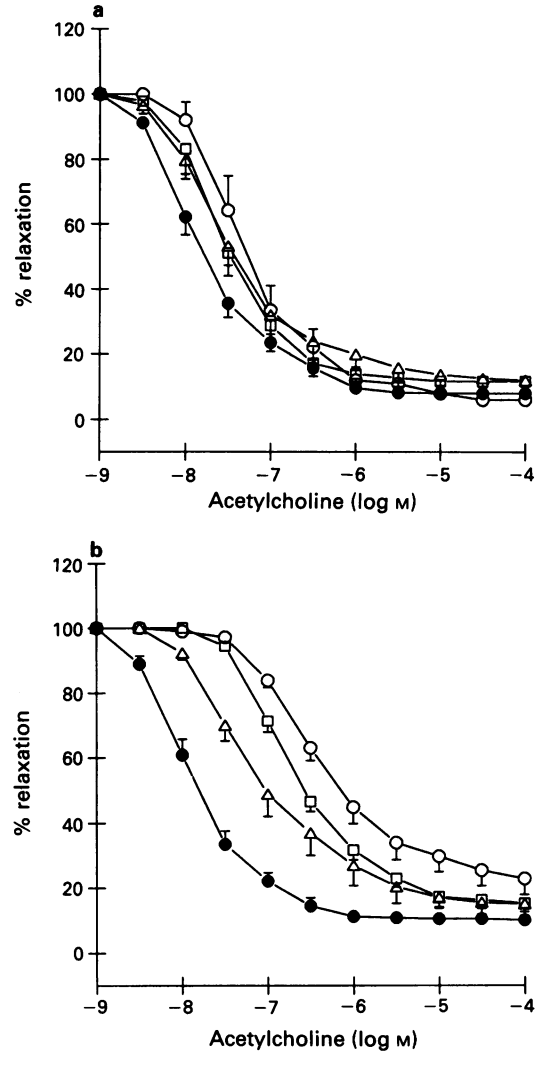

Figure 4 Effect of the preferential M_2 muscarinic antagonist methoctramine (a) and the preferential M_3 muscarinic antagonist 4-DAMP (b) on the endothelium-dependent relaxation evoked by acetylcholine in the SHR rat aorta in the presence of indomethacin (10^{-5} M). The experiments were performed on parallel rings with endothelium under control conditions (●) and in the presence of either methoctramine (a: 10^{-6} M (Δ), 3×10^{-6} M (□), 10^{-5} M (○)) or 4-DAMP (b: 10^{-9} M (Δ), 3×10^{-9} M (□), 10^{-8} M (○)). The data are given as mean ± s.e.mean and are expressed as percentage of the contraction to phenylephrine (3×10^{-8} M to 3×10^{-7} M). In the set of experiments involving methoctramine (a), the contraction induced by phenylephrine averaged 1.5 ± 0.2 g (control), 1.8 ± 0.3 g (methoctramine 10^{-6} M), 1.4 ± 0.3 g (methoctramine 3×10^{-6} M) and 1.4 ± 0.2 g (methoctramine 10^{-5} M) ($n = 6$). In the experiments with 4-DAMP (b), the contraction evoked by phenylephrine averaged 1.5 ± 0.2 g (control), 1.7 ± 0.3 g (4-DAMP 10^{-9} M),1.4 ± 0.2 g (4-DAMP 3×10^{-9} M) and 1.5 ± 0.2 g (4-DAMP 10^{-8} M) ($n = 6$).

Table 1 pA_2 values (mean ± s.e.mean of 6 observations) for muscarinic antagonist versus acetylcholine in the SHR aorta (rings with endothelium)

Antagonist	*Effect*	pA_2 ($-\log M$)	*Slope*
Atropine	Relaxation	9.15 ± 0.23	1.04
	Contraction	9.48 ± 0.07	0.99
Pirenzepine	Relaxation	–	1.71*
	Contraction	6.74 ± 0.22	1.19
Methoctramine	Relaxation	–	–
	Contraction	6.30 ± 0.20	0.83
4-DAMP	Relaxation	9.63 ± 0.28	1.02
	Contraction	9.39 ± 0.22	0.99

These parameters were obtained from Arunlakshana-Schild plot analysis when the slope of the plot was not different from unity. The asterisk denotes a slope which is significantly different from unity.

Discussion

The present results confirm that acetylcholine causes both endothelium-dependent relaxation and contraction in the aorta from SHR. These effects are mediated by activation of muscarinic receptors since atropine, a non-preferential muscarinic antagonist, displayed an 'apparent' competitive antagonism of the responses to acetylcholine. The muscarinic receptor subtype(s) that mediate(s) the endothelium-dependent contraction and relaxation to acetylcholine was characterized by use of preferential muscarinic receptor antagonists. Using functional studies, three muscarinic receptor subtypes have been identified on endothelial cells: the M_1 subtype (Komori & Suzuki, 1987; Orphanos & Catravas, 1989; Garcia-Villalon *et al.*, 1991), the M_2 subtype (Hynes *et al.*, 1986; Duckles, 1988) and the M_3 subtype (McCormack *et al.*, 1988; Duckles & Garcia-Villalon, 1990; Dauphin & Hamel, 1990; Brunner *et al.*, 1991; Jaiswal *et al.*, 1991; Garcia-Villalon *et al.*, 1991; Alonso *et al.*, 1991; Shimizu *et al.*, 1993). Each muscarinic receptor subtype may contribute to the local control of vascular reactivity.

Endothelium-dependent contraction to acetylcholine was obtained in the presence of N^G-nitro-L-arginine to negate the contribution of endothelium-derived nitric oxide (Ito *et al.*, 1991; Schini & Vanhoutte, 1992; Auch-Schwelk *et al.*, 1992). Endothelium-dependent relaxation to acetylcholine was obtained in the presence of indomethacin, to prevent the formation of vasoactive prostanoids and to abolish the effect of endothelium-derived contracting factor (Lüscher & Vanhoutte, 1986). Both responses to acetylcholine appear to be mediated by activation of the muscarinic M_3 receptor subtype. This conclusion is based on the fact that 4-DAMP, a preferential antagonist of muscarinic M_3 receptors, displays competitive antagonism of the endothelium-dependent contraction and relaxation to acetylcholine and yields for both responses a pA_2 value that is consistent with activation of an homologous population of muscarinic M_3 receptors (McCormack *et al.*, 1988; Michel *et al.*, 1989; Alonso *et al.*, 1991; 1993 Receptor Nomenclature). Although certain endothelium-dependent responses to acetylcholine are mediated by activation of M_1 or M_2 receptors (Rubanyi *et al.*, 1987; Komori & Suzuki, 1987; Orphanos & Catravas, 1989; Garcia-Villalon *et al.*, 1991), this does not appear to be the case in the SHR aorta. For example, the pA_2 value of pirenzepine for endothelium-dependent contraction to acetylcholine is consistent with activation of both M_2 and M_3 muscarinic receptor subtypes (range from 5.6 to 7.0; Eglen *et al.*, 1989; Fuder *et al.*, 1989; Van Charldorp & Van Zwieten, 1989; range 6.4 to 7.6; Duckles, 1988; Van Charldorp & Van Zwieten, 1989; Mei *et al.*, 1989), but the pA_2 for methoctramine is lower than that reported for an homologous population of M_2 muscarinic receptors (about 7.9; Michel & Whiting, 1988; Duckles & Garcia-Villalon, 1990; 1993 Receptor Nomenclature). The conclusion that M_3 muscarinic receptors mediate endothelium-dependent relaxation to acetylcholine is prompted also by the fact that pirenzepine only affects the relaxations to acetylcholine at concentrations which are at least one hundred times higher than the reported affinity of the antagonist for M_1 receptors (pA_2 8.00; 1993 Receptor Nomenclature). Furthermore, methoctramine, a preferential antagonist of muscarinic M_2 receptors, does not affect endothelium-dependent relaxation to acetylcholine, even at higher concentrations.

Methoctramine displayed different effects on endothelium-dependent contraction and relaxation to acetylcholine in the SHR aorta. Indeed, endothelium-dependent contractions to acetylcholine were reduced by methoctramine, while endothelium-dependent relaxation was not. Both the release of EDCF and the direct contractile effect of acetylcholine on smooth muscle contribute to the endothelium-dependent contraction in the present experiments. Although the direct effect of acetycholine on preparations without endothelium is too small to allow proper pharmacological identification of the receptor subtype involved, its antagonism by methoctramine could be responsible for the rightward shift of the concentration-dependent contraction to acetylcholine by the preferential M_2 muscarinic antagonist, while the release of EDCF would be mediated by activation of a M_3 receptor. However, the present experiments do not rule out the possibility that different subtypes of muscarinic M_3 receptors mediate endothelium-dependent relaxation and contraction to acetylcholine in the SHR aorta. This possibility is further supported by the fact that the release of the contractile factor occurs in response to higher concentrations of acetylcholine than are required to elicit the release of EDRF (Lüscher & Vanhoutte, 1986).

The endothelium-dependent relaxation mediated by activation of muscarinic M_3 receptors is well documented in mice and rabbit pial arteries, the rabbit aorta, the bovine coronary artery, the rat pulmonary artery and the cat cerebral artery (McCormack *et al.*, 1988; Dauphin & Hamel, 1990; Duckles & Garcia-Villalon, 1990; Alonso *et al.*, 1991; Brunner *et al.*, 1991; Garcia-Villalon *et al.*, 1991; Jaiswal *et al.*, 1991; Shimizu *et al.*, 1993). The results in these as well as the SHR rat aorta are at variance with those obtained in blood vessels such as the bovine pial artery (Garcia-Villalon *et al.*, 1991), the rabbit saphenous artery (Komori & Suzuki, 1987), the rabbit pulmonary artery (Orphanos & Catravas, 1989) and the canine femoral artery (Rubanyi *et al.*, 1987) where the M_1 subtype mediates endothelium-dependent responses to acetylcholine. Other endothelium-dependent responses to acetylcholine are caused by activation of the M_2 subtype such as in the bovine coronary artery (Duckles, 1988), the rabbit ear artery (Hynes *et al.*, 1986), the porcine cerebral artery (Van Charldorp & Van Zwieten, 1989) and the canine femoral arteries (Rubanyi *et al.*, 1987). This may reflect species heterogeneity, which is common in mammalian blood vessels (Lüscher & Vanhoutte, 1990).

In conclusion, the present results suggest that the release of both endothelium-derived contracting (EDCF) and relaxing (EDRF) factors upon stimulation with acetylcholine is mediated by activation of M_3 muscarinic receptors in the SHR aorta.

The authors wish to thank Barnabas Desta, Nusret Didzik and Shawn Latta for their technical assistance and Joanna Bale for secretarial help. This work was supported, in part, by a grant from the National Institute of Health (HL 35614) and a Grant-in-Aid from the 'Institut de Recherches Internationales Servier', Paris (F).

References

ALONSO, M.J., ARRIBAS, S., MARIN, J., BALFAGON, G. & SALAICES, M. (1991). Presynaptic M_2-muscarinic receptors on noradrenergic nerve endings and endothelium-derived M_3 receptors in cat cerebral arteries. *Brain Res.*, **567**, 76–82.

ARUNLAKSHANA, O. & SCHILD, O.H. (1959). Some quantitative uses of drug antagonists. *Br. J. Pharmacol. Chemother.*, **14**, 48–58.

AUCH-SCHWELK, W., KATUSIC, Z.S. & VANHOUTTE, P.M. (1990). thromboxane A_2 receptor antagonists inhibit endothelium-dependent contractions. *Hypertension*, **15**, 699–703.

AUCH-SCHWELK, W., KATUSIC, Z.S. & VANHOUTTE, P.M. (1992). Nitric oxide inactivates endothelium-derived contracting factor in the rat aorta. *Hypertension*, **19**, 442–445.

BASSENGE, E. & HEUSCH, G. (1990). Endothelial and neuro-humoral control of coronary blood flow in health and disease. *Rev. Physiol. Biochem. Pharmacol.*, **116**, 77–165.

BRUNNER, F., KÜHBERGER, E., GROSCHNER, K., POCH, G. & KULOVETZ, W.R. (1991). Characterization of muscarinic receptors mediating endothelium-dependent relaxation of bovine coronary artery. *Eur. J. Pharmacol.*, **200**, 25–33.

CHEN, G., SUZUKI, H. & WESTON, A.H. (1988). Acetylcholine releases endothelium-derived hyperpolarizing factor and EDRF from rat blood vessels. *Br. J. Pharmacol.*, **95**, 1165–1174.

DAUPHIN, F. & HAMEL, E. (1990). Muscarinic receptor subtype mediating vasodilatation in feline middle cerebral artery exhibits M_3 pharmacology. *Eur. J. Pharmacol.*, **178**, 203–213.

DUCKLES, S.P. (1988). Vascular muscarinic receptors: pharmacological characterization in the bovine coronary artery. *J. Pharmacol. Exp. Ther.*, **246**, 929–934.

DUCKLES, S.P. & GARCIA-VILLALON, A.L. (1990). Characterization of vascular muscarinic receptors: rabbit ear artery and bovine coronary artery. *J. Pharmacol. Exp. Ther.*, **253**, 608–613.

EGLEN, R.M., MICHEL, A.D. & WHITING, R.L. (1989). Characterization of the muscarinic receptor subtype mediating contractions of the guinea-pig uterus. *Br. J. Pharmacol.*, **96**, 497–499.

FUDER, H., SCHOPF, J., UNCKELL, J., WESNER, J., MELCHIORRE, C., TACKE, R.M., MUTSCHLER, E. & LAMBRECHT, G. (1989). Different muscarinic receptors mediate the prejunctional inhibition of [^{3}H]-noradrenaline release in rat or guinea-pig iris and the contraction of the rabbit iris sphincter muscle. *Naunyn-Schmied. Arch. Pharmacol.*, **340**, 597–604.

FURCHGOTT, R.F. & VANHOUTTE, P.M. (1989). Endothelium-derived relaxing and contracting factors. *FASEB J.*, **3**, 2007–2018.

FURCHGOTT, R.F. & ZAWADZKI, J.V. (1980). The obligatory role of endothelial cells in the relaxation of arterial smooth muscle by acetylcholine. *Nature*, **299**, 373–376.

GARCIA-VILLALON, A.L., KRAUSE, D.N., EHLERT, F.J. & DUCKLES, S.P. (1991). Heterogeneity of muscarinic receptor subtype in cerebral blood vessels. *J. Pharmacol. Exp. Ther.*, **258**, 304–310.

HYNES, M.R., BANNER, W., YAMAMURA, H.I. & DUCKLES, S.P. (1986). Characterization of muscarinic receptors of the rabbit ear artery smooth muscle and endothelium. *J. Pharmacol. Exp. Ther.*, **238**, 100–105.

ITO, T., KATO, T., IWAMA, Y., MURAMATSU, M., SHIMIZU, K., ASANO, H., OKUMURA, K., HASHIMOTO, H. & SATAKE, T. (1991). Prostaglandin H_2 as an endothelium-derived contracting factor and its interaction with endothelium-derived nitric oxide. *J. Hypertension*, **9**, 729–736.

JAISWAL, N., LAMBRECHT, G., MUTSCHLER, E., TACKE, R. & MALIK, K.U. (1991). Pharmacological characterization of the vascular muscarinic receptors mediating relaxation and contraction in rabbit aorta. *J. Pharmacol. Exp. Ther.*, **258**, 842–850.

KOMORI, K. & SUZUKI, H. (1987). Heterogeneous distribution of muscarinic receptors in the rabbit saphenous artery. *Br. J. Pharmacol.*, **92**, 657–664.

LÜSCHER, T.F. & VANHOUTTE, P.M. (1986). Endothelium-dependent contractions to acetylcholine in the aorta of the spontaneously hypertensive rat. *Hypertension*, **8**, 344–348.

LÜSCHER, T.F. & VANHOUTTE, P.M. (1990). Endothelium-derived relaxing factor. In *The Endothelium: Modulator of Cardiovascular Function*. ed. Lüscher, T.F. & Vanhoutte, P.M. pp. 23–43. Boca Raton: CRC Press.

MCCORMACK, D.G., MAK, J.C., MINETTE, P. & BARNES, P.J. (1988). Muscarinic receptor subtypes mediating vasodilation in the pulmonary artery. *Eur. J. Pharmacol.*, **158**, 293–297.

MEI, L., ROESKE, W.R. & YAMAMURA, H.I. (1989). Molecular pharmacology of muscarinic receptor heterogeneity. *Life Sci.*, **45**, 1831–1851.

MICHEL, A.S., STEFANICH, E. & WHITING, R.L. (1989). Direct labelling of rat M_3-muscarinic receptors by [^{3}H]4DAMP. *Eur. J. Pharmacol.*, **166**, 459–466.

MICHEL, A.S. & WHITING, R.L. (1988). Methoctramine, a polymethylene tetramine, differentiates three subtypes of muscarinic receptors in direct binding studies. *Eur. J. Pharmacol.*, **145**, 61–66.

MONCADA, S., PALMER, R.M.J. & HIGGS, E.A. (1991). Nitric oxide: physiology, pathophysiology and pharmacology. *Pharmacol. Rev.*, **43**, 109–142.

ORPHANOS, S.E. & CATRAVAS, J.D. (1989). Muscarinic receptor subtype (M_1) identification on rabbit pulmonary vascular endothelium *in vivo*. *Pharmacology*, **39**, 253–264.

RUBANYI, G.M., MCKINNEY, M. & VANHOUTTE, P.M. (1987). Biphasic release of endothelium-derived relaxing factor(s) by acetylcholine from perfused canine femoral arteries. Characterization of muscarinic receptors. *J. Pharmacol. Exp. Ther.*, **240**, 802–808.

SCHINI, V.B. & VANHOUTTE, P.M. (1992). Inhibitors of calmodulin impair the constitutive but not the inducible nitric oxide synthase activity in the rat aorta. *J. Pharmacol. Exp. Ther.*, **261**, 553–559.

SHIMIZU, T., ROSENBLUM, W.I. & NELSON, G.H. (1993). M_3 and M_1 receptors in cerebral arterioles in vivo: evidence for down-regulated or ineffective M_1 when endothelium is intact. *Am. J. Physiol.*, **264**, (*Heart Circ. Physiol.*, **33**): 665–669.

VAN CHARLDORP, K.J. & VAN ZWIETEN, P.A. (1989). Comparison of the muscarinic receptors in the coronary artery, cerebral artery and atrium of the pig. *Naunyn-Schmied. Arch. Pharmacol.*, **339**, 403–408.

YANAGISAWA, M. & MASAKI, T. (1989). Endothelin, a novel endothelium-derived peptide. *Biochem. Pharmacol.*, **38**, 1877–1883.

1993 Receptor Nomenclature Supplement, *Trends Pharmacol. Sci.*, **14**.

(Received December 29, 1993
Revised March 2, 1994
Accepted March 4, 1994)

Br. J. Pharmacol. (1994), **112**, 525–532

Pilocarpine-induced relaxation of rat tail artery by a non-cholinergic mechanism and in the absence of an intact endothelium

M.A. Tonta, [1]Helena C. Parkington, M. Tare & H.A. Coleman

Department of Physiology, Monash University, Clayton, Victoria 3168, Australia

1 The partial muscarinic agonist, pilocarpine, evoked concentration-dependent relaxation with an EC_{50} of 2.4×10^{-3} M in isolated segments of rat tail artery that were constricted with phenylephrine (10^{-8} to 2×10^{-7} M). Acetylcholine also evoked concentration-dependent relaxation but was more potent than pilocarpine (EC_{50}, 6.5×10^{-7} M).

2 The concentration-relaxation curves for pilocarpine were not affected by the muscarinic antagonists, atropine (10^{-9} M) or pirenzepine (5×10^{-7} M), while the concentration-relaxation curves for acetylcholine-evoked relaxation of the same tissues were shifted some 10 fold to the right by these concentrations of atropine and pirenzepine.

3 Acetylcholine failed to evoke relaxation following removal of the endothelium. The smooth muscle of the rat tail artery was some 10 fold more sensitive to the relaxing action of pilocarpine following denudation of the endothelium.

4 The effects of pilocarpine and acetylcholine on membrane potential were studied in tissues that were depolarized to -39 ± 1 mV with phenylephrine (5×10^{-8} to 2×10^{-7} M). In intact tissues, pilocarpine caused hyperpolarization, an effect that persisted in the presence of muscarinic antagonists. Acetylcholine also evoked hyperpolarization.

5 Following removal of the endothelium, pilocarpine (10^{-5} to 10^{-3} M) evoked hyperpolarization in 6 of 15 preparations and a decrease in the frequency of action potentials in the remainder. Both of these responses were associated with relaxation.

6 The effects of pilocarpine were compared with other agents that evoke endothelium-independent relaxation. The concentration-relaxation curves in response to pilocarpine and nitroprusside were shifted to the right by ferricyanide (10^{-5} M) and methylene blue (10^{-5} M). Glibenclamide (10^{-6} M) was without effect on the hyperpolarization and relaxation evoked by pilocarpine (10^{-4} to 10^{-3} M).

7 Thus, pilocarpine evokes relaxation of rat tail artery independently of the cholinergic system and it is suggested that this is achieved by decreasing the frequency of action potentials in the smooth muscle.

Keywords: Pilocarpine; endothelium; artery; relaxation; hyperpolarization; acetylcholine; nitroprusside; isoprenaline; cromakalim; smooth muscle

Introduction

Muscarinic agonists, such as acetylcholine, act on the endothelial cells of intact arteries to stimulate the release of factors that relax the underlying smooth muscle (Furchgott & Zawadski, 1980; Bolton *et al.*, 1984; Komori & Suzuki, 1987; Chen *et al.*, 1988; Feletou & Vanhoutte, 1988). More than one factor may be released from the endothelium. It is well established that endothelium-derived nitric oxide (NO) (Ignarro *et al.*, 1987; Palmer *et al.*, 1987; Furchgott, 1988) and prostacyclin (Moncada *et al.*, 1977; Lee *et al.*, 1990) relax arterial smooth muscle, and the hyperpolarization evoked by endothelium-derived hyperpolarizing factor (EDHF) (Chen *et al.*, 1988) would be expected to facilitate relaxation. The same type of muscarinic receptor is not necessarily involved in the release of the different endothelium-derived relaxing factors. Thus, activation of M_1 receptors is thought to be involved in the release of EDHF (Komori & Suzuki, 1987; Chen *et al.*, 1988), while M_2 receptors are coupled to the release of NO (Komori & Suzuki, 1987) and prostacyclin (Jaiswal & Malik, 1990).

Stimulation of the muscarinic receptors that are present on vascular smooth muscle cells most often results in contraction (Furchgott & Zawadski, 1980) and this is the predominant response to muscarinic agents in arteries denuded of their endothelium. However, Bolton and colleagues (1984) have described carbachol-induced relaxation of mesenteric arteries but not aortae, in the absence of endothelium. The type of muscarinic receptor involved was not identified.

The partial muscarinic agonist, pilocarpine, has been used to increase blood flux in the finger in human subjects (Lindblad, L-E., Westerman, R.A. & Wajnblum, D., personal communication). The drug was applied iontophoretically through the skin during measurement of blood flux with a laser doppler device. The site of action of the pilocarpine was unclear. It is likely that the laser doppler measured blood flux in the superficial blood vessels supplying the skin. Such vessels are likely to be influenced by temperature. In this study we used the tail artery from rats, a vessel that is involved in thermoregulation, to compare the effects of pilocarpine and acetylcholine and to investigate whether or not pilocarpine-induced vasorelaxation depended upon the presence of an intact endothelium.

Methods

Sprague-Dawley rats of either sex were decapitated and ring segments, 1–2 mm in length, of the ventral tail artery were isolated. Each segment was mounted on a myograph which allowed simultaneous recording of membrane potential and tension development (Parkington *et al.*, 1993). The tissues were continuously superfused with physiological saline solu-

[1] Author for correspondence.

tion containing (mM): NaCl 120, KCl 5, $CaCl_2$ 2.5, KH_2PO_4 1, $MgSO_4$ 1.2, $NaHCO_3$ 25 and glucose 11; at 29°C and gassed with 95% O_2 and 5% CO_2. The endothelium was removed as required (see Results) with a roughened wire. The success of the procedure was verified by the failure of acetylcholine to evoke relaxation of a contraction induced by phenylephrine. The tissues were stretched in increments until the transmural pressure was equivalent to 70–80 mmHg (the mean blood pressure in rats). Intracellular impalements were made from the adventitial surface using microelectrodes filled with 1 M KCl and having resistances of 80–120 MΩ.

For most experiments, acetylcholine, pilocarpine, nitroprusside, cromakalim and isoprenaline were injected for 10 s directly into the perfusion line. With this method the concentration of drug reached steady state at the tissue within 3–5 s (Parkington *et al.*, 1993). In some experiments, pilocarpine was added to the superfusate and was applied to the tissue for 1 min. Atropine, pirenzepine, N^{ω}-nitro-L-arginine methyl ester (L-NAME), ferricyanide, methylene blue and glibenclamide were added to the superfusate as described in Results.

Glibenclamide and cromakalim were kind gifts from Hoechst and Beecham, respectively. All other drugs were purchased from Sigma Chemicals (U.S.A.).

Active tension was raised in most preparations by adding phenylephrine to the superfusate. The maximal contractile capacity was determined for each tissue at the beginning of the day, using exposure to 10^{-5} M phenylephrine for 2 min. The phenylephrine was then washed out and the tissue was allowed to recover for 30 min. For all subsequent procedures, the concentration of phenylephrine in the superfusate was chosen to achieve a contraction that was approximately 30% of maximal. For some experiments (see Results) the thromboxane-mimetic, U46619 (15S)-hydroxy-11α,9α-(epoxymethano) prosta-5Z,13E-dienoic acid), was used instead of phenylephrine.

Concentration-relaxation curves were obtained by expressing the maximum amplitude of the relaxation as a % of the contraction evoked by phenylephrine. A sigmoid curve was fitted to these data using the least squares method, with the aid of the computer software package InPlot (GraphPad Inc.). The concentration of relaxant which was effective in producing a response that was 50% of maximal (EC_{50}) was determined. The statistic quoted with each mean is the standard error based on the number of animals used. A *t* test was used to test for significant differences between the values of EC_{50}. A significance level of $P<0.05$ was used throughout.

Results

Effect of pilocarpine and acetylcholine on the contraction evoked by phenylephrine

Phenylephrine, 10^{-8} to 2×10^{-7} M, constricted ring segments of rat tail artery to approximately 30% of maximal. Application of pilocarpine for 10 s caused concentration-dependent relaxation of this contraction (Figure 1). The relaxations evoked by 1 min exposure to lower concentrations of pilocarpine were similar in amplitude to those in response to 10 s application, but were appropriately longer in duration (Figure 2). At concentrations of approximately 3×10^{-3} M and above, the amplitude of the relaxation was larger when pilocarpine was applied for 60 s compared with 10 s (Figure 2).

The EC_{50} for the relaxation in response to 10 s application of pilocarpine was 2.4×10^{-3} M (pD_2, 2.62 ± 0.03, $n = 7$). This response was not affected by 10^{-9} M of the general

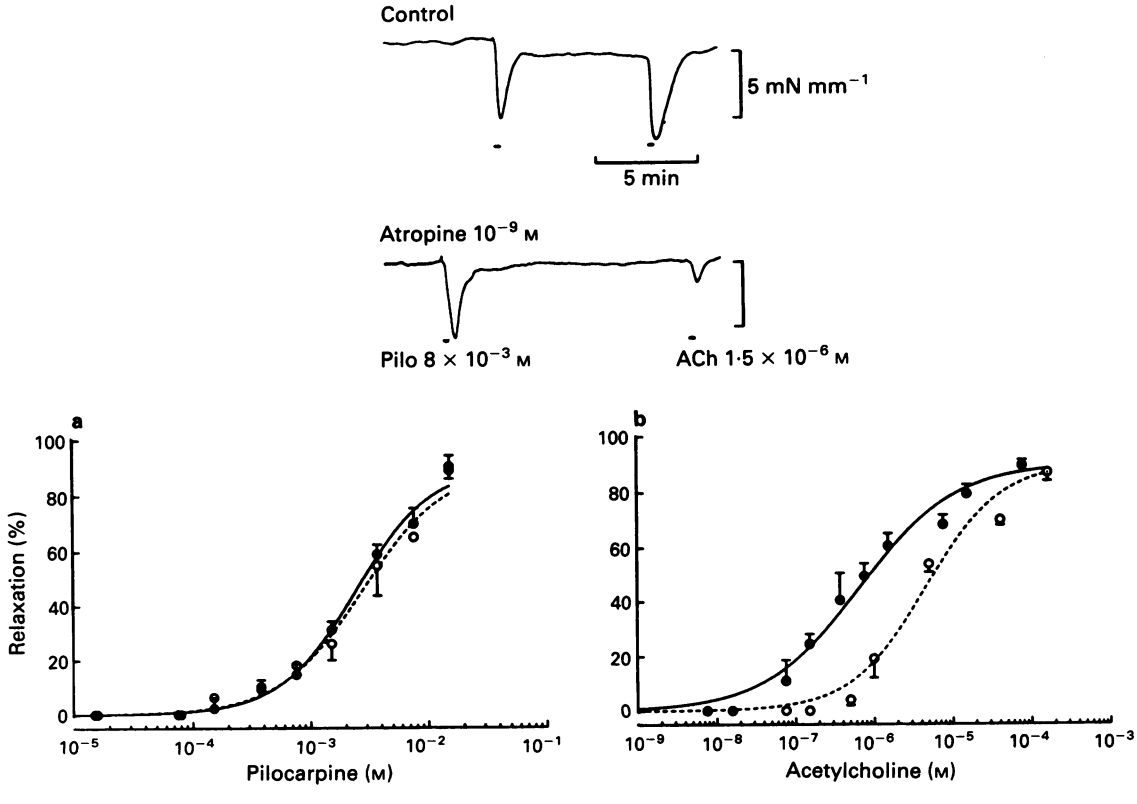

Figure 1 Pilocarpine (Pilo) and acetylcholine (ACh) evoked concentration-dependent relaxation of intact segments of rat tail artery that were constricted with phenylephrine (5×10^{-8} M). The EC_{50} for the relaxation evoked in 7 preparations of rat tail artery by pilocarpine (a) was 2.4×10^{-3} M (pD_2 2.62 ± 0.03) and was unaffected by 10^{-9} M atropine (EC_{50}, 2.7×10^{-3} M; pD_2, 2.57 ± 0.04). The EC_{50} for acetylcholine-evoked relaxation (b) was 6.5×10^{-7} M in control (pD_2, 6.19 ± 0.06) and was increased to 4.5×10^{-6} M by 10^{-9} M atropine (pD_2, 5.36 ± 0.08). In both (a) and (b): (●) control; (○) atropine 10^{-9} M.

muscarinic antagonist, atropine (EC_{50}, 2.7×10^{-3} M; pD_{20} 2.57 ± 0.04, $n = 7$) (Figure 1). Pirenzepine, another muscarinic antagonist also failed to block the relaxation induced by pilocarpine. In this series of experiments the EC_{50} for pilocarpine was 4.0×10^{-3} M (pD_2, 2.40 ± 0.03, $n = 5$) in control solution and was 4.9×10^{-3} M and 5.4×10^{-3} M in pirenzepine 10^{-7} M and 5×10^{-7} M, respectively (pD_2, 2.31 ± 0.03 and 2.27 ± 0.05, $n = 5$) (Figure 3). Acetylcholine also relaxed segments of rat tail artery. The EC_{50} for this response was 6.5×10^{-7} M (pD_2, 6.19 ± 0.06, $n = 7$) in control solution and this was increased to 4.5×10^{-6} M (pD_2, 5.36 ± 0.08, $n = 7$) by atropine (10^{-9} M) (Figure 1). In another series of experiments the EC_{50} for acetylcholine-evoked relaxation was increased from 5.2×10^{-7} M (pD_2, 6.28 ± 0.06, $n = 5$) in control to 2.3×10^{-6} M (pD_2, 5.64 ± 0.16, $n = 5$) in 10^{-7} M pirenzepine and to 6.5×10^{-6} M (pD_2, 5.18 ± 0.13, $n = 5$) in 5×10^{-7} M pirenzepine (Figure 3).

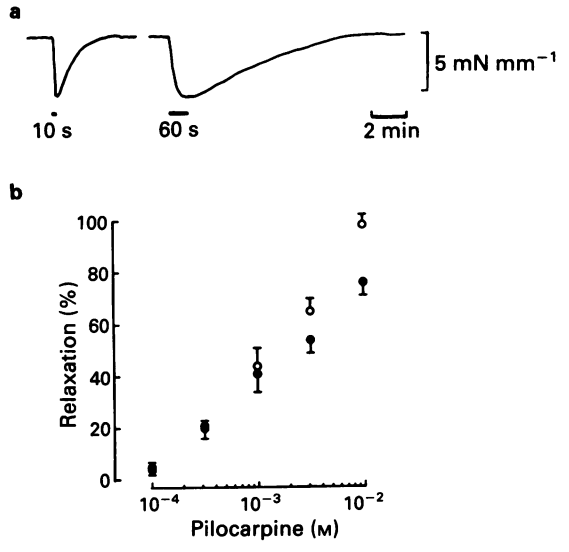

Figure 2 (a) An example of the effects of 10^{-3} M pilocarpine, applied for 10 and 60 s, on the contraction evoked by 10^{-7} M phenylephrine. (b) The amplitudes of the relaxation evoked in 3 preparations by concentrations of 10^{-3} M pilocarpine or below were not different whether they were applied at close range for 10 s (●) or included in the superfusate for 60 s (○), although the responses to the latter mode of exposure were of longer duration. The responses evoked by larger concentrations of pilocarpine were larger in amplitude when applied for 60 s than for 10 s.

Role of the endothelium

The apparent lack of effectiveness of muscarinic antagonists in blocking pilocarpine-evoked relaxation was puzzling, and prompted us to question the role of the endothelium in the response. Accordingly, the effects of pilocarpine and acetylcholine on the contraction evoked by phenylephrine were examined in segments of tail artery from 6 rats before and after removal of the endothelium. Acetylcholine failed to relax denuded segments, even at increased concentrations (Figure 4a). In contrast, pilocarpine continued to evoke relaxation following removal of the endothelium (Figure 4a). The EC_{50} of 1.5×10^{-4} M (pD_2, 3.82 ± 0.06) for pilocarpine-induced relaxation in 12 denuded preparations (those used as the controls in testing the effects of ferricyanide and methylene blue, see below) was some 10 fold shifted to the left compared with the EC_{50} of 2.4×10^{-3} M (pD_2, 2.62 ± 0.03) in 7 intact tissues (those used in the studies of the effects of atropine, see above) (Figure 4b).

In view of the resistance of pilocarpine-induced relaxation to both muscarinic antagonists and the integrity of the endothelium, the possibility was considered that the response to pilocarpine might be due to an antagonism of the constriction evoked by phenylephrine. Five tissues, denuded of endothelium, were superfused with 3×10^{-9} or 10^{-8} M of the thromboxane-mimetic, U46619, which produced similar levels of constriction to phenylephrine. Pilocarpine caused relaxation of the constriction evoked by U46619 that was indistinguishable from its effects when phenylephrine was used to constrict (not shown).

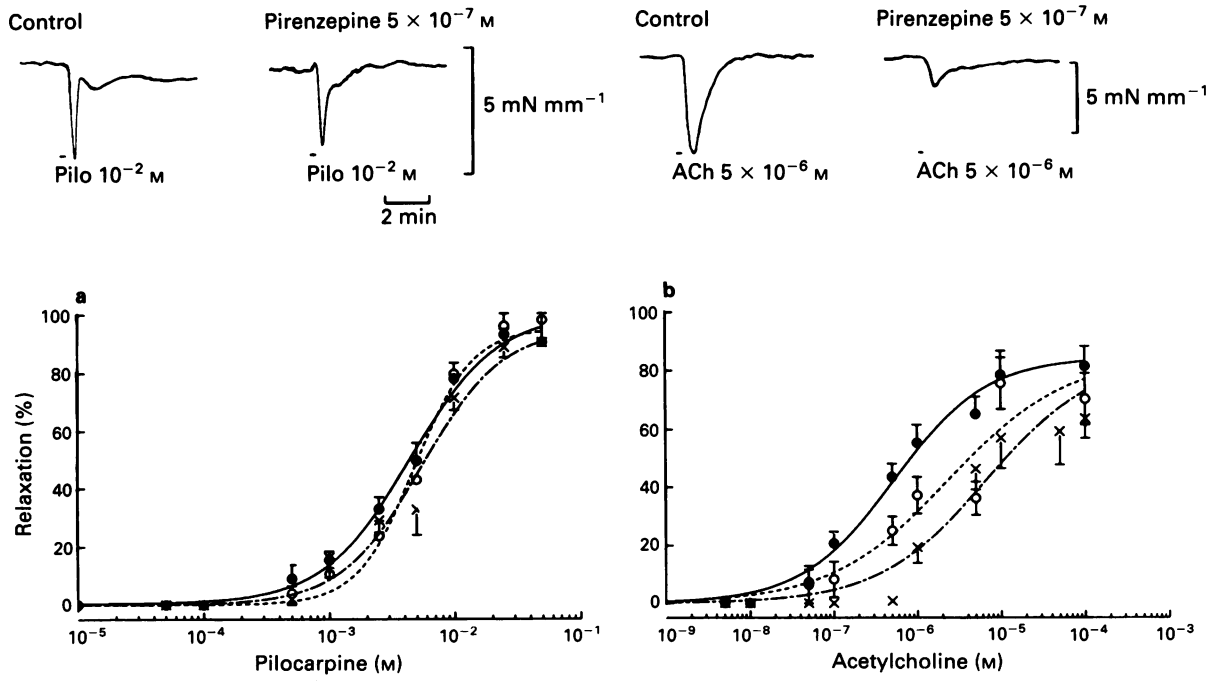

Figure 3 (a) Pilocarpine (Pilo)-induced relaxation in 5 preparations of rat tail artery (pD_2, 2.40 ± 0.03) was unaffected by pirenzepine (pD_2, 2.31 ± 0.03 and 2.27 ± 0.05 in 10^{-7} (○) and 5×10^{-7} M (X) pirenzepine, respectively); (●) control. (b) The relaxation evoked by acetylcholine (ACh) (EC_{50}, 5.2×10^{-7} M; pD_2, 6.28 ± 0.06) was progressively reduced by pirenzepine at 10^{-7} M (○) (EC_{50}, 2.3×10^{-6} M; pD_2, 5.64 ± 0.16) and 5×10^{-7} M (X) (EC_{50}, 6.5×10^{-6} M, pD_2, 5.18 ± 0.13); (●) control.

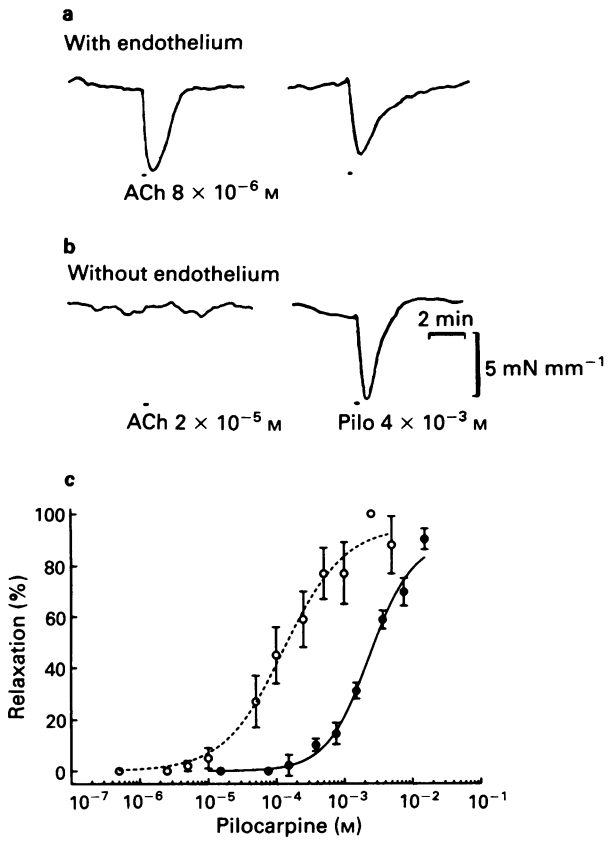

Figure 4 (a) Shows that both pilocarpine (Pilo) and acetylcholine (ACh) caused relaxation of rat tail artery with endothelium intact and constricted with phenylephrine (10^{-8} M). (b) Acetylcholine failed to relax the same preparation following removal of the endothelium, while pilocarpine continued to be effective in evoking relaxation. (c) In tissues from which the endothelium had been removed (the 12 tissues used to test the effects of ferricyanide (see Figure 8) and methylene blue (Figure 9)), the sensitivity to pilocarpine was significantly increased (EC_{50}, 1.5×10^{-4} M; pD_2, 3.82 ± 0.06) compared with the relaxation evoked in intact tissues (EC_{50}, 2.40×10^{-3} M; pD_2, 2.62 ± 0.03) the 7 tissues used when testing atropine, (see Figure 1): (●) with endothelium; (○) without endothelium.

It is now well established that nitric oxide (NO) is an important vasorelaxant produced by the vascular endothelium and the production of NO by vascular smooth muscle cells has also been described more recently (Schini & Vanhoutte, 1991). N^{ω}-nitro-L-arginine methyl ester (L-NAME) competes with L-arginine and reduces the biosynthesis of NO. Segments of intact tail artery from 7 rats were treated with L-NAME (2×10^{-5} M) for 20 min before and during application of pilocarpine. The relaxation evoked by application of 3×10^{-3} to 3×10^{-4} M pilocarpine was resistant to L-NAME. For example, the relaxation evoked by 3×10^{-3} M pilocarpine was $53 \pm 4\%$ in control and $53 \pm 5\%$ in L-NAME.

Vascular endothelium may also release the potent vasodilator prostaglandin, prostacyclin. In order to eliminate production of prostacyclin by either the endothelium or the smooth muscle cells, tissues from 4 rats were incubated with indomethacin (10^{-6} M) 20 min prior to and during application of pilocarpine. The relaxation in response to 3×10^{-3} M pilocarpine in control was $52 \pm 3\%$ and was $53 \pm 4\%$ in indomethacin.

Effects of pilocarpine on membrane potential

In order to gain further insights into the possible mechanisms whereby pilocarpine caused relaxation, membrane potential and tension were measured simultaneously in segments of rat tail artery. The membrane potential recorded from the smooth muscle cells of intact preparations at rest was -68 ± 1 mV ($n = 15$). Apart from spontaneous excitatory junction potentials, which were not associated with tension development, there were no fluctuations in membrane potential, and hence membrane potential was stable. Neither pilocarpine (10^{-4} to 10^{-2} M) nor acetylcholine (10^{-8} to 10^{-6} M) had any effect on membrane potential in 4 of these tissues at rest. The tension developed in preparations of rat tail artery resulting from stretching on the myograph was purely passive, and hence neither pilocarpine nor acetylcholine had an effect on tension at rest.

Inclusion of phenylephrine (5×10^{-8} M to 2×10^{-7} M) in the superfusing solution depolarized the membrane to -39 ± 1 mV ($n = 11$). The depolarization was not stable, and shallow oscillations occurred that consisted of peaks and troughs that were associated with phasic oscillations in tension (Figure 5). Application of pilocarpine to intact segments

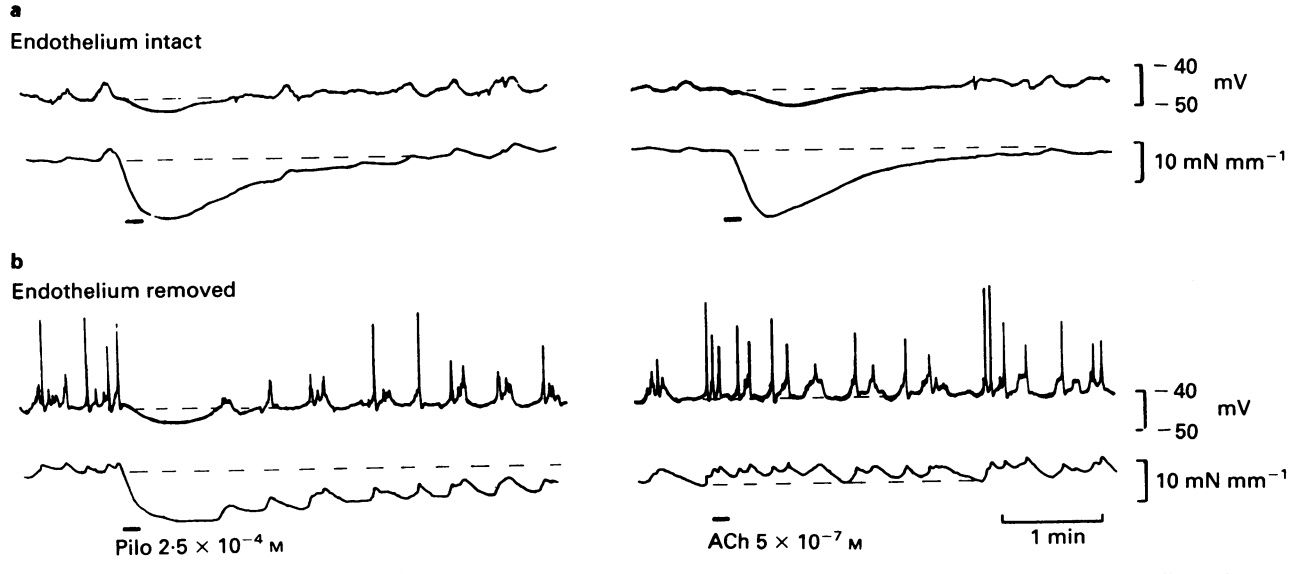

Figure 5 (a) Phenylephrine (5×10^{-8} M) depolarized intact segments of rat tail artery to approximately -39 mV. Pilocarpine (Pilo) and acetylcholine (ACh) both evoked repolarization and relaxation. (b) In segments without endothelium the oscillations in membrane potential evoked by phenylephrine were usually topped with slow action potentials of varying amplitudes. Pilocarpine evoked repolarization, reduced the frequency of action potentials and relaxed the tissue following removal of the endothelium. Acetylcholine failed to affect membrane potential or tension in segments denuded of endothelium.

for 10 s resulted in the disappearance of the oscillations in the membrane potential, hyperpolarization of up to 5 mV negative of the level of the troughs, and relaxation (Figure 5). In 3 tissues, hyperpolarization that was 3.7 ± 0.8 mV in control was 3.9 ± 0.6 mV in the presence of atropine. Acetylcholine similarly abolished oscillations and evoked hyperpolarization and relaxation in these tissues (Figure 5).

Removal of the endothelium

Following removal of the endothelium the resting potential was − 66 ± 2 mV ($n = 15$). In the presence of phenylephrine, the oscillations in membrane potential became more pronounced with troughs at − 43 ± 1 mV and peaks at − 40 ± 1 mV ($n = 15$). Slow, stunted action potentials of varying amplitudes usually occurred on the peaks of the oscillations. A phasic increase in tension was associated with each group of action potentials. Relaxation accompanied the brief cessations in action potential activity (Figures 5 and 6).

Pilocarpine abolished the action potentials, evoked hyperpolarization negative to the level of the troughs and produced relaxation (Figure 5). In contrast, acetylcholine never caused relaxation following removal of the endothelium and action potential activity was uninterrupted (Figure 5) or increased in frequency when the concentration of acetylcholine was increased to 10^{-3} M.

The effects of pilocarpine on membrane potential were difficult to quantify. The reasons can be appreciated from Figure 6, which shows the responses to increasing concentrations of pilocarpine in two endothelium-denuded preparations. At concentrations of less than approximately 10^{-5} M, pilocarpine was without effect on either membrane potential or tension in either of the tissues. At 2.5×10^{-5} M pilocarpine, the frequency of action potentials was decreased and this was associated with relaxation. Hyperpolarization was not observed in either tissue. In the responses illustrated in Figure 6a, higher concentrations of pilocarpine caused hyperpolarization, up to a maximum of 7 mV negative to the level of the troughs, and relaxation. This type of response was observed in 6 out of the 15 tissues studied.

Relaxation also occurred in another 5 of the 15 tissues, although hyperpolarization negative to the level of the troughs was absent (Figure 6b). In these tissues the decrease in tension was associated with a decrease in the frequency of

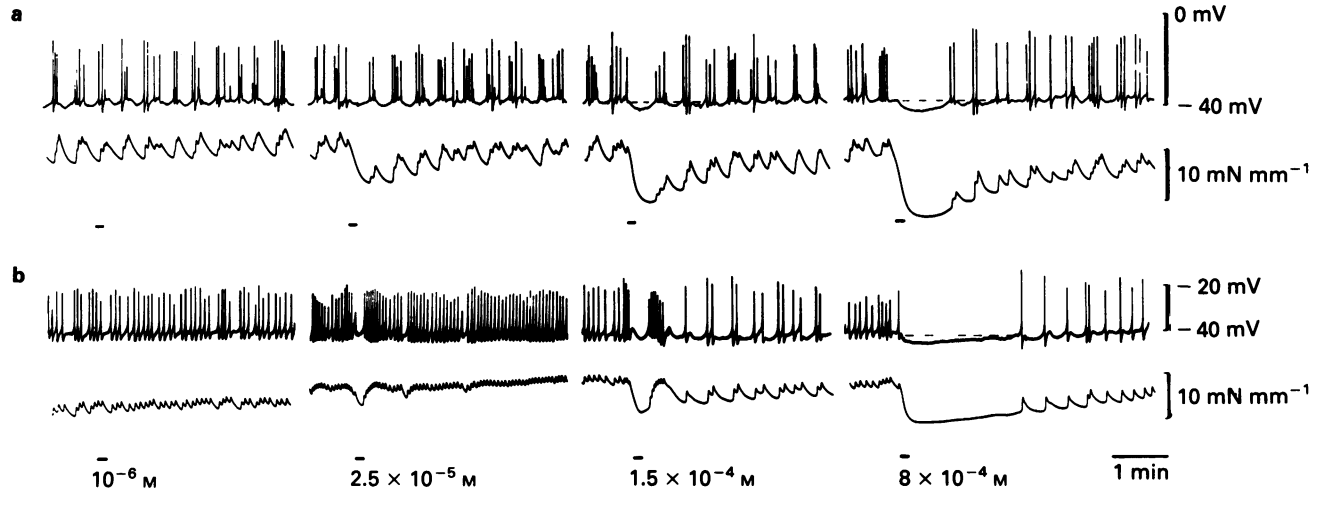

Figure 6 Examples of the effects of various concentrations of pilocarpine on membrane potential and tension in 2 preparations of rat tail artery denuded of endothelium and depolarized and constricted with phenylephrine (a, 3×10^{-8} M; b, 2.5×10^{-8} M). Pilocarpine (10^{-6} M) had no effect (a and b). At 2.5×10^{-5} M pilocarpine, the frequency of spike action potentials was decreased (a and b). In (a) 1.5×10^{-4} M pilocarpine repolarized the membrane, while this concentration reduced the frequency of action potentials in (b). At 8×10^{-4} M, pilocarpine evoked a larger repolarization in (a) and decreased the frequency of action potentials further in (b).

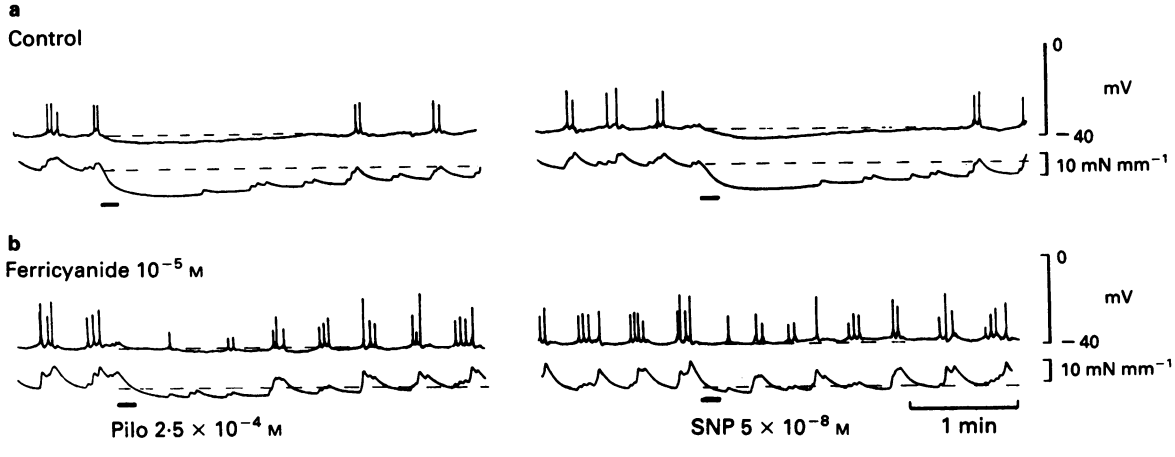

Figure 7 (a) In a segment of rat tail artery denuded of endothelium and depolarized and constricted with phenylephrine (3×10^{-8} M), pilocarpine (Pilo) and sodium nitroprusside (SNP) evoked repolarization negative to the troughs in the oscillations, cessation of action potentials and relaxation. (b) These responses to both agonists were markedly reduced by potassium ferricyanide.

spikes. In the remaining 4 of the 15 tissues an intermediate few mV of hyperpolarization occurred but the principal response was a decrease in the frequency of action potentials.

Comparison with other vasorelaxants

Since pilocarpine appeared capable of relaxing the rat tail artery in the absence of the endothelium, its effects on membrane potential and tension were compared with other agents that cause direct relaxation of vascular smooth muscle. Thus, in all subsequent experiments the segments of artery were denuded of endothelium, prior to stretching, to ensure that exogenously applied agents did not evoke the release of endogenous vasorelaxants that could contribute to the responses. The denuded preparations were then rested for 1 h before being stretched and continuously superfused with phenylephrine. Phenylephrine evoked oscillations in membrane potential and the peaks of the depolarizations were topped with small, slow action potentials and increased tension as described above. Every tissue was tested with acetylcholine to ensure that no functional endothelium remained.

Nitroprusside

Nitroprusside is thought to release NO and increase guanosine 3':5'-cyclic monophosphate (cyclic GMP) in vascular smooth muscle cells which causes relaxation that is independent of the integrity of the endothelium (Ignarro & Kadowitz, 1985; Waldman & Murad, 1987). In 8 preparations of rat tail artery, denuded of endothelium, pilocarpine and nitroprusside both caused cessation of the action potentials, hyperpolarization negative to the level of the troughs and relaxation (Figure 7). NO is oxidised by ferricyanide (Murad *et al.*, 1978). The hyperpolarization and relaxations induced by pilocarpine (10^{-4} to 10^{-3} M) and nitroprusside (3×10^{-8} to 10^{-7} M) were markedly attenuated by incubation for 10 min in potassium ferricyanide (10^{-5} M) (Figure 7). In 4 preparations the hyperpolarization evoked by 2.5×10^{-4} M pilocarpine was 4.6 ± 0.5 mV and this was reduced to 1.9 ± 0.4 mV by ferricyanide. In 8 preparations, the EC_{50} for the concentration-relaxation curve for pilocarpine was increased from 1.5×10^{-4} M (pD_2, 3.82 ± 0.06) in control to 2.3×10^{-3} M (pD_2, 2.64 ± 0.03) in 10^{-5} M ferricyanide, while the response to nitroprusside was shifted from 3.3×10^{-8} M (pD_2, 7.48 ± 0.02) to 1×10^{-6} M (pD_2, 6.00 ± 0.06) by ferricyanide (Figure 8).

Methylene blue

Soluble guanylate cyclase is thought to be blocked by methylene blue (Ignarro & Kadowitz, 1985; Waldman & Murad, 1987) and its effects on the relaxation evoked by pilocarpine and nitroprusside were studied in 4 preparations. Following 30 min incubation in methylene blue (10^{-5} M), the EC_{50} for the relaxation evoked by nitroprusside was significantly increased from 3.3×10^{-8} M (pD_2, 7.48 ± 0.02) to 1.9×10^{-7} M (pD_2, 6.73 ± 0.07) (Figure 9). The effect of methylene blue on the relaxation evoked by pilocarpine was small but significant, the EC_{50} was 1.3×10^{-4} M (pD_2, 3.89 ± 0.06) in control and 2.9×10^{-4} M (pD_2, 3.54 ± 0.11) in methylene blue (Figure 9).

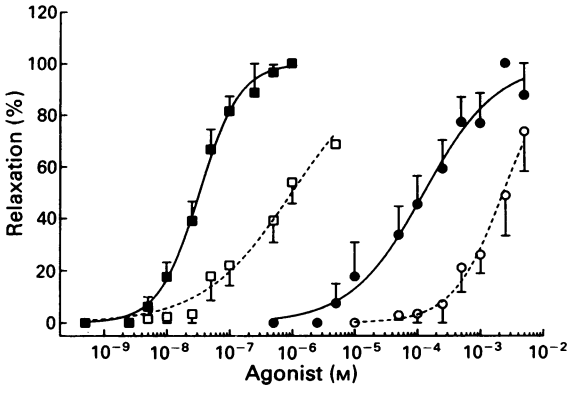

Figure 8 In 8 preparations of rat tail artery, potassium ferricyanide (10^{-5} M) (○, □) caused a significant shift in the EC_{50} for the relaxation evoked by pilocarpine (●, ○) (pD_2, from 3.82 ± 0.06 in control to 2.64 ± 0.03), and nitroprusside (■, □) (pD_2, from 7.48 ± 0.02 in control to 6.00 ± 0.06).

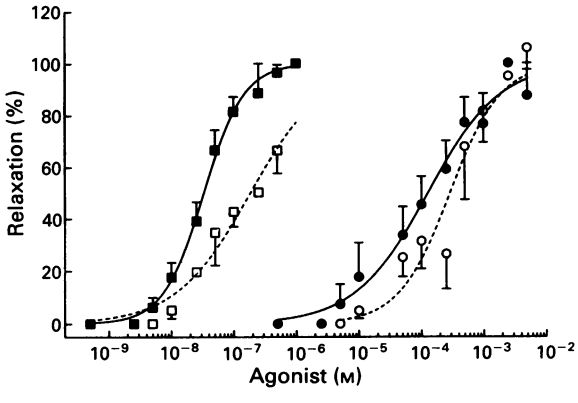

Figure 9 In 4 preparations of rat tail artery methylene blue (10^{-5} M) (○, □) caused a small but significant shift in the pD_2 for the relaxation evoked by pilocarpine (●, ○) from 3.89 ± 0.06 to 3.54 ± 0.11 ($P < 0.03$). The pD_2 for nitroprusside (■, □) was shifted from 7.48 ± 0.02 in control to 6.73 ± 0.07 by methylene blue.

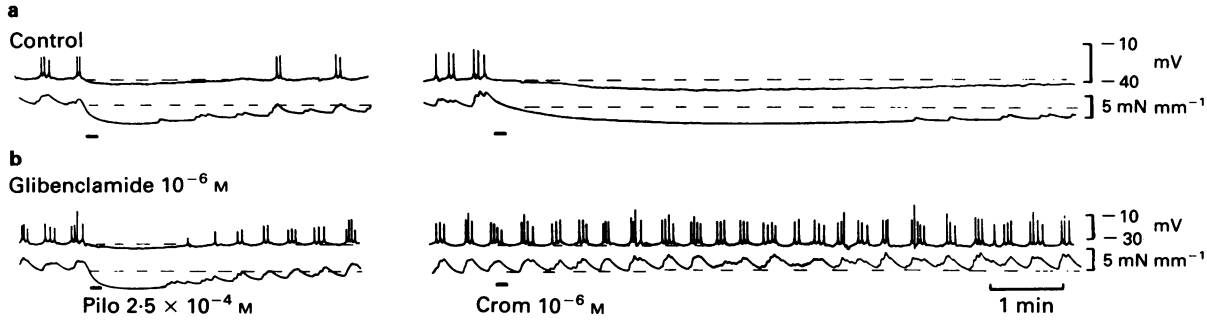

Figure 10 (a) In a segment of rat tail artery denuded of endothelium and depolarized and constricted with phenylephrine (7×10^{-8} M), pilocarpine (Pilo) and cromakalim (Crom) evoked repolarization negative to the troughs of the oscillations, cessation of action potentials and relaxation. (b) These responses to cromakalim were abolished by glibenclamide while the responses to pilocarpine persisted.

Isoprenaline

The β-adrenoceptor agonist, isoprenaline, stimulates cyclic AMP production in vascular smooth muscle and evokes relaxation in the absence of the endothelium. The rat tail artery is well supplied by adrenergic nerves containing noradrenaline. It was considered that the hyperpolarization and relaxation evoked by pilocarpine might result from the release of this noradrenaline. In 4 preparations of rat tail artery, denuded of endothelium, the hyperpolarization and relaxation in response to pilocarpine (10^{-4} to 10^{-3} M) was not affected by the β-adrenoceptor antagonist, propranolol (5×10^{-7} M). Furthermore, the hyperpolarization and relaxation evoked by isoprenaline (10^{-7} to 10^{-6} M) were not affected by ferricyanide (10^{-5} M) (not shown) while the responses to pilocarpine were reduced (see above).

Cromakalim

Cromakalim causes endothelium-independent hyperpolarization of vascular smooth muscle as a result of opening a class of potassium channels (Nakao *et al.*, 1988). This effect is accompanied by relaxation, presumably as a result of a reduction in calcium influx, since hyperpolarization would be expected to decrease the probability of opening of voltage-dependent calcium channels (Hirst & Edwards, 1989; Nelson *et al.*, 1990). In denuded segments of artery from 4 rats, both pilocarpine (10^{-4} to 10^{-3} M) and cromakalim (3×10^{-7} and 10^{-6} M) caused hyperpolarization, cessation of action potentials and relaxation (Figure 10). The responses to cromakalim were prolonged in duration. The 6.3 ± 0.3 mV hyperpolarization evoked by 10^{-6} M cromakalim was reduced to 0 mV by glibenclamide, while the 4.1 ± 0.4 mV hyperpolarization evoked by 2.5×10^{-4} M pilocarpine was unchanged at 4.0 ± 0.5 mV in glibenclamide.

Discussion

The results presented in this study demonstrate that, unlike acetylcholine, the ability of pilocarpine to hyperpolarize the depolarization and relax the constriction evoked by phenylephrine in the smooth muscle of rat tail artery does not depend on the presence of an intact endothelium and does not appear to result from interaction with muscarinic receptors. The ability of pilocarpine to hyperpolarize and relax the depolarization and constriction in response to α-adrenoceptors supports the observations of Bolton *et al.* (1984) in which they described relaxation in response to carbachol in guinea-pig mesenteric artery denuded of endothelium. In that study, the hyperpolarization evoked by carbachol in intact arteries was converted to depolarization following removal of the endothelium when the membrane was depolarized to around − 60 mV. Further depolarization of denuded tissues, to − 50 mV or more positive (see their Figure 11), restored the ability of carbachol to evoke hyperpolarization. In our study, in which phenylephrine depolarized the membrane to − 45 to − 35 mV, pilocarpine always evoked hyperpolarization or a decrease in the frequency of action potentials in preparations denuded of endothelium.

When compared with other agents that cause endothelium-independent hyperpolarization and relaxation, the responses to pilocarpine resemble most closely those induced by nitroprusside. Nitroprusside is believed to release NO within vascular smooth muscle (Ignarro & Kadowitz, 1985; Waldman & Murad, 1987). It has recently been demonstrated that arterial smooth muscle cells are capable of synthesizing NO (Schini & Vanhoutte, 1991). The relaxation evoked by pilocarpine was unaffected by agents that block biosynthesis of NO. Thus, it is unlikely that pilocarpine might be inducing NO production by the smooth muscle. Alternatively, pilocarpine might be releasing NO. The principal endogenous substrate for the biosynthesis of NO is a guanidino nitrogen of L-arginine (Palmer *et al.*, 1988), and production of NO from the imidazole ring of pilocarpine would require a completely different mechanism. If such a mechanism exists, it might be expected that both histidine and histamine could to act as sources of NO. We are unaware of any evidence supporting such an expectation.

The available evidence suggests that the NO liberated by nitroprusside stimulates soluble guanylate cyclase within vascular smooth muscle cells to bring about relaxation (Ignarro & Kadowitz, 1985; Waldman & Murad, 1987). Access of pilocarpine to directly stimulate a cytoplasmic cyclase, hence bypassing NO, seems unlikely. However, the cytoplasmic domain of the membrane-bound receptor for atrial-naturetic peptide is thought to be a guanylate cyclase. Stimulation of this receptor from the extracellular medium leads to an increase in cyclic GMP and relaxation of vascular smooth muscle (Winquist & Hintze, 1990).

Calcium influx through voltage-operated calcium channels is highly regulated within the range of membrane potential (− 50 to − 30 mV) evoked by phenylephrine in rat tail artery in this study (Nelson *et al.*, 1990). It is becoming increasingly clear that hyperpolarization of vascular smooth muscles is amongst the important mechanisms of vasodilatation (Standen *et al.*, 1989; Brayden, 1991). Pilocarpine evoked hyperpolarization in only 6 of the 15 preparations examined in this study. In the remaining 9 a decrease in the frequency of action potentials or a brief cessation of action potentials was observed. We have shown previously that the extent of the hyperpolarization induced by acetylcholine and exogenous NO in preparations of uterine artery was dependent upon the extent of the depolarization evoked by phenylephrine. Thus, when the membrane of the uterine artery was depolarized to around − 30 mV, that is, more depolarized than the range in which action potentials occurred, acetylcholine and NO evoked limited hyperpolarization. In contrast, these agents evoked concentration-dependent hyperpolarization when the membrane was less depolarized and were very effective in the range in which action potentials were prominent (Tare *et al.*, 1990). In the present study, low concentrations of phenylephrine (10^{-8}–2×10^{-7} M) rapidly depolarized intact segments of rat tail artery beyond the range of action potentials, while in denuded tissues it was difficult to drive the membrane potential beyond the range in which action potentials occurred. The tissues readily relaxed in the interval between bursts of action potentials evoked by phenylephrine. Pilocarpine appeared to exaggerate this situation by increasing the interval between action potentials or between bursts of action potentials. This is likely to explain the 10 fold increase in the sensitivity of denuded preparations of rat tail artery to the relaxing actions of pilocarpine. An effect of pilocarpine on membrane conductance is likely, although the magnitude or direction of such a change could not be tested in the myograph used in this study.

In conclusion, pilocarpine is capable of evoking relaxation of the smooth muscle of rat tail artery by a mechanism that is independent of muscarinic receptors and of the integrity of the endothelium. This is in stark contrast with the relaxation induced by acetylcholine. Of the agents tested that also induce relaxation that is independent of the endothelium, the actions of pilocarpine resembled those of nitroprusside most closely. The principal mechanism of this action of pilocarpine appears to involve a decrease in the frequency of firing of action potentials and presumably decreased calcium influx.

This study was supported by the National Heart Foundation of Australia. The authors thank Ms D. Clare for preparing the figures.

References

BOLTON, T.B., LANG, R.J. & TAKEWAKI, T. (1984). Mechanisms of action of noradrenaline and carbachol on smooth muscle of guinea-pig anterior mesenteric artery. *J. Physiol.*, **351**, 549–572.

BRAYDEN, J.E. (1991). Hyperpolarisation and relaxation of resistance arteries in response to adenosine diphosphate. *Circ. Res.*, **69**, 1415–1420.

CHEN, G., SUZUKI, H. & WESTON, A.H. (1988). Acetylcholine releases endothelium-derived hyperpolarising factor and EDRF from rat blood vessels. *Br. J. Pharmacol.*, **95**, 1165–1174.

FELETOU, M. & VANHOUTTE, P.M. (1988). Endothelium-dependent hyperpolarization of canine coronary smooth muscle. *Br. J. Pharmacol.*, **93**, 515–524.

FURCHGOTT, R.F. (1988). Studies on relaxation of rabbit aorta by sodium nitrite: the basis for the proposal that the acid-activatable inhibitory factor from bovine retractor penis is inorganic nitrite and the endothelium-derived relaxing factor is nitric oxide. In *Vasodilatation: Vascular Smooth Muscle, Peptides, Autonomic Nerves and Endothelium*. ed. Vanhoutte, P.M. pp. 401–414. New York: Raven Press.

FURCHGOTT, R.F. & ZAWADSKI, J.V. (1980). The obligatory role of endothelial cells in relaxation of arterial smooth muscle by acetylcholine. *Nature*, **288**, 373–376.

HIRST, G.D.S. & EDWARDS, F.R. (1989). Sympathetic neuroeffector transmission in arteries and arterioles. *Physiol. Rev.*, **69**, 546–604.

IGNARRO, L.J., BUGA, G.M., WOOD, K.S., BYRNS, R.E. & CHAUDHURI, G. (1987). Endothelium-derived relaxing factor produced and released from artery and vein is nitric oxide. *Proc. Natl. Acad. Sci. U.S.A.*, **84**, 9265–9269.

IGNARRO, L.J. & KADOWITZ, P.J. (1985). The pharmacological and physiological role of cyclic GMP in vascular smooth muscle relaxation. *Annu. Rev. Pharmacol. Toxicol.*, **25**, 171–191.

JAISWAL, N. & MALIK, K.U. (1990). Prostacyclin synthesis elicited by cholinergic agonists is linked to activation of M_2 alpha and M_2 beta muscarinic receptors in the rabbit aorta. *Prostaglandins*, **39**, 267–280.

KOMORI, K. & SUZUKI, H. (1987). Heterogeneous distribution of muscarinic receptors in the rabbit saphenous artery. *Br. J. Pharmacol.*, **92**, 657–664.

LEE, L., BRUNER, C.A. & WEBB, R.C. (1990). Prostanoids contribute to endothelium-dependent coronary vasodilatation in guinea-pigs. *Blood Vessels*, **27**, 341–351.

MONCADA, S., HERMAN, A.G., HIGGS, E.A. & VANE, J.R. (1977). Differential formation of prostacyclin (PGX or PGI_2) by layers of the arterial wall. An explanation for the anti-thrombotic properties of vascular endothelium. *Thromb. Res.*, **11**, 323–344.

MURAD, F., MITTAL, C.K., ARNOLD, W.P., KATSUKI, S. & KIMURA, H. (1978). Guanylate cyclase: activation by azide, nitro compounds, nitric oxide, and hydroxyl radical and inhibition by hemoglobin and myoglobin. *Adv. Cyclic Nucl. Res.*, **9**, 145–149.

NAKAO, K., OKABE, K., KITAMURA, K., KURIYAMA, H. & WESTON, A.H. (1988). Characteristics of cromakalim-induced relaxations in the smooth muscle cells of guinea-pig mesenteric artery and vein. *Br. J. Pharmacol.*, **95**, 795–804.

NELSON, M.T., PATLAK, J.B., WORLEY, J.F. & STANDEN, N.B. (1990). Calcium channels, potassium channels and voltage dependence of arterial smooth muscle tone. *Am. J. Physiol.*, **259**, C3–C18.

PALMER, R.M.J., FERRIGE, A.G. & MONCADA, S. (1987). Nitric oxide release accounts for the biological activity of endothelium-derived relaxing factor. *Nature*, **327**, 524–526.

PALMER, R.M.J., REES, D.D., ASHTON, D.S. & MONCADA, S. (1988). L-Arginine is the physiological precursor for the formation of nitric oxide in endothelium-dependent relaxation. *Biochem. Biophys. Res. Commun.*, **153**, 1251–1256.

PARKINGTON, H.C., TARE, M., TONTA, M.A. & COLEMAN, H.A. (1993). Stretch reveals three components in the hyperpolarisation of guinea-pig coronary artery in response to acetylcholine. *J. Physiol.*, **465**, 459–476.

SCHINI, V.B. & VANHOUTTE, P.M. (1991). L-Arginine evokes both endothelium-dependent and -independent relaxations in L-arginine-depleted aortas of the rat. *Circ. Res.*, **68**, 209–216.

STANDEN, N.B., QUAYLE, J.M., DAVIES, N.W., BRAYDEN, J.E., HUANG, Y. & NELSON, M.T. (1989). Hyperpolarising vasodilators activate ATP-sensitive K^+ channels in arterial smooth muscle. *Science*, **245**, 177–180.

TARE, M., PARKINGTON, H.C., COLEMAN, H.A., NEILD, T.O. & DUSTING, G.J. (1990). Hyperpolarisation and relaxation of arterial smooth muscle caused by nitric oxide derived from the endothelium. *Nature*, **345**, 69–71.

WALDMAN, S.A. & MURAD, F. (1987). Cyclic GMP synthesis and function. *Pharmacol. Rev.*, **39**, 163–196.

WINQUIST, R.J. & HINTZE, T.H. (1990). Mechanisms of arterial naturetic factor-induced vasodilatation. *Pharmacol. Ther.*, **48**, 417–426.

(Received July 6, 1993
Revised December 9, 1993
Accepted March 4, 1994)

Br. J. Pharmacol. (1994), **112**, 533–540

Nitrovasodilator-induced relaxation and tolerance development in porcine vena cordis magna: dependence on intact endothelium

[1]Georg Kojda, [2]Jan Klaus Beck, [3]Wilfried Meyer & Eike Noack

Institut für Pharmakologie, Heinrich-Heine Universität, Postfach 10 10 07, D-40001 Düsseldorf, Germany

1 Isolated segments of porcine vena cordis magna exhibited a reproducible contractile activity upon application of prostaglandin $F_{2\alpha}$ ($PGF_{2\alpha}$) or KCl, that was independent of the presence of intact endothelium. Substance P (3 nM) elicited strictly endothelium-dependent relaxations amounting to 46.1 ± 1.4% ($n = 206$) of contractions induced by 10 μM $PGF_{2\alpha}$.

2 S-nitroso-*N*-acetyl-D,L-penicillamine (SNAP), a compound that spontaneously liberates nitric oxide, concentration-dependently relaxed $PGF_{2\alpha}$-precontracted (50 μM) venous segments. Tolerance induction (incubation with 100 μM SNAP for 30 min) within the same segments resulted in a 3 fold attenuation of this effect, which was not further reduced after additional preincubation with glyceryl trinitrate (GTN). Removal of endothelium or the presence of N^{ω}-nitro-L-arginine methylester (L-NAME) significantly improved the potency of SNAP before and after tolerance induction.

3 Concentration-dependent relaxations induced by GTN in non-tolerant veins were similar in the presence and absence of endothelium but much more reduced in tolerant endothelium-denuded (75 fold) compared to intact (20 fold) segments. In contrast, the presence of L-NAME significantly improved GTN-activity solely in non-tolerant veins, which, therefore, also resulted in a more pronounced attenuation of activity due to tolerance induction (100 fold). Preincubation of intact veins with SNAP also reduced GTN-activity but to a lesser extent (10 fold).

4 The more delayed but much longer, and compared to GTN somewhat weaker, acting new nitrovasodilator N-(3-nitrato-pivaloyl)-1-cysteineethylester (SPM 3672) was more potent in denuded than intact non-tolerant venous segments. Induction of tolerance by GTN resulted in a 2 fold-attenuation of potency. This effect was increased to 15 fold in denuded veins but solely due to enhanced potency of SPM 3672 caused by removal of endothelium.

5 These data demonstrate that intact endothelium of porcine vena cordis magna attenuates the relaxant potency of nitrovasodilators but also probably participates in vascular bioactivation of GTN. We suggest that the reduced potency of nitrovasodilators is due to endogenous production of nitric oxide, which may affect the soluble guanylate cyclase/cyclic GMP-system or inhibit nitrate bioactivation pathways.

Keywords: Veins; nitrovasodilators; nitrate-tolerance; vascular smooth muscle; endothelium

Introduction

Nitrovasodilators are commonly used in the treatment of several cardiovascular disorders including coronary artery disease. The therapeutic benefit of these drugs is mainly based on their ability to relax vascular smooth muscle. The mechanism of action is not yet fully understood but previous results strongly indicate that nitrovasodilators must be considered as prodrugs, which require decomposition to their pharmacologically active principle (Ignarro *et al.*, 1981; Brian *et al.*, 1986), identified as nitric oxide (Feelisch & Noack, 1987). There are, however, profound differences between the various nitrovasodilators in their ability to liberate nitric oxide (Noack & Feelisch, 1991). *In vitro*, nitrate-ester containing drugs like glyceryl trinitrate liberate nitric oxide in significant amounts only in the presence of certain free thiols (e.g. cysteine). *In vivo*, enzymatic bioactivation within the vascular wall seems to dominate (Chung & Fung, 1990; Feelisch & Kelm, 1991; Bennet *et al.*, 1992). By contrast, 3-morpholinosydnonimine-*N*-ethylcarbamide (SIN-1), the active metabolite of molsidomine, or S-nitroso-*N*-acetyl-D,L-penicillamine (SNAP) spontaneously liberate nitric oxide in large amounts (Noack & Feelisch, 1991).

Furchgott & Zawadzki (1980) originally described the obligatory role of the vascular endothelium in arterial relaxation induced by acetylcholine. Later it was shown that this intimal monolayer represents a source of endogenous nitric oxide (Palmer *et al.*, 1987; Ignarro *et al.*, 1987). Furthermore, endothelial dysfunction and hence blunted or reduced endothelium dependent vasorelaxation, is an important factor in different pathological situations including atherosclerosis, which is considered to participate in the pathophysiology of coronary artery disease (Jayakody *et al.*, 1985; Freiman *et al.*, 1986; Moncada & Higgs, 1991). Previous reports described enhanced vasorelaxant activity of different nitrovasodilators in artery preparations with denuded compared to intact endothelium (Shirasaki & Su, 1985) or after treatment with inhibitors of endogenous nitric oxide synthesis (Busse *et al.*, 1989). The same effect was observed after systemic application of a nitric oxide synthase inhibitor to rats (Moncada *et al.*, 1991). It was suggested that the modulating effect of endothelium on vasorelaxation induced by nitrovasodilators in arteries is mediated by the endothelium-derived relaxing factor (EDRF), endogenous nitric oxide. The continuous production of EDRF could result in a desensitization of smooth muscle soluble guanylate cyclase, an effect that has been described for exogenous nitric oxide (Axelsson & Andersson, 1983; Schröder *et al.*, 1988). In addition, it seems possible that EDRF may also cause a reduced bioactivation of GTN in porcine coronary arteries

[1] Author for correspondence.
[2] Present address: j.h.o. Torbay Hospital, TQ2 7AA, Torquay, Devon
[3] Present address: Institut für Zoologie, Tierärztliche Hochschule, Bünteweg 17, D-30559 Hannover 71, Germany

(Kojda et al., 1992b). To elucidate the role of endothelium in nitrate activity in veins, the effects of three nitrates with different mechanisms of nitric oxide-liberation, GTN, SNAP and the new nitrovasodilator N-(3-nitrato-pivaloyl)-1-cysteineethylester (SPM 3672), were examined in porcine isolated vena cordis magna. In addition, endothelium-dependent nitrate-activity was also studied following induction of tolerance. Some of these results were presented at the Autumn Meeting of the German Society of Pharmacology and Toxicology in Graz, Austria (Kojda et al., 1992a).

Methods

Studies on isolated vessel segments

Hearts of 5–7 month old pigs (70–90 kg) were obtained from the local slaughterhouse. The vena cordis magna was carefully dissected within 10 to 15 min after slaughtering. The vein was cut through in the sulcus interventricularis and next to the auriculum and perfused with the aid of a cannula and a syringe with cold oxygenated (95% O_2 + 5% CO_2) Krebs-Henseleit solution (pH 7.4) of the following composition (mM): Na^+ 143.07, K^+ 5.87, Ca^{2+} 1.6, Mg^{2+} 1.18, Cl^- 124.78, HCO_3^- 25.00, $H_2PO_4^-$ 2.36, SO_4^{2-} 1.18 and glucose 5.05. The veins were cut from their muscle foundation and immediately stored in cooled buffer. In the laboratory, veins were carefully removed from the muscle and separated from the surrounding fatty tissue. Two segments from each heart (4 mm in length and 2 mm in diameter) were cut from the proximal end of the vessel next to the sinus coronarius, sometimes gently rubbed on their intimal surface with a small wooden stick in order to remove the endothelium, and then mounted between two stainless steel triangles in a water jacketed organ bath (37°C) as described by Kojda et al. (1992c). Preliminary experiments revealed an optimal resting tension of 1 g, which was achieved by separating the two triangles between which the rings were mounted leading to a slight stretching of the veins. Vessel tension was measured isometrically by Statham transducers.

After equilibration (1 h), contractile function of the segments was tested by application of KCl to reach a final concentration of 60 mM, which resulted in the development of an additional tension of approximately 2 g. The vessels relaxed to basal resting tension after repeated washings. The presence or absence of intact endothelium was then verified by relaxation of prostaglandin $F_{2\alpha}$ ($PGF_{2\alpha}$)-precontracted (10 μM) segments due to application of 3 nM of substance P. The presence or absence of endothelium was also verified by histological examination of some additionally prepared venous rings before and after mechanical denudation.

Application of 3 nM substance P to carefully prepared venous segments resulted in transient relaxations. These responses were absent if veins had been gently rubbed on their intimal surface. Intimal rubbing resulted in complete removal of endothelium but left the lamina elastica interna intact as evaluated by histological examination. Endothelium-dependent relaxations induced by substance P amounted to 46.1 ± 1.4% ($n = 204$) of the vasoconstriction induced by 10 μM $PGF_{2\alpha}$. Only tissues exhibiting at least 50% relaxation (veins with endothelium) or rubbed tissues were used in further experiments.

Vasorelaxant activity of GTN (0.01–100 μM), SPM 3672 (0.001–10 μM) and SNAP (0.001–10 μM) in veins with endothelium was studied by cumulative applications of the compounds following precontraction with 50 μM $PGF_{2\alpha}$. Development of tolerance to GTN and SNAP was induced by insertion of a 30 min incubation period with 100 μM of the respective nitrovasodilator between two cumulative applications within the same vessel segment. In the case of SNAP, a third cumulative concentration-response curve was added after a 30 min incubation period with 100 μM GTN. Incubation of the veins with 100 μM GTN and SNAP for 30 min did not change their contractile response to 50 μM $PGF_{2\alpha}$ after a washout period of 15 min. In contrast, incubation with 100 μM SPM 3672 followed by a washout period of 15 min markedly inhibited contractions of veins induced by 50 μM $PGF_{2\alpha}$, indicating the necessity of a prolonged washout period as demonstrated previously in rat aorta (Kojda & Noack, 1993). Therefore, single concentration-response curves for SPM 3672 were constructed with and without a 30 min preincubation period with 100 μM GTN to study a possible cross-tolerance phenomenon.

To investigate the influence of intact endothelium on the activity of nitrovasodilators, the experiments delineated above were also performed in rubbed veins and in veins with intact endothelium in the presence of 100 μM N^{ω}-nitro-L-arginine methylester (L-NAME), an inhibitor of endothelial nitric oxide-synthase (Mülsch & Busse, 1990). L-NAME, 100 μM, was added to the organ bath 15 min before precontraction with 50 μM $PGF_{2\alpha}$ and the following first cumulative application of GTN or SNAP and remained until all experiments were finished. In order to elucidate possible side-effects of L-NAME, we investigated its actions in the venous segments before and after precontraction. In some venous rings application of L-NAME slightly increased basal tension. However, these contractions never exceeded 10% of the vasoconstriction induced by 50 μM $PGF_{2\alpha}$ in the same vessel. A similar effect of L-NAME was observed in $PGF_{2\alpha}$-precontracted veins. We also investigated the influence of 1 mM L-NAME on the basal and stimulated (500 μM SNAP) activity of soluble guanylate cyclase partially purified from human platelets (Kojda & Noack, 1993) and observed no influence on basal activity, whereas the stimulated activity was slightly (less than 10%) reduced.

Substances and solutions

SNAP was synthesized in our laboratory according to Field et al. (1978). The reaction product was recrystallized once in methanol. Analysis of SNAP included a thin layer chromatography on Merck RP18 plates with methanol/water 7/3 (v/v) as eluent. To determine free sulphide-groups, spray detection was performed with 1.5 g of sodium nitroprusside dissolved in an aliquot of a solution containing 5 ml 2 N hydrochloric acid, 95 ml methanol and 10 ml ammonia (25%) and exhibited no detectable amount of free sulphides. Spray detection of the nitroso-group was achieved by two steps: spraying of Zn-powder (particle size < 60 μm) suspended in methanol was followed by spraying sulphanilic acid/α-naphthylamin 250 mg each in acetic acid (30%) and brief warming of the chromatography plate. This procedure resulted in a coloured area indicating an intact nitroso-group. In addition, the nitric oxide liberating property of synthesized SNAP was determined by the oxyhemoglobin assay (Feelisch & Noack, 1987) and yielded a nitric oxide formation rate of 1.28 ± 0.01 μM min^{-1} ($n = 3$) with 1 mM of SNAP in the reaction tube.

GTN and SPM 3672 were generously provided by Schwarz-Pharma AG, Monheim, Germany; $PGF_{2\alpha}$ and substance P were obtained from Sigma, Deisenhofen, Germany; all other chemicals were obtained from Merck, Darmstadt, Germany.

GTN (stock 1 mM) and $PGF_{2\alpha}$ (stock 10 mM) were available as aqueous solutions and an aqueous stock solution of L-NAME (10 mM) was freshly prepared every day. Stock solutions of SPM 3672 and SNAP (100 mM) were also prepared daily in dimethylsulphoxide, diluted with buffer as required and kept on ice until use. All concentrations indicated in the text, figures and tables are expressed as final bath concentrations.

Up to a final concentration of 0.01% in the organ bath, which was achieved by application of 10 μM of either SNAP or SPM 3672, dimethylsulphoxide alone did not modify basal or stimulated (50 μM $PGF_{2\alpha}$) vessel tension. However, starting at a concentration of 0.1%, dimethylsulphoxide alone

relaxed venous segments precontracted with 50 μM $PGF_{2\alpha}$. This relaxation, which was concentration-dependent and exceeded 90% (related to precontraction) at 5% dimethylsulphoxide as evaluated by concentration-response curves, prevented the use of SNAP and SPM 3672 in concentrations higher than 10 μM.

Statistics

Vasorelaxation due to treatment with the drugs is expressed as percentage of the contractile response achieved with 50 μM $PGF_{2\alpha}$ at the beginning of the experiments. The concentrations of the nitrovasodilators for half-maximal inhibition of $PGF_{2\alpha}$-induced vasoconstriction (pD_2-values) were calculated from the individual concentration-effect-curves by the method of Hafner *et al.* (1977). All data were analysed by one-way analysis of variance (ANOVA) with subsequent Student-Newman Keuls test (SAS PC Software 6.04, PROC ANOVA, also used to calculate the plotted concentration-response curves) and are expressed as mean values and standard error of the mean (s.e.mean). pD_2 values were used to test for significant differences and a P value less than 0.05 was considered as significant.

Results

Contractile activity

Application of KCl (60 mM) to freshly isolated segments of porcine vena cordis magna with intact endothelium resulted in rapidly developing stable contractions that reached 2.17 ± 0.12 g ($n = 72$). In rubbed segments the magnitude of this contraction was not significantly different (1.79 ± 0.12 g, $n = 41$).

Isolated segments of porcine vena cordis magna with intact endothelium exhibited a contractile response after application of 50 μM $PGF_{2\alpha}$ reaching 1.57 ± 0.08 g ($n = 72$). The initially phasic-tonic contraction was stable after 10 min and maintained for more than 2 h. Removal of endothelium did not significantly affect the vasoconstriction induced by 50 μM $PGF_{2\alpha}$ (1.46 ± 0.07 g, $n = 68$).

Effects of nitrovasodilators

All nitrovasodilators studied caused a concentration-dependent relaxation of precontracted porcine vena cordis magna with and without intact endothelium and after preincubation of endothelium-intact vessels with L-NAME.

SNAP was the most potent vasorelaxant within the group of nitrovasodilators investigated (Figure 1, Table 1). In veins with intact endothelium a second cumulative application of SNAP to the same vessel segement resulted in a significant displacement to the right of the concentration-effect curve (Table 1) without a change in the maximal response (Figure 1). No further change in the concentration-response curve to SNAP was seen after exposure to GTN (Table 1). Removal of endothelium or preincubation of intact veins with L-NAME induced a significant and comparable shift to the left of the concentration-effect curve of SNAP and there was no significant difference between the two respective pD_2-values (Table 1). In both experimental settings, the second cumulative application of SNAP revealed a decreased vasorelaxant potency as observed in enothelium-intact veins. A third cumulative application of SNAP after a preincubation with GTN exhibited a further significant reduction in vasodilator potency (Table 1). However, in veins tolerant to SNAP and GTN, SNAP was more potent after removal of endothelium as compared to the presence of L-NAME, which itself did not change significantly the activity of SNAP in GTN-tolerant venous segments (Table 1).

Glyceryl-trinitrate induced a concentration-dependent relaxation of venous segments precontracted with 50 μM $PGF_{2\alpha}$. The concentration-response curves of GTN were nearly iden-

Table 1 The vasodilator potencies of glyceryl trinitrate (GTN), S-nitroso-*N*-D,L-penicillamine (SNAP) and N-(3-nitratopivaloyl)-1-cysteineethylester (SPM 3672) as evaluated by a first (non-tolerant) and a second (tolerant) cumulative application to ring segments of porcine vena cordis magna precontracted with 50 μM $PGF_{2\alpha}$

Substance, condition	*With endothelium*	n	*Without endothelium*	n
GTN, non-tolerant,	6.522 ± 0.122	7	6.434 ± 0.058	11
GTN, tolerant,	5.198 ± 0.090	7	4.739 ± 0.158#	11
GTN, non-tolerant after L-NAME,	7.187 ± 0.084	5		
GTN, tolerant after L-NAME,	5.188 ± 0.095	5		
GTN after SNAP,	5.500 ± 0.101	7		
SNAP, non-tolerant	7.412 ± 0.064	10	8.051 ± 0.188#	11
SNAP, tolerant	6.960 ± 0.063	10	7.579 ± 0.078#	11
SNAP, tolerant after GTN	6.870 ± 0.083	10	7.259 ± 0.088#	11
SNAP, non-tolerant presence of L-NAME	7.741 ± 0.101	9		
SNAP, tolerant presence of L-NAME	7.190 ± 0.065	9		
SNAP, tolerant after GTN and in presence of L-NAME	6.911 ± 0.069	9		
SPM 3672, non-tolerant	6.205 ± 0.065	11	7.069 ± 0.071#	7
SPM 3672, tolerant to GTN	5.688 ± 0.079	6	5.858 ± 0.068	8

In some experiments preincubation with GTN or SNAP (0.1 mM) preceded cumulative applications (tolerant vessel segments) or N^{ω}-nitro-L-arginine methyl-ester (L-NAME, 0.1 mM) was present (for details see Methods). Given are the mean pD_2-values (in $-\log$ mol l^{-1}) and standard error of the mean (s.e.mean) of n individual experiments (#, significant difference from the value obtained in veins with endothelium; *, significant difference as indicated by the lines, $P > 0.05$).

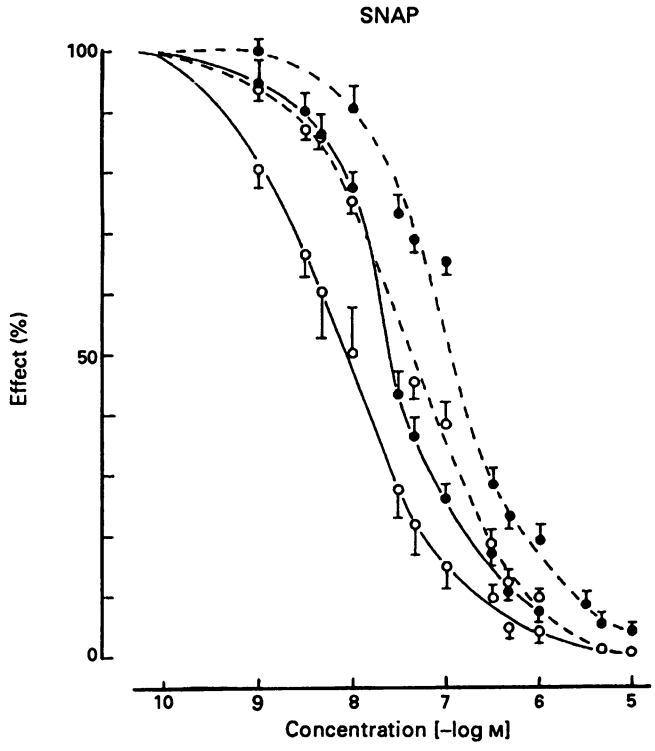

Figure 1 Vasodilator activity of S-nitroso-*N*-acetyl-D,L-penicillamine (SNAP) in the presence (– – –) and absence (——) of intact endothelium before (open symbols) and after (closed symbols) induction of tolerance within the same vessel segments precontracted by prostaglandin $F_{2\alpha}$ (50 μM). Each concentration-response curve is plotted by taking the respective mean values of 10–11 individual experiments; s.e.mean are shown.

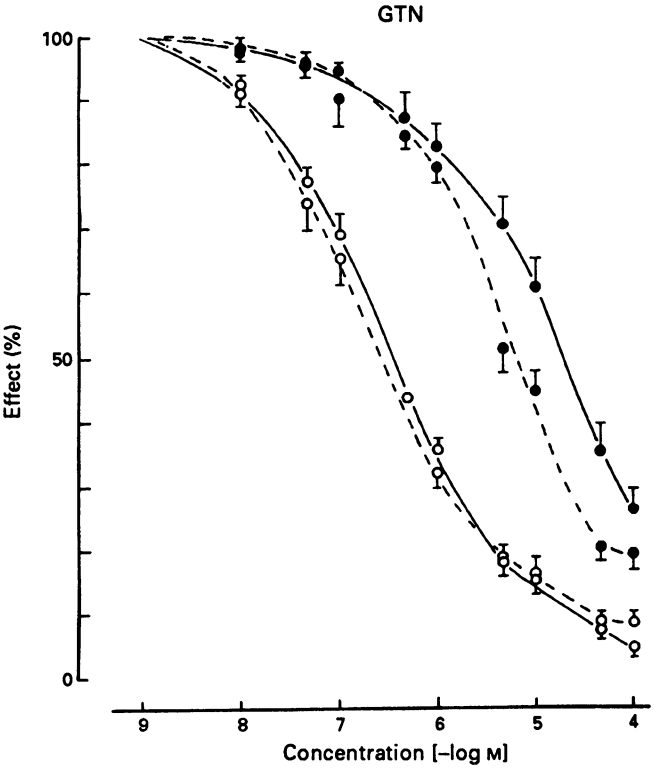

Figure 2 Vasodilator activity of glyceryl trinitrate (GTN) in the presence (– – –) and absence (——) of intact endothelium before (open symbols) and after (closed symbols) induction of tolerance within the same vessel segments precontracted by prostaglandin $F_{2\alpha}$ (50 μM). Each concentration-response curve is plotted by taking the respective mean values of 7–11 individual experiments; s.e.mean are shown.

tical in the presence and absence of endothelium (Figure 2) and there was no significant difference between the calculated pD_2-values (Table 1). A second cumulative application after tolerance induction within the same rings resulted in a pronounced rightward shift of the concentration-response curves for GTN in the presence and absence of endothelium and the maximal concentration of GTN used did not induce a complete relaxation (Figure 2). Furthermore, tolerant endothelium-denuded veins were significantly less sensitive and the respective pD_2-value of GTN was the lowest observed in the study (Table 1). Repetition of the experiment in non-tolerant veins with intact endothelium but in the presence of L-NAME, a known inhibitor of endothelial nitric oxide synthase, resulted in a significant displacement to the left of the concentration-response curve of GTN, which, however, disappeared during the second cumulative application after tolerance induction (Table 1). Thus, removal of endothelium or pretreatment with L-NAME increased development of tolerance to GTN in a different manner. Endothelial denudation resulted in attenuation of the potency of GTN in tolerant veins, while treatment with L-NAME caused an improved potency of GTN in non-tolerant segments. A significant shift to the right of the concentration-response curve of GTN ($P<0.001$) in endothelium-intact veins was also observed after a 30 min preincubation period with 100 μM SNAP, a compound, which spontaneously liberates large amounts of nitric oxide. However, development of tolerance to the activity of GTN induced by SNAP was lower than that induced by GTN itself as indicated by the significant difference between the respective pD_2-values (Table 1).

SPM 3672, the new nitrovasodilator, induced concentration-dependent relaxations of $PGF_{2\alpha}$-precontracted vessels. Cumulative application in non-tolerant veins with intact endothelium (Figure 3) revealed a slightly but significantly ($P<0.05$) lower potency than GTN (Table 1). In addition, the concentration-response curve of SPM 3672 in intact veins tolerant to GTN showed only a small shift to the right (Figure 3) indicating a negligible degree of cross-tolerance. Removal of endothelium significantly improved the potency of SPM 3672 in non-tolerant veins. In contrast, this difference was absent in veins tolerant to GTN (Figure 3, Table 1). Thus, removal of endothelium enhanced cross-tolerance between SPM 3672 and GTN.

Discussion

Endothelium-dependent relaxation in porcine vena cordis magna elicited by substance P was rather low compared to the almost complete relaxation observed in porcine coronary artery after the same experimental procedure (Kojda *et al.*, 1990; 1992c). Similar results have been reported from other experiments with vascular tissue from animals (De Mey & Vanhoutte, 1982; Vanhoutte & Miller, 1985) and human coronary (Ku *et al.*, 1992) and peripheral blood vessels (Thom *et al.*, 1987; Thulesius *et al.*, 1988; Lüscher *et al.*, 1988). In human coronary veins the magnitude of endothelium-dependent relaxation has been shown to be dependent on the agonist used and varied between 59 and 41% (Ku *et al.*, 1992). It seems unlikely that these observations are due to a reduced capacity of venous endothelial cells to produce vasorelaxant factors, since D'Orleans-Juste *et al.* (1992) recently reported a comparable release of EDRF and prostacyclin from endothelial cells cultured from either bovine aorta or bovine vena cava. Therefore, it may be suggested that the reduced endothelium-dependent relaxation in veins may be due to a more rapid destruction of endogenous vasodilators or caused by a decreased response of the underlying smooth muscle cells to these compounds. This is supported by the results of Lüscher *et al.* (1988), who demonstrated that endothelium-denuded strips of human

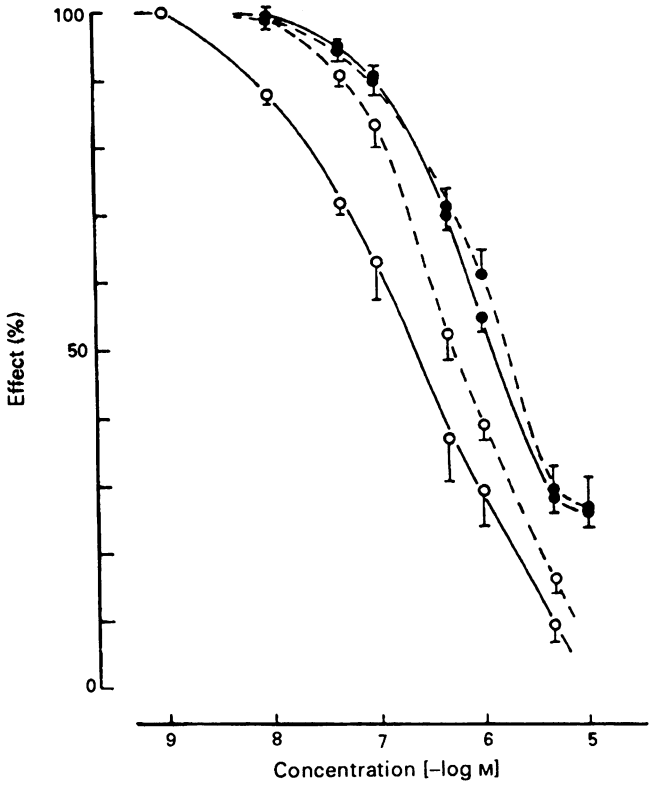

Figure 3 Vasodilator activity of N-(3-nitrato-pivaloyl)-1-cysteine-ethylester (SPM 3672) in the presence (- - -) and absence (——) of intact endothelium before (open symbols) and after (closed symbols) induction of tolerance to glyceryl trinitrate within the same vessel segments precontracted by prostaglandin $F_{2\alpha}$ (50 μM). Each concentration-response curve is plotted by taking the respective mean values of 6–11 individual experiments; s.e.mean are shown.

saphenous vein, mounted in a sandwich preparation parallel to intact strips of human mammary artery, relax only half-maximally due to stimulated release of arterial EDRF.

In order to elucidate the role of endothelium on nitrate activity in veins, we examined the effects of SNAP, GTN and SPM 3672 in isolated porcine vena cordis magna in the presence and absence of endothelium. These drugs exhibit substantial differences concerning their ability and mechanism to liberate nitric oxide, a compound that probably represents their pharmacologically active principle (Feelisch & Noack, 1987; Noack & Feelisch, 1991; Kojda & Noack, 1993). Furthermore, we intended to determine if the endogenous production of nitric oxide by the endothelium (Palmer *et al.*, 1987; Ignarro *et al.*, 1987) is involved and conducted experiments using L-NAME, an inhibitor of endothelial nitric oxide synthase (Mülsch & Busse, 1990). Our results revealed a substantial influence of endothelium and endogenous nitric oxide on the vasodilator potency of the nitrovasodilators, which, however, differed markedly between the drugs examined.

Removal of endothelium or pretreatment with L-NAME significantly potentiated vasorelaxation induced by SNAP (Figure 1). This compound spontaneously liberates large amounts of nitric oxide (see Methods) and maximally activates soluble guanylate cyclase partially purified from human platelets (Kojda & Noack, 1993). Therefore, its vasodilator action on porcine vena cordis magna is probably mediated by activation of smooth muscle soluble guanylate cyclase and subsequent formation of guanosine 3':5'-cyclic monophosphate (cyclic GMP). According to previous investigations (Axelsson & Andersson, 1983; Schröder *et al.*, 1988) it seems possible, that a desensitization of soluble guanylate cyclase caused by continuous basal liberation of EDRF (D'Orleans-Juste *et al.*, 1992), which also stimulates soluble guanylate cyclase, is responsible for the observed attenuation of vasorelaxation induced by SNAP in intact compared to denuded veins. Such densensitization might also explain the occurrence of a minor tolerance as well as GTN-induced cross tolerance to the action of SNAP described here (Figure 1, Table 1). On the other hand, it seems possible that the occurrence of tolerance development to SNAP-induced vasorelaxation in porcine vena cordis magna might be due simply to enhanced levels of intracellular cyclic GMP generated by stimulated soluble guanylate cyclase as pointed out by Jackson & Busse (1990). Although our results cannot discriminate between these two possible mechanisms, they indicate that prolonged exposure to nitric oxide, irrespective of its origin, may attenuate its own action in vascular smooth muscle of porcine vena cordis magna.

In view of this endothelium-dependent desensitization of venous smooth muscle to nitric oxide mediated by nitric oxide it seems surprising that we and others found no influence of endothelium on GTN-induced relaxation in veins (Figure 2, Table 1; Forster *et al.*, 1990). However, formation of nitric oxide from GTN probably requires several as yet undefined vascular bioactivation steps (Feelisch & Noack, 1987; Chung & Fung, 1990; Feelisch & Kelm, 1991), which may also be affected by endothelium-derived nitric oxide. As shown in Table 1, exposure of the veins to high concentrations of exogenous nitric oxide derived from SNAP resulted in an approximately 10 fold attenuation in potency of GTN. This finding cannot be completely explained by a nitric oxide-mediated desensitization of soluble guanylate cyclase or a reduced effectiveness of cyclic GMP, because results obtained from experiments in which the veins were pretreated with high concentrations of SNAP, revealed only a 3 fold attenuation in potency of SNAP (Table 1). In addition, a third cumulative application of SNAP was not affected by a 30 min incubation with GTN (100 μM). Therefore, nitric oxide derived from SNAP seems to decrease the activity of GTN by an additional mechanism. This mechanism may reflect an interference of nitric oxide with vascular bioactivation of GTN to nitric oxide, because the necessity of this metabolic conversion distinguishes the biological activity of the two nitrovasodilators (Noack & Feelisch, 1991). We also found a pronounced potentiation of vasorelaxation induced by GTN in veins with intact endothelium if L-NAME, an inhibitor of endothelial nitric oxide synthesis, was present in the organ bath throughout the experiments (Table 1). This observation indicates that not only exogenous but also endogenous nitric oxide affects the activity of GTN in porcine coronary veins. The fact that L-NAME induced a more pronounced increase in potency of GTN (5 fold) than in potency of SNAP (2 fold, Table 1) further indicates that the bioactivation pathway converting GTN to nitric oxide and other metabolites may also be affected by endogenous nitric oxide. However, the increase in potency of GTN in venous rings incubated with L-NAME seems to contradict the obvious lack of effect on potency of GTN observed after endothelium denudation. This inconsistency is probably due to the recently reported ability of endothelial cells to metabolize GTN to nitric oxide (Feelisch & Kelm, 1991; Salvemini *et al.*, 1992). This implies that denudation of endothelium produces two different and contrary effects. The destruction of the GTN-bioactivation pathway occurring in endothelial cells is expected to reduce the potency of GTN. On the other hand, the absence of the endothelial production of endogenous nitric oxide enhances the potency of GTN, as indicated by the results obtained in veins with intact endothelium treated with L-NAME.

As shown in Figure 4 (shaded areas), we suggest multiple actions of nitric oxide, whether derived from endogenous or exogenous sources, on relaxation of porcine vena cordis magna induced by GTN consisting of (1) desensitization of soluble guanylate cyclase or attenuation of the effects of cyclic GMP and (2) attenuation of the GTN-bioactivation

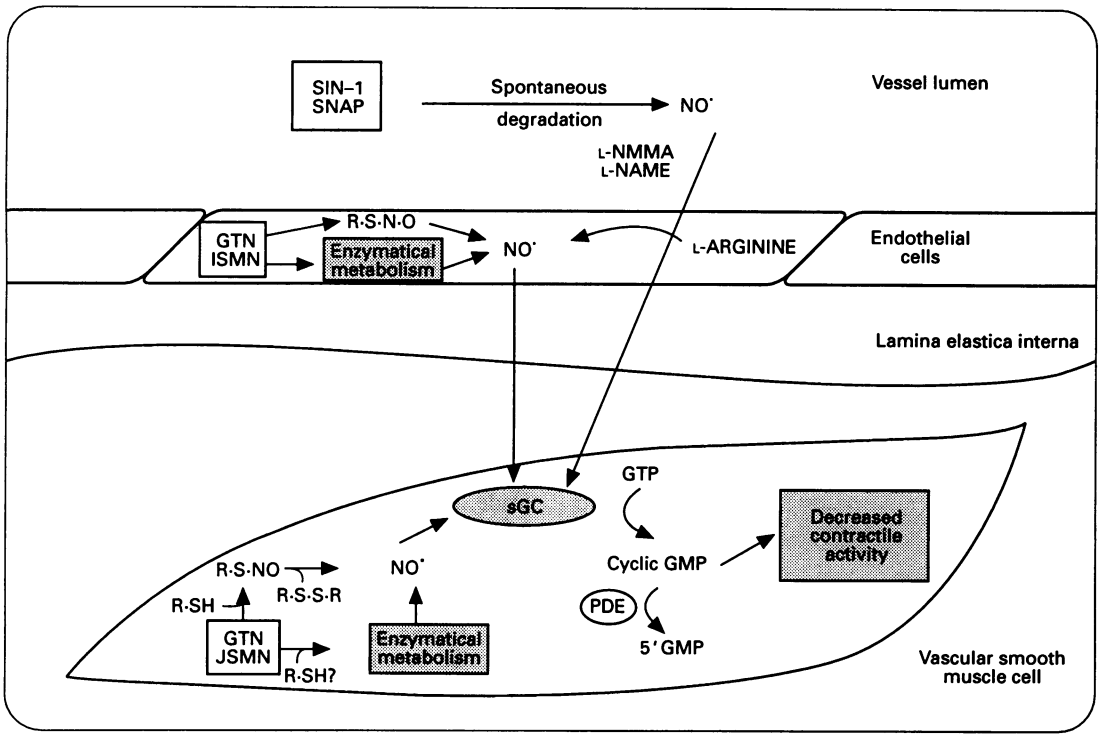

Figure 4 Scheme of the suggested mechanisms by which endogenous and exogenous nitric oxide (NO) may attenuate its own action as well as endothelial and vascular smooth muscle bioactivation of glyceryl trinitrate (GTN) in porcine vena cordis magna. The pathways or enzymes involved are indicated by the shaded areas. A desensitization of soluble guanylate cyclase (soluble guanylate cyclase) by exogenous and endogenous nitric oxide and a decreased activity of cyclic GMP due to an increased concentration have been reported previously (Axelsson & Andersson, 1983; Schröder *et al.*, 1988; Jackson & Busse, 1991; Moncada *et al.*, 1991). According to the results of the present study, bioactivation of GTN in vena cordis magna probably occurs in both endothelial and smooth muscle cells. It is proposed, that the possible inhibition of this pathway by nitric oxide might be involved in the development of nitrate tolerance.

within vascular smooth muscle and endothelial cells. The inhibition of nitric oxide formation in endothelial cells by L-NAME may result in a supersensitivity of smooth muscle to nitric oxide (Moncada *et al.*, 1991) accompanied by an enhanced bioactivation of GTN in endothelial and vascular smooth muscle cells and thus explain the high potency of GTN in L-NAME-treated veins (Table 1). In the absence of endothelium and endothelium-derived nitric oxide, any increase in the sensitivity of soluble guanylate cyclase and in the bioactivation of GTN in smooth muscle cells would be counteracted by the lack of GTN-bioactivation in endothelial cells, so that no significant influence on the activity of GTN was observed (Table 1).

That nitric oxide may induce an attenuation of potency of GTN is also supported by the results obtained in venous segments made tolerant to GTN (Table 1; Figure 4). We observed the weakest potency of GTN in tolerant veins without endothelium. This is a situation where the GTN-bioactivation pathway in smooth muscle cells is reduced and its endothelial counterpart is missing. Our results, therefore, indicate that inhibition of intravascular bioactivation of GTN induced by nitric oxide as the endproduct of this pathway might reflect a mechanism that is involved in experimentally and clinically (Ahlner *et al.*, 1991) documented tolerance. The influence of nitric oxide on the metabolism of GTN may be mediated by an unspecific mechanism e.g. by alterations in the redox status within the smooth muscle cytosol and we recently measured enhanced levels of free thiols and reduced levels of disulphides in vascular smooth muscle cells of porcine coronary arteries after endothelial denudation (Kojda *et al.*, 1993). The direct inhibition of metabolizing enzymes by nitric oxide (Wink *et al.*, 1993) may be involved as well.

The new nitrovasodilator SPM 3672 was less potent than GTN or SNAP. The action of SPM 3672 more closely resembles the action of SNAP than that of GTN with respect to the influence of endothelial denudation on its vascular activity (compare Figures 2 and 3). To our surprise we recently found that SPM 3672 spontaneously liberates nitric oxide in only very small amounts, two orders of magnitude lower than the spontaneous production of nitric oxide from SNAP (Kojda & Noack, 1993). Nevertheless, SPM 3672 markedly activated human isolated guanylate cyclase and enhanced vascular content of cyclic GMP. We suggested that a direct interaction of SPM 3672 with soluble guanylate cyclase resulting in liberation of nitric oxide is responsible for vasorelaxation. As observed with SNAP, the vasorelaxant potency of SPM 3672 was significantly attenuated by the presence of intact endothelium. Furthermore, the small degree of cross-tolerance to GTN also parallels the results obtained with SNAP and might be explained by desensitization of soluble guanylate cyclase or a reduced efficacy of cyclic GMP. But unlike SNAP and GTN, the effect of SPM 3672 occurred with a slow onset and persisted for more than 1 h (see Methods), which may favour this new nitrate for clinical investigation in the future.

At present, it is difficult to estimate the clinical importance of the endothelium-dependent activity of nitrovasodilators reported previously for arteries (Shirasaki & Su, 1985; Busse *et al.*, 1989) and in this study also for veins. It has, however, been demonstrated that systemic application of a nitric oxide synthase inhibitor caused a significant improvement of the response to GTN in rats *in vivo* (Moncada *et al.*, 1991). Taken together, these results support the speculation that the activity of nitrovasodilators like GTN is enhanced in certain regions of the vascular system, which exhibit a damaged

and/or dysfunctional endothelium as is found after balloon catheterization for example (Shimokawa & Vanhoutte, 1987) or induction of atherosclerosis (Jayakody *et al.*, 1985; Freiman *et al.*, 1986; Moncada & Higgs, 1991). Such a mechanism raises the question to what degree a vasorelaxant activity of GTN within the coronary circulation contributes to its beneficial anti-anginal effect. Additional evaluation of concentration-response relationships of nitrovasodilators in pathologically damaged vessels are required to gain a more detailed insight into the interaction between the vascular endothelium and the action of nitrovasodilators.

In summary, the results presented demonstrate that intact endothelium of porcine vena cordis magna significantly attenuates the vasorelaxant potency of different nitrovasodilators. We suggest that this influence of endothelium on the activity of nitrovasodilators is due to endogenous production of nitric oxide, which may act by two different mechanisms; (1) desensitization of soluble guanylate cyclase or reduced action of cyclic GMP and/or; (2) inhibition of intravascular nitrate bioactivation pathways. Our results also revealed that the endothelial cell layer of veins probably participates in vascular bioactivation of GTN. In addition, it is proposed that the inhibition of the intravascular bioactivation of GTN in endothelial and vascular smooth muscle cells induced by nitric oxide as the endproduct of this pathway might be partially responsible for the well known development of tolerance to GTN. The new nitrovasodilator, SPM 3672, exhibits a pattern of endothelium-dependent action which resembles more closely that of SNAP than that of GTN.

References

AHLNER, J., ANDERSSON, R.G.G., TORFGÅRD, K. & AXELSSON, K.L. (1991). Organic nitrate esters: clinical use and mechanism of actions. *Pharmacol. Rev.*, **43**, 351–423.

AXELSSON, K.L. & ANDERSSON, R.G.G. (1983). Tolerance towards glyceryl trinitrate, induced in vivo, is correlated to a reduced cGMP response and an alteration in cGMP turnover. *Eur. J Pharmacol.*, **88**, 71–79.

BENNET, B.M., MCDONALD, B.J. & ST. JAMES, M.J. (1992). Hepatic cytochrome P-450-mediated activation of rat aortic guanylyl cyclase by glyceryl trinitrate. *J. Pharmacol. Exp. Ther.*, **261**, 716–723.

BRIAN, J.F., MCLAUGHLIN, B.E., BREEDON, T.H., BENNET, B.M., NAKATSU, K. & MARKS, G.S. (1986). Biotransformation of glyceryl trinitrate occurs concurrently with relaxation of rabbit aorta. *J. Pharmacol. Exp. Ther.*, **237**, 608–614.

BUSSE, R., POHL, U., MÜLSCH, A. & BASSENGE, E. (1989). Modulation of the vasodilator action of SIN-1 by the endothelium. *J. Cardiovasc. Pharmacol.*, **14** (Suppl), S81–S85.

CHUNG, S.J. & FUNG, H.L. (1990). Identification of the subcellular site for nitroglycerin metabolism to nitric oxide in bovine coronary smooth muscle cells. *J. Pharmacol. Exp. Ther.*, **253**, 614–619.

D'ORLEANS-JUSTE, P., MITCHELL, J.A., WOOD, E.G., HECKER, M. & VANE, J.R. (1992). Comparison of the release of vasoactive factors from venous and arterial bovine cultured endothelial cells. *Can. J. Physiol. Pharmacol.*, **70**, 687–694.

DE MEY, J.G. & VANHOUTTE, P.M. (1982). Heterogeneous behaviour of the canine arterial and venous wall: importance of the endothelium. *Circ. Res.*, **51**, 439–447.

FEELISCH, M. & KELM, M. (1991). Biotransformation of organic nitrates to nitric oxide by vascular smooth muscle and endothelial cells. *Biochem. Biophys. Res. Commun.*, **180**, 286–293.

FEELISCH, M. & NOACK, E. (1987). Correlation between nitric oxide formation during degradation of organic nitrates and activation of guanylate cyclase. *Eur. J. Pharmacol.*, **139**, 19–30.

FIELD, L., RAVICHANDRAN, R., LENHERT, G. & CARNAHAN, G.E. (1978). An unusual stable thionitrate from N-acetyl-D,L-penicillamine; x-ray crystal and molecular structure of 2-(acetylamina)-2-carboxy-1,1-dimethylethyl thionitrate., *J. Chem. Soc. Chem. Commun.*, **1157**, 249–250.

FORSTER, C., MAIN, J.S. & ARMSTRONG, P.W. (1990). Endothelium modulation of the effects of nitroglycerin on blood vessels from dogs with pacing-induced heart failure. *Br. J. Pharmacol.*, **101**, 109–114.

FREIMAN, P.C., MITCHELL, G.G., HEISTADT, D.D., ARMSTRONG, M.L. & HARRISON, D.G. (1986). Atherosclerosis impairs endothelium-dependent vascular relaxation to acetylcholine and thrombin in primates. *Circ. Res.*, **58**, 783–789.

FURCHGOTT, R.F. & ZAWADZKI, J.V. (1980). The obligatory role of endothelial cells in the relaxation of arterial smooth muscle by acetylcholine. *Nature*, **288**, 373–376.

HAFNER, D., HEINEN, E. & NOACK, E. (1977). Mathematical analysis of concentration-response-relationships. *Arzneim. Forsch.*, **27**, 1871–1873.

IGNARRO, L.J., LIPTON, H., EDWARDS, J.C., BARICOS, W.H., HYMAN, A.L., KADOWITZ, P.J. & GUETTER, C.A. (1981). Mechanism of vascular smooth muscle relaxation by organic nitrates, nitrites, nitroprusside and nitric oxide: evidence for the involvement of S-nitrosothiols as active intermediates. *J. Pharmacol. Exp. Ther.*, **218**, 739–749.

IGNARRO, L.J., BUGA, G.M., WOOD, K.S., BYRNS, R.E. & CHAUDHURI, G. (1987). Endothelium-derived relaxing factor produced and released from artery and vein is nitric oxide. *Proc. Natl. Acad. Sci. U.S.A.*, **84**, 9265–9269.

JACKSON, W.F. & BUSSE, R. (1991). Elevated guanosine 3':5'-cyclic monophosphate mediates the depression of nitrovasodilator reactivity in endothelium-intact blood vessels. *Naunyn-Schmied. Arch. Pharmacol.*, **344**, 345–350.

JAYAKODY, T.L., SENARATNE, M.P.J., THOMPSON, A.B.R. & KAPPAGODA, C.T. (1985). Cholesterol feeding impairs endothelium-dependent relaxation of rabbit aorta. *Can. J. Physiol. Pharmacol.*, **63**, 1206–1209.

KOJDA, G., KLAUS, W., WERNER, G. & FRICKE, U. (1990). Reduced responses of nitrendipine in PGF2α-precontracted porcine isolated arteries after pretreatment with methylene blue. *Basic Res. Cardiol.*, **85**, 461–466.

KOJDA, G., BECK, J.K. & NOACK, E. (1992a). Nitrate action and tolerance in porcine vena cordis magna. *Naunyn-Schmied. Arch. Pharmacol.*, **346**, R35.

KOJDA, G., BEHNE, M. & NOACK, E. (1992b). Attenuation of nitrate activity and tolerance by intact endothelium. *J. Vasc. Res.*, **29**, 151.

KOJDA, G., KLAUS, W., WERNER, G. & FRICKE, U. (1992c). Intervascular and stimulus selectivity of nitrendipine and related derivatives in KCl and prostaglandin $F_{2\alpha}$ precontracted porcine arteries. *Br. J. Pharmacol.*, **106**, 85–90.

KOJDA, G., MEYER, W. & NOACK, E. (1993). Changes in intracellular free thiols and disulphides induced by nitrovasodilators and endothelium in porcine coronary arteries. *Naunyn-Schmied. Arch. Pharmacol.*, **347**, R247.

KOJDA, G. & NOACK, E. (1993). Nitric oxide liberating, soluble guanylate cyclase stimulating and vasorelaxing properties of the new nitrate-compound SPM 3672. *J. Cardiovasc. Pharmacol.*, **22**, 103–111.

KU, D.D., CAULFIELD, J.B. & KIRKLIN, J.K. (1992). Endothelium-dependent responses on human coronary blood vessels. In *Endothelial Regulation of Vascular Tone*. Ryan, U.S. & Rubanyi, G.M. pp. 197–223. New York: Marcel Dekker, Inc.

LÜSCHER, T.F., DIEDRICH, D., SIEBENMANN, R., LEHMANN, K. & STÜLZ, P. (1988). Difference between endothelium-dependent relaxation in arterial and in venous coronary bypass grafts. *N. Engl. J. Med.*, **319**, 462–467.

MONCADA, S. & HIGGS, E.A. (1991). Endogenous nitric oxide: physiology, pathology and clinical relevance. *Eur. J. Clin. Invest.*, **21**, 361–374.

MONCADA, S., REES, D.D., SCHULZ, R. & PALMER, R.M.J. (1991). Development and mechanism of a specific supersensitivity to nitrovasodilators after inhibition of vascular nitric oxide sythesis in vivo. *Proc. Natl. Acad. Sci. U.S.A.*, **88**, 2166–2170.

MÜLSCH, A. & BUSSE, R. (1990). N^G-nitro-L-arginine (N5-[imino-(nitroamino)methyl]-L-ornithine) impairs endothelium-dependent dilations by inhibiting cytosolic nitric oxide synthesis from L-arginine. *Naunyn-Schmied. Arch. Pharmacol.*, **341**, 143–147.

NOACK, E. & FEELISCH, M. (1991). Molecular mechanism of nitrovasodilator bioactivation. In *Endothelial Mechanism of Vasomotor Control*, ed. Drexler, H., Zeiher, A.M., Bassenge, E. & Just, H. pp. 37–50. Darmstadt, Germany: Steinkopff Verlag.

PALMER, R.M., FERRIGE, A.G. & MONCADA, S. (1987). Nitric oxide accounts for the biological activity of endothelium derived relaxing factor. *Nature*, **327**, 524–526.

SALVEMINI, D., MOLLACE, V., PISTELLI, A., ANGGARD, E. & VANE, J. (1992). Metabolism of glyceryl trinitrate to nitric oxide by endothelial cells and smooth muscle cells and its induction by *Escherichia coli* lipopolysaccharide. *Proc. Natl. Acad. Sci. U.S.A.*, **89**, 982–986.

SCHRÖDER, H., LEITMAN, D.C., BENNET, B.M., WALDMAN, S.A. & MURAD, F. (1988). Glyceryl trinitrate-induced desensitisation of guanylate cyclase in cultured rat lung fibroblasts. *J. Pharmacol. Exp. Ther.*, **245**, 413–418.

SHIMOKAWA, H. & VANHOUTTE, P.M. (1987). Porcine coronary arteries with regenerated endothelium have a reduced endothelium-dependent responsiveness to aggregating platelets and serotonin. *Circ. Res.*, **61**, 256–270.

SHIRASAKI, Y. & SU, C. (1985). Endothelium removal augments vasodilation by sodium nitroprusside and sodium nitrite. *Eur. J. Pharmacol.*, **114**, 93–96.

THOM, S.M., HUGHES, A.D., MARTIN, G. & SEVER, P.S. (1987). The role of endothelium in the control of venous tone: studies on isolated human veins. *Clin. Physiol.*, **73**, 547–552.

THULESIUS, O., UGAILY-THULESIUS, L., NEGLEN, P. & SHUHAIBER, H. (1988). The role of endothelium in the control of venous tone: studies on isolated human veins. *Clin. Physiol.*, **8**, 359–366.

VANHOUTTE, P.M. & MILLER, V.M. (1985). Heterogeneity of endothelium-dependent responses in mammalian blood vessels. *J. Cardiovasc. Pharmacol.*, **7**, S12–S13.

WINK, D.A., OSAWA, Y., DARBYSHIRE, J.F., JONES, C.R., ESHENAUR, S.C. & NIMS, R.W. (1993). Inhibition of cytochromes P450 by nitric oxide and a nitric oxide-releasing agent. *Arch. Biochem. Biophys.*, **300**, 115–123.

(Received April 23 1993
Revised February 18, 1994
Accepted March 7, 1994)

Br. J. Pharmacol. (1994), **112**, 541–546

Competitive and non-competitive effects of 5-hydroxyindole on 5-HT_3 receptors in N1E-115 neuroblastoma cells

André R. Kooyman, Johannes A. van Hooft, [1]Patrick M.L. Vanderheijden & [2]Henk P.M. Vijverberg

Research Institute of Toxicology, Utrecht University, P.O. Box 80.176, NL-3508 TD Utrecht, The Netherlands

1 Effects of 5-hydroxyindole (5-OH-indole) (the aromatic moiety of 5-hydroxytryptamine (5-HT)) on 5-HT-evoked ion current and the nature of these effects on 5-HT_3 receptors have been investigated in whole-cell voltage clamp and radioligand binding experiments on cultured N1E-115 mouse neuroblastoma cells.

2 The amplitude of 10 μM 5-HT-evoked ion currents was enhanced up to 150% of the control value by increasing concentrations up to 10 mM 5-OH-indole with half maximum effect of 0.8 mM. At concentrations between 10 mM and 50 mM, 5-OH-indole blocked the 5-HT-evoked ion current. Both the enhancement and the block by 5-OH-indole were accompanied by a marked slowing of the kinetics of decay of the 5-HT-evoked inward currents.

3 The blocking effect was surmounted when the 5-HT concentration was raised from 10 μM to 100 μM. Conversely, the increase in amplitude and the slowing of the decay of the 5-HT-evoked ion current induced by 1 mM 5-OH-indole were not reversed by the same increase of 5-HT concentration.

4 The binding of the selective antagonist [^{3}H]-GR65630 to 5-HT_3 receptors was displaced by 5-OH-indole in a concentration-dependent manner with a pK_i of 1.96. In saturation binding experiments 10 mM 5-OH-indole reduced the affinity of [^{3}H]-GR65630, whereas the total number of binding sites remained unaffected.

5 It is concluded that the blocking effect of high concentrations of 5-OH-indole is due to a competitive interaction with the antagonist recognition sites of 5-HT_3 receptors, whereas the potentiating effect of lower concentrations of 5-OH-indole appears to be mediated by a distinct non-competitive interaction.

Keywords: 5-Hydroxytryptamine; 5-HT_3 receptor; desensitization; block; 5-hydroxyindole; voltage clamp; ion current; radioligand binding; [^{3}H]-GR65630; N1E-115 mouse neuroblastoma cells

Introduction

The 5-HT_3 receptor belongs to the group of ligand-gated ion channels. The direct coupling of the 5-HT_3 receptor to an intrinsic ion channel has been established by the molecular cloning of a 5-HT_3 receptor subunit, which expresses both the receptor and the ion channel on reconstitution (Maricq *et al.*, 1991). Agonist interaction with the 5-HT_3 receptor ion current is unaffected by any of the known second messenger systems (Hoyer & Neijt, 1988; Yakel & Jackson, 1988; Yakel *et al.*, 1991; Yang, 1990).

In N1E-115 mouse neuroblastoma cells the interaction of 5-HT with the 5-HT_3 receptor causes the activation of ion current, which rapidly reaches its peak value and subsequently decays to a small steady level in the continuous presence of agonist. The pharmacology of this 5-HT-evoked ion current indicates that it is carried solely by 5-HT_3 receptor-operated ion channels (Neijt *et al.*, 1988). The rate of decay of ion current depends on the concentration of 5-HT. In the continuous presence of 5-HT, the ion current decays at the same rate at which the maximum attainable 5-HT-evoked ion current is reduced. Both inward current decay and the reduction of the maximum response reflect the equilibration between so-called desensitized and non-desensitized states of the ligand-gated ion channels during exposure to the agonist (Neijt *et al.*, 1989).

Recently, we found that millimolar concentrations of tetraethylammonium ions (TEA) block 5-HT_3 receptor-operated ion current and prevent its desensitization by a competitive interaction at (part of) the agonist recognition site (Kooyman *et al.*, 1993b). Conversely, 5-OH-indole, the aromatic moiety of the endogenous ligand 5-HT, enhances the amplitude of 5-HT_3 receptor agonist-evoked ion current in N1E-115 cells and, concomitantly, slows the kinetics of ion current decay (Kooyman *et al.*, 1993a).

Since the exact nature of the interaction of 5-OH-indole with 5-HT_3 receptors in N1E-115 cells remains to be established, we have investigated the concentration-dependent effects in whole-cell voltage clamp and radioligand binding experiments. The combined results show dual effect of 5-OH-indole on the 5-HT_3 receptor.

Methods

Cell culture

Mouse neuroblastoma cells of the clone N1E-115 (Amano *et al.*, 1972) were grown under the conditions described previously by Neijt *et al.* (1989). Subcultures of passage numbers 31–42 were used. For ligand binding studies, undifferentiated cells, grown up to a density of 60×10^6 cells per dish (Falcon, 500 cm^2), were harvested by scraping the bottom of the culture dish and stored in external solution at −80°C. For electrophysiological experiments, cells were cultured in tissue culture T-flasks, up to a density of 70×10^3 cells cm^{-2} and were resuspended every five days after dissociation in phosphate buffered saline containing 1% trypsin. Subcultures were grown in 3.5 cm tissue culture dishes. On day 2 in subculture differentiation of the cells was initiated in culture medium additionally supplemented with 1 mM dibutyryl cyclic AMP and 1 mM 3-isobutyl-1-methylxanthine. This medium was refreshed about every other day. Cells were used for experiments 7–12 days after the initiation of differentiation.

[1] Present address: Organon International BV, Dept. Neuropharmacology, P.O. Box 20, NL-5340 BH Oss, The Netherlands.
[2] Author for correspondence.

Electrophysiology

Ion currents were recorded by a suction pipette technique for whole-cell voltage clamp (Lee *et al.*, 1978) as described previously by Neijt *et al.* (1989). Cells were voltage clamped at − 70 mV. Series resistance, initially estimated from the instantaneous voltage jump in response to a constant current stimulus, was compensated under voltage clamp for about 80–85%. To maintain cells at holding potential in the absence of any stimulation, a steady inward current injection was required that varied between cells in the range of 0.1–0.5 nA. Membrane currents were low-pass filtered (− 3 dB at 1 kHz, 12 dB/oct), digitized (8 bits, 1024 points/record) and stored on a magnetic disc for off-line computer analysis.

Solutions

The ionic composition of the pipette solution was (in mM): K-glutamate 100, Na-HEPES 20, sucrose 120. The pH was adjusted to 7.25 with L-glutamic acid. The external solution contained (in mM): NaCl 125, KCl 5.5, HEPES 20, $CaCl_2$ 1.8, $MgCl_2$ 0.8, glucose 24 and sucrose 37, and the pH was adjusted to 7.3 with approximately 7 mM NaOH. The incubation buffer used in ligand binding studies was identical to the external solution.

Application of drugs

In the electrophysiological studies, cells were continuously superfused with external solution and ion currents were evoked by changing to agonist- and, optionally, drug-containing external solutions. The time constant of solution exchange was $\leqslant$ 1 s (Neijt *et al.*, 1989). Frozen concentrated stock solutions of 10 mM 5-HT and 1 M 5-OH-indole (dissolved in dimethylsulphoxide) were freshly thawed prior to the experiments. Unless the experimental protocol required otherwise, cells were repetitively exposed to the agonist at intervals of at least 100 s in order to allow complete recovery from desensitization. All experiments were performed at room temperature (20–24°C).

Ligand binding

Cells stored at − 80°C were thawed and diluted in cold incubation buffer to obtain a final concentration of 4×10^5 cells ml^{-1}. Cells were homogenized with a Polytron homogenizer for 20 s at maximal setting. The radioligand [^{3}H]-GR65630 was used as selective 5-HT_3 receptor antagonist (Kilpatrick *et al.*, 1987; 1988; 1989; Lummis *et al.*, 1990; Sharif *et al.*, 1991). For binding assays 400 µl of cell homogenate, 50 µl [^{3}H]-GR65630 and 50 µl of either control buffer or compound containing buffer were incubated at room temperature (20–24°C). Experiments were started by the addition of cell homogenates to glass incubation vials that contained radioligand and drug. The incubation was stopped by rapid filtration over Whatman GF/B glass fibre filters on a Brandell MR24 cell harvester. Filters were washed three times for 5 s with ice-cold 5 mM Tris HCl buffer (pH 7.4). Filter bound radioactivity was counted for 3 min in scintillation vials containing 2.5 ml Ultima Gold MV (Packard) using a Packard instruments 2200CA liquid scintillation spectrophotometer. Non-specific binding was determined in the presence of 100 µM MDL 72222. The exact concentration of radioligand was calculated from the total radioactivity added to the incubation mixture. Protein contents were measured according to Lowry *et al.* (1951). The association rate of 0.03 nM [^{3}H]-GR65630 was determined from samples incubated for various periods. The dissociation rate of the radioligand was determined from samples initially incubated with the radioligand for 15 min and subsequently diluted with 100 µM MDL 72222 for various periods. Saturation binding was performed by the incubation of membranes with increasing concentrations of the radioligand for 15 min. For competition experiments, samples were incubated for 15 min using 6 concentrations of drug at approximately 0.3 nM [^{3}H]-GR65630. All experiments were carried out in triplicate.

Data analysis and statistics

The dissociation rate constant (k_{-1}) was determined from the monoexponential loss of bound radioligand after dilution with 100 µM MDL 72222. The association rate constant (k_1) was calculated from the equation:

$$k_{+1} = (k_{obs} - k_{-1})/[L] \qquad [1]$$

in which [L] is the concentration of free radioligand and k_{obs} the rate of radioligand binding with time. K_D values were calculated from the kinetic rate constants and from saturation binding data by fitting a Langmuir adsorption isotherm. Apparent dissociation constants (K_i) were calculated from IC_{50} values according to the equation:

$$K_i = IC_{50}/(1 + [L]/K_D) \qquad [2]$$

(Cheng & Prusoff, 1973) using the K_D value obtained from saturation binding with [^{3}H]-GR65630. Scatchard transformation of saturation binding data were tested for linearity by least-squares regression analysis. Results are expressed as means ± s.d. of n independent experiments. Concentration-effect curves were fitted according to the function:

$$i = i_{max}/(1 + \{EC_{50}/[drug]\}^n) \qquad [3]$$

All non-linear curve fitting was performed using a Levenberg-Marquardt non-linear least squares algorithm (Marquardt, 1963).

Drugs

[^{3}H]-GR65630 ([^{3}H]-3-(5-methyl-1H-imidazol-4-yl)-1-(1-methyl-1H-indol-3-yl)-1-propanone, specific activity 79.2 Ci $mmol^{-1}$) was obtained from DuPont NEN, The Netherlands; tropisetron (ICS 205-930; (3 α-tropanyl)-1H-indol-3-carboxylic acid ester) from Sandoz, Basle, Switzerland; MDL 72222 (3-tropanyl-3,5-dichloro-benzoate) and 2-Me-5-HT ((±)-2-methyl-5-hydroxytryptamine maleate) from Research Biochemicals Inc., Natick, U.S.A.; 5-HT (5-hydroxytryptamine creatinine sulphate) and 5-OH-indole (5-hydroxyindole) from Sigma, St. Louis, U.S.A. and TEA (tetraethylammonium bromide) from Merck-Schuchardt, Munich, Germany.

Results

Modulation of the 5-HT-evoked ion current by 5-OH-indole

Ion currents evoked by superfusion of voltage-clamped N1E-115 cells with 10 µM 5-HT changed markedly in the presence of external 5-OH-indole. In the range of 100 µM to 10 mM, 5-OH-indole enhanced the amplitude and slowed the kinetics of decay of the 5-HT-evoked inward current (Figure 1a–c). The onset of these effects was rapid, since no difference was observed between 5-HT responses evoked during continuous superfusion of 5-OH-indole and responses evoked by intermittent coapplications of 5-HT and 5-OH-indole. On removal of 5-OH-indole its effects were also readily reversed. Higher concentrations of 5-OH-indole caused block of the 5-HT-evoked ion current, but the kinetics of the remaining ion current remained slow. In addition, slow tail currents, which indicate reversal of block, were observed on washing after 5-OH-indole concentrations $>$ 1 mM (Figure 1c–e). No effects were detected when up to 50 mM 5-OH-indole was superfused alone in otherwise normally responding cells (Figure 1f). Internal application of 10 mM 5-OH-indole neither affected the 5-HT-evoked ion current, nor caused an effect by itself (result not shown).

The concentration-dependence of the effects of 5-OH-indole on peak amplitude and on the kinetics of decay of the 5-HT-evoked ion current is shown in Figure 2. The peak amplitude of 5-HT-evoked inward current increased in a sigmoidal manner with increasing concentrations of 5-OH-indole up to 10 mM. A steep decrease of the peak inward current amplitude to a level below the amplitude of control responses, was observed when the concentration of 5-OH-indole was further increased. The concentration-effect curve fitted to the normalized peak amplitudes in the range up to 10 mM 5-OH-indole yielded an EC_{50} value of 0.8 ± 0.1 mM 5-OH-indole and a slope factor of 1.4 ± 0.2. The effects on the time constant of inward current decay showed a similar concentration-dependence, but did not appear to saturate at the maximum potentiation of the peak amplitude observed.

The effect of 1 mM 5-OH-indole was the same, irrespective of whether ion current was evoked by the nearly maximal effective concentration of 10 μM or by the supramaximal concentration of 100 μM 5-HT (Figure 3a). In the presence of 1 mM 5-OH-indole, the peak amplitude of the 10 μM 5-HT-evoked ion current was increased to $123 \pm 11\%$ and the time constant of decay to $319 \pm 37\%$ ($n = 5$) of control values obtained in the absence of 5-OH-indole. The peak amplitude of the 100 μM 5-HT-evoked ion current in the same cells was enhanced by 1 mM 5-OH-indole to $127 \pm 11\%$ and the time constant of decay to $352 \pm 66\%$ ($n = 5$) of control values. The results obtained at the two 5-HT concentrations did not differ significantly (Student's t test, $P = 0.36-0.58$). Conversely, the blocking effect of 5-OH-indole depended on the agonist concentration. Figure 3b shows that the amplitude of the 5-HT-evoked ion current in the presence of 25 mM 5-OH-indole is significantly enhanced when the agonist concentration is raised from 10 μM to 100 μM. In the presence of 25 mM 5-OH-indole, the peak amplitude of the 10 μM 5-HT-evoked ion current was $104 \pm 7\%$ ($n = 3$) and the peak amplitude of the 100 μM 5-HT-evoked current was $157 \pm 26\%$ ($n = 3$) of control values ($P = 0.03$). In some cells a simultaneous acceleration of the response kinetics was observed. These results show that the blocking effect of a high concentration of 5-OH-indole is surmounted by increasing the agonist concentration, whereas the enhancing effects of a lower concentration of 5-OH-indole cannot be surmounted.

Ligand binding to the 5-HT$_3$ receptor

The binding of [^{3}H]-GR65630 to N1E-115 cell homogenates was rapid and reversible (Figure 4a,b). The dissociation

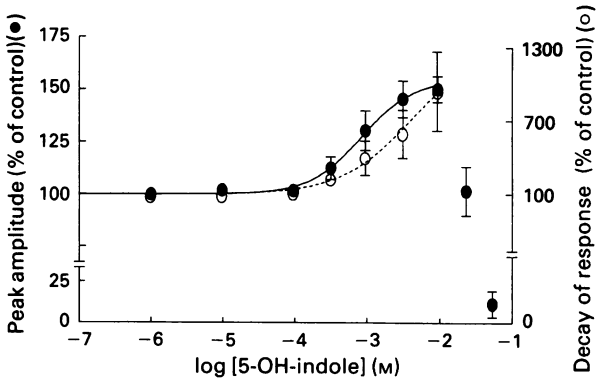

Figure 2 Concentration-dependence of the effects of 5-hydroxyindole (5-OH-indole) on the peak amplitude (●) and on the time constant of decay (○) of the 10 μM 5-hydroxytryptamine (5-HT)-induced inward current. Data points are mean values of 3–6 independent determinations obtained from a total of 38 cells. The solid line represents the concentration-effect curve fitted to the data obtained with concentrations ≤ 10 mM 5-OH-indole. The estimated EC_{50} value was 0.8 ± 0.1 mM, the slope factor 1.4 ± 0.2, and the maximum increase of the amplitude $56 \pm 2\%$. Both the peak amplitude and the time constant of inward current decay in the presence of 5-OH-indole are expressed as a percentage of control values obtained in the same cells.

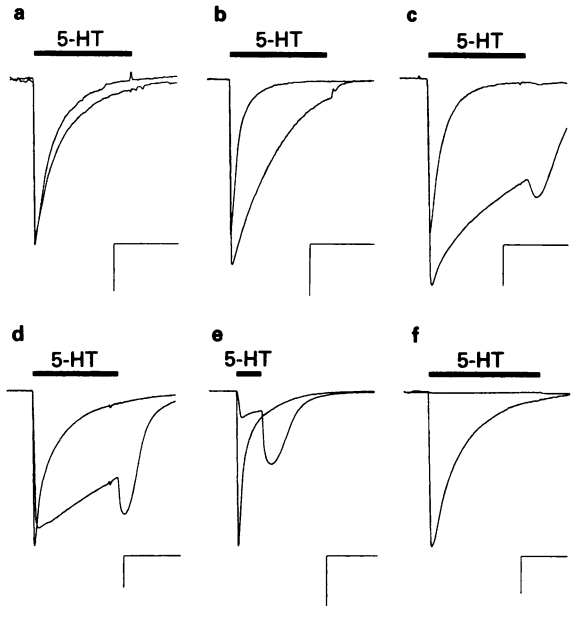

Figure 1 Effects of 5-hydroxyindole (5-OH-indole) on 5-hydroxytryptamine (5-HT)-induced inward current in N1E-115 cells. Voltage clamped cells were superfused with 10 μM 5-HT, as indicated by the bars above the traces, in the absence and in the presence of 5-OH-indole at concentrations of 100 μM (a); 1 mM (b); 10 mM (c); 25 mM (d) and 50 mM (e). At low concentrations 5-OH-indole enhanced the amplitude and slowed the decay of the 5-HT-induced inward current (a–c), whereas at high concentrations of 5-OH-indole additional block of the inward current was observed (d–e). Note the occurrence of tail currents on washing following 5-OH-indole application at concentrations ≥ 10 mM (c–e). In contrast to 5-HT, superfusion of 50 mM 5-OH-indole (bar) did not induce a detectable response in voltage clamped N1E-115 cells (f). Each pair of traces of inward current was recorded from a single cell and the data from different cells were scaled for matching peak amplitudes of the control inward currents. Vertical calibrations: 2 nA (a,d); 5 nA (c); 10 nA (b,e,f). Horizontal calibrations 20 s (a–c,e); 10 s (d,f).

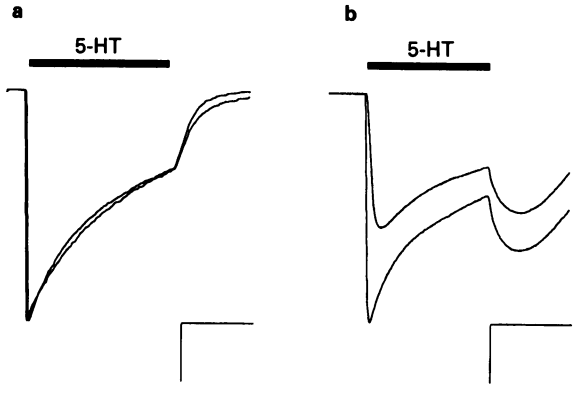

Figure 3 Dependence of the effects of 5-hydroxyindole (5-OH-indole) on agonist concentration. (a) Superimposed traces of inward current evoked in the same cell by 10 μM and 100 μM 5-hydroxytryptamine (5-HT, horizontal bar) in the continuous presence of 1 mM 5-OH-indole. Neither the amplitude nor the kinetics of inward current decay are changed by increasing the agonist concentration. Note that 100 μM 5-HT is a supra-maximal concentration. (b) Superimposed traces of inward current evoked in the same cell by 10 μM and 100 μM 5-HT (horizontal bar) in the continuous presence of 25 mM 5-OH-indole. The amplitude of the inward current is increased at 100 μM 5-HT, i.e., the blocking effect of 25 mM 5-OH-indole is surmounted by increasing the agonist concentration. Vertical calibrations: 5 nA. Horizontal calibrations: 20 s (a); 10 s (b).

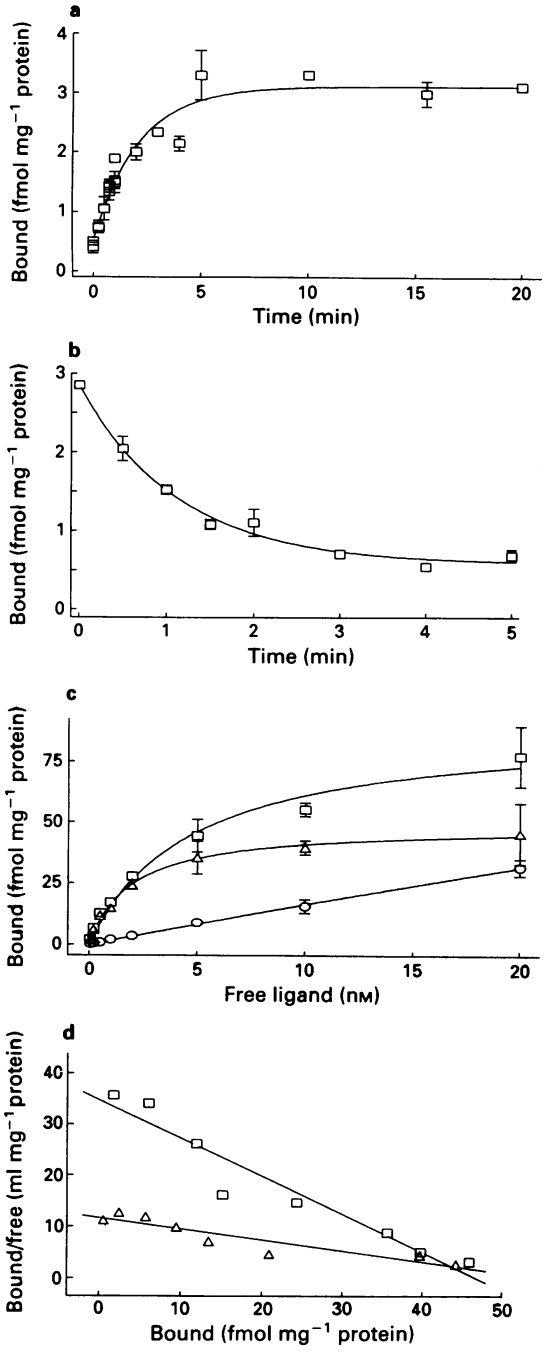

Figure 4 Binding of [^{3}H]-GR65630 to N1E-115 cell homogenates. (a) Association of the radioligand. The data represent the specific binding of 78 pM [^{3}H]-GR65630, determined by subtracting non-specific binding in the presence of 100 μM MDL 72222 from total binding, versus incubation time. Single exponential association curves were fitted according to the equation $B_t = B_\infty \times (1-\exp(-k_{obs} \times t))$. Estimated values of k_{obs} and B_∞ were 0.76 min^{-1} and 2.96 fmol mg^{-1} protein (s.e. of fit = 1.16×10^5). Imposing k_{obs} = 0.840 (calculated using the K_D value of 0.68 nM obtained from saturation binding and the k_{-1} value of 0.753 min$_{-1}$ obtained from radioligand dissociation, according to eqn. (1) yielded a fitted value for B_∞ of 2.89 fmol mg^{-1} protein (s.e. of fit = 1.07×10^5). (b) Dissociation of the radioligand measured at various periods after the addition of an excess of 100 μM MDL 72222 to samples that were first incubated for 15 min with 30 pM of the radioligand. The drawn dissociation curve was fitted according to the equation $B_t = B_0 \times \exp(-k_{-1} \times t) + C$, in which B represents total binding as a function of time and C the non-specific binding, which was not displaced in the presence of MDL 72222. (c) Saturation binding of the radioligand. Samples were incubated with various concentrations of [^{3}H]-GR65630 in the absence (□) to determine total binding and in the presence of 100 μM MDL 72222 (○) to determine non-specific binding. Specific binding (△) was calculated by subtracting non-specific binding from total binding. The specific binding curve represents the fitted Langmuir adsorption isotherm. (d) Scatchard transformation of the saturation binding of [^{3}H]-GR65630 in the absence (□) and in the presence (△) of 10 mM 5-OH-indole. Drawn lines were obtained by linear regression. All data points represent the mean values of triplicate determinations.

kinetics were fitted by a single exponential decay to a steady level of non-specific binding. The mean dissociation rate constant (k_{-1}) was 0.75 ± 0.12 min^{-1} ($n = 3$) and the non-specific binding represented $21 \pm 7\%$ of the radioactivity bound at $t = 0$. Fitting the monoexponential association kinetics obtained in 3 experiments using final radioligand concentrations of 45, 78 and 24 pM yielded rate constants (k_{obs}) of 0.68, 0.76 and 1.71 min^{-1}, respectively. The estimated k_{obs} varied too much to calculate a reliable K_D value. However, the association data were equally well fitted by k_{obs} values which were consistent with the K_D value from saturation binding (see Figure 4 and below). This indicates that, within the range of variability of the data, the same apparent radioligand affinities can be deduced from kinetic and saturation binding experiments.

The receptor binding profile was further characterized in competition binding experiments using the selective 5-HT$_3$ receptor antagonists, tropisetron and MDL 72222 and by the agonists, 5-HT and 2-Me-5-HT. The affinities of these compounds to displace the binding of [^{3}H]-GR65630 to the N1E-115 cell homogenates are listed in Table 1 and are compared to values obtained in other studies. At the highest concentrations, all competing drugs tested displaced the binding of [^{3}H]-GR65630 to the same extent as did 100 μM MDL 72222, which was used to monitor non-specific binding. This suggests that [^{3}H]-GR65630 and the competing drugs act on the same population of binding sites.

Modulation of ligand binding by 5-OH-indole

The 5-HT moiety, 5-OH-indole, displaced specifically bound [^{3}H]-GR65630 with a low pK_i value of 1.96 ± 0.53 ($n = 6$). The fraction of specifically bound radioligand that was displaced by 1 mM 5-OH-indole was $4.7 \pm 4.5\%$. It has been shown previously that external tetraethylammonium (TEA) is also a low affinity ligand of 5-HT$_3$ receptors in N1E-115 cells (Hoyer & Neijt, 1988). In the present experiments, TEA displaced [^{3}H]-GR65630 with a pK_i value of 3.03 ± 0.36 ($n = 3$) (see Table 1). Although electrophysiological experiments have demonstrated that TEA is a competitive 5-HT$_3$ receptor antagonist (Kooyman *et al.*, 1993b), a similar conclusion with respect to the nature of the interaction of 5-OH-indole cannot yet be drawn. The nature of the interaction between the binding of the unlabelled drug 5-OH-indole and that of [^{3}H]-GR65630 was investigated in saturation binding experiments (Figure 4c). 5-OH-indole causes an increase in the K_D but does not affect the B_{max} of the radioligand. In the absence of 5-OH-indole, the mean B_{max} and K_D values were 42.3 ± 1.9 fmol mg^{-1} protein ($\sim 2 \times 10^4$ sites/cell) and 0.68 ± 0.10 nM ($n = 3$), respectively, whereas in the presence of 10 mM 5-OH-indole the respective values were 46.9 ± 3.8 fmol mg^{-1} protein and 1.94 ± 0.36 nM ($n = 3$). Linear regression analysis of the Scatchard transforms (Figure 4d) showed that the two slopes, and consequently the K_D values, differed significantly at the $P < 0.001$ level. B_{max} values were within the 95% confidence limits and did not differ significantly. Both lines did not deviate significantly from linear, indicating that the radioligand labels a single affinity population of sites. Thus, 10 mM 5-OH-indole reduces the affinity of the radioligand without affecting the total number of sites, indicating a competitive interaction with the 5-HT$_3$ receptor.

Table 1 Displacement of radioligand binding to 5-HT$_3$ receptors in N1E-115 neuroblastoma cells by various unlabelled compounds

Ligand	*[^{3}H]-GR65630* (homogenate)[a]	*[^{3}H]-tropisetron* (homogenate)[b]	*[^{3}H]-GR65630* (intact cells)[c]
Tropisetron	9.10 ± 0.04 (3)	9.09	9.30
MDL 72222	7.59 ± 0.07 (4)	8.21	7.91
5-HT	6.31 ± 0.70 (3)	6.42	6.25
2-Me-5-HT	5.21 ± 0.43 (3)	5.89	5.81
5-OH-indole	1.96 ± 0.53 (6)	–	–
TEA	3.03 ± 0.36 (3)	2.36	–

Affinities of the ligands are expressed as pK_i values.
[a]This report, mean ± s.d. (*n*).
[b]After Hoyer & Neijt (1988).
[c]Calculated from radioligand concentration, IC_{50} and K_D values after Lummis *et al.* (1990).

Discussion

The interaction of 5-OH-indole with 5-HT$_3$ receptors in N1E-115 neuroblastoma cells has been investigated in whole-cell voltage clamp and radioligand binding experiments. The electrophysiological results agree with the previous observation that 1 mM 5-OH-indole potentiates the 5-HT$_3$ receptor-mediated ion current by enhancing the peak amplitude and by preventing desensitization (Kooyman *et al.*, 1993a). Potentiation of 5-HT$_3$ receptor-mediated ion current by ethanol in NCB-20 cells (Lovinger, 1991) and by trichloroethanol in rat nodose ganglion neurones (Lovinger & Zhou, 1993) has been reported before. This potentiation was associated with an enhanced rate of decay of the 5-HT-induced ion current, in contrast to the effect of 5-OH-indole.

The present description of the concentration-dependence of the electrophysiological effects of 5-OH-indole shows an additional blocking effect at high concentrations. The latter is reflected by a decrease of the peak amplitude of the 5-HT-induced inward current and by the occurrence of tail currents on washing. The electrophysiological results demonstrate that potentiation and block are distinct effects of 5-OH-indole. Firstly, the data on the concentration-dependent effects (Figure 1 and 2) show that potentiation is caused by low concentrations and block by high concentrations of 5-OH-indole. Secondly, the blocking effect is surmounted at increased agonist concentration in contrast to the potentiating effect (Figure 3). These results indicate that the two effects are due to interactions of 5-OH-indole with different sites. At intermediate 5-OH-indole concentrations, a mixture of potentiating and blocking effects is observed (Figure 1c,d). At 10 mM 5-OH-indole, enhancement of the amplitude of the 5-HT-induced ion current occurs simultaneously with a slow tail current. The tail current indicates that block has occurred in the presence of 5-OH-indole and is reversed on washing. With increasing concentration of 5-OH-indole the potentiating effect is reduced and reverses into a reduction of peak amplitude and the tail current becomes more pronounced (Figure 1c,e). These results indicate that the concentration-dependence of potentiation is distinct from that of block and that the concentration-ranges in which the two effects occur overlap. Since potentiation and block have oppositely effects on the 5-HT-induced ion current, it is not possible to determine the exact concentrations that cause half maximum potentiation and block. However, it can be inferred that half maximum block occurs at a concentration beyond 1 mM, since the absence of a tail current indicates that block does not occur at this concentration of 5-OH-indole (Figure 1b).

In order to corroborate the electrophysiological findings, the effects of 5-OH-indole were also investigated in receptor binding experiments. The radiolabelled antagonist [^{3}H]-GR65630 labels 5-HT$_3$ receptors in N1E-115 cell homogenates with a K_D value of 0.68 nM (Figure 4), i.e., with similar high affinity as previously reported for intact N1E-115 cells (Lummis *et al.*, 1990) and for NCB-20 cell homogenates (Sharif *et al.*, 1991). The radioligand is also displaced by a number of selective 5-HT$_3$ receptor (ant)agonists with apparent affinities which are similar to values reported for the displacement of [^{3}H]-tropisetron in N1E-115 homogenates (Hoyer & Neijt, 1988) and of [^{3}H]-GR65630 in intact N1E-115 cells (Lummis *et al.*, 1990) as can be seen from the compilation of data in Table 1. Half maximum displacement of [^{3}H]-GR65630 was obtained at a concentration of approximately 10 mM 5-OH-indole, whereas at 1 mM only 5% of the specifically bound radioligand was displaced. In addition, the binding experiments showed that 10 mM 5-OH-indole displaces the radioligand in a competitive manner (Table 1; Figure 4d). A comparison of the electrophysiological and binding results shows that 5-OH-indole causes a surmountable block of the 5-HT-induced ion current and competitively displaces the radioligand with similar low affinities. Therefore, it is concluded that high concentrations of 5-OH-indole block 5-HT$_3$ receptors by an interaction with the ligand recognition site. The non-surmountable potentiation of 5-HT-induced ion current, which is observed at concentrations of 5-OH-indole which fail to displace the radioligand, appears to be due to a non-competitive effect.

Similar to 5-OH-indole, high concentrations of TEA displace the binding of [^{3}H]-tropisetron (Hoyer & Neijt, 1988) as well as that of [^{3}H]-GR65630 (Table 1). Functional competition, as between the agonist and 5-OH-indole, was previously demonstrated to occur between 5-HT and TEA (Kooyman *et al.*, 1993b). Thus, both compounds appear to interact with the ligand recognition site of the 5-HT$_3$ receptor, but agonistic effects of 5-OH-indole, TEA, and of the combination of the two have never been observed (A.R. Kooyman, unpublished observation). From the binding properties of chemically distinct antagonists it has been proposed that ligand binding at the 5-HT$_3$ receptor involves interactions with a cationic and an aromatic site (Gozlan & Langlois, 1992). It is conceivable that TEA and 5-OH-indole compete with antagonist binding at the cationic and aromatic site, respectively. The large difference between the affinity of 5-HT and the affinities of 5-OH-indole and TEA (Table 1) as well as the absence of agonistic effects of TEA and 5-OH-indole suggest that the interaction of 5-HT with its recognition site involves more than a two point interaction with a cationic and an aromatic site. A further investigation of the site at which 5-OH-indole causes the non-competitive potentiation of the 5-HT$_3$ response and of other ligands interacting with this site is of interest in view of its prominent modulatory role in the neuronal response to 5-HT.

We are grateful to Ms Paula Martens for maintaining the cell cultures; Ing. Aart de Groot for electronics and computer support and Eric van der Haar for experimental assistance. Drs Gé Ruigt and Thijs de Boer of Organon International B.V., Oss, The Netherlands are acknowledged for providing facilities to perform radioligand binding experiments. This investigation has been supported by the NWO-foundation for Medical and Health Research (grant no. 900-553-021).

References

AMANO, T., RICHELSON, E. & NIRENBERG, P.G. (1972). Neurotransmitter synthesis by neuroblastoma clones. *Proc. Natl. Acad. Sci. U.S.A.*, **69**, 258–263.

CHENG, Y.C. & PRUSOFF, W.H. (1973). Relationship between inhibition constant (K_i) and the concentration of inhibitor which causes 50 percent inhibition (IC_{50}) of an enzymatic reaction. *Biochem. Pharmacol.*, **22**, 3099–3108.

GOZLAN, H. & LANGLOIS, M. (1992). Structural analysis of receptor-ligand interactions. In *Central and Peripheral 5-HT$_3$ Receptors*. ed. Hamon, M. pp. 59–88. London: Academic Press.

HOYER, D. & NEIJT, H.C. (1988). Identification of serotonin 5-HT$_3$ recognition sites in membranes of N1E-115 neuroblastoma cells by radioligand binding. *Mol. Pharmacol.*, **33**, 303–309.

KILPATRICK, G.J., JONES, B.J. & TYERS, M.B. (1987). Identification and distribution of 5-HT$_3$ receptors in rat brain using radioligand binding. *Nature*, **330**, 746–748.

KILPATRICK, G.J., JONES, B.J. & TYERS, M.B. (1988). The distribution of specific binding of the 5-HT$_3$ receptor ligand [^{3}H]-GR65630 in rat brain using quantitative autoradiography. *Neurosci. Lett.*, **94**, 156–160.

KILPATRICK, G.J., JONES, B.J. & TYERS, M.B. (1989). Binding of the 5-HT$_3$ ligand, [^{3}H]-GR65630, to rat area postrema, vagus nerve and the brains of several species. *Eur. J. Pharmacol.*, **159**, 157–164.

KOOYMAN, A.R., VAN HOOFT, J.A. & VIJVERBERG, H.P.M. (1993a). 5-Hydroxyindole slows desensitization of 5-HT$_3$ receptor-mediated ion current in N1E-115 neuroblastoma cells. *Br. J. Pharmacol.*, **108**, 287–289.

KOOYMAN, A.R., ZWART, R. & VIJVERBERG, H.P.M. (1993b). Tetraethylammonium ions block 5-HT$_3$ receptor-mediated ion current at the agonist recognition site and prevent desensitization in cultured mouse neuroblastoma cells. *Eur. J. Pharmacol.*, **246**, 247–254.

LEE, K.S., AKAIKE, N. & BROWN, A.M. (1978). Properties of internally perfused voltage clamp isolated nerve cell bodies. *J. Gen. Physiol.*, **71**, 489–507.

LOVINGER, D.M. (1991). Ethanol potentiation of 5-HT$_3$ receptor-mediated ion current in NCB-20 neuroblastoma cells. *Neurosci. Lett.*, **122**, 57–60.

LOVINGER, D.M. & ZHOU, Q. (1993). Trichloroethanol potentiation of 5-hydroxytryptamine$_3$ receptor-mediated ion current in nodose ganglion neurons from the adult rat. *J. Pharmacol. Exp. Ther.*, **265**, 771–776.

LOWRY, O.H., ROSEBROUGH, N.J., FARR, A.L. & RANDALL, R.J. (1951). Protein measurement with the Folin phenol reagent. *J. Biol. Chem.*, **193**, 265–275.

LUMMIS, S.C.R., KILPATRICK, G.J. & MARTIN, I.L. (1990). Characterization of 5-HT$_3$ receptors in intact N1E-115 neuroblastoma cells. *Eur. J. Pharmacol.*, **189**, 223–227.

MARICQ, A.V., PETERSON, A.S., BRAKE, A.J., MYERS, R.M. & JULIUS, D. (1991). Primary structure and functional expression of the 5-HT$_3$ receptor, a serotonin-gated ion channel. *Science*, **254**, 432–437.

MARQUARDT, D.W. (1963). An algorithm for least-squares estimation of nonlinear parameters. *J. Soc. Indust. Appl. Math.*, **11**, 431–441.

NEIJT, H.C., TE DUITS, I.J. & VIJVERBERG, H.P.M. (1988). Pharmacological characterization of serotonin 5-HT$_3$ receptor-mediated electrical response in cultured mouse neuroblastoma cells. *Neuropharmacol.*, **27**, 301–307.

NEIJT, H.C., PLOMP, J.J. & VIJVERBERG, H.P.M. (1989). Kinetics of the membrane current mediated by serotonin 5-HT$_3$ receptors in cultured mouse neuroblastoma cells. *J. Physiol.*, **411**, 257–269.

SHARIF, N.A., WONG, E.H.F., LOURY, D.N., STEFANICH, E., MICHEL, A.D., EGLEN, R.M. & WHITING, R.L. (1991). Characteristics of 5-HT$_3$ binding sites in NG108-15, NCB-20 neuroblastoma cells and rat cerebral cortex using [^{3}H]-quipazine and [^{3}H]-GR65630 binding. *Br. J. Pharmacol.*, **102**, 919–925.

YAKEL, J.L. & JACKSON, M.B. (1988). 5-HT$_3$ receptors mediate rapid responses in cultured hippocampus and a clonal cell line. *Neuron*, **1**, 615–621.

YAKEL, J.L., SHAO, X.M. & JACKSON, M.B. (1991). Activation and desensitization of the 5-HT$_3$ receptor in a rat glioma X mouse neuroblastoma hybrid cell line. *J. Physiol.*, **436**, 293–308.

YANG, J. (1990). In permeation through 5-hydroxytryptamine-gated channels in neuroblastoma N18 cells. *J. Gen. Physiol.*, **96**, 1177–1198.

(Received December 22, 1993
Revised February 21, 1994
Accepted March 7, 1994)

Br. J. Pharmacol. (1994), **112**, 547–550

Effect of topical administration of L-arginine on formalin-induced nociception in the mouse: a dual role of peripherally formed NO in pain modulation

Atsufumi Kawabata, Sachiko Manabe, Yuki Manabe & [1]Hiroshi Takagi

Department of Pharmacology, Faculty of Pharmaceutical Sciences, Kinki University, 3-4-1 Kowakae, Higashi-Osaka 577, Japan

1 We investigated the effects of intraplantar (i.pl.) administration of L-arginine and N^G-nitro-L-arginine methyl ester (L-NAME) on formalin-induced behavioural nociception in the mouse.

2 L- but not D-arginine, at 0.1–1 μg per paw, coadministered with i.pl. formalin, enhanced the second- but not the first-phase nociceptive responses, whereas it was without significant effects at 3 μg per paw, and conversely, produced antinociception at 10 μg per paw, resulting in a bell-shaped dose-response curve.

3 L-NAME at 0.1–1 μg per paw, when administered i.pl., exhibited antinociceptive activity in the second phase in a dose-dependent manner, although its D-enantiomer produced no effect.

4 An antinociceptive dose (1 μg per paw) of L-NAME (i.pl.) considerably reduced the increase in second-phase nociception elicited by low doses (1 μg per paw) of i.pl. L-arginine. The second-phase nociception decrease induced by a large dose (10 μg per paw) of i.pl. L-arginine was markedly reversed by i.pl. L-NAME at 0.1 μg per paw, raising it to a level above that of the control (formalin only).

5 These results suggest that peripheral NO plays a dual role in nociceptive modulation, depending on the tissue level, inducing either nociceptive or antinociceptive responses.

Keywords: Nitric oxide (NO); L-arginine; N^G-nitro-L-arginine methyl ester; nociceptive modulation; pain; formalin-induced nociception

Introduction

Nitric oxide (NO), a labile gaseous substance which was first identified as an endothelium-derived relaxing factor (EDRF) (for review, see Moncada *et al.*, 1988), acts as a neuronal messenger in the central and peripheral nervous systems and is involved in various biological events such as synaptic plasticity and neurotoxicity (for review, see Vincent & Hope, 1992; Bredt & Snyder, 1992). NO is formed from L-arginine by the calcium-calmodulin-requiring enzyme NO synthase (NOS) under physiological conditions, and exerts its actions mainly via activation of soluble guanylate cyclase.

Recent studies have suggested a role of the L-arginine-NO-guanosine 3':5'-cyclic monophosphate (cyclic GMP) pathway in central and peripheral nociceptive processing. N^G-nitro-L-arginine methyl ester (L-NAME) and N^G-monomethyl-L-arginine (L-NMMA), both NOS inhibitors, and methylene blue, a soluble guanylate cyclase inhibitor, administered intracerebroventricularly (i.c.v.), produce opioid-independent antinociceptive effects in the mouse which are blocked by coadministration of dibutyryl cyclic GMP, suggesting a promotive or positive role of the NO-cyclic GMP system in supraspinal transmission of nociceptive information (Moore *et al.*, 1991; Babbedge *et al.*, 1993; Kawabata *et al.*, 1993). The role of this system in spinal nociceptive processing has also been demonstrated by behavioural, electrophysiological and histochemical studies (Dun *et al.*, 1992; Haley *et al.*, 1992; Kitto *et al.*, 1992; Lee *et al.*, 1992; 1993; Meller *et al.*, 1992a,b; Morris *et al.*, 1992; Valtschanoff *et al.*, 1992; Meller & Gebhart, 1993). The peripheral mechanism is complex, both inhibitory and promotive actions of NO having been reported. Topically administered L-arginine exhibits antinociceptive activity in rats with carrageenin-induced hyperalgesia, the effect being inhibited by NOS inhibitors and by methylene blue (Duarte *et al.*, 1990; Kawabata *et al.*, 1992). Topical administration of non-enzymatic NO donors such as sodium nitroprusside, nitroglycerin and 3-morpholino-sydnonimine, also produce antinociception in a methylene blue-reversible manner in hyperalgesic rats (Duarte *et al.*, 1990; 1992; Ferreira *et al.*, 1991; 1992). In contrast, spinal neural activity in response to formalin injected into the receptive field is reduced by coadministration of L-NAME (Haley *et al.*, 1992). L-NAME suppresses, while L-arginine and NO donors enhance, nociceptive or inflammatory responses elicited by bradykinin, substance P, carrageenin and dextran (Hughes *et al.*, 1990; Carrado *et al.*, 1992; Ialenti *et al.*, 1992; Khalil & Helme, 1992). Thus, there exists evidence for both nociceptive and antinociceptive roles of the NO-cyclic GMP pathway in the peripheral tissues.

In the present study, we investigated the effects of topically applied L-arginine and L-NAME, a NOS inhibitor, on behavioural nociceptive responses induced by formalin. The results obtained suggest that peripherally formed NO may play a dual role in formalin-elicited nociception, dependent on the tissue level.

Methods

Experimental animals

Male ddY mice, weighing 12–20 g, which were purchased from Japan. SLC. Inc., received free access to food and water for at least 1 day before experiments.

Formalin-induced nociception test

According to the method of Dubuisson & Dennis (1977), modified by Shibata *et al.* (1989), each mouse received an intraplantar (i.pl.) injection of 25 μl of 0.5% formalin solution in the right hindpaw. The duration of paw-licking (an index of nociception) was measured for 30 min immediately after i.pl. injection. Results were expressed as licking time in the first (0–5 min) and second (10–30 min) phases.

[1] Author for correspondence.

Experimental protocol

L-Arginine, in the dose range of 0.1–10 μg per mouse, or N^G-nitro-L-arginine methyl ester (L-NAME), in the dose-range of 0.01–1 μg per paw, were coadministered with formalin, in a final volume of 25 μl, and nociceptive responses were observed for subsequent 30 min. In experiments to determine the interaction between L-arginine and L-NAME, both agents were coadministered with formalin in the same final volume.

Drugs used

L-Arginine hydrochloride and its enantiomer were purchased from Nakalai Tesque (Japan), and L- and D-NAME hydrochloride were from Sigma (U.S.A.) and from Bachem (Switzerland), respectively.

Statistical analysis

All results obtained were expressed as means with s.e.mean. Differences between groups were analysed by Newman-Keuls' test for multiple data, and $P<0.05$ was taken to indicate significance.

Results

Effects of i.pl. administration of L-arginine on formalin-induced nociception

L-Arginine, at 0.1–10 μg per paw, coadministered i.pl. with formalin, did not significantly alter the duration of paw-licking (nociceptive responses) induced by formalin in the first phase (0–5 min after formalin injection). Second-phase responses (10–30 min after formalin injection) were significantly increased by L-arginine, at a dose range of 0.1–1 μg per paw. A higher dose of L-arginine, 3 μg per paw, produced smaller and non-significant enhancement of the second-phase nociception. Conversely, the highest dose of L-arginine administered, 10 μg per paw, produced significant antinociception in the second phase (Figure 1). Further increases in the dose of L-arginine did not result in further increases in the antinociceptive activity (data not shown). Thus, L-arginine, at low doses, enhanced nociception, but, at high doses, produced antinociception in the second phase in the formalin test, resulting in a bell-shaped dose-response curve; the cross over from nociception to antinociception appears to occur at a dose between 3 and 10 μg per paw.

Antinociception induced by i.pl. administration of L-NAME in the formalin-induced nociception test

L-NAME, in the dose-range of 0.1–1 μg per paw, coadministered with i.pl. formalin, revealed significant antinociceptive activity in the second phase in a dose-dependent manner, although, at the same dose-range, failed to produce any significant effect on the first-phase responses (Figure 2).

Lack of effects of D-arginine and D-NAME (i.pl.) on formalin-induced nociception

D-Arginine, at 1 and 10 μg per paw, coadministered i.pl. with formalin, did not significantly affect formalin-induced second-phase nociceptive responses. D-NAME at 1 μg per paw, coadministered with i.pl. formalin, failed to produce significant antinociception in the second phase. The duration (seconds) of paw-licking in the second phase were 151.2 ± 2.2 ($n=5$), 142.0 ± 8.9 ($n=5$), 142.2 ± 6.9 ($n=5$) and 129.2 ± 11.9 ($n=5$) in groups treated with formalin only (control), D-arginine at 1 and 10 μg per paw, and D-NAME at 1 μg per paw, respectively.

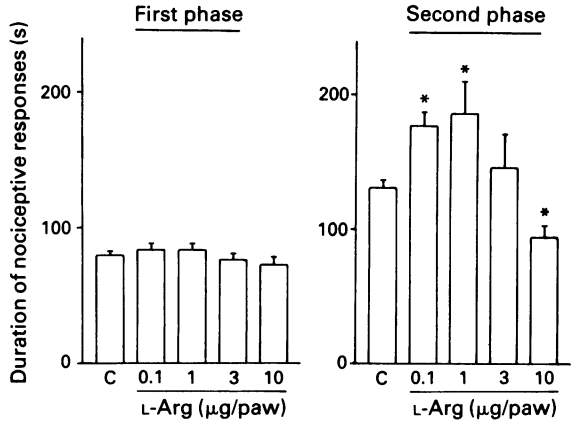

Figure 1 Effects of i.pl. administration of L-arginine (L-Arg) on formalin-induced nociception. L-Arg was co-administered i.pl. with formalin. Columns show mean with s.e.mean. $*P<0.05$ vs control (C). $n=32$ (control) and 16 (L-Arg).

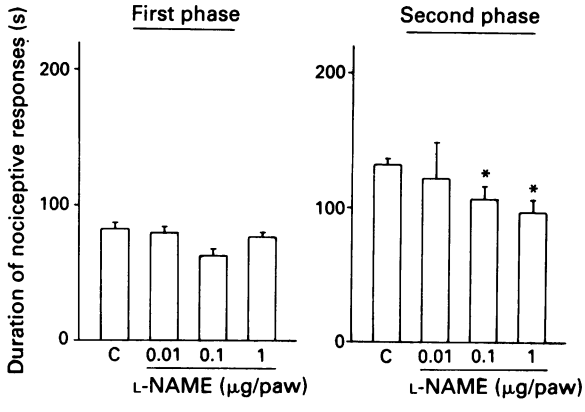

Figure 2 Effects of i.pl. administration of N^G-nitro-L-arginine methyl ester (L-NAME) on formalin-induced nociception. L-NAME was co-administered i.pl. with formalin. Columns show mean ± s.e.mean. $*P<0.05$ vs control (C). $n=18$ (control) and 5–8 (L-NAME).

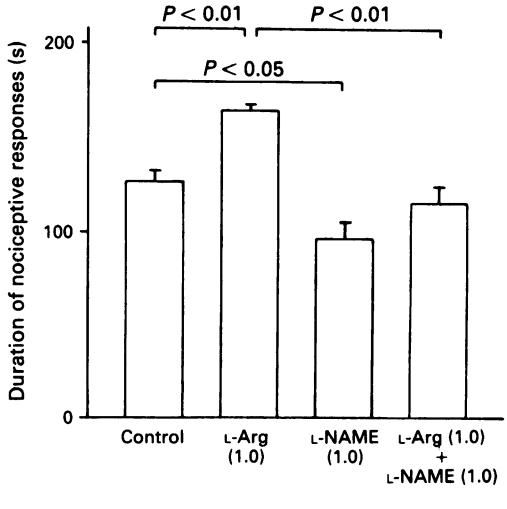

Figure 3 Effects of i.pl. N^G-nitro-L-arginine methyl ester (L-NAME) on second-phase nociception enhanced by low doses of L-arginine (L-Arg, i.pl.). L-Arg and/or L-NAME were coadministered i.pl. with formalin. Parentheses indicate the doses (μg per paw) of L-Arg and L-NAME. Columns show mean with s.e.mean. $n=6$.

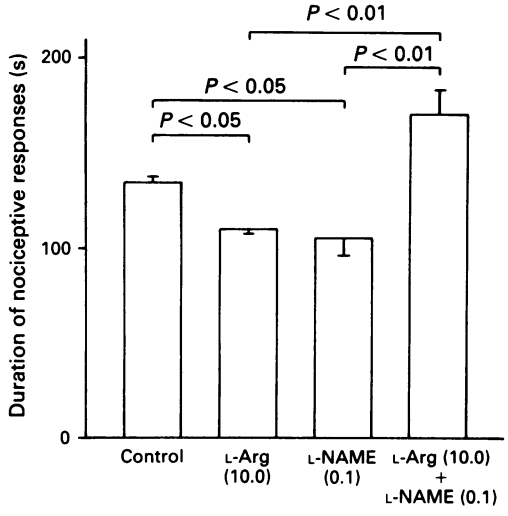

Figure 4 Effects of i.pl. N^G-nitro-L-arginine methyl ester (L-NAME) on second-phase antinociception induced by large doses of L-arginine (L-Arg, i.pl.). L-Arg and/or L-NAME were coadministered i.pl. with formalin. Parentheses indicate the doses (μg per paw) of L-Arg and L-NAME. Columns show mean with s.e.mean. $n = 7$.

Effects of L-NAME (i.pl.) on the second-phase nociceptive responses increased or decreased by L-arginine (i.pl.) in the formalin test

L-NAME, administered i.pl. at 1 μg per paw, which itself was antinociceptive, significantly reduced the increases in second-phase nociception (hyperalgesia) elicited by 1 μg per paw i.pl. L-arginine (Figure 3).

L-NAME (i.pl.) at a lower dose, 0.1 μg per paw, which itself produced antinociception, markedly reversed the decrease in second-phase nociception induced by 10 μg per paw i.pl. injection of L-arginine, raising it to a level above that of the control (Figure 4). L-NAME (i.pl.), at 1 μg per paw, which was also antinociceptive by itself, did not significantly alter L-arginine (10 μg per paw)-induced antinociception (data not shown).

Discussion

The present data indicate that L-arginine (i.pl.) induces enhancement and suppression of the second phase of formalin-induced nociception at low doses (0.1 – 1 μg per paw) and at a high dose (10 μg per paw), respectively, and that both the effects are mediated by enhancement in topical NO formation. Furthermore, L-NAME (0.1 – 1 μg per paw; i.pl.) appears to produce second-phase antinociception possibly by inhibiting NO formation.

L- but not D-arginine (i.pl.) produced two different actions on the second phase of formalin-induced nociception, depending on the concentration. The increase in second-phase nociception induced by low doses (1 μg per paw) of L-arginine (i.pl.) was blocked by the same dose of L-NAME (i.pl.), suggesting involvement of NO generated from L-arginine by NOS. The decreases in nociceptive responses induced by high doses (10 μg per paw) of L-arginine (i.pl.) were dramatically reversed by an antinociceptive dose (0.1 μg per paw) of L-NAME, increasing to a level above that of the control. This implies that L-arginine (10 μg per paw)-induced increases in topical formation of NO are inhibited by L-NAME (0.1 μg per paw) to a level equivalent to that brought about by a low dose (1 μg per paw) of L-arginine, which itself enhances nociception. A larger dose (1 μg per paw) of L-NAME appears to suppress L-arginine-induced NO formation to a level below that required to enhance nociception, since it did not notably enhance nociception suppressed by L-arginine. Thus, both enhancement and suppression of the second phase of formalin-induced nociception induced by L-arginine may possibly be mediated by NO generation by NOS. L-Arginine (i.pl.) has been reported to inhibit hyperalgesia induced by carrageenin via activation of the NO-cyclic GMP pathway, possibly by a direct effect on nociceptors (Duarte *et al.*, 1990; Kawabata *et al.*, 1992). In contrast, L-arginine (i.pl.) enhances carrageenin-induced oedema formation through topical NO formation, most probably by increasing vascular permeability (Ialenti *et al.*, 1992). This effect seems to promote nociception. Thus, there is evidence that L-arginine has opposing properties in the same hyperalgesic model. The nociceptive and antinociceptive effects in the second phase exerted by L-arginine in the present study may reflect dual actions on vascular permeability and on nociceptors, respectively, although additional studies should be conducted to elucidate this further. Recently, we also found that NO donors such as sodium nitroprusside and S-nitroso-*N*-acetylpenicillamine, coadministered i.pl. with formalin, produced enhancement and suppression of the second-phase nociception at a low dose (0.1 ng per paw) and at high doses (10 – 100 ng per paw), respectively (unpublished data), further supporting a dual action of peripheral NO.

L-NAME but not D-NAME (i.pl.) produced dose-dependent antinociception in the second phase in the formalin test, consistent with the electrophysiological study of Haley *et al.* (1992), who found that spinal neural activity in response to formalin injected into the receptive field was suppressed by L-NAME injected into the same site. Moore *et al.* (1991) reported that systemic administration of L-NAME produces both first- and second-phase antinociception in the formalin test, possibly by a central effect. However, the present results suggest that the peripheral mechanism may also contribute in part to the effect of systemic L-NAME. Further increases in the dose of L-NAME did not result in complete suppression of formalin-induced nociceptive responses in the second phase (data not shown), suggesting that NO is an important but not exclusive factor in the induction of the second-phase nociception. Topically applied L-NAME reduces oedema formation and/or increased vascular permeability induced by carrageenin, dextran, substance P and bradykinin by inhibiting NOS (Hughes *et al.*, 1990; Ialenti *et al.*, 1992; Khalil & Helme, 1992). Such effects of L-NAME probably result in antinociception, especially in chemically-mediated nociception models. It is well-known that the formalin-induced first- and second-phase nociceptive responses are related mainly to neural and inflammatory mechanisms, respectively (Dubuisson & Dennis, 1977; Shibata *et al.*, 1989). The antinociceptive effect of L-NAME may be secondary to its anti-inflammatory action, considering that L-NAME (i.pl.) suppressed second- but not first-phase nociception.

Taken together, formalin injected into the hindpaw possibly increases NO levels via the regional activation of NOS, this effect contributing to the induction of nociceptive responses in the second phase. L-NAME (i.pl.) first inhibits NOS, and then inhibits the formalin-induced increase in NO levels, thereby suppressing nociception (hypoalgesia). L-Arginine (i.pl.) at low doses enhances formalin-induced increases in NO formation, thus promoting nociception (hyperalgesia). At high doses, i.pl. L-arginine further increases tissue NO levels, resulting in hypoalgesia possibly due to suppressive effects on the nociceptor. In conclusion, peripheral NO may play a dual role in nociceptive modulation as assessed by the formalin test in the mouse.

This paper is the sixth report on 'Pain modulation by neuroactive amino acids'. Experiments were supported in part by research grant No. 05772045 from the Japanese Ministry of Education, Science and Culture.

References

BABBEDGE, R.C., HART, S.L. & MOORE, P.K. (1993). Anti-nociceptive activity of nitric oxide synthase inhibitors in the mouse: dissociation between the effect of L-NAME and L-NMMA. *J. Pharm. Pharmacol.*, **45**, 77–79.

BREDT, D.S. & SNYDER, S.H. (1992). Nitric oxide, a novel neuronal messenger. *Neuron*, **8**, 3–11.

CARRADO, A.P., BALLEJO, G., ANTUNES, E. & DE NUCCI, G. (1992). Mechanism of pain induced by radiocontrast media. *Toxicol. Lett.*, **64/65**, 739–743.

DUARTE, I.D.G., LORENZETTI, B.B. & FERREIRA, S.H. (1990). Peripheral analgesia and activation of the nitric oxide-cyclic GMP pathway. *Eur. J. Pharmacol.*, **186**, 289–293.

DUARTE, I.D.G., DOS SANTOS, I.R., LORENZETTI, B.B. & FERREIRA, S.H. (1992). Analgesia by direct antagonism of nociceptor sensitization involves the arginine-nitric oxide-cGMP pathway. *Eur. J. Pharmacol.*, **217**, 225–227.

DUBUISSON, D. & DENNIS, S.G. (1977). The formalin test: a quantitative study of the analgesic effects of morphine, meperidine and brain stem stimulation in rats and cats. *Pain*, **4**, 161–174.

DUN, N.J., DUN, S.L., FORSTERMANN, U. & TSENG, L.F. (1992). Nitric oxide synthase immunoreactivity in rat spinal cord. *Neurosci. Lett.*, **147**, 217–220.

FERREIRA, S.H., DUARTE, I.D.G. & LORENZETTI, B.B. (1991). The molecular mechanism of action of peripheral morphine analgesia: stimulation of the cGMP system via nitric oxide release. *Eur. J. Pharmacol.*, **201**, 121–122.

FERREIRA, S.H., LORENZETTI, B.B. & FACCIOLI, L.H. (1992). Blockade of hyperalgesia and neurogenic oedema by topical application of nitroglycerin. *Eur. J. Pharmacol.*, **217**, 207–209.

HALEY, J.E., DICKENSON, A.H. & SCHACHTER, M. (1992). Electrophysiological evidence for a role of nitric oxide in prolonged chemical nociception in the rat. *Neuropharmacology*, **31**, 251–258.

HUGHES, S.R., WILLIAMS, T.J. & BRAIN, S.D. (1990). Evidence that endogenous nitric oxide modulates oedema formation induced by substance P. *Eur. J. Pharmacol.*, **191**, 481–484.

IALENTI, A., IANARO, A., MONCADA, S. & ROSA, M.D. (1992). Modulation of acute inflammation by endogenous nitric oxide. *Eur. J. Pharmacol.*, **211**, 177–182.

KAWABATA, A., FUKUZUMI, Y., FUKUSHIMA, Y. & TAKAGI, H. (1992). Antinociceptive effect of L-arginine on carrageenin-induced hyperalgesia in rats: possible involvement of central opioidergic systems. *Eur. J. Pharmacol.*, **218**, 153–158.

KAWABATA, A., UMEDA, N. & TAKAGI, H. (1993). L-Arginine exerts a dual role in nociceptive processing in the brain: involvement of the kyotorphin-Met-enkephalin pathway and NO-cyclic GMP pathway. *Br. J. Pharmacol.*, **109**, 73–79.

KHALIL, Z. & HELME, R.D. (1992). The quantitative contribution of nitric oxide and sensory nerves to bradykinin-induced inflammation in rat skin microvasculature. *Brain Res.*, **589**, 102–108.

KITTO, K.F., HALEY, J.E. & WILCOX, G.L. (1992). Involvement of nitric oxide in spinally mediated hyperalgesia in the mouse. *Neurosci. Lett.*, **148**, 1–5.

LEE, J.H., PRICE, R.H., WILLIAMS, F.G., MAYER, B. & BEITZ, A.J. (1993). Nitric oxide synthase is found in some spinothalamic neurons and neuronal processes that appose spinal neurons that express Fos induced by noxious stimulation. *Brain Res.*, **608**, 324–333.

LEE, J.H., WILCOX, G.L. & BEIZ, A.J. (1992). Nitric oxide mediates Fos expression in the spinal cord induced by mechanical noxious stimulation. *Neuroreport*, **3**, 841–844.

MELLER, S.T., DYKSTRA, C. & GEBHART, G.F. (1992a). Production of endogenous nitric oxide and activation of soluble guanylate cyclase are required for N-methyl-D-aspartate-produced facilitation of the nociceptive tail-flick reflex. *Eur. J. Pharmacol.*, **214**, 93–96.

MELLER, S.T. & GEBHART, G.F. (1993). Nitric oxide (NO) and nociceptive processing in the spinal cord. *Pain*, **52**, 127–136.

MELLER, S.T., PECHMAN, P.S., GEBHART, G.F. & MAVES, T.J. (1992b). Nitric oxide mediates the thermal hyperalgesia produced in a model of neuropathic pain in the rat. *Neuroscience*, **50**, 7–10.

MONCADA, S., PALMAR, R.M.J. & HIGGS, E.A. (1988). Endothelium-derived relaxing factor: identification as nitric oxide and role in the control of vascular tone and platelet function. *Biochem. Pharmacol.*, **37**, 2495–2501.

MOORE, P.K., OLUYOMI, A.O., BABBEDGE, R.C., WALLACE, P. & HART, S.L. (1991). L-N^G-nitroarginine methyl ester exhibits antinociceptive activity in the mouse. *Br. J. Pharmacol.*, **102**, 198–202.

MORRIS, R., SOUTHAM, E., BRAID, D.J. & GARTHWAITE, J. (1992). Nitric oxide may act as a messenger between dorsal root ganglion neurones and their satellite cells. *Neurosci. Lett.*, **137**, 29–32.

SHIBATA, M., OHKUBO, T., TAKAHASHI, H. & INOKI, R. (1989). Modified formalin test, characteristic biphasic pain response. *Pain*, **38**, 347–352.

VALTSCHANOFF, J.G., WEINBERG, R.J., RUSTIONI, A. & SCHMIDT, H.H.H.W. (1992). Nitric oxide synthase and GABA colocalize in lamina II of rat spinal cord. *Neurosci. Lett.*, **148**, 6–10.

VINCENT, S.R. & HOPE, B.T. (1992). Neurons that say NO. *Trends Neurosci.*, **15**, 108–113.

(Received October 18, 1993
Revised February 14, 1994
Accepted March 7, 1994)

Br. J. Pharmacol. (1994), **112**, 551–556

Relationship between plasma lipids and palmitoyl-CoA hydrolase and synthetase activities with peroxisomal proliferation in rats treated with fibrates

M. Alegret, R. Ferrando, M. Vázquez, T. Adzet, M. Merlos & [1]J.C. Laguna

Unidad de Farmacología y Farmacognosia, Dept. Farmacología y Química Terapeutica, Facultad de Farmacia, Núcleo Universitario de Pedralbes, Barcelona 08028, Spain

1 The time-course of the effect of clofibrate (CFB), bezafibrate (BFB) and gemfibrozil (GFB) on lipid plasma levels and palmitoyl-CoA hydrolase and synthetase activities, as well as the correlations with the peroxisomal proliferation phenomenon have been studied in male Sprague-Dawley rats.

2 The administration of the three drugs caused a significant reduction in body weight gain, accompanied with a paradoxical increase in food intake in groups treated with BFB and GFB.

3 Drug treatment produced gross hepatomegaly and increase in peroxisomal β-oxidation, and these parameters were strongly correlated. The order of potency was BFB > CFB ≥ GFB.

4 Both plasma cholesterol (BFB ≈ CFB > GFB) and triglyceride (BFB ≈ GFB > CFB) levels were reduced in treated animals. There was an inverse correlation between these parameters and peroxisomal β-oxidation, although the peroxisomal proliferation seemed to explain only a small part of the hypolipidemic effect observed.

5 Cytosolic and microsomal (but not mitochondrial) palmitoyl-CoA hydrolase activities were increased by the three drugs (BFB > CFB > GFB), probably by inducing the hydrolase I isoform, which is insensitive to inhibition by fibrates *in vitro*. The increased hydrolase activities were directly and strongly correlated with peroxisomal β-oxidation.

6 Palmitoyl-CoA synthetase activity was also increased by the treatment with fibrates (BFB > CFB > GFB), probably as a consequence of the enhancement of hydrolase activities.

7 Some of the effects of fibrate treatment can be explained, at least in part, in terms of peroxisomal induction and caution should be exercised in the extrapolation of these results to species, such as man, that are insensitive to peroxisomal proliferation.

Keywords: Fibrates; peroxisomal proliferation; β-oxidation; palmitoyl-CoA hydrolase; palmitoyl-CoA synthetase

Introduction

Fibric acid derivatives are a well known group of hypolipidaemic drugs used mainly in the treatment of hypertriglyceridaemia and mixed hyperlipidaemia (Sirtori *et al.*, 1991; Klosiewicz-Latoszek & Szostak, 1991). Although they have been in therapeutic use for more than twenty years, the mechanism(s) by which they reduce blood lipis is not fully understood.

A considerable body of information has been gathered regarding the effect of fibric acid derivatives on several enzyme activities related to lipid biosynthesis (Bremer *et al.*, 1981; Reddy & Lalwani, 1983; Hawkins *et al.*, 1987). With few exceptions, most of these studies share similar drawbacks: (1) They are based on the effect of only one drug, clofibrate, accepted as a hypolipidaemic drug prototype, but which is gradually being replaced by more efficient drugs, like bezafibrate and gemfibrozil. (2) Usually, only one time point is studied per treatment (i.e. 7 or 15 days), making it difficult to relate the modification of one particular enzyme activity with the hypolipidaemic effect. (3) Fibrates are typical peroxisome inducers in rats (Esbenshade *et al.*, 1990; McGuire *et al.*, 1991); as the rat is usually the model studied, few authors give clear-cut information about the possible involvement of this phenomenon in the modification of the lipogenic enzyme activities reported. (4) There is a lack of information about the effect of fibrates *in vitro* on some of the enzyme activities studied *in vivo*. Given the prevailing role of fatty acids in lipoprotein metabolism (Desreumaux *et al.*, 1979; Vance & Vance, 1990), in the last few years we have studied the effect of fibric acid derivatives on enzyme activities related to fatty acid biosynthesis and its involvement in the hypolipidaemic activity (Alegret *et al.*, 1991; Sánchez *et al.*, 1992a,b; 1993a,b) In this paper, we report the effect *in vivo* of clofibrate, bezafibrate and gemfibrozil on two hepatic enzyme activities involved in fatty acid biosynthesis: palmitoyl-CoA hydrolase (EC 3.2.2.1) and palmitoyl-CoA synthetase (EC 6.2.1.3). Further, we have studied the temporal evolution of these activities and their relationship with the hypolipidaemic effect and peroxisome induction phenomena.

[1] Author for correspondence.

Methods

Animals

Male Sprague-Dawley rats (150) from Letica (Spain), weighing 110–120 g at the beginning of treatment, were maintained under conditions of constant humidity and temperature (22 ± 2°C) under a constant light-dark cycle and were fed standard diet (Panlab, Barcelona, Spain) for five days before the beginning of the studies. The animals were distributed randomly into four groups of 36 rats. Each group was fed, respectively, a control diet or a diet containing CFB, BFB or GFB. The six remaining rats were used as controls on day 0 of treatment to establish the basal values. Throughout the study, the weight and daily food intake of the animals was measured. The 36 rats in each group were killed randomly in groups of 6 after 1, 2, 4, 7, 10 and 15 days of treatment. The concentration of CFB administered in the diet was 0.3% w/w, as described by other authors (Berge &

Bakke, 1981; Stahlberg et al., 1989). The concentrations of the other two drugs (0.45% for BFB and 0.3% w/w for GFB) were chosen in such a way as to be equimolar to CFB. The diets were prepared as described by Berge & Bakke (1981), by soaking in an acetone solution of the drug. To avoid any possible effect of the solvent, the control diet was also soaked in acetone and dried.

Experimental

The animals were killed on the assigned day by decapitation between 08 h 00 min and 09 h 00 min. Blood samples were collected from the neck in EDTA tubes and plasma was obtained by centrifugation at 3000 *g*, for 10 min at 4°C. The livers were removed, perfused with ice-cold 0.9% NaCl, weighed and homogenized in eight volumes of 0.25 M sucrose, 50 mM Tris-HCl buffer, pH 7.4. The subcellular fractions were obtained by differential centrifugation as described previously (Nagi et al., 1989), and the protein content was determined by the method of Bradford (1976), with BSA used as standard. In order to check that the treatment did not affect the sedimentation distribution of cell organelles, fractions obtained from livers of control and CFB-treated rats were assayed for enzyme marker activities, succinate dehydrogenase activity (Earl & Korner, 1965) for heavy mitochondria, KCN insensitive palmitoyl-CoA β-oxidation (Lazarow, 1981) for light mitochondria, NADPH cytochrome c reductase (Alegret et al., 1991) for microsomes and glucose-6-phosphate dehydrogenase (Sánchez et al., 1993a) for cytosol. For the studies *in vitro*, cytosol obtained from control or GFB-treated rats was incubated with 5 mM GFB. The drug was added from a stock solution adjusted to pH between 7.5 and 8 with 0.1 N NaOH. The volume added did not modify the pH of the assay mixture.

Plasma cholesterol and triglyceride concentration measurement

Plasma cholesterol concentration was determined by the colorimetric test Monotest Cholesterol CHODPAP No. 290319, and triglyceride concentration was assayed by means of the Peridochrom Triglyceride GPO-PAP No. 701882 test, both from Boehringer Mannheim (Barcelona, Spain).

Enzyme assays

All enzyme activites were measured by spectrophotometric methods using a Perkin-Elmer 550 UV-Vis spectrophotometer with a recorder accessory. Palmitoyl-CoA hydrolase and palmitoyl-CoA synthetase activities were assayed as described in previous studies (Sánchez et al., 1992a; 1993b). Peroxisomal β-oxidation was determined in the postnuclear fraction by the method of Lazarow (1981). The incubation medium contained, in final concentrations: Tris-HCl buffer 50 mM, pH 8.0, KCN 1 mM, dithiothreitol 1 mM, FAD 10 μM, CoA 100 μM, BSA 75 μg ml^{-1}, Triton X-100 0.09 μl ml^{-1}, NAD 200 μM, and post-nuclear protein 400 μg. After 2 min of preincubation at 37°C the reaction was started by adding 20 μM palmitoyl-CoA, and the increase in absorbance at 340 nm with respect to a blank cuvette without palmitoyl-CoA was recorded.

Chemicals

Palmitic acid, palmitoyl-CoA, fatty-acid-free bovine serum albumin (BSA), HEPES, CoA, FAD and Trizma base (tris[hydroxymethyl]aminomethane) were obtained from Sigma Chemical Co. (Madrid, Spain); NADH, NADPH, DTNB and ATP were from Boehringer Mannheim (Barcelona, Spain); EDTA was from Merck (Barcelona, Spain) and Triton X-100 from Scharlau (Barcelona, Spain). Other general chemicals were obtained from commercial sources and were of the highest purity available.

Drugs

Clofibrate (CFB) was a generous gift from ICI-Farma (Pontevedra, Spain), bezafibrate (BFB) was a gift from Boehringer Mannheim (Barcelona, Spain) and gemfibrozil (GFB) was a gift from Parke-Davis (Barcelona, Spain).

Statistical evaluation

Results are expressed as means ± s.d. of *n* experiments performed in duplicate. By means of the FOUNDS computer programme, statistical differences were established by a two-way ANOVA test (treatment × time); when differences were found, multiple comparisons were performed between treatment groups at different time points using Duncan's test. Differences with $P<0.05$ were considered significant. Correlations between two variables were performed by linear regression using the GPIP computer programme.

Results

Non enzymatic parameters

Although all the animals showed a steady increase in body weight during the treatment, fibrate-treated animals gained less weight than control group from day 7 on (Figure 1a). Fibrate-treated animals weighed about 10% less than control in the last four days of treatment: on day 15, the average weight was 261.3 ± 15.9 g for control, and 239.5 ± 15.9, 236.2 ± 12.8 and 238.9 ± 21.9 g for the CFB, BFB and GFB treated groups. Surprisingly, this reduction in body weight gain was accompanied, in the case of BFB- and GFB-treated animals, by a significant increase in the daily food intake (Figure 1b). Thus, on day 11 of treatment, while daily food intake for control and CFB-treated animals was 28.9 ± 1.9 and 28.0 ± 2.1 g/day per rat, the animals treated with BFB and GFB consumed 36.6 ± 4.9 and 38.2 ± 7.9 g/day per rat.

The temporal evolution of the typical hepatomegaly produced by fibrates is shown in Figure 1c as the ratio between liver and body weight. As expected, while this ratio remained fairly constant in the control group, it increased from day 2 onwards for CFB, BFB and GFB-treated animals. While CFB and GFB showed similar capacity to produce hepatomegaly, BFB surpassed them at every time point studied; for instance, on day 15, the liver weight/body weight ratios (as percentages) were 4.9 ± 0.2, 7.4 ± 0.6, 8.5 ± 1.0, and 7.2 ± 0.6 for control, CFB, BFB and GFB-treated animals, respectively.

Effect of treatment on plasma cholesterol and triglyceride concentrations

Figures 2a and 2b show the temporal evolution of cholesterol and triglyceride levels in control and fibrate-treated animals. The hypocholesterolemic activity of fibrates was already evident on day 2 of treatment, but while CFB and BFB decreased cholesterol levels throughout the treatment (mean decrease of 31% and 37% versus control values for CFB and BFB), cholesterol concentration in GFB-treated animals reverted to control values on day 10 of treatment.

Triglyceride levels were significantly lower in the three treated groups than in the control one from day 1 of treatment. BFB and GFB showed similar hypotriglyceridemic potency, with mean reductions of triglyceride levels of 49 and 44%, respectively, while CFB was somewhat less effective (mean reduction of 31%).

Enzyme activities

As reported previously (Lazarow et al., 1982; Bodnar & Rachubinski, 1991), the sedimentation patterns of the various organelles were similar for both untreated and fibrate-treated

rats (data not shown). Liver protein content, measured in the post-nuclear homogenate was not significantly modifed by drug administration (data not shown).

As shown in Figure 3, the three fibric acid derivatives studied behaved as typical peroxisomal proliferators, significantly increasing the cyanide-insensitive palmitoyl-CoA oxidation from day 2 of treatment on, in the case of CFB and BFB, and from day 7 on in the case of GFB. Maximal increases were achieved on day 10 of treatment (6.4, 10 and 5.7 fold increase for CFB, BFB and GFB versus control values). Throughout the treatment, the order of potency as β-oxidation inducers was BFB > CFB > GFB.

The palmitoyl-CoA hydrolase activity present in the mitochondrial fraction (heavy and light) was practically unchanged by fibrate treatment (data not shown). Microsomal palmitoyl-CoA hydrolase was slightly increased by GFB-treatment, showing an average 30% increase in activity from day 2 to the end of treatment (Figure 4). Although CFB and BFB also increased this activity from day 2 to 7, the progressive increase in control values over time blunted this effect in the second week of treatment.

CFB, BFB and GFB strongly increased cytosolic palmitoyl-CoA hydrolase activity (Figure 5). Maximal induction was achieved on day 7 of treatment, with approximately 4, 7 and 2 fold increase over control values for CFB, BFB and GFB-treated animals, respectively. GFB was by far the least effective inducer; thus, while BFB-treated animals showed significant increases from the first day of treatment, in GFB-

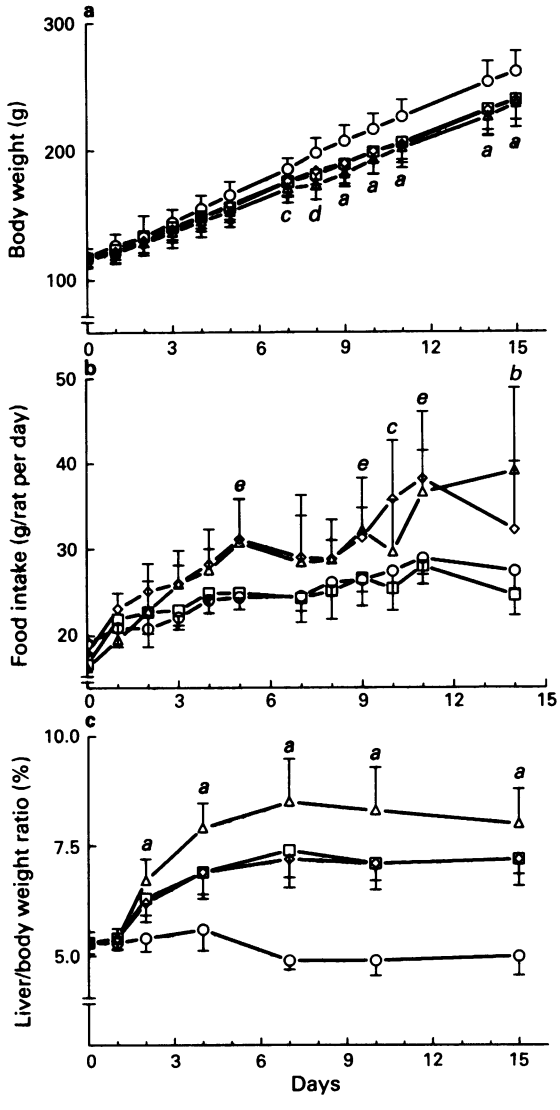

Figure 1 Time-course of the effect of a standard diet (○) or a diet supplemented with 0.3% w/w clofibrate (CFB) (□), 0.45% w/w bezafibrate (BFB) (△), and 0.3% w/w gemfibrozil (GFB) (◇) on (**a**) body weight, (**b**) daily food intake, and (**c**) liver/body weight ratio (%) of male Sprague-Dawley rats. Results are means ± s.d. of 6 experiments performed in duplicate. [a]means that values for CFB, BFB and GFB are all different from controls, $P<0.05$; [b]means that values for BFB are different from controls, $P<0.05$; [c]means that values for GFB are different from controls, $P<0.05$; [d]means that values for CFB and BFB are different from controls, $P<0.05$; [e]means that values for BFB and GFB are different from controls, $P<0.05$.

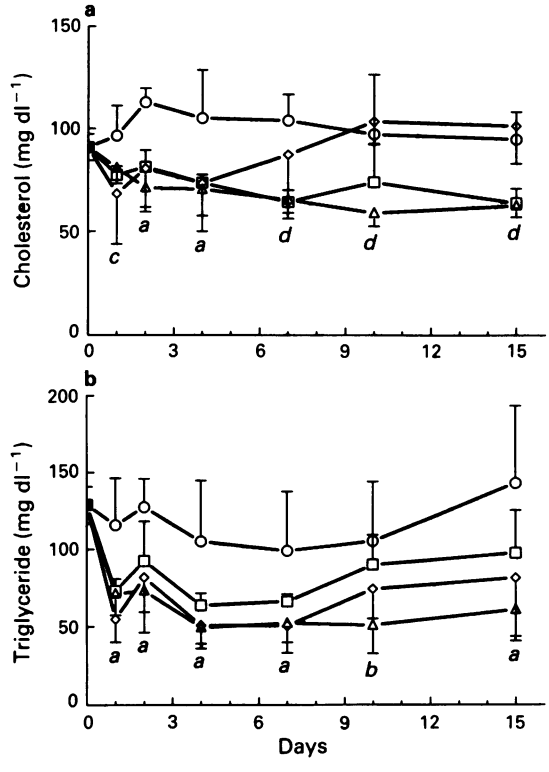

Figure 2 Time-course of the effect of a standard diet (○) or a diet supplemented with 0.3% w/w clofibrate (CFB) (□), 0.45% w/w bezafibrate (BFB) (△), and 0.3% w/w gemfibrozil (GFB) (◇) on (**a**) plasma cholesterol levels, and (**b**) plasma triglyceride levels of male Sprague-Dawley rats. Results are means ± s.d. of 6 experiments performed in duplicate. Legends for significance are the same as in Figure 1.

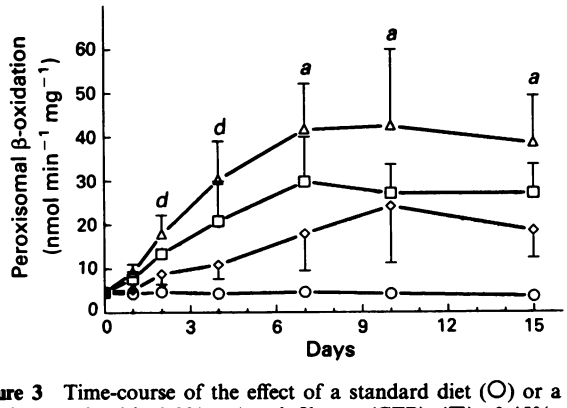

Figure 3 Time-course of the effect of a standard diet (○) or a diet supplemented with 0.3% w/w clofibrate (CFB) (□), 0.45% w/w bezafibrate (BFB) (△), and 0.3% w/w gemfibrozil (GFB) (◇) on cyanide-insensitive peroxisomal β-oxidation determined in the post-nuclear fraction of livers from male Sprague-Dawley rats. Results are means ± s.d. of 6 experiments performed in duplicate. Legends for significance are the same as in Figure 1.

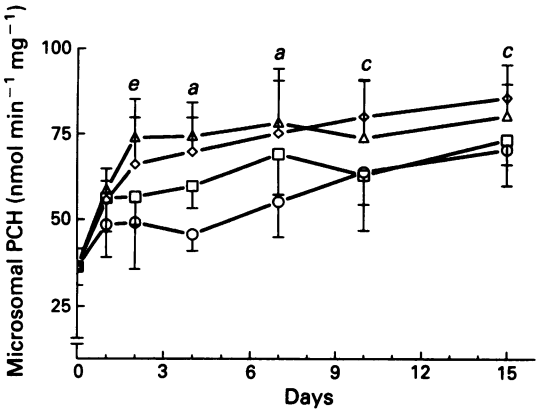

Figure 4 Time-course of the effect of a standard diet (○) or a diet supplemented with 0.3% w/w clofibrate (CFB) (□), 0.45% w/w bezafibrate (BFB) (△), and 0.3% w/w gemfibrozil (GFB) (◇) on palmitoyl-CoA hydrolase (PCH) activity in the microsomal fraction of livers from male Sprague-Dawley rats. Results are means ± s.d. of 6 experiments performed in duplicate. Legends for significance are the same as in Figure 1.

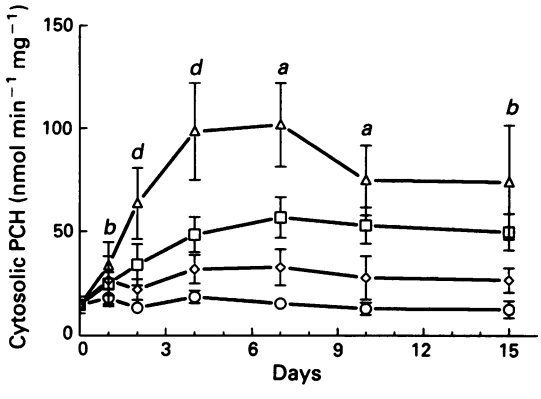

Figure 5 Time-course of the effect of a standard diet (○) or a diet supplemented with 0.3% w/w clofibrate (CFB) (□), 0.45% w/w bezafibrate (BFB) (△), and 0.3% w/w gemfibrozil (GFB) (◇) on palmitoyl-CoA hydrolase (PCH) activity in the cytosolic fraction of livers from male Sprague-Dawley rats. Results are means ± s.d. of 6 experiments performed in duplicate. Legends for significance are the same as in Figure 1.

treated animals this was accomplished after 7 days of drug consumption.

Palmitoyl-CoA hydrolase activity of cytosol from control animals was almost completely inhibited by 5 mM GFB *in vitro*, while only a partial inhibition of cytosol activity from GFB-treated animals was observed (Table 1).

As shown in Figure 6, the three drugs significantly increased microsomal palmitoyl-CoA synthetase activity from day 4 for the CFB- and BFB-treated groups and from day 7 for the GFB group. The order of potency was BFB > CFB- > GFB.

Discussion

Fibric acid derivatives are known to induce peroxisomal proliferation in rats. The typical manifestations of this process are hepatomegaly (Hawkins *et al.*, 1987) and increase in the specific activity of peroxisomal enzymes, such as the β-oxidation system (Reddy & Lalwani, 1983). In our study, both parameters increase quickly from the first day of administration (Figures 1c and 3). Moreover, there is a strong direct correlation between hepatomegaly expressed as

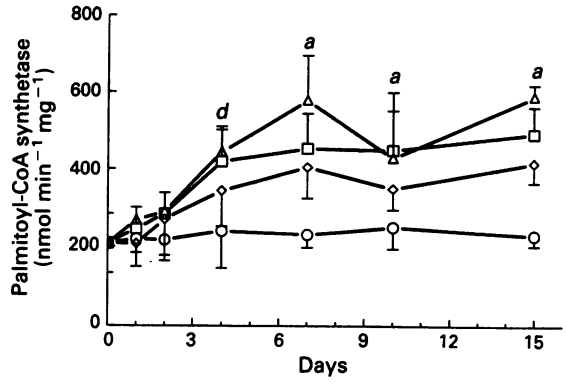

Figure 6 Time-course of the effect of a standard diet (○) or a diet supplemented with 0.3% w/w clofibrate (CFB) (□), 0.45% w/w bezafibrate (BFB) (△), and 0.3% w/w gemfibrozil (GFB) (◇) on palmitoyl-CoA synthetase activity in the microsomal fraction of livers from male Sprague-Dawley rats. Results are means ± s.d. of 6 experiments performed in duplicate. Legends for significance are the same as in Figure 1.

Table 1 Effect of gemfibrozil (GFB) on cytosolic palmitoyl-CoA hydrolase (PCH) activity *in vitro*, cytosol from control and GFB-treated rats

	Cytosol	
	Control	*GFB-treated*
No drug addition	11.5 ± 1.8	25.5 ± 5.1
+ 5 mM GFB	0.6 ± 0.7	14.3 ± 3.3

Activities are nmol min^{-1} mg^{-1} protein. Results are mean ± s.d. of three experiments performed in duplicate. Enzyme activities were assayed as described in Methods section.

Table 2 Correlation among enzymatic and non enzymatic parameters and peroxisomal proliferation (measured as peroxisomal β-oxidation activity)

	Peroxisomal β-oxidation	
	n	r^2
Liver/body weight	149	0.659
Plasma triglycerides	113	0.190*
Plasma cholesterol	115	0.248*
Palmitoyl-CoA synthetase	147	0.535
Cytosolic palmitoy-CoA hydrolase	149	0.473
Microsomal palmitoyl-CoA hydrolase	148	0.293

n are the number of pairs of data analysed. All r^2 values are statistically significant ($P < 0.001$).
*Means negative correlation.

the liver/body weight ratio and the increase in peroxisomal β-oxidation activity (Table 2), although β-oxidation increase could occur even without gross hepatomegaly (Lazarow *et al.*, 1982). Despite the correlation between these parameters, maximal enlargement of the liver is achieved earlier than maximal β-oxidation activities. This delay may be due to the time needed for the transcription and translation of the corresponding β-oxidation genes (Reddy *et al.*, 1986). BFB behaves as the most powerful peroxisomal inducer, whilst GFB is the least potent. As the presence of halogen atoms is a structural requirement for peroxisomal inducers (Esbenshade *et al.*, 1990; McGuire *et al.*, 1991), the lack of halogenation could account for the smaller effect of GFB.

A significant reduction in weight gain was observed in the fibrate-treated groups (Figure 1a), a phenomenon not des-

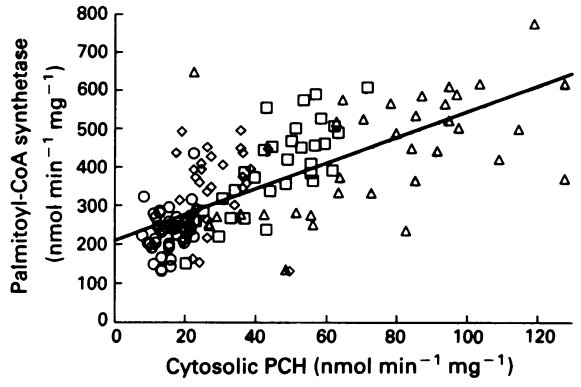

Figure 7 Relationship between palmitoyl-CoA synthetase and cytosolic palmitoyl-CoA hydrolase (PCH) activities in rats treated with a standard diet (○) or a diet supplemented with 0.3% w/w clofibrate (CFB) (□), 0.45% w/w bezafibrate (BFB) (△), and 0.3% w/w gemfibrozil (GFB) (◇). $n = 148$; $r^2 = 0.488$; $P < 0.0001$.

cribed by others (Stahlberg *et al.*, 1989; McGuire *et al.*, 1991). However, in the study by McGuire *et al.* (1991) a different strain of rats was used (CDS albino) while in the study by Stahlberg *et al.* (1989) although the rats were Sprague-Dawley, their higher initial weight (180 vs 120 g in our study) and the lower dose of BFB (0.1 vs 0.45%) make comparison difficult. Nonetheless, a significant increase was observed in the daily food intake of rats treated with BFB and GFB. It is noteworthy that the treatment with dehydroepiandrosterone (DHEA), a steroid hormone that induces peroxisomal proliferation, also causes a marked reduction in body weight of rats (Cleary, 1990; Rao *et al.*, 1992) and mice (Frenkel *et al.*, 1990). The anti-obesity effect of DHEA was thought to be due to the inhibition of glucose-6-phosphate dehydrogenase (Cleary, 1990), an enzyme which is inhibited by GFB *in vitro* (Sánchez *et al.*, 1993a). Nevertheless, the results concerning the action of DHEA are contradictory, and some authors report no effect on this enzymatic activity (Yamada *et al.*, 1991). Another hypothesis to explain the effect of DHEA could be the induction of a futile cycle of deacylation/reacylation of fatty acids in the liver of treated rats (Cleary, 1990). This argument could also be used to explain the effect of fibrates, as these drugs coordinately increase palmitoyl-CoA hydrolase and synthetase activities, as discussed below.

Administration of fibrates reduced plasma cholesterol and triglyceride levels in normolipidaemic rats (Figure 2a and b). The hypolipidaemic effect of these drugs showed a different profile in the study by McGuire *et al.* (1991), in which GFB reduced both cholesterol and triglyceride levels, while BFB showed only hypotriglyceridaemic activity and CFB even increased total cholesterol. However, in that study, experimental conditions were rather different, as animals were fed with a high-fat diet and they were fasted before they were killed. A slight, but significant, inverse correlation between β-oxidation and plasma cholesterol and triglyceride levels was found, suggesting that peroxisomal induction somehow contributes to the hypolipaemic effect of these drugs (Table 2). To our knowlege, only Pourbaix *et al.* (1984) have described a similar association between peroxisomal β-oxidation and plasma cholesterol levels in hamsters. In contrast, in a recent study by Pill *et al.* (1992) using Sprague-Dawley and Lewis rats, even though greater hypolipidaemic effect was achieved in the Lewis rats, which are more sensitive to peroxisomal proliferation, no linear relationship was found between the increase in the β-oxidation activity and the decrease in serum lipids. Moreover, in guinea-pigs (Vázquez *et al.*, 1993) and presumably in man (Hawkins *et al.*, 1987), the hypolipidaemic response to treatment with fibrates is not accompanied by peroxisomal proliferation.

The marked enhancement of liver cytosolic long-chain acyl-CoA hydrolase caused by the three fibrates had already been reported by other authors in CFB-treated rats (Berge *et al.*, 1984; Katoh *et al.*, 1987). Moreover, the increase observed by Katoh *et al.* (1987) correlated well with the induction of peroxisomal β-oxidation. The strong, direct correlation between cytosolic and microsomal acyl-CoA hydrolases and peroxisomal β-oxidation found in this study (Table 2) is in agreement with these reports. Furthermore, the potency order for the induction of palmitoyl-CoA hydrolase is identical to that of peroxisomal proliferating potency: BFB > CFB > GFB. These results also agree with those of Kawashima *et al.* (1983), who demonstrate that treatment with CFB increases hydrolase activity in rats and mice but not in guinea-pigs. Of the three fibrates, GFB is the most potent inhibitor of palmitoyl-CoA hydrolase *in vitro* (Sánchez *et al.*, 1992a). Nevertheless, the lower potency of GFB *in vivo* could not be attributed to the presence of the drug in the cytosolic fraction of treated animals, as activity is the same before and after dialysis of cytosol from GFB-treated rats (data not shown), a procedure which is known to eliminate the drug from the medium (Alegret *et al.*, 1991).

Kawashima *et al.* (1982) proposed the existence of two different inducible palmitoyl-CoA hydrolases in rat liver cytosol, other than the constitutive enzyme. The inducible enzymes were termed hydrolase I, which showed most of the inducible activity after the administration of peroxisomal proliferators, and hydrolase II. Our results *in vitro* confirm the hypothesis that fibrates inhibit the activity of the constitutive enzyme, while they do not affect the induced activity. Thus, if we consider the induced activity as the difference between GFB-treated and control activities, i.e. 25.5 minus 11.5 nmol min^{-1} mg^{-1}, this value closely reflects the activity remaining when cytosol obtained from GFB-treated rats is incubated with 5 mM GFB (about 14 nmol min^{-1} mg^{-1}), whereas this GFB concentration almost completely inhibited the enzyme activity of cytosol obtained from control animals. These results agree with those of previous studies *in vitro* in which the three fibrates were unable to inhibit cytosolic palmitoyl-CoA hydrolase from rat brain (Sánchez *et al.*, 1992a); this enzyme has similar properties to that of the inducible hepatic hydrolase I (Katoh *et al.*, 1987).

The three fibrates greatly increased microsomal palmitoyl-CoA synthetase activity, consistent with the results obtained by Yoshida & Singh (1990) in cell homogenates after treatment of rats with CFB for 14 days. These results cannot be explained by a direct effect of fibrates on the enzyme, as studies *in vitro* demonstrated no effect (CFB, BFB) or inhibition at supraphysiological concentrations (GFB) on palmitoyl-CoA synthetase activity (Sánchez *et al.*, 1993b). The order of potency *in vivo* is similar to that of peroxisomal induction, and in fact the two parameters are strongly correlated (Table 2). Nevertheless, as we found a direct correlation between palmitoyl-CoA synthetase and cytosolic palmitoyl-CoA hydrolase activities (Figure 7), and taking into account that maximal values are achieved earlier for the later enzyme, it seems likely that the induction of palmitoyl-CoA synthetase is an adaptive response to the increase in free CoA caused by the high hydrolase activites, rather than a direct consequence of the peroxisomal induction.

In summary, the time-course of the effect of CFB, BFB and GFB administration to male Sprague-Dawley rats on lipid plasma levels and palmitoyl-CoA hydrolase and synthetase activities, as well as the correlations with the peroxisomal proliferation phenomenon have been studied. From the results reported here, we can assume that: (a) peroxisomal proliferation explains only a relatively small percentage (reflected in the r^2 values) of the observed lipid-lowering effect and (b) given the strong interdependence between the proliferation of peroxisomes and the increase in palmitoyl-CoA synthetase and hydrolase activities, we could conclude that this phenomenon is not directly related to the hypolipidaemic effect of fibrates. Considering that fibrate

therapy is unlikely to cause peroxisomal induction in humans, the increase in these enzyme activities is not expected in humans after fibrate therapy. Thus, in interpreting results obtained from experiments designed to test the fibrate effect on rats, caution should be exercised in their extrapolation to species insensitive to the induction of peroxisomes.

This research was partly supported by grant 91/0147 from the Fondo de Investigaciones Sanitarias de la Seguridad Social and by grant SM91-0020 from DGICYT. M. Alegret and M. Vázquez were recipients of F.P.I. grants from the Generalitat de Catalunya. We also thank Mr Rycroft (Language Advice Service of the University of Barcelona) for his helpful assistance. Further, we greatly appreciate the technical support provided by Ms T. Iglesias.

References

ALEGRET, M., SANCHEZ, R.M., ADZET, T., MERLOS, M. & LAGUNA, J.C. (1991). In vitro effect of clofibric acid derivatives on rat hepatic microsomal electron transport chains. *Biochem. Pharmacol.*, **42**, 2057–2060.

BERGE, R.K. & AARSLAND, A. (1985). Correlation between the cellular level of long chain acyl-CoA, peroxisomal β-oxidation and palmitoyl-CoA hydrolase activity in rat liver. Are the two enzyme systems regulated by a substrate induced mechanism? *Biochim. Biophys. Acta*, **837**, 141–151.

BERGE, R.K. & BAKKE, O.M. (1981). Changes in lipid metabolizing enzymes of hepatic subcellular fractions from rats treated with tiadenol and clofibrate. *Biochem. Pharmacol.*, **30**, 2251–2256.

BERGE, R.K., FLATMARK, T. & OSMUNDSEN, H. (1984). Enhancement of long-chain acyl-CoA hydrolase activity in peroxisomes and mitochondria of rat liver by peroxisomal proliferators. *Eur. J. Biochem.*, **141**, 637–644.

BODNAR, A.G. & RACHUBINSKI, R.A. (1991). Characterization of the integral membrane polypeptides of rat liver peroxisomes isolate from untreated and clofibrate-treated rats. *Biochem. Cell. Biol.*, **69**, 499–508.

BRADFORD, M. (1976). A rapid sensitive method for the quantitation of microgram quantities of protein utilizing the principles of protein-dye binding. *Anal. Biochem.*, **72**, 248–254.

BREMER, J., ODMUNSEN, H., CRISTIANSEN, R.Z. & BORREBAEK, B. (1981). Clofibrate. *Methods Enzymol.*, **72**, 506–519.

CLEARY, M.P. (1990). Effect of dehydroepiandrosterone treatment on liver metabolism in rats. *Int. J. Biochem.*, **22**, 205–210.

DESREUMAUX, V., DEDONDER, E., DEWAILLY, P., SEZILLE, G. & FRUCHART, J.C. (1979). Effects of unsaturated fatty acids in phospholipids on the in vitro activation of the lipoprotein lipase and the triglyceride lipase. *Arzneim. Forsch.*, **29**, 1581–1583.

EARL, D.C.N. & KORNER, A. (1965). The isolation and properties of cardiac ribosomes and polysomes. *Biochem. J.*, **94**, 721–734.

ESBENSHADE, T.A., KAMANNA, V.S., NEWMAN, H.A.I., TORTORELLA, V., WITIAK, D.T. & FELLER, D.R. (1990). In vivo and in vitro peroxisome proliferation properties of selected clofibrate analogues in the rat. *Biochem. Pharmacol.*, **40**, 1263–1274.

FRENKEL, R.A., SLAUGHTER, C.A., ORTH, K., MOOMAW, C.R., HICKS, S.H., SNYDER, J.M., BENNET, M., PROUGH, R.A., PUTNAM, R.S. & MILEWICH, L. (1990). Peroxisome proliferation and induction of peroxisomal enzymes in mouse and rat liver by dehydroepiandrosterone feeding. *J. Steroid Biochem.*, **35**, 333–342.

HAWKINS, J.M., JONES, W.M., BONNER, F.W. & GIBSON, G.G. (1987). The effect of peroxisome proliferators on microsomal, peroxisomal and mitochondrial enzyme activities in the liver and kidney. *Drug Metab. Rev.*, **18**, 441–515.

KATOH, H., KAWASHIMA, Y., WATANUKI, H., KOZUKA, H. & ISONO, H. (1987). Effects of clofibric acid and tiadenol on cytosolic long-chain acyl-CoA hydrolase and peroxisomal β-oxidation in liver and extrahepatic tissues of rats. *Biochim. Biophys. Acta*, **920**, 171–179.

KAWASHIMA, Y., KATOH, H. & KOZUKA, H. (1982). Sex-related difference in the effect of clofibric acid in induction of two novel long-chain acyl-CoA hydrolases in rat liver. *Biochim. Biophys. Acta*, **712**, 48–56.

KAWASHIMA, Y., KATOH, H., NAKAJIMA, S. & KOZUKA, H. (1983). Induction of hepatic long-chain acyl-CoA hydrolase by clofibric acid administration. *Biochim. Biophys. Acta*, **752**, 182–185.

KLOSIEWICZ-LATOSZEK, L. & SZOSTAK, W.B. (1991). Comparative studies on the influence of different fibrates on serum lipoproteins in endogenous hyperlipoproteinaemia. *Eur. J. Clin. Pharmacol.*, **40**, 33–41.

LAZAROW, P.B. (1981). Assay of peroxisomal β-oxidation of fatty acids. *Methods Enzymol.*, **72**, 315–319.

LAZAROW, P.B., SHIO, H. & LEROY-HOUYET, M.A. (1982). Specificity in the action of hypolipidemic drugs: increase of peroxisomal β-oxidation largely dissociated from hepatomegaly and peroxisomal proliferation in the rat. *J. Lipid Res.*, **23**, 317–326.

MCGUIRE, E.J., LUCAS, J.A., GRAY, R.H. & DE LA IGLESIA, F.A. (1991). Peroxisome induction potential and lipid regulating activity in rats. Quantitative microscopy and chemical structure-activity relationships. *Am. J. Pathol.*, **139**, 217–229.

NAGI, M., LAGUNA, J.C., COOK, L. & CINTI, D.L. (1989). Disruption of rat hepatic microsomal electron transport chains by the selenium-containing anti-inflammatory agent Ebselen. *Arch. Biochem. Biophys.*, **2669**, 264–271.

PILL, J., VÖLKL, A., HARTIG, F. & FAHIMI, H.D. (1992). Differences in the response of Sprague-Dawley and Lewis rats to bezafibrate: the hypolipidemic effect and the induction of peroxisomal enzymes. *Arch. Toxicol.*, **66**, 327–333.

POURBAIX, S., HELLER, F. & HARVENGT, C. (1984). Effect of fenofibrate and LF 2151 on hepatic peroxisomes in hamsters. *Biochem. Pharmacol.*, **33**, 3661–3666.

RAO, M.S., MUSUNURI, S. & REDDY, J.K. (1992). Dehydroepiandrosterone-induced peroxisome proliferation in the rat liver. *Pathobiology*, **60**, 82–86.

REDDY, J.K., GOEL, S.K., NEMALI, M.R., CARRINO, J.J., LAFFLER, T.G., REDDY, M.K., SPERBECK, S.J., OSUMI, T., HASHIMOTO, T., LALWANI, N.D. & RAO, M.S. (1986). Transcriptional regulation of peroxisomal fatty acyl-CoA oxidase and enoyl-CoA hydratase/3-hydroxyacyl-CoA dehydrogenase in rat liver by peroxisomal proliferators. *Proc. Natl. Acad. Sci. U.S.A.*, **83**, 1747–1751.

REDDY, J.K. & LALWANI, N.D. (1983). Carcinogenesis by hepatic proliferators: evaluation of the risk of hypolipidaemic drugs and industrial plastisicers to man. *C.R.C. Crit. Rev. Toxicol.*, **12**, 1–58.

SANCHEZ, R.M., ALEGRET, M., ADZET, T., MERLOS, M. & LAGUNA, J.C. (1992a). Differential inhibition of long-chain acyl-CoA hydrolases by hypolipidemic drugs in vitro. *Biochem. Pharmacol.*, **43**, 639–644.

SANCHEZ, R.M., VAZQUEZ, M., ALEGRET, M., VIÑALS, M., ADZET, T., MERLOS, M. & LAGUNA, J.C. (1993a). Cytosolic lipogenic enzymes: effect of fibric acid derivatives *in vitro*. *Life Sci.*, **52**, 213–222.

SANCHEZ, R.M., VIÑALS, M., ALEGRET, M., VAZQUEZ, M., ADZET, T., MERLOS, M. & LAGUNA, J.C. (1992b). Inhibition of rat liver microsomal fatty acid chain elongation by gemfibrozil *in vitro*. *FEBS Lett.*, **300**, 89–92.

SANCHEZ, R.M., VIÑALS, M., ALEGRET, M., VAZQUEZ, M., ADZET, T., MERLOS, M. & LAGUNA, J.C. (1993b). Fibrates modify rat hepatic fatty acid elongation and desaturation *in vitro*. *Biochem. Pharmacol.*, **46**, 1791–1796.

SIRTORI, C.R., MANZONI, C. & LOVATI, M.R. (1991). Mechanisms of lipid-lowering agents. *Cardiology*, **78**, 226–235.

STAHLBERG, D., ANGELIN, B. & EINARSSON, K. (1989). Effects of the treatment with clofibrate, bezafibrate and ciprofibrate on the metabolism of cholesterol in rat liver microsomes. *J. Lipid Res.*, **30**, 953–957.

VANCE, J.E. & VANCE, D.E. (1990). Lipoprotein assembly and secretion by hepatocytes. *Annu. Rev. Nutr.*, **10**, 337–356.

VAZQUEZ, M., ALEGRET, M., ADZET, T., MERLOS, M. & LAGUNA, J.C. (1993). Gemfibrozil modifies acyl composition of liver microsomal phospholipids from guinea-pigs without promoting peroxisomal proliferation. *Biochem. Pharmacol.*, **46**, 1515–1518.

YAMADA, J., SAKUMA, M., IKEDA, T., FUKUDA, K. & SUGA, T. (1991). Characteristics of dehydroepiandrosterone as peroxisome proliferator. *Biochim. Biophys. Acta*, **1092**, 233–243.

YOSHIDA, Y. & SINGH, I. (1990). Effect of clofibrate on peroxisomal lignoceroyl ligase activity. *Biochem. J.*, **122**, 353–362.

(Received December 7, 1993
Revised February 14, 1994
Accepted March 7, 1994)

Br. J. Pharmacol. (1994), **112**, 557–565

Evidence for differential roles of nitric oxide (NO) and hyperpolarization in endothelium-dependent relaxation of pig isolated coronary artery

E.V. Kilpatrick & [1]T.M. Cocks

Department of Pharmacology, University of Melbourne, Parkville, Victoria 3052, Australia

1 The possible roles of endothelial and smooth muscle cell hyperpolarization and nitric oxide (NO) in endothelium-dependent relaxation were examined in isolated rings of pig right coronary artery.

2 The effects of hyperpolarization were prevented with high K^+ (30–125 mM), isotonic Krebs solutions. Functional antagonism due to high K^+-induced smooth muscle contraction was prevented with 0.3 μM nifedipine (in all treatments, for consistency). All rings were contracted with the thromboxane-mimetic U46619, (1–100 nM) to bring them to an initial active force of within 30–50% of maximum contraction.

3 High K^+ had no effects on the sensitivity (EC_{50}) or time course of endothelium-dependent (substance P, SP; bradykinin, BK; calcimycin, A23187) and -independent (sodium nitroprusside, SNP) agents. Maximum relaxations (R_{max}) to SP, BK and A23187 were reduced significantly by approximately 20% but only with 125 mM K^+.

4 In normal K^+ Krebs solution (5.9 mM), N^G-nitro-L-arginine (L-NOARG; 100 μM) caused 40%, 20% and no reduction in R_{max} for SP, BK and SNP respectively. EC_{50}s for SP and BK were decreased significantly by approximately two fold whereas that for SNP was increased significantly by approximately ten fold. At all high K^+ concentrations (30–125 mM), L-NOARG (100 μM) caused complete inhibition of relaxations to SP and BK but those to SNP were unaffected.

5 High K^+ (30 mM) unmasked potent and concentration-dependent inhibition of relaxations of SP by L-NOARG. At 10 μM L-NOARG, all relaxation responses to SP were abolished and at the higher concentrations of SP (1–10 nM) small but significant contractions were observed.

6 N^G-monomethyl-L-arginine (L-NMMA) had similar effects on relaxations to SP in the presence of 30 mM K^+ except that maximum inhibition (40%) of R_{max} was achieved at 10 μM L-NMMA and this was not increased with either 100 or 1000 μM L-NMMA. In normal K^+, L-NMMA (1000 μM) only decreased the EC_{50} by approximately two fold, without affecting R_{max}.

7 High choline$^+$ (25, 75 and 125 mM) isotonic Krebs also had no direct effect on the relaxations to SP, but like high K^+, enabled L-NOARG (100 μM) to inhibit these responses completely. Neither charybdotoxin (30 nM) nor substitution of 25 mM NaCl with 50 mM sucrose had any direct effect on relaxations to SP or on the block of relaxations to SP by L-NOARG (100 μM).

8 In conclusion, most if not all of the endothelium-dependent relaxation in the pig coronary artery *in vitro* is due to NO, but hyperpolarization can supplement 60%–80% of this response if NO synthesis is blocked. Multiple endothelium-derived factors could not only explain heterogeneity of the degree of block of endothelium-dependent relaxation responses by L-arginine analogues, but also constitute important 'back-up' mechanisms for control of arterial diameter.

Keywords: Endothelium; nitric oxide; L-NOARG; L-NMMA; KCl; hyperpolarization; vasodilatation; pig coronary artery

Introduction

Endothelium-derived relaxing factor (EDRF; Furchgott, 1981) or nitric oxide (NO; Palmer *et al.*, 1987; Palmer & Moncada, 1989; Moncada *et al.*, 1991a) is synthesized in endothelial and many other cell types from L-arginine by a family of isoforms of the dioxygenase enzyme nitric oxide synthase (NOS; see Nathan, 1992). Analogues of L-arginine modified in either one of the guanidino nitrogens like N^G-monomethyl-L-arginine (L-NMMA) and N^G-nitro-L-arginine (L-NOARG) inhibit NOS by competing at the active site with L-arginine (see Nathan, 1992; Marletta, 1993).

Most agents that activate release of NO from the endothelium also hyperpolarize both endothelial and smooth muscle cells. The type of K^+ channel involved in these responses, however, is contentious, as is the contribution of endothelium-dependent hyperpolarization to the physiological response, vasodilatation. Both Rusko *et al.* (1992) and Groschner *et al.* (1992) proposed that the increase in K^+ conductance associated with hyperpolarization in endothelial cells acts to enhance entry of extracellular Ca^{2+} and thus both promote and sustain activation of NOS and release of NO (see also Busse *et al.*,1988). This does not explain the ensuing hyperpolarization of the underlying smooth muscle unless the cells are electrotonically coupled (see Olesen *et al.*, 1988). Beny (1990a), however, found no evidence for either electrical or dye coupling between endothelial and smooth muscle cells in pig coronary arteries, although the smooth muscle cells were electrically coupled. Tare *et al.* (1990) found that NO itself caused smooth muscle hyperpolarization in guinea-pig uterine arteries and Pacicca *et al.* (1992) claimed that part of the hyperpolarization to both substance P (SP) and bradykinin (BK) in the pig coronary artery was due to NO. Many other studies, however (Chen *et al.*, 1988; Huang *et al.*, 1988; Komori *et al.*, 1988; Brayden, 1990; Komori & Vanhoutte, 1990; Garland & McPherson, 1992) have clearly discriminated between NO and whatever causes smooth muscle hyperpolarization in a range of arterial preparations (see Taylor & Weston, 1988). Feletou & Van-

[1] Author for correspondence.

houtte (1988) suggested that smooth muscle hyperpolarization was caused by a diffusible factor, separate from NO which was subsequently termed endothelium-derived hyperpolarizing factor (EDHF; see Taylor & Weston, 1988; Komori & Vanhoutte, 1990). Finally, Martin *et al.* (1992) proposed that differences in agonist efficacy and receptor reserve in a particular endothelium-dependent system should be considered before resistance to block by L-arginine analogues is taken as evidence for multiple EDRFs.

Studies in pig coronary arteries (Richard *et al.*, 1990; Illiano *et al.*, 1992; Nagao & Vanhoutte, 1992a,b; Pacicca *et al.*, 1992) have claimed that endothelium-dependent hyperpolarization, not NO-induced actions, is the predominant mechanism for relaxation to kinins like SP and BK. Similarly, Adeagbo & Triggle (1993) suggested that hyperpolarization plays a dominant role in control of basal arterial tone and a substantial role in the vasodilator responses to acetylcholine and histamine in the perfused mesenteric bed of the rat. Also, Fujii *et al.* (1992) claimed that the reduction in endothelium-dependent relaxation to acetylcholine in mesenteric arteries of the spontaneously hypertensive rat was due to loss of endothelium-dependent hyperpolarization. In each of these studies, high extracellular concentrations of potassium (high K^+) were used to negate the effect of hyperpolarization to various endothelium-dependent agents. In the present study, we also used high K^+ but blocked the ensuing smooth muscle contraction with nifedipine, which does not affect endothelium-dependent relaxation responses (Schoefter & Miller, 1986; Angus & Cocks, 1989). The level of initial active force (using the thromboxane A_2-mimetic, U46619) of the tissue was then set to similar values for all treatment groups to avoid any effects of functional antagonism. Our data indicate that in the pig epicardial coronary arteries: (1) hyperpolarization contributes to the relaxation response to SP, BK and A23187 when the release of NO is blocked and; (2) endothelium-dependent smooth muscle hyperpolarization is not mediated by NO. We propose that release of other endothelium-derived relaxing factors (in this case EDHF), together with, but distinct from, NO, and their differential contribution to the final relaxation response, may not only explain some of the heterogeneity of the effectiveness of L-arginine analogues as inhibitors of endothelium-dependent relaxations, but also constitute important 'back-up' systems for control of vascular tone.

Methods

Isolated tissues

Pig hearts were obtained from freshly-slaughtered animals (Large White pigs of either sex; 20–30 kg) at a local abattoir. The hearts were transported to the laboratory in cold (4°C), oxygenated Krebs solution (see below), the right coronary artery dissected free from surrounding myocardium and connective tissue and cut into 3 mm long rings. Some rings of artery had their endothelium removed by gently abrading the luminal surface with a Krebs-moistened filter paper taper (Cocks & Angus, 1983). Each artery ring was then mounted on two diametrically opposed stainless steel wire hooks in a water-jacketed, 25–30 ml organ bath containing Krebs maintained at 37°C and continually gassed with carbogen (95% O_2; 5% CO_2). The lower hook was attached to a micrometer-controlled plastic (PVC) support leg and the upper hook to a Grass force-displacement transducer. Changes in isometric, circumferential force were amplified and displayed on dual channel flat-bed chart recorders.

After an equilibration period of 60 min, the rings were stretched to 5 g passive force and allowed 30 min recovery after which time they were again stretched to 5 g. When a steady plateau of resting force was attained (30–40 min), the rings were contracted with an isotonic, maximally-depolarizing potassium physiological salt solution (KPSS, 125 mM K^+) in which all the NaCl of normal Krebs solution was replaced with KCl (see below). Once a steady maximal level of active force was obtained, the bathing solution was exchanged back to normal Krebs and the tissues allowed to return to resting levels of passive force. All tissues were then treated with 0.3 μM nifedipine and 30 min incubation time allowed. This concentration of nifedipine was predetermined as the lowest needed to inhibit contractions to 30–125 mM K^+ to a similar level (data not shown), and was maintained throughout every treatment.

The normal Krebs solutions for some tissues were again replaced with Krebs solution in which 25, 75 and 125 mM NaCl was replaced isotonically with either KCl, choline chloride or sucrose. Also, L-NOARG (0.01–100 μM) and L-NMMA (1–1000 μM) were added to some tissues and after a further 20 min equilibration period, all tissues were then contracted to between 30% and 50% of their respective maximum contractions to KPSS ($KPSS_{max}$) with the thromboxane A_2-mimetic, U46619 (1–100 nM). Upon reaching a steady level of contraction (initial active force), single or cumulative concentration-relaxation responses to the endothelium-dependent and -independent compounds being tested were obtained in each tissue. At the conclusion of each experiment, the maximum relaxation to sodium nitroprusside (SNP; 10 μM) was obtained, and all relaxation responses expressed as percentages of this maximum SNP relaxation response against initial active force. The composition (in mM) of the normal Krebs solution was as follows: Na^+ 143.1, K^+ 5.9, Ca^{2+} 2.5, Mg^{2+} 1.2, Cl^- 127.8, HCO_3^- 25, SO_4^{2-} 1.2, $H_2PO_4^-$ 1.2, glucose 11. The KPSS solution consisted of (mM): K^+ 124.9, Na^+ 25, Ca^{2+} 2.5, Mg^{2+} 1.2, Cl^- 128.7, HCO_3^- 25, SO_4^{2-} 1.2, $H_2PO_4^-$ 1.2, and glucose 6.1. The 30 mM and 77 mM K^+ and choline$^+$ modified Krebs solutions were normal Krebs with the same amount of NaCl removed to maintain ionic strength.

Statistics

All cumulative concentration-relaxation curves were normalized as percentages of the maximum relaxation to SNP. Each normalized curve was then computer-fitted with a sigmoidal regression curve of the following equation,

$$Y = P_1 + P_2/[1 + e^{P_3(\log x - P_4)}]$$

where x = drug concentration, P_1 = lower response plateau, P_2 = range between lower and upper response plateau, P_3 = a negative curvature index of slope, independent of P_2, $P_4 = \log_{10}$ of the molar concentration (EC_{50}) of relaxation agent necessary to give a 50% maximum response (see Elghozi & Head, 1990). Mean EC_{50} and R_{max} values and their standard errors (s.e.mean) were then calculated for each relaxation curve. Differences in mean EC_{50} and R_{max} values between two experimental groups (e.g. low and high K^+) were tested for significance by means of two-tailed, upaired *t* tests. Differences in mean EC_{50} and R_{max} values as well as mean levels of active force within each experimental group were analysed by one way analysis of variance (ANOVA) with multiple comparisons via Tukey-Kramer's modified *t* statistic. All differences were accepted as significant at the $P<0.05$ level.

Drugs and their source (parentheses)

U46619 (1,5,5-hydroxy-11,9-(epoxymethano)prosta-5Z,13E-dienoic acid, Upjohn: Kalamazoo, U.S.A.); substance P triacetate, N^G-nitro-L-arginine (L-NOARG), (all from Sigma, U.S.A.); N^G-monomethyl-L-arginine (L-NMMA; International Drug Technology, Melbourne, Australia), bradykinin triacetate (Fluka, Switzerland); sodium nitroprusside (Roche, Australia), charybdotoxin (kind gift from Prof J. Angus), (−)-nifedipine (Bayer), A23187 free base (Calbiochem). Stock solutions of nifedipine (10 mM), U46619 (1 mM) and A23187 (1 mM) were made up in absolute ethanol and that of

L-NOARG (100 mM) in 1 M $NaHCO_3$. All dilutions of these stocks were in distilled water. All other drugs were made up in distilled water.

Results

Effect of nifedipine on contraction responses to K^+

Contractions of coronary artery rings to increasing isotonic concentrations of K^+ (20–125 mM) were inhibited in a concentration-dependent manner by nifedipine (0.1–3 μM) with maximum block occurring at 0.3 μM. At this and higher concentrations of nifedipine, similar, small (5–10%) contractions were observed between 20 and 125 mM K^+. These nifedipine-resistant contractions were independent of the endothelium.

Effects of high K^+ on endothelium-dependent and -independent relaxation responses

The endothelium- and concentration-dependence of relaxation responses to substance P (SP; 0.01–3 nM), bradykinin (BK; 0.03–30 nM) and A23187 (0.01–1 μM) were confirmed by the abolition of all relaxation responses to these agents in rings of artery without endothelium (data not shown).

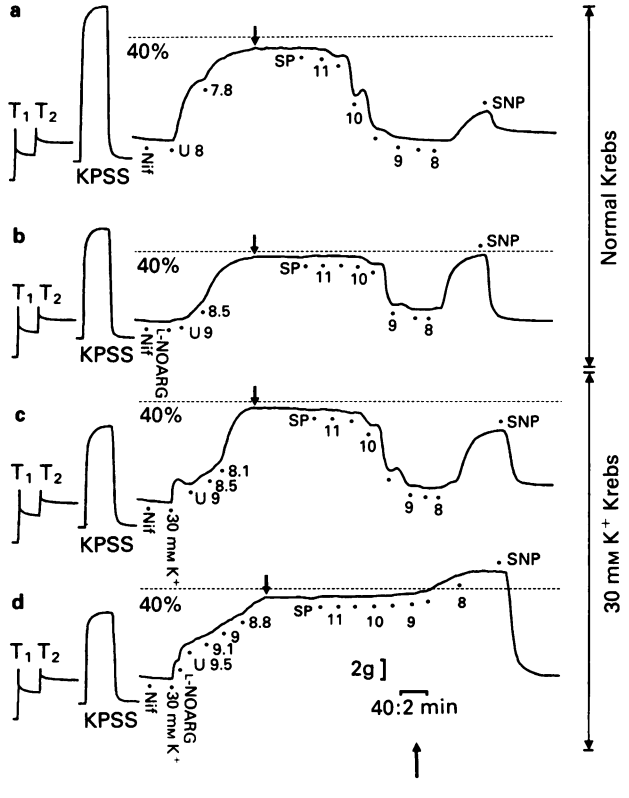

Figure 1 Digitized traces of original chart recordings from four separate rings of pig, isolated coronary artery, showing the effect of N^G-nitro-L-arginine (L-NOARG, 100 μM) on relaxation responses to cumulative half log concentrations of substance P (SP) in normal (a,b) and 30 mM K^+ concentration (c,d) Krebs solutions. In each case the dotted horizontal line indicates 40% of the maximum contraction to KPSS, to which each tissue was approximately set by the addition of the thromboxane A_2-mimetic, U46619 (1–30 nM). Also note that the gain was reduced to obtain the initial KPSS contraction. T_1 and T_2 represent the initial passive stretches. The time calibration bar indicates 40, and 2 min before, and after the arrow, respectively. Nif = 0.3 μM nifedipine; U = U46619; SNP = 10 μM sodium nitroprusside; SP = substance P. Concentrations are expressed as −log[M].

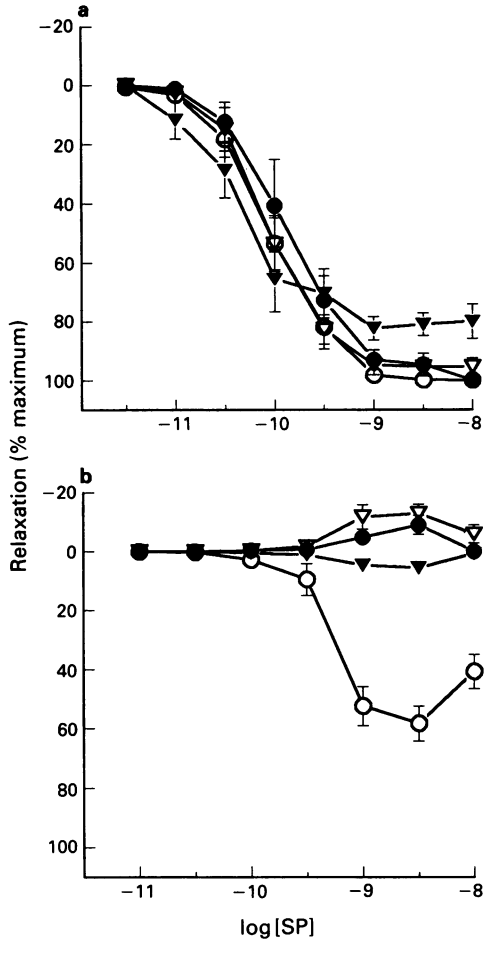

Figure 2 The effect of increasing concentrations of isotonic K^+ on cumulative concentration-relaxation curves to substance P (SP) in the absence (a) and presence (b) of 100 μM N^G-nitro-L-arginine (L-NOARG). Symbols (○), (●), (▽) and (▼) represent normal (5.9), 30, 77 and 125 mM K^+, respectively. Values (mean ± s.e.mean from 5 to 10 experiments) are expressed as percentages of the maximum relaxation to SNP (10 μM) from initial active force. Corresponding initial active forces were (32.6 ± 1.7, 35.7 ± 1.9, 43.1 ± 6.2, 38.0 ± 3.8)% of $KPSS_{max}$ and (42.9 ± 2.8, 52.5 ± 2.8, 38.3 ± 3.3, 43.7 ± 3.1)% of $KPSS_{max}$ in the absence, and presence of L-NOARG, respectively.

Table 1 Effect of increasing concentrations of K^+ on sensitivity (EC_{50}, −log [M]) and maximum relaxation (R_{max}, % maximum) to substance P (SP) in the absence and presence of 100 μM N^G-nitro-L-arginine (L-NOARG)

K^+ in Krebs (mM)	*L-NOARG* (100 μM)	*SP* EC_{50}	R_{max}	*n*
5.9 (Normal)	–	10.0 ± 0.1	100	10
30	–	9.9 ± 0.2	100	5
77	–	10.1 ± 0.1	95 ± 2.9	5
125	–	10.2 ± 0.2	82 ± 4.0*	5
5.9 (Normal)	+	9.3 ± 0.1*	58 ± 5.9*	10
30	+	–	−9.0 ± 3.3**	5
77	+	–	−13 ± 3.1**	5
125	+	–	5.6 ± 2.5**	5

n = number of experiments.
*Significant difference (two-tailed *P* value ≤0.05 for Student's unpaired *t* test) from corresponding treatment without L-NOARG.
*Significant differences (two-tailed *P* value ≤0.05 for one-way ANOVA and Tukey-Kramer modified *t* statistic) from control within each L-NOARG group.

In the presence of isotonic 30 mM K^+, with K^+-induced contraction prevented by nifedipine and the concentration of U46619 adjusted to give stable contractions between 30% and 50% $KPSS_{max}$, relaxation responses to the cumulative addition of increasing concentrations of SP were not different from those obtained in normal Krebs solution (5.9 mM K^+, Figure 1). In similar artery rings, L-NOARG (100 μM) caused significant small decreases in both sensitivity (EC_{50}) and maximum relaxation (R_{max}) to SP in normal K^+ Krebs but abolished the response to SP in high (30 mM) K^+ Krebs. Group data for these experiments with differing concentrations of K^+ is shown in Figure 2 and Table 1. EC_{50} for SP in normal Krebs (10.0 ± 0.1) was unaltered by all concentrations of K^+ whilst R_{max} was reduced significantly only with 125 mM K^+ (Table 1). Similarly, the highest concentration of K^+ (125 mM) had no significant effect on the EC_{50} values for BK and the endothelium-independent relaxing substance, sodium nitroprusside (SNP; see Figure 3 and Table 2). As for SP, R_{max} for BK was also significantly reduced by 125 mM K^+ whereas that for SNP was unaffected. In the presence of normal K^+, L-NOARG (100 μM) caused a small but significant decrease in both EC_{50} and R_{max} for SP and BK whereas for SNP the EC_{50} was significantly increased with no change in R_{max} (Figures 2 and 3; Tables 1 and 2). With high K^+, however, the relaxation curves to both SP and BK were abolished by L-NOARG (100 μM) whilst that to SNP was unaffected (Figures 2 and 3; Tables 1 and 2). Similar effects of high K^+ (125 mM) on the degree of block by L-NOARG of relaxations to the Ca^{2+} ionophore, A23187 (0.01–1 μM) were observed (data not shown). High K^+ (30 mM) also had

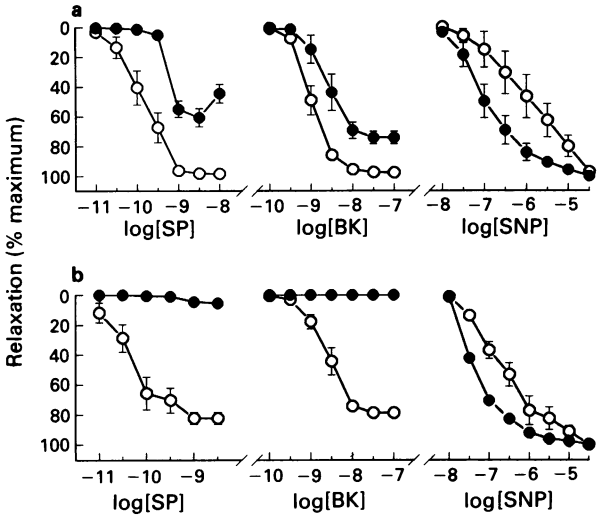

Figure 3 Effect of N^G-nitro-L-arginine (L-NOARG, 100 μM) on the cumulative relaxation-response curves to substance P (SP), bradykinin (BK) and sodium nitroprusside (SNP) in normal (a) and high (125 mM) K^+ (b) Krebs. Values (mean ± s.e.mean from 3 to 8 experiments) without (○), and with 100 μM L-NOARG (●), are expressed as percentages of the maximum relaxation to SNP (10 μM) from initial active force. Corresponding initial active forces were, in normal Krebs, (SP, 35.6 ± 2.8, 41.5 ± 2.1; BK, 35.6 ± 2.8, 41.5 ± 2.1; SNP, 32.9 ± 2.6, 39.2 ± 7.6)% of $KPSS_{max}$, and, in 125 mM K^+ Krebs, (SP, 38.0 ± 3.8, 43.7 ± 3.1; BK, 40.2 ± 4.2, 45.0 ± 2.2; SNP, 28.9 ± 4.11, 32.3 ± 1.2)% of $KPSS_{max}$.

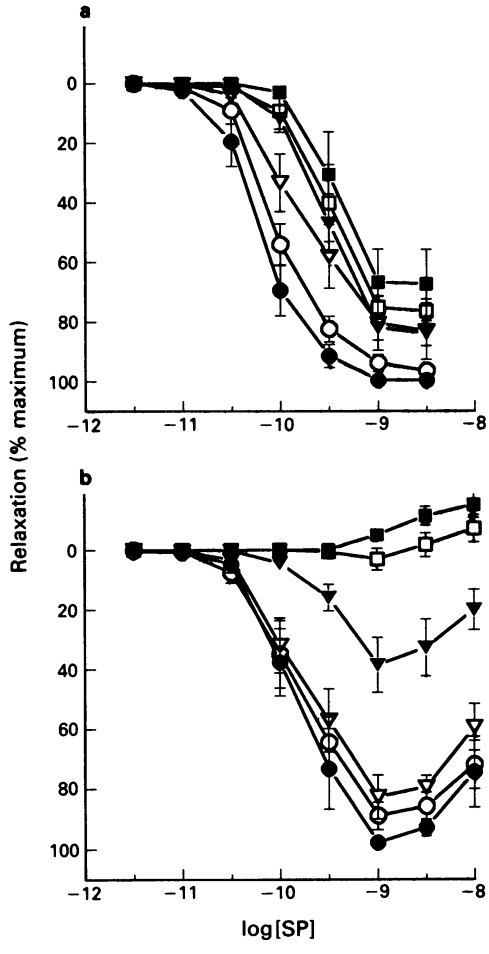

Figure 4 The effect of increasing concentrations of N^G-nitro-L-arginine (L-NOARG) on the cumulative concentration-relaxation curves to substance P (SP) in normal (a) and high K^+ (125 mM) Krebs (b). Symbols (○), (●), (▽), (▼), (□) and (■) represent 0, 0.01, 0.1, 1, 10 and 100 μM L-NOARG, respectively. Values (mean ± s.e.mean from 4 to 8 experiments) are expressed as percentages of the maximum relaxation to SNP (10 μM) from initial active force. Corresponding initial active forces were (37.6 ± 1.8, 35.7 ± 1.3, 34.3 ± 3.4, 43.7 ± 2.2, 36.9 ± 1.5, 38.3 ± 3.5)% of $KPSS_{max}$ and (38.2 ± 2.8, 44.2 ± 7.4, 42.4 ± 2.6, 45.7 ± 2.9, 35.0 ± 2.4)% of $KPSS_{max}$ in the normal (a) and 125 mM K^+ Krebs (b), respectively.

Table 2 Effect of N^G-nitro-L-arginine (L-NOARG, 100 μM) on sensitivity (EC_{50}, −log [M]) and maximum relaxation (R_{max}, % maximum) to substance P (SP), bradykinin (BK) and sodium nitroprusside (SNP) in normal (5.9 mM) and high potassium (125 mM K^+) Krebs solution

K^+ in Krebs (mM)	*L-NOARG* (100 μM)	*SP* EC_{50}	*SP* R_{max}	*n*	*BK* EC_{50}	*BK* R_{max}	*n*	*SNP* EC_{50}	*SNP* R_{max}	*n*
Normal	−	10.0 ± 0.1	100	10	9.0 ± 0.1	98 ± 1.1	5	5.9 ± 0.1	100	4
	+	9.3 ± 0.1*	58 ± 6*	10	8.6 ± 0.1	74 ± 4.3*	6	7.1 ± 0.2*	100	4
125 mM	−	10.2 ± 0.2	82 ± 4*	5	8.9 ± 0.3	78 ± 2.7*	3	6.7 ± 0.2	100	3
	+	−	5.6 ± 3	5	−	0	5	7.4 ± 0.01*	100	3

n = number of experiments.
* Significant difference within Krebs group.
* Significant differences between Krebs group for the same treatment (significance where two-tailed *P* value ≤0.05 for Student's unpaired *t* test).

no effect on either the amplitude or time course of the relaxation response to a submaximum concentration of SP (0.3 nM; data not shown).

Potency of L-NOARG

Since both 30 mM and 77 mM K^+ each by themselves had no effect on the relaxation curves to SP and BK, and since there was no difference between these concentrations of K^+ on the degree of block of SP relaxations by L-NOARG (Figure 2), the lowest concentration of K^+ (30 mM) was chosen to determine the concentration-dependence of the ability of L-NOARG (and L-NMMA, see below) to inhibit relaxation responses to SP.

In normal K^+ Krebs (5.9 mM), 1, 10 and 100 μM L-NOARG each caused the same approximate two fold significant decrease in EC_{50} for SP and, as mentioned above, at 100 μM, L-NOARG caused a significant 40% decrease in R_{max} for SP (Figures 4 and 6). In the presence of high K^+ (30 mM), however, L-NOARG now caused a concentration-dependent depression of R_{max} for SP which was blocked by approximately 60% at 1 μM and abolished at 10 μM L-NOARG. With high K^+, L-NOARG (1 μM) significantly reduced the EC_{50} for SP by the same amount (≃two fold) as

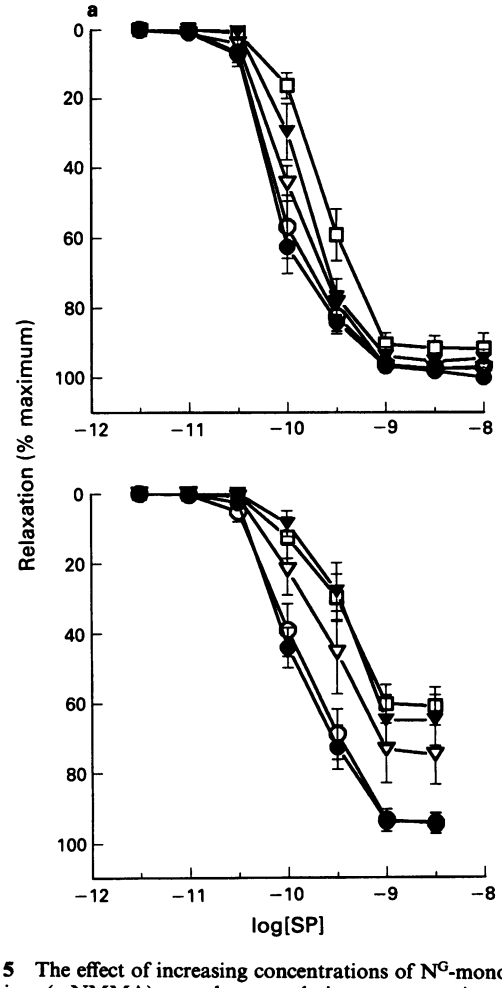

Figure 5 The effect of increasing concentrations of N^G-monomethyl-L-arginine (L-NMMA) on the cumulative concentration-response curve to substance P (SP) in normal (a) and high K^+ (125 mM) Krebs (b). Symbols (○), (●), (▽), (▼) and (□) represent 0, 1, 10, 100 and 1000 μM L-NMMA, respectively. Values (mean ± s.e.mean from 5 to 7 experiments) are expressed as percentages of the maximum relaxation to SNP (10 μM) from initial active force. Corresponding initial active forces were (38.3 ± 2.9, 35.4 ± 0.3, 35.4 ± 3.0, 38.4 ± 3.8, 40.3 ± 4.11)% of $KPSS_{max}$ and (37.0 ± 1.9, 40.0 ± 3.8, 43.0 ± 2.8, 38.5 ± 2.9, 39.8 ± 1.4)% of $KPSS_{max}$ in the normal (a) and 125 mM K^+ Krebs (b), respectively.

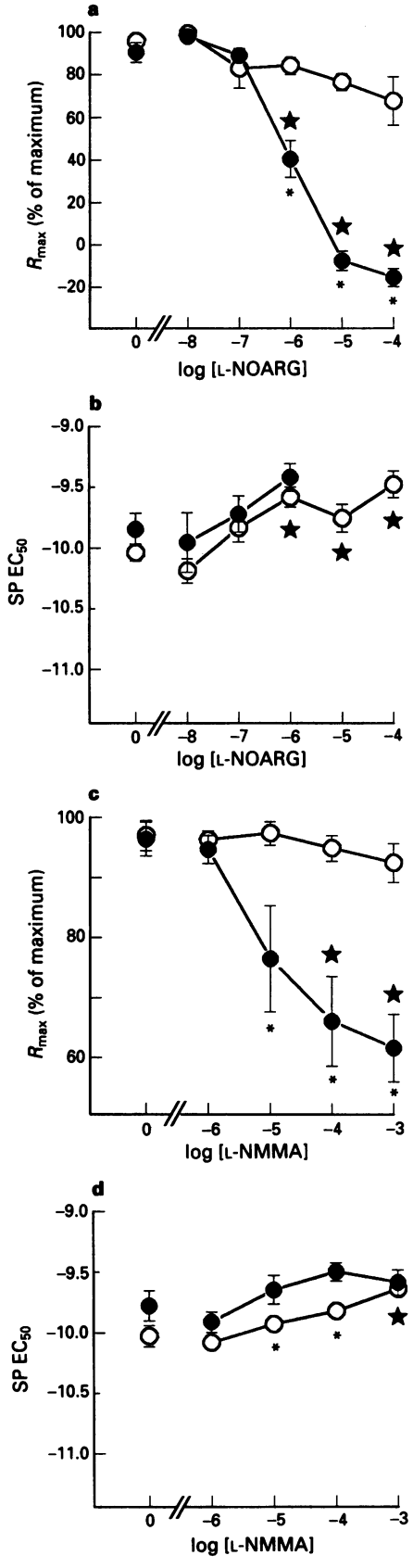

Figure 6 The effect of increasing concentrations of N^G-nitro-L-arginine (L-NOARG) (a and b) and N^G-monomethyl-L-arginine (L-NMMA) (c and d) in normal (○) and high K^+ (125 mM, ●) Krebs on EC_{50} and R_{max} data for substance P (SP) taken from curves shown in Figures 4 and 5. (★) represents values significantly different from control (○) (two-tailed P value <0.05 for Tukey-Kramer test for multiple comparisons after one-way ANOVA) for data within each group (i.e. horizontal analysis) and (*) represents values significantly different (two-tailed P value <0.05 for Student's t test) between normal and high K^+ groups.

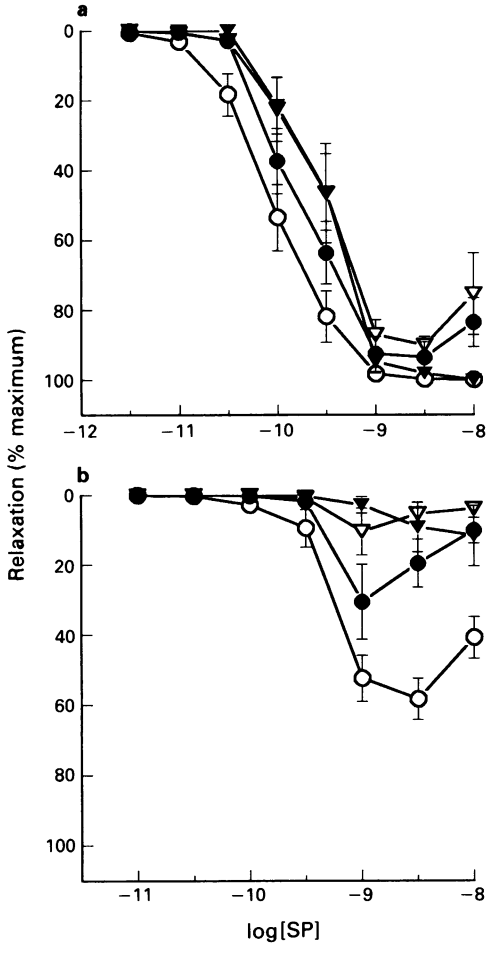

Figure 7 The effect of increasing concentrations of isotonic choline$^+$ on the cumulative concentration-relaxation curves to substance P (SP) in the absence (a) and presence (b) of 100 μM N^G-nitro-L-arginine (L-NOARG). Symbols (○), (●), (▽) and (▼) represent normal (5.9), 25, 75 and 125 mM choline$^+$, respectively. Values (mean ± s.e.mean from 3 to 10 experiments) are expressed as percentages of the maximum relaxation to SNP (10 μM) from initial active force. Corresponding initial active forces were (32.6 ± 1.7, 33.4 ± 0.9, 29.9 ± 0.8, 33.9 ± 2.0)% of $KPSS_{max}$ and (42.9 ± 2.8, 38.6 ± 2.1, 52.2 ± 2.6, 41.0 ± 2.0)% of $KPSS_{max}$ in the absence, and presence of L-NOARG, respectively.

L-NOARG (1–100 μM) in normal K^+ (Figures 4 and 6). At 10 and 100 μM L-NOARG, higher concentrations of SP (1–10 nM) caused contractions (Figure 4).

The increased degree of block of SP-mediated relaxations by L-NOARG in the presence of high K^+ was not observed when L-NOARG was incubated with high K^+ for 60 min and then the tissue returned to normal K^+ Krebs prior to initiating relaxations to SP (data not shown).

Potency of L-NMMA

In normal Krebs solution, L-NMMA (1–1000 μM) caused a small (approximate two fold) but significant rightwards shift in the relaxation curve to SP only at the highest concentration tested, 1000 μM (Figures 5 and 6). There was no significant effect on R_{max} to SP even at this concentration (Figure 6). In the presence of 30 mM K^+, 10, 100 and 1000 μM L-NMMA gave the same approximate but significant two fold decrease in EC_{50} for SP (Figures 5 and 6) as for 1 mM L-NMMA in normal K^+ Krebs solution. R_{max}, however, was now also significantly reduced by approximately 20% at 10 μM L-NMMA (Figure 6). There was a tendency for R_{max} to be decreased further with 100 and 1000 μM L-NMMA but this was not significantly lower than the level with 10 μM L-NMMA (Figure 6).

Effect of choline$^+$, sucrose and charybdotoxin on relaxation responses to SP

Choline$^+$ (25–125 mM) had no significant effect on the relaxation curve to SP but like high K^+, choline$^+$ significantly improved the degree of block of R_{max} for SP by L-NOARG (100 μM; Figure 7). Both isotonic 50 mM sucrose ad 30 nM charybdotoxin had no effect either on the relaxation response curve to SP or on the degree of inhibition by L-NOARG (100 μM) (data not shown).

Discussion

This study has demonstrated that whilst prevention of hyperpolarization of both endothelial and smooth muscle cells has no effect on endothelium-dependent relaxations *per se*, it converts L-NOARG from a relatively poor, to a potent, complete inhibitor of these responses in the pig coronary artery *in vitro*. This preparation was chosen for two reasons. First, it does not relax in response to prostacyclin (see Angus & Cocks, 1989), another endothelium-dependent factor that both relaxes and hyperpolarizes vascular smooth muscle (Jackson *et al.*, 1993). Second, and more important since membrane potential was not measured here, SP, BK and A23187 all cause both endothelium-dependent relaxation and hyperpolarization of endothelial (Brunet & Beny, 1989; Beny, 1990b; Rusko *et al.*, 1992; von der Weid & Beny, 1992) and smooth muscle (Beny *et al.*, 1986; Nagao & Vanhoutte, 1992a,b; Pacicca *et al.*, 1992) cells in this tissue.

The marked effect of high K^+ on the degree of block of endothelium-dependent relaxation by L-NOARG was also seen when Na^+ in normal Krebs was partially and isotonically replaced with choline$^+$, but not with sucrose. Thus, Na^+ depletion was unlikely to have caused the increased potency of L-NOARG observed with high K^+. The same effect of high choline$^+$ as high K^+ on the degree of block of SP relaxations by L-NOARG most likely indicates low potency, non-selective inhibition of K^+ channels by choline$^+$, similar to that reported for other cations like tetrabutylammonium (see Groschner *et al.*, 1992; Nagao & Vanhoutte, 1992a,b). Charybdotoxin had no effect on the ability of L-NOARG to inhibit relaxations to SP. Whilst Rusko *et al.* (1992) used charybdotoxin, albeit at high concentrations (100 nM), to implicate large conductance Ca^{2+}-activated K^+ channels in endothelial cell-mediated NO generation, Groschner *et al.* (1992) suggested that small conductance Ca^{2+}-activated K^+ channels in endothelial cells are involved in NO release. Adeagbo & Triggle (1993), however, claimed a role for apamin-sensitive K^+ channels in endothelium-dependent relaxation of rat mesenteric smooth muscle.

The concentration-dependent contractions to SP in the presence of both L-NOARG and high K^+, probably indicates the presence of tachykinin NK_2 receptors in smooth muscle cells, similar to those found in the rabbit pulmonary artery (Xiao *et al.*, 1992).

The findings here that (1) prevention of hyperpolarization with high extracellular K^+ alone did not alter the sensitivity, maximum relaxation or the time course of responses to substance P, bradykinin and A23187 and (2) L-NOARG produced only partial block of these responses in normal K^+ solutions, first suggest no role for hyperpolarization and only a partial role for NO in endothelium-dependent relaxation in the pig coronary artery *in vitro*. This is unlikely, however, since combination of high K^+ and L-NOARG abolished these responses. One explanation for the improved block by L-NOARG with high K^+ is simply that L-NOARG becomes a more potent inhibitor of NOS. This is also unlikely for two reasons. First, L-NOARG applied under high K^+ conditions followed by washout of the excess K^+ but not L-NOARG,

had no effect on the degree of block of SP responses seen in normal K^+ Krebs solution. Since L-NOARG is known to block constitutive NOS irreversibly (see below), the relaxations to SP should have been abolished in this case if the effect of high K^+ was simply to improve the ability of L-NOARG to inactivate NOS. Second, L-NOARG has been shown to be a potent and complete inhibitor of constitutive NOS in isolated endothelial cells (Mulsch & Busse, 1990; Stork & Cocks, unpublished observations) and of purified constitutive brain NOS (Furfine *et al.*, 1993; and see below). Furthermore, a study by Cowan *et al.* (1993) found that N^G-nitro-L-arginine methyl ester, which is known to block NOS in a similar manner to L-NOARG (Bogle *et al.*, 1992), abolished acetylcholine (ACh)-stimulated rise in guanosine 3′:5′-cyclic monophosphate (cyclic GMP) in rabbit abdominal aorta.

Therefore, given the assumption that L-NOARG abolishes NOS in endothelial cells, our results indicate, that in the pig coronary artery at least, both NO and hyperpolarization are entirely responsible for, but contribute differentially to, endothelium-dependent relaxation *in vitro*. Thus, NO can mediate all the relaxation response regardless of whether hyperpolarization is present, whilst hyperpolarization can account for 60%–80% of endothelium-dependent relaxation responses when NOS is inhibited. As such, hyperpolarization appears to act as a reserve or 'back-up' system, perhaps only important in terms of control of vessel calibre when the main system (NO) fails. Under what physiological or pathological circumstances such differential contribution of NO and hyperpolarization to endothelium-dependent vasodilatation occurs is unknown. Fujii *et al.* (1992) found that compared to mesenteric arteries taken from control, normotensive (WKY) rats, those from hypertensive (SHR) rats showed a reduction in ACh-mediated relaxation, which was probably due to loss of endothelium-dependent hyperpolarization. Also, Melkumyants *et al.* (1992) found no role for NO in endothelium-dependent arterial dilatation to increased flow in the hindquarters of the cat, although in an isolated endothelial cell model of flow-induced release of vasoactive factors, Cooke *et al.* (1991) reported that flow activated a Ca^{2+}-dependent K^+ channel in endothelial cells that lead to release of NO (see also Lamontagne *et al.*, 1992).

If the assumption that NOS activity is abolished by L-NOARG is valid, then our results do not necessarily support the hypothesis of Martin *et al.* (1992) as to why certain tissues show resistance to block of endothelium-dependent relaxation by L-arginine analogues. Martin *et al.* (1992) proposed that differences in the efficiency or 'reserve' in the mechanism of endothelium-dependent relaxation can adequately explain the variable inhibitory effects of L-arginine analogues, without the need to implicate other, non-NO relaxing factors. In support of this proposal, Martin *et al.* (1992) showed that by lowering the 'effector' reserve, of a particular tissue, for example by reducing receptor numbers or using less efficacious agonists at the same receptor site, the L-arginine analogue inhibitors could be changed from ones that showed little block to ones that caused near complete inhibition of endothelium-dependent relaxations. Martin *et al.* (1992) based their conclusion on the assumption that NO is the only factor involved in endothelium-dependent relaxation. A similar conclusion, however, could have been reached with the involvement of multiple factors, either released from endothelial cells at different concentrations of the same stimulating agonist, or at the same concentration but with different potencies as activators of smooth muscle relaxation. Simply by reducing the ability of the smooth muscle to relax, either by reducing the stimulus strength (Martin *et al.*, 1992) or by functional antagonism (see van den Brink, 1973a,b) would most affect the factor either released at the higher agonist concentrations or with the lower potency.

In the present study, any problems associated with functional antagonism were carefully avoided by use of nifedipine, and controlled titration of U46619-induced active force, since the pig coronary artery contracts to maximum to many vasoconstrictor agents including U46619. Thus, we observed marked functional antagonism of relaxations to both SP and SNP in arteries contracted with either U46619 or K^+ above approximately 50% of the tissue's maximum contraction (Kilpatrick & Cocks, unpublished observations). Others (Adeagbo & Triggle, 1993; Nagao & Vanhoutte, 1992a,b) similarly used high K^+ solutions to inhibit K^+ channel activity and thus hyperpolarization, but did not consider possible effects of functional antagonism. In fact, Nagao & Vanhoutte (1992a) contracted their pig coronary arteries with 60 mM K^+, which from our study would have caused a contraction of approximately 80% $KPSS_{max}$ and as such, marked functional antagonism of relaxation responses. Nagao & Vanhoutte (1992a) interpreted the reduction in potency and maximum response to BK in the presence of high K^+ as due to inhibition of the effects of hyperpolarization and concluded that hyperpolarization, not NO, is the main factor involved in endothelium-dependent relaxation in the pig coronary artery. Similar conclusions were reached by Richard *et al.* (1990), Pacicca *et al.* (1992) and Adeagbo & Triggle (1993). Our study, in which any complications of functional antagonism were avoided, suggests the opposite, that NO is the main relaxing factor with hyperpolarization providing 'back-up' if the NO/NOS system fails.

Endothelial cell hyperpolarization has been hypothesized to prolong NOS activation in response to agents that initially raise cell Ca^{2+} by increasing the electrochemical driving force for Ca^{2+} (see Rusko *et al.*, 1992; Groschner *et al.*, 1993). Therefore, by raising extracellular levels of K^+, the reinforcing effect of membrane hyperpolarization on Ca^{2+} entry would be reduced or negated, the efficiency of the NOS/NO system lowered and endothelium-dependent relaxations blocked to a greater degree with L-arginine analogues (see Martin *et al.*, 1992). However, such a mechanism is again unlikely to explain our results given the likelihood that NOS is completely blocked by L-NOARG. It is also unlikely that high extracellular K^+ affected the smooth muscle's ability to relax and in that way reduce efficiency of the tissue's response to NO, since relaxations to SNP were not affected by L-NOARG under high K^+ conditions to a greater degree than with normal K^+.

The increased sensitivity to SNP in the presence of L-NOARG in normal K^+ may be due to hypersensitivity of vascular smooth muscle to exogenous NO following removal of basally released NO, as previously suggested by Moncada *et al.* (1991b).

The reason for the inability of L-NMMA to abolish relaxation responses to SP, unlike L-NOARG, can be explained by differences in both the endothelial uptake mechanism and kinetics of block of NOS of the two analogues. L-NMMA and N-iminoethyl-L-ornithine (L-NIO; see Rees *et al.*, 1990), but not L-NOARG, compete with L-arginine for the system y^+ basic amino acid transporter (see Kavanaugh, 1993) in the plasma membrane of endothelial cells (Bogle *et al.*, 1992). In endothelial cells, the y^+ transporter is saturated between 1 and 100 μM L-arginine (Bogle *et al.*, 1992) and thus concentrations of extracellular L-NMMA above these concentrations would not allow further access of L-NMMA to NOS. Also, Kavanaugh (1993) has shown that endothelial cell hyperpolarization facilitates arginine entry via the y^+ transporter. Thus, inhibition of hyperpolarization (with high K^+ or choline$^+$) would further impede entry of L-NMMA but not L-NOARG. L-NMMA is also metabolized to L-citrulline then L-arginine in endothelial cells (Hecker *et al.*, 1990a,b), another factor that would limit the intracellular concentration of L-NMMA but not L-NOARG. Furthermore, whilst both L-NOARG and L-NMMA are competitive inhibitors of NOS, L-NOARG is a potent (K_i = 15 nM; see Furfine *et al.*, 1993) and effectively irreversible inhibitor due to its very slow rate of dissociation from the enzyme (Furfine *et al.*, 1993), whilst L-NMMA is rapidly reversible (Stork & Cocks, 1994). Finally, L-NMMA is not only less potent than L-NOARG,

but has to compete with intracellular L-arginine for the active site whereas L-NOARG irreversibly inactivates NOS possibly via a covalent interaction (Dwyer *et al.*, 1991) even in the presence of excess L-arginine (Stork & Cocks, unpublished observations; and see also Olken *et al.*, 1991). All these factors combine to make L-NOARG a much more effective NOS inhibitor than L-NMMA, particularly in studies as those reported here to evoke complete block of NOS.

Conclusion

In the pig isolated coronary artery, NO appears to be the main relaxing factor released in response to endothelium-dependent relaxing agents, but hyperpolarization can account for 60%–80% of relaxations to the same agents if synthesis of NO is blocked. This finding may not only explain the considerable heterogeneity in the degree of block of endothelium-dependent relaxation by L-arginine analogues between tissues and species, but it also raises the important question as to the relevance of endothelium-dependent hyperpolarization in vascular diseases like atherosclerosis and hypertension.

This work was supported by the National Health and Medical Research Council of Australia. We thank Drs Chris Garland, Didier Pruneau and Patrick Falckh for their helpful comments.

References

ADEAGBO, A.S.O. & TRIGGLE, C.R. (1993). Varying extracellular [K+]: a functional approach to separating EDHF- and EDNO-related mechanisms in perfused rat mesenteric arterial bed. *J. Cardiovasc. Pharmacol.*, **21**, 423–429.

ANGUS, J.A. & COCKS, T.A. (1989). Endothelium derived relaxing factor. *Pharmacol. Ther.*, **41**, 303–351.

BENY, J.-L. (1990a). Endothelial and smooth muscle cells hyperpolarized by bradykinin are not dye coupled. *Am. J. Physiol.*, **258**, H836–H841.

BENY, J.-L. (1990b). Thimerosal hyperpolarizes arterial smooth muscles in an endothelium-dependent manner. *Eur. J. Pharmacol.*, **185**, 235–238.

BENY, J.-L., BRUNET, P.C. & HUGGEL, H. (1986). Effect of mechanical stimulation, substance P and vasoactive intestinal polypeptide on the electrical and mechanical activities of circular smooth muscles from pig coronary arteries contracted with acetylcholine: role of endothelium. *Pharmacol.*, **33**, 61–68.

BOGLE, R.G., MONCADA, S., PEARSON, J.D. & MANN, G.E. (1992). Identification of inhibitors of nitric oxide synthase that do not interact with the endothelial cell L-arginine transporter. *Br. J. Pharmacol.*, **105**, 768–770.

BRAYDEN, J.E. (1990). Membrane hyperpolarization is a mechanism of endothelium-dependent cerebral vasodilation. *Am. J. Physiol.*, **259**, H668–H673.

BRUNET, P.C. & BENY, J.-L. (1989). Substance P and bradykinin hyperpolarize pig coronary artery endothelial cells in primary culture. *Blood Vessels*, **26**, 228–234.

BUSSE, R., FICHTNER, H., LUCKHOFF, A. & KOHLHARDT, M. (1988). Hyperpolarization and increased free calcium in acetylcholine-stimulated endothelial cells. *Am. J. Physiol.*, **255**, H965–H969.

CHEN, G., SUZUKI, H. & WESTON, A.H. (1988). Acetylcholine releases endothelium-derived hyperpolarizing factor and EDRF from rat blood vessels. *Br. J. Pharmacol.*, **95**, 1165–1174.

COCKS, T.M. & ANGUS, J.A. (1983). Endothelium-dependent relaxation of coronary arteries by noradrenaline and serotonin. *Nature*, **305**, 627–630.

COOKE, J.P., ROSSITCH, E., ANDON, N.A., LOSCALZO, J. & DZAU, V.J. (1991). Flow activates an endothelial potassium channel to release an endogenous nitrovasodilator. *J. Clin. Invest.*, **88**, 1663–1671.

COWAN, C.L., PALACINO, J.J., NAJIBI, S. & COHEN, R.A. (1993). Potassium channel-mediated relaxation to acetylcholine in rabbit arteries. *J. Pharmacol. Exp. Ther.*, **266**, 1482–1489.

DWYER, M.A., BREDT, D.S. & SNYDER, S.H. (1991). Nitric oxide synthase: irreversible inhibition by L-N^G-nitroarginine in brain in vitro and in vivo. *Biochem. Biophys. Res. Commun.*, **176**, 1136–1141.

ELGHOZI, J.-L. & HEAD, G.A. (1990). Spinal noradrenergic pathways and pressor responses to central angiotensin II. *Am. J. Physiol.*, **258**, H240–H246.

FELETOU, M. & VANHOUTTE, P.M. (1988). Endothelium-dependent hyperpolarization of canine coronary smooth muscle. *Br. J. Pharmacol.*, **93**, 515–524.

FUJII, K., TOMINAGA, M., OHMORI, S., KOBAYASHI, K., KOGA, T., TAKATA, Y. & FUJISHIMA, M. (1992). Decreased endothelium-dependent hyperpolarization to acetylcholine in smooth muscle of the mesenteric artery of spontaneously hypertensive rats. *Circ. Res.*, **70**, 660–669.

FURCHGOTT, R.F. (1981). The requirement for endothelial cells in the relaxation of arteries by acetylcholine and some other nitrovasodilators. *Trends Pharmacol. Sci.*, **2**, 173–176.

FURFINE, E.S., HARMON, M.F., PAITH, J.E. & GARVEY, E.P. (1993). Selective inhibition of constitutive nitric oxide synthase by L-N^G-nitroarginine. *Biochemistry*, **32**, 8512–8517.

GARLAND, C.J. & MCPHERSON, G.A. (1992). Evidence that nitric oxide does not mediate the hyperpolarization and relaxation to acetylcholine in the rat small mesenteric artery. *Br. J. Pharmacol.*, **105**, 429–435.

GROSCHNER, K., GRAIER, W.F. & KUKOVETZ, W.R. (1992). Activation of a small-conductance Ca^{2+}-dependent K^+ channel contributes to bradykinin-induced stimulation of nitric oxide synthesis in pig aortic endothelial cells. *Bioch. Biophys. Acta*, **1137**, 162–170.

HECKER, M., MITCHELL, J., HARRIS, H.J., KATSURA, M., THIEMERMANN, C. & VANE, J.R. (1990a). N^G-monomethyl-l-arginine but not N^G-nitro-l-arginine is metabolised by endothelial cells to l-citrulline. *Eur. J. Pharmacol.*, **183**, 648–649.

HECKER, M., MITCHELL, J., HARRIS, H.J., KATSURA, M., THIEMERMANN, C. & VANE, J.R. (1990b). Endothelial cells can metabolize N^G-monomethyl-l-arginine to l-citrulline and subsequently to l-arginine. *Biochem. Biophys. Res. Commun.*, **167**, 1037–1043.

HUANG, A.H., BUSSE, R. & BASSENGE, E. (1988). Endothelium-dependent hyperpolarization of smooth muscle cells in rabbit femoral arteries is not mediated by EDRF (nitric oxide). *Naunyn-Schmied. Arch. Pharmacol.*, **338**, 438–442.

ILLIANO, S., NAGAO, T. & VANHOUTTE, P.M. (1992). Calmidazolium, a calmodulin inhibitor, inhibits endothelium-dependent relaxations resistant to nitro-L-arginine in the canine coronary artery. *Br. J. Pharmacol.*, **107**, 387–392.

JACKSON, W.F., KONIG, A., DAMBACHER, T. & BUSSE, R. (1993). Prostacyclin-induced vasodilation in rabbit heart is mediated by ATP-sensitive potassium channels. *Am. J. Physiol.*, **264**, H238–H243.

KAVANAUGH, M.P. (1993). Voltage dependence of facilitated arginine flux mediated by the system y^+ basic amino acid transporter. *Biochemistry*, **32**, 5781–5785.

KOMORI, K., LORENZ, R.R. & VANHOUTTE, P.M. (1988). Nitric oxide, ACh, and electrical and mechanical properties of canine arterial smooth muscle. *Am. J. Physiol.*, **255**, H207–H212.

KOMORI, K. & VANHOUTTE, P.M. (1990). Endothelium-derived hyperpolarizing factor. *Blood Vessels*, **27**, 238–245.

LAMONTAGNE, D., POHL, U. & BUSSE, R. (1992). Mechanical deformation of vessel wall and shear stress determine the basal release of endothelium-derived relaxing factor in the intact rabbit coronary vascular bed. *Circ. Res.*, **70**, 123–130.

MARLETTA, M.A. (1993). Nitric oxide synthase structure and mechanism. *J. Biol. Chem.*, **268**, 12231–12234.

MARTIN, G.R., BOLOFO, M.L. & GILES, H. (1992). Inhibition of endothelium-dependent vasorelaxation by arginine analogues: a pharmacological analysis of agonist and tissue dependence. *Br. J. Pharmacol.*, **105**, 643–652.

MELKUMYANTS, A.M., BALASHOV, S.A., KLIMACHEV, A.N., KARTAMYSHEV, S.P. & KHAYUTIN, V.M. (1992). Nitric oxide does not mediate flow induced endothelium dependent arterial dilatation in the cat. *Cardiovasc. Res.*, **26**, 256–260.

MONCADA, S., PALMER, R.M.J. & HIGGS, E.A. (1991a). Nitric oxide: physiology, pathophysiology, and pharmacology. *Pharmacol. Rev.*, **43**, 109–142.

MONCADA, S., REES, D.D., SCHULZ, R. & PALMER, R.M.J. (1991b). Development and mechanism of a specific supersensitivity to nitrovasodilators after inhibition of vascular nitric oxide synthesis *in vivo*. *Proc. Natl. Acad. Sci. U.S.A.*, **88**, 2166–2170.

MULSCH, A. & BUSSE, A. (1990). N^G-nitroarginine (N^5-[imino(nitroamino)methyl]-1-ornithine) impairs endothelium-dependent dilations by inhibiting nitric oxide synthesis from L-arginine. *Naunyn-Schmied. Arch. Pharmacol.*, **341**, 143–147.

NAGAO, T. & VANHOUTTE, P.M. (1992a). Characterization of endothelium-dependent relaxations resistant to nitro-L-arginine in the porcine coronary artery. *Br. J. Pharmacol.*, **107**, 1102–1107.

NAGAO, T. & VANHOUTTE, P.M. (1992b). Hyperpolarization as a mechanism for endothelium-dependent relaxations in the porcine coronary artery. *J. Physiol.*, **445**, 355–367.

NATHAN, C. (1992). Nitric oxide as a secretory product of mammalian cells. *FASEB J.*, **6**, 3051–3064.

OLESEN, S.-P., DAVIES, P.F. & CLAPHAM, D.E. (1988). Muscarinic-activated K^+ current in bovine aortic endothelial cells. *Circ. Res.*, **62**, 1059–1064.

OLKEN, N.M., RUSCHE, K.M., RICHARDS, M.K. & MARLETTA, M.A. (1991). Inactivation of macrophage nitric oxide synthase activity by N^G-methyl-L-arginine. *Biochem. Biophys. Res. Commun.*, **177**, 828–833.

PACICCA, C., VON DER WEID, P.-Y. & BENY, J.-L. (1992). Effect of nitro-L-arginine on endothelium-dependent hyperpolarizations and relaxations of pig coronary arteries. *J. Physiol.*, **457**, 247–256.

PALMER, R.M.J., FERRIGE, A.G. & MONCADA, S. (1987). Nitric oxide release accounts for the biological activity of endothelium-derived relaxing factor. *Nature*, **327**, 524–526.

PALMER, R.M.J. & MONCADA, S. (1989). A novel citrulline-forming enzyme implicated in the formation of nitric oxide by vascular endothelial cells. *Biochem. Biophys. Res. Commun.*, **158**, 348–352.

REES, D.D., PALMER, R.M.J., SCHULZ, R., HODSON, H.F. & MONCADA, S. (1990). Characterization of three inhibitors of endothelial nitric oxide synthase *in vitro* and *in vivo*. *Br. J. Pharmacol.*, **101**, 746–752.

RICHARD, V., TANNER, F.C., TSCHUDI, M., & LUSCHER, T.F. (1990). Different activation of L-arginine pathway by bradykinin, serotonin, and clonidine in coronary arteries. *Am. J. Physiol.*, **259**, H1433–H1439.

RUSKO, J., TANZI, F., VAN BREEMAN, C. & ADAMS, D.J. (1992). Calcium activated potassium channels in native endothelial cells from rabbit aorta: conductance, Ca^{2+} sensitivity and block. *J. Physiol.*, **455**, 601–621.

SCHOEFFTER, P. & MILLER, R.C. (1986). Role of sodium-calcium exchange and effects of calcium entry blockers on endothelial-mediated responses in rat isolated aorta. *Mol. Pharmacol.*, **30**, 53–57.

TARE, M., PARKINGTON, H.C., COLEMAN, H.A., NEILD, T.O. & DUSTING, G.J. (1990). Hyperpolarization and relaxation of arterial smooth muscle caused by nitric oxide derived from the endothelium. *Nature*, **346**, 69–71.

TAYLOR, S.G. & WESTON, A.H. (1988). Endothelium-derived hyperpolarizing factor: a new endogenous inhibitor from the vascular endothelium. *Trends Pharmacol. Sci.*, **9**, 272–274.

VAN DEN BRINK, F.G. (1973a). The model of functional interaction. I. Development and first check of a new model of functional synergism and antagonism. *Eur. J. Pharmacol.*, **22**, 270–278.

VAN DEN BRINK, F.G. (1973b). The model of functional interaction. II. Experimental verification of a new model: the antagonism of a-adrenoceptor stimulants and other agonists. *Eur. J. Pharmacol.*, **22**, 279–286.

VON DER WEID, P.-Y. & BENY, J.-L. (1992). Effect of Ca^+ ionophores on membrane potential of pig coronary artery endothelial cells. *Am. J. Physiol.*, **262**, H1823–H1831.

XIAO, X.-H., MUSSAP, C.J. & BURCHER, E. (1992). Characterization of the tachykinin NK_2 receptor subtype in the rabbit pulmonary artery. *Peptides*, **13**, 281–285.

(Received November 8, 1993
Revised January 28, 1994
Accepted February 1, 1994)

Br. J. Pharmacol. (1994), **112**, 566–570

Effects of dietary marine oil supplementation on reactivity of human buttock subcutaneous arteries and forearm veins *in vitro*

[1]Jaye P.F. Chin, David M. Kaye, Robyn M. Hurlston, [2]James A. Angus, Garry L. Jennings & Anthony M. Dart

Alfred and Baker Medical Unit, Baker Medical Research Institute, Commercial Road, Prahran, Victoria, Australia 3181

1 The vascular reactivity of resistance arteries isolated from gluteal skin biopsies and veins isolated from forearms of subjects fed marine oils were examined.

2 Twenty seven healthy adult males were randomly allocated to one of two different treatment groups. The first group received maxEPA (eicosapentaenoic acid 0.178 g g^{-1}; docosahexaenoic acid 0.116 g g^{-1}) capsules 10 g per day for 28 days while the second group received an equivalent amount of mixed oil placebo capsules. Biopsies were performed on day 29 (13 for gluteal sections; 14 for forearm vein biopsies). Subcutaneous arteries and veins were mounted in myographs and standard organ baths, respectively.

3 The internal diameter of the subcutaneous arteries at a calculated transmural pressure of 100 mmHg averaged 183.7 ± 10.3 μm in the maxEPA group and 182.6 ± 19.8 μm in the placebo controls. Arteries from subjects on maxEPA demonstrated increased sensitivity to angiotensin II (maxEPA vs placebo: $-\log EC_{50}$ (M) -8.36 ± 0.18 vs -7.91 ± 0.14) but not to noradrenaline or 5-hydroxytryptamine. Concentration-response curves to acetylcholine, substance P and sodium nitroprusside obtained for noradrenaline precontracted vessels were unaltered with marine oil treatment as was the concentration-response curve to calcium in K^+-depolarized vessels.

4 Vein internal diameter at a calculated transmural pressure of 20 mmHg averaged 3.06 ± 0.23 mm in the maxEPA group and 2.96 ± 0.89 in the placebo group. Responses to noradrenaline, 5-hydroxytryptamine, angiotensin II and endothelin-1 were obtained in the absence and presence of indomethacin (1 μM) in veins from both maxEPA and placebo-treated subjects. Neither dietary supplementation with marine oils nor indomethacin had any effect on the responses obtained to these agonists.

5 The major finding of the present study was that in general, maxEPA supplementation did not affect responses to various vasoactive substances on isolated subcutaneous arteries or forearm veins. An exception was the observation of an enhanced response to angiotensin II in subcutaneous resistance arteries studied *in vitro*. This effect was selective for angiotensin II and was not apparent in veins isolated from the forearm.

Keywords: Fish oil; vascular reactivity (man)

Introduction

N-3 polyunsaturated fatty acids of marine origin (n-3 PUFA; marine oils) are reported to be cardioprotective. Oral supplementation with these oils lower plasma lipids (Nestel, 1990), blood pressure (Knapp & Fitzgerald, 1989) and the incidence of death following myocardial infarction (Burr *et al.*, 1989). We previously demonstrated that marine oils attenuate vasoconstrictor responses to noradrenaline and angiotensin II in human forearm resistance arteries *in vivo*. (Chin *et al.*, 1993a), without affecting vasodilator responses to either acetylcholine or sodium nitroprusside (Chin *et al.*, 1993b). This attenuating effect is, at least in part, antagonized by indomethacin (Chin *et al.*, 1993b). There was no evidence for an effect of marine oils on sympathetic activity in man at rest (Dart *et al.*, 1994).

To explore further the effects of marine oils on human vasculature, buttock subcutaneous resistance arteries and forearm veins were isolated from healthy volunteers fed marine oils. This enabled a more detailed pharmacological study than that possible using the *in vivo* forearm preparation. Since a similar attenuating effect of marine oils on responses to vasoconstrictor agonists to that seen in the human *in vivo* study has been reported in resistance vessels isolated from rats fed marine oils (Yin *et al.*, 1991), we sought to examine this phenomenon further in human isolated tissues. The effect of marine oils on endothelium-derived relaxing factor (EDRF) release was also explored following reports that arteries isolated from rats fed a marine oil diet demonstrate increased dilator responses to acetylcholine when compared with rats fed coconut oil (Yin *et al.*, 1988; 1990) and similarly for porcine coronary arteries (Shimokawa & Vanhoutte, 1989).

In a recent report, Hallaq & Leaf (1992) demonstrated that n-3 PUFAs reduced $^{45}Ca^{2+}$ influx into isolated neonatal cardiac myocytes of the rat. To test for a similar process in human resistance arteries, we examined the effects of marine oils on calcium concentration-response curves. Following our recent report that the attenuating effects of marine oils on vasoconstrictor responses are indomethacin-sensitive (Chin *et al.*, 1993b), we also sought to explore this further in isolated tissues.

Methods

A total of 27 healthy males (18–24 years) were recruited by advertisement and enrolled into either the gluteal subcutaneous artery biopsy protocol ($n = 14$) or the forearm vein biopsy protocol ($n = 13$). Criteria for inclusion in the study were non-smoking status, alcohol intake <2 standard alcoholic drinks/day, normotension (systolic blood pressure <140 mmHg; diastolic blood pressure <90 mmHg) and normocholesterolaemia (total cerum cholesterol <5.5 mmol l^{-1}; total triglyceride <2.0 mmol l^{-1}). In addition, all

[1] Author for correspondence.
[2] Present address: Department of Pharmacology, Melbourne University, Parkville 3001, Victoria, Australia.

volunteers had normal findings on physical examination as well as routine haematology and biochemical blood analyses. The study was approved by the Alfred Group of Hospitals Ethics Committee and written informed consent was obtained from all subjects.

Marine oil supplementation

A double-blind, placebo controlled, parallel study design was used. Upon recruitment into one of the two biopsy protocols, volunteers were further randomly assigned by an independent investigator into one of two dietary groups. The first group received maxEPA (eicosapentaenoic acid 0.178 g g^{-1}; docosahexaenoic acid 0.116 g g^{-1}) capsules, while the second group received mixed oil placebo. The contents of both capsules were similar to that used in our previous experiments and are as listed in Table 1. All subjects were instructed to take 10 capsules a day, every day, for 28 days (total n-3 PUFA content in maxEPA group: 2.94 g per day compared with approximately 2.5 g per 100 g mackeral or approximately 1.2 g per 100 g salmon) and were advised to maintain their lifestyle (i.e. in terms of diet and exercise) and refrain from any medication and in particular non-steroidal anti-inflammatory drugs. Compliance with capsule administration was confirmed by capsule count at the end of the 28-day period.

At 08 h 00 min on day 29, either buttock skin or forearm vein biopsies were performed under local anaesthesia (lignocaine, 1% s.c.) with strict aseptic conditions. Biopsies were immediately placed in ice cold Krebs Henseleit solution and transported to the laboratories.

Buttock subcutaneous arteries

Subcutaneous small arteries were isolated from buttock skin biopsies using a dissecting microscope (Nikon 102, zoom lens). As previously described (Mulvany & Halpern, 1977) segments of the arteries were threaded onto 40 μm diameter stainless steel wires and mounted as ring preparations (approximately 2 mm long) in an isometric myograph (JP Trading, Denmark). Vessels were bathed in Krebs solution (mM: NaCl 119, KCl 4.7, KH_2PO_4 1.18, $MgSO_4$ 1.17, $NaHCO_3$ 25, $CaCl_2$ 2.5, EDTA 0.026, glucose 5.5) bubbled with carbogen (95% O_2, 5% CO_2) at pH 7.4 and kept at a constant temperature of 37°C.

After an unstretched equilibration period of 30 min, each vessel was passively stretched to an internal circumference equal to $0.9 \times L_{100}$, where L_{100} denotes the internal circumference at the level of passive stretch equivalent to a transmural pressure of 100 mmHg. This was calculated using the length-tension relationship obtained in each vessel; $0.9 \times L_{100}$ was used since this has been shown to be optimal for maximal force production in arteries (Mulvany & Warshaw, 1979). This was important to ensure that arteries of different internal diameter were stretched passively to a similar point on their length-tension curve.

After a further 30 min, the viability of each vessel was confirmed by a 2 min exposure to a high potassium Krebs solution (KPSS; K^+ 124 mM) which was washed out and followed 5 min later with a single application of noradrenaline (10 μM) for 2 min. Cumulative concentration-response curves to acetylcholine, substance P and sodium nitroprusside (SNP) were obtained in log progression ratios of 0.5 in arteries contracted to a steady level of force (approximately 70–80% maximal constriction (E_{max})) by noradrenaline (1–3 μM). Cumulative concentration-response curves to the vasoconstrictor agents, noradrenaline, angiotensin II and 5-hydroxytryptamine (5-HT) were also obtained in each vessel. These concentration-response curves were constructed in a random order.

To examine the effect of marine oils on Ca^{2+} influx, a concentration-response curve to Ca^{2+} was obtained at the end of each experiment. Vessels were equilibrated with calcium-free Krebs solution for 15 min. To confirm the complete removal of calcium, calcium-free KPSS (Ca^{2+}-free, high (124 mM) K^+) was added every 5 min. The lack of contraction to calcium-free KPSS was taken as an indication that extracellular calcium was minimal. To test extracellular calcium entry into depolarized smooth muscle cells, a concentration-response curve to calcium (0–2.5 mM) was obtained in tissues bathed in calcium-free KPSS.

Forearm veins

Each segment of superficial vein biopsied from the forearm was carefully cleared of connective tissue and dissected into 2 × 3 mm rings. Each ring was mounted onto two L-shaped parallel wires (355 μm diameter) in a siliconised 25 ml jacketed glass organ bath, and bathed in Krebs solution (mM: NaCl 119, KCl 4.7, KH_2PO_4 1.18, $MgSO_4$ 1.17, $NaHCO_3$ 25, $CaCl_2$ 2.5, EDTA 0.026, glucose 11), under the same conditions as described above.

Vein preparations were passively stretched to an internal circumference equal to $0.9 \times L_{20}$ standard pressure (Sudhir *et al.*, 1990). After a further 30 min, each vessel ring underwent one of two protocols. All vessels were initially contracted with KPSS to ensure viability. In the first protocol, cumulative concentration-response curves in log concentration progression ratios of 0.5 were constructed to noradrenaline and 5-hydroxytryptamine (5-HT). Subsequently, indomethacin (10 μM) was added to the organ bath and after a 30 min incubation period, concentration-response curves to noradrenaline and angiotensin II were repeated in the presence of this cyclo-oxygenase inhibitor. Since angiotensin II displays tachyphylaxis at high concentrations in this preparation (Sudhir *et al.*, 1990), only a single curve was obtained for this agonist. Similarly, only a single concentration-response curve was constructed to endothelin-1 (ET-1) due to the limited availability of this compound. In the first protocol, both were obtained in the presence of indomethacin. Protocol two served as the time control experiment. Hence all concentration-response curves were constructed in protocol two as in protocol one, with the exception that indomethacin was not added in this series of experiments. In all the protocols used, a 30 min re-

Table 1 Oil capsule composition

Fatty acid composition per g	*Mixed oil placebo (g)*	*maxEPA (g)*
Total saturated fatty acids	0.296	0.254
18:1 + 16:1	0.309	0.283
Linoleic acid	0.395	–
Eicosapentaenoic acid	–	0.178
Docosahexaenoic acid	–	0.116
P/S ratio	1.340	1.610

*1 capsule = 1 g. P/S: polyunsaturated:saturated ratio

equilibration period was observed between each concentration-response curve.

Data analysis

Contractile responses were measured in mN for arterial preparations, and as g force normalized to the internal diameter for venous preparations. Individual concentration-response curves for each agonist were fitted to a logistic equation of the form $E = MA^P/(A^P \times K^P)$ where E is the response, M is the maximum response, A is the concentration eliciting E, K is the concentration eliciting 50% of the maximum response (i.e. EC_{50}) and P is the slope parameter (Nakashima *et al.*, 1982). From this equation, the concentrations corresponding to 10–90% (EC_{10-90}) of the maximum response were determined. The location of the EC_{50} value provided a measure of sensitivity. Since a maximum response was not achieved either to angiotensin II or ET-1 in the forearm vein preparation, responses to both these agonists were expressed as a percentage of the KPSS response.

Data are presented as mean ± standard error mean (s.e.mean) and analysed by Student's *t* test, where $P < 0.05$ is used as the criterion for statistical significance.

Drugs

Drugs used were (−)-noradrenaline bitartrate (Arterenol; Sigma), 5-hydroxytryptamine creatinine sulphate complex (Serotonin; Sigma), angiotensin II (Hypertensin; Ciba-Geigy), endothelin-1 (Sigma), indomethacin (Sigma), acetylcholine bromide (Upjohn) and sodium nitroprusside dihydrate (Nipride; Roche). Stock solutions of all drugs (with the exception of indomethacin) were made up on the day of study and diluted to the appropriate concentration in milli-Q distilled water. Indomethacin was dissolved in 0.1 M Na_2CO_3. All drugs were stored on ice until ready for use.

Results

Skin resistance arteries

The smallest viable vessel was obtained from each subject. Vessel internal diameter at L_{100} averaged 183.7 ± 10.3 μm ($n = 7$) in the maxEPA group and 182.6 ± 19.8 μm ($n = 7$) in the placebo group. The one-point contraction response to a single concentration of potassium (124 mM) obtained at the beginning of each experiment was unaffected by maxEPA (maxEPA vs placebo (mN): 3.01 ± 0.75 vs 2.45 ± 0.36, $P > 0.05$).

Subcutaneous arteries from subjects fed marine oils demonstrated an increased sensitivity to angiotensin II compared with subjects on placebo capsule (maxEPA vs placebo (− log EC_{50} M): − 8.36 ± 0.18 vs − 7.91 ± 0.14; $P < 0.05$; Figure 1). The − log EC_{50} values to noradrenaline and 5-HT and − log IC_{50} values to acetylcholine, substance P and SNP were not affected by dietary supplementation with marine oils. MaxEPA had no effect on the maximal responses obtained to any of the agonists used (see Table 2).

Contractile responses to calcium increased with increasing concentration. Dietary supplementation with maxEPA had no effect on either the − log EC_{50} value or maximal contractile response to calcium (Table 2).

Forearm veins

Two viable rings were obtained from all but one (where only one ring was viable) subject. Vessel internal diameter at L_{20} averaged 3.06 ± 0.23 mm ($n = 7$) in the maxEPA group and 2.96 ± 0.89 mm ($n = 6$) in the placebo group. The one-point contraction response (per diameter) to a single concentration of potassium (124 mM) obtained at the beginning of each experiment was unaffected by maxEPA (maxEPA vs placebo ($g\ mm^{-1}$): 1.58 ± 0.27 vs 1.46 ± 0.40).

The responses to noradrenaline (maxEPA vs placebo (− log EC_{50}): − 7.26 ± 0.27 vs − 7.75 ± 0.19) were not affected by dietary enrichment with marine oils. Similarly, maxEPA had no effect on the potency or maximal response

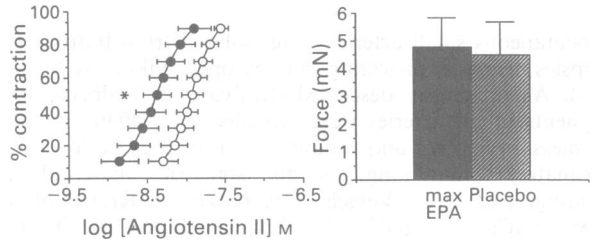

Figure 1 Concentration-contraction curves for angiotensin II in subcutaneous small arteries of maxEPA treated subjects (●, $n = 7$) compared with arteries from the placebo group (○, $n = 7$). Histograms represent the maximum contractions (force mN) ± s.e.mean, to angiotensin II for each group. These values was taken to be 100% to normalize the concentration-contraction curves shown at left. Horizontal error bars are ± s.e.mean at the EC_{50} value.

Table 2 Effect of maxEPA on potency and maximal responses of the vasoactive agents used on isolated subcutaneous small arteries

	Placebo		*MaxEPA*	
	Potency	E_{max}	*Potency*	E_{max}
	Contracting agents			
Agonists	EC_{50} *(− log M)*	*mN*	EC_{50} *(− log M)*	*mN*
Angiotensin II	7.91 ± 0.14	4.79 ± 0.94	8.36 ± 0.18*	4.55 ± 1.12
Noradrenaline	6.60 ± 0.35	5.86 ± 0.92	7.20 ± 0.20	5.86 ± 0.92
5-Hydroxytryptamine	6.77 ± 0.54	3.02 ± 1.75	6.99 ± 0.21	2.73 ± 1.12
Calcium	3.36 ± 0.37	3.00 ± 0.59	3.39 ± 0.10	4.02 ± 1.56
	Relaxing agents			
	IC_{50} *(− log M)*	*Maximum dilatation (%)*	IC_{50} *(− log M)*	*Maximum dilatation (%)*
Acetylcholine	7.10 ± 0.33	78.1 ± 10.4	7.50 ± 0.21	69.3 ± 15.3
Substance P	9.11 ± 0.14	87.7 ± 4.33	9.33 ± 0.08	73.5 ± 12.2
Sodium nitroprusside	7.27 ± 0.45	95.7 ± 1.60	7.19 ± 0.24	98.3 ± 1.11

E_{max} is the maximum contraction (mN) or maximum relaxation expressed as a percentage of the precontracted force to noradrenaline (0.3–3 μM). *$P < 0.05$ (Student's *t* test).

Table 3 Effect of maxEPA on potency (− log M) and maximal responses (g mm^{-1}) of noradrenaline and 5-hydroxytryptamine and on threshold concentrations (− log M) of angiotensin II and endothelin-1 in the absence and presence of indomethacin on human isolated fore-arm veins

	Placebo		*MaxEPA*	
Agonist	EC_{50} (− log M)	E_{max} (g mm^{-1})	EC_{50} (− log M)	E_{max} (g mm^{-1})
Noradrenaline	7.75 ± 0.19	1.92 ± 0.11	7.26 ± 0.27	2.42 ± 0.46
with indomethacin	7.31 ± 0.16	1.90 ± 0.13	7.32 ± 0.35	2.36 ± 0.38
5-Hydroxytryptamine	7.52 ± 0.17	2.34 ± 0.30	7.61 ± 0.12	2.76 ± 0.43
with indomethacin	7.32 ± 0.15	2.19 ± 0.22	7.45 ± 0.14	2.66 ± 0.42

	Threshold concentrations (− log M)	
	Placebo	*MaxEPA*
Noradrenaline	9.17 ± 0.40	8.50 ± 0.34
with indomethacin	8.75 ± 0.34	8.50 ± 0.39
5-Hydroxytryptamine	9.30 ± 0.54	8.57 ± 0.32
with indomethecin	8.90 ± 0.80	8.14 ± 0.18
Angiotensin II	9.00 ± 0.27	9.00 ± 0.33
with indomethacin	8.75 ± 0.14	9.42 ± 0.33
Endothelin-1	9.13 ± 0.47	9.33 ± 0.25
with indomethacin	9.88 ± 0.55	8.92 ± 0.15

E_{max} is the maximum contraction (g) per vessel diameter (mm) induced by the agonist.

induced by 5-HT (Table 3) or the threshold concentrations of angiotensin II or endothelin 1 (Table 3). Indomethacin did not alter the sensitivity of any of the agonists used in veins either from maxEPA or placebo fed subjects. The time-control experiments confirmed the stability of the preparation over the period of the experiment (data not shown).

Discussion

The major finding of the present study was that maxEPA supplementation failed to attenuate vascular reactivity *in vitro*. This is in marked contrast to findings from *in vivo* studies of forearm resistance arteries using identical marine oil and mixed oil placebo regimens (Chin *et al.*, 1993a,b). The difference between effects *in vivo* and *in vitro* were most pronounced with angiotensin II where an enhanced response was observed *in vitro*. This effect was selective for angiotensin II and was not apparent in veins isolated from the forearm.

The failure of marine oil supplementation to influence vascular responses *in vitro* is unlikely to be due to insufficient dosing of maxEPA since we previously demonstrated that this dose regimen of maxEPA is sufficient to produce an effect on vascular reactivity *in vivo* (Chin *et al.*, 1993a) and since an influence on the responses to angiotensin II was apparent in the present study. It is also unlikely to be due to tissue specificity as a general absence of effect was found in both subcutaneous arteries as well as forearm veins. The latter finding is particularly significant since these vessels were from the upper extremity, where the *in vivo* studies were conducted. We conclude therefore that dietary supplementation with marine oils most probably affects vascular reactivity *in vivo* by modifying circulating factors, possibly thromboxane A_2 of platelet origin since it is well documented that thromboxane A_3 is produced, at the expense of thromboxane A_2, following marine oil supplementation (Terano *et al.*, 1983; Yoshimura *et al.*, 1987). Furthermore, the *in vivo* effect of marine oil on vascular reactivity can be abolished by indomethacin (Chin *et al.*, 1993b). Once vessels were removed from their *in vivo* environment, the effect of marine oils was no longer apparent.

This theory is supported by the findings of Howe *et al.* (1992) who observed that vascular tone in the rat unstimulated *in situ* blood-perfused mesenteric preparation was significantly lower in rats fed fish oil. This was, however, not observed in their isolated buffer-perfused preparation (Head *et al.*, 1991), again raising the possibility that fish oil may be acting by affecting a blood-borne vasoactive substance such as TxA_2. Our conclusion is further supported by the lack of effect of indomethacin in the isolated vein preparations and the ensuing lack of effect of marine oils. The failure of indomethacin to influence responses obtained to the agonists used would suggest that locally generated cyclo-oxygenase metabolites do not play a major role in the modulation of responses in this preparation. It follows then that if marine oils were acting via the cyclo-oxygenase pathway (Chin *et al.*, 1993b) that it would have no effect on a preparation in which this pathway is of little importance. Not shown in this paper were preliminary experiments performed on subcutaneous resistance arteries isolated from skin biopsies obtained from two subjects treated with maxEPA capsules as described above and in addition, given indomethacin orally, 25 mg three times a day, on days 27 and 28. Four vessels (2 from each subject, average diameter 233.3 ± 30.65 μm) were obtained and a similar protocol to the one described above for subcutaneous arteries was followed in these preparations. Mean − log EC_{50} value for angiotensin II was 8.33 ± 0.18 M, a value not significantly different from that obtained for the maxEPA treated group, suggesting that the enhanced sensitivity to angiotensin following maxEPA supplementation is not indomethacin-sensitive. Responses to noradrenaline, 5-HT, sodium nitroprusside, acetylcholine, substance P and calcium were not significantly different compared with arteries from either placebo or maxEPA treated subjects, although this may reflect the small number of preparations in this group of experiments. In contrast, there are reports of a pronounced blunting effect in vessels isolated from animal models fed marine oils (Juan & Sametz, 1986; Yin *et al.*, 1989; 1990) and vascular prostacyclin has been shown to increase significantly (13.8 vs 8.6 ng g^{-1} saphenous vein) in patients receiving 4.3 g per day EPA and DHA capsules 28 days before coronary artery bypass surgery (DeCaterina *et al.*, 1989).

An unexpected finding from this study was the enhanced response to angiotensin II observed in subcutaneous resistance arteries studied *in vitro*. This finding was not observed in veins isolated from the forearms of subjects fed marine oils and conflicts with our original findings where a diminished response to angiotensin II was seen in *in vivo* forearm resistance arteries (Chin *et al.*, 1993). This increase in sensitivity appears to be selective for angiotensin II as responses to noradrenaline and histamine were not affected by marine oils, and was not due to alterations in Ca^{2+} influx into the vascular smooth muscle cell. As described above, this effect

of maxEPA is not indomethacin-sensitive and is thus unlikely to be due to changes in prostanoid profile. An unexplored possibility is that the enhanced sensitivity to angiotensin II observed in arteries from volunteers fed maxEPA is a result of changes in metabolism of angiotensin II.

In contrast to studies performed in arteries isolated from rats fed marine oils (Yin *et al.*, 1988; 1990) we found no effect of marine oils on vasodilator responses to the endothelium-dependent agonists, acetylcholine and substance P, in the subcutaneous arteries. The lack of effect of marine oils on endothelial cell function was consistent with our previous report that responses to acetylcholine in the *in vivo* forearm resistance arteries were unaffected by dietary enrichment with marine oils (Chin *et al.*, 1993b). From this we conclude that maxEPA does not modify endothelial function in healthy adults.

The effect of fish oils on calcium-mediated contractions and to a lesser extent on potassium-mediated contractions was also explored in the current study. Incorporation of EPA and DHA into platelet membrane following maxEPA at the dose given has previously been demonstrated (Chin *et al.*, 1993a). It is conceivable that a similar incorporation into vascular membrane might occur, changing the biophysical properties of the membrane and perhaps its function. Furthermore, marine oils have been reported to decrease calcium influx into neonatal myocytes following ouabain-induced toxicity (Hallaq & Leaf, 1992). An extension of this potential effect of marine oils on vascular smooth muscle could explain the changes in vascular reactivity observed. Although the concentration-response curve constructed to calcium does not give insight into intracellular calcium movements, it does provide a means by which calcium influx can be assessed. MaxEPA 10 g per day for 28 days did not modify either calcium or potassium responses in subcutaneous small arteries suggesting that any calcium blocking effects of maxEPA were not present.

In summary, the vascular reactivity of arteries and veins isolated from subjects fed marine oils were examined in this study. Dietary supplementation with marine oils had no effect on the potency or maximal response obtained to the vasoconstrictors noradrenaline, 5-HT and calcium or on the responses to the endothelium-dependent vasodilators, acetylcholine and substance P and the endothelium-independent vasodilator, sodium nitroprusside in subcutaneous resistance arteries. Sensitivity to angiotensin II was, on the other hand, enhanced in subcutaneous arteries isolated from subjects fed marine oils. Neither potency nor maximal response to the vasonconstrictors noradrenaline, 5-HT, angiotensin II and endothelin-1 were altered in veins isolated from subjects fed marine oils compared to those from subjects fed placebo capsules. Indomethacin had no effect on any of the agonists used in this preparation. These findings are consistent with the suggestion that dietary supplementation with marine oils affects vascular reactivity *in vivo* through changes in circulating prostanoids. The observation that maxEPA enhances the potency of angiotensin II in human isolated subcutaneous resistance arteries is novel and warrants further investigation.

This project was funded by an NHMRC institute grant awarded to the Baker Medical Research Institute. The authors would also like to acknowledge the generous support of R.P. Scherer Holdings Pty Ltd for donation of the maxEPA and mixed oil placebo capsules.

References

BURR, M.L., GILBERT, J.F., HOLLIDAY, R.M., ELWOOD, P.C., FEHILY, A.M., ROGERS, S., SWEETNAM, P.M. & DEADMAN, N.M. (1989). Effects of changes in fat, fish and fibre intakes on death and myocardial infarction: diet and reinfarction trial (DART). *Lancet*, **ii**, 757–761.

CHIN, J.P.F., GUST, A.P., NESTEL, P.J. & DART, A.M. (1993a). Marine oils dose-dependently inhibit vasoconstriction of forearm resistance arteries in man. *Hypertension*, **21**, 22–28.

CHIN, J.P.F., GUST, A.P. & DART, A.M. (1993b). Indomethacin inhibits the effects of dietary supplementation with marine oils on vasoconstriction of human forearm resistance vessels in vivo. *J. Hypertens.*, **11**, 1229–1234.

DART, A.M., CHIN, J.P.F. & ESLER, M.D. (1994). Effects of dietary supplementation with n-3 polyunsaturated fatty acids on sympathetic and haemodynamic responses to stress in man. *Nutr. Metab. Cardiovasc. Dis.* (in press).

DE CATERINA, R., GIANNESSI, D., MAZZONE, A., BERNINI, W., LAZZERNI, G., MAFFEI, S., CERRI, M., SALVATORE, L. & WEKSLER, B. (1990). Vascular prostacyclin is increased in patients ingesting ω-3 polyunsaturated fatty acids before coronary artery bypass graft surgery. *Circulation*, **82**, 428–438.

HALLAQ, H.A. & LEAF, A. (1992). Stabilization of cardiac arrhythmias by N-3 PUFS. *Third International Congress on Essential Fatty Acids and Eicosanoids* (Abstracts). Convenors: Gibson, R. & Sinclair, A. p. 54.

HEAD, R.J., MANO, M.T., BEXIS, S., HOWE, P.R.C. & SMITH, R.M. (1991). Dietary fish oil administration retards the development of hypertension and influences vascular neuroeffector function in the stroke prone spontaneously hypertensive rat (SHRSP). *Prostaglandin, Leukotrienes and Essential Fatty Acids*, **44**, 119–122.

HOWE, P.R.C., LUNGERSHAUSEN, Y.K., BEXIS, S., MANO, M.T. & HEAD, R.J. (1992). Effects of fish oil on blood pressure and vascular reactivity-variations between strains of genetically hypertensive rats. *Third International Congress on Essential Fatty Acids and Eicosanoids* (Abstracts), Convenors: Gibson, D. & Sinclair, A. p 212.

JUAN, H. & SAMETZ, W. (1986). Vasoconstriction induced by norepinephrine and angiotensin II is antagonized by eicosapentaenoic acid independent of formation of trienoic eicosanoids. *Naunyn-Schmied. Arch. Pharmacol.*, **332**, 288–292.

KNAPP, H.R. & FITZGERALD, G.A. (1989). The antihypertensive effects of fish oil: a controlled study of polyunsaturated fatty acid supplements in essential hypertension. *New Engl. J. Med.*, **32**, 1037–1043.

MULVANY, M.J. & HALPERN, W. (1977). Contractile properties of small resistance vessels in spontaneously hypertensive rats. *Circ. Res.*, **41**, 19–26.

MULVANY, M.J. & WARSHAW, D.M. (1979). The active tension-length curve of vascular smooth muscle-related to its cellular components. *J. Gen. Physiol.*, **74**, 85–104.

NAKASHIMA, A., ANGUS, J.A. & JOHNSTON, C.I. (1982). Comparison of angiotensin converting enzyme inhibitors captopril and MK421-diacid in guinea pig atria. *Eur. J. Pharmacol.*, **81**, 487–492.

NESTEL, P.J. (1990). Effects of n-3 fatty acids on lipid metabolism. *Annu. Rev. Nutr.*, **10**, 149–167.

SHIMOKAWA, H. & VANHOUTTE, P.M. (1989). Dietary ω3 fatty acids and endothelium-dependent relaxations in porcine coronary arteries. *Am. J. Physiol.*, **256**, H969–H973.

SUDHIR, K., ANGUS, J.A., ESLER, M.D., JENNINGS, G.L., LAMBERT, G.W. & KORNER, P.I. (1990). Altered venous responses to vasonconstrictor agonists and nerve stimulation in human primary hypertension. *J. Hypertens.*, **8**, 1119–1128.

TERANO, T., HIRAI, A., HAMAZAKI, T., KOBAYASHI, S., FUJITA, T., TAMURA, Y. & KUMAGAI, A. (1983). Effect of oral administration of highly purified eicosapentaenoic acid on platelet function, blood viscosity and red cell deformability in healthy human subjects. *Atherosclerosis*, **46**, 321–331.

YIN, K., CHU, Z.M. & BEILIN, L.J. (1990). Effect of fish oil feeding on blood pressure and vascular reactivity in spontaneously hypertensive rats. *Clin. Exp. Pharmacol. Physiol.*, **17**, 235–239.

YIN, K., CHU, Z.M. & BEILIN, L.J. (1991). Effect of fish oil feeding on blood pressure and vascular reactivity in spontaneously hypertensive rats. *Clin. Exp. Pharmacol. Physiol.*, **17**, 235–239.

YIN, K., CROFT, K.D. & BEILIN, L. (1988). Effects of pure EPA feeding on blood pressure and vascular reactivity in spontaneously hypertensive rats. *Clin. Exp. Pharmacol. Physiol.*, **15**, 275–280.

YOSHIMURA, T., MATSUI, K., ITO, M., YUNOHARA, T., KAWASAKI, N. & NAKAMURA, T. (1987). Effects of highly purified eicosapentaenoic acid on plasma beta thromboglobulin level and vascular reactivity to angiotensin II. *Artery*, **14**, 295–303.

(Received December 21, 1993
Accepted February 2, 1994)

Br. J. Pharmacol. (1994), **112**, 571–575

Stimulation by menthol of Cl secretion via a Ca^{2+}-dependent mechanism in canine airway epithelium

[1]A. Chiyotani, J. Tamaoki, S. Takeuchi, M. Kondo, K. Isono & K. Konno

First Department of Medicine, Tokyo Women's Medical College, 8-1 Kawada-cho, Shinjuku, Tokyo 162, Japan

1 To investigate the effect of menthol on airway epithelial ion transport function, we studied the bioelectrical properties of canine cultured tracheal epithelium by Ussing's short-circuit technique *in vitro*.

2 Addition of menthol (10^{-3} M) to the mucosal but not the submucosal solution increased the short-circuit current (I_{sc}) from 6.2 ± 0.9 to 14.0 ± 2.2 μA cm^{-2} ($P < 0.001$), and this effect was accompanied by increases in transepithelial potential difference and conductance. The response was dose-dependent, with the maximal increase from the baseline value and the concentration required to produce a half-maximal effect (EC_{50}) being 6.4 ± 0.9 μA cm^{-2} ($P < 0.001$) and 40 μM, respectively.

3 Other cyclic alcohols, including menthone and cyclohexanol, had no effect on the electrical properties.

4 The menthol-induced increase in I_{sc} was not altered by pretreatment of the cells with amiloride, indomethacin, or propranolol but was abolished by diphenylamine-2-carboxylate, furosemide or substitution of Cl with iodide in the medium.

5 Menthol (10^{-3} M) increased cytosolic levels of free calcium ([Ca^{2+}]i) from 98 ± 12 to 340 ± 49 nM ($P < 0.01$) in fura-2-loaded tracheal epithelium but did not affect the intracellular adenosine 3',5'-cyclic monophosphate content.

6 These results suggest that menthol stimulates Cl secretion across airway epithelium, probably through a Ca^{2+}-dependent mechanism, and might thus influence mucociliary transport in the respiratory tract.

Keywords: Menthol; airway epithelium; ion transport; calcium; mucociliary transport

Introduction

Airway epithelial cells play an important role in the regulation of mucociliary transport, which seems to be dependent on ciliary beating, the rheological properties of airway surface fluid, and mucus production (Wanner, 1977). It is known that the amount and the rheological properties of airway surface fluid can be influenced by the ion transport function of the airway epithelium. In particular, the electrochemical potential gradient produced by secretion of Cl towards, and absorption of Na from, the airway lumen may promote the subsequent water secretion and absorption, respectively, across the airway mucosa (Welsh *et al.*, 1980).

Menthol, a cyclic alcohol which is appreciated because it produces a cooling sensation, has been widely used as a component of food and drink, tobacco, cosmetics, etc. It has been reported that menthol increases the sensitivity of cutaneous cold receptors by modulating Ca^{2+} currents of neuronal membranes (Schäfer *et al.*, 1986; Swandulla *et al.*, 1986), and that peppermint oil, of which menthol is a major constituent, improves the symptoms of irritable bowel syndrome through a direct action on intestinal smooth muscle (Rees *et al.*, 1979; Taylor *et al.*, 1984). Although there are many ways in which inhaled menthol vapour can contact the surface of the respiratory mucosa, its action on airway epithelial function is unknown. Therefore, to elucidate the effect of menthol on epithelial ion transport and its mechanism of action, we studied the biolectric properties of canine cultured tracheal epithelium under short-circuit conditions *in vitro*.

Methods

Preparation of epithelium

Mongrel dogs of either sex weighing 21 to 38 kg were anaesthetized with intravenous pentobarbitone sodium (35 mg kg^{-1}), and the trachea was removed. After dissection of submucosal tissue and blood vessels, the resected tissues were placed in fresh medium containing Dulbecco's modified Eagle's medium (DMEM) and Ham's nutrient F-12 (1:1) with 0.05% protease type XIV (Sigma Chemical Co., St. Louis, Missouri, U.S.A.), and maintained at 4°C for 24 h. After mild agitation, the tissue sections were removed from the medium and cells were concentrated by centrifugation (1000 *g*, 10 min). The cell pellets were washed with medium containing 5% foetal calf serum to neutralize the protease. These cells were suspended in the mixture of DMEM and Ham's F-12 containing 5% foetal calf serum, 100 u ml^{-1} each of penicillin and streptomycin, 100 μg ml^{-1} gentamicin, 10 μg ml^{-1} insulin, 5 μg ml^{-1} transferrin, 25 ng ml^{-1} epidermal growth factor, and 7.5 μg ml^{-1} endothelial cell growth supplement. Our preliminary studies showed that this preparation of cells was composed of 98–99% epithelial cells and 1–2% fibroblasts and other nonepithelial cells, and the viability was between 86 and 97%, as assessed by trypan blue exclusion. The cells were then seeded at a density of 1.5×10^6 cm^{-2} using 1 ml of medium per Linbro tissue culture multiwell plate (15 mm diameter, 18 mm deep, Flow Lab Inc., McLean, Virginia, U.S.A.), and grown on nuclepore polycarbonate filters (13 mm diameter, 0.45 μm pore size) at 37°C in a CO_2 incubator (95% air:5% CO_2). The medium was changed every 24 h and on the 10th day of incubation, the cells became confluent and were used for measurement of bioelectric properties. Observation of cultured cells by transmission electron microscopy revealed that typical tight junctions separated two distinct membranes: the membrane facing the overlying medium contained microvilli and glycocalyx, while the membrane facing the filter surface was relatively unspecialized. These cells were not ciliated and did not contain goblet cells but maintained the electrical properties resembling those of the native tissue (Al-Bazzaz & Cheng, 1979).

[1] Author for correspondence.

Measurement of electrical properties

The short-circuit technique for measuring electrical properties of cultured epithelium has been described previously (Coleman *et al.*, 1984). Briefly, the filter on which tracheal epithelial cells were grown was mounted between Ussing chambers (0.5 cm^2 surface area) and bathed with Krebs-Henseleit solution of the following composition (in mM): Na 143.9, K 5.6, Ca 1.9, Mg 1.2, Cl 117.6, HCO_3 25.0, acetate 5.6, gluconate 3.8, H_2PO_4 1.3, SO_4 1.2 and glucose 5.6, oxygenated with 95% O_2:5% CO_2 and maintained at 37°C. Transepithelial potential difference (PD) was measured with two polyethylene bridges containing 3% agar in 1 M KCl, positioned within 1 mm of each side of the epithelial surface and connected to calomel electrodes (model 2080A-06T, Horiba Ltd, Tokyo, Japan) and a high-impedance voltmeter (model CEZ-9100, Nihon Kohden). Another pair of polyethylene bridges (3% agar in saline), positioned 10 mm from the orifice and connected to Ag/AgCl wires, was used to pass sufficient current through both the chamber and cells to bring the PD to zero. This short-circuit current (I_{sc}) was automatically corrected for solution resistance between the PD-detecting bridges, and recorded continuously on a pen recorder (model SR6335, Graphtec, Tokyo) except for 5 s every 3 min when the voltage clamp was turned off and the PD was recorded.

Tissue conductance (G) was calculated by dividing the measured I_{sc} per surface area by the PD. After a 20 min equilibration of cells when the PD did not vary by more than 0.2 $\mu A\ cm^{-2}$ in any 5-min intervals, cyclic alcohols including menthol, menthone and cyclohexanol (10^{-3} M) were added to either the mucosal or submucosal solution in the chamber. To assess the concentration-dependent relationship between menthol and I_{sc}, menthol was cumulatively added from 10^{-6} to 10^{-3} M in half-molar increments, during which the highest I_{sc} value recorded at each concentration was determined.

To assess whether the responses of I_{sc} were derived from Na absorption and/or Cl secretion by the epithelium, cells were pretreated for 30 min with each of the following: mucosal amiloride (10^{-4} M), a Na channel blocker (Al-Bazzaz & Zevin, 1984); mucosal diphenylamine-2-carboxylate (10^{-4} M), a Cl channel blocker (DiStefano *et al.*, 1986); submucosal furosemide (10^{-4} M), an inhibitor of the Na/K/2Cl cotransporter (Widdicombe *et al.*, 1983); or Cl-free medium on both sides in which Cl was substituted with iodide, which cannot be transported across the canine tracheal epithelium (Widdicombe & Welsh, 1980). Menthol (10^{-3} M) was then added to the chamber and the I_{sc} responses were compared with those of cells without pretreatment. To test possible involvement of prostaglandin synthesis or β-adrenoceptor activation in the action of menthol, we also examined the effects of pretreatment of cells with indomethacin (10^{-5} M) and propranolol (10^{-5} M).

Measurement of intracellular adenosine 3',5'-cyclic monophosphate (cyclic AMP)

We measured intracellular cyclic AMP levels, one of the important determinants for ion transport function (Welsh, 1987). The tracheal epithelial cells were incubated in the chambers, and menthol, menthone and cyclohexanol (10^{-3} M) were each added to the mucosal solution. For a positive control experiment, isoprenaline (10^{-6} M) was added to the submucosal solution. After 20 min, epithelia were removed from the chambers, and sonicated in a bath-type sonicator in ice-cold 10% trichloroacetic acid. After the extraction of trichloroacetic acid with ether, the residue was dissolved in acetate buffer. The cyclic AMP levels were determined in duplicate by a radioimmunoassay method (Brooker *et al.*, 1979), normalized for the protein content of the cells as determined by the method of Lowry *et al.* (1951), with bovine serum albumin as a standard, and corrected for the percentage recovery of [^{125}I]-cyclic AMP added as a tracer.

Measurement of $[Ca^{2+}]i$

Canine tracheal epithelial cells were cultured on round coverslips (15 mm diameter, Matsunami Ltd., Tokyo) coated with human placental collagen (20 $\mu g\ cm^{-2}$). After confluence was achieved, the coverslip was washed with Hank's balanced salt solution containing 10 mM N-2-hydroxyethylpiperazine-N'-2-ethanesulphonic acid (HEPES) at pH 7.4 and loaded with 2×10^{-6} M acetoxymethyl ester of fura-2 (fura 2-AM, Dojin Lab, Kumamoto, Japan) for 20 min at 37°C. After washing, the coverslip was held with a rigid holder in a continuously stirred cuvette containing HEPES-buffered Hank's solution maintained at 37°C, and the fluorescence intensity was measured by a spectrophotometer (model CAF-100, Japan Spectroscopic Co., Tokyo). Excitation at 340 and 380 nm was automatically exchanged at a rate of 50 Hz, and the emitted light from cells was detected by a photomultiplier tube through a 500 nm filter.

Maximal (R_{max}) and minimal (R_{min}) values for the ratio were determined in the presence of ionomycin (10^{-5} M) and ethylene glycol *bis* (β-amino-ethyl ether)-N,N,N',N'-tetra-acetic acid (EGTA, 5×10^{-3} M), and $[Ca^{2+}]_i$ values were calculated by the formula described by Grynkiewicz *et al.* (1985).

Drugs

The following drugs were used: menthol (2-isopropyl-5-cyclohexanol), amiloride, furosemide, indomethacin, (±)-propranolol, ionomycin, EGTA (Sigma Chemical Co.), diphenylamine-2-carboxylate, menthone, and cyclohexanol (Nacalai Tesque, Kyoto, Japan). Menthol was dissolved in dimethylsulphoxide (DMSO) and subsequently diluted in Krebs-Henseleit solution. The highest final concentration of DMSO in the Ussing chamber was 0.1%. Menthone and cyclohexanol were diluted in Krebs-Henseleit solution. Our preliminary studies showed that the vehicle (diluted DMSO) had no effect on the electrical properties of canine cultured tracheal epithelium.

Statistics

All values are expressed as means ± s.e.mean. Statistics analysis was performed by ANOVA or Newman-Keul multiple comparison test, and a P value of less than 0.05 was considered significant.

Results

Electrical properties

Addition of menthol (10^{-3} M) to the mucosal solution elicited an increase in I_{sc} of canine cultured tracheal epithelium, which peaked within 10 min (6.2 ± 0.9 to 14.0 ± 2.2 $\mu A\ cm^{-2}$, $P < 0.001$, $n = 9$) and remained elevated during the 30 min observation period (Figure 1). This menthol-induced increase in I_{sc} was accompanied by corresponding increases in PD and G ($P < 0.01$ and $P < 0.05$, respectively, $n = 9$) (Table 1). In contrast, submucosal addition of menthol did not alter these electrical properties. Menthone and cyclohexanol (10^{-3} M) when added to either the mucosal or submucosal solution had no effect on I_{sc} (Figure 1).

Cumulative addition of menthol to the mucosal solution increased I_{sc} in a concentration-dependent manner (Figure 2). The maximal increase from the baseline value (ΔI_{scmax}) and the concentration required to produce a half-maximal effect (EC_{50}) were 6.4 ± 0.9 $\mu A\ cm^{-2}$ ($P < 0.001$, $n = 10$) and 40 μM, respectively. The change of I_{sc} in response to the submucosal menthol did not reach a significant level.

Incubation of cells with amiloride, diphenylamine-2-carboxylate, furosemide and Cl-free medium *per se* decreased

Table 1 Effect of menthol on bioelectric properties of canine cultured tracheal epithelium

	Mucosal			*Submucosal*		
	Before	*After*	*Significance*	*Before*	*After*	*Significance*
I_{sc} ($\mu A\ cm^{-2}$)	6.2 ± 0.9	14.0 ± 2.2	$P<0.001$	6.8 ± 0.7	7.3 ± 0.7	NS
PD (mV)	2.2 ± 0.4	3.9 ± 0.4	$P<0.01$	2.3 ± 0.3	2.7 ± 0.4	NS
G ($mS\ cm^{-2}$)	2.8 ± 0.3	3.6 ± 0.4	$P<0.05$	2.9 ± 0.4	2.3 ± 0.3	NS

Definitions of abbreviations: I_{sc}, short-circuit current; PD, transepithelial potential difference; G, conductance; NS, not significant. Menthol (10^{-3} M) was added to either the mucosal or the submucosal solution of the Ussing chamber. Values are means ± s.e.; $n = 9$.

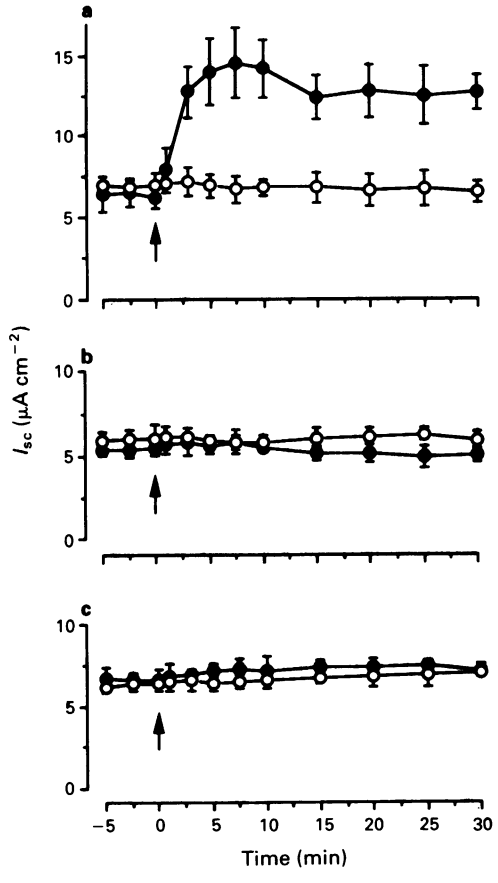

Figure 1 Time-course of the effects of menthol (10^{-3} M, a), menthone (10^{-3} M, b), and cyclohexanol (10^{-3} M, c) on short-circuit current (I_{sc}) of canine cultured tracheal epithelial cells. After establishing the baseline I_{sc}, each drug was added at time 0 (arrow) to either the mucosal (●) or submucosal solution (○) of the Ussing chamber. Each point represents the mean (with s.e.mean) of 9 experiments.

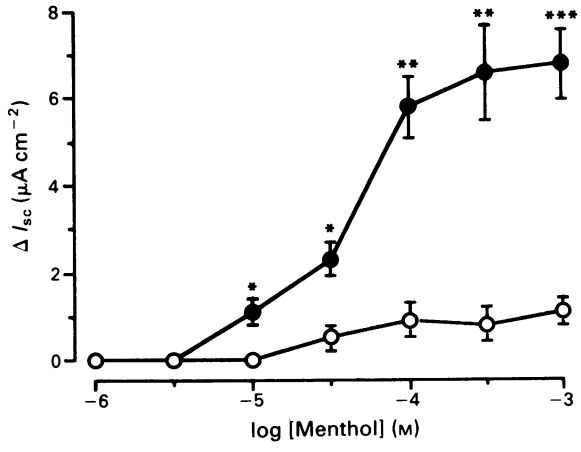

Figure 2 Concentration-dependent effect of menthol on short-circuit current (I_{sc}) of canine cultured tracheal epithelium. Menthol was added to either the mucosal (●) or submucosal (○) solution. Responses are expressed as the increase in I_{sc} (ΔIsc) from the baseline values obtained before the addition of menthol. Each point represents the mean (with s.e.mean) of 10 experiments. $*P<0.05$; $**P<0.01$; $***P<0.001$, significantly different from the baseline I_{sc}.

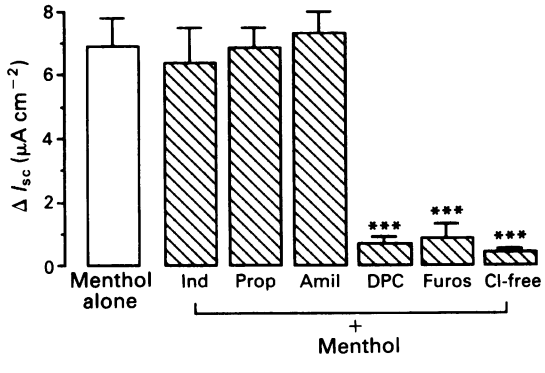

Figure 3 Effects of indomethacin (Ind, 10^{-5} M), propranolol (Prop, 10^{-5} M), amiloride (Amil, 10^{-4} M), diphenylamine-2-carboxylate (DPC, 10^{-4} M), furosemide (Furos, 10^{-4} M), and substitution of Cl in the bathing medium with iodide (Cl-free) on the increase in short-circuit current (ΔIsc) induced by mucosal addition of menthol (10^{-3} M) in canine cultured tracheal epithelial cells. Data are means (with s.e.mean) of 7 experiments. $***P<0.001$, significantly different from the response to menthol alone.

baseline I_{sc} of 3.5–9.4 $\mu A\ cm^{-2}$ by 1.9 ± 0.3, 4.2 ± 0.5, 3.7 ± 0.4 and 5.5 ± 0.4 $\mu A\ cm^{-2}$, respectively ($n = 7$, in each case). The increase in I_{sc} induced by the subsequent addition of menthol (10^{-3} M) to the mucosal solution was not altered by amiloride but greatly attenuated by diphenylamine-2-carboxylate, furosemide, and Cl-free medium ($P<0.001$, $n = 7$) (Figure 3). Pretreatment of cells with indomethacin and propranolol had no effect on the I_{sc} response to menthol.

Intracellular cyclic AMP levels

Incubation of epithelial cells with menthol (10^{-3} M), menthone (10^{-3} M), or cyclohexanol (10^{-3} M) did not significantly alter intracellular cyclic AMP levels (Figure 4). As a positive control experiment, the β-adrenoceptor agonist isoprenaline (10^{-6} M) increased cyclic AMP levels from 3.6 ± 0.29 to 121.5 ± 16.0 pmol mg^{-1} protein ($P<0.01$, $n = 5$).

Intracellular Ca^{2+} concentration

As shown in Figure 5, addition of menthol (10^{-3} M) increased $[Ca^{2+}]_i$ in canine cultured tracheal epithelium from 98 ± 12 to 340 ± 49 nM ($P<0.01$, $n = 5$), whereas menthone (10^{-3} M) and cyclohexanol (10^{-3} M) had little effect. The menthol-induced $[Ca^{2+}]_i$ response reached a plateau within 3 min and remained elevated as long as the drug was present.

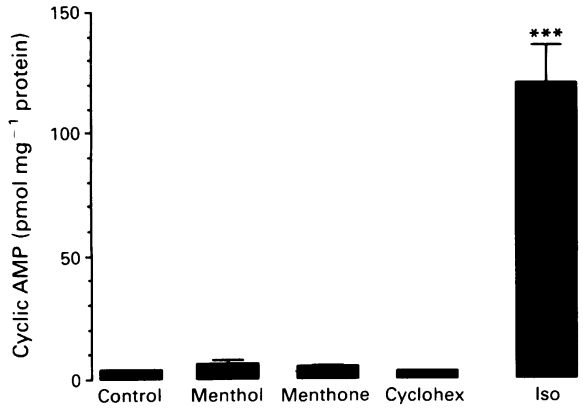

Figure 4 Effects of menthol, menthone and cyclohexanol (Cyclohex) at 10^{-3} M on cyclic AMP levels in canine tracheal epithelium. As a positive control, the effect of isoprenaline (Iso, 10^{-6} M) on cyclic AMP levels was assessed. Data are means (with s.e.mean) of 5 experiments. $***P<0.001$, significantly different from control tissues.

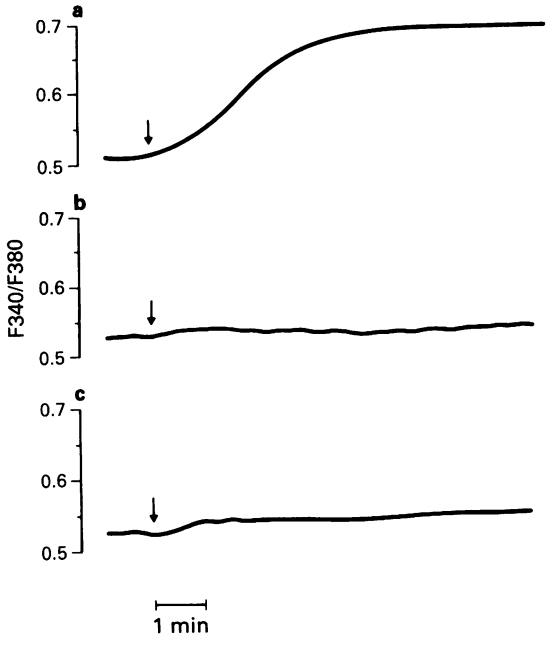

Figure 5 Typical recordings of fura-2 fluorescence ratios in canine tracheal epithelial cells exposed to menthol (a), menthone (b) and cyclohexanol (c) at 10^{-3} M, taken from 9–20 experiments. Immediately after the addition (arrows) of the compounds, menthol increased $[Ca^{2+}]_i$ whereas menthone and cyclohexanol had no effect.

Discussion

Our *in vitro* studies demonstrate that menthol alters the bioelectric properties of canine cultured tracheal epithelial cells. It is known that the alteration in the electrical properties of the airway epithelium is closely associated with functional changes of electrolyte transport across the cell consisting of Na absorption and Cl secretion (Boucher & Larsen, 1988). Although we did not measure ion fluxes directly in the present study, our results indicate that menthol may selectively stimulate the secretion of Cl across tracheal epithelial cells from the submucosal side toward the airway lumen. This conclusion is based on the following findings. First, menthol produced a concentration-dependent increase in I_{sc}, a bioelectric parameter that reflects net movement of actively transported ions (MacKnight *et al.*, 1980), and which was accompanied by increases in PD and G. Second, this increase in I_{sc} was not influenced by pretreatment of cells with amiloride, a Na channel blocker (Al-Bazzaz & Zevin, 1984), but was abolished by the Cl channel blocker, diphenylamine-2-carboxylate (DiStefano *et al.*, 1986), the inhibitor of the Na/K/2Cl cotransporter furosemide (Widdiscombe *et al.*, 1983), and the substitution of Cl in the medium with iodide, an anion that cannot be transported across the airway epithelium (Widdicombe & Welsh, 1980).

Because menthol is an alcohol, it could have acted on epithelial cells by inducing membrane labilization and/or modifying membrane fluidity due to its lipophilic properties (Grisham & Barnett, 1973; Haydon *et al.*, 1977). However, neither cyclohexanol, a highly lipid soluble cyclic alcohol from which menthol is derived, nor menthone, in which the hydroxy group of menthol is replaced with a keto group, produced any alteration in bioelectric properties, suggesting that the stimulation of Cl secretion may be specific for menthol. This specificity has also been reported in dihydropyridine-insensitive Ca^{2+} channels in human neuroblastoma cells (Sidell *et al.*, 1990).

In contrast to the responses to the mucosal addition of menthol, this drug did not alter the electrical properties of tracheal epithelium when it was added to the submucosal side. The reason for this difference is uncertain, but one possibility is that specific receptors for menthol could be located on the mucosal membrane rather than on the submucosal membrane of the epithelium.

It has been shown that activation of β-adrenoceptors can stimulate Cl secretion (Welsh, 1987) and that several agents stimulate Cl secretion through the synthesis and the release of cyclo-oxygenase products of arachidonic acid metabolism in canine tracheal mucosa (Eling *et al.*, 1986). To test the possible involvement of these mechanisms in the action of menthol, we examined the effects of the blockade of β-adrenoceptors and the cyclo-oxygenase pathway with propranolol and indomethacin, respectively. We found that the menthol-induced increase in I_{sc} was not reduced by these pharmacological blocking agents. Thus, the menthol-induced Cl secretion does not appear to be mediated by β-adrenoceptors or cyclo-oxygenase products.

Intracellular cyclic AMP and cytosolic Ca^{2+} are important second messengers regulating Cl secretion in the airway epithelium (Welsh, 1987). In the present study, cyclic AMP levels in tracheal epithelial cells were not changed by 10^{-3} M menthol, a concentration sufficient to increase epithelial I_{sc}. In contrast, the same concentration of menthol substantially increased $[Ca^{2+}]_i$ indicating that the effect of menthol on electrical properties may be associated with an increase in cytosolic free Ca^{2+}. In most cell types, a rapid transient increase and a sustained elevation of $[Ca^{2+}]_i$ may be derived from the Ca^{2+} release from intracellular stores and the Ca^{2+} influx from the extracellular solution, respectively (Williamson & Monck, 1989). Because the response of $[Ca^{2+}]_i$ to menthol was gradual and long-lasting, we speculate that it might be dependent on influx from the extracellular solution. To confirm this, further studies on $[Ca^{2+}]_i$ kinetics will be required.

In contrast to our findings, it has been reported that menthol does not stimulate but, instead, potently blocks Ca^{2+} currents through voltage-activated channels in cultured dorsal root ganglion cells from chick and rat embryos (Swandulla *et al.*, 1987), and that peppermint oil, of which menthol is a major constituent, improves some symptoms of irritable bowel syndrome (Swandulla *et al.*, 1986; Taylor *et al.*, 1984) probably through a mechanism involving Ca^{2+} antagonism (Hills & Aaronson, 1991). The reason for this contradictory action of menthol is uncertain, but it could be due to the difference in the cell types.

Active transport of Cl across the tracheal epithelium correlates to the movement of water toward the lumen (Welsh *et al.*, 1980). This water movement probably affects the depth of the periciliary sol layer of airway surface fluid and hydrates

airway mucus that interacts with ciliary function (Nadel *et al.*, 1985). Finally, it is appreciated that high concentrations of menthol are required to produce our observed effects but comparable concentrations are necessary in other systems (Swandulla *et al.*, 1986; Siddell *et al.*, 1990). Moreover, the concentration of menthol that may be achieved in the airways is unknown and it thus remains uncertain whether the drug may affect mucociliary transport function *in vivo*.

The authors thank Yoshimi Sugimura and Masayuki Shino for their technical assistance. This work was supported in part by a Grant for Scientific Research No. 04670476 from the Ministry of Education, Science and Culture, Japan.

References

AL-BAZZAZ, F.J. & CHENG, E. (1979). Effect of catecholamines on ion transport in dog tracheal epithelium. *Am. J. Physiol.*, **239,** C112–C117.

AL-BAZZAS, F.J. & ZEVIN, R. (1984). Ion transport and metabolic effects of amiloride in canine tracheal mucosa. *Lung*, **162,** 357–367.

BOUCHER, R.C. & LARSEN, E.H. (1988). Comparison of ion transport by cultured secretory and absorptive airway epithelia. *Am. J. Physiol.*, **254,** C535–C547.

BROOKER, G., HARPER, J.F., TERASAKI, W.L. & MOYLAN, R.D. (1979). Radioimmunoassay of cyclic AMP and cyclic GMP. *Adv. Cyclic Nucleotide Res.*, **10,** 1–33.

COLEMAN, D.L., TUET, I.K. & WIDDICOMBE, J.H. (1984). Electrical properties of dog tracheal epithelial cells grown in monolayer culture. *Am. J. Physiol.*, **246,** C355–C359.

DISTEFANO, A., WITTNER, M., SCHALATTER, E., LANG, F.J., ENGLERT, H. & GREGER, R. (1986). Diphenylamine-2-carboxylate, a blocker of the Cl^- conductive pathway in Cl-transporting epithelia. *Pflügers Arch.*, **405,** S95–S100.

ELING, T.E., DANILOWICZ, R.M., HENKE, D.C., SIVARAJAH, K., YANKASKAS, J.R. & BOUCHER, R.C. (1986). Arachidonic acid metabolism by canine tracheal epithelial cells: product formation and relationship to chloride secretion. *J. Biol. Chem.*, **261,** 12841–12849.

GRISHAM, C.M. & BARNETT, R.E. (1973). The effect of long chain alcohols on membrane lipids and the $(Na^+$-$K^+)$-ATPase. *Biochim. Biophys. Acta.*, **311,** 417–422.

GRYNKIEWICZ, G., POENIE, M. & TSIEN, R.Y. (1985). A new generation of Ca^{2+} indicators with greatly improved fluorescence properties. *J. Biol. Chem.*, **260,** 3440–3450.

HAYDON, D.A., HENDRY, B.M., LEVISON, S.R. & REQUENA, J. (1977). Anesthesia by the n-alkanes. A comparative study of nerve impulse blockage and the properties of black lipid bilayer membrane. *Biochim. Biophys. Acta*, **470,** 17–34.

HILLS, J.M. & AARONSON, P.I. (1991). The mechanism of action of peppermint oil on gastrointestinal smooth muscle. *Gastroenterology*, **101,** 55–65.

LOWRY, O.H., ROSENBROUGH, N.J., FARR, A.L. & RANDALL, R.J. (1951). Protein measurement with the Folin phenol reagent. *J. Biol. Chem.*, **193,** 265–275.

MACKNIGHT, A.D.C., DIBONA, D.R. & LEAF, A. (1980). Sodium transport across urinary bladder: a model 'Tight' epithelium. *Physiol. Rev.*, **60,** 615–715.

NADEL, J.A., WIDDICOMBE, J.H. & PEATFIELD, A.C. (1985). Regulation of airway secretions, ion transport, and water movement. In *Handbook of Physiology: The Respiratory Systems.* section 3, ed. Fishman, A.P. pp. 419–445. Bethesda: American Physiological Society.

REES, W.D.W., EVANS, B.K. & RHODES, J. (1979). Treating irritable bowel syndrome with peppermint oil. *Br. Med. J.*, **ii,** 835–836.

SCHÄFER, K., BRAUN, H.A. & ISENBERG, C. (1986). Effect of menthol on cold receptor activity. *J. Gen. Physiol.*, **88,** 757–776.

SIDELL, N., VERITY, M.A. & NORD, E.P. (1990). Menthol blocks dihydropyridine-insensitive Ca^{2+} channels and induces neurite outgrowth in human neuroblastoma cells. *J. Cell. Physiol.*, **142,** 410–419.

SWANDULLA, D., CARBONE, E., SCHÄFER, K. & LUX, H.D. (1987). Effect of menthol on two types of Ca currents in cultured sensory neurons of vertebrates. *Pflügers Arch.*, **409,** 52–59.

SWANDULLA, D., SCHÄFER, K. & LUX, H.D. (1986). Calcium channel current inactivation is selectively modulated by menthol. *Neurosci. Lett.*, **68,** 23–28.

TAYLOR, B.A., LUSCOMBER, D.K. & DUTHIE, H.L. (1984). Inhibitory effect of peppermint and menthol on human isolated coli. *Gut*, **25,** A1168–A1169.

WANNER, A. (1977). State of the art. Clinical aspects of mucociliary transport. *Am. Rev. Respir. Dis.*, **116,** 73–125.

WELSH, M.J. (1987). Electrolyte transport by airway epithelia. *Physiol. Rev.*, **67,** 1143–1184.

WELSH, M.J., WIDDISCOMBE, J.H. & NADEL, J.A. (1980). Fluid transport across the canine tracheal epithelium. *J. Appl. Physiol.*, **49,** 905–909.

WIDDISCOMBE, J.H. & NATHANSON, I.T. & HIGHLAND, E. (1983). Effects of 'loop' diuretics on ion transport by dog tracheal epithelium. *Am. J. Physiol.*, **245,** C388–C396.

WIDDISCOMBE, J.H. & WELSH, M.J. (1980). Anion selectivity of the chloride transport process in dog tracheal epithelium. *Am. J. Physiol.*, **239,** C112–C117.

WILLIAMSON, J.R. & MONCK, J.R. (1989). Hormone effects on cellular Ca^{2+} fluxes. *Annu. Rev. Physiol.*, **51,** 107–124.

(Received July 19, 1993
Revised January 27, 1994
Accepted February 3, 1994)

Br. J. Pharmacol. (1994), **112**, 576–578

Adrenoceptors mediating relaxation to catecholamines in rat isolated jejunum

[1]A. MacDonald, I.J. Forbes, D. Gallacher, G. Heeps & D.P. McLaughlin

Department of Biological Sciences, Glasgow Caledonian University, City Campus, Cowcaddens Road, Glasgow G4 0BA

1 The characteristics of adrenoceptors mediating relaxation to catecholamines in rat isolated jejunum were investigated.

2 Catecholamines and BRL 37344 produced relaxation of the KCl-contracted strips with an order of potency of isoprenaline (1.0) > BRL 37344 (0.63) > noradrenaline (0.1) > adrenaline (0.04).

3 In the presence of both prazosin (1 μM) and propranolol (1 μM) only small dextral shifts of the concentration-response curves to agonists were observed and an order of potency of BRL 37344 (2.5) > isoprenaline (1.0) > noradrenaline (0.2) > adrenaline (0.1) was obtained.

4 In the presence of prazosin (1 μM) and propranolol (1 μM), cyanopindolol (0.1–10 μM) produced a concentration-dependent rightward shift of the concentration-response curve to adrenaline with a Schild slope not significantly different from unity and a mean pA_2 value of 7.01.

5 The resistance of relaxant responses to propranolol, the relatively high potency of BRL 37344 compared to catecholamines and the competitive antagonism of relaxant responses to adrenaline by cyanopindolol suggest that β-adrenoceptors in rat small intestine are mainly atypical in nature.

Keywords: Adrenoceptors; atypical β-adrenoceptors; β_3-adrenoceptors; small intestine; jejunum

Introduction

Catecholamines can produce relaxation of non-sphincteric gastrointestinal muscle by an action on either postjunctional α- or β-adrenoceptors or a combination of both (Burnstock & Wong, 1981; Bülbring & Tomita, 1987). In addition to classical β_1- and β_2-adrenoceptors, evidence exists for the presence of a population of atypical β-adrenoceptors in the gastrointestinal tract with similarities to the atypical, or β_3-adrenoceptors of adipocytes (for review, see Zaagsma & Nahorski, 1990). The atypical β-adrenoceptors are characterized by a low affinity for classical β-adrenoceptor antagonists, e.g. propranolol, and by the high potency of a novel class of β-adrenoceptor agonists, e.g. BRL 37344 (Arch *et al.*, 1984).

The present study was carried out to examine the characteristics of adrenoceptors mediating relaxation in rat small intestine by looking at the effects of the classical α_1-and β-adrenoceptor antagonists, prazosin and propranolol, on responses to catecholamines and to BRL 37344. In addition, it has been reported that the non-selective β-adrenoceptor antagonist, cyanopindolol (Engel *et al.*, 1981) is a competitive and relatively potent antagonist at atypical β-adrenoceptors in the gut (Blue *et al.*, 1989; McLaughlin & MacDonald, 1990; 1991) and therefore the effect of cyanopindolol on responses to adrenaline was investigated.

A preliminary account of this work has been presented to the British Pharmacological Society (MacDonald *et al.*, 1991).

Methods

Male Wistar rats (200–300 g) were killed by a blow to the head and cervical dislocation. The jejunum was removed and immediately placed in Krebs physiological saline solution (PSS), at room temperature. Longitudinal smooth muscle strips (3 cm) of jejunum were suspended in organ baths containing PSS, at 37°C, for isotonic recording. The composition of the PSS was as follows (mM): NaCl 118, $CaCl_2$ 2.5, KCl 4.7, $NaHCO_3$ 25, KH_2PO_4 1.2, $MgSO_4$ 1.2 and glucose 11.1. The PSS solution also contained cocaine (3 μM), ascorbic acid (30 μM) and EDTA (30 μM) and was gassed with 95% O_2:5% CO_2. Strips were pre-contracted with a submaximal (approximately 70–80% of maximum) concentration of potassium chloride (40 mM) before cumulative concentration-response curves to agonists were carried out, responses being expressed as % relaxation. In the studies with propranolol and prazosin, one concentration-response curve (CRC) to one agonist was carried out in each tissue either in the presence or absence of propranolol (1 μM) and prazosin (1 μM). Tissues were allowed to equilibrate for 45 min before addition of agonists and the antagonists were present from the beginning of the equilibration period. To carry out a Schild analysis (see below) of the effects of cyanopindolol on adrenaline, four consecutive concentration-response curves to adrenaline were carried out at 1 h intervals in each tissue. Prazosin (1 μM) and propranolol (1 μM) were present throughout. Cyanopindolol was added after washing at the end of each CRC, allowing approximately 45 min equilibration time. Thus three different, increasing, concentrations of cyanopindolol were used in each experiment. Two concentration ranges of cyanopindolol were used: 0.1, 0.3 and 1 μM and 1, 3 and 10 μM. Some tissues received no cyanopindolol and served as controls to assess the magnitude of time-dependent changes.

Statistical analysis

Results are expressed as means ± s.e.mean with the number of observations, *n*, in parentheses with the exception of the regression line slope which is expressed as slope ± 95% confidence limits. Statistical significance between two data sets was tested by Student's *t* test. A probability level of $P < 0.05$ was considered to be statistically significant.

Schild plot

A Schild plot (Arunlakshana & Schild, 1959) for the antagonism of adrenaline by cyanopindolol was constructed as follows. Agonist concentration-ratios (CRs) were obtained from individual EC_{50} values with and without antagonist. The plot of log (CR − 1) versus log [antagonist] (Schild plot)

[1] Author for correspondence.

was analysed by linear regression. Antagonism was considered to be simple competitive in nature if the slope of the regression line was not significantly different from unity. A mean pA_2 value was obtained from individual estimates from the equation:

$$pA_2 = \log(CR - 1) - \log[\text{antagonist}]$$

after verifying that there was no significant regression of pA_2 on antagonist concentration (McKay, 1978).

Drugs used

The following drugs were dissolved in distilled water with the exception of cyanopindolol which was dissolved in 0.1 M tartaric acid: (−)-adrenaline (+)-bitartrate; BRL 37344 (sodium-4-[-2-[2-hydroxy-2-(-3-chlorophenyl) ethylamino] propyl] phenoxyacetate); (±)-cyanopindolol (Sandoz); (−)-isoprenaline (+)-bitartrate (Sigma); prazosin hydrochloride (Sigma); (±)-propranolol hydrochloride (Sigma); (−)-noradrenaline (+)-bitartrate (Sigma); UK 14,304 (5-bromo-6[2-imazolin-2-yl-amino]quinoxaline) bitartrate (Pfizer).

Results

In the absence of antagonists, catecholamines and BRL 37344 produced relaxation of the KCl-contracted strips with pD_2 values of (mean ± s.e.mean) 6.9 ± 0.1 (isoprenaline), 5.9 ± 0.2 (noradrenaline), 5.5 ± 0.15 (adrenaline) and 6.7 ± 0.3 (BRL 37344) giving an order of potency of isoprenaline (1.0) > BRL 37344 (0.63) > noradrenaline (0.1) > adrenaline (0.04) ($n = 4-10$) (Figure 1).

In three experiments the α_2-adrenoceptor agonist, UK 14,304 (up to 30 μM) caused no relaxation of the KCl-contracted jejunum (data not shown).

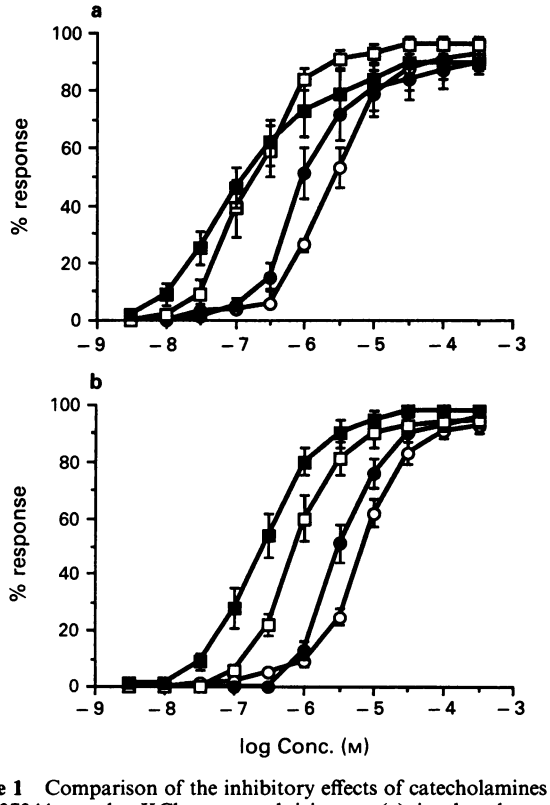

Figure 1 Comparison of the inhibitory effects of catecholamines and BRL 37344 on the KCl-contracted jejunum (a) in the absence of antagonists and (b) in the presence of prazosin (1 μM) and propranolol (1 μM). (■) BRL 37344; (□) isoprenaline; (●) noradrenaline; (○) adrenaline. Values are means ± s.e.mean of 4–10 experiments.

In the presence of both prazosin (1 μM) and propranolol (1 μM) only small dextral shifts of the concentration-response curves were observed (isoprenaline, 6.1 fold shift, $P < 0.001$; BRL 37344, 1.5, $P > 0.5$; noradrenaline, 3.3, $P < 0.05$; adrenaline, 2.7, $P < 0.05$), giving an order of potency of BRL 37344 (2.5) > isoprenaline (1.0) > noradrenaline (0.2) > adrenaline (0.1) (Figure 1).

In the presence of prazosin (1 μM) and propranolol (1 μM), cyanopindolol (0.1, 0.3, 1.0, 3 and 10 μM) produced a concentration-dependent rightward shift of the concentration-response curve to adrenaline with a Schild slope not significantly different from unity (0.82 ± 0.19, 95% CL, $n = 23$) and a mean pA_2 value of 7.01 ± 0.06 ($n = 23$) (Figure 2a,b,c).

Discussion

The order of potency of the catecholamines in the absence of antagonists suggests that the responses are mainly β in nature

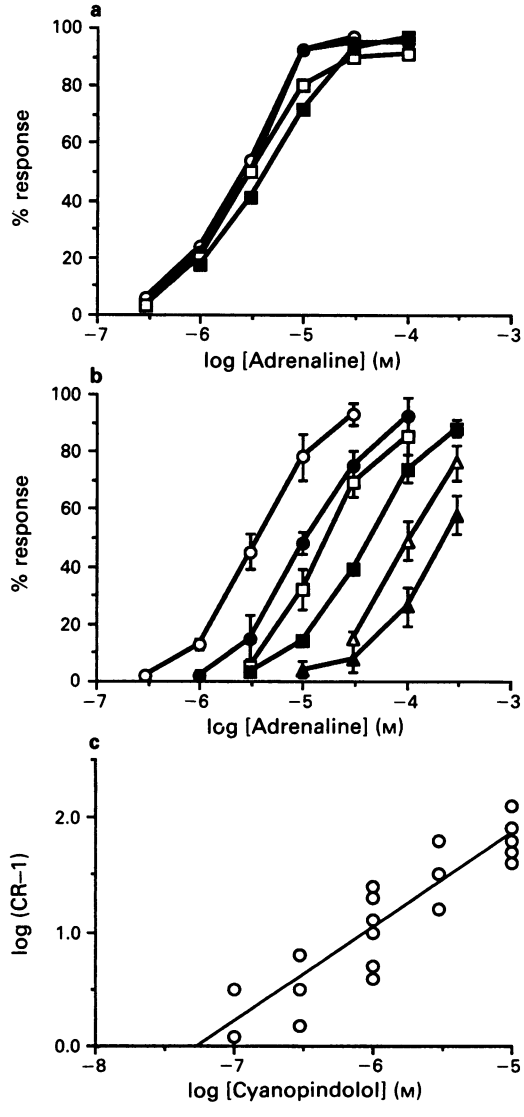

Figure 2 The effect of cyanopindolol on the inhibitory effects of adrenaline in the KCl-contracted rat jejunum. (a) Time control responses to adrenaline. Curves represent first (○), second (●), third (□), and fourth (■) CRCs. Values are means of eight experiments. Standard error bars are omitted for clarity. (b) Effect of cyanopindolol. Control, no cyanopindolol (○); 0.1 μM (●), 0.3 μM (□); 1 μM (■), 3 μM (△) and 10 μM (▲) cyanopindolol. Values are means ± s.e.mean of 3–8 experiments. (c) Schild plot of data from (b). The slope of the line was 0.82 ± 0.19, $n = 23$.

since isoprenaline was more potent than noradrenaline and adrenaline. The similar potencies of noradrenaline and adrenaline would suggest a β_1-adrenoceptor mediated response. However, the relatively high potency of BRL 37344 would further suggest a significant contribution to the response from atypical β-adrenoceptors. Bond & Clarke (1988) pointed out that the atypical β-adrenoceptor in guinea-pig ileum recognized catecholamines with a similar order of potency to the β_1-adrenoceptor but was distinguished from the β_1-adrenoceptor by the relatively high potency of BRL 37344.

Only small shifts of the agonist CRCs were obtained in the presence of prazosin and propranolol, indicating only a small contribution to the response of α_1 and/or classical β adrenoceptors. An α_2-adrenoceptor-mediated component was ruled out by the experiments which showed no response to the α_2-adrenoceptor agonist, UK 14304. We did not carry out further experiments to analyse these small shifts further but it seems likely that they were produced by blockade of classical β-adrenoceptors since (i) propranolol itself has been shown to produce similar shifts in rat colon and fundus (McLaughlin & MacDonald, 1990; 1991) and (ii) α-adrenoceptor mediated inhibitory effects in smooth muscle involve abolition of spontaneous spike discharge and hyperpolarization (Bülbring, 1954; 1957) and are not seen if the tissue is depolarized sufficiently to block spike generation (Magaribuchi & Kuriyama, 1972). The relative potencies of the catecholamines and BRL 37344 in the presence of prazosin and propranolol, with BRL 37344 becoming more potent than isoprenaline, are similar to those obtained by Bond & Clarke (1988) at the atypical β-adrenoceptors in guinea-pig ileum.

In the studies with the non-selective β-adrenoceptor antagonist cyanopindolol (Engel *et al.*, 1981), propranolol (1 μM) was present throughout to block classical β-adrenoceptors. These same conditions were employed in previous studies on rat distal colon (McLaughlin & MacDonald, 1990) and gastric fundus (McLaughlin & MacDonald, 1991). Under these conditions cyanopindolol produced further shifts of the CRCs to adrenaline. This supports previous reports of competitive antagonism of β_3-adrenoceptors by cyanopindolol (Blue *et al.*, 1989; McLaughlin & MacDonald, 1990; 1991). The pA_2 value of 7.01 obtained in the present study agrees reasonably well with the value obtained by Blue *et al.* (1989) in guinea-pig ileum (7.63) and by McLaughlin & MacDonald in rat colon (7.12) and gastric fundus (7.44).

A previous study of β-adrenoceptor-mediated relaxation of rat jejunum also concluded that relaxation was mediated via an atypical β-adrenoceptor (Van Der Vliet *et al.*, 1990). However, attempts to identify the atypical receptor with radiolabelled iodocyanopindolol proved to be unsuccessful because of the relatively low affinity of the ligand.

In conclusion, the resistance of catecholamine- and BRL 37344-induced relaxant responses to propranolol, the relatively high potency of BRL 37344 compared to catecholamines and the competitive antagonism of relaxant responses to adrenaline by cyanopindolol suggest that β-adrenoceptors in rat small intestine are mainly atypical in nature.

We are grateful to Glasgow Caledonian University for a research studentship (D.McL.) and small grants in support of this work. BRL 37344 and cyanopindolol were generous gifts from SmithKline Beecham and Sandoz respectively.

References

ARCH, J.R.S., AINSWORTH, A.T., CAWTHORNE, M.A., PIERCY, V., SENNIT, M.V., THODY, V.E., WILSON, C. & WILSON, S. (1984). Atypical β-adrenoceptor on brown adipocytes as target for anti-obesity drugs. *Nature*, **309**, 163–165.

ARUNLAKSHANA, O. & SCHILD, H.O. (1959). Some quantitative uses of drug antagonists. *Br. J. Pharmacol. Chemother.*, **14**, 48–58.

BLUE, D.R., BOND, R.A., ADHAM, N., DELMONDO, R., MICHEL, A., EGLEN, R.M., WHITING, R.L. & CLARKE, D.E. (1989). Interaction of dihydroalprenolol and cyanopindolol with atypical β-adrenoceptors in guinea-pig ileum. *Br. J. Pharmacol.*, **96**, 246P.

BOND, R.A. & CLARKE, D.E. (1988). Agonist and antagonist characterization of a putative adrenoceptor with distinct pharmacological properties from the α- and β-subtypes. *Br. J. Pharmacol.*, **95**, 723–734.

BÜLBRING, E. (1954). Membrane potentials of smooth muscle fibres of the taenia coli of the guinea-pig. *J. Physiol.*, **125**, 302–315.

BÜLBRING, E. (1957). Changes in configuration of spontaneously discharged spike potentials from smooth muscle of the guinea-pig's taenia coli. The effects of electrotonic currents and of adrenaline, acetylcholine and histamine. *J. Physiol.*, **135**, 412–425.

BÜLBRING, E. & TOMITA, T. (1987). Catecholamines action on smooth muscle. *Pharmacol. Rev.*, **39**, 49–96.

BURNSTOCK, G. & WONG, H. (1981). Systemic pharmacology of adrenergic agonists and antagonists: effects on the digestive system. In *Adrenergic Activators and Inhibitors*. ed. Szekeres, L. *Handbook of Experimental Pharmacology*, vol. 54, pp. 129–159. Berlin: Springer-Verlag.

ENGEL, G., HOYER, D., BERTOLD, R. & WAGNER, H. (1981). (±)[^{125}Iodo]cyanopindolol, a new ligand for beta-adrenoceptors: identification and quantitation of beta-adrenoceptors in guinea-pig. *Naunyn-Schmied. Arch. Pharmacol.*, **317**, 277–285.

MAGARIBUCHI, T. & KURIYAMA, H. (1972). Effects of noradrenaline and isoprenaline on the electrical and mechanical activities of guinea-pig depolarised taenia coli. *Jpn. J. Pharmacol.*, **22**, 253–270.

MCKAY, D. (1978). How should values of pA_2 and affinity constants for competitive antagonists be estimated? *J. Pharm. Pharmacol.*, **30**, 312–313.

MACDONALD, A., FORBES, I.J., GALLACHER, D., HEEPS, G. & MCLAUGHLIN, D.P. (1991). β-Adrenoceptors mediating relaxation in rat small intestine are atypical in nature. *Br. J. Pharmacol.*, **102**, 167P.

MCLAUGHLIN, D.P. & MACDONALD, A. (1990). Evidence for the existence of 'atypical' β-adrenoceptors (β_3-adrenoceptors) mediating relaxation in the rat distal colon *in vitro*. *Br. J. Pharmacol.*, **101**, 569–574.

MCLAUGHLIN, D.P. & MACDONALD, A. (1991). Characterization of catecholamine-mediated relaxations in rat isolated gastric fundus: evidence for an atypical β-adrenoceptor. *Br. J. Pharmacol.*, **103**, 1351–1356.

VAN DER VLIET, A., RADEMAKER, B. & BAST, A. (1990). A beta adrenoceptor with atypical characteristics is involved in the relaxation of the rat small intestine. *J. Pharmacol. Exp. Ther.*, **256**, 218–226.

ZAAGSMA, J. & NAHROSKI, S.R. (1990). Is the adipocyte β-adrenoceptor a prototype for the recently cloned atypical 'β_3-adrenoceptor'? *Trends Pharmacol. Sci.*, **11**, 3–7.

(Received December 13, 1993
Revised January 29, 1994
Accepted February 4, 1994)

Br. J. Pharmacol. (1994), **112**, 579–587

Differences in sensitivity of rat mesenteric small arteries to agonists when studied as ring preparations or as cannulated preparations

N.H. Buus, *E. VanBavel & [1]M.J. Mulvany

Danish Biomembrane Research Centre and Department of Pharmacology, Aarhus University, 8000 Aarhus C., Denmark and *Department of Medical Physics, University of Amsterdam, Amsterdam, The Netherlands

1 Pharmacological experiments on vascular tissue are normally performed on isometric ring or strip preparations. The aim of this study was to compare the isometric characteristics with the characteristics obtained if vessels were examined under the more physiologically appropriate isobaric condition.

2 Rat mesenteric small arteries were mounted either on two steel wires for isometric force measurement (wire-myograph) or cannulated for measurement of the internal diameter under isobaric conditions (pressure-myograph).

3 The passive pressure-diameter characteristics of the small arteries were similar on the wire- and pressure-myograph (using the Laplace relation to convert wall tension-internal circumference data from the wire-myograph to effective pressure-diameter characteristics).

4 In cumulative concentration-response experiments with noradrenaline and phenyelphrine, the threshold concentration was 8–10 times lower, and the EC_{50}-concentration was 4–5 times lower, in the pressure myograph compared to the wire-myograph. Thus vessels were not only more sensitive on the pressure myograph, but the slopes of the concentration-response curves were less steep. Similar experiments with vasopressin also showed this difference in the threshold-concentration and slope, but EC_{50} concentrations were similar.

5 Cumulative concentration-response experiments with K^+ showed no difference either in EC_{50} or in slope on the wire- and pressure-myographs.

6 On the wire-myograph, some vessels were stretched longitudinally (to mimic the longitudinal stretch which had to be used in the pressure-myograph to avoid buckling). Such stretch did not affect the passive characteristics.

7 The differences between the EC_{50} determined on the wire- and pressure-myographs as regards noradrenaline and phenylephrine were eliminated when neuronal noradrenaline uptake was inhibited by denervation. However, the slope of the concentration-response curves on the wire-myograph was not affected by denervation.

8 When vessels were exposed to cocaine (3 μM) the noradrenaline concentration-response curves were the same on the wire- and pressure-myographs as regards both EC_{50} and slope.

9 On the wire-myograph, the calcium antagonist, methoxyverapamil, (D600) reduced the maximal contractile effect of noradrenaline by 50%, but on the pressure-myograph D600 did not affect the maximal response.

10 The present results show that results obtained from vascular tissue under isometric conditions may differ substantially from the characteristics which would be obtained under isobaric conditions.

Keywords: Isometric; isotonic; myograph; concentration-response curve; amine uptake; calcium antagonist

Introduction

In vitro investigation of the contractile properties of intact vascular segments are performed by use of two principally different methods (Mulvany & Aalkær, 1990; Halpern & Kelley, 1991). Vessels can be mounted either as isometric preparations (on a 'wire-myograph', e.g. Mulvany & Halpern, 1977), when force development is measured at a certain diameter, or as cannulated isobaric preparations where the vessel is exposed to a transmural pressure and allowed to change diameter ('pressure-myograph', e.g. Halpern & Osol, 1985). Evidence is accumulating that certain characteristics of the vessels are critically dependent on which method is used. In particular, it has been suggested that the spontaneous basal tone (McCarron *et al.*, 1991; Vanbavel *et al.*, 1991) and myogenic behaviour (Halpern *et al.*, 1987; VanBavel *et al.*, 1991), which exists in most resistance arteries *in vivo*, are more easily reproduced *in vitro* in pressurized vessels than in wire-mounted vessels.

Indirect evidence for differences between wire- and pressure-myographs is also found in the literature as regards the concentration-response relations for e.g. noradrenaline (NA). Thus, for small rat mesenteric arteries, the NA pEC_{50}-values ($pEC_{50} = -\log(EC_{50}\ (M))$) on wire-myographs are reported in the range 5.52–5.96 (Whall *et al.*, 1980; Mulvany *et al.*, 1982; Nyborg & Mikkelsen, 1985; Nielsen & Mulvany, 1990), while the reported NA pEC_{50}-values for cannulated and pressurized rat mesenteric arteries of similar diameter are generally higher, e.g. in the range 6.3–6.45 (Marshall, 1977; Dohi & Lüscher, 1990; VanBavel & Mulvany, 1994). Furthermore, it appears that the slope of the NA concentration-response curves is steeper on wire-myographs than on pressure-myographs. Such differences have also been seen on a myograph where a cannulated preparation could be exposed to either isometric or isobaric conditions using a feed-back arrangement (VanBavel & Mulvany, 1994).

The possibility that the commonly used method of investigating vascular preparations isometrically may give results which are substantially different from results obtained isobar-

[1] Author for correspondence.

ically is potentially important: the isobaric method is clearly much closer to the *in vivo* situation than the isometric method. However, until now, there has been no systematic comparison of the two methods as regards agonist concentration-response relations. We have therefore performed concentration-response experiments using both a wire-myograph (Mulvany & Halpern, 1977) and a pressure-myograph (VanBavel *et al.*, 1990) to investigate the same preparation (a rat mesenteric small artery) and using the same solutions and protocols. The results confirmed the differences indicated above, and we have carried out further experiments to investigate possible reasons for the differences. In particular, we have investigated whether the results are specific to NA by determining the responses to other agonists (the α_1-adrenoceptor agonist, phenylephrine (PE) and vasopressin) and to high potassium solution. We have also investigated the possible influence of neuronal amine uptake. The results are consistent with the differences being due in part (a) to the effect of amine uptake on amine concentration-response relations being greater for wire-myographs than for pressure-myographs and (b) to the sensitivity to agonists being increased by force in the vascular wall. Some of these results have been presented previously in brief (Buus & Mulvany, 1992).

Methods

Male Wistar rats, aged 12–16 weeks, were killed with CO_2. Part of the intestinal tract was removed and kept in a physiological saline solution (PSS, for composition see below). Segments from a second or third order branch of the mesenteric superior artery were dissected and mounted in either a pressure-myograph or a wire-myograph, as explained below.

Pressure-myograph

Vessels mounted in the pressure-myograph (VanBavel *et al.*, 1990; 1991) were cannulated at both ends with small glass cannulae having an outer diameter of 110–150 μm and secured with 15 μm thin sutures. The cannulated segment was superfused with PSS, bubbled with 95% O_2 and 5% CO_2, at a flow rate of 10 ml min^{-1} from a 100 ml reservoir. The lumen was perfused at 10–100 μl min^{-1} with PSS containing 0.5% albumin and 40 mg l^{-1} of the fluorescent dye FITC-dextran (fluorescein isothiocyanat-dextran, molecular weight 487 kDa), the luminal pressure being controlled by adjustment of the height of the reservoirs feeding and receiving the perfusate. This flow rate is substantially lower than that which induces flow-mediated vasodilatation (Tesfarmariam *et al.*, 1985), as confirmed by our observation that stopping the flow did not affect lumen diameter. A pressure transducer connected to the feeding reservoir was used to record luminal pressure continuously. The flow rate of the perfusate was adjusted by maintaining a small difference in the height of the feeder and receiver reservoirs. It was important to choose segments without any side branches to avoid leakage of FITC-dextran or albumin from the lumen to the superfusate. After mounting, a transmural pressure of 80 mmHg (110 cmH_2O) was applied to the vessel, which was then lengthened until any bends in the vessel disappeared. The vessel chamber was placed under a microscope (Leitz Orthoplan) which was equipped with a fluorescence attachment. The luminal cross-sectional area was continuously measured by means of a fluorescence technique as described by VanBavel *et al.* (1990). In brief, the FITC-dextran present in the lumen was excited with a halogen light source. Excitation light was filtered to pass 400–800 nm with the aid of a dichroic mirror and the intensity of fluorescence light emitted from the vessel lumen was measured with a photomultiplier tube. The system was calibrated as follows. The temperature of the chamber was raised to 37°C, and the vessel diameter was set in turn to three or four different diameters (by adjustment of luminal pressure). For each diameter, measurements were made (a) of the intensity and (b) of the internal diameter by direct observation through the microscope by use of an ocular micrometer. Intensity was linearly related to the cross sectional area, as found previously (VanBavel *et al.*, 1990). Calibration was checked several times during each experiment.

Wire-myograph

Vessels were threaded on two 40 μm diameter stainless steel wires and mounted on a wire-myograph (model 500A, JP Trading) allowing direct determination of the vessel wall force while the internal circumference was controlled (Mulvany & Halpern, 1977). After the temperature had reached 37°C, arteries were stretched radially to their optimal lumen diameter, equal to (internal circumference)/π, for active tension development. This normalized effective lumen diameter (d_0), is an estimate of 90% of the diameter the vessel would have had, if it were relaxed and exposed to a transmural pressure of 100 mmHg (Mulvany & Halpern, 1977).

Experimental protocol

After normalization (wire-myograph) or calibration (pressure-myograph), vessels were activated for 2 min with K-PSS (125 mM) containing 10 μM NA. Vessels in the wire-myograph were accepted only if the calculated pressure against which they could contract (calculated according to the Laplace relation) exceeded 100 mmHg (Mulvany & Halpern, 1977), and vessels in the pressure-myograph were accepted only if visual inspection showed no side-branches leaking dye and the contraction was uniform along the whole segment length. With these criteria, all vessels in the wire-myograph were accepted, but 35% of the vessels in the pressure-myograph were discarded, nearly all because of dye leaking out of minute side-branches not visible during dissection. Most of the vessels in both the pressure- and wire-myographs were also tested to ensure that they relaxed to acetylcholine (1 μM) as an indication that the endothelium was still intact, and all met this criterion. The following protocols were followed.

(1) Passive pressure-diameter relationship

The vessel segment was first mounted on the pressure-myograph and the inner diameter measured at different transmural pressures. The same segment was then transferred to the wire-myograph and subjected to increasing degrees of radial distension. Full relaxation was ensured by the presence of papaverine (10 μM).

To investigate the effect of longitudinal stretch of the vessel on the wire-myograph, the normal mounting procedure was modified. The vessel was gently stretched with a forceps and clamped at both ends between the mounting wires and the metal jaws supporting the wires. After stretching, the normalization procedure was repeated and a new d_0 was found. With this modified procedure it was possible to obtain a degree of longitudinal stretch similar to that produced by the transmural pressure in the pressure-myograph.

(2) Active properties of vessels in pressure- and wire-myographs

Here concentration-response experiments with NA, PE, vasopressin and K^+ were performed on the pressure-myograph, or on the wire-myograph. Experiments in the pressure-myograph were made at a transmural pressure of 44 mmHg (60 cmH_2O). This pressure is similar to the calculated pressure at a distension of d_0 on the wire-myograph (ca. 55 mmHg, see Figure 1). NA and PE were added in a concentration range from 1 nM (NA) or 10 nM (PE) to 32 μM

in half log increments, AVP in a range from 0.039 to 5 u l^{-1} with doubling of concentrations, and K^+ (as K-PSS, see below) in seven different concentrations ranging from 5.9 mM to 125 mM. Each dose was added to the chamber for 2 min. To ensure that the experiments with PE involved only α_1-adrenoceptors, these were done in the presence of the α_2-antagonist yohimbine (0.1 μM). K^+ experiments were made in the presence of phentolamine (1 μM) to avoid the effect of NA released from depolarized sympathetic nerve endings.

(3) Investigation of a possible difference in the influence of sympathetic nerves in pressurized and wire-mounted arteries

(a) *Cocaine experiments* After the initial concentration-response curve with NA, cocaine (3 μM) was added and a new curve generated. To investigate an influence of the vessel diameter on NA reuptake a group of similar experiments were made at distensions of both d_0 and $0.5 \times d_0$.

(b) *Denervation experiments* After the initial NA concentration-response curve, vessels were denervated *in vitro* with 6-hydroxydopamine (457 mg l^{-1}). This was done in buffer-free PSS vigorously bubbled with N_2 (Aprigliano & Hermsmeyer, 1976), followed by a 2 h recovery period in standard PSS, after which a new concentration-response curve was obtained.

(4) Action of the calcium channel blocker D600 in pressurized and wire-mounted vessels

Vessels were set either to d_0 or to $0.4 \times d_0$. In each case, after the initial concentration-response curve with NA, 1 μM methoxyverapamil (D600) was added to the vessel chamber and a new curve was generated.

Time control experiments were not performed, since the aim of the studies was to compare the responses of wire-mounted and cannulated preparations when subjected to otherwise identical protocols. It should be noted, however, that for rat mesenteric small arteries both when wire-mounted (Mulvany *et al.*, 1982) and when cannulated (Van-Bavel & Mulvany, 1994), agonist concentration-response relations are repeatable for many hours.

Drugs and solutions

Drugs used were noradrenaline-HCl (NA, Sigma), D600 (methoxyverapmil, Knoll AG), vasopressin (Sandoz, where 1 u l^{-1} = ca. 2.5 nM), albumin (bovine, Sigma), fluorescein isothiocyanate-dextran (0.011 mol (mol glucose)$^{-1}$, Sigma), cocaine chloride (Pharmacy, Aarhus University Hospital), 6-hydroxydopamine (Sigma), phentolamine (Ciba-Geigy), phenylephrine (PE) and papaverine (SAD, Denmark), and yohimbine (Sigma). All drugs were dissolved in distilled water except D600 which was dissolved in 96% ethanol. The physiological saline solution was of the following composition (mM): NaCl 119, NaH_2CO_3 25, KCl 4.7, $CaCl_2 \cdot 2H_2O$ 2.5, $MgSO_4 \cdot 7H_2O$ 1.17, KH_2PO_4 1.18, Na_2EDTA 0.026 and glucose 5.5. K-PSS was similar to PSS except that NaCl was exchanged for KCl on an equimolar basis. The pH of the PSS was stabilized with HEPES ([N-(2-hydroxyethyl) piperazine-N'-[Z-ethane sulphonic acid]) at pH 7.40. Buffer-free PSS used for denervation consisted of (mM): NaCl 137, $MgCl_2$ 1, KCl 2.69, EDTA 0.03, $CaCl_2$ 1.8, glucose 7.8 and glutathione 0.02, pH 4.9.

Calculations and statistical considerations

The passive tension-diameter curves obtained on the wire-myograph were fitted to an exponential function: $T = a \times \exp(b \times d)$, where T is the passive tension, d the internal diameter, a and b constants. Based on the Laplace equation the effective pressure ($p = 2 \times T/d$) could be calculated (Mulvany & Halpern, 1977). For Figure 1, the diameters at various effective pressures on the fitted passive tension-diameter relation were determined; average diameters for the vessels investigated at each of these pressures were calculated. For Figure 2, the characteristics before and after stretch were determined by calculating the wall tensions and diameters at each distension (which ranged between 0.44 d_0 and 1.22 d_0); average tensions and diameters for the vessels investigated at each of these distensions was calculated.

All concentration-response curves were analyzed by iterative nonlinear regression analysis. Each regression line was fitted to a sigmoid equation: $R/R_{max} = A^n/(A^n + (EC_{50})^n)$ where R_{max} is the maximal response developed to the agonist, A is the concentration of agonist, EC_{50} is the concentration required for half maximum contraction and n is a constant which indicates the maximal slope of the concentration-response curve. The coefficients of determination for the fitted curves were $r^2 = 0.99$ both on the wire-myograph and the pressure-myograph. In each curve, the agonist concentration (A) corresponding to a certain degree of contraction (R/R_{max}) was calculated from the fitted curve; concentration-response data in the figures are therefore given with horizontal error bars. Sensitivities to NA, PE, K^+ and vasopressin are expressed as pEC_{50} equal to $-\log(EC_{50}(M))$ or, for vasopressin, $-\log(EC_{50}$ (u l^{-1})).

Results are given as mean ± s.e.mean. Differences between means were analyzed with Student's paired or unpaired two-tailed *t* test, as appropriate. In Table 2, to allow comparison between several group means, we used one way analysis of variance (one-way ANOVA) followed by Fisher's LSD (Least Significance Difference) test, having previously ensured that the data were normally distributed. The level of significance in all tests was set at $P < 0.05$.

Results

Passive properties of vessels

The passive pressure-diameter relationship of six vessels was determined first on the pressure-myograph and then on the wire-myograph. As shown in Figure 1 the relations were identical, even though on the pressure-myograph the vessels had to be stretched longitudinally by 76 ± 6% to keep the vessel straight when subjected to the highest pressure (80

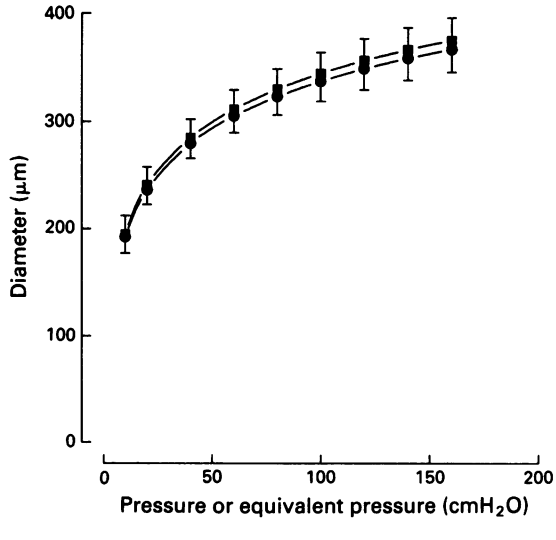

Figure 1 Pressure-diameter relation for six pressurized vessels (●) and equivalent pressure-diameter relation (■) obtained when these vessels were mounted on the wire-myograph. Equivalent pressures are calculated from the passive diameter-tension curves determined for each vessel as described in the text. Error bars show s.e.mean.

mmHg). Longitudinal stretch of vessels did not affect the normalised diameter: unstretched, d_0 was 290 ± 7 μm (n = 15); when stretched longitudinally by 56 ± 2%, d_0 was 281 ± 6 μm. Furthermore, as shown on Figure 2 longitudinal stretch did not influence the passive tension-diameter relationship.

Concentration-response experiments

Figure 3 shows typical traces obtained in NA concentration-response experiments, and Figure 4a and Table 1 show the average results. As indicated by the pEC_{50}-values in Table 1, the concentration needed to elicit half maximum response is almost 5 fold higher in the wire-myograph than in the pressure-myograph. The slope of the concentration-response curve was shallower in the pressure-myograph, consistent with the lower maximum slope (Table 1) and a 10 fold lower threshold concentration (measured as 10% of maximum responses, Figure 4a).

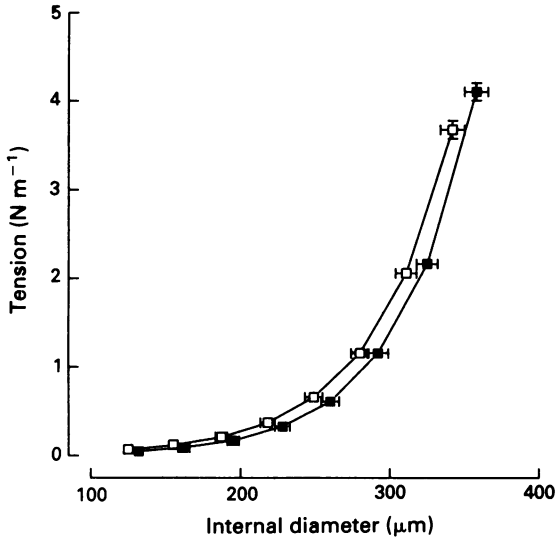

Figure 2 Effect of longitudinal stretch on passive diameter-tension characteristics of 15 vessels when mounted on the wire-myograph: unstretched (vessel length 1.92 ± 0.06 mm, ■) and when these vessels were stretched longitudinally (vessel length 2.92 ± 0.02 mm, □). Both curves are obtained from the fitted exponential passive diameter-tension curves as explained in the text. S.e.mean are shown where these exceed the size of the symbol.

To ensure that the findings concerning NA were mediated through α_1-adrenoceptors, concentration-response experiments with PE in the presence of α_2-adrenoceptor blockade (yohimbine, 0.1 μM) were also performed. These experiments also showed an increased sensitivity and lower maximum slope in the pressure-myograph compared to the wire-myograph (Table 1, Figure 4b). By contrast, experiments with K^+ (Table 1, Figure 4c) showed no significant difference in pEC_{50}-values or maximum slope. Concerning vasopressin, although the maximum slope and threshold concentration were lower on the pressure-myograph compared to the wire-myograph, there was no significant difference in the pEC_{50}-values (Table 1, Figure 4d). However, it should be noted that the effect of this drug was nearly an all-or-none response making the curve-fitting uncertain.

Inhibition of neuronal uptake by cocaine

Results from experiments with cocaine are outlined in Table 2a and Figure 5a. The increase in sensitivity to NA caused by cocaine is less in the pressure-myograph compared to the wire-myograph (Figure 5a), such that the initial differences in pEC_{50}-value and maximum slope disappeared. Cocaine did not affect the maximal active tension development in the wire-myograph (4.93 ± 0.26 N m^{-1} before and 4.47 ± 0.24 N m^{-1} after incubation with cocaine) or the maximal degree of contraction in the pressure-myograph (contracted to 22 ± 3% of relaxed diameter in the absence and to 23 ± 3% in the presence of cocaine). In ten experiments, we compared the effect of cocaine with vessels held at d_0 (257 ± 12 μm) and at 0.5 × d_0. There was a significant difference in the shift in NA-pEC_{50} caused by cocaine at these two distensions, being 0.67 ± 0.07 and 0.43 ± 0.06, respectively.

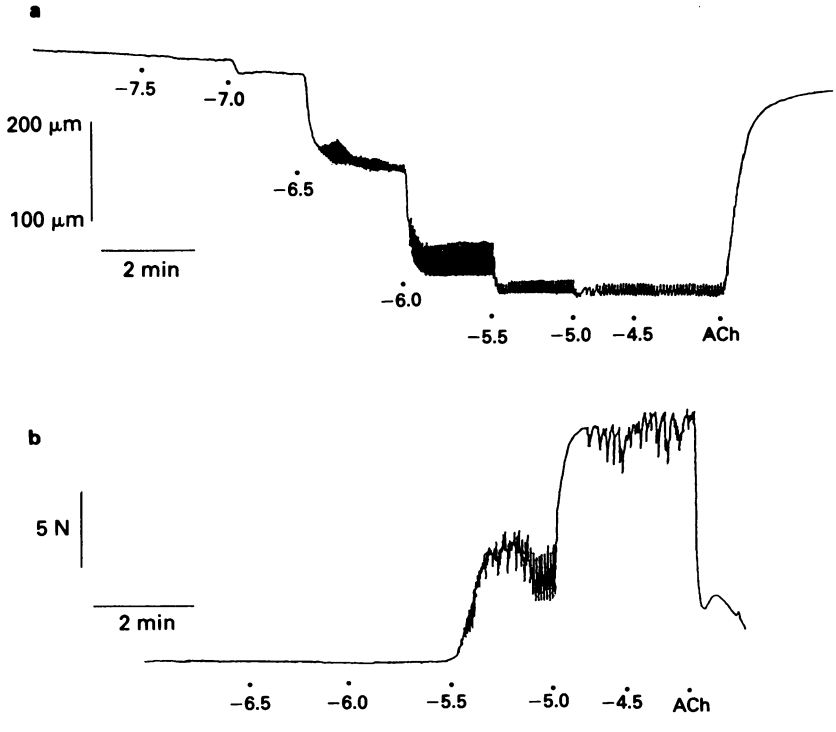

Figure 3 Traces showing noradrenaline (NA) concentration-response curves for a pressurized vessel (a), and a wire-mounted vessel (b). NA concentratons are given as log concentrations (M). ACh: acetylcholine 1 μM.

Table 1 Maximal contractions, pEC_{50} values and maximum slopes for concentration-response experiments

Agonist	*Experimental condition*	n	*Max. active tension* ($N\,m^{-1}$)	*Min. diameter* (% of relaxed diameter)	*pEC_{50}*	*Maximum slope*
Noradrenaline	Pressure-myograph	9		23 ± 4	6.42 ± 0.08[a]	1.65 ± 0.15[a]
	Wire-myograph	8	3.85 ± 0.25		5.77 ± 0.05[b]	2.60 ± 0.24[b]
Potassium	Pressure-myograph	7		30 ± 6	1.41 ± 0.02[a]	5.72 ± 0.79[a]
	Wire-myograph	7	3.36 ± 0.52		1.43 ± 0.01[a]	6.30 ± 0.20[a]
Vasopressin	Pressure-myograph	6		39 ± 7	0.54 ± 0.07[a]	3.49 ± 0.67[a]
	Wire-myograph	7	3.58 ± 0.47		0.38 ± 0.12[a]	6.18 ± 0.92[b]
Phenylephrine	Pressure-myograph	4		24 ± 4	6.00 ± 0.10[a]	2.29 ± 0.29[a]
	Wire-myograph	6	3.58 ± 0.29		5.65 ± 0.08[b]	3.94 ± 0.41[b]

Different superscripts designate within each group $P<0.05$ for pressure- v. wire-myograph by t test. $pEC_{50} = -\log (EC_{50}$ (M)) or for vasopressin $-\log (EC_{50}$ u $l^{-1})$). n is the number of vessels in each group. Values show mean ± s.e.mean.

Table 2 A Effect of cocaine (3 μM) on pEC_{50}-values and maximum slopes on vessels in the pressure- and wire-myographs

Experimental condition	n	*pEC_{50}* − Cocaine	*pEC_{50}* + Cocaine	*Maximum slope* − Cocaine	*Maximum slope* + Cocaine
Pressure-myograph	10	6.24 ± 0.07[a]	6.54 ± 0.07[c]	1.98 ± 0.21[a]	1.86 ± 0.13[a]
Wire-myograph	12	6.50 ± 0.03[b]	6.38 ± 0.09[c]	3.48 ± 0.17[b]	2.29 ± 0.23[a]

B Effect of *in vitro* denervation on pEC_{50}-values and maximum slopes on vessels in the pressure- and wire-myographs

Experimental condition	n	*pEC_{50}* Innervated	*pEC_{50}* Denervated	*Maximum slope* Innervated	*Maximum slope* Denervated
Pressure-myograph	6	6.16 ± 0.11[a]	6.56 ± 0.10[c]	1.72 ± 0.21[a]	1.50 ± 0.19[a]
Wire-myograph	8	5.85 ± 0.08[b]	6.67 ± 0.12[c]	3.07 ± 0.31[b]	3.35 ± 0.49[b]

In A and B different superscripts indicate differences between pEC_{50} and maximum slope values, respectively ($P<0.05$ by ANOVA followed by Fisher's LSD). n is the number of vessels. $pEC_{50} = -\log (EC_{50}$ (M)). Values show mean ± s.e.mean.

Two experiments on the wire-myograph provided indirect verification that PE was also taken up by the nerves, as observed in other preparations (Rawlaw *et al.*, 1980). After blocking reuptake with 3 μM cocaine, pEC_{50}-values for PE increased 0.58 and 0.44, respectively.

Inhibition of neuronal uptake by denervation

Following *in vitro* denervation, there was no difference in pEC_{50} for NA between wire- and pressure-myographs (Table 2b, Figure 5b), since, as with cocaine, denervation caused a greater change in sensitivity in the wire-mounted vessels. However, the denervation did not affect the maximum slope, so that the difference in the maximum slope remained. The denervation procedure did not alter the maximal force development of the vessels in the wire-myograph (maximal active tensions were 3.53 ± 0.32 $N\,m^{-1}$ before and 3.67 ± 0.33 $N\,m^{-1}$ after denervation) or in the pressure-myograph (contracted to 21 ± 3% of relaxed diameter before and 22 ± 3% after denervation).

D600

The effect of D600 (1 μM) on the NA concentration-response relation was investigated on the pressure-myograph ($n = 4$) and in the wire-myograph at distensions of d_0 ($n = 6$) and $0.4 \times d_0$ ($n = 6$). Results are shown in Figure 6. In all three cases, D600 was able to elicit a decrease in the pEC_{50} value for NA. In the wire-mounted vessels, D600 inhibited the maximal active tension, which declined from 4.99 ± 0.07 $N\,m^{-1}$ to 2.46 ± 0.25 $N\,m^{-1}$ and from 0.93 ± 0.03 $N\,m^{-1}$ to 0.18 ± 0.02 $N\,m^{-1}$ at distensions of d_0 and $0.4 \times d_0$, respectively. By contrast, D600 did not affect the maximal contraction in the pressure-myograph (26 ± 1% of the relaxed diameter before and 28 ± 2% after adding D600). However, in both the pressure- and wire-myographs, D600 (1 μM) eliminated vasomotion (i.e. rhythmic changes in the tension or diameter responses to the noradrenaline activation). At the end of each experiment, the vessel was stimulated with 125 mM K^+ in the presence of 1 μM D600 and 1 μM phentolamine: in both the wire- and pressure-myographs, D600 inhibited the sustained phase of the response to K^+.

Discussion

The main results are as follows. First, the passive pressure-internal diameter relationship of vessels tested on the wire-myograph (isometric conditions) was similar to that obtained on the pressure-myograph (isobaric conditions). Second, vessels on the pressure-myograph were 5–10 fold more sensitive to the α-adrenoceptor agonists NA and PE and ca. 3 fold more sensitive to threshold concentrations of vasopressin than on the wire-myograph; furthermore, the maximum slopes determined on the pressure-myograph were smaller than on the wire-myograph. By contrast, the characteristics with K^+ activation were similar. Third, as regards NA, inhibition of neuronal reuptake eliminated the difference in the pEC_{50}. Fourth, D600 decreased the maximal response to NA only in wire-mounted vessels.

Passive properties

Our finding that there was no difference in the pressure-diameter relationship between wire-mounted (calculated on the basis of the Laplace relation) and pressurized vessels suggests that lengthening caused by the intravascular pressure does not affect internal diameter. This interpretation is supported by the finding that longitudinal stretch of vessels on the wire-myograph did not affect the tension-diameter

relation (Figure 2). In contrast, Lew & Angus (1992) found that, at lower pressures, the pressurized vessels had larger diameters than the wire-mounted vessels. However, their pressurized vessels were cannulated only at one end, tied at the other end, and then pressurized like a balloon. Thus, at the lower pressure, the degree of longitudinal extension would have been less than under our conditions (where vessels were held at a fixed longitudinal extension), and this may explain the difference. In this respect, however, it should be emphasized that although under our conditions the wire- and pressure-myographs gave the same pressure-diameter relation, the longitudinal stretch used in the pressure-myograph will certainly reduce the wall thickness, as observed by Lew & Angus (1992), since the deformation involved is isovolumetric (Carew et al., 1968).

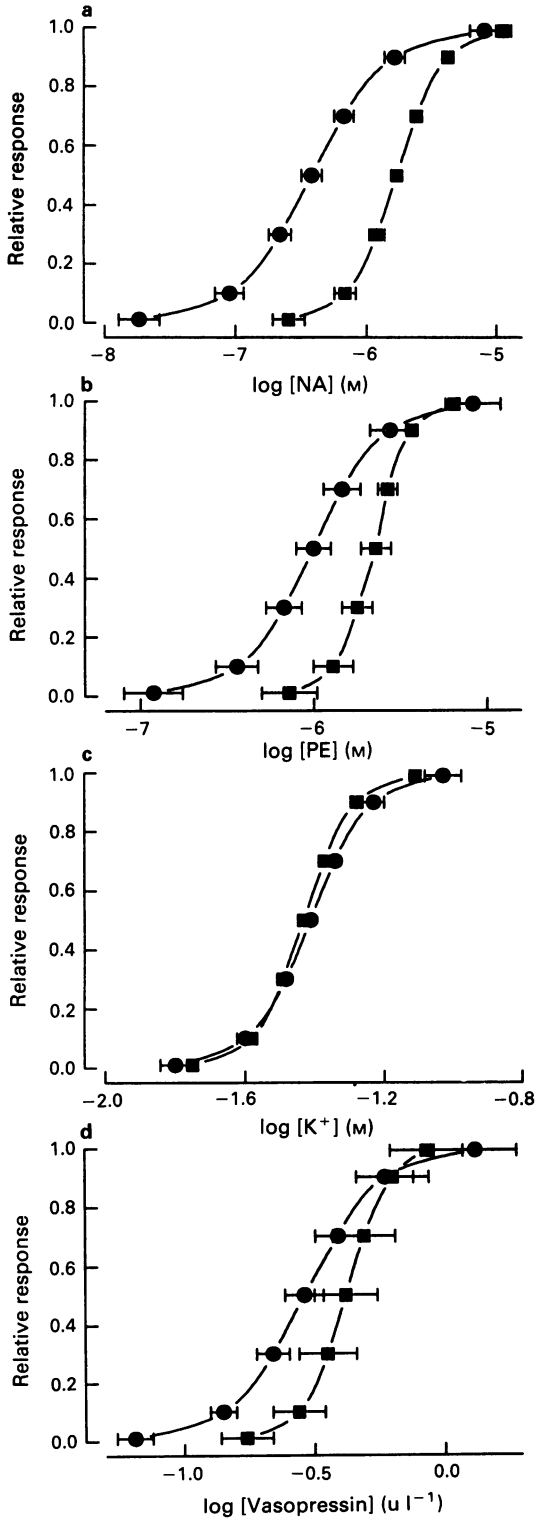

Figure 4 Concentration-response curves for (a) noradrenaline (NA), (b) phenylephrine (PE), (c) potassium (K^+) and (d) vasopressin, for (●) pressurized and (■) wire-mounted vessels. Responses are given as fraction of the maximal active tension (wire-myograph) or the maximal change in diameter (pressure-myograph). Analysis of the curves is shown in Table 1. S.e.means are shown where these exceed the size of the symbol.

Agonist responses in wire-mounted and pressurized vessels

The differences in the concentration-response relations seen in wire-mounted and pressurized vessels were of two types: changes in the pEC_{50} and changes in the maximum slope. These will be considered separately.

Changes in pEC_{50} On the basis of the experiments where the neuronal amine pump was inhibited either by cocaine or by denervation (Figure 5, Table 2), one reason for the lower pEC_{50} seen with NA activation on wire-myographs compared to pressure-myographs appears to be due to the amine pump being more effective in right-shifting the NA concentration-response relation in wire-mounted compared to pressurized vessels. The reason for this is not clear. It seems unlikely to be due to differences in adventitial v. luminal access (Venning & De la Lande, 1984; 1988; Tesfamariam & Halpern, 1988),

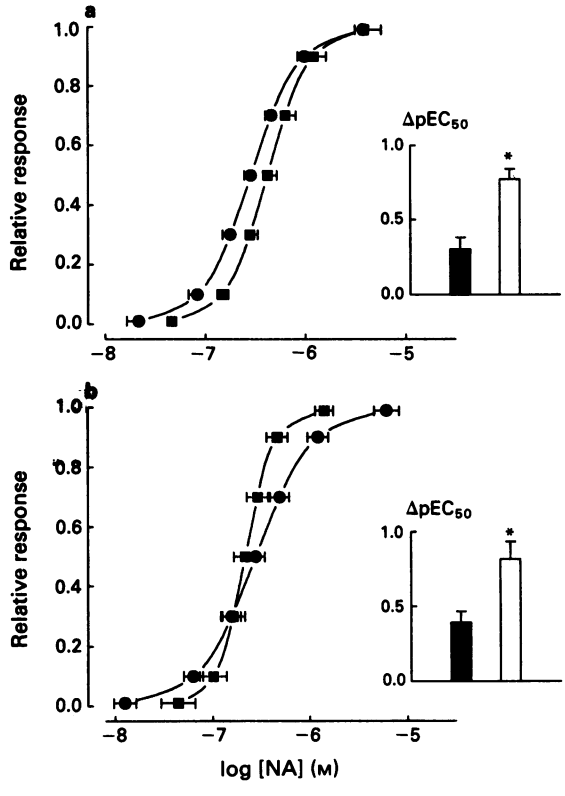

Figure 5 Effect of inhibition of neuronal amine uptake on noradrenaline (NA) concentration-response curves (a) in the presence of 3 μM cocaine and (b) after *in vitro* denervation: (●) pressurized; (■) wire-mounted vessels. Responses are given as a fraction of the maximal active tension (wire-myograph) or the maximal change in diameter (pressure-myograph). Insets show the increase in pEC_{50}-value: (a) after adding cocaine and (b) after denervation; solid columns represent pressurized and open columns wire-mounted vessels. Diameters of relaxed pressurized vessels were 323 ± 9 μm ($n = 16$) and the effective diameters of wire-mounted vessels were 280 ± 10 μm ($n = 20$). *$P < 0.05$ (unpaired t test). Analysis of the curves is shown in Table 2. S.e.means are shown where these exceed the size of the symbol.

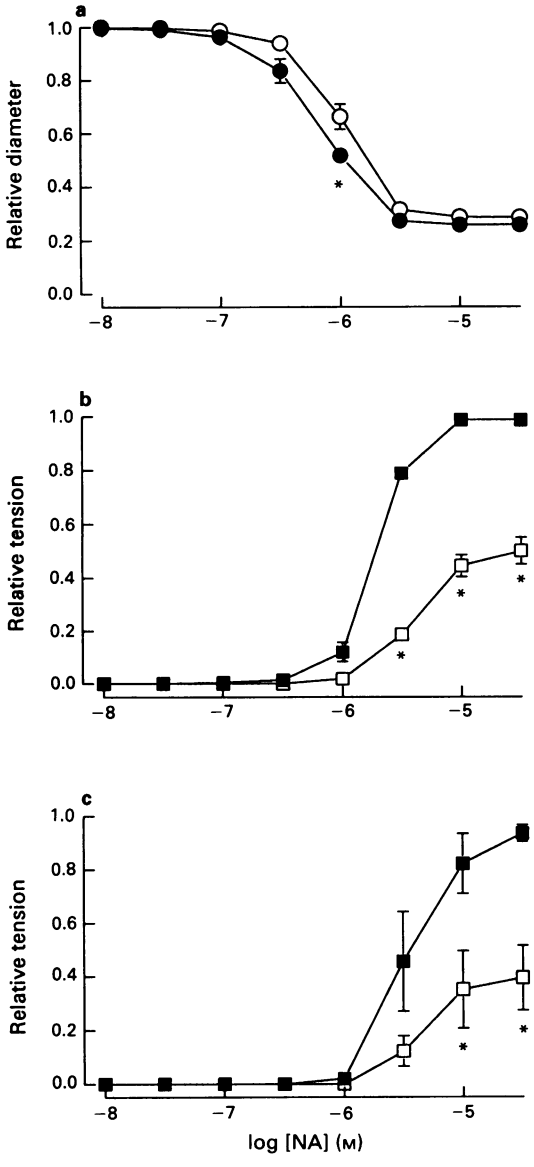

Figure 6 Concentration-response curves for noradrenaline (NA) in absence (closed symbols) and presence (open symbols) of 1 μM methoxyverapamil (D600). (a) Pressurized vessels (mean relaxed diameter 371 ± 25 μm, $n = 4$), where relative diameter given as fraction of the diameter of relaxed vessel. (b) Wire-mounted vessels at a distension of d_0 (294 μm, $n = 6$) and (c) $0.4 \times d_0$ (90 μm, $n = 6$); responses in (b) and (c) are given as fraction of the initial vessel response to the maximal concentration of noradrenaline. $^*P < 0.05$ (paired t test). S.e.means are shown where these exceed the size of the symbol.

since in both the wire- and the pressure-myographs, the NA had direct access to the adventitial surface. One possibility is that the longitudinal stretch imposed in the pressure-myograph results in the media surface area per amine pump being increased, so that the NA had freer access to the medial surface. Another possibility could be related to the observation that the effect of cocaine on the NA concentration-response relation was decreased when vessels were held at reduced diameter on the wire-myograph: in the pressure-myograph, the diameter is also greatly reduced with NA-activation. Further work is required to establish the true reason, but in any event the findings suggest that a major reason for the difference in NA pEC_{50}-values of wire-mounted and pressurized vessels is related to differences in the effectiveness of the neuronal amine pump under these conditions. This hypothesis is supported by the findings (a) that the pEC_{50} for PE (which also appears to be taken up by the amine pump, judging by the ability which we observed of cocaine to increase the pEC_{50} for PE) was also greater in pressurized vessels than for wire-mounted vessels, and (b) that the pEC_{50}-values for vasopressin and for K^+ (neither of which should be affected by the amine pump) were similar for pressurized and wire-mounted vessels.

Other mechanisms may also be responsible for differences in sensitivity on the wire- and pressure-myographs, for the NA threshold concentrations in the denervated and cocaine-exposed vessels were still slightly lower in the pressurized vessels than in the wire-mounted vessels (Figure 5), as were the vasopressin threshold concentrations (Figure 4). Such increased sensitivity is not observed when vessels are held under quasi-isobaric conditions on a wire-myograph in which the vessel distension is controlled by a motor to provide a constant pressure according to the Laplace relation (McPherson, 1992). Furthermore, threshold sensitivity in vessels held on a pressure-myograph under isometric conditions is similar to the sensitivity on such a myograph under isobaric conditions (VanBavel & Mulvany, 1994). Thus, it appears that the increased intravascular pressure itself may be causing the increase of threshold sensitivity to agonists, either directly through the increase in transmural pressure, or indirectly through the longitudinal extension caused by the increased transmural pressure. The present experiments do not show the mechanisms which are involved, but it must have some specificity, since no difference in the K^+ threshold was observed (Figure 4). The similarity of the results from NA and from PE (Figure 4, Table 1) indicate that neither α_2- nor β-adrenoceptors are involved.

Changes in maximum slope Under isobaric conditions, when a vessel contracts in response to activation, the equilibrium wall tension decreases according to the law of Laplace. This is a positive feedback mechanism, and thus isobaric activation might be expected to be an all-or-none phenomenon. That this does not happen in practice (e.g. with NA, Figure 4) is in part due to the vessel moving down the active tension-diameter curve (VanBavel & Mulvany, 1994). However, it is also likely that a myogenic mechanism is involved for, as Johnson (1980) has argued, it appears that wall tension is a regulator of vascular tone, such that a decrease in wall tension will reduce the level of activity. In isometric experiments, where resting wall tension has been varied by stretch, there is now substantial evidence that the sensitivity of vessels to α-agonists is reduced at low resting wall tensions, both in wire-mounted vessels (Price *et al.*, 1981; Nilsson & Sjøblom, 1985; McPherson, 1992) and in pressurized vessels (Lombard *et al.*, 1990; Meininger & Faber, 1991), as well as *in vivo* (Meininger & Trzeciakowski, 1988). It therefore seems plausible that the comparatively gradual maximum slope of the concentration-diameter curve, seen with agonist activation under isobaric conditions, is due to the decrease in wall tension which results from activation having a negative feedback action on vessel tone (VanBavel & Mulvany, 1994). By contrast, under isometric conditions, the increase in wall tension which accompanies activation will have a positive feedback action on vessel tone. Thus, it has been suggested (VanBavel & Mulvany, 1994) that the reason for the maximum slope being smaller for pressurized vessels compared to wire-mounted vessels may be the wall tension-regulating system proposed by Johnson (1980).

The present experiments provide some clues to a mechanism which could account for Johnson's (1980) proposed wall tension regulating system. On the basis that this system is responsible for the difference in the maximum slopes for wire-mounted and pressurized vessels, it appears that it is active not only for NA, but also for PE and vasopressin (Figure 4, Table 1). However, it does not appear to be active for K^+, where the maximum slopes for wire-mounted and pressurized vessels are the same. Furthermore, the sensitivity of wire-mounted vessels to K^+ activation is independent of

distension (Nilsson & Sjøblom, 1985). Moreover, the maximum slope of the NA concentration-response relation of wire-mounted vessels is decreased if the experiment is performed in a solution containing 30 mM K^+, which would limit any depolarizing effect of NA (Mulvany *et al.*, 1982). We can therefore hypothesize that the shallow slope of the agonist concentration-response curve of pressurized vessels is because under these conditions the agonist-induced depolarization is less than on wire-myographs. This hypothesis is supported by the finding that the verapamil analogue, D600 (which would block calcium influx through channels opened by depolarization) inhibited NA responses of wire-mounted vessels, but had little effect on pressurized vessels (Figure 6). The hypothesis does not explain, however, why cocaine (3 μM) caused a reduction of the maximum slope of wire-mounted vessels (Table 2a), a phenomenon which has been previously ascribed to high concentrations of noradrenaline causing saturation of the amine pump (Langer & Trendelenburg, 1969). Furthermore, we have found (Nilsson, Flatman & Mulvany, unpublished observations) that this concentration of cocaine does not affect the relation between force production and membrane potential in wire-mounted vessels, which argues against the maximum slope being dependent on this relation. More work, including measurements of membrane potential on a pressure-myograph, is required to elucidate this question.

Lack of action of D600 in pressurized vessels

Although the lack of action of D600 on the NA response of pressurized vessels could be explained as described above if such vessels did not depolarize in response to noradrenaline, that possibility remains to be tested. We have therefore considered other possibilities. The lack of action on pressurized vessels contrasts with the potent effect on isometric responses, as shown here (Figure 6), and previously (Nyborg & Mulvany, 1984). The lack of effect was not due to the D600 inactivating in the pressure-myograph chamber, since the vasomotion which was seen with NA activated vessels, disappeared in the presence of D600, as has been observed with other calcium antagonists (Gustafsson & Nilsson, 1991). Furthermore, the observed difference in action cannot be explained by an influence of the vessel diameter on the action of D600, since the response to NA was still reduced by about 50% at a low distension in the wire-myograph (Figure 6c). In support of our findings, an *in vivo* study on arterioles (De Clerck *et al.*, 1989) found no reduction in maximal vasoconstriction to NA, but only a reduction in sensitivity after treatment with verapamil. Further studies are required to determine the reason for this substantial difference between the responses of wire-mounted and pressurized vessels to a calcium-antagonist.

Perspectives

In summary, the results indicate that pressurized mesenteric vessels have a higher sensitivity to α-agonists (expressed as a pEC_{50}) than wire-mounted vessels under circumstances of the same initial smooth muscle cell length. This appears to be due to a smaller neuronal uptake of agonists in the pressurized vessel. But this only explains part of the difference as all the agonists, except potassium, showed a smaller threshold concentration in the pressure-myograph indicating that other factors are of importance. Furthermore, wire-mounted vessels have a steeper agonist concentration-response relation than pressurized vessels, while the calcium antagonist, D600, was a potent inhibitor of NA responses in wire-mounted vessels, but had little effect in pressurized vessels. Since the *in vivo* situation corresponds more closely to an isobaric condition than to an isometric condition, the results presented here raise the possibility that responses obtained under isometric conditions may in part be mediated by mechanisms which are less important under *in vivo* conditions. Thus, although isometric experiments are convenient to perform, our results provide additional cause for caution in interpreting them in terms of the *in vivo* situation.

We thank Dr Christian Aalkjær for critical discussion. This work was supported by the Danish Medical Research Council and the Danish Heart Foundation. The authors are members of the European Working Party on Resistance Artery Disease (EURAD), supported by the European Community under the BIOMED 1 programme. M.J.M. is a member of the Aarhus University Cardiovascular Research Centre.

References

APRIGLIANO, O. & HERMSMEYER, K. (1976). In vitro denervation of the portal vein and caudal artery of the rat. *J. Pharmacol. Exp. Ther.*, **198**, 568–577.

BUUS, N.H. & MULVANY, M.J. (1992). Noradrenaline sensitivity of rat mesenteric small arteries determined on a pressure myograph and a wire myograph. *Acta Physiol. Scand.*, **146** (suppl 608), 54 (abstract).

CAREW, T.E., VAISHNAV, R.N. & PATEL, D.J. (1968). Compressibility of the arterial wall. *Circ. Res.*, **23**, 61–68.

DE CLERCK, F., LOOTS, W., VOETEN, J. & JANSSEN, P.A.J. (1989). Differential effects of verapamil and flunarizine on epinephrine-induced vasoconstriction and on spontaneous vasomotion of arterioles in skeletal muscle in the rat in vivo. *J. Cardiovasc. Pharmacol.*, **13**, 76–83.

DOHI, Y. & LÜSCHER, T.F. (1990). Aging differentially affects direct and indirect actions of endothelin-1 in perfused mesenteric arteries of the rat. *Br. J. Pharmacol.*, **100**, 889–893.

GUSTAFSSON, H. & NILSSON, H. (1991). Rhythmic contractions of isolated small arteries. In *Resistance Arteries, Structure and Function*. ed. Mulvany, M.J., Aalkjær, C., Heagerty, A.M., Nyborg, N.C.B. & Strandgaard, S. pp. 196–198. Amsterdam: Elsevier Science Publishers.

HALPERN, W. & KELLEY, M. (1991). In vitro methodology for resistance arteries. *Blood Vessels*, **28**, 245–251.

HALPERN, W. & OSOL, G. (1985). Blood vessel diameter measurement. *Prog. Appl. Microcirc.*, **8**, 32–39.

HALPERN, W., OSOL, R. & OSOL, G. (1987). Activation induces myogenic-like diameter responses to dynamic pressure changes in isolated and pressurized small mesenteric arteries in the rat. In *Vascular Neuroeffect or Mechanisms*. ed. Bevan, J.A., Majewski, H., Maxwell, R.A. & Story, D.F. pp. 15–22. Washington DC: JRL Press Ltd.

JOHNSON, P.C. (1980). The myogenic response. In *Handbook of Physiology – The Cardiovascular System*. ed. Bohr, D.R., Somlyo, A.P. & Sparks, Jr, H.V. pp. 409–442. Bethesda: The American Physiological Society.

LANGER, S.Z. & TRENDELENBURG, U. (1969). The effect of a saturable uptake mechanism on the slopes of dose-response curves for sympathetic amines and on the shifts of dose-response curves produced by a competitive antagonist. *J. Pharmacol. Exp. Ther.*, **167**, 117–142.

LEW, M.J. & ANGUS, J.A. (1992). Wall thickness to lumen diameter ratios of arteries from SHR and WKY: comparison of pressurised and wire-mounted preparations. *J. Vasc. Res.*, **29**, 443–449.

LOMBARD, J.H., ESKINDER, H., KAUSER, K., OSBORN, J.L. & HARDER, D.R. (1990). Enhanced norepinephrine sensitivity in renal arteries at elevated transmural pressure. *Am. J. Physiol.*, **259**, H29–H33.

MARSHALL, J.M. (1977). The effect of uptake by adrenergic nerve terminals on the sensitivity of arterial vessels to topically applied noradrenaline. *Br. J. Pharmacol.*, **61**, 429–432.

McCARRON, J.G., QUAYLE, J.M., HALPERN, W. & NELSON, M.T. (1991). Cromakalim and pinacidil dilate small mesenteric arteries but not small cerebral arteries. *Am. J. Physiol.*, **261**, H287–H291.

McPHERSON, G.A. (1992). Assessing vascular reactivity of arteries in the small vessel myograph. *Clin. Exp. Pharmacol. Physiol.*, **19**, 815–825.

MEININGER, G.A. & FABER, J.E. (1991). Adrenergic facilitation of myogenic response in skeletal muscle arterioles. *Am. J. Physiol.*, **260**, H1424–H1432.

MEININGER, G.A. & TRZECIAKOWSKI, J.P. (1988). Vasoconstriction is amplified by autoregulation during vasoconstrictor-induced hypertension. *Am. J. Physiol.*, **254**, H709–H718.

MULVANY, M.J. & AALKJÆR, C. (1990). Structure and function of small arteries. *Physiol. Rev.*, **70**, 921–961.

MULVANY, M.J. & HALPERN, W. (1977). Contractile properties of small arterial resistance vessels in spontaneously hypertensive and normotensive rats. *Circ. Res.*, **41**, 19–26.

MULVANY, M.J., NILSSON, H. & FLATMAN, J.A. (1982). Role of membrane potential in the response of rat small mesenteric arteries to exogenous noradrenaline stimulation. *J. Physiol.*, **332**, 363–373.

NIELSEN, H. & MULVANY, M.J. (1990). The divergence in the excitation-contraction coupling of rat mesenteric resistance arteries lies distal to the receptor site. *Eur. J. Pharmacol.*, **179**, 1–7.

NILSSON, H. & SJÖBLOM, N. (1985). Distension-dependent changes in noradrenaline sensitivity in small arteries from the rat. *Acta Physiol. Scand.*, **125**, 429–435.

NYBORG, N.C.B. & MULVANY, M.J. (1984). Effect of felodipine, a new dihydropyridine vasodilator, on contractile responses to potassium, noradrenaline and calcium in mesenteric resistance vessels of the rat. *J. Cardiovasc. Pharmacol.*, **6**, 499–505.

NYBORG, N.C.B. & MIKKELSEN, E.O. (1985). In vitro studies on responses to noradrenaline, serotonin, and potassium of intramyocardial and mesenteric vessels from wistar rats. *J. Cardiovasc. Pharmacol.*, **7**, 417–423.

PRICE, J.M., DAVIS, D.L. & KNAUSS, E.B. (1981). Length-dependent sensitivity in vascular smooth muscle. *Am. J. Physiol.*, **241**, H557–H563.

RAWLAW, A., FLEIG, H., KURAHASHI, K. & TRENDELENBURG, U. (1980). The neuronal and extraneuronal uptake and deamination of ^{3}H-(−)-phenylephrine in the perfused rat heart. *Naunyn-Schmied. Arch. Pharmacol.*, **314**, 237–247.

TESFAMARIAM, B. & HALPERN, W. (1988). Asymmetry of responses to noradrenaline in perfused resistance arteries. *Eur. J. Pharmacol.*, **152**, 167–170.

TESFAMARIAM, B., HALPERN, W. & OSOL, G.K. (1985). Effects of perfusion and endothelium on the reactivity of isolated resistance arteries. *Blood Vessels*, **22**, 301–305.

VANBAVEL, E., GIEZEMAN, M.J.M.M., MOOIJ, T. & SPAAN, J.A.E. (1991). Influence of pressure alterations on tone and vasomotion of isolated mesenteric small arteries of the rat. *J. Physiol.*, **436**, 371–383.

VANBAVEL, E., MOOIJ, T., GIEZEMAN, M.J.M.M. & SPAAN, J.A.E. (1990). Cannulation and continuous cross-sectional area measurement of small blood vessels. *J. Pharmacol. Methods*, **24**, 219–227.

VANBAVEL, E. & MULVANY, M.J. (1994). Role of wall tension in the vasoconstrictor response of cannulated rat small arteries. *J. Physiol.*, (in press).

VENNING, M.G. & DE LA LANDE, I.S. (1984). Effects of uptake and surface of entry on the responses of the rat caudal artery to noradrenaline, adrenaline and methoxamine. *Blood Vessels*, **21**, 149–155.

VENNING, M.G. & DE LA LANDE, I.S. (1988). Role of sympathetic nerves in disposition and metabolism of intraluminal and extraluminal noradrenaline in the rabbit ear artery. *Blood Vessels*, **25**, 232–239.

WHALL, C.W., MYERS, M.M. & HALPERN, W. (1980). Norepinephrine sensitivity, tension development and neuronal uptake in resistance arteries from spontaneously hypertensive and normotensive rats. *Blood Vessels*, **17**, 1–15.

(Received September 6, 1993
Revised January 17, 1994
Accepted February 8, 1994)

Br. J. Pharmacol. (1994), **112**, 588–594

The effect of leukocyte depletion on pulmonary M_2 muscarinic receptor function in parainfluenza virus-infected guinea-pigs

Allison D. Fryer, Kathryn A. Yarkony & [1]*David B. Jacoby

Department of Environmental Health Sciences, School of Hygiene and Public Health, and *Division of Pulmonary and Critical Care Medicine, Johns Hopkins Asthma and Allergy Center, Johns Hopkins University, Baltimore, Maryland 21224, U.S.A.

1 Parainfluenza infections of the airways cause dysfunction of inhibitory M_2 muscarinic receptors on the pulmonary parasympathetic nerves. To distinguish the direct effects of virus from the effects of virus-induced airway inflammation on M_2 muscarinic receptor function, guinea-pigs were depleted of leukocytes by pretreating with cyclophosphamide (30 mg kg^{-1}, i.p. daily for 7 days) after which they were infected with parainfluenza virus type 1 (Sendai virus).

2 Guinea-pigs were anaesthetized, tracheotomized, and ventilated. The vagus nerves were isolated and cut, and the distal ends were electrically stimulated causing bronchoconstriction. In control animals, pilocarpine (1–100 μg kg^{-1}, i.v.) inhibited and gallamine (0.1–10 mg kg^{-1}, i.v.) potentiated vagally-induced bronchoconstriction by stimulating or blocking M_2 muscarinic receptors on the vagus. These effects of pilocarpine and gallamine were almost completely lost in virus-infected animals, demonstrating loss of M_2 receptor function.

3 Cyclophosphamide depleted peripheral blood leukocytes and inhibited the virus-induced influx of inflammatory cells into the lung. Depletion of leukocytes protected M_2 receptor function from viral infection in some, but not all, guinea-pigs tested.

4 Among infected animals that had been depleted of leukocytes, the viral content (expressed as the log of the number of tissue culture infectious doses per g lung tissue) of those that retained normal M_2 receptor function was 4.29 ± 0.05 (mean ± s.e.mean), while the viral content of those that lost M_2 receptor function despite leukocyte depletion was 5.45 ± 0.20 ($P = 0.011$). Thus the viral content of the lungs in which M_2 receptor function was lost was 16 times greater than that of the lungs in which M_2 receptor function was preserved. Viral content correlated with the inhibition of vagally-mediated bronchoconstriction after the maximum dose of pilocarpine (100 μg kg^{-1}; $r^2 = 0.81$, $P = 0.0004$).

5 In antigen-challenged animals, inhibitory M_2 muscarinic receptor function is restored when positively charged inflammatory cell proteins are bound and neutralized by heparin. However, heparin (2000 u kg^{-1}, i.v.) did not reverse virus-induced loss of M_2 muscarinic receptor function, even in those guinea-pigs with a lower viral titer.

6 Because leukocyte depletion protected M_2 muscarinic receptor function only in animals with mild viral infections, it appears that viruses have both an indirect, leukocyte-dependent effect on M_2 receptors and, in animals with more severe infections, a leukocyte-independent effect on M_2 receptors. The failure of heparin to restore M_2 receptor function demonstrates that the leukocyte-dependent loss of M_2 receptor function is not mediated by positively charged inflammatory cell proteins.

Keywords: Virus; parasympathetic nerves; vagus nerves; muscarinic receptors; airway inflammation; airway smooth muscle; asthma; cyclophosphamide; pilocarpine; gallamine

Introduction

Asthma exacerbations are frequently the result of viral airway infections (Welliver, 1983). Even in normal subjects, viral infections increase airway resistance (Johanson *et al.*, 1969) and airway responsiveness (Empey *et al.*, 1976; Aquilina *et al.*, 1980).

Much of this virus-induced airway hyperresponsiveness is mediated by the vagus nerves as it is blocked by atropine (Empey *et al.*, 1976; Aquilina *et al.*, 1980). Furthermore, it is the activity of the efferent cholinergic nerves which is increased since bronchoconstriction induced by electrical stimulation of these nerves is potentiated by viral infection (Buckner *et al.*, 1985). There is no evidence that the M_3 muscarinic receptors, which are responsible for airway smooth muscle contraction, are altered by viral infection (Buckner *et al.*, 1985; Jacoby *et al.*, 1988; Dusser *et al.*, 1989). However, the M_2 muscarinic receptors on the vagus nerves in the lung, which normally inhibit acetylcholine (ACh) release (Fryer & Maclagan, 1984), are no longer functional in virus infected guinea-pigs (Fryer & Jacoby, 1991).

Dysfunction of inhibitory M_2 muscarinic receptors may be a direct effect of viral neuraminidase, which cleaves sialic acid residues from the M_2 receptors, thereby decreasing agonist affinity for the receptors (Fryer *et al.*, 1990). Alternatively, inflammatory cells and their products may be important participants in loss of M_2 receptor function. In ozone-exposed and in antigen-challenged guinea-pigs, depletion of inflammatory cells protects the function of the neuronal M_2 muscarinic receptors (Fryer & Jacoby, 1992; Gambone & Fryer, 1992; Jacoby *et al.*, 1993). Furthermore, administering heparin to the antigen challenged guinea-pig acutely restores neuronal M_2 receptor function, probably by binding to and neutralizing positively charged inflammatory cell protins such as eosinophil major basic protein (Fryer & Jacoby, 1992; Jacoby *et al.*, 1993). In order to determine whether inflammatory cells are essential to virus-induced loss of neuronal M_2 muscarinic receptors, we tested the effect of leukocyte depletion on M_2 receptor function in parainfluenza virus-infected guinea-pigs. We also tested the effect of heparin in virus-infected guinea-pigs that were not depleted of leukocytes.

[1] Author for correspondence.

Methods

Leukocyte depletion

Pathogen-free guinea-pigs (Dunkin-Hartley, 250–350 g) were injected intraperitoneally with cyclophosphamide (30 mg kg^{-1}) daily for seven days. A separate group was injected with sterile saline.

Virus infection

Parainfluenza type 1 (Sendai virus; ATCC VT-105) was grown in Rhesus monkey kidney cell monolayers in L-15 medium for one week at 34°C. Cultures were frozen and thawed to disrupt cells, cleared by low-speed centrifugation, and stored in aliquots at −70°C.

Viral content was determined by exposing fresh Rhesus monkey kidney cell monolayers to serial 10 fold dilutions of the stock solution. After incubation for 1 week at 34°C, the monolayers were washed and the medium was replaced with a 0.5% suspension of guinea-pig erythrocytes. After 1 h, the erythrocytes were washed off, and the monolayers were examined under an inverted phase-contrast microscope (Olympus) for evidence of haemadsorption (sticking of erythrocytes to the surface of cells expressing the viral hemogglutinin on their surfaces) (Shelokov *et al.*, 1958). Viral content was determined as the multiple of the amount of stock solution required to produce infection in 50% of Rhesus monkey kidney monolayers, the $TCID_{50}$.

Guinea-pigs were anaesthetized with ketamine (45 mg kg^{-1}, i.m.) and xylazine (8 mg kg^{-1}, i.m.). Animals in the infected group were inoculated intranasally with 1 ml virus solution that contained 10^5 $TCID_{50}$ ml^{-1}, obtained by diluting the viral stock in Dulbecco's phosphate-buffered saline. Animals in the uninfected (control) group were inoculated intranasally with fluids obtained from virus-free Rhesus monkey kidney cells that were prepared and diluted in phosphate-buffered saline in the same way as the viral solutions. Control and infected animals were housed in separate laminar flow hoods.

Virus isolation and titration

After physiological studies were completed, the guinea-pig lungs were removed and stored at −70°C. Frozen samples were thawed, weighed, and homogenized in 2 ml phosphate-buffered saline (Polytron, Brinkman, Lucerne, Switzerland). Virus was eluted from the tissue homogenate by incubating at 34°C for 1 h. The suspensions were centrifuged at 400 *g* for 30 min, and the viral content of the supernatants was determined by inoculating Rhesus monkey kidney cell monolayers as above.

Anaesthesia and measurement of pulmonary inflation pressure (Ppi)

Four days after inoculation with virus or with control media, guinea-pigs were anaesthetized with urethane (1.5 g kg^{-1}) injected intraperitoneally. This dose of urethane produces a deep anaesthesia lasting 8–10 h (Green, 1982). None of the experiments described lasted longer than 3 h and the depth of anaesthesia was monitored by observing for fluctuations in heart rate and blood pressure. Guinea-pigs were handled in accordance with the standards established by the U.S.A. Animal Welfare Acts set forth in National Institute of Health guidelines and the Policy and Procedures Manual published by the Johns Hopkins University School of Hygiene and Public Health Animal Care and Use Committee.

Once the guinea-pigs were anaesthetized, a carotid artery was cannulated for measurement of blood pressure and heart rate. Cannulae were placed into both jugular veins for the administration of drugs. Both vagi were cut and the distal portions were placed on shielded platinum electrodes immersed in a pool of liquid paraffin. The animal's body temperature was maintained at 37°C with a heating blanket.

The animals were paralyzed with suxamethonium (infused at 10 μg kg^{-1} min^{-1}), tracheostomized, and ventilated with a positive pressure, constant volume animal ventilator (Harvard Apparatus Co., South Natick, MA, U.S.A.) (tidal volume 2.5–3.5 ml, 100–120 breaths min^{-1}). P_{O_2} and P_{CO_2} were measured from arterial blood samples at the beginning and the end of each experiment (Corning 170 pH/blood gas analyzer; Corning Glass, Medfield, MA, U.S.A.). Airflow was recorded as the pressure drop across a Fleish pneumotachograph (3/0) measured with a Grass differential pressure transducer (PT5B). The airflow signal was integrated to give tidal volume. Pulmonary inflation pressure (Ppi) was measured with a Spectromed pressure transducer (DTX). All signals were displayed on a Grass polygraph.

A positive pressure of 85–100 mmH_2O was needed for adequate ventilation of the animals. Given constant flow and volume, bronchoconstriction was measured as the increase in Ppi over the baseline inflation pressure (Dixon & Brody, 1903). The Ppi signal from the driver was fed into the input of the preamplifier of a second channel on the polygraph, and the baseline Ppi was subtracted electrically (Burden & Parkes, 1971). Thus Ppi was recorded on one channel and increases in Ppi were recorded on a separate channel at a higher sensitivity. Using this method it was possible to accurately measure increases in Ppi as small as 2 mmH_2O above baseline.

Vagal stimulation and M_2 receptor function

Simultaneous stimulation of both vagus nerves (2 and 15 Hz, 0.2 ms pulse duration, 5–20 V, 45 pulses per train) caused bronchoconstriction and a fall in heart rate. Both of these responses were rapidly reversed upon cessation of stimulation. Because the response of the neuronal M_2 receptor to endogenous agonists (ACh released from the nerves) is greater at high stimulus frequencies (Fryer & Maclagan, 1984), the effects of the M_2 antagonist, gallamine, were tested using stimulation at 15 Hz, while the effects of the muscarinic agonist, pilocarpine, were tested using stimulation at 2 Hz. The nerves were stimulated regularly at 1 min intervals. All animals were pretreated with guanethidine (5 mg kg^{-1}, i.v.). This dose of guanethidine depletes noradrenaline, and it produced a temporary reduction in the magnitude of the vagally-induced bronchoconstriction and bradycardia (Blaber *et al.*, 1985). Thirty minutes after guanethidine, when the responses to stimulation of the vagus nerves were back to pre-guanethidine values and were reproducible, cumulative dose-response curves measuring the effect of pilocarpine (1–100 μg kg^{-1}) or gallamine (0.1–10.0 mg kg^{-1}) on vagally-induced bronchoconstriction were performed. Doses of pilocarpine greater than 30 μg kg^{-1} produced a transient bronchoconstriction. Therefore, the effect of these doses of pilocarpine on vagally-induced bronchoconstriction was measured after the Ppi had returned to baseline. Doses of pilocarpine greater than 100 μg kg^{-1} were not used because they caused sustained bronchoconstriction via stimulation of muscarinic receptors on the airway smooth muscle. At the end of each experiment vagally-induced bronchoconstriction and bradycardia were abolished by atropine (1 mg kg^{-1}, i.v.) indicating that both of these responses were mediated via release of ACh onto muscarinic receptors.

In a group of virus-infected guinea-pigs that had not been pretreated with cyclophosphamide, heparin (2000 u kg^{-1}, i.v.) was given after the baseline response to vagal stimulation had been established but before administration of gallamine. We have previously shown that this treatment reverses the M_2 receptor dysfunction in antigen-challenged guinea-pigs (Fryer & Jacoby, 1992). In this way, the role of cationic inflammatory cell proteins such as eosinophil major basic protein was assessed.

Measurement of inflammatory cells

At the end of the each experiment, the lungs were lavaged four times with 10 ml aliquots of warm phosphate-buffered saline that contained 0.2 M EDTA and 10^{-4} M isoprenaline. Lavage fluids were centrifuged (400 *g*, 10 min) and the pellets were resuspended in normal saline. Cells were counted in a haemocytometer. Slides made of lavaged cells using a cytospin were stained with Diff-Quik (American Scientific Products) and used to determine cell differentials. Blood was also obtained via the carotid artery cannula. After eliminating the erythrocytes by hypotonic lysis, the remaining leukocytes were counted as above.

Drugs

Pilocarpine, suxamethonium, atropine, isoprenaline, urethane and L-15 medium were purchased from Sigma, St. Louis, Missouri, U.S.A.; guanethidine was supplied by CIBA, Summit, New Jersey, U.S.A.; and ketamine was purchased from Aveco Co Inc., Fort Dodge, Iowa, U.S.A. Xylazine was purchased from Mobay Corp, Shawnee, Kansas, U.S.A. All drugs were dissolved and diluted in 0.9% NaCl. Rhesus monkey kidney cells were purchased from Viromed, Minnetonka, Minnesota, U.S.A.

Statistics

The effects of viral infection and of leukocyte depletion on dose-response curves to pilocarpine were compared by two way analyses of variance. Viral content of the lungs and cell counts and differentials in various groups of animals were compared by one-way analysis of variance. A P value less than 0.05 was considered significant.

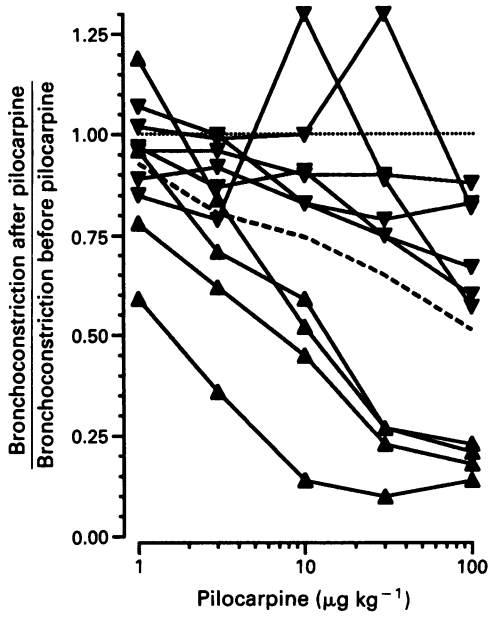

Figure 1 The effect of pilocarpine on vagally-induced bronchoconstriction in cyclophosphamide treated guinea-pigs. Animals were depleted of leukocytes by pretreating with cyclophosphamide before viral infection. Pilocarpine was administered before stimulating the vagus: (▲) represent results from individual animals that responded to pilocarpine; (▼) represent individual animals that were refractory to pilocarpine. The mean of all ten animals is shown by a dashed line. Results are expressed as the ratio of vagally-induced bronchoconstriction in the presence of pilocarpine to the response to vagal stimulation in the absence of pilocarpine (0.2 ms, 5–30 V, 2 Hz, 44 pulses train^{-1}).

Results

Viral infection

All animals that were exposed to parainfluenza virus became infected as shown by recovery of infectious virus from lung homogenates into Rhesus monkey kidney cells. Viral content was determined as the multiple of the amount of stock solution required to produce infection in 50% of Rhesus monkey kidney monolayers (the $TCID_{50}$). Viral content of lungs from non-cyclophosphamide treated animals was 4.4 ± 0.19 log$TCID_{50}$ g^{-1} lung tissue ($n = 10$) while that from cyclophosphamide treated animals was 5.0 ± 0.23 log$TCID_{50}$ g^{-1} lung tissue ($n = 12$; $P = 0.049$). No virus was recovered from control (uninfected) animals.

Inhibitory M_2 muscarinic receptor function

There was no difference in baseline Ppi (100 ± 8.2 mmH_2O controls, 107 ± 11.4 mmH_2O infected) or baseline heart rate (301 ± 11.3 beats min^{-1} controls, 288 ± 15.6 beats min^{-1} infected) between control and virus-infected guinea-pigs; these responses were also unaffected by cyclophosphamide treatment as well as by viral infection of leukocyte-depleted guinea-pigs (data not shown). Electrical stimulation of the vagus nerves caused bronchoconstriction (measured as an increase in Ppi) and bradycardia in both groups. Stimulus voltage was adjusted within a range of 5–20 V to yield comparable bronchoconstriction responses in all groups of animals. In the cyclophosphamide-treated, virus-infected group, pilocarpine inhibited the bronchoconstrictor response to vagal stimulation in 4 animals (showing preservation of M_2 receptor function (▲)), but failed to inhibit this response in 6 animals (showing loss of M_2 receptor function; (▼), Figures 1 and 2). In control (uninfected) guinea-pigs, stimulation of M_2 muscarinic receptors on the parasympathetic nerves by pilocarpine inhibited vagally-induced bronchoconstriction

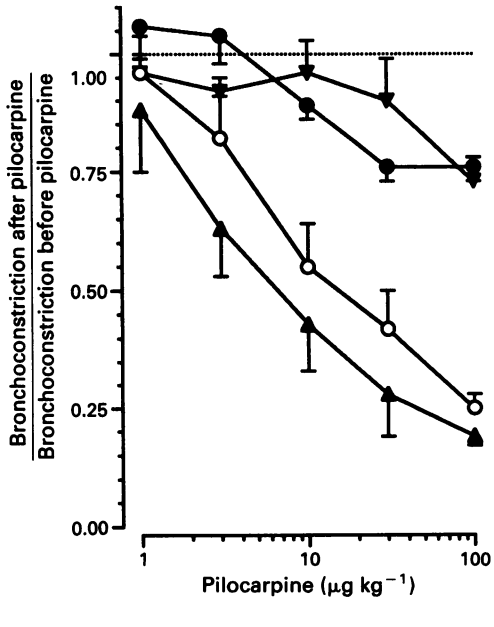

Figure 2 Cyclophosphamide does not protect the function of M_2 muscarinic receptors from viral infection in all guinea-pigs. The effect of pilocarpine on bronchoconstriction after vagal stimulation was measured in control (○, $n = 5$) or virus-infected guinea-pigs (●, $n = 5$). In animals that were depleted of leukocytes by pretreating with cyclophosphamide before viral infection, pilocarpine inhibited vagally-induced bronchoconstriction in 4 animals (▲) and did not in 6 animals (▼). Results are expressed as in Figure 1. Vagally-induced bronchoconstriction in the absence of pilocarpine was (in mmH_2O) for controls 20.8 ± 1.15, for virus infected 21.6 ± 9.8, for cyclophosphamide/pilocarpine-refractory 17.6 ± 2.3, and for cyclophosphamide/pilocarpine-responsive 22.6 ± 1.0.

in dose-dependent fashion ((○), Figure 2). In contrast, pilocarpine was not an effective inhibitor of vagally-induced bronchoconstriction in guinea-pigs infected with parainfluenza virus but not pretreated with cyclophosphamide ((●), Figure 2). The effect of pilocarpine on vagally-induced bronchoconstriction in guinea-pigs treated with cyclophosphamide and not infected with virus was not different from controls (data not shown).

Viral content of lungs from cyclophosphamide-treated animals

As noted above, the lungs of cyclophosphamide-treated, virus-infected animals contained 5.0 ± 0.23 log$TCID_{50}$ g^{-1} lung tissue. Because the cyclophosphamide-treated, virus-infected animals fell so clearly into two groups with respect to M_2 receptor function (see Figure 1), we analysed the viral content of the lungs of these two groups. We defined the group in which M_2 receptor function was preserved as those in which the response to vagal stimulation after the maximal dose of pilocarpine (100 $\mu g\ kg^{-1}$) was less than 50% (equivalent to a ratio of 0.5 in Figure 2) of the baseline response to vagal stimulation, and the group in which M_2 receptor function was lost as those in which the response to vagal stimulation after pilocarpine remained greater than 50% of the baseline response. The viral content of the lungs from those that lost M_2 receptor function was 5.45 ± 0.20, while among those in which receptor function was preserved the viral content was 4.29 ± 0.05 log$TCID_{50}$ g^{-1} lung tissue ($P = 0.011$; Figure 3). Thus, the lungs of those guinea-pigs that lost M_2 receptor function contained 16 times as much virus as the lungs of those that retained normal M_2 receptor function. Among these cyclophosphamide-treated animals, lung viral content correlated with the response to vagal stimulation after pilocarpine 100 $\mu g\ kg^{-1}$ ($r^2 = 0.81$, $P = 0.0004$; Figure 4).

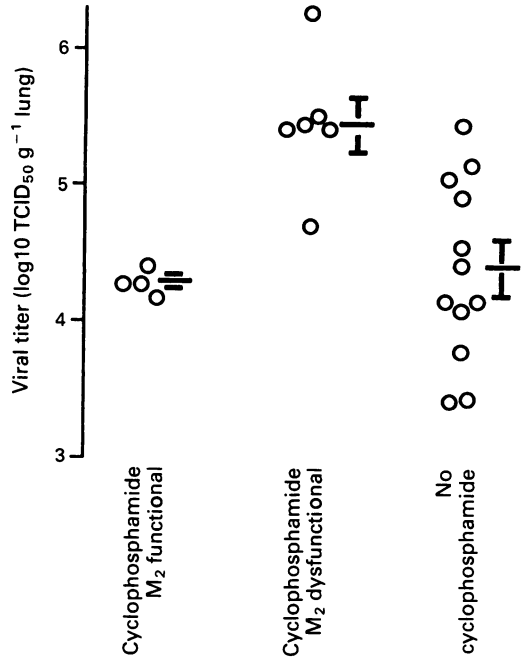

Figure 3 Viral contents of the lungs was significantly greater in the 6 animals that lost M_2 receptor function despite leukocyte depletion than it was in the 4 animals that retained normal M_2 receptor function ($P = 0.011$). The viral content of the lungs of non-cyclophosphamide-treated animals overlaps both of the cyclophosphamide-treated groups.

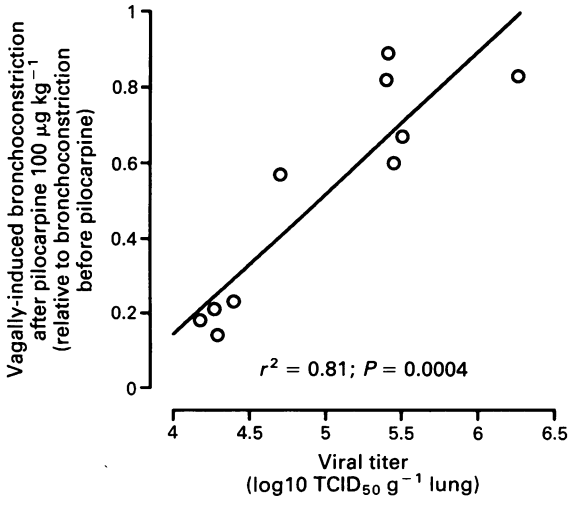

Figure 4 Viral content of the lungs of cyclophosphamide-treated guinea-pigs correlates with M_2 receptor function (expressed as the ratio of vagally-induced bronchoconstriction after pilocarpine 100 $\mu g\ kg^{-1}$, i.v. to the response to vagal stimulation in the absence of pilocarpine).

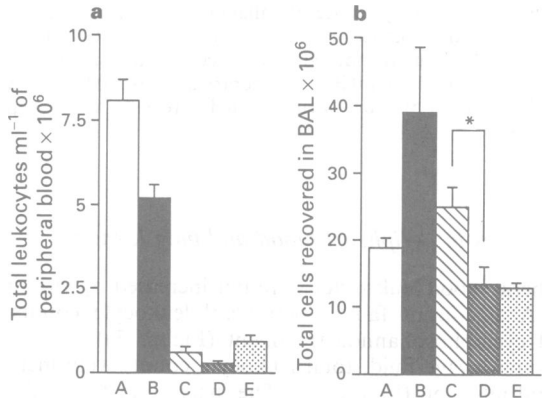

Figure 5 Effect of cyclophosphamide pretreatment on peripheral blood leukocytes (a) and lung lavage leukocytes (b). Controls are shown as (A); virus infected as (B); cyclophosphamide + low titer virus as (C); cyclophosphamide + high titer virus as (D) and cyclophosphamide alone as (E). Asterisk represents a significant difference between high and low viral titer animals ($P < 0.05$, t test with Bonferroni correction).

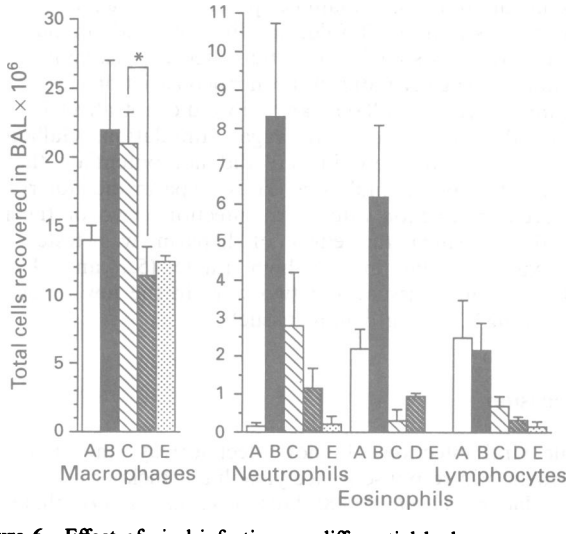

Figure 6 Effect of viral infection on differential leukocyte counts in lung lavage. Controls are shown as (A); virus infected as (B); cyclophosphamide + low titer virus as (C); cyclophosphamide + high titer virus as (D) and cyclophosphamide alone as (E). Asterisk represents a significant difference between high and low viral titer animals ($P < 0.05$, t test with Bonferroni correction).

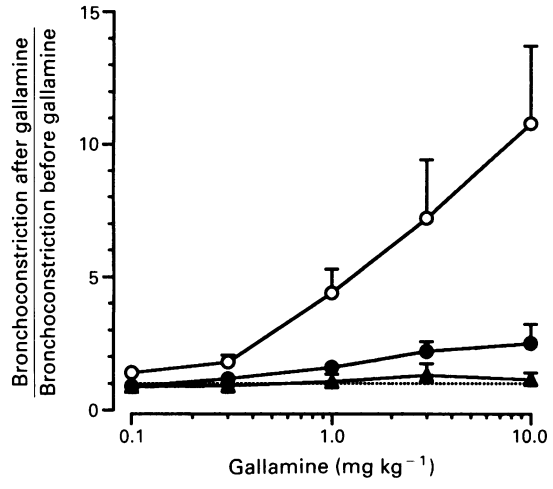

Figure 7 Effect of heparin on the function of neuronal M_2 muscarinic receptors in the lungs of infected guinea-pigs. Gallamine potentiation of bronchoconstriction was measured in control (○, $n = 4$), virus-infected (●, $n = 4$), or virus-infected + heparin (▲, $n = 4$). Results are expressed as the ratio of vagally-induced bronchoconstriction in the presence of gallamine to the response to vagal stimulation in the absence of gallamine (0.2 ms, 5–30 V, 15 Hz, 75 pulses train^{-1}). Vagally-induced bronchoconstriction in the absence of gallamine was (in $mmHO_2$) for controls, 15.6 ± 0.83; for virus-infected, 18.7 ± 1.5; for virus-infected treated with heparin, 14.8 ± 1.9.

Leukocytes in peripheral blood and lung lavage

Peripheral blood leukocytes were not increased by viral infection. A significant fall in peripheral leukocyte counts followed cyclophosphamide treatment (Figure 5a).

In lung lavage fluid, total leukocyte counts were increased by viral infection (Figure 5b). The increase in total cells was made up primarily of neutrophils and eosinophils, with a non-significant trend towards an increase in macrophages (Figure 6). These increases were prevented by pretreatment with cyclophosphamide (Figures 5 and 6).

Effect of heparin on M_2 receptor function in virus-infected guinea-pigs

In control animals, gallamine potentiated vagally-induced bronchoconstriction 10 fold. In virus-infected animals this potentiation was significantly attenuated and gallamine only potentiated vagally-induced bronchoconstriction by 2 fold (Figure 7). Heparin (2000 u kg^{-1}, i.v.) did not affect baseline Ppi or the Ppi response to vagal stimulation. Gallamine, given 30 min after heparin, still did not potentiate the Ppi response to vagal stimulation. Thus, heparin did not restore M_2 receptor function after viral infection. Two of the four animals in which the effect of heparin was tested had lung viral content in the high range (5.1 and 4.9 log-$TCID_{50}$ g^{-1} lung tissue) and two were in the low range (4.1 and 4.2 log$TCID_{50}$ g^{-1} lung tissue).

Discussion

While viral infections do not affect airway smooth muscle contraction in response to acetylcholine (Buckner *et al.*, 1981; 1985; Jacoby *et al.*, 1988; Dusser *et al.*, 1989), there are substantial changes in the neural control of airway smooth muscle. Increased vagally-mediated reflex bronchoconstriction has been reported in humans (Empey *et al.*, 1976; Aquilina *et al.*, 1980) and in experimental animals (Buckner *et al.*, 1981). Guinea-pigs infected with parainfluenza virus have an increased response to electrical stimulation of the vagus nerves (Buckner *et al.*, 1981), which results from dysfunction of inhibitory neuronal M_2 receptors (Fryer & Jacoby, 1991).

We have previously suggested that parainfluenza virus-induced pulmonary M_2 receptor dysfunction may be the result of cleavage of sialic acid residues from M_2 receptors by neuraminidase, an enzyme present on the virus (Fryer *et al.*, 1990; Fryer & Jacoby, 1991). Exposing M_2 receptors to parainfluenza virus *in vitro* decreases agonist affinity for the receptors by an order of magnitude. This effect can be blocked by the neuraminidase inhibitor, 2,3-dehydro-2-deoxy-N-acetylneuraminic acid (DDN), and can be mimicked by an equivalent concentration of purified neuraminidase (Fryer *et al.*, 1990). Thus, pulmonary M_2 receptor dysfunction maybe a direct effect of the parainfluenza virus on the receptor.

Alternatively, virus-induced airway inflammation may be responsible for pulmonary M_2 receptor dysfunction. Exposure to either ozone (Schultheis *et al.*, 1994) or antigen (Fryer & Wills-Karp, 1991) causes a similar dysfunction of these neuronal M_2 muscarinic receptors as viral infection. In the case of ozone exposure, depleting leukocytes by pretreating with cyclophosphamide prevents loss of M_2 receptor function (Gambone & Fryer, 1992). Furthermore, in antigen-exposed guinea-pigs, neutralizing positively charged inflammatory cell proteins, using either heparin or poly-l-glutamic acid, acutely reverses the M_2 receptor dysfunction (Fryer & Jacoby, 1992). Eosinophil major basic protein and eosinophil peroxidase, two such positively charged proteins, have previously been shown to be allosteric antagonists at the M_2 receptor (Jacoby *et al.*, 1993).

Neuronal M_2 muscarinic receptor function in the lungs was tested with either the muscarinic agonist, pilocarpine, or muscarinic antagonist, gallamine. In control guinea-pigs, pilocarpine inhibited vagally-induced bronchoconstriction by 75% (ratio of 0.25 in Figure 2) by stimulating the neuronal M_2 muscarinic receptor. Conversely, gallamine potentiated vagally-induced bronchoconstriction by 10 fold by blocking these receptors and removing the inhibition that they provide. In those guinea-pigs that were infected with parainfluenza virus, the effects of pilocarpine (Figure 2) and gallamine (Figure 7) were significantly attenuated. These results confirm loss of neuronal M_2 muscarinic receptor function in guinea-pigs infected with parainfluenza virus (Fryer & Jacoby, 1991).

In those guinea-pigs pretreated with cyclophosphamide, the effect of pilocarpine on vagally-induced bronchoconstriction in the virus-infected animals fell clearly into two groups. In one group of animals pilocarpine had little effect on vagally-induced bronchoconstriction (Figure 1, (▼)). In this group ($n = 6$), vagally-induced bronchoconstriction after even the maximum dose of pilocarpine (100 μg kg^{-1}) remained at greater than 50% (equal to a ratio of 0.5 on Figure 2) of that before pilocarpine (range of ratios, 0.60–0.88). In contrast, in the other group ($n = 4$), pilocarpine inhibited vagally-induced bronchoconstriction similarly to the controls (Figure 1, (▲)), and the response to vagal stimulation after the maximum dose of pilocarpine was less than 50% of that before pilocarpine (range of ratios, 0.14–0.23). Thus, it can be seen that not only is a significant difference between these groups apparent by analysis of variance ($P = 0.0006$) with no overlap between the maximal inhibition of pilocarpine in the two groups, but also that there is considerable separation between the ranges of the maximal effects of pilocarpine. Because the responses to pilocarpine were so dissimilar in these cyclophosphamide treated animals, the data from these groups was analysed separately (Figure 2).

Cyclophosphamide depleted inflammatory cells in the peripheral blood and prevented the virus-induced influx of inflammatory cells into the lung as reflected by the lavage data (Figure 5). These effects on inflammatory cells were present in both the group in which M_2 receptor function was preserved and the group in which it was lost. In fact, there

was a more pronounced depletion of inflammatory cells in the lavage fluid from the cyclophosphamide-treated group that lost M_2 receptor function ($25 \pm 3 \times 10^6$ cells) than in the cyclophosphamide-treated group that maintained M_2 receptor function ($13.4 \pm 2.6 \times 10^6$ cells; $P<0.05$ by t test with Bonferroni correction).

Virus production was increased in the lungs of guinea-pigs that had been depleted of leukocytes by pretreatment with cyclophosphamide. This increase has previously been described in mice infected with influenza virus (Singer *et al.*, 1972; Hurd & Heath, 1975). We compared the viral content of the lungs of the cyclophosphamide-treated animals divided into two groups based on M_2 receptor function as above. Cyclophosphamide-treated animals that retained normal M_2 receptor function produced significantly less virus than those that lost M_2 receptor function (Figure 3). This suggests that in animals with a more severe infection (defined by greater virus production) the virus itself is able to damage the M_2 receptor independently of inflammation. Among cyclophosphamide-treated animals, there was a significant correlation between lung viral content and the response to vagal stimulation after pilocarpine $100\,\mu g\,kg^{-1}$ ($r^2 = 0.81$, $P = 0.0004$; Figure 4). Thus, in the absence of leukocytes, neuronal M_2 muscarinic receptor function, or loss of function, is predicted by the severity of viral infection.

The data in this study show that lung inflammation is not a *sine qua non* for the loss of M_2 receptor function after viral infection. Since inflammatory cell depletion with cyclophosphamide protected M_2 muscarinic receptors in only a portion of the virus infected guinea-pigs, there are at least two mechanisms involved in virus-induced M_2 muscarinic receptor dysfunction. One mechanism is dependent upon inflammatory cells, and the other is independant of inflammatory cells. The inflammatory cell-independent mechanism is most apparent in the guinea-pigs with a more severe viral infection, but since the viral content of the lungs of animals that did not receive cyclophosphamide overlapped to a substantial extent the viral contents of the two groups of cyclophosphamide-treated animals (Figure 3), this severe infection does not require depletion of inflammatory cells.

It is not possible on the basis of these data to state which inflammatory cells are responsible for the loss of M_2 receptor function in mild viral infections. The virus-induced increases in both neutrophils and eosinophils in the lungs were prevented by cyclophosphamide pretreatment. Eosinophil major basic protein and eosinophil peroxidase, which are allosteric antagonists at the M_2 receptor (Jacoby *et al.*, 1993), as well as the positively charged neutrophil cationic protein, might be involved in leukocyte-mediated M_2 receptor dysfunction. However, the failure of heparin, a poly-anionic polysaccharide that binds and neutralizes many positively charged proteins (Frigas *et al.*, 1980; Fryer & Jacoby, 1992), to restore neuronal M_2 muscarinic receptor function in non-cyclophosphamide-treated guinea-pigs makes these proteins less attractive candidates as mediators of this effect in viral infections. The failure of heparin to restore M_2 receptor function cannot be attributed to a direct effect of virus on the M_2 receptor in these animals, since two of the four animals in which the effect of heparin was tested fell into the low virus-content group and would therefore be expected to have lost M_2 receptor function via a leukocyte-dependent mechanism.

Other inflammatory cell products may participate in M_2 receptor damage. Many mammalian cells contain neuramidinase, including inflammatory cells (Pilatte *et al.*, 1987; Schauer, 1983). Although the effect of viral infections on inflammatory cell neuraminidase has not been examined, the neuraminidase of macrophages, the predominant cell type in the lavage fluid in our study, is inducible by mycobacterial infection (Pilatte *et al.*, 1987). Inflammatory cell neuraminidases might also decrease agonist affinity for M_2 receptors by cleaving sialic acid residues from the receptor.

These results demonstrate that parainfluenza virus-induced loss of neuronal M_2 muscarinic receptor function in the lungs occurs via several mechanisms. One mechanism depends upon the presence of inflammatory cells, but not upon the presence of charged inflammatory cell proteins. The other mechanism is independent of inflammatory cells and may result from a direct effect of the virus on the M_2 muscarinic receptor. Thus, virus-induced loss of M_2 receptor function in the lungs occurs via very different mechanisms from those seen in antigen challenged- or ozone-exposed guinea-pigs.

The authors wish to thank Ms Constance L. Elbon and Ms Deborah Eastman for technical assistance. This work was supported by National Institute of Health grants HL-47120 (D.B.J.) and HL-44727 (A.D.F.) and by grants from the Tobacco Research Council (A.D.F.) and the American Lung Association (A.D.F.). D.B.J. is a recipient of the Edward Livingston Trudeau Scholarship from the American Lung Association.

References

AQUILINA, A.T., HALL, W.J., DOUGLAS, R.G. & UTEL, M.J. (1980). Airway reactivity in subjects with viral upper respiratory tract infections: the effects of exercise and cold air. *Am. Rev. Respir. Dis.*, **122**, 3–10.

BLABER, L.C., FRYER, A.D. & MACLAGAN, J. (1985). Neuronal muscarinic receptors attenuate vagally-induced contraction of feline bronchial smooth muscle. *Br. J. Pharmacol.*, **86**, 723–728.

BUCKNER, C.K., CLAYTON, D.E., AIN-SHOKA, A.A., BUSSE, W.W., DICK, E.C. & SHULT, P. (1981). Parainfluenza 3 infection blocks the ability of a beta adrenergic receptor to inhibit antigen-induced contraction of guinea pig isolated airway smooth muscle. *J. Clin. Invest.*, **67**, 376–384.

BUCKNER, C.K., SONGSIRIDEJ, V., DICK, E.C. & BUSSE, W.W. (1985). In vivo and in vitro studies of the use of the guinea pig as a model for virus-provoked airway hyperreactivity. *Am. Rev. Respir. Dis.*, **132**, 305–310.

BURDEN, D.T. & PARKES, M.W. (1971). Effect of β-adrenoceptive blocking agents on the response to bronchoconstrictor drugs in the guinea-pig overflow preparation. *Br. J. Pharmacol.*, **41**, 122–131.

DIXON, W.E. & BRODY, T.G. (1903). Contributions to the physiology of the lungs. Part 1, the bronchial muscles and their innervation and the action of drugs upon them. *J. Physiol.*, **29**, 97–173.

DUSSER, D.J., JACOBY, D.B., DJOKIC, T.D., RUBENSTEIN, I., BORSON, D.B. & NADEL, J.A. (1989). Virus induces airway hyperresponsiveness to tachykinins: role of neutral endopeptidase. *J. Appl. Physiol.*, **67**, 1504–1511.

EMPEY, D.W., LAITINEN, A., JACOBS, L., GOLD, W.M. & NADEL, J.A. (1976). Mechanisms of bronchial hyperreactivity in normal subjects following upper respiratory tract infection. *Am. Rev. Respir. Dis.*, **113**, 523–527.

FRIGAS, E., LOEGERING, D.A. & GLEICH, G.J. (1980). Cytotoxic effect of the guinea pig major basic protein on tracheal epithelium. *Lab. Invest.*, **42**, 35–43.

FRYER, A.D., EL-FAKAHANY, E.E. & JACOBY, D.B. (1990). Parainfluenza virus type 1 reduces the affinity of agonists for muscarinic receptors in guinea-pig heart and lung. *Eur. J. Pharmacol.*, **181**, 51–58.

FRYER, A.D. & JACOBY, D.B. (1991). Parainfluenza virus infection damages inhibitory M2 muscarinic receptors on pulmonary parasympathetic nerves in the guinea-pig. *Br. J. Pharmacol.*, **102**, 267–271.

FRYER, A.D. & JACOBY, D.B. (1992). Function of pulmonary M2 muscarinic receptors in antigen challenged guinea-pigs is restored by heparin and poly-l-glutamate. *J. Clin. Invest.*, **90**, 2292–2298.

FRYER, A.D. & MACLAGAN, J. (1984). Muscarinic inhibitory receptors in pulmonary parasympathetic nerves in the guinea-pig. *Br. J. Pharmacol.*, **83**, 973–978.

FRYER, A.D. & WILLS-KAPP, M. (1991). Dysfunction of M2 muscarinic receptors in pulmonary parasympathetic nerves after antigen challenge in guinea-pigs. *J. Appl. Physiol.*, **71**, 2255–2261.

GAMBONE, L.M. & FRYER, A.D. (1992). Inflammatory cell depletion preserves neuronal M2 receptor function in guinea-pigs exposed to ozone. *Am. Rev. Respir. Dis.*, **145**, A614.

GREEN, C.J. (1982). *Animal Anaesthesia.* Laboratory Animal Handbooks, vol. 8, pp. 81–82. London: Laboratory Animals Ltd.

HURD, J. & HEATH, R.B. (1975). Effect of cyclophosphamide on infections in mice caused by virulent and avirulent strains of influenza virus. *Infect. Immun.*, **11**, 886–889.

JACOBY, D.B., GLEICH, G.J. & FRYER, A.D. (1993). Human eosinophil major basic protein is an endogenous allosteric antagonist at the inhibitory muscarinic M2 receptor. *J. Clin. Invest.*, **91**, 1314–1318.

JACOBY, D.B., TAMAOKI, J., BORSON, D.B. & NADEL, J.A. (1988). Influenza infection causes airway hyperresponsiveness by decreasing enkephalinase. *J. Appl. Physiol.*, **64**, 2653–2658.

JOHANSON, W.G., PIERCE, A.K. & SANFORD, J.P. (1969). Pulmonary function in uncomplicated influenza. *Am. Rev. Respir. Dis.*, **100**, 141–144.

PILATTE, Y., BIGNON, J. & LAMBRE, C.R. (1987). Lysosomal and cytosolic sialidases in rabbit alveolar macrophages: demonstration of increased lysosomal activity after in vivo activation with bacillus Calmette-Guerin. *Biochem. Biophys. Acta*, **923**, 150–155.

SCHAUER, R. (1983). *Glycosidases with Special Reference to the Pathophysiological Role of Sialidases.* ed. Popper, H., Reutter, W., Kottgen, E. & Gudats, F. pp. 83–97. Boston: MTP Press Ltd.

SCHULTHEIS, A.H., BASSETT, B.J.P. & FRYER, A.D. (1994). Ozone-induced airway hyperresponsiveness and loss of neuronal M_2 muscarinic receptor function. *J. Appl. Physiol.*, (in press).

SHELOKOV, A., VOGEL, J.E. & CHI, L. (1958). Hemadsorption (adsorption-hemagglutination) test for viral agents in tissue culture with special reference to influenza. *Proc. Soc. Exp. Biol. Med.*, **97**, 802–809.

SINGER, S.H., FORD, M. & KIRSCHSTEIN, R.L. (1972). Respiratory diseases in cyclophosphamide-treated mice. II. Decreased virulence of PR8 influenza virus. *Infect. Immun.*, **5**, 957–960.

WELLIVER, R.C. (1983). Upper respiratory infections in asthma. *J. Allergy Clin. Immunol.*, **72**, 341–346.

(Received July 20, 1993
Revised January 18, 1994
Accepted February 8, 1994)

Br. J. Pharmacol. (1994), **112**, 595–603

Effects of chronic intravenous infusions of dopexamine and isoprenaline to rats on D_1-, β_1- and β_2-receptor-mediated responses

S.W. Martin & [1]Kenneth J. Broadley

Department of Pharmacology, Welsh School of Pharmacy, University of Wales, Cardiff, PO Box 13, Cardiff CF1 3XF

1 Rats received intravenous infusions of dopexamine, an agonist with selectivity for D_1-dopamine receptors and β_2-adrenoceptors (240 $\mu g\,kg^{-1}\,h^{-1}$), isoprenaline, a β_1- and β_2-adrenoceptor agonist (40 $\mu g\,kg^{-1}\,h^{-1}$) or vehicle (isotonic saline at pH 2.5) for 7 days via subcutaneously implanted osmotic minipumps. Tissues were then removed for determination of functional responsivenss to β_1-adrenoceptor, β_2-adrenoceptor and dopamine D_1-receptor stimulation.

2 The β_1-adrenoceptor-mediated responses of the spontaneously beating right atrium (increase in rate) and paced left atrium (increase in tension) showed significant reductions in sensitivity to isoprenaline following isoprenaline infusion. The EC_{50} values were significantly increased from 5.6 to 17.7 nM in right atria and from 7.4 to 27.1 nM in left atria. The maximum rate increase of right atria was also significantly less after isoprenaline infusion compared with controls (164.0 and 251.9 beats min^{-1}, respectively) but the maximum tension responses of left atria were not significantly different. After infusion with dopexamine, however, there was no change in sensitivity of the left or right atria to β_1-adrenoceptor stimulation by isoprenaline.

3 β_2-Adrenoceptor-mediated relaxation responses to isoprenaline of the pulmonary artery, constricted with noradrenaline (6×10^{-8} M), showed no significant difference in maximum response or EC_{50} in tissue from isoprenaline- or dopexamine-infused rats compared with vehicle-infused controls. β_2-Adrenoceptor-mediated vasodilator responses were also examined in the kidney perfused with the thromboxane A_2 analogue, U46619 (7.1×10^{-8} M) to raise perfusion pressure. As with the pulmonary artery, there was no significant difference in ED_{50} or maximum response to isoprenaline in kidneys from isoprenaline-infused animals compared with vehicle controls.

4 The D_1-receptor-mediated vasodilator responses to dopamine of the kidney perfused with U46619 were reduced after infusion of rats with dopexamine. The maximum fall in perfusion pressure (16.0 mmHg) and ED_{50} value (5.2 μg) were significantly different from those after vehicle infusion (31.5 mmHg; 1.5 μg).

5 These results show that functional responses mediated via β_1-adrenoceptors and D_1-receptors are reduced by intravenous infusions of isoprenaline and dopexamine, respectively. In contrast, the β_2-adrenoceptor-mediated vasodilator responses of the pulmonary artery and kidney are not reduced by these agonists. Thus, under identical conditions, there appears to be selective down-regulation of peripheral β_1- and D_1-receptors, but not of β_2-adrenoceptors.

Keywords: Rat renal vasculature; atria; pulmonary artery; dopexamine infusions; isoprenaline infusions; D_1-dopamine receptor desensitization; β_1-adrenoceptor desensitization

Introduction

Dopexamine hydrochloride, developed for the management of acute heart failure, selectively stimulates β_2-adrenoceptors and D_1-dopamine receptors. The β_2-adrenoceptor-mediated systemic vasodilatation, along with D_1-mediated mesenteric vasodilatation reduces afterload, whilst D_1-receptor-mediated renal vasodilatation improves kidney perfusion. Additionally, some inotropic support is provided by direct stimulation of cardiac β_2-adrenoceptors, by activation of reflex mechanisms arising from the vasodepressor action and by inhibition of $uptake_1$ which results in potentiation of the action of noradrenaline on β_1-adrenoceptors (Smith & O'Connor, 1988). Although β_1-adrenoceptors predominate over β_2-adrenoceptors in the human heart (Bristow *et al.*, 1986; Böhm *et al.*, 1989; Brodde *et al.*, 1989; Steinfath *et al.*, 1991), the smaller β_2-adrenoceptor population which also mediates contractile responses (Ablad *et al.*, 1974; Zerkowski *et al.*, 1986) may become more important in some forms of heart disease. In dilated cardiomyopathy (DCM) and possibly aortic valve disease, β_1-adrenoceptors are selectively down-regulated (Brodde *et al.*, 1989; Michel *et al.*, 1990; Steinfath *et al.*, 1991) whilst β_2-adrenoceptors are spared and in such cases, selective β_2-adrenoceptor stimulation may be advantageous.

Infusion of catecholamines in rats and guinea-pigs has been reported to result in decreased density of cardiac β_2-adrenoceptors (Nanoff *et al.*, 1989; Lu & Barnett, 1990; Molenaar *et al.*, 1990). Desensitization of vascular β_2-receptors has also been described in the aorta and portal vein of these animals following catecholamine infusions (Hayes *et al.*, 1986). This suggests the possibility that desensitization of the cardiac β_2-receptors could occur as a result of prolonged dopexamine administration in patients with heart failure and that the effectiveness of the treatment could also be reduced by concomitant desensitization of vascular β_2-receptors. Indeed, tolerance to the effects of dopexamine has been reported in clinical studies (Murphy & Hampton, 1988; Böhm *et al.*, 1990), and a reduction in β_2-receptor number has been observed in guinea-pig myocardium following a 7-day subcutaneous infusion of dopexamine (Williams *et al.*, 1990).

Also important, with respect to dopexamine in the treatment of heart failure, is the behaviour of the renal vascular D_1-dopamine receptor under conditions of chronic stimulation. Little is known of the susceptibility of this receptor to

[1] Author for correspondence.

desensitization; although decreased [^{3}H]-SCH23390 binding and reduced dopamine-stimulated adenosine 3':5'-cyclic monophosphate (cyclic AMP) production has been observed for central D_1-receptors in mouse neuroblastoma cells following incubation with dopamine (Barton & Sibley, 1990). Similarly, cyclic AMP production stimulated by dopamine acting via the D_1-receptor has been shown to be reduced by 50–60% in membrane homogenates prepared from rat striatal slices incubated with 10 μM dopamine for 30 min (Memo *et al.*, 1982). In addition, up-regulation of central D_1-receptors (assessed by [^{3}H]-SCH23390 binding) has been described by Hess *et al.* (1988) and Riva & Creese (1990) and following chronic treatment of rats with the selective antagonist SCH23390.

Studies on peripheral D_1-receptors, however, are sparse. Treatment of rats with SKF 102698, a dopamine-β-hydroxylase inhibitor, has been shown to result in a decreased stimulation of cyclic AMP accumulation by the D_1-receptor agonist, fenoldopam, in proximal convoluted tubules and a loss of [^{125}I]-SCH23390 binding (Kinoshita *et al.*, 1990). Presumably the raised levels of endogenous dopamine caused down-regulation of the D_1-receptors. Furthermore, incubation of cultured opossum kidney cells with dopamine has been reported to lead to rapid desensitization of D_1-receptor-stimulated adenylate cyclase and to a time-dependent decrease in receptor number as assessed by [^{125}I]-SCH23390 binding (Bates *et al.*, 1991). However, no functional studies appear to have been performed on renal vascular D_1-receptor-mediated responses. The present study was therefore undertaken to examine the effects of a 7-day infusion of dopexamine to rats, upon the functional responses to stimulation of D_1-receptors in the perfused renal vasculature, β_1-receptors of isolated atria and β_2-receptors of the renal vasculature and pulmonary artery. For comparison with the effects of dopexamine upon β_1- and β_2-receptors, a parallel study using a 7-day infusion of isoprenaline was also carried out. In all previous studies of the effects of prolonged *in vivo* infusion of isoprenaline upon cardiovascular β-adrenoceptor regulation, the isoprenaline has been delivered subcutaneously; the present study differs from these in that both isoprenaline and dopexamine were administered intravenously, which is the therapeutic route for dopexamine.

Methods

Male Wistar rats (220–260 g) were implanted subcutaneously with osmotic minipumps (Alzet, 2ML1, output 10 μl h^{-1}) delivering either isoprenaline (40 μg kg^{-1} h^{-1}), dopexamine (240 μg kg^{-1} h^{-1}) or vehicle (isotonic saline at pH 2.5) via a cannula in the jugular vein for 7 days. The dose of dopexamine was based on the clinical range, while that for isoprenaline was based on the previous literature which has used exclusively s.c. infusions of 40 (e.g. Lu & Barnett, 1990; Butterfield & Chess-Williams, 1993) or 400 μg kg^{-1} h^{-1} (e.g. Chang *et al.*, 1982; Kenakin & Ferris, 1983; Hayes *et al.*, 1986; Nanoff *et al.*, 1989). Prior to implantation, the minipumps were filled and left to prime for 4 h at room temperature or overnight at 4°C in a beaker of sterile saline; drops of fluid could then be seen leaving the flow moderator.

Implantation of osmotic minipumps

Rats were anaesthetized with midazolam (4.2 mg kg^{-1}, i.p.) followed after 5 min with fentanyl (0.26 mg kg^{-1}, i.p.) and droperidol (0.28 mg kg^{-1}, i.p.). An external jugular vein was cannulated with a length of saline-filled polythene catheter tubing (Portex, internal diameter 0.76, external diameter 1.2 mm). The free end of the cannula passed subcutaneously to the back of the neck where it emerged through a lateral 1.5 cm incision approximately 3 cm from the base of the skull. A subcutaneous pocket was formed on the animal's back and an Alzet osmotic minipump (Charles River, Margate, Kent), filled and primed with the appropriate solution, was inserted. The cannula was flushed with a sufficient volume of the same drug solution as the minipump to displace all of the saline and thus ensure immediate onset of drug action. The cannula was cut to length, fitted to the drug delivery portal of the osmotic minipump and secured with a cotton thread. Wounds were closed with silk sutures. Animals were then allowed to recover, with body temperature monitored by a rectal thermometer and maintained at 37 ± 1°C under a lamp.

Preparation of isolated tissues

Seven days after implantation, the minipumps were removed under pentobarbitone anaesthesia (60 mg kg^{-1}, i.p.). The cannulae were examined for blockages due to coagulated blood or, in the case of dopexamine, deposits of polymerized drug. The volume remaining within the minipump was measured to determine that the correct volume had been delivered. At a flow rate of 10 μl h^{-1} and pump capacity of 2 ml, after 7 days the residual volume should be $<$0.32 ml.

Isolated perfused kidney

While anaesthetized with pentobarbitone, the abdomen was opened and the descending aorta cannulated retrogradely below the level of the renal arteries. The polythene cannula (Portex, with luer mount, size 3FG external diameter 0.75 mm) was advanced until the tip was opposite the left renal artery. The mesenteric artery was tied with a cotton ligature and the aorta ligated immediately below the coeliac artery. Both kidneys were then perfused with carboxygenated (CO_2:O_2, 5%:95%) Krebs-bicarbonate solution at 37°C by means of a Watson-Marlow (502S) peristaltic pump (Falmouth, Cornwall, UK) at 11 ml min^{-1}. The Krebs-bicarbonate solution had the following composition (mM) in distilled water: NaCl 118.4, $NaHCO_3$ 24.9, KCl 4.7, $CaCl_2$ 1.9, $MgSO_4$ 1.15, KH_2PO_4 1.15 and glucose 11.7. The vena cava was cut between the left and right renal veins to allow escape of perfusate and the right renal artery was ligated. The thorax was then opened for removal of the left atrium, right atrium and pulmonary artery.

Alterations in perfusion pressure arising from changes in renal vascular resistance, were recorded on a Lectromed polygraph (MT8P, Welwyn Garden City, Hertfordshire) by means of a pressure transducer (Bell & Howell, type 4-327-L221) situated between the perfusion cannula and warming coil. A Condon manometer was also connected in series with the pressure transducer to accommodate some degree of volume change during drug responses. In order to observe vasodilator responses, the perfusion pressure was raised by perfusion with Krebs solution containing the thromboxane A_2 agonist, U46619 (7.1×10^{-8} M). Once the perfusion pressure had reached a stable plateau (vehicle controls, 204.6 ± 6.4; dopexamine pretreated, 199.8 ± 5.3; isoprenaline pretreated, 198 ± 4.1 mmHg), a dose-response curve for either isoprenaline or dopamine was constructed by bolus injection. Increasing doses were added sequentially in half logarithmic increments, each dose being added when perfusion pressure had returned to a stable level.

Isolated atria

After opening the thorax, the right atrium was removed with cotton threads through the inferior vena cava and atrioventricular junction for attachment to the tissue holder. A third cotton through the superior vena cava allowed connection to a Devices isometric force transducer (Lectromed, type UF1 57 g sensitivity range). Left atria were removed with a cotton loop through the atrioventricular junction which secured the atrium into close contact with a pair of platinum electrodes (Harvard, Edenbridge, Kent). A second cotton thread through the atrial appendage was used to connect the tissue

to a Devices isometric force transducer. Both atria were mounted in 50 ml organ baths containing gassed (5% CO_2/95% O_2) Krebs solution at 37°C. A resting diastolic tension of 0.75 g was applied and tension changes recorded on the polygraph. Left atria were paced at 2 Hz with pulses of threshold voltage plus 50% and 5 ms duration delivered by a Harvard Research stimulator. Rate of contraction of the spontaneously contracting right atrium was recorded by means of a ratemeter (Lectromed, type 5250) triggered by the tension signal.

Pulmonary artery

A ring segment (5–8 mm long) of the main pulmonary artery was removed and set up between two stainless steel pins placed through the lumen. One pin was fixed and the other linked by a stainless steel rod to a Devices isometric transducer. The tissues were immersed in a 50 ml organ bath containing Krebs solution at 37°C gassed with 95% O_2/5% CO_2. The resting tension was adjusted to 1 g and this was maintained during a 1 h equilibration period. The tissues were then contracted with noradrenaline at a concentration (6×10^{-8} M) causing 80–90% of the maximum effect. Relaxation responses to isoprenaline were then obtained by cumulative addition of increasing concentrations in half log increments until the maximum effect was achieved.

Measurement of responses and statistical analysis

Changes in rate and force of contraction in isolated atria were measured by subtraction of the resting rate or developed tension immediately preceding a concentration-response curve from the total rate or developed tension at the peak effect of each dose of isoprenaline. Relaxation of the pulmonary artery was the peak reduction of tension at each concentration of isoprenaline measured from the stable contraction induced by noradrenaline. Vasodepressor responses of the perfused kidney were measured as the peak fall in perfusion pressure for each dose of agonist from the stable U46619-induced vasoconstriction immediately preceding the dose-response curve.

For concentration-response curves, the responses were plotted as the absolute changes in rate (beats min^{-1}), tension (g) or perfusion pressure (mmHg) and as the percentage of maximum response. From the latter plots of individual experiments, the EC_{50} value was determined by linear interpolation between points on either side of the 50% response. Geometric mean EC_{50} values and their 95% confidence limits were then obtained.

Statistical analysis of differences in tissue sensitivity between vehicle-treated and isoprenaline- or dopexamine-infused animals was made by comparing EC_{50} values by means of Student's two-tailed t test. Additionally, the mean absolute maximum responses (± s.e.mean) were compared by Student's unpaired t test. Probability values of less than 0.05 were considered significant.

Drugs

In experiments to examine β_1-receptor-mediated responses of left and right atria, tissues were incubated throughout with the β_2-receptor antagonist, ICI 118,551 (10^{-7} M). In experiments to examine β_2-receptor-mediated responses of perfused kidney or pulmonary artery, tissues were perfused or incubated throughout with the β_1-receptor antagonist, atenolol (10^{-5} M). Additionally, the β_2-receptor-mediated responses of the kidney were examined in the presence of SCH23390 (10^{-8} M) and prazosin (10^{-6} M) to block D_1- and α_1-adrenoceptors, respectively. The D_1-receptor-mediated renal vasodilator activity of dopamine was examined in the presence of propranolol (10^{-6} M) and prazosin (10^{-6} M). In all preparations, metanephrine (10^{-5} M) was present throughout to block uptake$_2$ and cocaine (10^{-5} M) was included in the kidney perfusion solution to block uptake$_1$ of dopamine.

The following drugs were used: (±)-atenolol (ICI Pharmaceuticals, Macclesfield, Cheshire), cocaine hydrochloride (Hillcross Pharmaceuticals, Burnley), dopamine hydrochloride (Sigma, Poole, Dorset), dopexamine hydrochloride (Fisons, Loughborough, Leicester), droperidol (Sigma), fentanyl citrate (Sigma), ICI 118,551 hydrochloride (ICI), (−)-isoprenaline bitartrate (Sigma), (±)-metanephrine hydrochloride (Sigma), midazolam (Hypnovel, Roche, Welwyn Garden City, Herts), (−)-noradrenaline bitartrate (Sigma), phenobarbitone sodium (Sagatal, Rhone Mérieux, Dublin, Eire), prazosin hydrochloride (Pfizer, Sandwich, Kent), (±)-propranolol hydrochloride (Sigma), SCH23390 maleate (Schering Corporation, Bloomfield, NJ, USA) and U46619 ((15S)-hydroxy-11α,9α-(epoxymethano)prosta-5Z, 13E-dienoic acid) (Sigma).

Isoprenaline (0.08 mg ml^{-1}, as the salt) and dopexamine (7.92 mg ml^{-1}, as the salt) for inclusion in the minipumps were made up in 0.9% w/v saline containing 0.01% w/v EDTA. This solution was acidified to pH 2.5 using 0.01 M HCl and then filter sterilized (pore size 0.2 μM) into multidose vials for use. These solutions were stored in a refrigerator and used within 1 week. The vehicle was 0.9% w/v saline containing 0.01% w/v EDTA, acidifed to pH 2.5 and filtered as for the test solutions.

In the *in vitro* experiments, stock solutions of dopamine and isoprenaline were prepared in 0.01 M HCl in distilled water, while U46619 was dissolved in 1% w/v sodium bicarbonate. Dilutions were then made in Krebs bicarbonate solution. The vehicle exerted no pharmacological effects *in vitro*.

Results

β_1-Adrenoceptor-mediated responses of left and right atria

In right atria from isoprenaline-treated rats, there was a rightward shift of the concentration-response curve compared with tissues from vehicle-infused rats (Figure 1b). The EC_{50} value was significantly greater after isoprenaline infusion than in controls (Table 1). The increase in EC_{50} value was accompanied by a significant depression of mean maximum response in the isoprenaline-treated group compared with the vehicle-treated group (Figure 1a). Similar results were obtained in the paced left atria following isoprenaline infusion (Figure 1c & d). The EC_{50} for isoprenaline stimulation of tension was significantly larger in the isoprenaline-treated group than the vehicle-treated rats. Although the mean maximum tension increase was lower in the isoprenaline-treated group than in the vehicle-treated group, this was not significant (Table 1).

In contrast, infusion of dopexamine had no effect on the atrial β_1-receptor responsiveness. Mean EC_{50} and maximum values for isoprenaline-stimulated increases in right atrial rate or left atrial tension were not significantly different in tissues from dopexamine- and vehicle-treated rats (Table 2).

β_2-Adrenoceptor-mediated responses of pulmonary artery

The vasorelaxant β_2-receptor-mediated responses of the pulmonary artery were not significantly affected by the prolonged infusion with either isoprenaline or dopexamine. Although the maximum response for the relaxation by isoprenaline appears to be lower in the isoprenaline-treated group than in the vehicle-treated group when plotted as the absolute reduction in tension (Figure 2a), they were not significantly different (Table 1, Student's two-tailed unpaired t test, $P > 0.05$). When plotted as the percentage of maximum response, the curves were virtually superimposable (Figure 2b) and the EC_{50} values were not significantly different (Table 1).

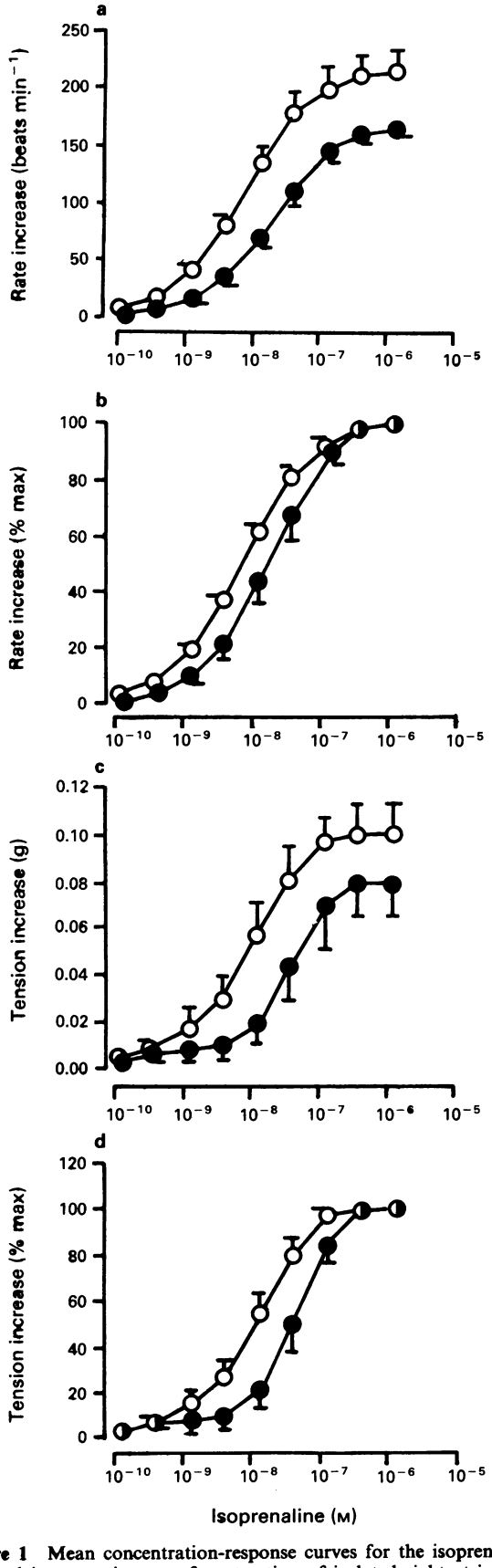

Figure 1 Mean concentration-response curves for the isoprenaline-induced increases in rate of contraction of isolated right atria (a,b) and increases in tension of isolated left atria (c,d) of rats. Atria were taken from rats that had received intravenous infusions of vehicle (○, $n = 4$ right atria, $n = 6$ left atria) or isoprenaline (●, $n = 5$ right atria, $n = 4$ left atria, 40 $\mu g\,kg^{-1}\,h^{-1}$) for 7 days. Responses are plotted as the increase in rate (beats min^{-1}) or tension (g) above baseline (a,c), or as increases in rate or tension expressed as a percentage of the maximum (b,d). Mean values are shown, with s.e.mean.

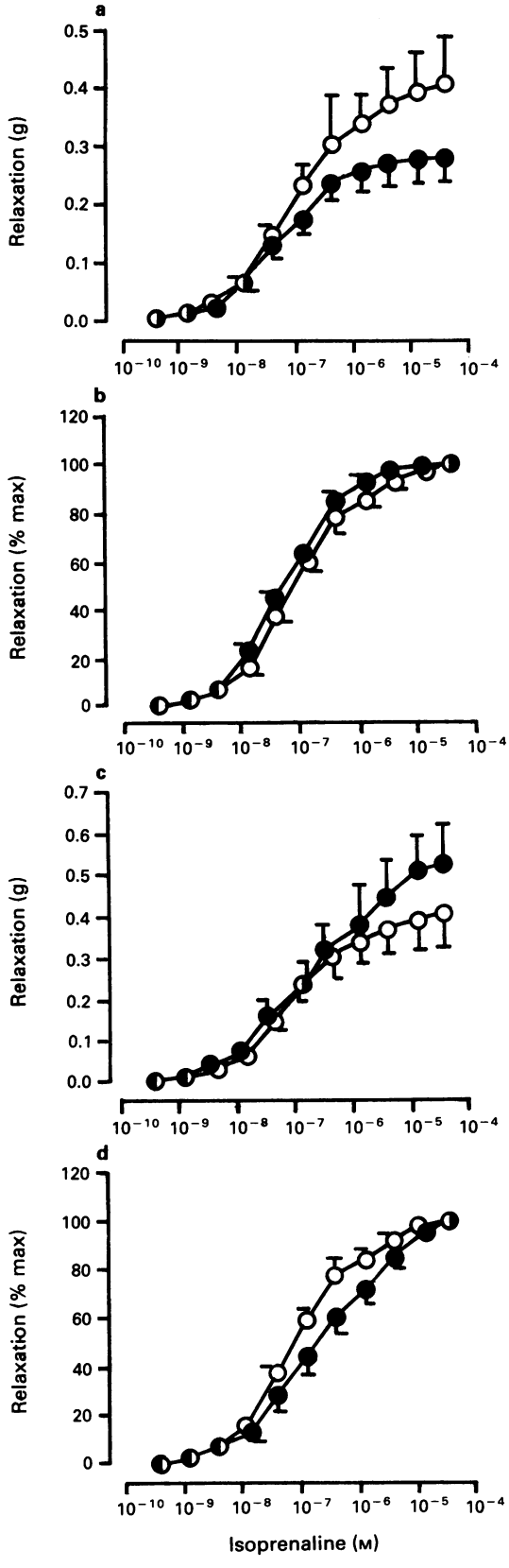

Figure 2 Mean concentration-response curves for the relaxation of noradrenaline-contracted rat isolated pulmonary arteries by isoprenaline. Pulmonary artery ring segments were taken from rats that had received intravenous infusions of isoprenaline (a,b) or dopexamine (c,d). The effects of infusions of isoprenaline (●, $n = 4$, 40 $\mu g\,kg^{-1}\,h^{-1}$) or dopexamine (●, $n = 6$, 240 $\mu g\,kg^{-1}\,h^{-1}$) for 7 days are compared with infusions of vehicle (○, $n = 7$) for 7 days. Responses are plotted as the reduction of tension (g) from the noradrenaline-induced plateau (a,c), or as the reduction in tension expressed as a percentage of maximum (b,d). Mean values are shown, with s.e. mean.

Table 1 Mean EC_{50} values[1] and maximum responses for isoprenaline in tissues from vehicle or isoprenaline-infused (40 $\mu g\ kg^{-1}\ h^{-1}$) rats

	Tissue			
	Right atrial rate	*Left atrial tension*	*Kidney perfusion pressure*	*Pulmonary artery*
Receptor type	β_1	β_1	β_2	β_2
$^1EC_{50}$	nM	nM	μg	nM
Vehicle	5.65	7.4	0.31	59.2
	(3.9–8.2)	(3.4–16.3)	(0.08–1.21)	(36.7–95.7)
Isoprenaline	17.7*	27.1*	0.18^{NS}	43.3^{NS}
	(13.6–23.1)	(10.1–72.9)	(0.11–0.32)	(22.6–85.1)
Maximum	beats min^{-1}	g	mmHg	g
Vehicle	215.9 ± 16.0	0.10 ± 0.013	38.25 ± 2.1	0.41 ± 0.08
n	4	6	4	7
Isoprenaline	164.0* ± 8.0	0.08^{NS} ± 0.01	32.7^{NS} ± 8.4	0.28^{NS} ± 0.04
n	5	4	4	4

[1]Geometric mean EC_{50} values (or ED_{50} values in the case of perfused kidney) together with the 95% confidence limits, in parentheses, are shown. Arithmetic means of maxima with s.e.mean are shown. A significant difference between vehicle- and isoprenaline-infused rats, as determined by Student's unpaired *t* test, is indicated by * and no significant difference by ^{NS}.

Table 2 Mean EC_{50} values[1] and maximum responses for isoprenaline or dopamine in tissues from vehicle- or dopexamine-infused (240 $\mu g\ kg^{-1}\ h^{-1}$) rats

	Tissue			
	Right atrial rate	*Left atrial tension*	*Kidney perfusion pressure*	*Pulmonary artery*
Agonist	Isoprenaline	Isoprenaline	Dopamine	Isoprenaline
Receptor type	β_1	β_1	D_1	β_2
$^1EC_{50}$	nM	nM	μg	nM
Vehicle	12.7	7.4	1.5	59.2
	(5.9–27.5)	(3.4–16.3)	(0.97–2.33)	(36.7–95.7)
Dopexamine	11.4^{NS}	6.4^{NS}	5.2*	137^{NS}
	(7.8–16.6)	(2.3–18.5)	(3.1–8.5)	(34.1–547)
Maximum	beats min^{-1}	g	mmHg	g
Vehicle	168.6 ± 8.3	0.10 ± 0.01	31.5 ± 4.6	0.41 ± 0.08
n	7	6	4	7
dopexamine	179.2^{NS} ± 27.0	0.10^{NS} ± 0.02	16.0* ± 1.9	0.53^{NS} ± 0.09
n	6	4	5	6

[1]Geometric mean EC_{50} values (or ED_{50} values in the case of perfused kidney) together with the 95% confidence limits, in parentheses, are shown. Arithmetic means of maxima with s.e.mean are shown. A significant difference between vehicle- and dopexamine-infused rats, as determined by Student's unpaired *t* test, is indicated by * and no significant difference by ^{NS}.

After infusion of rats with dopexamine, there was a small increase in the maximum response to isoprenaline of the pulmonary artery and an increase in EC_{50} value, however, these were not significantly different from the vehicle-treated group (Figure 2c and d, Table 2).

β_2-Adrenoceptor-mediated responses of the renal vasculature

As in the pulmonary artery preparations, β_2-receptor-mediated vasodilator responses of the rat perfused kidney following 7-day infusions of isoprenaline were not significantly changed from those obtained in kidneys from vehicle-treated animals (Figure 3a and b); mean ED_{50} and maximal values for isoprenaline-stimulated vasodilatation were not significantly different in the two treatment groups ($P > 0.05$, Table 1).

D_1-receptor-mediated responses of the renal vasculature

Figure 3c and d shows the D_2-receptor-mediated vasodilator responses to dopamine in perfused kidneys from dopexamine- and vehicle-infused rats. Infusion of dopexamine for 7 days resulted in a marked reduction in sensitivity to D_1-receptor stimulation by dopamine. The ED_{50} for vasodilatation by dopamine was increased and the maximum vasodilator response was significantly depressed in kidneys from the dopexamine-treated group compared with vehicle-treated rats (Table 2).

Discussion

Prolonged intravenous administration of isoprenaline to rats resulted in a marked loss of sensitivity to isoprenaline of isolated atria removed from these animals. This indicates that a functional desensitization of the atrial β_1-receptors had occurred. In contrast, there was no change in sensitivity of the β_2-receptor-mediated vasodilatation of the pulmonary artery and renal vascular bed removed from the same animals. Prolonged dopexamine infusion resulted in pronounced reduction in sensitivity of the renal vascular D_1-receptor-mediated responses to dopamine, but was without significant effect upon responses arising from stimulation of atrial β_1-receptors or the β_2-receptors of the pulmonary artery by isoprenaline. These results indicate desensitization by dopexamine of D_1-dopamine receptors, but not β_1 or β_2-receptors.

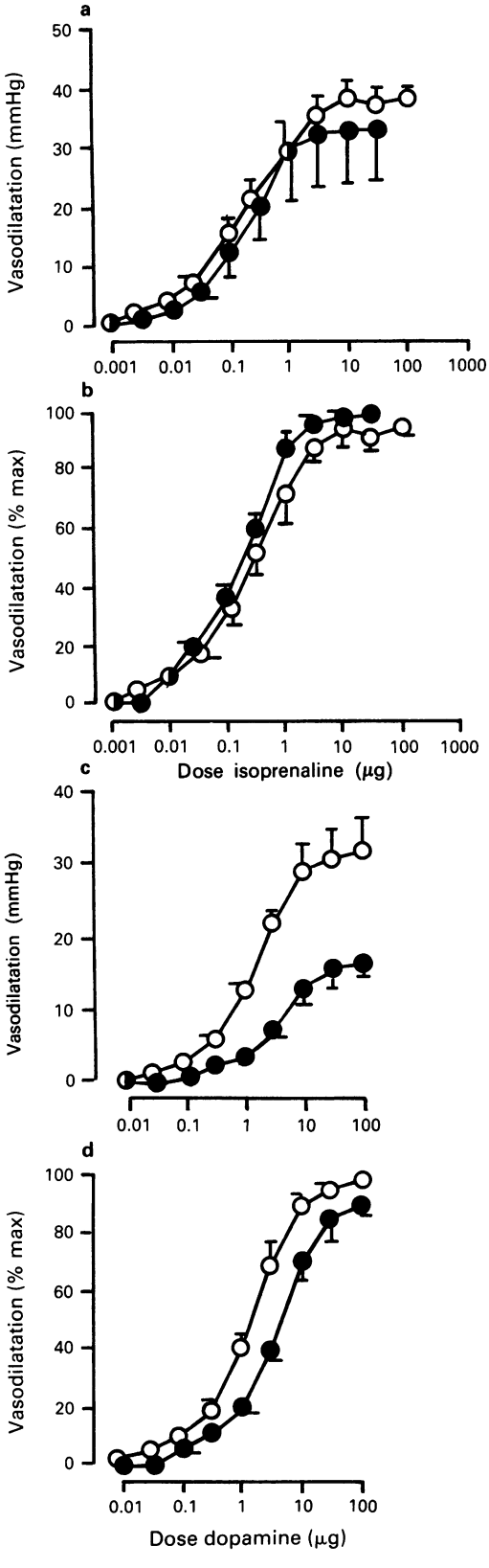

Figure 3 Mean concentration-response curves for the vasodilator responses of the rat perfused kidney to isoprenaline (a,b) or dopamine (c,d). Kidneys were perfused *in situ* in rats that had received intravenous infusions of isoprenaline (a,b) or dopexamine (c,d). The effects of infusions of isoprenaline (●, $n = 4$, 40 μg kg^{-1} h^{-1}) or dopexamine (●, $n = 5$, 240 μg kg^{-1} h^{-1}) for 7 days are compared with infusions of vehicle (○, $n = 4$) for 7 days. Responses are plotted as the reduction of perfusion pressure (mmHg) from the plateau level of vasoconstriction by U46619 (a,c), or as the reduction in perfusion pressure expressed as a percentage of the maximum (b,d). Mean values are shown, with s.e.mean.

β_1-Adrenoceptor-mediated atrial responses

Desensitization of the atrial β_1-receptors was not unexpected since the desensitizing/down regulatory effects upon cardiac β_1-receptors of prolonged elevation of catecholamine levels *in vivo* is a well documented phenomenon, observed in human heart failure (Bristow *et al.*, 1986; Michel *et al.*, 1988; Steinfath *et al.*, 1991) and experimentally in rats (Chang *et al.*, 1982; Kenakin & Ferris, 1983; Hayes *et al.*, 1986; Nanoff *et al.*, 1989; Lu & Barnett, 1990; Vleeming *et al.*, 1990; Butterfield & Chess-Williams, 1993); guinea-pigs (Elfellah & Reid, 1990) and cats (Hedberg *et al.*, 1984). Equally, lack of desensitization of atrial β_1-receptors following 7-day dopexamine infusion was not a surprising result since dopexamine has been reported to be only a weak agonist at the β_1-receptors of the guinea-pig right atria (Mitchell *et al.*, 1987), with an intrinsic activity of only 0.1 relative to isoprenaline (Brown *et al.*, 1985). In the guinea-pig left atria, it was found to have no intrinsic activity and therefore to act as a β_1-receptor antagonist (Williams *et al.*, 1990). In contrast to the present results, these workers detected a small, but non-significant increase in guinea-pig atrial β_1-adrenoceptors, after 7-day infusions of dopexamine (50 or 200 μg kg^{-1} h^{-1} s.c.), which was attributed to receptor up-regulation arising from competitive antagonism of noradrenaline by dopexamine.

β_2-Adrenoceptor-mediated vascular responses

Neither dopexamine nor isoprenaline infusions resulted in significant desensitization of the β_2-receptors of the pulmonary artery and isoprenaline infusion had no effect upon the β_2-receptors of the renal vascular bed. Nevertheless, desensitization of β_2-receptors has been observed in isolated vascular tissues and from binding studies by other investigators following isoprenaline infusions. For example, Snavely *et al.* (1984) reported equal losses of both β_1- and β_2-receptors in the rat renal cortex following a 14-day isoprenaline infusion (s.c.). By contrast, both Lu & Barnett (1990) and Nanoff *et al.* (1989) demonstrated significantly greater losses of myocardial β_2-receptors than β_1-receptors following s.c. isoprenaline pretreatments of 3 and 7 days. An autoradiographic study by Molenaar *et al.* (1990) would appear to support these observations in the guinea-pig atrio-ventricular conducting system. A similar pattern of β-receptor loss was noted following a 7-day s.c. pretreatment of guinea-pigs with isoprenaline, the loss of β_2-receptor binding sites of the gastrocnemius muscle being greater than for the β_1-receptors of the left ventricle (Elfellah & Reid, 1990). Tsujimoto & Hoffman (1985), however failed to detect any reduction of β_2-receptor number in rat mesenteric artery after prolonged s.c. infusion of adrenaline, but observed a reduction in the maximal relaxation promoted by isoprenaline. This highlights the dangers of extrapolating the results of binding studies to the physiological response; radioligand binding studies measure only receptor presence, whereas the functional response is dependent upon both receptor presence and stimulus-response coupling. Thus, measurement of receptor number does not distinguish between receptors which are functionally coupled to adenylate cyclase and those which are not. Neither can it distinguish between receptors that are functionally involved in the production of the tissue response of interest and those that mediate other responses. For instance, rat cardiomyocytes contain only β_1-receptors, whereas the β_2-receptors occur on non-myocyte cell types (Lau *et al.*, 1980; Buxton & Brunton, 1985; Juberg *et al.*, 1985) – mainly the coronary endothelium. Thus, down-regulation of the β_2 subtype would not correlate with changes in inotropic or chronotropic responses. Similarly, blood vessels may contain cells other than smooth muscle cells, such as endothelial cells and fibroblasts, and measurement of β-receptors would reflect a mixture of cell types (Tsujimoto & Hoffman, 1985). Another difficulty associated with binding studies arises in tissues having a large number of spare receptors; it is known

that both cardiac and vascular tissues possess sizeable β-receptor reserves that provide for maximal changes in force development when only a small fraction of receptors are occupied by agonists with high intrinsic efficacies (such as isoprenaline) (Venter, 1979; Cohen *et al.*, 1982; Hayes *et al.*, 1984). It may therefore be possible for a large number of receptors to be down-regulated without significantly affecting the functional response (Kenakin, 1987) and thus binding measurements may overestimate the extent of desensitization.

Unfortunately, in the literature, measurements of tissue responses rarely accompany binding data, and in fact binding studies greatly predominate over functional studies of β-receptor desensitization. However, functional studies do show similar variations in the extent of β_1- and β_2-receptor desensitization in different tissues following *in vivo* s.c. infusion of catecholamines. Cohen & Schenck (1987) examined the effect of isoprenaline s.c. infusion on the β-receptor-mediated responses of the rat jugular vein, where both β_1- and β_2-receptor subtypes mediate relaxation (Cohen *et al.*, 1982). They found that a 4-day infusion of isoprenaline resulted in virtual abolition of the β_1-receptor-mediated relaxation response but only a modest shift in the dose-response curve for β_2-mediated response. In another study, the potency and maximum response for isoprenaline was decreased to a comparable extent for the β_1-mediated responses of rat ventricular strips and β_2-mediated relaxation of rat portal vein (Hayes *et al.*, 1986). Similar results were obtained by Vleeming *et al.* (1990) who compared β_1- and β_2-receptors desensitization in the rat heart and aorta, respectively, after a 16 hour s.c. infusion of isoprenaline.

Thus, considering the results of both binding and functional studies, the literature is confusing with regard to β-receptor subtype desensitization in different tissues. It has been suggested that receptor desensitization may not be dependent on subtype alone but may also depend upon tissue type and species (Lu & Barnett, 1990; Elfellah & Reid, 1990). Given this, it may be possible that the β_2-receptors of the rat pulmonary artery and renal vascular bed observed in the present study are resistant to desensitization. At the cellular level, desensitization of β-adrenoceptors appears to involve three mechanisms. After short term exposure to agonists, there is uncoupling of the receptor from the GTP binding protein (G_s), the cleaved α-subunit of which stimulates adenylate cyclase to increase cyclic AMP production and activation of cyclic AMP-dependent protein kinase (PKA). This pathway is activated at low agonist concentrations and is associated with phosphorylation of the receptor. Another kinase, β-adrenoceptor kinase, also phosphorylates β-adrenoceptors but only in the agonist-occupied form (Lohse *et al.*, 1990). Phosphorylation and uncoupling is followed by the second component; sequestration of the receptor into the cytoplasm. Long-term exposure to agonists results in the third mechanism of down-regulation or loss of receptors through their degradation (Hausdorff *et al.*, 1990; Lefkowitz *et al.*, 1990). Since the short term mechanisms are readily reversed within minutes, it is only the latter long-term process that would apply to the present study. It is possible that this shows differences in susceptibility between tissues.

Another possible reason for the lack of β_2-receptor desensitization in the present study is that the dose of isoprenaline ($40\ \mu g\ kg^{-1}\ h^{-1}$) was too low to induce desensitization of vascular β_2-receptors whilst being sufficient to produce β_1-receptor desensitization. The potency of isoprenaline in the pulmonary artery was approximately 10 fold less than its potency in the left atria and 8 fold less than its potency in right atria. Although the dose of dopexamine was higher ($240\ \mu g\ kg^{-1}\ h^{-1}$), it has been shown that dopexamine is considerably less potent than isoprenaline in producing β_2-receptor-mediated relaxation of the guinea-pig uterus, where its intrinsic activity is also less than that of isoprenaline ($\alpha = 0.78$) (Williams *et al.*, 1990), although it acts as a full agonist in guinea-pig trachea (Brown *et al.*, 1985). Therefore, it is conceivable that the dose of dopexamine may also have been insufficient to induce desensitization of pulmonary arterial β_2-receptors, especially if dopexamine acts as a partial agonist in that tissue; partial agonists have been shown to be less effective in producing β-receptor desensitization than full agonists (Pittman *et al.*, 1984; Neve *et al.*, 1985). Nevertheless, a 45% reduction in β_2-receptor number in guinea-pig myocardium has been reported following an infusion of $200\ \mu g\ kg^{-1}\ h^{-1}$ dopexamine for 3 days (Williams *et al.*, 1990) and likewise, a $40\ \mu g\ kg^{-1}\ h^{-1}$ infusion of isoprenaline in rats for the same period resulted in a 66% decrease in ventricular β_2-receptors. Although, as previously discussed, decreases in receptor number determined by binding studies may not necessarily be reflected by decreases in tissue responsiveness to agonists, the substantial reductions reported in these ligand binding studies indicate that both dopexamine and isoprenaline are capable of effecting major changes in β_2-receptor populations at the concentrations used in the present study. It is worth noting that in these previous studies, the isoprenaline and dopexamine was infused subcutaneously whereas in the present study it was via the intravenous route. Although it is difficult to relate the concentrations administered by these routes, it is reasonable to expect that the concentration of agonist reaching the receptor is greater by the i.v. than s.c. route. That the concentrations of isoprenaline and dopexamine used here did not produce significant desensitization in the tissues examined may therefore be due to genuine resistance of the β_2-receptors therein to undergo that process. This is confirmed by the results of our previous *in vitro* studies in which incubation of lung parenchymal strips or rat pulmonary artery or aorta with isoprenaline failed to induce desensitization of the β_2-receptor-mediated relaxation responses (Martin & Broadley, 1990; Herepath & Broadley, 1992).

D_1-receptor-mediated responses

The marked desensitization of the D_1-receptor-mediated responses in the renal vascular bed following dopexamine infusion suggests that the D_1-receptor is readily desensitized in that tissue. Although no other reports of peripheral D_1-receptor desensitization in intact tissue are available, the results of the present study are supported by the observations of Kinoshita *et al.* (1990) and Bates *et al.* (1991). These authors demonstrated respectively, a reduction of D_1-receptor binding sites in rat proximal convoluted tubules after pretreatment with the dopamine-β-hydroxylase inhibitor, SKF 102698, and in cultured opossum kidney cells after incubation with dopamine. If the desensitization of D_1-receptors indicated by the present results also occurs in man, one of the major therapeutic effects of dopexamine (i.e. renal vasodilatation) may be subject to tachyphylaxis. In clinical studies, both Böhm *et al.* (1990) and Murphy & Hampton (1988) have reported tolerance to the haemodynamic improvements attributed to the action of dopexamine on β-receptors (e.g. increased cardiac index, increased stroke volume and decreased systemic vascular resistance) after intravenous infusions ($6\ \mu g\ kg^{-1}\ min^{-1}$) exceeding 6 h and 18 h to patients with heart failure. When $4\ \mu g\ kg^{-1}\ min^{-1}$ was infused for 48 h, the haemodynamic improvements produced by dopexamine were well maintained with the exception of heart rate which returned to control levels after 1 h of treatment (Baumann *et al.*, 1990). This suggests the possibility that only dopexamine infusion rates in excess of $4\ \mu g\ kg^{-1}\ min^{-1}$ are great enough to induce tolerance and although in the present study $4\ \mu g\ kg^{-1}\ min^{-1}$ ($= 240\ \mu g\ kg^{-1}\ h^{-1}$) was sufficient to produce desensitization of D_1-receptor-mediated renal vasodilator responses; this may have been due to the much extended duration of the infusion (168 h).

This work was supported by Fisons Pharmaceuticals, Loughborough, Leicestershire, UK. We are grateful for the assistance of Dr J.B. Farmer of that company for his help and guidance. We are also grateful to the companies concerned for their generous gifts of atenolol, dopexamine, ICI 118,551, prazosin and SCH 23390.

References

ABLAD, B., CARLSSON, B., CARLSSON, E., DAHLOF, C., EK, L. & HULTBERG, E. (1974). Cardiac effects of β-adrenergic receptor antagonists. *Adv. Cardiol.*, **12**, 290–302.

BARTON, A.C. & SIBLEY, D.R. (1990). Agonist-induced desensitization of D_1-dopamine receptors linked to adenylyl cyclase activity in NS20Y neuroblastoma cells. *Mol. Pharmacol.*, **38**, 531–541.

BATES, M.D., CARON, M.G. & RAYMOND, J.R. (1991). Desensitization of DA_1 dopamine receptors coupled to adenylyl cyclase in opossum kidney cells. *Am. J. Physiol.*, **297**, F937–F945.

BAUMANN, G., FELIX, S.B. & FILEK, S.A.L. (1990). Usefulness of dopexamine hydrochloride versus dobutamine in chronic congestive heart failure and effects on haemodynamics and urine output. *Am. J. Cardiol.*, **65**, 748–754.

BOHM, M., PIESKE, B., SCHNABEL, P., SCHWINGER, R., KEMKOS, B., KLOVEKORN, W.-P. & ERDMANN, E. (1989). Reduced effects of dopexamine on force of contraction in the failing human heart despite a preserved β_2-adrenoceptor subpopulation. *J. Cardiovasc. Pharmacol.*, **14**, 549–559.

BOHM, M., REUSCHEL-JANETSCHEK, E. & ERDMANN, E. (1990). Lack of sustained haemodynamic effects of the β_2-adrenoceptor agonist dopexamine in end-stage congestive heart failure. *Am. J. Cardiol.*, **65**, 395–396.

BRISTOW, R., GINSBURG, R., UMANS, V., FOWLER, M., MINOBE, W., RASMUSSEN, R., ZERA, P., MENLOVE, R., SHAH, P., JAMIESON, S. & STINSON, E.B. (1986). β_1- and β_2-adrenergic-receptor subpopulations in nonfailing and failing human ventricular myocardium: coupling of both subtypes to muscle contraction and selective β_1-receptor down-regulation in heart failure. *Circ. Res.*, **59**, 297–309.

BRODDE, O.-E., ZERKOWSKI, H.-R., BORST, H.G., MAIER, W. & MICHEL, M. (1989). Drug- and disease-induced changes of human cardiac β_1- and β_2-adrenoceptors. *Eur. Heart J.*, **10** (suppl B), 38–44.

BROWN, R.A., DIXON, J., FARMER, J.B, HULL, J.C., HUMPHRIES, R.G., INCE, F., O'CONNOR, S.E., SIMPSON, W.T. & SMITH, G.W. (1985). Dopexamine: a novel agonist at peripheral dopamine receptors. *Br. J. Pharmacol.*, **85**, 599–608.

BUTTERFIELD, M.C. & CHESS-WILLIAMS, R. (1993). Potentiation of α-adrenoceptor-mediated responses following chronic β-adrenoceptor stimulation in the rat heart. *Br. J. Pharmacol.*, **108**, 658–662.

BUXTON, I.L.O. & BRUNTON, L.L. (1985). Direct analysis of β-adrenergic receptor subtypes on intact adult ventricular myocytes of the rat. *Circ. Res.*, **56**, 126–132.

CHANG, H.Y., KLEIN, R.M. & KUNOS, G. (1982). Selective desensitization of cardiac beta adrenoceptors by prolonged *in vivo* infusion of catecholamines in rats. *J. Pharmacol. Exp. Ther.*, **221**, 784–789.

COHEN, M.L. & SCHENCK, K.W. (1987). Selective down regulation of vascular β_1-adrenergic receptors after prolonged isoproterenol infusion. *J. Cardiovasc. Pharmacol.*, **10**, 365–368.

COHEN, M.L., WILEY, K.S. & BEMIS, K.G. (1982). Analysis of the $beta_1$ and $beta_2$ adrenoceptor interactions of the partial agonist, Clenbuterol (NAB 365) in the rat jugular vein and atria. *Naunyn-Schmied. Arch. Pharmacol.*, **320**, 145–151.

ELFELLAH, M.S. & REID, J.L. (1990). Regulation of β-adrenoceptors in the guinea-pig left ventricle and skeletal muscle following chronic agonist treatment. *Eur. J. Pharmacol.*, **182**, 387–392.

HAUSDORFF, W.F., CARON, M.G. & LEFKOWITZ, R.J. (1990). Turning off the signal: desensitization of β-adrenergic function. *FASEB J.*, **4**, 2881–2889.

HAYES, J.S., BOWLING, N. & BODER, G.B. (1984). Contractility and protein phosphorylation in cardiomyocytes: effects of isoproterenol and AR-L57. *Am. J. Physiol.*, **16**, H157–H160.

HAYES, J.S., WYSS, V.L., SCHENCK, K.S. & COHEN, M.L. (1986). Effects of prolonged isoproterenol infusion on cardiac and vascular responses to adrenoceptor agonists. *J. Pharmacol. Exp. Ther.*, **237**, 757–763.

HEDBERG, A., MATTSSON, H., NERME, V. & CARLSSON, E. (1984). Effects of in vivo treatment with isoprenaline or prenalterol on beta-adrenoceptor mechanisms in the heart and soleus muscle of the cat. *Naunyn-Schmied. Arch. Pharmacol.*, **325**, 251–258.

HEREPATH, M.L. & BROADLEY, K.J. (1992). Resistance of β_2-adrenoceptor-mediated responses of lung strips to desensitization by long-term agonist exposure – comparison with atrial β_1-adrenoceptor-mediated responses. *Eur. J. Pharmacol.*, **215**, 209–219.

HESS, E.J., NORMAN, A.B. & CREESE, I. (1988). Chronic treatment with dopamine receptor antagonists. Behavioural and pharmacologic effects on D_1 and D_2 dopamine receptors. *J. Neurosci.*, **8**, 2261–2370.

JUBERG, E.N, MINNEMAN, K.P.L. & ABEL, P.W. (1985). β_1- and β_2-adrenoceptor binding and functional responses in the left and right atria of rat heart. *Naunyn-Schmied. Arch. Pharmacol.*, **330**, 193–202.

KENAKIN, T.P. (1987). *Pharmacologic Analysis of Drug-Receptor Interaction.* New York: Raven Press.

KENAKIN, T.P. & FERRIS, R.M. (1983). Effects of *in vivo* β-adrenoceptor down-regulation on cardiac responses to prenalterol and pirbuterol. *J. Cardiovasc. Pharmacol.*, **5**, 90–97.

KINOSHITA, S., OHLSTEIN, E.H. & FELDER, R.A. (1990). Dopamine-1 receptors in rat proximal convoluted tubule: regulation by intrarenal dopamine. *Am. J. Physiol.*, **258**, F1068–F1074.

LAU, Y.H., ROBINSON, R.B., ROSEN, M.R. & BILEZKIAN, J.P. (1980). Subclassification of β-adrenergic receptors in cultured rat cardiac myoblasts and fibroblasts. *Circ. Res.*, **47**, 41–48.

LEFKOWITZ, R.J., HAUSDORFF, W.P. & CARON, M.G. (1990). Role of phosphorylation in desensitization of the β-adrenoceptor. *Trends Pharmacol. Sci.*, **11**, 190–194.

LOHSE, M.J., BENOVIC, J.L., CARON, M.G. & LEFKOWITZ, R.J. (1990). Multiple pathways of rapid β_2-adrenergic receptor desensitization. *J. Biol. Chem.*, **265**, 3202–3209.

LU, X. & BARNETT, D.B. (1990). Differential rates of down regulation and recovery of rat myocardial β-adrenoceptor subtypes in vivo. *Eur. J. Pharmacol.*, **182**, 481–486.

MARTIN, S.W. & BROADLEY, K.J. (1990). Comparison of in vitro desensitization at cardiac β_1- and vascular β_2-adrenoceptors. *J. Pharm. Pharmacol.*, **42** (Suppl), 187P.

MEMO, M., LOVENBERG, W. & HANBAUER, I. (1982). Agonist-induced subsensitivity of adenylyl cyclase coupled with a dopamine receptor in slices from rat corpus striatum. *Proc. Natl. Acad. Sci. U.S.A.*, **79**, 4456–4460.

MICHEL, M.C., MAISEL, A.S. & BRODDE, O.-E. (1990). Mitigation of β_1- and/or β_2-adrenoceptor function in human heart failure. *Br. J. Clin. Pharmacol.*, **30** (suppl 1), 375–425.

MICHEL, M.C., PINGSMANN, A., BECKERINGH, J.J., ZERKOWSKI, H.-R., DOETSCH, N. & BRODDE, O.-E. (1988). Selective regulation of β_1- and β_2-adrenoceptors in the human heart by chronic β-adrenoceptor antagonist treatment. *Br. J. Pharmacol.*, **94**, 685–692.

MITCHELL, P.D., SMITH, G.W., WELLS, E. & WEST, P.A. (1987). Inhibition of $uptake_1$ by dopexamine hydrochloride (*in vitro*). *Br. J. Pharmacol.*, **92**, 265–270.

MOLENAAR, P., SMOLICH, J.J., RUSSELL, F.D., MCMARTIN, L.R. & SUMMERS, R.J. (1990). Differential regulation of *beta*-1 and *beta*-2 adrenoceptors in guinea-pig atrioventricular conducting system after chronic (−)-isoproterenol infusion. *J. Pharmacol. Exp. Ther.*, **255**, 393–400.

MURPHY, J.J. & HAMPTON, J.R. (1988). Failure of dopexamine to maintain haemodynamic improvement in patients with chronic heart failure. *Br. Heart J.*, **60**, 45–49.

NANOFF, C., FREISSMUTH, M., TUISL, E. & SCHULTZ, W. (1989). A different desensitization pattern of cardiac β-adrenoceptor subtypes by prolonged in vivo infusion of isoprenaline. *J. Cardiovasc. Pharmacol.*, **13**, 198–203.

NEVE, K.A., BARRETT, D.A. & MOLINOFF, P.B. (1985). Selective regulation of beta-1 and beta-2 adrenergic receptors by atypical agonists. *J. Pharmacol. Exp. Ther.*, **235**, 657–664.

PITTMAN, R.N., REYNOLDS, E.E. & MOLINOFF, P.B. (1984). Relationship between intrinsic activities of agonists in normal and desensitized tissue and agonist-induced loss of beta adrenergic receptors. *J. Pharmacol. Exp. Ther.*, **230**, 614–618.

RIVA, M.A. & CREESE, I. (1990). Effect of chronic administration of dopamine receptor antagonists on D_1 and D_2 dopamine receptors and sigma/haloperidol binding sites in rat brain. *Mol. Neuropharmacol.*, **1**, 17–22.

SMITH, G.W. & O'CONNOR, S.E. (1988). An introduction to the pharmacologic properties of Dopacard (dopexamine hydrochloride). *Am. J. Cardiol.*, **52**, 9c–17c.

SNAVELY, M.D., ZIEGLER, M.G. & INSEL, P.A. (1984). A new approach to determine rates of receptor appearance and disappearance in vivo: Application to agonist-mediated down-regulation of rat renal cortical β_1- and β_2-adrenergic receptors. *Mol. Pharmacol.*, **27**, 19–26.

STEINFATH, M., GEERTZ, B., SCHMITZ, W., SCHOLZ, H., HAVERICH, A., BREIL, I., HANRATH, P., REAPCKE, E., SIGMUND, M. & LO, H.-B. (1991). Distinct down-regulation of cardiac β_1- and β_2-adrenoceptors in different human heart diseases. *Naunyn-Schmied. Arch. Pharmacol.*, **343**, 217–220.

TSUJIMOTO, G. & HOFFMAN, B.B. (1985). Desensitization of β-adrenergic receptor-mediated vascular smooth muscle relaxation. *Mol. Pharmacol.*, **27**, 210–217.

VENTER, J.C. (1979). High efficiency of coupling between beta-adrenergic receptors and cardiac contractility: direct evidence for 'spare' beta adrenergic receptors. *Mol. Pharmacol.*, **16**, 429–440.

VLEEMING, W., VAN ROOIJ, H.H., WEMER, J. & PORSIUS, A.J. (1990). Modulation of adrenoceptor-mediated cardiovascular effects by short-term in vivo infusion of isoproterenol in rats. *J. Cardiovasc. Pharmacol.*, **16**, 584–593.

WILLIAMS, D.W., ELNATAN, J., MOLENAAR, P. & SUMMERS, R.J. (1990). Effects of prolonged infusion of dopexamine on β_1- and β_2-adrenoceptors in guinea-pig myocardium. *J. Auton. Pharmacol.*, **10**, 127–137.

ZERKOWSKI, H.-R., IBEZONO, K., ROHM, N., REIDEMEISTER, J.C. & BRODDE, O.-E. (1986). Human myocardial β-adenoceptors: a demonstration of both β_1- and β_2-adrenoceptors mediating contractile responses to β-agonists on the isolated right atrium. *Naunyn-Schmied. Arch. Pharmacol.*, **332**, 142–147.

(Received September 20, 1993
Revised January 27, 1994
Accepted February 8, 1994)

Br. J. Pharmacol. (1994), **112**, 604–610

Sensitivity to protein kinase C inhibitors of nicardipine-insensitive component of high K^+ contracture in rat and guinea-pig aorta

[1]A.M. Low, [2]J.C.P. Loke, [3]C.Y. Kwan & E.E. Daniel

Smooth Muscle Research Program and the Department of Biomedical Sciences, McMaster University, Hamilton, Ontario, L8N 3Z5 Canada

1 In the rat and guinea-pig aorta, we observed that the contraction to hypertonically-added K^+, unlike the isotonic K^+-induced contraction, was only partially sensitive to nicardipine (0.1, 1 and 10 μM), an L-type Ca^{2+} channel blocker and occurred in Ca^{2+}-free medium containing 50 μM EGTA. We have characterized this nicarpidine-insensitive hypertonically-added K^+ contraction.

2 The contraction induced by an equi-osmolar concentration of mannitol was similar in size to that evoked by hypertonically-added K^+.

3 When the tissue was depleted of its internal Ca^{2+} stores with various agents such as phenylephrine (10 μM), cyclopiazonic acid (30 μM), thapsigargin (1 μM) or ryanodine (30 μM), or by incubation in Ca^{2+}-free medium over 30 min, little effect was observed on the high K^+ contracture in the presence of L-type Ca^{2+} channel blockade.

4 Phentolamine (10 μM) or indomethacin (10 μM) did not reduce the contraction induced by high K^+.

5 Application of a protein kinase C inhibitor, H7 (10, 30 and 100 μM) or calphostin C (1 μM), reduced the high K^+ contraction but not that caused by an equi-osmolar concentration of mannitol.

6 The data suggest that hypertonic K^+-induced contraction differs from that caused by hypertonicity or depolarization *per se* and invokes membrane enzyme activation.

Keywords: Hyperosmolarity; vascular contraction; H7; calphostin C

Introduction

It is well established that in most smooth muscle a depolarizing agent, such as high K^+, evokes contraction via an elevation of cytosolic Ca^{2+} through dihydropyridine-sensitive Ca^{2+} channels (Bolton, 1979). However, Jenkin and his coworkers (1991) demonstrated that the high K^+-induced contraction in the guinea-pig aorta was relatively insensitive to nifedipine compared to the rat aorta. Several investigators have provided evidence for the release of intracellularly-stored Ca^{2+} by high K^+ in rat aortic smooth muscle cells (e.g. Kobayashi *et al.*, 1985) and rat parotid cells (Takemura & Ohshika, 1987; 1988). In the rat vas deferens, accumulation of inositol 1,4,5-trisphosphate (IP_3) was reported to accompany the contraction induced by high K^+ and this occurred in tissue from animals treated with reserpine or in the presence of an α-adrenoceptor antagonist, prazosin (Khoyi *et al.*, 1989).

Involvement of protein kinase C (PKC) in high K^+ contraction in the rat vas deferens has also been suggested (Rice & Abraham, 1992) and this appears to be consistent with the report that high K^+ stimulates the translocation of PKC and activates it (Haller *et al.*, 1990). More recently, a study reported differential relaxation effects by Ca^{2+} channel blockers on high K^+ contracture which was induced by two commonly used techniques: iso-osmolar substitution of NaCl with KCl and hyperosmolar addition of KCl (Nielsen-Kudsk *et al.*, 1992). The findings of the present study show that hyperosmolar addition of KCl causes nicardipine-insensitive contraction in the rat and guinea-pig aorta which can be reduced by blockers of PKC.

[1] Author for correspondence.
[2] Present address: Malignant Hyperthermia Investigation Unit, Department of Anaesthesia, University of Toronto, Toronto, Ontario M5G 2C4.
[3] Present address: Department of Physiology, University of Hong Kong, Hong Kong.

Methods

Male Hartley guinea-pigs (250–300 g) and Wistar rats (300–350 g) were used. The animals were killed by stunning and decapitation by use of a procedure approved by our University Animal Care Committee. The thoracic aorta was isolated and placed in Krebs solution at pH 7.4 containing (mM): NaCl 119, KCl 5, $CaCl_2$ 2.5, $MgCl_2$ 2, $NaHCO_3$ 25, NaH_2PO_4 1 and glucose 11. Fat and connective tissue were removed under a dissecting microscope and 3–4 mm rings were prepared. The endothelium was removed with the teeth of a pair of forceps and the rings were mounted on a 15 ml organ bath connected to a force transducer (Grass FT03C) and a chart recorder (Gould 2800). The presence or absence of the endothelial cells was tested functionally with 10 μM carbachol.

The organ baths and Krebs solution were bubbled continuously with 95% O_2/5% CO_2 and warmed to 37°C. The rings were equilibrated for 20 min before stretching to the optimal resting force of around 3 g for the guinea-pig aorta and 2 g for the rat aorta. Stimulation of the arteries with 120 mM K^+ added hypertonically was repeated every 15–20 min until reproducible contractions were obtained. For Ca^{2+}-free Krebs, $CaCl_2$ was replaced by 50 μM EGTA.

Cumulative concentration-response curves for K^+ were constructed in the absence or the presence of the drug of interest. Increasing concentrations of K^+ were added to the baths without omitting any other ion, i.e. producing hypertonic solutions. Substitution of 100 mM KCl for 100 mM NaCl constituted iso-osmolar solution of high K^+.

Following an equilibration period of about 1 h, all arterial rings were stimulated with increasing concentrations of K^+ to construct a concentration-response curve. The response to a maximum concentration of K^+ of this concentration-response curve was used as 100% for subsequent concentration-response curves for each arterial ring. It has been suggested that a use-dependent phenomenon is associated with repeated high K^+ stimulation in the rat aorta (Wright,

1991). Therefore, time control experiments were performed in parallel but results showed no use-dependent phenomenon.

Thapsigargin (1 μM), cyclopiazonic acid (CPA, 30 μM), ryanodine (30 μM) or calphostin C (1 μM) was added to the arterial rings and incubation continued for 60–90 min. The effects of these compounds are maximal at these concentrations (Deng & Kwan, 1991; Low *et al.*, 1991; 1992; Shimamoto *et al.*, 1993). Low Cl^- Krebs solution was made by substituting NaCl with sodium isethionate (Sigma).

Drugs

Thapsigargin (Sigma), CPA (Sigma), 12-*o*-tetradecanoylphorbol-13-acetate (TPA, Sigma), phorbol 12, 13-dibutyrate (PDBu, Sigma) and calphostin C (Kamiya Biomedical Company) were dissolved in dimethyl sulphoxide (DMSO) to make a stock solution of 10 mM. Calphostin C was protected from light and was made up fresh before use. Ryanodine (Research Biochemical Inc) and nicardipine (Sigma) were prepared in absolute ethanol as a stock solution of 10 mM. Indomethacin (Sigma) was dissolved in NaOH and the stock was titrated with HCl to pH 7.4. 1-(5-isoquinolinylsulfonyl)-2-methyl-piperazine (H7, Sigma) was dissolved in H_2O to a stock solution of 10 mM. All other chemicals were of laboratory standard from various commercial sources. None of the solvents affected the tissue response when the pharmacological agents were omitted.

Statistical analysis

Data are expressed as the mean ± standard error of mean (s.e.mean). Significant differences were analysed by Student's paired two-tailed test or one-way analysis of variance where appropriate. When the F ratio is significant, the significantly-differing pairs were determined by Bonferroni's method. The minimal P value accepted for statistical significance was 0.05. n refers to the number of experiments from not less than three animals.

Results

Differential effects of nicardipine on high K^+-induced contraction in rat and guinea-pig aorta

Concentration-response curves to K^+ were constructed for both the guinea-pig aorta and rat aorta in parallel. In normal Krebs solution, it was observed that rat aorta had a lower threshold for contraction to K^+ elevation and reached maximum contraction at a lower K^+ concentration (Figure 1a) compared to guinea-pig aorta which was relatively less sensitive to K^+ (Figure 1b). In the guinea-pig aorta, the tissue concentration-response curve fell off at around 300 mM K^+ (not shown).

The effects of nicardipine on hypertonically-added K^+-induced contraction in the aorta of (a) rat and (b) guinea-pig are shown in Figure 1. When the tissue was pretreated with 0.1, 1 or 10 μM nicardipine prior to the construction of the concentration-response curve to K^+, the guinea-pig aorta still contracted in a concentration-dependent fashion in response to K^+. The slope of the concentration-response curve was lowered by nicardipine. Nicardipine reduced the contractile response by about 20–55% ($P<0.05$) but did not abolish the responses.

In the rat aorta, contraction to K^+ also occurred in nicardipine but it was inhibited by 40–60% ($P<0.05$) by the L-type Ca^{2+} channel antagonist. There was no significant difference between responses in the presence of varying concentrations of nicardipine.

After 5 min of pre-incubation in Ca^{2+}-free medium, increasing K^+ concentrations contracted the rat aorta: the contraction was not significantly different from that in the presence of nicardipine (Figure 1a). Similarly, the guinea-pig aorta responded in Ca^{2+}-free medium as it did in the

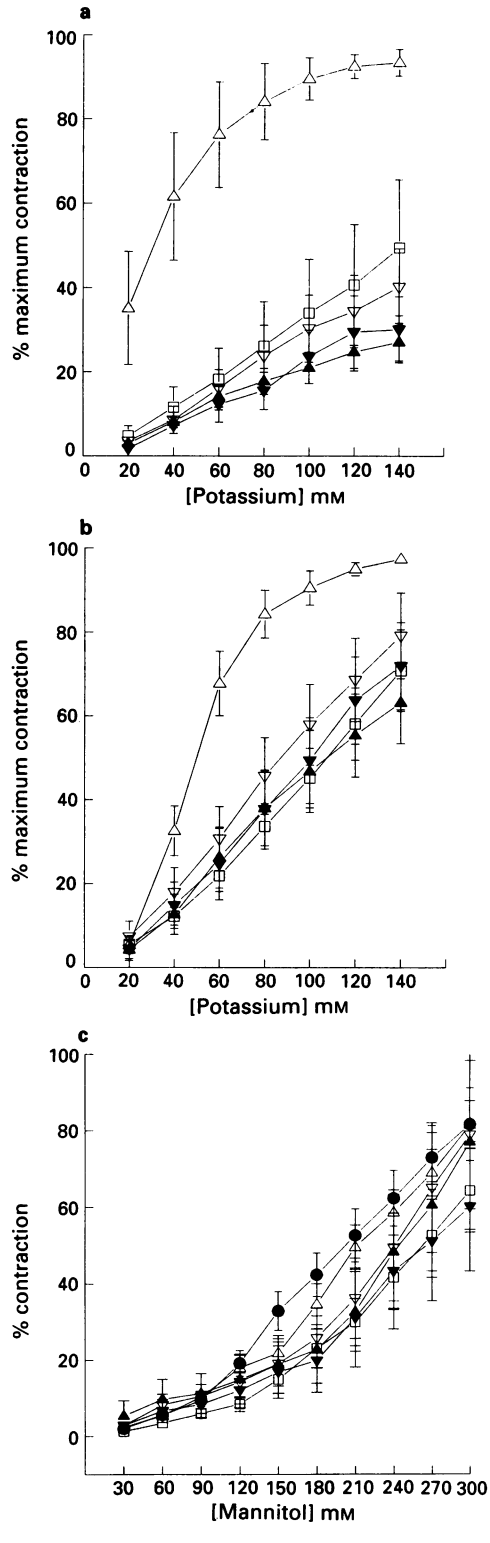

Figure 1 Concentration-dependent contraction to K^+ in the (a) rat ($n = 6$) and (b) guinea-pig aorta ($n = 8$). Some of the rat arterial rings were pre-incubated with 0.1 (▲), 1 (▽) or 10 (▼) μM nicardipine or were pre-incubated in Ca^{2+}-free Krebs solution (□) prior to the construction of a concentration-response curve to K^+. In the rat aorta, a substantially greater portion of the contraction was blocked by nicardipine or by the absence of external Ca^{2+} compared to controls (△). In contrast, a fair portion of K^+ contraction in the guinea-pig was insensitive to nicardipine or to the absence of external Ca^{2+} compared to controls (△). (c) Concentration-dependent responses to mannitol in the rat (△, $n = 18$) and guinea-pig (○, $n = 12$) aorta in normal Krebs solution. Concentration-response curves to mannitol were also constructed in the rat aorta in Ca^{2+}-free Krebs solution (□, $n = 9$) and in the presence of 0.1 (▲, $n = 6$), 1 (▽, $n = 6$) or 10 (▼, $n = 6$) μM nicardipine.

presence of nicardipine in the Ca^{2+}-containing medium (Figure 1b). In both tissues, the increase in tension with increments of K^+ concentration in Ca^{2+}-free medium was less steep compared to that in normal Krebs similar to the responses in the presence of nicardipine. After the completion of the concentration-response curve, addition of 10 mM EGTA or 3 mM nickel did not affect the contraction, confirming that the contraction did not involve an influx of Ca^{2+} from an extracellular source.

Concentration-response curves to mannitol in Ca^{2+}-containing Krebs solution, Ca^{2+}-free Krebs solution or in the presence of nicardipine (0.1, 1 or 10 μM) in the rat aorta are shown in Figure 1c. The responses to mannitol in normal Krebs solution obtained from the guinea-pig aorta are also shown in Figure 1c. The contractions are expressed as a percentage of maximum K^+ response in Ca^{2+}-containing Krebs solution. In general, while the responses to mannitol in normal Krebs solution, in Ca^{2+}-free medium and in the presence of nicardipine were overlapping, at higher concentrations of mannitol (>240 mM), contractions were significantly greater compared to those evoked by hypertonically-added K^+ under similar conditions. The size of the responses from the guinea-pig aorta were similar (not significantly different) to those evoked by hypertonically-added K^+ in Ca^{2+}-free medium or in the presence of nicardipine. Addition of 10 mM EGTA for 10 min prior to the construction of mannitol concentration-response curve in Ca^{2+}-free medium did not have a significant effect when compared to controls which were not pre-exposed to high EGTA.

Comparison between K^+ contracture induced by hypertonic addition and isotonic substitution

Figure 2 shows contraction in Ca^{2+}-free medium expressed as a percentage of contraction in the presence of 2.5 mM Ca^{2+} in rat and guinea-pig aorta. The contractions were induced by hypertonic addition of 100 mM KCl, KCl substituted isotonically for NaCl (100 mM) and KCl added hypertonically to low Cl^- Krebs solution made by isethionate substitution.

Hypertonically-added K^+ caused significantly larger contraction compared to isotonic substitution ($P<0.05$). As expected, contractions to isotonic K^+ addition in the absence of extracellular Ca^{2+} were very small. Hypertonically-added K^+ to normal Krebs doubles the Cl^- ion concentration. So, to investigate if this ion contributes to the 'hypertonic effect', NaCl was substituted with sodium isethionate. In this modified Krebs solution, referred to as 'low Cl^- solution', the only ion that was elevated was the K^+ ions when KCl was added hypertonically. Under these conditions, the contraction was significantly potentiated compared to results obtained when KCl was added hypertonically ($P<0.05$). Therefore, the contraction induced by hypertonically-added KCl in normal Krebs medium was not due to an increased concentration of Cl^- ions.

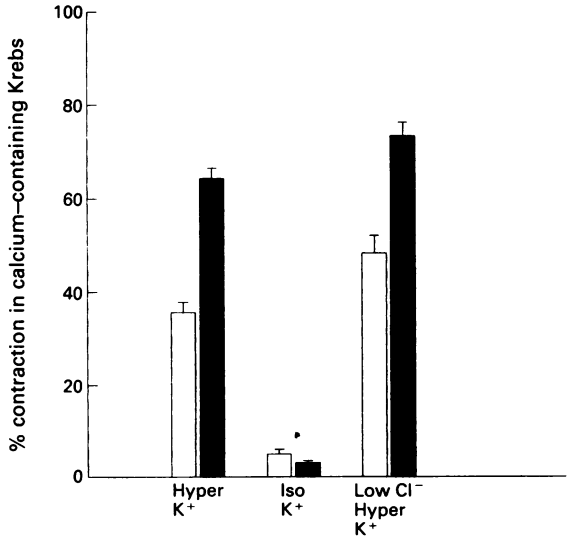

Figure 2 Aortic rings of rat (open columns, $n = 13$) and guinea-pig (solid columns, $n = 17-23$) aorta were stimulated in Ca^{2+}-free Krebs with high K^+ (100 mM) either added hypertonically (Hyper K^+) or isotonically-substituted (Iso K^+). Responses are expressed as a percentage of the contraction evoked when 2.5 mM Ca^{2+} was added to the bath. 'LowCl Hyper K^+' denotes hypertonically-added K^+ to low Cl^- Krebs medium. Contraction by LowCl Hyper K^+ was significantly larger than Hyper K^+ alone. Iso K^+ is significantly less compared to all groups.

Lack of effects of pretreatment with phentolamine and indomethacin

Inclusion of 10 μM phentolamine, an α_1- and α_2-adrenoceptor antagonist, did not affect significantly the K^+-induced contraction eliminating the possibility of noradrenaline release from depolarized nerve terminals observed to be present on the guinea-pig aorta (Morris, 1991). Furthermore, since the contraction persisted in Ca^{2+}-free medium, it is unlikely that any release of neurotransmitter occurred.

Indomethacin was used to inhibit phospholipase A_2, the enzyme responsible for production of such potent vasoconstrictor prostanoids as thromboxane A_2. After an incubation period of 30 min with 10 μM indomethacin, there was no significant change on the concentration-responses to elevated K^+ in either normal or Ca^{2+}-free Krebs solution in either rat or guinea-pig aorta (not shown).

Role of intracellular Ca^{2+} stores

Various modulators of the internal Ca^{2+} stores were used to investigate the possible contribution of the internal Ca^{2+} stores to hypertonically-added K^+-induced contraction. Guinea-pig aortic rings were treated with CPA (30 μM), thapsigargin (1 μM) or ryanodine (30 μM). CPA and ryanodine had no significant effect on K^+ concentration-response curves in normal Krebs solution compared to controls (Figure 3a). On the other hand, pretreatment with thapsigargin potentiated the responses to high K^+ significantly compared to controls ($P<0.05$).

Although CPA, thapsigargin or ryanodine apparently shifted significantly the concentration-response curve to K^+ in the presence of nicardipine (10 μM) when compared with untreated controls in the presence of nicardipine (Figure 3b), the responses of treated tissue in the presence and absence of nicardipine were not significantly different (cf. CPA, thapsigargin and ryanodine in Figure 3a and Figure 3b). Therefore, this may indicate that nicardipine had no effect on the concentration-response curves to high K^+ in the presence of CPA, thapsigargin or ryanodine. However, nicardipine inhibited significantly the contraction to hypertonically-added K^+ by about 20–40% (cf. control in Figure 3a and Figure 3b) as was the case in Figure 1b. It is also interesting to note the lack of inhibition by nicardipine in CPA, thapsigargin or ryanodine-treated tissues on concentration-response curves to K^+, suggesting that these compounds can induce Ca^{2+} influx through non-L-type Ca^{2+} channels, thereby enhancing contraction due to elevated K^+. These observations are consistent with results which have previously been reported that modulators of the Ca^{2+} release and uptake mechanisms of the SR can induce Ca^{2+} influx through non-dihydropyridine-sensitive channels (Low *et al.*, 1991; Xuan *et al.*, 1992).

In another series of experiments, the tissues were incubated in Ca^{2+}-free medium for 5 min prior to a challenge with 10 μM phenylephrine (Figure 3c). In controls, the transient contraction was followed by a contraction which was lower in amplitude and longer in duration and the latter was manifest by a 25% increase in basal contraction as seen in

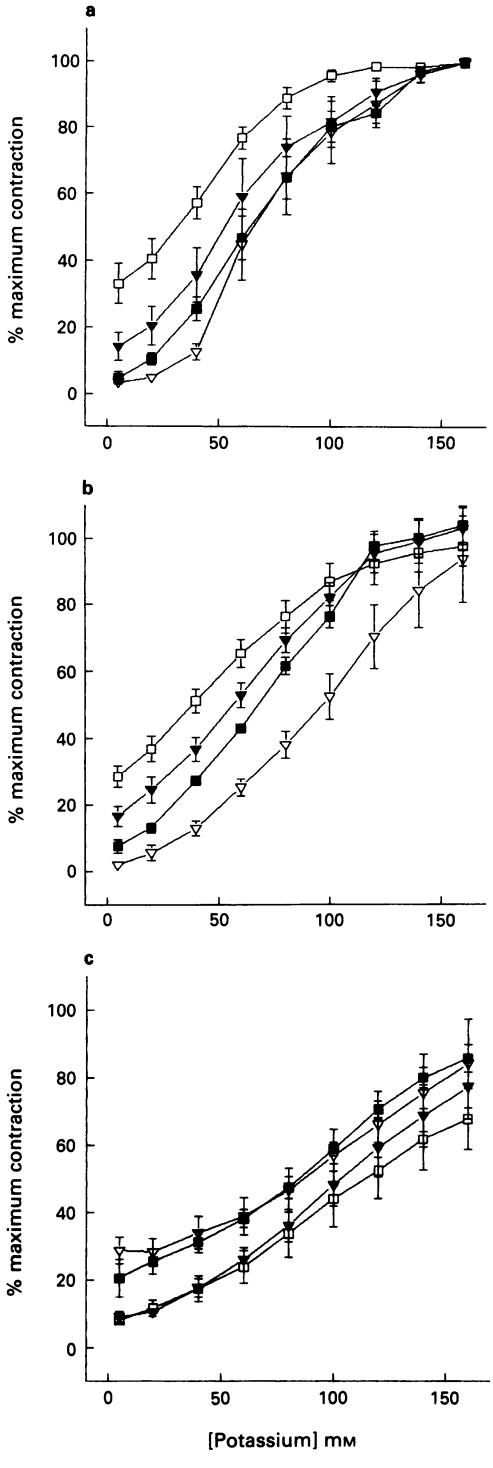

Figure 3 Concentration-dependent responses to K^+ in the guinea-pig aorta in the absence (∇, $n = 5$) and presence of the modulators of internal Ca^{2+} uptake (cyclopiazonic acid (CPA), 10 μM, ▼, $n = 5$; thapsigargin, 1 μM, □, $n = 6$) and release (ryanodine, 30 μM, ■, $n = 5$). (a) In normal Krebs solution, there was no significant effect of CPA or ryanodine on the concentration-dependent responses to K^+. Thapsigargin significantly enhanced K^+ contraction. (b) Procedure is as in (a) except, nicardipine (10 μM) was present. The responses obtained from pretreatment with CPA, ryanodine or thapsigargin were similar to those in (a). The control responses to K^+ were inhibited by nicardipine. Therefore, the apparent enhancement of responses by CPA, ryanodine or thapsigargin could be accounted for by the effect of nicardipine on the control. (c) Procedure as in (a) except the experiments were carried out in Ca^{2+}-free Krebs after the stimulation of the tissue with phenylephrine (10 μM). Phenylephrine induced a transient contraction followed by a fairly sustained contraction in Ca^{2+}-free medium in control. In the rings treated with CPA or thapsigargin, phenylephrine-induced contraction (both transient and sustained) was absent. In the ryanodine-treated tissue, the transient was absent, although the sustained contraction due to phenylephrine was not blocked. None of these manipulations affected the nicardipine-insensitive high K^+ contraction.

Figure 3c at 5 mM K^+ (significantly different from responses of CPA- or thapsigargin-treated tissues). The transient contraction associated with the addition of phenylephrine was absent in the tissue-pretreated with CPA, thapsigargin or ryanodine but present in controls. While the transient contraction was absent in ryanodine-treated tissues, phenylephrine stimulation in these tissues gave rise to a sustained contraction of lower amplitude which was not significantly different from control responses. The maximum amplitude of hypertonically-added K^+ contraction in Ca^{2+}-free medium was not significantly different in tissues pretreated with CPA, thapsigargin or ryanodine compared with controls. These results suggest that the ryanodine-sensitive Ca^{2+} pool may be different from that which is sensitive to CPA, thapsigargin and phenylephrine in the guinea-pig aorta.

Phenylephrine still induced a transient contraction when the tissue was incubated for around 5 min in Ca^{2+}-free medium. In order to ensure that the internal Ca^{2+} stores were emptied particularly when there was some evidence for multiple Ca^{2+} stores in this tissue (guinea-pig aorta), pre-incubation of the tissue in Ca^{2+}-free medium containing 50 μM EGTA was prolonged from 5 to 30 min. Successful depletion was denoted by the absence of phenylephrine-induced contraction. The concentration-response curves to K^+ constructed after 5 or 30 min were not significantly different (not shown). These observations together with those made with the selective modulators of the internal Ca^{2+} stores eliminate any direct participation of intracellular stores in sustaining hypertonically-induced K^+ contraction in Ca^{2+}-free medium.

Effects of H7

Contractions in the rat and guinea-pig aorta were induced by hypertonically added 100 mM K^+ or equi-osmolar concentration of mannitol in Ca^{2+}-free Krebs solution. This contraction was expressed as 100%. Figure 4 shows that in the guinea-pig and rat aorta, H7, a non-selective inhibitor of protein kinases, relaxed in a concentration-dependent manner the arterial rings contracted with hypertonically-added K^+. It had little effect on the contraction to hypertonic mannitol. Addition of H7 on the plateau of mannitol-induced contraction caused a further increase in tension in the guinea-pig aorta. Larger maximum relaxations (~65%) to H7 were observed in the rat aorta compared to those observed in the guinea-pig aorta (~12%). The relaxation in the rat but not in the guinea-pig aorta was statistically significant.

Effects of calphostin C

The participation of PKC in the high K^+-induced contraction was further investigated with a highly selective inhibitor of PKC, calphostin C (Shimamoto *et al.*, 1993) in the guinea-pig aorta. Figure 5 shows the results obtained with calphostin C. Pre-incubation with calphostin C (1 μM) significantly inhibited the maximum high K^+ contraction in normal Krebs solution by about 25% ($P<0.05$, Figure 5a) and by about 50% in Ca^{2+}-free solution ($P<0.05$, Figure 5b). In both cases, inhibition by calphostin C occurred at KCl concentrations greater than 60 mM. Following stimulation of the arterial rings with phenylephrine (10 μM), hypertonic addition of KCl caused concentration-dependent increase in contraction. In the presence of calphostin C, the phenylephrine and KCl-induced responses at all concentrations tested were reduced by about 20% ($P<0.05$, Figure 5c).

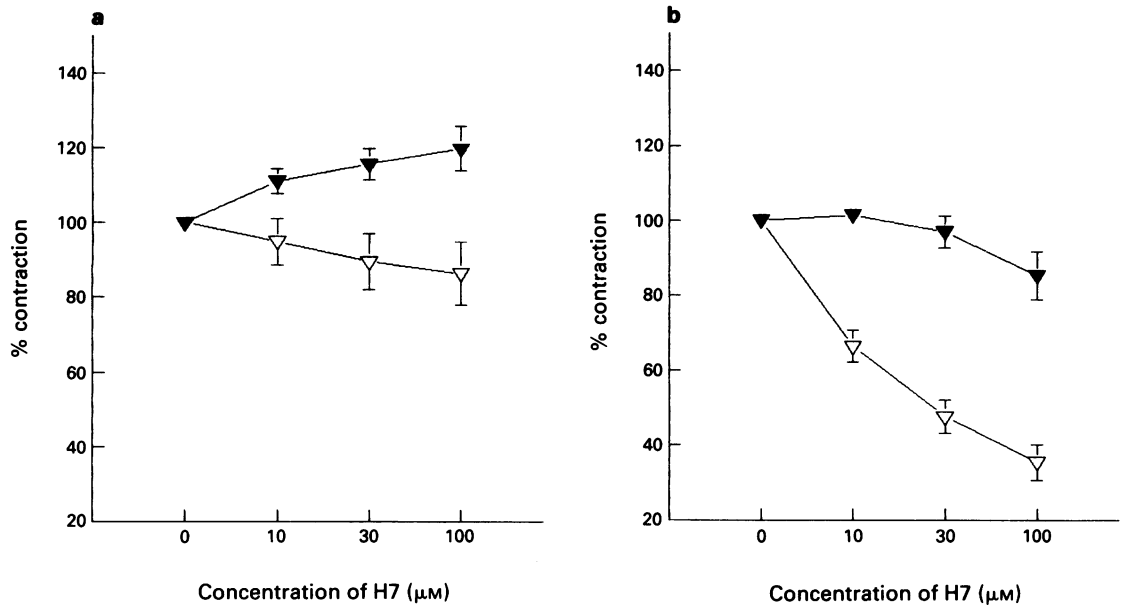

Figure 4 Concentration-dependent relaxation effect of H7 in (a) guinea-pig ($n = 9-10$) and (b) rat ($n = 11-12$) aorta to hypertonically-added K^+ (100 mM, ▽) or mannitol (200 mM, ▼). Contraction to hypertonically-added K^+ or mannitol in Ca^{2+}-free Krebs solution is represented as 100%.

Parallel studies using TPA (1 μM) and PDBu (1 μM), activators of PKC were performed. In guinea-pig aortic rings pretreated with calphostin C (1 μM), PDBu-induced contractions were significantly inhibited (14.7 ± 5.3% of maximum K^+ contraction in Ca^{2+}-containing Krebs solution, $n = 6$) compared to controls (54.3 ± 8.9%, $n = 6$). In two guinea-pig aortic rings, TPA-induced contractions were completely inhibited while control rings underwent a mean contraction of 35.7 ± 9.9% ($n = 2$).

It has been reported that PKC activation can either be dependent or independent of external Ca^{2+} and Ca^{2+} release. Therefore, in order to remove Ca^{2+} completely, the arterial rings were pre-incubated with high EGTA (10 mM) for at least 10 min prior to the construction of concentration-response curve to high K^+. These tissues could no longer respond to phenylephrine in Ca^{2+}-free Krebs solution. Contraction to hypertonic KCl still persisted under these conditions (data not shown). This suggests that activation of PKC in the guinea-pig aorta may well be a Ca^{2+}-independent mechanism.

Discussion

Hypertonically-added KCl causes vascular contraction independent of Ca^{2+} and insensitive to nicardipine

Influx of Ca^{2+} through the voltage-dependent, L-type Ca^{2+} channels occurs following depolarization in smooth muscle. KCl is a depolarizing agent commonly used by hypertonic addition, but it can also be applied by isotonic substitution. In this study, we have shown that in the rat and guinea-pig aorta, contractions produced by these two techniques occurred via different mechanisms. This finding is consistent with results reported by Nielsen-Kudsk *et al.* (1992) that contraction induced by isotonic substitution of KCl could be wholly antagonized by Ca^{2+} channel blockers, but contraction induced by hypertonic addition could only be partially antagonized. The nicardipine-sensitive component of high K^+ contraction accounts for approximately 50% and 20%, respectively, of the contractions of rat and guinea-pig aorta in normal Krebs solution containing 2.5 mM Ca^{2+}.

Nicardipine-insensitive KCl contraction cannot be solely explained by hyperosmolarity

Nielsen-Kudsk *et al.* (1992) suggested that hyperosmolarity *per se* contributes to contraction when KCl was added hypertonically in guinea-pig airway smooth muscle. In the present study, although the contraction induced by mannitol of equal osmolarity to that of KCl was similar to or larger than that induced by hypertonically-added K^+, the contraction induced by mannitol was resistant to relaxation by H7. This shows that the mannitol-induced contraction does not depend on an H7-sensitive kinase. It also suggests that contracture induced by hypertonically-added K^+ in vascular smooth muscle cannot be wholly accounted for by hyperosmolarity *per se*. Instead, this contracture appears to be mediated by more than one mechanism.

Nicardipine-insensitive KCl contraction is sensitive to PKC inhibitors

PKC is present at high concentrations in smooth muscle and can be activated by diacylglycerol or phorbol esters at near resting intracellular Ca^{2+} levels and remains active in the absence of Ca^{2+} (Nishizuka, 1984; 1992). It is a cytosolic protein the activation of which has been directly demonstrated to involve its low Ca^{2+}-dependent movement from the cytosol to the surface membrane (Khalil & Morgan, 1991). A fraction of the basal tone of vascular smooth muscle has been suggested to involve the activation of Ca^{2+}-independent isozyme of PKC (Collin *et al.*, 1992). This observation is consistent with a report on various arterial tissues including the rat aorta, carotid artery, tail artery, rabbit aorta and mesenteric artery, that a phorbol ester, 12-deoxyphorbol 13-isobutyrate, caused contraction independent of a rise in intracellular Ca^{2+} and this was thought to be due to increased cross-bridge cycling, independent of the phosphorylation of the myosin light chain (Sato *et al.*, 1992).

In this study, we provide evidence for a role played by PKC in hypertonically-induced KCl contraction. Hypertonically-added K^+ appears to cause contraction in part via the activation of PKC since the contraction was blocked by the PKC inhibitors, H7 and calphostin C. These compounds inhibit PKC activation by interacting with the

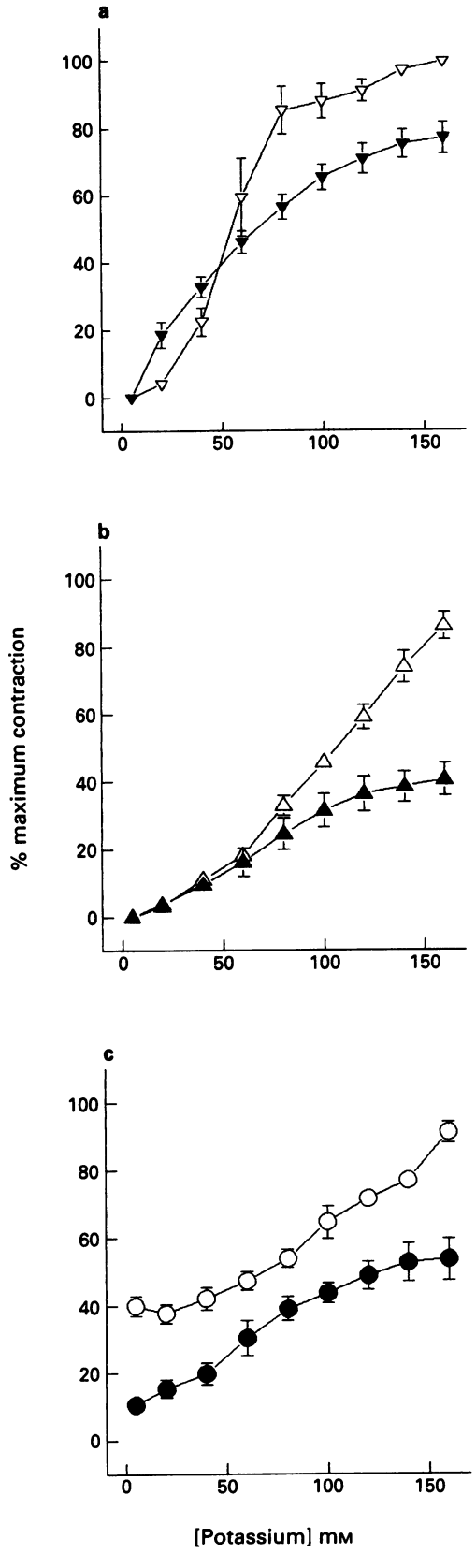

Figure 5 Effects of calphostin C (1 μM) on the concentration-responses to K^+ in the guinea-pig aorta. (a) In normal Krebs solution ($n = 6$), calphostin C (▼) reduced the responsiveness of the tissue by about 20% compared to controls (▽). (b) In Ca^{2+}-free medium ($n = 6$), contraction to high K^+ was significantly inhibited by 50% in calphostin C (▲)-treated tissues compared with controls (△). (c) Pretreatment of the tissue with calphostin C (●) significantly reduced the phenylephrine- and KCl-induced contractions in Ca^{2+}-free medium ($n = 6$) compared with controls (○).

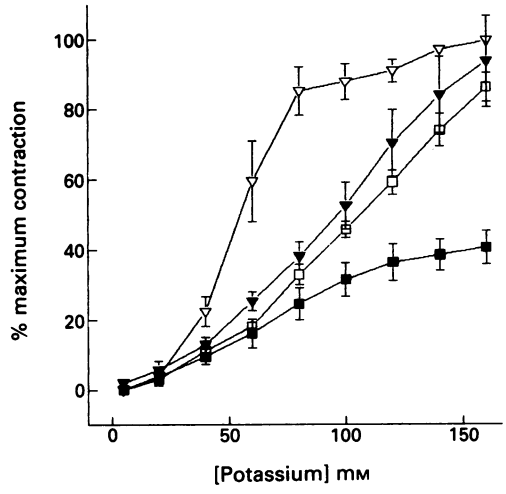

Figure 6 A summary of the main findings of this study in the guinea-pig aorta: components of hypertonically-added K^+ contraction. The relationship of concentration-responses to K^+ in normal Krebs solution ($n = 8$, ▽), in Krebs containing nicardipine (10 μM, $n = 8$, ▼), in Ca^{2+}-free Krebs ($n = 6$, □) and in Ca^{2+}-free Krebs containing calphostin C (1 μM, $n = 6$, ■).

catalytic (Hidaka *et al.*, 1984) or regulatory diacylglycerol binding domain, respectively (Kobayashi *et al.*, 1989).

Nicardipine-insensitive KCl contraction is not due to Ca^{2+} release from the intracellular store

A recent report demonstrated that a large membrane hyperpolarization can inhibit noradrenaline-induced synthesis of inositol 1,4,5-trisphosphate (IP_3) in the rabbit mesenteric artery although depolarization did not appear to affect the synthesis of IP_3 in the study (Itoh *et al.*, 1992). On the other hand, the release of internally-stored Ca^{2+} by high K^+ in other smooth muscle has been demonstrated directly with a fluorescent dye in a Ca^{2+}-free environment (rat aorta; Kobayashi *et al.*, 1985) or indirectly by measurement of IP_3 levels after ruling out effects from neurotransmitter release (rat vas deferens; Khoyi *et al.*, 1989). In non-excitable cells such as the rat parotid cells, high K^+ elevated free Ca^{2+} concentration in both normal and Ca^{2+}-free medium. It was concluded that this results from the mobilization of Ca^{2+} from internal storage sites since high K^+ did not affect $^{45}Ca^{2+}$ uptake into the cells (Takemura & Ohshika, 1987; 1988). Their findings suggest that high K^+ can activate phospholipase C in some vascular muscles. The mechanism by which a depolarizing agent, such as K^+, activates membrane-bound or intracellular enzymes is not known but such a phenomenon has been previously reported (Itoh *et al.*, 1992; Quast, 1993). This interesting phenomenon in excitation-contraction coupling warrants further investigation.

In our experiments, using agents which affect uptake and release from Ca^{2+} stores, we were not able to attribute the high K^+-induced contraction in Ca^{2+}-free medium directly to any form of Ca^{2+} release from storage sites. This is expected since the release of Ca^{2+} is transient and limited by the available amount of stored Ca^{2+}. Nevertheless, the transient release of Ca^{2+} can activate PKC and phosphorylate the myosin light chain kinase. These events may possibly contribute to the sustained contraction but are unlikely to play a role in this study. When we performed an experiment in which the arteries were incubated with 10 mM EGTA to remove all the intracellular Ca^{2+} stores prior to the hypertonic addition of K^+, a concentration-dependent increase in tension was still observed. Furthermore, in most of the experiments, by the time we added H7 or calphostin C, at least 30 min had lapsed with the arterial rings bathed in

Ca^{2+}-free Krebs. A 30 min period of incubation in Ca^{2+}-free medium containing 50 μM EGTA was found to abolish the phenylephrine-induced contraction, an observation which suggests that most of the Ca^{2+} in the cell had dissipated.

Collins and her co-workers (1992) have suggested the presence of Ca^{2+}-independent isozyme of PKC in ferret aortic cells. Such an isozyme could account for our observations on high K^+ induced contraction. Since the activation of phospholipase C not only gives rise to IP_3 but also to diacylglycerol, it is not surprising that high K^+-induced depolarization can also activate PKC. It is interesting that in the guinea-pig aorta, calphostin C also significantly inhibited phenylephrine induced contraction in Ca^{2+}-free medium (Figure 5).

Summary

Figure 6 summarizes the components of contraction induced by hypertonically-added K^+ in the guinea-pig aorta. The EC_{50} of the concentration-response curve to hypertonically-added K^+ is around 50 mM in normal Krebs solution whereas in Ca^{2+}-free Krebs or with nicardipine pretreatment, the EC_{50} is around 100 mM. The addition of calphostin C at 1 μM reduced the maximum contraction by about 50%. The nature of the residual contraction in Figure 6 following blockade by calphostin C was not investigated in this study but may be accounted for by hyperosmolarity *per se*.

Results from the present study also suggest that the ryanodine-sensitive Ca^{2+} pool may be different from that which is sensitive to CPA, thapsigargin and phenylephrine in the guinea-pig aorta. Therefore, multiple Ca^{2+} stores may exist in this tissue just as in dog mesenteric artery (Low *et al.*, 1992) and other tissues (bovine adrenal chromaffin cells, Robinson & Burgoyne, 1991; sea urchin egg, Rakow & Shen, 1990 and guinea-pig papillary muscle, Lynch III, 1991).

Conclusion

Our results suggest that hypertonically-added K^+, in contrast to isotonically-added K^+, causes contraction not only via L-type Ca^{2+} channel but also by activating membrane-bound enzymes. This mechanism is not the same as that by which hyperosmolar mannitol causes contraction. A significant portion of the high K^+ contracture in Ca^{2+}-free medium can apparently be accounted for by an isozyme of PKC independently of extracellular or intracellular Ca^{2+}.

This work was supported by the Heart and Stroke Foundation and Medical Research Council of Canada. A.M.L. is an MRC of Canada post-doctoral fellow.

References

ABRAHAM, S.T. & RICE, P.J. (1992). Protein kinase C-mediated contractile response of the rat vas deferens. *Eur. J. Pharmacol.*, **218**, 243–249.

BOLTON, T.B. (1979). Mechanisms of action of transmitters and other substances on smooth muscle. *Physiol. Rev.*, **59**, 607–718.

COLLINS, E.M., WALSH, M.P. & MORGAN, K.G. (1992). Contraction of single vascular smooth muscle cells by phenylephrine at constant $[Ca^{2+}]_i$. *Am. J. Physiol.*, **262**, H754–H762.

DENG, H.W. & KWAN, C.Y. (1991). Cyclopiazonic acid is a sarcoplasmic reticulum Ca^{2+} pump inhibitor of rat aortic muscle: a functional study. *Acta Pharmacol. Sinica*, **12**, 53–58.

HALLER, H., SMALLWOOD, J.I. & RASMUSSEN, H. (1990). Protein kinase C translocation in intact vascular smooth muscle strips. *Biochem. J.*, **270**, 375–381.

HIDAKA, H., INAGAKI, M., KAWAMOTO, S. & SASAKI, Y. (1984). Isoquinolinesulfonamides, novel and potent inhibitors of cyclic nucleotide dependent protein kinase and protein kinase C. *Biochemistry*, **23**, 5036–5041.

ITOH, T., SEKI, N., SUZUKI, S., ITO, S., KAJIKURI, J. & KURIYAMA, H. (1992). Membrane hyperpolarization inhibits agonist-induced synthesis of inositol 1,4,5-trisphosphate in rabbit mesenteric artery. *J. Physiol.*, **451**, 307–328.

JENKIN, R.A., BALDI, M.A., IWANOV, V. & MOULDS, R.F.W. (1991). Differences between rat and guinea pig aorta in postreceptor mechanisms of α_1-adrenoceptors. *J. Cardiovasc. Pharmacol.*, **18**, 566–573.

KHALIL, R.A. & MORGAN, K.G. (1991). Imaging of protein kinase C distribution and translocation in living vascular smooth muscle cells. *Circ. Res.*, **69**, 1626–1631.

KHOYI, M.A., SMITH, M.A., BUXTON, I.L.O. & WESTFALL, D.P. (1989). Factors involved in the generation of tension during contraction to high K^+ in the rat vas deferens. *Cellular Signalling*, **6**, 599–605.

KOBAYASHI, S., KANAIDE, H. & NAKAMURA, M. (1985). K^+-depolarization induces a direct release of Ca^{2+} from intracellular storage sites in cultured vascular smooth muscle cells. from rat aorta. *Biochem. Biophys. Res. Commun.*, **129**, 877–884.

KOBAYASHI, E., NAKAMO, H., MORIMOTO, M. & TAMAOKI, T. (1989). Calphostin C (UCN-1028C), a novel microbial compound, is a highly potent and specific inhibitor of protein kinase C. *Biochem. Biophys. Res. Commun.*, **159**, 548–553.

LOW, A.M., GASPAR, V., KWAN, C.Y., DARBY, P.J., BOURREAU, J.P. & DANIEL, E.E. (1991). Thapsigargin inhibits repletion of the phenylephrine-sensitive intracellular pool in vascular smooth muscles. *J. Pharmacol. Exp. Ther.*, **258**, 105–1113.

LOW, A.M., KWAN, C.Y. & DANIEL, E.E. (1992). Evidence for two types of internal Ca^{2+} stores in canine mesenteric artery with different refilling mechanisms. *Am. J. Physiol.*, **262**, H31–H37.

LYNCH, III C. (1991). Pharmacological evidence for two types of myocardial sarcoplasmic reticulum Ca^{2+} release. *Am. J. Physiol.*, **260**, H785–H795.

MORRIS, J.L. (1991). Roles of neuropeptide Y and noradrenaline in sympathetic neurotransmission to the thoracic vena cava and aorta of guinea-pigs. *Regul. Pept*, **32**, 297–310.

NIELSEN-KUDSK, J.E., NIELSEN, C.B. & MELLEMKJAER, S. (1992). Influence of osmolarity of solutions used for K^+ contraction on relaxant responses to pinacidil, verapamil, theophylline and terbutaline in isolated airway smooth muscles. *Pharmacol. Toxicol.*, **70**, 46–49.

NISHIZUKA, Y. (1984). The role of protein kinase C in cells surface signal transduction and tumor promotion. *Nature*, **308**, 693–698.

NISHIZUKA, Y. (1992). Intracellular signalling by hydrolysis of phospholipids and activation of protein kinase C. *Science*, **258**, 607–614.

QUAST, U. (1993). Do the K^+ channel openers relax smooth muscle by opening K^+ channels? *Trends Pharmacol. Sci.*, **14**, 332–337.

RAKOW, T.L. & SHEN, S.S. (1990). Multiple stores of Ca^{2+} are released in the sea urchin egg during fertilization. *Proc. Natl. Acad. Sci. U.S.A.*, **87**, 9285–9289.

ROBINSON, I.M. & BURGOYNE, R. (1991). Characterisation of distinct inositol 1,4,5-trisphosphate-sensitive and caffeine-sensitive Ca^{2+} stores in digitonin-permeabilized adrenal chromaffin cells. *J. Neurochem.*, **56**, 1587–1593.

SATO, K., HORI, M., OZAKI, H., TAKANO-OHMURO, H., TSUCHIYA, T., SUGI, H. & KARAKI, J. (1992). Myosin phosphorylation-independent contraction induced by phorbol ester in vascular smooth muscle. *J. Pharmacol. Exp. Ther.*, **261**, 497–505.

SHIMAMOTO, Y., SHIMAMOTO, H., KWAN, C.Y. & DANIEL, E.E. (1993). Differential effects of putative protein kinase C inhibitors on contraction of rat aortic smooth muscle. *Am. J. Physiol.*, **265**, H1300–H1306.

TAKEMURA, H. & OHSHIKA, H. (1987). Effects of Ca^{2+} agonist and antagonists on cytosolic free Ca^{2+} concentration: studies on Ca^{2+} channels in rat parotid cells. *Comp. Biochem. Physiol.*, **88**, 219–224.

TAKEMURA, H. & OHSHIKA, H. (1988). K^+ elevates cytosolic free Ca^{2+} concentration due to mobilization from internal storage sites in rat parotid cells. *Comp. Biochem. Physiol.*, **89A**, 173–178.

WRIGHT, G. (1991). Use-dependent decline in rat aorta sensitivity to contraction by K^+. *Can. J. Physiol. Pharmacol.*, **69**, 921–928.

XUAN, Y.-T., WANG, O.-L. & WHORTON, R. (1992). Thapsigargin stimulates Ca^{2+} entry in vascular smooth muscle cells: nicardipine-sensitive and -insensitive pathways. *Am. J. Physiol.*, **262**, C1258–C1265.

(Received July 20, 1993
Revised January 19, 1994
Accepted February 8, 1994)

Br. J. Pharmacol. (1994), **112**, 611–615

Cell inward transport of L-DOPA and 3-O-methyl-L-DOPA in rat renal tubules

[1]P. Soares-da-Silva, [2]M.H. Fernandes & P.C. Pinto-do-Ó

Institute of Pharmacology and Therapeutics, Faculty of Medicine, 4200 Porto, Portugal

1 The present study has determined the kinetics of the uptake of L-3,4-dihydroxyphenylalanine (L-DOPA) and 3-O-methyl-L-DOPA (3-OMDOPA) in rat renal tubules and examined the effect of 3-OMDOPA on the inward transport of L-DOPA and on its conversion into dopamine in kidney homogenates.

2 The accumulation of both L-DOPA and 3-OMDOPA in renal tubules was found to occur through non-saturable and saturable mechanisms. The kinetics of the saturable component of L-DOPA and 3-OMDOPA uptake in renal tubules were as follows: L-DOPA, $V_{max} = 11.1$ nmol mg^{-1} protein h^{-1} and $K_m = 216\ \mu M$ ($n = 6$); 3-OMDOPA, $V_{max} = 8.1$ nmol mg^{-1} protein h^{-1} and $K_m = 231\ \mu M$ ($n = 5$). The diffusion constant of the non-saturable component for the accumulation of L-DOPA and 3-OMDOPA was 0.0010 and 0.0014 μmol^{-1}, respectively.

3 3-OMDOPA (100 to 2000 μM) was found to produce a concentration-dependent decrease (29% to 81% reduction) of the saturable component of the tubular uptake of L-DOPA; the K_i value of 3-OMDOPA for inhibition of L-DOPA uptake was found to be 181 μM ($n = 5$). The accumulation of L-DOPA obtained in experiments conducted at 4°C was not affected by 3-OMDOPA.

4 In experiments conducted in kidney homogenates only L-DOPA (10 to 5000 μM) was found to be decarboxylated. The V_{max} and K_m values for aromatic L-amino acid decarboxylase determined in the absence of 3-OMDOPA ($V_{max} = 14.1$ nmol mg^{-1} protein h^{-1}; $K_m = 62\ \mu M$) were not significantly different from those observed when the decarboxylation of L-DOPA was carried out in the presence of 1000 μM 3-OMDOPA ($V_{max} = 15.7$ nmol mg^{-1} protein h^{-1}; $K_m = 68\ \mu M$).

5 It is concluded that the tubular uptake of both L-DOPA and 3-OMDOPA occur through non-saturable and saturable mechanisms; only the saturable tubular uptake of L-DOPA was found to be inhibited by 3-OMDOPA. It is further shown that 3-OMDOPA neither undergoes decarboxylation into 3-MT nor affects the decarboxylation of L-DOPA.

Keywords: L-DOPA; 3-O-methyl-L-DOPA (3-O-methylDOPA); kidney; dopamine

Introduction

After almost three decades of clinical use, L-3,4dihydroxyphenylalanine (L-DOPA) in combination with a peripheral aromatic L-amino acid decarboxylase (AAAD) inhibitor still remains widely used in the treatment of Parkinson's disease. Major problems with this type of therapy are the L-DOPA-induced dyskinesias which it has been suggested are related to kinetic factors that affect the absolute and relative plasma concentrations of L-DOPA and 3-O-methyl-L-DOPA (3-OMDOPA) (Furgeson *et al.*, 1976; Rivera-Calimlim *et al.*, 1977); patients with L-DOPA-induced dyskinesias have been reported to present higher plasma concentrations of 3-OMDOPA (Reilly *et al.*, 1980). Although the decarboxylation of L-DOPA is believed to represent a major pathway of its metabolism, methylation into 3-OMDOPA by catechol-*O*-methyltransferase (COMT) may also occur, this assuming particular relevance in conditions of AAAD inhibition (Sharpless *et al.*, 1973; Männistö & Kaakkola, 1989). The proposed mechanisms through which 3-OMDOPA may predispose to dyskinesias include inhibition of L-DOPA uptake at the blood-brain barrier and competition for decarboxylation by AAAD (Reilly *et al.*, 1980).

In kidney, it has been suggested that dopamine may be of some physiological importance in the regulation of tubular reabsorption of sodium (Lee, 1993). The synthesis of dopamine in renal tissues has been demonstrated to result from the decarboxylation of circulating or filtered L-DOPA in epithelial cells of proximal convoluted tubules. This type of cell is endowed with high AAAD activity and the formation of dopamine is believed to occur after the uptake of L-DOPA into this cellular compartment (Soares-da-Silva & Fernandes, 1990). The tubular uptake of L-DOPA has been demonstrated to occur through an energy-dependent and stereo-selective carrier-mediated process, the rate of transport being 2 fmol cm^{-1} s^{-1} (Chan, 1976). There is, however, lack of objective information concerning the mechanism(s) involved and the nature of the process(es) of cell membrane transport of L-DOPA in epithelial cells of renal tubules. However, given the considerable high AAAD in renal tissues (Soares-da-Silva *et al.*, 1993), it is possible that the rate limiting step in the renal formation of dopamine from plasma L-DOPA resides in the cell inward transport of the substrate.

The aim of the present work was to determine the nature and the kinetic characteristics of the tubular uptake of both L-DOPA and of its O-methylated derivative 3-OMDOPA. In the studies reported here we took advantage of the fact that 3-OMDOPA is the only compound known to inhibit the cell inward transport of L-DOPA at the level of the blood-brain barrier, and decided to examine also the extent to which 3-OMDOPA is inhibiting the tubular uptake of L-DOPA. In addition, given the structural similarities between L-DOPA and 3-OMDOPA we thought it of interest to study the extent to which these compounds undergo decarboxylation by renal AAAD.

Methods

Uptake studies of L-DOPA and 3-OMDOPA into renal tubules were performed in male Wistar rats (Biotério do

[1] Author for correspondence.
[2] Permanent address: Faculty of Medical Dentistry, 4200 Porto, Portugal.

Instituto Gulbenkian de Ciência, Oeiras, Portugal), aged 45–60 days, given benserazide (10 mg kg^{-1}, i.p.) 60 min before they were killed, in order to inhibit peripheral AAAD (DaPrada *et al.*, 1987). In some experiments, the uptake of 3-OMDOPA was performed in renal tubules obtained from rats given saline (0.9% NaCl), instead of benserazide, 60 min before they were killed. Animals were killed by decapitation under ether anaesthesia and the kidneys removed through a midline abdominal incision, after which they were decapsulated, cut in half and placed in ice-cold Collins solution [containing (in mM): KH_2PO_4 15, K_2HPO_4 50, KCl 15, $NaHCO_3$ 15, $MgSO_4$ 60 and glucose 140, pH = 7.4]. The outer cortex was cut out with fine scissors and minced with a scalpel into a fine paste. The cortical paste was filtered sequentially through a series of Nybolt nylon sieves, first 180 μm and then 75 μm. Unseparated cortex remained on the upper (180 μm) sieve, while the lower one (75 μm) retained predominantly proximal nephron segments. The sieves were continuously rinsed with cold Collins solution throughout. The retained tubules were then washed off with cold Collins solution and collected into a pellet by centrifugation at 200 *g*, for 5 min, 4°C; renal tubules used in incubation experiments were suspended in Hanks medium. The Hanks medium had the following composition (mM): NaCl 137, KCl 5, $MgSO_4$ 0.8, Na_2HPO_4 0.33, KH_2PO_4 0.44, $CaCl_2$ 0.25, $MgCl_2$ 1.0, Tris HCl 0.15 and sodium butyrate 1.0, pH = 7.4. Pargyline (0.1 mM) and tolcapone (1 μM) were also added to the Hanks medium in order to inhibit the enzymes, monoamine oxidase (MAO) and COMT, respectively (Fernandes *et al.*, 1991; Soares-da-Silva & Vieira-Coelho, 1993). The viability of proximal renal tubules used in this study was assessed by the trypan blue (0.2% w/v) exclusion method; nephron segments were pipetted on to a glass slide and observed 90 s after exposure to the dye, with a Leica microscope. Under these conditions, more than 90% of the renal tubules excluded the dye.

The preincubation and incubation of renal tubules (500 μl) were carried out in glass test tubes, continuously shaken and gassed (95% O_2 and 5% CO_2) throughout the experiment. Some experiments were performed to define the kinetic characteristics of the tubular uptake of L-DOPA and 3-OMDOPA. The non-saturable component of L-DOPA and 3-OMDOPA uptake was determined in experiments conducted at 4°C; the saturable component was derived from the total amount of L-DOPA and 3-OMDOPA accumulated in renal tubules at 37°C, subtracted with the values obtained for the non-saturable component. After preincubation, renal tubules were incubated for 15 min in Hanks medium with increasing concentrations (50 to 2000 μM) of L-DOPA or 3-OMDOPA. The incubation was stopped by cooling and an aliquot (300 μl) of the incubation medium containing the renal tubules was immediately transferred to Spin-X (Costar) centrifuge filter (0.22 μm) tubes and centrifuged (4 min, 3000 *g*, 4°C); the renal tubules were washed twice with ice-cold medium (500 μl). The extraction of L-DOPA and 3-OMDOPA from renal tubules was performed by the addition of 500 μl of 0.2 M perchloric acid to the Spin-X centrifuge filter tubes at the end of the second washing period; the centrifuge filter tubes were then centrifuged and 50 μl of the filtered aliquot containing the compounds of interest was then injected directly into the column of a high pressure liquid chromatograph for the quantification of L-DOPA and 3-OMDOPA. The filters were found not to retain L-DOPA or 3-OMDOPA and the extraction process employed was also found to remove both compounds completely from the renal tubules.

In experiments conducted with the aim of studying the interference of 3-OMDOPA with the tubular uptake of L-DOPA, renal tubules were preincubated for 15 min with increasing concentrations of 3-OMDOPA (50, 100, 250, 500, 1000 and 2000 μM); the incubation was performed in the presence of 250 μM L-DOPA. As mentioned above, the saturable component of L-DOPA uptake was derived from the total amount of L-DOPA accumulated in renal tubules at 37°C subtracted with the values obtained in paired experiments conducted at 4°C. At the end of the incubation, renal tubules were washed twice with ice-cold Hanks medium and the assay of L-DOPA and 3-OMDOPA was performed as described above.

In experiments designed to study the decarboxylation of L-DOPA or 3-OMDOPA and the interference of 3-OMDOPA with the decarboxylation of L-DOPA, kidney homogenates instead of renal tubules were used. Whole kidneys were homogenized in a modified Krebs solution with Duall-Kontes homogenizers and kept continuously on ice. The composition of the modified Krebs solution was as follows (in mM): NaCl 50, choline chloride 68, KCl 4.7, $CaCl_2$ 2.4, $MgSO_4$ 1.2, $NaHCO_3$ 25, KH_2PO_4 1.2, EDTA 0.4, glucose 10 and sodium butyrate 1; pH = 7.4. L-α-Methyl-*p*-tyrosine (50 μM) and copper sulphate (10 μM) were also added to the Krebs solution in order to inhibit the enzyme, tyrosine hydroxylase and inhibit the endogenous inhibitors of dopamine β-hydroxylase, respectively. Aliquots of 1.0 ml of kidney homogenates plus 1.0 ml Krebs solution were placed in glass test tubes and incubated for 30 min in the presence of tolcapone (1 μM) and pargyline (0.1 mM); thereafter, L-DOPA or 3-OMDOPA (10 to 5000 μM) was added to the medium for a further 15 min. In experiments in which the effect of 3-OMDOPA (1000 μM) was tested on the decarboxylation of L-DOPA, the methylated compound was present during the preincubation and incubation periods. During incubation, kidney homogenates were continuously shaken and gassed (95% O_2 and 5% CO_2) and maintained at 37°C. The reaction was stopped by the addition of 250 μl of 2 M perchloric acid and the preparations kept at 4°C for 60 min; this procedure has been found to result in a complete extraction of catecholamines from the tissues (Fernandes *et al.*, 1991). The samples were then centrifuged (200 *g*, 2 min, 4°C) and 50 μl aliquots of the supernatant filtered on Millipore microfilters (MF1) and injected directly into the column of a high performance liquid chromatograph (h.p.l.c.) for the quantification of dopamine and 3-methoxytyramine.

The h.p.l.c. system consisted of a pump (Gilson model 302; Gilson Medical Electronics, Villiers le Bel, France) connected to a mannometric module (Gilson model 802 C) and a stainless-steel 5 μm ODS column (Biophase, Bioanalytical Systems, West Lafayette, IN, U.S.A.), 25 cm in length; samples were injected by means of an automatic sample injector (Gilson model 231) connected to a Gilson dilutor (model 401). The mobile phase was a degassed solution of citric acid (0.1 mM), sodium octylsulphate (0.5 mM), sodium acetate (0.1 M), EDTA (0.17 mM), dibutylamine (1 mM) and methanol (8% v/v), adjusted to pH 3.5 with perchloric acid (2 M) and pumped at a rate of 1.0 ml min^{-1}. The detection was carried out electrochemically with a glassy carbon electrode, an Ag/AgCl reference electrode and an amperometric detector (Gilson model 141); the detector cell was operated at 0.75 V. The current produced was monitored using the Gilson 712 h.p.l.c. software. The lower limits for detection of L-DOPA, 3-OMDOPA, dopamine and 3-methoxytyramine ranged from 350 to 500 fmol.

The protein content of the suspensions of renal tubules and kidney homogenates was determined by the method of Bradford (1976), with human serum albumin as a standard.

V_{max} and K_m values for the saturable component of L-DOPA and 3-OMDOPA uptake and AAAD activity were calculated by linear regression analysis. The diffusion constant represents the slope of the accumulation of L-DOPA and 3-OMDOPA measured in experiments carried out at 4°C (Neame & Richards, 1972). For the calculation of the IC_{50} s the parameters of the Hill-equation for multisite inhibition were fitted to the experimental data (Segel, 1975). The K_i s were calculated from the corresponding IC_{50} s as described by Cheng & Prussof (1973). Geometric means are given with 95% confidence limits and arithmetic means are given with s.e.mean.

L-3,4-dihydroxyphenylalanine (L-DOPA), dopamine hydrochloride, 3-methyl-L-DOPA, pargyline hydrochloride and trypan blue were purchased from Sigma Chemical Company (St Louis, MO, U.S.A.); tolcapone was kindly donated by the producer (Hoffmann La Roche, Basle, Switzerland).

Results

Incubation of renal tubules at 4°C in the presence of increasing concentrations of L-DOPA and 3-OMDOPA, results in a concentration-dependent accumulation of the substrates (Figure 1); under these experimental conditions the accumulation of both L-DOPA and 3-OMDOPA was found to be linear and of similar magnitude. When the experiments were carried out at 37°C, the accumulation of both L-DOPA and 3-OMDOPA in renal tubules was found to be greater than that occurring at 4°C and showed a trend for saturation. The saturable component of both L-DOPA and 3-OMDOPA uptake (Figure 1) was derived from the total amount of L-DOPA or 3-OMDOPA accumulated in renal tubules at 37°C with the values obtained in experiments conducted at 4°C subtracted. The V_{max} and K_m values for the saturable component of L-DOPA and 3-OMDOPA uptake in renal tubules were as follows: L-DOPA, $V_{max} = 11.1 \pm 2.5$ nmol mg^{-1} protein h^{-1} and $K_m = 216$ (95% confidence limits: 96,487) μM ($n = 6$); 3-OMDOPA, $V_{max} = 8.1 \pm 2.1$ nmol mg^{-1} protein h^{-1} and $K_m = 231$ (93,575) μM ($n = 5$). The diffusion constant (in μmol^{-1}) of the non-saturable component for the accumulation of L-DOPA and 3-OMDOPA was 0.0014 (0.0011, 0.0019; $n = 6$) and 0.0010 (0.0005, 0.0019; $n = 5$), respectively.

Figure 2 shows the effect of increasing concentrations (50 to 2000 μM) of 3-OMDOPA on the saturable component of L-DOPA uptake into renal proximal tubules. 3-OMDOPA was found to produce a concentration-dependent decrease in the tubular uptake of L-DOPA. The lowest concentration of 3-OMDOPA (100 μM) resulting in some inhibition of L-DOPA uptake was found to reduce its tubular uptake by 29%; the greatest inhibitory effect on the tubular uptake of L-DOPA (81% reduction) was obtained with 1000 μM 3-OMDOPA. The K_i value (in μM) of 3-OMDOPA for inhibition of L-DOPA uptake was found to be 181 (98,333) ($n = 5$). This K_i value for 3-OMDOPA agrees with the K_m value of 3-OMDOPA uptake obtained in saturation experiments. The accumulation of L-DOPA obtained in experiments conducted at 4°C was found not to be affected by 3-OMDOPA (data not shown).

Incubation of kidney homogenates, in conditions of catechol-*O*-methyltransferase (COMT) and monoamine

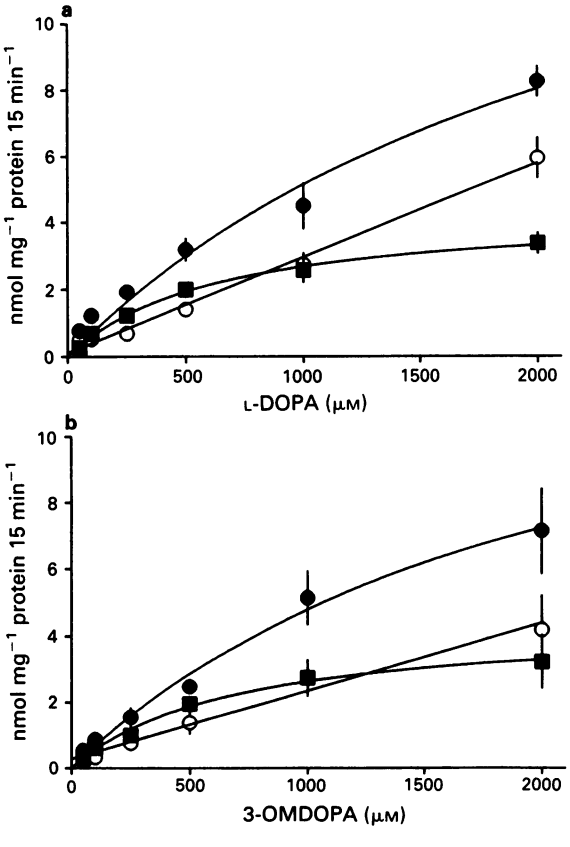

Figure 1 Accumulation of (a) L-DOPA and (b) 3-OMDOPA in suspensions of rat isolated renal tubules. The non-saturable component of substrate uptake (○) was obtained in experiments conducted at 4°C and was found to be linear with the concentration of the substrate. The saturable component (■) was derived from the total (●) amount of L-DOPA or 3-OMDOPA accumulated in renal tubules at 37°C with the values obtained for the non-saturable component subtracted. Each point is the mean with s.e.mean of five to six experiments per group.

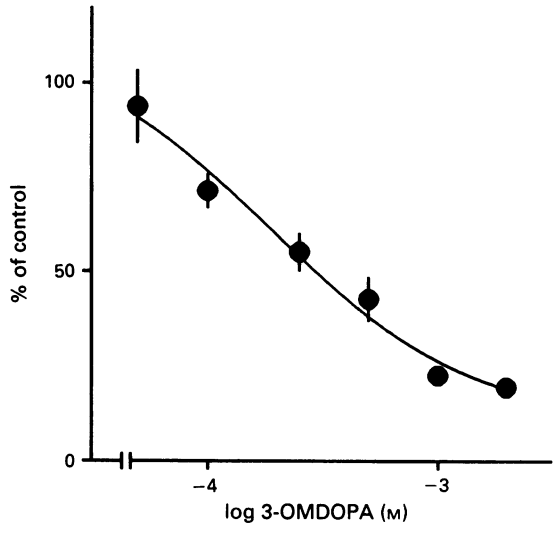

Figure 2 Concentration-dependent inhibition by 3-OMDOPA (50 to 2000 μM) of the saturable transport of L-DOPA in suspensions of rat isolated renal tubules incubated with 250 μM L-DOPA. Each point represents the mean with s.e.mean of six experiments per group.

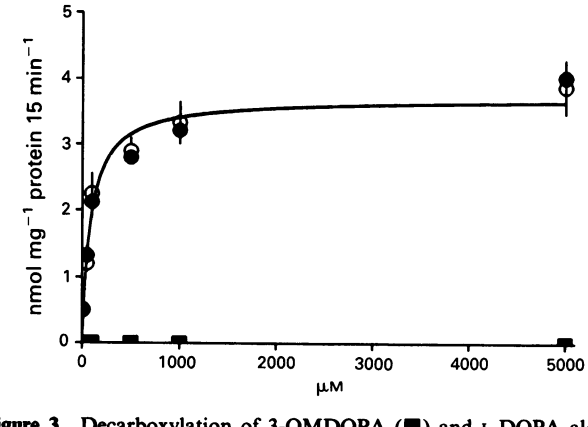

Figure 3 Decarboxylation of 3-OMDOPA (■) and L-DOPA alone (○) or in combination with 3-OMDOPA (1000 μM; ●) in rat kidney homogenates incubated with increasing concentrations (10 to 5000 μM) of the substrates. The results show levels (in mol mg^{-1} protein 15 min^{-1}) of dopamine and 3-methoxytyramine formed, respectively, from added L-DOPA and 3-OMDOPA during a 15 min incubation period. Since no formation of 3-methoxytyramine from added 3-OMDOPA was found to occur, the levels indicated in the figure are the detection limit of the method for 3-methoxytyramine. Each point represents the mean with s.e.mean of four experiments per group.

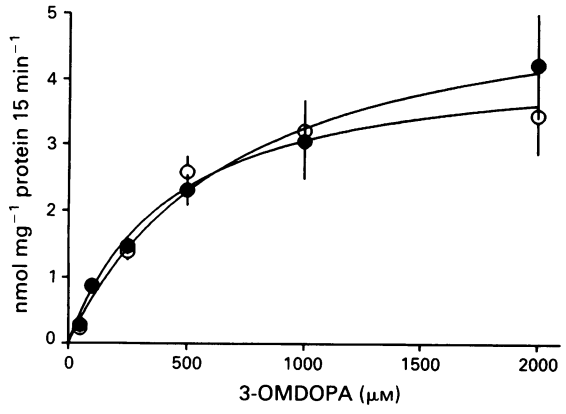

Figure 4 Accumulation of 3-OMDOPA in suspension of rat isolated renal tubules obtained from control animals (●) and benserazide-treated animals (○). The results are levels (in nmol mg^{-1} protein 15 min^{-1}) of 3-OMDOPA accumulated in renal tubules through the saturable transporter. The saturable component was derived from the total amount of 3-OMDOPA accumulated in renal tubules at 37°C with the values obtained for the non-saturable component subtracted. Each point is the mean with s.e.mean of five experiments per group.

oxidase (MAO) inhibition, with L-DOPA (10 to 5000 μM) resulted in a concentration-dependent formation of dopamine, as shown in Figure 3. However, the incubation of kidney homogenates with 3-OMDOPA (10 to 5000 μM) did not result in the formation of 3-methoxytyramine, the compound expected to result from the decarboxylation of 3-OMDOPA. The addition of 1000 μM 3-OMDOPA to the incubation medium did not affect the formation of dopamine in kidney homogenates incubated with increasing concentrations of L-DOPA (10 to 5000 μM). The V_{max} and K_m values for AAAD determined in the absence of 3-OMDOPA (V_{max} = 14.1 ± 0.6 nmol mg^{-1} protein h^{-1}; K_m = 62 [43, 87] μM) were not significantly different from those observed when the decarboxylation of L-DOPA was carried out in the presence of 1000 μM 3-OMDOPA (V_{max} = 15.7 ± 1.0 nmol mg^{-1} protein h^{-1}; K_m = 68 [54, 87] μM).

In Figure 4 are shown the results on the saturable component of 3-OMDOPA uptake in renal tubules obtained from non-treated rats and animals given benserazide 60 min before they were killed. As indicated in the figure, no significant difference was observed on the tubular uptake of 3-OMDOPA in control and benserazide-treated rats. The accumulation of 3-OMDOPA through the non-saturable uptake component was similar in benserazide treated rats to that observed in the corresponding control animals (data not shown).

Discussion

The data presented here show that both L-DOPA and 3-OMDOPA are taken up into renal tubules through saturable and non-saturable mechanisms. The maximum rate of uptake of these two substrates through the saturable transporter and their affinity for the transporter unit, as shown by the V_{max} and K_m values, were found to be similar. The finding that 3-OMDOPA exerts a concentration-dependent inhibition upon the saturable component of tubular transport of L-DOPA, suggests that the two compounds are taken up by the same transporter. This suggestion is further supported by the result that 3-OMDOPA does not affect the non-saturable accumulation of L-DOPA, which is also in agreement with the view that the accumulation of both L-DOPA and 3-OMDOPA in renal tubules may not be related to the binding of these compounds to tissue components. At concentrations of the substrates approaching half saturation, diffusional uptake accounts for 49% and 36% of the total accumulation of 3-OMDOPA and L-DOPA, respectively. On the other hand, the similarity between K_i values of 3-OMDOPA for inhibition of L-DOPA uptake and K_m values of 3-OMDOPA tubular uptake agree with the view that 3-OMDOPA exerts a competitive type of inhibition upon the tubular uptake of L-DOPA. The results reported here for renal tissues are in accordance with those obtained in brain tissues, where it has been demonstrated that 3-OMDOPA competes with L-DOPA for its transport at the level of the blood-brain barrier (Wade & Katzman, 1975). Like that found to occur in renal tubules, the transport of both 3-OMDOPA and L-DOPA was found to occur through saturable and non-saturable mechanisms. In brain, however, the affinity of 3-OMDOPA (K_t = 0.13 mM) for the saturable transporter was found to be higher than that for L-DOPA (K_t = 0.34 mM).

An additional mechanism by which 3-OMDOPA has been suggested to interfere with the action of L-DOPA is that concerning the competition between the two compounds for AAAD (Reilly *et al.*, 1980). The experiments described here on kidney homogenates show, in contrast, that 3-OMDOPA was neither decarboxylated by AAAD nor interfered with the decarboxylation of L-DOPA. These results agree with those of Ferrini & Glasser (1964) while showing that 3-OMDOPA is in fact a poor substrate for AAAD, as determined in the guinea-pig kidney and mouse brain. After confirming that 3-OMDOPA does not undergo decarboxylation by renal AAAD it was decided to test the possibility of the interference of benserazide on the tubular accumulation of this compound. In experiments carried out in renal tubules prepared from renal tissues obtained from benserazide-treated and the corresponding controls (animals given the vehicle) it was found that the rate of maximum uptake of 3-OMDOPA through the saturable transporter was similar in both experimental conditions and the diffusional uptake of 3-OMDOPA was also not affected by pretreatment with the AAAD inhibitor. The dose of benserazide used has been demonstrated by other authors (DaPrada *et al.*, 1987) to produce an almost complete inhibition of the enzyme in peripheral tissues; the finding that no formation of dopamine was observed in renal tubules incubated with L-DOPA agrees with the view that this dose of benserazide is effective in inhibiting renal AAAD. Thus, in spite of the structural similarities between benserazide and L-DOPA or 3-OMDOPA, it might be suggested that the AAAD inhibitor does not interfere with the cell inward transport of these compounds.

The functional relevance of 3-OMDOPA is most probably shown in parkinsonian patients treated with L-DOPA in combination with a peripheral AAAD inhibitor, a condition which facilitates the *O*-methylation of L-DOPA (Männistö & Kaakkola, 1989). Even so, the plasma levels of 3-OMDOPA after the administration of 500 mg of L-DOPA to non-parkinsonian subjects has been found to exceed by far those of L-DOPA, dopamine or the amine metabolites, 3-methoxytyramine, 3,4-dihydroxyphenylacetic acid (DOPAC) and homovanillic acid (HVA) (Shigetomi *et al.*, 1991). In contrast to that described for normotensive subjects, salt-sensitive essential hypertensive patients fail to excrete larger amounts of dopamine in the urine, in conditions of increased renal delivery of sodium (for a review, see Lee, 1993) and appear to present an enhanced ability to deaminate and *O*-methylate renal dopamine (Shigetomi *et al.*, 1991). Apparently no differences were observed between the pattern of 3-OMDOPA formation after the administration of L-DOPA between control subjects and hypertensive patients (Shigetomi *et al.*, 1991). Plasma 3-OMDOPA does not, however, reflect exclusively the ability of renal tissues to *O*-methylate L-DOPA and it remains to be determined whether the increased renal COMT activity suggested to occur in hypertensive patients is accompanied by an increased *O*-methylation of endogenous circulating L-DOPA; if this

should occur, then the increased availability of 3-OMDOPA at the renal tubules would tend to decrease the tubular uptake of L-DOPA and the formation of renal dopamine. Circulating L-DOPA has been demonstrated to be converted to dopamine in the human kidney (Zimlichman *et al.*, 1988; Wolfovitz *et al.*, 1993), where the amine is expected to exert a natriuretic effect (Lee, 1993), and thereafter is excreted into the urine.

In conclusion, the results presented suggest that L-DOPA and 3-OMDOPA are using the same transporter in order to be taken up into renal tubular cells, 3-OMDOPA exerts a competitive type of inhibition upon the tubular uptake of L-DOPA. It is further shown that 3-OMDOPA neither undergoes decarboxylation into 3-MT nor affects the decarboxylation of L-DOPA.

The present study was supported by grant number PBIC/C/CEN 1139/92 from the Junta Nacional de Investigação Cientifica e Tecnológica (JNICT).

References

BRADFORD, M.M. (1976). A rapid method for the quantitation of microgram quantities of protein utilizing the principle of protein-dye binding. *Anal. Biochem.*, **72,** 248–254.

CHAN, Y.L. (1976). Cellular mechanisms of renal tubular transport of L-DOPA and its derivatives in the rat: microperfusions studies. *J. Pharmacol. Exp. Ther.*, **199,** 17–24.

CHENG, Y.-C. & PRUSSOFF, W.H. (1973). Relationship between the inhibition constant (K_i) and the concentration of the inhibitor which causes 50 per cent inhibition (IC_{50}) of an enzymatic reaction. *Biochem. Pharmacol.*, **22,** 3099–3108.

DAPRADA, M., KETTLER, R., ZURCHER, G., SCHAFFNER, R. & HAEFLEY, W.E. (1987). Inhibition of decarboxylase and levels of dopa and 3-O-methyldopa: a comparative study of benserazide versus carbidopa in rodents and of madopar standard versus madopar HBS in volunteers. *Eur. Neurol.*, **27** (suppl. 1), 9–20.

FERNANDES, M.H., PESTANA, M. & SOARES-DA-SILVA, P. (1991). Deamination of newly-formed dopamine in rat renal tissues. *Br. J. Pharmacol.*, **102,** 778–782.

FERRINI, R. & GLASSER, A. (1964). In vitro decarboxylation of new phenylalanine derivatives. *Biochem. Pharmacol.*, **13,** 798–801.

FURGESON, M.D., DILL, R.E. & DORIS, R.L. (1976). Importance of O-methylation in dopamine-induced motor and behavioural phenomena. *Brain Res.*, **105,** 163–167.

LEE, M.R. (1993). Dopamine and the kidney: ten years on. *Clin. Sci.*, **84,** 357–375.

MÄNNISTÖ, P.T. & KAAKKOLA, S. (1989). New selective COMT inhibitors: useful adjuncts for Parkinson's disease? *Trends Pharmacol. Sci.*, **10,** 54–56.

NEAME, K.D. & RICHARDS, T.G. (1972). *Elementary Kinetics of Membrane Carrier Transport.* Oxford: Blackwell Scientific Publications.

REILLY, D.K., RIVERA-CALIMLIM, L. & VAN DYKE, R. (1980). Catechol-O-methyltransferase activity: a determinant of levodopa response. *Clin. Exp. Pharmacol.*, **28,** 278–286.

RIVERA-CALIMLIM, L., DEEPAK, T., ANDERSON, R. & JOYNT, R. (1977). The clinical picture and plasma levodopa metabolite profile of parkinsonian non-responders. *Arch. Neurol.*, **34,** 228–232.

SEGEL, I.H. (1975). *Enzyme Kinetics: Behavior Analysis of Rapid Equilibrium and Steady-State Enzyme Systems.* New York: John Wiley.

SHARPLESS, N.S., TYCE, G.M. & OWEN, C.A. (1973). Effect of chronic administration of L-DOPA on catechol-O-methyltransferase in rat tissues. *Life Sci.*, **12,** 97–106.

SHIGETOMI, S., BUU, N.T. & KUCHELL, O. (1991). Dopaminergic abnormalities in borderline essential hypertensive patients. *Hypertension*, **17,** 997–1002.

SOARES-DA-SILVA, P. & FERNANDES, M.H. (1990). Regulation of dopamine synthesis in the rat kidney. *J. Auton. Pharmacol.*, **10** (Suppl. 1), s25–s30.

SOARES-DA-SILVA, P., FERNANDES, M.H. & PESTANA, M. (1993). A comparative study on the synthesis of dopamine in the human, dog and rat kidney. *Acta Physiol Scand.*, **148,** 347–351.

SOARES-DA-SILVA, P. & VIEIRA-COELHO, M.A. (1993). Increased sensitivity of renal catechol-O-methyltransferase to inhibition by tolcapone. *J. Am. Soc. Nephrol.*, **4,** 896 (abstact).

WADE, L.A. & KATZMAN, R. (1975). 3-O-methylDOPA uptake and inhibition of L-DOPA at the blood brain barrier. *Life Sci.*, **17,** 131–136.

WOLFOVITZ, E., GROSSMAN, E., FOLIO, C.J., KEISER, H.R., KOPIN, I.J. & GOLDSTEIN, D.S. (1993). Derivation of urinary dopamine from plasma dihydroxyphenylalanine in humans. *Clin. Sci.*, **84,** 549–557.

ZIMLICHMAN, R., LEVINSON, P.D., KELLY, G., STULL, R., KEISER, H.R. & GOLDSTEIN, D.S. (1988). Derivation of urinary dopamine from plasma dopa. *Clin. Sci.*, **75,** 515–520.

(Received December 16, 1993
Revised February 7, 1994
Accepted February 8, 1994)

Br. J. Pharmacol. (1994), **112**, 616–624

Block by capsaicin of voltage-gated K^+ currents in melanotrophs of the rat pituitary

S.J. Kehl

Department of Physiology, University of British Columbia, Vancouver, B.C., V6T 1Z3, Canada

1 Whole-cell recordings of macroscopic K^+ currents were made from acutely dissociated and cultured melanotrophs isolated from the pars intermedia of the adult rat pituitary.

2 In acutely dissociated cells, external capsaicin reversibly decreased the amplitude both of the fast-activating, fast-inactivating potassium current $I_K(f)$ and the slowly-activating, slowly-inactivating potassium current $I_K(s)$. To simplify the investigation of the mechanism of action of capsaicin experiments were conducted on cultured melanotrophs that express only $I_K(s)$.

3 In control cells the activation rate and the amplitude of $I_K(s)$ increased with depolarization and the current showed very little inactivation at any voltage during pulses lasting for 100–300 ms. In capsaicin, the decrease of the current amplitude was associated with an increased rate of current decay ('inactivation'). At a given voltage, the extent and the rate of the capsaicin-induced inactivation was proportional to the capsaicin concentration; and, at a given concentration, the extent and rate of the inactivation increased with membrane depolarization.

4 The fit of the Hill equation to data derived from the steady-state block of $I_K(s)$ evoked at 10 mV indicated an equilibrium dissociation constant (K_D) of 17.4 μM (95% confidence limits 15.8–19.0) and a Hill coefficient of 1.8 (95% CI 1.5–2.2) suggesting that at least two molecules of capsaicin must bind to the channel to block it.

5 Analysis of the voltage-dependence of the steady-state block in 100 μM capsaicin showed that half-maximal block occurred at -29 ± 2 mV ($n = 10$). Two-pulse experiments designed to study the time-dependence of channel block in 100 μM capsaicin indicated that the blocking kinetics were well fitted by a single exponential and that the rate of block increased with depolarization. The value for τ_{block} at 0 mV was 24 ± 7 ms ($n = 4$).

6 Recovery from block in 100 μM capsaicin was also well fitted by a single exponential. The recovery time constant ($\tau_{recovery}$) was 708 ± 140 ms at -50 mV, 70 ± 6 ms at -70 mV and 19 ± 1.3 ms at -90 mV ($n = 4$).

7 In 50–100 μM capsaicin, the decay of the tail current was biexponential, the values for τ_{fast} and τ_{slow} being, respectively, less than and greater than the single time constant fitted to the control tail current. Inward and outward K^+ currents were equally affected by capsaicin.

8 Most of these effects of capsaicin on the $I_K(s)$ of melanotrophs can be accounted for by a kinetic scheme in which capsaicin binds to and blocks open K^+ channels.

Keywords: Pituitary; slow outward potassium current; capsaicin; open channel block, melanotrophs

Introduction

Melanotrophs, the cells of the pars intermedia of the rat pituitary that secrete the peptide, α-melanocyte stimulating hormone (α-MSH), possess at least two types of voltage-gated K^+ current (Kehl, 1989; Schneggenburger & Lopez-Barneo, 1992) which are easily distinguished by their biophysical properties. The $I_K(f)$, a fast-activating, fast-inactivating current, resembles the transient outward or A-current found in many excitable tissues; and, the $I_K(s)$ is a slowly-activating, slowly-inactivating current of the delayed rectifier type. These two currents are also distinguishable to some extent by their pharmacology. Thus, whereas $I_K(f)$ and $I_K(s)$ are blocked by 4-aminopyridine (Kehl, 1990; Schneggenburger & Lopez-Barneo, 1992) external tetraethylammonium ions (TEA) selectively block the $I_K(s)$ (Kehl, 1989).

Capsaicin is the active component of hot peppers of the genus *Capsicum* which, when applied in low micromolar concentrations, causes the opening of non-selective cation channels and consequently depolarizes dorsal root ganglion (DRG) cells (Bevan & Szolcsányi, 1990). In higher concentrations capsaicin also affects voltage-operated channels (Dubois, 1982; Erdélyi & Such, 1984; Petersen *et al.*, 1987, 1989; Bleakman *et al.*, 1990; Docherty *et al.*, 1991). The report by Dubois (1982) that capsaicin blocks the fast- but not the slowly-inactivating outward K^+ current in the frog node of Ranvier prompted this investigation of the effects of capsaicin on the $I_K(f)$ and $I_K(s)$ of melanotrophs. I found that externally applied capsaicin reduced the amplitude and increased the rate of decay both of $I_K(f)$ and $I_K(s)$. Experiments to determine the mechanism of action of capsaicin focused on its effects on the $I_K(s)$ in cultured melanotrophs and the results suggest that capsaicin acts as an open channel blocker.

Methods

Male Wistar rats (200–300 g) were anaesthetized with CO_2 prior to decapitation and techniques described previously were used to prepare acutely dissociated and cultured melanotrophs (Kehl, 1989, 1990).

The patch electrodes used to record macroscopic (whole-cell) currents at room temperature were pulled from Corning No. 7052 glass and coated near the tip with Sylgard 184 (Dow Corning) to reduce capacitive currents. Current signals referenced to an agar bridge containing 150 mM NaCl were recorded with an EPC-7 patch clamp amplifier. The holding potential was -70 mV, except where indicated, and the pulse frequency was 0.25 Hz.

Signals recorded on magnetic tape were filtered at 2–3 kHz

[1] Author for correspondence.

(– 3 dB) and digitized at a 5–6 kHz sampling frequency by a 12-bit Lab Master A/D interface (Scientific Solutions, OH, U.S.A.). Digitized data were analysed on an Intel-based computer using BASIC-Fastlab software (Indec, CA, U.S.A.).

The standard external recording solution contained (mM): NaCl 140, KCl 3.5, $MgCl_2$ 1, $CaCl_2$ 2, N-2-hydroxyethylpiperazine-N'-2-ethanesulphonic acid (HEPES) 10 and glucose 5. In some experiments $I_K(s)$ was blocked by substituting 20 mM TEA chloride for an equivalent amount of NaCl in the standard external recording solution. The fast inward Na^+ current was blocked with 1–2 μM tetrodotoxin. The patch pipette (internal) recording solution contained (mM): KCl 140, $MgCl_2$ 5, $CaCl_2$ 1, ethyleneglycol-*bis*-(β-aminoethyl ether)-N,N,N',N'-tetraacetic acid (EGTA) 10, HEPES 10 and Na_2ATP 1. In the latter solution the free Ca^{2+} concentration is approximately 5 nM. The pH of the internal and external solutions was adjusted to 7.4 with KOH and NaOH, respectively.

Capsaicin was obtained from Aldrich and Sigma. The supply for Aldrich contained approximately 65% capsaicin and 35% dihydrocapsaicin while that supplied by Sigma contained 98% capsaicin. Since experiments with dihydrocapsaicin (Sigma, 90% pure) suggested that it was equipotent with capsaicin (data not shown) the concentration of either lot of capsaicin is expressed without any correction for impurities. All other chemicals were obtained from Sigma. On the day of experiment, capsaicin was dissolved in ethanol to give a 20 mM stock solution from which test solutions were made. Ethanol was added when necessary to equalize its concentration (0.5% v/v) in control and test solutions. The same effects were observed when dimethylsulphoxide (0.5% v/v) was the vehicle for the capsaicin. All drugs were applied by perfusion.

Except where noted, curve fitting was by use of regression routines in BASIC-Fastlab or SYSTAT (Evanston, IL, U.S.A.). Programmes written in QuickBASIC (Microsoft, WA, U.S.A.) were used for simulations.

Results

Capsaicin blocks $I_K(f)$ and $I_K(s)$ in acutely dissociated melanotrophs

As discussed previously, in the control solution the outward current evoked by an unconditioned test pulse to 20 mV consists of two components (Figure 1a(i)) which can be distinguished by differences of their biophysical and pharmacological properties: the $I_K(f)$ is eliminated by a pre-pulse that inactivates the $I_K(f)$ channels, and the $I_K(s)$ is selectively blocked by external TEA.

Figure 1a(i) shows the current evoked in standard external medium by an unconditioned test pulse to 20 mV. When the test pulse was applied immediately after a 500 ms conditioning pulse to – 20 mV only the $I_K(s)$ persisted (Figure 1a(ii)). The current obtained by subtracting $I_K(s)$ from the non-conditioned current represents the $I_K(f)$ and is shown in Figure 1b. The typical effect of 100 μM capsaicin on the K^+ currents of an acutely dissociated melanotroph is illustrated in Figure 1c,d. After switching to external medium containing 100 μM capsaicin the unconditioned test current showed two distinct peaks (Figure 1c(i)) each of which was followed by rapid current decay. When the test pulse was preceded by a conditioning pre-pulse the first of the two peaks was eliminated and the amplitude of the second was reduced (Figure 1c(ii)). The current eliminated by the pre-pulse was obtained by subtracting the conditioned from the non-conditioned currents and is shown in Figure 1d.

No significant or consistent change in the holding current was observed during the application of the capsaicin suggesting that the membrane does not contain capsaicin-gated cation channels of the type found in sensory neurones (Bevan & Szolcsányi, 1990). There was also no evidence for any desensitization of the response to capsaicin either with prolonged or repeated applications.

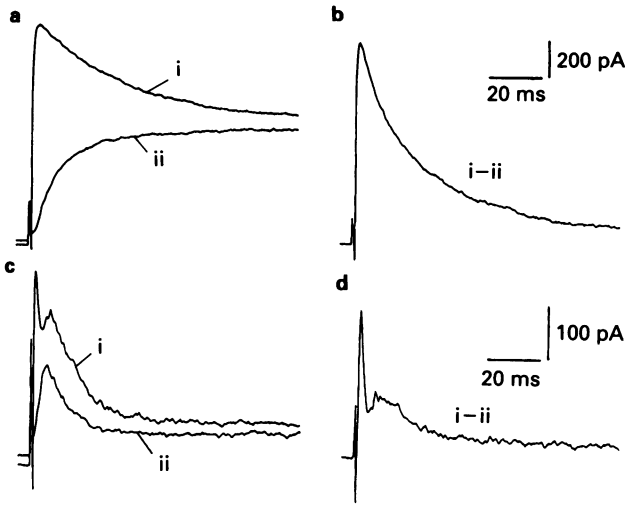

Figure 1 (a) In an acutely dissociated melanotroph in control medium a depolarizing command from – 70 mV to 20 mV evoked an outward current that activated rapidly and then partially inactivated (i). When preceded by a 500 ms conditioning pulse to – 20 ms the current at 20 mV activated slowly and did not inactivate (ii). This non-inactivating current is the $I_K(s)$. The difference current shown in (b) represents the $I_K(f)$ and was obtained by subtracting the conditioned current (a(ii)) from the non-conditioned current (a(i)). (c) In the same cell, while exposed to 100 μM capsaicin, a depolarizing step to 20 mV elicited two current peaks in the non-conditioned response (c(i)). A 500 ms conditioning pulse to – 20 mV eliminated the first peak and reduced the amplitude of the second peak (c(ii)). The current eliminated by the conditioning pulse was obtained by subtraction and is shown in (d).

The effects of 20 mM external TEA on the biphasic current evoked in 100 μM capsaicin are illustrated in Figure 2. This concentration of TEA was chosen because it substantially reduces $I_K(s)$ but has little or no effect on $I_K(f)$ (Kehl, 1989). Shown superimposed on the control current in Figure 2a are the currents evoked in medium containing either 100 μM capsaicin or 100 μM capsaicin plus 20 mM TEA. The higher gain traces of Figure 2b clearly show that TEA eliminates the second but not the first of the two current peaks evoked in capsaicin.

The simplest conclusion that can be drawn from the results of experiments such as those illustrated in Figures 1 and 2 is that, because of its insensitivity to TEA and its elimination by a depolarizing pre-pulse, the first component of the biphasic current recorded in capsaicin-containing solutions reflects the altered behaviour of $I_K(f)$. Similarly, the second component, because of its sensitivity to TEA and its persistence following a depolarizing pre-pulse, reflects the altered behaviour of $I_K(s)$.

The effects of *internal* capsaicin were tested in five cells by adding it to the patch pipette solution (final concentration 200 μM). In every case after 10–20 min of whole-cell recording there was no evidence for any change of the current amplitude or current kinetics.

It appears therefore that external capsaicin affects $I_K(s)$ and $I_K(f)$ in the same way: the current amplitude is reduced and there is an increased rate of current decay. Subsequent experiments designed to determine the mechanism of action of capsaicin focused on its effects on $I_K(s)$. Fortuitously, the $I_K(f)$ of cultured melanotrophs, as in cultured sympathetic neurones (Sacchi & Belluzzi, 1993), is usually not detectable (Kehl, 1989; Cota & Armstrong, 1988). Consequently by using cultured cells the $I_K(s)$ can be studied in isolation without resorting to pharmacological or other experimental interventions. In the text that follows the terms

'inactivation' and 'block' are used interchangeably to describe the capsaicin-induced changes of I_K(s).

Capsaicin blocks the I_K(s) in cultured melanotrophs

The traces of Figure 3 confirm that capsaicin has effects on the I_K(s) of cultured cells that are identical to those described above in acutely dissociated cells. In medium containing 40 μM capsaicin, the current activated at the same rate as the control current, reached a single peak and then rapidly decayed to a non-zero steady-state level. If the inactivating current recorded in capsaicin does represent the altered behaviour of I_K(s) then, unlike the I_K(f), it would be expected to be eliminated by TEA and this is indeed what is found. Following a 2 min perfusion with medium containing 40 μM capsaicin plus 20 mM TEA, the transient current was eliminated and the amplitude of the steady-state current was reduced. After returning to medium containing only the 40 μM capsaicin the 'inactivating' current reappeared and complete recovery to the control current amplitude was observed after a 2 min perfusion with drug-free medium (Figure 3).

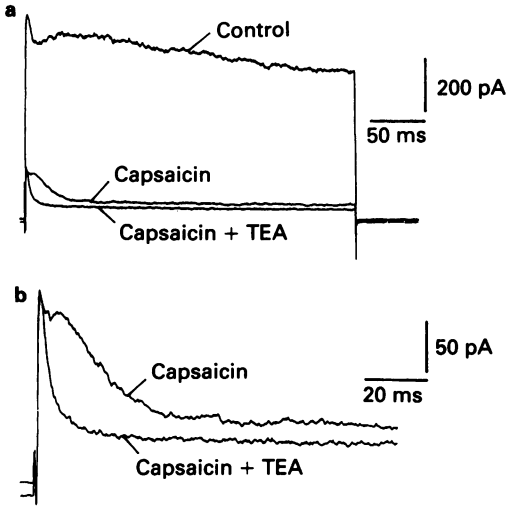

Figure 2 The control traces show I_K(f) and I_K(s) (which here shows some inactivation) evoked in an acutely dissociated melanotroph by a 300 ms pulse to 20 mV. After switching to medium containing 100 μM capsaicin the amplitude of the outward current decreased. (b) Traces recorded at a higher gain and time resolution show the biphasic nature of the current (cf. Figure 1c(i)). After switching to saline that contained both 100 μM capsaicin and 20 mM tetraethylammonium (TEA) the second component of the outward current was selectively eliminated. These results and those of Figure 1 suggest that the first and second components of the biphasic current in capsaicin reflect the altered behaviour of I_K(f) and I_K(s), respectively.

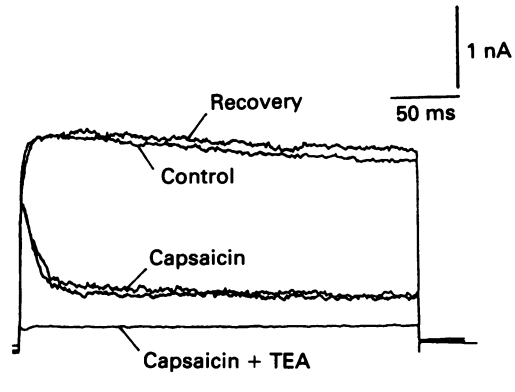

Figure 3 In a melanotroph maintained in culture for 6 days a depolarizing command to 20 mV evoked only the I_K(s) which inactivated very slowly during the 300 ms pulse. In 40 μM capsaicin, the activation time course matched that of the control response, as indicated by the overlap of the rising phase of the currents; however, the current peaked much earlier and then rapidly decayed to a non-zero steady-state. After switching to an external solution containing 40 μM capsaicin and 20 mM tetraethylammonium (TEA) the inactivating current was eliminated and the amplitude of the steady-state current was reduced. These results suggest that the inactivating current recorded in capsaicin reflects the interaction of capsaicin molecules with open I_K(s) channels. In acutely dissociated cells treated with capsaicin, this TEA-sensitive, inactivating current appears as the second component of the biphasic current (cf. Figure 2b).

In control cells, either cultured or acutely dissociated, the I_K(s) was unaffected by conditioning pre-pulses. However, the 'inactivating' I_K(s) recorded in 50–100 μM capsaicin was reduced by up to 60% by a 500 ms conditioning pre-pulse to – 20 mV (e.g. Figure 1c). This effect of a conditioning pulse reflects the voltage-dependence of the block by capsaicin and is discussed below in reference to Figure 6.

The steady-state block of I_K(s) is concentration-dependent

The relationship between the degree of block of I_K(s) and the capsaicin concentration is shown in Figure 4. For these experiments $I_{control}$ was recorded and the bath solution was then replaced by capsaicin-containing medium to measure $I_{capsaicin}$. The normalized or fractional current was defined as the ratio of the steady-state current in capsaicin to that in control medium ($I_{capsaicin}/I_{control}$). A problem encountered in several cells was the gradual increase of the amplitude of I_K(s) over the first 20–30 min of recording, a phenomenon that has also been observed in melanotrophs in the pituitary slice (Schneggenburger & Lopez-Barneo, 1992). Responses were included for analysis only when the recovery current was 90–110% of the control response. The data of Figure 4 were pooled from 11 cells for currents evoked at 10 mV. A least squares regression routine used to fit the data points to the Hill equation,

$$\frac{I_{capsaicin}}{I_{control}} = \frac{1}{1+\left(\frac{[Capsaicin]}{K_D}\right)^H}, \quad (1)$$

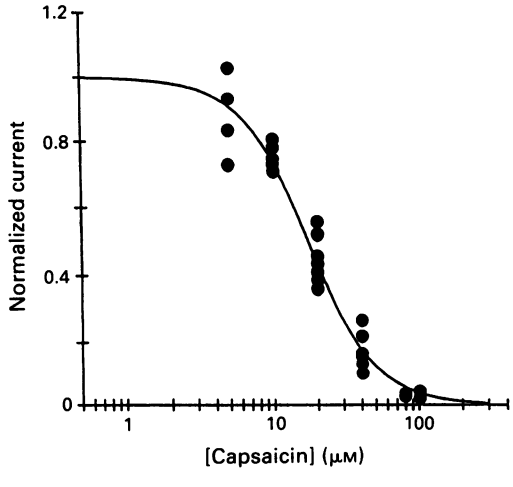

Figure 4 The relationship between the concentration of external capsaicin and the normalized (fractional) steady-state current. Responses were evoked at 10 mV and the steady-state current was normalized with respect to the control current ($I_{capsaicin}/I_{control}$) at the same potential. The smooth line represents the best fit of the points to the Hill equation for which the K_D was 17.4 μM and the value for the Hill coefficient (H) was 1.84. That at least two molecules of capsaicin must bind to block the channel is suggested by the value of 1.84 for H.

indicated an equilibrium dissociation constant (K_D) of 17.4 μM (95% confidence limits 15.8–19.0 μM) and a Hill coefficient (H) of 1.84 (95% CI 1.5–2.2). The value for H suggests that at least two molecules of capsaicin must bind to the channel to block it. For currents evoked at 30 mV (not shown) the fitted value for the K_D was 16.4 μM (95% CI 15–17.8 μM) and H was 1.63 (95% CI 1.4–1.9) ($n = 7$ cells).

The rate of decay of $I_K(s)$ in capsaicin is affected by membrane voltage

Figure 5 shows typical responses to varying concentrations of capsaicin at three different membrane voltages. In the example shown, the cell was depolarized for 300 ms to − 10 mV (a), 10 mV (b), and 30 mV (c). Each family of traces shows, from above downwards, the current evoked in 0, 10, 20, 40 and 100 μM capsaicin. At − 10 mV there was little or no current decay and the fractional current ($I_{capsaicin}/I_{control}$) in 10, 20 and 40 μM capsaicin was much greater than it was at the same concentrations at 10 and 30 mV. For example, in 20 μM capsaicin the fractional current was 0.8, 0.45 and 0.41 at − 10, 10 and 30 mV, respectively. Additionally, in all of the traces the activation rate was unchanged, as indicated by the overlap of the rising phase of the currents. Finally, the traces in Figure 5b,c show that the rate of current 'inactivation' increased with an increase of the capsaicin concentration and that at a given concentration of capsaicin the rate of current 'inactivation' increased with membrane depolarization.

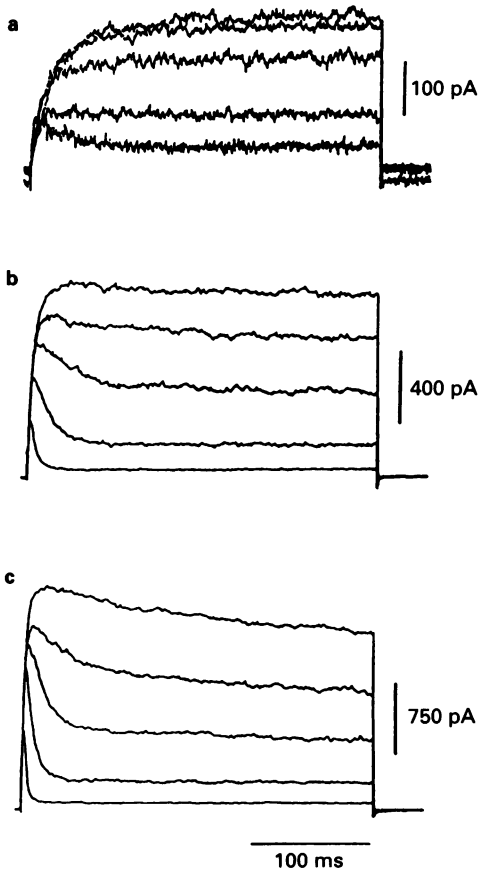

Figure 5 Membrane currents at − 10 mV (a), 10 mV (b) and 30 mV (c) in, for each set of traces and from above downwards, 0, 10, 20, 40 and 100 μM capsaicin. Note that except in the 100 μM capsaicin there was no overshoot of the currents evoked at − 10 mV. The fractional steady-state block at − 10 mV, particularly with the lower capsaicin concentrations, was much less than that at 10 or 30 mV. The responses also show that for a given concentration of capsaicin the degree of 'inactivation' of the current increases with membrane depolarization.

The block of $I_K(s)$ by capsaicin is voltage- and time-dependent

To measure the time-dependence of the block of I_K(s) at potentials ⩽ 0 mV, a double pulse protocol involving a conditioning and a test pulse was used. The rationale behind this pre-pulse–test-pulse protocol is entirely analogous to that commonly used to study inactivation kinetics in channels with an intrinsic inactivation process (Hille, 1991). Channels could become blocked ('inactivated') during the conditioning pulse (depending on its intensity and duration) and the proportion of channels that had not become blocked (i.e., those available for activation) could then be estimated from the amplitude of the test current evoked immediately thereafter. In the experiments with capsaicin, the cell was exposed to a 100 μM concentration of the drug and test pulses to 30 or 50 mV were preceded by conditioning pulses of varying duration (5 to 500 ms) and intensity (− 60 to 0 mV) (Figure 6a). The test current amplitude was calculated as the difference between the peak and steady-state current. Results typical of those obtained in four such experiments are shown in Figure 6b. A conditioning depolarization to − 40 mV did not affect the amplitude of the subsequent test current. However, as has been reported for the open channel block by nimodipine of slowly-inactivating Ca^{2+} current in clonal pituitary cells (Cohen & McCarthy, 1987), with stronger conditioning

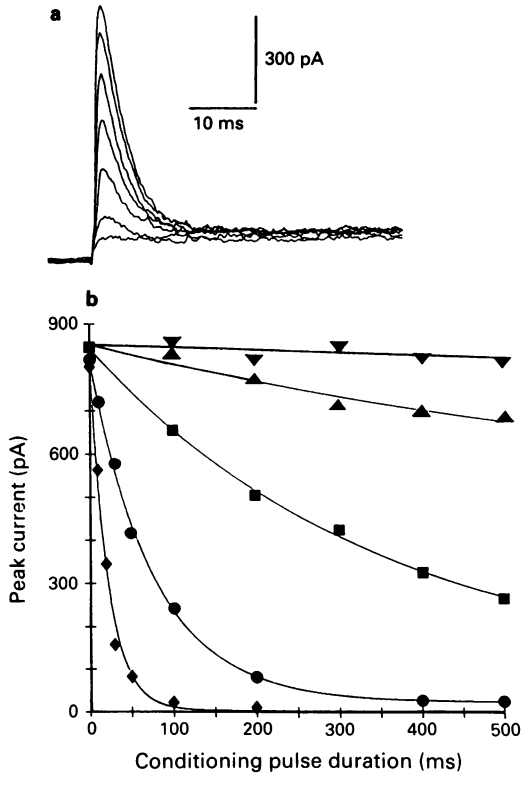

Figure 6 The voltage- and time-dependence of the block of I_K(s) by capsaicin. (a) Currents recorded from a cell bathed in 100 μM capsaicin, held at − 70 mV and stepped to a test potential of 50 mV immediately after applying conditioning pulses (not shown) to − 10 mV and lasting, from above downwards, for 0, 10, 30, 50, 100, 200 or 400 ms. (b) The conditioning pulse duration versus the peak amplitude of the test current. Conditioning pulses were varied in duration between 10 and 500 ms and in intensity between − 40 and 0 mV. Test current amplitude was calculated as the difference between the peak and the steady-state current. Pre-pulses to − 40 mV (▼) and lasting for up to 500 ms did not affect the amplitude of the test current. As the intensity of the depolarizing pre-pulse was increased from − 30 mV (▲), to − 20 mV (■), to − 10 mV (●) and finally to 0 mV (◆) there was a progressive increase of the rate and extent of the block of the test current.

depolarizations the extent and the speed of the block increased. For example, following a 500 ms conditioning pulse to − 30 mV (Figure 6b, ▲) the test current was reduced by 10–30% ($n = 3$ cells) and the time constant of the exponential fitted to the data points varied from 210 to 690 ms. At 0 mV (Figure 6b, ◆) the time course of the decline of the peak amplitude of test currents was well fitted by a single exponential with a time constant of 24 ± 7 ms ($n = 4$ cells). By comparison, at 50 mV the pulse current decayed exponentially with a time constant less than 10 ms (e.g. Figures 6a, 8a).

For the analysis of the steady-state voltage dependence of the channel block the same approach was used but the pre-pulse had a fixed duration of 1 s. Except for very small depolarizations this long pre-pulse assured that the equilibrium condition had been reached before the application of the test pulse. The capsaicin concentration was 100 μM. Again, the relative amplitude of the test current ($I_{conditioned}/I_{unconditioned}$) reflected the proportion of channels that remained in the resting state at the end of the conditioning pulse. The test current amplitude was calculated as described for Figure 6b and the normalized current was defined as $I_{conditioned}/I_{unconditioned}$. Data obtained from 10 cells and fitted to the Boltzmann equation indicated that in 100 μM capsaicin, half-maximal block occurred at − 29 ± 2 mV. In other words, on average, half of the channels remained in the resting state following a 1 s conditioning pulse to − 29 mV. This voltage-dependence of the block by capsaicin probably accounts for the ≈50% reduction of the 'inactivating' $I_K(s)$ in Figure 1c following a 500 ms conditioning pulse to − 20 mV.

Effects of capsaicin on the $I_K(s)$ tail current

Experiments to examine the tail current behaviour in 100 μM capsaicin were carried out in symmetrical K^+ solutions (140 mM K_o/140 mM K_i, $E_K = 0$ mV) so that large inward tail currents could be evoked by stepping back to − 70 mV following the application of a strong but brief depolarization to open $I_K(s)$ channels. For the traces shown in Figure 7a a 5 ms depolarization to 20 mV was used. In the control response the outward pulse current gave way to a large inward instantaneous tail current when the membrane potential suddenly returned to − 70 mV. The difference in the size of the outward and inward current immediately preceding and following the step to − 70 mV is accounted for by the 3.5 fold greater driving force for inward K^+ movement ($I = g \times (V\text{-}E_K)$). The current recorded in 100 μM capsaicin is shown superimposed on the control current in Figure 7a. In Figure 7b the current has been scaled so that the peak of the *inward* current matches that in the control response. This scaling procedure illustrates two points. First, from the fact that the *outward* current in capsaicin at the end of the depolarizing command is also matched to the control outward current, it is evident that inward and outward K^+ currents are equally affected by capsaicin. Second, the tail current in capsaicin has two components, one of which decays faster, the other slower, than the control tail current. Similar results were obtained in each of the five cells tested. When longer depolarizing pulses were used, the envelope of the peak inward tail current paralleled the time-dependent decline of the pulse current amplitude at the end of the depolarizing command (not shown).

The traces of Figure 7c,d represent the simulated behaviour of the tail current in an open channel blocking scheme and are included to allow comparisons to the experimental data. The details of the model and the parameters used for the simulation are given below.

The recovery from capsaicin block is voltage- and time-dependent

To study the voltage-dependence of the recovery of $I_K(s)$ from capsaicin block I used a paired-pulse protocol in which

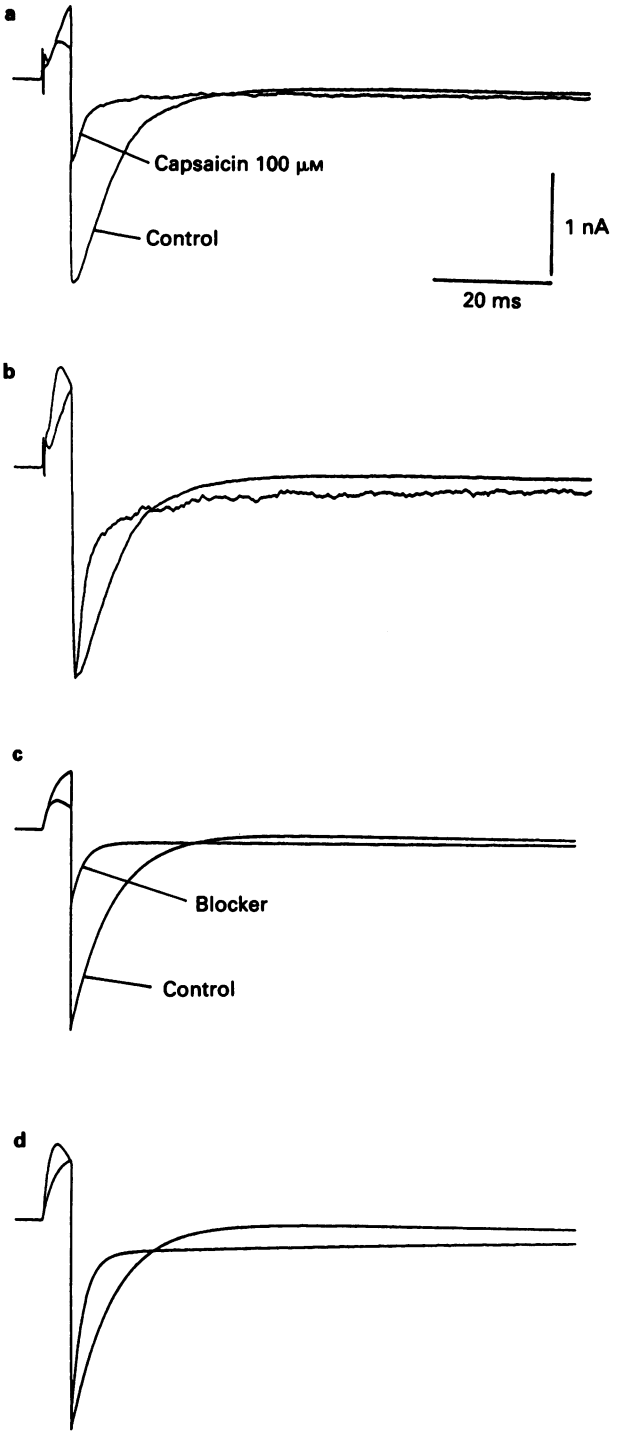

Figure 7 The effect of capsaicin on tail current relaxations. (a) For the control responses the potential was stepped from − 70 to 20 mV for 5 ms in a cell in which E_K was ≈0 mV. The decay of the tail current at − 70 mV was well fitted by a single exponential with a time constant of 7.8 ms. Shown superimposed on the control response is the smaller current recorded in 100 μM capsaicin. (b) For these traces the current in capsaicin was scaled 2.5 fold to allow comparison with the control response. Note that the tail in capsaicin is biexponential, one component being faster, the other slower than the control value. (c) The output of the open channel blocking model programmed to approximate the stimulus conditions used in (a). For the tail kinetics, α_1 was zero and β_1 was 0.13 ms^{-1} ($\tau_{deactivation} = 7.8$ ms), the concentration of blocker was 100 μM, the proportionally constant (δ) was 0.000035 $\mu M^{-2} ms^{-1}$ and the unblocking rate constant was 0.024 ms^{-1}. The traces in (c) and (d) are presented in the same format as (a) and (b), respectively. The computed traces have been scaled to match the responses in (a) and (b) but have no vertical calibration; the time base is the same as for (a). The current calibration applies only to the traces in (a).

two identical voltage commands, lasting for 100 ms and taking the potential to 20–50 mV, were separated by a interpulse interval of 5–800 ms (e.g., Figure 8a). Cells were exposed to 100 μM capsaicin and the holding potential, which was the same as the interpulse potential, was set at − 50, − 70 or − 90 mV. The test current amplitude was measured as described previously. Figure 8b shows the typical relationship between the interpulse and the normalized ($I_{conditioned}/I_{unconditioned}$) test current. When the holding potential was − 50 mV, recovery was well fitted by a single expotential with a time constant of 530 ms. At − 70 mV and − 90 mV the recovery time constant decreased to 61 and 21 ms, respectively. In four such experiments the time constants for recovery from the block were 708 ± 140 ms at − 50 mV, 70 ± 6 ms at − 70 mV and 19 ± 1.3 ms at − 90 mV.

Discussion

Externally-applied capsaicin produces a time-dependent block of I_K(f) and I_K(s) in melanotrophs that is manifest as a decrease of the peak current amplitude and, except with small depolarizations, an increased rate of current decay. In the frog node of Ranvier (Dubois, 1982) 10 μM capsaicin reduces the K^+ current, 'in a time-dependent manner but only for large depolarizations', and although a similar effect of capsaicin on K^+ currents has been reported in other preparations (Erdélyi & Such, 1984; Petersen *et al.*, 1987) there has not been a detailed analysis of the mechanism of action of capsaicin.

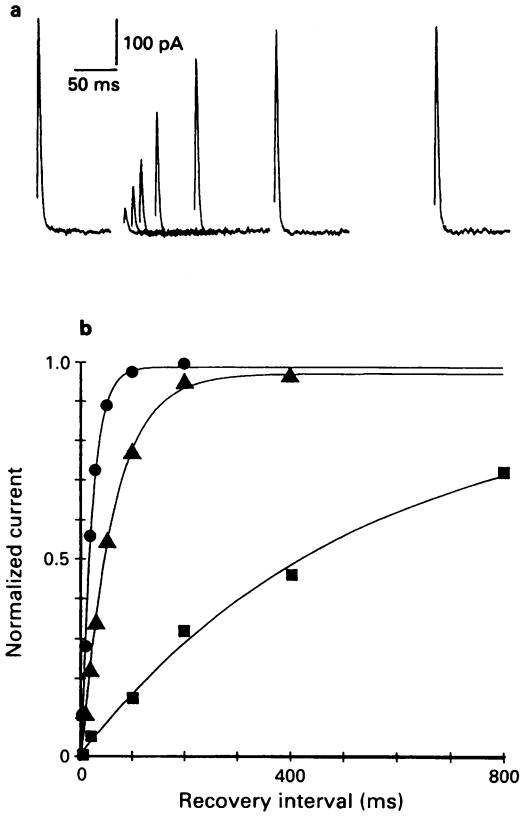

Figure 8 The time course of recovery from block in 100 μM capsaicin. (a) The voltage clamp protocol consisted of paired 100 ms pulses separated by a 10 to 400 ms interval and taking the membrane to 50 mV from the holding potential of − 70 mV. The traces show, from left to right, the unconditioned test current and the current evoked 10, 20, 30, 50, 100, 200 and 400 ms after the end of the first pulse. For clarity the initial 1.5 ms of the rising phase of the current have been blanked. (b) For the same cell the graph of the normalized test current versus the interpulse interval. The time constant of the exponential fitted to the recovery time course at − 50 (■), − 70 (▲) and − 90 mV (●) was 531, 61 and 21 ms, respectively.

An important feature of the block of I_K(s) by capsaicin was that the initial rising phase of the current was unaffected. Since at the beginning of the voltage pulse dI/dt will be proportional to the number of channels available for activation and since the initial dI/dt is unchanged in capsaicin this is interpreted as showing the absence of any significant resting block of I_K(s) channels. Without any resting block, and if the single channel conductance (γ) is unaffected by capsaicin, then the reduction of the steady-state current must be due to a decrease of the open probability (P_o) since the macroscopic current is equal to $NP_o\gamma(V\text{-}E_K)$ where N is the number of activatable channels and $V\text{-}E_K$ is the driving force for ion flow.

There are two mechanistically-distinct processes that could underlie a decrease of P_o in capsaicin: either capsaicin increases the rate of intrinsic inactivation (which must then be assumed to be coupled to channel opening) or it acts as an open channel blocker. The former mechanism seems unlikely not only because this would require that the inactivation rate be increased by up to two orders of magnitude but because it would also require a very large hyperpolarizing shift of the voltage-dependence of inactivation to account for the increased rate of decay of the I_K(s) tail current in capsaicin-treated cells (Figure 7b). It seems more likely therefore that capsaicin is acting as an open channel blocker. Though it has not yet been systematically studied, a similar action could conceivably account for the effects of capsaicin on I_K(f).

Simulation of the block of I_K(s) by capsaicin

I have assumed in the following analysis of the actions of capsaicin that the I_K(s) represents the activity of a single class of K^+ channels there being no evidence to the contrary. Single channel recordings in physiological saline have revealed that melanotrophs express a ≈100 pS calcium- and voltage-activated K^+channel (BK) but with the 5 nM Ca^{2+} in the internal recording solution the contribution of this BK channel to the macroscopic K^+ current is probably significant only with depolarizations beyond + 60 mV (Kehl, unpublished observations).

To simulate the actions of capsaicin, I followed the approach used by Armstrong (1969; 1971) to model the open channel block by TEA and its structural analogues of the delayed rectifier K^+current of the squid giant axon. In an open channel blocking scheme, the channel must be in the open state for the drug to occupy its binding site(s). Consequently the essential features of the gating of I_K(s) channels and the open channel binding of capsaicin can be expressed in a Markov chain model:

$$C \underset{\beta_1}{\overset{\alpha_1}{\rightleftharpoons}} O \underset{\beta_2}{\overset{\alpha_2}{\rightleftharpoons}} OB$$

where C represents the closed or resting conformation, O the open, conducting channel and OB the open but capsaicin-blocked channel. The opening and closing rate constants, α_1 and β_1 respectively, are voltage-dependent; the blocking rate constant (α_2) is proportional to the concentration of capsaicin and β_2, the unblocking rate constant, is concentration-independent. In the gating scheme presented there is only one closed state even though the time course of I_K(s) activation, which is usually sigmoidal (e.g., Figure 1a), suggests there are at least two closed states.

Computer-generated traces based on the three-state kinetic scheme and shown in Figure 9 represent the ensemble average of a single channel simulation (DeFelice & Clay, 1983) in which α_2, the blocking rate constant, was, from above downwards, 0, 0.03, 0.12 or 0.48 ms^{-1}. Increasing the blocking rate constant is equivalent to increasing the concentration of the blocking drug. The unblocking reaction, β_2,

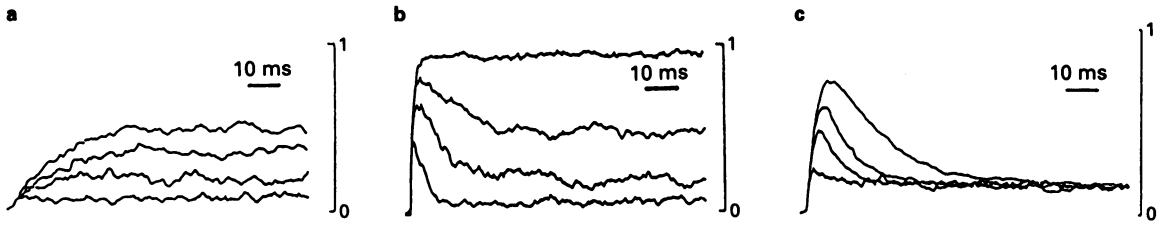

Figure 9 Ensemble averages of a single channel simulation of the open channel block of a non-inactivating current. The traces actually represent the channel open probability (P_o) which varies between 0 and 1 but can be taken as being representative of membrane currents. Shown superimposed in (a) and (b) are control responses (top traces) and the responses at three different concentrations of blocker. In (a), α_1 and β_1 were 0.033 ms^{-1}; in (b), α_1 and β_1 were set to 0.633 and 0.033 ms^{-1}, respectively, to mimic the consequences of a stronger depolarization. The effect of increasing the external concentration of the blocker was mimicked by setting α_2, the blocking rate, to 0.03, 0.12 or 0.48 ms^{-1}; β_2 was concentration-independent and was assigned a value of 0.033 ms^{-1}. Two important points are illustrated by the simulation. First, the degree of block at any given concentration of blocker is greater in (b) than in (a), and, second, 'inactivation' is seen only in the traces in (b). This apparent voltage-dependence of steady-state block and 'inactivation' reflects the fact that the blocking reaction (here assumed to be voltage-independent) is in series with the voltage-dependent gating reaction. For the traces shown in (c), α_1 and β_1 were 0.33 and 0.003 ms^{-1} respectively so that without channel block (not shown) the steady-state P_o would be 0.99. For the simulation β_2 was, from above downwards, 0.05, 0.125, 0.25 or 1.0 ms^{-1} and α_2 was always equal to $5\beta_2$ so that the steady-state P_o for each trace was $\approx$0.16 (equation 2). The traces illustrate how, under the conditions of a fixed α_2/β_2 ratio, increasing the value for α_2 decreases the amplitude of the transient component and increases the rate of decay of the current. This feature of the model was used in the process of fitting simulated currents to experimental data in Figure 10.

was fixed at 0.033 ms^{-1} to reflect its concentration-independence. Both the blocking and unblocking reactions were assumed to be voltage-independent. In Figure 9a the opening and closing rate constants, α_1 and β_1, were 0.033 ms^{-1} to give an activation time constant (τ) of 15 ms ($1/(\alpha_1 + \beta_1)$) and a control steady-state open probability (P_o) of 0.5 (i.e., $\alpha_1/(\alpha_1 + \beta_1)$). For Figure 9b the only change made was to increase α_1 to 0.633 ms^{-1} (τ = 1.5 ms, P_o = 0.95). Increasing the activation rate constant is equivalent to giving a stronger depolarization.

All of the qualitative features of the experimental data are apparent in the simulated currents (compare Figure 9a,b and Figure 5). First, the initial activation rate is not affected by the blocker. Second, at a given 'concentration' of blocker, inactivation is evident only with the faster activation rate (Figure 9b). The latter feature reflects the fact that the decay rate is affected by the rate at which the channels are delivered to the blocking reaction. With small depolarizations the slow delivery of open channels limits the blocking rate whereas with large depolarizations, where the activation rate is greater, the rate of current decay more closely reflects the microscopic blocking rate. Third, the fractional steady-state current ($I_{blocker}/I_{control}$) is affected by the channel gating. For example, when the blocking rate constant was 0.03 ms^{-1} (the second trace from the top) the fractional current was 0.69 and 0.54 in Figure 9a and 9b, respectively. Knowing that at equilibrium $\alpha_1 C = \beta_1 O$, $\alpha_2 O = \beta_2 OB$ and that the total number of channels N_T is equal to C + O + OB, the equilibration open probability in the presence of the blocker is

$$\frac{O}{N_T} = \frac{1}{1 + \frac{\beta_1}{\alpha_1} + \frac{\alpha_2}{\beta_2}}, \qquad (2)$$

which simplifies to $\alpha_1/(\alpha_1 + \beta_1)$ for the control response. The fractional current at a given voltage is then,

$$\frac{I_{blocker}}{I_{control}} = \frac{\frac{1}{1 + \frac{\beta_1}{\alpha_1} + \frac{\alpha_2}{\beta_2}}}{\frac{\alpha_1}{\alpha_1 + \beta_1}} = \frac{1}{1 + n_\infty \frac{\alpha_2}{\beta_2}}, \qquad (3)$$

where n_∞, the control steady-state open probability, is $\alpha_\alpha/(\alpha_1 + \beta_1)$. Thus, although in the model the binding/unbinding of the blocking molecule is constrained to be voltage-independent, the block is voltage-dependent because α_1 and β_1 (and consequently n_∞) are voltage-dependent. In other words, the blocking reaction is voltage-dependent because it is in series with the voltage-dependent gating reaction. The same situation can exist in channels where inactivation is coupled to channel opening (Hille, 1991).

The traces of Figure 9c illustrate the output of the simulation when the opening rate, the closing rate and the ratio α_2/β_2 were fixed and the value for α_2 was changed. For the simulation the value for β_2, the unblocking rate constant, from the top trace downwards was 0.01, 0.025, 0.05, and 0.2 ms^{-1}; the value for α_2, the blocking rate constant, was in every case 5 times the value for β_2 (i.e., $\alpha_2/\beta_2 = 5$); and, the opening and closing rate constants were 0.33 and 0.033 ms^{-1}, respectively. Since α_2/β_2 was fixed, the mean steady-state open probability is the same ($\approx$0.16, equation 2) for each trace. The traces show how changing the blocking rate (α_2) in the face of a fixed α_2/β_2 ratio influences the transient portion of the $I_K(s)$ current. When α_2 is increased there is a decrease of the peak current amplitude and an increase in the rate of current decay. The latter aspect of the model behaviour has been used in the fitting procedure to estimate the values for α_2 and β_2 for Figure 10.

Fitting of blocking and unblocking rates to experimental data

The smooth lines fitted by eye to the experimental data of Figure 10 were generated as follows. As for Figure 9, current activation was modelled as a first order reaction except that, for convenience, β_1 was set to zero. By setting β_1 to zero the block becomes independent of channel gating (n_∞ = 1 in equation 3) and consequently the fitting routine overestimates the K_D when P_o is low. Any error in the estimate of the K_D is reduced at potentials above $\approx$30 mV where P_o is near maximal. An apparent molecularity of 2 was chosen based on the estimated Hill coefficient (Figure 4) and was incorporated in a pseudo first-order reaction in which the blocking rate constant (α_2) was related to the square of the capsaicin concentration by a proportionality constant (δ) having the units of $\mu M^{-2} ms^{-1}$. Mechanistically the latter approach is an oversimplification since it assumes that two molecules of capsaicin interact instantaneously with the channel. The unblocking rate constant, β_2, was concentration-independent and, like the blocking rate, was assumed to have no voltage-dependence. Though very slow inactivation was sometimes evident in control responses, particularly with depolarizations beyond 20 mV (e.g., Figure 2a), no attempt was made to include an intrinsic inactivation process in the model.

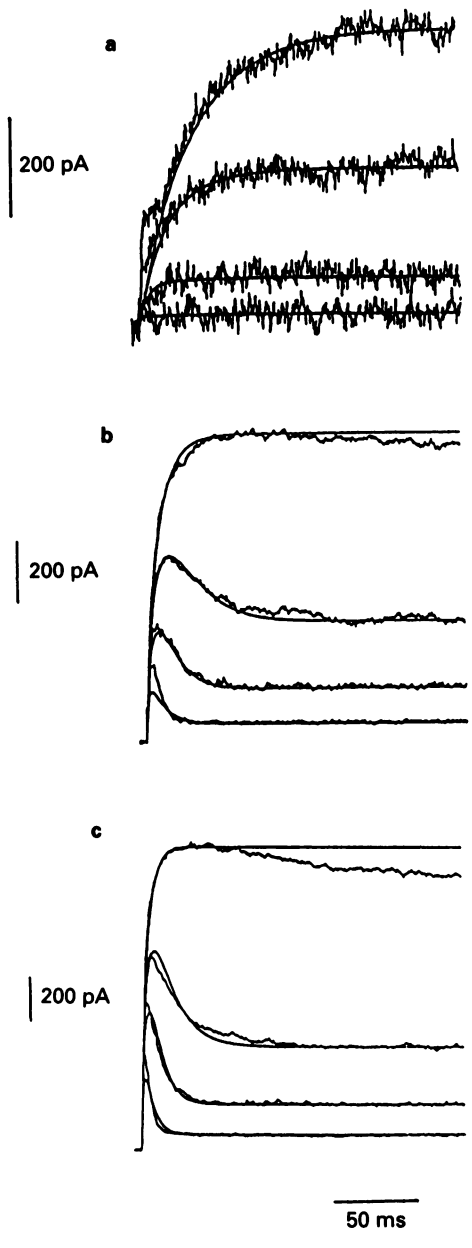

Figure 10 The fit of simulated currents to experimental data. Each family of traces shows from above downwards the currents evoked in 0, 20, 40 and 80 μM capsaicin at − 10 mV (a), 10 mV (b) and 30 mV (c). See text for the details of the fitting procedure. The value for α_1 was 0.03, 0.11 and 0.23 ms^{-1} at − 10, 10 and 30 mV, respectively. Table 1 lists the values assigned to δ and β_2 to generate the lines superimposed on the experimental data.

The procedure for fitting the model output to the experimental data followed a rationale based on the outcome of the simulation in Figure 9c. First, a value for α_1 was set to obtain the best fit, by eye, to the activation kinetics of the control current. Then, since the steady-state current in the presence of the blocker depends on the ratio α_2/β_2 (equation 2), the next step in the fitting procedure was to use a fixed value for β_2 and then to vary α_2 (by altering δ) until the steady-state levels of the model and the experimental data were the same. Next, keeping the ratio α_2/β_2 constant, the value of α_2 was adjusted to obtain the best fit to the transient component of the $I_K(s)$. Table 1 indicates the values for δ and β_2 fitted to the current evoked at − 10, 20, 30 and 50 mV. The K_D calculated from the fitted values for δ and β_2 (right column of Table 1) is similar to that derived from the analysis of steady-state currents (Figure 4).

Tail current kinetics in the open channel blocking scheme

A consequence of the open channel blocking scheme is that the $I_K(s)$ tail current will be altered in two ways. First, since in the presence of the blocker there are two reactions that lead away from the open state (i.e., closing of the activation gate (deactivation) or channel block), part of the current should decay faster than control responses where only deactivation occurs. Second, because blocked channels might then undergo several opening-blocking transitions before finally closing, part of the tail current should decay more slowly than the control tail current. The output of the tail current simulation with and without channel block is shown in Figure 7c,d (see figure legend for the values used for the gating and blocking rate constants). In the control response a 5 ms 'depolarization' evokes a non-inactivating outward current, and, after returning to the holding potential, the time course of the decay of the inward tail current decays monoexponentially with a time constant equal to $1/\beta_1$. In the presence of the blocker the simulated pulse current inactivates and the appearance of two components in the tail current is apparent in Figure 7d where the peak of the tail current in the presence of the blocker has been scaled to match the control peak inward current. The similarity between the experimental (Figure 7b) and simulated currents (Figure 7d) offers additional support for open channel block as the basis for the action of capsaicin.

Recovery from channel block by capsaicin is faster than predicted

Voltage-dependent recovery from the block by capsaicin is also predicted by the blocking scheme. If the channel cannot close from the blocked state, and since the open→closed transition is favoured whenever the closing rate constant (β_1) is greater than the blocking rate constant (α_2), then membrane hyperpolarization, which under the constraints of the

Table 1 Values used in the fitting of simulated currents to experimental data in Figure 10

Membrane potential (mV)	*[Capsaicin]* (μM)	δ (μM^{-2} ms^{-1})	α_2 (ms^{-1})	β_2 (ms^{-1})	$(\beta_2/\delta)^{\frac{1}{2}}$ (μM)
− 10	20	0.000075	0.03	0.033	20.9
10	20	0.00011	0.044	0.024	14.8
30	20	0.00014	0.056	0.027	13.9
50	20	0.00016	0.064	0.033	14.4
− 10	40	0.00011	0.176	0.033	17.3
10	40	0.000098	0.157	0.025	16.0
30	40	0.00011	0.176	0.025	15.1
50	40	0.00012	0.192	0.032	16.3
− 10	80	0.00011	0.704	0.033	17.3
10	80	0.000096	0.614	0.015	12.5
30	80	0.000097	0.621	0.020	14.4
50	80	0.00011	0.704	0.025	15.1

model increases β_1 but has no effect on α_2 or β_2, would increase the rate at which blocked channels recover to the activatable state. The experimental data showed that recovery was indeed voltage-dependent and, at least qualitatively, in the manner expected: hyperpolarization speeds recovery. However, in a computer simulation (not shown) where β_1 was 0.1 ms^{-1} (to approximate the deactivation rate at -70 or -90 mV) α_2 was 1 ms^{-1} (0.0001 $\mu M^{-2} ms^{-1}$) (100 $\mu M)^2$) and β_2 was 0.033 ms^{-1}, the recovery time constant was $\approx$330 ms. This value is similar to the recovery time constant of 313 ms calculated from,

$$\tau_{recovery} = \left(\frac{\beta_1}{1+\frac{\alpha_2}{\beta_2}}\right)^{-1}$$

(Neher & Steinbach, 1978). However both values are 3–10 times larger than the actual recovery time constants measured at -70 and -90 mV. There are two possible explanations for this difference between the theoretical and experimental results. The first is that the blocking and unblocking rates are voltage-dependent. The second is that there is an additional and faster recovery route involving an open-blocked→closed-blocked→closed pathway.

Two theories have been proposed to account for state-dependent binding. One, the modulated receptor theory (MRT), assumes that the affinity of the blocker for the binding site is affected by the channel state. The other, the guarded receptor theory (GRT), supposes that the binding site is not exposed until the channel is in a particular state. The weight of evidence strongly supports the idea that the channel must open before the block by capsaicin can occur but it is not yet known if the binding results from the removal of a diffusion barrier (the activation gate?) or whether the affinity of the binding site increases after the channel opens.

Although qualitatively similar to the block of the delayed rectifier by TEA (Armstrong, 1969; 1971) there are differences between the block by TEA and the block of I_K(s) in melanotrophs by capsaicin. First, internal but not external TEA blocks the K^+ current of the squid giant axon whereas external but not internal capsaicin blocks the I_K(s) in melanotrophs and the I_K(f) of DRG neurones (Petersen *et al.*, 1987). Second, whereas the block of the delayed rectifier by internal TEA is affected by the direction of the current flow (so that inward rectification of tail currents is apparent), inward and outward currents are equally affected by capsaicin. The inward rectification recorded in TEA has been attributed to the 'sweeping' of the TEA from the pore by inward-going K^+ but no such sweeping effect is evident with the block of I_K(s) by capsaicin, perhaps because the binding is more stable. Alternatively, the lack of any sweeping effect might mean that, rather than blocking the pore 'like a cork in a bottle', capsaicin acts allosterically at a site remote from the influence of ion fluxes. Adding to the difficulties in analysis of the mechanism of action of capsaicin is the uncertainty about whether it acts from the aqueous and/or the lipid phase since capsaicin is a lipophilic compound.

Capsaicin has been shown here to exert a potent and state-dependent block of K^+ currents in melanotrophs. The potency of the block of I_K(s) by capsaicin ($K_D \approx 20\ \mu M$ at 10 mV) is similar to that produced by long chain analogues of TEA. Indeed, preliminary studies have shown that low micromolar concentrations of tetrapentyl ammonium (TPA) cause a similar time- and voltage-dependent block of the I_K(s) of melanotrophs, however, in contrast to the situation with capsaicin, the block by TPA reverses slowly, if at all. Unfortunately, the usefulness of capsaicin as a blocker of ionic currents is limited by its 'voltage-dependence' and by its lack of specificity since it has also been reported to affect voltage-gated Na^+ and Ca^{2+} channels (see Introduction). Nonetheless, like other naturally-occurring toxins (Castle *et al.*, 1989), capsaicin might prove to be a useful pharmacological probe in the analysis of the molecular structure of voltage-gated channels.

Supported by grants from the B.C. Health Research Foundation and the Natural Sciences and Engineering Research Council of Canada.

References

ARMSTRONG, C.M. (1969). Inactivation of the potassium conductance and related phenomena caused by quaternary ammonium ion injection in squid axons. *J. Gen. Physiol.*, **54**, 553–575.

ARMSTRONG, C.M. (1971). Interaction of tetraethylammonium ion derivatives with the potassium channels of giant axons. *J. Gen. Physiol.*, **58**, 413–437.

BEVAN, S. & SZOLCSÁNYI, J. (1990). Sensory neuron-specific actions of capsaicin: mechanisms and applications. *Trends Pharmacol. Sci.*, **11**, 330–333.

BLEAKMAN, D., BRORSON, J.R. & MILLER, R.J. (1990). The effect of capsaicin on voltage-gated calcium currents and calcium signals in cultured dorsal root ganglion cells. *Br. J. Pharmacol.*, **101**, 423–431.

CASTLE, N.A., HAYLETT, D.G. & JENKINSON, D.J. (1989). Toxins in the characterization of potassium channels. *Trends Neurosci.*, **12**, 59–65.

COHEN, C.J. & MCCARTHY, R.T. (1987). Nimodipine block of calcium channels in rat anterior pituitary cells. *J. Physiol.*, **387**, 195–225.

COTA, G. & ARMSTRONG, C.M. (1988). Potassium channel 'inactivation' induced by soft-glass patch pipettes. *Biophys. J.*, **53**, 107–109.

DEFELICE, L.J. & CLAY, J.R. (1983). Membrane current and membrane potential from single-channel kinetics. In *Single-Channel Recording*. ed. Sakmann, B. & Neher, E. pp. 323–342. New York: Plenum Press.

DOCHERTY, R.J., ROBERTSON, B. & BEVAN, S. (1991). Capsaicin causes prolonged inhibition of voltage-activated calcium currents in adult rat dorsal root ganglion neurons in culture. *Neurosci.*, **40**, 513–521.

DUBOIS, J.M. (1982). Capsaicin blocks one class of K^+ channels in the frog node of Ranvier. *Brain Res.*, **245**, 372–375.

ERDÉLYI, L. & SUCH, G. (1984). The effects of capsaicin on the early outward current in identified snail neurones. *Neurosci. Lett.*, **48**, 349–353.

HILLE, B. (1991). *Ionic Channels of Excitable Membranes*. Sunderland: Sinauer.

KEHL, S.J. (1989). Cultured melanotrophs of the adult rat pituitary possess a voltage-activated fast transient outward current. *J. Physiol.*, **411**, 457–468.

KEHL, S.J. (1990). 4-aminopyridine causes a voltage-dependent block of the transient outward current in acutely dissociated adult rat melanotrophs. *J. Physiol.*, **431**, 512–528.

NEHER, E. & STEINBACH, J.H. (1978). Local anaesthetics transiently block currents through single acetylcholine-receptor channels. *J. Physiol.*, **277**, 153–176.

PETERSEN, M., PIERAU, FR.-K. & WEYRICH, M. (1987). The influence of capsaicin on membrane currents in dorsal root ganglion neurones of guinea-pig and chicken. *Pflügers Arch. Eur. J. Physiol.*, **409**, 404–410.

PETERSEN, M., WAGNER, G. & PIERAU, FR.-K. (1989). Modulation of calcium-currents by capsaicin in a subpopulation of sensory neurones of guinea pig. *Naunyn-Schmied Arch Pharmacol.*, **339**, 184–191.

SACCHI, O. & BELLUZZI, O. (1993). The action potential in mammalian neurons: new perspectives. *News Physiol. Sci.*, **8**, 42–44.

SCHNEGGENBURGER, R. & LOPEZ-BARNEO, J. (1992). Patch-clamp analysis of voltage-gated current in intermediate lobe cells from rat pituitary thin slices. *Pflügers Arch. Eur. J. Physiol.*, **420**, 302–312.

(Received September 1, 1993
Revised January 19, 1994
Accepted February 8, 1994)

Br. J. Pharmacol. (1994), **112**, 625–629

Measurement and pharmacokinetic analysis of imipramine and its metabolite by brain microdialysis

Yuji Sato, Shinji Shibanoki, Megumi Sugahara & [1]Koichi Ishikawa

Department of Pharmacology, Nihon University School of Medicine, Oyaguchi-Kami Machi, Itabashi, Tokyo 173, Japan

1 The feasibility of the brain microdialysis method for direct measurement and pharmacokinetic study of imipramine (Imip) and its metabolite desipramine (DMI) was investigated in the rat brain.

2 A dialysis tube was inserted into the right striatum of male Wistar rats, which were administered i.p. with 12.5 mg kg^{-1} Imip. Thirty μl dialysate was collected every 15 min, and the levels of Imip and DMI were measured by high-performance liquid chromatography with electrochemical detection (h.p.l.c.–e.c.d.). SKF-525A and aminopyrine were concomitantly administered in order to assess their respective effects on the pharmacokinetics of Imip and DMI in the brain.

3 The intracerebral half life ($t_{1/2}$) of Imip was 2.4 ± 0.3 h with Imip alone. Premedication with SKF-525A, an inhibitor of drug-metabolizing enzymes, significantly prolonged the $t_{1/2}$ of Imip, while at the same time production of DMI from Imip was accordingly inhibited. Concomitant administration of aminopyrine did not induce any significant change in the concentrations of Imip, but significantly inhibited the concentrations of DMI through its competitive antagonism in the demethylation pathway.

4 The present results suggest that the brain microdialysis method reflects the intracerebral pharmacokinetics of Imip and DMI well and may be applicable to further pharmacokinetic investigations of psychotropic agents.

Keywords: Brain microdialysis; pharmacokinetics; high-performance liquid chromotography with electrochemical detection; imipramine

Introduction

Imipramine (Imip) is one of the most widely used antidepressants in the clinical practice of psychiatry, and its demethylated metabolite, desipramine (DMI), is also known to exert significant antidepressant activity. While their concentrations in plasma and brain homogenate samples have been often detected by the high performance liquid chromatography (h.p.l.c.) method (Suckow & Cooper, 1981; Sugita *et al.*, 1987; Foglia *et al.*, 1991), the time course of their concentrations in the brain has rarely been reported, with the exception of an early pharmacokinetic study by Daniel *et al.* (1981) in which the concentrations of the drugs from animals killed at specific time points were assayed spectrofluorometrically.

Recent advances in brain microdialysis techniques have enabled the direct measurement of various neurotransmitters in the brain (Ungerstedt & Hallstroem, 1987), but pharmacokinetic investigations of psychotropic agents by this method are limited (Dubey *et al.*, 1989; Matos *et al.*, 1992; Tellez *et al.*, 1992). Since pharmacokinetic drug monitoring is crucial for the rational therapeutic use of drugs, the feasibility of employing the brain microdialysis method for pharmacokinetic studies is of particular importance. One of the methological advantages of brain microdialysis is that, in particular, time-dependent changes in the concentrations of a psychotropic drug administered to a single animal can be easily traced for a length of time that is sufficient to calculate the biological half life and other pharmacokinetic parameters of the drug correctly. This is not achievable by the traditional measurement of drug concentration in the plasma by h.p.l.c., which requires too large an amount of blood to be sampled from one animal.

We established a method for directly monitoring the time-course of the concentrations of Imip and DMI in the brain of rats by applying the brain microdialysis method and h.p.l.c. with electrochemical detection (e.c.d.). This paper describes the method employed, the pharmacokinetic data obtained for Imip and DMI in brain of rats, and the effects of SKF-525A and aminopyrine of the pharmacokinetics of Imip and DMI. SKF-525A, a well-known inhibitor of liver enzymes involved in drug metabolism (Kato *et al.*, 1964; Galeotti *et al.*, 1983) and aminopyrine, which, together with Imip, is metabolized mainly through demethylation, were administered concomitantly with Imip. The aim was to determine whether or not the time-dependent changes in concentrations of Imip and DMI measured by brain microdialysis correctly reflected the actual pharmacokinetics of Imip and DMI in the rat brain which is influenced by both SKF-525A and aminopyrine.

Methods

Animals and surgical procedures

Twenty-one adult male Wistar rats (Shizuoka Laboratory Animal Center, Hamamatsu, Japan), weighing about 300 to 350 g, were used for the experiments. The animals were housed for at least one week prior to the experiments in a room where the temperature (23 ± 0.5°C), humidity (60 ± 5%) and light cycle (12-h illumination with the light turned on at 07 h 00 min) were controlled. The rats were fed on laboratory chow regularly and water *ad libitum*. They were anaesthetized with a single i.p. injection of 50 mg kg^{-1} pentobarbitone and positioned in a stereotaxic frame with atraumatic ear bars. After exposing the skull, a guide cannula (G-8, Eicom, Kyoto, Japan) was implanted stereotaxically into the right striatum (coordinates with respect to the bregma: anterior, 0; lateral, 3; ventral, 4 mm) according to the atlas of Paxinos & Watson (1982). After implantation, the cannula was fixed firmly to the skull with anchor screws and dental cement, and then occluded with a dummy cannula. The dialysis experiment was performed at least 2 days after the operation in order to avoid possible interfering effects.

[1] Author for correspondence.

Drug administration

Imip at a dose of 12.5 mg kg^{-1} was injected i.p. into all the animals. In order to evaluate the influence of SKF-525A on the elimination of Imip, 50 mg kg^{-1} SKF-525A was injected i.p. into 5 animals 30 min before the administration of Imip. Aminopyrine was co-administered with Imip to 11 animals at dose levels of 25, 50, and 100 mg kg^{-1} i.p. (the number of the animals given each dose of aminopyrine were 3, 4 and 4, respectively) to determine how it affected the demethylation of Imip and the production of DMI. All the drugs were given in a volume of 0.1 ml 100 g^{-1} 2 h after dialysis started.

Dialysis

On the day of the experiment, the dummy cannula was removed from the guide cannula and an I-shaped dialysis probe (BDP-I-8-03, Eicom; mol. wt. cutoff :50000; exposed surface for striatum :3.0 mm). was inserted which was then perfused with Ringer solution (composition mM: NaCl 147, KCl 4.0, $CaCl_2$ 2.4) at a constant flow rate of 2 μl min^{-1} using a perfusion pump (Microliter syringe pump, Harvard, U.S.A.). Following a 2-h period for stabilization of the baseline, dialysate samples (30 μl) were collected directly into an autoinjector every 15 min throughout the whole experiment. All rats were placed in a plexiglass container (30 × 30 × 35 cm) during the experiment, kept freely moving and allowed free access to food and water.

The *in vitro* recovery rates of Imip and DMI were estimated by placing probes in Ringer solution containing Imip and DMI. Collection of the perfusate and assay of the Imip and DMI contained in the perfusate were undertaken in the same manner as described above. The recovery rates of Imip and DMI so calculated were 15.1 ± 2.1% and 15.0 ± 2.2%, respectively (mean ± s.d., $n = 4$). The following results have not been corrected for recovery for convenience.

Chromatographic conditions

The concentrations of Imip and DMI in the dialysates were measured by h.p.l.c.-e.c.d. The h.p.l.c.-e.c.d. system consisted of a pump (880-PU, JASKO, Tokyo, Japan) with an autoinjector (AS-10, Eicom, Kyoto, Japan; injector loop size: 100 μl), an electrochemical detector (CB-100, Eicom, Kyoto, Japan) with a thin-layer carbon graphite electrode (6-GE, Eicom) and a chromatographic column (average particle size, 5 μm; 150 × 6.4 mm i.d.; Puresil C18 ODS column, Millipore, U.S.A.). The mobile phase consisted of a mixture of 0.1 M sodium acetate buffer (pH 4.0), acetonitrile and H_2O (5:3:2), and the flow rate was set at 1.5 ml min^{-1}. The chromatographic column was maintained at 37°C with a waterbath (Thermo Minder Mini-80, Taiyo, Tokyo, Japan). The detector potential was set at 800 mV versus an Ag/AgCl reference electrode. After the experiment, rats were killed by i.p. injection of thiopentone sodium and the location of each probe was verified histologically.

Drugs and chemicals

Imipramine hydrochloride was purchased from Nihon Ciba-Geigy Co. (Hyogo, Japan). Desipramine hydrochloride was purchased from Sigma, St. Louis, U.S.A. Each drug was dissolved in saline immediately prior to injection. Acetonitrile and sodium acetate were obtained from Wako Pure Chemicals, Osaka, Japan. N,N-diethylaminoethyl-2,2-diphenylvalerate hydrochloride (SKF-525A hydrochloride) was purchased from Research Biochemicals Inc., U.S.A. Aminopyrine was purchased from Sigma.

Statistics

Statistical analysis of the data for multiple comparisons was performed by two-way analysis of variance (ANOVA) with repeated measures on one factor and *post-hoc* tests (Fisher's protected least significance difference; significance level, 5%). For single comparisons, the significance of differences between means was determined by Student's two-tailed t tests.

Results

Static experiments

Hydrodynamic voltammograms of Imip and DMI are plotted in Figure 1. Both Imip and DMI started their electrical responses at 450 mV. The responses increased steadily up to about 850 mV and then decreased. The maximum response was higher in DMI than in Imip.

Chromatograms

A chromatogram for authentic standard Imip and DMI, a blank chromatogram, and a typical chromatogram obtained from a rat sample after i.p. administration of Imip are illustrated in Figure 2. The retention times of authentic Imip and DMI were 9.80 min and 8.78 min, respectively. The blank chromatogram did not demonstrate peaks corresponding to those of the authentic standards, while two peaks with the same retention times as those of the authentic standards appeared on the chromatogram from the sample. The present chromatographic conditions thus revealed no significant interference by biological substances in the accurate determination of the drugs, and we can therefore identify the two peaks on the chromatogram from the sample as representing Imip and DMI.

Concentrations of Imip and DMI in dialysate

The time-course changes in the extracellular concentrations of Imip and DMI in 30 μl dialysate after a single administration of Imip are shown in Figure 3a. Imip reached a peak at about 60 min after its administration, while DMI reached its maximal concentration about 180 min after administration. Notably also, the concentrations of DMI decreased more slowly than those of Imip.

Figure 3b illustrates the time course changes of Imip and DMI following premedication with SKF-525A. The concentrations of DMI at every point were significantly lower ($F(1,39) = 17.984$, $P < 0.0001$) in the group to which SKF-525A was administered prior to Imip than in group injected with Imip alone. It is also evident that the concentrations of

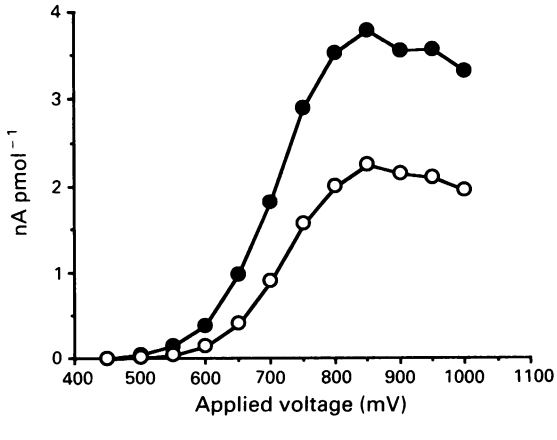

Figure 1 Hydrodynamic voltammograms of imipramine (Imip, ○) and desipramine (DMI, ●). Detector, CB-100, Eicom; mobile phase, 0.1 M sodium acetate buffer (pH 4.0): acetonitrile: H_2O (5:3:2). Each curve represents 400 ng of Imip and DMI.

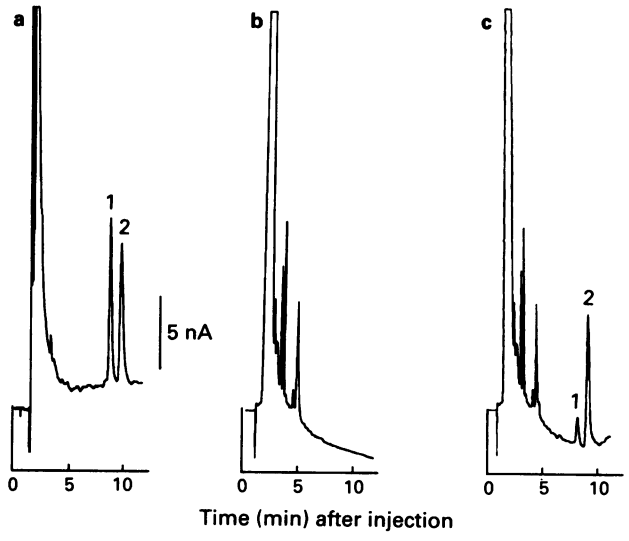

Figure 2 Typical chromatograms of dialysates. (a) Standard substances (400 pg of imipramine (Imip) and desipramine (DMI)); (b) blank; (c) sample after injection of Imip 12.5 mg kg^{-1}. (1) DMI; (2) Imip. The applied voltage of the electrochemical detector was set at 850 mV.

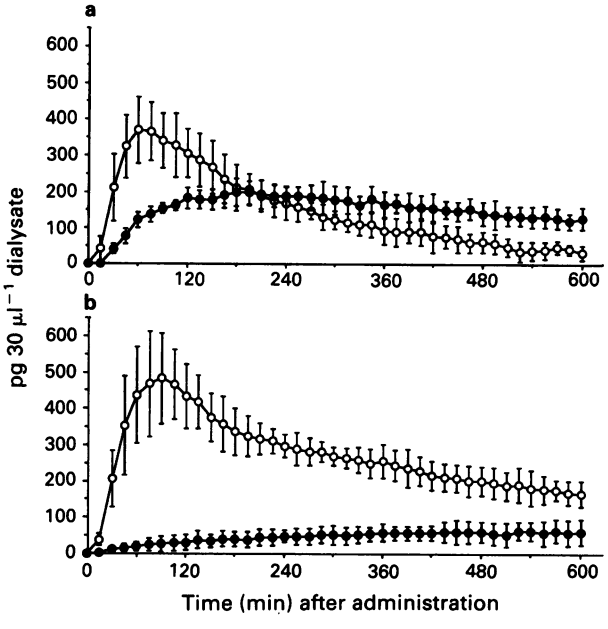

Figure 3 Extracellular concentrations of imipramine (Imip, ○) and desipramine (DMI, ●) (pg 30 µl^{-1} dialysate) after intraperitoneal administration of 12.5 mg kg^{-1} of Imip without (a; $n = 5$) and with 50 mg kg^{-1} of SKF-525A (b, $n = 5$). Premedication with SKF-525A significantly lowered the concentrations of DMI, while the concentrations of IMP became significantly higher (by ANOVA; $F(1,39) = 17.984$, $P < 0.0001$).

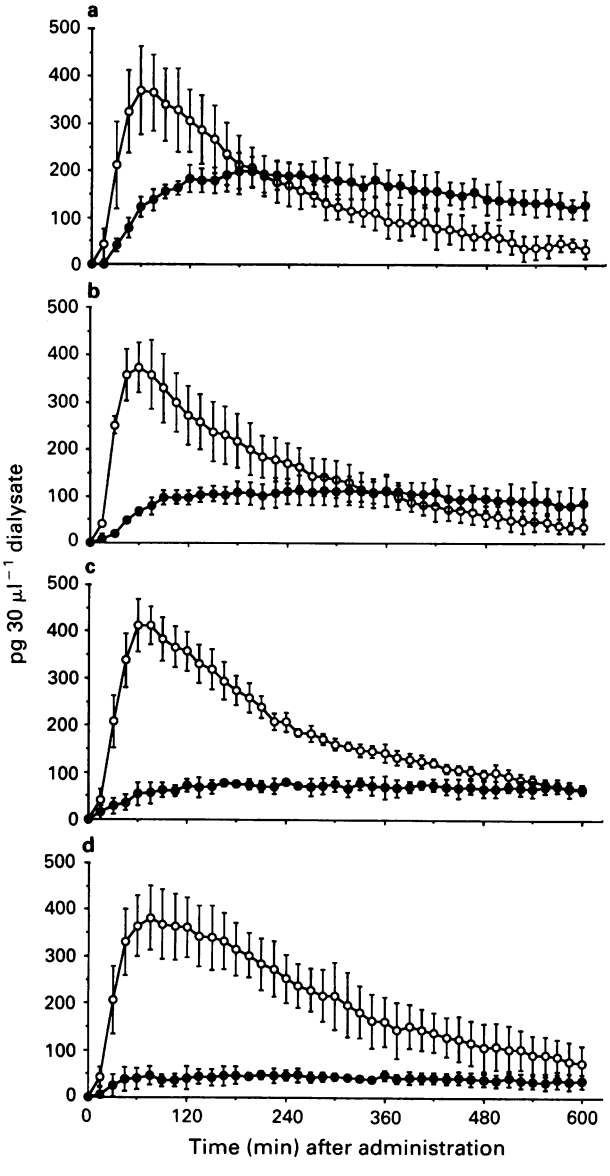

Figure 4 Time-course of imipramine (Imip, ○) and desipramine (DMI, ●) with concomitant administration of aminopyrine (AMP). (a) ($n = 5$), Imip only; (b) ($n = 3$), Imip + 25 mg kg^{-1} AMP; (c) ($n = 4$), Imip + 50 mg kg^{-1} AMP; (d) ($n = 4$), Imip + 100 mg kg^{-1} AMP. The extracellular concentrations of DMI showed significant differences in proportion to the given dosage of AMP (by ANOVA; $F(3,177) = 3.337$, $P < 0.0001$), while the concentrations of Imip were not significantly different with or without concomitant administration of AMP (by ANOVA; $F(3,117) = 0.969$, $P > 0.01$).

Table 1 Biological half life and other pharmacokinetic parameters of imipramine (Imip)

Treatment	C_o (pg 30 µl^{-1})	C_{max} (pg 30 µl^{-1})	$t_{1/2}$ (h)	k_e (h^{-1})
Imip alone	502.9 ± 128.3	369.5 ± 92.7	2.4 ± 0.3 (2.1–2.9)	0.29 ± 0.0034
Imip + SKF	479.6 ± 87.9	441.1 ± 93.2	6.7 ± 1.4 (4.6–7.8)*	0.11 ± 0.0026
Imip + 25AMP	516.8 ± 196.6	373.8 ± 53.1	2.7 ± 0.6 (1.9–3.0)	0.27 ± 0.073
Imip + 50AMP	559.5 ± 81.7	412.1 ± 40.3	3.5 ± 0.2 (3.2–3.6)*	0.19 ± 0.014
Imip + 100AMP	494.5 ± 54.9	382.2 ± 68.4	3.5 ± 0.7 (2.6–4.4)**	0.21 ± 0.043

Biological half life ($t_{1/2}$), elimination rate constant (k_e) and initial concentration (C_o) are theoretical values calculated from regression coefficients given by applying the least square method to the log/linear concentrations/time curves of Imip of each rat. C_{max} represents the mean maximal concentrations of Imip, derived from the linear/linear plots of concentrations of Imip. Significant differences in $t_{1/2}$ were observed between the Imip alone group and the Imip + SKF-525A, Imip + 50 mg and 100 mg aminopyrine (AMP) groups, respectively (*$P < 0.01$; **$P < 0.05$).

Imip in the SKF-525A group were significantly higher than those in the group to which Imip alone was administered ($F(1,39) = 42.548$, $P < 0.0001$). This difference in concentrations of Imip and DMI is considered to be attributable to the effect of SKF-525A, which inhibits the drug metabolism by liver enzymes, such as cytochrome P450, by suppressing the production of DMI from Imip and prolonging the elimination of Imip.

Figure 4 shows the time-course changes in the extracellular concentrations of Imip and DMI with concomitant administration of aminopyrine at dose levels of 25, 50, and 100 mg kg^{-1}. Significant differences ($F(3,117) = 3.337$, $P < 0.0001$) were noted among the extracellular concentrations of DMI in proportion to the given dosages of aminopyrine. These differences are thought to reflect the competitive antagonism between Imip and aminopyrine, both of which are metabolized mainly through demethylation. The fact that the concentrations of Imip with and without concomitant administration of aminopyrine were not significantly different ($F(3,117) = 0.969$, $P > 0.01$) implies that aminopyrine affected only the metabolic pathway through demethylation, so leaving other pathways and the metabolism of Imip as a whole intact.

Pharmacokinetic data

The biological half life ($t_{1/2}$), maximal (C_{max}) as well as initial (C_o) concentrations and elimination rate constant (k_e) of Imip are listed in Table 1. C_o, $t_{1/2}$ and k_e were calculated from the regression coefficients given by applying the least square method to the log/linear concentrations/time curves of Imip between 60–600 min after the administration of Imip in each rat. The correlation coefficients of the regression curves all exceeded 0.98 and were statistically significant ($P < 0.001$). C_{max} represents the actual mean value derived from the linear/linear plots of concentrations of Imip as shown in Figures 3 and 4.

Significant differences in $t_{1/2}$ were observed between the Imip alone group and the Imip + 50 mg, 100 mg aminopyrine (AMP) and Imip + SKF-525A (SKF) groups, respectively (Student's two-tailed t tests).

The significant prolongation of the $t_{1/2}$ of Imip as a result of concomitant administration of SKF-525A or aminopyrine implies that demethylation plays a major role in the metabolism of Imip and that the prolongation of $t_{1/2}$ due to inhibition of drug metabolizing enzymes has a clinical significance. Since it has already been reported that the plasma levels of both Imip and DMI are significantly correlated with their clinical effect (Reisby *et al.*, 1977), the prolonged intracerebral concentration of Imip and resultant low production of DMI may bring about some important differences in the clinical pharmacodynamic effects. No significant difference was demonstrated for C_o (the initial concentration of Imip) or C_{max} (the maximal concentration of Imip), implying that its uptake into the brain was unaffected by the concomitant administration of either SKF-525A or aminopyrine.

Discussion

The present findings demonstrate that the brain microdialysis technique, while having been applied almost solely to pharmacodynamic investigations of various neurotransmitters, can also be utilized for pharmacokinetic studies in psychopharmacology which have previously been undertaken mainly by means of the determination of psychotropic drugs in homogenized brain samples from animals (Imip by Masada *et al.*, 1986). The application of microdialysis to the pharmacokinetic study of psychotropic agents, although still limited (diazepam by Dubey *et al.*, 1989; phenobarbitone by Tellez *et al.*, 1992), is of great importance, since microdialysis can detect quite small amounts of psychotropic drugs in the brain directly (detection limit for Imip: 8.9 pg 30 μl^{-1} dialysate) and also because it reflects the intracerebral drug metabolism quite well in free-moving rats without gross damage to the brain.

In our experiments, the feasibility and accuracy of the brain microdialysis technique for the pharmacokinetic study of psychotropic agents have been endorsed. First, premedication with SKF-525A prior to the administration of Imip significantly prolonged the elimination of Imip and inhibited the increase in concentration of DMI in the collected dialysates. This means that the concentration of DMI, a demethylated metabolite of Imip, in dialysates from the brain reflected the general drug metabolism through liver enzymes, mainly cytochrome P-450, being inhibited by the administration of SKF-525A. It is well known that there is substantial cytochrome P-450 activity in the brain mitochondria (Ghersi-Egea & Livertoux, 1992). Thus, it must be taken into consideration that Imip may be metabolized in part also in the CNS. However, if SKF-525A crosses the blood-brain-barrier in parallel with Imip and affects the cytochrome P-450 localized in the brain, the drug metabolism in the CNS must be inhibited by the systemic administration of SKF-525A to the same extent as the cytochrome P-450 localized in the liver.

Concomitant administration of aminopyrine suppressed the production of DMI from Imip significantly in a dose-dependent manner, while it did not affect the time-course changes in concentration of Imip. This is considered to be due to competitive antagonism between aminopyrine and Imip, both of which are metabolized through demethylation. The fact that the elimination of Imip did not change significantly is due to the availability of alternative metabolic pathways other than demethylation, such as hydroxylation (Potter *et al.*, 1982). We thus found, by the brain microdialysis technique, that the dose-dependent competitive antagonism between Imip and aminopyrine, both administered i.p., was well reflected in the dialysates collected through the microdialysis probe. There are several reports in which the competitive antagonism between aminopyrine and other drugs has been investigated (Renton, 1985; Gellert *et al.*, 1986; Moochhala *et al.*, 1986; Floreani & Carpenedo, 1990). Similar results were obtained in our present experiments.

In a previous study, in which we measured the concentrations of drugs in homogenized brain samples (Shibanoki *et al.*, 1989), the biological half lives of Imip and DMI in the rat brain after intravenous injection of Imip were estimated to be 114 ± 24 min and 210 ± 54 min, respectively. Despite the difference in mode of administration of Imip, the difference in biological half life of Imip between our two different methods is relatively small, considering that the Imip measured in dialysis only reflected the concentration of the free compound. This confirms that the brain dialysis method, in comparison with previous detection techniques, holds good for the measurement of psychotropic agents.

Daniel *et al.* (1981) found some deviation from linearity in the Imip and DMI time curves in the blood and the brain and suggested that the pharmacokinetics of Imip and DMI follows the equations for a multi-compartment system. However, the correlation coefficients of the Imip and DMI time curves in our experiment suggested their linearity, which implies a single compartment model for their pharmacokinetics. In our experiment, concentrations of Imip and DMI were measured from the dialysates collected through the probe in the striatum which can be regarded as a single compartment in the pharmacokinetics of Imip and DMI, whereas Daniel *et al.* (1981) measured Imip and DMI from homogenized samples of the whole brain which must serve as a multi-compartment system.

In conclusion, brain microdialysis combined with h.p.l.c.-e.c.d. represents a sensitive procedure for the direct measurement of the time-course concentrations of psychotropic agents in the brain. It is hoped that through the use of this

method, the pharmacokinetics of various psychotropic agents and their pharmacodynamic effects on neurotransmitters will be examined further, so that the actual mechanisms and metabolism of psychotropic drugs will be better understood and permit their more rational clinical usage.

References

DANIEL, W., ADAMUS, A., MELZACKA, M., SZYMURA, J. & VETULANI, J. (1981). Cerebral pharmacokinetics of imipramine in rats after single and multiple dosages. *Naunyn-Schmied. Arch. Pharmacol.*, **317**, 209–213.

DUBEY, R.K., MCALLISTER, C.B., INOUE, M. & WILKINSON, G.R. (1989). Plasma binding and transport of Diazepam across the blood-brain barrier. *J. Clin. Invest.*, **84**, 1155–1159.

FLOREANI, M. & CARPENEDO, F. (1990). Inhibition of rat liver monooxygenase activities by 2-methyl-1,4-naphthoquinone (menadione). *Toxicol. Appl. Pharmacol.*, **105**, 333–339.

FOGLIA, J.P., SORISIO, D. & PEREL, J.M. (1991). Determination of imipramine, despiramine and their hydroxy metabolites by reversed-phase chromatography with ultraviolet and coulometric detection. *J. Chromatogr.*, **572**, 247–258.

GALEOTTI, T., EBOLI, M., PALOMBINI, G. VAN ROSSUM, G.D.V. & KAPOOR, S.C. (1983). Inhibition of mitochondrial oxidative metabolism by SKF-525A in intact cells and isolated mitochondria. *Biochem. Pharmacol.*, **32**, 3285–3295.

GELLERT, J., ALDERMAN, J. & LIEBER, C.S. (1986). Interaction between ethanol metabolism and mixed-function oxidation in alcohol dehydrogenase positive and negative deermice. *Biochem. Pharmacol.*, **35**, 1037–1041.

GHERSI-EGEA, J.F. & LIVERTOUX, M.H. (1992). Evidence for drug metabolism as a source of reactive species in the brain. *Exper. Suppl.* (Basel), **62**, 219–226.

KATO, R., CHIESARA, E. & VASSANELLI, P. (1964). Further studies on the inhibition and stimulation of microsomal drug-metabolizing enzymes of rat liver by various compounds. *Biochem. Pharmacol.*, **13**, 69–83.

MASADA, M., SUZUKI, K., KIKUTA, S., YAMASHITA, S., NAKANISHI, K., NADAI, T., IGARASHI, Y. & NOGUCHI, T. (1986). Regional distribution and elimination kinetics of imipramine in rat brain after a single intraperitoneal administration. *Chem. Pharm. Bull.*, **34**, 2173–2177.

MATOS, F.F., ROLLEMA, H. & BASBAUM, A.I. (1992). Simultaneous measurement of extracellular morphine and serotonin in brain tissue and CSF by microdialysis in awake rats. *J. Neurochem.*, **58**, 1773–1781.

MOOCHHALA, S.M. & RENTON, K.W. (1986). Inhibition of hepatic microsomal drug metabolism by the immunosuppressive agent cyclosporin A. *Biochem. Pharmacol.*, **35**, 1499–1503.

PAXINOS, G. & WATSON, C. (1982). *The Rat Brain in Stereotaxic Coordinates*, 2nd Edition. New York: Academic Press.

POTTER, W.Z., CALIL, H.M., SUTFIN, T.A., ZAVADIL, A.P., JUSKO, W.J., RAPOPORT, J. & GOODWIN, F.K. (1982). Active metabolites of impramine and desipramine in man. *Clin. Pharmacol. Ther.*, **31**, 393–401.

REISBY, N., GRAM, L., BECH, P., NAGY, A., PETERSEN, G., ORTMANN, J., IBSEN, I., DENCKER, S., JACOBSEN, O., KRAUTWALD, O., SONDERGAARD, I. & CHRISTIANSEN, J. (1977). Imipramine: clinical effects and pharmacokinetic variability. *Psychopharmacology*, **54**, 263–272.

RENTON, K.W. (1985). Inhibition of hepatic microsomal drug metabolism by the calcium channel blockers diltiazem and verapamil. *Biochem. Pharmacol.*, **34**, 2549–2553.

SHIBANOKI, S., IMAMURA, Y., KUBO, T., KOGURE, M., GOTOH, Y. & ISHIKAWA, K. (1989). Difference in the biological fate of dosulepin and imipramine in rats. *Neurosciences*, **15**, 359–370.

SUCKOW, R.F. & COOPER, T.B. (1981). Simultaneous determination of imipramine, desipramine, and their 2-hydroxy metabolites in plasma by ion-pair reversed-phase high-performance liquid chromatography with amperometric detection. *J. Pharm. Sci.*, **70**, 257–261.

SUGITA, S., KOBAYASHI, A., SUZUKI, S., YOSHIDA, T. & NAKAZAWA, K. (1987). High-performance liquid chromatographic determination of imipramine and its metabolites in rat brain. *J. Chromatogr.*, **421**, 412–417.

TELLEZ, S., FORGES, N., ROUSSIN, A. & HERNANDEZ, L. (1992). Coupling of microdialysis with capillary electrophoresis: a new approach to the study of drug transfer between two compartments of the body in freely moving mouse. *J. Chromatogr.*, **581**, 257–266.

UNGERSTEDT, U. & HALLSTROEM, A. (1987). In vivo microdialysis: a new approach to the analysis of neurotransmitters in the brain. *Life Sci.*, **41**, 861–864.

(Received September 21, 1993
Revised December 14, 1993
Accepted February 9, 1994)

Br. J. Pharmacol. (1994), **112**, 630–634

Requirement for endothelium-derived nitric oxide in vasodilatation produced by stimulation of cholinergic nerves in rat hindquarters

K.E. Loke, C.G. Sobey, *G.J. Dusting & [1]O.L. Woodman

Departments of Pharmacology and *Physiology, University of Melbourne, Parkville, Victoria 3052, Australia

1 We aimed to determine whether nitric oxide (NO) and/or the endothelium is involved in cholinergic neurogenic vasodilatation in the rat isolated hindquarters.

2 The abdominal aorta was cannulated for perfusion of the rat hindquarters with Krebs bicarbonate solution containing phenylephrine, to induce basal constrictor tone. In the presence of noradrenergic neurone blockade with guanethidine (200 mg kg^{-1}, i.p.) electrical stimulation of peri-aortic nerves induced frequency-dependent decreases in hindquarters perfusion pressure, indicating vasodilatation. Both the endothelium-dependent vasodilator, acetylcholine (ACh) and the endothelium-independent vasodilator, sodium nitroprusside (SNP) induced dose-dependent decreases in perfusion pressure. In each experiment, responses to either nerve stimulation, ACh or SNP were recorded before and after treatment with saline vehicle, atropine (1 μM), N^G-nitro-L-arginine (L-NOARG, 100 μM), L-arginine (1 mM), L-arginine plus L-NOARG, or 3-3 cholamidopropyl dimethylammonio 1-propanesulphonate (CHAPS, 30 mg). Hindquarters dilatation after each treatment was expressed as a percentage of the control response.

3 Following treatment with saline, responses to nerve stimulation and ACh were 99 ± 9% and 107 ± 10% of control, respectively demonstrating the reproducibility of these responses. Nerve stimulation-induced dilatation was abolished by atropine (0 ± 0% of control, $P<0.05$) or reduced to 14 ± 10% of control by NO synthase inhibition with L-NOARG ($P<0.05$). Dilator responses to ACh were also abolished by atropine (0 ± 0% of control, $P<0.05$) or inhibited by L-NOARG (59 ± 10% of control, $P<0.05$), indicating that the neurogenic dilatation is cholinergic and is mediated by NO. The administration of the NO precursor, L-arginine, prevented the inhibitory effect of L-NOARG on dilator responses to nerve stimulation and ACh (L-arginine plus L-NOARG: 89 ± 13% and 122 ± 24% of control, respectively). In addition CHAPS, which removes endothelial cells, inhibited responses to both nerve stimulation (0 ± 0% of control, $P<0.05$) and ACh (33 ± 8% of control, $P<0.05$). In contrast, no treatment significantly reduced the vasodilator responses to SNP.

4 These observations suggest that cholinergic neurogenic vasodilatation in the rat isolated hindquarters requires the synthesis and release of NO from the endothelium.

Keywords: Acetylcholine; 3-3 cholamidopropyl dimethylammonio 1-propanesulphonate (CHAPS); cholinergic neurogenic dilatation; endothelium; nitric oxide; N^G-nitro-L-arginine

Introduction

It is well established that vasodilatation by exogenous acetylcholine (ACh) involves the release of endothelium-derived nitric oxide (NO) (Furchgott & Zawadzki, 1980; Moncada *et al.*, 1991a). However, the role of NO and/or the endothelium in vasodilatation caused by neuronally-released ACh is not yet clearly established.

Recent attempts to determine whether NO does mediate cholinergic neurogenic vasodilatation have involved the use of NO synthase inhibitors such as N^G-nitro-L-arginine (L-NOARG) and its methyl ester (L-NAME) as well as N^G-monomethyl-L-arginine (L-NMMA) (Broten *et al.*, 1992; McMahon *et al.*, 1992; Andriantsitohaina & Suprenant, 1992; Loke *et al.*, 1994). These studies all concluded that NO mediates cholinergic neurogenic dilatation although the results of the two studies using L-NAME (McMahon *et al.*, 1992; Broten *et al.*, 1992) must be viewed with some caution due to the subsequent report that L-NAME possesses muscarinic receptor antagonist activity (Buxton *et al.*, 1993). Furthermore, although the authors of two of those reports concluded that the endothelium was the source of the NO (Broten *et al.*, 1992; Andriantsitohaina & Suprenant, 1992) no direct evidence was provided to support that conclusion. In addition others reported that stimulation of cholinergic nerves causes vasodilatation of the cat posterior auricular and rabbit lingual arteries (Brayden & Bevan, 1985; Brayden & Large, 1986) through an action independent of the endothelium. Thus the role of endothelium-derived NO in cholinergic neurogenic vasodilatation remains to be clarified.

The aims of this study were twofold. Firstly, to establish whether NO mediates dilator responses to the stimulation of cholinergic nerves in the rat hindquarters by examining the influence of the NO synthase inhibitor L-NOARG. L-NOARG has been reported to have no interaction with muscarinic receptors (Buxton *et al.*, 1993). Secondly, to determine whether removal of the endothelium with the biological detergent, 3-3 cholamidopropyl dimethylammonio 1-propanesulphonate (CHAPS) (Bhardwaj & Moore, 1988) prevents cholinergic neurogenic dilatation.

Methods

General procedures

Sprague-Dawley rats of either sex (250–400 g) were anaesthetized with pentobarbitone sodium (60 mg kg^{-1}, i.p.; Boehringer Ingelheim, Australia). Following a midline abdominal incision, the aorta was cannulated adjacent to the iliac bifurcation. The hindquarters were then perfused with Krebs-bicarbonate solution (37°C bubbled with 95% O_2, 5% CO_2) containing (mM): NaCl 118, KCl 4.7, KH_2PO_4 1.2, $MgSO_4$

[1] Author for correspondence.

1.2, (+)-glucose 11.0, $NaHCO_3$ 25.0 and $CaCl_2$ 2.5, using a roller pump (TSE, McLennan Ltd.). The hindquarters were perfused at a constant rate of 10–16 ml min^{-1} (0.04 ml min^{-1} per g body wt). Phenylephrine (0.3–100 μM) was added to the perfusate to constrict the vasculature, resulting in a baseline perfusion pressure of 79 ± 3 mmHg. The vena cava was sectioned to permit the perfusate to escape. Drugs were injected into the perfusion circuit. A side-arm of the perfusion circuit was connected to a pressure transducer (Spectromed) and perfusion pressure was recorded on a Grass polygraph (Model 7E, Quincy, MA, U.S.A.). In this constant flow system changes in perfusion pressure reflected changes in vascular tone. After hindlimb perfusion was commenced, the rat was killed by an intracardiac injection of 4 M KCl and 15 min was then allowed for the preparation to stabilize.

Removal of endothelium from the rat hindquarters vasculature

In 16 rats the endothelium was removed from the hindquarters vasculature by infusion of the biological detergent CHAPS (5 mg ml^{-1}) for 30 s (total dose 30 mg). Specific endothelial damage was confirmed in each experiment by a reduced dilator response to ACh but not to sodium nitroprusside (SNP).

Protocols

Group I: Effects of atropine, L-NOARG, L-arginine and CHAPS on vasodilator responses to peri-aortic nerve stimulation Rats were pretreated with guanethidine sulphate 24 and 3 h prior to experimentation (100 mg kg^{-1}, i.p. on each occasion). The abdominal aorta was cannulated as described above and a bipolar electrode was placed around the aorta. Peri-aortic nerves were electrically stimulated (10 ms, 2–10 Hz) with a Grass stimulator (Model SD9, Quincy, MA, U.S.A.) for 20 s at supramaximal voltage (60–100 V). Stimulation-induced changes in perfusion pressure were examined in 6 groups of rats before and 15 min after treatment with saline vehicle, atropine, L-NOARG, L-arginine, L-arginine plus L-NOARG or CHAPS. The protocol for each group was: (A) In 5 rats, saline was added to the perfusate in place of an antagonist to assess the stability of the preparation. (B) In 5 rats, the effect of peri-aortic nerve stimulation on perfusion pressure was examined before and 15 min after addition of atropine (1 μM) to the perfusate. (C) In 6 rats, stimulation-induced responses were re-examined 15 min after L-NOARG (100 μM) was added to the perfusate. (D) In 6 rats, dilator responses to electrical stimulation were examined before and 15 min after addition of L-arginine (1 mM) to the perfusate. (E) In 6 rats, control dilator responses to nerve stimulation were first established in the presence of L-arginine (1 mM) and re-examined 15 min after the further addition of L-NOARG (100 μM) to the perfusate. (F) In 6 rats, dilator responses were examined before and 15 min after infusion of CHAPS (30 mg). Baseline perfusion pressure during L-NOARG administration or after CHAPS infusion was maintained equivalent to the control levels by reducing the concentration of phenylephrine in the perfusate.

Group II: Effects of atropine, L-NOARG, L-arginine and CHAPS on vasodilator responses to ACh Bolus (1–3 μl) injections of ACh (1–100 ng) were given 5 min apart to a second group of rats to induce control vasodilator responses in the hindquarters. As in Group I, responses were re-examined 15 min after treatment with: (A) saline vehicle ($n = 6$), (B) atropine ($n = 4$), (C) L-NOARG ($n = 6$), (D) L-arginine ($n = 6$), (E) L-arginine plus L-NOARG ($n = 6$) or (F) CHAPS ($n = 5$).

Group III: Effects of L-NOARG, L-arginine and CHAPS on vasodilator responses to SNP Bolus injections (1–10 μl) of the endothelium-independent vasodilator, SNP (0.1–10 μg) were administered in a third group of rats before and 15 min after treatment with (A) saline vehicle ($n = 5$), (B) atropine ($n = 4$), (C) L-NOARG ($n = 5$), (D) L-arginine ($n = 6$), (E) L-arginine plus L-NOARG ($n = 6$) or (F) CHAPS ($n = 5$).

Drugs

Acetylcholine perchlorate, L-arginine hydrochloride, atropine methylbromide, 3-3 cholamidopropyl dimethylammonio 1-propane sulphonate (CHAPS), guanethidine sulphate, N^G-nitro-L-arginine, L-phenylephrine hydrochloride and sodium nitroprusside. All drugs were obtained from the Sigma Chemical Co. (St Louis, MO, U.S.A.), except for ACh (BDH, England). All drugs were dissolved and diluted in saline.

Statistical analysis

Decreases in perfusion pressure indicating vasodilatation are presented as mean ± s.e.mean of n experiments. Each dilator response recorded after treatment was expressed as a percentage of the control response in that preparation, and one average value was obtained from all doses in each experiment. Thus each animal acted as its own control and any variability between animals was negated. The effects of treatments were then assessed by one-way analysis of variance (ANOVA). Responses to nerve stimulation, ACh and SNP obtained before and after treatment were evaluated by ANOVA which treated all frequencies or doses as a group, to observe whether the treatment had any significant effect on these responses. The effects of treatments on baseline perfusion pressure were analysed by Student's paired t test, comparing baseline values obtained before and after each treatment. Statistical significance was achieved when $P < 0.05$.

Results

Group I: Effects of atropine, L-NOARG, L-arginine and CHAPS on vasodilator responses to peri-aortic nerve stimulation

In the presence of elevated vascular tone (phenylephrine, 0.3–100 μM) aortic perivascular nerve stimulation (2–10 Hz) caused frequency-dependent decreases in hindquarters perfusion pressure in rats pretreated with guanethidine (200 mg kg^{-1}, i.p.) (Figures 1a and 2a). These responses were not altered by addition of saline vehicle to the perfusate confirming that there was no significant change in responses with time (99 ± 9% of control). Hindquarters neurogenic responses were abolished by atropine (1 μM; 0 ± 0% of control, $P < 0.05$) indicating cholinergic dilatation. The stimulation-induced decreases in perfusion pressure were significantly attenuated by L-NOARG (100 μM) (Figure 1a). L-Arginine alone had no effect on the stimulation-induced decreases in perfusion pressure (96 ± 12% of control). However, pretreatment with L-arginine prevented the inhibitory effect of L-NOARG on these responses (89 ± 13% of control). Vasodilator responses to nerve stimulation were abolished by treatment with CHAPS (30 mg) (Figure 2a).

Group II: Effects of atropine, L-NOARG, L-arginine and CHAPS on vasodilator responses to ACh

Bolus injections of ACh (1–100 ng) caused dose-dependent decreases in perfusion pressure of the rat hindquarters under elevated vascular tone (Figures 1b and 2b). Control decreases in perfusion pressure induced by ACh were not altered by administration of the saline vehicle (107 ± 10% of control), but were inhibited by either atropine (0 ± 0% of control, $P < 0.05$) or L-NOARG (Figure 1b). As in Group I, L-arginine had no effect on the response to ACh, but prevented

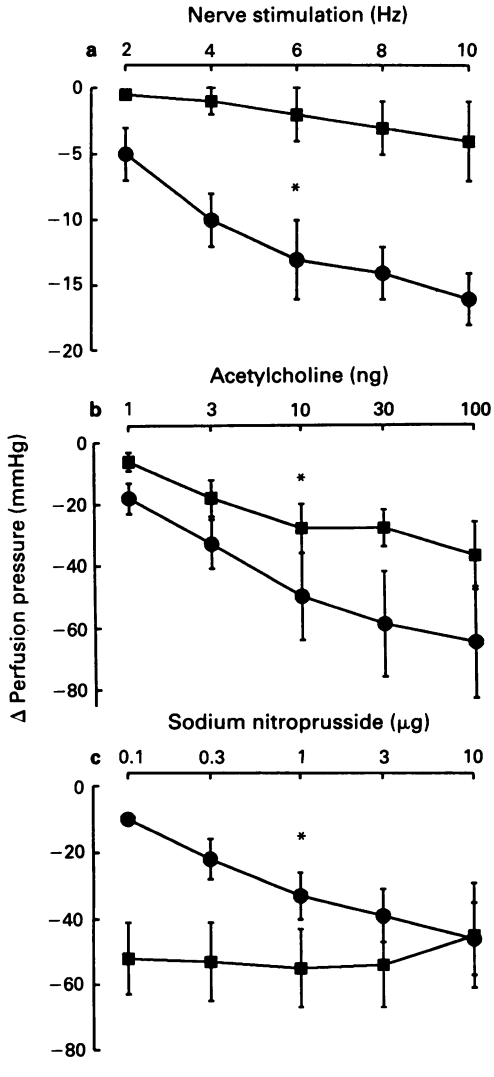

Figure 1 Control (●) frequency- and dose-dependent decreases in perfusion pressure indicating vasodilatation in the rat isolated hindquarters in response to (a) peri-aortic nerve stimulation (2–10 Hz) after noradrenergic neurone blockade with guanethidine ($n = 6$), (b) acetylcholine (1–100 ng, $n = 6$) and (c) sodium nitroprusside (0.1–10 μg, $n = 5$). Responses obtained in the presence of NO synthase inhibition by N^G-nitro-L-arginine (L-NOARG, 100 μM) are shown for each group by (■). L-NOARG significantly inhibited responses to both nerve stimulation and acetylcholine but enhanced dilatation caused by sodium nitroprusside. *Different from control, $P < 0.05$, analysis of variance. The hindquarters vasculature was pre-constricted by inclusion of phenylephrine in the perfusate. The values shown are the mean with s.e.mean.

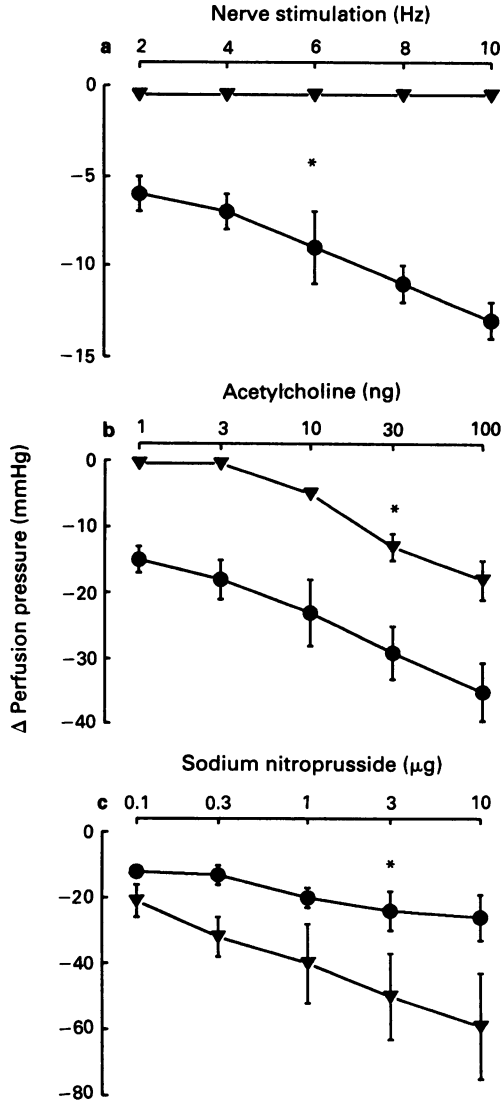

Figure 2 Control (●) frequency- and dose-dependent decreases in perfusion pressure indicating vasodilatation in the rat isolated hindquarters in response to (a) peri-aortic nerve stimulation (2–10 Hz) after noradrenergic neurone blockade with guanethidine ($n = 6$), (b) acetylcholine (1–100 ng, $n = 5$) and (c) sodium nitroprusside (0.1–10 μg, $n = 5$). Responses obtained after removal of endothelial cells with 3-3 cholamidopropyl dimethylammonio 1-propanesulphonate (CHAPS, 30 mg) are shown for each group by (▲). CHAPS significantly inhibited responses to both nerve stimulation and acetylcholine but enhanced dilatation caused by sodium nitroprusside. *Different from control, $P < 0.05$, analysis of variance. The hindquarters vasculature was pre-constricted by inclusion of phenylephrine in the perfusate. The values shown are the mean with s.e.mean.

the inhibitory effect of L-NOARG on the ACh-induced dilatation (L-arginine: 97 ± 9% of control; L-arginine plus L-NOARG: 122 ± 24% of control). In addition, vasodilator responses to ACh were significantly reduced after the administration of CHAPS (Figure 2b).

Group III: Effects of L-NOARG, L-arginine and CHAPS on vasodilator responses to SNP

SNP (1–10 μg) caused dose-dependent decreases in hindquarters perfusion pressure (Figures 1c and 2c) which were unaffected by either atropine (133 ± 16% of control) or the saline vehicle (114 ± 9% of control). These responses were enhanced by treatment with L-NOARG (Figure 1c). L-Arginine alone had no effect on dilator responses to SNP; however, the potentiation of SNP responses by L-NOARG was prevented in the presence of L-arginine (L-arginine: 83 ± 8% of control; L-arginine plus L-NOARG: 118 ± 7% of control). Dilator responses to SNP were also enhanced by treatment with CHAPS (Figure 2c).

Baseline perfusion pressure

In each experiment, the concentration of phenylephrine in the perfusate was adjusted so that there was no significant difference in the baseline perfusion pressure before and after each treatment (data not shown).

Discussion

Extensive studies have established that NO released from vascular endothelial cells mediates vasodilator responses to exogenous ACh. However, no previous study has provided direct evidence supporting a role for endothelium-derived NO in cholinergic neurogenic vasodilatation. In this study, vasodilatation in response to stimulation of cholinergic nerves was found to be mediated by NO in the rat hindquarters. Moreover, for the first time we have presented additional evidence in the same preparation that the source of NO is the endothelium.

In the rat hindquarters, vasodilator responses to peri-aortic nerve stimulation and exogenous ACh were inhibited by atropine, and also L-NOARG, an arginine analogue reported to have no interaction with muscarinic receptors (Buxton *et al.*, 1993), indicating that cholinergic neurogenic vasodilatation is mediated by NO. In addition, the inhibitory effect of L-NOARG on dilator responses to both nerve stimulation and ACh were prevented by treatment with the NO precursor, L-arginine, confirming the involvement of NO synthesis in this process.

Consistent with our findings that cholinergic neurogenic vasodilatation involves NO synthesis, Andriantsitohaina & Surprenant (1992) reported that activation of cholinergic nerves induced dilatation which was mediated by NO in the guinea-pig submucosal vasculature *in vitro*. In that study, vasodilator responses to ganglionic stimulation and exogenous muscarine were inhibited by the muscarinic receptor antagonist, 4-diphenylacetoxy-*N*-methyl-piperidine methiodide, and by the NO synthase inhibitor L-NMMA. As we observed with L-NOARG, the inhibitory effect of L-NMMA was prevented by L-arginine. The presents results are also consistent with *in vivo* findings in the dog hindlimb (Loke *et al.*, 1994), dog coronary (Broten *et al.*, 1992) and cat pulmonary (McMahon *et al.*, 1992) beds suggesting that arginine analogues inhibit cholinergic neurogenic vasodilatation. In the dog hindlimb, we induced neurogenic vasodilatation via electrical stimulation of specific sites in the hypothalamus and observed that, like dilatation by exogenous ACh, those responses were attenuated by either muscarinic receptor antagonists (atropine and tropicamide) or L-NOARG. Furthermore, the inhibitory effect of L-NOARG was reversed by administration of L-arginine. Previous findings from experiments in the dog coronary (Broten *et al.*, 1992) and cat pulmonary (McMahon *et al.*, 1992) beds indicated that cholinergic vasodilatation evoked by vagal stimulation and exogenous ACh were reduced after administration of L-NAME. However, L-NAME has since been reported to have muscarinic receptor antagonist activity (Buxton *et al.*, 1993). As L-arginine did not prevent or reverse the effects of L-NAME in those studies (Broten *et al.*, 1992; McMahon *et al.*, 1992), the inhibition by L-NAME of cholinergic responses may have been at least partly due to the blockade of muscarinic receptors.

Having established that NO mediates cholinergic neurogenic vasodilatation in the rat hindquarters, we investigated the role of the endothelium in this mechanism. In this model, we removed endothelial cells from the rat hindquarters vasculature using the biological detergent, CHAPS. Following endothelial removal, vasodilator responses to both nerve stimulation and exogenous ACh were abolished or substantially reduced. Importantly, the vasodilator responses to SNP were not inhibited by CHAPS indicating that vascular smooth muscle function remained intact after endothelial removal. Thus the endothelial cells are the source of NO that mediates cholinergic neurogenic vasodilatation.

L-NOARG and CHAPS appeared to have similar effects on responses to nerve stimulation and exogenous ACh. If stimuli that produced a similar level of dilatation are compared (e.g. 10 Hz nerve stimulation and 1 ng ACh) L-NOARG and CHAPS caused a similar level of attenuation of the dilator responses. Higher doses of ACh (10–100 ng) did cause some dilatation that was resistant to treatment with L-NOARG or CHAPS. Further investigation is required to determine whether this is a result of the level of inhibition produced by the single doses of L-NOARG and CHAPS that were used or whether ACh at higher doses is able to cause dilatation independently of NO and the endothelium.

The dilator response to SNP was enhanced in the presence of L-NOARG or CHAPS. This observation is consistent with previous reports whereby nitrovasodilator responses were potentiated in the presence of L-arginine analogues, or in the absence of functional endothelium (Shirasaki & Su, 1985; Mugge *et al.*, 1991). Since baseline perfusion pressure was not significantly altered after treatment with L-NOARG or CHAPS, the enhanced dilator response to SNP is likely to be due to the reported increased sensitivity of guanylate cyclase to exogenous NO when basal NO release is impaired (Moncada *et al.*, 1991b).

The present findings are in contrast to those from some earlier *in vitro* studies indicating that cholinergic neurogenic relaxation is not endothelium-dependent in the cat posterior auricular and rabbit lingual arteries (Brayden & Bevan, 1985; Brayden & Large, 1986). Those findings suggested vasorelaxation by neuronally released ACh was mediated through muscarinic receptors located on vascular smooth muscle cells. However, in both of those arteries, dilator responses to exogenous ACh were also found to be endothelium-independent. In contrast, we confirmed in this study that ACh acts by the release of NO from the endothelium in the rat hindquarters. More recently cholinergic relaxation of isolated arteries from the rabbit middle cerebral bed was reported to be attenuated after removal of endothelium by rubbing or by treatment with the α-toxin of *Staphylococcus aureus*, suggesting that cholinergic neurogenic relaxation of those vessels is endothelium-dependent (Van Riper & Bevan, 1992). Consistent with that finding, an *in vivo* study in the rat gastric mucosa has demonstrated that stimulation-induced increases in gastric mucosal blood flow, indicated by an increase in gastric mucosal haemoglobin and oxygen saturation of haemoglobin, were reduced by atropine or by removal of the endothelium with collagenase (Kitagawa *et al.*, 1987). Although no evidence was provided in either model that NO is involved, those studies support the role of endothelium in cholinergic neurogenic vasodilatation. Thus it appears that in order to cause vasodilatation, neuronally released ACh must diffuse from the nerves through layers of smooth muscle to the endothelial cells to release NO.

In contrast to suggestions that ACh released from nerves in some vascular beds cannot diffuse to the vascular endothelium (Brayden & Bevan, 1985; Brayden & Large, 1986), Angus *et al.* (1983) reported that ACh applied topically to the adventitial surface of the dog femoral artery *in vivo* can traverse the artery wall and cause endothelium-dependent dilatation. In addition, histological examination of coronary arteries has shown that cholinergic nerves terminate in the adventitio-medial border in large arteries (Denn & Stone, 1976) and penetrate the media in resistance vessels (Pillay & Reid, 1982). Moreover, since there are fewer smooth muscle layers in resistance vessels in comparison to large vessels (Rhodin, 1967), ACh released from cholinergic nerves in the rat hindquarters vasculature may more readily diffuse to the vascular endothelium of resistance vessels than in large arteries.

In conclusion, this is the first study to demonstrate clearly that vasodilatation in response to cholinergic nerve stimulation is mediated by endothelium-derived NO. At least in this preparation neurogenic cholinergic dilatation involves diffusion of neuronally-released ACh from cholinergic nerve terminals in the arterial wall to the endothelium, wherein the vasodilator NO is released.

This study was supported by the National Health and Medical Research Council of Australia. K.E.L. received an Overseas Postgraduate Research Scholarship from the Australian Government.

References

ANGUS, J.A., CAMPBELL, G.R., COCKS, T.M. & MANDERSON, J.A. (1983). Vasodilatation by acetylcholine is endothelium-dependent: a study by sonomicrometry in canine femoral artery *in vivo*. *J. Physiol.*, **344**, 209–222.

ANDRIANTSITOHAINA, R. & SUPRENANT, A. (1992). Acetylcholine released from guinea-pig submucosal neurones dilates arterioles by releasing nitric oxide from endothelium. *J. Physiol.*, **453**, 493–502.

BRAYDEN, J.E. & BEVAN, J.A. (1985). Neurogenic muscarinic vasodilatation in the cat: an example of endothelial cell-independent cholinergic relaxation. *Circ. Res.*, **56**, 205–211.

BRAYDEN, J.E. & LARGE, W.A. (1986). Electrophysiological analysis of neurogenic vasodilatation in the isolated lingual artery of the rabbit. *Br. J. Pharmacol.*, **89**, 163–171.

BHARDWAJ, R. & MOORE, P.K. (1988). Endothelium-derived relaxing factor and the effects of acetylcholine and histamine on resistance blood vessels. *Br. J. Pharmacol.*, **95**, 835–843.

BROTEN, T.P., MIYASHIRO, J.K., MONCADA, S. & FEIGL, E.O. (1992). Role of endothelium-derived relaxing factor in parasympathetic coronary vasodilatation. *Am. J. Physiol.*, **262**, H1579–H1584.

BUXTON, I.L.O., CHEEK, D.J,. ECKMAN, D., WESTFALL, D.P., SANDERS, K.M. & KEEF, K.D. (1993). N^G-nitro-L-arginine methyl ester and other alkyl esters of arginine are muscarinic receptor antagonists. *Circ. Res.*, **72**, 387–395.

DENN, M.J. & STONE, H.L. (1976). Autonomic innervation of dog coronary arteries. *J. Appl. Physiol.*, **41**, 30–35.

FURCHGOTT, R.F. & ZAWADZKI, J.V. (1980). The obligatory role of endothelial cells in the relaxation of arterial smooth muscle by acetylcholine. *Nature*, **288**, 373–376.

KITAGAWA, H., TAKEDA, F. & KOHEI, H. (1987). Endothelium-dependent increases in rat gastric mucosal hemodynamics induced by acetylcholine and vagal stimulation. *Eur. J. Pharmacol.*, **133**, 57–63.

LOKE, K.E., SOBEY, C.G., DUSTING, G.J. & WOODMAN, O.L. (1994). Cholinergic neurogenic vasodilatation is mediated by nitric oxide in the dog hindlimb. *Cardiovasc. Res.* (in press).

MONCADA, S., PALMER, R.M.J. & HIGGS, E.A. (1991a). Nitric oxide: physiology, pathophysiology, and pharmacology. *Pharmacol. Rev.*, **43**, 109–142.

MONCADA, S., REES, D.D., SCHULZ, R. & PALMER, R.M.J. (1991b). Development and mechanism of a specific supersensitivity to nitrovasodilators after inhibition of vascular nitric oxide synthesis *in vivo*. *Proc. Natl. Acad. Sci. U.S.A.*, **88**, 2166–2170.

MCMAHON, T.J., HOOD, J.S. & KADOWITZ, P.J. (1992). Pulmonary vasodilator response to vagal stimulation is blocked by N^{ω}-nitro-L-arginine methyl ester in the cat. *Circ. Res.*, **70**, 364–369.

MUGGE, A., ANTONIO, J., LOPEZ, G., PIEGORS, D.J., BREESE, K.R. & HEISTAD, D.D. (1991). Acetylcholine-induced vasodilatation in rabbit hindlimb *in vivo* is not inhibited by analogues of L-arginine. *Am. J. Physiol.*, **260**, H242–247.

PILLAY, C.V. & REID, J.V.O. (1982). Histochemical localization of acetylcholinesterase in the wall of cardiac blood vessels in the baboon, dog and vervet monkey. *Basic Res. Cardiol.*, **77**, 213–219.

RHODIN, J.A.G. (1967). The ultrastructure of mammalian arterioles and precapillary sphincters. *J. Ultrastruct. Res.*, **18**, 181–223.

SHIRASAKI, Y. & SU, C. (1985). Endothelium removal augments vasodilatation by sodium nitroprusside and sodium nitrite. *Eur. J. Pharmacol.*, **114**, 93–96.

VAN RIPER, D.A. & BEVAN, J.A. (1992). Electrical field stimulation-mediated relaxation of rabbit middle cerebral artery: evidence of a cholinergic endothelium-dependent component. *Circ. Res.*, **70**, 1104–1112.

(Received September 20, 1993
Revised February 4, 1994
Accepted February 10, 1994)

Br. J. Pharmacol. (1994), **112**, 635–639

Effects of isocarbacyclin, a stable prostacyclin analogue, on monkey isolated cerebral and peripheral arteries

[1]Yasuaki Kawai & Toshio Ohhashi

The First Department of Physiology, Shinshu University School of Medicine, 3-1-1 Asahi Matsumoto, 390 Japan

1 The effects of isocarbacyclin (TEI 7165), a stable prostacyclin analogue, were examined in monkey isolated cerebral and peripheral arteries.

2 Addition of TEI 7165 (0.1 nM–10 μM) produced a dose-dependent relaxation in cerebral arteries pre-contracted with 1 μM 5-hydroxytryptamine (5-HT). High concentrations (more than 1 μM) of TEI 7165 elicited a transient contraction followed by a sustained relaxation.

3 TEI 7165 also elicited a dose-dependent relaxation in the peripheral (except popliteal) arteries. The maximum relaxation induced by 10 μM TEI 7165 was greater ($P<0.05$) in the mesenteric artery than in the cerebral artery. The negative logarithm of the EC_{50} value for the mesenteric, 7.6 ± 0.3, was greater ($P<0.05$) than that for the cerebral artery, 6.4 ± 0.3. The decreasing order of potency for the TEI 7165-induced relaxation was as follows: mesenteric > renal > cerebral > coronary > popliteal.

4 Removal of the endothelium did not significantly affect TEI 7165-induced relaxations.

5 The transient contraction produced by high concentrations of TEI 7165 was not observed in cerebral arteries precontracted with 1 nM U46619, a stable analogue of thromboxane A_2 (TXA_2). Furthermore, the TEI 7165-induced contraction was markedly suppressed ($P<0.05$) by treatment with 10 nM S1452, a TXA_2 blocking agent.

6 These results suggest that TEI 7165 causes an endothelium-independent relaxation in monkey cerebral and peripheral arteries, and that there is a marked regional difference in the TEI 7165-induced relaxations. A high concentration of TEI 7165 also produces a transient contraction which is probably through activation of TXA_2 (TP-) receptors.

Keywords: Cerebral artery; isocarbacyclin; prostacyclin; vascular smooth muscle; thromboxane A_2

Introduction

Prostacyclin (PGI_2) causes a relaxation of vascular smooth muscles of cerebral arteries (Chapleau & White, 1979) and increases cerebral blood flow (Pickard *et al.*, 1980). PGI_2 also inhibits aggregation of platelets (Moncada & Vane, 1978). These effects of PGI_2 suggest a possible therapeutic use in ischaemic cerebral disorders (Hoshi & Mizushima, 1990). Isocarbacyclin, (+)-9(0)-methano-$\Delta^{6(9\alpha)}$-PGI_1, has recently been synthesized as a stable analogue of PGI_2 (Shibasaki *et al.*, 1983). This compound shows antithrombotic (Mizushima *et al.*, 1987) and angiogenic activities (Ohtsu *et al.*, 1988). Kawai & Ohhashi (1991) reported that isocarbacyclin produced a relaxation of vascular smooth muscles in monkey cerebral arteries. Since PGI_2 also dilates peripheral arteries (Toda, 1980), however, it is important to compare the relative potency of isocarbacyclin between cerebral and other arteries.

It is known that high concentrations of PGI_2 produce contractile responses in cat (Uski *et al.*, 1983), dog (Chapleau & White, 1979), and human (Uski *et al.*, 1983) cerebral arteries. Other prostanoids also cause marked contraction of isolated cerebral arteries, TXA_2 showing the highest potency (Uski & Andersson, 1984). To the best of our knowledge, however, a possible role of TP-receptors in PGI_2-induced contraction of vascular smooth muscles has not been examined in detail.

The purpose of the present study was (1) to compare the potency for isocarbacyclin-induced relaxation between monkey isolated cerebral and extracerebral arteries and (2) to investigate the mechanism of contraction produced by high concentrations of isocarbacyclin with special reference to the TP-receptor.

[1] Author for correspondence at present address: Department of Physiology, Faculty of Medicine, Tottori University, 86 Nishi-machi Yonago, 683 Japan.

Methods

Eighteen adult macaque monkeys of either sex, weighing 6.5 ± 0.6 kg, were anaesthetized with ketamine hydrochloride (50 mg kg^{-1}, i.m.) and killed by bleeding from the common carotid artery. Cerebral (basilar and intracranial vertebral), coronary, mesenteric, renal, and popliteal arteries (outer diameter, 1.5–2.0 mm for popliteal arteries and 0.8–1.3 mm for other arteries) were rapidly dissected. The arterial segments were cut into helical strips, approximately 15 mm long and 1.5 mm wide. Each strip was fixed vertically between hooks in a 10 ml organ bath which was perfused with Krebs solution at a constant rate of 4 ml min^{-1}. The hook anchoring the lower end of the strip was fixed to the bottom of the bath, and the upper end was connected to the lever of a force-displacement transducer (Shinko Tsushin UL-10). The composition of the Krebs solution (mM) was as follows: NaCl 120.0, KCl 5.9, $NaHCO_3$ 25.0, NaH_2PO_4 1.2, $CaCl_2$ 2.5, $MgCl_2$ 1.2 and glucose 5.5. The solution was maintained at 36.5 ± 0.5°C and aerated with a gas mixture of 95% O_2 and 5% CO_2 to give a pH of 7.3–7.4. The resting tension was adjusted to the optimal level for obtaining maximum contractile response to 80 mM KCl solution in each arterial preparation. Changes in the isometric tension were recorded on a direct writing oscillograph (Sanei Sokki 8K 20).

Following a 90 min equilibration, the preparations were contracted by perfusion with Krebs solution containing 1 μM 5-hydroxytryptamine (5-HT). In the previous study, TEI 7165-induced relaxation was observed in the preparations without precontraction because isolated monkey cerebral arteries developed a high myogenic tone in an organ bath perfused with Krebs solution (Kawai & Ohhashi, 1991). Since isolated peripheral arteries failed to show sufficient myogenic tone in Krebs solution in the current study, these arteries were precontracted when the relaxant responses to TEI 7165 were examined. Therefore, cerebral arteries were also contracted before addition of TEI 7165 in order to compare their responses with those of peripheral arteries. The

precontraction level produced by 1 μM 5-HT solution seems to be most suitable for elucidating the dose-response relationship for relaxant agents (Kawai & Ohhashi, 1989). The basal tension of the preparations did not change significantly throughout the experiment. After the precontraction reached a plateau, the response to isocarbacyclin (TEI 7165) was evaluated by cumulative addition of the agent to the bathing medium with a microsyringe. The concentration of TEI 7165 was increased by a factor of 10 as soon as a steady response to the previous administration had been achieved. At the end of each experiment, 10 μM sodium nitroprusside (SNP) was added to obtain maximum relaxation in each preparation. The extent of TEI 7165-induced relaxation is expressed as a percentage of the SNP-induced relaxation.

In order to examine the possibility that TEI 7165 acts by releasing nitric oxide from endothelium, the responses to TEI 7165 were also examined in preparations from which endothelial cells had been removed by mechanically rubbing the intimal surface with a filter paper following Furchgott's technique (Furchgott & Zawadzki, 1980). The absence or presence of endothelium was confirmed histologically by the silver staining procedure (Poole *et al.*, 1958).

The amount of contraction induced by isocarbacyclin was expressed as a percentage of the 1 μM 5-HT-induced contraction. In some experiments, the effect of isocarbacyclin was examined in cerebral and mesenteric arteries which were contracted by 1 nM–10 nM U46619, a stable analogue of TXA_2. When the effect of S1452 (the calcium salt of (+)-S-145), an antagonist of the TXA_2 receptor (Arita *et al.*, 1992), on isocarbacyclin-induced contraction was tested, the preparations were treated for 30 min with S1452 and contracted with 1 μM 5-HT before the responses to isocarbacyclin were determined.

The following drugs were used: 5-hydroxytryptamine creatinine sulphate (5-HT, Sigma, St. Louis, MO, U.S.A.), isocarbacyclin (TEI 7165, Teijin, Tokyo, Japan), sodium nitroprusside (SNP, Merk, Darmstadt, Germany), S1452 (Calcium 5(Z)-1**R**, 2**S**, 3**S**, 4**S**-7-[3-phenylsulphonylaminobicyclo [2. 2. 1] hept-2-yl]-5-heptenoate hydrate) (Shionogi, Osaka, Japan), and U46619 (9,11-dideoxy-11α, 9α-epoxymethano-prostaglandin $F_{2\alpha}$) (Sigma, St.Louis, MO, U.S.A.). TEI 7165, S1452 and U46619 were dissolved in ethanol if not otherwise stated and diluted with distilled water just before use. 5-HT and SNP were diluted in fresh stock Krebs solution. The doses of drugs are expressed as a final organ bath concentration.

Experimental values shown in the text and tables are means ± s.e. The n values represent the number of animals used. The concentration of TEI 7165 causing a 50% relaxation of 10 μM TEI 7165-induced relaxation is expressed as the EC_{50} value. For multiple comparisons, one-way analysis of variance was used. The differences between two groups were analysed by Student's paired or unpaired t test. The differences in means were considered significant at $P<0.05$.

Results

Effects of TEI 7165 on monkey isolated cerebral arteries

Perfusion with 1 μM 5-HT caused a contraction of cerebral arteries (Figure 1a and Table 1). TEI 7165 (0.1 nM–10 μM) produced a dose-dependent relaxation in a monkey vertebral artery (Figure 1a). High concentrations of TEI 7165 (1 μM and 10 μM) elicited a transient contraction followed by a sustained relaxation. This transient contraction was also induced by TEI 7165 when it was dissolved in dimethyl sulphoxide (DMSO, Sigma, St. Louis, MO, U.S.A.) but was not produced by solvent only e.g. either ethanol or DMSO. No significant difference was observed between the responses of basilar and vertebral arteries. The threshold concentration for relaxant response to TEI 7165 was 1 nM (Figure 2).

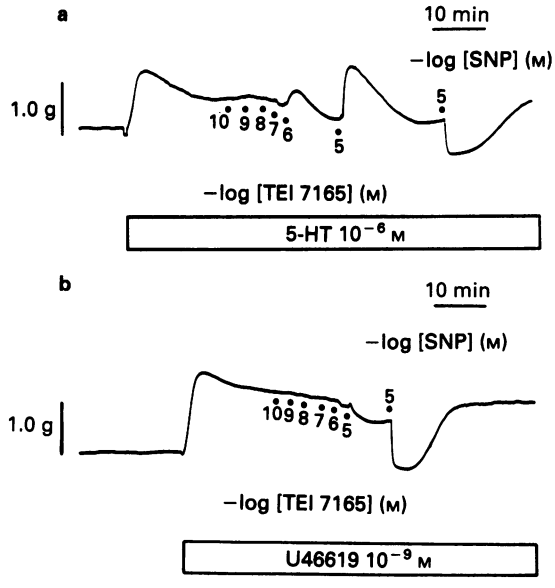

Figure 1 Typical responses to isocarbacyclin (TEI 7165) in concentrations ranging from 0.1 nM to 10 μM and sodium nitroprusside (SNP) 10 μM in a monkey vertebral artery which was contracted by (a) 1 μM 5-hydroxytryptamine 5-HT and (b) 1 nM U46619.

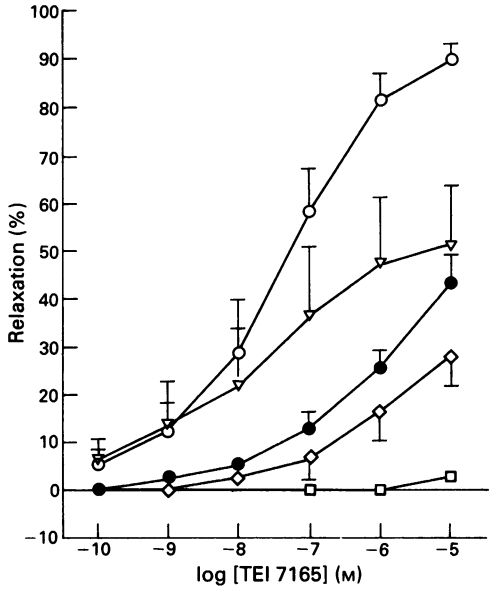

Figure 2 Cumulative dose-response curves for isocarbacylin (TEI 7165) in monkey mesenteric (○, $n=8$), renal (▽, $n=5$), cerebral (●, $n=5$), coronary (◇, $n=5$), and popliteal arteries (□, $n=6$) which had been contracted by 1 μM 5-hydroxytryptamine.

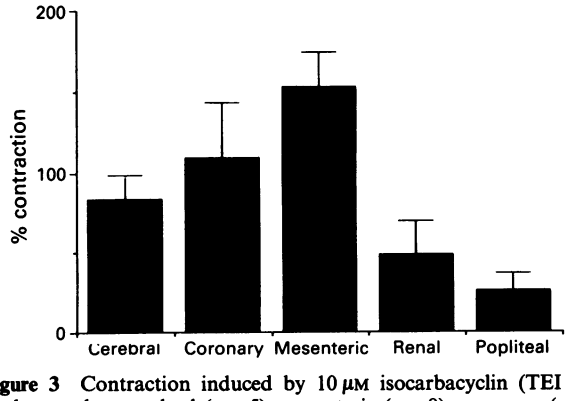

Figure 3 Contraction induced by 10 μM isocarbacyclin (TEI 7165) in the monkey cerebral ($n=5$), mesenteric ($n=8$), coronary ($n=5$), renal ($n=5$), and popliteal arteries ($n=6$) treated with 1 μM 5-hydroxytryptamine.

Effects of TEI 7165 on monkey isolated peripheral arteries

The degree of contraction produced by 5-HT in coronary and popliteal arteries was significantly greater than that in cerebral arteries (Table 1). In all peripheral arteries, addition of 10 μM SNP produced a remarkable relaxation which was almost 100% (90–112%) of the 5-HT-induced precontraction.

There was a marked regional difference in the TEI 7165-induced relaxation, expressed as percentage of the SNP-induced relaxation, among various monkey arteries which had been contracted by 1 μM 5-HT (Figure 2). TEI 7165 elicited the greatest relaxation in mesenteric arteries. The threshold concentration was less than 0.1 nM, and maximum relaxation induced by 10 μM TEI 7165 was 89.6 ± 3.5% in the mesenteric arteries. On the other hand, popliteal arteries were much less sensitive to TEI 7165, the threshold concentration and maximum relaxation being 1 μM and 2.9 ± 1.4% (statistically not significant comparing with time-control), respectively. Table 2 demonstrates the EC_{50} values and E_{max} values (maximum relaxations induced by 10 μM TEI 7165). The decreasing order of potency for the TEI 7165-induced relaxation in monkey isolated arteries contracted by 5-HT was as follows: mesenteric > renal > cerebral > coronary > popliteal. A high concentration (10 μM) of TEI 7165 produced transient contraction not only in cerebral but also in coronary and mesenteric arteries (Figure 3). In renal and popliteal arteries, the contraction was statistically not significant because of variability between preparations.

Effects of endothelium removal on TEI 7165-induced relaxation

The responses to TEI 7165 were also examined in cerebral and mesenteric arteries from which endothelial cells had been removed. The amount of contraction produced by 1 μM 5-HT was not significantly different from that obtained in the endothelium-intact preparations. Addition of 10 μM SNP relaxed the endothelium-denuded preparations almost to the same extent as in endothelium-intact preparations (Table 1). There was no significant difference in EC_{50} and E_{max} values between preparations with and without endothelium in both cerebral and mesenteric arteries (Table 2).

Contractile responses to high concentration of TEI 7165

The transient contraction of cerebral artery preparations induced by high concentrations of TEI 7165 was almost abolished when the preparation was contracted with 1 nM U46619 (Figure 1b). Addition of U46619 (1 nM–10 nM) increased the tension by 730 ± 110 mg in five cerebral arteries. The amount of contraction elicited by 10 μM TEI 7165 was only 8.1 ± 4.8% of the U46619-induced contraction ($n = 5$).

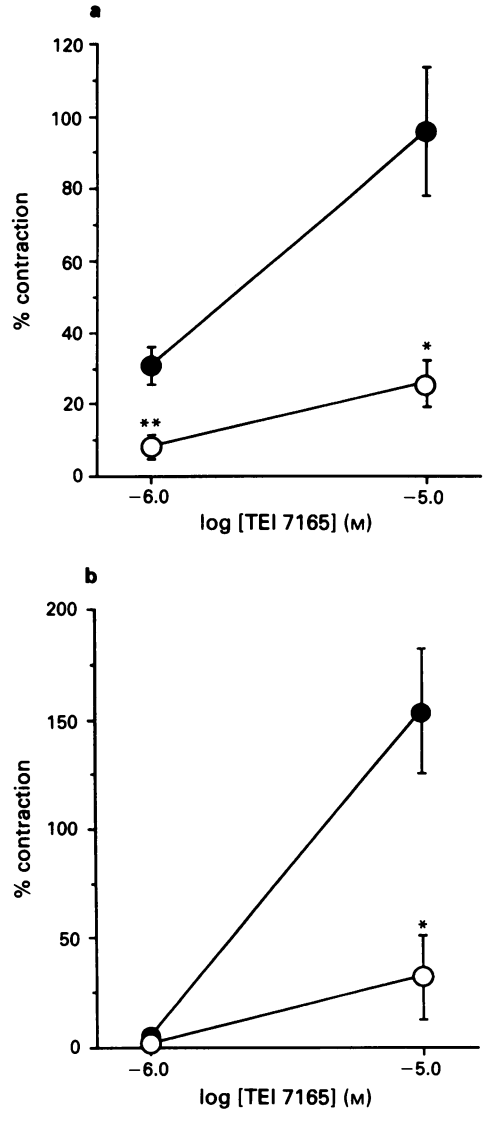

Figure 4 Effects of S1452 on isocarbacyclin (TEI 7165)-induced contraction of monkey (a) cerebral ($n = 6$), and (b) mesenteric arteries ($n = 6$): (●) and (○) indicate the results from control and 1 μM S1452-treated preparations, respectively. $^{**}P < 0.05$; $^{*}P < 0.01$.

Treatment with 10 nM S1452 did not significantly affect contraction produced by 1 μM 5-HT; 710 ± 70 mg in control vs 580 ± 90 mg after treatment with S1452 ($n = 6$). On the other hand, S1452 attenuated the TEI 7165-induced contraction of cerebral (Figure 4a) and mesenteric arteries (Figure 4b).

Table 1 5-Hydroxytryptamine (5-HT)-induced precontraction and sodium nitroprusside (SNP)-induced relaxation of monkey isolated arteries

Artery	n	*5-HT* (mg)	*SNP* (mg)	*% of precontraction*[a] (%)
Cerebral	5	520 ± 90	1240 ± 120	258 ± 32
Cerebral E(−)[b]	5	420 ± 60	1040 ± 160	251 ± 28
Coronary	5	1010 ± 130*	1150 ± 130	112 ± 7*
Mesenteric	8	880 ± 160	930 ± 160	107 ± 3*
Mesenteric E(−)[b]	6	1230 ± 170*	1400 ± 150	119 ± 10*
Renal	5	580 ± 100	620 ± 90*	110 ± 4*
Popliteal	6	2740 ± 480*	2550 ± 480*	90 ± 5*

*Significantly different from results obtained in endothelium-intact cerebral artery, $P < 0.05$.
[a]Percentage of SNP-induced relaxation relative to 5-HT-induced contraction.
[b]E(−): preparations without endothelium.

Table 2 Relaxant response of monkey isolated arteries to isocarbacyclin (TEI 7165)

Artery	n	$-logEC_{50}$	E_{max} (%)
Mesenteric	8	7.6 ± 0.3*	89.6 ± 3.5*
Mesenteric E(−)[b]	6	7.3 ± 0.1*	94.9 ± 1.4*
Renal	5	7.6 ± 0.6	51.4 ± 12.6
Cerebral	5	6.4 ± 0.3	43.4 ± 6.0
Cerebral E(−)[b]	5	6.3 ± 0.2	39.3 ± 5.4
Coronary	5	6.1 ± 0.2	28.5 ± 6.2
Popliteal	6	–[a]	2.9 ± 1.4*

EC_{50}: concentration of TEI 7165 causing 50% of each maximum response.
E_{max}: maximum relaxation expressed as percentage of SNP-induced relaxation.
[a]Not evaluated.
[b]E(−): preparation without endothelium.
*Significantly different from results obtained with endothelium-intact cerebral artery, $P<0.05$.

Discussion

PGI_2 causes a marked relaxation in human cerebral arteries (Brandt *et al.*, 1981; Uski *et al.*, 1983), and in cerebral arteries of dogs (Chapleau & White, 1979; Toda, 1980), cats (Uski *et al.*, 1983), and baboons (Hayashi *et al.*, 1985). Isocarbacyclin (TEI 7165) is a stable analogue of PGI_2 (Shibasaki *et al.*, 1983; Mizuno-Yagyu *et al.*, 1987; Mizushima *et al.*, 1987). However, there is little information about its vasorelaxant activity except in our recent report which examined the effect of TEI 7165 on monkey isolated cerebral arteries (Kawai & Ohhashi, 1991). The present results demonstrate that TEI 7165 produces a dose-dependent relaxation in monkey isolated cerebral and peripheral (except popliteal) arteries. High concentrations of TEI 7165 (1 μM and 10 μM) caused a transient contraction followed by a sustained relaxation (Figure 1a). Although the dose-response curves for TEI 7165 did not reach a plateau at concentrations up to 10 μM, higher concentrations of TEI 7165 were not examined in the present study because preliminary experiments indicated that such concentrations of TEI 7165 elicited sustained contractions of monkey cerebral arteries.

There was a marked regional difference in the TEI 7165-induced relaxation. In preparations contracted by 5-HT, TEI 7165 produced the greatest relaxation in mesenteric arteries followed by renal, cerebral, coronary, and popliteal arteries in decreasing order (Figure 2). The maximum relaxation induced by 10 μM TEI 7165 was significantly greater in the mesenteric artery and significantly smaller in the popliteal artery compared with responses obtained in the cerebral artery (Table 2). Although the dose-response curves for TEI 7165 did not reach a plateau for the reasons mentioned above, we calculated apparent EC_{50} values on the assumption that TEI 7165 exerts its maximum relaxant effect at a concentration of 10 μM. The negative logarithm of the EC_{50} for the mesenteric artery, 7.6 ± 0.3, was significantly greater than that for the cerebral artery, 6.4 ± 0.3 (Table 1). The EC_{50} value for the popliteal artery was not evaluated because TEI 7165 produced no relaxation in some of the preparations. Toda (1980) reported that PGI_2 Na or PGI_2 methylester produced a dose-dependent relaxation in canine isolated arteries contracted by $PGF_{2\alpha}$ or high K^+ with a decreasing order of effect on mesenteric > renal > coronary > cerebral. Our result is consistent with those of Toda (1980) except that the cerebral artery is more sensitive to PGI_2 than is the coronary artery. Our results also show that monkey popliteal artery is much less sensitive to isocarbacyclin than the cerebral or other peripheral arteries.

There are several possibilities which account for the regional difference in TEI 7165-induced relaxation: (1) the contractile effect of TEI 7165 may decrease its relaxant effects in some arteries, (2) TEI 7165 may release nitric oxide from the endothelium to cause smooth muscle relaxation and (3) receptor and/or intracellular signal transduction system for TEI 7165 are different. The first and second possibilities are, however, unlikely for the following reasons: (1) contraction induced by TEI 7165 was lowest in popliteal arteries in which the relaxant response was not observed, whereas the contraction was greatest in the mesenteric arteries where the relaxation response was also greatest. (2) TEI 7165 caused almost the same relaxation response in endothelium-denuded cerebral and mesenteric arteries as in the endothelium-intact preparations (Table 2). Therefore, a difference in the ability of the endothelium to produce nitric oxide cannot explain the regional difference in TEI 7165-induced relaxation. Thus, differences in receptor and/or the intracellular signal transduction system seem to be the most likely reason for the regional difference. PGI_2 relaxes vascular smooth muscle through stimulation of the PGI_2 receptor, increasing the intracellular concentration of adenosine 3':5'-cyclic monophosphate (cyclic AMP) (Oliva *et al.*, 1984) which, in turn, activates protein kinase A in smooth muscle cells. Further studies are needed to clarify the heterogeneity of receptor and signal transduction mechanisms for TEI 7165-induced relaxation.

According to standard nomenclature (see TIPS, 1993) prostanoid receptors are classifed into five main classes; DP, EP (including EP_1, EP_2 and EP_3), FP, IP and TP. Activation of EP (except EP_2), FP and TP-receptors leads to the contraction of smooth muscle cells (Kennedy *et al.*, 1982). Several findings suggest that PGI_2 may act on EP and FP as well as IP-receptors. For example, Dong *et al.* (1986) showed that isocarbacyclin contracted the guinea-pig trachea through activation of EP_1-receptors. Uski *et al.* (1983) showed that PGI_2 relaxed isolated feline cerebral arteries contracted with $PGF_{2\alpha}$, but not when contracted with noradrenaline or 5-HT, and suggested that the relaxant effect was due to PGI_2 competing with $PGF_{2\alpha}$ for the same contraction-inducing prostanoid receptors (probably FP-receptors). On the other hand, a role of TP-receptors in PGI_2-induced contraction has not been examined in detail. In the present study, high concentrations of TEI 7165 (1 μM and 10 μM) elicited a transient contraction of cerebral, coronary, and mesenteric arteries (Figure 3). This is consistent with the observations that PGI_2 causes a contraction in cerebral arteries (Chapleau & White, 1979; Uski *et al.*, 1983), coronary artery (Dusting *et al.*, 1977) and various veins (Levy, 1978). In this study, the TEI 7165-induced contraction seems to be produced by stimulation of TP-receptors on vascular smooth muscle cells since a TXA_2 antagonist, S1452, attenuated the contraction observed (Figure 4). S1452 is a highly potent and selective antagonist for platelet TP-receptors with no ability to displace the specific binding of [^{3}H]-PGD_2 and [^{3}H]-$PGF_{2\alpha}$ (Hanasaki & Arita, 1988). However, since we used a relatively high concentration of S1452 to observe its maximum effect the involvement of EP- and/or FP-receptors in the mechanism of TEI 7165-induced blood vessel contraction cannot be excluded. That TEI 7165 failed to contract monkey cerebral arteries when precontracted with U46619 may support the above hypothesis i.e. that high concentrations of TEI 7165 contract monkey

arteries through activation of TP-receptors. Although the mechanism of this effect remains somewhat obscure the following two possibilities may be suggested: (1) U46619 may produce a partial desensitization of the preparation and/or (2) TEI 7165 may compete with U46619 at the same TP-receptors.

The possibility that high concentrations of TEI 7165 stimulate the synthesis and release of endogenous TXA_2 in the vascular wall also cannot be excluded. However, Hadhazy *et al.* (1984) showed that high concentrations of PGI_2 cause a contraction of rabbit isolated arteries in the presence of indomethacin. Thus, the contractile effect of TEI 7165 in monkey isolated arteries is likely to be due, at least in part, to its direct action on TP-receptors in vascular smooth muscle.

In conclusion, TEI 7165 produces an endothelium-independent relaxation in monkey isolated cerebral and peripheral (except popliteal) arteries. A marked regional difference in TEI 7165-induced relaxation of monkey isolated arteries was observed. High concentrations of TEI 7165 cause a transient contraction of these blood vessels probably due to stimulation of TP-receptors on vascular smooth muscle.

The authors are grateful to Teijin Co. and Shionogi Co. for their generous gift of isocarbacyclin and S1452, respectively. They also thank R. Ballard for the assistance with statistics and G. Murthy and K. Hutchinson for manuscript preparation.

References

ARITA, H., KUROSAWA, A., OGUMA, T., KITAMURA, T., EBIHARA, A. & NARISADA, M. (1992). S1452 – A novel TXA2 receptor antagonist. *Cardiovasc. Drug Rev.*, **10**, 280–295.

BRANDT, L., LJUNGGREN, B., ANDERSSON, K.E., HINDFELDT, B. & USKI, T. (1981). Effects of indomethacin and prostacyclin on isolated human pial arteries contracted by CSF from patients with aneurysmal SAH. *J. Neurosurg.*, **55**, 877–883.

CHAPLEAU, C.E. & WHITE, R.P. (1979). Effects of prostacyclin on the canine isolated basilar artery. *Prostaglandins*, **17**, 573–580.

DONG, Y.J., JONES, R.L. & WILSON, N.H. (1986). Prostaglandin E receptor subtypes in smooth muscle: agonist activities of stable prostacyclin analogues. *Br. J. Pharmacol.*, **87**, 97–107.

DUSTING, G.J., MONCADA, S. & VANE, J.R. (1977). Prostacyclin (PGI2) is a weak contractor of coronary arteries of the pig. *Eur. J. Pharmacol.*, **45**, 301–304.

FURCHGOTT, R.F. & ZAWADZKI, J.V. (1980). The obligatory role of endothelial cells in the relaxation of arterial smooth muscle by acetylcholine. *Nature*, **288**, 373–376.

HADHAZY, P., MALOMVOLGYI, B. & MAGYAR, K. (1984). Differential contractile responsiveness of isolated rabbit arteries from different vascular beds to cyclooxygenase inhibitors and PGI_2. *Eur. J. Pharmacol.*, **98**, 323–330.

HANASAKI, K. & ARITA, H. (1988). Characterization of a new compound, S-145, as a specific TXA2 receptor antagonist in platelets. *Thrombosis Res.*, **50**, 365–376.

HAYASHI, S., PARK, M.K. & KUEHL, T.J. (1985). Relaxant and contractile responses to prostaglandins in premature, newborn and adult baboon cerebral arteries. *J. Pharmacol. Exp. Ther.*, **233**, 628–635.

HOSHI, K. & MIZUSHIMA, Y. (1990). A preliminary double-blind cross-over trial of lipo-PGI_2, a prostacyclin derivative incorporated in lipid microspheres, in cerebral infarction. *Prostaglandins*, **40**, 155–164.

KAWAI, Y. & OHHASHI, T. (1989). Heterogeneity in responses of isolated monkey arteries and veins to atrial natriuretic peptide. *Can. J. Physiol. Pharmacol.*, **67**, 326–330.

KAWAI, Y. & OHHASHI, T. (1991). Prostaglandin F2α-induced endothelium-dependent relaxation in isolated monkey cerebral arteries. *Am. J. Physiol.*, **260**, H1538–H1543.

KENNEDY, I., COLEMAN, R.A., HUMPHREY, P.P.A., LEVY, G.P. & LUMLEY, P. (1982). Studies on the characterisation of prostanoid receptors: a proposed classification. *Prostaglandins*, **24**, 667–689.

LEVY, J.V. (1978). Contractile responses to prostacyclin (PGI2) of isolated human saphenous and rat venous tissue. *Prostaglandins*, **16**, 93–97.

MIZUNO-YAGYU, Y., HASHIDA, R., MINEO, C., IKEGAMI, S., OHKUMA, S. & TAKANO, T. (1987). Effects of PGI_2 on transcellular transport of fluorescein dextran through an arterial endothelial monolayer. *Biochem. Pharmacol.*, **36**, 3809–3813.

MIZUSHIMA, Y., IGARASHI, R., HOSHI, K., SIM, A.K., CLELAND, M.E., HAYASHI, H. & GOTO, J. (1987). Marked enhancement in antithrombotic activity of isocarbacyclin following its incorporation into lipid microspheres. *Prostaglandins*, **33**, 161–168.

MONCADA, S. & VANE, J.R. (1978). Unstable metabolites of arachidonic acid and their role in haemostasis and thrombosis. *Br. Med. Bull.*, **34**, 129–135.

OHTSU, A., FUJII, K. & KUROZUMI, S. (1988). Induction of angiogenic response by chemically stable prostacyclin analogs. *Prostaglandins, Leuko. Essent. Fatty Acids*, **33**, 35–39.

OLIVA, D., NOE, A., NICOSIA, S., BERNINI, F., FUMAGALLI, R., WHITTLE, B.J.R., MONCADA, S. & VANE, J.R. (1984). Prostacyclin-sensitive adenylate cyclase in cultured myocytes: differences between rabbit aorta and mesenteric artery. *Eur. J. Pharmacol.*, **105**, 207–213.

PICKARD, J.D., TAMURA, A., STEWART, M., MACGEORGE, A. & FITCH, W. (1980). Prostacyclin, indomethacin and the cerebral circulation. *Brain Res.*, **197**, 425–431.

POOLE, J.C.F., SANDERS, A.G. & FLOREY, H.W. (1958). The regeneration of aortic endothelium. *J. Path. Bact.*, **75**, 133–143.

SHIBASAKI, M., TORISAWA, Y. & IKEGAMI, S. (1983). Synthesis of 9(0)-Methano-$\Delta 6^{(9\alpha)}$-PGI_1; the highly potent carbon analog of prostacyclin. *Tetrahedron Lett.*, **24**, 3493–3496.

TIPS RECEPTOR NOMENCLATURE SUPPLEMENT (1993). *Trends Pharmacol. Sci.*, 31.

TODA, N. (1980). Responses to prostaglandins H2 and I2 of isolated dog cerebral and peripheral arteries. *Am. J. Physiol.*, **238**, H111–H117.

USKI, T.K. & ANDERSSON, K.-E. (1984). Effects of prostanoids on isolated feline cerebral arteries. *Acta Physiol. Scand.*, **120**, 131–136.

USKI, T., ANDERSSON, K.E., BRANDT, L., EDVINSSON, L. & LJUNGGREN, B. (1983). Responses of isolated feline and human cerebral arteries to prostacyclin and some of its metabolites. *J. Cereb. Blood Flow Metab.*, **3**, 238–245.

(Received September 14, 1993
Revised January 4, 1994
Accepted February 11, 1994)

Br. J. Pharmacol. (1994), **112**, 640–648

Improvement of cardiovascular effects of metoprolol by replacement of common salt with a potassium- and magnesium-enriched salt alternative

[1]Eero M.A. Mervaala, *Juha Laakso, Heikki Vapaatalo & Heikki Karppanen

Department of Pharmacology and Toxicology, P.O. Box 8 (Siltavuorenpenger 10), FIN-00014 University of Helsinki, Finland and *Mila Ltd., Sirrikuja 4 B, FIN-00940 Helsinki, Finland

1 The influence of sodium chloride (NaCl)-enrichment of the diet (6% of the dry weight) and that of a novel sodium-reduced, potassium-, magnesium-, and L-lysine-enriched salt alternative on the cardiovascular effects of the β_1-adrenoceptor blocking drug, metoprolol, was studied in stroke-prone spontaneously hypertensive rats.

2 Increased dietary sodium chloride intake produced a marked rise in blood pressure and induced left ventricular and renal hypertrophy. By contrast, the salt alternative did not increase blood pressure and caused remarkably less cardiac and renal hypertrophy than did sodium chloride.

3 Metoprolol treatment at a daily dose of 250 mg kg^{-1} lowered blood pressure and decreased left ventricular hypertrophy index during the control diet. Sodium chloride-enrichment blocked the antihypertensive effect of metoprolol, while a partial protective effect on left ventricular and renal hypertrophy persisted. In the presence of the salt alternative-enrichment both at the level of 6% and 10.5% (corresponding to a NaCl level of 6%), metoprolol was fully able to exert its beneficial cardiovascular and renal effects.

4 Both salt supplementations, irrespective of metoprolol treatment, induced a 3 to 4 fold increase in the urinary excretion of calcium. There was a linear correlation between the urinary excretions of sodium and calcium. The urinary excretion of magnesium rose by 90% and that of potassium by 110% in the salt alternative group.

6 Our findings suggest that replacement of common salt by a potassium-, and magnesium-enriched salt alternative in the diet produces beneficial cardiovascular effects and improves the antihypertensive efficacy of metoprolol in stroke-prone spontaneously hypertensive rats. Increased intake of potassium and/or magnesium and L-lysine from the salt alternative is involved in the beneficial effects of the salt alternative. The NaCl-induced myocardial and renal hypertrophies appear to be partially mediated by β-adrenoceptor activation.

Keywords: Stroke-prone spontaneously hypertensive rats; cardiac hypertrophy; renal hypertrophy; metoprolol; dietary salt intake; sodium; potassium; magnesium; calcium

Introduction

β-Adrenoceptor blocking agents belong to a group of first-line drugs in the treatment of essential hypertension and ischaemic heart disease. The high intake of sodium chloride (NaCl), typical of most industrialized societies (Law *et al.*, 1991), interferes with the therapeutic effects of diuretics (Ram *et al.*, 1981; Pecker, 1990) and angiotensin converting enzyme inhibitors (ACEI) (MacGregor *et al.*, 1987; Waeber *et al.*, 1990).

There is evidence which suggests that sodium chloride may interfere also with the effects of β-adrenoceptor blocking drugs (Owens & Brackett, 1978; Erwteman *et al.*, 1984). Unlike common salt, a novel sodium-reduced, potassium-, magnesium-, and L-lysine-enriched salt alternative, even in high doses did not raise blood pressure and produced little of any left ventricular hypertrophy in spontaneously hypertensive rats (Mervaala *et al.*, 1992). Moreover, replacement of common salt in the diet by the salt alternative markedly improved the cardiovascular effects of ACEI (Mervaala *et al.*, 1994a,b). The beneficial effects of the salt alternative were, to a great extent, mediated by natriuresis induced by potassium and/or magnesium (Mervaala *et al.*, 1992). Since diuretics improve the efficacy of the β-adrenoceptor blocking drug, metoprolol (Bengtsson, 1979; Asplund, 1981), it was of interest to examine the influence of the novel salt alternative on the effects of metoprolol. Therefore, using stroke-prone spontaneously hypertensive rats as a model we studied the effects of metoprolol during the salt alternative or sodium chloride supplementation on blood pressure and the development of left ventricular hypertrophy. The possible effects of the different salt supplementations and metoprolol treatment on renal mass were also examined.

[1] Author for correspondence.

Methods

Experimental animals and diets

Experiment I: Equal dietary levels of sodium chloride (NaCl) and the salt alternative Sixty inbred male stroke-prone spontaneously hypertensive rats (SHRSP), originally developed by Okamoto *et al.* (1974), were used. The rats, from our own breeding programme, were housed five animals in a cage in an animal laboratory (illuminated from 06 h 30 min to 18 h 30 min, room temperature 22–24°C). At the beginning of the study, the nine week-old, blood pressure- and weight-matched rats (body weights ranging from 163 g to 236 g) were divided into six subgroups to receive different diet and drug regimens for five weeks. The NaCl-enriched diet was produced by adding 6.0 g of NaCl to 94.0 g of the standard rat chow (Finnewos Aqua, Helsinki, Finland). The salt alternative-enriched diet was produced by adding 6.0 g of the commercially available salt alternative (PANSALT, Oriola Oy, Espoo, Finland), to 94.0 g of the chow. This salt alterna-

tive has the following composition: NaCl 57%, KCl 28%, $MgSO_4 \cdot 7H_2O$ 12%, L-lysine hydrochloride 2% and anticaking agents ($MgCO_3$, SiO_2) 1%. Therefore, the sodium chloride concentration was 43% lower in the salt alternative-enriched diet than in the NaCl-enriched diet. The contents of sodium, potassium, magnesium and other nutrients in the different diets are given in Table 1. The rats had free access to tap water and chow. Metoprolol was added to the chow (6.0 g metoprolol tartrate corresponding to 2.3 g metoprolol free base kg^{-1} dry weight of the chow) to produce an approximate daily dose of 250 mg kg^{-1} body weight. Systolic blood pressure of the pretrained rats was measured weekly by a tail cuff method (Blood pressure recorder, model no. 8002e, W + W Electronics Inc., Basel, Switzerland). The same technician made all blood pressure measurements. Details of the procedure have been described earlier (Mervaala *et al.*, 1992). The animals were examined daily for survival and signs of stroke throughout the study. Assessment of stroke was based on the presence of evident and stable hemiplegia, akinesia, lethargy, and hyporesponsiveness according to the symptomatological classification described by Yamori *et al.* (1982). During the fifth week of the experiment the rats were housed individually in metabolic cages. Food intake was recorded and urine was collected over a 24 h period. After the five-week experimental period, the rats were anaesthetized with sodium pentobarbitone (65 mg kg^{-1}, i.p.), the hearts were excised, great vessels, atria and the free wall of the right ventricle were dissected and the left ventricular mass was measured. The left ventricular wet weight-to-body weight ratio was calculated as an index of left ventricular hypertrophy. The kidneys were washed with ice-cold saline and weighed. The weight of the kidneys-to-body weight ratio was calculated as an index of renal hypertrophy. The experimental design of the study was approved by the Animal Experimentation Committee of the University of Helsinki, Finland.

Experiment II: Equal dietary levels of sodium chloride in the NaCl and the salt alternative groups Sixteen male SHRSP were used in this study. At the beginning of the study, the nine week-old, blood pressure and weight-matched rats (body weights ranging from 164 g to 227 g) were divided into two subgroups to receive either a NaCl-enriched diet (6.0 g of NaCl was added to 94.0 g of the standard rat chow) or a salt alternative-enriched diet (10.5 g of PANSALT was added to 89.5 g of the standard rat chow). The content of sodium chloride in the chow was thereby adjusted to the same level in the different diets. The contents of sodium, potassium, magnesium and other nutrients in the different diets are given in Table 1. All rats received metoprolol. Otherwise Experiment II was performed in the same way as Experiment I.

Determination of electrolyte concentrations

The concentrations of the elements sodium, potassium, magnesium, calcium, phosphorus and zinc in urine were determined with a Baird PS-4 inductively-coupled plasma emission spectrometer (Baird Co, Bedford, MA, U.S.A.) as described in detail elsewhere (Laakso *et al.*, 1991). For magnesium the intra-assay imprecision was 1.5% and the interassay imprecision was 0.5%. The intra-assay imprecision for the other elements was better than 3% and the inter-assay imprecision was not more than 5%. The mean levels obtained for the NIST (National Institute of Standards, Washington, U.S.A.) 1577b reference material were within 3.5% of NIST certified values.

Drugs

Metoprolol tartrate (kindly donated by Dr Margareta Nordlander from Astra Hässle AB, Mölndal, Sweden) was used in the present study.

Table 1 Contents of sodium, potassium, magnesium and other nutrients in the different diets

	Control diet	*NaCl-enriched diet*	*Salt alternative-enriched diet*
Mineral element			
Sodium			
Experiment I[1])	0.3*	2.6*	1.6*
Experiment II[2])		2.6*	2.6*
Potassium			
Experiment I[1])	0.8*	0.8*	1.7*
Experiment II[2])		0.8*	2.3*
Magnesium			
Experiment I[1])	0.2*	0.2*	0.27*
Experiment II[2])		0.2*	0.3*
Mineral elements (contents common for all diets)			
Calcium	1.0*		
Phosphorus	0.75*		
Iron	178 mg kg^{-1}		
Zinc	115 mg kg^{-1}		
Manganese	89 mg kg^{-1}		
Copper	18 mg kg^{-1}		
Iodine	2 mg kg^{-1}		
Cobalt	1 mg kg^{-1}		
Major constituents (contents common for all diets)			
Water	11.7*		
Crude fat	5.3*		
Crude protein	21.0*		
Fibre	2.8*		
Carbohydrate	52.2*		
Ash	7.0*		
Metabolizable energy	13.0 MJ kg^{-1}		

*Values are expressed as % (g 100 g^{-1}) of the dry weight of the pellets.
[1]Experiment I: equal dietary levels of sodium chloride and the salt alternative.
[2]Experiment II: equal dietary levels of sodium chloride in the NaCl and the salt alternative groups.

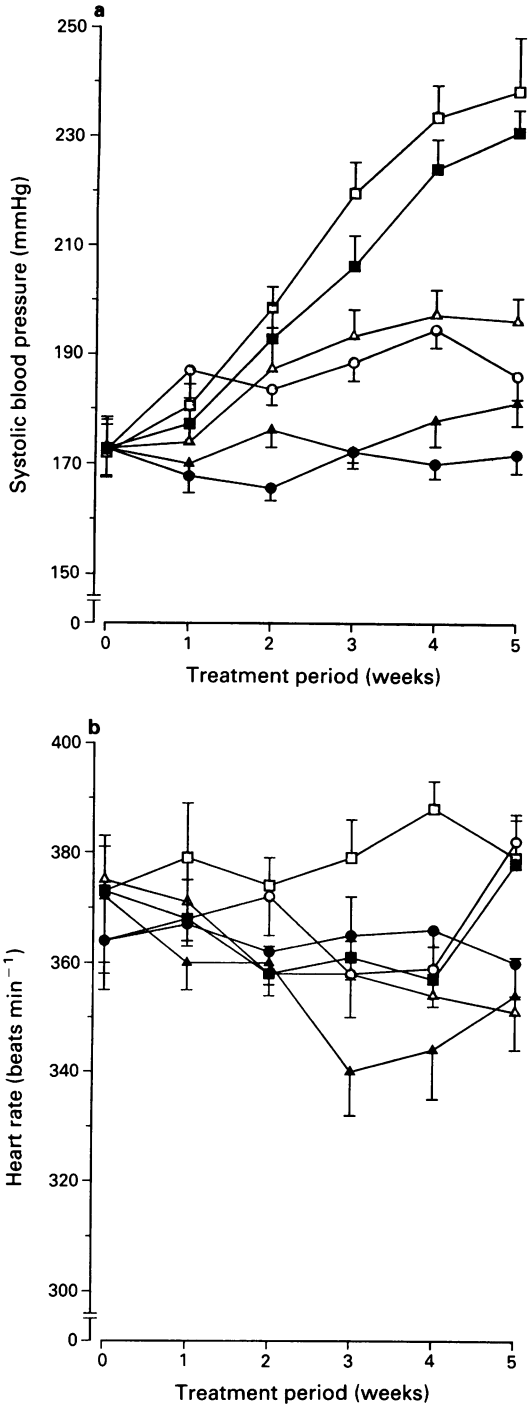

Figure 1 Effects on blood pressure (a) and heart rate (b) in stroke-prone, spontaneously hypertensive rats (SHRSP) during different diet and drug regimens: (○), controls on normal diet ($n = 10$); (□) NaCl-enriched diet (NaCl 6%, $n = 8-10$); △, salt alternative-enriched diet (Pansalt 6%, $n = 10$); (●) metoprolol during control diet ($n = 10$); (■), metoprolol during NaCl-enriched diet ($n = 10$); (▲) metoprolol during the salt alternative-enriched diet ($n = 10$). Blood pressure; repeated analysis of variance between-subjects effects, $P < 0.0001$; within-subject effects, $P < 0.0001$; time-group interaction, $P < 0.0001$. NaCl-enrichment, in the presence or in the absence of metoprolol produced a rise in blood pressure ($P < 0.01$ to 0.001 *versus* all other groups). Metoprolol treatment (250 mg kg^{-1} day^{-1}) significantly decreased blood pressure during control diet ($P < 0.001$ *versus* control group) and the salt alternative-enriched diet ($P < 0.05$ *versus* control group). Heart rate; repeated analysis of variance between-subjects effects, $P < 0.0001$; within-subject effects, $P = 0.0961$; time-group interaction, $P = 0.6158$. Heart rate of the NaCl group was higher than that of all metoprolol-treated groups and the salt alternative group ($P < 0.05-0.01$). The heart rate of the metoprolol treatment group during the salt alternative-enriched diet was decreased even in comparison with the control group ($P < 0.05$). Symbols indicate means with s.e.mean.

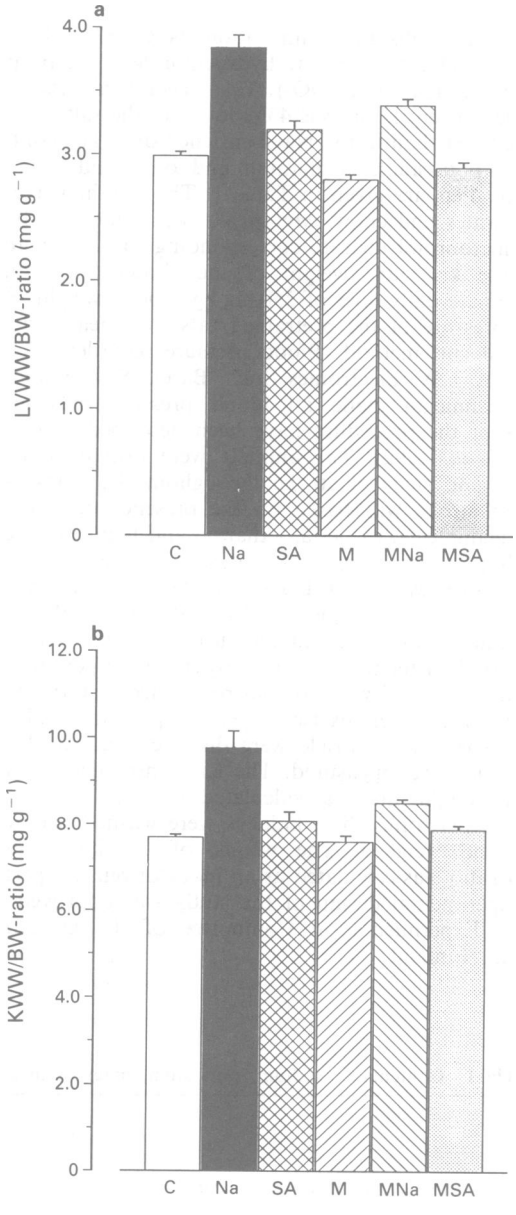

Figure 2 Left ventricular hypertrophy index (a) expressed as left ventricular wet weight (LVWW) to body weight (BW) ratio, and renal hypertrophy index (b) expressed as left + right kidney wet weight (KWW) to body weight (BW) ratio, of stroke-prone, spontaneously hypertensive rats (SHRSP) after five weeks on the different diet and drug regimens. C, controls on normal diet ($n = 10$); Na, NaCl-enriched diet (NaCl 6%, $n = 8$); SA, salt alternative-enriched diet (Pansalt 6%, $n = 10$); MC, metoprolol during control diet ($n = 10$); MNa, metoprolol during NaCl-enriched diet ($n = 10$); MSA, metoprolol during the salt alternative-enriched diet ($n = 10$). NaCl-enrichment produced left ventricular hypertrophy (analysis of variance $P < 0.0001$, $P < 0.001$ *versus* all other groups), which was partially prevented by metoprolol treatment (250 mg kg^{-1} day^{-1}). Metoprolol treatment during the control diet decreased left ventricular hypertrophy ($P = 0.002$ *versus* control group). NaCl-enrichment produced renal ventricular hypertrophy (analysis of variance $P < 0.0001$, $P < 0.001$ *versus* all other groups), which was partially prevented by metoprolol treatment. Columns indicate means with s.e.mean.

Statistical analysis

Statistical analysis was carried out by one-way analysis of variance (ANOVA) supported by the Tukey's test. Data for multiple observations over time were analysed by two-way ANOVA with repeated measures for overall treatment effect, and Tukey's test was used for multiple paired comparisons of

treatment groups at different times. The area under the curve (AUC) (blood pressure *versus* time) of each individual rat in different treatment groups was also calculated mathematically by the methods outlined by Matthews *et al.* (1990). The AUCs were then tested by ANOVA, supported by Tukey's test. Regression lines were calculated by the least squares method. The data were analysed by SAS statistical Software (SAS Institute Inc., Cary, NC., U.S.A.). The results are expressed as means ± s.e.mean.

Results

Experiment I

Death-rate and stroke During the five-week experiment, two of the 10 SHRSP receiving the NaCl-enriched diet died following clinically diagnosed stroke, while the other eight were asymptomatic. By contrast, none of the 10 SHRSP receiving the salt alternative-enriched diet died or suffered from stroke. In the presence of the metoprolol treatment, no deaths occurred and there was no evidence of stroke in the SHRSP supplemented either with sodium chloride or the salt alternative.

Blood pressure, and left ventricular and renal mass Enrichment of the diet with sodium chloride produced a marked further elevation of blood pressure as compared to the age-related increase in blood pressure of the control SHRSP (Figure 1a). The rats receiving the salt alternative-enriched diet showed no significant increase in blood pressure when compared to the control SHRSP (Figure 1a). Metoprolol treatment lowered blood pressure during the control and the salt alternative-enriched diets. NaCl-enrichment blocked the antihypertensive effect of metoprolol (Figure 1a). The blood pressure level of the 14-week-old Wistar-Kyoto rats from our breeding during the control diet was 138 ± 2 mmHg ($n = 19$).

NaCl-enrichment produced a marked left ventricular hypertrophy as indicated by an increase in the left ventricular wet weight-to-body weight ratio (Figure 2a). In the salt alternative supplemented rats, the left ventricular hypertrophy index was not significantly increased when compared to the control group, and it was clearly decreased when compared to the NaCl group (Figure 2a). Metoprolol decreased the left ventricular hypertrophy index during the control diet ($P = 0.002$). NaCl-enrichment attenuated the cardioprotective effect of metoprolol ($P < 0.001$ *versus* control group and $P < 0.001$ *versus* NaCl group without metoprolol) (Figure 2a). The cardioprotective effect of metoprolol persisted during the salt alternative-enriched diet ($P < 0.001$ *versus* metoprolol during NaCl-enriched diet) (Figure 2a). The left ventricular hypertrophy correlated very strongly with the systolic blood pressure (AUC) (multiple regression $r = 0.79$, $P < 0.0001$, $n = 58$). The left ventricular wet weight-to-body weight ratio of the 14-week-old Wistar-Kyoto rats from our breeding during the control diet was 2.17 ± 0.07 mg g^{-1} ($n = 19$).

NaCl-enrichment produced a marked renal hypertrophy as indicated by an increase in the right + left kidney wet weight-to-body weight ratio (Figure 2b). In the salt alternative supplemented rats the renal hypertrophy index did not differ from that of the control group (Figure 2b). Metoprolol did not decrease the renal hypertrophy index during the control diet, but it prevented the NaCl-induced increase in the renal hypertrophy index (Figure 2b). The renal hypertrophy correlated very strongly with the systolic blood pressure (AUC) (multiple regression $r = 0.62$, $P < 0.001$, $n = 58$) and with the left ventricular hypertrophy (multiple regression, $r = 0.88$, $P < 0.0001$, $n = 58$). The weight of the kidneys-to-body weight ratio of the 14-week-old Wistar-Kyoto rats from our breeding during the control diet was 6.54 ± 0.08 mg g^{-1} ($n = 19$).

Table 2 Twenty-four hour food consumption, urine volume and urinary excretion rates of various mineral elements of stroke-prone, spontaneously hypertensive rats after four weeks on the different diet and drug regimens

	C	*Na*	*SA*	*MC*	*MNa*	*MSA*	*ANOVA*	*Difference between groups at* $P < 0.05$
Food intake ($g\,d^{-1}$)	21.9 ± 1.8	18.0 ± 1.2	21.1 ± 1.0	25.3 ± 1.3	26.8 ± 1.6	29.2 ± 2.0	0.0001	Na vs. MC, MNa and MSA MSA vs. C, Na and SA
Urine								
volume ($ml\,d^{-1}$)	16.4 ± 1.1	61.1 ± 5.7	47.5 ± 1.9	20.2 ± 3.8	52.4 ± 5.8	38.9 ± 2.8	< 0.0001	C and MC vs. Na, SA, MNa and MSA MSA vs. Na
sodium ($mmol\,d^{-1}$)	2.0 ± 0.2	14.4 ± 1.4	12.6 ± 0.6	2.8 ± 1.1	15.8 ± 2.2	11.4 ± 0.6	< 0.0001	C and MC vs. Na, SA, MNa and MSA
potassium ($mmol\,d^{-1}$)	3.0 ± 0.2	2.4 ± 0.09	6.4 ± 0.4	3.2 ± 0.5	2.3 ± 0.4	6.5 ± 0.4	< 0.0001	SA and MSA vs C, Na, MC and MNa
magnesium ($mmol\,d^{-1}$)	0.24 ± 0.02	0.32 ± 0.02	0.45 ± 0.03	0.24 ± 0.03	0.35 ± 0.06	0.46 ± 0.03	< 0.0001	SA and MSA vs. C, MC and Na
phosphorus ($mmol\,d^{-1}$)	0.96 ± 0.08	1.30 ± 0.09	1.14 ± 0.06	0.80 ± 0.02	1.26 ± 0.10	1.00 ± 0.06	0.0001	Na vs. C Na, SA and MNa vs. MC
calcium ($mmol\,d^{-1}$)	0.038 ± 0.003	0.19 ± 0.02	0.15 ± 0.01	0.036 ± 0.02	0.17 ± 0.02	0.13 ± 0.01	< 0.0001	C and MC vs. Na, SA, MNa and MSA MSA vs. Na
zinc ($\mu mol\,d^{-1}$)	0.11 ± 0.01	0.28 ± 0.04	0.26 ± 0.03	0.14 ± 0.02	0.25 ± 0.03	0.21 ± 0.02	< 0.0001	C and MC vs. Na, SA and MNa

The control group (C, $n = 10$) and the metoprolol group (MC, $n = 10$; metoprolol mixed in the chow to produce an approximate daily dose of 250 mg kg^{-1}) received standard rat chow (Na 0.3%). The chow of the high sodium chloride group (Na, $n = 10$) and that of the high sodium chloride + metoprolol group (MNa, $n = 10$; metoprolol as above) was supplemented with common salt (6% NaCl). The chow of the salt alternative group (SA, $n = 10$) and that of the salt alternative + metoprolol group (MSA, $n = 10$; metoprolol as above) was supplemented with 6% of the salt alternative (Pansalt).

Heart rate Overall during the five-week experiment the heart rate of the NaCl group was higher than that of all metoprolol-treated groups and the salt alternative group (Figure 1b). The heart rate of the metoprolol-treated group during the salt alternative-enriched diet was decreased as compared to the controls (Figure 1b).

Metabolic variables and indicators NaCl supplemented SHRSP weighed less than the other SHRSP at the end of the experimental period (body weight: 272 ± 4 g in the control group, 220 ± 7 g in the NaCl group, 268 ± 5 g in the salt alternative group, 257 ± 7 g in the metoprolol group during the control diet, 262 ± 4 g in the metoprolol group during the NaCl-enriched diet and 260 ± 4 g in the metoprolol group during the salt alternative-enriched diet, ANOVA $P<0.001$). The food intake in all metoprolol-treated groups during the fifth study week was slightly increased but significantly so, only in comparison to the NaCl group (Table 2). The food intake of the metoprolol-treated group during the salt alternative-enriched diet was bigger than that of the groups which did not receive metoprolol. However, it did not differ from the intake in the other metoprolol-treated groups (Table 2). All groups with salt supplements had an increased diuresis (Table 2).

The calculated average daily dose of metoprolol free base was 233 ± 16 mg kg^{-1} body weight in the control diet group, 240 ± 17 mg kg^{-1} in the NaCl-enriched diet group and 262 ± 17 mg kg^{-1} in the salt alternative-enriched diet group (ANOVA $P = 0.47$).

Urine electrolytes The 24 h urinary excretion of sodium was increased in all groups with salt supplements when compared to the control group (Table 2). The urinary excretions of potassium and magnesium were increased in the salt alternative supplemented rats both in the presence and in the absence of metoprolol. The urinary excretion of calcium was markedly increased in all groups with either of the salt supplements. The urinary output of calcium was smaller in the salt alternative group than in the NaCl group ($P = 0.04$). The excretion of phosphorus was increased in the NaCl supplemented rats and that of zinc in the NaCl and the salt alternative supplemented rats (Table 2).

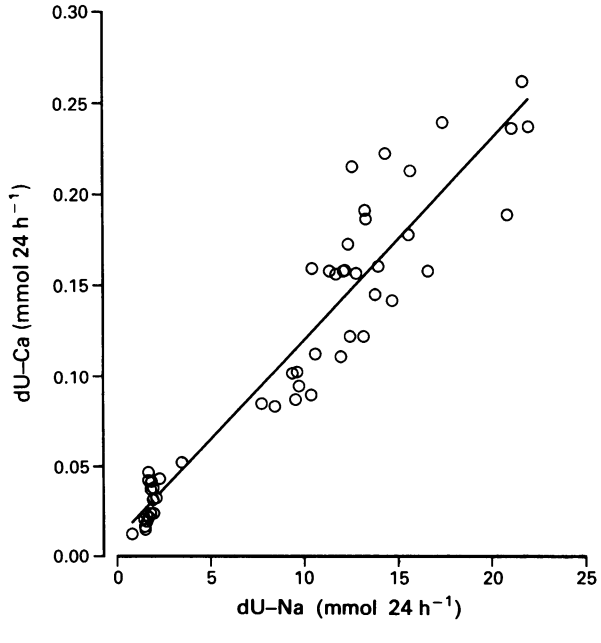

Figure 3 Scatter plot shows positive linear correlation between the 24 h urinary excretions of sodium (dU-Na) and calcium (dU-Ca) in stroke-prone, spontaneously hypertensive rats during different diet and drug regimens ($r = 0.95$, $P<0.0001$, $n = 58$).

The urinary excretion of sodium correlated with the left ventricular hypertrophy (multiple regression $r = 0.47$, $P = 0.0007$, $n = 58$) and with the renal hypertrophy (multiple regression $r = 0.45$, $P = 0.001$, $n = 58$). The urinary excretion of calcium correlated also with the left ventricular hyper-

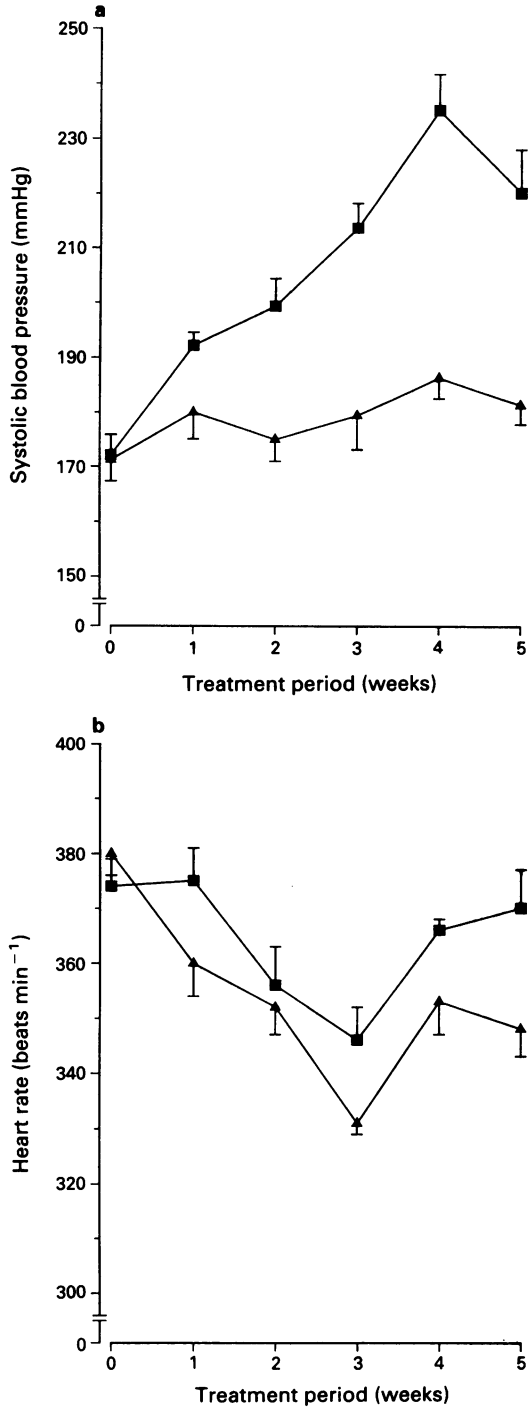

Figure 4 Effects on blood pressure (a) and heart rate (b) in stroke-prone, spontaneously hypertensive rats (SHRSP) during different diet and drug regimens: (■) metoprolol during NaCl-enriched diet (NaCl 6%, $n = 8$); (▲) metoprolol during the salt alternative-enriched diet (Pansalt 10.5%, corresponding to 6% of NaCl, $n = 8$). The blood pressure of the metoprolol-treated SHRSP was higher during the NaCl-enriched diet than during the salt alternative-enriched diet (repeated analysis of variance between-subjects effects, $P<0.0001$; within-subject effects, $P<0.0001$; time-group interaction, $P<0.0001$). The heart rate of the metoprolol-treated group was slightly higher during the NaCl-enriched diet (repeated analysis of variance between-subjects effects, $P = 0.04$; within-subject effects, $P<0.0001$; time-group interaction, $P = 0.06$). Symbols indicate means with s.e.mean.

trophy (multiple regression $r = 0.54$, $P = 0.0001$, $n = 58$) and with the renal hypertophy (multiple regression, $r = 0.50$, $P = 0.0002$, $n = 58$). There was a linear correlation between the urinary excretions of sodium and calcium (Figure 3).

Experiment II

Death rate and stroke None of the metoprolol-treated SHRSP in the experiment II died or showed any evidence of stroke during the five-week experimental period.

Blood pressure, heart rate and left ventricular and renal mass Overall during the five-week experiment the blood pressure and the heart rate were higher in the NaCl group than in the salt alternative group (Figures 4a and b). The left ventricular hypertrophy index (Figure 5a) and the renal hypertrophy index (Figure 5b) of the NaCl group were higher than those of the salt alternative group. The left ventricular hypertrophy correlated with the systolic blood pressure (multiple regression $r = 0.63$, $P = 0.02$, $n = 16$). The renal hypertrophy correlated with the systolic blood pressure (multiple regression $r = 0.63$, $P = 0.01$, $n = 16$) and with the left ventricular hypertrophy (multiple regression $r = 0.74$, $P = 0.003$, $n = 16$).

Metabolic variables and indicators There was no difference between the groups in the body weight (248 ± 6 g in the NaCl group and 246 ± 6 g in the salt alternative group, $P = 0.78$) at the end of the experimental period. There were no differences between the groups in the food intake or diuresis (Table 3). The calculated average daily dose of metoprolol free base was 267 ± 21 mg kg^{-1} body weight in the NaCl group and 235 ± 10 mg kg^{-1} in the salt alternative group ($P = 0.19$).

Urine electrolytes The 24 h urinary excretions of potassium and magnesium were higher in the salt alternative group than in the NaCl group (Table 3). There were no significant differences between the groups in the urinary excretion of sodium, calcium, phosphorus or zinc (Table 3). There was a linear correlation between the urinary excretions of sodium and calcium (Figure 6). The urinary excretion of sodium did not significantly correlate either with the left ventricular hypertrophy (multiple regression $r = 0.44$, $P = 0.13$, $n = 16$) or with the renal hypertrophy (multiple regression $r = -0.03$, $P = 0.93$, $n = 16$). The correlation between urinary excretion of calcium and the left ventricular hypertrophy did not quite reach statistical significance (multiple regression $r = 0.48$, $P = 0.09$, $n = 16$). The urinary excretion of calcium did not correlate with the renal hypertrophy (multiple regression $r = -0.01$, $P = 0.96$, $n = 16$).

Table 3 Twenty-four hour food consumption, urine volume and urinary excretion rates of various mineral elements of stroke-prone, spontaneously hypertensive rats after four weeks on the different diet and drug regimens

	MNa	*MSA*	t *test* (P-*value*)
Food intake (g d^{-1})	26.4 ± 1.6	23.8 ± 1.2	0.22
Urine			
volume (ml d^{-1})	49.9 ± 5.2	54.3 ± 2.4	0.44
sodium (mmol d^{-1})	13.9 ± 1.6	13.1 ± 0.7	0.67
potassium (mmol d^{-1})	2.4 ± 0.3	7.3 ± 0.3	<0.001
magnesium (mmol d^{-1})	0.31 ± 0.04	0.44 ± 0.02	0.02
phosphorus (mmol d^{-1})	1.1 ± 0.1	1.0 ± 0.03	0.23
calcium (mmol d^{-1})	0.17 ± 0.03	0.17 ± 0.01	0.85
zinc (μmol d^{-1})	0.23 ± 0.05	0.18 ± 0.03	0.39

The chow of the high sodium chloride + metoprolol group (MNa, $n = 8$; metoprolol mixed in the chow to produce an approximate daily dose of 250 mg kg^{-1}) was supplemented with common salt (6% NaCl). The chow of the salt alternative + metoprolol group (MSA, $n = 8$; metoprolol as above) was supplemented with 10.5% of the salt alternative (Pansalt) to produce equal dietary levels of sodium chloride.

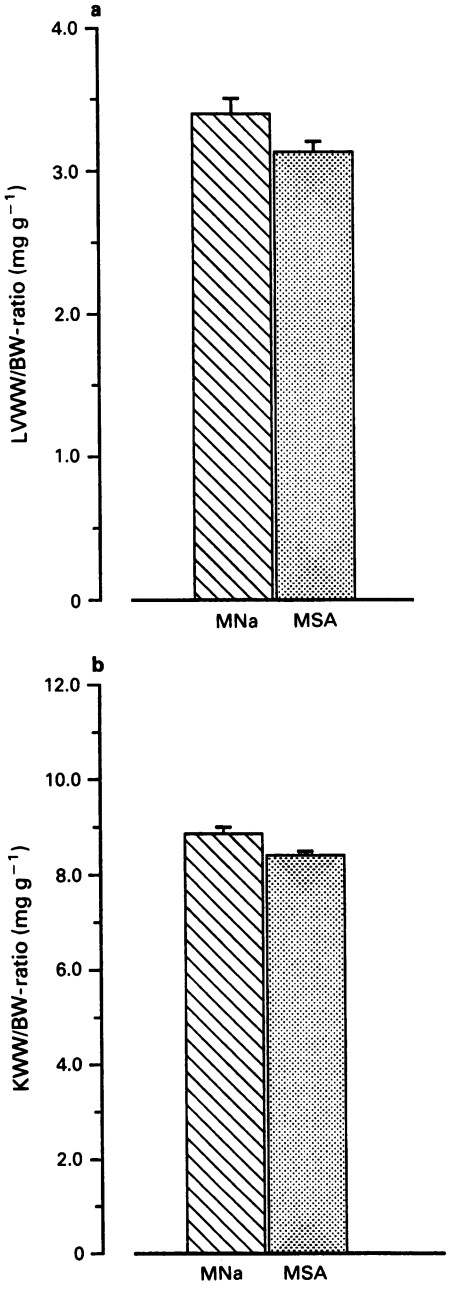

Figure 5 Left ventricular hypertrophy index (a) expressed as left ventricular wet weight (LVWW) to body weight (BW) ratio, and renal hypertrophy index (b) expressed as left + right kidney wet weight (KWW) to body weight (BW) ratio, of stroke-prone, spontaneously hypertensive rats (SHRSP) after five weeks on the different diet and drug regimens. MNa, metoprolol during NaCl-enriched diet (NaCl 6%, $n = 8$); MSA, metoprolol during the salt alternative-enriched diet (Pansalt 10.5% corresponding to 6% of NaCl, $n = 8$). The differences in the left ventricular hypertrophy index did not quite reach statistical significance ($P = 0.06$). The renal hypertrophy index of the metoprolol-treated SHRSP was higher in the NaCl group than in the salt alternative group ($P = 0.02$). Columns indicate means with s.e.mean.

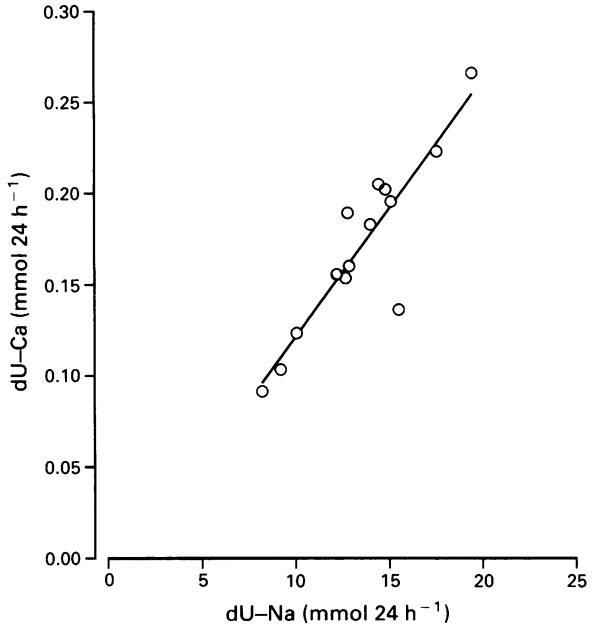

Figure 6 Scatter plot shows positive linear correlation between the 24 h urinary excretions of sodium (dU-Na) and calcium (dU-Ca) in the metoprolol-treated stroke-prone, spontaneously hypertensive rats during common salt and the salt alternative diets ($r = 0.90$, $P < 0.0001$, $n = 16$).

Discussion

In stroke-prone SHR, an increased intake of sodium chloride (NaCl) over a five-week period produced a marked further elevation of blood pressure and increase in left ventricular hypertrophy as compared to the age-related increases in the control group. These effects of sodium chloride are in agreement with previous findings in SHR and SHRSP (Oparil *et al.*, 1988; Tobian, 1988; Karppanen, 1989; Mervaala *et al.*, 1992). A raised intake of sodium chloride also produced renal hypertrophy. This finding is in agreement with the observations on previous studies in normotensive rats (Wilson *et al.*, 1973), salt-sensitive and -resistant rats (Sapirstein *et al.*, 1950; McCormick *et al.*, 1989) and renal hypertensive rats (Vapaatalo *et al.*, 1970). The development of renal hypertrophy might be a defence mechanism against the increased salt and volume load, induced by the increased intake of sodium chloride and the concomitant increase in the fluid intake. However, the persistence of an increased volume load is suggested by our previous finding that, during an increased intake of sodium chloride, the levels of atrial natriuretic peptide were elevated both in spontaneously hypertensive and in hypertension-resistant Wistar-Kyoto rats (Mervaala *et al.*, 1992). Recently McCormick *et al.* (1989) showed that a high intake of sodium chloride elevated the renal hypertrophy index, increased protein and DNA content, and decreased the protein/DNA-ratio in Dahl salt-sensitive rats without any significant effect on water content of the kidney.

By contrast, the potassium-, magnesium-, and L-lysine-enriched salt alternative at the same intake level as common salt did not induce any significant rise in blood pressure. The salt alternative caused significantly less left ventricular and renal hypertrophy than did common salt. Our previous studies (Karppanen, 1989; Mervaala *et al.*, 1992), using higher levels of the salt alternative, demonstrated that the increased intake of potassium and/or magnesium and L-lysine from the salt alternative protected against the harmful effects of the increased intake of sodium chloride. A protective effect of potassium supplementation against stroke and mortality in sodium chloride-loaded rats has been reported (Tobian *et al.*, 1985; Tobian, 1988). Previously it has been shown that, potassium supplementation prevents the rise in blood pressure during sodium chloride loading by attenuating the increase in cardiac output, mainly as a result of the natriuresis (Young *et al.*, 1976; Fujita & Ando, 1984). Moreover, potassium supplementation protected against dysfunction of endothelial cells in stroke-prone spontaneously hypertensive rats (Sugimoto *et al.*, 1988) and preserved endothelial function also in Dahl rats during the high sodium chloride diet (Sudhir *et al.*, 1993). In the present study the increased intake of the protective agents from the salt alternative may have mediated its beneficial effects. However, the smaller intake of sodium chloride in the salt alternative group may also have contributed to the favourable effect.

In agreement with previous findings (Ljung *et al.*, 1976; 1978; Weiss & Lundgren, 1978; Christensen *et al.*, 1989) metoprolol lowered blood pressure and prevented the development of left ventricular hypertrophy in stroke-prone spontaneously hypertensive rats during a low-sodium diet. The antihypertensive effect of metoprolol was blocked by the increased intake of sodium chloride. As adverse influence of dietary sodium chloride on the effects of β-adrenoceptor blocking drugs has been reported (Samizadeh *et al.*, 1977; Erwteman *et al.*, 1984; Tsuda & Masuyama, 1991). Unlike common salt, the novel sodium-reduced, potassium-, magnesium- and L-lysine enriched salt alternative did not block the antihypertensive effect of metoprolol. Even when the dietary sodium chloride intake was adjusted to the same level in the common salt and the salt alternative groups, a remarkable beneficial interaction between metoprolol and the salt alternative existed. This finding indicates that an increase in the intakes of potassium, magnesium and/or L-lysine is responsible for at least a part of the beneficial effects of the salt alternative. We have previously found very similar interactions between sodium chloride, the salt alternative and the angiotensin converting enzyme inhibitors, enalapril (Mervaala *et al.*, 1994a) and ramipril (Mervaala *et al.*, 1994b). Consistent with our finding, Suppa *et al.* (1988) found that replacement of common salt by a low-sodium/high-potassium salt substitute induced a further reduction in the systolic blood pressure of hypertensive patients treated with metoprolol. In the first part of the present study the lower intake of sodium chloride probably also contributed to the beneficial effects of the salt alternative. This assumption is supported by the fact that, in the presence of a low dietary sodium chloride level in the control SHRSP, metoprolol produced remarkable cardiovascular effects in spite of the fact that potassium, magnesium and L-lysine levels were the same as in the sodium chloride group. Consistent with our findings is the demonstration in clinical studies that salt restriction or combination with a natriuretic diuretic enhances the cardiovascular effects of metoprolol (Bengtsson, 1979; Asplund, 1981; Erwteman *et al.*, 1984).

The mechanisms by which sodium chloride antagonizes and the salt alternative maintains the effects of metoprolol are not completely understood. A decrease in cardiac output, a suppression of renin release, a reduction of sympathetic tone and an improvement of baroreceptor sensitivity have been implicated in the antihypertensive effect of β-adrenoceptor blocking drugs (Bolli *et al.*, 1990). A high intake of sodium chloride increases extracellular fluid volume and cardiac output (Fujita & Ando, 1984), and also sympathetic tone (Oparil *et al.*, 1989). Such effects of sodium chloride are likely to attenuate the antihypertensive effect of metoprolol.

We have recently found that the salt alternative may prevent the NaCl-induced volume load, since the plasma level of atrial natriuretic peptide (ANP) was increased in the sodium chloride group but remained normal in the salt alternative group (Mervaala *et al.*, 1992). Our previous findings also suggest that the salt alternative may not increase sympathetic tone (Mervaala *et al.*, 1992).

It has been shown that a high intake of sodium chloride inhibits sodium-potassium-ATPase (Hamlyn *et al.*, 1982;

Blaustein & Hamlyn, 1984) and increases the level of intracellular calcium (Alexiewicz *et al.*, 1992), an effect which is known to produce vasoconstriction. Potassium and magnesium activate sodium-potassium-ATPase (Lindenmayer & Schwartz, 1973). Magnesium also acts as a calcium-channel antagonist (Altura & Altura, 1990). Consistent with these findings common salt, but not the salt alternative, increased contractile responses to noradrenaline of isolated endothelium-intact mesenteric arterial rings (Mervaala *et al.*, 1994b). These differences in the effects between sodium chloride and the salt alternative are likely to explain, at least in part, the marked improvement of the antihypertensive effect of metoprolol when common salt was replaced by the salt alternative.

In spite of the fact that metoprolol did not significantly lower blood pressure, it did produce a partial protection against the development of the left ventricular hypertrophy during the high intake of sodium chloride. This suggests that the NaCl-induced left ventricular hypertrophy is mediated, at least in part, by the activation of the sympathetic nervous system, as supported by previous studies (Östman-Smith, 1981; Lindpaintner & Sen, 1985; Meggs *et al.*, 1988; Oparil *et al.*, 1988; 1989; Fields *et al.*, 1991; Muntzel & Drueke, 1992). The activation of the sympathetic nervous system is also suggested by the increased heart rate of the NaCl supplemented rats in the present study. However, an increased volume load during the high sodium chloride diet also appears to be involved in the production of the NaCl-induced left ventricular hypertrophy (Mervaala *et al.*, 1992). The NaCl-induced renal hypertrophy also appeared to be mediated, at least in part, by the activation of the sympathetic nervous system, since metoprolol treatment antagonized the increase in renal mass in the present study.

In the present study an increase in the intake of sodium chloride was associated with a 3 to 4 fold increase in the urinary excretion of calcium. The urinary excretion of calcium correlated very strongly with the urinary excretion of sodium. On the other hand, increased calcium intake dose-dependently augmented urinary excretion of sodium and reduced the arterial wall sodium/potassium ratio suggesting an important interaction between these two electrolytes in the regulation of blood pressure and vascular responses (Wuorela *et al.*, 1992). The calcium metabolism might also have important implications in the development of the NaCl-induced cardiac hypertrophy. A crucial cardiovascular interaction between sodium and calcium is also suggested by the finding that calcium supplementation decreased blood pressure and improved vascular relaxation in salt-sensitive spontaneously hypertensive rats (Pörsti *et al.*, 1990; Wuorela *et al.*, 1992). Interestingly, in the present study, replacement of common salt by the sodium-reduced salt alternative decreased the urinary excretion of calcium. There is evidence suggesting that an increased intake of sodium chloride causes bone resorption (Chan *et al.*, 1992) as indicated by an increase in the urinary excretion of hydroxyproline. Moreover, it has been shown that, salt restriction reduces bone resorption, at least in postmenopausal women (Need *et al.*, 1991). These findings lend further support to the suggestion that the high sodium chloride diet is a dietary risk factor for osteoporosis (Shortt & Flynn, 1990). In addition to the beneficial cardiovascular effects, the present salt alternative also influenced the urinary calcium loss more favourably than did sodium chloride.

In conclusion, a novel sodium-reduced, potassium-, magnesium- and L-lysine-enriched salt alternative elevated blood pressure, produced cardiac and renal hypertrophy and induced loss of calcium into the urine markedly less than did common salt in stroke-prone spontaneously hypertensive rats. Metoprolol treatment effectively lowered blood pressure and prevented left ventricular hypertrophy during a low-sodium diet. A high intake of sodium chloride almost completely blocked the cardiovascular effects of metoprolol, while during the salt alternative-enriched diet, even at very high concentrations, the effects of metoprolol persisted. The beneficial interaction between metoprolol and the salt alternative appeared to be mainly due to the increased intake of potassium, magnesium and/or L-lysine. The lower sodium content apparently also contributed to the beneficial effects of the salt alternative.

This study was supported by grants from the Academy of Finland, the University of Helsinki, the Yrjö Jahnsson Foundation and the Sigrid Jusélius Foundation. The gift of metoprolol from Dr Margareta Nordlander from Astra Hässle AB, Mölndal, Sweden, is gratefully acknowledged. We thank Ms Pirkko Olkkonen, Ms Toini Siiskonen and Ms Aila Urjansson for providing excellent technical assistance.

References

ALEXIEWICZ, J.M., GACIONG, Z., PARISE, M., KARUBIAN, F., MASSRY, S.G. & CAMPESE, V.M. (1992). Effect of dietary sodium intake on intracellular calcium in lymphocytes of salt-sensitive hypertensive patients. *Am. J. Hypertens.*, **5**, 536–541.

ALTURA, B.M. & ALTURA, B.T. (1990). Role of magnesium in the pathogenesis of hypertension: relationship to its actions on cardiac and vascular smooth muscle. In *Hypertension: Pathophysiology, Diagnosis and Management*. ed. Laragh, J.H. & Brenner, B.M. pp. 1003–1025. New York: Raven Press Ltd.

ASPLUND, J. (1981). A fixed-ratio combination of metoprolol and hydrochlorothiazide ('Co-Betaloc') in essential hypertension: a comparison between the individual drugs. *Curr. Ther. Res.*, **29**, 387–394.

BENGTSSON, C. (1979). Metoprolol and hydrochlorothiazide in fixed combination in the treatment of arterial hypertension. *Curr. Ther. Res.*, **26**, 394–401.

BLAUSTEIN, M.P. & HAMLYN, J.M. (1984). Sodium transport inhibition, cell calcium, and hypertension. The natriuretic hormone/Na^+-Ca^{2+} exchange/hypertension hypothesis. *Am. J. Med.*, **5**, 45–59.

BOLLI, P., FERNANDEZ, P.G. & BÜHLER, F.R. (1990). Beta-blockers in the treatment of hypertension. In: *Hypertension: Pathophysiology, Diagnosis, and Management*. ed. Laragh, J.H. & Brenner, B.M. pp. 2181–2208. New York: Raven Press Ltd.

CHAN, E.L.P., HO, C.S., MACDONALD, D., HO, S.C., CHAN, T.Y.K. & SWAMINATHAN, R. (1992). Interrelationships between urinary sodium, calcium, hydroxyproline and serum PTH in healthy subjects. *Acta Endocrinol.*, **127**, 242–245.

CHRISTENSEN, K.L., JESPERSEN, L.T. & MULVANY, M.J. (1989). Development of blood pressure in spontaneously hypertensive rats after withdrawal of long-term treatment related to vascular structure. *J. Hypertens.*, **7**, 83–90.

ERWTEMAN, T.M., NAGELKERKE, N., LUBSEN, J., KOSTER, M. & DUNNING, A.J. (1984). β-blockade, diuretics, and salt restriction for the management of mild hypertension: a randomised double blind trial. *Br. Med. J.*, **289**, 406–409.

FIELDS, N.G., YUAN, B. & LEENEN, F.H.H. (1991). Sodium-induced cardiac hypertrophy. Cardiac sympathetic activity versus volume load. *Circ. Res.*, **68**, 745–755.

FUJITA, T. & ANDO, K. (1984). Hemodynamic and endocrine changes associated with potassium supplementation in sodium-loaded hypertensives. *Hypertension*, **6**, 184–192.

HAMLYN, J.M., RINGEL, R., SCHAEFFER, J., LEVINSON, P.D., HAMILTON, B.P., KOWARSKI, A.A. & BLAUSTEIN, M.P. (1982). A circulating inhibitor of ($Na^+ + K^+$)ATPase associated with essential hypertension. *Nature*, **300**, 650–652.

KARPPANEN, H. (1989). New oral salt in treatment of high blood pressure. *Magnesium*, **8**, 274–287.

LAAKSO, J.T., TIKKANEN, H. & MICHELSSON, J.-E. (1991). Element concentrations in normal and immobilization-induced necrotic rabbit muscles. *Trace Elem. Med.*, **8**, 34–42.

LAW, M.R., FROST, C.D. & WALD, N.J. (1991). By how much does dietary salt reduction lower blood pressure? I- Analysis of observational data among populations. *Br. Med. J.*, **302**, 811–815.

LINDENMAYER, G.E. & SCHWARTZ, A. (1973). Nature of the transport adenosine triphosphatase digitalis complex. *J. Biol. Chem.*, **248**, 1291–1300.

LINDPAINTNER, K. & SEN, S. (1985). Role of sodium in the hypertensive cardiac hypertrophy. *Circ. Res.*, **57**, 610–617.

LJUNG, B., ÅBLAD, B., ALMGREN, O., DAHLÖF, C.-G. & ERIKSSON, B.-M. (1978). Effects of metoprolol on adrenergic mechanisms during long- and short term antihypertensive treatment of spontaneously hypertensive rats. *Acta Physiol. Scand.*, **625**, 36–40.

LJUNG, B., ÅBLAD, B., DREWS, L., FELLENIUS, E., KJELLSTEDT, A. & WALLBORG, M. (1976). Anti-hypertensive effect of metoprolol in spontaneously hypertensive rats. *Clin. Sci. Mol. Med.*, **51**, S443–S445.

MACGREGOR, G.A., MARKANDU, N.D., SINGER, D.R., CAPPUCCIO, F.P. & SHORE, A.C. (1987). Moderate sodium restriction with angiotensin converting enzyme inhibitor in essential hypertension: a double blind study. *Br. Med. J.*, **294**, 531–534.

MATTHEWS, J.N.S., ALTMAN, D.G., CAMPBELL, M.J. & ROYSTON, P. (1990). Analysis of serial measurements in medical research. *Br. Med. J.*, **300**, 230–235.

MCCORMICK, C.P., RAUCH, A.L. & BUCKALEW, V.M.J. (1989). Differential effect of dietary salt on renal growth in Dahl salt-sensitive and salt-resistant rats. *Hypertension*, **13**, 122–127.

MEGGS, L.G., BEN-ARI, J., GAMMON, D. & GOODMAN, A.I. (1988). Myocardial hypertrophy: the effect of sodium and the role of sympathetic nervous system activity. *Am. J. Hypertens.*, **1**, 11–15.

MERVAALA, E.M.A., HIMBERG, J.-J., LAAKSO, J., TUOMAINEN, P. & KARPPANEN, H. (1992). Beneficial effects of a potassium- and magnesium-enriched salt alternative. *Hypertension*, **19**, 535–540.

MERVAALA, E.M.A., LAAKSO, J., HIMBERG, J.-J. & KARPPANEN, H. (1994a). Replacement of regular salt by a noval salt alternative improves the cardiovascular effects of the ACE enalapril. *Hypertension Res.*, (in press).

MERVAALA, E.M.A., PAAKKARI, I., LAAKSO, J., NEVALA, R., TERÄVÄINEN, T., FYHRQUIST, F., VAPAATALO, H. & KARPPANEN, H. (1994b). Replacement of salt by a novel potassium- and magnesium-enriched salt alternative improves the cardiovascular effects of ramipril. *Br. J. Pharmacol.*, (in press).

MUNTZEL, M. & DRUEKE, T. (1992). A comprehensive review of the salt and blood pressure relationship. *Am. J. Hypertens.*, **5**, 1–42.

NEED, A.G., MORRIS, H.A., CLEGHORN, D.B., DE NICHILO, D., HOROWITZ, M. & NORDIN, B.E.G. (1991). Effect of salt restriction on urine hydroxyproline excretion in postmenopausal women. *Arch. Int. Med.*, **151**, 757–759.

OKAMOTO, K., YAMORI, Y. & NAGAOKA, A. (1974). Establishment of the stroke-prone spontaneously hypertensive rat (SHR). *Circ. Res.*, **34/35**, (Suppl I), 143–153.

OPARIL, S., CHEN, Y.-F., YANG, R.-H., JIN, H., MENG, Q.C., CRAGOE, E.J. & WYSS, J.M. (1989). The neuronal basis of salt sensitivity. In: *Salt and Hypertension*. ed. Rettig, R., Ganten, D. & Luft, F. pp. 83–96. Berlin-Heidelberg: Springer-Verlag.

OPARIL, S., MENG, Q.C., CHEN, Y.-F., YANG, R.-H., JIN, H. & WYSS, J.M. (1988). Genetic basis of NaCl-sensitive hypertension. *J. Cardiovasc. Pharmacol.*, **12**, S56–S69.

ÖSTMAN-SMITH, I. (1981). Cardiac sympathetic nerves as the final common pathway in the induction of adaptive cardiac hypertrophy. *Clin. Sci.*, **61**, 265–272.

OWENS, C.J. & BRACKETT, N.C. (1978). Role of sodium intake in the antihypertensive effect of propranolol. *Southern Med. J.*, **71**, 43–46.

PECKER, M.S. (1990). Pathophysiologic effects and strategies for long-term diuretic treatment of hypertension. In: *Hypertension: Pathophysiology, Diagnosis, and Management*. ed. Laragh, J.H. & Brenner, B.M. pp. 2143–2167. New York: Raven Press Ltd.

PÖRSTI, I., WUORELA, H., ARVOLA, P., SÄYNÄVÄLAMMI, P., NURMI, A.-K., HUHTALA, H., LAIPPALA, P. & VAPAATALO, H. (1990). Effects of calcium and deoxycorticosterone on blood pressure, plasma renin activity and vascular reactivity in spontaneously hypertensive rats. *Clin. Exp. Hypertens,*, **A12**, 1159–1174.

RAM, C.V.S., GARRETT, B.N. & KAPLAN, N.M. (1981). Moderate sodium restriction and various diuretics in the treatment of hypertension. Effects of potassium wastage and blood pressure control *Arch. Int. Med.*, **141**, 1015–1019.

SAMIZADEH, A., LOSSE, H. & WESSELS, F. (1977). Einfluß von Kochsalz und Beta-Sympathikolytica auf den Blutdruckverlauf der erblichen spontanen Hypertonie der Ratte. *Med. Welt.*, **28**, 2050–2054.

SAPIRSTEIN, L.A., BRANDT, W.L. & DRURY, D.R. (1950). Production of hypertension in the rat by substituting hypertonic sodium chloride solutions for drinking water. *Proc. Soc. Exp. Biol. Med.*, **73**, 82–85.

SHORTT, C. & FLYNN, A. (1990). Sodium-calcium inter-relationships with specific reference to osteoporosis. *Nutr. Rev.*, **3**, 101–115.

SUDHIR, K., KURTZ, T.W., YOCK, P.G., CONNOLLY, A.J. & MORRIS, R.C.J. (1993). Potassium preserves endothelial function and enhances aortic compliance in Dahl rats. *Hypertension*, **22**, 315–322.

SUGIMOTO, T., TOBIAN, L. & GANGULI, M.C. (1988). High potassium diets protect against dysfunction of endothelial cells in stroke-prone spontaneously hypertensive rats. *Hypertension*, **11**, 579–585.

SUPPA, G., POLLAVINI, F., ALBERTI, D., SAVONITTO, S. & THE ITALIAN GROUP FOR THE PREVENTION AND CARE OF ARTERIAL HYPERTENSION (GIPCIA) (1988). Effects of a low-sodium high-potassium salt in hypertensive patients treated with metoprolol: a multicentre study. *J. Hypertens.*, **6**, 787–790.

TOBIAN, L. (1988). Potassium and sodium in hypertension: the Volhard Lecture. *J. Hypertens.*, **6** (suppl 4), 12–24.

TOBIAN, L., LANGE, J., ULM, K., WOLD, L. & IWAI, J. (1985). Potassium reduces cerebral hemorrhage and death rate in hypertensive rats, even when blood pressure is not lowered. *Hypertension*, **7** (suppl-I), 110–114.

TSUDA, K. & MASUYAMA, Y. (1991). Inhibition of norepinephrine release from vascular adrenergic neurons by oral administration of β-blocker in DOCA-salt hypertension. *Am. J. Hypertens.*, **4**, 68–71.

VAPAATALO, H.I., LAHOVAARA, S. & HACKMAN, R. (1970). Studies with renal hypertensive rats. *Ann. Med. Exp. Fenn.*, **48**, 28-32.

WAEBER, B., NUSSBERGER, J. & BRUNNER, H.R. (1990). Angiotensin-converting-enzyme inhibitors in hypertension. In: *Hypertension: Pathophysiology, Diagnosis and Management*. ed. Brenner, B.M. & Laragh, J.H. pp. 2209–2232. New York: Raven Press Ltd.

WEISS, L. & LUNDGREN, Y. (1978). Left ventricular hypertrophy and its reversability in young spontaneously hypertensive rats. *Cardiovasc. Res.*, **12**, 635–638.

WILSON, R.B., SMITH, D.M. & NEWBERNE, P.M. (1973). Excess sodium chloride intake in neonatal rats. *Arch. Pathol.*, **96**, 372–376.

WUORELA, H., PÖRSTI, I., ARVOLA, P., MÄKYNEN, H. & VAPAATALO, H. (1992). Three levels of dietary calcium-effects on blood pressure and electrolyte balance in spontaneously hypertensive rats. *Naunyn-Schmied. Arch. Pharmacol.*, **346**, 542–549.

YAMORI, Y., HORIE, R., AKIGUCHI, I., KIHARA, M., NARA, Y. & LOVENBERG, W. (1982). Symptomatological classification in the development of stroke in stroke-prone spontaneously hypertensive rats. *Jpn. Circ. J.*, **46**, 274–283.

YOUNG, D.B., MCCAA, R.E., PAN, Y.-J. & GUYTON, A.C. (1976). The natriuretic and hypotensive effects of potassium. *Circ. Res.*, **38**, 84–89.

(Received November 25, 1993
Revised February 3, 1994
Accepted February 10, 1994)

Br. J. Pharmacol (1994), **112**, 649–653

Effects of glibenclamide on systemic and splanchnic haemodynamics in conscious rats

[1]Richard Moreau, Hirokazu Komeichi, Philippe Kirstetter, Song Yang, *Brigitte Aupetit-Faisant, Stéphane Cailmail & Didier Lebrec

Laboratoire d'Hémodynamique Splanchnique, Unité de Recherches de Physiopathologie Hépatique, INSERM U-24, Hôpital Beaujon, 92118 Clichy, France and *Service de Biochimie, CHU Pitié-Salpétrière, 75634 Paris, Cedex 13, France

1 The effects of the sulphonylurea, glibenclamide (20 mg kg^{-1}, i.v.), at a dose that blocks vascular potassium channels, on systemic and splanchnic haemodynamics (radioactive microspheres) were studied in conscious rats.

2 Glibenclamide significantly decreased cardiac index and hepatic artery blood flow while it significantly increased vascular resistance in systemic, portal and hepatic arterial territories.

3 In rats with suppressed cardiovascular reflexes, glibenclamide induced vasoconstriction in systemic, portal and hepatic arterial territories.

4 Intracerebroventricular administration of glibenclamide did not alter systemic or regional vascular tone.

5 Glibenclamide blunted the vasodilator effect of the potassium channel opener, diazoxide but not that of the L-type calcium channel blocker, nicardipine.

6 Another sulphonylurea, glipizide (20 mg kg^{-1}, i.v.), induced significant systemic and splanchnic vasoconstriction.

7 Thus, the glibenclamide-induced blockade of vascular potassium channels caused a vasoconstriction in the systemic and splanchnic vascular beds. In these territories, therefore, the opening of glibenclamide-sensitive potassium channels might be responsible for a basal vasodilator tone.

Keywords: Glibenclamide; glipizide; sulphonylurea; K^+-channels; vascular tone

Introduction

While the vasodilator effect of potassium channel openers, such as cromakalim or diazoxide has been clearly established (Quast & Cook, 1989; Weston & Edwards, 1991), the vascular effect of the sulphonylureas, such as glibenclamide, which are potassium channel blockers, is unclear. On one hand, since it has been shown that glibenclamide inhibits the vasodilator effect of potassium channel openers (Wilson *et al.*, 1988; Buckingham *et al.*, 1989; Quast & Cook, 1989; Winquist *et al.*, 1989), glibenclamide *per se* may be a vasoconstrictor. On the other hand, it has been shown that glibenclamide *per se* has no effect on vascular tone *in vitro* or *in vivo* at doses that block the effects of cromakalim administration (Buckingham *et al.*, 1989; Quast & Cook, 1989). In these latter studies, however, the *in vivo* effects of glibenclamide were assessed by measuring blood pressure and not vascular resistance (Buckingham *et al.*, 1989; Quast & Cook, 1989). Moreover, since the work by Quast & Cook (1989) was performed in anaesthetized rats, anaesthesia might have altered the response to this substance. Elucidation of the vascular effects of glibenclamide is important since if this substance is shown to be a vasoconstrictor, this would suggest that potassium channels play a role in the control of basal vascular tone. Therefore, the aim of the present study was to examine the effects of glibenclamide administration on the systemic and splanchnic haemodynamics of conscious rats.

Methods

Animals

Sixty-three adult male Sprague-Dawley rats (Charles River Laboratories, Saint-Aubin-Lès-Elbeuf, France) were used in the present study. All rats were caged and allowed free access to food and water until 14–16 h before the study, when food was withdrawn. Protocols performed in this laboratory were approved by the French Agricultural Office in conformity with European legislation for research involving animals.

Protocols

Protocol 1 Eight sets of experiments were carried out to examine haemodynamic responses to: a sulphonylurea alone (glibenclamide or glipizide), a combination of glibenclamide and a potassium channel opener, a combination of glibenclamide and an L-type calcium channel blocker. (1) Haemodynamic values were measured prior to and 20 min after the administration of glibenclamide (20 mg kg^{-1}, i.v. bolus) (Quast & Cook, 1989; Cavero *et al.*, 1989; Buckingham *et al.*, 1989) in 8 rats. Plasma glucose concentrations were measured at the same time as the haemodynamic values; (2) haemodynamic values were measured prior to and 20 min after the administration of the vehicle of glibenclamide in 7 rats; (3) haemodynamic values were measured prior to and 20 min after the administration of glipizide (20 mg kg^{-1}) in 8 rats; (4) haemodynamic values were measured prior to and 10 min after the administration of the potassium channel opener, diazoxide (30 mg kg^{-1}, i.v. bolus) (Quast & Cook, 1989) in 6 rats; (5) haemodynamic values were measured prior to and 10 min after the administration of diazoxide in 6 rats pretreated with glibenclamide (in these animals, diazoxide was given 10 min after the administration of glibenclamide); (6) haemodynamic values were measured prior to and 10 min after the administration of the L-type calcium channel blocker, nicardipine (1 mg kg^{-1}, i.v. bolus) (Guc *et al.*, 1990) in 6 rats; (7) haemodynamic values were measured prior to and 10 min after the administration of nicardipine in 6 rats pretreated with glibenclamide (in these animals, nicardipine was given 10 min after the administration of glibenclamide);

[1] Author for correspondence.

(8) the last set of experiments was performed to examine whether the haemodynamic response to glibenclamide was related to a central effect of this substance. For this, haemodynamic values were measured prior to and 20 min after the intracerebroventricular administration (Wright *et al.*, 1986) of glibenclamide (1 mg kg^{-1}) in 4 rats.

Protocol 2 This set of experiments was carried out to examine whether the haemodynamic response to glibenclamide was related to cardiovascular reflexes. For this, haemodynamic values were measured prior to and 20 min after the administration of glibenclamide (20 mg kg^{-1}) in 6 rats in which cardiovascular reflexes were suppressed. This suppression was achieved by the administration of a combination of: hexamethonium [three bolus injections (total dose: 15 mg kg^{-1}), followed by a 0.45 mg kg^{-1} min^{-1} infusion throughout the experiment], atropine methyl bromide (0.005 mg kg^{-1} min^{-1} infusion throughout the experiment), the α_1-adrenoceptor blocker, prazosin (1 mg kg^{-1}, i.v.), and the non selective β-adrenoceptor blocker, propranolol (0.4 mg kg^{-1} for 10 min). Glibenclamide was administered 20 min after the start of the hexamethonium infusion.

Protocol 3 Plasma corticosterone concentrations were measured 24 h after surgery in 3 rats to verify whether animals had fully recovered from surgery. In addition, these plasma concentrations were measured in 3 rats which did not undergo surgery.

Haemodynamic measurements

Twenty-four hours before haemodynamic measurements, catheters were inserted under light diethyl ether anaesthesia. A catheter was inserted in a femoral vein to give drugs (see above). Arterial pressure and heart rate were measured using a catheter inserted into a femoral artery. Portal pressure was measured via a catheter inserted into the portal vein. Briefly, the abdomen was opened and a polypropylene catheter (0.7 mm of diameter) was inserted into a small ileal vein and gently advanced to the bifurcation of the superior mesenteric and the splenic veins. The abdominal incision was closed with catgut. The left ventricle was cannulated via the right carotid artery. All catheters were attached to the external vascular walls and then tunneled subcutaneously to the back of the neck. Haemodynamic studies were performed in conscious unrestrained rats. Cardiac index and regional blood flows were measured by the radioactive microsphere method and the reference sample method as previously described (Lee *et al.*, 1985). For the first set of haemodynamic measurements, a precounted aliquot of approximately 60,000, 16 ± 1 μm diameter, ^{141}Ce-labelled microspheres (sp. act. 10 mCi/g; New England Nuclear, Boston, MA), suspended in Ficoll 70 (10% Pharmacia Fine Chemicals AB, Uppsala, Sweden) and Tween 80 (0.01%) and ultrasonically agitated, was injected into the ventricular catheter and flushed with 1 ml of isotonic saline for 45 seconds. During microsphere injection, a reference blood sample was drawn from the catheter in the femoral artery into a motor-driven syringe at 0.8 ml min^{-1} for 1 min. For the set of second haemodynamic measurements, an injection of ^{113}Sn-labelled microspheres was given and the same technique was used. The animal was then killed with an overdose of pentobarbitone sodium. Individual organs were dissected and placed in separate tubes for counting with a gamma-counter (Computer Gamma G 4000; Kontron, Montigny-Le-Bretonneux, France) at energy settings of 70–210 and 280–1000 keV for ^{113}Sn and ^{141}Ce, respectively. Errors due to the spillover of the ^{113}Sn and ^{141}Ce channel were corrected using ^{113}Sn and ^{141}Ce standards. Adequate microsphere mixing was assumed with a difference $<10\%$ between the left and right kidneys. Cardiac index (CI) was calculated by the following formula: CI (ml min^{-1} 100 g^{-1}) = [radioactivity injected (c.p.m./reference blood sample radioactivity (c.p.m.)] × [100/body wt (g)] × 0.8 (ml min^{-1}). Systemic vascular resistance (SVR) was calculated by the following formula: SVR [(dyn s cm^{-5} 100 g) × 10^3] = mean arterial pressure (mmHg) × 80/Cl (ml min^{-1} 100 g^{-1}). Regional blood flows were calculated by the following formula: organ blood flow (ml min^{-1} 100 g^{-1}) = [organ radioactivity (c.p.m.)/radioactivity injected (c.p.m.)] × Cl (ml min^{-1} 100 g^{-1}). Portal tributary blood flow was calculated as the sum of stomach, intestine, colon, spleen, and mesenteric-pancreas blood flows. Portal territory vascular resistance (PTVR) was calculated by the following formula: PTVR [(dyn s cm^{-5} 100 g) × 10^3] = [mean arterial pressure (mmHg) − portal pressure (mmHg)] × 80/portal tributory blood flow (ml min^{-1} 100 g^{-1}). Hepatic artery vascular resistance (HAVR) was calculated by the following formula: HAVR [(dyn s cm^{-5} 100 g) × 10^5] = mean arterial pressure (mmHg) × 80/hepatic artery blood flow (ml min^{-1} 100 g^{-1}).

Other measurements

Arterial (femoral artery) plasma glucose concentrations were measured by a glucose oxidase method (Trinder, 1969). Plasma corticosterone concentrations were determined in duplicate by a radioimmunoassay method using rabbit polyclonal antibodies (Aupetit-Faisant *et al.*, 1993).

Drugs

Glibenclamide and diazoxide were purchased from Sigma Chemical (St. Louis, MO, U.S.A.). Nicardipine was purchased from Sandoz Laboratory (Division Sandoz, Laboratoires Sandoz S.A.R.L., Rueil-Malmaison, France). Thirty mg of glibenclamide was dissolved in 1 ml 0.1 N NaOH + 4 ml 5% dextrose. Thirty mg of diazoxide was dissolved in 300 μl *N,N*-dimethyl-formamide. Ten mg of nicardipine was diluted in 10 ml of sterile water (pH 3.5).

Statistical analysis

Values are expressed as the means ± s.e.mean. Results were analyzed by one-way analysis of variance. $P<0.05$ was considered significant.

Results

Twenty-four hours after surgery, plasma corticosterone concentrations were 184 ± 7 ng ml^{-1}. These concentrations were 190 ± 17 ng ml^{-1} in animals which did not undergo surgery. At the time of haemodynamic studies rats weighed 321 ± 7 g. Glibenclamide alone significantly decreased the cardiac index (17%) and hepatic artery blood flow (43%) while it increased systemic vascular resistance (31%), portal territory vascular resistance (35%) and hepatic artery vascular resistance (114%) (Table 1). Plasma glucose concentrations were not significantly affected by glibenclamide administration [1.04 ± 0.02 g l^{-1} (i.e., 5.8 ± 0.1 mmol l^{-1}) and 1.16 ± 0.09 g l^{-1} (i.e., 6.4 ± 0.5 mmol l^{-1}) before and after glibenclamide, respectively]. The vehicle did not change systemic and regional haemodynamics (Table 1).

Diazoxide alone significantly increased cardiac index and significantly decreased arterial pressure, and systemic and hepatic artery vascular resistances (Table 2). In rats which received a combination of glibenclamide and diazoxide, arterial pressure, cardiac index, systemic and hepatic artery vascular resistances did not change (Table 2).

Nicardipine alone significantly increased cardiac index and significantly decreased arterial pressure, and systemic and portal territory vascular resistance (Table 3). In rats which received a combination of glibenclamide and nicardipine the cardiac index significantly increased while arterial pressure and systemic vascular resistance significantly decreased (Table 3).

In rats with suppressed cardiovascular reflexes, gliben-

Table 1 Effects of glibenclamide or vehicle on haemodynamics in conscious normal rats

	Glibenclamide ($n = 8$)		*Vehicle* ($n = 7$)	
	Baseline	*After*	*Baseline*	*After*
Heart rate (beats min^{-1})	381 ± 12	371 ± 9	390 ± 10	407 ± 11
Mean arterial pressure (mmHg)	103 ± 2	107 ± 4	100 ± 3	104 ± 4
Cardiac index (ml min^{-1} 100 g^{-1})	28.1 ± 2.5	22.9 ± 2.3*	31.5 ± 3.1	31.5 ± 2.7
Stroke volume index (μl 100 g^{-1})	74 ± 6	62 ± 6*	80 ± 7	77 ± 5
Systemic vascular resistance (10^3 × dyn s cm^{-5} 100 g)	308 ± 30	393 ± 32*	267 ± 23	274 ± 20
Portal tributary blood flow (ml min^{-1} 100 g^{-1})	4.6 ± 0.6	3.6 ± 0.4	6.0 ± 0.8	5.3 ± 0.6
Portal territory vascular resistance (10^3 × dyn s cm^{-5} 100 g)	1875 ± 247	2379 ± 229*	1339 ± 172	1539 ± 159
Hepatic artery blood flow (ml min^{-1} 100 g^{-1})	1.33 ± 0.32	0.65 ± 0.15*	1.37 ± 0.38	1.34 ± 0.28
Hepatic artery vascular resistance (10^5 × dyn s cm^{-5} 100 g)	104 ± 29	179 ± 34*	81 ± 18	77 ± 13

Values are means ± s.e. Animals received 20 mg kg^{-1} glibenclamide (i.v. bolus). Vehicle contained 0.1 N NaOH and 5% dextrose.
*Significantly different from baseline: $P < 0.05$.

Table 2 Effects of diazoxide or glibenclamide plus diazoxide on haemodynamics in conscious normal rats

	Diazoxide ($n = 6$)		*Glibenclamide + diazoxide* ($n = 6$)	
	Baseline	*After*	*Baseline*	*After*
Heart rate (beats min^{-1})	367 ± 10	541 ± 30*	406 ± 21	425 ± 12
Mean arterial pressure (mmHg)	101 ± 3	80 ± 2*	111 ± 3	112 ± 3
Cardiac index (ml min^{-1} 100 g^{-1})	24.3 ± 1.6	37.5 ± 1.7*	22.8 ± 1.0	22.6 ± 1.9
Stroke volume index (μl 100 g^{-1})	66 ± 4	71 ± 7	57 ± 4	53 ± 4
Systemic vascular resistance (10^3 × dyn s cm^{-5} 100 g)	339 ± 27	173 ± 12*	386 ± 15	405 ± 19
Portal tributary blood flow (ml min^{-1} 100 g^{-1})	5.4 ± 0.5	5.7 ± 0.7	5.0 ± 0.4	3.4 ± 0.5*
Portal territory vascular resistance (10^3 × dyn s cm^{-5} 100 g)	1483 ± 211	1067 ± 162	1691 ± 171	2741 ± 325*
Hepatic artery blood flow (ml min^{-1} 100 g^{-1})	1.23 ± 0.12	1.54 ± 0.13	0.86 ± 0.26	0.66 ± 0.17
Hepatic artery vascular resistance (10^5 × dyn s cm^{-5} 100 g)	72 ± 7	43 ± 4*	147 ± 32	177 ± 36

Values are means ± s.e. Doses were 20 mg kg^{-1} (i.v. bolus) for glibenclamide and 30 mg kg^{-1} (i.v. bolus) for diazoxide.
*Significantly different from baseline: $P < 0.05$.

Table 3 Effects of nicardipine or glibenclamide plus nicardipine on haemodynamics in conscious normal rats

	Nicardipine ($n = 6$)		*Glibenclamide + nicardipine* ($n = 6$)	
	Baseline	*After*	*Baseline*	*After*
Heart rate (beats min^{-1})	387 ± 18	524 ± 29*	377 ± 12	534 ± 30*
Mean arterial pressure (mmHg)	109 ± 4	84 ± 4*	112 ± 4	75 ± 4*
Cardiac index (ml min^{-1} 100 g^{-1})	32.7 ± 1.5	46.3 ± 6.3*	24.3 ± 0.9	35.8 ± 2.6*
Stroke volume index (μl 100 g^{-1})	85 ± 4	90 ± 13	65 ± 4	67 ± 3
Systemic vascular resistance (10^3 × dyn s cm^{-5} 100 g)	270 ± 16	153 ± 14*	373 ± 27	171 ± 9*
Portal tributary blood flow (ml min^{-1} 100 g^{-1})	4.7 ± 0.3	6.1 ± 0.9	4.9 ± 0.7	3.7 ± 0.6
Portal territory vascular resistance (10^3 × dyn s cm^{-5} 100 g)	1816 ± 183	1074 ± 141*	1902 ± 284	1580 ± 251
Hepatic artery blood flow (ml min^{-1} 100 g^{-1})	1.28 ± 0.39	1.46 ± 0.22	0.90 ± 0.09	1.00 ± 0.07
Hepatic artery vascular resistance (10^5 × dyn s cm^{-5} 100 g)	101 ± 24	49 ± 5	105 ± 12	61 ± 4

Values are means ± s.e. Doses were 20 mg kg^{-1} (i.v. bolus) for glibenclamide and 1 mg kg^{-1} (i.v. bolus) for nicardipine.
*Significantly different from baseline: $P < 0.05$.

Table 4 Effects of glibenclamide on haemodynamics in conscious rats in which cardiovascular reflexes were suppressed ($n = 6$)

	Baseline	*After glibenclamide*
Heart rate (beats min^{-1})	400 ± 8	311 ± 16
Mean arterial pressure (mmHg)	77 ± 4	92 ± 2*
Cardiac index (ml min^{-1} 100 g^{-1})	31.0 ± 1.6	28.6 ± 1.4*
Stroke volume index (μl 100 g^{-1})	100 ± 4	93 ± 4
Systemic vascular resistance (10^3 × dyn s cm^{-5} 100 g)	201 ± 10	261 ± 11*
Portal tributary blood flow (ml min^{-1} 100 g^{-1})	4.8 ± 0.2	4.1 ± 0.3*
Portal territory vascular resistance (10^3 × dyn s cm^{-5} 100 g)	1209 ± 70	1724 ± 135*
Hepatic artery blood flow (ml min^{-1} 100 g^{-1})	1.96 ± 0.15	0.63 ± 0.13*
Hepatic artery vascular resistance (10^5 × dyn s cm^{-5} 100 g)	32 ± 2	143 ± 26*

Values are means ± s.e. Animals received 20 mg kg^{-1} glibenclamide (i.v. bolus) and were pretreated with a combination of hexamethonium (15 mg kg^{-1} i.v. bolus + 0.45 mg kg^{-1} min^{-1} infusion), methyl atropine bromide (0.005 mg kg^{-1} min^{-1}), prazosin (1 mg kg^{-1} min^{-1} i.v. bolus), propranolol (0.4 mg min^{-1} for 10 min).
*Significantly different from baseline: $P < 0.05$.

Table 5 Effects of intracerebroventricular administration of glibenclamide on haemodynamics in conscious rats ($n = 4$)

	Baseline	*After glibenclamide*
Heart rate (beats min^{-1})	385 ± 10	395 ± 10
Mean arterial pressure (mmHg)	111 ± 8	112 ± 6
Cardiac index (ml min^{-1} 100 g^{-1})	26.5 ± 1.6	27.5 ± 1.8
Stroke volume index (μl 100 g^{-1})	69 ± 5	70 ± 5
Systemic vascular resistance (10^3 × dyn s cm^{-5} 100 g)	339 ± 36	333 ± 36
Portal tributary blood flow (ml min^{-1} 100 g^{-1})	3.8 ± 0.4	3.3 ± 0.2
Portal territory vascular resistance (10^3 × dyn s cm^{-5} 100 g)	2349 ± 480	2581 ± 235
Hepatic artery blood flow (ml min^{-1} 100 g^{-1})	1.46 ± 0.32	1.87 ± 0.20
Hepatic artery vascular resistance (10^5 × dyn s cm^{-5} 100 g)	70 ± 14	50 ± 4

Values are means ± s.e. Animals received 1 mg kg^{-1} glibenclamide.

Table 6 Effects of glipizide on haemodynamics in conscious rats ($n = 8$)

	Baseline	*After glipizide*
Heart rate (beats min^{-1})	364 ± 13	359 ± 15
Mean arterial pressure (mmHg)	95 ± 3	110 ± 5*
Cardiac index (ml min^{-1} 100 g^{-1})	39.4 ± 3.2	35.2 ± 3.8
Stroke volume index (μl 100 g^{-1})	108 ± 8	101 ± 12
Systemic vascular resistance (10^3 × dyn s cm^{-5} 100 g)	205 ± 21	277 ± 37*
Portal tributary blood flow (ml min^{-1} 100 g^{-1})	7.7 ± 0.7	6.7 ± 0.8
Portal territory vascular resistance (10^3 × dyn s cm^{-5} 100 g)	1070 ± 188	1366 ± 185*
Hepatic artery blood flow (ml min^{-1} 100 g^{-1})	0.97 ± 0.18	0.46 ± 0.07*
Hepatic artery vascular resistance (10^5 × dyn s cm^{-5} 100 g)	102 ± 20	223 ± 34*

Values are means ± s.e. Animals received 20 mg kg^{-1} glipizide (i.v. bolus).
*Significantly different from baseline: $P < 0.05$.

clamide significantly decreased cardiac index, portal tributary blood flow and hepatic artery blood flow while it significantly increased arterial pressure and vascular resistance in the portal, hepatic artery, and systemic territories (Table 4).

Intracerebroventricular administration of glibenclamide did not significantly change regional and systemic haemodynamics (Table 5).

Glipizide administration significantly increased arterial pressure (16%) and vascular resistance in systemic, portal, and hepatic artery territories (35%, 35% and 149%, respectively) (Table 6).

Discussion

This study examined the haemodynamic responses to glibenclamide administration in conscious rats. These animals had fully recovered from surgery since they had no increase in plasma corticosterone concentrations. This result confirms previous findings which showed that normal rats had fully recovered from surgery 24 h after the operation (Fenoy *et al.*, 1989; Harrison-Bernard *et al.*, 1991). The finding that plasma glucose concentrations were not altered following glibenclamide differs from previous results which showed that a same dose of this substance induced hypoglycaemia (Quast & Cook, 1989). Since the vehicle of glibenclamide contained glucose in the present study, and not in the previous one, the discrepancy between the studies might be related to the composition of the vehicle. On the other hand, glibenclamide induced systemic vasoconstriction but did not increase arterial pressure. The lack of vasopressor effect was due to a decrease in cardiac index (related to a reduction in stroke volume). These findings show that arterial pressure alone cannot be used to assess the vasoconstrictor effect of glibenclamide.

Glibenclamide elicited hepatic arterial vasoconstriction, which, in turn caused a decline in hepatic arterial blood flow. In addition, this substance induced a vasoconstriction in the portal territory which elicited a decrease in portal tributary blood flow. This decrease, however, was not significant.

Since the suppression of cardiovascular reflexes did not abolish glibenclamide-induced systemic and splanchnic vasoconstriction, the vasoconstrictor action of this substance does not appear to be due to an indirect mechanism, i.e., a reflex increase in sympathetic vascular tone. On the other hand, the intracerebroventricular administration of glibenclamide did not alter systemic and regional vascular resistance. Thus, the vasoconstrictor effect of intravenous glibenclamide was not due to an interaction of this substance with central mechanisms which control the cardiovascular system. Taken together, these findings show that glibenclamide elicited vasoconstriction by acting directly on vessels. In fact, this substance has been shown to block vascular potassium channels directly (Standen *et al.*, 1989; Antoine *et al.*, 1992), a result that is confirmed in the present study, and in a previous one (Clapham *et al.*, 1991), by the finding that glibenclamide abolished the vasodilator effect of an opener of vascular potassium channels, diazoxide, but not that of a L-type calcium channel blocker, nicardipine. Consequently, glibenclamide-induced vasoconstriction appears to be the result of the blockade of vascular potassium channels. This view is also supported by the results which showed that glipizide, another sulphonylurea which blocks vascular potassium channels, induced a systemic and splanchnic vasoconstriction. This last result shows that vasoconstriction was not an idiosyncratic action by glibenclamide.

In the pancreatic β-cell, the blockade of potassium channels (i.e., reduction of potassium efflux from the cell) by glibenclamide induces membrane depolarization (Ashcroft, 1988; Boyd, 1992) which then activates L-type calcium channels and allows calcium to enter the cell (Boyd, 1992). A similar mechanism may occur in the smooth muscle cells and account for glibenclamide-induced vasoconstriction. Indeed, membrane depolarization should occur in smooth muscle cells since glibenclamide blocks vascular potassium channels (see above). In addition, glibenclamide administration seems to be associated with the opening of vascular L-type calcium channel since blockade of these channels by dihydropyridines suppressed the vasoconstrictor action of the sulphonylurea in the present study.

Since glibenclamide-induced vasoconstriction was due to a blockade of potassium efflux from the smooth muscle cells, this suggests that under baseline conditions a potassium efflux was responsible for a certain degree of vasorelaxation. In other words, the results of the present study support the existence of a baseline vasodilator tone which is related to the opening of glibenclamide-sensitive potassium channels.

In conclusion, the present study shows that the blockage of potassium channels by glibenclamide induces a vasoconstriction in the systemic and splanchnic territories. These findings suggest that under baseline conditions the opening of glibenclamide-sensitive potassium channels might be responsible for vasodilator tone.

References

ANTOINE, M.H., BERKENBOOM, G., FANG, Z.Y., FONTAINE, J., HERCHUELZ, A. & LEBRUN, P. (1992). Mechanical and ionic response of rat aorta to diazoxide. *Eur. J. Pharmacol.*, **216**, 299–306.

ASHCROFT, F.M. (1988). Adenosine 5'-triphosphate-sensitive potassium channels. *Annu. Rev. Neurosci.*, **11**, 97–118.

AUPETIT-FAISANT, B., BATTAGLIA, C., ZENATTI, M., EMERIC-BLANCHOUIN, N. & LEGRAND, J.C. (1993). Hypoaldosteronism accompanied by normal or elevated mineralocorticosteroid pathway steroid: a marker of adrenal carcinoma. *J. Clin. Endocrinol. Metab.*, **76**, 38–43.

BOYD, A.E. III. (1992). The role of ion channels in insulin secretion. *J. Cell. Biochem.*, **48**, 234–241.

BUCKINGHAM, R.E., HAMILTON, T.C, HOWLETT, D.R., MOOTOO, S. & WILSON, C. (1989). Inhibition of glibenclamide of the vasorelaxant action of cromakalim in the rat. *Br. J. Pharmacol.*, **97**, 57–64.

CAVERO, I., MONDOT, S. & MESTRE, M. (1989). Vasorelaxant effects of cromakalim in rats are mediated by glibenclamide-sensitive potassium channels. *J. Pharmacol. Exp. Ther.*, **248**, 1261–1268.

CLAPHAM, J.C., HAMILTON, T.C., LONGMAN, S.D., BUCKINGHAM, R.E, CAMPBELL, C.A., ILSLEY, G.L. & GOUT, B. (1991). Antihypertensive and haemodynamic properties of the potassium channel activating (−) enantiomer of cromakalim in animal models. *Arzneim. -Forsch.*, **41**, 385–391.

FENOY, F.J., QUESADA, T., GARCIA-SALOM, M., ROMERO, J.C. & SALAZAR, F.J. (1989). Hemodynamic effects of chronic infusion of rANP in renal hypertensive rats. *Am. J. Physiol.*, **256**, H1393–H1398.

GUC, M.O., FURMAN, B.L. & PARRATT, J.R. (1990). Endotoxin-induced impairment of vasopressor and vasodepressor responses in the pithed rat. *Br. J. Pharmacol.*, **101**, 913–919.

HARRISON-BERNARD, L.M., VARI, R.C., HOLLEMAN, W.H., TRIPPODO, N.C. & BARBEE, R.W. (1991). Chronic vs. acute hemodynamic effects of atrial natriuretic factor in conscious rats. *Am. J. Physiol.*, **260**, R247–R254.

LEE, S.S., GIROD, C., VALLA, D., GEOFFROY, P. & LEBREC, D. (1985). Effects of pentobarbital anesthesia on splanchnic hemodynamics of normal and portal-hypertensive rats. *Am. J. Physiol.*, **249**, G528–G532.

QUAST, U. & COOK, N.S. (1989). *In vitro* and *in vivo* comparison of two channel K^+ openers, diazoxide and cromakalim, and their inhibition by glibenclamide. *J. Pharmacol. Exp. Ther.*, **250**, 261–271.

STANDEN, N.B., QUAYLE, J.M., DAVIES, N.W., BRAYDEN, J.E, HUANG, Y. & NELSON, M.T. (1989). Hyperpolarizing vasodilators activate ATP-sensitive K^+ channels in arterial smooth muscle. *Science*, **245**, 177–180.

TRINDER, P. (1969). Determination of glucose in blood using glucose oxidase with an alternative oxygen acceptor. *Annu. Clin. Biochem.*, **6**, 24–27.

WESTON, A.H. & EDWARDS, G. (1991). Latest developments in K-modulator pharmacology. *Z. Cardiol.*, **80**, Suppl. 7, 1–8.

WILSON, C., COLDWELL, M.C., HOWLETT, D.R., COOPER, S.M. & HAMILTON, T.C. (1988). Comparative effects of K channel blockage on the vasorelaxant activity of cromakalim, pinacidil and nicorandil. *Eur. J. Physiol.*, **152**, 331–339.

WINQUIST, R.J., HEANEY, L.A., WALLACE, A.A., BASKIN, E.P., STEIN, R.B., GARCIA, M.L. & KACZOROWSKI, G.J. (1989). Glyburide blocks the relaxation response to BRL 34915 (cromakalim), minoxidil sulfate and diazoxide in vascular smooth muscle. *J. Pharmacol. Exp. Ther.*, **248**, 149–156.

WRIGHT, J.W., SULLIVAN, M.J., QUIRK, W.S., BATT, C.M. & HARDING, J.W. (1987). Heightened blood pressure and drinking responsiveness to intracerebroventricularly applied angiotensins in the spontaneously hypertensive rat. *Brain Res.*, **420**, 289–294.

(Received November 22, 1993
Revised January 24, 1994
Accepted February 14, 1994)

Br. J. Pharmacol. (1994), **112**, 654–658

Metabolic disposition of leukotriene B_4 (LTB_4) and oxidation-resistant analogues of LTB_4 in conscious rabbits

[1]Sylvie Marleau, Nancy Dallaire, Patrice E. Poubelle & [2]Pierre Borgeat

Centre de recherche en Rhumatologie et Immunologie, Centre de recherche du CHUL et Université Laval, 2705 Boulevard Laurier, Québec, Canada, G1V 4G2

1 The kinetics of leukotriene B_4 (LTB_4), after single i.v. injections of doses of 0.1 to 1 $\mu g\,kg^{-1}$, were investigated in conscious rabbits and compared with those of the Ω- and β-oxidation resistant bioactive analogues, 20, 20, 20-trifluoro-LTB_4 (20-F_3-LTB_4) and 3-thio-LTB_4, respectively.

2 Immunoreactive LTB_4 (IR-LTB_4) elimination was first-order, as shown by a constant systemic clearance (Cl_{LTB_4}) and a proportional increase in the area under the curve (AUC) of the plasma concentration versus time curve over the dose-range studied. Our results showed a good correlation between observed steady-state plasma concentrations (Css) of IR-LTB_4 after continuous infusion of LTB_4 and those predicted by using the mean estimated Cl_{LTB_4} of 93 ± 4 ml $min^{-1}\,kg^{-1}$, further confirming the linearity of IR-LTB_4 elimination.

3 The half-life ($t_{\frac{1}{2}}$) or IR-LTB_4 increased from 0.47 ± 0.02 to 0.63 ± 0.04 min as a consequence of a change in the apparent volume of distribution (V_d) from 72 ± 5 to 109 ± 13 ml kg^{-1}, for the 0.1 and 1 $\mu g\,kg^{-1}$ doses injected, respectively.

4 Single i.v. injections of [^{3}H]-LTB_4 (4.7 ng kg^{-1}) were administered, and the decay of plasma [^{3}H]-LTB_4 following h.p.l.c. purification was used to estimate the kinetic parameters. The kinetic parameters of [^{3}H]-LTB_4 were characterized by a mean systemic clearance (Cl) of 96 ± 11 ml $min^{-1}\,kg^{-1}$, a $t_{\frac{1}{2}}$ of 0.53 ± 0.03 min, and an apparent V_d of 85 ± 9 ml kg^{-1}, similar to the parameters obtained after LTB_4 boluses.

5 The disposition of LTB_4 analogues, whether resistant to Ω- or to β-oxidation *in vitro*, did not differ significantly from the disposition of the LTB_4 molecule. The half-lives of 20-F_3-LTB_4 and 3-thio-LTB_4 in the circulation were 0.52 ± 0.07 min and 0.70 ± 0.11 min, respectively.

6 In summary, our results showed that LTB_4, as well as Ω-oxidation- and β-oxidation-resistant analogues were cleared very rapidly from the rabbit circulation and indicate that *in situ*, metabolism in blood is not a rate-limiting factor for the elimination of LTB_4.

Keywords: Leukotriene B_4 (LTB_4) kinetics; oxidation-resistant LTB_4 analogues; LTB_4; conscious rabbit

Introduction

Leukotriene B_4 (LTB_4), a 5-lipoxygenase metabolite of arachidonic acid in leukocytes, stimulates phagocyte functional responses such as chemotaxis, adherence, superoxide anion synthesis and degranulation (Naccache *et al.*, 1989; Ford-Hutchinson, 1990). In support of its putative role in inflammation, increased local concentrations of LTB_4 have been observed in inflammatory conditions, such as purulent peritoneal exudates (Kikawa *et al.*, 1986), inflammatory bowel diseases (Fretland *et al.*, 1990), or psoriatic skin lesions (Brain *et al.*, 1984). Moreover, plasma LTB_4 levels may also be transiently elevated, as observed during reperfusion following hindlimb ischaemia in rodents (Goldman *et al.*, 1992) and rabbits (Welbourn *et al.*, 1990), and during anaphylaxis in guinea-pigs (Lee *et al.*, 1986).

Despite important progress in the characterization of the biological activities of LTB_4, knowledge of the mechanisms regulating its local or systemic levels *in vivo* is limited. On the one hand, it is well documented that Ω-oxidation represents the major metabolic pathway for LTB_4 in human isolated neutrophils (Nadeau *et al.*, 1984; Powell, 1984; Shak & Goldstein, 1984; 1985), although reduction may be favoured in neutrophils from other species (Powell, 1984; Powell & Gravelle, 1990). However, the contribution of these metabolic pathways to the regulation of LTB_4 levels *in vivo* is unclear. Indeed, Gresele *et al.* (1986) found reduced catabolism of LTB_4 in whole blood compared with isolated leukocytes and Taylor & Sun (1985) showed that massive infiltration of neutrophils in the rat pleural cavity did not modify the disappearance of LTB_4 from the chest. On the other hand, rat hepatic and renal microsomal preparations possess Ω- and Ω-1 oxidation activities for LTB_4 (Newton *et al.*, 1985; Romano *et al.*, 1987), and the proposed routes of metabolism of LTB_4 in rat hepatocytes include Ω-oxidation and β-oxidation from the Ω-end of the 20-carboxy-LTB_4 metabolite as well as β-oxidation from the carboxyl end of LTB_4 (Harper *et al.*, 1986). These studies suggest that metabolism in the liver and kidney may be important in the regulation of LTB_4 levels *in vivo*. Accordingly, evaluation of the metabolic disposition of LTB_4 *in vivo* confirmed extensive β-oxidation of LTB_4 in the monkey and the rabbit (Serafin *et al.*, 1984) and intrahepatic Ω-oxidation followed by β-oxidation from the Ω-end in the rat (Hagmann & Korte, 1990), leading mainly to the production of volatile derivatives, with no intact LTB_4 detected in the bile or the urine. In the present study, we provide a detailed kinetic analysis of LTB_4 in conscious rabbits after single i.v. injections of unlabelled or labelled LTB_4 and further document the systemic disposition of Ω- and β-oxidation resistant analogues.

Methods

Animals

Male New Zealand rabbits (2.5–3.5 kg) purchased from Charles River (St. Constant, Québec, Canada) were used

[1] Present address: Faculté de pharmacie, Université de Montréal, C.P. 6128, Succ. A, Montréal, Québec, Canada, H3C 3J7.
[2] Author for correspondence.

throughout the studies. They were maintained in individual cages with free access to food (Purina pellets) and water for at least 5 days before any experimental work was undertaken.

Single injection procedures

The rabbits were placed in restraining cages (Fenco, Boston, MA, U.S.A.); two catheters were installed, one in the marginal vein of an ear (PE-50; Clay Adams, Parsipanny, NJ, U.S.A.) to allow the injection of LTB_4, and one in the central artery of an ear (Butterfly-21; Abbott Ireland LTD., North Chicago, IL, U.S.A.) to allow blood sampling. An infusion of 0.9% NaCl-5% glucose (74:26 v/v) was started at the rate of 23 ml h^{-1} to compensate for fluid loss and for blood volume replacement. After a 60 min stabilization period, LTB_4 was injected i.v. at doses of 0.1, 0.5, or 1 $\mu g\,kg^{-1}$ in 1 ml vehicle. Multiple blood samples (1.2 ml) were withdrawn at $t = -30$ and $t = -5$ before and at $t = 0.5$, 1, 1.5, 2, 3, 5, 8, 12, 16 and 20 min after the bolus. The blood samples were collected in chilled polypropylene tubes containing potassium EDTA (3.7 mM, final concentration) and centrifuged for 10 min at 600 *g* at 4°C. Plasma was collected and kept at − 70°C until assayed for LTB_4. The same blood-sampling intervals were used to assess the decay of LTB_4 analogues in plasma. 20-F_3-LTB_4 was injected at the dose of 0.5 $\mu g\,kg^{-1}$, whereas the dose of the 3-thio-LTB_4 analogue (available in limited quantity) was 0.16 $\mu g\,kg^{-1}$. In the study of LTB_4 radioactive tracer disposition, 0.3 $\mu Ci\,kg^{-1}$ (4.7 ng kg^{-1}) of [14, 15-^{3}H]-LTB_4 was injected.

Analytical methods

Plasma concentration of LTB_4 was determined by enzyme immunoassay (EIA) (Cayman Chemical Co., Ann Arbor, MI, U.S.A.) after reverse-phase h.p.l.c. purification of the samples, as described previously (Marleau *et al.*, 1993). Briefly, protein precipitation in plasma samples (0.4 ml) was accomplished by the addition of 4 vol of ice-cold acetonitrile containing prostaglandin B_2 (PGB_2, 20 ng ml^{-1}) as an internal standard. The supernatants (0.6 ml fractions) were diluted to 2 ml with water and purified by reverse-phase h.p.l.c. (Borgeat *et al.*, 1990). The h.p.l.c. fractions containing LTB_4 or LTB_4 analogues were collected and evaporated under reduced pressure using a Speed-Vac concentrator (Savant Instr., Farmingdale, NY, U.S.A.); the dry residues were dissolved with 50 μl of ethanol and diluted to 1 ml with EIA buffer (0.1 M phosphate buffer, pH 7.4, containing 0.4 M NaCl, 1 mM EDTA, 0.1% BSA and 0.01% sodium azide). The recovery of LTB_4 after extraction from blood and h.p.l.c. purification was 92 ± 10% ($n = 6$) (data not shown). A typical calibration curve for the assay of LTB_4 showed a slope factor of 1.002, an ED_{50} of 38 pg ml^{-1}, and a minimal detectable amount of 9 pg ml^{-1}. Amounts of LTB_4 or LTB_4 analogues in plasma samples were quantified with calibration curves generated with the respective compounds. Plasma samples containing tritiated LTB_4 were deproteinized and purifed by h.p.l.c. as described. Fractions were collected at 1 min intervals, and the radioactivity content was determined by liquid scintillation.

Kinetic determinations

The kinetic parameters were estimated by a nonlinear regression curve-fitting programme (PC-NONLIN) according to an open one-compartment model. The mean basal IR-LTB_4 concentration was subtracted from the IR-LTB_4 concentrations observed after the administration of exogenous LTB_4.

Chemicals

5(S),12(R)-dihydroxy-6,14-*cis*-8,10-*trans*-eicosatetraenoic acid (LTB_4) and 3-thio-LTB_4 were generous gifts from Dr Robert Young (Merck Frost, Pointe-Claire, Québec, Canada), and 20,20,20-trifluoro-5(S), 12(R,S)-dihydroxy-6,14-*cis*-8,10-*trans*-eicosatetraenoic acid (20-F_3-LTB_4) was obtained from Cayman Chemical Co. (Ann Arbor, MI, U.S.A.). Stock solutions of LTB_4 and LTB_4 analogues (200 $\mu g\,ml^{-1}$ in ethanol) were kept at − 20°C and diluted in phosphate buffered saline containing 0.01% bovine serum albumin (BSA) (vehicle) immediately before use. We obtained [14, 15-^{3}H]-LTB_4 (specific activity 21.5 Ci $mmol^{-1}$) from Dupont (Boston, MA, U.S.A.) and BSA (low endotoxin) from Sigma Chemical Company (St. Louis, MO, U.S.A.).

Statistical analysis

The results are expressed as mean ± s.e.mean. Statistical analysis was carried out by one-way analysis of variance, using Dunnett's distribution table to assess statistical significance ($^*P < 0.05$; $^{**}P < 0.01$).

Results

Kinetics of IR-LTB_4 and [^{3}H]-LTB_4 after a single injection

Mean arterial basal IR-LTB_4 plasma concentrations in these groups of conscious rabbits were 0.18 ± 0.03 nM (60.2 ± 9.4 pg ml^{-1}) ($n = 19$). Thirty seconds after LTB_4 injections, arterial IR-LTB_4 concentrations increased to 2.3 ± 0.2 nM and 18.3 ± 3.5 nM ($n = 6$), for the 0.1 and 1.0 $\mu g\,kg^{-1}$ doses, respectively, and rapidly declined to basal levels. The data were analysed according to an open one-compartment model, as the semilogarithmic plots of plasma IR-LTB_4 concentrations versus time showed monoexponential declines until basal concentrations were reached (Figure 1). The kinetic parameters (Table 1) revealed a proportional increase in the area under the curve (AUC) of the plasma concentration versus the time curve function of the dose, resulting in a constant systemic clearance (Cl) over the dose-range studied. However, the apparent volume of distribution (V_d) increased

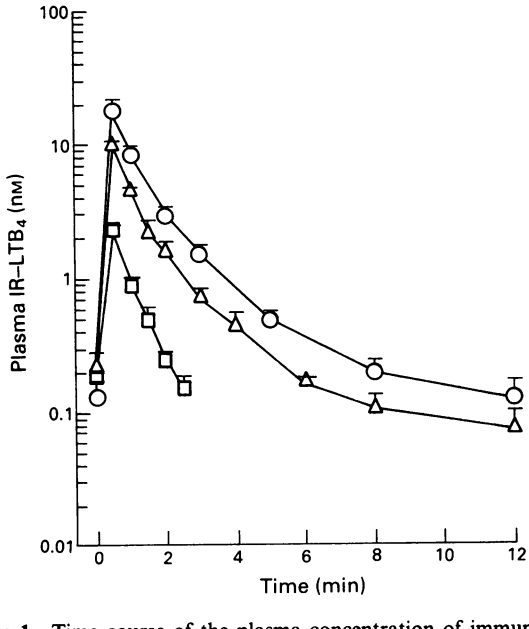

Figure 1 Time course of the plasma concentration of immunoreactive leukotriene B_4 (IR-LTB_4) after a single injection of LTB_4: 0.1 $\mu g\,kg^{-1}$ ($n = 6$) (□); 0.5 $\mu g\,kg^{-1}$ ($n = 7$) (△); 1 $\mu g\,kg^{-1}$ ($n = 6$) (○). The mean basal IR-LTB_4 concentration (0.18 ± 0.03 nM) was subtracted from all IR-LTB_4 concentrations measured. LTB_4 was purified by h.p.l.c. and assayed by ELISA. The results are expressed as mean (± s.e.mean).

Table 1 Kinetic parameters of immunoreactive leukotriene B_4 (IR-LTB_4) after a single i.v. injection of three different doses

Dose ($\mu g\ kg^{-1}$)	*AUC*[a] ($pg\ min\ ml^{-1}$)	Cl_{LTB_4}[b] ($ml\ min^{-1}\ kg^{-1}$)	V_d[c] ($ml\ kg^{-1}$)	$t_{\frac{1}{2}}$ (min)
0.1 ($n = 6$)	1177 ± 96[d]	88 ± 7	72 ± 5	0.47 ± 0.02
0.5 ($n = 7$)	5592 ± 412	92 ± 6	84 ± 5	0.57 ± 0.05
1.0 ($n = 6$)	10897 ± 1452	98 ± 10	109 ± 13**	0.63 ± 0.04*

[a]Total area under the concentration-time curve from zero to infinity; [b]systemic clearance of IR-LTB_4; [c]apparent volume of distribution; [d]mean (± s.e.mean).
*$P < 0.05$; **$P < 0.01$.

significantly, from 72 ± 5 to 109 ± 13 $ml\ kg^{-1}$ for the 0.1 and 1 $\mu g\ kg^{-1}$ doses, respectively, which was accompanied by a 34% increase in the half-life. Nevertheless, the mean calculated systemic Cl could be used to predict steady-state plasma concentrations (Css) after different infusion rates (Table 2). In addition, plasma concentrations of LTB_4 increased proportionally with the infusion rate ($r^2 = 0.9990$), further supporting first-order elimination kinetics (Table 2). Figure 2 illustrates the radioactivity decay from plasma before and after purification of plasma [^{3}H]-LTB_4 by h.p.l.c. Kinetic analysis of the data revealed a systemic Cl of [^{3}H]-LTB_4 of 96 ± 11 $ml\ min^{-1}\ kg^{-1}$, an apparent V_d of 85 ± 9 ml kg^{-1}, and a $t_{\frac{1}{2}}$ of 0.53 ± 0.03 min ($n = 3$). These parameters were not significantly different from those calculated after the bolus (0.1 $\mu g\ kg^{-1}$ dose).

Disposition of LTB_4 analogues

The kinetic parameters estimated from the disappearance curves of immunoreactive 20-F_3-LTB_4 and 3-thio-LTB_4 (Figure 3) are summarized in Table 3. Overall, the parameters were not statistically different from those calculated after a bolus of LTB_4 (0.1 $\mu g\ kg^{-1}$). Both analogues were rapidly cleared from plasma, the 20-F_3-LTB_4 with a $t_{\frac{1}{2}}$ of 0.52 ± 0.06 min ($n = 4$) and the 3-thio-LTB_4 with a half-life of 0.71 ± 0.06 min ($n = 3$).

Table 2 Plasma concentrations of immunoreactive leukotriene B_4 (IR-LTB_4) at steady state (Css) after a continuous infusion at different rates compared with the predicted Css calculated using the kinetic parameters of LTB_4 estimated after a single injection of LTB_4

Infusion rate ($ng\ min^{-1}\ kg^{-1}$)	*Css (observed)*[a] (nM)	*Css (predicted)* (nM)
10	0.31 ± 0.01[b]	0.32[c]
25	0.68 ± 0.05	0.80
50	1.30 ± 0.10	1.60
100	2.68 ± 0.09	3.20

[a]The results showed a good correlation between the Css (observed) and the infusion rate (linear regression: 0.0191 ± 0.0266x, $r^2 = 0.9990$); [b]the results are expressed as mean (± s.e.mean) ($n = 4$); [c]Css (predicted) were estimated using a mean Cl_{LTB4} of 93 $ml\ min^{-1}\ kg^{-1}$.

Discussion

Intravenous administration of LTB_4 produced a transient increase in arterial plasma concentrations of IR-LTB_4. The systemic Cl_{LTB_4} was constant over the dose-range studied, as indicated by the proportional increments in the AUC and the doses injected (Table 1). The mean calculated systemic Cl of LTB_4 of 93 $ml\ min^{-1}\ kg^{-1}$, representing about 30% of the cardiac output in conscious rabbits (Woods *et al.*, 1989) was used to estimate the Css of LTB_4 following different infusion rates (Table 2). Indeed, the LTB_4 plasma concentrations actually measured under steady-state conditions (Marleau *et al.*, 1993) were very close those predicted and were highly

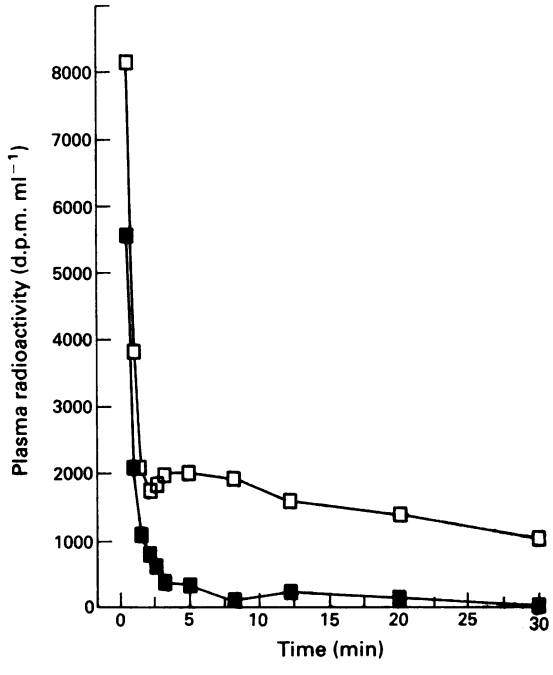

Figure 2 Decay of the total radioactivity in plasma (□) and of the radioactivity associated with [^{3}H]-leukotriene B_4 ([^{3}H]-LTB_4) following h.p.l.c. purification (■) after a single i.v. injection of [^{3}H]-LTB_4 (0.3 $\mu Ci\ kg^{-1}$) (results are from one experiment representative of three).

Table 3 Kinetic parameters of leukotriene B_4 (LTB_4) analogues after a single i.v. injection

Analogue	*Dose* ($\mu g\ kg^{-1}$)	Cl_{LTB_4}[a] ($ml\ min^{-1}\ kg^{-1}$)	V_d[b] ($ml\ kg^{-1}$)	$t_{\frac{1}{2}}$ (min)
20-F_3-LTB_4 ($n = 5$)	0.5	123 ± 22[c]	125 ± 35	0.52 ± 0.07
3-thio-LTB_4 ($n = 4$)	0.16	NC[d]	NC[d]	0.70 ± 0.11*

[a]Systemic clearance of immunoreactive LTB_4; [b]apparent volume of distribution; [c]mean (± s.e.mean); [d]not calculated.
*$P < 0.05$

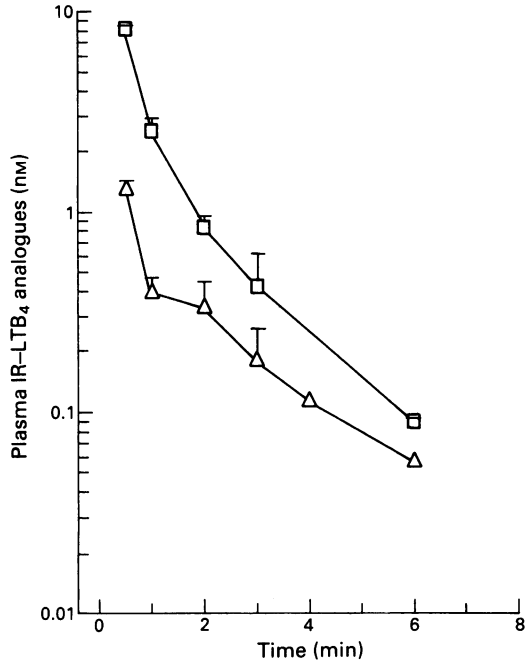

Figure 3 Time course of the plasma concentrations of immunoreactive leukotriene B_4 (IR-LTB_4) analogues after a single i.v. injection of the 20-F_3-LTB_4 (0.5 $\mu g\,kg^{-1}$; $n = 4$) (□); or of the 3-thio-LTB_4 (0.16 $\mu g\,kg^{-1}$; $n = 3$) (△). LTB_4 analogues were purified by h.p.l.c. and assayed by ELISA. The results are expressed as mean (± s.e.mean).

correlated to the infusion rate (Table 2). Taken together, these observations further confirmed that removal of IR-LTB_4 from the circulation was proportional to the plasma concentrations over the dose-range studied.

Our results showed that LTB_4 was distributed in a volume close to the estimated plasma volume (82–102 ml kg^{-1}) in rabbits (Marleau *et al.*, 1989), suggesting that the distribution of LTB_4 is largely limited to the vascular compartment. The data also showed that the apparent V_d increased by 51%, with a 10 fold increase in the dose of LTB_4 injected (Table 1). A slight increase in the free fraction of drugs that are highly bound to plasma proteins in the vascular compartment (which is likely to be the case for a fatty acid derivative) is associated with an increase in the apparent V_d, but it should have little effect on the clearance of highly cleared drugs (Gibaldi & Perrier, 1982). From the present data, it cannot be ascertained whether the high and transient elevation of LTB_4 plasma concentrations (up to 100 fold over basal levels 30 s after the 1 $\mu g\,kg^{-1}$ bolus) were indeed associated with nonlinear binding of LTB_4 in the vascular compartment. However, the finding that the transient elevation in LTB_4 plasma concentrations after the bolus did not modify the mean arterial pressure (Marleau *et al.*, 1993) excludes a significant redistribution of LTB_4 secondary to haemodynamic changes. Whatever the causative factors underlying the increase in the apparent V_d with the dose, these changes were accompanied by a slight decrease in the $t_{\frac{1}{2}}$, from 0.47 ± 0.02 to 0.63 ± 0.04 min, over the dose-range studied (Table 1).

In other experiments, tracer amounts of LTB_4 were administered as a bolus. As shown in Figure 2, about 80% of the total plasma radioactivity disappeared in the first 2 min after the injection; this decline was largely associated with the disappearance of [^{3}H]-LTB_4. In the subsequent minutes, the radioactivity associated with [^{3}H]-LTB_4 continued to decline steadily, whereas the residual radioactivity in plasma was relatively stable up to 30 min after the i.v. injection. About 50% of the radioactivity present in plasma from 3 to 30 min after the bolus injection of [^{3}H]-LTB_4 was found in the washings of the octadecylsilyl silica extraction cartridge (ahead of the h.p.l.c. column), strongly suggesting the appearance of small-molecular-weight polar metabolites, such as tritiated water, in the plasma. Very similar radioactivity profiles were observed after arresting an infusion of [^{3}H]-LTB_4 in the monkey, with parallel initial decay of total and nonvolatile ^{3}H-labelled metabolites. This was followed by the appearance of volatile labelled metabolites (mainly tritiated water) that accounted for more than 85% of the total radioactivity in plasma (Serafin *et al.*, 1984).

Previous studies on the metabolism of LTB_4 *in vitro* and *in vivo* (Harper *et al.*, 1986; Hagmann & Korte, 1990) have suggested that Ω- and β-oxidation-resistant analogues of LTB_4 might be protected from rapid degradation *in vivo*. Our results show that, despite its *in vitro* Ω-oxidation resistant property (Tanaka *et al.*, 1988), 20-F_3-LTB_4 is rapidly and efficiently removed from the circulation after a single i.v. injection (Figure 3, Table 3). We also studied the disposition of the β-oxidation resistant, 3-thio-analogue of LTB_4; the half-life of this analogue was only slightly prolonged to 0.7 min. Taken together, the present studies on the kinetics of LTB_4 and oxidation-resistant analogues *in vivo* indicate that LTB_4 is rapidly cleared from the circulation through an uptake mechanism and that Ω- and/or β-oxidation at the level of the vascular compartment do not have a significant impact on the elimination of LTB_4 from the rabbit circulation. Our studies also demonstrated that the oxidation-resistant analogues of LTB_4 are not likely to be useful in *in vivo* studies, as their uptakes and clearances from the rabbit circulation were similar to that of LTB_4. It is, however, likely that the hepatic and/or renal metabolism of 20-F3-LTB_4 and 3-thio-LTB_4 differs significantly from that of LTB_4, which could not be assessed in the present study.

It is noteworthy that relatively long half-lives of LTB_4 have been observed after local administration. Indeed, following intradermal injections, the half-life of LTB_4 in skin sites was approximately 5 min (Aked & Foster, 1987), whereas the half-life of [^{14}C]-LTB_4 from the inflamed pleural cavity in rats was 46 min (Taylor & Sun, 1985). In these studies, the local metabolism of LTB_4 did not appear to be a major route of elimination and it has been suggested that the stability of LTB_4 at inflammatory sites is the consequence of protein binding (Taylor & Sun, 1985). Similarly, studies in our laboratory have shown that plasma drastically reduces the metabolism of LTB_4 by human neutrophils (Palmantier & Borgeat, unpublished data; Nadeau *et al.*, 1984). In contrast, the very rapid disappearance of LTB_4 as well as of LTB_4 Ω- and β-oxidation-resistant analogues following their systemic administration suggests that protein binding in the vascular compartment would rather play a carrier role for the rapid delivery of LTB_4 at sites of uptake, possibly in the renal and hepatic vasculature.

This work was supported by grants from the Medical Research Council of Canada and by the Merck Frosst Center for Therapeutic Research. S.M. is recipient of a postdoctoral fellowship from the Medical Research Council of Canada. P.B. and P.E.P. are recipients of scholarships from le Fonds de la Recherche en Santé du Québec.

References

AKED, D.M. & FOSTER, S.J. (1987). Leukotriene B_4 and prostaglandin E_2 mediate the inflammatory response of rabbit skin to intradermal arachidonic acid. *Br. J. Pharmacol.*, **92,** 545–552.

BORGEAT, P., PICARD, S., VALLERAND, P., BOURGOIN, S., ODEIMAT, A., SIROIS, P. & POUBELLE, P.E. (1990). Automated on-line extraction and profiling of lipoxygenase products of arachidonic acid by high performance liquid chromatography. In *Methods In Enzymology. Arachidonate related Lipid Mediators.* ed. Murphy, R.C. & Fitzpatrick, F. pp. 98–116. New York: Academic Press.

BRAIN, S.D., CAMP, R.D.R., CUNNINGHAM, F.M., DOWD, P.M., GREAVES, M.W. & KOBZA BLACK, A. (1984). Leukotriene B_4-like material in scale of psoriatic skin lesions. *Br. J. Pharmacol.*, **83,** 313–317.

FORD-HUTCHINSON, A.W. (1990). Leukotriene B_4 in inflammation. *Crit. Rev. Immunol.*, **10,** 1–12.

FRETLAND, D.J., DJURIC, S.W. & GAGINELLA, T.S. (1990). Eicosanoids and inflammatory bowel disease: regulation and prospects or therapy. *Prostaglandins Leukot. Essent. Fatty Acids*, **41,** 215–233.

GIBALDI, M. & PERRIER, D. (1982). Apparent volume of distribution. In *Pharmacokinetics.* ed. Swarbrick, J. pp. 199–210. New York: Marcel Dekker, Inc.

GOLDMAN, G., WELBOURN, R., KLAUSNER, J.M., KOBZIK, L., VALERI, C.R., SHEPRO, D. & HECHTMAN, H.B. (1992). Mast cells and leukotrienes mediate neutrophil sequestration and lung edema after remote ischemia in rodents. *Surgery*, **112,** 578–586.

GRESELE, P., ARNOUT, J., COENE, M.C., DECKMYN, H. & VERMYLEN, J. (1986). Leukotriene B_4 production by stimulated whole blood: comparative studies with isolated polymorphonuclear cells. *Biochem. Biophys. Res. Commun.*, **137,** 334–342.

HAGMANN, W. & KORTE, M. (1990). Hepatic uptake and metabolic disposition of leukotriene B_4 in rats. *Biochem. J.*, **267,** 467–470.

HARPER, T.W., GARRITY, M.J. & MURPHY, R.C. (1986). Metabolism of leukotriene B4 in isolated rat hepatocytes. Identification of a novel 18-carboxy-19,20-dinor leukotriene B_4 metabolite. *J. Biol. Chem.*, **261,** 5414–5418.

KIKAWA, Y., SHIGEMATSU, Y. & SUDO, M. (1986). Leukotriene B_4 and 20-OH-LTB_4 in purulent peritoneal exudates demonstrated by GC-MS. *Prostaglandins Leuko. Med.*, **23,** 85–94.

LEE, T.H., ISRAEL, E., DRAZEN, J.M., LEITCH, A.G., RAVALESE III, J., COREY, E.J., ROBINSON, D.R., LEWIS, R.A. & AUSTEN, K.F. (1986). Enhancement of plasma levels of biologically active leukotriene B compounds during anaphylaxis in guinea-pigs pretreated by indomethacin or by a fish oil-enriched diet. *J. Immunol.*, **136,** 2575–2582.

MARLEAU, S., FORTIN, C., POUBELLE, P.E. & BORGEAT, P. (1993). In vivo desensitization to leukotriene B_4 (LTB_4) in the rabbit. Inhibition of LTB_4-induced neutropenia during intravenous infusion of LTB_4. *J. Immunol.*, **150,** 206–213.

MARLEAU, S., ONG, H., DE LEAN, A. & DU SOUICH, P. (1989). Disposition and dynamics of atrial natriuretic factor in conscious rabbits. *J. Pharmacol. Exp. Ther.*, **251,** 328–333.

NACCACHE, P.H., SHA'AFI, R.I. & BORGEAT, P. (1989). Mobilization, metabolism and biological effects of eicosanoids in polymorphonuclear leukocytes. In *The Neutrophil: Cellular Biochemistry and Physiology.* ed. Hallett, M.B. pp. 116–140. Boca Raton (Florida): CRC Press.

NADEAU, M., FRUTEAU DE LACLOS, B., PICARD, S., BRAQUET, P., COREY, E.J. & BORGEAT, P. (1984). Studies on leukotriene B_4 Ω-oxidation in human leukocytes. *Can J. Biochem. Cell. Biol.*, **62,** 1321–1326.

NEWTON, J.F., ECKARDT, R., BENDER, P.E., LEONARD, T. & STAUB, K. (1985). Metabolism of leukotriene B_4 in hepatic microsomes. *Biochem. Biophys. Res. Commun.*, **128,** 733–738.

POWELL, W.S. (1984). Properties of leukotriene B_4 20-hydroxylase from polymorphonuclear leukocytes. *J. Biol. Chem.*, **259,** 3082–3089.

POWELL, W.S. & GRAVELLE, F. (1990). Biosynthesis and metabolism of leukotriene B_4 by rat polymorphonuclear leukocytes. In *Advances in Prostaglandin, Thromboxane, and Leukotriene Research.* ed. Samuelsson, B., Paoletti, R. & Ramwell, P.W. pp. 181–184. New York: Raven Press, Ltd.

ROMANO, M.C., ECKARDT, R.D., BENDER, P.E., LEONARD, T.B., STRAUB, K.M. & NEWTON, J.F. (1987). Biochemical characterization of hepatic microsomal leukotriene B_4 hydroxylases. *J. Biol. Chem.*, **262,** 1590–1595.

SERAFIN, W.E., OATES, J.A. & HUBBARD, W.C. (1984). Metabolism of leukotriene B_4 in the monkey. Identification of the principal nonvolatile metabolite in the urine. *Prostaglandins*, **27,** 899–911.

SHAK, S. & GOLDSTEIN, I.M. (1984). Ω-oxidation is the major pathway for the catabolism of leukotriene B_4 in human polymorphonuclear leukocytes. *J. Biol. Chem.*, **259,** 10181–10187.

SHAK, S. & GOLDSTEIN, I.M. (1985). Leukotriene B_4 Ω-hydroxylase in human polymorphonuclear leukocytes. Partial purification and identification as a cytochrome P-450. *J. Clin. Invest.*, **76,** 1218–1228.

TANAKA, Y., KLAUCK, T.M., JUBIZ, W., TAGUCHI, T., HANZAWA, Y., IGARASHI, A., INAZAWA, K., KOBAYASHI, Y. & BRIGGS, R.G. (1988). Biosynthesis of 20,20,20-trifluoroleukotriene B_4 from 20,20,20-trifluoroarachidonic acid: a metabolically stable analog of leukotriene B_4 and its application to a study of stimulation of leukotriene B_4 synthesis by immunoglobulin G. *Archiv. Biochem. Biophys.*, **263,** 178–190.

TAYLOR, B.M. & SUN, F.F. (1985). Disappearance and metabolism of leukotriene B_4 during carrageenan-induced pleurisy. *Biochem. Pharmacol.*, **34,** 3495–3498.

WELBOURN, R., GOLDMAN, G., KOBZIK, L., PATERSON, I., VALERI, C.R., SHEPRO, D. & HECHTMAN, H.B. (1990). Neutrophil adherence receptors (CD 18) in ischemia. Dissociation between quantitative cell surface expression and diapedesis mediated by leukotriene B_4. *J. Immunol.*, **145,** 1906–1911.

WOODS, R.L., OLIVER, J.R. & KORNER, P.I. (1989). Direct and neurohumoral cardiovascular effects of atrial natriuretic peptide. *J. Cardiovasc. Pharmacol.*, **13,** 177–185.

(Received December 15, 1993
Revised February 8, 1994
Accepted February 15, 1994)

Br. J. Pharmacol. (1994), **112**, 659–665

Effects of the new A_2 adenosine receptor antagonist 8FB-PTP, an 8 substituted pyrazolo-triazolo-pyrimidine, on *in vitro* functional models

[1]Silvio Dionisotti, Annamaria Conti, Daniele Sandoli, Cristina Zocchi, *Franco Gatta & Ennio Ongini

Research Laboratories, Schering-Plough S.p.A., 20060 Comazzo, Milan, Italy and *Laboratory of Medicinal Chemistry, Istituto Superiore di Sanità, 00161 Rome, Italy

1 We have characterized the *in vitro* pharmacological profile of putative A_2 adenosine antagonists, two non-xanthine compounds, 5-amino-8-(4-fluorobenzyl)-2-(2-furyl)-pyrazolo [4,3-e]-1,2,4-triazolo[1,5-c] pyrimidine (8FB-PTP) and 5-amino-9-chloro-2-(2-furyl 1,2,4-triazolo [1,5-c] quinazoline (CGS 15943), and the xanthine derivative (E)7-methyl-8-(3,4-dimethoxystyryl)-1,3-dipropyl-xanthine (KF 17837).

2 In binding studies on bovine brain, 8FB-PTP was the most potent (K_i = 0.074 nM) and selective (28 fold) drug on A_2 receptors, whereas CGS 15943 and KF 17837 exhibited affinity in the low and high nanomolar range, respectively, and showed little selectivity.

3 In functional studies, 8FB-PTP antagonized 5'-N-ethyl-carboxamidoadenosine (NECA)-induced vasorelaxation of bovine coronary artery (pA_2 = 7.98) and NECA-induced inhibition of rabbit platelet aggregation (pA_2 = 8.20). CGS 15943 showed weak activity in the platelet aggregation model (pA_2 = 7.43) and failed to antagonize NECA-induced vasodilatation. KF 17837 was ineffective in both models up to micromolar concentrations.

4 Antagonism of A_1-mediated responses was tested versus 2-chloro-N^6-cyclopentyladenosine (CCPA) in rat atria. 8FB-PTP and CGS 15943 also antagonized competitively the negative chronotropic response induced by CCPA. Conversely, KF 17837 was unable to reverse A_1-mediated responses.

5 8FB-PTP is a potent and competitive antagonist of responses mediated by A_2 adenosine receptors. The data provided a basis to reduce, by further chemical modifications, the affinity at A_1 receptor and therefore enhance A_2 receptor selectivity.

Keywords: Adenosine receptors; A_1 and A_2 receptors; A_2 antagonists; bovine coronary artery; platelet aggregation; CGS 15943; KF 17837; 5-amino-8-(4-fluorobenzyl)-2-(2-furyl)-pyrazolo [4,3-e]-1,2,4-triazolo[1,5-c]pyrimidine (8FB-PTP)

Introduction

Adenosine effects are mediated by two cell surface receptors, termed A_1 and A_2, and coupled to adenylate cyclase in an inhibitory or stimulatory manner, respectively (Van Calker *et al.*, 1979; Londos *et al.*, 1980). The A_2 receptor has been divided into high and low affinity subtypes, A_{2a} and A_{2b}, on the basis of biochemical studies (Bruns *et al.*, 1986) and confirmed by molecular cloning (Maenhaut *et al.*, 1990; Libert *et al.*, 1991). More recent studies led to the identification of other adenosine receptors, tentatively designated as A_3 and A_4, the definitive classification of which still awaits further pharmacological characterization and molecular biology data (Abbracchio *et al.*, 1993).

Efforts made over several years have led to the discovery of a series of adenosine analogues which stimulate selectively either A_1 or A_2 receptors (Van Galen *et al.*, 1992). As for antagonists, several xanthine derivatives have been synthesized in an attempt to improve affinity and selectivity of the natural compounds, caffeine and theophylline, and avoid interactions with other biochemical systems, e.g. phosphodiesterase (PDE) inhibition (Rall, 1985; Bruns *et al.*, 1986). A number of 8-substituted xanthines have been found to be highly selective for the A_1 receptor with little or no interaction with phosphodiesterase and one of them, the drug 8-cyclopentyl-1,3-dipropylxanthine (DPCPX) is widely used as a prototypical A_1-selective antagonist (Bruns *et al.*, 1987). More recently, interesting progress has been made with the discovery that 8-styryl-xanthines are selective A_2 antagonists (Shimada *et al.*, 1992; Jacobson *et al.*, 1993a). In binding studies, some of these compounds appear to be relatively potent at A_2 receptors (e.g. K_i values ranging between 10 and 30 nM) with a good separation versus A_1 receptors (e.g. A_1/A_2 more than 100 fold). For example, the drug (E)7-methyl-8-(3,4-dimethoxystyryl)-1,3-dipropyl-xanthine (KF 17837) (Figure 1) has been reported to have a K_i of 7.8 nM and an A_1/A_2 ratio of 190 (Shimada *et al.*, 1992). However, there are no data available as to their A_2 antagonist properties in functional assays. A variety of other non-xanthine derivatives which potently interact with A_2 receptors have been intensively studied over the last few years (Jacobson *et al.*, 1992). The reference compound 5-amino-9-chloro-2-(2-furyl)1,2,4-triazolo[1,5-c]quinazoline (CGS 15943) (Figure 1) has high affinity for A_2 receptors (K_i = 3 nM), but it is also very potent at A_1 receptors (A_1/A_2 about 7 fold) (Williams *et al.*, 1987). It follows that CGS 15943 does not discriminate between A_1- and A_2-mediated functional responses.

In an attempt to improve A_2-selectivity, we have recently synthesized some analogues of CGS 15943 in which the phenyl group was replaced by a heterocyclic ring such as pyrazolo or imidazolo (Gatta *et al.*, 1993). One of these compounds, the 8-substituted pyrazolo-triazolo-pyrimidine derivative, 5-amino-8-(4-fluorobenzyl)-2-(2-furyl)-pyrazolo-[4,3-e]-1,2,4-triazolo[1,5-c]pyrimidine (8FB-PTP) (Figure 1), showed an affinity for A_1 and A_2 receptors comparable to that of CGS 15943, but displayed a higher potency in blocking the functional response in platelets, an effect mediated by A_2 receptors (Gatta *et al.*, 1993). Moreover, our previous and ongoing experience with selective adenosine agonists has allowed us to set up experimental techniques which are suitable for discriminating between responses specifically mediated by either the A_1 or A_2 receptor (Dionisotti *et al.*, 1992; Conti *et al.*, 1993). Thus, antagonism of the A_2-

[1] Author for correspondence.

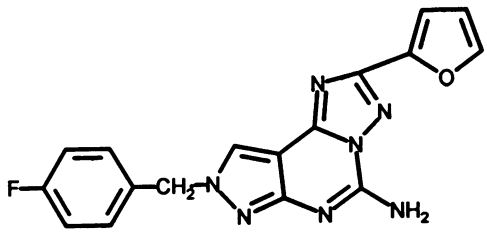

8FB-PTP

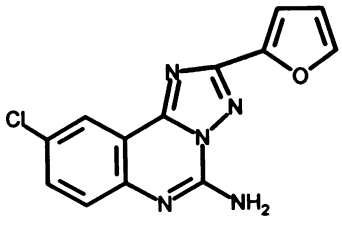

CGS 15943

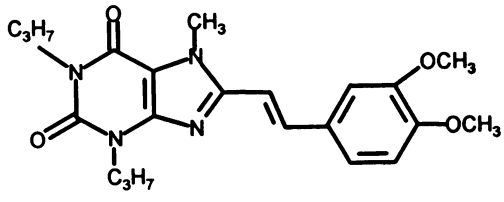

KF 17837

Figure 1 Chemical structures of 5-amino-8-(4-fluorobenzyl)-2-(2-furyl)-pyrazolo[4,3-e]-1,2,4-triazolo[1,5-c] pyrimidine (8FB-PTP), 5-amino-9-chloro-2-(2-furyl)1,2,4-triazolo[1,5-c]quinazoline (CGS 15943) and (E)7-methyl-8-(3,4-dimethoxystyryl-1,3-dipropyl-xanthine (KF 17837).

mediated effect was tested on both bovine coronary artery relaxation and antiaggregatory activity in rabbit platelets induced by 5'-N-ethyl-carboxamidoadenosine (NECA). Antagonism of the negative chronotropic A_1-mediated response induced by 2-chloro-N^6-cyclopentyladenosine (CCPA) was assayed in rat atria. Using these sensitive experimental models, we have characterized the pharmacological profile of the new A_2 antagonist, 8FB-PTP, in comparison with CGS 15943 and the xanthine derivative, KF 17837.

Methods

Receptor binding assay

Bovine brain was obtained from a local abattoir within 10 min of the animal being killed. Frontal cortex and striatum were dissected on ice and disrupted with a Polytron PTA 10 probe (setting 5, 30 s) in 24 vol of 50 mM Tris-HCl buffer, pH 7.4. Cortical and striatal homogenates were then centrifuged (for 10 min at 4°C), at 40,000 (twice) and 48,000 *g*, respectively. The pellets were resuspended in buffer containing 2 iu ml^{-1} adenosine deaminase. After 30 min of incubation at 37°C the membranes were centrifuged and the pellet was stored at −70°C. A_1 and A_2 receptor binding affinity was assayed on cortical and striatal membranes using [^{3}H]-N^6-cyclohexyladenosine ([^{3}H]-CHA) (Bruns *et al.*, 1980) and [^{3}H]-2-[*p*-(2-carboxyethyl)-phenetylamino]-5'-*N*-ethylcarboxamidoadenosine ([^{3}H]-CGS 21680) (Jarvis *et al.*, 1989) as radioligands, respectively. Saturation studies were carried out by incubating membranes with concentrations of [^{3}H]-CHA between 0.03 and 64 nM for A_1 receptors and [^{3}H]-CGS 21680 between 1 and 192 nM for A_2 receptors. Non specific binding was defined in the presence of CHA 10 μM and 5'-N-ethylcarboxamidoadenosine (NECA) 100 μM for A_1 and A_2 receptors respectively, and was ≤10% of total binding. Competition studies were performed with at least 8 different concentrations of each compound. Bound and free radioligands were separated by rapid filtration through Whatman GF/B filters, using a Brandel cell harvester (Brandel, Gaithersburg, MD, U.S.A.). Radioactivity was determined in an LS-6000 Beckman liquid scintillation counter (Beckman Instruments Inc., Fullerton, CA, U.S.A.), at an efficiency of between 50 to 60%. Protein concentration was determined by the method of Lowry *et al.* (1951), with bovine serum albumin used as standard.

Phosphodiesterases assay

The activity of the selected adenosine antagonists on PDE enzymes was assayed on type III phosphodiesterase (PDE) and carried out according to Ahn *et al.* (1991). The final reaction mixture (0.2 ml) contained 50 mM Tris-HCl buffer (pH 7.5), 5 mM $MgCl_2$, 0.1 mg ml^{-1} bovine serum albumin, 1 μM adenosine 3':5'-cyclic monophosphate (cyclic AMP), [^{3}H]-cyclic AMP (about 80,000 c.p.m.) and 25 ng type III PDE from bovine heart.

Platelet aggregation assay

The antagonism to NECA-induced antiaggregatory activity was tested in rabbit platelets. Platelet aggregation was performed according to the Born turbidimetric technique (Born & Cross, 1963) using a DIC PA-3220 Aggrecorder (Kyoto Daiichi Kagaku Co. Ltd., Japan) and adenosine diphosphate (5 μM) was used as the aggregatory agent.

Citrated blood from New Zealand White male rabbits (Bettinardi Farm, Alzate, Novara, Italy) of body weight 3–4 kg was collected from the left carotid artery during pentobarbitone anaesthesia (20 mg kg^{-1}, i.v.). Platelet-rich plasma preparation and the platelet aggregation assay were performed as previously described (Gatta *et al.*, 1993).

Bovine coronary artery

Bovine hearts obtained from a local abattoir were used, according to a method described elsewhere (Conti *et al.*, 1993). The hearts were taken within 10 min of slaughter and the main branch of the left anterior descending coronary artery was used. Arterial segments were cleaned of connective tissue, cut into rings and allowed to equilibrate for at least 60 min in an organ bath containing Krebs-Henseleit solution at 37°C and aerated with a mixture of 95% O_2 and 5% CO_2. The rings were placed under a resting tension of 1 g. Submaximal contractions of vascular tissues were produced by prostaglandin $F_{2\alpha}$ ($PGF_{2\alpha}$ 3 μM). Cumulative dose-response curves were constructed, using increasing concentration of NECA (1 nM–10 μM), in the absence or presence of the antagonist.

Rat atria

Male Sprague-Dawley rats (150–200 g) were supplied by Charles River (Calco, Como, Italy). After acclimatization to standard laboratory conditions, the animals were killed by decapitation and the hearts were removed. The method used to test adenosine agonists is described elsewhere (Conti *et al.*,1993). Briefly, atria were isolated and allowed to beat spontaneously in an organ bath containing Krebs-Henseleit solution aerated with a mixture of 95% O_2 and 5% CO_2 at 37°C. The isometric contractions were recorded by a strain

gauge transducer (Mod. 83F M.A.R.B.) connected on line to a PC Olivetti M386/25. After a period of equilibration (1 h), the decrease in atrial rate evoked by cumulative addition of the A_1-selective agonist, 2-chloro-N^6-cyclopentyladenosine (CCPA) was measured. The concentration dose-response curves of the agonist were then repeated in the presence of each antagonist.

Statistical analysis

Binding parameters were estimated by the computerized non-linear fitting programme LIGAND (Munson & Rodbard, 1980). As for the PDE assay, IC_{50} values (when calculation was possible) were obtained by linear regression.

The relationship between platelet aggregation or isolated tissue response (y) and agonist log-dose was fitted after logit transformation of dependent variables by a weighted least squares method. The average dose-response function was obtained as a mean constant curve based on the constants estimated from each preparation using the programme PROC GLM, from SAS Institute (1987). Since the dose-response curves shared the same sigmoid shape and shifted to the right as the concentration of the competitive antagonist increased (Waud, 1975), all the experimental points were simultaneously fitted by a reparameterized logistic function with agonist and antagonist log-doses used as independent variables, and pA_2 as the further parameter to be estimated. Nonlinear least square estimates were obtained according to Marquardt and using the programme PROC NONLIN, from SAS Institute (1987).

As described by Gaddum (Tallarida *et al.*, 1979), the value (A') of the agonist's ED_{50} in the presence of an antagonist concentration (B) was expressed as a function of B, of the agonist's ED_{50} (A) in the absence of the antagonist, and of pA_2 (i.e. $-\log K_b$; K_b being the dissociation constant of the antagonist):

$$\log 10\ A' = \log 10\ A + \log 10\ (1 + 10^{(\log 10\ B + pA_2)}) \quad \text{(eq. 1)}$$

According to Finney (1978), the response (y) is linked to the agonist dose (x) by the following logistic function:

$$y = [1 + \exp \beta\ (\log 10 \times - \log 10\ A')]^{-1} \quad \text{(eq. 2)}$$

where β is the maximum slope of logistic function.

By substitution of the right part of the eq. 1 for log 10 A' and introduction of an extra-parameter τ which denotes the Schild-plot slope, eq. 2 becomes:

$$y = \{1 + \exp \beta\ [\log 10 \times - \log 10\ A - \log 10(1 + 10^{(\tau \log 10\ B + pA_2)})]\}^{-1}$$

This equation provides a direct approach to test the hypothesis of competitive antagonism (i.e. $\tau = 1$) and to estimate the pA_2 value.

Chemicals

5-Amino-9-chloro-2-(2-furyl)1,2,4-triazolo[1,5-c]quinazoline (CGS 15943) was kindly supplied by Ciba-Geigy (Summit, NJ, U.S.A.). (E)7-methyl-8-(3,4-dimethoxystyryl)-1,3-dipropylxanthine (KF 17837) and 5-amino-8-(4-fluorobenzyl)-2-(2-furyl)-pyrazolo[4,3-e]-1,2,4-triazolo[1,5-c]pyrimidine (8FB-PTP) were synthesized by Dr F. Gatta (Laboratory of Medicinal Chemistry, Istituto Superiore di Sanità, Rome, Italy). 5'-N-ethylcarboxamidoadenosine (NECA), 8-cyclopentyl-1,3-dipropylxanthine (DPCPX) and 2-chloro-N^6-cyclopentyladenosine (CCPA), were from Research Biochemicals Inc. (Natick, MA, U.S.A.). [^{3}H]-N^6-cyclohexyl-adenosine ([^{3}H]-CHA) (specific activity 30.2 Ci mM^{-1}), [^{3}H]-2-[*p*-(2-carboxyethyl)-phenetylamino]-5'-*N*-ethyl-carboxamidoadenosine ([^{3}H]-CGS 21680) (specific activity 47.2 Ci mM^{-1}) and [^{3}H]-adenosine 3':5'-cyclic monophosphate ([^{3}H]-cyclic AMP) (specific activity 31.2 Ci mM^{-1}) were from NEN Research Products (Boston, MA, U.S.A.). Cyclic AMP and prostaglandin $F_{2\alpha}$ ($PGF_{2\alpha}$) were from Sigma Chemical Co. (St. Louis, MO, U.S.A.). Adenosine diphosphate (ADP) and adenosine deaminase were supplied by Boehringer Mannheim GmbH (Mannheim, Germany). Milrinone was from Sterling Winthrop Inc. (Rensselaer, NY, U.S.A.). Bovine heart type III PDE was from Dr B. Mutus (Department of Chemistry and Biochemistry, University of Windsor, Ontario, Canada). All other reagents were from commercial sources.

Table 1 Comparison of the affinity of selected adenosine antagonists in inhibiting [^{3}H]-CHA and [^{3}H]-CGS 21680 binding in bovine brain membranes

Antagonist	A_1 K_i (nM)	A_2 K_i (nM)	A_1/A_2 *ratio*
8FB-PTP	2.04 (1.77–2.34)	0.074 (0.064–0.086)	27.6
CGS 15943	2.40 (2.07–2.78)	0.95 (0.79–1.14)	2.5
KF 17837	237.03 (163.8–342.9)	73.59 (60.75–89.13)	3.2
DPCPX	0.14 (0.11–0.17)	122.90 (120.0–125.9)	0.0011

Each value represents the geometric mean, with 95% confidence limits in parentheses, of at least 4–6 different experiments. For abbreviations, see text.

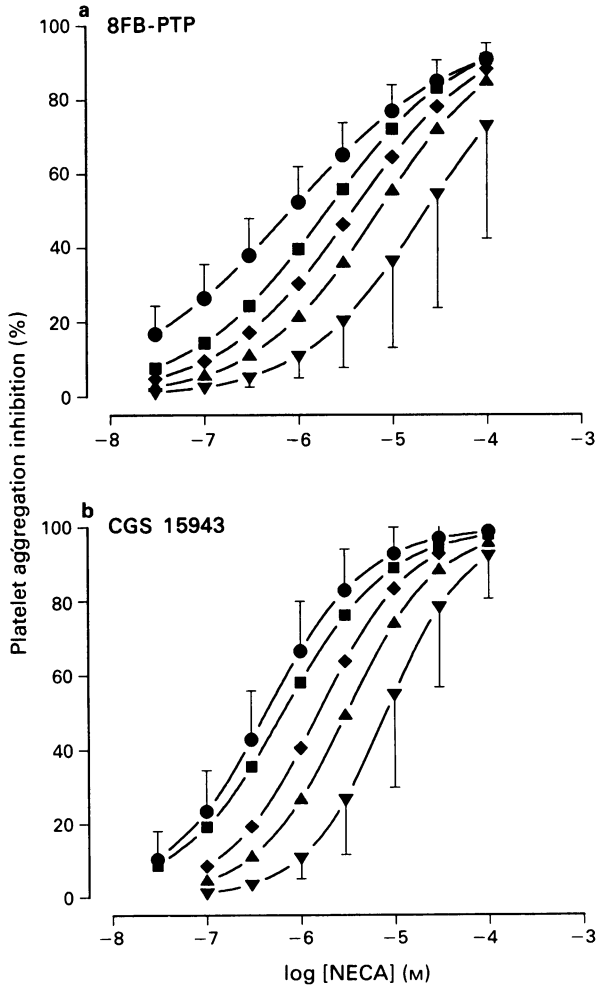

Figure 2 Effects of A_2 adenosine antagonists on NECA-induced platelet aggregation inhibition. ADP 5 μM was used as aggregatory agent. Each point represents the geometric mean, with 95% confidence limits, of 4–5 replications. (a) Dose-response curve for NECA alone (●) and in the presence of 8FB-PTP: 0.003 μM (■), 0.01 μM (◆), 0.03 μM (▲), 0.1 μM (▼). (b) Dose-response curve for NECA alone (●) and in the presence of CGS 15943: 0.03 μM (■), 0.1 μM (◆), 0.3 μM (▲), 1.0 μM (▼). For abbreviations, see text.

The composition of the Krebs Henseleit solution was as follows (mM): NaCl 118, KCl 4.7, $MgSO_4$ 1.2, $NaHCO_3$ 25, KH_2PO_4 1.2, $CaCl_2$ 2.5, glucose 11 (pH 7.4).

Results

Receptor binding assay

Saturation experiments ($n = 4$) showed that [^{3}H]-CHA and [^{3}H]-CGS 21680 bound to a single class of receptors in frontal cortex and striatum bovine brain, with a K_d of 0.42 (0.36–0.48) and 6.2 (5.8–6.6) nM, and an apparent B_{max} value of 815 (726–914) and 670 (558–806) fmol mg^{-1} of protein, respectively (95% confidence limits in parentheses). In competition studies, the affinity of selected adenosine antagonists for A_1 and A_2 receptors was examined (Table 1). 8FB-PTP was the most potent compound in inhibiting [^{3}H]-CGS 21680 binding with a K_i value of 0.074 nM and a selectivity for A_2 versus A_1 receptors of 28 fold. CGS 15943 and KF 17837 exhibited affinity at A_2 receptors in the low and high nanomolar range, respectively, but they did not show A_2 versus A_1 selectivity. The reference A_1 antagonist, DPCPX, showed the highest affinity ($K_i = 0.14$ nM) and selectivity (about 900) for the A_1 receptors.

Phosphodiesterases assay

The ability of the drugs to inhibit the hydrolysis of cyclic AMP was evaluated on Type III PDE from bovine heart. Milrinone, which was tested as positive reference compound, showed an IC_{50} value of 0.6 μM. None of the compounds tested showed appreciable activity (% of inhibition from 6 to 37) at concentrations up to 100 μM.

Platelet aggregation assay

The antiaggregatory activity of the adenosine agonist, NECA was assayed in rabbit platelets and its IC_{50} value (with 95% confidence limits in parentheses) was 0.70 μM (0.36–1.38). 8FB-PTP and CGS 15943 reversed the platelet aggregation inhibition produced by NECA. The compounds shifted the dose-response curves to the right in a concentration-dependent manner without changing the shape or the maximal inhibitory effect induced by NECA on platelet aggregation (Figure 2). The pA_2 values estimated were of 8.20 and 7.43, respectively (Table 2), indicating that 8FB-PTP is about 10 fold more active than CGS 15943. When tested alone at high concentrations, neither 8FB-PTP (0.1 μM) nor CGS 15943 (1 μM), showed intrinsic activity on platelet aggregation. The xanthine derivative, KF 17837, was unable to antagonize the antiaggregatory activity of NECA at concentrations up to 1 μM. As expected, the A_1 antagonist, DPCPX, at 1 μM had no effect.

Isolated smooth and cardiac tissue preparations

Bovine coronary artery NECA-induced vasorelaxation was studied in bovine coronary artery rings precontracted with $PGF_{2\alpha}$ (3 μM). NECA produced concentration-dependent relaxation and its EC_{50} value (with 95% confidence limits in parentheses) was 98 nM (66–144). The dose-response curves of NECA were shifted towards the right in a parallel manner by 8FB-PTP at 0.1, 0.3 and 1 μM, therefore showing a competitive antagonism. The pA_2 value obtained was 7.98 (Table 2). Conversely, CGS 15943 and KF 17837 (which have been reported to have affinity for the A_2 receptor subtype in the nanomolar range) at concentrations as high as 1 μM failed to antagonize NECA-induced relaxation. As expected, the selective A_1 antagonist, DPCPX (0.1 μM and 1 μM) did not shift the dose-response curve of NECA (Figure 3).

Rat atria The A_1-selective agonist, CCPA, induced a concentration-dependent decrease in the spontaneous rate of rat atrial preparations. The EC_{50} value (with 95% confidence limits in parentheses) was 8.2 (5.8–11.7) nM. The A_1 antagonist, DPCPX (1–10 nM), antagonized in a competitive manner the negative chronotropic response induced by CCPA ($pA_2 = 9.22$). 8FB-PTP and CGS 15943 (1–10 nM) also antagonized CCPA-induced responses competitively in rat atria, with pA_2 values of 8.71 and 9.62, respectively (Table 2). KF 17837 failed to antagonize CCPA-induced effects at a concentration as high as 1 μM.

Discussion

The present data show that a non-xanthine heterocyclic compound, an 8-substituted pyrazolo-triazolo-pyrimidine derivative, designated 8FB-PTP, has potent A_2 antagonistic properties in selected functional assays. The drug has very high affinity, being in the pM range, for the A_2 bovine striatal receptors and displays an A_1/A_2 ratio of 28 fold. In specific and reliable biological assays which permit the measurement of A_2-mediated responses, such as the models of coronary vasodilatation and platelet aggregation, the drug 8FB-PTP was found to be potent and produce parallel rightward shifts in the agonist concentration-response curve. Thus, the data clearly indicate the competitive nature of this antagonism. Moreover, the drug is devoid of effects on Type III phosphodiesterases, it potently blocks A_2-stimulated adenylate cyclase in human platelets (Gatta *et al.*, 1993), and it does not bind to other receptor systems commonly linked to G-protein (data not shown). To our knowledge, this is the first compound that combines high affinity for the A_2 receptor and clear antagonistic properties on A_2-mediated biological responses. 8FB-PTP, having affinity in the low nanomolar range for the A_1 receptor, was also found to antagonize readily agonist-induced depression of spontaneous rate in rat atria, a typical A_1-mediated

Table 2 Functional activity of selected adenosine antagonists in tissues containing A_1 and A_2 receptors

	Rabbit platelet[a]		*Bovine coronary artery*[b]		*Rat atria*[c]	
Antagonist	pA_2	*Schild-plot slope*	pA_2	*Schild-plot slope*	pA_2	*Schild-plot slope*
8FB-PTP	8.20 (7.69–8.69)	0.97 (0.90–1.03)	7.98 (6.92–9.03)	1.08 (0.91–1.24)	8.71 (8.07–9.35)	0.96 (0.88–1.04)
CGS 15943	7.43 (6.66–8.19)	1.04 (0.92–1.16)	NM (1 μM)	–	9.62 (8.72–10.5)	1.00 (0.89–1.11)
KF 17837	NM (1 μM)	–	NM (1 μM)	–	NM (1 μM)	–
DPCPX	NM (1 μM)	–	NM (1 μM)	–	9.22 (8.51–9.93)	0.96 (0.87–1.04)

NM: not measurable. 95% confidence limits or highest concentrations tested in parentheses.
[a]Antagonism to NECA-induced antiaggregatory activity in rabbit platelets.
[b]Antagonism to NECA-induced vasorelaxation in bovine coronary artery.
[c]Antagonism to CCPA-induced negative chronotropic effect in rat atria.

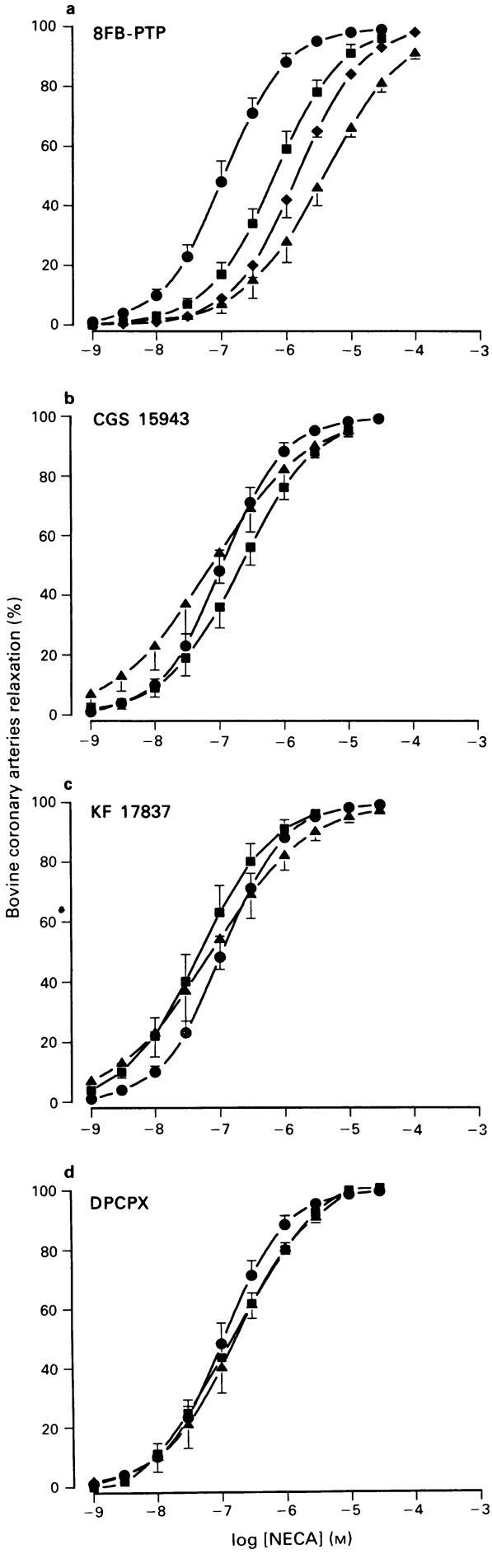

response. It follows that the drug may be a useful pharmacological tool in selected tissues where only the activity of A_2 receptors is expressed.

The drug 8FB-PTP is an analogue of the triazoloquinazoline, CGS 15943, which has been considered a potent A_2 antagonist, useful for studying adenosine receptor function (Williams *et al.*, 1987). However, several drawbacks associated with its biochemical and pharmacological profile have hampered its widespread use as a reference A_2 antagonist. CGS 15493 has similar nanomolar affinity for both A_1 and A_2 receptors therefore showing little or no selectivity (Williams *et al.*, 1987). Moreover, in functional tests the drug is equally potent on both A_1 and A_2 receptors (Ghai *et al.*, 1987). In our studies, CGS 15943 was found to have equal affinity, in the low nanomolar range, for both A_1 and A_2 receptors. In platelet aggregation, it displayed competitive antagonism in reversing the effect induced by NECA with a potency 10 fold weaker than that of 8FB-PTP, but it was unable to antagonize NECA-induced vasodilatation in bovine coronary arteries. Likewise, in previous studies devoted to the evaluation of A_2 agonists (Conti *et al.*, 1993), we tested CGS 15943 in the rat aorta model and did not find any relevant antagonistic activity up to 1 μM (unpublished data). This is in agreement with the results of other authors who have been unable to find antagonistic properties in functional models for CGS 15943. For example, in human mammary arteries and saphenous veins, CGS 15943 does not antagonize vasodilatation induced by A_2 agonists (Sabouni *et al.*, 1990; Makujina *et al.*, 1992). However, the same authors reported an action on human coronary arteries, at the high concentration of 10 μM. Conversely, the original report by Ghai *et al.* (1987) describes its marked antagonist actions in dog coronary arteries. These conflicting data could be partially explained by possible species differences in receptor density or subtypes. In the light of this, it is clear why CGS 15943 has not become a reference A_2 antagonist.

But the most surprising results were obtained with KF 17837 which was presented as an A_2-selective xanthine (Shimada *et al.*, 1992). At variance with the original work in the rat brain (K_i = 7.8 nM; Shimada *et al.*, 1992), in our binding studies the drug did not display marked affinity for A_2 receptors either in bovine (K_i = 74 nM; Table 1) or in rat brain (K_i = 64 nM). In agreement with our finding, Jacobson *et al.* (1993a) found a weaker affinity (K_i = 31 nM) in the rat brain. The differences may in part be explained by considering that Shimada *et al.* (1992) used [^{3}H]-NECA as radioligand instead of the A_{2a}-selective agonist, [^{3}H]-CGS 21680 used by Jacobson *et al.* (1993a) and in the present study. But the most unexpected finding emerged in the functional studies where the drug did not antagonize the effects induced by NECA in two models sensitive to A_2 receptor modulation. After completion of these studies, Nonaka *et al.* (1993) reported that the dissolution of KF 17837, in particular at low concentrations, determines rapid photoisomerization of the compound whereas the crystalline form is stable. Thus, the original E-isomer (KF 17837) becomes an equilibrium mixture of E- and Z-isomers when exposed to the light. In view of this finding, we have performed the h.p.l.c. analysis of drug solutions used in our study confirming both the

Figure 3 Effects of selected adenosine A_2 antagonists on vasorelaxation induced by NECA in bovine coronary arteries. Each point represents the geometric mean, with 95% confidence limits, of at least 7 replications. (a) Dose-response curve for NECA alone (●) and in the presence of 8FB-PTP: 0.1 μM (■), 0.3 μM (◆), 1.0 μM (▲). (b) Dose-response curve for NECA alone (●) and in the presence of CGS 15943: 0.1 μM (■), 1.0 μM (▲). (c) Dose-response curve for NECA alone (●) and in the presence of KF 17837: 0.1 μM (■), 1.0 μM (▲). (d) Dose-response curve for NECA alone (●) and in the presence of DPCPX: 0.1 μM (■), 1.0 μM (▲). For abbreviations, see text.

stability of KF 17837 as the crystalline form and its photoisomerization when dissolved in dimethylsulphoxide 1% (data not shown). These data are still in contrast with those of Nonaka *et al.* (1993) who indicate a K_i value of 8 nM for the equilibrium mixture as measured in rat striatal membranes using the A_{2a} selective agonist, [^{3}H]-CGS 21680. Moreover, the fact remains that in our experimental conditions, KF 17837 was inactive up to 1 μM in functional *in vitro* studies. Thus, the identification of the E- and Z-isomers clarifies only which chemical structure interacts with the A_2 receptor but does not explain why the test compound does not show any meaningful A_2 antagonistic properties in *in vitro* pharmacological assays. Whether or not the data obtained with KF 17837 may extend to the new chemical class of 8-styryl-xanthines is not known. Among the xanthines synthesized by Jacobson *et al.* (1993a), 8-(3-chlorostyryl)caffeine has been reported to have A_2 antagonist properties in both *in vitro* and *in vivo* studies (Jacobson *et al.*, 1993b). Additional studies are therefore necessary to define better the profile of the A_2 antagonist xanthines before their use as reference tools in experimental studies.

There are comments to be made on the models which have been examined. In binding studies with bovine cerebral tissues the test compounds were more effective than in rat tissues. This is in agreement with our experience using both adenosine agonists and antagonists, and with other results showing greater sensitivity of the bovine versus rat brain tissues (Ferkany *et al.*, 1986; Stone *et al.*, 1988). Having used the bovine coronary arteries as a functional model for the measurement of the A_2 receptor responses, it seemed that the bovine brain could be the most appropriate tissue for binding studies. The two functional models used for assessing the A_1- and A_2-mediated responses appear to be reliable but differences between the models preclude any comparison of drug selectivity in functional assays (Conti *et al.*, 1993). Thus, despite the 28 fold difference in binding potency, the apparent paradox that the drugs seem to be more effective in the A_1 model should be viewed in the context of the different experimental models examined.

Classification of the adenosine receptors has recently become rather complex (Abbracchio *et al.*, 1993). While the classification into two main receptor types, A_1 and A_2, still remains valid, there is discussion as to whether other receptor types such as A_3 and A_4 should also be included in the overall scheme. This complexity is mainly due to the fact that molecular biology has provided peptide sequences which go beyond the A_1/A_2 hypothesis, and some biology data do not fit with the two-receptor classification scheme. For example, binding data obtained with the non-selective adenosine agonist [^{3}H]-CV 1808 have been interpreted by considering the existence of a different type of adenosine receptor, which has been tentatively designated as A_4 (Cornfield *et al.*, 1992). In these experimental conditions, also CGS 15943 has been found to antagonize the so-called A_4 receptor, therefore showing again lack of selectivity. Unfortunately, as [^{3}H]-CV 1808 is not available from commercial sources, the possible interaction of 8FB-PTP with this new adenosine receptor was not investigated and thus cannot be excluded. More recently, Gurden *et al.* (1993) have suggested that the response in guinea-pig aorta occurs via the A_{2b} receptor, which is usually associated with fibroblasts, rather than the classical A_{2a} receptors. On these grounds, the physiological role of each receptor type and consequently the receptor nomenclature can be clarified only with the discovery of new ligands possessing the ability to interact more specifically with each receptor subtype. From the present data, the new non-xanthine heterocyclic drug, 8FB-PTP, has emerged as a potent A_2 antagonist in functional assays and can provide useful information as to the function of the A_2 receptor. Since the compound is highly potent at A_2 receptors, it provides a basis to progress with further synthetic efforts in order to reduce affinity at A_1 receptors and therefore enhance A_2 receptor selectivity.

We are very grateful to Dr Erminio Bonizzoni for the development of the statistical methodology in pA_2 analysis. We also thank Dr Ho Sam Ahn and Dr Carolyn Foster for phosphodiesterase studies (Department of Pharmacology, Schering-Plough Research Institute, Kenilworth, NJ, U.S.A.).

References

ABBRACCHIO, M.P., CATTABENI, F., FREDHOLM, B.B. & WILLIAMS, M. (1993). Purinoceptor nomenclature: a status report. *Drug Dev. Res.*, **28**, 207–213.

AHN, H.S., FOSTER, M., FOSTER, C., SYBERTZ, E. & WELLS, J.N. (1991). Evidence for essential histidine and cysteine residues in calcium/calmodulin-sensitive cyclic nucleotide phosphodiesterase. *Biochemistry*, **30**, 6754–6760.

BORN, G.V.R. & CROSS, M.J. (1963). The aggregation of blood platelets. *J. Physiol.*, **168**, 178–195.

BRUNS, R.F., DALY, J.W. & SNYDER, S.H. (1990). Adenosine receptors in brain membranes: binding of N^6-cyclohexyl [^{3}H] adenosine and 1,3-diethyl-8[^{3}H] phenylxanthine. *Proc. Natl. Acad. Sci. U.S.A.*, **77**, 5547–5551.

BRUNS, R.F., FERGUS, J.H., BADGER, E.W., BRISTOL, J.A., SANTAY, L.A., HARTMAN, J.D., HAYS, S.J. & HUANG, C.C. (1987). Binding of the A_1-selective adenosine antagonist 8-cyclopentyl-1,3-dipropylxanthine to rat brain membranes. *Naunyn-Schmied. Arch. Pharmacol.*, **335**, 59–63.

BRUNS, R.F., LU, G.H. & PUGSLEY, T.A. (1986). Characterization of the A_2 adenosine receptor labeled by [^{3}H]NECA in rat striatal membranes. *Mol. Pharmacol.*, **29**, 331–346.

CONTI, A., MONOPOLI, A., GAMBA, M., BOREA, P.A. & ONGINI, E. (1993). Effects of selective A_1 and A_2 adenosine receptor agonists on cardiovascular tissues. *Naunyn-Schmied. Arch. Pharmacol.*, **348**, 108–112.

CORNFIELD, L.J., HU, S., HURT, S.D. & SILLS, M.A. (1992). [^{3}H]2-Phenylaminoadenosine ([^{3}H]CV 1808) labels a novel adenosine receptor in rat brain. *J. Pharmacol. Exp. Ther.*, **263**, 552–561.

DIONISOTTI, S., ZOCCHI, C., VARANI, K., BOREA, P.A. & ONGINI, E. (1992). Effects of adenosine derivatives on human and rabbit platelet aggregation. Correlation of adenosine receptor affinities and antiaggregatory activity. *Naunyn-Schmied. Arch. Pharmacol.*, **346**, 673–676.

FERKANY, J.W., VALENTINE, H.L., STONE, G.A. & WILLIAMS, M. (1986). Adenosine A_1 receptors in mammalian brain: species differences in their interactions with agonists and antagonists. *Drug Dev. Res.*, **9**, 85–93.

FINNEY, D.J. (1978). *Statistical Methods in Biological Assay*, 3rd ed. pp. 80–82. London: Griffin.

GATTA, F., DEL GIUDICE, M.R., BORIONI, A., BOREA, P.A., DIONISOTTI, S. & ONGINI, E. (1993). Synthesis of imidazo [1,2-c]pyrazolo [4,3-e]pyrimidines, pyrazolo [4,3-e]1,2,4-triazolo[1,5-c]pyrimidines and triazolo[5,1-i]purines: new potent A2 adenosine receptor antagonists. *Eur. J. Med. Chem.*, **28**, 569–577.

GHAI, G., FRANCIS, J.E., WILLIAMS, M., DOTSON, R.A., HOPKINS, M.F., COTE, D.T., GOODMAN, F.R. & ZIMMERMAN, M.B. (1987). Pharmacological characterization of CGS 15943A: a novel non-xanthine adenosine antagonist. *J. Pharmacol. Exp. Ther.*, **242**, 784–790

GURDEN, M.F., COATES, J., ELLIS, F., EVANS, B., FOSTER, M., HORNBY, E., KENNEDY, I., MARTIN, D.P., STRONG, P., VARDEY, C.J. & WHEELDON, A. (1993). Functional characterization of three adenosine receptor types. *Br. J. Pharmacol.*, **109**, 693–698.

JACOBSON, K.A., GALLO-RODRIGUEZ, C., MELMAN, N., FISCHER, B., MAILLARD, M., VAN BERGEN, A., VAN GALEN, P.J.M. & KARTON, Y. (1993a). Structure-activity relationships of 8-styryl-xanthines as A_2-selective adenosine antagonists. *J. Med. Chem.*, **36**, 1333–1342.

JACOBSON, K.A., NIKODIJEVIC', O., PADGETT, W.L., GALLO-RODRIGUEZ, C., MAILLARD, M. & DALY, J.W. (1993b). 8-(3-Chlorostyryl)caffeine (CSC) is a selective A2-adenosine antagonist in vitro and in vivo. *FEBS*, **323**, 141–144.

JACOBSON, K.A., VAN GALEN, P.J.M. & WILLIAMS, M. (1992). Adenosine receptors: pharmacology, structure-activity relationships, and therapeutic potential. *J. Med. Chem.*, **35**, 407–422.

JARVIS, M.F., SCHULZ, R., HUTCHISON, A.J., DO, U.H., SILLS, M.A. & WILLIAMS, M. (1989). [^{3}H]CGS 21680, a selective A_2 adenosine receptor agonist directly labels A_2 receptors in rat brain. *J. Pharmacol. Exp. Ther.*, **251**, 888–893.

LIBERT, F., SCHIFFMANN, S.F., LEFORT, A., PARMENTIER, M., GERARD, C., DUMONT, J.E., VANDERHAEGEN, J.J. & VASSART, G. (1991). The orphan receptor cDNA RDC7 encodes an A1 adenosine receptor. *EMBO J.*, **10**, 1677–1682.

LONDOS, C., COOPER, D.M.F. & WOLFF, J. (1980). Subclasses of external adenosine receptors. *Proc. Natl. Acad. Sci. U.S.A.*, **77**, 2551–2554.

LOWRY, O.H., ROSEBROUGH, N.J., FARR, A.I. & RANDALL, R.J. (1951). Protein measurement with Folin phenol reagent. *J. Biol. Chem.*, **193**, 265–275.

MAENHAUT, C., VAN SANDE, J., LIBERT, F., ABRAMOWICZ, M., PARMENTIER, M., VANDERHAEGEN, J.J., DUMONT, J.E., VASSART, G. & SCHIFFMANN, S. (1990). RDC8 codes for an adenosine A2 receptor with physiological constitutive activity. *Biochem. Biophys. Res. Commun.*, **173**, 1169–1178.

MAKUJINA, R.R., SABOUNI, M.H., BHATIA, S., DOUGLAS, F.L. & MUSTAFA', S.J. (1992). Vasodilatory effects of adenosine A_2 receptor agonists CGS 21680 and CGS 22492 in human vasculature. *Eur. J. Pharmacol.*, **221**, 243–247.

MUNSON, P.J. & RODBARD, P. (1980). LIGAND: a versatile computerized approach for characterization of ligand-binding systems. *Anal. Biochem.*, **107**, 220–239.

NONAKA, Y., SHIMADA, J., NONAKA, H., KOIKE, N., AOKI, N., KOBAYASHI, H., KASE, H., YAMAGUCHI, K. & SUZUKI, F. (1993). Photoisomerization of a potent and selective adenosine A2 antagonist, (E)-1,3-dipropyl-8-(3,4-dimethoxystyryl)-7-methylxanthine. *J. Med. Chem.*, **36**, 3731–3733.

RALL, T.W. (1985). Central nervous system stimulants: the methylxanthine. In *The Pharmacological Basis of Therapeutics*, 7th ed. ed. Gilman, A.G., Goodman, L.S., Rall, T.W. & Murad, F. pp. 589–602. New York: Macmillan Publishing Co.

SABOUNI, M.H., BROWN, G.L., KOTAKE, A.N., DOUGLAS, F.L. & MUSTAFA', S.J. (1990). Effects of CGS 15943 on the relaxation produced by adenosine analogs in human blood vessels. *Eur. J. Pharmacol.*, **187**, 525–530.

SAS/STAT GUIDE FOR PERSONAL COMPUTER. VERSION 6 EDITION (1987). SAS Institute Inc., Cary, NC, USA. pp. 549–640 (PROC GLM), pp. 675–693 (PROC NONLIN).

SHIMADA, J., SUZUKI, F., NONAKA, H., ISHII, A. & ICHIKAWA, S. (1992). (E)-1,3-dialkyl-7-methyl-8-(3,4,5-trimethoxy-styryl) xanthines: potent and selective adenosine A2 antagonists. *J. Med. Chem.*, **35**, 2342–2345.

STONE, G.A., JARVIS, M.F., SILLS, M.A., WEEKS, B., SNOWHILL, E.W. & WILLIAMS, M. (1988). Species differences in high-affinity adenosine A_2 binding sites in striatal membranes from mammalian brain. *Drug Dev. Res.*, **15**, 31–46.

TALLARIDA, R.J., COWAN, A. & ADLER, M.W. (1979). pA_2 and receptor differentiation: a statistical analysis of competitive antagonism. *Life Sci.*, **25**, 637–654.

VAN CALKER, D., MULLER, M. & HAMPRECHT, B. (1979). Adenosine regulates via two different types of receptors the accumulation of cyclic AMP in cultured brain cells. *J. Neurochem.*, **33**, 999–1005.

VAN GALEN, P.J.M., STILES, G.L., MICHAELS, G.S. & JACOBSON, K.A. (1992). Adenosine A_1 and A_2 receptors: structure function relationships. *Med. Res. Rev.*, **12**, 423–471.

WAUD, D.R. (1975). Analysis of dose-response curves. *Methods in Pharmacology*, vol. 3. *Smooth Muscles*. ed. Daniel, E.E. & Paton, D.M. pp. 471–506. New York: Plenum Press.

WILLIAMS, M., FRANCIS, J., GHAI, G., BRAUNWALDER, A., PSYCHOYOS, S., STONE, G.A. & CASH, W.D. (1987). Biochemical characterization of the triazoloquinazoline, CGS 15943, a novel, non-xanthine adenosine antagonist. *J. Pharmacol. Exp. Ther.*, **241**, 415–420.

(Received October 18, 1993
Revised January 10, 1994
Accepted January 31, 1994)

Br. J. Pharmacol. (1994), **112**, 666–670

Evaluation of a series of novel CCK_B antagonists using a functional assay in the rat central nervous system

[1]P.R. Boden, R.D. Pinnock, M.C. Pritchard & G.N. Woodruff

Parke-Davis Neuroscience Research Centre, Addenbrookes Hospital Site, Hills Road, Cambridge CB2 2QB

1 Electrophysiological recordings from rat ventromedial hypothalamus (VMH) *in vitro* have been used to compare the effects of novel chemical entities on CCK_B receptor activation in the rat central nervous system.

2 Twenty compounds from three different chemical series were evaluated for their ability to reduce pentagastrin-induced increases in action potential firing rate.

3 All twenty compounds studied were found to be CCK_B antagonists, with equilibrium constants spanning a concentration-range of several orders of magnitude. The rank order for their ability to block pentagastrin responses correlated well with values obtained for their relative affinities for the mouse cortex CCK_B binding site.

4 It is concluded that the VMH preparation provides a good functional correlate to binding assays in the rodent central nervous system for a structurally diverse series of CCK_B antagonists.

Keywords: Novel CCK_B antagonists; hypothalamus; electrophysiology

Introduction

Cholecystokinin (CCK) is an important hormone, existing in both the mammalian gastrointestinal tract and central nervous system. In the latter CCK exists predominantly as the sulphated octapeptide (Dockray, 1976; Innis *et al.*, 1979), acting either at the gastrin/CCK_B receptor or at the more discretely localized CCK_A receptor to modify a wide variety of centrally-mediated behavioural events, including feeding (Gibbs & Smith, 1973; Dourish *et al.*, 1989), analgesia (Jurna & Zetler, 1981; Faris *et al.*, 1983; Watkins *et al.*, 1983) and anxiety (Bradwejn *et al.*, 1990). The relative importance of the two CCK receptor types in modulation of each of these behavioural states is unclear but the design and synthesis of highly selective antagonists for both CCK_A (Chang & Lotti, 1986) and CCK_B (Lotti & Chang, 1989; Hughes *et al.*, 1990) receptors has provided the opportunity to isolate the events following activation of a particular CCK receptor sub-type in the central nervous system.

Novel CCK_B antagonists, notable for their structural dissimilarities, are now available. Non-peptide CCK_B antagonists have been derived from three different approaches. The gastrin/CCK_B antagonist L365,260 was produced following modification of the selective CCK_A receptor antagonist devazepide (Evans *et al.*, 1986; 1988). L365,260 displays a 100 fold greater affinity for the CCK_B receptor than for the CCK_A receptor (Lotti & Chang, 1989). Research at Lilly has produced a series of CCK_B antagonists following screening and structure-activity work based on early lead compounds culminating in the synthesis of LY-262691. This compound shows improved selectivity for the CCK_B receptor when compared to L365,260 (400 fold cf. 100 fold) although its affinity for the CCK_B receptor *per se* is lower (Bock, 1991). Horwell (1991) using a peptoid approach to modify the smallest active fragment of CCK, CCK-4, has produced CI-988. This compound has the highest CCK_B binding affinity when compared to the aforementioned compounds and is the most selective CCK_B receptor antagonist to date (Woodruff *et al.*, 1991) it is also a very effective anxiolytic in a number of animal models (Hughes *et al.*, 1990; Woodruff *et al.*, 1991) and enhances morphine-induced analgesia in rats (Weisenfeld-Hallen *et al.*, 1990).

At present, the number of functional assays for central CCK_B receptors is limited. The best characterized is the rat ventromedial hypothalamus (VMH) which possesses neurones the spontaneous action potential firing rate of which is increased by CCK (Boden & Hill, 1988). A great majority (>90%) of VMH neurones are CCK-sensitive and the preparation has a high density of CCK_B receptors (Woodruff *et al.*, 1991). Using this model we have shown that peptoid CCK_B ligands are powerful antagonists of CCK-8s induced excitation (Hughes *et al.*, 1990) but the use of a non-selective agonist such as the sulphated C-terminal octapeptide can sometimes lead to activation of a mixture of both CCK_B and CCK_A receptors (Pinnock *et al.*, 1992), leading to possible under-estimation of functional activity. To overcome this difficulty in CCK_B antagonist studies we have used the selective agonist, pentagastrin, sometimes in combination with the selective CCK_A antagonist, devazepide, in an attempt to eliminate all possible interactions arising from activation of CCK_A receptors.

The aims of the present study were 2 fold. Firstly, to validate the use of an *in vitro* brain slice VMH preparation for quantitative pharmacological studies of CCK_B antagonists in the central nervous system. To this end the CCK_B antagonist activity of a number of novel chemical entitites spanning a wide range of binding affinities from the same chemical series were investigated. Secondly, to compare the three chemically distinct CCK_B antagonist classes in the same paradigm at least one representative from each of the aforementioned drug design strategies was included in the present study.

Methods

Electrophysiology

Extracellular recordings were made from rat VMH neurones contained in coronal slices of rat midbrain. Hypothalamic slices were prepared from the brains of male Wistar rats (100–200 g) as described previously (Boden & Hill, 1988) and incubated in pre-gassed (95% O_2:5% CO_2) artificial cerebrospinal fluid of the following composition (mM); NaCl 124, KCl 5, $CaCl_2$ 2.4, NaH_2PO_4 1.2, $MgCl_2$ 1.2, glucose 11, $NaHCO_3$ 25 at room temperature (21–23°C). One hour prior to recording, one slice was pinned to the Sylgard base of a Perspex chamber where it was submerged in ACSF and perfused by a gravity-fed perfusion system with ACSF at 37°C flowing at 4 ml min^{-1}. Drugs were applied directly

[1] Author for correspondence.

dissolved in the perfusing medium, three-way taps being used to switch to a drug-containing ACSF. When included in the perfusing ACSF, devazepide((S)-N-(2,3-dihydro-1-methyl-2-oxo-5- phenyl-1H-1, 4-benzodiazepin-3-yl)- 1H-indole-2-carboxamide) was added at a concentration of 10 nM for at least 20 min prior to recording. No detectable difference was found between shifts in pentagastrin dose-response curves using relatively low concentrations of CCK_B antagonists when devazepide was omitted from the ACSF but the CCK_A antagonist was used routinely at a concentration of 10 nM in studies assessing the actions of powerful CCK_B antagonists at high concentrations when the amounts of pentagastrin required to overcome the block might reach levels sufficient to activate CCK_A receptors. CCK_B antagonists were included in the perfusing solution for 30 min before construction of a second pentagastrin concentration-response curve in the presence of the antagonist. No change in the magnitude of the block produced by the antagonists was found when longer (up to 2 h) pre-incubation times were used. Data collection and analysis were performed with previously described methodology (Boden & Hill, 1987; Hughes *et al.*, 1990; Pinnock *et al.*, 1992). Final ratemeter histograms and dose-response curves were obtained by importing the files into a graphics and statistics software package (RS1, BBN software products, Cambridge, MA, U.S.A.). The same software was used to generate the correlation curve shown in Figure 1.

Receptor binding

Male mice were stunned and decapitated and the whole brain removed. The cerebral cortex was dissected free, weighed and homogenized in 10 volumes of ice-cold Tris buffer (pH 6.9 at 21°C) in a Polytron (setting 6 for 10–15 s). The homogenate was then centrifuged for 15 min at 20,000 *g* and the resulting pellet washed by re-suspension in Tris-HCl using a Polytron followed by re-centrifugation.

The final pellet was re-suspended in a standard assay buffer (10 mM HEPES, 130 mM NaCl, 4.7 mM KCl, 5 mM $MgCl_2$, 1 mM EGTA containing 0.25 mg ml^{-1} bacitracin) at a tissue concentration of 2 mg of original wet weight ml^{-1} of assay buffer.

For binding assays, aliquots (400 µl) of cortical membranes were incubated with a fixed concentration (35 pM) of [^{125}I]-Bolton-Hunter CCK-8 ([^{125}I]-CCK-8 specific activity, 2000 Ci $mmol^{-1}$) for 120 min at 21°C in the absence and presence of a range of concentrations (3×10^{-11} to 1×10^{-6} M) of unlabelled test compound to give a final assay volume of 500 µl. Non-specific binding was that remaining in the presence of either 1 µM CCK-8s or CI-988. Non-specific binding defined by either the peptide or non-peptide ligands was equivalent.

Following the end of the incubation of washing (3 × 4 ml) in ice-cold NaCl, the assay was terminated by rapid filtration under vacuum through Whatman GF/B filter strips. The filters were transferred to vials containing 5 ml of Beckman HP scintillant and radioactivity was measured in a Packard series 5000 gamma counter. Binding results were analyzed using Graphpad INPLOT (Graphpad Software Inc.). Competition data were transformed by non-linear regression to obtain IC_{50} values, which were then converted to K_i values by the Cheng-Prussoff equation.

Clog P determinations

Clog P represents the calculated log P value as determined from the PCMODELS programme (Daylight Chemical Information Systems).

Sources of drugs

Pentagastrin (Boc-β-alanine CCK tetrapeptide) was purchased from Cambridge Research Biochemicals or Peninsula Laboratories. CCK_B antagonists were synthesized in the Medicinal Chemistry Department, Parke-Davis Neuroscience Research Centre (PDNRC), Cambridge, U.K., with the exception of PD141949, PD144598 and PD145942 which were synthesized in the Medicinal Chemistry Department, Warner-Lambert, Ann Arbor, Michigan, U.S.A.

Results

Tables 1 and 2 list the novel CCK_B ligands synthesized at PDNRC and used in the study, showing the side chain modifications to the core molecule. Synthesis of two CCK_B ligands of the pyrazolidinone series developed at Lilly, (compounds 20 and 17 in Howbert *et al.*, 1992) purported to show both good CCK_B binding and CCK_B/CCK_A selectivity, was undertaken to yield compounds **12** and **13** in the present study. The Merck, Sharp & Dohme CCK_B/gastrin antagonist L365260 was also screened (compound **20**), thus providing a list of compounds derived from different chemical strategies.

The results described in this paper to novel CCK_B antagonists in the rat VMH were obtained from a total of 78 preparations. All of the compounds were evaluated on at least three separate occasions to provide equilibrium constant (K_e) values. These results are summarized, together with the data for binding affinities (K_i) for the same compounds, in Table 3 and the relationship between pK_i from binding studies and pK_e from the functional assay is shown graphically in Figure 1. The best fit line for the data had a slop of 1.0 and a coefficient of determination (R^2) of 0.72.

Peptoid antagonists

Seventeen of the compounds tested were developed from the peptoid strategy, compounds exemplified by compound **2**

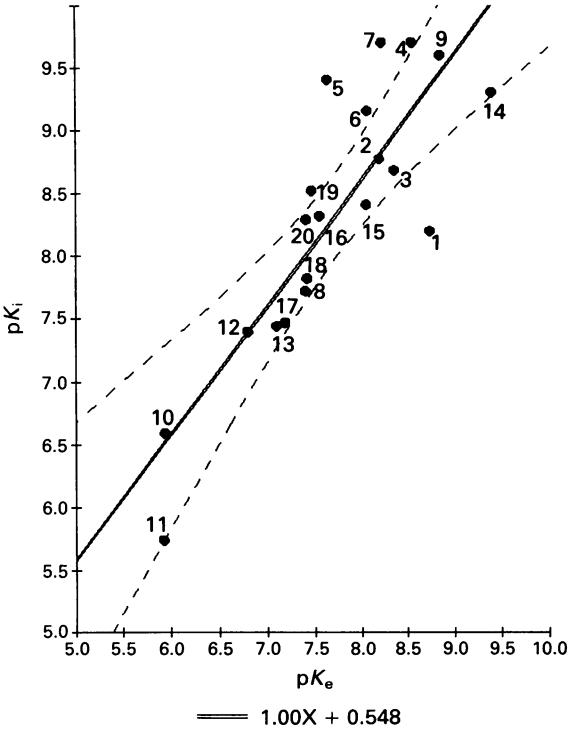

Figure 1 Summary of pK values for CCK_B antagonists. Plotted on the ordinate scale are pK_i values derived from binding studies on mouse cortex, against pK_e values on the abscissa scale from the functional assay (rat VMH, with pentagastrin used as the agonist in the presence of devazepide). The data shown are for 20 compounds spanning five orders of magnitude in the two tests. The best fit line, indicated by the solid line, has a slope (m) of 1.00 and a coefficient of determination (R^2) of 0.72. The dashed lines indicate the 95% confidence limits for the line.

Table 1 Chemical structures of 'peptoid' CCK_B ligands

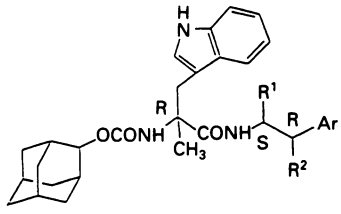

Compound	*R¹*	*R²*	*Ar*
(1)PD132461	CH_2OH	H	Ph
(2)PD134308	H	$NHCO(CH_2)_2CO_2H$	Ph
(3)PD135158[a]	H	$NHCO(CH_2)_2CO_2H$	Ph
(4)PD135666	CH_2CO_2H	H	Ph
(5)PD135667	$CH_2SCH_2CO_2H$	H	Ph
(6)PD136450[b]	H	$NHCOCH{:}CHCO_2H$	Ph
(7)PD137649	$CH_2SO_2CH_2CO_2H$	H	Ph
(8)PD140015	H	H	2-Pyridyl
(9)PD140376	CH_2CO_2H	H	4-Aminophenyl
(10)PD140548[c]	CH_2CO_2H	H	Ph
(14)PD142308	CH_2CO_2H	H	3-Iodo-4-aminophenyl
(15)PD142898[d]	CH_2CO_2H	H	Ph
(16)PD148101	CH_2OH	H	3-Pyridyl

[a]N-terminal blocking group is 1S endobornyloxycarbonyl; [b] olefin has E configuration; [c]S stereochemistry at Trp centre and **R** configuration at homo-Phe α-carbon; [d]N-terminal blocking group is S,S-2-methylcyclohexyloxycarbonyl.

Table 2 Chemical structures of 'peptoid' CCK_B ligands

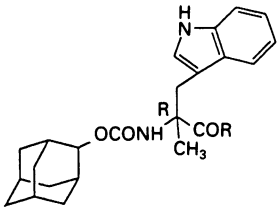

Compound	*R*
(11)PD141745	(S)Asp(S)$PheNH_2$
(17)PD141949	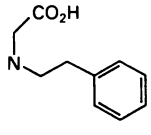
(18)PD144598	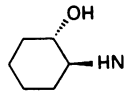
(19)PD145942	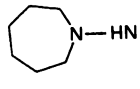

(PD134308, which is now called CI-988). In the present study the K_e for compound **2** against pentagastrin was 6.5 nM (range 0.8–10.4 nM), which agrees with previous reports showing this compound to be a powerful CCK_B antagonist (Hughes *et al.*, 1990). Compound **3** (PD135158) was also found to antagonize pentagastrin responses, with a K_e of 4.4 nM (range 1.7–7.4 nM). Both of the values differ slightly from those found using CCK as the agonist (Hughes *et al.*, 1990), possibly as a result of CCK_A receptor influence in the assays using the non-selective CCK agonist. Compounds **2** and **3** are carboxylic acids, as is compound **4** (PD135666), although this compound was somewhat less active in the functional assay than would have been predicted from binding assays.

Compound **14**(PD142308), which is the *m*-iodo *p*-amino phenyl derivative of compound **4**, was the most powerful antagonist tested in the VMH assay. No difference was found between the K_i value obtained in receptor binding and its equivalent K_e value of 400 pM. Figure 2 shows typical data obtained using this compound in the rat VMH. Compound **5**(PD135667) was less effective than might have been predicted in the functional assay. This compound has a high clog P value (5.8) but this is also found in compounds exhibiting a good correlation between binding and functional data from both the peptoid series e.g. compound **3** (PD135158) and entities from other classes e.g. compound **12**. Another more pertinent structural feature of compound **5**(PD135667) may be the inclusion of a sulphur-containing acid side chain. This feature is also found in compound **7**(PD137649) which is the corresponding sulphone derivative, whereas compound **5**(PD135667) has a thio-ether side chain moiety. Compound **7**(PD137649) was also less effective in the functional test than would be expected.

Compound **10**(PD140548) was tested as an example of a CCK_A receptor selective compound, having relatively low affinity for the CCK_B compared to the CCK_A binding site (compound 30p in Boden *et al.*, 1993). This compound still antagonized pentagastrin responses with a K_e in line with that expected, despite having only weak affinity for the CCK_B receptor. The same was true for compound **11**(PD141745) which is a weak, non-selective CCK antagonist, characteristics which were exemplified in its relatively poor pK_i and pK_e values. Compound **15**(PD142898) is a non-selective CCK antagonist with high affinity for both CCK_A and CCK_B receptors (compound 28 h in Boden *et al.*, 1993). The pK_e value obtained in the present study confirmed compound **15**(PD142898) to be a powerful CCK_B antagonist.

CCK_B antagonists from other chemical strategies

Compounds from two other, differing, chemical classes were tested in the rat VMH model. Compounds **12**, **13** and **20** were all CCK_B antagonists with K_e values in good agreement with those expected from the more extensive range of peptoid antagonists used in the present study.

Table 3 Summary of equilibrium constant (K_e) values and binding affinity constant values (K_i) for novel CCK_B antagonists

(N) *PD number*	K_e (nM)	K_e (range)	K_i (nM)	pK_e	pK_i
(1)PD132461	1.8	(0.8–3.3)	6.3	8.7	8.2
(2)PD134308	6.5	(1.8–10.4)	1.7	8.2	8.8
(3)PD135158	4.4	(1.7–7.4)	2.1	8.4	8.7
(4)PD135666	2.8	(0.1–8.4)	0.2	8.5	9.7
(5)PD135667	22.7	(19.0–28.0)	0.4	7.7	9.4
(6)PD136450	8.6	(6.1–9.7)	0.7	8.1	9.2
(7)PD137649	5.9	(3.2–10.3)	0.2	8.2	9.7
(8)PD140015	39.7	(10.1–83.0)	19.0	7.4	7.7
(9)PD140376	1.4	(0.8–2.0)	0.2	8.9	9.6
(10)PD140548	1150	(520–2500)	260.0	5.9	6.6
(11)PD141745	1200	(1010–1320)	1800	5.9	5.7
(12)	158.1	(100–235)	40.0	6.8	7.4
(13)	79.6	(27.3–162.3)	36.0	7.1	7.4
(14)PD142308	0.4	(0.3–0.5)	0.5	9.4	9.3
(15)PD142898	8.8	(5.4–10.8)	3.9	8.1	8.4
(16)PD148101	27.9	(23.4–31.2)	4.8	7.6	8.3
(17)PD141949	64.8	(53.7–102.7)	34.6	7.2	7.5
(18)PD144598	38.1	(17.2–64.1)	15.0	7.4	7.8
(19)PD145942	33.5	(25.2–41.7)	3.0	7.5	8.5
(20)	39.0	(33.6–43.8)	5.1	7.4	8.3

Functional assay for K_e value determination was the rat VMH with pentagastrin used as the agonist.
Binding assays were performed on the mouse cerebral cortex.
Compounds **12** and **13** are pyrazolidinone derivatives (compounds 20 and 17 in Howbert *et al.*, 1992). Compound **20** is L365260.

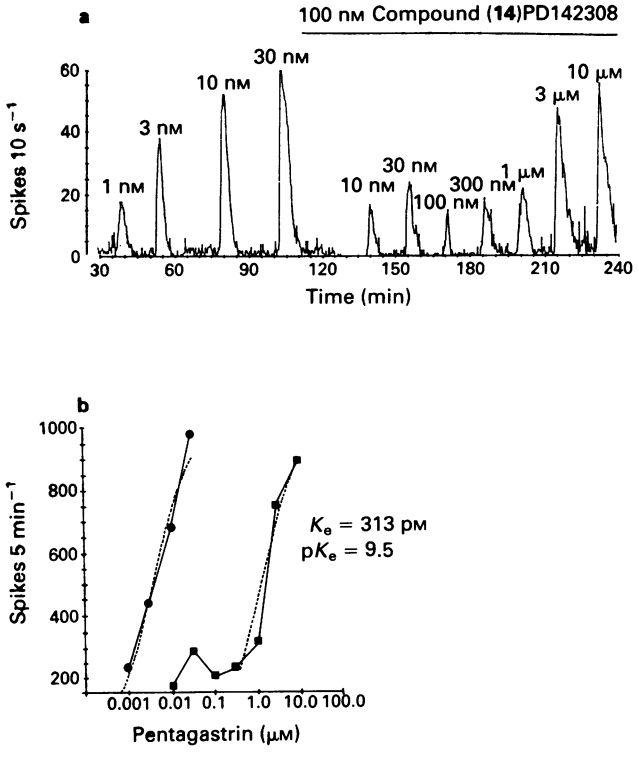

Figure 2 Ratemeter histogram showing typical trace obtained with one of the peptoid CCK_B antagonists: (a) shows the firing rate of a spontaneously active VMH neurone, given as firing rate (spikes $10\,s^{-1}$ epoch) against time course of the experiment along the abscissa scale in min. Pentagastrin was applied directly dissolved in the perfusing ACSF for 1 min (shown by ●) at the concentrations given to yield a control dose-response curve (● in b). Compound **14** was perfused for 30 min before repeating the pentagastrin dose-response curve in the continued presence of compound **14**. The responses to 10 nM and 30 nM pentagastrin were reduced. After 1 h in the presence of compound **14**, subsequent applications of increasing doses of the agonist were used to produce the data given by (■) in (b). The equilibrium constant for compound **14** in this experiment was 313 pM.

Discussion

The majority of the compounds shown in Table 1 were selected for evaluation in an electrophysiological assay on the basis of their high affinity and selectivity in the mouse cortex CCK_B receptor binding assay and their structural diversity. Comparison of functional data with results from binding assays revealed a highly positive correlation. One notable feature is that, irrespective of chemical class, there is a consistent difference between the absolute values obtained in the two tests, with binding values being around one-half an order of magnitude better than seen in the functional studies. Whether this is due to under-estimation of functional antagonism because of poor penetration of the compounds is not known. It is unlikely to be a result of insufficient equilibration time since compounds were always included for 30 min prior to construction of a second pentagastrin concentration-response curve. One other possible explanation would be that the binding of K_i values are over-estimates resulting from the use of a non-selective ligand for displacement experiments. The relatively low specific activity of [^{3}H]-pentagastrin restricts the use of this radioligand in binding studies because of the possible errors which may be introduced with the requirement for higher tissue concentrations.

Included in the selection of compounds were examples of carboxylic acids e.g. compounds **2**(PD134308), **3**(PD135158) and **4**(PD135666), pyridine bases e.g. compound **8** and **16** and neutral alcohols e.g. compounds **1**(PD132461) and **19**(PD145942). Log P values for the series span almost two orders of magnitude, from 4.1 (compound **8**,PD140015) to 5.8 (compound **5**,PD135667). The pK_a values for the acids is even more wide-ranging (4.16 for compound **6**(PD136450) to 6.16 for compound **2**(PD134308)). Despite this physicochemical diversity, only one compound **1**(PD132461) yielded a pK_e value greater than its pK_i counterpart. The reason for this is unclear since compound **1**(PD132461) is a neutral alcohol derivative similar to compounds **16** (PD148101) and **19** (PD145942) with an unexceptional log P value of 5.19.

In summary, the results presented herein from *in vitro* functional studies confirm all 20 compounds to be antagonists at CCK_B receptors in the rat brain. Thus, we can conclude that the VMH slice preparation provides a robust CNS assay and provides a good functional adjunct to obtain a rank order which mirrors that found in binding studies for novel CCK_B antagonists.

References

BOCK, M.G. (1991). Development of non-peptide cholecystokinin type B receptor antagonists. *Drugs of the Future*, **16**, 631–640.

BODEN, P.R., HIGGINBOTTOM, M., HILL, D.R., HORWELL, D.C., HUGHES, J., REES, D.C., ROBERTS, E., SINGH, L., SUMAN-CHAUHAN, N. & WOODRUFF, G.N. (1993). Cholecystokinin dipeptoid antagonists: design, synthesis and anxiolytic profile of some novel CCK-A and CCK-B selective and 'mixed' CCK-A/CCK-B antagonists. *J. Med. Chem.*, **36**, 552–565.

BODEN, P. & HILL, R.G. (1987). Effects of cholecystokinin and pentagastrin on neuronal activity in the ventromedial nucleus of the rat hypothalamic slice preparation. *Br. J. Pharmacol.*, **92**, 585P.

BODEN, P. & HILL, R.G. (1988). Effect of cholecystokinin and related peptides on neuronal activity in the ventromedial nucleus of the rat hypothalamus. *Br. J. Pharmacol.*, **94**, 246–252.

BRADWEJN, J., KOSZYCKI, D. & METERISSIAN, G. (1990). Cholecystokinin tetrapeptide induces panic attacks in patients with panic disorder. *Can. J. Psychiatry*, **35**, 83–85.

CHANG, R.S.L. & LOTTI, V. (1986). Biochemical and pharmacological characterization of an extremely potent and selective non-peptide cholecystokinin antagonist. *Proc. Natl. Acad. Sci. U.S.A.*, **83**, 4923–4926.

DOCKRAY, G.J. (1976). Immunochemical evidence for cholecystokinin-like peptides in brain. *Nature*, **2264**, 568–570.

DOURISH, C.T., RUCKERT, A.C., TATTERSALL, F.D. & IVERSEN, L.L. (1989). Evidence that decreased feeding induced by systemic injection of cholecystokinin is mediated by CCK_A receptors. *Eur. J. Pharmacol.*, **173**, 233–234.

EVANS, B.E., BOCK, M.G., RITTLE, K.E., DiPARDO, R.M., WHITTER, W.L., VEBER, D.F., ANDERSON, P.S. & FREIDINGER, R.M. (1986). Design of potent, orally effective, nonpeptidal antagonists of the peptide hormone cholecystokinin. *Proc. Natl. Acad. Sci. U.S.A.*, **83**, 4918–4922.

EVANS, B.E., RITTLE, K.E., BOCK, M.G., DiPARDO, R.M., FREIDINGER, R.M, WHITTER, W.L., LUNDELL, G.F., VEBER, D.F., ANDERSON, P.S., CHANG, R.S.L., LOTTI, V.J., CERINO, D.J., KLING, P.J., KUNKEL, K.A., SPRINGER, J.P. & HIRSHFELD, J. (1988). Methods for drug discovery: Development of potent, selective, orally effective cholecystokinin antagonists. *J. Med. Chem.*, **31**, 2235–2246.

FARIS, P.L., KOMISURAK, B.R., WATKINS, L.R. & MAYER, D.J. (1983). Evidence for the neuropeptide cholecystokinin as an antagonist of opiate analgesia. *Science*, **219**, 310–312.

GIBBS, J. & SMITH, G.P. (1973). Cholecystokinin-decreased food intake in rats. *J. Comp. Physiol.*, **84**, 488–495.

HOWBERT, J.J., LOBB, K.L., BROWN, R.F., REEL, J.K., NEEL, D.A., MASON, N.R., MENDELSOHN, L.G., HODGKISS, J.P. & KELLY, J.S. (1992). A novel series of non-peptide CCK and gastrin antagonists: medicinal chemistry and electrophysiological demonsration of antagonism. In *Multiple Cholecystokinin Receptors – Progress Towards CNS Therapeutic Targets*. ed. Dourish, C., Cooper, S.J., Iversen, S.D. & Iversen, L.L. Oxford University Press: London.

HORWELL, D.C. (1991). Development of CCK_B antagonists. *Neuropeptides*, **19** (Suppl.), 57–64.

HUGHES, J., BODEN, P., COSTALL, B., DOMENEY, A., KELLY, E., HORWELL, D.C., HUNTER, J.C., PINNOCK, R.D. & WOODRUFF, G.N. (1990). Development of a class of cholecystokinin type B receptor antagonists having potent anxiolytic activity. *Proc. Natl. Acad. Sci. U.S.A.*, **87**, 6728–6732.

INNIS, R.B., CORREA, F.M.A., UHL, G.R., SCHNEIDER, B. & SNYDER, S.H. (1979). Cholecystokinin octapeptide-like immunoreactivity: histochemical localization in rat brain. *Proc. Natl. Acad. Sci. U.S.A.*, **76**, 521–525.

JURNA, I. & ZETLER, G. (1981). Antinociceptive effect of centrally administered caeurlein and cholecystokinin (CCK). *Eur. J. Pharmacol.*, **73**, 323–331.

LOTTI, V. & CHANG, R.S.L. (1989). A potent and selective non-peptide gastrin antagonist and brain (CCK_B) receptor ligand: L365,260. *Eur. J. Pharmacol.*, **162**, 273–280.

PINNOCK, R.D., RICHARDSON, R.S., BODEN, P.R. & WOODRUFF, G.N. (1992). Cholecystokinin receptors in the rat brain *in vitro*: sensitivity to CCK_A and CCK_B receptor agonists and antagonists. *Mol. Neuropharmacol.*, **1**, 211–218.

WATKINS, L.R., KINSHECK, I.B. & MAYER, D.J. (1983). Potentiation of opiate analgesia and apparent reversal of morphine tolerance by proglumide. *Science*, **224**, 395–396.

WEISENFELD-HALLIN, Z., XU, X.-J., HUGHES, J., HORWELL, D.C. & HOKFELT, T. (1990). PD134308, a selective antagonist of cholecystokinin type B receptor, enhances the analgesic effect of morphine and synergistically interacts with intrathecal galanin to depress spinal nociceptive reflexes. *Proc. Natl. Acad. Sci. U.S.A.*, **87**, 7105–7109.

WOODRUFF, G.N., HILL, D.R., BODEN, P.R., PINNOCK, R.D., SINGH, L. & HUGHES, J. (1991). Functional role of brain CCK receptors. *Neuropeptides*, **19** (Suppl.), 45–56.

(Received November 18, 1993
Revised February 14, 1994
Accepted February 16, 1994)

Br. J. Pharmacol. (1994), **112**, 671–675

Importance of the intestine as a site of metformin-stimulated glucose utilization

[1]C.J. Bailey, K.J. Mynett & T. Page

Department of Pharmaceutical & Biological Sciences, Aston University, Birmingham B4 7ET

1 The intestine has been implicated as a site of increased glucose utilization by the antihyperglycaemic drug, metformin. This study makes a quantitative assessment of this effect.

2 Glucose utilization by the intestine and hind limb region was determined by arterial-venous glucose difference adjusted for blood flow rate in fasted rats receiving a hyperglycaemic hyperinsulinaemic infusion.

3 Intrajejunal administration of metformin, 250 mg kg^{-1}, increased glucose disposal during the infusion procedure, associated with increased glucose utilization in the intestine by 69% and in the hind limb region by 40%.

4 Metformin, 250 mg kg^{-1}, increased glucose disappearance during an intravenous glucose tolerance test. This was accompanied by increased uptake of tritiated 2-deoxy-D-glucose into the intestinal mucosa to a greater extent than into skeletal muscles (per unit wet weight of tissue).

5 The results demonstrate that the intestinal mucosa is a quantitatively important site of increased glucose utilization during the blood glucose-lowering effect of metformin.

Keywords: Metformin; glucose utilization; intestine; hind limbs

Introduction

The antihyperglycaemic agent, metformin (dimethylbiguanide), increases glucose utilization, reduces hepatic glucose production and reduces the rate of intestinal glucose absorption (Bailey, 1992; 1993). The blood glucose-lowering effect requires the presence of at least some insulin, but metformin does not increase insulin concentrations (Bailey & Mynett, 1994). Metformin augments insulin-stimulated glucose uptake and metabolism by skeletal muscle and fat, and increases the suppression of hepatic gluconeogenesis by insulin (Bailey, 1992; 1993).

Recent studies have shown that metformin increases glucose utilization by the intestine (Penicaud *et al.*, 1989; Bailey *et al.*, 1992). This occurs in the fasted state as well as in the fed state, indicating that the drug can increase the intestinal extraction of glucose from the vascular compartment. The intestine requires the presence of insulin to undertake normal glucose metabolism, but it does not show an insulin concentration-related utilization of glucose as seen with muscle and fat (Kellett *et al.*, 1984). Moreover, the intestinal wall accumulates much higher concentrations of metformin than other tissues (Wilcock & Bailey, 1994), raising the possibility that the drug may have a different mode of action in the intestine than in other tissues.

The present study investigates the contribution of the intestine to the overall effect of metformin on glucose uptake from the circulation. The study examines whether metformin alters blood flow through the intestine, and compares glucose utilization by the intestine and hind limb region after i.v. glucose administration. The uptake of glucose by different tissues has also been assessed using the non-metabolized glucose analogue, 2-deoxy-D-glucose.

Methods

Animals

Adult male Wistar rats weighing 150–200 g were maintained as previously described (Bailey *et al.*, 1992). Anaesthesia was induced with sodium pentobarbitone (60 mg kg^{-1}, i.p.) and maintained with further doses of 15 mg kg^{-1} h^{-1}. Rectal temperature was held at 34–36°C. A cannula was introduced into the right internal jugular vein for i.v. administration of test substances.

Blood flow

Rats were fasted for 24 h, anaesthetized, and the abdomen was opened. Transonic ultrasound flow sensors (2 mm) were coupled around the hepatic portal vein (HPV) and lower abdominal vena cava (IVC) using acoustic lubricating jelly. The sensors were connected to a T106 transonic volume flow meter (Transonic System Inc, Ithaca, New York, U.S.A.) supplied by Linton Instrumentation, Diss, Norfolk. Blood flow was monitored continuously (Drost *et al.*, 1984) and recorded on a flat-bed chart recorder.

Hyperglycaemic hyperinsulinaemic infusion

Twenty-four hours fasted, anaesthetized rats received an i.v. infusion of the following via the jugular cannula: adrenaline bitartrate (0.08 μg kg^{-1} min^{-1}), propranolol hydrochloride (1.7 μg kg^{-1} min^{-1}), glucose (16 mg kg^{-1} min^{-1}) and bovine insulin (3 miu kg^{-1} min^{-1}) as described by Reaven *et al.* (1983). This produced a steady hyperglycaemia (about 11 mmol l^{-1}) and hyperinsulinaemia (about 5 ng ml^{-1}) by 60–90 min. This steady state was maintained in control animals throughout the remainder of the experiment (until 180 min). The effect of metformin was determined by administration of metformin hydrochloride (250 mg kg^{-1}) into the proximal jejunum at 90 min. Control animals received an equivalent volume of PBS, 10 ml kg^{-1}. Blood samples were taken from the tail tip at 30 min intervals throughout the study for determination of plasma glucose and insulin concentrations.

At the end of the infusion period (180 min), simultaneous blood samples were taken for plasma glucose determination from the lower abdominal aorta, lower abdominal vena cava, and hepatic portal vein.

[1] Author for correspondence.

Tissue uptake of 2-deoxy-D-glucose

Glucose uptake into different tissues was measured using 2-deoxy-D-[1-^{3}H]-glucose administered during an intravenous glucose tolerance test (IVGTT). Twenty-four hour fasted, anaesthetized rats received either metformin hydrochloride (250 mg kg^{-1}) or an equivalent volume of PBS (10 ml kg^{-1}) delivered into the proximal jejunum at −60 min. At 0 min the rats received an i.v. glucose bolus (0.5 g kg^{-1}), and at 5 min an i.v. injection of 2-deoxy-D-[1-^{3}H]-glucose (5 μCi per 100 g body weight) and [U-^{14}C]-sucrose (1.67 μCi per 100 g body weight). Blood samples for plasma glucose determination were taken from the tail tip at −60, 0, 5 and 30 min. The rate of plasma glucose disappearance (% min^{-1}) was determined ($69.3/t_{\frac{1}{2}}$) between 5 and 30 min. At 30 min a venous blood sample and the following tissues were quickly removed: quadriceps femoris, soleus, transverse abdominal muscle, diaphragm, heart ventricular apex, epididymal white fat, antral region of stomach, mid-jejunum, mid-small intestine (halfway between ligament of Treitz and ileo-caecal valve), mid-ileum, descending colon, and cerebral hemisphere of brain. Samples of intestinal mucosa were carefully separated by scraping with a microscope slide. Pieces of tissue weighing about 50 mg and 50 μl of plasma were digested in 0.5 ml 1 mmol l^{-1} NaOH at 80°C, and 5 ml Hisafe II scintillant was added for counting on a Packard 1800 TR liquid scintillation analyser. The tissue accummulation of 2-deoxy[1-^{3}H]-glucose-6-phosphate was determined as d.p.m. mg^{-1} wet weight of tissue corrected for the sucrose space.

Glucose and insulin assays

Plasma glucose was measured by an automated glucose oxidase procedure (Stevens, 1971) and plasma insulin was determined by radioimmunoassay using a polyethylene glycol separation method (Desbuquois & Aurbach, 1971).

Chemicals

All chemicals were obtained from Sigma Chemical Company, Poole or BDH, Poole except: PBS tablets from Unipath, Basingstoke; metformin hydrochloride from Lipha Pharmaceuticals, West Drayton; sodium pentobarbitone (Sagatal) from RMB Animal Health Ltd, Dagenham; anti-insulin serum from Linco Research, St. Louis, U.S.A.; [^{125}I]-insulin from Amerlite Diagnostics, Amersham; [U-^{14}C]-sucrose, 621 mCi mmol^{-1}, and 2-deoxy-D-[1-^{3}H]-glucose, 14.4 Ci mmol^{-1} from Amersham International, Amersham.

Statistical analysis

Data are presented as mean ± s.e.mean. Data were evaluated for the effect of metformin by one-way analysis of variance, and differences between individual groups were compared by Student's unpaired t test. Differences were considered to be significant if $P<0.05$.

Results

Blood flow

Blood flow measurements were undertaken in fasted anaesthetized rats by use of transonic flow sensors around the HPV and lower abdominal IVC. Under conditions of basal glycaemia, blood flow rates were about 60 and 40 ml min^{-1} kg^{-1} for the HPV and IVC respectively. Flow rates in the HPV were temporarily (5–10 min) increased by about 10% when hyperglycaemia (10–15 mmol l^{-1}) was induced by intravenous administration of glucose.

Metformin (250 mg kg^{-1}, intrajejunally) did not significantly alter blood flow rates in either the HPV or IVC under basal or hyperglycaemic conditions.

Hyperglycaemic hyperinsulinaemic infusion

The infusion of glucose and insulin together with adrenaline and propranolol in fasted anaesthetized rats created a steady hyperglycaemia (about 11 mmol l^{-1}) and hyperinsulinaemia (about 5 ng ml^{-1}) between 90 and 180 min as shown in Figure 1. Administration of metformin (250 mg kg^{-1}, intrajejunally) at 90 min produced a progressive fall in the venous plasma glucose concentration, whereas plasma insulin was not significantly altered.

An indication of the importance of the intestine and the hind limbs as sites of metformin-stimulated glucose disposal was obtained by comparing the plasma glucose concentration in blood samples taken from the aorta (A), lower abdominal IVC and HPV at the end of the infusion period (180 min). As shown in Table 1, the arterial plasma glucose concentrations of control and metformin-treated rats were not significantly different. The metformin-treated rats showed a slightly greater fall in plasma glucose in the IVC (A-IVC) compared with control rats. The fall in plasma glucose in the HPV (A-HPV) was more pronounced in the metformin-treated rats, implicating the intestine as an important site of glucose utilization in these rats. Taking account of blood flow rates, it was estimated that glucose utilization by the intestine (HPV drainage) was 69% greater in metformin-treated rats (194.5 ± 20.3 μmol min^{-1} kg^{-1}) than controls (114.8 ± 8.5 μmol min^{-1} kg^{-1}; $P<0.01$). Glucose disposal by the hind limb region (drainage into the lower abdominal IVC) was 40% higher in metformin-treated rats (86.1 ± 8.5 μmol min^{-1} kg^{-1}) than controls (60.6 ± 8.5 μmol min^{-1} kg^{-1}; $P<0.05$).

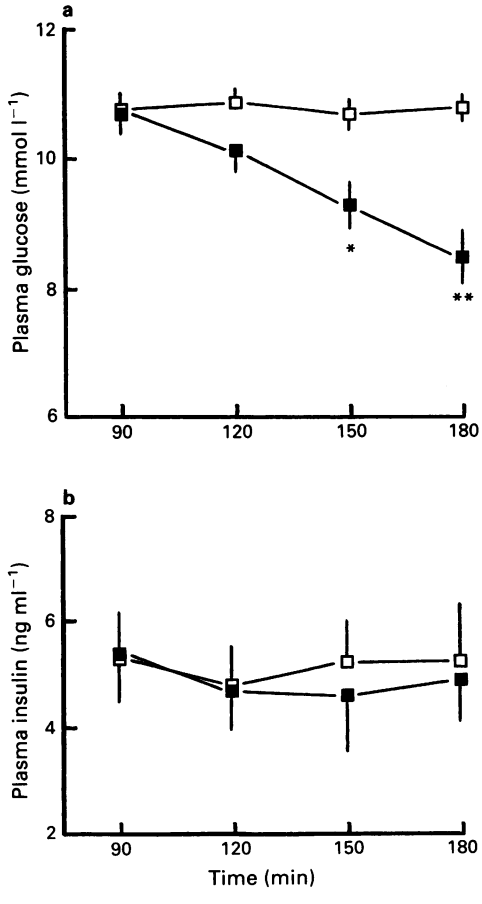

Figure 1 Plasma glucose (a) and insulin (b) concentrations of fasted anaesthetized rats during a hyperglycaemic hyperinsulinaemic infusion. At time 90 min, when a steady hyperglycaemia had been achieved, either 250 mg kg^{-1} metformin (■) or saline as control (□) was given intrajejunally. Values are mean with s.e.mean, $n=6$. *$P<0.05$, **$P<0.01$ versus control, Student's unpaired t test.

Tissue uptake of 2-deoxy-D-glucose

Tissue accumulation of 2-deoxy-D-glucose phosphate (2DGP) was measured during an IVGTT in fasted anaesthetized rats treated with metformin (250 mg kg^{-1}, intrajejunally) at 60 min before the i.v. glucose injection. Intravenous glucose tolerance was improved in the metformin-treated rats as shown in the inset to Figure 2, confirming previous experiments (Bailey & Mynett, 1994). The metformin-treated rats showed higher mean values for 2DGP accumulation into the muscle and fat, with a significant increase in 2DGP accumulation by soleus muscle. This is consistent with increased glucose utilization by the hind limb region during the hyperglycaemic hyperinsulinaemic infusion experiments. A substantial increase in 2DGP accumulation occurred in the mucosa of jejunum (by 30%) and the mid-small intestine (by 60%) of the metformin-treated rats. However, 2DGP accumulation by tissues from other regions of the gastrointestinal tract, and by brain and liver was not significantly altered.

As metformin passes down the intestine it initially produces a high concentration of the drug in the wall of the jejunum, and subsequently in the wall of ileum (Wilcock & Bailey, 1994). During the time course of the present study (up to 90 min), intrajejunally administered metformin increased 2DGP accumulation in the jejunum and mid-small intestine, but not in the ileum. Intravenous administration of metformin produces a more even distribution of drug along the length of the small intestine, although the absolute levels achieved are lower than after enteral administration (Wilcock & Bailey, 1993). Thus the tissue accumulation of 2DGP was determined after i.v. administration of metformin (250 mg kg^{-1}) at 60 min before i.v. glucose injection. The i.v. administration of metformin reduced basal plasma concentrations, and improved i.v. glucose tolerance as shown in the inset to Figure 3. After i.v. metformin, there was no significant change in 2DGP accumulation by muscle and fat. However, 2DGP accumulation in the intestinal mucosa was increased in each of the three regions examined: in the jejunum (by 20%), in the mid-small intestine (by 105%) and in the ileum (by 64%).

Table 1 Effect of metformin (250 mg kg^{-1}, intrajejunally at 90 min) on plasma glucose concentrations in aorta (A), lower abdominal inferior vena cava (IVC) and hepatic portal vein (HPV) of rats at termination (180 min) of a hyperglycaemic hyperinsulinaemic infusion

	Plasma glucose (mmol l^{-1})	
	Control $n = 6$	*Metformin* $n = 6$
Aorta	11.4 ± 0.3	10.07 ± 0.3
IVC	10.0 ± 0.4	8.7 ± 0.4*
HPV	9.7 ± 0.3	7.5 ± 0.5**
A-IVC	1.4 ± 0.1	2.0 ± 0.2*
A-HPV	1.7 ± 0.1	3.2 ± 0.2**
IVC-HPV	0.35 ± 0.1	1.2 ± 0.1**

*$P<0.05$, **$P<0.01$.

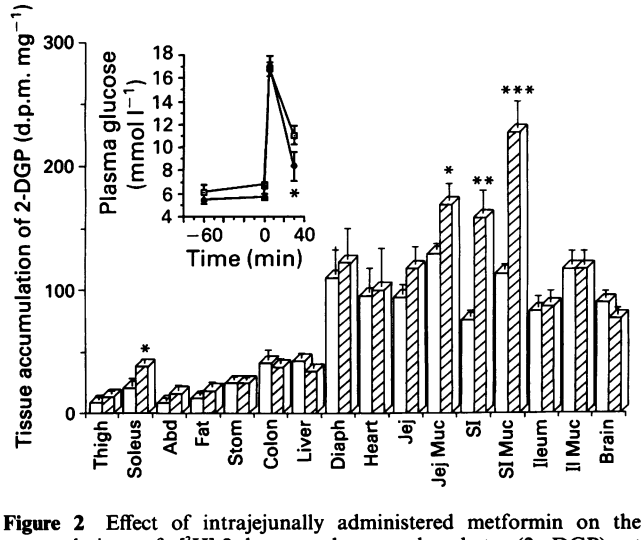

Figure 2 Effect of intrajejunally administered metformin on the accumulation of [^{3}H]-2-deoxy-D-glucose phosphate (2 DGP) at 30 min during an intravenous glucose tolerance test in fasted anaesthetized rats. At time −60 min, 250 mg kg^{-1} metformin (hatched columns) or saline as control (open columns) was given intrajejunally. Inset shows plasma glucose concentrations during the glucose tolerance test: metformin (■), control (□). The rate of glucose disappearance (% min^{-1}) was 1.7 ± 0.3 and 2.5 ± 0.3 for control and metformin-treated rats respectively. Values are mean with s.e.mean, $n = 6$. *$P<0.05$, **$P<0.01$, ***$P<0.001$ versus control, Student's unpaired t test.

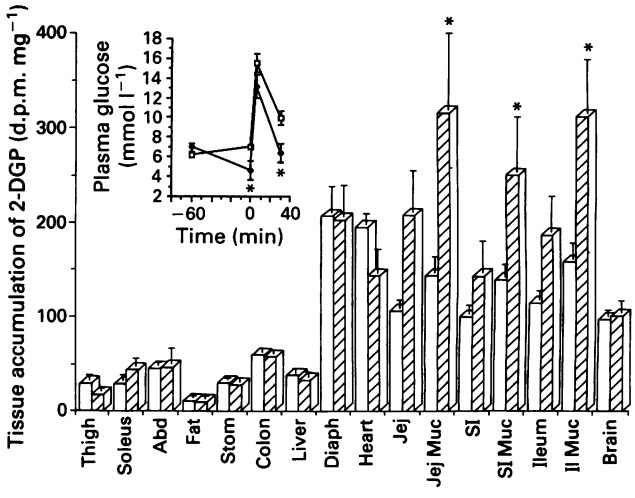

Figure 3 Effect of intravenously administered metformin on the accumulation of [^{3}H]-2-deoxy-D-glucose phosphate (2DGP) at 30 min during an intravenous glucose tolerance test in fasted anaesthetized rats. At time −60 min, 250 mg kg^{-1} metformin (hatched columns) or saline as control (open columns) was given intravenously. Inset shows plasma glucose concentrations during the glucose tolerance test: metformin (■), control (□). The rate of glucose disappearance (% min^{-1}) was 1.7 ± 0.3 and 2.5 ± 0.2 for control and metformin-treated rats respectively. Values are mean with s.e.mean, $n = 6$. *$P<0.05$ versus control, Student's unpaired t test.

Discussion

The ability of metformin to enhance insulin-mediated glucose disposal is well established (Nosadini *et al.*, 1987; DeFronzo *et al.*, 1991; Riccio *et al.*, 1991), and skeletal muscle has been implicated as an important destination of that glucose (Frayn & Adnitt, 1972; Bailey & Puah, 1986; Rossetti *et al.*, 1990). Recent studies have indicated that the intestine is also an important site of metformin-stimulated glucose utilization (Penicaud *et al.*, 1989; Wilcock & Bailey, 1990; Bailey *et al.*, 1992). However, a quantitative determination of the effect of metformin on glucose utilization by the intestine *in vivo* has not been reported.

Glucose utilization is sensitive to changes in regional blood flow (DeFronzo *et al.*, 1981), and it has been claimed that metformin may alter hepatic blood flow (Ohnhaus *et al.*, 1978). Since 70–80% of hepatic blood flow derives from the intestinal drainage into the hepatic portal vein (Greenway & Stark, 1971), it was pertinent to check the effect of metformin on blood flow in this vessel. Measurements of portal blood

flow in laboratory rodents which were hitherto estimated indirectly (Greenway & Stark, 1971; Aardal *et al.*, 1978), can now be determined directly with transonic flow sensors (Drost *et al.*, 1984).

A previous study, using internal calorimetry with thermocouples implanted into the liver, suggested that a high dose of metformin (500 mg kg^{-1}) increased liver blood flow by 10–25% over 2 h but a lower dose (175 mg kg^{-1}) had no effect (Ohnhaus *et al.*, 1978). Using the transonic flow sensors we noted that a rise in plasma glucose produced a small increase in blood flow from the intestine (Abumrad *et al.*, 1982), but there was no effect of metformin (250 mg kg^{-1}) on blood flow in the HPV or lower abdominal IVC under conditions of basal or raised glycaemia.

During the hyperglycaemic hyperinsulinaemic infusion, glucose utilization by the hind limb region (about 60 μmol min^{-1} kg^{-1}) was comparable with, but predictably slightly higher than, glucose utilization during euglycaemic hyperinsulinaemic clamp studies (Brichard *et al.*, 1992). The 40% greater utilization of glucose by the hind limb region of metformin-treated rats is also consistent with clinical estimates of the effect of metformin on whole body glucose utilization during hyperinsulinaemic glucose clamp procedures in diabetic patients (Nosadini *et al.*, 1987; DeFronzo *et al.*, 1991; Riccio *et al.*, 1991).

Our *in vivo* estimate of glucose utilization by the intestine (drainage into HPV) of rats during the hyperglycaemic hyperinsulinaemic infusion studies (about 115 μmol min^{-1} kg^{-1}) was higher than estimated in the hyperinsulinaemic state in dogs (Abumrad *et al.*, 1982; Barrett *et al.*, 1985) and during *in vitro* gut perfusion studies in rats (Windmueller & Spaeth, 1971). This may partly reflect the combination of hyperglycaemia and hyperinsulinaemia which enhances intestinal glucose utilization (Barrett *et al.*, 1982), and increased intestinal blood flow during pentobarbitone anaesthesia (Aardal *et al.*, 1978). Clinical studies have not discriminated glucose utilization by the intestine from net glucose exchange by all splanchnic tissues due to the difficulty of hepatic portal cannulation (Ferrannini *et al.*, 1985).

The 69% greater utilization of glucose by the intestine of metformin-treated rats suggests that metformin exerts a stronger effect on glucose utilization by this tissue than the predominantly skeletal muscle of the hind limb region. This is supported by the 2DGP accumulation studies showing that metformin produced a greater increase in 2DG uptake by tissues of the small intestine than by skeletal muscles. The intestinal effect of metformin was exerted mainly on the mucosa, and was evident in the jejunum and mid-small intestine after intrajejunal administration of the drug. However, after i.v. administration of metformin, which gives a more even distribution of the drug along the small intestine (Wilcock & Bailey, 1994), 2DG uptake was also increased in ileal mucosa.

Since the intestinal mucosa accumulates much higher concentrations of metformin (up to 10^{-3} mol kg^{-1}) compared with other tissues such as skeletal muscle (in the range of 10^{-5} mol kg^{-1}), it is possible that the drug acts differently on the intestinal tissue (Wilcock & Bailey, 1994). Whereas therapeutic doses of metformin do not significantly increase lactate production by skeletal muscle (Bailey & Puah, 1986; Jackson *et al.*, 1987), there is a substantial increase in lactate production by the intestine (Wilcock & Bailey, 1990; Bailey *et al.*, 1992). Thus the exposure of intestinal tissue to very high concentrations of metformin may stimulate anaerobic glycolysis, while lower concentrations of the drug in skeletal muscle enhance mainly glycogenesis and glucose oxidation (Bailey & Puah, 1986; Rossetti *et al.*, 1990; Reddi & Jyothirmayi, 1992). Preliminary evidence suggests that metformin increases glucose uptake in muscle and fat by increasing the translocation of the glucose transporter GLUT1, and possibly GLUT4, into the plasma membrane (Matthaei *et al.*, 1991; Sarabia *et al.*, 1992). Since these particular isoforms of the transporter are not expressed (to any extent) in the intestinal mucosa (Pessin & Bell, 1992) the mechanism through which metformin promotes glucose uptake in this tissue remains to be determined. Although the presence of some insulin is required for normal glucose metabolism by the intestine, the insulin dose-response effect is different from muscle and fat (Kellet *et al.*, 1984). This supports the possibility that metformin may enhance glucose utilization in the intestine through a different mechanism from that which appears to operate in muscle and fat (Bailey, 1993).

The contention that very high concentrations of metformin in the intestine may compromise ATP formation locally has not been examined, despite the evidence that metformin increases intestinal lactate production. A significant proportion of this lactate is extracted by the liver under conditions of basal glycaemia (Bailey *et al.*, 1992). There is also an adjustment of lactate metabolism after a glucose challenge which results in net lactate utilization by the periphery (Jackson *et al.*, 1987; Bailey *et al.*, 1992). Thus it is likely that metformin-stimulated glucose utilization by the intestine makes an important contribution to increased glucose recycling (Penicaud *et al.*, 1989). This is envisaged to include an intrasplanchnic substrate cycle in which glucose is converted to lactate in the intestine, released into the portal circulation and extracted by the liver to form glucose (Bailey, 1993).

The authors gratefully acknowledge the technical help of Ms Susan L. Turner, constructive discussions with Dr H.C.S. Howlett, and the support of Lipha Pharmaceuticals.

References

AARDAL, N.P., SVANES, K. & EGENBERG, K.E. (1973). Effect of hypothermia and pentobarbital anaesthesia on the distribution of cardiac output in rabbits. *Eur. Surg. Res.*, **5**, 362–372.

ABUMRAD, N.N., CHERRINGTON, A.D., WILLIAMS, P.E., LACY, W.W. & RABIN, D. (1982). Absorption and disposition of a glucose load in the conscious dog. *Am. J. Physiol.*, **242**, E398–E406.

BAILEY, C.J. (1992). Biguanides in NIDDM. *Diabetes Care*, **15**, 755–772.

BAILEY, C.J. (1993). Metformin – an update. *Gen. Pharmacol.*, **24**, 1299–1309.

BAILEY, C.J. & MYNETT, K.J. (1994). Insulin requirement for the antihyperglycaemic effect of metformin. *Br. J. Pharmacol.* (in press).

BAILEY, C.J. & PUAH, J.A. (1986). Effect of metformin on glucose metabolism in mouse soleus muscle. *Diab. Metab.*, **12**, 212–218.

BAILEY, C.J., WILCOCK, C. & DAY, C. (1992). Effect of metformin on glucose metabolism in the splanchnic bed. *Br. J. Pharmacol.*, **105**, 1009–1013.

BARRETT, E.J., FERRANNINI, E., GUSBERG, R., BEVILACQUA, S. & DEFRONZO, R.A. (1985). Hepatic and extrahepatic splanchnic glucose metabolism in the postabsorptive and glucose fed dog. *Metabolism*, **34**, 410–419.

BRICHARD, S.M., ONGEMBA, L.N. & HENQUIN, J.C. (1992). Oral vanadate decreases muscle insulin resistance in obese fa/fa rats. *Diabetologia*, **35**, 522–527.

DEFRONZO, R.A., BARZILAI, N. & SIMONSON, D.C. (1991). Mechanism of metformin action in obese and lean non-insulin-dependent diabetic subjects. *J. Clin. Endocrinol. Metab.*, **73**, 1294–1301.

DEFRONZO, R.A., FERRANNINI, E., SATO, Y., FELIG, P. & WAHREN, J. (1981). Synergistic interaction between exercise and insulin on peripheral glucose uptake. *J. Clin. Invest.*, **68**, 1468–1474.

DESBUQUOIS, B. & AURBACH, G.D. (1971). Use of polyethylene glycol to separate free and antibody-bound peptide hormones in radioimmunoassay. *J. Clin. Endocrinol. Metabol.*, **33**, 732–738.

DROST, C.J., DOBSON, A., SELLARS, A.F., BARNES, R.J. & COMLINE, R.S. (1984). An implantable transit-time ultrasonic flowmeter for long term measurement of blood volume flow. *Fed. Proc.*, **43,** 538.

FERRANNINI, E., BJORKMAN, O., REICHARD, G.A., PILO, A., OLSSON, M., WAHREN, J. & DEFRONZO, R.A. (1985). The disposal of an oral glucose load in healthy subjects. A quantitative study. *Diabetes*, **34,** 580–588.

FRAYN, K.N. & ADNITT, P.I. (1972). Effects of metformin on glucose uptake by isolated diaphragm from normal and diabetic rats. *Biochem. Pharmacol.*, **21,** 3153–3162.

GREENWAY, C.V. & STARK, R.D. (1971). Hepatic vascular bed. *Physiol. Rev.*, **51,** 23–65.

JACKSON, R.A., HAWA, M.I., JASPAN, J.B., SIM, B.M., DISILVIO, L., FEATHERBE, D. & KURTZ, A.B. (1987). Mechanism of metformin action in non-insulin-dependent diabetes. *Diabetes*, **36,** 632–640.

KELLETT, G.L., JAMAL, A., ROBERTSON, J.P. & WOLLEN, N. (1984). Acute regulation of glucose absorption, transport and metabolism in rat small intestine by insulin in vivo. *Biochem. J.*, **219,** 1027–1035.

MATTHAEI, S., JAMMAN, A., KLEIN, H.H., BENECKE, H., KREYMANN, G.L., GLIER, J.S. & GRETEN, H. (1991). Association of metformin's effects to increase insulin-stimulated glucose transport with potentiation of insulin-induced translocation of glucose transporters from intracellular pool to plasma membrane in rat adipocytes. *Diabetes*, **40,** 850–857.

NOSADINI, R., AVOGARO, A., TREVISAN, R., VALERIO, A., TESSARI, P., DUNER, E., TIENGO, A., VELUSSI, M., DEL PRATO, S., DE KREUTZENBERG, S., MUGGEO, M. & CREPALDI, G. (1987). Effect of metformin on insulin-stimulated glucose turnover and insulin binding to receptors in type II diabetes. *Diabetes Care*, **10,** 62–67.

OHNHAUS, E.E., BERGER, W. & NARS, P.W. (1978). The effect of different doses of dimethylbiguanide (DMB) on liver blood flow, blood glucose and plasma immunoreactive insulin in anaesthetized rats. *Biochem. Pharmacol.*, **27,** 789–793.

PENICAUD, L., HITIER, Y., FERRE, P. & GIRARD, J. (1989). Hypoglycaemic effect of metformin in genetically obese (fa/fa) rats results from an increased utilization of blood glucose by intestine. *Biochem. J.*, **262,** 881–885.

PESSIN, J.E. & BELL, G.I. (1992). Mammalian facilitative glucose transporter family: structure and molecular regulation. *Annu. Rev. Physiol.*, **54,** 911–930.

REAVEN, E., WRIGHT, D., MONDON, C.E., SOLOMON, R., HO, H. & REAVEN, G.M. (1983). Effect of age and diet on insulin secretion and insulin action in the rat. *Diabetes*, **32,** 175–180.

REDDI, A.S. & JYOTHIRMAYI, G.N. (1992). Effect of chronic metformin treatment on hepatic and muscle glycogen metabolism in KK mice. *Biochem. Med. Metab. Biol.*, **47,** 124–132.

RICCIO, A., DEL PRATO, S., KREUTZENBERG, S.V. & TIENGO, A. (1991). Glucose and lipid metabolism in non-insulin-dependent diabetes. Effects of metformin. *Diabetes Metab.*, **17,** 180–184.

ROSSETTI, L., DEFRONZO, R.A., GHERZI, R., STEIN, P., ANDRAGHETTI, G., GLAZETTI, G., SHULMAN, G.I., KLEIN-ROBBENHAAR, E. & CORDERA, R. (1990). Effect of metformin treatment on insulin action in diabetic rats: in vivo and in vitro correlations. *Metabolism*, **39,** 425–435.

SARABIA, V., LAM, L., BURDETT, E., LEITER, L.A. & KLIP, A. (1992). Glucose transport in human skeletal muscle cells in culture: stimulation by insulin and metformin. *J. Clin. Endocrinol. Metab.*, **90,** 1386–1395.

STEVENS, J.F. (1971). Determination of glucose by an automatic analyser. *Clin. Chim. Acta*, **32,** 199–201.

WILCOCK, C. & BAILEY, C.J. (1994). Accumulation of metformin by tissues of normal and diabetic mice. *Xenobiotica*, **24,** 49–57.

WILCOCK, C. & BAILEY, C.J. (1990). Sites of metformin-stimulated glucose metabolism. *Biochem. Pharmacol.*, **39,** 1831–1834.

WINDMUELLER, J.G. & SPAETH, A.E. (1971). Fat transport and lymph and plasma lipoprotein biosynthesis by isolated intestine. *J. Lipid Res.*, **13,** 92–105.

(Received December 20, 1993
Accepted February 24, 1994)

Br. J. Pharmacol. (1994), **112**, 676–682

Nitric oxide-mediated inhibitory response of rat proximal colon: independence from changes in membrane potential

Naowarat Suthamnatpong, Muneaki Hosokawa, Tadayoshi Takeuchi, [1]Fumiaki Hata & *Tadashi Takewaki

Department of Veterinary Pharmacology, College of Agriculture, University of Osaka Prefecture, Sakai 593 and *University of Gifu, Gifu 501-11 Japan

1 We studied the relation of nitric oxide-mediated relaxation of smooth muscle to changes in membrane potential of cells in the proximal colon of rats.

2 The resting membrane potential and electrical field stimulation (EFS)-induced junction potentials were recorded from the circular and longitudinal muscle cells.

3 Localized distension with a small balloon caused relaxation of the circular muscle on the anal side of the distended region (descending relaxation). Relaxation of the longitudinal muscle was also induced by EFS.

4 Inhibitory junction potentials (i.j.ps) were recorded from all circular muscle cells tested, but rarely from the longitudinal muscle cells.

5 The i.j.ps were recorded only in the presence of atropine but relaxations of both muscles were induced even in the absence of atropine.

6 Apamin (100 nM) completely abolished the i.j.ps recorded in both circular and longitudinal muscle cells, but had no significant effect on the relaxations of either.

7 In contrast to apamin, N^G nitro-L-arginine (10 μM) inhibited the relaxations of both muscles, but did not affect the i.j.ps.

8 Exogenously added nitric oxide (0.1–10 μM) induced relaxations of both muscles concentration-dependently, but did not affect the membrane potentials at these concentrations.

9 These data strongly suggest that nitric oxide-mediated relaxation of rat proximal colon is not associated with the i.j.ps of the cell membrane.

Keywords: Nitric oxide; rat proximal colon; apamin; nonadrenergic noncholinergic transmission; descending relaxation

Introduction

Nitric oxide has been reported to mediate an inhibitory response in various regions of the gastrointestinal tract, such as the ileocolonic junction (Bult *et al.*, 1990; Boeckxstaens *et al.*, 1990; Ward *et al.*, 1992b), duodenum (Toda *et al.*, 1990) and the proximal colon (Dalziel *et al.*, 1991; Thornbury *et al.*, 1991; Ward *et al.*, 1992a) of dogs, proximal colon (Hata *et al.*, 1990a) and gastric fundus (Li & Rand, 1991; Boeckxstaens *et al.*, 1991) of rats, and the lower oesophagus (Murray *et al.*, 1991; Tottrup *et al.*, 1991) and internal anal sphincter (Rattan *et al.*, 1992) of opossums. The mechanism of the inhibitory action of nitric oxide is still unknown, but two possible mechanisms have been proposed. One is a pathway involving a guanosine 3′,5′-cyclic monophosphate (cyclic GMP) generating system. Increase in the cyclic GMP level is reported to be associated with the relaxation of the lower oesophageal sphincter of opossums (Torphy *et al.*, 1986; Barnette *et al.*, 1989) and man (Barnette *et al.*, 1991), and the internal anal sphincter of dogs (Grous *et al.*, 1991). Moreover, increase in the cyclic GMP content also seems to be associated with nitric oxide-induced relaxation in preparations of taenia coli of guinea-pigs (Shikano *et al.*, 1988), the proximal colon of dogs (Ward *et al.*, 1992) and rats (Suthamnatpong *et al.*, 1993b) and the ileum of rats (Kanada *et al.*, 1992). Nitric oxide has been reported to activate soluble guanylate cyclase and increase the cyclic GMP level in various preparations (Arnold *et al.*, 1977). These findings strongly suggest that a nitric oxide-cyclic GMP generating system is responsible for the inhibitory neuronal pathway in the gastrointestinal tract, though the mechanism beyond the production of cyclic GMP is still unclear.

The other possible mechanism of nitric oxide-mediated relaxation is based on studies on the membrane potentials of smooth muscle cells. A nitric oxide synthetase inhibitor, N^G-nitro-L-arginine methyl ester (L-NAME) was found to inhibit the inhibitory junction potentials (i.j.ps) evoked by electrical field stimulation (EFS; Dalziel *et al.*, 1991) and hyperpolarization induced by exogenous nitric oxide in the proximal colon (Thornbury *et al.*, 1991) and small intestine (Stark *et al.*, 1991) of dogs. L-NAME also abolished the i.j.ps recorded by the double sucrose gap method from circular muscle of opossum esophagus and dog intestine (Christinck *et al.*, 1991). Thornbury *et al.* (1991) suggested that nitric oxide enhanced the open probability of Ca^{2+}-activated K^+ channels which mediate the hyperpolarization response to inhibitory neurotransmission in colonic muscle cells.

We previously suggested that nitric oxide mediates relaxation of longitudinal (Suthamnatpong *et al.*, 1993a) and circular (Hata *et al.*, 1990a) muscle of rat proximal colon. Thus, it was of interest to study whether nitric oxide-mediated relaxation of the rat proximal colon was related to the i.j.ps of the cell membrane. In the present work, we examined the effect of N^G-nitro-L-arginine, an inhibitor of nitric oxide synthase, and some K^+-channel antagonists on the i.j.ps induced by EFS and the inhibitory responses of both longitudinal and circular smooth muscles of the rat proximal colon. The data strongly suggest that nitric oxide-mediated relaxation of both muscles of the proximal colon of rats is independent of the i.j.ps. Some of the results present in this paper have been reported in preliminary form (Suthamnatpong *et al.*, 1993c).

[1] Author for correspondence.

Methods

Male Wistar rats (250–350 g) were used. They were lightly anaesthetized with ether and then stunned by a blow on the head and bled via the carotid arteries. Proximal segments of the colon were removed and placed in Tyrode solution consisting of (in mM): NaCl 137, KCl 2.7, $CaCl_2$ 1.8, $MgCl_2$ 1.1, NaH_2PO_4 0.42, $NaHCO_3$ 11.9 and glucose 5.6. The contents of the excised segments were gently flushed out with Tyrode solution.

Recording of i.j.ps in longitudinal and circular muscles of proximal colon induced by EFS

The segments of the proximal colon were mounted in a 1.5 ml organ bath maintained at 30°C and perfused continuously with Tyrode solution at a rate of 3 ml min^{-1}. Atropine (1 μM) and guanethidine (5 μM) were added to the bathing solution throughout the experiment to block cholinergic and noradrenergic responses, respectively. Membrane potentials were recorded with a conventional glass microelectrode filled with 3 M KCl with a resistance of 50–80 MΩ. The electrode impalement were made into the longitudinal muscle cells of the superficial layer or circular muscle cells of the deep layer from the serosal side (Takewaki & Ohashi, 1977). Intramural nerves within the segment were stimulated by a pair of Ag wire electrodes, one on the serosal surface 1–2 mm from the impaled glass microelectrode and the other in the solution. The distance between the two electrodes was about 20 mm.

Recording of responses of colonic longitudinal muscle to EFS

Segments of the proximal colon (2.5–3.0 cm in length) were suspended in an organ bath containing 20 ml of Tyrode solution maintained at 37°C and bubbled with 95% O_2:5% CO_2. After an equilibration period of 30 min, responses of the longitudinal muscle to EFS with trains of 100 pulses of 0.3 ms width and supramaximal voltage (20 V) at a frequency of 10 Hz were recorded isotonically, with 10 min intervals between tests.

Recording of responses of colonic circular muscle to the stimulus of distension

Colonic segments were held horizontally in a specially designed organ bath described elsewhere (Hata *et al.*, 1990b). The middle of the segment was connected by a hook at the joint of the mesentery to an anchor fixed to the bottom of the bath. A rubber balloon connected to a syringe by thin polyethylene tubing was introduced into the lumen and positioned in the middle of the segment. The balloon was inflated with 0.1 to 0.2 ml of warm water from the syringe to produce slightly greater local distension than that produced by a faecal bolus. The duration of distension was 20 or 30 s. The mechanical response of the circular muscle about 1.0 cm anal to the balloon was recorded by connecting a frog heart clip to a small area of the wall opposite the anchor and then connecting the clip via a thread to an isotonic transducer. Both ends of the segment were free. This arrangement allowed preferential recording of the response of the circular muscle. The circular muscle was subjected to a resting load of 0.5 g.

Drugs

Apamin, glibenclamide and N^G-nitro-L-arginine (L-NOARG) were purchased from Sigma Chemical Co., St. Louis, U.S.A. Charybdotoxin was from the Peptide Institute, Osaka, Japan. Gaseous nitric oxide was dissolved in Tyrode solution just before experiments, as described by Gillespie & Sheng (1988), and added to the organ bath in volumes of 0.3–300 μl. These volumes of Tyrode solution alone did not affect the spontaneous contractile activity or the muscle tone. Drugs were added to the organ bath as solutions in redistilled water in volumes of less than 1.0% of the bathing solution. A similar volume of redistilled water alone also had no affect on the muscle. Data are expressed as means ± s.e.

Results

Effects of EFS on the membrane potentials of the longitudinal and circular smooth muscle cells of rat proximal colon

The resting membrane potentials of longitudinal and circular muscle cells of the rat proximal colon were −62.7 ± 1.2 mV ($n = 87$) and −63.4 ± 1.1 mV ($n = 133$), respectively. In the absence of atropine and guanethidine, EFS (1–10 pulses) at 0.5 Hz induced excitatory junction potentials of the membrane of longitudinal and circular smooth muscle cells. In contrast, in the presence of atropine (1 μM) and guanethidine (5 μM), EFS induced transient hyperpolarization in all circular muscle cells tested. These hyperpolarizations were inhibitory junction potentials (i.j.ps), since they were abolished by tetrodotoxin (0.1 μM). The i.j.ps reached a peak in about 250 ms, and their total duration varied from 800 to 1300 ms. Repetitive nerve stimulation at frequencies of 0.5–1 Hz resulted in facilitation of the i.j.ps. At higher frequencies than 2 Hz, successive i.j.ps summed up resulting in large hyperpolarization (Figure 1). The maximal hyperpolarization was approximately 20 mV, and its latency was about 100 ms. Occasionally the hyperpolarization was followed by rebound depolarization. In the following experiments, atropine and guanethidine were added to the bathing fluid throughout the experiments for recording the i.j.ps. In contrast to the circular muscle, a single pulse of EFS did not affect the membrane potential in 82 of 87 longitudinal muscle cells in the presence of atropine and guanethidine and induced only a small transient hyperpolarization in the other 5 cells.

Effects of apamin and N^G-nitro-L-arginine on i.j.ps of circular and longitudinal muscle cells evoked by EFS

N^G-nitro-L-arginine (L-NOARG) even at the highest concentration tested (200 μM) did not have any significant effect on

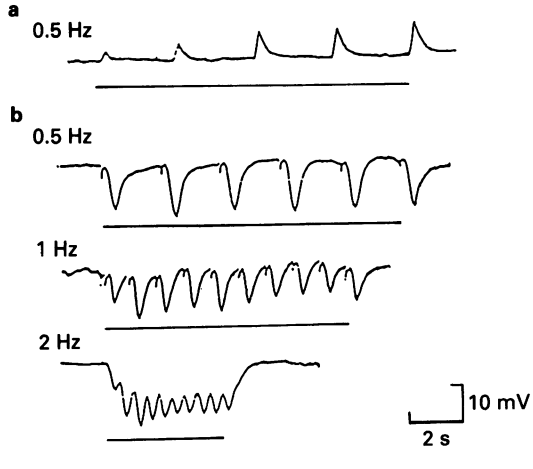

Figure 1 Facilitation or summation of junction potentials recorded from a circular muscle cell of the rat proximal colon in response to repetitive stimulation of intramural nerves. Junction potentials were induced by electrical field stimulation (EFS) at the indicated frequencies in the absence (a) or presence (b) of 1 μM atropine and 5 μM guanethidine. Lines indicate the duration of EFS.

the resting membrane potential or the i.j.ps recorded in either circular or longitudinal muscle (Figure 2). Apamin, a blocker of the small conductance Ca^{2+}-activated K^+-channel, did not have any significant effect on the resting membrane potential at 20–100 nM, but it concentration-dependently reduced the amplitude of the i.j.ps induced by a single pulse or train of pulses in both circular and longitudinal muscle cells and abolished them at 100 nM (Figures 2 and 3).

Effects of apamin and L-NOARG on descending inhibitory responses of circular muscle of rat proximal colon to local distension

On local distension, colonic segments showed relaxation of the circular muscle anal to the distended region in the absence or presence of atropine and guanethidine. Apamin at 0.1–1.0 μM gradually increased the amplitude of the spontaneous contractile activity, but did not affect the descending relaxation ($n = 6$; Figure 4). L-NOARG at 10 μM inhibited the descending relaxation, as shown previously (Hata *et al.*, 1990a).

Effects of apamin and L-NOARG on inhibitory responses of longitudinal muscle of rat proximal colon to EFS

EFS of the proximal segment induced rapid, transient relaxation and subsequent contraction of the longitudinal muscle, in the absence or presence of atropine and guanethidine. Apamin increased the tone of the longitudinal muscle and the frequency of spontaneous contractile activity, slightly at 0.1 μM and moderately at 1 μM, but did not have any significant effect on EFS-induced relaxation at these concentrations ($n = 6$; Figure 5). L-NOARG at 10 μM markedly inhibited EFS-induced relaxation, as shown previously (Suthamnatpong *et al.*, 1993a).

Effects of exogenous nitric oxide on contractile activity and membrane potential of circular muscle cells

Exogenous nitric oxide inhibited spontaneous contractile activity and decrease in tone of the circular muscle concentration-dependently. Significant inhibitions were observed in the micromolar range of nitric oxide (Figure 6). However, lower concentrations (<20 μM) of nitric oxide induced no detectable change in the membrane potential of circular muscle cells ($n = 6$). At 20 μM, it induced only weak hyperpolarization of 2.1 ± 0.7 mV ($n = 5$), whereas at 40–100

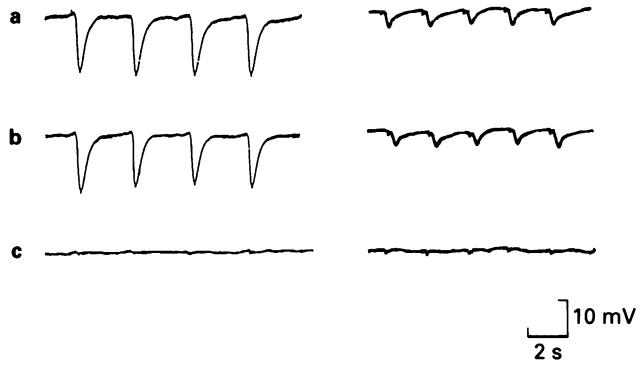

Figure 2 Effects of N^G-nitro-L-arginine (L-NOARG) and apamin on the inhibitory junction potentials (i.j.ps) induced by EFS in circular (left) and longitudinal (right) muscle cells of the rat proximal colon: i.j.ps induced by EFS at 0.5 Hz were recorded before (a) and 10 min after application of 200 μM L-NOARG (b) or L-NOARG plus 100 nM apamin (c). Atropine (1 μM) and guanethidine (5 μM) were added to the bathing fluid throughout the experiment.

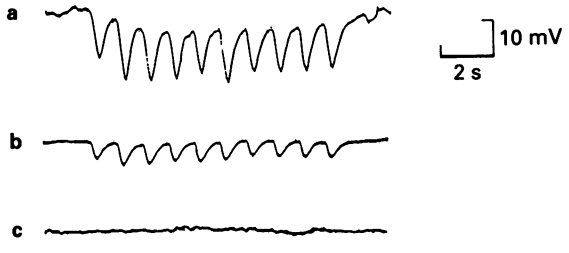

Figure 3 Concentration-dependent inhibition of i.j.ps by apamin in a circular muscle cell of the rat proximal colon: i.j.ps were induced by EFS at 1 Hz in the absence (a) or presence of 30 (b) or 100 (c) nM apamin. All records were from the same circular muscle cell in the presence of atropine and guanethidine.

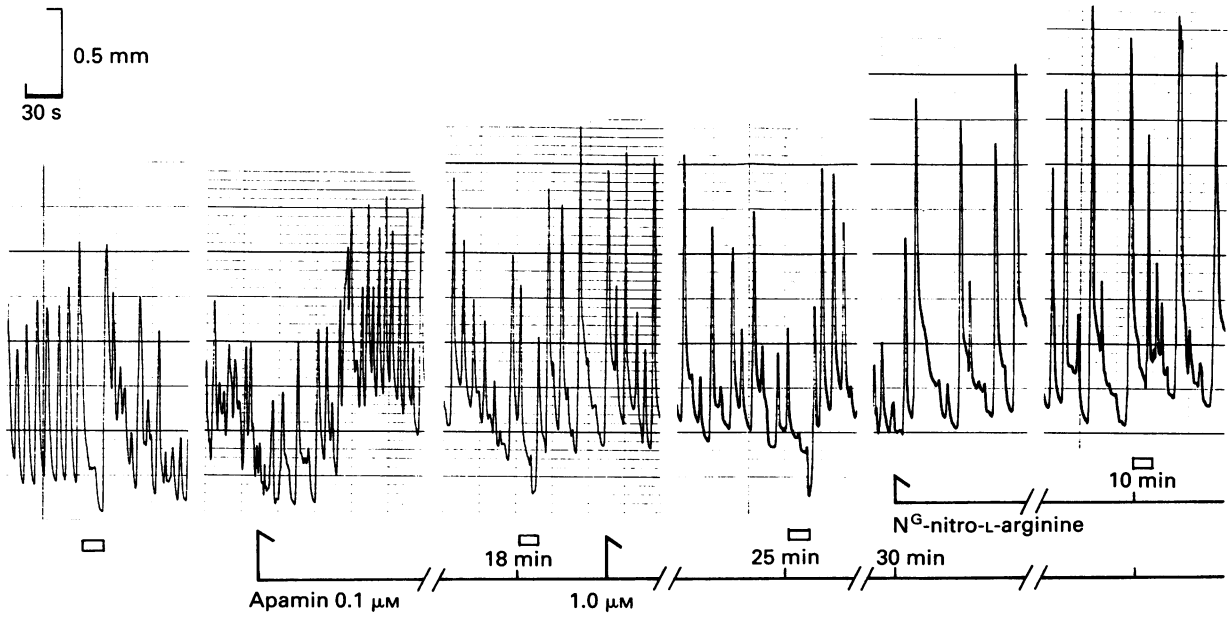

Figure 4 Effects of apamin and N^G-nitro-L-arginine (L-NOARG) on descending relaxation of rat proximal colon. Small rectangles indicate 20 s distension. Apamin at the indicated concentrations and L-NOARG at 10 μM were added at the times indicated by arrows. The continuous lines indicate the presence of apamin and L-NOARG in the bathing fluid. Times noted on the lines are those after addition of the drugs. Atropine (1 μM) and guanethidine (5 μM) were present throughout.

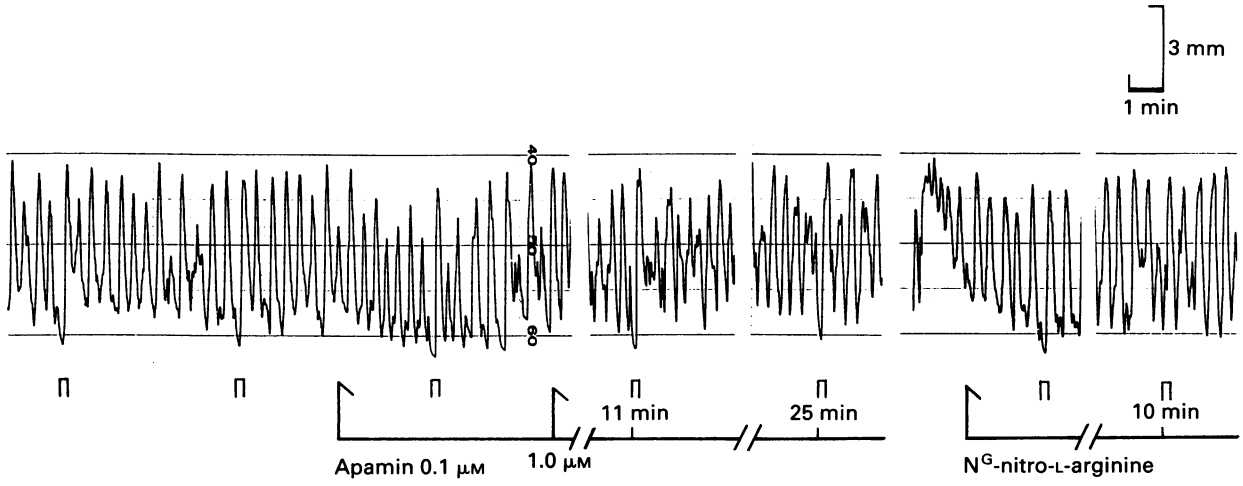

Figure 5 Effects of apamin and N^G-nitro-L-arginine on EFS-induced relaxation of longitudinal muscle of rat proximal colon. A segment of rat proximal colon was stimulated electrically at the times marked with small bars for 10 s at 10 Hz and relaxation of the longitudinal muscle was recorded. Further details were as for Figure 4.

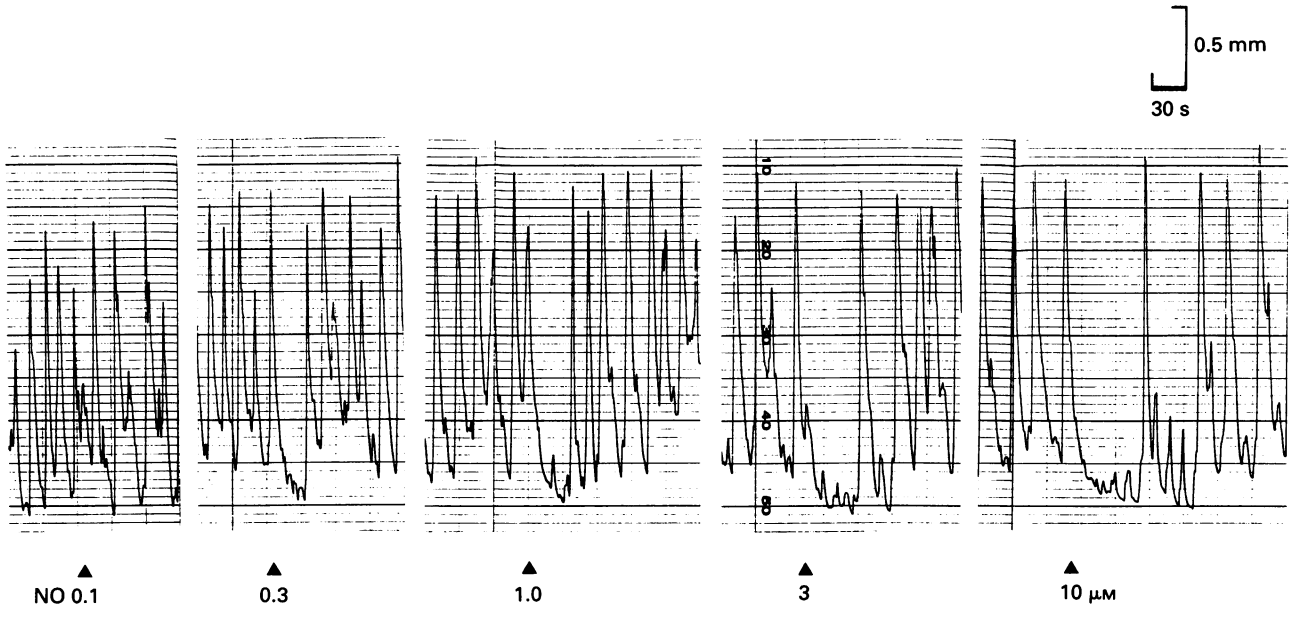

Figure 6 Relaxation of circular muscle of rat proximal colon in response to nitric oxide (NO). Spontaneous contractile activity of the circular muscle was recorded and various concentrations of NO were added at the times indicated by (▲). This record is typical of those from 6 preparations.

μM, it inhibited spontaneous discharges of action potentials, in addition to causing moderate hyperpolarization, and at 100 μM it induced further hyperpolarization of 16.1 ± 0.4 mV reproducibly ($n = 9$; Figure 7).

Effects of exogenous nitric oxide on the contractile activity and membrane potential of longitudinal muscle cells

The longitudinal muscle also responded dose-dependently to exogenous nitric oxide in the micromolar range, as observed previously (Suthamnatpong *et al.*, 1993a). However, 40 μM nitric oxide induced only slight hyperpolarization of the longitudinal muscle cell membrane, although a maximal amplitude of 15.3 ± 0.5 mV ($n = 7$) was recorded at 100 μM.

Effects of charybdotoxin and glibenclamide on inhibitory responses and the i.j.ps of circular muscle cells

Charybdotoxin, a blocker of the Ca^{2+}-activated large conductance K^+ channel, did not have any appreciable effects on EFS-induced relaxation of longitudinal muscle ($n = 4$) and descending inhibitory responses of circular muscle ($n = 3$) at 1 nM–1 μM. The EFS-induced i.j.ps recorded in circular muscle cells were also not affected by these concentrations of charybdotoxin ($n = 4$; not shown).

Glibenclamide, a blocker of the ATP-sensitive K^+ channel, at concentrations up to 1 μM had no effect on the relaxation of either circular or longitudinal muscle ($n = 4$) or on the i.j.ps of circular muscle ($n = 6$; not shown).

Discussion

In the presence, but not the absence, of atropine, i.j.ps in response to EFS were recorded from all circular smooth muscle cells of rat proximal colon tested, but rarely from longitudinal muscle cells. Furthermore, when recorded, the amplitudes of the i.j.ps from longitudinal muscle cells were small. Therefore, it seems likely that innervation of non-adrenergic, noncholinergic inhibitory neurones that induce

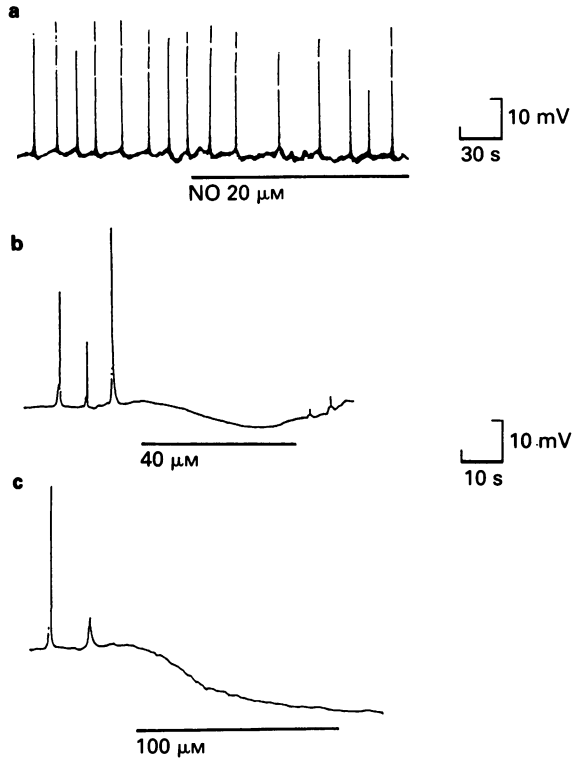

Figure 7 Effects of exogenous nitric oxide (NO) on discharges of spontaneous action potentials and the membrane potential in a circular muscle cell of the rat proximal colon. Membrane potentials of the cell which discharged spontaneously were recorded in the presence of atropine (1 μM) and guanethidine (5 μM). Lines (a), (b) and (c) indicate the presence of 20, 40 and 100 μM NO, respectively.

the i.j.ps is abundant in the circular muscle but scarce in the longitudinal muscle of the rat proximal colon.

In contrast to the i.j.ps, relaxations of the circular and longitudinal muscles were induced even in the absence of atropine. Apamin completely abolished the EFS-induced i.j.ps of the circular and longitudinal muscle cells, but did not affect relaxations of either induced by EFS or local distension. In contrast, L-NOARG inhibited the relaxations of both circular and longitudinal muscles as shown previously (Hata *et al.*, 1990a; Suthamnatpong *et al.*, 1993a), but did not affect the i.j.ps recorded in either. Furthermore, exogenously added nitric oxide induced relaxations of both muscles dose-dependently at 0.1–10 μM, but did not affect the membrane potential at these concentrations. These data strongly suggest that nitric oxide-mediated relaxation of rat proximal colon is not associated with the i.j.ps.

Several studies in vascular smooth muscle have suggested a dissociation of nitric oxide-mediated relaxation of smooth muscle from the i.j.ps: exogenous nitric oxide caused relaxation of canine isolated mesenteric (Komori *et al.*, 1988), rabbit femoral (Huang *et al.*, 1988), cerebral (Brayden, 1990) and basilar (Rand & Garland, 1992; Plane & Garland, 1993) artery without inducing hyperpolarization. Moreover L-NOARG partly inhibited relaxation, but not hyperpolarization of rat femoral veins induced by ACh (Nagao & Vanhoutte, 1991). Haemoglobin, which binds and inactivates nitric oxide, also inhibited relaxation, but not hyperpolarization induced by ACh in rat aorta and the main pulmonary artery (Chen *et al.*, 1988). Methylene blue inhibited ACh- and histamine-induced relaxation, but not hyperpolarization (Chen & Suzuki, 1989). The potassium channel blocker, glibenclamide, inhibited hyperpolarization but not relaxation induced by nitric oxide in the mesenteric artery of rats (Garland & McPherson, 1992) and it also completely inhibited hyperpolarization but only partly inhibited relaxation induced by ACh in the cerebral artery of rabbits (Brayden, 1990). All these data strongly suggest that the nitric oxide-mediated relaxation of smooth muscle of all kinds of blood vessels tested is independent of hyperpolarization of the smooth muscle cell membrane.

Many studies have indicated that ACh releases a hyperpolarizing factor (EDHF) from the endothelium which is different from the endothelium-derived relaxing factor (EDRF), and that hyperpolarization of the cell membrane results in relaxation of smooth muscle (Chen *et al.*, 1988; Komori *et al.*, 1988; Chen & Suzuki, 1989; Brayden, 1990; Nagao & Vanhoutte, 1991; Garland & McPherson, 1992; Rand & Garland, 1992). The results in most of these studies suggested that ACh-induced relaxation also involves a nitric oxide-mediated component that is independent of changes in the membrane potential, although the results in two studies (Garland & McPherson, 1992; Rand & Garland, 1992) suggested that nitric oxide does not participate in the relaxation. However, none of the results indicated that a nitric oxide-mediated component is involved in the coupling, activation of muscarinic cholinoceptors-hyperpolarization of the cell membrane-relaxation of the smooth muscle. Therefore, it is reasonable to postulate that in vascular smooth muscle cells, the agonist induces the production of EDRF and EDHF separately by activating the receptors on the membrane of endothelial cells, and these in turn induce relaxation of the smooth muscle.

One report is inconsistent with this postulation. Namely, L-NOARG was found to inhibit ACh-induced relaxation and hyperpolarization of the uterine artery of guinea-pigs, and L-arginine was found to reverse these inhibitions in a parallel fashion (Tare *et al.*, 1990). The reason for this discrepancy between uterine artery and other blood vessels is unknown. Possibly there may be differences in different regions of the blood vessels.

A few reports suggest an association of hyperpolarization with relaxation of the smooth muscles in the gastrointestinal tract: EFS induced nitric oxide-mediated i.j.ps and exogenous nitric oxide (0.1–30 μM) dose-dependently induced hyperpolarization of circular muscle cells of canine proximal colon (Thornbury *et al.*, 1991; Dalziel *et al.*, 1991). In a subsequent study in the same laboratory, a membrane permeable analogue of cyclic GMP, 8-bromo cyclic GMP, was shown to induce relaxation of the muscle as well as hyperpolarization of the cell membrane (Ward *et al.*, 1992a). These results suggested that cyclic GMP may be a second messenger that transduces the enteric inhibitory transmitter signal into the i.j.ps and subsequent relaxation of the proximal colon. However, as we pointed out above, definite evidence for the coupling of nitric oxide-(cyclic GMP)-hyperpolarization-relaxation has been obtained only from results on the uterine artery of guinea-pigs.

EDHF was suggested to increase the potassium conductance of smooth muscle cell membranes of rat arteries (Chen & Suzuki, 1989). It was also suggested that Ca^{2+}-activated K^+ channels were important in termination of electrical slow waves in canine colonic myocytes (Carl & Sanders, 1989). Various results have been obtained on the effects of several kinds of K^+-channel antagonist on agonist-induced hyperpolarization or relaxation of smooth muscles in different tissue preparations, but there are several reports of inhibitory effects of K^+ channel antagonists on nitric oxide-mediated responses: apamin was found to block partially nitric oxide-associated relaxation of canine intestine circular muscle (Christinck *et al.*, 1991), charybdotoxin to block nitrovasodilator-induced relaxation of bovine tracheal smooth muscle (Hamaguchi *et al.*, 1992) and glibenclamide to block ACh-induced hyperpolarization of rabbit cerebral artery (Brayden, 1990) and also nitric oxide-induced hyperpolarization of rat mesenteric artery (Garland & McPherson, 1992). Recently, it was also suggested that endothelium-dependent hyperpolarization in response to ACh was not important for

relaxation of the basilar artery, since glibenclamide abolished ACh-induced hyperpolarization, but not relaxation (Plane & Garland, 1993). Thus, it seemed interesting to examine the effects of K^+ channel antagonists on nitric oxide-mediated relaxation and on EFS-induced i.j.ps in the proximal colon of rats. However, apamin inhibited only EFS-induced i.j.ps that were insensitive to L-NOARG. The EFS-induced relaxation sensitive to L-NOARG and the exogenous nitric oxide-induced relaxation were not inhibited by the K^+ channel antagonists tested. These results strongly suggested that nitric oxide-mediated relaxation of the rat proximal colon does not involve activation of the K^+ channels that are sensitive to these antagonists.

The present findings in the rat proximal colon suggest that EFS activates two pathways separately: a nitric oxide-mediated pathway coupled to relaxation of the muscle, and a neurogenic pathway that induces hyperpolarization of the membrane of the muscle cells. In the rat proximal colon, unlike in blood vessels, where endothelial cells produce EDHF, some inhibitory neurotransmitter(s) released from the myenteric plexus activates apamin-sensitive K^+ channels. But the hyperpolarization is not associated *per se* with relaxation of the muscle. Thus, it is likely that the nitric oxide-mediated component is important in inducing relaxation of the rat proximal colon and that the hyperpolarization-related component has a minor role, if any.

This work was supported in part by a Grant-in-Aid for Scientific Research from Ministry of Education, Science and Culture of Japan.

References

ARNOLD, W.P., MITTAL, C.K., KATSUKI, S. & MURAD, F. (1977). Nitric oxide activates guanylate cyclase and increases guanosine 3':5'-cyclic monophosphate levels in various tissue preparations. *Proc. Natl. Acad. Sci. U.S.A.*, **74**, 3203–3207.

BARNETTE, M., BARONE, F.C., FOWLER, P.J., GROUS, M., PRICE, W.J. & ORMSBEE, H.S. (1991). Human lower oesophageal sphincter relaxation is associated with raised cyclic nucleotide content. *Gut*, **32**, 4–9.

BARNETTE, M., TORPHY, T.J., GROUS, M., FINE, C. & ORMSBEE, H.S.3. (1989). Cyclic GMP: a potential mediator of neurally- and drug-induced relaxation of opossum lower esophageal sphincter. *J. Pharmacol. Exp. Ther.*, **249**, 524–528.

BOECKXSTAENS, G.E., PELCKMANS, P.A., BOGERS, J.J., BULT, H., DE MAN, J.G., OOSTERBOSCH, L., HERMAN, A.G. & VAN MAERCKE, Y.M. (1991). Release of nitric oxide upon stimulation of non-adrenergic, non-cholinergic nerves in the rat gastric fundus. *J. Pharmacol. Exp. Ther.*, **256**, 441–447.

BOECKXSTAENS, G.E., PELCKMANS, P.A., BULT, H., DE MAN, J.G., HERMAN, A.G. & VAN MAERCKE, Y.M. (1990). Non-adrenergic non-cholinergic relaxation mediated by nitric oxide in the ileocolonic junction. *Eur. J. Pharmacol.*, **190**, 239–246.

BRAYDEN, J.E. (1990). Membrane hyperpolarization is a mechanism of endothelium-dependent cerebral vasodilation. *Am. J. Physiol.*, **259**, H668–H673.

BULT, H., BOECKXSTAENS, G.E., PELCKMANS, P.A., JORDAENS, F.H., VAN MAERCKE, Y.M. & HERMAN, A.G. (1990). Nitric oxide as an inhibitory non-adrenergic noncholinergic neurotransmitter. *Nature*, **345**, 346–347.

CARL, A. & SANDERS, K.M. (1989). Ca^{2+}-activated K channels of canine colonic myocytes. *Am. J. Physiol.*, **257**, C470–C480.

CHEN, G. & SUZUKI, H. (1989). Some electrical properties of the endothelium-dependent hyperpolarization recorded from rat arterial smooth muscle cells. *J. Physiol.*, **410**, 91–106.

CHEN, G., SUZUKI, H. & WESTON, A.H. (1988). Acetylcholine releases endothelium-derived hyperpolarizing factor and EDRF from rat blood vessels. *Br. J. Pharmacol.*, **95**, 1165–1174.

CHRISTINCK, F., JURY, J., CAYABYAB, F. & DANIEL, E.E. (1991). Nitric oxide may be the final mediator of nonadrenergic, noncholinergic inhibitory junction potentials in the gut. *Can. J. Physiol. Pharmacol.*, **69**, 1448–1458.

DALZIEL, H.H., THORNBURY, K.D., WARD, S.M. & SANDERS, K.M. (1991). Involvement of nitric oxide synthetic pathway in inhibitory junction potentials in canine proximal colon. *Am. J. Physiol.*, **260**, G789–G792.

DESAI, J.M., SESSA, W.C. & VANE, J.R. (1991). Involvement of nitric oxide in the reflex relaxation of the stomach to accomodate food or fluid. *Nature*, **351**, 477–479.

GARLAND, C.J. & MCPHERSON, G.A. (1992). Evidence that nitric oxide does not mediate the hyperpolarization and relaxation to acetylcholine in the rat small mesenteric artery. *Br. J. Pharmacol.*, **105**, 429–435.

GILLESPIE, J.S. & SHENG, H. (1988). Influences of haemoglobin and erythrocytes on the effects of EDRF, a smooth muscle inhibitory factor and nitric oxide on vascular and non-vascular smooth muscle. *Br. J. Pharmacol.*, **95**, 1151–1156.

GROUS, M., JOSLYN, A.F., THOMPSON, W. & BARNETTE, M.S. (1991). Change in intracellular cyclic nucleotide content accompanies relaxation of the isolated canine internal anal sphincter. *J. Gastrointest. Motil.*, **3**, 46–52.

HAMAGUCHI, M., ISHIBASHI, T. & IMAI, S. (1992). Involvement of charybdotoxin-sensitive K+ channel in the relaxation of bovine tracheal smooth muscle by glyceryl trinitrate and sodium nitroprusside. *J. Pharmacol. Exp. Ther.*, **262**, 263–270.

HATA, F., ISHII, T., KANADA, A., YAMANO, N., KATAOKA, T., TAKEUCHI, T. & YAGASAKI, O. (1990a). Essential role of nitric oxide in descending inhibition in the rat proximal colon. *Biochem. Biophys. Res. Commun.*, **172**, 1400–1406.

HATA, F., KATAOKA, T., TAKEUCHI, T., YAGASAKI, O. & YAMANO, N. (1990b). Differences in control of descending inhibition in the proximal and distal regions of rat colon. *Br. J. Pharmacol.*, **101**, 1011–1015.

HUANG, H., BUSSE, R. & BASSENGE, E. (1988). Endothelium dependent hyperpolarization of smooth muscle cells in rabbit femoral arteries is not mediated by EDRF (nitric oxide). *Naunyn-Schmied. Arch. Pharmacol.*, **338**, 438–442.

KANADA, A., HATA, F., SUTHAMNATPONG, N., MAEHARA, T., ISHII, T., TAKEUCHI, T. & YAGASAKI, O. (1992). Key roles of nitric oxide and cyclic GMP in nonadrenergic and noncholinergic inhibition in rat ileum. *Eur. J. Pharmacol.*, **216**, 287–292.

KOMORI, K., LORENZ, R.R. & VANHOUTTE, P.M. (1988). Nitric oxide, ACh, and electrical and mechanical properties of canine arterial smooth muscle. *Am. J. Physiol.*, **255**, H207–H212.

LI, C.G. & RAND, M.J. (1991). Evidence that part of the NANC relaxant response of guinea pig trachea to electrical field stimulation is mediated by nitric oxide. *Br. J. Pharmacol.*, **102**, 91–94.

MURRAY, J., DU, C., LEDLOW, A., BATES, J.N. & CONKLIN, J.L. (1991). Nitric oxide: mediator of nonadrenergic, noncholinergic responses of opossum esophageal muscle. *Am. J. Physiol.*, **261**, G401–G406.

NAGAO, T. & VANHOUTTE, P.M. (1991). Hyperpolarization contributes to endothelium-dependent relaxations to acetylcholine in femoral veins of rats. *Am. J. Physiol.*, **261**, H1034–H1037.

PLANE, F. & GARLAND, C.J. (1993). Differential effects of acetylcholine, nitric oxide and levcromakalim on smooth muscle membrane potential and tone in the rabbit basilar artery. *Br. J. Pharmacol.*, **110**, 651–656.

RAND, V.E. & GARLAND, C.J. (1992). Endothelium-dependent relaxation to acetylcholine in the rabbit basilar artery: importance of membrane hyperpolarization. *Br. J. Pharmacol.*, **106**, 143–150.

RATTAN, S., SARKAR, A. & CHAKDER, S.A. (1992). Nitric oxide pathway in rectoanal inhibitory reflex of opossum internal anal sphincter. *Gastroenterology*, **103**, 43–50.

SHIKANO, K., LONG, C.J., OHLSTEIN, E.H. & BERKOWITZ, B.A. (1988). Comparative pharmacology of endothelium-derived relaxing factor and nitric oxide. *J. Pharmacol. Exp. Ther.*, **247**, 873–881.

STARK, M.E., BAUER, A.J. & SZURSZEWSKI, J.H. (1991). Effect of nitric oxide on circular muscle of the canine small intestine. *J. Physiol.*, **444**, 743–761.

SUTHAMNATPONG, N., HATA, F., KANADA, A., TAKEUCHI, T. & YAGASAKI, O. (1993a). Mediators of nonadrenergic, noncholinergic inhibition in the proximal, middle and distal regions of rat colon. *Br. J. Pharmacol.*, **108**, 348–355.

SUTHAMNATPONG, N., MAEHARA, T., KANADA, A., TAKEUCHI, T. & HATA, F. (1993b). Dissocation of cyclic GMP level from relaxation of the distal, but not the proximal colon of rats. *Jpn. J. Pharmacol.*, **62**, 387–393.

SUTHAMNATPONG, N., TAKEUCHI, T., HATA, F. & TAKEWAKI, T. (1993c). Nitric oxide-mediated relaxation in rat proximal colon does not involve inhibitory junction potentials. *Jpn. J. Pharmacol.*, **61**, 311P.

TAKEWAKI, T. & OHASHI, H. (1977). Non-cholinergic excitatory transmission to intestinal smooth muscle cells. *Nature*, **268**, 749–750.

TARE, M., PARKINGTON, H.C., COLEMAN, H.A., NEILD, T.O. & DUSTING, G.J. (1990). Hyperpolarization and relaxation of arterial smooth muscle caused by nitric oxide derived from the endothelium. *Nature*, **346**, 69–71.

THORNBURY, K.D., WARD, S.M., DALZIEL, H.H., CARL, A., WESTFALL, D.P. & SANDERS, K.M. (1991). Nitric oxide and nitrosocysteine mimic nonadrenergic, noncholinergic hyperpolarization in canine proximal colon. *Am. J. Physiol.*, **261**, G553–G557.

TODA, N., BABA, H. & OKAMURA, T. (1990). Role of nitric oxide in non-adrenergic, non-cholinergic nerve-mediated relaxation in dog duodenal longitudinal muscle strips. *Jpn. J. Pharmacol.*, **53**, 281–284.

TORPHY, T.J., FINE, C.F., BURMAN, M., BARNETTE, M.S. & ORMSBEE, H.S.3. (1986). Lower esophageal sphincter relaxation is associated with increased cyclic nucleotide content. *Am. J. Physiol.*, **251**, G786–G793.

TOTTRUP, A., SVANE, D. & FORMAN, A. (1991). Nitric oxide mediating NANC inhibition in opossum lower esophageal sphincter. *Am. J. Physiol.*, **260**, G385–G389.

WARD, S.M., DALZIEL, H.H., BRADLEY, M.E., BUXTON, I.L.O., KEEF, K., WESTFALL, D.P. & SANDERS, K.M. (1992a). Involvement of cyclic GMP in non-adrenergic, non-cholinergic inhibitory neurotransmission in dog proximal colon. *Br. J. Pharmacol.*, **107**, 1075–1082.

WARD, S.M., MCKEEN, E.S. & SANDERS, K.M. (1992b). Role of nitric oxide in non-adrenergic, non-cholinergic inhibitory junction potentials in canine ileocolonic sphincter. *Br. J. Pharmacol.*, **105**, 776–782.

(Received January 21, 1994
Revised February 22, 1994
Accepted March 1, 1994)

Br. J. Pharmacol. (1994), **112**, 683–689

Agonistic and antagonistic properties of the bradykinin B_2 receptor antagonist, Hoe 140, in isolated blood vessels from different species

[1]Michel Félétou, Martine Germain, Christophe Thurieau, Jean-Luc Fauchère & Emmanuel Canet

Institut de Recherches Servier, 11 rue des Moulineaux, 92150 Suresnes, France

1 Hoe 140, a recently described bradykinin B_2 antagonist, and NPC 567 from an earlier generation of bradykinin B_2 antagonists, were tested in rabbit and sheep isolated blood vessels.

2 In rabbit jugular vein, a bradykinin B_2 preparation, NPC 567 was an antagonist (apparent pA_2: 8.67 ± 0.16) with marked residual agonistic activity ($\log[EC_{50}]$: -7.29 ± 0.13). Hoe 140 was a potent non-competitive antagonist devoid of agonistic properties (slope of the Schild plot: 2.02; estimated pA_2: 9.04).

3 In rabbit aorta, a bradykinin B_1 preparation, NPC 567 was a competitive antagonist (pA_2: 6.32 ± 0.13) but Hoe 140 was ineffective. The two antagonists did not show any agonistic properties in this tissue.

4 In sheep femoral artery without endothelium, bradykinin and Hoe 140 induced contractions with identical efficacy and similar potency ($\log[EC_{50}]$: -8.05 ± 0.12, -7.73 ± 0.10; maximal contraction in % of KCl [60 mM]: 59.5 ± 15.1, 62.0 ± 13.1; for bradykinin and Hoe 140, respectively). In contrast NPC 567 was an extremely weak agonist. The contractile responses to bradykinin and Hoe 140 were inhibited by NPC 567 (apparent pK_B: 6.89 ± 0.22 and 6.58 ± 0.08 versus bradykinin and Hoe 140, respectively) but not by a B_1 bradykinin antagonist, suggesting that the receptor involved was a bradykinin B_2 receptor.

5 In sheep femoral artery with endothelium, bradykinin induced a biphasic response: an endothelium-dependent relaxation and a contraction which were both inhibited by NPC 567 (apparent pK_B: 7.10 ± 0.15) and Hoe 140 (pA_2: 8.38 ± 0.12). As bradykinin B_2 receptor antagonists, Hoe 140 and NPC 567 were less potent in the sheep femoral artery than in the rabbit jugular vein. Neither Hoe 140 nor NPC 567 were agonists for the endothelial receptor.

6 This study demonstrates that Hoe 140, a new bradykinin B_2 receptor antagonist, is more selective and more potent than NPC 567; however, it may possess, depending on the tissue studied, marked residual agonistic properties. Furthermore, bradykinin B_2 receptors are subject to important species specificity. Finally, two different bradykinin B_2 receptor subtypes may coexist in the sheep femoral artery with endothelium.

Keywords: Bradykinin; B_2 receptor; sheep femoral artery; rabbit jugular vein; aorta; Hoe 140; NPC 567

Introduction

Bradykinin is a potent and ubiquitous inflammatory mediator which produces vascular leakage, endothelium-dependent vasodilatation, and vascular and bronchial smooth muscle contraction (Bhoola *et al.*, 1992). Based on studies in isolated vascular smooth muscle, kinin receptors have been divided into two main classes: B_1 and B_2 (Regoli & Barabé, 1980; Rhaleb *et al.*, 1990); but most of the early inflammatory effects of bradykinin are thought to be mediated through the B_2 receptor subtype. Hoe 140 is a novel, potent and long-acting selective bradykinin B_2 antagonist which possesses only minimal residual agonistic activity on a variety of isolated smooth muscle preparations (Hock *et al.*, 1991; Wirth *et al.*, 1991; Lembeck *et al.*, 1991) unlike some earlier antagonists such as NPC 567 (Rhaleb *et al.*, 1991). However the bradykinin B_2 receptor family may be further divided into presynaptic (i.e. 'neuronal') and postsynaptic (i.e. 'smooth muscle') subtypes based on the pharmacological responses, or the binding of some bradykinin analogues (Llona *et al.*, 1987; Braas *et al.*, 1988; Burch & Kyle, 1992; Seguin *et al.*, 1992; Seguin & Widdowson, 1993). It may also vary according to the species (Hock *et al.*, 1991).

The allergic sheep is an interesting model of antigen-induced airway inflammation and hyperresponsiveness, sensitive to bradykinin B_2 antagonists such as NPC 567 (Solèr *et al.*, 1990). However, to our knowledge there is no information available concerning the antagonistic activity of Hoe 140 in sheep isolated smooth muscle preparations. The purpose of our study was to characterize the pharmacology of the B_2 bradykinin antagonist (Hoe 140) in isolated blood vessels of sheep and rabbit, and to compare it with a bradykinin antagonist of an earlier generation (NPC 567).

Methods

Experiments were performed in male New-Zealand rabbits (12 weeks old; Charles River, France) and sheep of either sex (6–8 months old; Charles River). Rabbits and sheep were anaesthetized with an overdose of pentobarbitone (40 mg kg^{-1} in the ear vein for the rabbits; 60 mg kg^{-1} in the humeral vein for the sheep). The rabbit aorta and jugular veins and the sheep femoral arteries were excised, immersed in cold (4°C) physiological salt solution and cleaned of adherent connective tissue. Arteries and veins were cut into rings (4 mm long) and mounted in an organ bath for isometric tension recording. In rabbit aortic rings and in some sheep femoral arterial rings, the endothelium was carefully removed by inserting a pair of watchmaker forceps into the lumen and rolling them back and forth on saline-wetted paper.

[1] Author for correspondence.

Endothelium removal was demonstrated by the disappearance of the relaxation to acetylcholine (10^{-6} M). The tissues were bathed in modified Krebs-Ringer solution (37°C, bubbled with a 95% O_2:5% CO_2 gas mixture; pH 7.4) of the following composition (mM): NaCl 118.3, KCl 4.7, $CaCl_2$ 2.5, $MgSO_4$ 1.2, KH_2PO_4 1.2, $NaHCO_3$ 25, calcium-disodium EDTA 0.026 and glucose 11.1. The tissues were connected to a UC_2 force transducer (Gould, France) and changes in tension were recorded on a polygraph (Gould, France).

Rings were stretched step by step (1 g of passive tension for the rabbit jugular vein, 8–10 g for the rabbit aorta and the sheep femoral artery) until optimal and reproducible contraction to KCl (40 mM added to the bath) was achieved. Then a reference contraction was produced with a concentration of KCl (60 mM added to the bath) which gave the maximum contraction to the depolarizing solution in those tissues. After repeated rinses, rings were subjected to a resting period of 45 min. Antagonists (e.g. Hoe 140) were allowed to equilibrate for 45 min before the cumulative addition of agonist (e.g. bradykinin). Experiments were performed in parallel in the rings from the same tissue. Only one agonist concentration-response curve was performed on a single ring.

Calculation and statistical evaluation

Data are shown as means ± s.e.mean. n represents the number of animals from which tissue was taken. Data were expressed as % of the reference contraction (KCl: 60 mM) or normalized (0–100%). In precontracted tissues, the changes in tension are expressed as % of the level of precontraction. Statistical evaluation was performed with a three-way analysis of variance (treatment × concentration × tissue). When a significant interaction was observed ($P<0.05$) a complementary analysis was undertaken (Newman-Keul's test) to identify differences among groups. EC_{50} calculation was performed with linear regression within the two half log concentrations surrounding the 50% value. Apparent antagonist dissociation constants were determined according to the equation: $K_B = [Ant]/(\text{concentration ratio} - 1)$ where [Ant] is the concentration of the antagonist and concentration ratio is the EC_{50} in the presence of the antagonist divided by the EC_{50} of the agonist in the absence of the antagonist. These results were then expressed as the negative logarithm of the K_B (i.e. $-\log(K_B) = pK_B$). pA_2 values were calculated according to Tallarida's method; the slope of the Schild plot was constrained to unity (Tallarida *et al.*, 1979).

Materials

Acetylcholine, bradykinin, Des-Arg^9-bradykinin, Des-Arg^9-Leu^8-bradykinin, indomethacin, N^G-nitro-L-arginine, papaverine, phenylephrine, NPC 567 (D-Arg[Hyp^3, D-Phe^7] bradykinin) (Sigma: La Verpillère, France). Hoe 140 (D-Arg-[Hyp^3, Thi^5, D-Tic^7, Oic^8] bradykinin) was synthesized in our institute (IdRS, Suresnes, France). The synthesis was performed by the solid-phase method on a Milligen 9050 peptide synthesizer and the crude peptide was purified to homogeneity by reverse-phase h.p.l.c. Fractions corresponding to 98% purity or higher were pooled and analysed. Peptide content was determined by amino-acid analysis with a Varian LC90 Star system. The molecular weight was determined by FAB-MS on a Nermag R10-10C apparatus.

All drugs were freshly dissolved in distilled water on the day of the experiment.

Results

Rabbit jugular vein

In rabbit isolated jugular vein, bradykinin (10^{-10}–10^{-5} M), NPC 567 (10^{-10}–10^{-5} M) and Des-Arg^9-bradykinin (10^{-10}–10^{-5} M) produced a concentration-dependent contraction. Des-Arg^9-Leu^8-bradykinin (up to 10^{-5} M) and Hoe 140 (up to 10^{-6} M) did not induce any changes in tone (Figure 1; Table 1). The rank order of potency of the bradykinin analogues was: bradykinin > NPC 567 > Des-Arg^9-bradykinin >>> Des-Arg^9-Leu^8-bradykinin, Hoe 140. NPC 567 (3×10^{-8}, 10^{-7}, and 10^{-6} M) induced a rightward shift in the bradykinin concentration-response curve. At the two highest doses (10^{-7} and 10^{-6} M), NPC 567 induced a contraction linked to its residual agonistic activity (Figure 1). This may explain the lower maximum reached by bradykinin in presence of NPC 567 at these two concentrations. The slope of the Schild plot was not significantly different from unity, indicating an apparently competitive antagonism (Figure 2, Table 2).

Hoe 140 (5×10^{-10}, 10^{-9}, 3×10^{-9} M) induced a rightward shift of the bradykinin concentration-response curves and a profound depression of the maximal response indicating a non-competitive antagonism. An attempt to calculate an affinity constant was made, using the Schild analysis, from the average EC_{50} obtained under control conditions or in presence of Hoe 140. The slope of the Schild plot differed significantly from unity, confirming the non-competitive antagonism produced by Hoe 140 (Figure 2, Table 2).

The presence of indomethacin (5×10^{-6} M) and N^G-nitro-L-arginine (10^{-4} M) did not modify the antagonistic effects of Hoe 140 (data not shown).

Rabbit aorta

In rabbit isolated aorta without endothelium, bradykinin (10^{-10}–10^{-5} M) and Des-Arg^9-bradykinin (10^{-10}–10^{-5} M) produced a concentration-dependent contraction. NPC 567 (up to 10^{-5} M), Des-Arg^9-Leu^8-bradykinin (up to 10^{-5} M) and

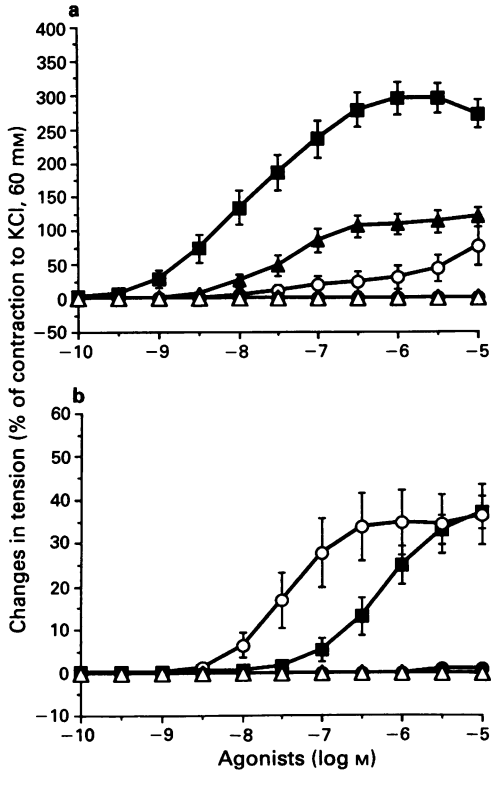

Figure 1 Agonistic effects of bradykinin analogues in rabbit isolated vascular tissue. Data are shown as mean ± s.e.mean. (a) Jugular vein: bradykinin, $n = 13$ (■); Des-Arg^9-bradykinin, $n = 6$ (○); NPC 567, $n = 6$ (▲); Des-Arg^9-Leu^8-bradykinin, $n = 2$ (●); Hoe 140, $n = 2$ (△). (b) Aorta: bradykinin, $n = 6$ (■); Des-Arg^9-bradykinin, $n = 6$ (○); NPC 567, $n = 4$ (▲); Des-Arg^9-Leu^8-bradykinin, $n = 4$ (●); Hoe 140, $n = 2$ (△).

Table 1 Agonistic effects of bradykinin analogues in rabbit vascular tissue

		Bradykinin	*Des-Arg⁹-BK*	*NPC 567*	*Des-Arg⁹-Leu⁸-BK*	*Hoe 140*
Jugular vein	$\log(EC_{50})$	-7.76 ± 0.18 (13)	> -5.6 (6)	-7.29 ± 0.13 (6)	In (2)	In (2)
	Max (% KCl)	295.0 ± 21.1 (13)	76.8 ± 29.3 (6)	119.4 ± 15.0 (6)		
	Potency (BK = 1)	1	<0.007	0.34		
Aorta	$\log(EC_{50})$	-6.28 ± 0.14 (6)	-7.30 ± 0.14 (6)	In (4)	In (4)	In (2)
	Max (% KCl)	37.3 ± 3.6 (6)	36.7 ± 6.9 (6)			
	Potency (BK = 1)	1	10			

Data are shown as mean ± s.e.mean. Numbers in parentheses indicate the number of animals from which tissue was taken. In: inactive: lack of agonistic activity. BK: bradykinin.

Table 2 Effects of the bradykinin antagonists

Rabbit	*Agonist*	*NPC 567*	*Hoe 140*	*Des-Arg⁹Leu⁸-BK*
Jugular vein	Bradykinin	pA_2: 8.67 ± 0.16 (4) Slope: 0.81 ± 0.26	pA_2*: 9.04 ± 0.28 (7) Slope: 2.02 ± 0.66	ND
Aorta	Des-Arg⁹-BK	pA_2: 6.32 ± 0.13 (4) Slope: 0.82 ± 0.16	In (6)	pA_2: 7.03 ± 0.16 (4) Slope: 0.87 ± 0.08
Sheep femoral artery (without endothelium)				
Contraction	Bradykinin	pK_B: 6.89 ± 0.22 (6)	ND	In (6)
	Hoe 140	pK_B: 6.58 ± 0.08 (6)		In (6)
	Des-Arg⁹-BK	In (3)	ND	In (2)
Sheep femoral artery (with endothelium)				
Relaxation	Bradykinin	pK_B: 7.10 ± 0.15 (6)	pA_2: 8.38 ± 0.12 (6) Slope: 1.14 ± 0.29	In (6)
Contraction	Bradykinin	pK_B: 6.58 ± 0.40 (6)	pK_B: 7.66 ± 0.23 (6)	In (6)
	Hoe 140	pK_B: 6.56 ± 0.34 (6)		In (6)

Data are shown as mean ± s.e.mean. Numbers in parentheses indicate the number of animals from which tissue was taken. In: inactive: lack of agonistic activity. ND: not determined. BK: bradykinin.
The slope value of the Schild plot is indicated. The pA_2 values have been calculated with the slope of the Schild plot constrained to unity. *Indicates that the pA_2 value is an estimated value.

Hoe 140 (up to 10^{-6} M) did not induce any significant changes in tone (Figure 1, Table 1). The rank potency of the bradykinin analogues was: Des-Arg⁹-bradykinin > bradykinin >>> NPC 567, Des-Arg⁹-Leu⁸-bradykinin, Hoe 140.

Des-Arg⁹-Leu⁸-bradykinin (10^{-6}, 3×10^{-6}, 10^{-5} M) and NPC 567 (10^{-7}, 10^{-6}, 10^{-5} M) induced a parallel rightward shift of the Des-Arg⁹-bradykinin concentration-response curve. The maximal response to Des-Arg⁹-bradykinin was not affected by the two compounds and the slopes of the Schild plots were not significantly different from unity, indicating an apparently competitive antagonism (Figure 3). Hoe 140 (10^{-6}, 10^{-5} M) did not influence the contractile response to the B_1 bradykinin agonist (Table 2).

Sheep femoral artery without endothelium

In isolated sheep femoral artery without endothelium, bradykinin (10^{-10}–10^{-5} M), NPC 567 (10^{-10}–10^{-5} M), Des-Arg⁹-bradykinin (10^{-10}–10^{-5} M), Des-Arg⁹-Leu⁸-bradykinin (10^{-10}–10^{-5} M) and Hoe 140 (10^{-10}–3×10^{-6} M) produced a concentration-dependent contraction (Figure 4, Table 3). The rank potency order of the bradykinin analogues was: bradykinin ≥ Hoe 140 >> Des-Arg⁹-bradykinin > NPC 567, Des-Arg⁹-Leu⁸-bradykinin. The contractile responses were not inhibited by indomethacin (5×10^{-6} M; data not shown).

The contractile response induced by Hoe 140 had a rapid onset, although less so than with bradykinin; however, the plateau phase of the contraction to Hoe 140 was more stable than with bradykinin.

NPC 567 (10^{-7}, and 10^{-6} M) induced a parallel rightward shift of the bradykinin and the Hoe 140 concentration-response curves (Figure 5, Table 2). The maximal responses to bradykinin and Hoe 140 were not affected by NPC 567 suggesting an apparently competitive antagonism. Des-Arg⁹-Leu⁸-bradykinin (up to 3×10^{-6} M) did not influence the response to either bradykinin or Hoe 140 (Figure 5, Table 2).

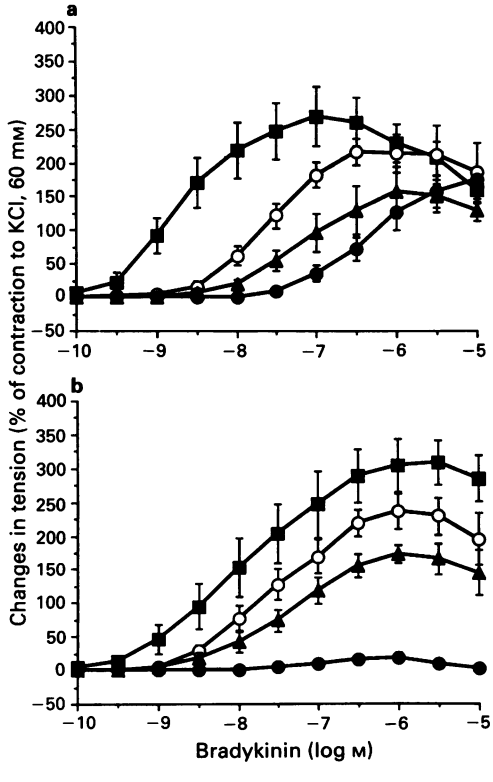

Figure 2 Bradykinin concentration-response curves: effects of bradykinin B_2 antagonists in rabbit isolated jugular vein. Data are shown as mean ± s.e.mean. (a) Effect of NPC 567 ($n = 4$). Control (■); NPC 567 (3×10^{-8} M) (○); NPC 567 (10^{-7} M) (▲); NPC 567 (10^{-6} M) (●). (b) Effect of Hoe 140 ($n = 7$). Control (■); Hoe 140 (5×10^{-10} M) (○); Hoe 140 (10^{-9} M) (▲); Hoe 140 (3×10^{-9} M) (●).

The contractile response to Des-Arg^9-bradykinin was not influenced by NPC 567 (up to 10^{-6} M) or Des-Arg^9-Leu^8-bradykinin (up to 3×10^{-6} M) (Table 2).

Sheep femoral artery with endothelium

In sheep isolated femoral artery contracted with phenylephrine (2×10^{-7} M) and in the presence of indomethacin (5×10^{-6} M), the cumulative addition of bradykinin (10^{-10}–10^{-5} M) produced a biphasic response. The first phase of the response was an endothelium-dependent relaxation followed by an endothelium-independent contraction. None of the other bradykinin analogues tested: Des-Arg^9-bradykinin (up to 10^{-5} M), NPC 567 (up to 10^{-5} M), Hoe 140 (up to 10^{-6} M) induced an endothelium-dependent relaxation. Hoe 140 provoked a concentration-dependent increase in tension (Figure 6, Table 3).

The endothelium-dependent relaxation to bradykinin was inhibited by NPC 567 and Hoe 140 but not by Des-Arg^9-Leu^8-bradykinin (up to 3×10^{-6} M). NPC 567 (10^{-6} M) and Hoe 140 (10^{-8}, 3×10^{-8}, 10^{-7} M) induced a parallel rightward shift of the bradykinin concentration-response curves suggestive of competitive antagonism (Figure 7, Table 2).

The increase in tension induced by either bradykinin or Hoe 140 was inhibited by NPC 567 (10^{-6} M) but not by Des-Arg^9-Leu^8-bradykinin (3×10^{-6} M) (Table 2). Hoe 140 also inhibited the increase in tension evoked by bradykinin. The presence of either antagonist (NPC 567 or Des-Arg^9-Leu^8-bradykinin) did not unmask an endothelium-dependent relaxation to either Hoe 140 or Des-Arg^9-bradykinin (Table 2).

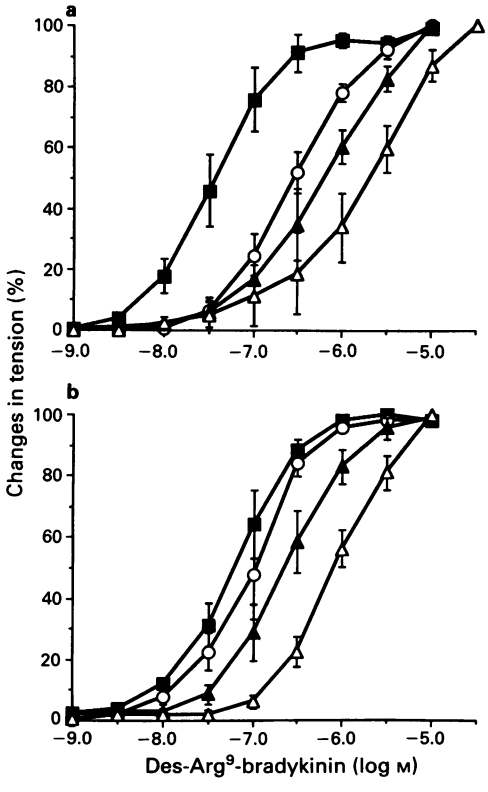

Figure 3 Des-Arg^9-bradykinin concentration-response curves: effects of bradykinin antagonists in rabbit isolated aorta. Data are shown as mean ± s.e.mean. (a) Des-Arg^9-Leu^8-bradykinin ($n = 4$). Control (■); Des-Arg^9-Leu^8-BK (10^{-6} M) (○); Des-Arg^9-Leu^8-BK (3×10^{-6} M) (▲); Des-Arg^9-Leu^8-BK (10^{-5} M) (△). (b) NPC 567 ($n = 4$). Control (■); NPC 567 (10^{-7} M) (○); NPC 567 (10^{-6} M) (▲); NPC 567 (10^{-5} M) (△).

Discussion

This study confirms that the bradykinin B_2 receptor is a heterogeneous class of receptor with tissue and species variation. Furthermore Hoe 140, a new peptidic B_2 receptor antagonist thought to be devoid of agonistic properties, can still present, *in vitro*, a partial agonistic activity, depending on the tissue and species studied.

Rabbit smooth muscle preparations

In the rabbit jugular vein, bradykinin induced a contraction probably due to the direct activation of smooth muscle cell bradykinin B_2 receptors (Rhaleb *et al.*, 1991). Indeed, the B_1

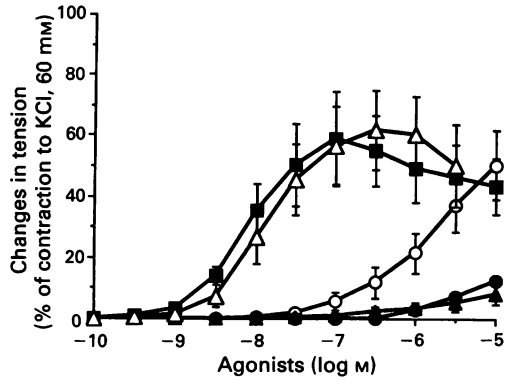

Figure 4 Agonistic effects of bradykinin analogues in sheep isolated femoral artery without endothelium. Data are shown as mean ± s.e.mean. Bradykinin, $n = 8$ (■); Des-Arg^9-bradykinin, $n = 8$ (○); NPC 567, $n = 6$ (▲); Des-Arg^9-Leu^8-bradykinin, $n = 2$ (●); Hoe 140, $n = 10$ (△).

Table 3 Agonistic effects of bradykinin analogues in sheep femoral artery

		Bradykinin	*Des-Arg^9-BK*	*NPC 567*	*Des-Arg^9-Leu^8-BK*	*Hoe 140*
Without endothelium						
Contraction	log(EC_{50})	− 8.05 ± 0.12 (8)	> − 5.9 (8)	> − 5.6 (6)	> − 5.6 (2)	− 7.73 ± 0.10 (10)
	Max (% KCl)	59.5 ± 15.1 (8)	50.7 ± 11.2 (8)	5.2 ± 2.8 (6)	7.1 ± 0.0 (2)	62.0 ± 13.1 (10)
	Potency (BK = 1)	1	< 0.007	< 0.004	< 0.004	0.48
With endothelium						
Relaxation	log(EC_{50})	− 8.76 ± 0.09 (12)	In (4)	In (3)	ND	In (6)
	Max (% papaverine)	59.6 ± 9.2 (12)				
Contraction	log(EC_{50})	− 6.30 ± 0.18 (12)	In (4)	In (3)	ND	− 7.65 ± 0.12 (6)
	Max (% KCl)	49.6 ± 11.8 (12)				48.3 ± 13.3 (6)
	Potency (BK = 1)	1				22

Data are shown as mean ± s.e.mean. Numbers in parentheses indicate the number of animals from which tissue was taken. In: inactive: lack of agonistic activity. ND: not determined. BK: bradykinin.

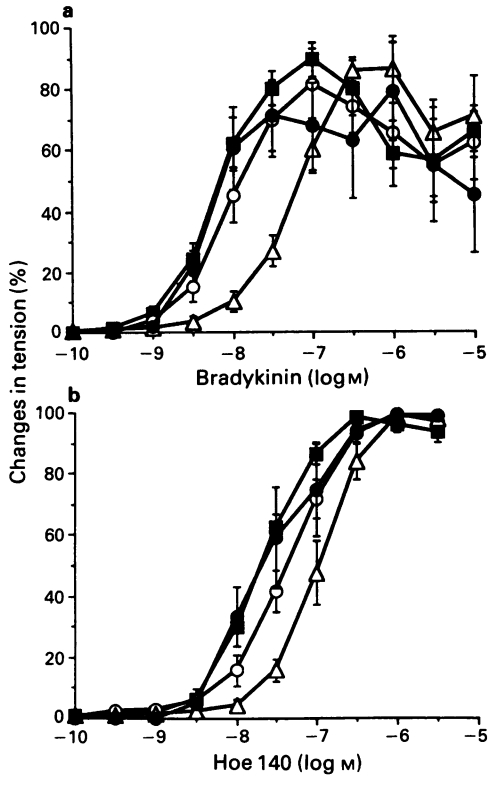

Figure 5 Effects of NPC 567 (a bradykinin B_2 receptor antagonist), and Des-Arg^9-Leu^8-bradykinin (a bradykinin B_1 receptor antagonist) in sheep isolated femoral vein without endothelium. Data are shown as mean ± s.e.mean. (a) Bradykinin concentration-response curves ($n = 6$). Control (■); NPC 567 (10^{-7} M) (○); NPC 567 (10^{-6} M) (△); Des-Arg^9-Leu^8-BK (3×10^{-6} M) (●). (b) Hoe 140 concentration-response curves ($n = 6$). Control (■); NPC 567 (10^{-7} M) (○); NPC 567 (10^{-6} M) (△); Des-Arg^9-Leu^8-BK (3×10^{-6} M) (●).

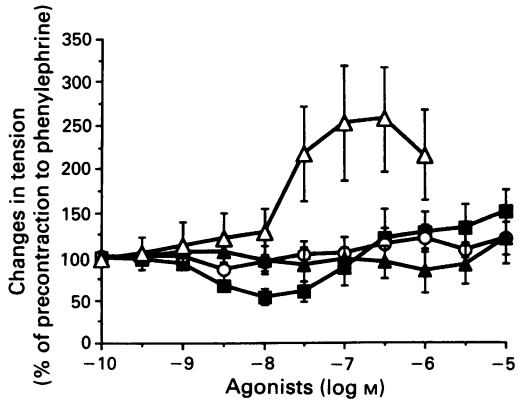

Figure 6 Agonistic effects of bradykinin analogues in sheep isolated femoral artery with endothelium. Data are shown as mean ± s.e.mean. Bradykinin, $n = 12$ (■); Des-Arg^9-bradykinin, $n = 4$ (○); NPC 567, $n = 3$ (▲); Hoe 140, $n = 6$ (△).

agonist, Des-Arg^9-bradykinin, evoked only a minor contractile response. On this tissue, NPC 567 was a partial agonist and apparently a competitive antagonist (confirming previously published data; Rhaleb *et al.*, 1991; 1992a,b). In previous work, it has been clearly demonstrated that the B_1 antagonist, Des-Arg^9-Leu^8-bradykinin, is inactive (Rhaleb *et al.*, 1992a,b).

In the rabbit aorta, a preparation with B_1 bradykinin receptors, Des-Arg^9-bradykinin was, as expected, a potent agonist and its effect was inhibited by Des-Arg^9-Leu^8-bradykinin. The contraction induced by bradykinin in rabbit aorta was probably due to its degradation into Des-Arg^9-bradykinin, by local carboxypeptidase N. This contraction can be prevented by mergepta, an inhibitor of this enzyme (Regoli *et al.*, 1990). The non-specific nature of NPC 567 was confirmed as this compound was also an apparently competitive antagonist in this tissue. However, NPC 567 was 224 times more potent in the jugular vein than in the aorta. Furthermore, there was no residual agonistic activity for NPC 567 in the rabbit aorta (Rhaleb *et al.*, 1992a).

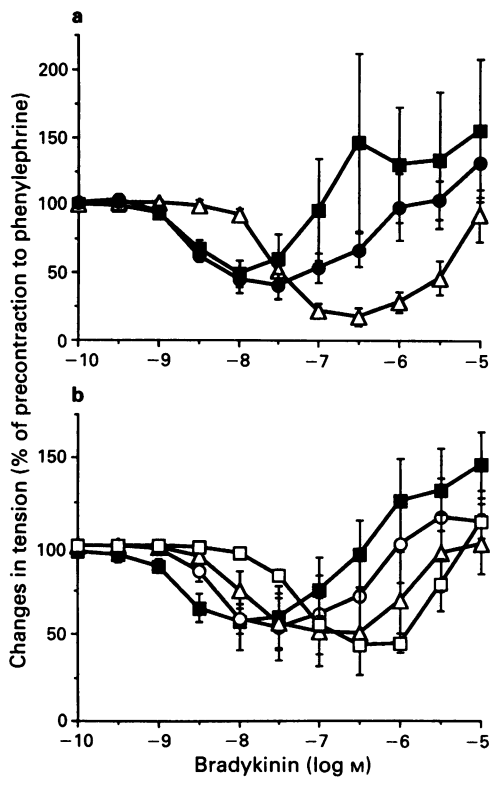

Figure 7 Bradykinin concentration-response curves: effects of bradykinin receptor antagonists in sheep isolated femoral artery with endothelium, precontracted with phenylephrine. Data are shown as mean ± s.e.mean. (a) NPC 567 and Des-Arg^9-Leu^8-bradykinin ($n = 6$). Control (■); NPC 567 (10^{-6} M) (△); Des-Arg-Leu^8-BK (3×10^{-6} M) (●). (b) Hoe 140 ($n = 6$). Control (■); Hoe 140 (10^{-8} M) (○); Hoe 140 (3×10^{-8} M) (△); Hoe 140 (10^{-7} M) (□).

In contrast, Hoe 140 was a potent selective antagonist of bradykinin B_2 receptors with no residual agonistic activity either in the jugular vein or in the aorta. The non-competitive nature of the Hoe 140 antagonism in the jugular vein has been observed in this and other tissues (Rhaleb *et al.*, 1992b). The affinity value calculated under our experimental conditions should be interpreted with caution; nevertheless, in the rabbit jugular vein, Hoe 140 was markedly more potent than NPC 567. A 'tight binding' of this compound to the bradykinin receptor, due to the presence of the two hydrophobic synthetic amino-acid 'D-Tic' and 'Oic', has been suggested (Lembeck *et al.*, 1991; Griesbacher & Lembeck, 1992).

Sheep femoral artery

In the sheep femoral artery, bradykinin stimulated an endothelial receptor which produced endothelium-dependent relaxation and a non-endothelial receptor which produced a prostaglandin-independent smooth muscle contraction. None of the other bradykinin analogues tested produced an endothelium-dependent relaxation. The apparently competitive inhibition of the bradykinin-induced relaxation shown by NPC 567 and Hoe 140 confirms that the bradykinin endo-

thelial receptor is a B_2 subtype (Schini *et al.*, 1990; Félétou *et al.*, 1992). There was no evidence for the presence of an endothelial B_1 receptor in this tissue unlike some other preparations such as bovine pulmonary artery endothelial cells (Sung *et al.*, 1988).

In contrast, each bradykinin analogue tested had, to a varying extent, residual agonistic contractile activity on the sheep femoral artery smooth muscle. Des-Arg^9-bradykinin was able to produce a contraction that was not influenced by the B_2 and B_1 antagonists. Kinins release histamine from mast cells by a mechanism that is independent of B_1 or B_2 bradykinin receptor stimulation. In a non-pathological tissue, mast cell infiltration in the blood vessel wall should be minimal. However, as we did not use histamine receptor antagonists, we cannot exclude the possibility that the effect of Des-Arg^9-bradykinin is related to mast cell degranulation; but first-generation B_2 antagonists such as NPC 567 are much more potent in releasing histamine than B_1 agonists (Devillier *et al.*, 1988). In the sheep femoral artery without endothelium, NPC 567 was an extremely weak agonist. So the mechanism involved in the contraction to Des-Arg^9-bradykinin cannot be determined at present and may involve an uncharacterized receptor similar to the one described by Calixto & Medeiros (1992) in the rat fundus.

Interestingly, Hoe 140 had a dramatic contractile effect; it had the same efficacy (identical maximal effect) and very similar potency to bradykinin in sheep femoral artery without endothelium. The contraction induced by Hoe 140 and bradykinin could be attributed to B_2 receptor stimulation since NPC 567 antagonized the response but not by Des-Arg^9-Leu^8-bradykinin. This may indicate that in the sheep femoral artery, two subtypes of B_2 bradykinin receptors are present.

Hoe 140 was able to distinguish between the endothelial and the non-endothelial receptor (possibly on the smooth muscle cells). Indeed this antagonist had an agonistic activity only in the non-endothelial receptor (contractile response). Even in the presence of B_1 or B_2 bradykinin receptor antagonists, Hoe 140 was unable to elicit an endothelium-dependent relaxation. Furthermore, the contractile response induced by Hoe 140 was hardly shifted by the presence of the endothelium (shift: 1.2); in contrast, the bradykinin contractile response was significantly shifted by the endothelial cell presence (shift: 56). In the rat, the existence of multiple mRNA species of the bradykinin B_2 receptor suggests the likelihood of receptor subtypes (McEachern *et al.*, 1991). Binding studies have also demonstrated the existence of B_2 bradykinin receptor subtypes in the guinea-pig (Seguin *et al.*, 1992; Seguin & Widdowson, 1993). In the epithelium membranes of guinea-pig ileum, a new binding site different from the well known bradykinin B_2 receptor has been described. This site interacts exclusively with some bradykinin receptor antagonists such as Tyr-D-Arg-[Hyp^3,D-Phe^7, Leu^8] bradykinin (Tousignant *et al.*, 1992). To demonstrate the presence of bradykinin B_2 receptor subtypes in the sheep femoral artery, the effects of various agonists and antagonists should be studied. However, it was beyond the scope of this paper to identify precisely the existence (or not) of these receptor subtypes.

Similarly, the bradykinin B_2 receptor in the jugular vein is clearly distinct from the B_2 subtype(s) present in the sheep femoral artery. Hoe 140 and NPC 567 as antagonists are more potent in the rabbit jugular vein than in the sheep femoral artery (Hoe 140: 5–24; NPC 567: 40–130 times more potent). NPC 567 was an antagonist with marked residual agonistic activity in the jugular vein but with hardly any intrinsic activity in the sheep. Conversely, Hoe 140 had no residual agonistic activity in the rabbit jugular vein, but was an agonist at the non-endothelial receptor in the sheep femoral artery. Furthermore, the Hoe 140 inhibition in the rabbit jugular vein was non-competitive, but apparently competitive in the sheep femoral artery.

In conclusion, this study demonstrates that Hoe 140, a new bradykinin B_2 receptor antagonist, is more selective and more potent than NPC 567. However, depending on the tissue studied, it may possess marked residual agonistic properties. Furthermore, bradykinin B_2 receptors are subject to important species specificity. Finally, two different bradykinin B_2 receptor subtypes may coexist in the sheep femoral artery with endothelium.

References

BHOOLA, K.D., FIGUEROA, C.D. & WORTHY, K. (1992). Bioregulation of kinins: kallikreins, kininogens, and kininases. *Pharmacol. Rev.*, **44**, 1–80.

BRAAS, K.M., MANNING, D.C., PERY, D.C. & SNYDER, S.H. (1988). Bradykinin analogues: differential agonist and antagonist activities suggesting multiple receptors. *Br. J. Pharmacol.*, **94**, 3–5.

BURCH, R.M. & KYLE, D.J. (1992). Recent developments in the understanding of bradykinin receptors. *Life Sci.*, **50**, 829–838.

CALIXTO, J.B. & MEDEIROS, Y. (1991). Bradykinin-induced biphasic response in the rat isolated stomach fundus: functional evidence for a novel bradykinin receptor. *Life Sci.*, **50**, PL47–PL52.

DEVILLIER, P., RENOUX, M., DRAPEAU, G. & REGOLI, D. (1988). Histamine release from rat peritoneal mast cells by kinin antagonists. *Eur. J. Pharmacol.*, **149**, 137–140.

FÉLÉTOU, M., GERMAIN, M. & TEISSEIRE, B. (1992). Converting-enzyme inhibitors potentiate bradykinin-induced relaxation in vitro. *Am. J. Physiol.*, **262**, H839–H845.

GRIESBACHER, T. & LEMBECK, F. (1992). Analysis of the antagonistic actions of Hoe140 and other novel bradykinin analogues on the guinea-pig ileum. *Eur. J. Pharmacol.*, **211**, 393–398.

HOCK, F.J., WIRTH, K., ALBUS, U., LINZ, W., GERHARDS, H.J., WIEMER, G., HENKE, S., BREIPOHL, G., KÖNIG, W., KNOLLE, J. & SCHÖLKENS, B.A. (1991). Hoe140 a new potent and long acting bradykinin-antagonist: *in vitro* studies. *Br. J. Pharmacol.*, **102**, 769–773.

LEMBECK, F., GRIESBACHER, T., ECKHARDT, M., HENKE, S., BREIPOHL, G. & KNOLLE, J. (1991). New, long-acting, potent bradykinin antagonists. *Br. J. Pharmacol.*, **102**, 297–304.

LLONA, I., VAVREK, R., STEWART, J. & HUIDOBRO-TORO, J.P. (1987). Identification of pre- and postsynaptic bradykinin receptor sites in the vas deferens: evidence for different structural prerequisites. *J. Pharmacol. Exp. Ther.*, **241**, 608–614.

MCEACHERN, A.E., SHELTON, E.R., BHAKTA, S., OBERNOLTE, R., BACH, C., ZUPPAN, P., FUJISAKI, J., ALCRICH, R.W. & JARNAGIN, K. (1991). Expression cloning of a rat B_2 bradykinin receptor. *Proc. Natl. Acad. Sci. U.S.A.*, **88**, 7724–7728.

REGOLI, D. & BARABE, J. (1980). Pharmacology of bradykinin and related kinins. *Pharmacol. Rev.*, **32**, 1–46.

REGOLI, D., RHALEB, N.E., DRAPEAU, G. & DION, S. (1990). Kinin receptor subtypes. *J. Cardiovasc. Pharmacol.*, **15** (Suppl. 6), S30–S38.

RHALEB, N.E., GOBEIL, F. & REGOLI, D. (1992a). Non-selectivity of new bradykinin antagonists for B_1 receptors. *Life Sci.*, **51**, 125–129.

RHALEB, N.E., ROUISSI, N., DRAPEAU, G., JUKIC, D. & REGOLI, D. (1990). Characterization of bradykinin receptors in peripheral organs. *Can. J. Physiol. Pharmacol.*, **69**, 938–943.

RHALEB, N.E., ROUISSI, N., JUKIC, D., REGOLI, D., HENKE, S., BREIPOHL, G. & KNOLLE, J. (1992b). Pharmacological characterization of a new highly potent B_2 receptor antagonist (Hoe140: D-Arg-[Hyp3,Thi5,D-Tic7,Oic8]bradykinin). *Eur. J. Pharmacol.*, **210**, 115–120.

RHALEB, N.E., TELEMAQUE, S., ROUISSI, N., DION, S., JUKIC, D., DRAPEAU, G. & REGOLI, D. (1991). Structure-activity studies of bradykinin and related peptides. *Hypertension*, **17**, 107–115.

SEGUIN, L. & WIDDOWSON, P.S. (1993). Effects of nucleotides on [3H]bradykinin binding in guinea pig: further evidence for multiple B_2 receptor subtypes. *J. Neurochem.*, **60**, 752–757.

SEGUIN, L., WIDDOWSON, P.S. & GIESEN-CROUSE, E. (1992). Existence of three subtypes of bradykinin B_2 receptor in guinea pig. *J. Neurochem.*, **59**, 2125–2133.

SCHINI, V., BOULANGER, C., REGOLI, D. & VANHOUTTE, P.M. (1990). Bradykinin stimulates the production of cyclic GMP via activation of B_2 kinin receptors in cultured porcine aortic endothelial cells. *J. Pharmacol. Exp. Ther.*, **252**, 581–585.

SOLER, M., SIELCZACK, M. & ABRAHAM, W.M. (1990). A bradykinin-antagonist blocks antigen-induced airway hyperresponsiveness and inflammation in sheep. *Pulm. Pharmacol.*, **3**, 9–15.

SUNG, C.P., ARLETH, A.J., SHIKANO, K. & BERKOWITZ, B.A. (1988). Characterization and function of bradykinin receptors in vascular endothelial cells. *J. Pharmacol. Exp. Ther.*, **247**, 8–13.

TALLARIDA, R.J., COWAN, A. & ADLER, M.W. (1979). pA2 and receptor differentiation: a statistical analysis of competitive antagonism. *Life Sci.*, **25**, 637–654.

TOUSIGNANT, C., REGOLI, D., RHALEB, N.E., JUKIC, D. & GUILLEMETTE, G. (1992). Characterization of a novel binding site for 125I-Tyr-D-Arg-[Hyp3,D-Phe7,Leu8]bradykinin on epithelial membranes of guinea pig ileum. *Eur. J. Pharmacol.*, **225**, 235–244.

WIRTH, K., HOCK, F.J., ALBUS, U., LINZ, W., ALPERMANN, H.G., ANAGNOSTOPOULOS, H., HENKE, S., BREIPOHL, G., KÖNIG, W., KNOLLE, J. & SCHÖLKENS, B.A. (1991). Hoe140 a new potent and long acting bradykinin-antagonist: *in vivo* studies. *Br. J. Pharmacol.*, **102**, 774–777.

(Received December 6, 1993
Revised February 28, 1994
Accepted March 2, 1994)

Br. J. Pharmacol. (1994), **112**, 690–694

Blockade by 4,4′-diisothiocyanatostilbene-2,2′-disulphonate (DIDS) of P_{2X}-purinoceptors in rat vas deferens

[1]Ralph Bültmann & Klaus Starke

Pharmakologisches Institut, Universität Freiburg, Hermann-Herder-Strasse 5, D-79104 Freiburg i.Br., Germany

1 The possibility of an antagonist effect of 4,4′-diisothiocyanatostilbene-2,2′-disulphonate (DIDS) at P_{2X}-purinoceptors was studied in rat vas deferens.

2 DIDS reduced contractions elicited by α,β-methylene ATP 3 μM, IC_{50} 1.6 μM, but did not change contractions elicited by K^+ 35 mM. DIDS 3.2 μM slightly shifted the concentration-response curve of α,β-methylene ATP to the right and reduced the maximum. DIDS 10 μM markedly decreased and DIDS 32 μM abolished contractions over the entire range of the α,β-methylene ATP concentration-response curve. DIDS 32 μM also abolished contractions elicited by ATP but did not change contractions elicited by noradrenaline. The antagonist effect of DIDS was only slowly reversible.

3 The presence of either suramin 320 μM or α,β-methylene ATP 10 μM during the exposure to DIDS protected the tissue from the long-lasting blocking effect of DIDS.

4 4,4′-Diisothiocyanatodihydrostilbene-2,2′-disulphonate (H_2DIDS) was equipotent with DIDS whereas several analogues in which one or both of the isothiocyanate residues were replaced were less effective or without effect against α,β-methylene ATP.

5 DIDS attenuated the purinergic component of neurogenic contractions elicited by electrical field stimulation, IC_{50} 3.9 μM, but did not change the adrenergic component.

6 It is concluded that DIDS causes a selective, long-lasting, non-equilibrium blockade of P_{2X}-purinoceptors in rat vas deferens. Due to this effect it also selectively blocks the purinergic component of neurogenic contractions.

Keywords: Rat vas deferens; DIDS; α,β-methylene ATP; P_{2X}-purinoceptor; P_2-purinoceptor antagonists; co-transmission; purinergic transmission

Introduction

4,4′-Diisothiocyanatostilbene-2,2′-disulphonate (DIDS), commonly used as an anion transport inhibitor (see Cabantchik & Greger, 1992), blocks a number of presumably purinoceptor-mediated responses, namely ADP-induced bovine platelet aggregation (Kitagawa *et al.*, 1983), ATP-induced ion fluxes in murine erythroleukemia cells (Chahwala & Cantley, 1984), the ATP-induced entry of calcium into rat parotid acinar cells (McMillian *et al.*, 1988; Soltoff *et al.*, 1993), the ATP-induced cation current in smooth muscle cells of the rabbit ear artery (Amédée *et al.*, 1990), ATP-induced currents in chick skeletal muscle (Thomas *et al.*, 1991), the ATP-induced acidification of the cytosol of rat cardiac cells (Pucéat *et al.*, 1991), an ATP-activated Cl^- current in human airway epithelial cells (Stutts *et al.*, 1992), and nucleotide-induced contractions of the guinea-pig trachea (Fedan *et al.*, 1993). Most of these effects of DIDS have been attributed to blockade of anion transport mechanisms or Cl^- channels. In rat parotid acinar cells, however, DIDS also decreased the binding of [^{32}P]-ATP (McMillian *et al.*, 1988); moreover, purinoceptor ligands protected the cells from the irreversible effect of DIDS, indicating that DIDS blocked the (P_{2Z}) purinoceptor rather than the subsequent transduction mechanism (Soltoff *et al.*, 1993; see Cusack, 1993, for a review on P_2-purinoceptors).

The possibility of a blockade by DIDS of P_{2X}-purinoceptors has not been investigated. We used rat vas deferens to examine this possibility. In rat vas deferens, P_{2X}-purinoceptors mediate contractions to the prototypic P_{2X}-purinoceptor agonist, α,β-methylene ATP (Burnstock & Kennedy, 1985), as well as the purinergic component of neurogenic contractions (Mallard *et al.*, 1992) and part of the response to exogenous ATP (Bültmann & Starke, 1994).

[1] Author for correspondence.

Methods

Male Wistar rats (240–300 g) were decapitated and the vasa deferentia removed and cleaned of adherent tissue. The medium used for incubation and superfusion contained (mM): NaCl 118, KCl 4.8, $CaCl_2$ 2.5, $MgSO_4$ 1.2, KH_2PO_4 0.9, $NaHCO_3$ 25, glucose 11, ascorbic acid 0.3 and disodium EDTA 0.03. It was saturated with 95% O_2/5% CO_2 and kept at 37°C.

Contraction

Whole vasa deferentia or (experiments with α,β-methylene ATP) prostatic thirds were suspended vertically in a 5.7 ml organ bath. The lower end was fixed and the upper end attached to an isometric force transducer (K30, Hugo Sachs Elektronik, Hugstetten, Germany) under an initial tension of 9.8 mN. The medium was replaced every 15 min (occasionally 25 min). Tissues relaxed to about 3 mN during a 60 min equilibration period. This final resting tension remained constant for the rest of the experiments. The tension was recorded on a Graphtec thermal pen recorder (Ettlingen, Germany).

Contractions were elicited by α,β-methylene ATP, high K^+, ATP, noradrenaline or electrical field stimulation, of which only one was tested on a single preparation. Unless stated otherwise, agonists and high K^+ were washed out immediately after contractions had peaked. High K^+ was added as 35 mM KCl, the final K^+ concentration was therefore 40.7 mM, without osmotic compensation. Field stimulation (single pulses, 0.3 ms pulse width, 100 mA) was applied via platinum electrodes located at the top and the bottom of the organ bath (Stimulator II, Hugo Sachs Elektronik). Where reasonable, concentration-response data were analysed by logistic curve fitting to the weighted mean contraction values using equation No. 25 of Waud (1976) and non-linear regression. The calculation yielded the maximal

effect and the IC_{50} or EC_{50}, i.e. the concentration producing 50% of the maximum.

Tritium overflow

Experiments with [^{3}H]-noradrenaline were carried out as described (Bültmann *et al.*, 1993b). Briefly, slices of the prostatic portion of the vas deferens were preincubated with [^{3}H]-noradrenaline and then superfused with medium of the above composition. The stimulation periods (S_1 to S_6) consisted of 50 pulses per 5 Hz. Drugs or solvent were added after S_3. For evaluation of their effects on basal tritium efflux, ratios were calculated of efflux in the 2 min before S_4 over efflux in the 2 min before S_1. For evaluation of effects on stimulation-evoked tritium overflow, the sum of the overflow elicited by S_1 to S_3 (S_{1-3}) and the sum of the overflow elicited by S_4 to S_6 (S_{4-6}) was formed and ratios S_{4-6}/S_{1-3} were then calculated.

Materials

Adenosine 5'-triphosphate disodium salt (ATP), α,β-methylene ATP lithium salt, 4,4'-diisothiocyanatostilbene-2,2'-disulphonic acid disodium salt (DIDS), (−)-noradrenaline bi-(+)-tartrate (Sigma, Deisenhofen, Germany), 4,4'-diazidostilbene-2,2'-disulphonic acid disodium salt, 4,4'-dinitrostilbene-2,2'-disulphonic acid disodium salt, 4-acetamido-4'-isothiocyanatostilbene-2,2'-disulphonic acid disodium salt (SITS; Aldrich, Steinheim, Germany), 4,4'-diisothiocyanatodihydrostilbene-2,2'-disulphonic acid disodium salt (H_2DIDS; Molecular Probes, Eugene, U.S.A.) and suramin (Bayer, Wuppertal, Germany) were dissolved in distilled water. KCl for high K^+ was dissolved in medium. 4,4'-Diaminostilbene-2,2'-disulphonic acid (Aldrich) was dissolved in water with addition of twice the molar amount of sodium hydroxide. Solutions of stilbenes and suramin were prepared freshly before each experiment. Drug solutions were added to the organ bath in aliquots not exceeding 100 μl.

Statistics

The arithmetic mean ± s.e.mean (for IC_{50} or EC_{50} values of fitted curves the s.e. as defined by Waud, 1976) is given throughout.

Differences between means were tested for significance by the Mann–Whitney test. Differences between fitted curves were tested according to p. 371 of Motulsky & Ransnas (1987). Differences with error probabilities <0.05 were taken to be statistically significant.

Results

Contraction

In initial experiments, α,β-methylene ATP was given every 60 min at the same concentration, 3 μM. It elicited rapid transient contractions of 9.9 ± 0.3 mN ($n = 54$; first addition; see Figure 3 below). The contractions increased upon repeated addition in the presence of solvent (by 68 ± 5% at 6th addition; $n = 5$). Increasing concentrations of DIDS, H_2DIDS and SITS reduced and finally abolished the contractions, with IC_{50} values of 1.6 ± 0.3, 2.0 ± 0.3 and 8.9 ± 1.0 μM, respectively (Figure 1). 4,4'-Diazidostilbene-2,2'-disulphonate and 4,4'-dinitrostilbene-2,2'-disulphonate reduced contractions elicited by α,β-methylene ATP 3 μM only at very high concentrations. 4,4'-Diaminostilbene-2,2'-disulphonate was without effect at concentrations of up to 1 mM (Figure 1). The interaction of DIDS with K^+ 35 mM was studied with the same protocol. DIDS (0.32–32 μM) did not alter contractions elicited by high K^+ ($n = 4$ and 5 for solvent and DIDS, respectively).

The effect of DIDS on the concentration-response curves of α,β-methylene ATP, ATP and noradrenaline was then determined. Increasing concentrations of α,β-methylene ATP elicited increasing contraction with an EC_{50} of 3.5 ± 0.4 μM ($n = 15$; all first concentration-response curves pooled). A second concentration-response curve after addition of solvent was very similar to the first one (EC_{50} 3.6 ± 0.6 μM, $n = 4$; (○) in Figure 2a). DIDS 3.2 μM shifted the concentration-response curve of α,β-methylene ATP slightly to the right (EC_{50} 8.5 ± 1.0 μM; $P<0.05$) and decreased the maximum (by 33%; $P<0.01$). DIDS 10 and 32 μM markedly depressed and abolished, respectively, contractions over the entire range of α,β-methylene ATP concentrations (Figure 2a).

Increasing concentrations of ATP and noradrenaline likewise elicited increasing contractions. For both agonists, a second concentration-response curve after addition of solvent could be superimposed on the first one ($n = 4$ each). DIDS 32 μM abolished contractions elicited by ATP (Figure 2b) but did not alter contractions elicited by noradrenaline (Figure 2c).

The antagonism of DIDS against α,β-methylene ATP was only slowly reversible. The blockade by DIDS 32 μM of the

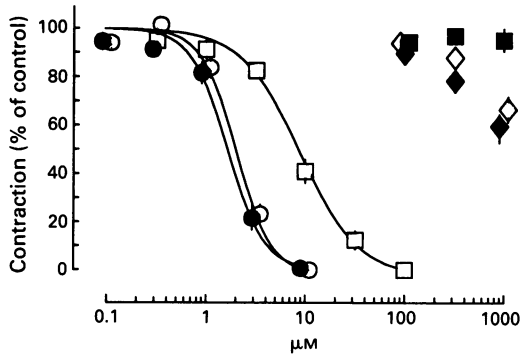

Figure 1 Effect of DIDS and related compounds on contractions elicited by α,β-methylene ATP. α,β-Methylene ATP 3 μM was added to the bath at 60 min intervals and washed out immediately after the contraction had peaked. DIDS (●), H_2DIDS (○), SITS (□), 4,4'-diazidostilbene-2,2'-disulphonate (◆), 4,4'-dinitrostilbene-2,2'-disulphonate (◇) or 4,4'-diaminostilbene-2,2'-disulphonate (■) was added at increasing concentrations immediately after the first and all following responses to α,β-methylene ATP. Abscissae: antagonist concentration. Ordinates show contraction as a percentage of first, pre-antagonist, contraction, corrected for any change observed in controls (solvent). Means ± s.e.mean from 3 to 5 experiments.

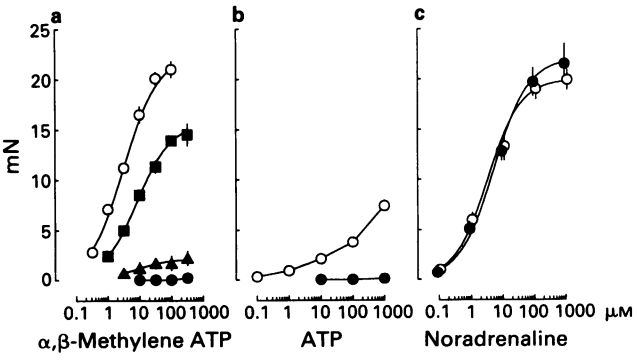

Figure 2 Effect of DIDS on concentration-response curves of (a) α,β-methylene ATP, (b) ATP and (c) noradrenaline. Increasing concentrations of antagonists were added every 30 min and washed out immediately after the contraction had peaked. Two concentration-response curves for the agonist studied were determined in each tissue. Solvent or DIDS was added to the medium after completion of the first curve and the second curve was determined 60 min later. Abscissae: agonist concentration. Ordinates show contractions (mN) in second curves in the presence of solvent (○) or DIDS 3.2 (■), 10 (▲) or 32 μM (●). Means ± s.e.mean from 3 to 5 experiments.

effect of α,β-methylene ATP 3 μM, for example, initially complete, still amounted to 58% after 3 h of washout (application of α,β-methylene ATP every 60 min, of DIDS for 60 min; $n = 3$).

A long-lasting, non-equilibrium blockade of P_{2X}-purinoceptors might explain the non-competitive character of the antagonism of DIDS against α,β-methylene ATP (Figure 2a). Receptor protection experiments were performed to examine this possibility. α,β-Methylene ATP 3 μM was administered twice, with an interval of 130 min. In controls, the second contraction slightly exceeded the first one (by 20 ± 2%; $n = 6$). Compared with (and corrected for) these controls, incubation with DIDS 32 μM for 60 min followed by 60 min washout reduced the subsequent response to α,β-methylene ATP 3 μM by 77 ± 2% ($P < 0.01$; $n = 5$; Figure 3a). Suramin 320 μM and α,β-methylene ATP 10 μM, the protecting drugs, were applied immediately after the first addition of α,β-methylene ATP 3 μM for 70 min and then washed out for 60 min. After exposure to suramin 320 μM or α,β-methylene ATP 10 μM alone, the second contraction elicited by α,β-methylene ATP 3 μM again slightly exceeded the first one (by 4 ± 6 and 33 ± 4%, respectively; $n = 4$ each). Compared to (and corrected for) the 'suramin alone' group, incubation with DIDS 32 μM in the presence of suramin 320 μM reduced the subsequent response to α,β-methylene ATP 3 μM by 22 ± 6% ($P < 0.05$; $n = 4$; Figure 3b), much less than the 77% reduction produced by DIDS alone. Presence of α,β-methylene ATP 10 μM afforded even better protection: exposure to DIDS 32 μM in the presence of α,β-methylene ATP 10 μM did not lead to a significant decrease of the subsequent response to α,β-methylene ATP 3 μM (12 ± 4% reduction compared to and corrected for the 'α,β-methylene ATP 10 μM alone' group; $n = 4$; $P > 0.05$; Figure 3c).

Electrical stimulation of vasa deferentia with single pulses every 60 min elicited biphasic contractions (Figure 4) which remained approximately constant in solvent controls ($n = 4$). DIDS reduced the rapid (purinergic) phase in a concentration-dependent manner but did not alter the slow (adrenergic) phase (Figure 4). For further analysis, purinergic and adrenergic phases were isolated by prazosin and suramin, respectively (Bültmann *et al.*, 1993a). In the presence of prazosin 0.3 μM, contractions amounted to 9.1 ± 0.6 mN (first contraction; $n = 10$) and remained approximately constant upon repeated stimulation in solvent controls ($n = 5$). DIDS progressively reduced and eventually abolished these purinergic contractions, IC_{50} 3.9 ± 0.6 μM (Figure 5). In the presence of suramin 300 μM, contractions amounted to 12.8 ± 1.5 mN (first contraction; $n = 8$) and again remained approximately constant in controls ($n = 4$). DIDS did not alter the adrenergic contractions (Figure 5).

Tritium overflow

Experiments with [^{3}H]-noradrenaline were carried out in order to examine whether DIDS, like suramin (Kurz *et al.*,

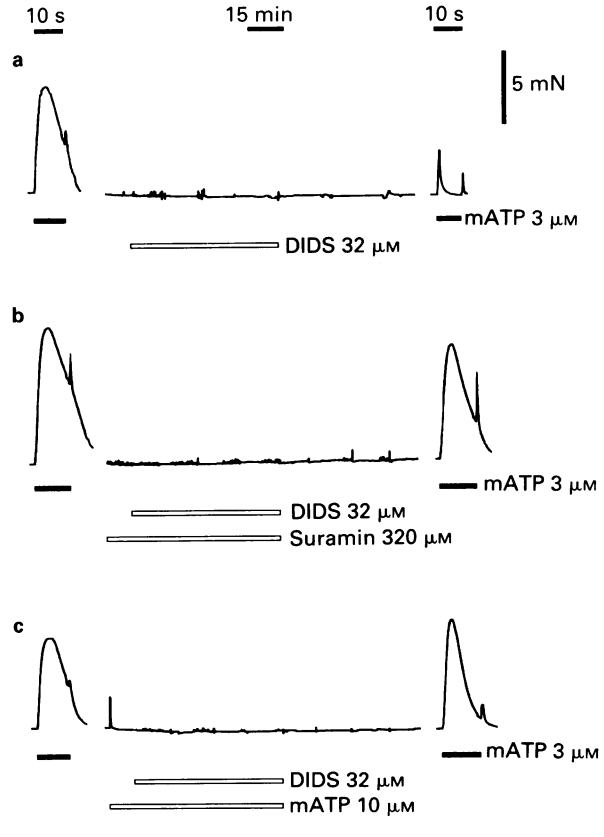

Figure 3 Protection by suramin and α,β-methylene ATP (mATP) against the long-lasting blocking effect of DIDS. α,β-Methylene ATP 3 μM was added twice, at an interval of 130 min. DIDS 32 μM was administered about 11 min after the first addition of α,β-methylene ATP 3 μM and left in the bath for 60 min. DIDS was administered either alone (a) or in the presence of suramin 320 μM (b) or α,β-methylene ATP 10 μM (c) which were given immediately after the first response to α,β-methylene ATP 3 μM and washed out together with the latter. Note different time calibrations for middle tracings on the one hand and left- and right-hand tracings on the other. Due to desensitization, α,β-methylene ATP 10 μM elicited only a very small contraction (c). Representative tracings from 4 or 5 experiments.

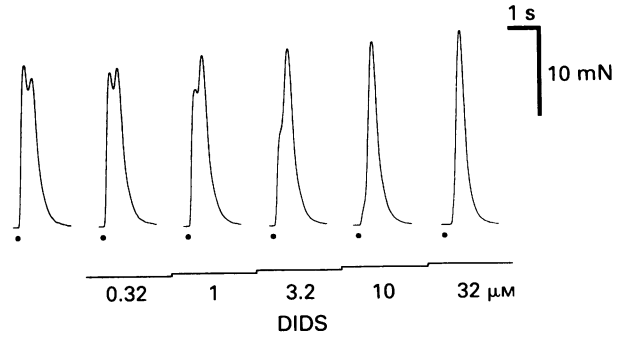

Figure 4 Effect of DIDS on neurogenic contractions. Tissues were electrically stimulated by single pulses every 60 min (dots). DIDS was added at increasing concentrations immediately after the first and all following stimulations. Representative tracings from 6 experiments.

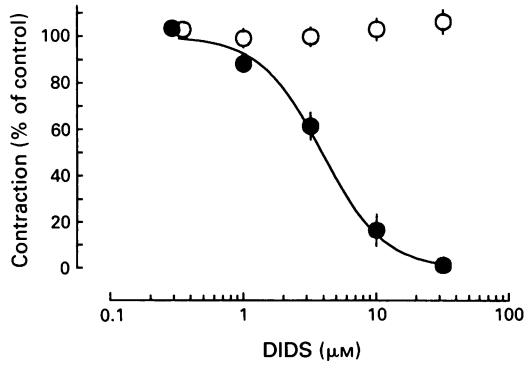

Figure 5 Effect of DIDS on purinergic and adrenergic components of neurogenic contractions. The medium contained either prazosin 0.3 μM (●) or suramin 300 μM (○) from the beginning. Tissues were electrically stimulated by single pulses every 60 min. DIDS was added at increasing concentrations immediately after the first and all following stimulations. Abscissae: DIDS concentration. Ordinates show contraction as a percentage of the first, pre-DIDS, contraction, corrected for any change observed in controls (solvent). Means ± s.e.mean from 4 or 5 experiments.

1993), affected sympathetic transmitter release. There were 6 stimulation periods (S_1 to S_6). Solvent, suramin or DIDS was added after S_3, 64 min before S_4, and kept for the remainder of the experiment. The fractional rate of tritium efflux immediately before S_1 was $0.00155 \pm 0.00003\ min^{-1}$. The overflow evoked by S_1 to S_3 (sum of S_1, S_2 and S_3) amounted to $0.168 \pm 0.007\%$ of tissue tritium ($n = 23$). In solvent controls, the evoked overflow remained approximately constant ($S_{4-6}/S_{1-3} = 1.06 \pm 0.06$; $n = 8$). Suramin 320 μM increased the evoked overflow ($S_{4-6}/S_{1-3} = 1.35 \pm 0.03$; $n = 7$; $P < 0.005$). DIDS 32 μM, in contrast, caused no change ($S_{4-6}/S_{1-3} = 0.94 \pm 0.05$; $n = 8$; $P > 0.05$). Neither suramin nor DIDS changed the basal outflow of tritium.

Discussion

DIDS reduced contractions elicited by α,β-methylene ATP in a concentration-dependent manner (Figures 1 and 2a). Contractions elicited by high K^+ or (Figure 2c) noradrenaline, in contrast, were not changed, thus raising the possibility that the inhibition was due to P_{2X}-purinoceptor blockade.

The blockade produced by DIDS was long-lasting. This at best slowly reversible, non-equilibrium type of effect also showed up in the non-competitive change of the concentration-response curve of α,β-methylene ATP (Figure 2a). The persistent blockade was prevented when the tissue was exposed to DIDS in the presence of either suramin or α,β-methylene ATP (Figure 3). Suramin acts on sites in addition to P_2-purinoceptors (Voogd *et al.*, 1993), and the desensitization produced by α,β-methylene ATP may lead to changes other than those of the P_{2X}-purinoceptor. However, the fact that both compounds protected the tissue from the long-lasting effect of DIDS supports the view that DIDS blocked the P_{2X}-purinoceptor, specifically, its nucleotide binding site.

The IC_{50} value of DIDS against α,β-methylene ATP 3 μM was 1.6 μM. DIDS was, hence, more potent than suramin (IC_{50} 10.1 μM) and about equipotent with pyridoxalphosphate-6-azophenyl-2',4'-disulphonic acid (PPADS; IC_{50} 2.1 μM) when the latter were tested against α,β-methylene ATP with the same protocol (Bültmann & Starke, 1994). It should be noted that DIDS blocked the rat vas deferens P_{2X}-purinoceptor with about the same potency with which it irreversibly blocks the human red blood cell Cl^- exchanger, the anion transporter most sensitive to DIDS (IC_{50} 2 μM; Table 4 of Cabantchik & Greger, 1992).

Several of the present findings resemble results obtained in rat parotid acinar cells where ATP, by activation of P_{2Z}-purinoceptors, stimulated the uptake of $^{45}Ca^{2+}$ (Soltoff *et al.*, 1993). As in the rat vas deferens, the effect of ATP on rat parotid cells was blocked by DIDS, the blockade (tested against ATP instead of α,β-methylene ATP) persisted despite washout, and in protection experiments the blockade was prevented by P_2-purinoceptor ligands. Moreover, as in the present results, H_2DIDS was about equipotent with DIDS, DIDS was about 3 times more potent that SITS, and 4,4'-dinitrostilbene-2,2'-disulphonate had no effect, in rat parotid cells (Soltoff *et al.*, 1993). Therefore, at P_{2X}-purinoceptors as well as at P_{2Z}-purinoceptors, isothiocyanate residues may be decisive for the blockade produced by stilbene disulphonates, as suggested by Soltoff *et al.* (1993). In further support of the suggestion, two additional non-isothiocyanato stilbene disulphonates, 4,4'-diazidostilbene-2,2'-disulphonate and 4,4'-diaminostilbene-2,2'-disulphonate, were at best weak blocking agents. DIDS was more potent at rat vas deferens P_{2X}-purinoceptors (IC_{50} 1.6 μM against α,β-methylene ATP 3 μM) than at rat parotid P_{2Z}-purinoceptors (IC_{50} about 35 μM against ATP 300 μM; Soltoff *et al.*, 1993). This was not due to the longer exposure periods used in the present study (60 min as compared to 10 or 20 min in rat parotid cells), since DIDS also was more potent in rat vas deferens when the exposure per concentration was reduced to 10 min (IC_{50} 6.6 μM against α,β-methylene ATP 3 μM; R. Bültmann, unpublished data).

As well as against exogenous contraction-producing agents, DIDS also acted selectively against the components of neurogenic contractions: the purinergic, P_{2X}-receptor-mediated (Mallard *et al.*, 1992) component was decreased with an IC_{50} (3.9 μM) similar to that found against α,β-methylene ATP, whereas the adrenergic component was unchanged. The pattern of antagonism confirms postganglionic sympathetic noradrenaline-ATP co-transmission in rat vas deferens (see Burnstock, 1990; von Kügelgen & Starke, 1991). Suramin increased the evoked overflow of tritium, and hence the release of noradrenaline, from tissues preincubated with [^{3}H]-noradrenaline. The increase has been demonstrated previously and explained by the interruption of a negative feedback mediated by prejunctional P_{2Y}-like autoreceptors (Kurz *et al.*, 1993; von Kügelgen *et al.*, 1993; 1994). DIDS did not share this effect with suramin and, hence, apparently does not block the prejunctional receptors (see also Fuder & Muth, 1993).

Whereas α,β-methylene ATP and the purinergic transmitter contract the rat vas deferens exclusively through P_{2X}-purinoceptors, exogenous ATP seems to act through three receptors: P_{2X}, P_{2Y} and a non-P_{2X}-non-P_{2Y}-receptor; suramin blocks the P_{2X}- and P_{2Y}-, PPADS the P_{2X}- and the non-P_{2X}-non-P_{2Y}-receptor (Bültmann & Starke, 1994). The complete suppression by DIDS of the effect of ATP (Figure 2b) suggests that DIDS may block all three receptors.

An interaction of DIDS with ATP in guinea-pig vas deferens has been mentioned in a review article: DIDS 100 μM caused only a moderate depression of the amplitude of contractions induced by ATP 0.1 μM–10 mM and in addition prolonged the contractions (Fedan & Lamport, 1990). The reason may be the brief duration, 15 min, of the exposure to DIDS (Fedan & Lamport, 1990). A species difference seems unlikely: incubation of the guinea-pig vas deferens with DIDS 1–32 μM for 60 min per concentration progressively reduced and finally abolished contractions elicited by α,β-methylene ATP 3 μM as well as the purinergic component of neurogenic contractions, in accord with the results on rat vas deferens (R. Bültmann, unpublished data).

This study was supported by the Deutsche Forschungsgemeinschaft (SFB 325). We thank Bayer for suramin.

References

AMÉDÉE, T., LARGE, W.A. & WANG, Q. (1990). Characterization of chloride currents activated by noradrenaline in rabbit ear artery cells. *J. Physiol.*, **428**, 501–516.

BÜLTMANN, R. & STARKE, K. (1994). P_2-purinoceptor antagonists discriminate three contraction-mediating receptors for ATP in rat vas deferens. *Naunyn-Schmied. Arch. Pharmacol.*, **349**, 74–80.

BÜLTMANN, R., SZABO, B. & STARKE, K. (1993a). Inhibition by ethanol of contractions of rat vas deferens: no evidence for selective blockade of P_{2X}-purinoceptors. *Naunyn-Schmied. Arch. Pharmacol.*, **347**, 527–533.

BÜLTMANN, R., VON KÜGELGEN, I. & STARKE, K. (1993b). Effects of nifedipine and ryanodine on adrenergic neurogenic contractions of rat vas deferens: evidence for a pulse-to-pulse change in Ca^{2+} sources. *Br. J. Pharmacol.*, **108**, 1062–1070.

BURNSTOCK, G. (1990). Co-transmission. *Arch. Int. Pharmocodyn.*, **304**, 7–33.

BURNSTOCK, G. & KENNEDY, C. (1985). Is there a basis for distinguishing two types of P_2-purinoceptor? *Gen. Pharmacol.*, **16**, 433–440.

CABANTCHIK, Z.I. & GREGER, R. (1992). Chemical probes for anion transporters of mammalian cell membranes. *Am. J. Physiol.*, **262,** C803–C827.

CHAHWALA, S.B. & CANTLEY, L.C. (1984). Extracellular ATP induces ion fluxes and inhibits growth of Friend erythroleukemia cells. *J. Biol. Chem.*, **259,** 13717–13722.

CUSACK, N.J. (1993). P_2 receptor: subclassification and structure-activity relationships. *Drug. Dev. Res.*, **28,** 244–252.

FEDAN, J.S., BELT, J.J., YUAN, L.X. & FRAZER, D.G. (1993). Contractile effects of nucleotides in guinea pig isolated, perfused trachea: involvement of respiratory epithelium, prostanoids and Na^+ and Cl^- channels. *J. Pharmacol. Exp. Ther.*, **264,** 210–216.

FEDAN, J.S. & LAMPORT, S.J. (1990). P_2-purinoceptor antagonists. *Ann. N.Y. Acad. Sci.*, **603,** 183–197.

FUDER, H. & MUTH, U. (1993). ATP and endogenous agonists inhibit evoked [^{3}H]-noradrenaline release in rat iris via A_1 and P_{2Y}-like purinoceptors. *Naunyn-Schmied. Arch. Pharmacol.*, **348,** 352–357.

KITAGAWA, S., ENDO, J., KUBO, R. & KAMETANI, F. (1983). Inhibitory effects of 4,4′-diisothiocanostilbene-2,2′-disulfonate (DIDS) on the ADP-stimulated aggregation of gel-filtered bovine blood platelets. *Biochem. Biophys. Res. Commun.*, **111,** 306–311.

KURZ, K., VON KÜGELGEN, I. & STARKE, K. (1993). Prejunctional modulation of noradrenaline release in mouse and rat vas deferens: contribution of P_1- and P_2-purinoceptors. *Br. J. Pharmacol.*, **110,** 1465–1472.

MALLARD, N., MARSHALL, R., SITHERS, A. & SPRIGGS, B. (1992). Suramin: a selective inhibitor of purinergic neurotransmission in rat isolated vas deferens. *Eur. J. Pharmacol.*, **220,** 1–10.

MCMILLIAN, M.K., SOLTOFF, S.P., LECHLEITER, J.D., CANTLEY, L.C. & TALAMO, B.R. (1988). Extracellular ATP increases free cytosolic calcium in rat parotid acinar cells. *Biochem. J.*, **255,** 291–300.

MOTULSKY, H.J. & RANSNAS, L.A. (1987). Fitting curves to data using nonlinear regression: a practical and nonmathematical review. *FASEB J.*, **1,** 365–374.

PUCÉAT, M., CLÉMENT, O. & VASSORT, G. (1991). Extracellular MgATP activates the Cl^-/HCO_3^- exchanger in single rat cardiac cells. *J. Physiol.*, **444,** 241–256.

SOLTOFF, S.P., MCMILLIAN, M.C., TALAMO, B.R. & CANTLEY, L.C. (1993). Blockade of ATP binding site of P_2 purinoceptors in rat parotid acinar cells by isothiocyanate compounds. *Biochem. Pharmacol.*, **45,** 1936–1940.

STUTTS, M.J., CHINET, T.C., MASON, S.J., FULLTON, J.M. CLARKE, L.L. & BOUCHER, R.C. (1992). Regulation of Cl^- channels in normal and cystic fibrosis airway epithelial cells by extraceullar ATP. *Proc. Natl. Acad. Sci. U.S.A.*, **89,** 1621–1625.

THOMAS, S.A., ZAWISA, M.J., LIN, X. & HUME, R.I. (1991). A receptor that is highly specific for extracellular ATP in developing chick skeletal muscle *in vitro*. *Br. J. Pharmacol.*, **103,** 1963–1969.

VON KÜGELGEN, I., KURZ, K. & STARKE, K. (1993). Axon terminal P_2-purinoceptors in feedback control of sympathetic transmitter release. *Neuroscience*, **56,** 263–267.

VON KÜGELGEN, I., KURZ, K. & STARKE, K. (1994). P_2-purinoceptor-mediated autoinhibition of sympathetic transmitter release in mouse and rat vas deferens. *Naunyn-Schmied. Arch. Pharmacol.*, **349,** 125–132.

VON KÜGELGEN, I. & STARKE, K. (1991). Noradrenaline-ATP cotransmission in the sympathetic nervous system. *Trends Pharmacol. Sci.*, **12,** 319–324.

VOOGD, T.E., VANSTERKENBURG, E.L.M., WILTING, J. & JANSSEN, L.H.M. (1993). Recent research on the biological activity of suramin. *Pharmacol. Rev.*, **45,** 177–203.

WAUD, D.R. (1976). Analysis of dose-response relationships. In *Advances in General and Cellular Pharmacology*, vol. 1. ed. Narahashi, T. & Bianchi, C.P. pp. 145–178. London: Plenum.

(Received January 11, 1994
Revised February 20, 1994
Accepted March 2, 1994)

Br. J. Pharmacol. (1994), **112**, 695–703

Effects of DAU 6215, a novel 5-hydroxytryptamine$_3$ (5-HT$_3$) antagonist on electrophysiological properties of the rat hippocampus

M.B. Passani, A.M. Pugliese, M. Azzurrini & [1]R. Corradetti

Dipartimento di Farmacologia Preclinica e Clinica, Universita' di Firenze, Viale Morgagni 65, 50134 Firenze, Italy

1 The aim of the present study was to test the effects of DAU 6215 (endo-*N*-(8-methyl-8-azabicyclo-[3.2.1]-octo-3-yl)-2,3-dihydro-2-oxo-1H-benzimidazole-1-carboxamide hydrochloride), a newly synthesized, selective 5-hydroxytryptamine$_3$ (5-HT$_3$) antagonist, on the cell membrane properties and on characterized 5-HT-mediated responses of pyramidal neurones in the hippocampal CA1 region.

2 Administration of DAU 6215, even at concentrations several hundred fold its K_i, did not affect the cell membrane properties of pyramidal neurones, nor modify extracellularly recorded synaptic potentials, evoked by stimulating the Schaffer's collaterals.

3 Micromolar concentrations (15–30 μM) of 5-HT elicited several responses in pyramidal neurones that are mediated by distinct 5-HT receptor subtypes. DAU 6215 did not antagonize the 5-HT$_{1A}$-induced membrane hyperpolarization and conductance increase, a response that was blocked by the selective 5-HT$_{1A}$ antagonist NAN-190 (1-(2-methoxyphenyl)-4-[4-(2-phtalamido)butyl-piperazine). Similarly, DAU 6215 did not affect the membrane depolarization and decrease in amplitude of the afterhyperpolarization, elicited by the activation of putative 5-HT$_4$ receptors.

4 5-HT increased the frequency of spontaneous postsynaptic potentials (s.p.s.ps) recorded in pyramidal neurones loaded with chloride. In agreement with previous observations, most of the s.p.s.ps were reversed GABAergic events, produced by the activation of 5-HT$_3$ receptors on interneurones, because they persisted in the presence of the glutamate NMDA and non NMDA antagonists, D-aminophosphonovaleric acid (APV; 50 μM) and 6,7-dinitroquinoxaline-2,3-dione (DNQX; 25 μM), and were elicited by the selective 5-HT$_3$ agonist, 2-methyl-5-HT (2-Me-5-HT, 50 μM).

5 The increase in frequency of s.p.s.ps induced by 5-HT was significantly antagonized by DAU 6215 in 70% of the cases, whereas the 5-HT$_3$ antagonist always suppressed the effect of 2-Me-5-HT, at concentrations as low as 60 nM.

6 The antagonistic effect of DAU 6215 was also tested on the 5-HT$_3$-mediated block of induction of long-term potentiation (LTP), elicited by a primed burst (PB) stimulation. Extracellular recordings showed that low concentrations (60 nM) of DAU 6215 suppressed the inhibitory action of 5-HT on PB-induced LTP, without affecting the 5-HT$_{1A}$-induced reduction in the amplitude of the population spike.

7 These results provide evidence that DAU 6215 is an effective antagonist of the 5-HT$_3$-mediated responses in the central nervous system and may offer a cellular correlate for the pharmacological effects of DAU 6215 as an anxiolytic and cognition enhancer.

Keywords: 5-HT (5-hydroxytryptamine); 5-HT$_3$ receptor; DAU 6215; spontaneous postsynaptic potentials; NAN-190; hippocampus; long-term potentiation (LTP); primed burst stimulation (PB)

Introduction

In the last few years a novel class of 5-hydroxytryptamine$_3$ (5-HT$_3$) receptor antagonist has been synthesized (Turconi *et al.*, 1990) and the potency and selectivity of these new molecules have been tested in isolated preparations and *in vivo* models. Among these compounds, DAU 6215 (endo-*N*-(8-methyl-8-azabicyclo-[3.2.1]-octo-3-yl)-2,3-dihydro-2-oxo-1H-benzimidazole-1-carboxamide hydrochloride), a benzimidazolone derivative, exhibits a high affinity for the [^{3}H]-ICS 205-930 binding site in rat brain tissue, and it is equipotent with ICS 205-930 in inhibiting 5-HT-induced bradycardia in rats (Turconi *et al.*, 1990; 1991a). DAU 6215 was also found to be a weak, partial agonist at the 5-HT$_4$ receptor, as demonstrated by the ability of this compound to stimulate adenosine 3':5'-cyclic monophosphate (cyclic AMP) production in colliculi neurones in cultures (Dumuis *et al.*, 1991). Several central pharmacological effects of DAU 6215 have been described: it is a potent antiemetic (Sagrada *et al.*, 1990; 1991), an anxiolytic in animal models (Borsini *et al.*, 1993), and it decreases the morphine-induced reward in animal models (Turconi *et al.*, 1991b). Recently, it was found that DAU 6215, also reduces scopolamine-induced behavioural deficits in rats (Brambilla *et al.*, 1993; Pitsikas *et al.*, 1994). Electrophysiological recordings *in vivo*, have shown that chronic administration of DAU 6215 reduces the number of spontaneously firing dopaminergic neurones in the rat ventral tegmental area, suggesting a potential antipsychotic activity of this compound (Prisco *et al.*, 1992). In spite of the biochemical evidence that DAU 6215 is a selective 5-HT$_3$ receptor antagonist, the effect of this ligand on the neuromodulatory action of 5-HT in the CNS has not yet been tested. We studied the pharmacological profile of DAU 6215 in the hippocampal slice preparation for the following reasons. The hippocampus displays different patterns of activity that have been correlated with long-term synaptic potentiation and some forms of learning and memory storage (Teyler *et al.*, 1987); it is a region enriched with 5-HT receptors (Köhler, 1984) and 5-hydroxytryptaminergic terminals originating in the raphe nuclei (Swanson *et al.*, 1987) and electrophysiological studies *in vivo* and *in vitro* have demonstrated that 5-HT has an inhibitory action on evoked synaptic potentials (Segal, 1975; 1976; 1980; Jahnsen, 1980; Ropert,

[1] Author for correspondence.

1988) and long-term potentiation (LTP; Corradetti et al., 1992a). Applications of micromolar concentrations of 5-HT exert multiple and well characterized actions on CA1 pyramidal neurones through distinct 5-HT receptor subtypes (Anwyl, 1990). Postsynaptic actions of 5-HT on CA1 pyramidal neurones include hyperpolarization of the cell membrane associated with decreased input resistance, and a reduction of the afterhyperpolarization (AHP; Segal, 1980; Andrade & Nicoll, 1987; Colino & Halliwell, 1987; Ropert, 1988). Activation of an inwardly rectifying potassium channel mediates the membrane hyperpolarization and decrease in input resistance, through a 5-HT_{1A} receptor (Andrade & Nicoll, 1987; Colino & Halliwell, 1987) associated with a G protein (Andrade et al., 1986). The slow excitatory action and reduction of the amplitude of the AHP (Chaput et al., 1990; Andrade & Chaput, 1991) is due to the closing of calcium-dependent K^+ channels (I_{AHP}; Andrade & Nicoll, 1987; Colino & Halliwell, 1987), supposedly through the activation of 5-HT_4-like receptors (Chaput et al., 1990; Andrade & Chaput, 1991). Up till now, no direct effect of 5-HT on CA1 pyramidal neurones in hippocampal slices has been ascribed to 5-HT_3 receptor stimulation. Activation of 5-HT_3 receptors is apparently responsible for the 5-HT-induced increase in spontaneous post-synaptic potentials (s.p.s.ps); this effect has been attributed to enhanced activity of GABAergic interneurones (Ropert & Guy, 1991), although a non-5-HT_3 component has also been described (Van den Hooff & Galvan, 1991).

Recently, it was demonstrated that the simultaneous activation of both 5-HT_{1A} and 5-HT_3 receptors is responsible for the inhibitory action of 5-HT on the induction of LTP produced by a primed burst (PB) stimulation *in vitro*, (Corradetti et al., 1992a).

These properties make the hippocampal slice a suitable preparation to study the action of DAU 6215 on well characterized electrophysiological responses of CA1 pyramidal neurones to 5-HT and also its antagonistic effects on the neuromodulatory action of 5-HT on synaptic activity, mediated by 5-HT_3 receptors. Part of the results described here have been published previously (Corradetti et al., 1992b).

Methods

Preparation of hippocampal slices

Experiments were carried out on *in vitro* hippocampal preparations as previously described (Corradetti et al., 1992a). Charles River male Wistar rats (100–200 g body weight) were anaesthetized with ether and decapitated. The hippocampi were rapidly removed and placed in ice cold oxygenated (95% O_2:5% CO_2) artificial cerebrospinal fluid (aCSF) of the following composition (mM): NaCl 124, KCl 3.33, KH_2PO_4 1.25, $MgSO_4$ 2, $CaCl_2$ 2.5, $NaHCO_3$ 25, D-glucose 10 (pH 7.4). Slices (400 μm thick) were cut with a McIlwain tissue chopper from the dorsal half of the hippocampus and kept in oxygenated aCSF for at least 1 h at room temperature (20–23°C). A single slice was then placed on a nylon mesh and completely submerged in a small chamber and superfused with oxygenated aCSF (30–32°C) at a constant flow rate of 2–3 ml min^{-1}. Drugs were administered through a three-way tap and complete exchange of the chamber volume occurred in 1 min.

Intracellular recordings

CA1 pyramidal neurones were recorded in current clamp mode with either 3 M potassium-methylsulphate- (50–100 MΩ) or KCl- (35–50 MΩ) filled electrodes. Electrical signals were filtered at 30 kHz and amplified with an Axoclamp 2A (Axon Instruments, Foster City, CA, U.S.A.) and displayed on an oscilloscope and chart recorder (2800 Gould Instruments, Cleveland OH, U.S.A.). Traces were stored on a digital tape (DTR 1200, Biologic, France; 48 kHz sampling frequency) and on computer using a pClamp programme (Axon Instruments) for off-line measurements (sampling frequency = 3–10 kHz). Only neurones with stable resting membrane potentials (r.m.p.; range − 54/−80 mV) and input resistances (R_{in}; range 31–86 MΩ) throughout the recording were included in the analysis. When cells appeared to have reached a stable membrane potential, pulses of hyperpolarizing current (200–400 pA, 400 ms) were delivered through the recording electrode to monitor changes in input resistance during drug application. To study the s.p.s.ps, 3 M KCl-filled electrodes were used with a resistance not exceeding 50 MΩ. Low resistance electrodes were used to obtain a good diffusion of chloride within the impaled cells. Neurones were maintained at a negative potential (− 90/− 100 mV) by current injection to load the cell with chloride and prevent them from firing action potentials due to reversed inhibitory postsynaptic potentials. The cells were allowed to load with chloride for 15–20 min and to reach a stable membrane potential before results were recorded. Experiments aimed at studying the effects of DAU 6215 on the AHP were carried out in the presence of 1 μM tetrodotoxin (TTX), 5 mM tetraethylammonium chloride (TEA) and 1 μM NAN-190 (1-(2-methoxyphenyl)-4-[4-(2-phthalamido)butil piperazine), a 5-HT_{1A} antagonist, to allow for the generation of calcium spikes (Andrade & Nicoll, 1987) and eliminate the 5-HT_{1A} component of the response. These compounds were perfused for at least 30 min before testing 5-HT. Under these conditions, injections of positive current pulses (100 ms) through the recording electrode elicited a calcium spike, followed by a large calcium-dependent K^+-activated AHP (Schwartzkroin & Slawsky, 1977; Madison & Nicoll, 1986, Andrade & Nicoll, 1987). This procedure was used, as opposed to examining the AHP following a burst of spikes, because the large amplitude, reproducible AHP produced by the calcium spike, enables the systematic examination of the effects of 5-HT and its antagonists (Chaput et al., 1990).

Extracellular recordings

Experiments were performed in 41 slice preparations. The Schaffer's collateral/commissural fibres were stimulated through bipolar nichrome electrodes with 80–110 μs, 0.017 Hz test pulses. Evoked potentials were recorded with 3 M NaCl-filled electrodes (3–6 MΩ) placed in the stratum pyramidale of the CA1 region. Responses were amplified (Neurolog NL104, Digitimer Ltd., England), displayed on an oscilloscope, digitized and stored on floppy disks for later analysis (sample rate 33 kHz; DATA 6000, Analogic, Danvers, MA, U.S.A.). Input-output curves were obtained at the beginning of each experiment by gradually increasing the stimulus strength. The test stimulus pulse was then adjusted at an intensity that elicited population spikes of an amplitude 30–40% of the maximum, and was maintained constant for the duration of the experiment. After 30 min equilibrium, a 25 min control period was used to generate baseline values. LTP was induced with a primed burst (PB) stimulation, consisting of a pulse followed by a burst of five pulses at 100 Hz, after a 170 ms interval. The strength of the pulses during the high frequency burst was kept at the same intensity as the test pulse. 5-HT was applied for 5 min and the PB stimulation delivered during the fifth min of application of the drug, which was washed out immediately after the patterned stimulation. DAU 6215 was allowed to equilibrate for at least 15 min before adding 5-HT and was left for at least 15 min after the PB stimulation and wash out of the agonist.

Data analysis

The instantaneous frequency of occurrence of spontaneous postsynaptic events was measured with a DATA 6000 (sampling frequency 3–5 kHz). A reference level was manually

chosen to detect only events of an amplitude exceeding background noise (0.5–1 mV). The programme then, automatically calculated the instantaneous average frequency, measured as the reciprocal of the average of the time intervals between 'paired' crossings of the reference y-level on the time axis. Paired crossings were defined as adjacent crossings of the same polarity with one crossing of opposite polarity between the two. Although the reference level used probably cut off most of miniature s.p.s.ps, it is possible that in some cells these were included in our measurements. The occasional inclusion of miniature potentials in the measurements, though, should not be relevant to our results, since 5-HT does not affect either the frequency or the amplitude of miniature i.p.s.p. (Ropert & Guy, 1991). The sampling was performed on 20 s periods and the average frequencies grouped in 3–4 min bins.

Chemical substances

The following drugs were applied in the perfusion solution: 5-hydroxtryptamine (5-HT) creatinine sulphate or hydrochloride salts, 2-methyl-5-hydroxytryptamine maleate (2-Me-5-HT), 1-(2-methoxyphenyl)-4-[4-(2-phthalamido)butil-piperazine (NAN-190), all from Research Biomedical Inc. Wayland, U.S.A.: endo-*N*-(8-methyl-8-azabicyclo-[3.2.1]-octo -3-yl)-2,3-dihydro-2-oxo-1H-benzimidazole-1-carboxamide hydrochloride (DAU 6215-Cl; gift of Dr Borsini, Boehringer Ingelheim, Milan, Italy); D-aminophosphonovaleric acid (D-APV) and 6,7-dinitroquinoxaline-2,3-dione (DNQX), both from Tocris Neuramin, (Essex, England); tetrodotoxin (TTX) and tetraethylammonium chloride (TEA), both from Sigma, St Louis MO, U.S.A.

Statistics

All numerical data are given as means ± s.e.mean; Student's paired *t* test and multiple comparison ANOVA, followed by Fisher LSD *post hoc* test, were used where appropriate; a value of $P<0.05$ was considered statistically significant.

Results

In a first series of experiments we investigated the selectivity of the antagonistic action of DAU 6215 on well characterized 5-HT responses of hippocampal neurones, mediated by different receptor subtypes.

DAU 6215 does not block 5-HT$_{1A}$-mediated responses

In 14 pyramidal neurones (resting membrane potential: r.m.p. = − 68 ± 1.5 mV; input resistance: R_{in} = 52 ± 4.9 MΩ), 3–5 min applications of 30 μM 5-HT, a concentration that elicits a maximal effect, consistently induced a membrane hyperpolarization (7 ± 1 mV) and reduced the input resistance by an average of 30 ± 2.9% (Figure 1a). The decrease in membrane resistance was still observable when the membrane potential was manually clamped at the control resting potential during 5-HT application, which eliminated the possibility that the change in resistance was due to non-linearities of the current/voltage relationship. DAU 6215 up to micromolar concentrations, did not significantly change the cell membrane potential and input resistance and was ineffective in antagonizing the 5-HT-induced responses (Figures 1a,b; Table 1). On the other hand, 1 μM NAN-190, a 5-HT$_{1A}$ ligand (Glennon *et al.*, 1988a,b) with antagonist effects in the hippocampus (Fletcher *et al.*, 1993; see also Discussion), significantly antagonized the membrane potential change and reduction in input resistance induced by 30 μM 5-HT (n = 4; Figure 1a). NAN-190, *per se*, had no effect on either the input resistance or the resting membrane potential (R_{in} and r.m.p. in control medium were 41.8 ± 3.9 MΩ and − 67 ± 2 mV, respectively; in 1 μM NAN-

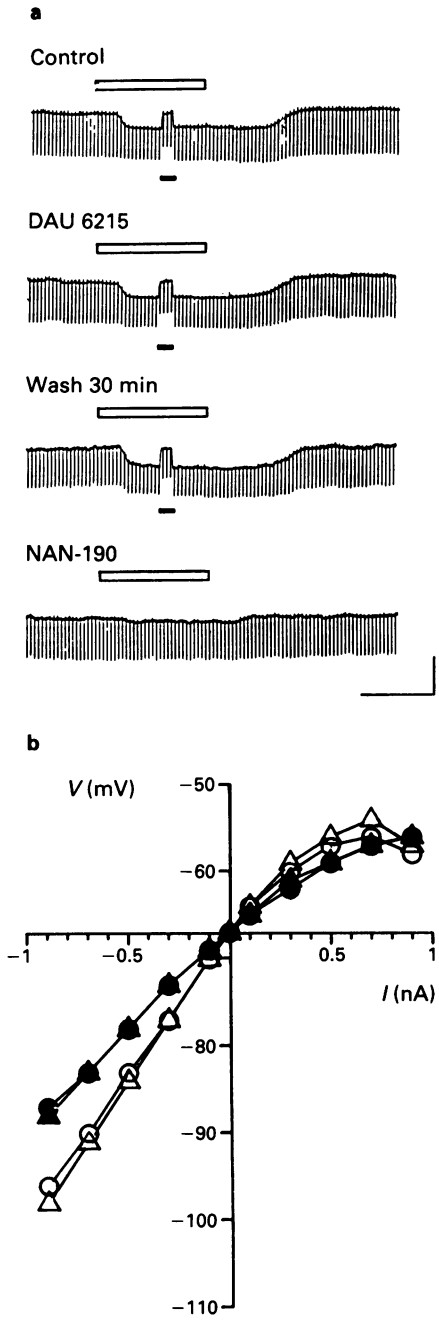

Figure 1 The hyperpolarization and conductance increase produced by 5-hydroxytryptamine (5-HT) are not antagonized by DAU 6215. (a) Chart records of resting membrane potential of a CA1 pyramidal cell in which 5-HT (30 μM, open bars) was applied (from top trace): in normal aCSF, in the presence of DAU 6215 (3 μM, 15 min), after 30 min washout of DAU 6215; and in the presence of the 5-HT$_{1A}$-receptor antagonist NAN-190 (1 μM, 20 min). Downward deflections are electrotonic cell membrane responses to constant current pulses (0.3 nA, 400 ms) injected through the recording electrode to monitor total input resistance. During 5-HT application, the membrane potential was manually clamped at the control value (− 67 mV) by injecting + 0.18 nA through the recording electrode (filled bars) to rule out the possibility that the decrease in input resistance was only apparent and was due to cell hyperpolarization. Note that the response to 5-HT was almost completely blocked by NAN-190, but was not affected by DAU 6215. (b) Plot of current-voltage relationships (I/V curves) recorded in a pyramidal neurone bathed in tetrodotoxin (1 μM) to prevent cell firing at positive potentials: control (Δ), 30 μM 5-HT (▲), 3 μM DAU 6215 (○), 5-HT in the presence of DAU 6215 (●). During the application of 5-HT, membrane potential was manually clamped at the control value by injecting positive current (d.c. = + 0.42 nA). Note that 5-HT both in control aCSF and in the presence of DAU 6215, produced similar changes of the I/V relationship, whereas DAU 6215 by itself did not affect the I/V curve. Calibration bars: 10 mV, 3 min.

Table 1 DAU 6215 has no direct effect on cell membrane properties, nor does it antagonize the changes in membranes potential (Δ MP), input resistance (ΔR_{in}) and population spike (PS) amplitude produced by 5-HT

Treatment	*ΔMP* (MV)	(n)	*ΔR_{in}* (%)	(n)	*PS amplitude* (% control)	(n)
DAU 6215 60 nM	0 ± 0	(3)	2 ± 1.4	(3)	106 ± 6	(11)
DAU 6215 300 nM	−2.5 ± 1.1	(5)	−4 ± 3.5	(5)	97 ± 1	(6)
DAU 6215 1 μM	NT		NT		104 ± 4	(6)
DAU 6215 3 μM	0.8 ± 0.7	(6)	1.3 ± 2.5	(6)	NT	
5-HT 30 μM	−4.3 ± 0.4	(3)	−40 ± 4.2	(3)	34 ± 6	(5)
+ DAU 6215 60 nM	−4.7 ± 0.3	(3)	−42 ± 6.9	(3)	29 ± 7	(5)
5-HT 30 μM	−10 ± 2.4	(5)	−33 ± 5.4	(5)	44 ± 14	(4)
+ DAU 6215 300 nM	−9.4 ± 2.4	(5)	−29 ± 13	(5)	45 ± 12	(4)
5-HT 30 μM	NT		NT		9 ± 7	(4)
+ DAU 6215 1 μM	NT		NT		12 ± 9	(4)
5-HT 30 μM	−5.8 ± 0.7	(6)	−23 ± 3	(6)	NT	
+ DAU 6215 3 μM	−6.7 ± 0.6	(6)	−23 ± 3	(6)	NT	

Number of experiments are indicated in parentheses (*n*). NT, not tested.

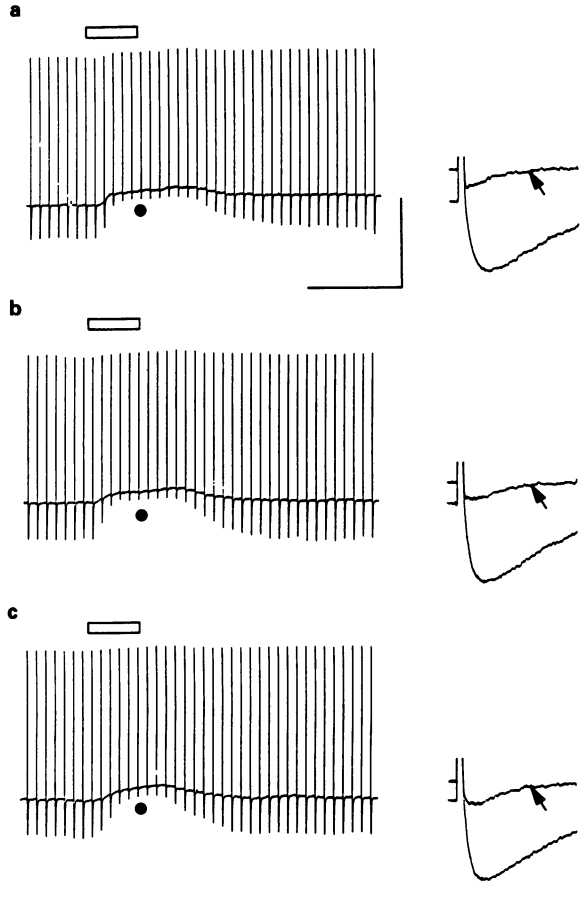

Figure 2 DAU 6215 does not antagonize the 5-hydroxytryptamine (5-HT)-induced reduction of the afterhyperpolarization (AHP) in hippocampal pyramidal cells. Chart record of calcium spikes evoked by depolarizing current pulses (+ 300 pA; 100 ms) delivered every 30 s in the presence of tetrodotoxin (1 μM), tetraethylammonium (5 mM) and NAN-190 (1 μM, see Methods). The calcium spike was followed by a large AHP (downward deflections). (a) 5-HT (15 μM, open bar) elicited a decrease in the amplitude of the AHP (− 71%) and a depolarization of the membrane potential (6 mV). (b) The action of 5-HT persisted in the presence of 1 μM DAU 6215 and (c) after 15 min washout of DAU 6215. R.m.p. = − 54 mV. Calibration bars: 30 mV, 5 min. In the panels at the right, a control response before application of 5-HT and the response taken at time indicated by the spot in the corresponding left panel, are amplified at different voltage gain and timebase (calibrations: 15 mV, 1 s) and superimposed to show the effect of 5-HT (arrows) on AHP more clearly.

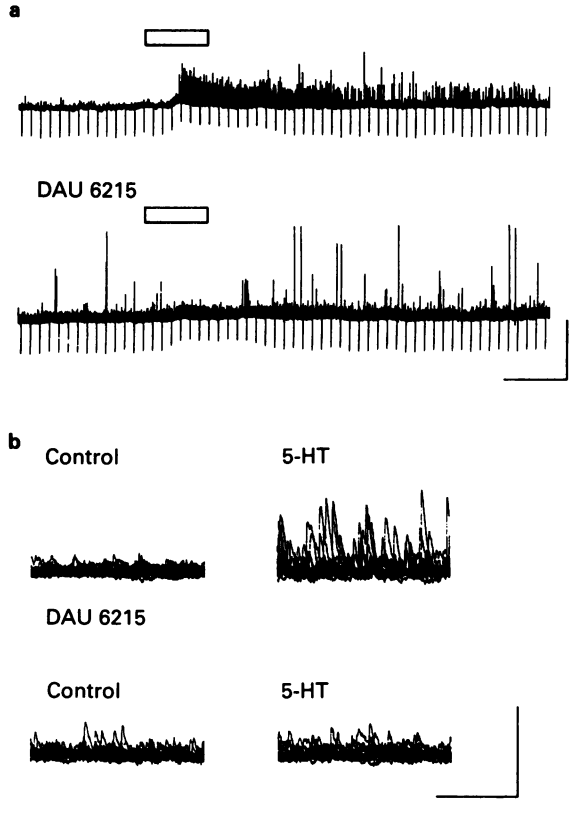

Figure 3 DAU 6215 antagonizes 5-hydroxytryptamine (5-HT) induced increase in the frequency of GABA-mediated spontaneous postsynaptic potentials (s.p.s.ps). (a) Voltage chart recording of a pyramidal neurone maintained at − 95 mV by injecting − 0.9 nA of current through the recording electrode filled with KCl. Upper trace: superfusion of 30 μM 5-HT (open bar) augmented the frequency and amplitude of s.p.s.ps, an effect that outlasted the application of the amine. Lower trace: DAU 6215 (300 nM) antagonized the effect of 5-HT. Downward deflections are electrotonic responses to constant current pulses (− 0.3 nA, 400 ms). Note the reduction of input resistance during 5-HT applications. Calibration bars: 20 mV, 3 min. (b) Voltage chart recording of the same neurone as in (a) plotted on a different time scale and voltage gain (sampling rate, 3.3 kHz). Each panel shows 14 superimposed sweeps taken in control conditions immediately before (upper left panel), and during 5-HT application (upper right panel). In the lower panels, s.p.s.ps were recorded in the presence of DAU 6215 alone (left) and during application of 30 μM 5-HT in the presence of the antagonist. Calibration bars: 10 mV, 300 ms.

190 R_{in} = 41.9 ± 5 MΩ and r.m.p. = − 67 ± 1.1 mV). In the presence of NAN-190, the hyperpolarizing response to 5-HT was greatly reduced (− 1.8 ± 1 mV versus − 5.3 ± 0.8 mV; $P<0.05$), as well as the percentage decrease in input resistance (7.3 ± 4.3% versus 24 ± 4%; $P<0.01$). In these cells, 30 μM 5-HT never elicited a depolarizing response. The small hyperpolarization still present in NAN-190 suggests an incomplete block of the 5-HT$_{1A}$ response that hindered the 5-HT$_4$-mediated depolarization. However, when a lower concentration (15 μM) of 5-HT was used, the 5-HT$_{1A}$ effect was completely antagonized and the 5-HT$_4$-mediated response was revealed (see below). The effects of 5-HT and DAU 6215 were also studied on the input/voltage relationship in four cells (r.m.p. = − 58 ± 1.8 mV; R_{in} = 45 ± 4.6 MΩ) bathed in 1 μM TTX to prevent cell firing at positive potentials. 5-HT (30 μM) induced a reduction of the slope of the *I/V* curve (Figure 1b). DAU 6215 (3 μM) *per se* did not affect the *I/V* curve and it did not modify the action of 5-HT on the slope resistance (Figure 1b).

DAU 6215 does not antagonize the 5-HT-induced depolarization and AHP amplitude decrease

We tested DAU 6215 on the slow depolarization and reduction of the AHP produced by 5-HT through a putative 5-HT$_4$ receptor subtype. In five pyramidal neurones (r.m.p. = − 54 ± 2 mV; R_{in} = 65 ± 4.8 mΩ), the AHP amplitude following a calcium spike was 13.1 ± 2 mV. In the presence of 15 μM 5-HT the reduction of the AHP amplitude, measured at the peak of the effect, was 78 ± 2.7%, accompanied in all cells by a depolarization (4.5 ± 1.1 mV; Figure 2a). The calcium spike amplitude did not significantly change during the treatment (62.7 ± 5.4 mV in control conditions and 60.5 ± 5.5 mV during 5-HT application). Fifteen to twenty min superfusion with 1 μM DAU 6215 did not affect the calcium spike amplitude, nor antagonize the effect of 5-HT on the membrane potential and AHP amplitude. In the

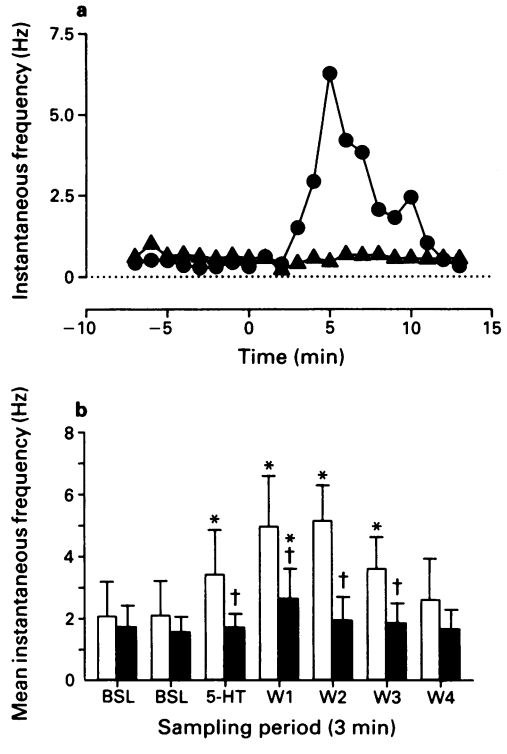

Figure 4 Analysis of the effects of DAU 6215 on 5-hydroxytrytamine (5-HT)-elicited spontaneous postsynaptic potentials (s.p.s.ps). (a) Effect of 5-HT (30 μM) on the instantaneous frequency of s.p.s.ps (e.g., see Figure 3) in the absence (●) or in the presence of 300 nM DAU 6215 (▲). 5-HT was bath-applied at time 0 for 3 min. Each point represents the average instantaneous frequency measured in 1 min recordings from a CA1 pyramidal cell maintained at − 98 mV by − 0.68 nA of steady current. (b) Effect of 5-HT in the absence (open columns) and in the presence of 300 nM DAU 6215, (solid columns). Each column is the mean ± s.e.mean of values from 5 pyramidal cells. Values were obtained measuring the average instantaneous frequency during 3 min recordings. Abbreviations: BSL, baseline; W1–W4, washout. *Values are statistically significant when compared to corresponding BSL values ($P<0.05$, Student's one-tailed paired *t* test): †Values are significantly different ($P<0.05$, multiple comparison ANOVA followed by Fisher LSD *post-hoc* test) from corresponding periods in the absence of DAU 6215.

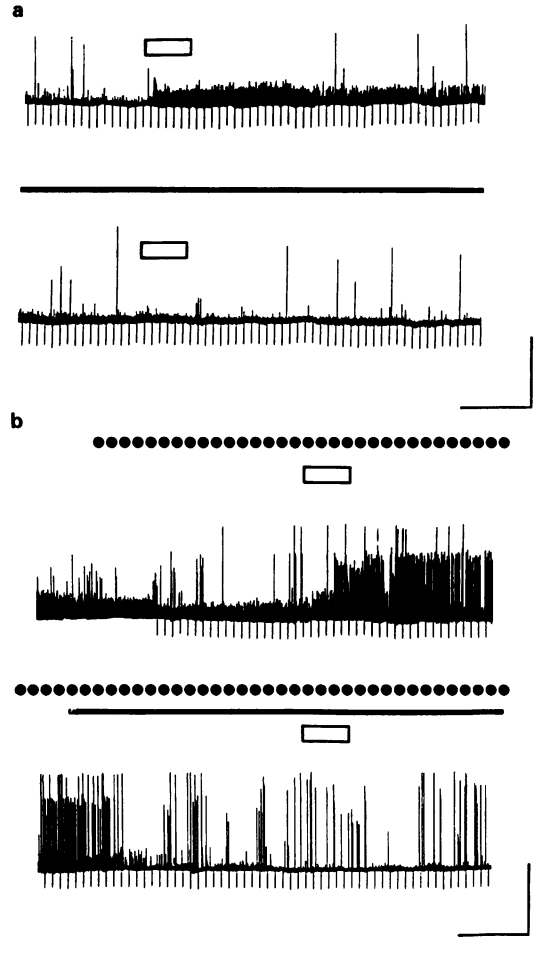

Figure 5 The 5-HT$_3$ selective agonist 2-methyl-5-hydroxytryptamine (2-Me-5-HT) mimics the effect of 5-HT on spontaneous postsynaptic potentials (s.p.s.ps) and its action is antagonized by DAU 6215. (a) Voltage chart recording of a pyramidal neurone held at − 92 mV by injecting − 0.84 nA of current through the recording electrode filled with KCl. Application of 50 μM 2-Me-5-HT (open bar, upper trace) produced an increase in the frequency of s.p.s.ps. This effect was abolished by 60 nM DAU 6215 (filled bar, lower trace). Downward deflections are electrotonic responses to current pulses (− 0.3 nA, 400 ms) to monitor input resistance. Note that 2-Me-5-HT did not change the input resistance, indicating the lack of 5-HT$_{1A}$ or 5-HT$_4$ mediated effects on cell conductance. (b) In a pyramidal cell held at − 93 mV membrane potential by injection of − 0.85 nA, the frequency of s.p.s.ps is only slightly decreased by application of NAN-190 (1 μM; upper trace, dotted line), which did not block the increase in s.p.s.ps elicted by 2-Me-5-HT (open bar). Note that the largest upward deflections are 30–35 mV, reversed i.p.s.ps that reached threshold for triggering action potentials (traces are clipped by chart record frequency response). In contrast, when DAU 6215 (300 nM, filled bar) was applied, still in the presence of NAN-190 (dotted line), a noticeable decrease in the frequency of s.p.s.ps occurred and the effect of 2-Me-5-HT was antagonized. Downward deflections represent electrotonic responses to constant current pulses. Calibration bars: 40 mV, 6 min for (a) and (b).

presence of DAU 6215, 5-HT elicited a 74 ± 2.7% reduction in the amplitude of the AHP and a 4.6 ± 1.5 mV depolarization, values not significantly different from those obtained in the presence of 5-HT alone (Figure 2b and c). Similar results were obtained with 30 μM 5-HT ($n = 2$; not shown).

DAU 6215 antagonizes the increase in frequency of spontaneous synaptic potentials elicited by 5-HT

Neurones impaled with 3 M KCl-filled electrodes and held at a negative potential by constant current injections exhibited depolarizing s.p.s.ps (Figure 3) that have been characterized as reversed $GABA_A$-mediated inhibitory postsynaptic potentials (Alger & Nicoll, 1980). As illustrated in Figure 3a, 5-HT (30 μM; $n = 17$) increased the frequency and amplitude of s.p.s.ps; the effect of 5-HT developed rapidly and outlasted the application of the drug by several minutes. The action of 5-HT did not decrease with time, since repeated applications to the same cell at intervals ranging between 15 and 60 min, produced comparable responses ($n = 6$; not shown). When the cells were maintained near the reversal potential for potassium (− 89 mV ± 1.7), the hyperpolarizing effect of 5-HT was not observed, and the only direct postsynaptic action of 5-HT on pyramidal neurones was a reduction in input resistance (Figure 3a). 5-HT increased the frequency of s.p.s.ps in the presence of 50 μM APV and 25 μM DNQX, compounds that at these concentrations block NMDA and non NMDA glutamate receptors ($n = 5$; not shown). Conversely, 5-HT had no effect in the presence of bicuculline (10 μM; $n = 3$) that abolished the reversed i.p.s.ps (not shown). These results are in agreement with previous observations indicating that these depolarizing events are GABA-mediated, reversed potentials (Ropert & Guy, 1991). Applications of DAU 6215 (300 nM) suppressed the 5-HT-mediated increase in spontaneous synaptic potentials in six out of nine cases (Figure 3). DAU 6215 required 20–30 min equilibration to exert its maximal effect, which was long-lasting since it persisted for over 1 h, after washing out the compound. For these reasons, recovery of the response to 5-HT was achieved only in 3 cases. The instantaneous frequency of the s.p.s.ps was analysed in five out of the six cells, chosen on the basis of a signal-to-noise ratio that allowed a reliable detection of synaptic events (see methods). In these preparations the instantaneous frequency of s.p.s.ps in control conditions varied from cell to cell (range 0.4–6.5 Hz) but was rather constant over time in individual cells, allowing good estimation of the effect of 5-HT on this parameter. Figure 4 illustrates the results of this analysis applied to responses in a pyramidal neurone. 5-HT elicited a 6 fold increase in instantaneous frequency of s.p.s.p. and this effect was antagonized by 300 nM DAU 6215. Figure 4b shows the means and the statistical significance of measures taken from the 5 similar experiments analysed.

As mentioned in the introduction, the 5-HT-induced increase in the frequency of s.p.s.ps presumably involved more than one 5-HT receptor subtype. In an attempt to isolate the 5-HT_3 component of the response to 5-HT, we applied 2-Me-5-HT, a selective 5-HT_3 agonist. Three-five min applications of 50 μM 2-Me-5-HT caused an increase in the frequency of synaptic events, in a manner comparable to the effect of 5-HT ($n = 4$, Figure 5). In all cases, DAU 6215 was effective in blocking the 2-Me-5-HT response at concentrations as low as 60 nM ($n = 3$, Figure 5a). The fact that in two cells DAU 6215 blocked the increase in instantaneous frequency of s.p.s.ps elicited by either 2-Me-5-HT (Figure 5b) or 5-HT in the presence of NAN-190 (not shown) confirms that in these cases the effect was not mediated by 5-HT_{1A} receptors. In two cases, 5-HT (30 μM) applied to neurones that had not responded to 2-Me-5-HT, elicited an increase in the frequency of spontaneous synaptic events. In these preparations,

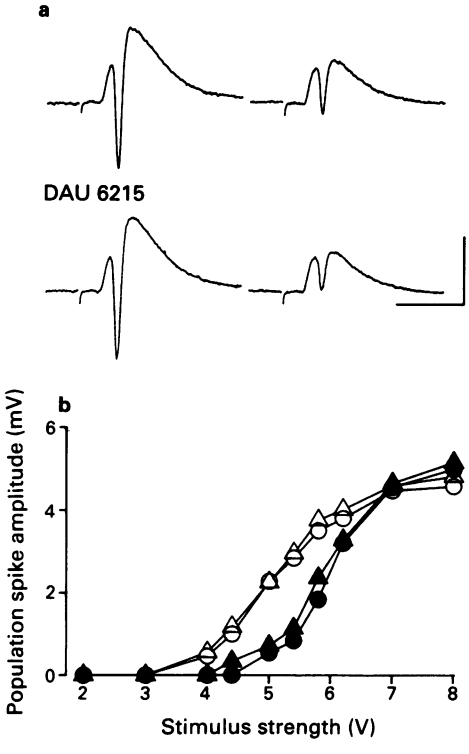

Figure 6 DAU 6215 does not modify the reduction of population spike amplitude induced by 5-hydroxytryptamine (5-HT). (a) Stimulation of the stratum radiatum evoked an excitatory postsynaptic potential and a population spike (upper left). Superfusion with 5-HT (30 μM; 15 min) decreased the amplitude of the population spike (upper right). DAU 6215 did not affect the evoked response (300 nM, 20 min; lower left), nor antagonize the action of 5-HT (lower right). Stimulus artifacts are partially blanked (first small downward deflection). Calibration bars: 2 mV, 10 ms. (b) Input/output curves were constructed in control conditions (○) by increasing the strength of the pulse delivered to the stratum radiatum. This was repeated starting from the fifth minute of application of 5-HT (30 μM; ●); after 20 min superfusion with DAU 6215 (1 μM, △); and at the fifth min of 5-HT application in the presence of DAU 6215 (▲).

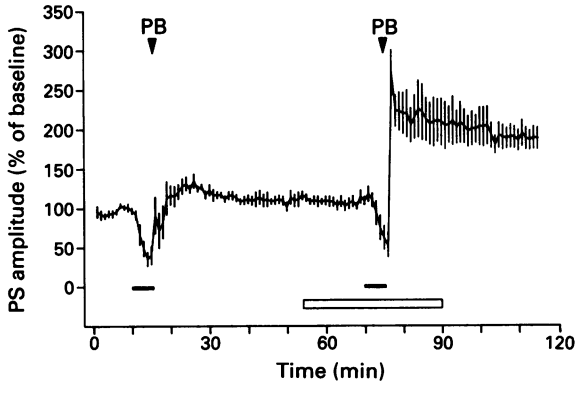

Figure 7 DAU 6215 antagonizes the 5-hydroxytryptamine (5-HT)-mediated block of long-term potentiation (LTP) produced by primed burst (PB) stimulation. The graph shows the mean amplitude (± s.e.mean; $n = 7$) of population spikes (PS) evoked by test pulses. For each experiment, the amplitude of the population spike was expressed as a percentage of the average of the population spike amplitudes obtained during a 10 min period before starting the experiment. Application of 5-HT (30 μM, filled bars) for 5 min decreased the amplitude of population spikes and blocked the induction of LTP by a PB, delivered at the fifth min of 5-HT application. When the PB was delivered at the fifth min of 5-HT application in the presence of DAU 6215 (60 nM, open bar), a long-lasting increase in the amplitude of the population spike was obtained.

300 nM DAU 6215 failed to antagonize the 5-HT-mediated response. In addition, in 4 experiments DAU 6215 (300 nM) failed to block the response elicited by 30 μM 5-HT in the presence of D-APV (50 μM), DNQX (25 μM) and 1 μM NAN-190 (not shown). These results suggest that in some preparations receptors other than the 5-HT$_3$ and 5-HT$_{1A}$ subtype participated in the 5-HT-mediated response.

DAU 6215 antagonizes the 5-HT-mediated block of LTP

In the following experiments we tested the effects of DAU 6215 on synaptic hippocampal potentials and LTP and its antagonistic action on the inhibitory effects that 5-HT exerts on the same parameters.

Micromolar concentrations of 5-HT reduced the amplitude of the population spike evoked by low frequency stimulation of the Schaffer's collaterals (Figure 6), a response apparently due to the activation of 5-HT$_{1A}$ receptors (Beck *et al.*, 1985; Corradetti *et al.*, 1992a). As reported previously (Segal, 1980; Corradetti *et al.*, 1992a), the effect of 5-HT decreased at higher intensities of stimulation (Figure 6b). Applications of DAU 6215 at concentration up to 1 μM, (about 250 times its K_i had, *per se*, no effect on the amplitude of the population spike evoked with different stimulus intensities, and the inhibitory action of 5-HT on the amplitude of the population spike was not antagonized by any of the concentrations of DAU 6215 tested (Figure 6b; Table 1). We than investigated the effect of DAU 6215 on the inhibition exerted by 5-HT on the LTP induced by PB stimulation (see methods). A PB stimulation delivered to the stratum radiatum evoked an LTP that was prevented by the application of 30 μM 5-HT (Figure 7). When the PB stimulation was repeated in the presence of both 30 μM 5-HT and DAU 6215 (60 nM; $n = 7$), a long-lasting increase in the amplitude of the evoked response was observed (Figure 7).

Discussion

The results of our investigation demonstrate that DAU 6215 exerts a powerful antagonism of the presumed 5-HT$_3$-mediated effects of 5-HT on synaptic activity in the hippocampal CA1 region. Our data indicate that DAU 6215 antagonizes the effect of 5-HT on GABA-mediated spontaneous potentials and on the induction of LTP, through the selective blockade of 5-HT$_3$ receptors. The biochemical evidence that DAU 6215 binds to 5-HT$_3$ receptor subtypes in the CNS (Turconi *et al.*, 1990), was confirmed by several of our results. Our intracellular recordings from pyramidal neurones showed that DAU 6215 does not exert any direct action on cell membrane properties; concentrations of DAU 6215 up to 3 μM did not change the membrane potential of pyramidal neurones, nor the *I/V* relationship. Consistently, extracellular recordings of evoked responses did not show any modification of the synaptic response.

Two receptor subtypes, 5-HT$_{1A}$ and 5-HT$_4$ mediate direct effects of 5-HT on pyramidal neurones (Beck *et al.*, 1985; 1993; Chaput *et al.*, 1990; Andrade & Chaput, 1991). DAU 6215 did not antagonize the 5-HT$_{1A}$-mediated hyperpolarization and shift of the *I/V* curve slope. On the other hand, NAN-190 that itself did not elicit any response, almost completely blocked the 5-HT changes in resting membrane potential and input resistance. Although NAN-190 may act as a partial agonist in the raphe, our results demonstrate that this compound exerts an effective antagonism of 5-HT$_{1A}$-mediated responses of hippocampal pyramidal cells. The different behaviour of the compound in these tissues may reside in the absence of a 5-HT$_{1A}$ receptor reserve in the hippocampus, as suggested by Fletcher *et al.* (1993).

The absence of any antagonism by DAU 6215 at the 5-HT$_{1A}$ receptor was confirmed by the results obtained with extracellular recordings. The use of selective agonists and antagonists (Beck *et al.*, 1985) demonstrated that the inhibitory effect of 5-HT on evoked potentials is mediated by 5-HT$_{1A}$ receptors. DAU 6215 applied at concentrations as high as 1 μM, did not modify the inhibitory effect of 5-HT on evoked synaptic potentials.

It has been reported that DAU 6215 behaves as a weak partial agonist at the 5-HT$_4$ receptor of colliculi neurones (Dumuis *et al.*, 1991; Baxter *et al.*, 1992), although the affinity of DAU 6215 for the 5-HT$_3$ receptor is in the nM range (Turconi *et al.*, 1991a) and that for the 5-HT$_4$ receptor is in the μM range (Dumuis *et al.*, 1991). Our results, though, did not reveal any agonist or antagonist effect of DAU 6215 on 5-HT$_4$-mediated responses in CA1 pyramidal neurones.

Although 5-HT$_3$ receptors do not appear to mediate any direct action of 5-HT on pyramidal neurones, there is increasing evidence indicating that GABAergic interneurones may express 5-HT$_3$ receptors. Binding studies demonstrated the presence of 5-HT$_3$ receptors in the hippocampus (Kilpatrick *et al.*, 1987) and anatomical observations showed that 5-hydroxytryptaminergic projections from raphe nuclei impinge on hippocampal GABAergic interneurones (Kosofsky & Molliver, 1987; Hornung & Celio, 1992). Electrophysiological studies in hippocampal primary cultures showed the activation of a 5-HT$_3$ receptor-mediated current in a subset of neurones (Yakel & Jackson, 1988; Yakel *et al.*, 1988). Although the experiments were directed at studying pyramidal cells, it is possible that these were interneurones. Recently, Ropert & Guy (1991) demonstrated that 5-HT increases both frequency and amplitude of spontaneous GABA-mediated synaptic activity in the CA1 region. This action can be mimicked by the selective 5-HT$_3$ agonist 2-Me-5-HT and blocked by 5-HT$_3$ antagonists such as ICS 205-930 at nanomolar concentrations. The inhibitory potentials, that, when recorded with KCl-loaded electrodes in cells maintained at negative potentials appear as depolarizing events (Alger & Nicoll, 1980), are suppressed by bicuculline and persist when NMDA and non-NMDA receptors are blocked by selective antagonists (Ropert & Guy, 1991 and present results). Our results confirm that 5-HT increases the frequency and amplitude of s.p.s.ps. Although only the increase in frequency was quantified, a qualitative analysis of the responses showed that 5-HT augmented the amplitude of spontaneous events, as well. DAU 6215 blocked the 5-HT-mediated increase in synaptic activity at concentrations within the nM range. It was suggested that the activation of receptor subtypes other than 5-HT$_3$ may participate in this response (e.g., 5-HT$_{1A}$; Van den Hooff & Galvan, 1991). Our experiments conducted in the presence of a 5-HT$_{1A}$ antagonist (NAN-190) or using the selective agonist 2-Me-5-HT, also indicate that other components may be involved in the 5-HT-induced increase in s.p.s.p. frequency. In those cases in which the 5-HT$_3$ component was predominant (approximately 70%), DAU significantly antagonized the increase in synaptic activity produced by either 5-HT or 2-Me-5-HT. The participation of receptors other than 5-HT$_3$ would explain why in a few circumstances 2-Me-5-HT did not exert any effect, whereas 5-HT augmented the synaptic activity, a response not blocked by DAU 6215. Also, in a few cases DAU 6215 failed to block the response elicited by 5-HT in the presence of NAN-190, DNQX and D-APV, suggesting that other, still unidentified 5-HT receptor subtype(s) may be involved. Due to the intrinsic limitations of the protocol used, we were unable to construct a concentration-effect relationship for DAU 6215; however, the fact that antagonism of the 2-Me-5-HT induced response was obtained with concentrations as low as 60 nM indicates that DAU 6215 exerts its action within the range of concentrations consistent with its selective antagonism of 5-HT$_3$ receptors. Our results, therefore, confirm the presence of a 5-HT$_3$ component in the 5-HT induced increase in the frequency of inhibitory s.p.s.ps, and demonstrate that DAU 6215, at nM concentrations, significantly affects the modulatory action of 5-HT on the hippocampal synaptic activity, by blocking 5-

HT_3 receptors presumably located on GABAergic interneurones.

Our extracellular recordings show that DAU 6215 is able to antagonize the inhibitory effect of 5-HT on the induction of LTP produced by PB stimulation. In a previous study (Corradetti *et al.*, 1992a), we have demonstrated that the inhibition of PB-induced LTP can be achieved by the blockade of either 5-HT_{1A} or 5-HT_3 receptors, because the activation of both receptor subtypes seems to be necessary for the action of 5-HT. Since DAU 6215 is devoid of 5-HT_{1A} antagonistic effects at nM concentrations, the action of DAU 6215 in this experimental protocol appears to be mediated by antagonism at the 5-HT_3 receptor. Indeed, the effect of DAU 6215 was comparable to that obtained in the presence of other selective 5-HT_3 antagonists such as ICS 205-930 and ondansetron (Corradetti *et al.*, 1992a).

The hippocampal region is physiologically involved in emotional and cognitive functions, therefore the effects of DAU 6215 on the synaptic activity of this structure may be relevant for its pharmacological actions *in vivo*. In particular, DAU 6215 has been shown to act as an anxiolytic in animal models (Borsini *et al.*, 1993), and, like other 5-HT_3 antagonists (Barnes *et al.*, 1990; Chugh *et al.*, 1991; Domeney *et al.*, 1991; Carey *et al.*, 1992), it exerts a cognition enhancing effect (Brambilla *et al.*, 1993; Pitsikas *et al.*, 1993; 1994). The results of our investigation showing the antagonism of the 5-HT-mediated inhibition of LTP, a phenomenon of synaptic plasticity possibly involved in learning (Teyler & DiScenna 1987), may provide a cellular correlate for the pharmacological effects of DAU 6215 on cognition.

We thank Dr G. Pepeu and Dr F. Borsini for their comments on the manuscript. This work was supported by grants from CNR (92. 02556. CT04; 93. 04345. CT04) and from M.U.R.S.T. (60%; 1991, 1992).

References

ALGER, B.E. & NICOLL, R.A. (1980). Spontaneous inhibitory postsynpatic potentials in hippocampus: mechanism for tonic inhibition. *Brain Res.*, **200**, 195–200.

ANDRADE, R. & CHAPUT, Y. (1991). 5-hydroxytryptamine$_4$-like receptors mediate the slow excitatory response to serotonin in the rat hippocampus. *J. Pharmacol. Exp. Ther.*, **257**, 930–937.

ANDRADE, R., MALENKA, R.C. & NICOLL, R.A. (1986). A G protein couples serotonin and $GABA_B$ receptors to the same channel in hippocampus. *Science*, **234**, 1261–1265.

ANDRADE, R. & NICOLL, R.A. (1987). Pharmacological distinct actions of serotonin on single pyramidal neurons of the rat hippocampus recorded *in vitro*. *J. Physiol.*, **394**, 99–124.

ANWYL, R. (1990). Neurophysiological actions of 5-hydroxytryptamine in the vertebrate nervous system. *Prog. Neurobiol.*, **35**, 451–468.

BARNES, J.M., COSTALL, B., COUGHLAN, J., DOMENEY, A.M., GERRARD, P.A., KELLY, M.E., NAYLOR, R.J., ONAIVI, E.S., TOMKINS, D.M. & TYERS, M.B. (1990). The effects of ondansetron, a 5-HT_3 receptor antagonist on cognition in rodents and primates. *Pharmacol. Biochem. Behav.*, **35**, 955–962.

BAXTER, G.S. & CLARKE, D.E. (1992). Benzimidazolone derivatives act as 5-HT_4 receptor ligands in rat oesophagus. *Eur. J. Pharmacol.*, **212**, 225–229.

BECK, S.G., CHOI, K.C. & LIST, T.J. (1993). Comparison of 5-hydroxytryptamine$_{1A}$-mediated hyperpolarization in CA1 and CA3 hippocampal pyramidal cells. *J. Pharmacol. Exp. Ther.*, **263**, 350–359.

BECK, S.G., CLARKE, W.P. & GOLDFARB, J. (1985). Spiperone differentiates multiple 5-hydroxytryptamine responses in rat hippocampal slices in vitro. *Eur. J. Pharmacol.*, **116**, 195–197.

BORSINI, F., BRAMBILLA, A., CESANA, R. & DONETTI, A. (1993). The effect of DAU 6215, a novel 5HT-3 antagonist, in animal models of anxiety. *Pharmacol. Res.*, **27**, 151–164.

BRAMBILLA, A., GHIORZI, A., PITSIKAS, N. & BORSINI, F. (1993). DAU 6215, a novel 5-HT_3 receptor antagonist, selectively antagonizes scopolamine-induced deficit in a passive avoidance task, but not scopolamine-induced hypermotility in rats. *J. Pharm. Pharmacol.*, **45**, 841–843.

CAREY, G.J., COSTALL, B., DOMENEY, A.M., GERRARD, P.A., JONES, D.N.C., NAYLOR, R.J. & TYERS, M.B. (1992). Ondansetron and arecoline prevent scopolamine-induced cognitive deficits in the marmoset. *Pharmacol. Biochem. Behav.*, **42**, 75–83.

CHAPUT, Y., ARANEDA, R.C. & ANDRADE, R. (1990). Pharmacological and functional analysis of a novel serotonin receptor in the rat hippocampus. *Eur. J. Pharmacol.*, **182**, 441–456.

CHUGH, Y., SAHA, N., SANKARANARAYANAN, A. & SHARMA, P.L. (1991). Memory enhancing effects of granisetron (BRL 43694) in a passive avoidance task. *Eur. J. Pharmacol.*, **203**, 121–123.

COLINO, A. & HALLIWELL, J.V. (1987). Differential modulation of three separate K-conductances in hippocampal CA1 neurons by serotonin. *Nature*, **328**, 73–77.

CORRADETTI, R., BALLERINI, L., PUGLIESE, A.M. & PEPEU, G. (1992a). Serotonin blocks the long-term potentiation induced by primed burst stimulation in the CA1 region of the rat hippocampal slices. *Neurosci.*, **46**, 511–518.

CORRADETTI, R., PUGLIESE, A.M., BALLERINI, L. & PEPEU, G. (1992b). Primed-burst induced long-term potentiation: a more flexible model to study cognition enhancing activity of drugs? *Pharmacol. Res.*, **26**, 214.

DOMENEY, A.M., COSTALL, B., GERRARD, P.A., JONES, D.N.C., NAYLOR, R.J. & TYERS, M.B. (1991). The effects of ondansetron on cognitive performance in the marmoset. *Pharmacol. Biochem. Behav.*, **38**, 169–175.

DUMUIS, A., SEBBEN, M., MONFERINI, E., NICHOLA, M., TURCONI, M., LADINSKY, H. & BOCKAERT, J. (1991). Azabicycloalkyl benzimidazolone derivatives as a novel class of potent agonists at the 5-HT_4 receptor positively coupled to adenylate cyclase in brain. *Naunyn-Schmied. Arch. Pharmacol.*, **343**, 245–251.

FLETCHER, A., CLIFFE, I.A. & DOURISH, C.T. (1993). Silent 5-HT_{1A} receptor antagonists: utility as research tools and therapeutic agents. *Trends Pharmacol. Sci.*, **14**, 441–448.

GLENNON, R.A., NAIMAN, N.A., LYON, R.A. & TITELER, M. (1988a). Azylpiperazine derivatives as high-affinity 5-HT_{1A} serotonin ligands. *J. Med. Chem.*, **31**, 1968–1971.

GLENNON, R.A., NAIMAN, N.A., PIERSON, M.E., TITELER, M., LYON, R.A. & WEIBERGE, E. (1988b). NAN-190: an azylpiperazine analog that antagonizes the stimulus effects of the 5-HT_{1A} agonist 8-hydroxy-2-(di-n-propylamino)tetraline (8-OH-DPAT). *Eur. J. Pharmacol.*, **154**, 339–341.

HORNUNG, J.P. & CELIO, M.R. (1992). The selective innervation by serotonergic axons of calbindin-containing interneurons in the neocortex and hippocampus of the marmoset. *J. Comp. Neurol.*, **320**, 457–467.

JAHNSEN, H. (1980). The action of 5-hydroxytryptamine on neuronal membranes and synpatic transmission in the area CA1 of the hippocampus *in vitro*. *Brain Res.*, **197**, 83–94.

KILPATRICK, G.I., JONES, B.J. & TYERS, M.B. (1987). Identification and distribution of 5-HT_3 receptors in rat brain using radioligand binding. *Nature*, **330**, 746–748.

KÖHLER, C. (1984). The distribution of serotonin binding sites in the hippocampal region of the rat brain. An autoradiographic study. *Neurosci.*, **13**, 667–680.

KOSOFSKY, B.E. & MOLLIVER, M.E. (1987). The serotoninergic innervation of cerebral cortex: different classes of axon terminals arise from dorsal and median raphe nuclei. *Synapse*, **1**, 153–168.

MADISON, D.V. & NICOLL, R.A. (1986). Action of noradrenaline recorded intracellularly in rat hippocampal CA1 pyramidal neurons, *in vitro*. *J. Physiol.*, **372**, 221–244.

PITSIKAS, N., BRAMBILLA, A. & BORSINI, F. (1993). DAU 6215, a novel 5-HT_3 receptor antagonist, improves performance in the aged rat in the Morris water maze task. *Neurobiol. Aging*, **14**, 561–564.

PITSIKAS, N., BRAMBILLA, A. & BORSINI, F. (1994). Effect of DAU 6215, a novel 5-HT_3 receptor antagonist, on scopolamine-induced amnesia in the rat in a spatial learning task. *Pharmacol. Biochem. Behav.*, **47**, 95–99.

PRISCO, S., PESSIA, M., CECI, A., BORSINI, F. & ESPOSITO, E. (1992). Chronic treatment with DAU 6215, a new 5-HT$_3$ receptor antagonist, causes a selective decrease in the number of spontaneously active dopaminergic neurons, in the rat tegmental area. *Eur. J. Pharmacol.*, **214,** 13–19.

ROPERT, N. (1988). Inhibitory action of serotonin in the CA1 hippocampal neurons *in vitro*. *Neurosci.*, **26,** 69–81.

ROPERT, N. & GUY, N. (1991). Serotonin facilitates GABAergic transmission in the CA1 region of rat hippocampus *in vitro*. *J. Physiol.*, **441,** 121–136.

SAGRADA, A., NICOLA, M., MICHELETTI, R. & TEMPLETON, D. (1990). Antiemetic activity of DAU 6215 against vomiting induced by different chemotherapeutic drugs. *The Second IUPHAR Satell. Meet. Serotonin*, Basel, Abst 154.

SAGRADA, A., TURCONI, M., BONALI, P., SCHIANTARELLI, P., MICHELETTI, R., MONTAGNA, E., NICOLA, M., ALGATE, D.R., RIMOLDI, E.M. & DONETTI, A. (1991). Antiemetic activity of the new 5-HT$_3$ antagonist DAU 6215 in different animal models of cancer chemotherapy and irradiation. *Cancer Chemother. Pharmacol.*, **28,** 470–474.

SCHWARTZKROIN, P.A. & SLAWSKY, M. (1977). Probable calcium spikes in hippocampal neurons. *Brain Res.*, **135,** 157–161.

SEGAL, M. (1975). Physiological and pharmacological evidence for a serotonergic projection to the hippocampus. *Brain Res.*, **94,** 115–131.

SEGAL, M. (1976). 5-HT antagonists in the hippocampus. *Brain Res.*, **103,** 161–166.

SEGAL, M. (1980). The action of serotonin in the rat hippocampal slice preparation. *J. Physiol.*, **303,** 423–439.

SWANSON, L.W., KÖHLER, C. & BJÖRKLUND, A. (1987). The limbic region. I: the septohippocampal system. In *Handbook of Chemical Neuroanatomy*. ed. Björklund, A., Hökfelt, T. & Swanson, L.W. pp. 125–227. Amsterdam: Elsevier.

TEYLER, T.J. & DISCENNA, P. (1987). Long-term potentiation. *Annu. Rev. Neurosci.*, **10,** 131–161.

TURCONI, M., DONETTI, A., SCHIAVONI, A., SAGRADA, A., MONTAGNA, E., NICOLA, M., CESANA, R., RIZZI, C. & MICHELETTI, R. (1991a). Pharmacological properties of a novel class of 5-HT$_3$ receptor antagonists. *Eur. J. Pharmacol.*, **203,** 203–211.

TURCONI, M., NICOLA, M., QUINTERO, M.G., MAIOCCHI, L., MICHELETTI, R., GIRALDO, E. & DONETTI, A. (1990). Synthesis of a new class of 2,3-dihydro-2oxo-1H-benzimidazole-1-carboxyl acid derivatives as highly potent 5-HT$_3$ receptor antagonists. *J. Med. Chem.*, **33,** 2101–2108.

TURCONI, M., SCHIANTARELLI, P., BORSINI, F., RIZZI, C.A., LADINSKY, H. & DONETTI, A. (1991b). Azabicycloalkyl benzimidazolones: interactions with serotonergic 5-HT$_3$ and 5-HT$_4$ receptors and potential therapeutic implications. *Drugs of the Future*, **16,** 1011–1026.

VAN DEN HOOFF, P. & GALVAN, M. (1991). Electrophysiology of the 5-HT$_{1A}$ ligand MDL 73005EF in the rat hippocampal slice. *Eur. J. Pharmacol.*, **196,** 291–298.

YAKEL, J.L. & JACKSON, M.B. (1988). 5-HT$_3$ receptors mediate rapid responses in cultured hippocampus and a clonal cell line. *Neuron*, **1,** 615–621.

YAKEL, J.L., TRUSSELL, L.O. & JACKSON, M.B. (1988). Three serotonin responses in cultured mouse hippocampal and striatal neurons. *J. Neurosci.*, **8,** 1273–1285.

(Received November 18, 1993
Revised February 18, 1994
Accepted March 7, 1994)

Br. J. Pharmacol. (1994), **112**, 704–708

Evidence for a differential location of vasoconstrictor endothelin receptors in the vasculature

[1]Suzanne Moreland, Diane McMullen, Benoni Abboa-Offei & Andrea Seymour

Department of Pharmacology, Bristol-Myers Squibb Pharmaceutical Research Institute, P.O. Box 4000, Princeton, New Jersey 08543, U.S.A.

1 There are at least two subtypes of vascular endothelin (ET) receptors. Stimulation of the ET_A receptors on vascular smooth muscle cells leads to vasoconstriction, whereas activation of the ET_B receptors on endothelial cells elicits vasodilatation. Several reports in the literature have suggested the presence of a vasoconstrictor non-ET_A receptor on vascular smooth muscle which has pharmacological similarities to the ET_B receptor. The present study was undertaken to determine the location of this ET_B-like receptor within the vascular system.

2 Fourteen vascular smooth muscle preparations from six species were used to determine the effect of the ET_A receptor antagonist, BQ-123, on concentration-response curves elicited by ET-1 and the ability of the ET_B receptor agonist, sarafotoxin S6c, to cause contraction. The vessels fell into two categories. One group was sensitive to BQ-123 and insensitive to sarafotoxin S6c and, thus, probably contained ET_A receptors. The other group, with vasoconstrictor ET_B-like receptors, was insensitive to BQ-123 and sensitive to sarafotoxin S6c.

3 Vessels from cynomolgus monkeys, when studied *in vitro*, appeared to contain primarily ET_A receptors, although the potency of BQ-123 was quite variable, suggesting the possibility of ET_A receptor subtypes. In contrast, both ET-1 and sarafotoxin S6c, given as intravenous injections in conscious monkeys, produced transient, equipotent, and dose-related increases in blood pressure. The highest dose of sarafotoxin S6c (1 nmol kg^{-1}, i.v.) also caused a marked secondary depressor response (-80 ± 6 mmHg) that lasted approximately 10 min. The pressor responses suggest that the vasoconstrictor ET_B-like receptors are present in cynomolgus monkeys.

4 The data suggest the presence of two distinct vasoconstrictor ET receptor subtypes on smooth muscle cells. The ET_A receptors are primarily located on the high pressure side of the circulation. The vasoconstrictor ET_B-like receptors appear to be concentrated on the low pressure side.

Keywords: Vascular smooth muscle; endothelin; blood pressure; ET receptors

Introduction

Three isoforms of the endothelin (ET) receptor have been cloned. ET_A receptors preferentially bind ET-1 over ET-3 (Arai *et al.*, 1990) and are present on vascular smooth muscle cells (Lin *et al.*, 1991) where their stimulation leads to vasoconstriction. The ET_B receptors are non-selective for ET-1 and ET-3 (Sakurai *et al.*, 1990) and are located on endothelial cells where their stimulation leads to vasodilatation (Saeki *et al.*, 1991; Takayanagi *et al.*, 1991). The ET_C receptor binds ET-3 with a higher affinity than ET-1 and was recently cloned from *Xenopus* melanophores (Karne *et al.*, 1993). It remains to be established whether this amphibian ET_C receptor has a mammalian counterpart.

Although it is well accepted that ET_A receptors mediate contraction in vascular smooth muscle, recent data have suggested that activation of a non-ET_A receptor subtype constricts some vascular and non-vascular smooth muscles. Both Williams *et al.* (1991) and Clozel *et al.* (1992) reported that administration of the selective ET_B receptor agonist, sarafotoxin S6c, to pithed rats elicited a pressor response. We (Moreland *et al.*, 1992b) and others (Sumner *et al.*, 1992; Panek *et al.*, 1992) have shown that ET_B-selective agonists contract certain isolated smooth muscle preparations and that ET_A-selective antagonists have little or no effect in those tissues. These data support the hypothesis that an ET_B-like receptor subtype is present on vascular smooth muscle obtained from certain locations in the vasculature and that stimulation of this receptor leads to contraction. The present study was undertaken to map the location of vasoconstrictor ET receptors in the vasculature from a variety of species.

[1] Author for correspondence.

Methods

In vitro *studies*

Tissues were prepared by a modification of techniques described previously (Moreland *et al.*, 1992b). Hog carotid arteries were obtained at slaughter from Hatfield Packing Company. Male Sprague-Dawley rats (250–300 g), New Zealand white rabbits (2–3 kg), and mongrel dogs (12–16 kg) were used in these studies. Male and female cynomolgus monkeys (2.5–4 kg) were purchased from Charles River and Hazelton. Before the surgical removal of the necessary tissues, the rats were killed with CO_2 and the rabbits were anaesthetized with sodium methohexitone. Dogs were anaesthetized with sodium pentobarbitone, treated with heparin, then intubated and ventilated. Monkeys were sedated with ketamine (10 mg kg^{-1}, i.m.), then a peripheral venous catheter was placed in the forearm and an overdose of Nembutal was administered. All tissues were exposed gently, then removed and quickly placed in ice-cold MOPS-buffered physiological salt solution (PSS) where they were cleaned of connective tissue.

Dog left anterior descending coronary arteries, dog saphenous veins, monkey iliac arteries, monkey jugular veins, monkey saphenous veins, rat aortae, rabbit carotid arteries, rabbit renal arteries, and rabbit saphenous veins were cut into rings 3–4 mm wide. The endothelium was removed by gently rubbing the intimal surface. Two stainless steel self-closure wires (0.001–0.003 inch diameter) were inserted through each ring. Rat portal veins, approximately 1 cm in length, were mounted intact. Rabbit pulmonary arteries and monkey vena cavae were prepared as circumferential strips with the endothelium removed as described above. Hog carotid thin medial strips were prepared by removing the

intima and adventitia (Moreland *et al.*, 1992a), then cut into 1.5–2.5 mm widths.

All preparations were mounted for isometric force recording between two gold clips. One clip was connected to a micrometer for control of tissue length, the other to a Grass FT 03 force transducer and Grass model 7D polygraph. The mounted preparations were placed in individual water-jacketed muscle chambers in bicarbonate-buffered PSS at 37°C, aerated with 5% CO_2 in O_2. During an equilibration period of at least 1 h, the tissues were brought to the following preloads (in g): dog coronary artery (10), dog saphenous vein (2), monkey iliac artery (5), monkey jugular vein (2), monkey saphenous vein (1.5), monkey vena cava (1), rabbit carotid artery (4), rabbit pulmonary artery (1), rabbit renal artery (1), rabbit saphenous vein (0.5), rat aorta (2), and rat portal vein (2). The hog carotid artery was adjusted to L_o, the optimal length for active contraction. Next the effectiveness of the endothelium removal was determined by confirming the absence of the characteristic relaxation of a phenylephrine (10 μM)-induced contraction by acetylcholine (10 μM). If any relaxation occurred, the preparation was re-rubbed to complete the removal. No attempts were made to remove the endothelium from the human saphenous veins or rat aortae.

Bicarbonate-buffered PSS contained, in mM: NaCl 118.4, KCl 4.7, KH_2PO_4 1.2, $MgSO_4$ 1.2, $CaCl_2$ 1.9, $NaHCO_3$ 25 and D-glucose 10.1. The pH was maintained at 7.4 by aeration with 5% CO_2 in O_2. MOPs-buffered PSS contained, in mM: NaCl 140, KCl 4.7, $NaHPO_4$ 1.2, $MgSO_4$ 1.2, $CaCl_2$ 1.6, 2 MOPS (3-[N-morpholino]propane sulphonic acid), Na_2EDTA 0.2 (ethylenediamine tetraacetic acid), and D-glucose 5.6. The pH was adjusted to 7.4 with 5 N NaOH.

In all tissues except rat portal veins, cumulative concentration-response curves were obtained for ET-1 in the absence and presence of the ET_A receptor antagonists BQ-123 (cyclo(D-tryptophyl-D-aspartyl-L-prolyl-D-valyl-L-leucine); Ihara *et al.*, 1992) or FR139317 ((**R**)2-[(**R**)-2-[(**S**)-2-[[1-hexahydro-1H-azepinyl)]carbonyl]amino-4-methyl pentanoyl] amino-3-[3-(1-methyl-1H-indoyl)]propionyl]amino-3-(2-pyridyl) propionic acid; Sogabe *et al.*, 1993). A 20 min incubation time was allowed with the antagonists before exposure of the tissue to the first concentration of ET-1. Three to five concentrations of ET_A antagonist were tested. Concentrations were chosen in half-log increments between 0.3 and 100 μM BQ-123 and between 1 and 100 μM FR139317. The antagonists were also tested for their ability to block spontaneous contractions in rat portal veins. A separate group of tissues was exposed to sarafotoxin S6c (100 nM) and, if force developed, full concentration-response curves were obtained and EC_{50} values determined.

Data are shown as mean ± s.e. Agonist potency is expressed as an EC_{50} value, the concentration of agonist producing half-maximal force, which was calculated by linear regression analysis for each tissue. Antagonist activity (apparent K_B) was calculated with multiple concentrations of antagonist from the following equation: apparent $K_B = B/[(A'/A)-1]$, where B is the concentration of antagonist, A′ is the EC_{50} value for the agonist in the presence of antagonist, and A is the EC_{50} value of the agonist alone. $n = 3-6$ tissues from separate animals for each concentration of antagonist.

In vivo *studies*

Male and female cynomolgus monkeys were selected at random from a colony of trained animals implanted with chronic catheters in the abdominal aorta and vena cava as described by Scalese *et al.* (1990). The routine care and maintenance of our primate colony was described in a previous publication (Scalese *et al.*, 1990) and is in accordance with the principles of humane animal care and use established by the American Association for the Accreditation of Laboratory Animal Care. On the morning of an experiment, the conscious monkeys were seated in restraining chairs and the arterial catheters were connected via Gould-Statham strain gauge transducers to a Beckman recorder for measurement of mean arterial blood pressure. The monkeys were left undisturbed for at least 30 min in order to establish the baseline mean arterial pressure.

ET-1 and sarafotoxin S6c were dissolved in saline so that each dose was administered in a volume of 1 ml kg^{-1}. The blood pressure responses to increasing doses of 0.03, 0.1, 0.3 nmol kg^{-1} i.v. of ET-1 and 0.03, 0.1, 0.3 and 1 nmol kg^{-1} i.v. of sarafotoxin S6c were determined in two groups of monkeys ($n = 4$/peptide). Enough time was allowed between doses to permit blood pressure to return to baseline values before a higher dose was delivered. The maximal pressor and depressor responses were measured after each dose of sarafotoxin S6c to generate dose-response curves. In addition, the time course of the blood pressure changes produced by 1 nmol kg^{-1} i.v. of sarafotoxin S6c was determined.

Results

In vitro *studies*

ET-1 contracted all the isolated smooth muscles examined in a concentration-dependent fashion. The EC_{50} values ranged from 0.32 nM in the monkey vena cava to 3.3 nM in the rabbit saphenous vein (Table 1). Concentrations of the ET_B agonist, sarafotoxin S6c, as high as 100 nM were unable to elicit contraction in any of the preparations from the high pressure side of the circulation, with the exception of one monkey iliac artery. However, sarafotoxin S6c did produce contractions in several of the isolated smooth muscles on the low pressure side. This finding suggests that the vasoconstrictor ET_B-like receptor is localized primarily on the venous side of the circulation. The EC_{50} values for sarafotoxin S6c ranged from 0.4 nM in the dog saphenous vein to 2.1 nM in the rabbit saphenous vein.

The selective ET_A receptor antagonists were tested for their ability to depress contractions in the isolated smooth muscle preparations elicited by ET-1 (Figure 1). Generally, the ET_A receptor antagonists were effective in tissues that did not contract in response to sarafotoxin S6c and ineffective in those that did (Table 1). The potency (apparent K_B) of BQ-123 ranged from 35 nM in the rabbit carotid artery to 2.4 μM in the dog saphenous vein. The potency of FR139317 was similar to that of BQ-123 in the tissues in which it was studied. With the exception of the dog saphenous vein, tissues which responded to sarafotoxin S6c were unaffected by the ET_A receptor antagonists. The peak force of the sarafotoxin S6c contractions in the dog saphenous vein was a small percentage (<10%) of the force elicited by ET-1 (Table 1). Likewise, a minor component of ET-1-induced force was unaffected by the ET_A receptor antagonists. These data suggest that there is a mixed population of ET_A and ET_B-like receptors in the dog saphenous vein.

The effect of BQ-123 on spontaneous activity in the rat portal vein was also examined. At concentrations as high as 10 μM, BQ-123 had no effect on the peak force or rate of spontaneous contractions suggesting that the ET_A receptor is not an important mediator of spontaneous contractions in the rat portal vein.

The vessels isolated from the cynomolgus monkeys did not fit the simple pattern of effects observed in the dog, hog, rabbit, or rat. In the monkey iliac artery, 100 nM sarafotoxin S6c elicited a contraction in only one specimen which contracted to 32% of the maximal ET-1-induced force. In the monkey jugular vein, 100 nM sarafotoxin S6c elicited small (10% of ET-1-induced force) contractions in most preparations. Sarafotoxin S6c (100 nM) did not contract the monkey saphenous vein. At 100 nM, sarafotoxin S6c produced variable amounts of force ranging from 0–78% of the force elicited by ET-1 in the monkey vena cava. The relative lack

Table 1 Potency of ET receptor agonists and antagonists in isolated smooth muscle preparations

Tissue	*ET-1* EC_{50} (nM)	*Sarafotoxin S6c* EC_{50} (nM)	*BQ-123* K_B (nM)	*FR139317* K_B (nM)
Dog				
coronary artery	0.44 ± 0.071 (8.2 ± 1.4 g)	> 100	70 ± 16	55 ± 14
saphenous vein	1.3 ± 0.42 (16 ± 2.0 g)	0.4 ± 0.12 (1.3 ± 0.4 g)	2400 ± 1100	780 ± 440
Hog				
carotid artery	1.3 ± 0.45 (8.8 ± 1.8 g)	> 100	77 ± 16	NT
Monkey				
iliac artery	0.55 ± 0.22 (16 ± 1.8 g)	> 100	290 ± 55	NT
jugular vein	0.34 ± 0.25 (4.0 ± 0.5 g)	> 100	> 1000	NT
saphenous vein	1.1 ± 0.70 (7.6 ± 1.5 g)	> 100	710 ± 430	NT
vena cava	0.32 ± 0.23 (2.0 ± 0.1 g)	> 100	44 ± 17	NT
Rabbit				
carotid artery	0.59 ± 0.16 (6.0 ± 0.3 g)	> 100	35 ± 14	51 ± 10
pulmonary artery	1.8 ± 0.22 (3.4 ± 0.3 g)	1.5 ± 0.40 (2.9 ± 0.3 g)	> 300	NT
renal artery	2.8 ± 0.60 (10 ± 1.2 g)	> 100	> 300	NT
saphenous vein	3.3 ± 0.98 (5.2 ± 0.8 g)	2.1 ± 1.0 (5.3 ± 0.8 g)	> 300	NT
Rat				
aorta	0.52 ± 0.11 (6.1 ± 0.4 g)	> 100	64 ± 10	NT

K_B = apparent K_B, calculated as described in the Methods. Maximum force for contractions elicited by ET-1 or sarafotoxin S6c is shown in parentheses below the corresponding EC_{50} values. Data are shown as mean ± s.e. NT: not tested.

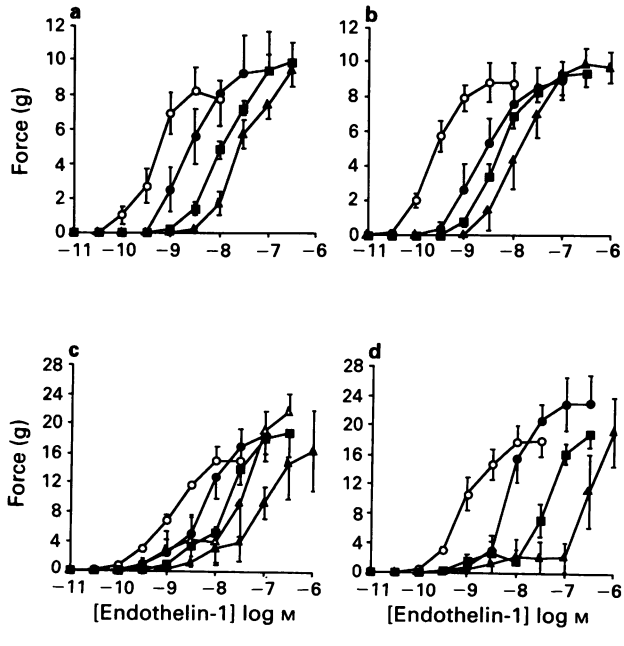

Figure 1 Cumulative concentration-response curves for endothelin-1 (ET-1) in various isolated vascular smooth muscle preparations: (a) shows data collected in dog coronary artery in the absence (○) and presence of 0.3 (●), 1 (■), or 3 (▲) μM BQ-123; $n = 4$ animals, (b) shows data obtained in rabbit carotid artery in the absence (○) and presence of 0.3 (●), 1 (■), or 3 (▲) μM FR139317; $n = 3$ animals. Panel (c) shows results collected in dog saphenous vein in the absence (○) and presence of 3 (●), 10 (■), 30 (△), or 100 (▲) μM BQ-123; $n = 4$ animals; (d) shows curves obtained in dog saphenous vein in the absence (○) and presence of 3 (●), 10 (■), or 100 (▲) μM FR139317; n = 3–4 animals.

of effect of sarafotoxin S6c on the monkey isolated vessels compared with the other preparations suggested that the vasoconstrictor ET_B-like receptor might not play an important role in the primates. Therefore, sarafotoxin S6c was tested in the human isolated saphenous vein where it was found to cause a concentration-related contraction (EC_{50} = 1.4 ± 0.21 nM).

In vivo *studies*

The effects of sarafotoxin S6c were also determined in conscious cynomolgus monkeys. Mean arterial pressure was 112 ± 3, 110 ± 4, 109 ± 4 and 114 ± 2 mmHg before administration of 0.03, 0.1, 0.3 and 1 nmol kg^{-1} i.v. of sarafotoxin S6c in the monkeys. The lower doses of sarafotoxin S6c (0.03–0.3 nmol kg^{-1}, i.v.) produced predominantly pressor responses in the conscious monkeys (Figure 2). This activity reached its peak within 1 min then gradually waned during the next 10 to 15 min. A higher dose of 1 nmol kg^{-1} i.v. of sarafotoxin S6c caused an initial pressor response followed within minutes by a profound reduction in mean arterial pressure (Figures 2 and 3). Blood pressure then returned toward pretreatment levels within 10 min. All monkeys were observed to cough and gag after administration of the highest dose of sarafotoxin S6c, perhaps due to the activation of airway ET_B-like receptors (Hay, 1992).

ET-1 was equipotent with sarafotoxin S6c and also produced dose-related increases in mean arterial pressure in conscious cynomolgus monkeys (Figure 2). Mean arterial pressures were 116 ± 7, 114 ± 6 and 116 ± 7 mmHg before administration of 0.03, 0.1 and 0.3 nmol kg^{-1} i.v. of ET-1. The magnitudes of the responses to ET-1 were similar to the activities of equimolar doses of the ET_B agonist sarafotoxin S6c in the conscious monkeys. Because 1 nmol kg^{-1} of sarafotoxin S6c elicited a large depressor response in the

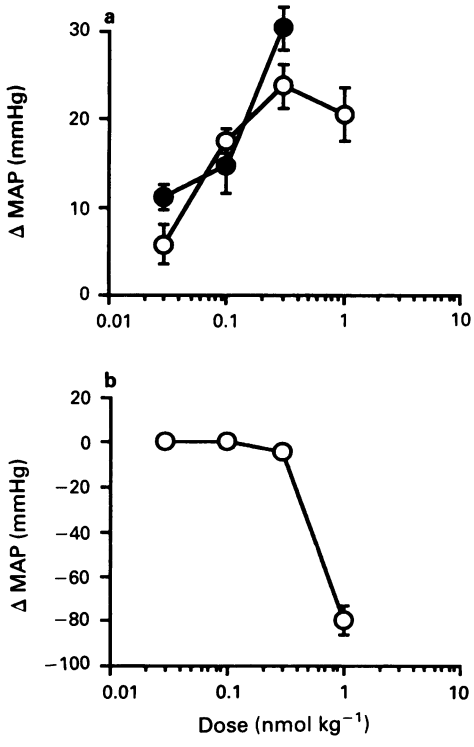

Figure 2 Effects of sarafotoxin S6c (○) and endothelin-1 (ET-1) (●) on mean arterial pressure (MAP) in conscious monkeys. Peak pressor (a) and depressor (b) effects are plotted as mean ± s.e. $n = 4$ animals/peptide.

primates, doses > 0.3 nmol kg^{-1} of ET-1 were not tested. The coughing produced by sarafotoxin S6c was not evident with ET-1. However, ET-1 induced emesis in one monkey.

Discussion

This survey of tissues was undertaken to map the location of functional ET_A and ET_B-like receptors within the vasculature and across species. The isolated smooth muscles used in this study can be divided into two major groups. Those which were sensitive to the effects of BQ-123 and FR139317, and did not contract in response to sarafotoxin S6c were defined as containing ET_A receptors. This group included the dog coronary artery, hog carotid artery, monkey saphenous vein, rabbit carotid artery, and rat aorta. The preparations which were not affected by BQ-123 or FR139317, but contracted in response to sarafotoxin S6c were defined as containing the vasoconstrictor ET_B-like receptors. Tissues with the ET_B-like receptors included the rabbit pulmonary artery and rabbit saphenous vein. The human saphenous vein probably also contains ET_B-like receptors which were responsible for the contraction induced by sarafotoxin S6c. A few of the tissues appeared to contain a variable mixture of both types of receptors, such as the dog saphenous vein, monkey iliac artery, and monkey jugular vein. The rabbit renal artery did not contract in response to sarafotoxin S6c nor were the contractions elicited by ET-1 antagonized by BQ-123 suggesting that the ET receptor in rabbit renal artery is functionally distinct from either the ET_A or ET_B-like isoforms. A similar ET receptor, insensitive to BQ-123 and to sarafotoxin S6c, was described in rat vas deferens (Eglezos *et al.*, 1993).

To date, we have not found functional evidence for ET_B-like receptors on the high pressure side of the circulation, although Harrison *et al.* (1992) have suggested their presence in the pig coronary artery. In contrast, ET_A receptors are apparently present on both high and low pressure sides of the circulation. This appears to be particularly true in the vessels

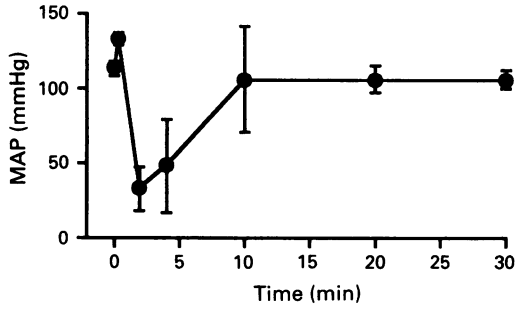

Figure 3 Time course of effects of 1 nmol kg^{-1} i.v. of sarafotoxin S6c on mean arterial pressure (MAP) in conscious monkeys. Data are plotted as mean ± s.e. $n = 4$ animals.

isolated from the cynomolgus monkey. However, intravenous injection of sarafotoxin S6c produced substantial increases in mean arterial pressure in conscious cynomolgus monkeys. Thus, the lack of evidence for ET_B-like receptors in the isolated tissues probably resulted from choosing large vessels for study. It is possible that the resistance vessels responsible for the control of blood pressure contain ET_B-like receptors.

Sarafotoxin S6c causes a hypertensive response upon intravenous injection, presumably by activation of ET_B-like receptors which would also be stimulated by ET-1. Thus, activation of the ET_B-like receptors may be important in pressor responses elicited by ET-1. It is difficult to imagine how substantial increases in blood pressure would result from stimulation of the ET_B-like receptor present relatively rarely on only the low pressure side of the circulation. It may be that functional ET_B-like receptors are also on large vessels on the high pressure side of the circulation or that they occur with more frequency in the resistance vessels. If this were true, we would have missed sampling the arterial ET_B-like receptors by chance. An alternative possibility is that sarafotoxin S6c activation of endothelial ET_B receptors releases a constrictor factor. However, neither a thromboxane receptor nor an angiotensin II receptor antagonist affected contractions elicited by sarafotoxin S6c in the rabbit isolated saphenous vein (data not shown).

The responses to sarafotoxin S6c and ET-1 in the monkeys differed from the biphasic activity of ET-1 reported previously in rats (King *et al.*, 1989). In the rodents, doses of ET-1 similar to those used in the present study produced a transient depressor response that preceded a sustained increase in blood pressure. The immediate fall in blood pressure has been attributed to stimulation of the endothelial ET_B receptors (Saeki *et al.*, 1991; Takayanagi *et al.*, 1991). In the present study, the lower doses of 0.03 to 0.3 nmol kg^{-1} i.v. of sarafotoxin S6c or ET-1 transiently increased blood pressure without an initial depressor response in conscious monkeys. This monophasic pressor activity was similar to previous reports that ET-1 infusions increased blood pressure in conscious dogs (Goetz *et al.*, 1988; Donckier *et al.*, 1991) and reduced cardiac contractility (Donckier *et al.*, 1991). This finding raises the possibility that the secondary fall in blood pressure produced by the highest dose of 1 nmol kg^{-1} i.v. of sarafotoxin S6c in the present study may have resulted from decreases in cardiac performance rather than activation of endothelial ET_B receptors.

In summary, we have shown that ET_A receptors occur throughout the vasculature but are concentrated primarily on the high pressure side of the circulation. Vasoconstrictor ET_B-like receptors are located on the low pressure side of the circulation in many species. These ET_B-like receptors can apparently mediate pressor responses elicited by sarafotoxin S6c in conscious cynomolgus monkeys.

The authors thank Drs John A. Bevan and Ismail Laher in the Department of Pharmacology at the University of Vermont College of Medicine for providing the data from the human saphenous vein.

References

ARAI, H., HORI, S., ARAMORI, I., OHKUBO, H. & NAKANISHI, S. (1990). Cloning and expression of a cDNA encoding an endothelin receptor. *Nature*, **348**, 730–732.

CLOZEL, M., GRAY, G.A., BREU, V., LÖFFLER, B.-M. & OSTERWALDER, R. (1992). The endothelin ET_B receptor mediates both vasodilation and vasoconstriction *in vivo*. *Biochem. Biophys. Res. Commun.*, **186**, 867–873.

DONCKIER, J.E., HANET, C., BERBINSCHI, A., GALANTI, L., ROBERT, A., VAN MECHELEN, H., POULEUR, H. & KETELSLEGERS, J.-M. (1991). Cardiovascular and endocrine effects of endothelin-1 at pathophysiological and pharmacological plasma concentrations in conscious dogs. *Circulation*, **84**, 2476–2484.

EGLEZOS, A., CUCCHI, P., PATACCHINI, R., QUARTARA, L., MAGGI, C.A. & MIZRAHI, J. (1993). Differential effects of BQ-123 against endothelin-1 and endothelin-3 on the rat vas deferens: evidence for an atypical endothelin receptor. *Br. J. Pharmacol.*, **109**, 736–738.

GOETZ, K.L., WANG, B.C., MADWED, J.B., ZHU, J.L. & LEADLEY Jr, R.J. (1988). Cardiovascular, renal, and endocrine responses to intravenous endothelin in conscious dogs. *Am. J. Physiol.*, **255**, R1064–R1068.

HARRISON, V.J., RANDRIANTSOA, A. & SCHOEFFTER, P. (1992). Heterogeneity of endothelin-sarafotoxin receptors mediating contraction of pig coronary artery. *Br. J. Pharmacol.*, **105**, 511–513.

HAY, D.W.P. (1992). Pharmacological evidence for distinct endothelin receptors in guinea-pig bronchus and aorta. *Br. J. Pharmacol.*, **106**, 759–761.

IHARA, M., NOGUCHI, K., SAEKI, T., FUKURODA, T., TSUCHIDA, S., KIMURA, S., FUKAMI, T., ISHIKAWA, K., NISHIKIBE, M. & YANO, M. (1992). Biological profiles of highly potent novel endothelin antagonists selective for the ET_A receptor. *Life Sci.*, **50**, 247–255.

KARNE, S., JAYAWICKREME, C.K. & LERNER, M.R. (1993). Cloning and characterization of an endothelin-3 specific receptor (ET_C receptor) from *Xenopus laevis* dermal melanophores. *J. Biol. Chem.*, **268**, 19126–19133.

KING, A.J., BRENNER, B.M. & ANDERSON, S. (1989). Endothelin: a potent renal and systemic vasoconstrictor peptide. *Am. J. Physiol.*, **256**, F1051–F1058.

LIN, H.Y., KAJI, E.H., WINKEL, G.K., IVES, H.E. & LODISH, H.F. (1991). Cloning and functional expression of a vascular smooth muscle endothelin 1 receptor. *Proc. Natl. Acad. Sci. U.S.A.*, **88**, 3185–3189.

MORELAND, R.S., CILEA, J. & MORELAND, S. (1992a). Staurosporine decreases stiffness but not stress in endothelin-1 stimulated arterial muscle. *Am. J. Physiol.*, **262**, C862–C869.

MORELAND, S., MCMULLEN, D.M., DELANEY, C.L., LEE, V.G. & HUNT, J.T. (1992b). Venous smooth muscle contains vasoconstrictor ET_B-like receptors. *Biochem. Biophys. Res. Commun.*, **184**, 100–106.

PANEK, R.L., MAJOR, T.C., HINGORANI, G.P., DOHERTY, A.M., TAYLOR, D.G. & RAPUNDALO, S.T. (1992). Endothelin and structurally related analogs distinguish between endothelin receptor subtypes. *Biochem. Biophys. Res. Commun.*, **183**, 566–571.

SAEKI, T., IHARA, M., FUKURODA, T., YAMAGIWA, M. & YANO, M. (1991). [$Ala^{1,3,11,15}$]Endothelin-1 analogs with ET_B agonistic activity. *Biochem. Biophys. Res. Commun.*, **179**, 286–292.

SAKURAI, T., YANAGISAWA, M., TAKUWA, Y., MIYAZAKI, H., KIMURA, S., GOTO, K. & MASAKI, T. (1990). Cloning of a cDNA encoding a non-isopeptide-selective subtype of the endothelin receptor. *Nature*, **348**, 732–735.

SCALESE, R.J., DEFORREST, J.M., HAMMERSTONE, S., PARENTE, E. & BURKETT, D.E. (1990). Long term vascular catheterization of the cynomolgus monkey. *Lab. Anim. Sci.*, **40**, 530–532.

SOGABE, K., NIREI, H., SHOUBO, M., NOMOTO, A., AO, S., NOTSU, Y. & ONO, T. (1993). Pharmacological profile of FR139317, a novel, potent endothelin ET_A receptor antagonist. *J. Pharmacol. Exp. Ther.*, **264**, 1040–1046.

SUMNER, M.J., CANNON, T.R., MUNDIN, J.W., WHITE, D.G. & WATTS, I.S. (1992). Endothelin ET_A and ET_B receptors mediate vascular smooth muscle contraction. *Br. J. Pharmacol.*, **107**, 858–860.

TAKAYANAGI, R., KITAZUMI, K., TAKASAKI, C., OHNAKA, K., AIMOTO, S., TASAKA, K., OHASHI, M. & NAWATA, H. (1991). Presence of non-selective type of endothelin receptor on vascular endothelium and its linkage to vasodilation. *FEBS Lett.*, **282**, 103–106.

WILLIAMS, D.L., JONES, K.L., PETTIBONE, D.J., LIS, E.V. & CLINESCHMIDT, B.V. (1991). Sarafotoxin S6c: an agonist which distinguishes between endothelin receptor subtypes. *Biochem. Biophys. Res. Commun.*, **175**, 556–561.

(Received August 2, 1993
Revised February 23, 1994
Accepted March 7, 1994)

Br. J. Pharmacol. (1994), **112**, 709–715

The effects of sigma ligands and of neuropeptide Y on N-methyl-D-aspartate-induced neuronal activation of CA_3 dorsal hippocampus neurones are differentially affected by pertussin toxin

François P. Monnet, [1]Guy Debonnel, Richard Bergeron, Benjamin Gronier & Claude de Montigny

Neurobiological Psychiatry Unit, Department of Psychiatry, McGill University, 1033 Pine Avenue, West, Montréal, Québec, Canada H3A 1A1

1 The *in vivo* effects of the high affinity sigma ligands 1,3-di(2-tolyl)guanidine (DTG), (+)-N-cyclopropylmethyl-*N*-methyl-1,4-diphenyl-1-ethyl-but-3-en-1-ylamine hydrochloride (JO-1784), (+)-pentazocine and haloperidol, as well as of those of neuropeptide Y (NPY), on *N*-methyl-D-aspartate (NMDA)- and quisqualate (Quis)-induced neuronal activations of CA_3 pyramidal neurones were assessed, using extracellular unitary recording, in control rats and in rats pretreated with a local injection of pertussis toxin (PTX), to evaluate the possible involvement of $G_{i/o}$ proteins in mediating the potentiation of the neuronal response to NMDA by the activation of sigma receptors in the dorsal hippocampus.

2 Microiontophoretic applications as well as intravenous injections of (+)-pentazocine potentiated selectively the NMDA response in control rats as well as in PTX-pretreated animals. In contrast, the PTX pretreatment abolished the potentiation of the NMDA response by DTG, JO-1784 and NPY. Moreover, microiontophoretic applications of DTG induced a reduction of NMDA-induced neuronal activation. Neither in control nor in PTX-treated rats, did the sigma ligands and NPY have any effect on Quis-induced neuronal response.

3 In PTX-treated rats, the potentiation of the NMDA response induced by (+)-pentazocine was suppressed by haloperidol, whereas the reduction of the NMDA response by DTG was not affected by haloperidol.

4 This study provides the first *in vivo* functional evidence that sigma ligands and NPY modulate the NMDA response by acting on distinct receptors, differentiated by their PTX sensitivity.

Keywords: NMDA; $G_{i/o}$ protein; pertussis toxin; sigma receptors; haloperidol; 1,3-di(2-tolyl)guanidine (DTG); JO-1784; (+)-pentazocine; neuropeptide Y; BMY-14802

Introduction

The recent synthesis of selective and high affinity sigma ligands has led to the identification of some of the pharmacological characteristics of sigma receptors. We have shown that several sigma ligands selectively and markedly potentiate *N*-methyl-D-aspartate (NMDA)-induced neuronal activation of rat CA_3 dorsal hippocampus pyramidal neurones using an *in vivo* electrophysiological paradigm (Monnet *et al.*, 1990; 1992b). This potentiation of the NMDA response is suppressed by other sigma ligands such as haloperidol, BMY-14802 and (+)-*N*-n-propyl-3-(3-hydroxyphenyl) piperidine [(+)-3-PPP] which by themselves, at low doses, do not affect the NMDA response. Therefore, the former are tentatively denoted agonists and the later antagonists in the present manuscript.

These results suggest the existence of a functional interaction between sigma and NMDA receptors. Further support for this notion has been provided by data obtained in both A9 and A10 regions (Iyengar *et al.*, 1990a) and in the hypothalamic-pituitary-adrenal axis (Iyengar *et al.*, 1990b; 1991). Neuropeptide Y (NPY), which has been reported to bind to sigma receptors (Roman *et al.*, 1989; 1993; Bouchard *et al.*, 1993), behaves like sigma agonists in our *in vivo* electrophysiological model (Monnet *et al.*, 1992c,d) as well as in various *in vivo* and *in vitro* paradigms (Roman *et al.*, 1989; 1991b; Riviere *et al.*, 1990), suggesting that it might act on sigma receptors.

Guanosine triphosphate (GTP)-binding regulatory G proteins (guanine nucleotide-binding proteins) might be involved in the biological effects of several high affinity sigma ligands (Itzhak & Khouri, 1988; Chattarji *et al.*, 1989; Itzhak, 1989). Indeed, in rat brain membrane preparations, GTP and Gpp(NH)p reduce the high affinity component of the binding of the sigma ligands (+)-*N*-allylnormetazocine [(+)-SKF-10,047], (+)-3-PPP and pentazocine, this phenomenon being attributed to the conversion of sigma receptors from a high to a low affinity state (Irzhak & Khouri, 1988; Beart *et al.*, 1989). As Gpp(NH)p reduces the slower dissociative component of sigma binding, it has been proposed that, in their high affinity state, at least a subpopulation of sigma receptors are coupled to G proteins (Itzhak, 1989). In addition, pretreatment with pertussis toxin (PTX), which inactivates $G_{i/o}$ proteins by ADP-ribosylation, reduces the high affinity binding component and prevents the effects of Gpp(NH)p on [^{3}H]-(+)-3PPP binding (Itzhak, 1989), suggesting the coupling of sigma receptors to $G_{i/o}$ proteins (Gilman, 1987; Fredholm & Lindgren, 1988; Hertting & Allgaier, 1988).

Sigma receptors have been separated, to date, into two classes, denoted σ_1 and σ_2 (Quirion *et al.*, 1992). The sigma ligands, haloperidol, 1,3-di(2-toly)guanidine (DTG) and (+)-3-PPP, do not discriminate between σ_1 and σ_2 sites, whereas the (+)-benzomorphans, (+)-SKF-10,047 and (+)-pentazocine as well as JO-1784, bind preferentially to σ_1 sites with a nanomolar affinity (Quirion *et al.*, 1992).

[1] Author for correspondence.

The goal of the present study was thus to assess, *in vivo*, whether the effect of sigma ligands on the NMDA response involved a $G_{i/o}$ type of protein. To this end, using *in vivo* extracellular unitary recording of CA_3 dorsal hippocampus pyramidal neurones, we compared in control rats and in rats pretreated with PTX, the capacity of high affinity sigma ligands (DTG, JO-1784, (+)-pentazocine) and of NPY, to potentiate NMDA-induced neuronal activation in the CA_3 dorsal hippocampus.

Methods

Pertussis toxin pretreatment

Male Sprague-Dawley rats (175–200 g) were obtained from Charles River (Saint-Constant, Québec, Canada) and housed four per cage. They were kept on a 12 h:12 h light/dark cycle with free access to water and Purina chow. Following anaesthesia with chloral hydrate (400 mg kg^{-1}, i.p.), the rats were mounted in a stereotaxic apparatus. The pretreatment with PTX (1 μg in 2 μl of physiological saline, Sigma Chemical Co., St-Louis, MO, U.S.A.) consisted in lowering unilaterally the tip of a 5-μl Hamilton syringe into the dorsal hippocampus at A: 4.5, L: 4 and D: 4, according to the atlas of Paxinos & Watson (1986). Pertussis toxin was slowly injected over a period of 5 min. Control rats received an equal volume of physiological salines. *In vivo* electrophysiological experiments were carried out 3 to 11 days later. This interval was chosen because it was observed, in the same *in vivo* electrophysiological experiments, that the efficacy of microiontophoretic applications of 5-hydroxytryptamine (5-HT) in suppressing the firing activity of CA_3 hippocampal pyramidal neurones, an effect which is $G_{i/o}$ protein-dependent (Andrade *et al.*, 1986), was drastically reduced during this time period (Blier *et al.*, 1992).

Recordings from CA_3 dorsal hippocampus pyramidal neurones

Recordings were obtained as previously described (Monnet *et al.*, 1992d). In brief, rats were anaesthetized with urethane (1.25 g kg^{-1}, i.p.), and mounted in a stereotaxic apparatus. Body temperature was maintained at 37°C throughout the experiment. Five-barrelled glass micropipettes, were used for extracellular unitary recordings of the activity of CA_3 dorsal hippocampus pyramidal neurones. One side barrel, filled with 2 M NaCl, was used for automatic current balancing. The other side barrels, used for microiontophoresis, were filled with NMDA (10 mM in 200 mM NaCl, pH 8), Quis (1.5 mM in 400 mM NaCl, pH 8), acetylcholine (ACh) (1.5 mM in 200 mM NaCl, pH 8) and one of the following solutions: DTG (1 mM in 200 mM NaCl, pH 4), JO-1784 (1 mM in 200 mM NaCl, pH 4), (+)-pentazocine (0.5 mM in 200 mM NaCl, pH 4), NPY (0.1 mM in 150 mM NaCl and bovine serum albumin 0.1%, pH 4), or haloperidol (0.2 mM in 50 mM NaCl, pH 3.5).

The micropipette was lowered into the CA_3 region of the dorsal hippocampus (L: 4.2 mm and A: 4.2 mm, at a depth of 3.5 to 4.5 mm from the cortical surface; Paxinos & Watson, 1986). Action potentials, monitored on an oscilloscope, triggered square pulses fed to a computer. The duration of the microiontophoretic applications and the intensities of the currents used were also stored in the computer, permitting the calculation of the total number of spikes generated per nC. For a given neurone, the currents of NMDA and Quis were adjusted to obtain a firing frequency in between 7 and 15 Hz and were thereafter maintained constant for the reminder of the experiment. All applications of NMDA and Quis were of 50 s, while those of the sigma ligands and of NPY were of 15 to 20 min.

Experimental series

In a first series of experiments, since NPY does not cross the blood brain barrier and could only be applied by microiontophoresis, the sigma ligands DTG, JO-1784, (+)-pentazocine and haloperidol were also applied by microiontophoresis in control and PTX-treated animals. The effects of the microiontophoretic applications of the sigma ligands were assessed by determining the number of spikes generated per nC of NMDA and Quis before and during the microiontophoretic application of the substance studied.

In a second series, DTG, (+)-pentazocine and haloperidol were administered intravenously. The effects of these sigma ligands were assessed by determining the number of spikes generated per nC of NMDA and Quis before and after the injection. Only one neurone was tested in each rat which received only one dose of DTG or (+)-pentazocine.

Drugs

The following substances were used: NMDA and PTX (Sigma Chemical, St. Louis, MO, U.S.A.), Quis (Tocris Neuramin, Buckhurst Hill, Essex, U.K.), DTG (Aldrich, Milwaukee, WI, U.S.A.), haloperidol (McNeil Laboratories, Stouffville, ONT, Canada). JO-1784 [(+)-N-cyclopropylmethyl-*N*-methyl-1,4-diphenyl-1-ethyl-but-3-en-1-ylamine, hydrochloride] was kindly provided by Dr J.L. Junien (Institut de Recherche Jouveinal, Fresnes, France), (+)-pentazocine by Dr B.C. deCosta (N.I.H., Bethesda, MD, U.S.A.) and NPY was a generous gift from Dr A. Fournier (Institut National de la Recherche Scientifique-Santé, Pointe-Claire, Québec, Canada).

Statistical analysis

All results are expressed as the mean ± s.e.mean of the number of spikes generated per nC of NMDA or Quis, *n* being the number of neurones tested. Statistical significance was assessed by Student's paired *t* test with Dunnett's correction for multiple comparisons. Probability values less than 0.05 were considered as significant.

Results

Microiontophoretic applications of NMDA and Quis produced consistent activation of all CA_3 pyramidal neurones recorded. Pertussis toxin, which inactivates $G_{i/o}$ proteins by ADP-ribosylation, was used to document the possible involvement of these proteins in the modulation of NMDA-induced neuronal activation in the CA_3 region of the rat dorsal hippocampus by high affinity sigma ligands and NPY. The *in vivo* PTX pretreatment did not affect the spontaneous firing activity or NMDA- or Quis-induced neuronal activity. None of the sigma ligands tested nor NPY had any effect on the spontaneous activity of pyramidal neurones in the CA_3 region, consistent with previous observations (Brooks *et al.*, 1987; Lodge *et al.*, 1988; Monnet *et al.*, 1992b,c,d).

Effects of microiontophoretic applications of JO-1784, NPY, DTG and (+)-pentazocine

In a first series of experiments, the high affinity sigma ligands JO-1784 (Roman *et al.*, 1990), (+)-pentazocine (Su, 1982), DTG (Weber *et al.*, 1986), as well as NPY (Roman *et al.*, 1989) were applied microiontophoretically for successive periods of 10 to 20 min with 5, 10 and 20 nA ejecting currents, in control and PTX-treated rats.

In naive rats, JO-1784 (from 10 and 20 nA) produced a selective and current-dependent enhancement of the NMDA response, 20 nA inducing a three fold increase of NMDA-induced firing activity (Figures 1a, 2a). In PTX-treated rats, JO-1784, even at a current of 20 nA, failed to induce any

significant potentiation of the NMDA response (Figures 1b, 2a). As in control rats, JO-1784 did not modify the neuronal response to Quis.

Similarly, when applied microiontophoretically with a current of 10 nA, NPY produced in control rats a two fold enhancement of the NMDA response (Figure 2b), but had no effect on the Quis response. In PTX-treated rats, the potentiating effect of NPY on the NMDA response was abolished (Figure 2b).

In control animals, microiontophoretic applications of DTG produced a greater than two fold increase in the neuronal activation induced by microiontophoretic applications of NMDA, (Figure 2c). After pretreatment with PTX however, DTG induced a slight but significant reduction of the NMDA-induced firing activity (Figure 2c). The Quis response was not modified by the microiontophoretic application of DTG in either control or PTX-pretreated rats.

The microiontophoretic application of (+)-pentazocine produced, in naive rats, a 150% increase of NMDA-induced neuronal activation (Figure 2d), without affecting the response to Quis. In PTX-treated rats, (+)-pentazocine, unlike the other sigma ligands, still produced a potentiation of the NMDA response (Figure 2d), without modifying that of Quis.

As in previous studies, in control animals, the microiontophoretic application, as well as the intravenous administration of a low dose (10 $\mu g\,kg^{-1}$), of haloperidol concurrently with the application of DTG, (+)-pentazocine, JO-1784 or NPY, suppressed the potentiation of the NMDA response induced by these sigma ligands (data not shown). In PTX-treated rats, the potentiation induced by the microiontophoretic application of (+)-pentazocine was also suppressed by haloperidol (10 $\mu g\,kg^{-1}$, i.v., Figure 2d). However, the

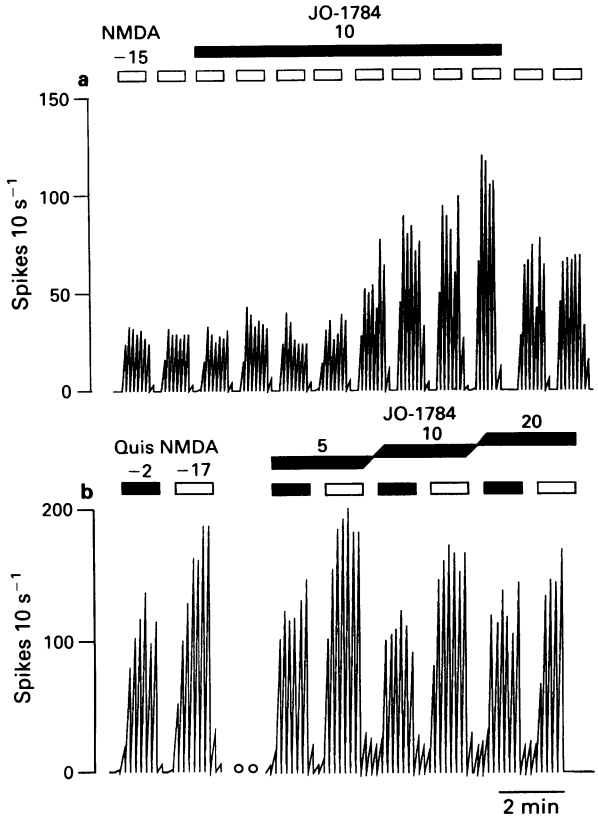

Figure 1 Integrated firing rate histograms of CA_3 dorsal hippocampus pyramidal neurones showing the effects of microiontophoretic applications of *N*-methyl-D-aspartate (NMDA) and quisqualate (Quis) before and during the microiontophoretic application of JO-1784 in a control rat (a) and in a rat pretreated with pertussis toxin (b). Bars indicate the duration of applications for which currents are given in nA and dots correspond to 10–15 min interruption, of the trace, in this and subsequent figures. Time base applies to both traces.

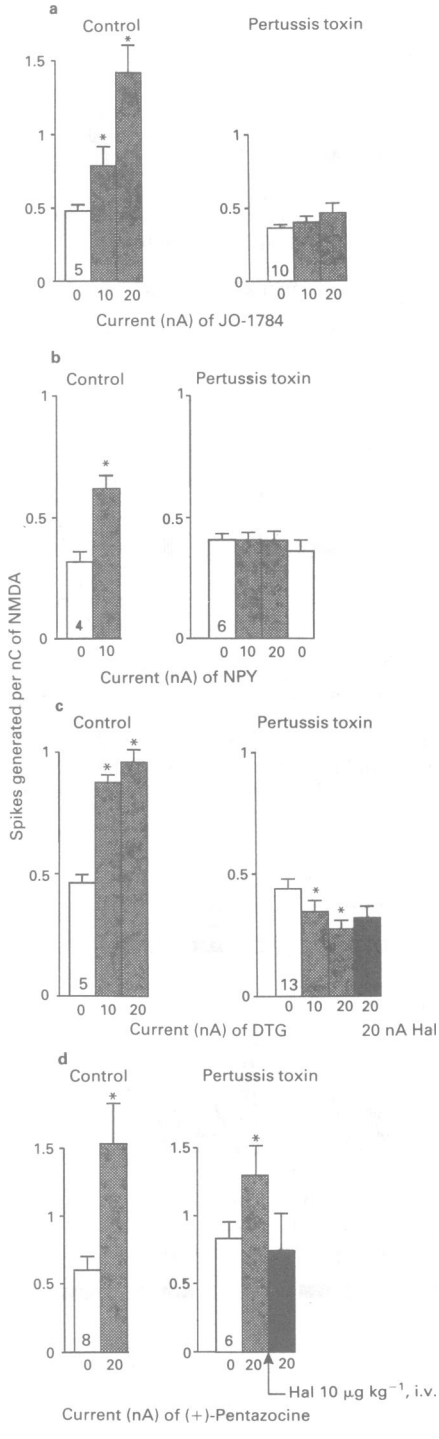

Figure 2 Responsiveness expressed as the number of spikes generated per nanocoulomb (nC; mean ± s.e.mean) of CA_3 dorsal hippocampus neurones to microiontophoretic applications of *N*-methy-D-aspartate (NMDA) before (open column), during (stippled columns) microiontophoretic applications of JO-1784 (a), neuropeptide Y (NPY), (b), 1,3-di(2-tolyl)guanidine (DTG) (c) and (+)-pentazocine (d), and following the microiontophoretic application or the intravenous administration (solid column) of haloperidol in control and pertussis toxin treated rats. The number at the base of the first column of each histogram in this and in subsequent figures indicates the number of neurones tested. In all series of experiments, the same neurones were recorded from during the complete sequence. All applications of NMDA and Quis were of 50 s. $*P<0.01$.

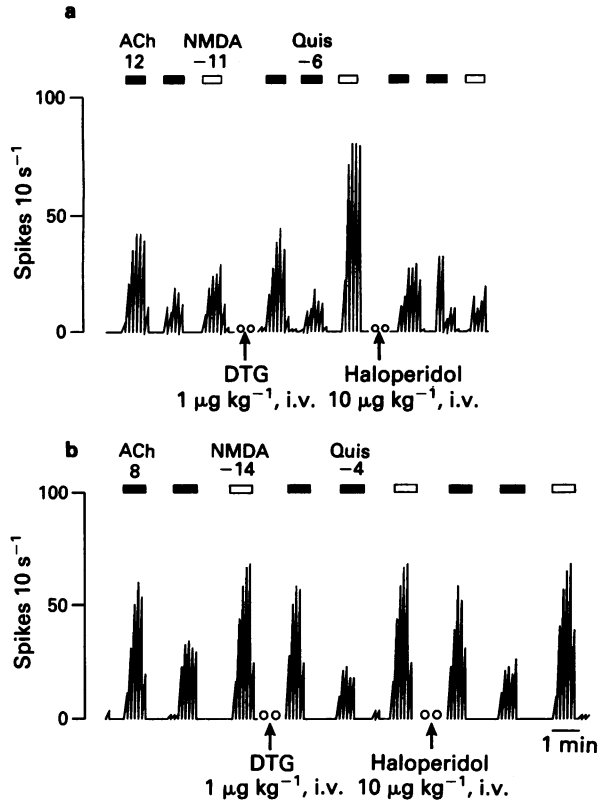

Figure 3 Integrated firing rate histograms showing the response of CA_3 dorsal hippocampus pyramidal neurones to microiontophoretic applications of acetylcholine (ACh), *N*-methyl-D-aspartate (NMDA) and quisqualate (Quis) before and following the intravenous administration of 1,3-di(2-tolyl)guanidine (DTG) and following the intravenous injection of haloperidol, in a control (a) and a pertussis toxin treated rat (b).

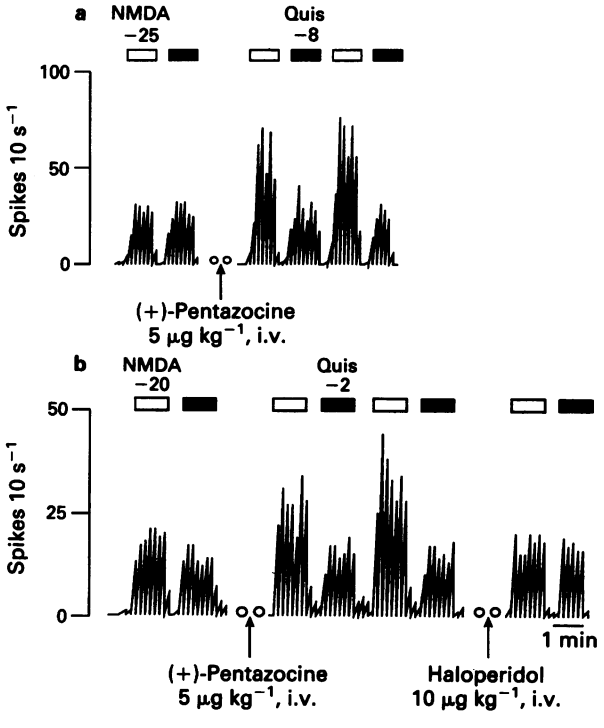

Figure 4 Integrated firing rate histograms showing the response of CA_3 dorsal hippocampus pyramidal neurones to microiontophoretic applications of *N*-methyl-D-aspartate (NMDA) and quisqualate (Quis) before and following the intravenous administration of (+)-pentazocine and following the intravenous injection of haloperidol, in a control (a) and a pertussis toxin treated rat (b).

DTG-induced attenuation of the NMDA response obtained in PTX-treated rats was not reversed by haloperidol (Figure 2c).

Effects of the intravenous administrations of DTG and (+)-pentazocine

In a second series of experiments, the two sigma ligands DTG and (+)-pentazocine, which were found to modulate the NMDA response when applied by microiontophoresis in PTX-treated rats, were administered intravenously. As illustrated in Figures 3a and 4a, DTG, at a dose of 1 $\mu g\,kg^{-1}$, and (+)-pentazocine, at a dose of 5 $\mu g\,kg^{-1}$, selectively enhanced by three fold the firing activity of CA_3 pyramidal neurones to microiontophoretic applications of NMDA in control rats (Figure 5), consistent with previous reports (Monnet *et al.*, 1990; 1992b). When injected in PTX-treated rats, DTG (1 $\mu g\,kg^{-1}$, i.v.) neither enhanced nor reduced the NMDA-induced neuronal activation (Figures 3b, 5b). However, in PTX-treated rats, (+)-pentazocine (5 $\mu g\,kg^{-1}$, i.v.) produced a marked and selective potentiation of the NMDA response, similar to that obtained in the control animals (Figures 4, 5a). The subsequent intravenous administration of a low dose of haloperidol (10 $\mu g\,kg^{-1}$) completely abolished the (+)-pentazocine-induced potentiation of the NMDA-induced firing activity of CA_3 pyramidal neurones in PTX-treated rats (Figures 4b, 5a). Neither the intravenous administration of DTG nor (+)-pentazocine modified the

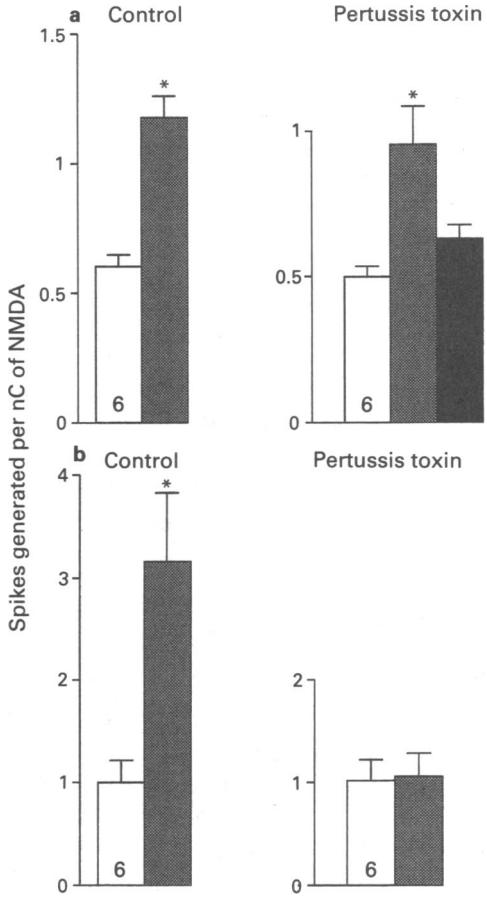

Figure 5 Responsiveness expressed as the number of spikes generated per nanocoulomb (mean ± s.e.mean) of CA_3 dorsal hippocampus neurones to microiontophoretic applications of *N*-methy-D-aspartate (NMDA) before (open columns) and after (stippled columns) the intravenous administration of (+)-pentazocine, 5 $\mu g\,kg^{-1}$ (a) and 1,3-di(2-tolyl)guanidine, (DTG) 1 $\mu g\,kg^{-1}$ (b). Since (+)-pentazocine still induced a potentiation of NMDA response in pertussis toxin-treated rats, a subsequent injection of haloperidolol (10 $\mu g\,kg^{-1}$, i.v.) was administered (solid column).

neuronal activation induced by microiontophoretic applications of Quis or ACh in control and PTX-treated rats (Figures 3–5).

Discussion

The present results obtained *in vivo*, in the CA_3 region of the rat dorsal hippocampus, show that the inactivation of $G_{i/o}$ proteins by PTX abolished the potentiating effects of DTG, JO-1784 and NPY on the NMDA response, but not that of (+)-pentazocine. In addition, in PTX-treated rats, haloperidol reversed the potentiating effect of (+)-pentazocine on the NMDA response.

The unaltered effects of NMDA and Quis on the firing activity of CA_3 pyramidal neurones, following $G_{i/o}$ protein inactivation by a PTX pretreatment, are consistent with previous observations in rat striatal neurones (Sladeczek *et al.*, 1985), cerebellar granule cells (Nicoletti *et al.*, 1986), hippocampal slices (Beaudry *et al.*, 1986) and forebrain synaptosomes (Recaens *et al.*, 1987) suggesting that the excitatory effects of these amino acids are not mediated by G proteins.

The observation that microiontophoretic applications of DTG, (+)-pentazocine, JO-1784 and NPY, as well as the intravenous administration of low doses of DTG and (+)-pentazocine, potentiated NMDA-induced neuronal activation of CA_3 dorsal hippocampus in control animals is consistent with previous *in vivo* studies (Monnet *et al.*, 1990; 1992b; Martin *et al.*, 1992) and with the data obtained by Iyengar *et al.* (1990b, 1991), who demonstrated that several sigma ligands also potentiated NMDA-dependent adrenocorticotropic hormone and prolactin release in pituitary cells as well as dopamine turnover in the striatum and olfactory tubercles.

The lack of effect of PTX-treatment on (+)-pentazocine-induced potentiation of the NMDA response (Figures 2, 4 and 5) suggests that this sigma ligand activates a subtype of sigma receptor not coupled to $G_{i/o}$ proteins. Haloperidol is known to bind with high affinity to dopamine, α_1-adrenoceptor, 5-HT, muscarinic and sigma receptors (Burt *et al.*, 1977; Peroutka *et al.*, 1977; Su, 1982). However, the only binding sites that haloperidol, DTG, JO-1784 and (+)-pentazocine share are the sigma sites (Su, 1982; Weber *et al.*, 1986; Roman *et al.*, 1990). Therefore, the suppression by haloperidol of the potentiating effect of (+)-pentazocine on the NMDA response in the present series of experiments constitutes conducive evidence that (+)-pentazocine potentiates the NMDA response by activating sigma receptors. These results differ from those of Itzhak (1989) who found that the binding of racemic pentazocine to sigma sites labelled with [^{3}H]-3-PPP was altered by GTP and Gpp(NH)p, suggesting that these sites were coupled to G proteins. Furthermore, (+)-pentazocine is considered to bind selectively to σ_1 receptors which have been suggested to be associated with a $G_{i/o}$ protein (Quirion *et al.*, 1992). However, De-Haven-Hudkins *et al.* (1992) have reported that the binding of [^{3}H]-(+)-pentazocine was insensitive to GTP and Gpp(NH)p, suggesting that [^{3}H]-(+)-pentazocine binds to sigma receptors not coupled to $G_{i/o}$ proteins. The apparently discrepant data of these two binding studies could be explained by the different forms of pentazocine and/or species used (guinea-pigs vs rats). The present results, in keeping with the observations of De Haven-Hudkins *et al.* (1992), suggest that the potentiating effect of (+)-pentazocine on the NMDA response is mediated by a subtype of σ_1 receptor not coupled to a $G_{i/o}$ protein and sensitive to haloperidol.

The high affinity sigma ligand, JO-1784, as well as NPY, have previously been shown to enhance the NMDA response *in vivo* as well as *in vitro* (Riviere *et al.*, 1990; Roman *et al.*, 1991b; Monnet *et al.*, 1992a,b,d), the effect of NPY being mediated via a non-Y_1, non-Y_2, non-Y_3 receptor, probably corresponding to a subtype of sigma receptor (Monnet *et al.*, 1992c,d). The similarity of some of the effects of JO-1784 and NPY has been reported in other models (Riviere *et al.*, 1990; 1993; Roman *et al.*, 1991a,b; Gué *et al.*, 1992a,b; Pascaud *et al.*, 1993). Thus, the prevention by PTX pretreatment of the potentiating effect of JO-1784 and NPY (Figure 1 and 2) is fully consistent with previous observations suggesting that they exert their effects on the NMDA response via a subtype of sigma receptor coupled to $G_{i/o}$ proteins (Junien *et al.*, 1991; Monnet *et al.*, 1992a).

Following the inactivation of $G_{i/o}$ proteins by PTX, the intravenous administration of DTG did not modify the neuronal response to NMDA and Quis, whereas the microiontophoretic application of DTG produced a slight but significant reduction of the excitatory effect of NMDA, but not of Quis, (Figures 2, 3 and 5). At present, we do not have a definite explanation for the differential effects of DTG when applied by microiontophoresis and intravenously. The suppression of the potentiating effect of DTG following PTX is consistent with the results obtained with JO-1784 and NPY. However, in addition, PTX pretreatment unveiled a second component ($G_{i/o}$ protein-insensitive) of the effect of DTG on the NMDA response, consisting of reduction in the NMDA response. Some reports have described an inhibitory effect of high doses of sigma ligands on NMDA-induced effects, albeit to a weaker degree than phencyclidine (PCP)-like drugs (Anis *et al.*, 1983; Lodge & Anis, 1984; Malouf *et al.*, 1988). This inhibitory effect of sigma ligands has been ascribed, however, to their low affinity for the PCP binding site (Lodge *et al.*, 1988; Malouf *et al.*, 1988; Church & Lodge, 1990; Monnet *et al.*, 1992b). Two groups have reported an inhibitory effect of DTG at low doses. First, Roth *et al.* (1993) have observed in the rat prepiriform cortex that concentrations of DTG as low as 1 nM produced an anticonvulsant effect, via a reduction of the NMDA response (Roth *et al.*, 1993). Second, Connick *et al.* (1992a) reported a reduction of the NMDA response by low doses of DTG in the CA_1 region of the rat dorsal hippocampus. One intriguing finding here is that the suppressant effect of DTG was not reversed by haloperidol (Figure 2c). In this and in previous experiments, haloperidol consistently suppressed the potentiating effects of sigma ligands. The reversal of the effects of (+)-pentazocine, DTG and JO-1784 by haloperidol has also been observed in the peripheral nervous system (Massamiri & Duckles, 1990), in behavioural models (Tam *et al.*, 1988; Steinfels *et al.*, 1989) as well as in the central nervous system both *in vivo* (Tam *et al.*, 1988; Monnet *et al.*, 1990; 1992b) and *in vitro* (Roman *et al.*, 1989; Connor *et al.*, 1992). Hence, since DTG and haloperidol both bind to both σ_1 and σ_2 receptors (Quirion *et al.*, 1992), it is possible that the suppressant effect of DTG on the NMDA responses in PTX-treated rats might not be ascribed to sigma receptors. However, some reports have provided evidence for the existence of more than two subtypes of sigma receptors. Zhou & Musacchio (1991) have suggested the existence of at least four subtypes of sigma receptors, one of them, R_4 having a moderately low affinity for DTG and very low affinity for haloperidol. Connick *et al.* (1992b), have proposed that this R_4 subtype of sigma receptor might not be coupled to a G protein. Moreover, the anticonvulsant effect of low doses of DTG is also insensitive to haloperidol (Roth *et al.*, 1993). Therefore, the observation that, in PTX-treated rats, the DTG-induced reduction of the NMDA response was not reversed by haloperidol (Figure 2c) raises the possibility that DTG might exert its inhibitory effect via a haloperidol-insensitive sigma receptor not coupled to $G_{i/o}$ protein, possibly corresponding to the R_4 subtype.

In conclusion, the present results provide further support for the notion that several types of sigma receptors exist in the central nervous system and that some sigma receptors are coupled to $G_{i/o}$ proteins.

We wish to thank T. Vo for computer programming, statistical analysis and illustrations, and L. Martin for her secretarial assis-

tance. This work was supported, in part, by the Medical Research Council of Canada, by the Royal Victoria Hospital Research Institute and by the Fonds de la Recherche en Santé du Québec (F.R.S.Q.). F.P.M. was in receipt of a Convention Industrielle de la Formation par la Recherche Fellowship from the Ministère de la Santé, France. G.D. and R.B. are in receipt of a Scholarship and a Fellowship from the F.R.S.Q., respectively and B.G. of a Fellowship from the Fondation pour la Recherche Médicale.

References

ANDRADE, R., MALENKA, R.C. & NICOLL, R.A. (1986). A G protein couples serotonin and $GABA_B$ receptors to the same channels in hippocampus. *Science*, **234**, 1261–1265.

ANIS, A., BERRY, S.C., BURTON, N.R. & LODGE, D. (1983). The dissociative anaesthetics, ketamine and phencyclidine, selectively reduce excitation of central mammalian neurones by N-methyl-aspartate. *J. Pharmacol. Exp. Ther.*, **79**, 565–575.

BEART, P.M., OSHEA, R.D. & MANALLAK, D.T. (1989). Regulation of sigma-receptors – high-affinity and low-affinity agonist states, GTP shifts, and up-regulation by rimcazole and 1,3-di(2-tolyl)guanidine. *J. Neurochem.*, **53**, 779–788.

BEAUDRY, M., EVANS, J. & LYNCH, G. (1986). Excitatory amino acids inhibit stimulation of phosphatidylinositol metabolism by aminergic agonists in hippocampus. *Nature*, **319**, 329–331.

BLIER, P., LISTA, A. & DE MONTIGNY, C. (1992). Differential properties of pre- and postsynaptic 5-hydroxytryptamine$_{1A}$ receptors in the dorsal raphe and hippocampus: II. Effect of pertussis and cholera toxins. *J. Pharmacol. Exp. Ther.*, **265**, 16–23.

BOUCHARD, P., DUMONT, Y., FOURNIER, A., ST-PIERRE, S. & QUIRION, R. (1993). Evidence for in vivo interactions between neuropeptide Y-related peptides and sigma receptors in the mouse hippocampal formation. *J. Neurosci.*, **13**, 3926–3931.

BROOKS, P.A., KELLY, J.S., ALLEN, J.M., SMITH, D.A.S. & STONE, T.W. (1987). Direct excitatory effects of neuropeptide Y (NPY) on rat hippocampal neurons *in vitro*. *Brain Res.*, **408**, 295–298.

BURT, D.R., CREESE, I. & SNYDER, S.H. (1977). Antischizophrenic drugs: chronic treatment elevates dopamine receptor binding in brain. *Science*, **196**, 326–328.

CHATTARJI, S., STANTON, P.K. & SEJNOWSKI, T.J. (1989). Commissural synapses, but not mossy fiber synapses, in hippocampal field CA_3 exhibit associative long-term potentiation and depression. *Brain Res.*, **495**, 145–150.

CHURCH, J. & LODGE, D. (1990). Failure of sigma-receptor ligands to reduce the excitatory actions of N-methyl-DL-aspartate on rat spinal neurons *in vivo*. *J. Pharm. Pharmacol.*, **42**, 56–57.

CONNICK, J.H., ADDAE, J.I., NICHOLSON, C.D. & STONE, T.W. (1992a). The σ ligand 1,3-di-o-tolyguanidine depresses amino acid-induced excitation non-selectively in rat brain. *Eur. J. Pharmacol.*, **214**, 169–173.

CONNICK, J.H., HANLON, G., ROBERTS, J., FRANCE, L., FOX, P.K. & NICHOLSON, C.D. (1992b). Multiple σ binding sites in guinea-pig and rat brain membranes: G-protein interactions. *Br. J. Pharmacol.*, **107**, 726–731.

CONNOR, M., PATTERSON, T. & CHAVKIN, C. (1992). Zinc is a potential endogenous ligand for one form of the haloperidol-sensitive sigma receptor. *Soc. Neurosci. Abst.*, **18**, 195.6.

DEHAVEN-HUDKINS, D.L., FLEISSNER, L.C. & FORD-RICE, F.Y. (1992). Characterization of the binding of [^{3}H](+)-pentazocine to σ recognition sites in guinea pig brain. *Eur. J. Pharmacol.: Mol. Pharmacol.*, **227**, 371–378.

FREDHOLM, B.B. & LINDGREN, E. (1988). Effects of N-ethylmaleimide and forskolin on noradrenaline release from rat hippocampal slices. Evidence that prejunctional adenosine and α-receptors are linked to N-proteins but not adenylate cyclase. *Acta Physiol. Scand.*, **130**, 95–105.

GILMAN, A.G. (1987). G proteins: Transducers of receptor-generated signals. *Annu. Rev. Biochem.*, **56**, 615–649.

GUÉ, M., JUNIEN, J.L., DEL RIO, C. & BUENO, L. (1992a). Neuropeptide Y and sigma ligand (JO 1784) suppress stress-induced colonic motor disturbances in rats through sigma and cholecystokinin receptors. *J. Pharmacol. Exp. Ther.*, **261**, 850–855.

GUÉ, M., YONEDA, M., MÖNNIKES, H., JUNIEN, J.-L. & TACHÉ, Y. (1992b). Central neuropeptide Y and the sigma ligand, JO 1784, reverse corticotropin-releasing factor-induced inhibition of gastric acid secretion in rats. *Br. J. Pharmacol.*, **107**, 642–647.

HERTTING, G. & ALLGAIER, C. (1988). Participation of protein kinase C and regulatory G proteins in modulation of the evoked noradrenaline release in brain. *Cell Mol. Neurobiol.*, **8**, 105–114.

ITZHAK, Y. (1989). Multiple affinity binding states of the sigma-receptor effect of GTP-binding protein-modifying agents. *Mol. Pharmacol.*, **36**, 512–517.

ITZHAK, Y. & KHOURI, M. (1988). Regulation of the binding of sigma- and phencyclidine (PCP)-receptor ligands in rat brain membranes by guanine nucleotides and ions. *Neurosci. Lett.*, **85**, 147–152.

IYENGAR, S., DILWORTH, V.M., MICK, S.J., CONTRERAS, P.C., MONAHAN, J.B., RAO, T.S. & WOOD, P.L. (1990a). Sigma receptors modulate both A9 and A10 dopaminergic neurons in the rat brain – functional interaction with NMDA receptors. *Brain Res.*, **524**, 322–326.

IYENGAR, S., MICK, S., DILWORTH, V., MICHEL, J., RAO, T.S., FARAH, J.M. & WOOD, P.L. (1990b). Sigma receptors modulate the hypothalamic-pituitary-adrenal (Hpa) axis centrally - evidence for a functional interaction with NMDA receptors, *in vivo*. *Neuropharmacology*, **29**, 299–303.

IYENGAR, S., WOOD, P.L., MICK, S.J., DILWORTH, V.M., GRAY, N.M., FARAH, J.M., RAO, T.S. & CONTRERAS, P.C. (1991). (+)-3-[3-Hydroxyphenyl-*N*-(1-propyl) piperidine] selectively differentiates effects of sigma ligands on neurochemical pathways modulated by sigma receptors. Evidence for subtypes, *in vivo*. *Neuropharmacology*, **30**, 915–922.

JUNIEN, J.L., GUÉ, M. & BUENO, L. (1991). Neuropeptide Y and sigma ligand (JO 1784) act through a Gi protein to block the psychological stress and corticotropin-releasing factor-induced colonic motor activation in rats. *Neuropharmacology*, **30**, 1119–1124.

LODGE, D. & ANIS, N.A. (1984). Effects of ketamine and three other short acting anaesthetics on spinal reflexes and inhibitions in the cat. *Br. J. Anaesth.*, **56**, 1143–1151.

LODGE, D., ARAM, J.A., CHURCH, J., DAVIES, S.N., FLETCHER, E. & MARTIN, D. (1988). Electrophysiological studies of the interaction between phencyclidine/sigma receptor agonists and excitatory amino acid neurotransmission on central mammalian neurons. In *Sigma and Phencyclidine-like Compounds as Molecular Probes in Biology*. ed. Domino, E.F. & Kamenka, J.M. pp. 239–250. Ann Arbor: NPP Books.

MALOUF, A.T., SWEARENGEN, E. & CHAVKIN, C. (1988). Comparison of the actions of phencyclidine and sigma ligands on CA1 hippocampal pyramidal neurons in the rat. *Neuropharmacology*, **27**, 1161–1170.

MARTIN, W.J., ROTH, J.S. & WALKER, J.M. (1992). The effects of sigma compounds on both NMDA- and non NMDA-mediated neuronal activity in rat hippocampus. *Soc. Neurosci. Abst.*, **18**, 16.6.

MASSAMIRI, T. & DUCKLES, S.P. (1990). Multiple vascular effects of sigma-ligands and PCP ligands-inhibition of amine uptake and contractile responses. *J. Pharmacol. Exp. Ther.*, **253**, 124–129.

MONNET, F.P., DEBONNEL, G., JUNIEN, J.L. & DE MONTIGNY, C. (1990). *N*-methyl-D-aspartate-induced neuronal activation is selectively modulated by sigma receptors. *Eur. J. Pharmacol.*, **179**, 441–445.

MONNET, F.P., BLIER, P., DEBONNEL, G. & DE MONTIGNY, C. (1992a). Modulation by sigma ligands of *N*-methyl-D-aspartate-induced [^{3}H]noradrenaline release in the rat hippocampus: G-protein dependency. *Naunyn-Schmied. Arch. Pharmacol.*, **346**, 32–39.

MONNET, F.P., DEBONNEL, G. & DE MONTIGNY, C. (1992b). *In vivo* electrophysiological evidence for a selective modulation of *N*-methyl-D-aspartate-induced neuronal activation in rat CA_3 dorsal hippocampus by sigma ligands. *J. Pharmacol. Exp. Ther.*, **261**, 123–130.

MONNET, F.P., DEBONNEL, G., FOURNIER, A. & DE MONTIGNY, C. (1992c). Neuropeptide Y potentiates the *N*-methyl-D-aspartate response in the CA_3 dorsal hippocampus. II. Involvement of a subtype of sigma receptor. *J. Pharmacol. Exp. Ther.*, **263**, 1219–1225.

MONNET, F.P., FOURNIER, A., DEBONNEL, G. & DE MONTIGNY, C. (1992d). Neuropeptide Y potentiates selectively the *N*-methyl-D-aspartate response in the rat CA_3 dorsal hippocampus. I. Involvement of an atypical neuropeptide Y receptor. *J. Pharmacol. Exp. Ther.*, **263**, 1212–1218.

NICOLETTI, F., IADAROLA, M.J., WROBLEWSKI, J.T. & COSTA, E. (1986). Excitatory amino acids recognition sites-coupled with inositol phospholipid metabolism: developmental changes and interaction with α_1-adrenoceptors. *Proc. Natl. Acad. Sci. U.S.A.*, **83,** 1931–1934.

PASCAUD, X.B., CHOVET, M., ROZE, C. & JUNIEN, J.-L. (1993). Neuropeptide Y and σ receptor agonists act through a common pathway to stimulate duodenal alkaline secretion in rats. *Eur. J. Pharmacol.*, **231,** 389–394.

PAXINOS, G. & WATSON, C. (1986). *The Rat Brain in Stereotaxic Coordinates*. 2nd edition. San Diego, CA: Academic press.

PEROUTKA, S.J., U'PRICHARD, D.C., GREENBERG, D.A. & SNYDER, S.H. (1977). Neuroleptic drug interactions with norepinephrine α receptor binding sites in rat brain. *Neuropharmacology*, **16,** 549–556.

QUIRION, R., BOWEN, W.D., ITZHAK, Y., JUNIEN, J.L., MUSACCHIO, J.M., ROTHMAN, R.B., SU, T.P., TAM, S.W. & TAYLOR, D.P. (1992). Classification of sigma binding sites: a proposal. In *Multiple Sigma and PCP Receptor Ligands: Mechanisms for Neuromodulation and Neuroprotection*? ed. Kamenka, J.M. & Domino, E.F. pp. 927–933. Ann Arbor: NPP Books.

RECAENS, M., SASSETTI, I., NOURIGAT, A., SLADECZEK, F. & BOCKAERT, J. (1987). Characterization of subtypes of excitatory amino acid receptors involved in the stimulation of inositol phosphate synthesis in rat brain synaptosomes. *Eur. J. Pharmacol.*, **141,** 87–93.

RIVIERE, P.J.M., PASCAUD, X., JUNIEN, J.L. & PORRECA, F. (1990). Neuropeptide-Y and JO 1784, a selective sigma ligand, alter intestinal ion transport through a common, haloperidol-sensitive site. *Eur. J. Pharmacol.*, **187,** 557–559.

RIVIERE, P.J.M., RAO, R.K., PASCAUD, X., JUNIEN, J.L. & PORRECA, F. (1993). Effects of neuropeptide Y, peptide YY and sigma ligands on ion transport in mouse jejunum. *J. Pharmacol. Exp. Ther.*, **264,** 1268–1274.

ROMAN, F.J., PASCAUD, X., DUFFY, O., VAUCHE, D., MARTIN, B. & JUNIEN, J.L. (1989). Neuropeptide-Y and peptide – YY interact with rat brain sigma and PCP binding sites. *Eur. J. Pharmacol.*, **174,** 301–302.

ROMAN, F.J., PASCAUD, X., DUFFY, O. & JUNIEN, J.L. (1991a). *N*-methyl-D-aspartate receptor complex modulation by neuropeptide Y and peptide YY in rat hippocampus *in vitro*. *Neurosci. Lett.*, **122,** 202–204.

ROMAN, F.J., PASCAUD, X., DUFFY, O. & JUNIEN, J.L. (1991b). Modulation by neuropeptide Y and peptide YY of NMDA effects in hippocampal slices: Role of sigma receptors. In *NMDA Receptor Related Agents: Biochemistry, Pharmacology and Behavior* ed. Kameyama, T., Nabeshima, T. & Domino, E.F. pp. 211–218. Ann Arbor: NPP Books.

ROMAN, F.J., MARTIN, B. & JUNIEN, J.L. (1993). In vivo interaction of neuropeptide Y and peptide YY with σ receptor sites in the mouse brain. *Eur. J. Pharmacol.*, **242,** 305–307.

ROMAN, F.J., PASCAUD, X., MARTIN, B., VAUCHE, D. & JUNIEN, J.L. (1990). JO-1784, a potent and selective ligand for rat and mouse brain sigma sites. *J. Pharm. Pharmacol.*, **42,** 439–440.

ROTH, J.E., FRANKLIN, P.H. & MURRAY, T.F. (1993). The σ receptor ligand 1,3-di(2-tolyl)guanidine is anticonvulsant in the rat prepiriform cortex. *Eur. J. Pharmacol.*, **236,** 327–331.

SLADECZEK, F., PIN, J.P., RECAENS, M., BOCKAERT, J. & WEISS, S. (1985). Glutamate stimulates inositol phosphate formation in striatal neurons. *Nature*, **317,** 717–719.

STEINFELS, G.F., TAM, S.W. & COOK, L. (1989). Electrophysiological effects of selective sigma-receptor agonists, antagonists, and the selective phencyclidine receptor agonist MK-801 on midbrain dopamine neurons. *Neuropsychopharmacology*, **2,** 201–208.

SU, T.P. (1982). Evidence for sigma opioid receptor: binding of [^{3}H]SKF-10047 to etorphine-inaccessible sites in guinea-pig brain. *J. Pharmacol. Exp. Ther.*, **223,** 284–290.

TAM, S.W., STEINFELS, G.F. & COOK, L. (1988). Biochemical and behavioural aspects of sigma and phencyclidine receptors: Similarities and differences. In *Sigma and Phencyclidine-like Compounds as Molecular Probes in Biology*. ed. Domino, E.F. & Kamenka, J.-M. pp. 383–396. Ann Arbor: NPP Books.

WEBER, E., SONDERS, M., QUARUM, M., MCLEAN, S., POU, S. & KEANA, J.F.W. (1986). 1,3-Di(2-[5-3H]tolyl)guanidine: a selective ligand that labels sigma-type receptors for psychotomimetic opiates and antipsychotic drugs. *Proc. Natl. Acad. Sci. U.S.A.*, **83,** 8784–8788.

ZHOU, G.Z. & MUSACCHIO, J.M. (1991). Computer-assisted modelling of multiple dextromethrophan and sigma binding sites in guinea pig brain. *Eur. J. Pharmacol: Mol. Pharmacol.*, **206,** 261–269.

(Received December 10, 1993
Revised March 2, 1994
Accepted March 8, 1994)

British Journal of Pharmacology

VOLUME 112 (2) JUNE 1994

BRITISH JOURNAL OF PHARMACOLOGY

The *British Journal of Pharmacology* welcomes contributions in all fields of experimental pharmacology including neuroscience, biochemical, cellular and molecular pharmacology. The Board of Editors represents a wide range of expertise and ensures that well-presented work is published as promptly as possible, consistent with maintaining the overall quality of the journal.

Edited for the British Pharmacological Society by

A.T. Birmingham
(Chairman)

R.W. Horton **W.A. Large**
(Secretaries)

Submission of manuscripts: Manuscripts (two copies) should be sent to The Editorial Office, British Journal of Pharmacology, St. George's Hospital Medical School, Cranmer Terrace, London SW17 0RE.

Authors should consult the Instructions to Authors and the Nomenclature Guidelines for Authors in Vol. **111,** 378–387. These Instructions and Guidelines also appear with the journal Index for Volumes **108–110**, 1993. A checklist of the essential requirements is summarised in each issue of the journal, or as the last page of the issue.

The *British Journal of Pharmacology* is published monthly by the Scientific & Medical Division, Macmillan Press Ltd.

The journal is covered by *Current Contents*, *Excerpta Medica* and *Index Medicus*.

All business correspondence and reprint requests should be addressed to the Scientific & Medical Division, Macmillan Press Ltd., Houndmills, Basingstoke, Hampshire RG21 2XS, UK. Telephone: (0256) 29242; Fax: (0256) 810526.

Enquiries concerning advertising space or rates should be addressed to: Michael Rowley, Advertisement Manager, Macmillan Press Ltd., Hasler House, High Street, Great Dunmow, Essex CM6 1AP. Tel: 0371 874613; Fax: 0371 872273.

Annual subscription prices for 1994 EC £540, elsewhere £595/US$950 (sterling rate is definitive). Orders must be accompanied by remittance. Cheques should be made payable to Macmillan Press, and sent to: Macmillan Press Ltd., Subscription Department, Brunel Road, Houndmills, Basingstoke, Hampshire RG21 2XS, UK.
Overseas subscribers may make payments into UK Post Office Giro Account No. 5192455. Full details must accompany the payment.

British Journal of Pharmacology (ISSN 0007–1188) is published monthly by Macmillan Publishers Ltd, c/o Mercury Airfreight International Ltd, 2323 Randolph Avenue, Avenel, NJ 07001, USA. Subscription price is $950.00 per annum. 2nd class postage is paid at Rahway NJ. *Postmaster*: send address corrections to Macmillan Publishers, c/o Mercury Airfreight International Ltd, 2323 Randolph Avenue, Avenel NJ 07001.

ISSN 0007–1188
0007–1188/94 $9.00 + $0.00

PREPARATION OF MANUSCRIPTS

Authors are strongly recommended to read the full *Instructions to Authors* and *Nomenclature Guidelines for Authors* (*Br. J. Pharmacol.* 1994, **111,** 378–387) before submitting a manuscript for publication in the *British Journal of Pharmacology*. The manuscript and cover letter should be checked against the following list before mailing.

The original and one copy of the manuscript must be supplied. Manuscripts must be typed in double-line spacing on one side of A4 paper, in type not smaller than 12 characters per inch or 10 point. Both copies to include Tables and a set of labelled Figures. One set of Figures without numbers or letters is also to be included. The text to be arranged in the following subsections:

1. **Title**—To have no more than 150 characters on a separate page, which should also include a Short Title (50 characters maximum) and the name and address of the author for correspondence.
2. **Summary**—To be arranged in numbered paragraphs (Full Papers) or a single paragraph (Special Reports).
   —to include aims, principal results and conclusions.
   —to include Key words (10 maximum) at end of summary.
3. **Introduction**—To contain concise statements of the problem and the aims of the investigation.
4. **Methods**—To have brief but adequate account of the procedures; *full names of drugs (including those referred to by manufacturer's code)*, sources of drugs and statistical tests to be stated.
5. **Results**—To have no repetition of data in Figures, Tables and text.
6. **Discussion**—Findings and conclusions to be placed in context of other relevant work.
   NB Simple repetition of results and unwarranted speculation are not acceptable.
7. **Acknowledgements**—Sources of support. Sources of drugs not widely available commercially.
8. **References**—All references in the text to be included in the Reference List and *vice versa*. References in alphabetical order with complete citations; Journals publishing 'in press' papers identified.
   References to manuscripts submitted to other journals but not yet accepted are not allowed.
9. **Tables**—Each on a separate page and prepared in accordance with current requirements of the Journal.
10. **Figures**—Both labelled and non-labelled Figures to be prepared in accordance with current requirements of the Journal (see *Instructions to Authors*, 1993, **108,** 275–281) and provided with Figure Number and Authors' names on back (*in pencil*).
    —each legend to be typed on a separate page and carrying keys to symbols.
    —keys to symbols and histograms must not appear on the figures themselves, but in the respective legends.
    —'box style' figures are not in keeping with the Journal style; line drawings etc must have only left-hand and bottom axes.
11. **Manuscripts**—To be accompanied by a declaration signed by each author that
    (a) results are original
    (b) approval of all persons concerned has been given to submit manuscripts for consideration (see also 12b)
    (c) the same material is neither 'in press' (i.e. is in proof or has definitely been accepted for publication) nor under consideration elsewhere. Furthermore it will not be submitted or published elsewhere before a decision has been reached by the Editorial Board of the *British Journal of Pharmacology* and will not be submitted elsewhere if accepted by the *British Journal of Pharmacology*.
    (d) Copyright assignment is included.
12. **Cover letter**—To state clearly
    (a) Corresponding author's full postal address, telephone, telex or Fax number
    (b) where appropriate, that *either* ethical approval has been given for investigation *or* Company or Institutional permission to publish work has been received.
13. **Reminder**—Packaging to be sufficiently robust to protect Figures and to withstand mailing.

Failure to comply with *Instructions to Authors* may lead to substantial delays in processing, review and publication and may even jeopardize acceptance of the manuscript.

NOMENCLATURE

Authors are reminded that accepted receptor and associated terminology is laid out in *Nomenclature Guidelines for Authors*, as published in the *British Journal of Pharmacology, Br. J. Pharmacol.*, 1994, **111,** 385–387.

SPECIAL REPORTS

The purpose of *Special Reports* is to provide rapid publication for **new** and **important** results which the Editorial Board considers are likely to be of special pharmacological significance. *Special Reports* will have publication priority over all other material and so authors are asked to consider carefully the status of their work before submission.

In order to speed publication there is normally no revision allowed beyond very minor typographical or grammatical corrections. If significant revision is required, the Board may either invite rapid re-submission or, more probably, propose that it be re-written as a Full Paper and be re-submitted for consideration. In order to reduce delays, proofs of *Special Reports* will be sent to authors but **essential corrections must reach the Production Office within 48 hours of receipt.** Authors should ensure that their submitted material conforms exactly to the following requirements.

Special Reports should normally occupy no more than two printed pages of the Journal; two illustrations (Figures or Tables, with legends) are permitted. As a guideline, with type face of 12 pitch and double-line spacing, a page of A4 paper could contain about 400 words. The absolute maximum length of the *Special Report* is 1700 words. For each Figure or Table, please deduct 200 words. The manuscript should comprise a Title page with key words (maximum of 10), a Summary consisting of a single short paragraph, followed by Introduction, Methods, Results, Discussion and References (maximum of 10). In all other respects, the requirements are the same as for Full Papers (see current 'Instructions to Authors').

BRITISH JOURNAL OF PHARMACOLOGY VOLUME 112 (2) 1994

SPECIAL REPORTS

PAPERS

Contents continue inside back cover

Typeset by Elite Typesetting Techniques, Southampton, Hampshire
and printed in Great Britain by Unwin Brothers Ltd., The Gresham Press, Old Woking, Surrey